PB2005-102288

U.S. Department
of Transportation
Federal Highway Administration

Office of Bridge Technology
400 Seventh Street S.W.
Washington D.C. 20590

Application of Geophysical Methods to Highway Related Problems

August 2004

Publication No. FHWA-IF-04-021

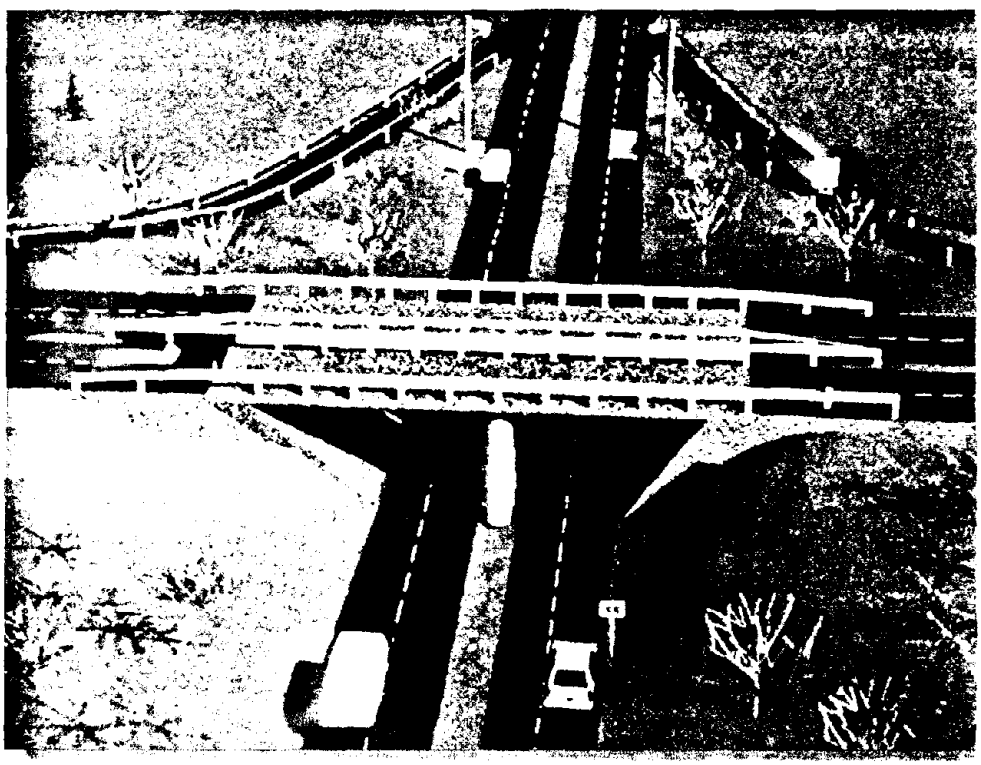

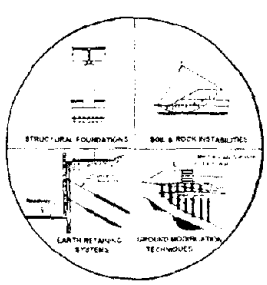

NOTICE

This report is disseminated under the sponsorship of the Department of Transportation in the interest of information exchange. The United States Government assumes no liability for its contents or use thereof.

The United States Government does not endorse products or manufacturers. Trademarks or manufacturers' names appear herein only because they are considered essential to the object of this document.

The contents of this report reflect the views of the authors, who are responsible for the facts and accuracy of the data presented herein. The contents do not necessarily reflect the official policy of the Department of Transportation.

This report does not constitute a standard, specification, or regulation.

1. Report No.	2. Government Accession No.	3. Recipient's Catalog No.

4. Title and Subtitle	5. Report Date
Application of Geophysical Methods to Highway Related Problems	September 2003
	6. Performing Organization Code

7. Author(s)	8. Performing Organization Report No.
W. Ed Wightman, Ph.D., Geophysics; Frank Jalinoos, MS Geophysics Philip Sirles, MS, Geophysics; Kanaan Hanna, MS, Mining Engineering	

9. Performing Organization Name and Address	10. Work Unit No. (TRAIS)
Blackhawk GeoSciences, A Division Of Blackhawk GeoServices	
	11. Contract or Grant No. DTFH68-02-P-00083

12. Sponsoring Agency Name and Address	13. Type of Report and Period Covered
Federal Highway Administration Central Federal Lands Highway Div. 555 Zang Street Lakewood, Co 80228	Technical Manual, 2002-2003
	14. Sponsoring Agency Code

15. Supplementary Notes
Contracting Officer's Technical Representative: Khamis Y. Haramy
A web page is available based on this report at http://girs.cflhd.gov

16. Abstract
This document is designed to provide highway engineers with a basic knowledge of geophysics and nondestructive test (NDT) methods for solving specific transportation related problems. The document is not intended to make engineers experts in the field of geophysics, but rather to provide them with tools that will assist them in the use of suitable geophysical and NDT techniques to evaluate problems for design, planning, construction, or remediation efforts. A table is included to provide the user with a simplified approach of suggested method(s) for various highway engineering problems.
In this document, the term NDT is used to refer to condition evaluation of engineered structures. Condition evaluation includes integrity assessment for defects and corrosion, and the determination of unknown geometry, such as unknown foundation depths or extent of foundations. A broad range of practical methods are presented, including most traditional geophysical methods. These have been adapted to provide solutions more specific to a variety of engineering problems.
The document is divided into two parts. The first part is problem oriented and provides a range of geophysical imaging and NDT methods that can be used to solve particular highway-related problems. The second part provides more comprehensive discussions of the geophysical methods and theory.

17. Key Word	18. Distribution Statement
Geophysical surveys, Non Destructive Testing, Drilled Shafts, Decks, Pavements, Vibration Evaluation, Geological Evaluations, Engineering Properties	No restrictions

19. Security Classif. (of this report)	20. Security Classif. (of this page)	21. No. of Pages	22. Price
Unclassified	Unclassified	742	

Form DOT F 1700.7 (8-72) Reproduction of completed page authorized

SI CONVERSION FACTORS				
APPROXIMATE CONVERSION FROM SI UNITS				
Symbol	**When You Know**	**Multiply By**	**To Find**	**Symbol**
LENGTH				
mm	millimeters	0.039	inches	in
m	meters	3.28	feet	ft
m	meters	1.09	yards	yd
km	kilometers	0.621	miles	mi
AREA				
mm^2	square millimeters	0.0016	square inches	in^2
m^2	square meters	10.764	square feet	ft^2
m^2	square meters	1.195	square yards	yd^2
ha	hectares	2.47	acres	ac
km^2	square kilometers	0.386	square miles	mi^2
VOLUME				
ml	millimeters	0.034	fluid ounces	fl oz
m^3	liters	0.264	gallons	ga
m^3	cubic meters	35.71	cubic feet	ft^3
l	cubic meters	1.307	cubic yards	yd^3
MASS				
g	grams	0.035	ounces	oz
kg	kilograms	2.202	pounds	lb
TEMPERATURE				
°C	Celsius	1.8C+32	Fahrenheit	°F
WEIGHT DENSITY				
kN/m^3	kilonewton / cubic meter	6.36	poundforce / cubic foot	pcf
FORCE and PRESSURE or STRESS				
N	newtons	0.225	poundforce	lbf
kN	kilonewtons	225	poundforce	lbf
kPa	kilopascals	0.145	poundforce / square inch	psi
kPa	kilopascals	20.9	poundforce / square foot	psf

ACKNOWLEDGEMENTS

The authors would like to express their appreciation to Mr. Khamis Y. Haramy, COTR of the Federal Highway Administration (FHWA), Central Federal Lands Highway Division (CFLHD), for guiding, directing, and providing valuable technical assistance and review during the preparation of the document. The authors would also like to thank the following individuals who provided a technical review of the document:

- Roger Surdahl
- Justin Henwood
- Linden Snyder
- Benjamin Rivers
- Barry Berkovitz
- Thomas Lefchik
- Hamilton Duncan
- Silas Nichols

The authors would like to thank the following senior reviewers for providing helpful technical comments and reviewing the document:

- Gary Young, Geomedia Research and Development
- Neil Anderson, Ph.D., School of Mines and Metallurgy, University of Missouri-Rolla
- Erick Westman, Ph.D., Virginia Polytechnic University

The authors would like to thank the following individuals for contributing and providing information used for the development of this document:

- Michael Klosterman, U.S. Army Corps of Engineers – HQ02
- Greg Hempen, Ph.D., U.S. Army Corps of Engineers – St. Louis District
- John Diehl, GeoVision, a division of Blackhawk GeoServices
- Carl Rascoe, GeoVision, a division of Blackhawk GeoServices
- Francisco Romero, GeoVision, a division of Blackhawk GeoServices
- Gary Young, Geomedia Research and Development
- Wayne Peeples, Ph.D., Geomedia Research and Development
- Choon Park, Ph.D., Kansas Geological Survey
- Michael Culig, Colog, a division of Layne Christensen
- Nathan Davis, Colog, a division of Layne Christensen

The authors would like to thank the manufacturers and consulting companies for providing the copyrighted materials used in this document. Reference to these materials is included in the document.

The authors would like to thank Mr. Manuel Montoya, Computer Services, and Messrs. Linden Snyder and Alex Stefanacci, CFLHD, for the web page design of this document.

Finally, the authors would like to thank Ms. Cecelia Slivick, Blackhawk GeoServices, and Ms. Jean Rau, NSA Geotechnical Services, for editing, word processing, and layout of the document, Messrs. Herman Vialpando and James Vialpando, Blackhawk GeoServices, for drafting and art work, and Ms. Alisa Green, Blackhawk GeoServices for obtaining copyrighted materials.

PREFACE

The purpose of this document is to provide highway engineers with a basic knowledge of geophysics and nondestructive test (NDT) methods for solving specific engineering problems during geotechnical investigation, construction, and maintenance of highways. The document is not intended to make engineers experts in the field of geophysics, but rather to provide them with tools that will assist them in the use of suitable geophysical and NDT techniques to evaluate problems for design, planning, construction, or remediation efforts.

The application of geophysical imaging and NDT methods has been increasing in site characterization and geotechnical investigations during highway constructions because they offer accurate and timely information for design quality and performance. Detailed knowledge of unforeseen, highly variable subsurface ground conditions reduces project risk and costs associated with "change of conditions" claims, and improve construction and safety. In this document, the term NDT is used to refer to condition evaluation of engineered structures. Condition evaluation includes integrity assessment for defects and corrosion, and the determination of unknown geometry, such as unknown foundation depths or extent of foundations.

This document provides a broad range of practical methods, including almost all traditional geophysical methods. These have been adapted to provide solutions more specific to a variety of engineering problems pertaining to transportation. For example, conventional geophysical methods have been used to evaluate the physical properties of soil and rock, such as seismic methods which are used to calculate the depth to bedrock or locate underground voids. In the NDT applications, the same seismic methods have been adapted for condition evaluation with great success, producing a technique known as the Ultraseismic test method. In this method, the concrete structure itself is used instead of the earth for the transmission of the acoustic energy with reflection events coming from either the bottom of a structure, as in a bridge foundation, or a defect zone. Similarly, the ground penetrating radar (GPR) geophysical method, originally developed for high resolution imaging of the subsurface, is now used routinely in condition evaluation of pavements, concrete slabs, and walls. These types of NDT geophysical investigations are used in the transportation and infrastructure systems to evaluate new procedures for Quality Assurance (QA) and existing structures for forensic and Quality Control (QC) purposes. To this end, many state and federal Department of Transportations (DOT's) have added various NDT testing standard specifications to their construction codes and will continue to do so with continued deployment of geophysics and NDT in the construction projects.

This document is divided into two parts. The first part is problem oriented and provides a range of geophysical and NTD methods that can be used to solve a particular problem. The second part describes the geophysical techniques in greater detail.

TABLE OF CONTENTS

CHAPTER 1 INTRODUCTION 1

1.1 PURPOSE 1
1.2 BACKGROUND 1
1.2.1 An Overview of Geophysics 1
1.2.2 Application of Geophysics and NDT Methods in Transportation 2
1.2.3 Advantages and Limitations 2
1.3 EVALUATION OF APPROPRIATE GEOPHYSICAL METHODS 3
1.4 DOCUMENT ORGANIZATION 3

GEOPHYSICAL IMAGING AND NONDESTRUCTIVE TESTING FOR HIGHWAY APPLICATIONS – PART I 7

CHAPTER 2 BRIDGE SYSTEM – SUBSTRUCTURE 7

2.1 DETERMINING THE UNKNOWN DEPTH OF FOUNDATIONS 7
2.1.1 Surface NDT Methods 8
2.1.1.1 Sonic Echo(SE)/Impulse Response (IR) 8
2.1.1.2 Bending Waves 12
2.1.1.3 Ultraseismic (US) 14
2.1.1.4 Seismic Wave Reflection Survey 18
2.1.1.5 Transient Forced Vibration Survey 20
2.1.2 Borehole Nondestructive Testing Methods 21
2.1.2.1 Parallel Seismic (PS) 21
2.1.2.2 Induction Field (IF) 23
2.1.2.3 Borehole Logging Methods 25
2.1.2.4 Dynamic Foundation Response 26
2.1.2.5 Borehole Radar 27
2.1.2.6 Borehole Sonic 28
2.1.2.7 Cross-borehole Seismic Tomography 29
2.1.3 Determining Depth of Foundation Socketing Into Bedrock 31
2.2 INTEGRITY TESTING 32
2.2.1 Integrity Testing of Foundations 32
2.2.1.1 Crosshole Sonic Logging (CSL) 32
2.2.1.2 Crosshole Sonic Logging Tomography (CSLT) 35
2.2.1.3 Gamma-gamma Density Logging (GDL) 38
2.2.1.4 Sonic Echo/Impulse Response (SE/IR) 40
2.2.1.5 Single Hole Sonic Logging (SSL) 44
2.2.1.6 Ultraseismic (US) Profiling 45
2.2.2 Integrity Testing of Other Bridge Substructure Elements 48
2.2.2.1 Ultrasonic Pulse Velocity (UPV) 51
2.2.2.2 Impact Echo (IE) 53
2.2.2.3 Ground Penetrating Radar (GPR) 55

2.2.2.4 Spectral Analysis of Surface Waves (SASW) 56
2.2.2.5 Acoustic Emissions (AE) 59
2.2.2.6 High Energy Radiography 60
2.3 REBAR QUALITY AND BONDING TO CONCRETE WITHIN CONCRETE ELEMENTS 61
2.3.1 Direct Measurement Methods 64
2.3.1.1 Half-cell Potential 64
2.3.1.2 Linear Polarization Resistance (LPR) 67
2.3.1.3 Galvanostatic Pulse Technique 69
2.3.1.4 Electrochemical Noise 70
2.3.1.5 Acoustic Emissions 71
2.3.1.6 Magnetic Field Disturbance (MFD) 72
2.3.2 Indirect Measurement Methods 72
2.3.2.1 Potentiodynamic Polarization Curves 72
2.3.2.2 Electrochemical Impedance Spectroscopy (EIS) and Harmonic Analysis 73
2.3.2.3 Zero Resistance Ammetry 73
2.3.3 General Discussion and Conclusions 74
2.4 BRIDGE FOUNDATION SCOUR 74
2.4.1 Time Domain Reflectrometry (TDR) 76
2.4.2 Parallel Seismic (PS) 79
2.4.3 Ground-Penetrating Radar (GPR) 84
2.4.4 Continuous Seismic Reflection Profiling 88
2.4.5 Fathometer 91

CHAPTER 3 BRIDGE SYSTEM – SUPERSTRUCTURE 95

3.1 DECK STABILITY ANALYSIS 96
3.1.1 Initial Monitoring or Structural Verification 97
3.1.2 Periodic Monitoring 98
3.1.3 Permanent Monitoring 98
3.1.4 Recommendations 99
3.2 QA/QC OF NEW DECKS 99
3.2.1 QA Using Geophysical Methods 101
3.2.1.1 Ground Penetrating Radar (GPR) 103
3.2.1.2 Impact Echo (IE) 103
3.2.1.3 Spectral Analysis of Surface Waves (SASW) and Ultrasonic Surface Waves Methods 104
3.2.1.4 Spectral Analysis of Surface Waves (SASW) and Impact Echo (IE) Combined 104
3.3 BASELINE CONDITION ASSESSMENT 104
3.3.1 Baseline Condition Assessment Using Geophysical Methods 105
3.3.1.1 Ground Penetrating Radar (GPR) 106
3.3.1.2 Electromagnetic (EM) Instruments Sensitive to Ferrous Content in Steel 108
3.3.1.3 Ultrasonic-Seismic Techniques 109
3.3.1.4 Ultrasonic Seismic and Impact Echo (Combined) 109
3.3.1.5 Half-Cell Corrosion Potential Mapping 110

3.3.1.6 Infrared (IR) Thermography *111*
3.4 CONDITION EVALUATION OF EXISTING DECK **113**
3.4.1 Presence, Pattern and Density (PPD) of Rebar **113**
3.4.1.1 Ground Penetrating Radar (GPR) *114*
3.4.2 Rebar Condition/Corrosion **114**
3.4.2.1 Ground Penetrating Radar (GPR) *116*
3.4.2.2 Half-Cell Corrosion Potential *117*
3.4.3 Concrete Condition/Integrity **118**
3.4.3.1 Ground Penetrating Radar (GPR) *120*
3.4.3.2 Impact Echo (IE) *121*
3.4.3.3 Surface Wave Methods: SASW/MASW and USW Spectral Analysis of Surface Waves (SASW)/Multiple Channel Analysis of Surface Waves (MASW) and Ultrasonic Surface Waves (USW) *121*
3.4.4 Incipient Spalling **125**
3.4.4.1 Ground Penetrating Radar (GPR) *126*
3.4.4.2 Impact Echo (IE) *126*
3.4.4.3 Surface Wave Methods: Spectral Analysis of Surface Waves (SASW)/Multiple Channel Analysis of Surface Waves (MASW) and Ultrasonic Surface Waves (USW) *126*
3.4.5 Vehicle Mounted Ground Penetrating Radar (GPR) Systems **127**
3.4.5.1 GPR Method One: *127*
3.4.5.2 GPR Method Two: *128*
3.4.5.3 GPR Method Three: *129*

CHAPTER 4 PAVEMENTS **135**

4.1 QA/QC OF NEW PAVEMENTS **136**
4.1.1 Ground Penetrating Radar (GPR) **137**
4.1.2 Impact Echo (IE) **139**
4.1.3 Spectral Analysis of Surface Waves (SASW) and Ultra Sonic Surface Wave (USW) Methods **140**
4.1.4 Multichannel Analysis of Surface Waves (MASW) Method **145**
4.2 CONDITION EVALUATION OF EXISTING PAVEMENTS **150**
4.2.1 Segregation in Hot Mix Asphalt **150**
4.2.2 Moisture Variation **151**
4.2.3 Rock Pockets **152**
4.2.4 Voids Beneath Pavements **152**
4.2.5 Cracking **152**
4.2.6 Pavement Condition/Integrity **153**
4.2.7 Structural Changes **153**
4.3 TRANSPORTATION / GEOTECHNICAL METHODS **154**

CHAPTER 5 ROADWAY SUBSIDENCE **157**

5.1 MAPPING VOIDS, SINKHOLES, ABANDONED MINES, AND OTHER CAVITIES **157**
5.1.1 Gravity Method **157**
5.1.2 Ground Penetrating Radar **160**

5.1.3 Resistivity Methods **163**
5.1.4 Seismic Refraction **168**
5.1.5 Shear Wave Reflection Surveys **169**
5.1.6 Rayleigh Waves Recorded with a Common Offset Array **172**
5.1.7 Cross-borehole Seismic Tomography **174**
5.2 ROADBED CLAY PROBLEMS **177**
5.2.1 Estimating Clay Content **177**
5.2.1.1 Conductivity Measurements *178*
5.2.1.2 Resistivity Measurements *181*
5.2.1.3 Time Domain Electromagnetic Soundings *183*
5.2.1.4 Induced Polarization *185*
5.2.2 Identifying Roadbed Underlain by Expansive Clays (Determine Clay Content in Swelling Soils) **186**
5.2.2.1 Conductivity Measurements *189*
5.2.2.2 Resistivity Methods *191*
5.2.2.3 Time Domain Electromagnetic Soundings *195*
5.2.2.4 Induced Polarization *196*

CHAPTER 6 SUBSURFACE CHARACTERIZATION **199**

6.1 SUBSURFACE GEOPHYSICAL MAPPING AND IMAGING **199**
6.1.1 Determination of the Depth/Structure/Fractures of Bedrock **199**
6.1.1.1 Ground Penetrating Radar (GPR) *200*
6.1.1.2 Seismic Refraction *202*
6.1.1.3 Seismic Reflection *206*
6.1.1.4 Resistivity *208*
6.1.1.5 Time Domain Electromagnetic Soundings *209*
6.1.1.6 Conductivity Measurements using the EM31 and EM34 ..... *212*
6.1.1.7 Spectral Analysis of Surface Waves *214*
6.1.1.8 Gravity *218*
6.1.1.9 Conductivity Measurements to Map Fractures *221*
6.1.1.10 Ground Penetrating Radar to Map Fractures *222*
6.1.1.11 Rayleigh Waves Recorded with a Common Offset Array to Map Fractures *223*
6.1.1.12 Seismic Refraction to Map Fractures *225*
6.1.1.13 Shear Wave Seismic Reflection to Map Fractures *226*
6.1.1.14 Resistivity Measurements to Map Fractures *227*
6.1.1.15 Geophysical Methods to Map Faults *228*
6.1.2 Mapping Fractures and Identifying Weak Zones Within the Bedrock **229**
6.1.2.1 Resistivity *232*
6.1.2.2 Time Domain Electromagnetic Soundings *235*
6.1.2.3 Conductivity Measurements *237*
6.1.2.4 Rayleigh Waves Recorded with a Common Offset Array *238*
6.1.2.5 Shear Wave Seismic Reflection *239*
6.1.2.6 Seismic Refraction *241*
6.1.2.7 Ground Penetrating Radar *243*
6.1.2.8 Very Low Frequency Electromagnetic Surveys *245*

6.1.2.9 Borehole Televiewers (Optical & Acoustic) *247*
6.1.3 Mapping Lithology **249**
6.1.3.1 Seismic Refraction *253*
6.1.3.2 Seismic Reflection *255*
6.1.3.3 Time Domain Electromagnetic Soundings *257*
6.1.3.4 Resistivity *259*
6.1.3.5 Magnetic *261*
6.1.3.6 Induced Polarization *263*
6.1.3.7 Borehole Gamma Logs (Natural Gamma or Gamma Ray) *266*
6.1.4 Locating Shallow Sand and Gravel Deposits **268**
6.1.4.1 Resistivity; Soundings, and Traverses *270*
6.1.4.2 Conductivity Measurements *273*
6.1.4.3 Time Domain Electromagnetic Soundings *275*
6.1.4.4 Airborne Resistivity *276*
6.1.4.5 Seismic Refraction *278*
6.1.4.6 Ground Penetrating Radar *280*
6.1.5 Mapping Groundwater Surface and Flow **281**
6.1.5.1 Resistivity Soundings *283*
6.1.5.2 Time Domain Electromagnetic Soundings *286*
6.1.5.3 Seismic Refraction *287*
6.1.5.4 Ground Penetrating Radar *289*
6.1.5.5 Nuclear Magnetic Resonance *290*
6.1.5.6 Self Potential *293*
6.1.5.7 The Electroseismic *295*
6.1.5.8 Borehole HydroPhysical™ Logging *298*
6.2 GEOPHYSICAL METHODS TO DETERMINE PHYSICAL PROPERTIES **299**
6.2.1 Determining Engineering Properties of the Subsurface **299**
6.2.1.1 Seismic Refraction *303*
6.2.1.2 Nuclear Magnetic Resonance *305*
6.2.1.3 Ground Penetrating Radar *307*
6.2.1.4 Spectral Analysis of Surface Waves *308*
6.2.2 Borehole Logging **310**
6.2.2.5 Suspension logging *310*
6.2.2.6 Integrated Logging System *313*
6.2.2.7 Crosshole Shear logging *315*
6.2.3 Determining the Rippability of Rocks **318**
6.2.3.1 Seismic Refraction *320*
6.3 GEOPHYSICAL METHODS TO IMAGE BURIED MANMADE FEATURES **322**
6.3.1 Detecting Subsurface Utilities **322**
6.3.1.1 Magnetic *323*
6.3.1.2 Electromagnetic *325*
6.3.1.3 Ground Penetrating Radar *330*
6.3.1.4 Acoustic Pipe Tracer *332*
6.3.2 Detecting Underground Storage Tanks **332**

6.3.2.1 Magnetic Methods *332*
6.3.2.2 Electromagnetic *335*
6.3.2.3 Metal Detectors *337*
6.3.2.4 Ground Penetrating Radar *339*
6.3.3 Mapping Contaminant Plumes **342**
6.3.3.1 Electromagnetic *343*
6.3.3.2 Resistivity *346*
6.3.3.3 Ground Penetrating Radar *350*
6.3.3.4 Induced Polarization *351*
6.3.3.5 Electromagnetic Methods to Map Aquitard Topography *353*
6.3.3.6 Seismic Refraction to Map Aquitard Topography *354*
6.3.4 Detecting Unexploded Ordnance (UXO) **358**
6.3.4.1 Magnetic *359*
6.3.4.2 Electromagnetic *365*
6.3.4.3 Ground Penetrating Radar *367*

CHAPTER 7 VIBRATION MEASUREMENTS **371**

7.1 VIBRATIONS CAUSED BY TRAFFIC, CONSTRUCTION, AND BLASTING **371**
7.1.1 Traffic Vibrations **371**
7.1.2 Blasting Vibrations **380**
7.1.3 Construction Vibrations **382**
7.1.4 Vibration Recommendations **384**

GEOPHYSICAL METHODS, THEORY, AND DISCUSSION – PART II **389**

CHAPTER 8 GEOPHYSICAL QUANTITIES **391**

8.1 ELECTRICAL CONDUCTIVITY (σ) AND RESISTIVITY (ρ) **391**
8.1.1. Factors Influencing Electrical Conductivity **391**
8.1.1.1 .Metal Content *391*
8.1.1.2 Porosity *391*
8.1.1.3 Clay Content *392*
8.1.1.4 Permeability *393*
8.1.1.5 Skin Depth *395*
8.1.2 Ground Penetrating Radar Attenuation **396**
8.1.3 Induced Polarization (Ip) And Complex Resistivity **397**
8.1.4 Dielectric Permittivity ε **399**
8.1.4.1 Velocity of EM Radiation *401*
8.1.4.2 Reflection Coefficient *401*
8.1.4.3 Water Content *401*
8.2 MAGNETIC SUSCEPTIBILITY (K) **402**
8.2.1 Geomagnetic Field **403**
8.2.1.1 Susceptibility and Magnetite *404*
8.2.1.2 Magnetization of Soils *404*
8.3 DENISTY **404**
8.4 POROSITY **404**
8.5 SEISMIC VELOCITIES (VS, VP) **405**

8.6 REFLECTIVITY 406
8.7 GEOMECHANICAL (ENGINEERING) PROPERTIES 407

CHAPTER 9 SURFACE GEOPHYSICAL METHODS 409

9.1 POTENTIAL FIELD METHODS 409
9.1.1 Magnetic Methods 409
9.1.2 Gravity Methods 414
9.2 SEISMIC METHODS 425
9.2.1 Seismic Reflection Methods 430
9.2.1.1 Common-Offset Seismic Reflection Method 433
9.2.1.2 Subbottom Profiling 437
9.2.1.3 Fathometer Surveys 440
9.2.2 Surface Wave Methods 443
9.2.2.1 Spectral Analysis of Surface Waves (SASW) 443
9.2.2.2 Common-Offset Rayleigh Wave Method 446
9.3 ELECTRICAL METHODS 449
9.3.1 Self-Potential (SP) Method 453
9.3.2 Equipotential and Mise-a-la-Masse Methods 458
9.3.3 Resistivity Methods 461
9.3.4 Induced Polarization 482
9.4 ELECTROMAGNETIC METHODS 489
9.4.1 Frequency Domain Electromagnetic Methods 490
9.4.1.1 Tilt Angle Method 491
9.4.1.2 Terrain Conductivity Method 493
9.4.2 Time-Domain Electromagnetic Methods 501
9.4.3 Ground-Penetrating Radar 516
9.4.4 Very Low-Frequency (VLF) Method 524
9.4.5 Seismoelectrical Method 527
9.4.6 Metal Detectors 531
9.5 NUCLEAR METHODS 534
9.5.1 Nuclear Magnetic Resonance (NMR) Method 534

CHAPTER 10 BOREHOLE GEOPHYSICAL METHODS 539

10.1 GENERAL IN-HOLE PROCEDURES 539
10.2 GENERAL CROSSHOLE PROCEDURES 556
10.3 SURFACE TO BOREHOLE PROCEDURES 567
10.3.1. Overview of Borehole Seismic Methods 567
10.3.2 Velocity Surveys 572
10.3.3 Vertical Incidence VSP 575
10.4 LOGGING TECHNIQUES AND TOOLS 583
10.4.1 Electrical Methods 583
10.4.1.1 Spontaneous Potential Log 583
10.4.1.2 Single-Point Resistance Log 587
10.4.1.3 Normal Resistivity Log 589
10.4.1.4 Lateral Resistivity Log 595
10.4.1.5 Focused Resistivity Log 595
10.4.1.6 Microresistivity Log 596

10.4.1.7 Dipmeter Log *596*
10.4.1.8 Induction Logging *597*
10.4.2 Nuclear Logging **599**
10.4.2.1 Gamma logging *603*
10.4.2.2 Gamma-Gamma Logging *605*
10.4.2.3 Neutron Logging *608*
10.4.3 Acoustic Logging **610**
10.4.3.1 Acoustic-Velocity Logs *611*
10.4.3.2 Acoustic Waveform Logging *614*
10.4.3.3 Cement-Bond Logging *619*
10.4.3.4 AcousticTeleviewer *619*
10.4.4 Other Methods of Logging **624**
10.4.4.1 Caliper Logging *624*
10.4.4.2 Fluid *626*
10.4.4.3 Temperature Logging *626*
10.4.4.4 Conductivity Logging *630*
10.4.5 Flow Logging **631**
10.4.5.1 Impeller Flowmeter *632*
10.4.5.2 Heat-Pulse Flowmeters *632*
10.4.6 Hydrophysical Logging **634**
10.4.7 Well-Completion Logging **637**
10.4.7.1 Casing Logging *637*
10.4.7.2 Logging Annular Materials *638*
10.4.7.3 Borehole-Deviation *640*
10.4.8 Hole-to-Hole Logging **640**
10.4.8.1 Crosshole Seismic/Sonic Logging Survey *640*
10.4.8.2 Crosshole Seismic/Sonic Tomography Survey *646*

BIBLIOGRAPHY **649**

GLOSSARY **698**

LIST OF FIGURES

Figure 1. Source and receiver locations for a Sonic Echo/Impulse Response test for three shaft geometric configurations. 9
Figure 2. Data from the Sonic Echo method and depth calculations. 11
Figure 3. Depth calculations using frequency domain data for the Impulse Response method. 11
Figure 4. Field setup for the Bending Wave method for piles. 13
Figure 5. Ultraseismic test method and vertical profiling test geometry. 16
Figure 6. Ultraseismic test method and horizontal profiling test geometry 16
Figure 7. Example Ultraseismic-Vertical Profiling dataset from a bridge pier. 17
Figure 8. Example Ultraseismic-Horizontal Profiling dataset from a wall structure. 18
Figure 9. Shot and receiver layout for SeismicRreflection survey (plan view) 19
Figure 10. Geophone and shot positions for Common Depth Point recording 20
Figure 11. Parallel Seismic survey setup. 22
Figure 12. Parallel Seismic data and velocity lines. 23
Figure 13. Induction Field method setup. 25
Figure 14. Borehole Radar system. 28
Figure 15. Schematic of the Borehole Sonic method. 29
Figure 16. Tomographic survey design. 30
Figure 17. Tomograms showing: (a) socketed piles and (b) caisson on top of bedrock 31
Figure 18. Crosshole Sonic Logging instruments. 33
Figure 19. Crosshole Sonic Logging method with various kinds of defects. 34
Figure 20. Travel time plot for Crosshole Sonic Logging. 35
Figure 21. Ray paths for Crosshole Sonic Logging and Crosshole Sonic Logging Tomography (S is source, R is receiver). 36
Figure 22. Comparison of Crosshole Sonic Logging and Crosshole Sonic Logging Tomography results. 37
Figure 23. Gamma-gamma denisty logging equipment 38
Figure 24. Gamma-gamma density logs and results. 40
Figure 25. Defects in shafts and seismic waves used to image these defects. 42
Figure 26. Sonic Echo record and depth calculation. 43
Figure 27. Depth calculations using frequency domain data for the Impulse Response method. 44
Figure 28. Single Hole Sonic Logging instrument. 46
Figure 29. Ultraseismic test method showing the vertical profiling test geometry. 48
Figure 30. Measurement points for Ultrasonic Pulse Velocity method. 52
Figure 31. Relation between pulse velocity and compressive strength. 53
Figure 32. Schematic diagram of Impact Echo method 54
Figure 33. Ground Penetrating Radar system over a defect. 55
Figure 34. Plot of Ground Penetrating Radar data from a post-tension tendon survey. 56
Figure 35. Schematic showing variation of Rayleigh wave partical motion with depth. 57
Figure 36. Basic configuration of Spectral Analysis Surface Waves measurements. 58
Figure 37. High Energy Radiography equipment and operation 61

Figure 38. Power equipment to test rebar bonding: (a) Preparation Kit, and (b) Power equipment. 62
Figure 39. Half-cell measuring circuit for detecting rebar corrosion. 65
Figure 40. Half-cell instrument. 66
Figure 41. Example Half-cell Potential results. 66
Figure 42. Linear Polarization Resistance probe 67
Figure 43. Guard ring setup for Linear Polarization Resistance measurements. 68
Figure 44. Example Tafel graph. 69
Figure 45. GalvaPulse© instrument. 70
Figure 46. Scour mechanism. 75
Figure 47. Cable configurations for use in the Time Domain Reflectometry method. 77
Figure 48. Time Domain Reflectrometry signals from cable ends and a thinner section of the cable. 77
Figure 49. Cable installation for Time Domain Reflectrometry measurements at a pier. 78
Figure 50. Parallel Seismic setup. 80
Figure 51. No scour case. Data not filtered. Note the uniform data amplitudes across the water-sediment interface. The linear refraction first-arrival pattern A-B changes to the hyperbolic first-break pattern C-D at C, which occurs at the base of the pier. 81
Figure 52. Scour case. Data not filtered. Note strong attenuation of data amplitudes where energy traverses the mud-filled scour zone. 82
Figure 53. No scour case. Seismic data after digital filtering with a strong low-cut filter. Note the uniform amplitudes across the water-sediment interface. 83
Figure 54. Scour case: Seismic data after digital filtering with a strong low-cut filter. Note the severe energy attenuation of data transmitted through the mud filled scour zone. 83
Figure 55. Unprocessed 300 MHz Ground Penetrating Radar data collected 2 feet upstream from a pier. 85
Figure 56 . Digitally filtered and migrated 300 MHz Ground Penetrating Radar data. 85
Figure 57. Unpositioned 300 MHz Ground Penetrating Radar data collected four feet from a central pier. 86
Figure 58. Ground Penetrating Radar data processed and interpreted to different stages. 87
Figure 59. The Seismic Reflection method. 89
Figure 60. Continuous Seismic Profiling data recorded with a 14.4- kHz transducer. Data have been filtered, spatially corrected, and deconvolved. 90
Figure 61. Continuous Seismic Profiling swept frequency data using 2-16 kHz transducer. 91
Figure 62. Fathometer data recorded with 200 kHz transducer 92
Figure 63. Fathometer data recorded using a 3.5 kHz transducer. 93
Figure 64. Collapse of Tacoma Narrows Bridge. 96
Figure 65. Ground Penetrating Radar image of rebar. 103
Figure 66. Horn antenna (air-coupled) setup and measurement: Basic horn antenna setup (single antenna) is used for bridge deck or pavement evaluation at high speed. Individual Ground Penetrating Radar methods. 107
Figure 67. Ultrasonic-Seismic and Impact Echo test methods (basic setup and measurement). 110
Figure 68. Half-Cell Corrosion Potential method (basic setup and measurement). 111

Figure 69. Geophysical method results (Ground Penetrating Radar and Half-Cell Corrosion Potential contour plots) from double-blind test. 116
Figure 70. Portable Pavement Seismic Analyzer correlated to initial, moderate and severe delamination development (fair, poor, serious), respectively. Results plotted on plan-view map and compared with chain drag. 123
Figure 71. Condition levels obtained by using integrated Ultrasonic-Seismic method. 125
Figure 72. Ground Penetrating Radar Method One: high speed, high resolution, Dual-Polarization Horn Antenna Method 128
Figure 73. Ground Penetrating Radar Method Two: low speed and high-resolution using four 1.5 GHz antennas spaced equal distance apart 129
Figure 74. Comparison of Ground Penetrating Radar Methods with "ground truth" 131
Figure 75. Example Impact Echo Systems. 140
Figure 76. Seismic waves generated. 141
Figure 77. Recorded waveforms 141
Figure 78. Velocity calculation. 142
Figure 79. Spectral Analysis of Surface Waves Instruments 143
Figure 80. Schematic illustrating a typical Multichannel Analysis of Surface Waves survey setup. 145
Figure 81. A 3-step processing scheme for Multichannel Analysis of Surface Waves data. 147
Figure 82. Overall procedure to construct a 2-D Vs map from an Multichannel Analysis of Surface Waves survey 149
Figure 83. Definition of a source-receiver configuration and increment of the configuration. 150
Figure 84. Gravity field over a void 158
Figure 85. Graviton-EG gravity meter 158
Figure 86. Correction for topography. 159
Figure 87. Ground Penetrating Radar system over a void. 161
Figure 88. Ground Penetrating Radar data showing reflections thought to indicate voids. 162
Figure 89. Ground Penetrating Radar data from a pavement survey showing its interpretation. 162
Figure 90. Electrode arrays used to measure resistivity. 164
Figure 91. Electrode array for measuring the resistivity of the ground, and resistivity-sounding curve. 165
Figure 92. Electrode layout for a resistivity survey 166
Figure 93. Data from a resistivity survey over a sinkhole plotted as a pseudosection 167
Figure 94. Seismic refraction across a fracture zone. 168
Figure 95. The Microvib shear wave generator. 170
Figure 96. Ray paths for shear waves over a water/air-filled void. 170
Figure 97. Results from a Microvib survey showing an interpreted void. 171
Figure 98. Voids interpreted from shear wave reflection data 172
Figure 99. Rayleigh wave particle motion and displacement over a void. 173
Figure 100. Data from a Rayleigh wave survey over a void/fracture zone. 174
Figure 101. Source and receiver locations for a tomographic survey 175
Figure 102 . Isometric view of the low velocity zone 176
Figure 103. EM38 instrument being used in vertical dipole mode 179
Figure 104. Relation between soil conductivity and clay content. 180

Figure 105. Syscal Junior automated resistivity system. 182
Figure 106. Dipping clay/shale layer. 188
Figure 107. Clay in alluvium. 188
Figure 108. Conductivity data along a road and the interpretation 191
Figure 109. Resistivity data plotted to form a depth vs resistivity section. 194
Figure 110. Induced Polarization waveform 197
Figure 111. Ground Penetrating Radar system. 201
Figure 112. Ground Penetrating Radar instrument. 201
Figure 113. Ground Penetrating Radar antenna (100 MHz) used in a survey. 202
Figure 114. Seismic Refraction: field set up and data recorder. 203
Figure 115. Basic Generalized Reciprocal method interpretation. 204
Figure 116. Generalized Reciprocal method interpretation. 205
Figure 117. Example of a SeismicRefraction interpretation. 206
Figure 118. The Seismic Reflection method 207
Figure 119. Resistivity Sounding (a) Data recording geometry, and (b) Sounding curve 209
Figure 120. Time Domain Electromagnetic Sounding. 210
Figure 121. A Time Domain Electromagnetic Sounding curve. 211
Figure 122. Model conductivity results over a conductive bedrock. 212
Figure 123. SeisOpt® 2D velocity in an area with strong lateral velocity gradient. 217
Figure 124. Shear-wave profile interpretation from a SeisOpt survey. 217
Figure 125. Gravitational pull over a bedrock depression. 218
Figure 126. Model D1a gravity meter 219
Figure 127. Bedrock fractures and potentially useful attributes. 221
Figure 128. Anomaly from an EM31/34 used in vertical dipole mode over a conductive fracture zone. 222
Figure 129. Ground Penetrating Radar data illustrating a section over a fracture zone. 223
Figure 130. Rayleigh wave particle motion and displacement over a fracture zone. 224
Figure 131. Seismic Refraction for locating fracture zones. 225
Figure 132. Resistivity measurements used for locating water-bearing fractures. 228
Figure 133. Seismic Reflection section showing faults. 229
Figure 134. Two conceptual examples showing weak zones. 230
Figure 135. Resistivity data over a fracture zone. 235
Figure 136. Protem transmitter and receiver for Time Domain Electromagnetic sounding measurements: (a) Protem transmitter, and (b) Protem receiver. 236
Figure 137. Example seismic section showing interpreted faults. 241
Figure 138. Ground Penetrating Radar equipment. 243
Figure 139. A 250 MHz antenna being used in a field survey. 244
Figure 140. Very Low Frequency instrument. 246
Figure 141. Very Low Frequency anomaly over a vertical conductor. 246
Figure 142. Examples of typical borehole images, optical and acoustic. 247
Figure 143. Projection of a planar intersection with a cylindrical borehole. 248
Figure 145. Resistivities of different rock types. 250
Figure 146. Seismic velocities of different rock types. 251
Figure 147. Seismic time-distance graph over four-layer ground. 253
Figure 148. The Minivib seismic source 256
Figure 149 . Resistivity data showing stratigraphic changes. 260

Figure 150. Magnetic anomaly over a magnetite rich zone....262
Figure 151. Induced Polarization instrument....264
Figure 152. Chargeability pseudosection....265
Figure 153. Measured (apparent) resistivity pseudosection....265
Figure 154. Interpreted Induced Polarization data....266
Figure 155. Example of gamma CPS vs. depth....267
Figure 156. Sand and gravel - geological model....269
Figure 157. Sand and gravel deposit resting on bedrock slope....270
Figure 158. Fixed wing airborne conductivity system....277
Figure 159 . Helicopter conductivity measuring system....277
Figure 160. Results from an airborne survey for sand and gravel....278
Figure 161. Section showing drill results and resistivity values over a sand and gravel deposit....278
Figure 162. Two common groundwater occurrences....282
Figure 163. Resistivity instrument....284
Figure 164. Schematic of the Nuclear Magnetic Resonance method....290
Figure 165. Instrument for measuring Nuclear Magnetic Resonance....291
Figure 166. Field data and interpretation of a Nuclear Magnetic Resonance survey....292
Figure 167. Self Potential anomaly expected over water flowing into fracture zone....293
Figure 168. Self Potential anomaly expected over water flowing out of a fracture zone....293
Figure 169. Methods of recording Self Potential data....295
Figure 170. The GroundFlow 2500 instrument....296
Figure 171. System layout for Electroseismic surveys....297
Figure 172. Examples of ambient flow characterization and 10 gpm production test, respectively....299
Figure 173. Schematic showing suspension logging system....311
Figure 174. Sample suspension logging waveform record....313
Figure 175. Examples of engineering rock property traces as calculated from density and sonic logs....314
Figure 176. Schematic of crosshole method....316
Figure 177. Rippability versus seismic velocity....320
Figure 178. Magnetic field from a cylindrical object....324
Figure 179. Magnetic locating instrument....324
Figure 180. Magnetic locator using two sensors to measure the gradient....324
Figure 181. Utility-locating instrument....326
Figure 182. Utility-locating instrument in use....326
Figure 183. The EM31-MK2 instrument....328
Figure 184. The EM61-MK2 instrument....329
Figure 185. The EM61-HH2 hand held instrument....329
Figure 186. 400 MHz Ground Penetrating Radar antenna....330
Figure 187. Ground Penetrating Radar data from a utility trench....331
Figure 188. Grad-601 magnetic gradiometer system....333
Figure 189. Magnetometer with Global Positioning System....334
Figure 190. Concept diagram for electromagnetic methods....336
Figure 191. The GEM2 electromagnetic instrument....337
Figure 192. Metal detector using two magnetic sensors....338

Figure 193. Ground Penetrating Radar over a tank. 340
Figure 194. Ground Penetrating Radar instrument. 340
Figure 195. Ground Penetrating Radar images over three Underground Storage Tanks 341
Figure 196. Ground Penetrating Radar signal from three Underground Storage Tanks. 342
Figure 197. The EM34 being used in horizontal dipole mode. 344
Figure 198. EM31 conductivity data - vertical dipole mode. 344
Figure 199. EM34 conductivity data – horizontal dipole mode. 345
Figure 200. The Ohm-Mapper. 348
Figure 201. SuperSting R1 IP resistivity meter. 348
Figure 202. Example data recorded with the Sting-Swift System. 349
Figure 203. Ground Penetrating Radar data over a hydrocarbon plume. 351
Figure 204. Using conductivity to map aquitard topography. 354
Figure 205. Seismic refraction principles. 355
Figure 206. Basic Generalized Reciprocal Methods interpretation. 356
Figure 207. Generalized Reciprocal Methods interpretation. 357
Figure 208. Example of a seismic refraction interpretation. 357
Figure 209. Cesium magnetometer with GPS 360
Figure 210. Gradiometer using two cesium sensors. 360
Figure 211. Total magnetic field strength and vertical gradient anomalies. 361
Figure 212. The MTADS UXO detection system 361
Figure 213. STOLS UXO detection system. 362
Figure 214. Helicopter-mounted magnetometer system. 363
Figure 215. Analytic Signal 363
Figure 216. Total magnetic field data from a helicopter magnetic survey 364
Figure 217. Analytic signal for data. 364
Figure 218. An array of two EM61 instruments. 366
Figure 219. The GEM-3 electromagnetic instrument. 366
Figure 220. Ground Penetrating Radar data across buried metal and plastic mines. 368
Figure 221. High resolution sensor for ambient vibration monitoring. 376
Figure 222. GPS-3™ general purpose seismograph. 381
Figure 223. Safe level blasting criteria from OSMRE. 382
Figure 224. CVM-2 continuous vibration monitor. 383
Figure 225. Electrical resistivity of rocks with various wt % of sulfide. 393
Figure 226. A layered aquifer model. 394
Figure 227. Schematic relationship between hydraulic conductivity, porosity and resistivity. 395
Figure 228. Skin depth as a function of resistivity and frequency. 396
Figure 229. Schematic of the phase shift between an applied voltage and the resulting current when ρ is complex. 397
Figure 230. Conductivity ranges of some materials.. 398
Figure 231. Schematic of decay time associated with complex resistivity, IP. 399
Figure 232. Variation of resistivity (upper) and phase as function of frequency for some montmorillonite clays. 400
Figure 233. Schematic displacement of charge within a molecule by an electric field E. 401
Figure 234. Dielectric constant of a water-saturated rock as a function of porosity 402
Figure 235. Dielectric constant range for some common materials. 402

Figure 236. Susceptibility as a function of magnetite content.....404
Figure 237. Susceptibility range of common materials.....405
Figure 238. Density ranges in common materials.....405
Figure 239. P-wave velocities as a function of porosity.....406
Figure 240. S-wave velocity ranges for common materials.....407
Figure 241. P wave velocity ranges for common materials.....407
Figure 242. Magnetic field vector examples for two anomalous fields.....414
Figure 243. Actual and measured fields due to magnetic inclination.....415
Figure 244. Normalized peak vertical attraction versus depth to diameter for a spherical body.....416
Figure 245. Gravity anomalies for long horizontal cylindrical cavities as a function of depth, size, and distance from peak.....417
Figure 246. Geologic model (bottom) including water- and air-filled voids; theoretical gravity anomaly (top) due to model; and possible observed gravity (middle).....423
Figure 247. Geologic model (bottom) including water and air filled voids, theoretical gravity anomaly (top) due to model; and possible observed gravity (middle).....424
Figure 248. Gravity traverse and interpreted model.....425
Figure 249. Schematic of the seismic reflection method.....431
Figure 250. Multichannel recordings for seismic reflection.....432
Figure 251. Illustration of common depth point.....432
Figure 252. Simple seismic reflection record.....432
Figure 253. Optimum offset distance determination for the common offset method.....434
Figure 254. Common offset method schematic.....434
Figure 255. Sample common offset record.....435
Figure 256. Reflected subbottoming signal amplitude cross section.....439
Figure 257. Density cross section in Gulfport ship canal, Mississippi.....439
Figure 258. Fathometer data recorded with 200 kHz transducer.....441
Figure 259. Fathometer data recorded using a 3.5 kHz transducer.....442
Figure 260. Typical Spectral Analysis of Surface Waves data.....445
Figure 261. Inversion results of typical Spectral Analysis of Surface Waves data.....445
Figure 262. Rayleigh wave particle motion and displacement.....447
Figure 263. Data from a Rayleigh wave survey over a void/fracture zone.....448
Figure 264. Schematic of flow-induced negative streaming potentials.....454
Figure 265. Electrode configurations at the Harris-Hunter sinkhole site.....458
Figure 266. Principle of the mise-a-la-masse method.....459
Figure 267. Location of a buried ammunition magazine by equipotential methods.....460
Figure 268. Potential pattern from current source in test position.....460
Figure 269. Potential pattern from current source in H-1 zone.....460
Figure 270. Equipotentials and current lines for a pair of current electrodes A and B on a homogeneous half-space.....463
Figure 271. Electrode array configurations for resistivity measurements.....466
Figure 272. Asymptotic behavior of the apparent resistivity curves at very small and very large electrode spacings.....467
Figure 273. Example data sheet for Schlumberger vertical sounding.....472
Figure 274. Example data sheet for Wenner array.....472
Figure 275. Example data sheet for dipole-dipole array.....473

Figure 276. Two-layer master set of sounding curves for the Schlumberger array.....477
Figure 277. Four types of three-layer VES curves. 478
Figure 278. Wenner horizontal resistivity profile over a vertical fault.....480
Figure 279. Wenner horizontal resistivity profiles over a filled sink. 481
Figure 280. Theoretical Wenner profiles across a circular cylinder.....481
Figure 281. Overvoltage on a metallic particle in electrolyte.....483
Figure 282. Nonmetallic induced polarization agent.....483
Figure 283. Apparent resistivity and apparent chargeability (IP) sounding curves for a four-layer model. 485
Figure 284. Dipole-dipole plotting method. 486
Figure 285. Geoelectric section, VES and IP sounding curves at alluvial deposits. 487
Figure 286. Plan profiles for η_a and ρ_a using the gradient array in Baima, China, over a buried cable.....488
Figure 287. Network of SRP-IP profiles with contours of IP vs ηa (%) and extent of contaminant interpreted on the basis of the geophysical survey.. 488
Figure 288. Generalized picture of electromagnetic induction prospecting. 489
Figure 289. Generalized picture of the frequency domain EM method. 492
Figure 290. In-phase and out-of-phase response of a sphere in a uniform alternating magnetic field. 492
Figure 291. Terrain conductivity meter response over conductive dike.....495
Figure 292. Cumulative response curves for both vertical coplanar and horizontal coplanar dipoles.....495
Figure 293. Contours of apparent conductivity for an acid mine dump site in Appalachia from terrain conductivity meter. 498
Figure 294. Contours of apparent conductivity measured with ground conductivity meter over dry farm land. Alberta, Canada. 498
Figure 295. Typical resistivity sounding and interpretation, Dungeness, England. 499
Figure 296. Contours of ground conductivity in mS/m, Dungeness, England. 500
Figure 297. Apparent conductivity contours in ohm-m from a terrain conductivity meter survey in southern Australia. 501
Figure 298. Transmitter current wave form. 502
Figure 299. Central loop sounding configuration. 502
Figure 300. Transient current flow in the ground. 503
Figure 301. Receiver output wave form. 504
Figure 302. Receiver gate locations. 505
Figure 303. Log plot-receiver output voltage versus time (one transient). 505
Figure 304. Wenner array: apparent resistivity, two layer curve 507
Figure 305. Time Domain Electromagnetic apparent resistivity, homogeneous half space.....508
Figure 306. Time Domain Electromagnetic receiver output voltage, two layer earth.....508
Figure 307. Time Domain Electromagnetic apparent resistivity, two layered earth. 509
Figure 308. Forward layered-earth calculations 510
Figure 309. Forward layered earth calculations.....512
Figure 310. Offset Rx locations to check lateral homogeneity. 513
Figure 311. Oscillations induced in receiver response by power line. 515
Figure 312. Common offset and common midpoint acquisition modes. 520
Figure 313. Schematic illustration of common offset single-fold profiling. 521

Figure 314. Ground Penetrating Radar received signal and graphic profile display.....521
Figure 315. Format of a Ground Penetrating Radar reflection section with radar events.....523
Figure 316. Schematic of a set of targets surveyed by Ground Penetrating Radar.....523
Figure 317. Actual Ground Penetrating Radar record over a culvert, pipe, and two tunnels.....524
Figure 318. Tilt of the VLF field vector over a conductor.....525
Figure 319. Comparison of VLF instruments.....526
Figure 320. VLF profile, Burkina Faso, Africa.....526
Figure 321. VLF profile over buried telephone line.....527
Figure 322. Seismoelectrical conversion at an interface.....528
Figure 323. Generation of an electric field by a head wave.....528
Figure 324. Ground Flow 1500 instrument.....529
Figure 325. System layout for electroseismic surveys.....530
Figure 326. Approximate metal detector detection depths for various targets with two coil sizes.....532
Figure 327. Block diagram of one metal dectector coil arrangement and associated electronics.....533
Figure 328. Test survey using a metal detector and a magnetic gradiometer.....534
Figure 329. Schematic of the Nuclear Magnetic Resonance methods.....535
Figure 330. Field data and interpretation of a Nuclear Magnetic Resonance survey.....537
Figure 331. Log selection chart.....542
Figure 332. Computer plot of gamma and neutron logs of three test holes in the Chicago area.....547
Figure 333. Cross section of four test holes in the Chicago area.....548
Figure 334. Cross plot of acoustic transit time versus neutron porosity, Madison limestone test well No. 1, Wyoming.....549
Figure 335. Three-dimensional "Z-plot" of gamma, density, and neutron log response of a test hole in the Chicago area.....550
Figure 336. Effect of drilling technique on hole diameter.....551
Figure 337. Schematic of crosshole method.....558
Figure 338. Crosshole SV-wave paired borehole records at five depths.....559
Figure 339. Illustration of refracted ray path geometries in crosshole seimsic tests.....562
Figure 340. Crosshole SV-waves showing direct (D) and refracted (R) arrivals.....563
Figure 341. Example problem.....567
Figure 342. Correlation between crosshole survey, velocity log synthetic seismogram, and surface seismic reflection section.....569
Figure 343. Recording of a vertical seismic profile; direct arrivals, reflected primaries, and examples of downgoing and upgoing multiples.....569
Figure 344. Example of correlation between Vertical Seismic Profiling and surface seismic profiling.....570
Figure 345. Model of a fault structure.....571
Figure 346. Travel path used for converting total travel time to vertical travel time.....573
Figure 347. Summary of possible corrections to tie velocity survey to surface seismic data.....574
Figure 348. Vertical time depth plot corrected to Seismic Reference Datum.....574
Figure 349. Example of final display from velocity survey with sonic log.....575
Figure 350. Basic concept of upgoing and downgoing wave fields.....576

Figure 351. Example of a Vertical Seismic Profiling recording in one-way time with gain correction applied. 577
Figure 352. Simple synthetic Vertical Seismic Profiling illustrating effects of multiples. 578
Figure 353. Comparison of real and synthetic Vertical Seismic Profiles. 579
Figure 354. Tube wave amplitudes as a function of source offset. 581
Figure 355. Correlation of time-scaled logs with Vertical Seismic Profile and surface seismic section. 582
Figure 356. Example of tying a Vertical Seismic Profiling to a log derived from lithiofacies analysis. 583
Figure 357. Tying the sum stack to log-derived volumetric analysis of lithology, porosity, and hydrocarbon saturation. 584
Figure 358. Flow of current at typical bed contacts and the resulting spontaneous potential curve and static values. 584
Figure 359. System used to make conventional single-point resistance spontaneous potential logs. 586
Figure 360. Caliper, gamma, spontaneous potential, normal resistivity, single point resistance and neutron logs compared to lithology; Kipling, Saskatchewan, Canda. 587
Figure 361. Caliper, differential and conventional single-point resistance logs in a well in fractured crystalline rocks. 589
Figure 362. Borehole correction chart for 16-in normal resistivity log. 590
Figure 363. Electrically equivalent sodium chloride solution plotted as a function of conductivity or resistance and temperature. 590
Figure 364. Principles of measuring resistivity in Ohm-meter. 591
Figure 365. System used to make 40- and 162 cm (16- and 64-in) normal resistivity logs. 592
Figure 366. System for calibrating normal resistivity equipment. 593
Figure 367. Relation of bed thickness to electrode spacing for normal devics at two thicknesses. 594
Figure 368. System used to make induction logs. 598
Figure 369. Relative response of an induction probe with radial distance from borehole axis. 599
Figure 370. Comparison of open hole induction log with 16-in normal log and induction log made after casing was installed. 600
Figure 371. Comparison of a digital recording of a gamma signal with 1-s samples to an analog recording with 1-s time constant. 601
Figure 372. Theoretical response of a neutron probe to changes in porosity and bed thickness. 602
Figure 373. Relative radioactivity of common rocks. 604
Figure 374. Plot of laboratory measurements of bulk density versus gamma-gamma log response in the same borehole. 607
Figure 375. Comparison of laboratory measurements of porosity versus acoustic, neutron and density log response in the same borehole. 607
Figure 376. Calibration data for a compensated neutron-porosity probe in the API limestone pit. 610
Figure 377. Acoustic waveforms for a two-receiver system. 612

Figure 378. Relation of acoustic-transit time to porosity for a tuff, sandstone and siltstone, Raft River geothermal reservoir, Idaho. 615
Figure 379. Composite of logs showing the location of permeable fractures indicated by the arrows at changes in temperature gradient and by low tube and shear wave amplitude. 616
Figure 380. Engineering properties calculated from geophysical logs of a core hole compared with rock quality determination (RQD) from the core. 618
Figure 381. Plot showing a comparison of a tube wave amplitude calculated from acoustic waveform data and hydraulic fracture aperture calculated from straddle packer tests. 618
Figure 382. Three-dimensional view of a fracture and appearance of the same fracture on an acoustic televiewer log. 620
Figure 383. Diagram showing comparison of reconstructed fracture data from borehole television, and a detailed core log, with a copy of an acoustic televiewer log. 621
Figure 384. Acoustic-televiewer log of fracture-producing zone A in a geothermal well, Roosevelt Hot Springs, Utah. 622
Figure 385. Mechanical and acoustic-caliper logs of fracture-producing zone A in a geothermal well, Roosevelt Hot Springs, Utah. 623
Figure 386. Caliper logs from probes having four independent arms, three averaging arms, and a single arm. Madison limestone test well No 1, Wyoming. 625
Figure 387. Temperature, differential temperature, caliper, and acoustic televiewer logs of Sears test well No 1, near Raleigh, NC. 629
Figure 388. Selected temperature logs of a monitoring hole 12 m from a recharge well, high plains, Texas. 629
Figure 389. Diurnal temperature cycles and travel times 630
Figure 390. Equipment for making heat pulse flow meter logs 633
Figure 391. Analog record of a heat pulse from a thermal flowmeter 633
Figure 392. Calibration data for an impeller flowmeter. 634
Figure 393. Schematic drawing of equipment used for hydrophysical logging after injection of deionized water; and time series of fluid conductivity logs 635
Figure 394. Single arm caliper log on the right and data from heat pulse flowmeter showing zones of water entry and exit. 636
Figure 395. Dual spaced and 4π density logs in a cased monitoring well showing completion as interpreted from the logs. 639
Figure 396. Basic wave elements 641
Figure 397. Crosshole Sonic Logging method with various kinds of defects/anomalies. 645
Figure 398. Travel time plot for a Crosshole Sonic Logging log. 646
Figure 399. Ray paths for Crosshole Sonic Logging and Crosshole Sonic Logging Tomography; S-source, R-receiver 647
Figure 400. Comparison of Crosshole Sonic Logging and Crosshole Sonic Logging Tomography results 648

LIST OF TABLES

Table 1. Application of geophysical methods to highway engineering problems. 5
Table 2. Nondestructive testing of concrete - point of interest/damage type. 50
Table 3. Corrosion rates of steel in concrete. 64
Table 4. Proposed relationship between corrosion rate and remaining service life. 64
Table 5. Likelihood of corrosion damage as a function of the corrosion potential. 64
Table 6. Bridge deck monitoring. 100
Table 7. Optimum acquisition parameters — rules of thumb. 147
Table 8. Cation Exchange Capacities (CEC) of common clay types. 187
Table 9. Ordnance penetration and detection using magnetic and electromagnetic methods. .359
Table 10. Approximate strength of perception for various magnitudes of weighted vibration. (M.J. Griffin, 1990, p. 262) 373
Table 11. Summary of vibration recommendations. 385
Table 12. Comparison of electric and hydraulic properties. 394
Table 13. Approximate magnetic susceptibility of representative rock types. 410
Table 14. Density approximations for representative rock types. 422
Table 15. Typical/representative field values of VP, pb and v for various materials. 427
Table 16. Seismic reflection use differences by methodology. 436
Table 17. Typical electrical resistivities of earth materials. 452
Table 18. Electromagnetic properties of earth materials. 519
Table 19. Compressional-wave velocity and transit time in common rocks and fluids (single values are averages). 614
Table 20. Numerical relationship between path length, transit time, frequency, period, velocity, and wavelength. 643
Table 21. Required number of access tubes versus shaft diameter. 644

CHAPTER 1 INTRODUCTION

1.1 PURPOSE

The purpose of this document is to provide highway engineers with a basic knowledge of geophysics and nondestructive test (NDT) methods for solving specific engineering problems during geotechnical site investigation, construction, and maintenance of highways. The document is not intended to make engineers experts in the field of geophysics, but rather to provide them with tools that will assist them in the use of suitable geophysical and NDT techniques to evaluate problems for design, planning, construction, or remediation efforts.

The document is divided into two parts. The first part provides descriptions of geophysical imaging and NDT methods for solving specific transportation problems. The reader can select an appropriate method and understand its applications and limitations. The second part provides the reader with indepth knowledge of geophysical methods and theories. The following general background is offered to assist the reader with a better understanding of geophysics.

1.2 BACKGROUND

1.2.1 An Overview of Geophysics

Geophysics is the science of applying the principles of physics to investigations related to the structure and properties of the earth. It has been said that geophysics essentially is the measurement of contrasts in the physical properties of materials beneath the surface of the earth and an attempt to deduce the nature and distribution of the materials responsible for these observations. Geophysical exploration has been utilized in numerous fields to study a wide range of targets within the earth from discovering the deep structure of the earth at thousands of meters to near surface structures and properties at depths of a few tens of meters. Some of the latest geophysical technologies are targeted at studying engineered material, such as pavements and bridge decks at only a few centimeters depth. Geophysical surveys are conducted on the ground surface, within drill holes, and from the water and air. A partial list of applications includes: mineral and petroleum exploration and production, environmental contaminant mapping, mapping subsurface ground conditions for civil engineering projects, solution cavity detection, hydrological mapping, mapping near surface utilities, detection and mapping of unexploded ordnance, and archeological and forensic investigations.

In this document, NDT geophysical investigations are applied in two modes; parametric studies such as measuring and analyzing seismic velocity for determining the modulus of concrete pavement, and imaging and mapping studies such as using ground penetrating radar (GPR) to look for trends that can be correlated to delaminations on a bridge deck.

1.2.2 Application of Geophysics and NDT Methods in Transportation

The application of geophysical imaging and NDT methods has been increasing in site characterization and geotechnical investigations throughout state and federal highway departments. Transportation personnel use geophysical methods to assist in highway design, construction, repair, and maintenance phases. Detailed knowledge of unforeseen, highly variable subsurface ground conditions reduces project risk and costs associated with "change of conditions" claims, and improve construction and safety.

In this document, the term NDT is used to refer to condition evaluation of engineered structures, including concrete, asphalt, masonry, timber, and steel structure. Condition evaluation includes integrity assessment for defects and corrosions, and the determination of unknown geometry, such as foundation depths or extent of foundations.

A broad range of practical methods, including almost all traditional geophysical methods, have been adapted to provide NDT solutions more specific to a variety of engineering problems. For example, conventional geophysical methods have been used to evaluate the physical properties of soil and rock, such as seismic methods, which are used to calculate the depth to bedrock or locate underground voids. In NDT applications, the same seismic methods have been adapted for condition evaluation of concrete structure with great success, producing a technique known as the Ultraseismic test method. In this method, the concrete structure itself is used instead of the earth for the transmission of the acoustic energy with reflection events coming from either the bottom of a structure, as in a bridge foundation, or a defect zone. Similarly, the GPR geophysical method, originally developed for high resolution imaging of the subsurface, is now used routinely in condition evaluation of pavements, concrete slabs, and walls. These types of NDT geophysical investigations are used in the transportation and infrastructure systems to evaluate new and existing structures for Quality Assurance (QA) and Quality Control (QC) and forensic purposes. To this end, many state and federal Department of Transportations (DOT) have added various NDT testing standard specifications to their construction codes and will continue to do so with continued deployment of geophysics and NDT in the construction projects.

1.2.3 Advantages and Limitations

In general, the subsurface characterization provided by geophysical exploration methods is valuable for highway evaluation for the following reasons:

1. They allow nondestructive investigation below the surface of the ground, pavement, bridge deck, or other structure.

2. They provide information between and below standard geotechnical borings most common to transportation projects.

3. They allow collection of data over large areas in very much shorter times than most destructive methods.

4. They cost less per data point than most invasive methods.

5. They can offer accurate and timely information for design quality and performance.

Although geophysical methods provide the above advantages, it is important to remember that the information obtained in geophysical surveys is often subject to more than one reasonable interpretation. Also, depending on specific site-conditions such as geology, target dimensions, cultural interface, and the engineering problem to be investigated, a combination of methods or techniques may be utilized in a given investigation. In other words there is no one, unique interpretation to a set of geophysical data. Also more than one method may be used to solve a particular engineering problem. Therefore, it is recommended that before conducting any geophysical investigation, as much knowledge as possible be obtained about the target and site. For subsurface characterization for example, this can be accomplished by obtaining geotechnical, geological, hydrological, or other investigative reports. Boring logs, which are normally included in these reports, can be extremely valuable if the borings were performed in the vicinity of the site. U.S. Government literature, including Federal Highway Administration (FHWA) and U.S. Geological Survey (USGS) publications, and U.S. Department of Agriculture (USDA) soil surveys, can also provide useful information. In essence, a priori knowledge of geological conditions and all previous surveys completed in the vicinity of the site should greatly assist engineers in designing a geophysical survey and selecting a suitable method(s). Additionally, it will help assure the most reasonable interpretation of the results once these data are collected.

1.3 EVALUATION OF APPROPRIATE GEOPHYSICAL METHODS

This document presents a summary of the state-of-practice of geophysical imaging and NDT methods appropriate for a wide range of transportation problems. Advancements in computing capabilities, analysis software, graphic software, and survey methodology have contributed to significant gains in the value of geophysical and NDT methods, and have produced results that are more accurate and reliable than traditional approaches. Therefore, there is a need to provide geotechnical engineers with suitable geophysical tools to assist in the rational development of the survey methodology as well as in the selection of the appropriate methods, and interpretations.

Table 1 is prepared to provide an overview of suggested geophysical imaging and NDT methods used for highway geotechnical investigations, as described in Part I. These methods are listed in terms of engineering problems and applications of these technologies to highway design, construction, repair, and maintenance. The table is designed as a "Solution Matrix" that guides the user, without reading the entire document, to obtain an answer during the initial design phase of the survey. For more complex highway engineering problem, it is recommended that the user review specific sections to assess the most appropriate method(s) for solving highway engineering problems. Finally, the table has been organized in order of the subject material presented in the document.

1.4 DOCUMENT ORGANIZATION

To assist the reader, this document is divided into two parts. Part I is problem oriented and provides a range of geophysical imaging and NDT methods that can be used to solve the particular problem. For each problem described, the suitable method(s) are discussed

presenting a brief description of the basic concept. Data acquisition, data processing and interpretation, and advantages and limitations of each method are discussed with reference to the particular problem to be solved. Part II provides a more comprehensive discussion of the geophysical methods and theory. The intent of Part II is to give a conceptual understanding of the methods, using equations only when needed. The text is prepared for readers who are not familiar with geophysics but require a deeper understanding without being burdened by excessive theory.

Bibliographies are provided at the end of the document and divided into Part I and II. The references in each part are listed for each topic and by engineering problem within the chapter or particular section. For example, the references in Chapter 2, Bridge System, and Section 2.1 Determining the Unknown Depth of Foundation provides readers with a more rigorous description of the methods and their applications along with more theory and mathematical treatment. Since some references may be appropriate for more than one topic, hence they may be listed more than once.

Following Chapter 1, the remainder of Part I and Part II is organized as follows:

Part I – Geophysical Imaging and Nondestructive Testing for Highway Applications

- *Chapter 2 – Bridge System – Substructure.* This chapter describes geophysical or NDT methods used for condition evaluation of bridge substructure including the unknown depth and geometry of the foundation as well as assessing the integrity of bridge substructure elements and bridge scour.
- *Chapter 3 – Bridge System – Superstructure.* This chapter describes geophysical or NDT methods used for evaluating bridge decks. Discussions of methods used for deck stability analysis and condition evaluation of new and existing decks are presented.
- *Chapter 4 – Pavements.* This chapter presents geophysical or NDT methods used for condition evaluation of new and existing pavements.
- *Chapter 5 – Roadway Subsidence.* This chapter discusses geophysical or NDT methods used for mapping/imaging voids, sinkholes, abandoned mines, and other subsurface cavities beneath roadways.
- *Chapter 6 – Subsurface Characterization.* This chapter describes geophysical or NDT methods used for mapping subsurface ground properties including bedrock depth, fractures, lithology, and other subsurface features.
- *Chapter 7 – Vibration Measurements.* This chapter covers geophysical or NDT methods used for monitoring vibrations caused by traffic, construction, and blasting.

Table 1. Application of geophysical methods to highway engineering problems.

Engineering Problem	Application	Geophysical/NDT Solutions
CHAPTER 2 - BRIDGE SYSTEM SUBSTRUCTURE	Unknown Depth of Foundations	Sonic Echo/Impulse Response, Bending wave, Ultraseismic, Seismic Wave Reflection, Transient Force Vibration, Parallel Seismic, Induction Field, Borehole logging, Dynamic Foundation Response, Borehole Radar, Borehole Seismic
	Integrity Testing of Foundations and Structures	Crosshole Sonic Logging, Crosshole Sonic Logging Tomography, Gamma-Gamma Density Logging, Singlehole Sonic Logging, Sonic Echo/Impulse Response, Ultraseismic Profiling, Ultrasonic Pulse Velocity, Impact Echo, Ground Penetrating Radar, Spectral Analysis of Surface Waves, Acoustic Emissions, Radiography
	Rebar Quality and Bonding	Half-cell Potential, Linear Polarization Resistance, Galvanostatic Pulse Technique, Electrochemical Noise, Acoustic Emissions, Magnetic Field Disturbance
	Foundation Scour	Time Domain Reflectometry, Parallel Seismic, Ground Penetrating Radar, Continuous Seismic Reflection Profiling, Fathometer
CHAPTER 3 - BRIDGE SYSTEM SUPERSTRUCTURE	Bridge Deck Stability	Vibration Monitoring, Ground Penetrating Radar, Electromagnetic, Impact Echo, Spectral Analysis of Surface Waves and Ultrasonic Surface Waves Methods, Half-Cell Corrosion Potential Mapping, Infrared Thermography
	New Decks	
	Baseline Assessment	
	Existing Decks	
CHAPTER 4 - PAVEMENTS	QA/QC Of New Pavements	GPR, Impact Echo, Spectral Analysis of Surface Waves, Ultra Sonic Surface Wave (USW), Multichannel Analysis of Surface Waves (MASW)
	Existing Pavements	
	Transportation / Geotechnical Methods	
CHAPTER 5 - ROADWAY SUBSIDENCE	Mapping Voids, Sinkholes, Abandoned Mines, and Other Cavities	Gravity, GPR, Resistivity , Seismic Refraction, Seismic Reflection, Rayleigh Waves Recorded with a Common Offset Array, Cross-borehole Seismic Tomography
	Roadbed Clay Problems	Conductivity Measurements, Resistivity Measurements, Time Domain Electromagnetic Soundings, Induced Polarization
CHAPTER 6 - SUBSURFACE CHARATERIZATION	Mapping Bedrock, Lithologies, Sand & Gravel Deposits, Groundwater Surface, and Flow	Ground Penetrating Radar, Seismic Refraction, Compressional and Shear Wave Reflection, Resistivity, Time Domain Electromagnetic, Conductivity Measurements, Spectral Analysis of Surface Waves, Gravity, Very Low Frequency Electromagnetic, Borehole Televiewer, Induced Polarization, Borehole Gamma and HydroPhysical Logging, Nuclear Magnetic Resonance, Self Potential, Electroseismic
	Determining Engineering Properties and Rippability of Soil and Rock	Seismic Refraction, Nuclear Magnetic Resonance, Ground Penetrating Radar, Spectral Analysis of Surface Waves, Suspension Logging, Full Waveform Sonic Logging, Crosshole Shear
	Utility Locator, Detecting Underground Storage Tank, UXO and Contaminant Plums	Magnetic, Electromagnetic, Ground Penetrating Radar, Acoustic Pipe Tracer, Metal Detectors, resistivity, Induced Polarization, Refraction
CHAPTER 7 - VIBRATION MEASUREMENTS	Vibration Caused By Traffic, Construction, and Blasting	Vibration Monitoring

Part II – Geophysical Methods, Theory, and Discussions

- *Chapter 8 – Geophysical Quantities.* This chapter provides information on physical properties and quantities which are involved in an understanding of geophysics and geophysical methods. In addition, the units of measurement, relationships such as saturated porosity vs. dielectric constant, and some of the physical properties of the earth are discussed.
- *Chapter 9 – Surface Geophysical Methods.* This chapter describes surface geophysical methods including gravity, seismic, electrical, electromagnetic, and nuclear methods.
- *Chapter 10 – Borehole Geophysical Methods.* This chapter provides general information on in-hole and cross-hole procedures, surface to borehole procedures, and methods. In addition, logging techniques including electrical, nuclear, acoustic, flow, hydrophysical, well completion, and hole-to-hole methods are included.

GEOPHYSICAL IMAGING AND NONDESTRUCTIVE TESTING FOR HIGHWAY APPLICATIONS – PART I

CHAPTER 2 BRIDGE SYSTEM – SUBSTRUCTURE

In a bridge system, bridge superstructure is defined as all structure above bridge bearing elevation and bridge substructure is defined as everything below the superstructure. Therefore, bridge substructure includes all foundation elements such as columns, wall piers, footings, pile caps, precast or auger-cast concrete piles, drilled shafts, etc. The substructure can be generalized as an abutment or pier, which can be made of concrete, masonry, stone, steel and/or timber.

Bridges play a key role in the national transportation system, and the ability to assess their condition is vital for safe transportation operations. Some of the bridges that comprise the system traverse waterways, where bridge failures most commonly occur due to scour damage. The loss of support from scour damage can result in settlement, which, in turn, can affect the superstructure and lead to subsequent failure. These problems are not always easily detected. Furthermore, many older bridges in the United States have no plans of the foundation system.

There are approximately 580,000 highway bridges in the National Bridge Inventory. The type and/or depth of the foundations of about 104,000 of these bridges are unknown. For a large number of older non-federal-aid bridges, and to a lesser extent federal-aid bridges, there are no design or as-built bridge plans available to document the type, depth, geometry, or materials incorporated in the foundations.

These unknown bridge foundations pose a significant problem to State Department of Transportations from scour volunerability concerns. Because of the risk of scour undermining bridge foundations and the threat to public safety, there is a need to screen and evaluate all bridges over rivers, streams, and in coastal areas, both on and off state systems. To determine the susceptibility of a bridge to scour, information on the foundation type and depth is needed to perform an accurate scour evaluation of each bridge. It would be quite beneficial to have a method, or methods, that can detect and evaluate the structural conditions beneath bridge piers. One promising approach is nondestructive testing.

In this chapter, nondestructive test (NDT) methods used for condition evaluation of bridge substructure are described. The term "condition evaluation" includes determination of the unknown depth and geometry of the foundations as well as assessing the integrity of bridge substructure elements and bridge scour. In Chapter 3, NDT methods used for evaluating bridge superstructure are discussed.

2.1 DETERMINING THE UNKNOWN DEPTH OF FOUNDATIONS

Bridge foundations can be divided into shallow footings or deep foundations. Footings are mostly square or rectangular in shape. They may also be pedestal masonry stone footings or massive cofferdam footings in shape. Piles might be present with or without pile caps and may be battered or vertical. Piles can be made of concrete (round, square, or octagonal),

steel (H-piles or round pipe sections), or timber. Deep foundations can be pre-cast concrete piles, or more recently, drilled shafts and auger-cast concrete piles. The top of footings or pile caps may be buried underneath riprap, backfill mud and/or channel soils.

Nondestructive tests (NDT) that are used for the determination of the unknown depth of foundations usually involve seismic methods and are often called small strain tests. The term "small strain test" is used to describe tests where a small seismic energy source, such as a hammer, is used to generate the seismic waves.

These tests can be divided into two groups: Surface NDT, if access is required only at the surface of a foundation, or Borehole NDT, if a borehole is drilled close to the foundation structure and extends along its length.

Five potential surface NDT methods used to determine foundation depths. These are Sonic Echo, Bending Waves, Ultraseismic Vertical Profiling, Seismic Wave Reflection Survey, and Transient Forced Vibration Survey. Borehole NDT methods include Parallel Seismic, Borehole Radar, Magnetic Methods, Dynamic Foundation Response, Borehole Sonic, cross-borehole tomography, and, where the substructures contain steel, Induction Field. The application of each method to specific engineering problem, the basic concept for each method, field data acquisition, processing and interpretation are described below. Advantages and limitations are also discussed.

2.1.1 Surface NDT Methods

As mentioned above, surface methods are applied from the accessible surface of the foundation element. Therefore, the foundation structure is used directly as the medium for the transmission of the acoustic energy.

2.1.1.1 Sonic Echo(SE)/Impulse Response (IR)

Sonic Echo/Impulse Response (SE/IR) tests are performed to evaluate the integrity and determine the length of deep foundations. This method can be used to detect defects, soil inclusions and pile necking, diameter increases (bulbing) as well as approximate pile lengths.

SE/IR tests are performed on drilled shafts and driven piles (concrete or timber) or auger-cast piles. These tests can also be performed on shallow wall structures such as an abutment or a wall pier of a bridge, provided the top of the wall is accessible.

Basic Concept: The Sonic Echo method requires a measurement of the travel time of seismic waves (time domain), and the Impulse Response method uses spectral analysis (frequency domain) for interpretation. These two methods are sometimes called Pile Integrity Testing methods (PIT). The Sonic Echo method is also known as Echo, Seismic, Sonic, Impulse Echo and Pulse Echo methods. Other names for the Impulse Response Method include Sonic Mobility, Transient Dynamic Response, Impulse Response Spectrum, Impedance, Shock, Transient Response, Transient Dynamic Response, and Sonic.

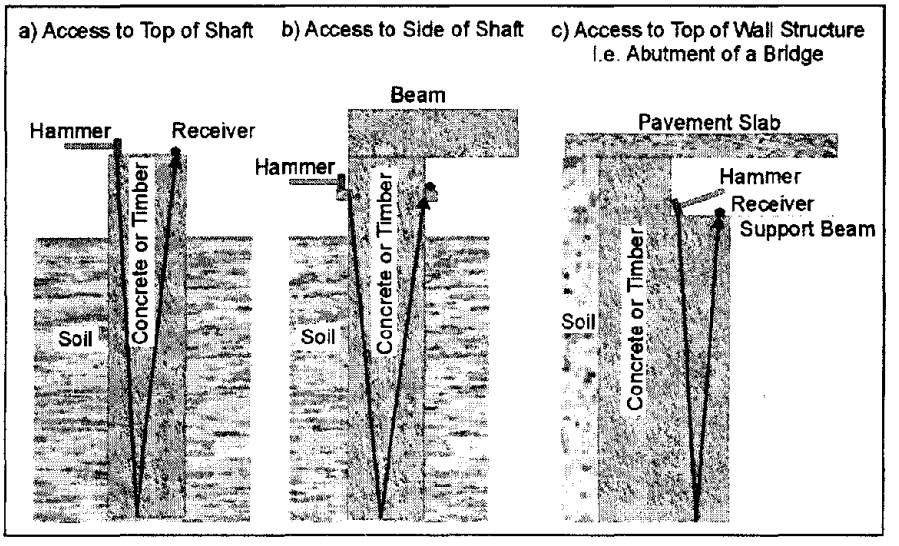

Figure 1. Source and receiver locations for a Sonic Echo/Impulse Response test for three shaft geometric configurations.

In both (SE/IR) tests, the reflection of compressional waves (also called P waves by geophysicists) from the bottom of the tested structural element or from a discontinuity such as a crack or a soil intrusion is measured. The generated wave from an impulse hammer travels down a shaft or a pile until a change in acoustic impedance (depends on velocity, density, and changes in diameter) is encountered where the wave reflects back and is recorded by a receiver placed next to the impact point.

Data Acquisition: For drilled shafts and piles, the best results from SE/IR tests are obtained if the top of the drilled shaft or the pile is exposed for receiver attachment and hammer hitting (see figure 1a). If the top is not exposed, then the SE/IR tests are performed on the side. This requires at least the upper 30 to 60 cm of the shaft to be exposed (see figure 1b). For wall-like shallow structures, the top of an abutment or a pier should be exposed for SE/IR testing (see figure 1c). In these cases where the superstructure is in place, the SE/IR data becomes more difficult to interpret because of the many reflecting boundaries, and two or more receivers should be used to track reflections (please refer to the Ultraseismic method in section 2.1.1.3).

In an SE/IR test, a hammer strikes the foundation top, and a receiver monitors the response of the foundation. A digital signal analyzer records the hammer input and the receiver output. Sonic Echo (SE) tests are typically performed with different frequency filtering to optimize reflections coming from the bottom of the foundation and to reduce the effect of surface waves or reflections from a discontinuity at a shallow depth where the frequencies associated with these two conditions are high. In an Impulse Response (IR) test, a digital analyzer automatically calculates the transfer and coherence functions after transforming the time records of the hammer and the receiver to the frequency domain.

Data Processing: To aid in interpreting SE/IR data, certain processing techniques can be applied to enhance weak echoes. SE signals, which are measurements of acceleration, are commonly integrated to produce velocity and exponentially amplified to enhance weak reflections and to compensate for the damping of energy. For cases where echoes are not

easily identified in the data, other processing, such as the Cepstrum technique, is used. In this technique, an autocorrelation function is calculated to help better determine the time separation between two echoes. In simple cases, the SE data can be used to obtain an image of the shaft through a process called impedance imaging.

For best results, it is important to know the P wave velocity in the structure being tested. It is not safe to assume the concrete velocity is known from other empirical data. Velocities of concrete can vary based on the aggregate used, age of the structure, and state of weathering, ASR or other degradation. It is easy to measure local velocity if two sides of the structure are available or if a sufficient length of the body is available for access. A source placed a measured distance from a receiver can be used to get a first arrival signal to compute the P-wave velocity.

Data Interpretation: Sonic Echo data are used to determine the depth of the foundation based on the time separation between the first arrival and the first reflection events or between any two consecutive reflection events (Δt) according to the following equation:

$$D = V \times \frac{\Delta t}{2}, \tag{1}$$

where D is the reflector depth, and V is the velocity of compressional waves. A reflector can be the bottom of the foundation or any discontinuity along the embedded part of the foundation. The Sonic Echo data can also be used to determine the existence of a bulb or a neck in a shaft or the end conditions of the shaft based on the polarity of the reflection events. Figure 2 illustrates the data from a Sonic Echo survey along with the depth calculation computed between the second and third echoes. The multiple echoes are all interpreted as coming from the same reflector since the time separations of the echoes are all equal. Any pair can be used to calculate the two-way travel time between the source and the reflector. In this case the clearest pair of echoes were the second and third, which were used to calculate the depth using the formula above, giving a depth of 2.01 m.

The Impulse Response data are also used to determine the depth of reflectors according to the following equation:

$$D = \frac{V}{(2 \times \Delta f)}, \tag{2}$$

where

Δf = distance between two peaks in the transfer function plot $\left(\frac{\text{velocity}}{\text{force versus frequency}} \right)$,

or between zero frequency and the first peak for soft bottom conditions.

The multiple echoes from a discontinuity or bottom, as seen in the Sonic Echo method, result in increased energy at the frequency of the echo. This causes a peak in the frequency spectrum. Under conditions where there is a hard material beneath the structure, the second harmonic of the echo is also evident. Using the frequency difference between zero and the main echo

frequency or between the first and second harmonic frequencies in the formula above gives the depth of the structure. In addition, the Impulse Response data provides information about the dynamic stiffness of the foundation. This value can be used to predict foundation behavior under working loads or correlated with the results of load tests to more accurately predict foundation settlement.

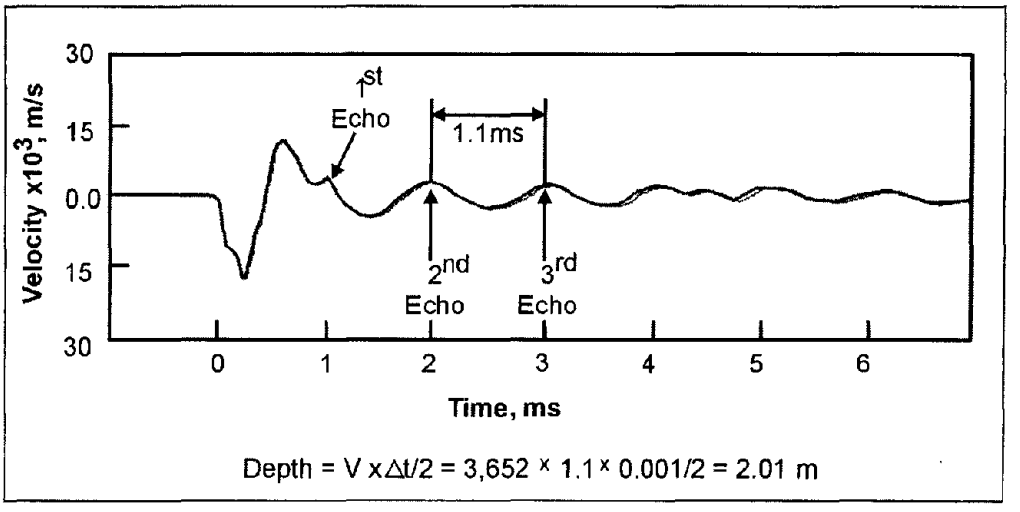

Figure 2. Data from the Sonic Echo method and depth calculations.

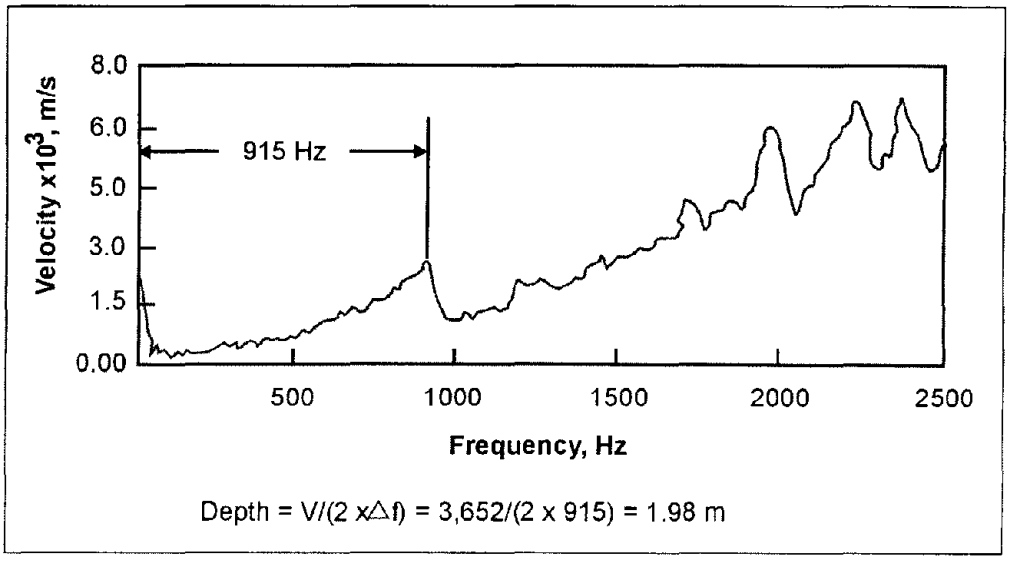

Figure 3. Depth calculations using frequency domain data for the Impulse Response method.

Example data for the Impulse Response method are shown in figure 3, along with the depth calculations showing a reflector depth of 1.98 m.

Advantages: This is a quick and economical test method used mostly in columnar shaped foundations without access tubes. Any defects can be found early with minimal delays to construction.

Limitations: The SE/IR method works best for free-standing columnar-shaped foundations, such as piles and drilled shafts, without any structure on top. Typically, SE/IR tests are performed on shafts or piles of length-to-diameter ratios of up to 20:1. Higher ratios (30:1) are possible in softer soils. The method can only detect large defects with cross-sectional area changes greater than 5%.

A toe reflection is not possible if the pile is socketed in bedrock of similar stiffness (or acoustic impedance) as concrete. If the pile is embedded in very stiff soils, penetration may be limited up to 8 m. For the softer soils, echoes can be observed from piles of up to 80 m in length. This method cannot be used for steel H-piles.

2.1.1.2 Bending Waves

This method uses flexural (bending) waves, rather than the compressional waves used in the Sonic Echo/Impulse Response method to determine integrity and unknown depth of deep foundations. It is limited to applications on rod-like deep foundations such as timber piles, concrete piles, and drilled shafts that extend above the ground or water surface.
The Bending wave method has been used experimentally on timber piles, but will also work on other, more slender members. The method has been used on timber piles up to 18.3 m in length. The key feature of this method is that only a horizontal blow is required, which is easy to apply to the side of a substructure.

Basic Concept: This method uses the propagation of flexural or bending waves in piles that are highly dispersive in nature. The bending wave velocity decreases with increasing wavelength, with most of the velocity decrease occurring at wavelengths that are longer than the pile diameter. These longer waves propagate as flexural or bending wave energy.

Correspondingly, as wavelengths become shorter than the diameter of a pile, the bending wave velocity limit is approximately that of the surface (Rayleigh) wave velocity, and this wave energy propagates as surface waves. Compressive waves are also dispersive in piles, but in a different way that, in practice, results in a velocity decrease only when a deep foundation has a low length-to-diameter ratio of about 2:1 or less, which is uncommon for deep foundations.

The classical wave equation, often called the traditional wave solution, does not account for dispersion. It is an ideal mathematical description of the behavior of the pulse, with its solution implying that a wave will travel through a rod without affecting the shape of the rod. This is the difference with dispersive signal analysis; dispersive analysis of the wave data extracts a selected group of frequencies. These frequencies are then analyzed for the individual time required to travel to the tip of the pile and back or from their tops to the location of an area of damage such as a void, break, soil intrusion, or material deterioration.

Since the method involves striking the pile on a side and placing the receivers on the side of the pile, the method is potentially useful in cases where the top of the pile is obscured by a structure. The Sonic Echo/Impulse Response methods either require the top of the pile to be accessible or a small structure needs to be rigidly attached to the side of the structure to allow hammer blows to create compressional waves.

Data Acquisition: The Bending Wave method involves horizontally impacting the pile to generate flexural or bending waves that travel up and down the pile as illustrated in figure 4. The receivers are in a plane with the hammer blow on the same side of the pile. The equipment consists of a recording oscilloscope or dynamic signal analyzer, small to large hammers or other impact sources ranging from rubber to hard plastic to steel, and cushioning materials to protect and dampen the blow to the timber pile for metal-tipped hammers. Two accelerometers (G1 and G2) are used to measure the initial bending wave arrivals and subsequent reflections. The bending wave propagation is monitored by two horizontal accelerometer receivers mounted on the same side of the pile as the impact (see figure 4).

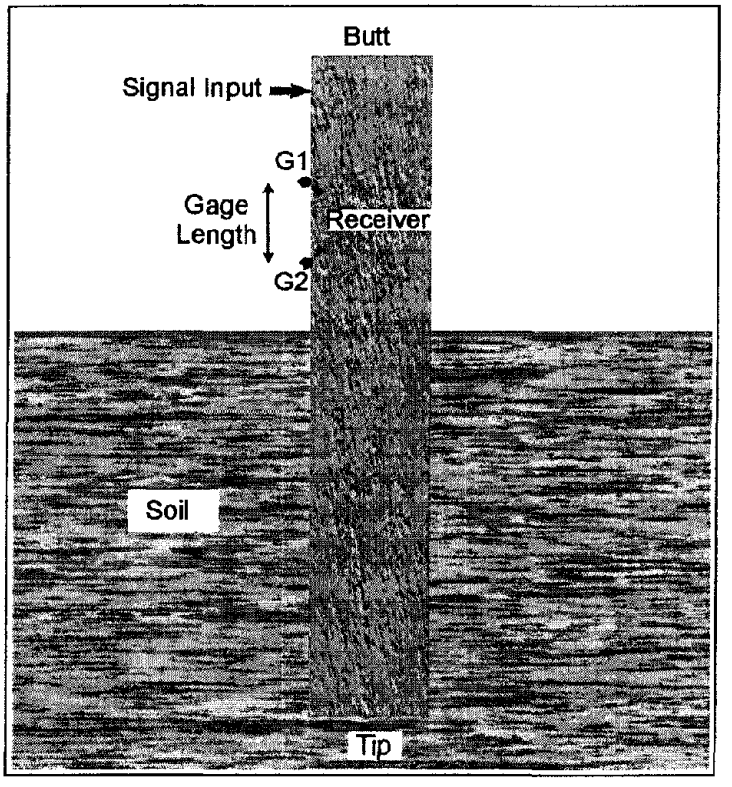

Figure 4. Field setup for the Bending Wave method for piles.

Data Processing: The Bending Wave method with the Short Kernel Method (SKM) analysis can be thought of as being the bending wave equivalent of the Sonic Echo method, which uses the faster compressional (longitudinal) waves. This method involves determining the velocity of wave travel, then identifying initial wave arrivals and subsequent reflections (echoes), and finally calculating the depths and locations of the reflection events. In the SKM method, one or more cycles are used as "Kernel Seed" in order to cross-correlate with number of seed frequencies between 500-4000 Hz.

Data Interpretation: The cross-correlation function amplifies the bending wave response at the seed frequency. Using two receivers, bending wave velocity is computed as the difference of cross-correlated peak responses. Also, upward versus downward traveling reflection events are distinguished by their travel-time moveout characteristics.

Advantages: This method provides a quick and economical test that does not require access tubes inside the foundation or boreholes outside.

Limitations: Theoretical studies have shown that for a 12-m-long, 1-m-diameter concrete shaft, depth predictions may not be able to be made for depths greater than 5 m due to the high attenuation associated with flexural waves as compared to compressional waves traveling down a rod. Stiff soil layers can result in apparent short pile lengths being predicted. Reflection events from top of the grade may be present in the data records resulting in false interpretation of the data. This method cannot be used for steel H-piles.

2.1.1.3 Ultraseismic (US)

The Ultraseismic (US) method is performed to evaluate the integrity and determine the length of shallow and deep foundations. US tests can be performed on drilled shafts and driven or auger-cast piles. The tests can also be performed on shallow wall-shaped substructures such as an abutment or a wall pier of a bridge provided at least 1.5 to 1.8 m of the side of the structural element is exposed for testing. The method is particularly useful in testing abutments and wall piers of bridges because of the relatively large exposed areas available for testing.

The Ultraseismic tests can be performed on concrete, masonry, stone, and wood foundations. Steel pile foundations can also be tested, but damping of the energy in this case is much greater than that of concrete and wood due to the large surface areas and small cross-sectional areas of steel piles.

Ultraseismic method was developed by Mr. Frank Jalinoos as part of NCHRP 21-5 research program in response to the difficulty encountered in interpreting the Sonic Echo/Impulse Response and Bending wave methods from complex structures (such as a bridge) where many reflecting boundaries are present. This method is an adaptation of multi-channel seismic reflection method to bounded engineered structures.

Basic Concept: The Ultraseismic method uses multi-channel, three-component (vertical and two perpendicular horizontal receivers, i.e., triaxial receiver) recording acoustic data followed by computer processing techniques adapted from seismic exploration methods. Seismograph records are typically collected by using impulse hammers as the source, and accelerometers as receivers that are mounted on the surface or side of the accessible bridge substructure at intervals of 30 cm or less. The bridge substructure element is used as the medium for transmission of the seismic energy. Four wave modes of longitudinal (compressional) and torsional (shear) body waves as well as flexural (bending) and Rayleigh surface waves can be recorded by this method. Seismic processing can greatly enhance data quality by identifying and clarifying reflection events that are from the foundation bottom and minimizing the effects of undesired wave reflections from the foundation top and attached beams. For concrete bridge elements, useful wave frequencies up to 4 to 5 kHz are commonly recorded.

This method can be used in two modes: Ultraseismic Vertical Profiling (VP), presented below, and Horizontal Profiling (HP).

Data Acquisition: The Vertical Profiling test geometry is presented in figure 5 and shows the accelerometers and impact point. The impact point can be located either at the top or the

bottom of the receiver line. Vertical impacts to the substructure are comparatively rich in compressional wave energy, although more flexural/Rayleigh (surface) wave energy is generated. Horizontal impacts are rich in flexural wave energy when the impacts generate wavelengths that are longer than the thickness of the substructure element. Impacts that generate wavelengths shorter than the thickness will be rich in Rayleigh wave energy. The VP accelerometer array is useful for differentiating downgoing events from the upgoing events based on their characteristic time moveout, and accurately measure their velocity. A VP accelerometer array is also used to tie reflection events from the bottom to a corresponding horizon in an HP section. For a medium with a bounded geometry, such as a bridge column, four types of stress waves are generated that include longitudinal (compressional), torsional (shear), surface (Rayleigh), and flexural (bending) waves. In longitudinal vibration, each element of the column extends and contracts along the direction of wave motion that is along the column axis. In torsional vibration, each transverse section of the column remains in its own plane and rotates about its center. Finally, in flexural vibration, the axis of the column moves laterally in a direction perpendicular to the axis of the column. Each wave type can independently provide information about the depth of the foundation or the presence of significant flaws within the bridge substructure. However, practically, longitudinal (P-wave, compressional) and flexural (bending) waves are much easier to generate on bridge substructures than torsional waves. Consequently, compressional and flexural wave energy were generated by orienting impacts to substructures vertically and horizontally, respectively.

The Ultraseismic Horizontal Profiling Method (HP), presented in figure 6, was developed for potential use on massive abutment and wall substructure elements and dam like structures, which typically have greater widths of top or side surfaces. This permits access to a line of receivers to be placed at a common elevation. The HP method uses the same basic equipment as the VP test, but since the receivers are at the same elevation, reflection events from footing bottoms should have the same arrival time in the seismic records.

Data Processing: The recorded receiver outputs from the many receiver locations are stacked together much like stacking of reflection seismic geophysical data. The stacking of many traces improves the signal-to-noise ratio and provides better tracking of the reflected waves. In addition, the slope of coherent events in the stacked records determines the velocity of the direct and reflected waves to be used in the depth calculation. Confidence in the interpretation of the US data is higher than in the SE/IR and SKM test data because of the use of many receiver locations.

In addition to stacking the data from US tests, other geophysical data processing techniques can be used. Applications of digital filters, Automatic Gain Control (AGC), source deconvolution, and migration techniques can be applied to the data to enhance weak echoes. Also, separation of downgoing events from upgoing events enhances the weak echoes coming from the bottom of the foundation or any discontinuity along the buried length of the foundation.

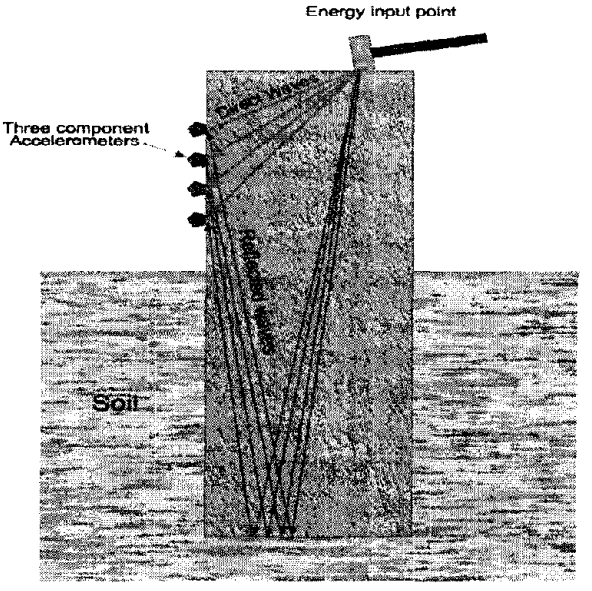

Figure 5. Ultraseismic test method and vertical profiling test geometry.

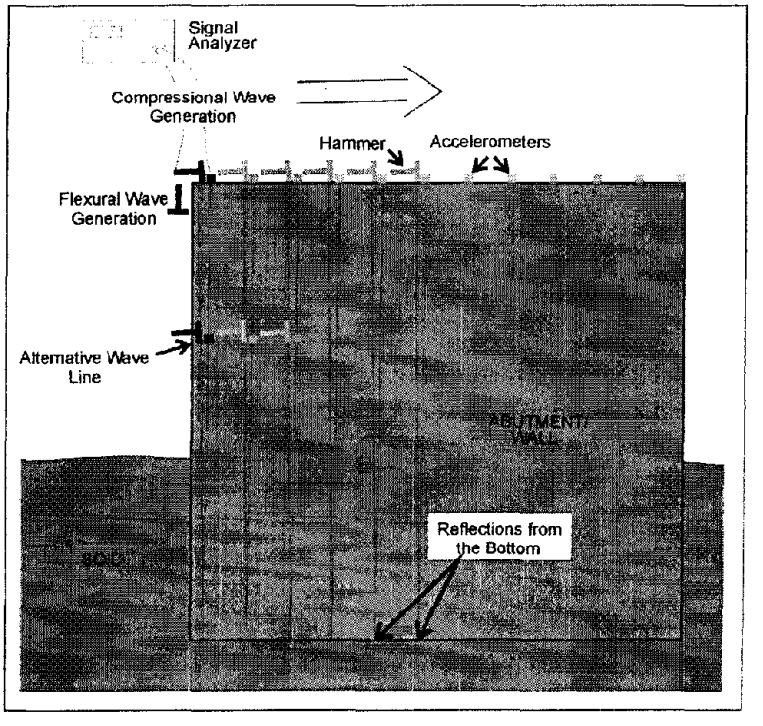

Figure 6. Ultraseismic test method and horizontal profiling test geometry

Data Interpretation: An example US-Vertical Profiling dataset from a concrete pier foundation is shown in figure 7. In this figure, the seismic record from the horizontal impact of a 1.4-kg hammer and horizontal component accelerometer recording is shown at 4-μs sampling interval after bandpass filtering and automatic gain control (AGC) being applied. The 1.4-kg hammer was located at the top of the bridge pier and the receiver survey line was laid out below the source using 0.3 m intervals. Therefore, trace 2 is located 0.3 m below the source location and trace 22 (the last trace) at 6.4 m below the source location. The downgoing flexural waves have a linear positive moveout with travel time increasing with distance and upgoing events having a negative linear moveout. For this field geometry, the depth of the foundation is easily calculated from the intersection of downgoing and upgoing events at about 9 m below the top of the pier beam.

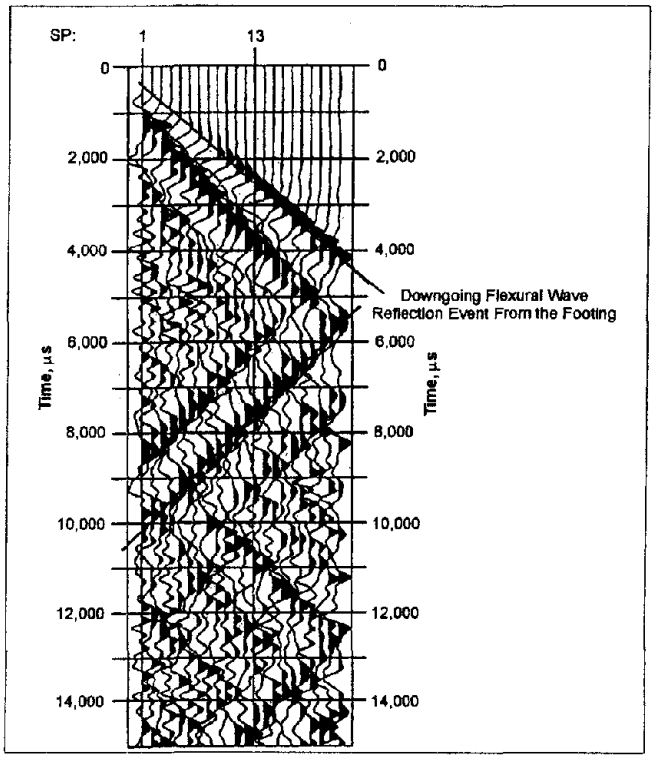

Figure 7. Example Ultraseismic-Vertical Profiling dataset from a bridge pier.

An example US-Horizontal Profiling dataset from a pier wall structure is shown in figure 8. In this figure, the seismic "shot record" from the vertical impact of a 1.4-kg hammer and vertical component accelerometer recording is indicated at 4-μs sampling interval after bandpass filtering and automatic gain control (AGC) gain being applied. The 1.4-kg hammer was located at the center of the wall and the receiver survey line was laid out at 0.3 m intervals across the top of the wall along its centerline. Weak bottom reflection events from the wall bottom are present and processing techniques adapted from seismic data processing method can be used to image bottom reflections.

The data records also clearly indicate Rayleigh surface wave events that are reverberating from both ends of the wall in a X-pattern. The Spectral Analysis of Surface Waves (SASW)

method has been used to determine unknown depths of foundations in bridge abutments. With multi-receiver US-Horizontal profiling recording, the more generalized Multichannel Analysis of Surface Waves (MASW) method can be used in this application in assessing integrity and depth.

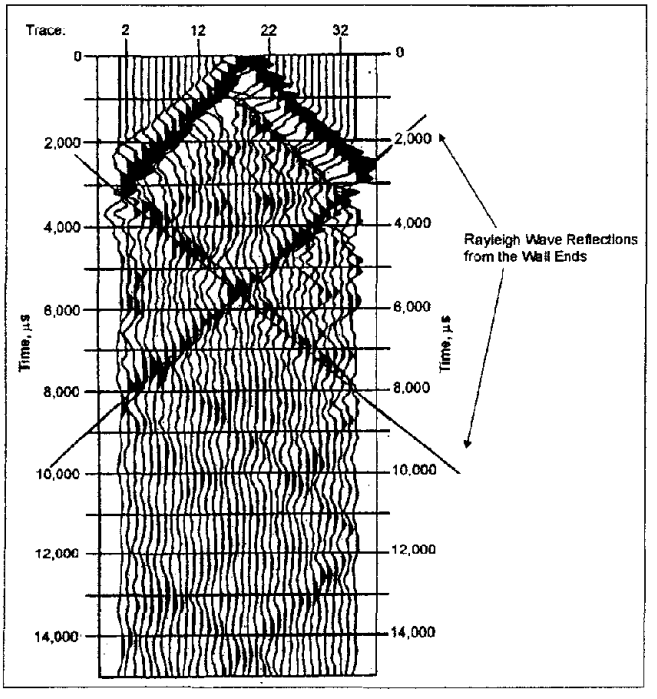

Figure 8. Example Ultraseismic-Horizontal Profiling dataset from a wall structure.

Advantages: This method can be used to obtain two-dimensional reflection images from complex structures, such as bridges, buildings, and dams. It uses well-proven processing techniques developed in the seismic exploration method. Multiple-channel recording allows for differentiation of bottom echoes from other complex wave modes far more reliably than single-channel Sonic/Pulse Echo or Bending wave methods. Ultraseismic tests can determine the depth of foundations with an accuracy of about 95%.

Limitations: The Ultraseismic method requires at least 1.5 to 1.8 m of the structural member to be exposed, which is not always possible. For very deep foundations, echoes from the bottom may not be obtained because of the attenuation of energy in the surrounding soil. The Ultraseismic method is not capable of determining the depths of buried piles, especially steel H-piles, beneath a buried pile cap.

2.1.1.4 Seismic Wave Reflection Survey

An application of Seismic Wave Reflection survey method, used to image the toe of a pile column, is described in Use of Geophysical Methods in Construction, edited by Soheil Nazarian and John Diehl is included herein.

Basic Concept: In this method, the seismic survey involved setting up shot points on one side of the pier and two horizontal component geophones on the other side of the pier. The

toe of the pier will diffract seismic waves passing under it. The depth of the pier can be found from the position of the diffractions on the seismic records.

Data Acquisition: Figure 9 shows the layout of the seismic lines and the pier location.Reflection seismic data are usually considered to image a point midway between the shot and the receiver. This point is called the Common Depth Point (CDP) (as illustrated in figure 10). Seismic traces that occur at a CDP are usually summed together to form a single trace. For each shot, the geophones record the ground surface motion in two orthogonal directions. Repeating a number of hammer blows at the same location allows the data recorded at the geophones to be stacked, thus improving the signal-to-noise ratio.

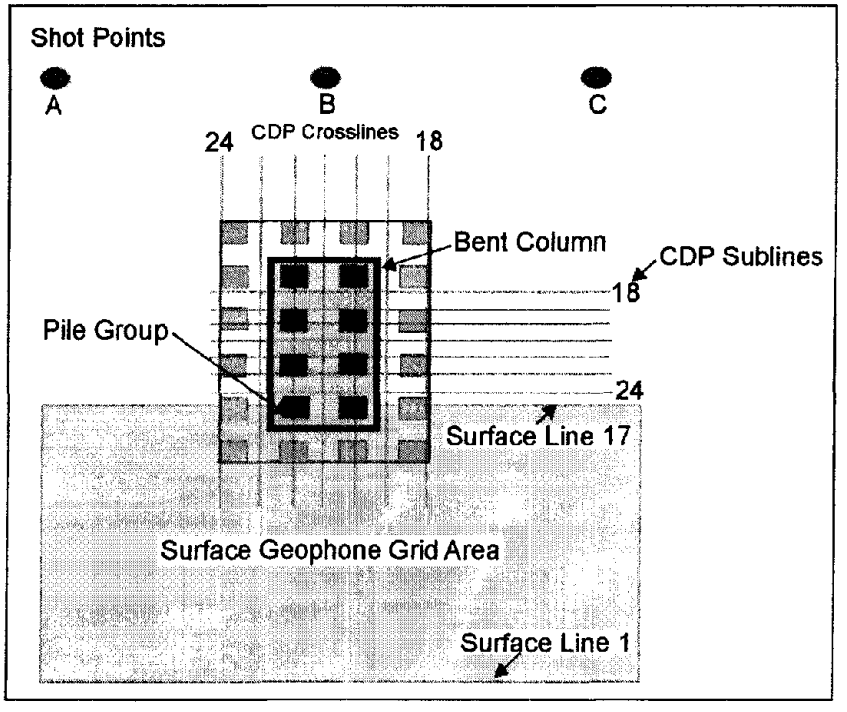

Figure 9. Shot and receiver layout for SeismicRreflection survey (plan view).

Data Processing: If a diffracting surface exists below the ground surface, its geophysical signature along any subline will appear as a hyperbola. The seismic data were processed using standard seismic processing procedures, including migration to collapse the diffraction patterns.

Data Interpretation: The data are interpreted by observing the time on the processed seismic record at which the reflections from the toe of the pile occur. Using this time along with the measured rock/soil velocity allows the depth of the pile to be calculated.

Advantages and Limitations: Because seismic pulses have a finite wavelength and hence bandwidth, the pulses "see" the bottoms of the piles as a zone that is a fraction of the length of the waves. It would take very high-frequency energy to see the precise locations of the bottoms of the piles. Having a finite wavelength produces some uncertainty about the depth of the pile, with shorter wavelengths providing less uncertainty. Generally, for field conditions, a

depth resolution to about one-half of one wavelength can be expected. If the peak frequency is about 550 Hz, and the velocity of the waves is about 500 m/sec, then the wavelength is about 0.9 m. Thus, the resolution will be about 0.45 m.

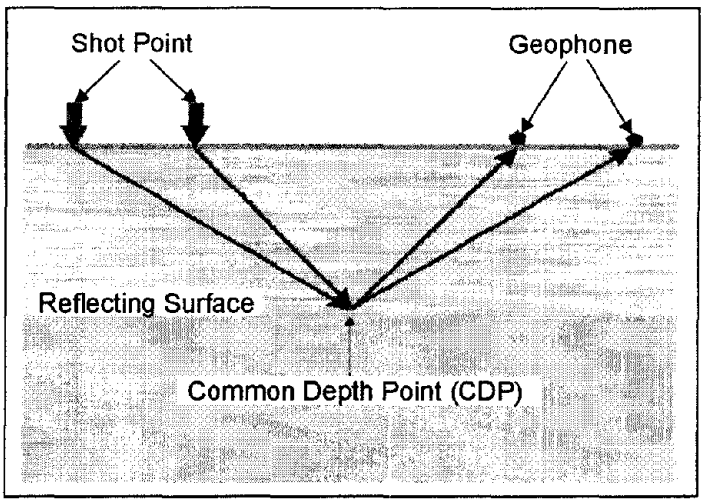

Figure 10. Geophone and shot positions for Common Depth Point recording.

2.1.1.5 Transient Forced Vibration Survey

The transient forced vibration survey method is used to image the toe of a pile column. This method is described in Use of Geophysical Methods in Construction, edited by Soheil Nazarian and John Diehl is included herein.

Data Acquisition: For this survey, geophones are mounted on the vertical column that extends above the ground surface. A hammer is used to strike the column in a horizontal direction, producing shear waves; the shear wave data are recorded by geophones. This process is repeated by impacting the opposite side of the column. This allows the compressional wave component of the signal to be removed from the total signal, thereby isolating just the shear wave signal.

Data Processing: For the survey described in the above-referenced book, autocorrelation, automatic gain control, and filtering were used to process the data. Upgoing and downgoing waves are separated using velocity filters. Autocorrelation functions were then developed between the downgoing waves, the upgoing waves, and the summation of upgoing and downgoing waves after gain equalization to achieve equal power in both sets of waves.

Data Interpretation: The data are interpreted using the autocorrelation functions for upgoing, downgoing, and summed waves. In the example, survey peaks in these functions are observed, corresponding to the periodicity of the column and the drilled shaft. Using velocity information, the distances from the source to these reflection points can be obtained. These distances correlate well with the known distances.

Advantages and Limitations: It is not possible to interpret the data using simple reflection times. The autocorrelation function is needed to identify major periodicities. The method

sees the average of pile depths with multiple piers and cannot resolve the number of individual piles or their individual lengths.

2.1.2 Borehole Nondestructive Testing Methods

These NDT methods require access from a borehole drilled close to the foundations.

2.1.2.1 Parallel Seismic (PS)

The Parallel Seismic (PS) method is a borehole test method for determining depths of foundations. The method can also detect major anomalies within a foundation as well as provide the surrounding soil velocity profile. The method requires the installation of cased borehole close to the foundation being tested. The method can be used when the foundation tops are not accessible or when the piles are too long and slender (such as H piles or driven piles) to be testable by sonic echo techniques.

Basic Concept: The Parallel Seismic (PS) method involves hammer impacts at any part of the exposed structure that is connected to the foundation (or impacting the foundation itself, if accessible). A hydrophone or a three-component geophone located in a nearby borehole records the compressional and/or shear waves traveling down the foundation. Therefore, the PS test requires drilling a 5- to 10-cm-diameter hole as close as possible to the foundation being tested (preferably within 1.5 m). The borehole should extend at least 3 to 5 m below the expected bottom of the foundation. If hydrophones are used, the hole must be cased, capped at the bottom, and the casing and hole filled with water. For geophone use, the hole must usually be cased and grouted to prevent the soil from caving in during testing.

PS tests can be performed on concrete, wood, masonry, and steel foundations. Some portion of the structure that is connected to the foundation must be exposed for the hammer impacts.

Data Acquisition: The field setup for Parallel Seismic tests is shown in figure 11. In a PS test, a hammer strikes the structure, and the response of the foundation is monitored by a hydrophone or a geophone receiver placed in the borehole. A signal analyzer records the hammer input and the receiver output. The receiver is first lowered to the bottom of the hole, and a measurement is taken. Then, the receiver is moved up 30 or 60 cm, and the second measurement is made. This process is continued until the receiver has reached the top of the boring.

Data Processing: Analysis of the PS data is performed in the time domain. In PS tests, one relies on identifying direct arrival times of compressional and shear waves at the receiver locations, as well as the wave amplitudes. The PS tests are performed at 30 to 60 cm vertical receiver intervals in the borehole. Figure 11 shows the pile and borehole configuration used for the test. The first arrival times are plotted as a function of depth, and the depth where a change of slope occurs is observed to find the foundation depth. Also, the foundation depth can be obtained by observing the depth where the signal amplitude of the first arrival energy is significantly reduced. In addition, geophysical processing techniques can be used to help optimize the Parallel Seismic data. These techniques include Automatic Gain Control (AGC) and filtering to enhance weak events.

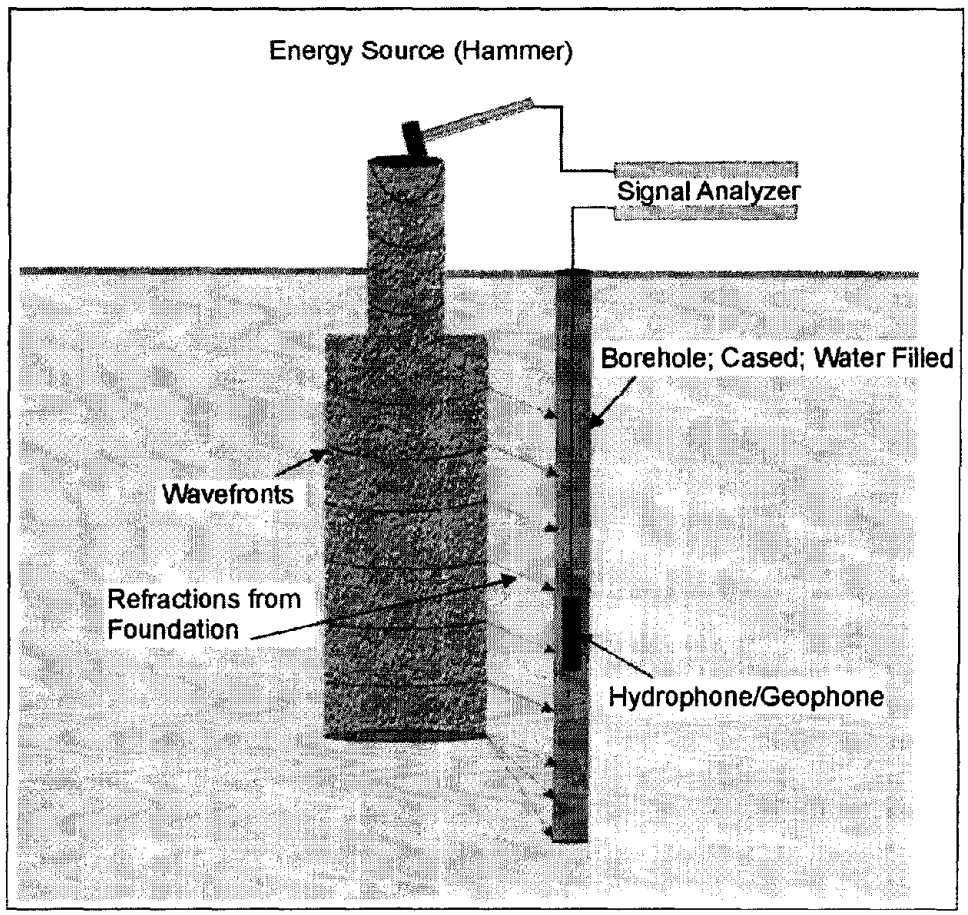

Figure 11. Parallel Seismic survey setup.

Data Interpretation: For hydrophone data, the time arrival of compressional waves is picked from the data for all receiver locations. A plot of the time arrival-versus-depth is prepared, an example of which is illustrated in figure 12.

In figure 12, the velocity of the concrete in the shaft is 5,155 m/s. A break in the graph occurs at a depth of 8.5 m indicating the depth of the shaft.

For uniform soil conditions, two lines are identified in the plot as shown in figure 12. The slope of the upper line is indicative of the velocity of the tested foundation, and the second line is indicative of the velocity of the soil below the bottom of the foundation. The intersection of the two lines gives the depth of the foundation. For nonuniform soil conditions, the interpretation of data from hydrophone use can be difficult due to the nonlinearity of the first time arrival. For geophone data in uniform soil conditions, the data can be interpreted in a way similar to the hydrophone data. When variable soil velocity conditions exist, an alternative to the first arrival time in data interpretation is used. All the traces are stacked, and a V-shape is searched for in the data because the bottom of the foundation acts as a strong source of energy (a point diffractor and a reflector), which produces upward and downward traveling waves. When a geophone is used, the borehole is

generally not filled with water. As a result, tube waves are minimized so that later arrival of reflected and diffracted shear and compressional waves can be identified.

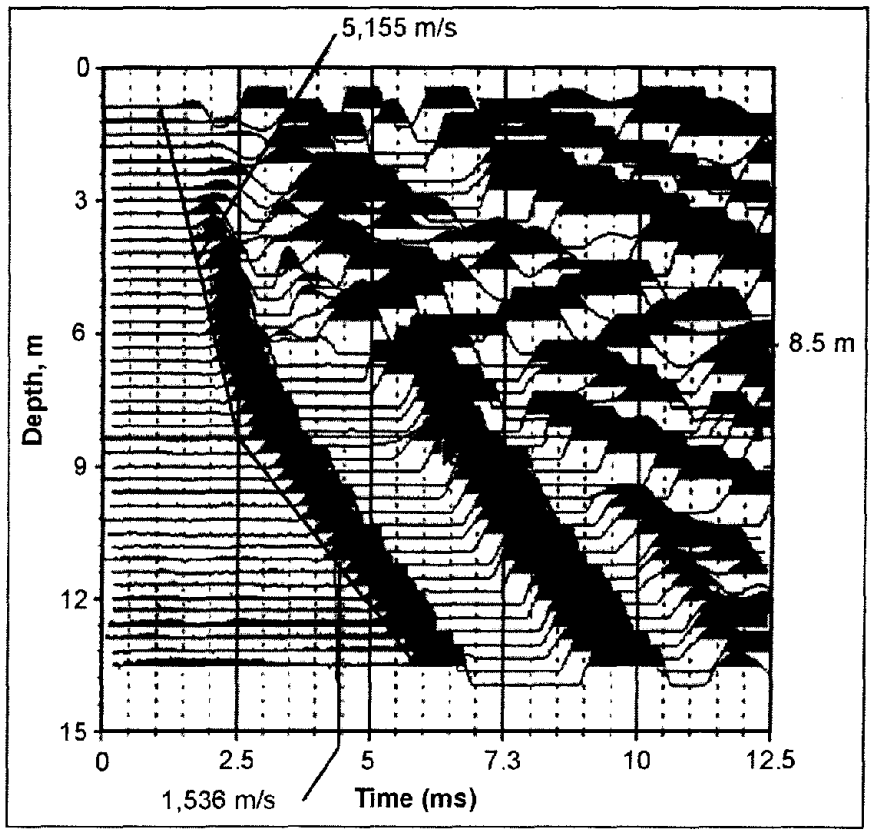

Figure 12. Parallel Seismic data and velocity lines.

Advantages: The Parallel Seismic method is more accurate and more versatile than other nondestructive surface techniques for determining unknown foundation depths. The accuracy of the method depends on the variability of the velocity of the surrounding soil and the spacing between the borehole and the foundation element. Depths are normally determined with 95% accuracy or better.

Limitations: A borehole is needed for Parallel Seismic tests, which adds to the cost of the investigation (unless borings are also required for other geotechnical purposes). The borehole should be within 1.5 m of the foundation, which sometimes cannot be achieved. Note that for very uniform soils (such as saturated sands), a successful test can be performed with up to 4.5 to 6 m spacing between the source and the borehole. As the borehole moves away from the foundation, interpretation of the PS data becomes more difficult, and the uncertainty in the tip depth determination becomes greater.

2.1.2.2 Induction Field (IF)

Induction Field (IF) method is used for the determination of the unknown depth of steel or continuously reinforced concrete piles.

Basic Concept: This is an electrical method that relies on detecting the magnetic field in in response to an oscillating current impressed into a steel pile. In order for this method to work, the pile must, therefore, contain electrically conductive materials. For reinforced concrete piles, this usually implies that reinforcing rebar extends along its full length.

A sensor is placed down a drillhole located close to the pile and detects the changing magnetic field strength. This sensor could be a magnetic field sensor or a coil. Along the length of the pile, the magnetic field strength will be relatively strong. However, the magnetic field strength will be significantly diminished at levels in the drillhole beneath the bottom of the pile to a residual conductivity value of the soil or bedrock. This change in the magnetic field strength is used to determine the depth of the pile.

Data Acquisition: An electrical contact must be made to the pile in question when conducting an Induction Field survey. Another electrode must be placed some distance from the pile. This can be another pile or simply an electrode placed in the ground. Oscillating current is then made to flow between these two electrodes. Figure 13 shows the layout of the pile, borehole and electrodes.

Data Processing: The detector measures the voltage and the data stored in the recorder. The magnitude of the measured voltage is plotted against the depth of the detector. This plot will show a significant decrease in magnetic field strength when the detector is beneath the toe of the pile.

Data Interpretation: Interpretation of the Induction Field method simply requires a visual observation of the voltage decay with depth down the borehole. The voltage will usually stabilize beneath the pile at a low voltage whose magnitude will depend on the resistivity of the ground.

Advantages: The Induction Field method is a proven technology for the determination of unknown depth of piles containing electrically conductive material, such as rebar. If the reinforcement is continuous in a concrete foundation, it can be used to detect the presence of piles underneath a footing.

Limitations: The interpretation of data is complicated by the existence of conductive materials in the bridge structure and the surrounding ground (including the water-table). Probably the most restrictive requirement is that there must be metal (usually reinforcing rebar) inside the pile, and it must extend continuously along the length of the pile. In addition, an electrical contact with the metal must be possible near the top of the pile. A PVC cased borehole is required. No signal would be received through a steel-cased borehole.

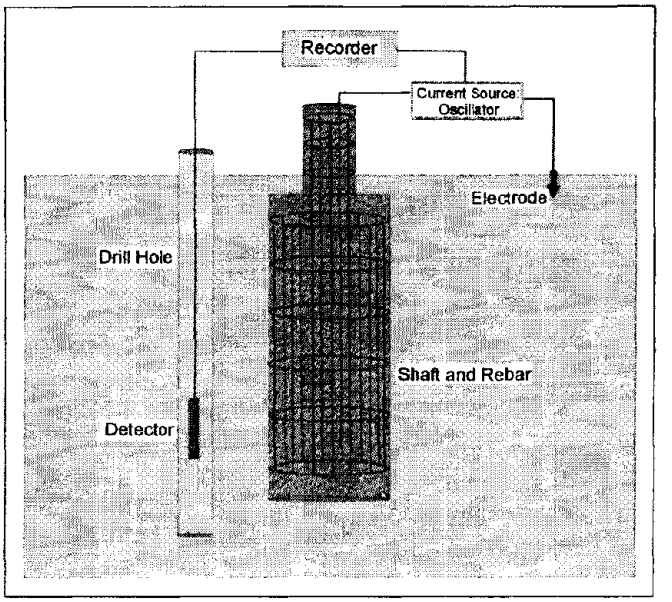

Figure 13. Induction Field method setup.

2.1.2.3 Borehole Logging Methods

Two borehole geophysical logging methods, magnetic logging and electromagnetic induction logging methods, can be used for the determination of unknown depth of steel of reinforced concrete piles.

No information was found on the use of these methods for measuring pile depths. However, it seems clear that these methods should work if the conditions are appropriate. In view of their simplicity and ease of use, it is included herein as methods that could be tested.

A borehole magnetometer could be used to find the depth of piles if they contain reinforcing rebar along the length of the pile. The reinforcing rebar will have induced magnetization due to the influence of the Earth's magnetic field and will radiate a secondary magnetic field. A magnetometer will respond to both the Earth's magnetic field and the secondary field. Beneath the toe of the pile, the secondary field will rapidly diminish resulting in a decrease in the magnetic field strength. A magnetometer in a nearby drill hole will detect this magnetic field change from which the toe of the pile can be induced.

Alternatively, borehole electrical methods, such as induction logging, can be used. In the induction logging method, an AC current is transmitted into the ground by the source coil and another coil is used for receiving the returning signal. The transmitted AC current generates a time-varying primary magnetic field, which induces eddy currents in the conductive ground or steel reinforcing rebar. These eddy currents set up secondary magnetic fields, which induces a voltage in the receiving coil. The magnitude of the received current can be used to determine the pile toe.

These two geophysical logging methods were not found in any of the references and are under investigation by Blackhawk GeoServices.

2.1.2.4 Dynamic Foundation Response

The Dynamic Foundation Response uses the resonant frequencies of structures to differentiate foundation types. The vibration response of a bridge substructure will exhibit lower resonant frequency responses when excited for a shallow foundation versus the comparatively higher resonant frequency response of a deep foundation system.

Basic Concept: The method is unproven for this use in bridges, but is based on the dynamic analysis theory for vibration design of foundations (soil dynamics) and geotechnical analyses of foundations subjected to earthquake loading.

Data Acquisition: A hammer with a built-in dynamic force transducer is used as the vibration source. A triaxial block of seismic accelerometers records the resulting signals. Typically, a bridge is excited at five to six locations, and the triaxial response is measured at five to six locations giving rise to 25 to 36 source-receiver combinations. The bridges are impacted in the vertical and horizontal directions to excite these modes as well as rocking modes along the frame of the substructures. This type of testing is known as modal testing; when the impulse force is measured and the resultant vibration response is measured, the transfer function can be calculated as in the Impulse Response test.

Data Processing: In its most basic form, a transfer function is calculated by taking the Fast Fourier Transforms of the input (impact force (F) and the output accelerometer receiver responses in acceleration units (A) as functions of frequency (f). The transfer function is obtained by dividing the output by the input (A/F). Plots of the transfer function versus frequency indicate the frequencies and amplitudes of resonance for a tested structure.

Data Interpretation: The dynamic foundation response of bridges, especially bridge piers, is much more complex than simple footing and pile foundation cases. Consequently, there will be many resonances present in transfer function results. Also, fundamental resonances of bridges are generally less than 20 Hz, and frequently less than 10 Hz. To determine the various resonances and their vibration mode shapes, the transfer function test must excite the range of frequencies of interest, and a number of locations must be tested to identify the mode shapes. The process of determining the full vibration behavior of a bridge abutment or pier then requires curve fitting of the experimental data, and can also involve theoretical dynamic analysis of the bridge with dynamic structural analysis programs.

Limitations: In tests, the Dynamic Foundation Response method showed some sensitivity in the response of the foundation as a function of depth and existence of piles, particularly for vertical vibrations. However, in practice, the bridges generally could not be excited with the 5.5 kg hammer at frequencies comparable to the natural frequencies identified in the theoretical modeling. More research is needed to explore different sources to generate the very low frequencies required for the experimental modal tests and then to perform curve fitting techniques to experimental data to be able to extract the mode shapes from the experimental data to compare with the theoretical mode shapes.

Practical tests showed that a 5.5 kg hammer was not sufficient to generate the required waves in bridges at the required frequencies. However, the method showed some response of the

foundation as a function of depth and existence of piles. This was particularly true for vertical vibrations. It is possible that this method may be appropriate for monitoring over time, where changes in the response could be detected. However, no references were found indicating that this is currently done.

2.1.2.5 Borehole Radar

Borehole Radar uses a borehole ground penetrating radar (GPR) antenna to obtain reflection echoes from a foundation for the determination of unknown depth and geometry of foundation.

Data Acquisition: In borehole radar, an antenna transmits radar energy into the surrounding rock and soil, and a receiver then records reflections that occur as the radar signals encounter and reflect from interfaces with different dielectric properties. The method is very similar to the borehole sonic method, where seismic waves are used rather than electromagnetic waves.

Borehole radar can be used in reflection mode or in cross-hole tomography mode. The radar measurements are either directional or omnidirectional, depending on the type of equipment and antennas. Only the reflection mode will be discussed in this document.

Radar uses radio waves with frequencies varying generally between 10 and 2,000 MHz. These waves are influenced primarily by the dielectric properties of the medium through which they are traveling and the electrical conductivity of the medium. Highly conductive materials attenuate the radar signals and limit its depth of penetration. Although the lower frequencies penetrate more than higher frequencies, they have less resolution.

For radar frequencies of 100 MHz, penetration varies from 10 to 40 m in resistive rocks. In conductive, clay-rich rocks, penetration will be less than 5 m. Figure 14 shows the borehole radar system.

Data Interpretation: In the unknown depth of foundation application, the borehole radar signal will be reflected from the foundation until the bottom of the foundation is reached. There will be no reflections beneath the foundation, except for those emanating from geologic conditions. The observed change in the reflected signal is used to locate the bottom of the foundation.

Limitations: Borehole radar requires a PVC-cased borehole; the method will not work if the hole is steel-cased. The depth of penetration is significantly influenced by the electrical conductivity of the rocks and soil surrounding the borehole, which may not be known before the radar survey is completed. Penetration up to about 10 m may be achieved in resistive conditions. In conductive materials, since the penetration of the GPR signal will be limited, getting the borehole as close to the pile as possible will be advantageous.

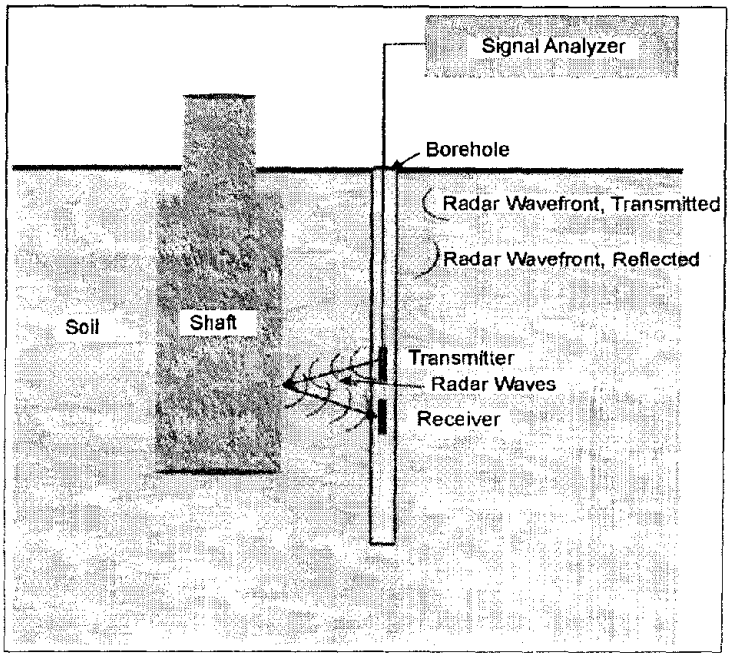

Figure 14. Borehole Radar system.

2.1.2.6 Borehole Sonic

This method is similar to Sonar and is based on using borehole seismic sources and geophones to obtain reflection echoes from a foundation for the determination of unknown depth and geometry of foundations.

Basic Concept: This method is a borehole equivalent of the surface reflection seismic method. It requires a borehole close to the pile into which a sonde is lowered containing a seismic source and a seismic wave detector. The requirement for the method to work is that there is a seismic impedance contrast between the pile (for example, concrete) and the soil into which the borehole is drilled. It is likely that this will frequently be the case since the velocity of seismic waves in soil is typically much lower than those in concrete. Figure 15 shows the method and seismic waves.

Data Acquisition: The borehole sonic surveys are conducted using a single borehole utilizing borehole logging sondes with low frequency sources or alternatively using separate boreholes for the source and receiver that are held at the same measurement depths. The survey is conducted by taking measurements at various depths within the borehole. In many logging methods, readings are taken when the sonde is ascending.

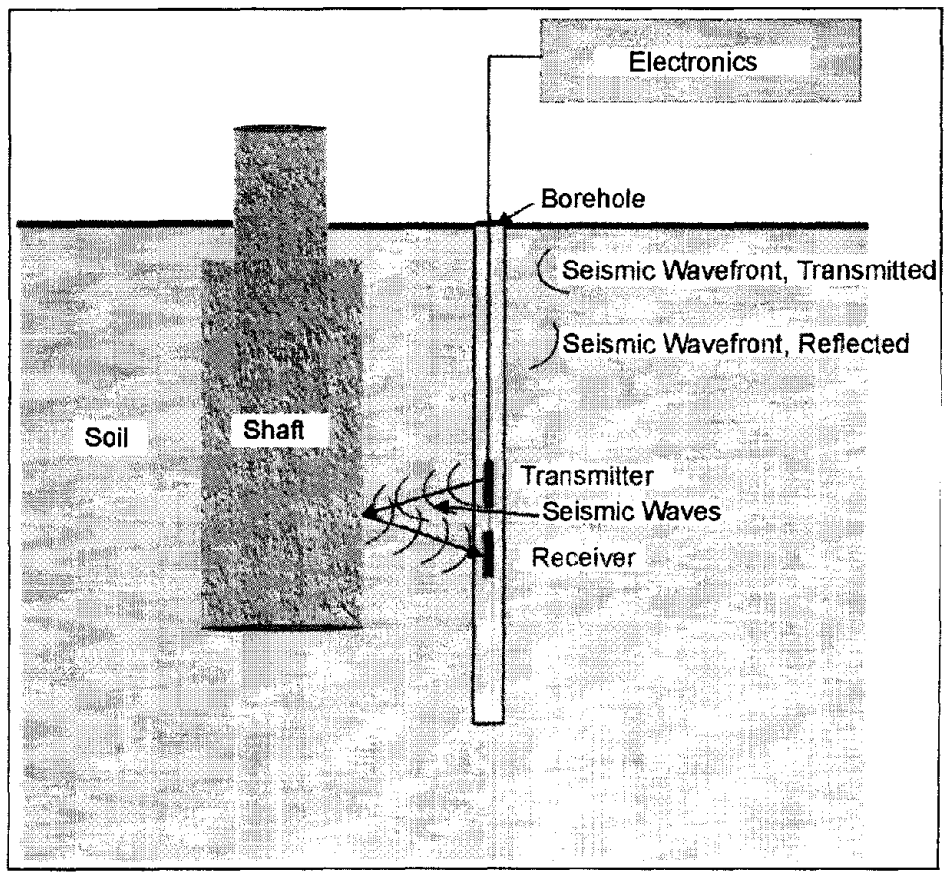

Figure 15. Schematic of the Borehole Sonic method.

Limitations: Seismic waves in soil are attenuated significantly with distance and may also be dispersive, thus limiting the higher frequency content of the signal. In addition, the waves are reflected from a curved surface (the pile), which may provide less returned energy than a plane surface as is common in surface seismic reflection methods. To this date, this method is not proven for the determination of the unknown foundation depths.

2.1.2.7 Cross-borehole Seismic Tomography

Two- and three-dimensional tomography is used for the high resolution imaging of the subsurface between boreholes.

Basic Concept: Tomography is an inversion procedure that provides for two- or three-dimensional (2-D and 3-D) velocity (and/or attenuation) images between boreholes from the observation of transmitted first arrival energy.

Data Acquisition: Tomography data collection involves scanning the region of interest with many combinations of source and receiver depth locations, similar to medical CAT-SCAN (figure 16). Typical field operation consists of holding a string of receivers (geophones or hydrophones) at the bottom of one borehole and moving the source systematically in the opposite borehole from bottom to top. The receiver string is then moved to the next depth

location and the test procedure is repeatuntil all possible source-receiver combinations are incorporated.

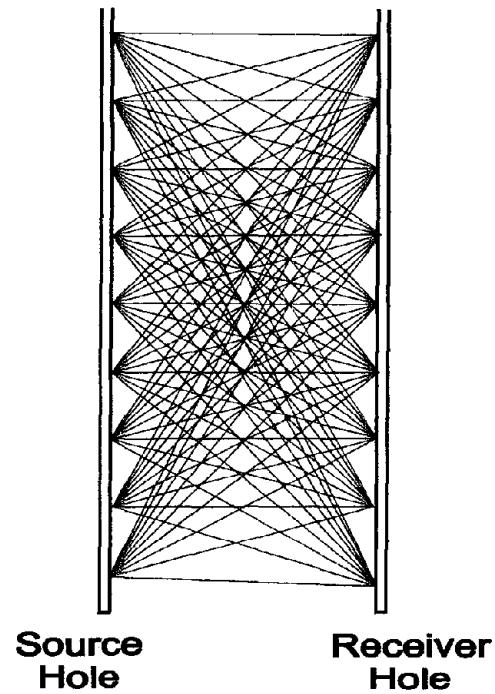

Figure 16. Tomographic survey design.

Data Processing: In the tomographic inversion technique, the acoustic wavefield is initially propagated through a presumed theoretical model and a set of travel times are obtained by ray-tracing (forward modeling). The travel time equations are then inverted iteratively in order to reduce the root mean square (RMS) error between the observed and computed travel times. The inversion results can be used for imaging the velocity (travel time tomography) and attenuation (amplitude tomography) distribution between boreholes.

Data Interpretation: Described below in figure 17a is a tomographic survey designed to investigate the foundation of an existing bridge. In this example, cross-hole velocity tomography surveys were conducted by pairing a seismic source in one borehole and a string of receivers in an adjacent borehole to propagate and capture seismic signals transmitted between source and receiver boreholes. Steel or concrete piles that existed within the surveyed area were indicated in the tomograms as relatively higher seismic velocity zones than the surrounding ground. The pile group, as depicted in Figure 17a, appeared as relatively higher seismic velocity anomalies within the fill and soil material above the bedrock. There was also a clear indication of low-velocity anomaly pockets in the top of the bedrock where the piles were driven into the bedrock. The seismic tomography survey indicated that the piles were point-bearing on rock, and, in fact, the piles were driven into the bedrock surface when installed.

The example shown in figure 17a is a tomographic survey designed to investigate the depth of four drilled shafts supported by a pile cap under a bridge column. The shafts were

originally thought to be 2m socketed in the bedrock. The tomogram sections, however, show that the shafts rested on top of bedrock. The results were also confirmed using the parallel seismic method. In figure 17b, the top of bedrock was well defined with no low-velocity anomalies apparent. In this figure, the water-saturated alluvial sediments, shown in blue, lies above bedrock, shown in green.

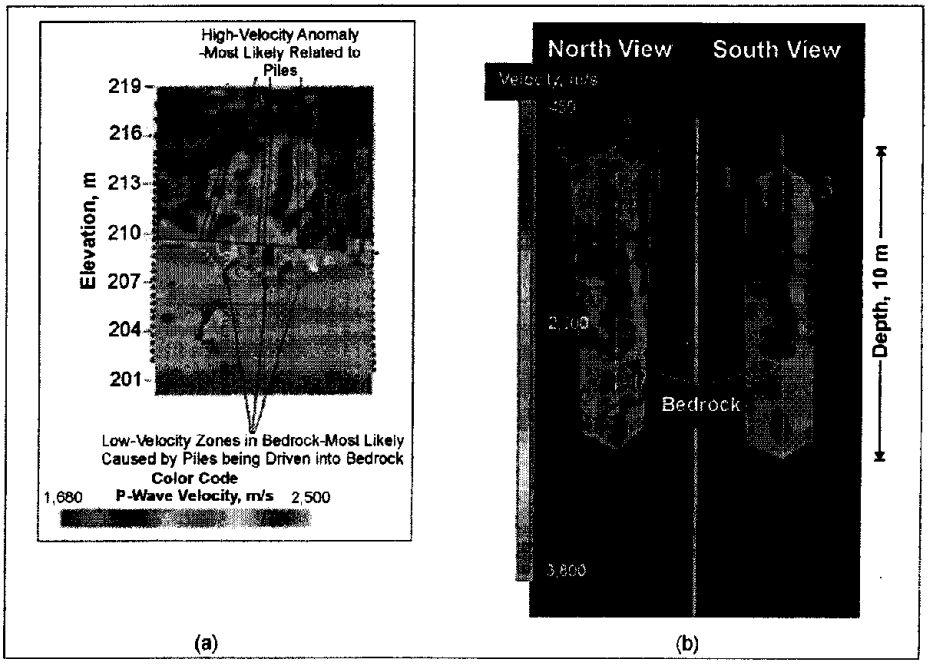

Figure 17. Tomograms showing: (a) socketed piles and (b) caisson on top of bedrock. (NSA Geotechnical Services, Inc. and Blackhawk GeoServices, Inc., respectively)

Advantages: Tomography provides high-resolution two-dimensional area or three-dimensional volumetric imaging of target zones for immediate engineering remediation. Tomography can then be used in before and after surveys for monitoring effectiveness of remediation. Tomography can also be used in before and after surveys for monitoring fluid injections between test holes or for assessing the effectiveness of soil improvement techniques.

Attenuation tomography can be used for the delineating fracture zones. Wave equation processing can be used for a high-resolution imaging of the reflection events in the data including those outside and below the area between the boreholes.

Limitations: Tomography is data-intensive and specialized 3-D analyses software is required for true three-dimensional imaging. Artifacts can be present due to limited ray coverage near the image boundaries.

2.1.3 Determining Depth of Foundation Socketing Into Bedrock

Finding the depth of socketing of foundations into bedrock involves finding two depths—the foundation and the bedrock. Finding the depth of the foundations was discussed in sections

2.1.1 and 2.1.2. Bedrock depths can be found using either surface geophysical methods or borehole methods for those piles with a borehole close by.

Alternatively, cross-borehole tomographic imaging can be used to determine the depth of foundation socketing, as was discussed in section 2.1.2.7. Several methods can be used to find bedrock depth. The particular method to use depends on the expected depth and the local conditions. The methods include Ground Penetrating Radar (GPR), Seismic Refraction, Seismic Reflection, Resistivity, and Time Domain Electromagnetic Soundings methods. These methods are discussed in Chapter 6.1.1.

2.2 INTEGRITY TESTING

Road features such as bridges often use drilled shafts to bear the load of the bridge. During construction, the drilled shafts can be imaged using various testing methods for integrity assessments. This is important since defects in the shaft may result in structural instability and/or safety concerns. These tests are called Nondestructive Tests (NDT) and involve measuring various physical properties of the shafts. NDT are increasingly being used in the United States for quality assurance (QA) and quality control (QC) on highway projects that use deep foundations, and to assess the integrity of other civil engineering structures.

2.2.1 Integrity Testing of Foundations

Several methods can be used to test the integrity of concrete foundations, including crosshole sonic logging (CSL), crosshole sonic logging tomography (CSLT), single hole sonic logging (SSL), gamma-gamma density logging (GDL), and sonic echo (SE)/impulse response (IR) methods. A brief discussion of each of these methods is given below listing their advantages and limitations.

2.2.1.1 Crosshole Sonic Logging (CSL)

The Crosshole Sonic Logging (CSL) method is developed for integrity testing of concrete foundations, such as drilled shafts, slurry walls, and auger cast piles. This cross-hole logging technique is performed using water-filled PVC or steel access tube pairs.

Basic Concept: Crosshole Sonic Logging (CSL) uses high frequency compressional sonic waves as the energy source. The sonic source produces an impulse whose frequency content is usually 30 to 40 kHz. Sonic waves passing through concrete are influenced by the density and elastic modulus of the concrete. Fractured or "weak" concrete zones lower the velocity of the sonic waves and, therefore, can be detected. In addition, the amplitude of a seismic pulse is affected by these defects although this is not extensively used at the present time. The frequency content of the seismic energy pulse determines the resolution and penetration of the signal. High frequencies have high amplitude attenuation but can image small targets. Conversely, lower frequencies have less attenuation but image larger targets.

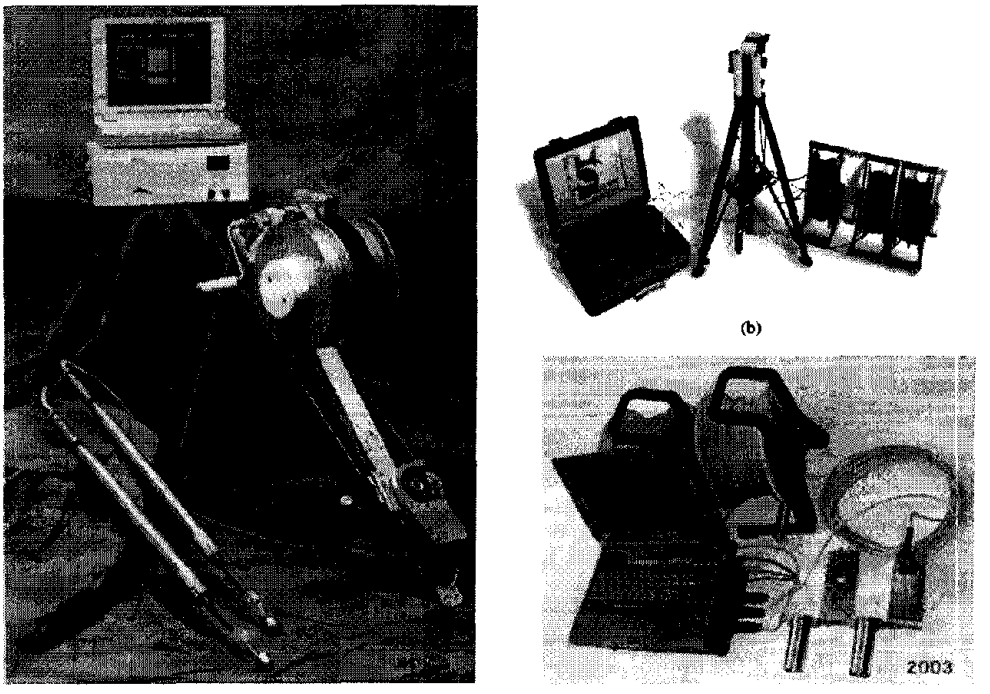

Figure 18. Crosshole Sonic Logging instruments. (a) InfraSeis, Inc., (b) Olson Instruments, Inc., and (c) GeoSciences Testing and Research, Inc.

Several companies manufacture instruments for the CSL system; three sets of such system are shown in figure 18.

Data Acquisition: Figure 19 illustrates the CSL method. Steel or PVC access tubes must be attached to the inside of the reinforcing rebar cage prior to the concrete placement and be filled with water. At least two schedule 40 access tubes, usually having a inside diameter of 50 mm, are required. Special care must be taken when installing access tubes to avoid debonding between the concrete and the tubes. Poor bonding between access tubes and concrete can cause complete signal loss. One of the tubes is used for the transmitter and the other for the receiver probe. The transmitter and receiver probes can be oriented such that the path between them is horizontal (zero offset, as seen in figures 19 and 21) or with some offset. Zero offset logging is called standard Crosshole Sonic Logging. Readings are taken at regular 6 cm intervals down the shaft while maintaining the same offset. Defects are observed as a reduction in the travel time of the seismic wave from the transmitter to the receiver. It is important that the tubes are vertical, and that the distance between them is constant for their entire length so that seismic travel time differences do not result from these distance differences rather than defects in the concrete. In addition, unrecognized distance differences in the distance between tubes may result in false interpretations of defects.

Other variations in the geometric configuration are also used. These include the source and receiver lowered into the same tube, or a source and multiple receivers lowered into separate holes. The most commonly used configuration is the one described above.

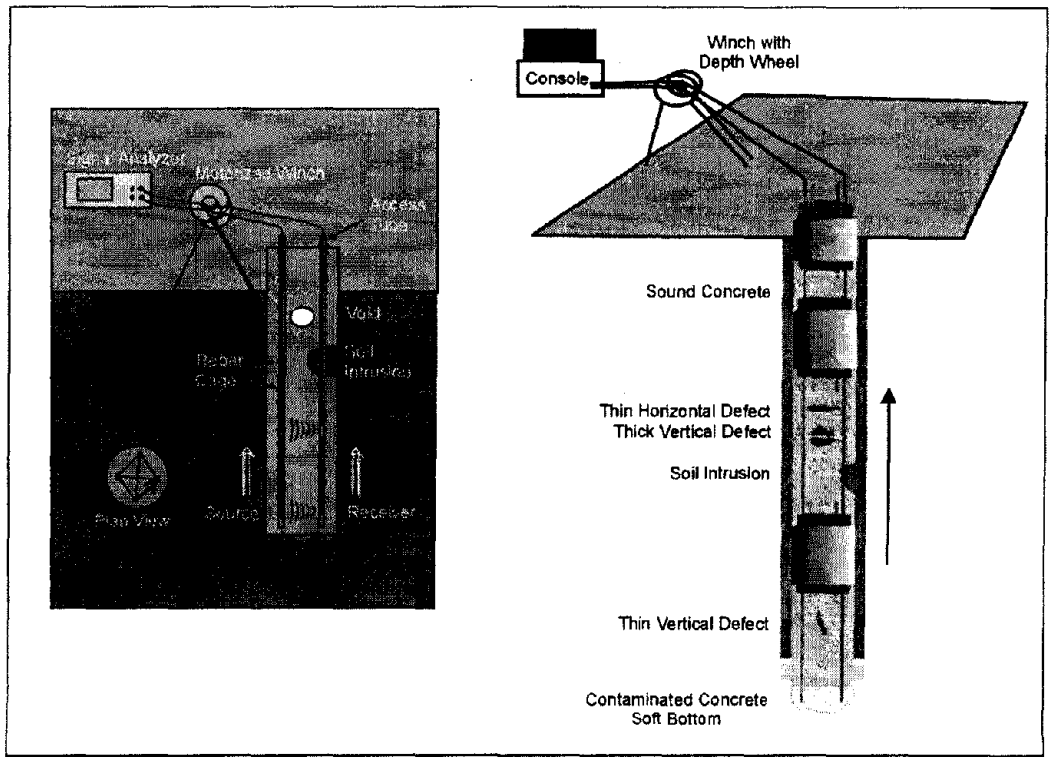

Figure 19. Crosshole Sonic Logging method with various kinds of defects. (Blackhawk GeoServices, Inc.)

Figure 19 shows the CSL method and the ray paths. Common defects are also shown illustrating their influence on the seismic wave travel times.

Data Processing: The received data must plotted and presented such that any defects in the shaft are clearly observed. Figure 20 shows a typical CSL travel time plot. If only two access tubes are available and only one offset between the transmitter and receiver is used, then anomalies may exist anywhere between the two tubes. It is then difficult to determine the geometry and exact location of the anomaly with respect to the tube location. However, if data are collected with several different offsets between the transmitter and receiver, then a more definitive location can be given for any anomalies.

Advantages: CSL allows for accurate characterization of soil intrusions or other anomalies throughout the shaft inside the rebar cage (between the tubes). Several levels of defects can be detected by this method with high precision. It can be used to identify young (heavy retarted) un-cured concrete.

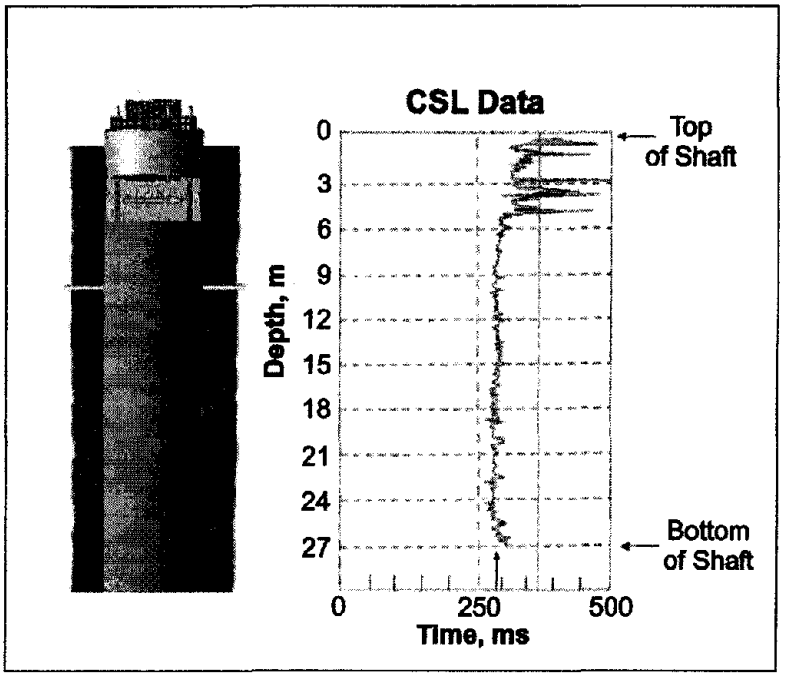

Figure 20. Travel time plot for Crosshole Sonic Logging. (Blackhawk GeoServices, Inc.)

Limitations: Access tubes must be installed prior to concrete placement and special care must be taken to avoid tube debonding between concrete and the tubes. Tube debonding condition can occur with PVC access tubes above the water table. No signal is obtained in the tube debonding zone. Only defects along the path of the sonic wave will be detected; it cannot detect anomalies outside the rebar cage. It cannot be used to detect shaft bulbing (increase in diameter); although this can easily be checked by the Sonic Echo (SE)/Impulse Response (IR) test, described in section 2.2.1.4.

2.2.1.2 Crosshole Sonic Logging Tomography (CSLT)

Tomography is an inversion procedure that provides two- or three-dimensional (2-D and 3-D) velocity (and/or attenuation) images between access tubes from the observation of transmitted first arrival energy. This method can be used for delineating internal flaws in man-made structures; such as buildings, bridges, slurry diaphragm walls, and dams.

Basic Concept: Tomography data collection involves scanning the region of interest with many combinations of source and receiver depth locations. Typical field operation consists of holding the receiver tool at the bottom of one hole/surface and moving the source tool systematically in the opposite hole/surface from bottom to the top. The receiver is then moved to the next depth location and the test procedure is repeated until all possible source-receiver combinations are incorporated.

Data Acquisition: *Offset-Tomography* (CSLT shown in figure 21) consists of running a zero-offset (CSL) log in combination with several positive offset (receiver is shallower) and negative offset (source is shallower) logs to create a two-dimensional tomographic panel

between a pair of tubes. This procedure is repeated for all possible inspection tube combinations to form a three-dimensional tomography dataset.

Data Processing: In the tomographic inversion technique, the acoustic wavefield is initially propagated through a presumed theoretical model and a set of travel times are obtained by ray-tracing (forward modeling). The travel time equations are then inverted iteratively in order to reduce the root mean square (RMS) error between the observed and computed travel times. The inversion results can be used for imaging the velocity (travel time tomography) and attenuation (amplitude tomography) distribution between boreholes.

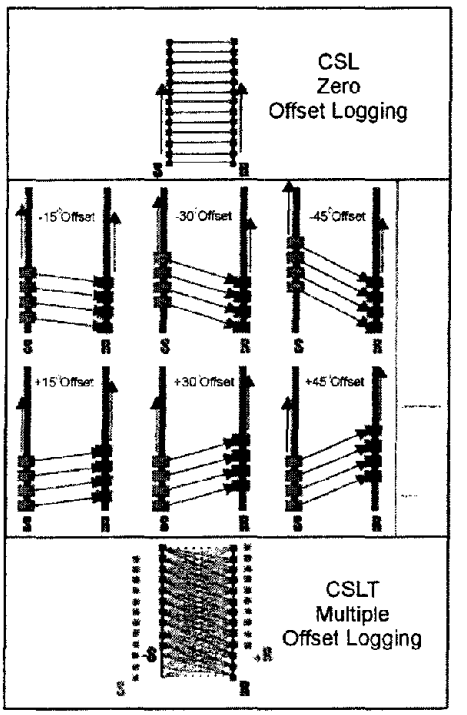

Figure 21. Ray paths for Crosshole Sonic Logging and Crosshole Sonic Logging Tomography (S is source, R is receiver).

Data Interpretation: Figure 22 illustrates the results of a CSL survey compared to a CSLT survey. The two drawings on the left side of the figure show the ray paths for the CSL and CSLT systems. The third drawing shows the location of the defects in the shaft, and the fourth drawing illustrates the results of the CSL survey. As can be seen, the top and bottom of the defect are observed. However, it is not possible to identify the exact location of the defect from the CSL data. With CSLT 2-D and 3-D tomographic images, it is possible to provide a more accurate volumetric definition of the defect zones within the shaft than the CSL method.

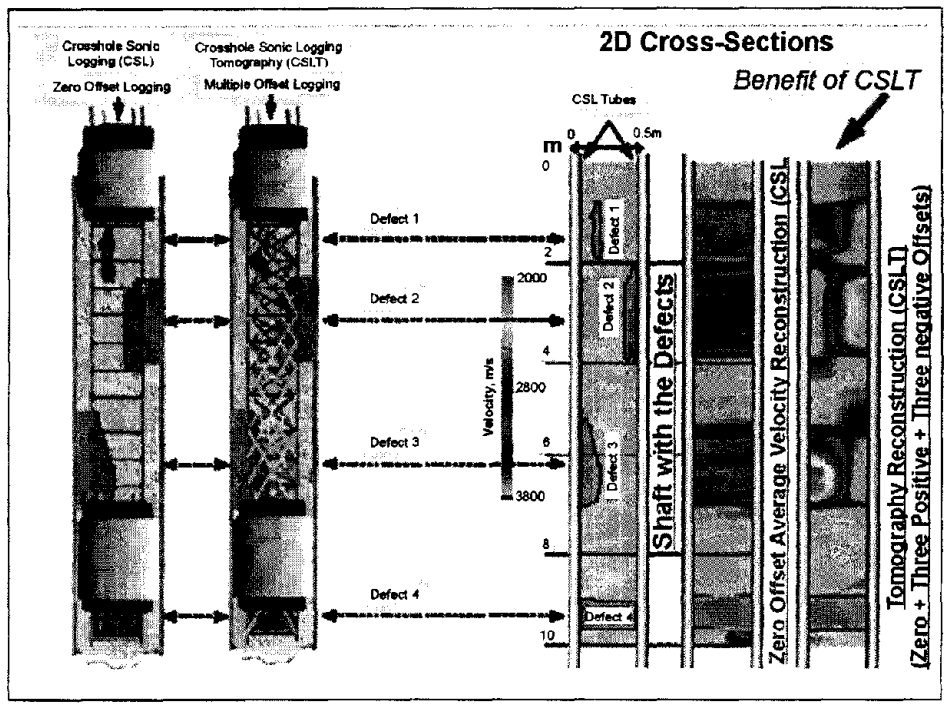

Figure 22. Comparison of Crosshole Sonic Logging and Crosshole Sonic Logging Tomography results. (Blackhawk GeoServices, Inc.)

Advantages: CSLT Provides for two-dimensional area or three-dimensional volumetric imaging of defect zones for immediate engineering remediation. Tomography is used in before and after surveys for monitoring the effectiveness of remediation. Tomographic processing can identify horizontally elongated defects, such as cold joints, that are missed by standard CSL technique (amplitude or travel time). Attenuation tomography can be used for the delineating fracture zones.

There are three main benefits of tomographic imaging:

1. Tomographic imaging provides better spatial resolution of defects for confirmation through coring followed by remedial action;

2. Tomography provides a more accurate correlation between percentage drop in velocity with percentage drop in concrete strength for shaft acceptance criteria;

3. Two and three dimensional tomography, when performed routinely, will provide engineers in the owner agencies a tool for assessing the integrity of drilled shaft foundations without further costly delays to construction.

Limitations: Tomography is data-intensive for non-automated CSL field systems. Specialized 3-D analyses software is required for true three-dimensional imaging. Artifacts can be present due to limited ray coverage near the image boundaries.

Currently this method cannot be used to image defects outside the rebar cage.

2.2.1.3 Gamma-gamma Density Logging (GDL)

The 4-pi Gamma-Gamma Density Logging (GDL) method is developed for integrity testing of concrete foundations, such as drilled shafts, slurry walls, and auger cast piles. This single-hole logging technique is performed using air or water-filled PVC or steel access tubes.

Basic Concept: The technique is able to detect drops in average bulk density that is indicative of anomalies in the material surrounding the inspection tube. The gamma-gamma logger measures the intensity of reflected radiation, or backscatter, from the material around the borehole. The intensity of the backscatter is largely a function of the density of the material. Variations in backscatter intensity, therefore, indicate variations in density. The method is used for QA of concrete in large-diameter caissons and mass concrete foundations where access tubes can be installed with the reinforcing cage before the concrete is placed. Figure 23 shows the equipment used for gamma-gamma logging.

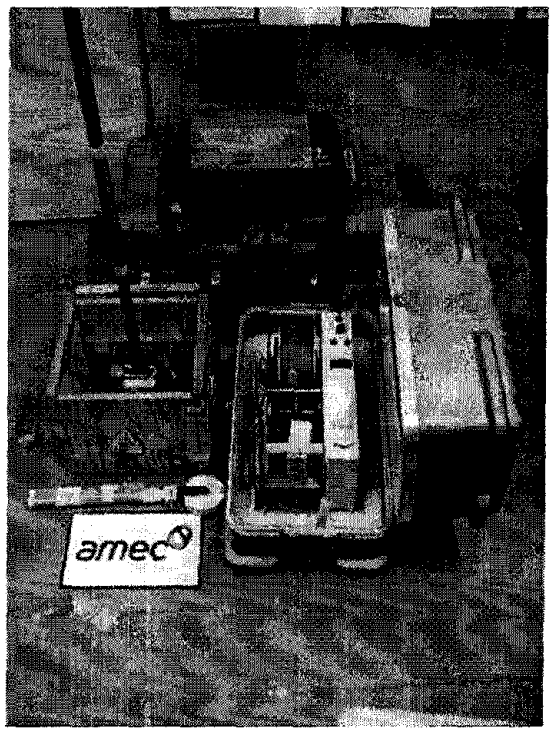

Figure 23. Gamma-gamma denisty logging equipment. (AMEC Earth & Environmental, Inc.)

Current gamma-gamma logging equipment is based on lightweight geophysical logging systems that use a laptop computer for computer control, data acquisition, and storage. One person can operate this equipment.

The gamma-gamma log can be used as a comparative form of testing, where variations in backscatter intensity indicate anomalies in concrete quality. If the anomalies must be quantified, or actual density values are required, the gamma backscatter values must be correlated with a reference density value. For calibration purposes, a test block should be

constructed of the same concrete, with an access tube of the same material as those used in the structure to be tested. Gamma-gamma tests performed under controlled conditions on the test block then provide reference measurements from which a factor can be calculated that will relate gamma intensity to density.

Data Acquisition: In the GDL test method, a weak Cesium-137 source is used to emit gamma rays into the surrounding material. A small fraction of the gamma ray photons are reflected back to the probe (due to compton scattering) and their intensity are recorded by a NaI scintillation crystal as counts per second (cps). The measured count rate (cps) depends on the electron density of the surrounding medium which is proportional to the mass per unit volume. The tool is calibrated by placing the probe in an environment of known density in order to convert the measured count rate (cps) into the units of density in gr/cm^3 or lbs/ft^3.

In the GDL test, the radius of investigation is largely governed by 1/2 of the source-detector spacing. An optimal spacing is selected (generally about 35 cm) and the GDL test is performed from all tubes in order to obtain uniform coverage around the perimeter of the shaft. Good concrete condition will result in a near continuous alignment of the data. Anomalous zones—due to soil intrusions, poor concrete, or voids—are characterized by large low density (high count rate) deflection in the data.

Gamma-gamma logs can be conducted in water or air-filled access tubes. The access tubes can be PVC or steel. Gamma-gamma logs can be effective even when the access tube has become debonded from the cement.

Data processing: Data processing is conducted with a microcomputer similar to that used for acquisition. The data are usually processed for bulk density. These calculations are preformed during real-time data acquisition or post-acquisition with a software analysis package.

Data Interpretation: Figure 24 shows the data and exposed upper portion of a shaft.

In figure 24, the data from Tube 1 (left trace) indicated possible flaws in the upper 3 m of the shaft. Excavation of the top of the shaft at Tube 1 revealed rebar without proper concrete cover. Very low readings of 2,306 to 2,403 kg/m^3 in the upper 30 to 60 cm of Tube 1 were corroborated by an absence of concrete along that tube at the upper four horizontal rebars. Concrete was present for the next few meter as was indicated by density readings between 2,419 and 2,451 kg/m^3. Measured densities then dropped down from 2,419 kg/m^3 to 2,322 kg/m^3 at depths of about 1.5 to 3 m. The picture shows that neither Tube 1 nor the horizontal rebar in this area were covered by concrete.

Advantages: GDL allows for precise characterization of soil intrusions or other anomalies at a radius of about 18 cm both inside and outside of the rebar cage. It can be used in fresh concrete while restoration is still feasible as the density of concrete changes minimally as it sets. GDL can provide information related to the quality of the concrete. The tube debonding condition minimally affects the GDL data.

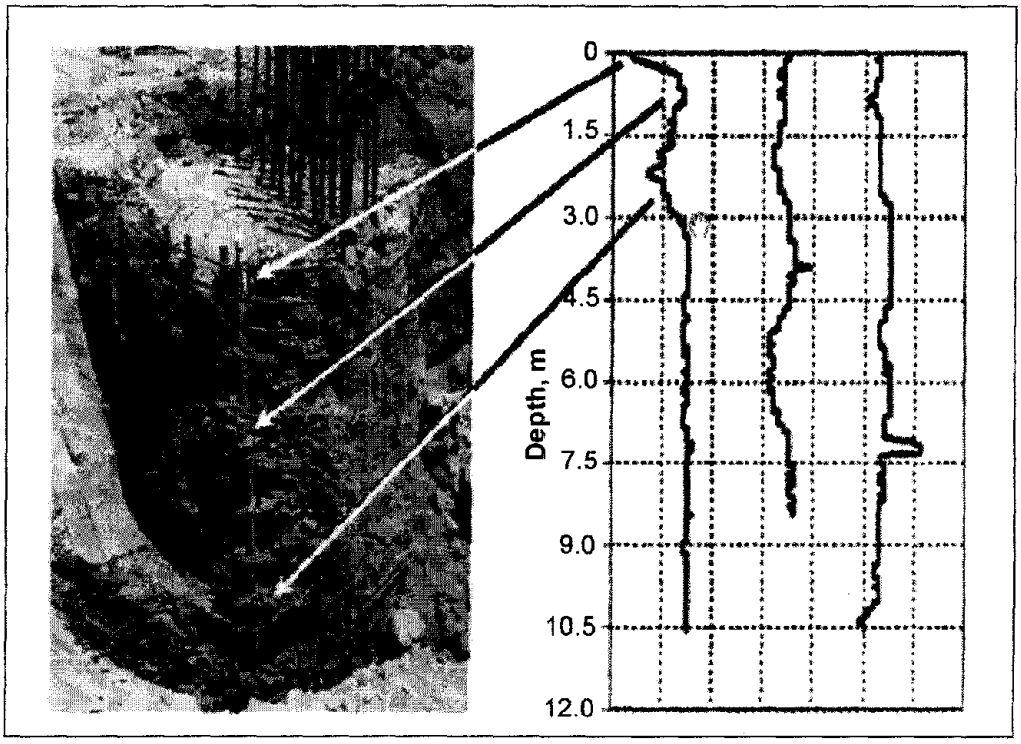

Figure 24. Gamma-gamma density logs and results. (Geophysics, 2002)

Limitations: GDL cannot be used to detect anomalies inside the shafts, only along the outer perimeter of the shaft at about 18 cm radius from each tube or 36 cm tube-tube spacing. It can not be used to identify young, heavily-retarded uncured concrete. GDL cannot detect shaft bulbing (increase in diameter). GDL requires special handling for the use of radioactive sources. As mentioned above, an obvious limitation of the method is the limited depth of penetration. Generally, with the gamma-gamma method, the location of the defect within the shaft cannot be determined, only its existence and depth. Combining the CSL/CSLT methods with the gamma-gamma density method provides a good solution.

2.2.1.4 Sonic Echo/Impulse Response (SE/IR)

Sonic Echo/Impulse Response (SE/IR) tests are performed to evaluate the integrity and determine the length of deep foundations. This method can be used to detect defects, soil inclusions and pile necking, diameter increases (bulbing) as well as approximate pile lengths.

SE/IR tests are performed on drilled shafts and driven piles (concrete or timber) or auger-cast piles. The test can also be performed on shallow wall structures such as an abutment or a wall pier of a bridge provided the top of the wall is accessible.

Basic Concept: The Sonic Echo method requires a measurement of the travel time of seismic waves (Time domain) and the Impulse Response Method uses spectral analysis (Frequency domain) for interpretation. These two methods are sometimes called Pile Integrity Methods (PIT).

Additional names for the Sonic Echo Method include Echo, Seismic, Sonic, Impulse Echo, and Pulse Echo Methods. Other names for the Impulse Response Method include Sonic Mobility, Transient Dynamic Response, Impulse Response Spectrum, Impedance, Shock, Transient Response, Transient Dynamic Response, and Sonic.

In both the sonic echo and impulse response tests, compressional waves (P waves by geophysicists) are reflected from the bottom of the tested structural element or from a discontinuity such as a crack or a soil intrusion. The generated wave from an impulse hammer travels down a shaft or a pile until a change in acoustic impedance (depends on velocity, density, and changes in diameter) is encountered, and the wave reflects back and is recorded by a receiver placed next to the impact point. This change in impedance can occur and be observed from significantly large defects within the shaft, as illustrated in figure 25.

Data Acquisition: For drilled shafts and piles, the best results from SE/IR tests are obtained if the top of the drilled shaft or the pile is exposed to allow receiver attachment and hammer strikes (see figure 25a). If the top is not exposed, then the SE/IR tests are performed on the side that provides at least the upper 30 to 60 cm of the shaft be exposed (see figure 25b). In those cases where the superstructure is in place, the SE/IR data become more difficult to interpret because of the many reflecting boundaries, and two or more receivers should be used to track reflections (please refer to the Ultraseismic method in section 2.2.1.6).

In an SE/IR test, a hammer strikes the foundation top, and a receiver monitors the response of the foundation. A digital analyzer records the hammer input and the receiver output. SE tests are typically performed with different frequency filtering to optimize reflections coming from the bottom of the foundation and to reduce the effect of surface waves or reflections from a discontinuity at a shallow depth where the frequencies associated with these two conditions are high. In an IR test, a digital analyzer automatically calculates the transfer and coherence functions after transforming the time records of the hammer and the receiver to the frequency domain.

Data Processing: To help interpret SE/IR data, processing techniques can be applied to enhance weak echoes. SE signals, which are measurements of acceleration, are commonly integrated to produce velocity and treated with a gain function that increases exponentially with travel time from the source to enhance weak reflections and to compensate for the damping of energy. For cases where echoes are not easily seen in the data, other sophisticated signal processing techniques are available. In simple cases, the SE data can be used to obtain an image of the shaft through a process called impedance imaging.

For best results, it is important to know the P wave velocity in the structure being tested. It is not safe to assume the concrete velocity is known from general rules of thumb. Velocities of concrete can vary based on the aggregate used, age of the structure, and state of weathering, ASR or other degradation. It is easy to measure local velocity if two sides of the structure are available or if an exposed section of the body of sufficient length is available. A source placed a measured distance from a receiver can be used to get a first arrival signal to compute the P-wave velocity.

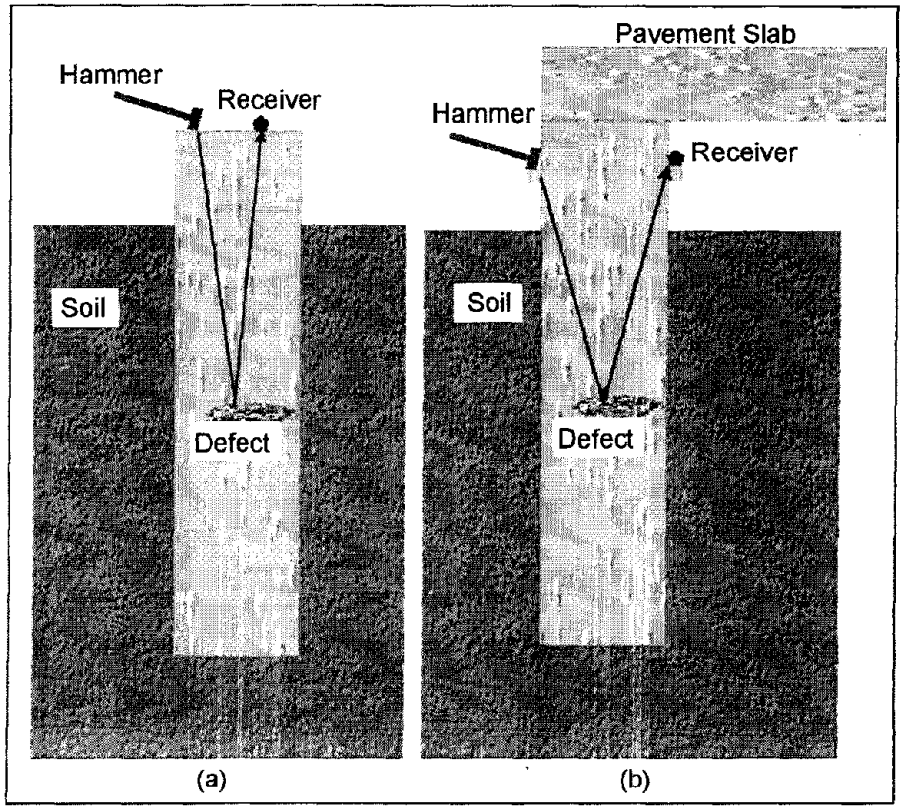

Figure 25. Defects in shafts and seismic waves used to image these defects.

Data Interpretation: Sonic Echo data are used to determine the depth of the foundation based on the time separation between the first arrival and the first reflection events or between any two consecutive reflection events (Δt) according to the following equation:

$$D = V \times \frac{\Delta t}{2}, \tag{3}$$

where D is the reflector depth, and V is the velocity of compressional waves. Figure 26 shows a sonic echo record and the depth calculation using the second and third echoes. The multiple echoes are all interpreted as coming from the same reflector since they are an equal time apart on the record. Any pair can be used to calculate the two-way travel time between the source and the reflector. In this case the clearest pair of echoes were the second and third, which were used to calculate the depth using the formula above, giving a depth of 2.01 m. A reflector can be the bottom of the foundation or any discontinuity along the embedded part of the foundation. Sonic Echo data can also be used to determine the existence of a bulb or a neck in a shaft or the end conditions of the shaft based on the polarity of the reflection events.

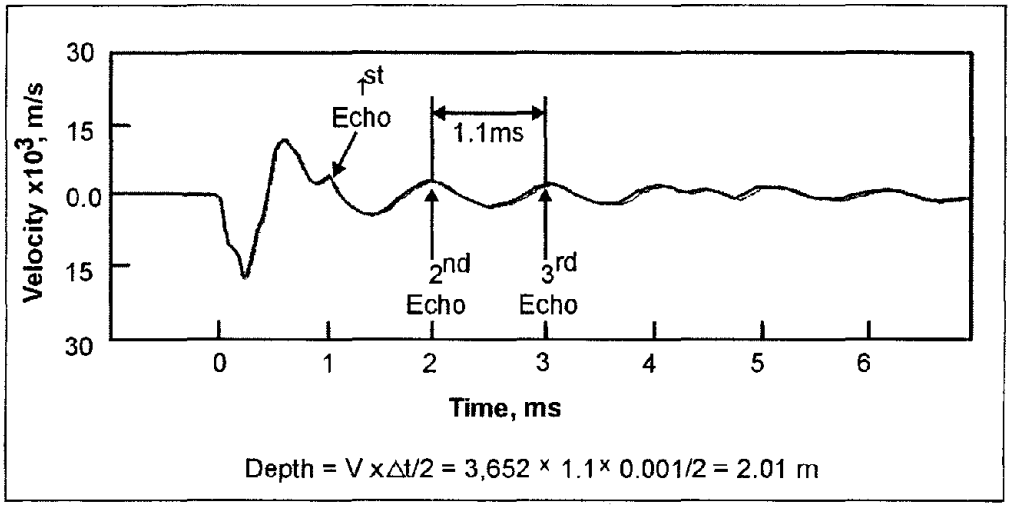

Figure 26. Sonic Echo record and depth calculation.

Impulse Response data are used to determine the depth of reflectors according to the following equation:

$$D = \frac{V}{(2 \times \Delta f)}, \tag{4}$$

where

Δf = distance between two peaks in the transfer function plot $\left(\frac{\text{velocity}}{\text{force versus frequency}}\right)$,

or between zero frequency and the first peak for soft bottom conditions.

where Δf is the distance between two peaks in the frequency spectrum plot (velocity/force versus frequency) or between zero frequency and first peak for soft bottom conditions. The multiple echoes from a discontinuity or bottom, as seen in the Sonic Echo method, result in increased energy at the frequency of the echo. This causes a peak in the frequency spectrum. Under conditions where there is a hard material beneath the structure, the second harmonic of the echo is also evident. Using the frequency difference between zero and the main echo frequency or between the first and second harmonic frequencies in the formula above gives the depth of the structure. IR data also provide information about the dynamic stiffness of the foundation. This value can be used to predict foundation behavior under working loads or correlated with the results of load tests to more accurately predict foundation settlement.

Example data for the Impulse Response method is shown in figure 27, along with the depth calculations showing a reflector depth of 1.98 m.

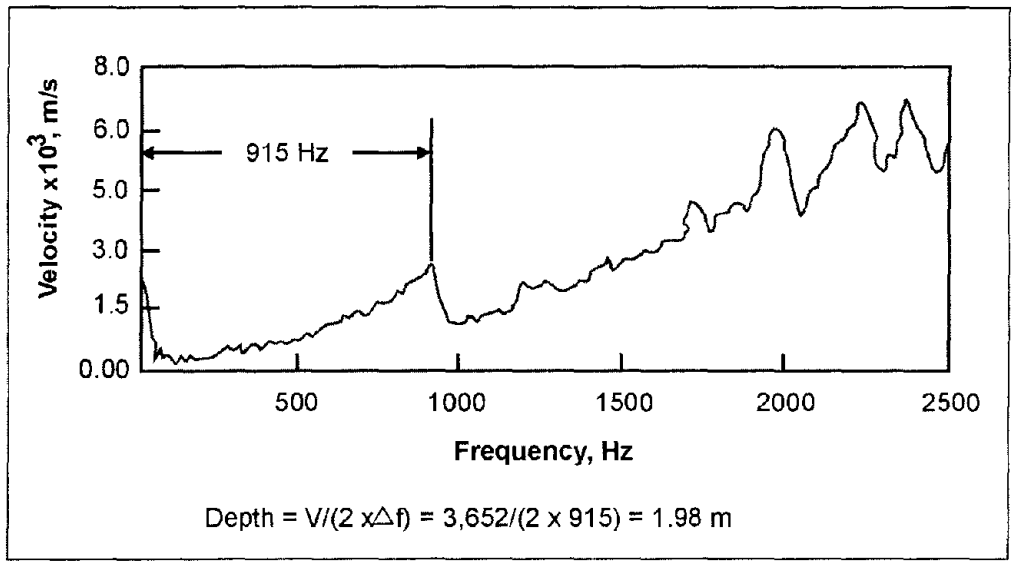

Figure 27. Depth calculations using frequency domain data for the Impulse Response method.

Advantages: This is a quick and economical test method used mostly in columnar shaped foundations without access tubes. The defects can be found early with minimal delays to construction.

Limitations: The SE/IR method works best for free-standing columnar-shaped foundations, such as piles and drilled shafts, without any structure on top.

Typically, SE/IR tests are performed on shafts or piles of length-to-diameter ratios of up to 20:1. Higher ratios (30:1) are possible in softer soils. The method can only detect large defects with cross-sectional area change of greater than 5%.

A toe reflection is not possible if the pile is socketed in bedrock of similar stiffness (or acoustic impedance) as concrete. If the pile is embedded in very stiff soils, penetration may be limited to about 8 m. For the softer soils, echoes can be observed from piles of up to 75 m in length. This method cannot be used for steel H-piles.

A much more detailed analysis, with detection of much smaller defects, can be done using Crosshole Seismic Logging (CSL), gamma-gamma density logging (GDL), and Crosshole Seismic Tomography (CSLT).

2.2.1.5 Single Hole Sonic Logging (SSL)

The single hole sonic logging (SSL) method is developed for integrity testing of concrete foundations in water-filled PVC or steel access tubes.

Basic Concept: The single hole sonic logging (SSL) method measures the speed of a sonic pulse around a single water-filled access tube to provide quality assurance of concrete placement. The method is particularly suited to small-diameter piles that penetrate rockfill with large cavities and are then socketed into rock. It is also suitable for small- diameter piles where the installation of two tubes may be impractical. The method can also be used to

confirm CSL defects and for confirmation of debonded conditions between an access tube and the surrounding concrete. The probe consists of a transmitter and a receiver, as illustrated in figure 28.

Data Acquisition: A single water-filled tube is required for the instrument. Similar to sonic logging in boreholes, this method measures the refracted arrival time between a sonic transmitter and receiver probe as a function of logging depth interval of typically 6 cm.

Generally, the method should be run after the concrete has been allowed to set for about six days. As reported by J.M. Amir in the piletest.com website, this method was tested in both steel and PVC-cased tubes and it was found that the PVC tube worked best. The steel tube prevented the wave from exiting the tube because of its high velocity. Tube diameter was also investigated using two tubes having diameters of 40 and 50 mm. It was found that the smaller tube filters noise more effectively and facilitates processing of the signal. In investigating probe separation, it was found that increasing the probe separation enhanced the anomaly. As expected, the detection range for the system depends on the size of the defect. A 50% reduction in signal may be observed even when the defect is only 30 mm high, providing it surrounds the tube.

Advantages: The method can be used to confirm CSL defects and for confirmation of debonded conditions between an access tube and the surrounding concrete.

Limitations: Access tubes must be installed prior to concrete placement and special care must be taken to avoid tube debonding between concrete and the tubes. No signal is obtained in the tube debonding zone.

SSL can only detect defects within centimeters of the access tubes. SSL does not define the depth extent of anomalies as accurately as CSL. It cannot be used to detect shaft bulbing (increase in diameter); although this can easily be checked by the Sonic Echo (SE)/Impulse Response (IR) test.

2.2.1.6 Ultraseismic (US) Profiling

Ultraseismic (US) tests are performed to evaluate the integrity and determine the length of shallow and deep foundations. US tests can be performed on drilled shafts and driven or auger-cast piles. The test can also be performed on shallow wall-shaped substructures such as an abutment or a wall pier of a bridge provided at least 1.5 to 1.8 m of the side of the structural element are exposed for testing. The method is particularly useful in testing abutments and wall piers of bridges because of the relatively large exposed areas available for testing.

Ultraseismic tests can be performed on concrete, masonry, stone, and wood foundations. Steel pile foundations can also be tested, but damping of the energy in this case is much greater than that of concrete and wood due to the large surface areas and small cross-sectional areas of steel piles.

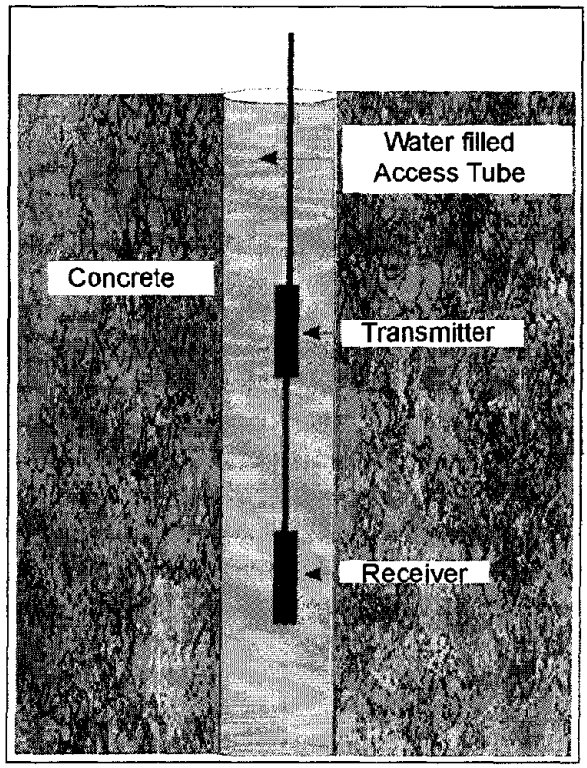

Figure 28. Single Hole Sonic Logging instrument.

The Ultraseismic method was developed by Mr. Frank Jalinoos as part of NCHRP 21-5 research program in response to the difficulty encountered in interpreting the Sonic Echo/Impulse Response and Bending wave methods from complex structures (such as a bridge) where many reflecting boundaries are present. This method is an adaptation of multi-channel seismic reflection method to bounded engineered structures.

Basic Concept: The Ultraseismic method uses multi-channel, three-component (vertical and two perpendicular horizontal receivers, i.e., triaxial receiver) recording of acoustic data followed by computer processing techniques adapted from seismic exploration methods. Seismogram records are typically collected by using impulse hammers (experimented with 0.090, 0.453, 1.36, and 5.4-kg hammers) as the source and accelerometers as receivers that are mounted on the surface or side of the accessible bridge substructure at intervals of 30 cm or less. The bridge substructure element is used as the medium for the transmission of the seismic energy. Four wave modes of longitudinal (compressional) and torsional (shear) body waves as well as flexural (bending) and Rayleigh surface waves can be recorded by this method. Seismic processing can greatly enhance data quality by identifying and clarifying reflection events that are from the foundation bottom and minimizing the effects of undesired wave reflections from the foundation top and attached beams. For concrete bridge elements, useful wave frequencies up to 4-5 kHz are commonly recorded. This method can be used in two modes—one called Ultraseismic Vertical Profiling (VP), presented below, and the Horizontal Profiling Method (HP).

Data Acquisition: The Vertical Profiling test geometry is presented in figure 29 and shows the accelerometers and impact point. The impact point can be located either at the top or the bottom of the receiver line. Vertical impacts to the substructure are comparatively rich in compressional wave energy, although more flexural/Rayleigh (surface) wave energy is generated. Horizontal impacts are rich in flexural wave energy when the impacts generate wavelengths that are longer than the thickness of the substructure element. Impacts that generate wavelengths shorter than the thickness will be rich in Rayleigh wave energy. The VP lines are useful in differentiating downgoing events from the upgoing events based on their characteristic time moveout, and accurately measure their velocity. A VP line is also used to tie reflection events from the bottom to a corresponding horizon in a HP section. For a medium with a bounded geometry, such as a bridge column, four types of stress waves are generated, including longitudinal, torsional, surface (Rayleigh), and flexural (bending) waves. In longitudinal vibration, each element of the column extends and contracts along the direction of wave motion that is along the column axis. In torsional vibration, each transverse section of the column remains in its own plane and rotates about its center. Finally, in flexural vibration, the axis of the column moves laterally in a direction perpendicular to the axis of the column. Each wave type can independently provide information about the depth of the foundation or the presence of significant flaws within the bridge substructure. However, practically, longitudinal (P-wave, compressional) and flexural (bending) waves are much easier to generate on bridge substructures than torsional. Consequently, compressional and flexural wave energy was generated by orienting impacts to substructures vertically and horizontally, respectively.

Advantages: The Ultraseismic (US) method uses well-proven processing techniques developed in the seismic reflection exploration method. Multiple-channel recording allows for differentiation of bottom echoes from other complex wave modes far more reliably than single-channel Sonic/Pulse Echo or Bending wave methods.

US can be used for assessing the integrity of bridge foundations as well as columns, like determining the post-earthquake damage of steel-cased concrete columns. For wall structures, this method can be used to obtain two-dimensional reflection images containing defect zones.

Limitations: The strength of the echo depends on the surrounding soil, and the signal-to-noise ratio decreases as the length-to-diameter ratio of columnar shape structures exceeds 20 to 30. Defects below a large defect may be indistinguishable and defects near the bottom of the pile may be difficult to detect.

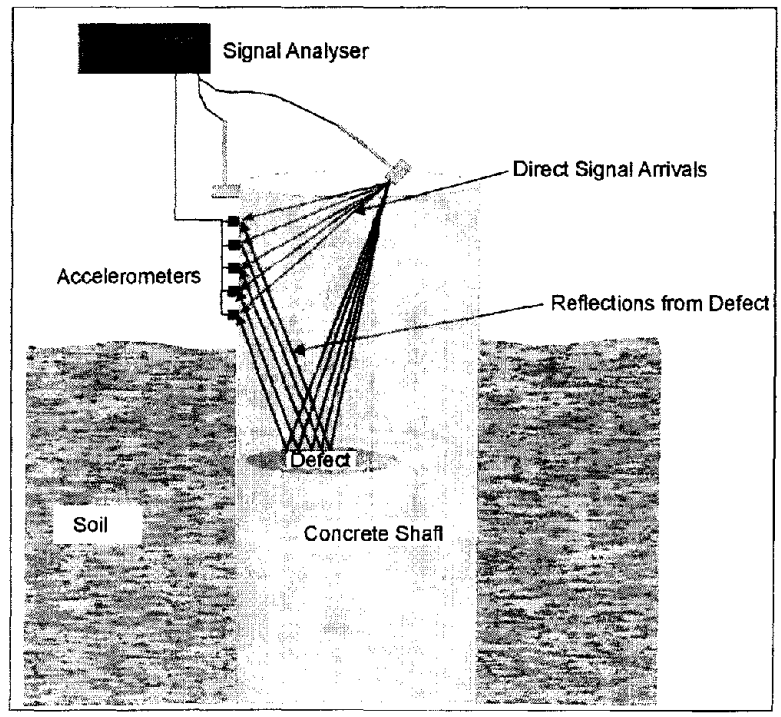

Figure 29. Ultraseismic test method showing the vertical profiling test geometry.

2.2.2 Integrity Testing of Other Bridge Substructure Elements

Concrete structures, such as bridge structures, are normally cast on site using locally available materials. Although the concrete material itself is usually prepared according to careful design and quality controlled by the manufacturer, inconsistencies in the final product may appear due to variations in the quality of the materials. The casting of large volumes of concrete in heavily reinforced and awkwardly configured structures is difficult and not always successful. The uniqueness of most large structures can introduce unpredictable factors that may increase the risk of unforeseen difficulties during pours and the intervals between pours. Innovative techniques intended to make the work more efficient can lead to quality and conformance problems of the finished product. Unfortunately, the outward appearance of the concrete surface may not reveal internal defects.

Quality control of the finished product may be carried out by visual inspection and by performance monitoring, e.g., measuring concrete strain under load or, in the long term, due to creep. The general behavior and appearance of the structure is thus checked. However, critical damage and deterioration to concrete structures are often less dependent on the general condition than on specific defects, particularly in the case of pre- and/or post-tensioned structures or those in a potentially aggressive environment.

For in-service structures, the construction plans and records may not be available. Also, environmental and service conditions may have caused changes in the integrity of the structural components. Concrete has a heterogeneous nature; it is susceptible to change in uniformity and properties, locally at the fresh stage, and, in the long term, due, for instance, to the effects of moisture movement.

Defects in concrete must also be treated from the point of view of engineering significance and not purely on type, size, and position. A nondestructive survey of a large concrete structure must, therefore, be made efficiently, using techniques with predictable behavior, reliability, and capability. The interpretation of the survey results must include an understanding of the significance of defects from an engineering perspective. This requires harmony between structural engineering expertise, preferably with historic knowledge of the structure in question, and inspection personnel with access to nondestructive technology with proven performance for the case in question. Qualitative surveys of concrete are relatively simple to carry out, but usually leave many questions unanswered. Quantitative surveys are possible with the techniques available today, although a key factor is pre-survey information. It helps to know what the problem might be and to then tailor the specific technique to locate the potential problem.

The condition of concrete structures should be tested to:

- Obtain information that can be used in the prediction of service life.
- Determine the ability of the structure to safely handle the design loads or anticipated loads.
- Determine conformance of the "as-built" structure with contract plans, specifications, and approved changes.

The service life of a structure may be affected over time by corrosion of embedded steel. The "as-built" condition of a structure may be different from the contract plans and specifications and approved changes for two reasons: on-site detail changes may not have been recorded, or workmanship-related problems may be present.

In the majority of cases, the more ambitious inspection programs, some of them involving NDT, are initiated by observations of deterioration at a late stage. It may also be necessary to establish parameters, which can be used in load-bearing capacity calculations or simply to determine the position of reinforcement prior to intrusive works.

Extensive cracking of concrete can lead to loss of reinforcement bond, as can settlement of the concrete at its plastic stage during casting. Voids can constitute weak zones and loss of anchorage capacity and, in some circumstances, can lead to serious corrosion of embedded steel.

One problem that has received much attention due to catastrophic failure of some major civil engineering structures is that of corrosion to pre- and/or post-tensioned reinforcing cables or bars. These are normally placed inside ducts, which are either injected with a cement grout or filled with some other corrosion-inhibiting material such as oil or grease. In the former case, there is no possibility of removing the cables for inspection. Voids inside cable ducts may occur due to unsuccessful grout injection, increasing the risk of corrosion to pre-stressed steel. Inspection of these cables requires location, usually behind one or more layers of reinforcing, detection of voids, and inspection of the physical condition of the cables

themselves. Table 2 summarizes the potential defect/damage types and problem cases frequently encountered.

Table 2. Nondestructive testing of concrete - point of interest/damage type.

Item/Object of test	Description
1	Cracking perpendicular to surface concrete
2	Cracking (internal) parallel with concrete surface
3	Deterioration of concrete with time
4	Damaged (weak) concrete layers
5	Elastic properties of concrete (E-modulus)
6	Elastic properties of concrete (G-modulus)
7	Thickness of concrete member or layer
8	Voids and inhomogeneities
9	Reinforcement location
10	Reinforcement diameter
11	Damage to reinforcement
12	Location of pre-stressed cable ducts
13	Detection of voids in pre-stressed cable ducts

In section 2.2.1, the techniques that are appropriate for evaluating the condition of concrete in new foundation elements were discussed. If the definition is expanded from concrete foundation elements to concrete structures in general, then other techniques can also be used. This section includes some of these other techniques.

Geophysical methods discussed in section 2.2.1 for integrity testing of concrete in foundations are listed below:

1. Crosshole Sonic Logging (CSL)/Crosshole Sonic Logging Tomography (CSLT).
2. Sonic Echo (SE) / Impulse Response (IR).
3. Gamma-gamma Density Logging (GDL).
4. Single Hole Sonic Logging (SSL).
5. Ultraseismic Profiling (US).

Methods that are used for concrete structures in general include the following:

1. Ultrasonic Pulse Velocity (UPV).
2. Impact Echo (IE).
3. Ground Penetrating Radar (GPR).
4. Spectral Analysis of Surface Waves (SASW) / Multichannel Analysis of Surface Waves (MASW).

In addition to the geophysical methods, there are several methods that use traditional NDT methods. These techniques are listed below. Some of these methods, although providing good results for thin concrete, may not be appropriate for concrete foundations where the method needs to penetrate much thicker concrete.

1. High Resolution Acoustic Mapping.
2. Neutron Computer Tomography.
3. Acoustic Emission (AE) Analysis.
4. High Energy Radiography.
5. Thermographic Imaging.
6. Laser Interferometry.
7. X-Rays.

Of the above methods, only Acoustic Emissions and High Energy Radiography are briefly discussed. These are presented merely as examples of the traditional NDT methods and can be used to illustrate the differences between the geophysics and other methods. Non-geophysical methods include the Rebound hammer, core analysis, and Penetration Resistance Probe. These techniques are not discussed in this document.

2.2.2.1 Ultrasonic Pulse Velocity (UPV)

This method is used for computing the ultrasonic pulse velocity of structural concrete. UPV can be used for assessing integrity of structural concrete elements of up to 7.5 m thick with two-sided access. UPV tests can also be performed on wood, masonry, and metal structures.

Basic Concept: This technique involves measuring the travel time of acoustic pulses through material with a known thickness. The frequencies of the transmitted signals vary from 50 to 300 kHz. Under certain conditions, it is possible to estimate the compressive strength using the ultrasonic pulse velocity method. The method requires that objects to be tested have two sides available for access. Voids, honeycomb, cracks, delaminations, and other damage to concrete can be located. This method is used to predict the strength of early stage concrete and as a relative indication of concrete quality.

Data Processing and Interpretation: An example survey is presented in which a concrete column having a cross- sectional area of 1 m was measured. A grid interval of 150 mm by 150 mm was drawn on the surface of the column giving the measurement locations. Figure 30 shows the column and the measuring points.

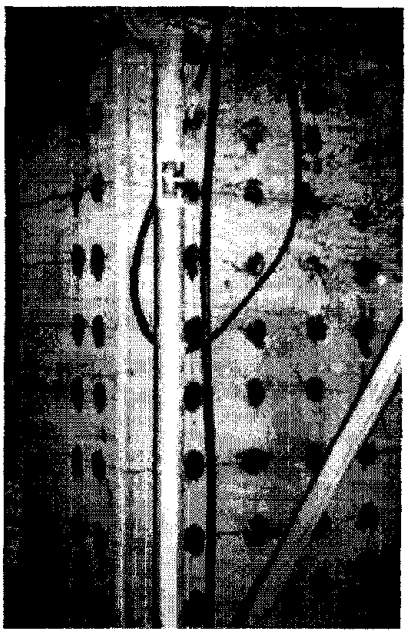

Figure 30. Measurement points for Ultrasonic Pulse Velocity method. (Rösch, 2003)

Core samples were taken for this particular survey to establish the relationship between pulse velocity and compressive strength of the concrete the results are presented in figure 31.

When applying ultrasonic pulse velocity (UPV) measurements to assess concrete quality in compound units, it is important to base the interpretation on more than just a few measurements. It is also helpful to present the results in a 3-D diagram as shown here.

Advantages: The method has provided reliable in-situ delineations of the extent and severity of cracks, areas of deterioration, and general assessments of the condition of concrete structures. The equipment can penetrate over 90 m of continuous concrete with the aid of amplifiers and is easily portable. Although most surveys are done in dry conditions, the transducers can be waterproofed for underwater surveys. Tomographic inversion techniques can be used for two and three-dimensional imaging of defects by scanning the tested element with many combination of source and receiver measurement locations.

Limitations: The method requires two-sided access of the tested element.

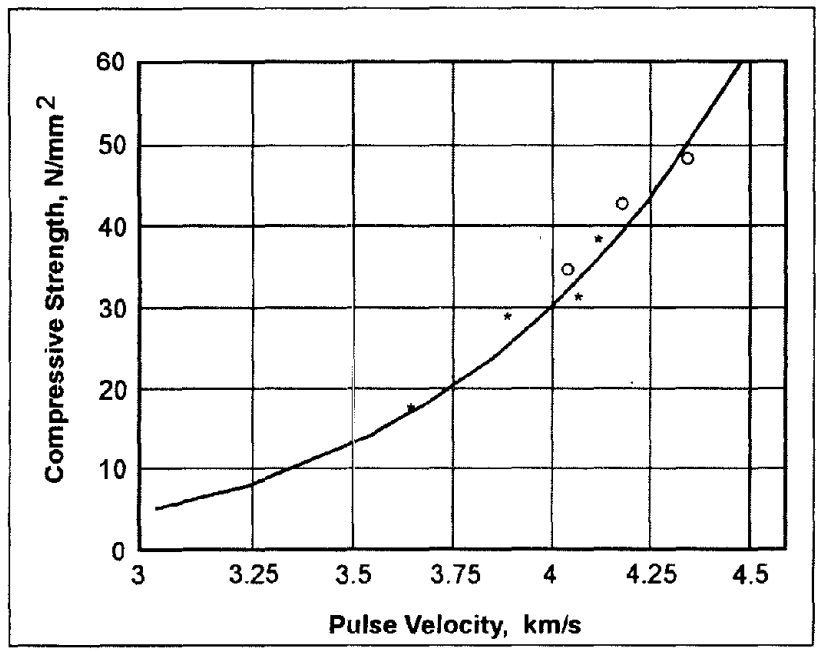

Figure 31. Relation between pulse velocity and compressive strength.

2.2.2.2 Impact Echo (IE)

Impact Echo (IE) is an acoustic nondestructive test method used for evaluating concrete, masonry, and timber structures. For bridge substructure investigations, IE tests are performed to assess the conditions of slabs, beams, columns, and retaining walls. IE is also used to assess the integrity of pavements, runways, tunnels, and dams. Voids, honeycomb, cracks, delaminations and debonding in plain and reinforced structures can be found with this method. Thickness measurements are done according to ASTM Standard C 1383-98a.

A team of researchers at the National Institute of Standards and Technology (formerly the National Bureau of Standards) initiated a study in 1983 that developed the rudimentary basis for this method. Subsequently, research carried out at Cornell University, under the direction of Dr. Mary Sansalone, has refined the theoretical basis of the method, extended its applications to a broad spectrum of problems and lead to the development of several field systems.

Basic Concept: The IE tests rely on reflection of compressional waves from the bottom of the structural member or from flaws. An instrumented hammer, or an impactor, is used as a source to generate compressional waves which are sensed by a receiver after being reflected several times. The receiver is typically placed about 5 to 7.5 cm from the impact point. The selection of a hammer versus a smaller impactor depends on the thickness of the member so that appropriate frequencies are generated.

Data Acquisition: In conventional IE tests (figure 32), the hammer or a short duration mechanical impactor is used to generate low-frequency compressional waves (up to about 80 kHz), which reflects back from the bottom of the tested member or from a discontinuity. A

receiver, placed next to the impact point, measures the response of the system. The wavelengths of these compressional waves are typically between 50mm and 2000mm which is longer than natural inhomogeneities in concrete (aggregate, air bubbles, micro-cracks, etc.). As a result they propagate through concrete almost as though it were a homogeneous elastic medium.

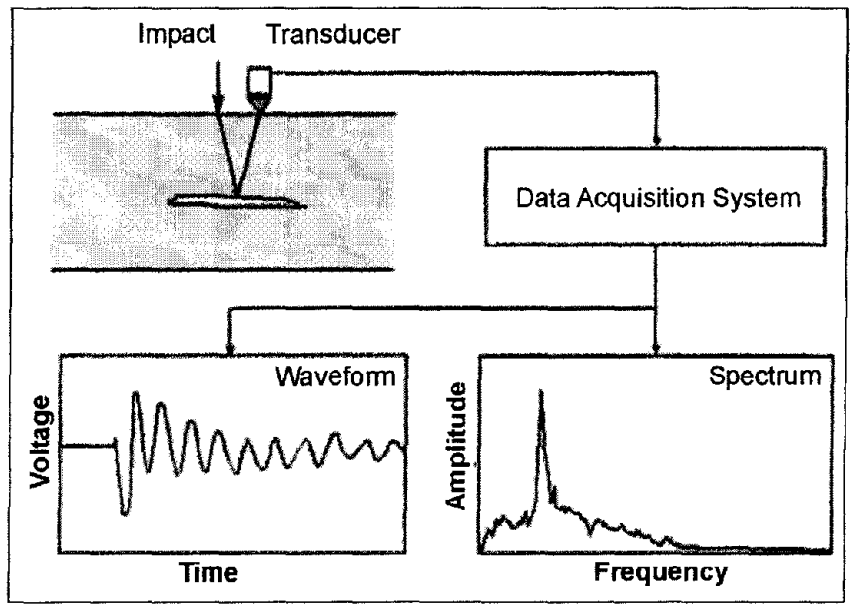

Figure 32. Schematic diagram of Impact Echo method.

Data Processing: Since the reflections are more easily identified in the frequency domain, the time traces are then transformed to the frequency domain for calculations of the transfer function. Pronounced peaks in the transfer function or frequency spectrum test records typically indicate reflections. These peaks correspond to thickness or flaw depth resonant frequencies.

Data Interpretation: The Frequency spectrum of the receiver is used to determine the depth of reflectors according to:

$$D = V_p / (2 \times f_r)$$

where D is the reflector depth, f_r is the large dominant frequency peak identified in the response, and V_p is the compressional wave velocity. If the velocity of the concrete is known or can be measured, then the depth of a reflector can be calculated from the reflection echo peak frequency. The wave speed V_p can be measured by observing the travel time of a compressional wave between two transducers held a fixed distance apart on the concrete surface or by performing a calibration test on a slab of known thickness and observing the dominant frequency.

The highest amplitude frequency peak is the main indicator of a reflector depth (thickness echo). The presence of additional echo peaks can also be significant, indicating the presence of possible defects or other interfaces in the concrete.

Advantages: Similar to Ground Penetrating Radar (GPR), described in section 2.2.2.3, only one-sided access is required for this test.

Limitations: For accurate thickness and flaw calculations, accurate measurement of compressional wave velocity is required.

2.2.2.3 Ground Penetrating Radar (GPR)

GPR uses electromagnetic wave to assess integrity and thickness of concrete, masonry and timber structures. For concrete structures, GPR can be used to map the rebar and tendons as well as locate voids underneath slabs.

Basic Concept: GPR is most commonly used for evaluating roadbed surfaces (concrete, asphalt) and requires one surface to be exposed. The GPR antenna is placed on this surface to image the internal structure or the other side of the structure. The GPR instrument consists of a recorder and a transmitting and receiving antenna. Different antennas provide different frequencies. Lower frequencies provide greater depth penetration but lower resolution. Figure 33 provides a drawing illustrating GPR reflections from the bottom of a concrete surface and from a defect within the concrete.

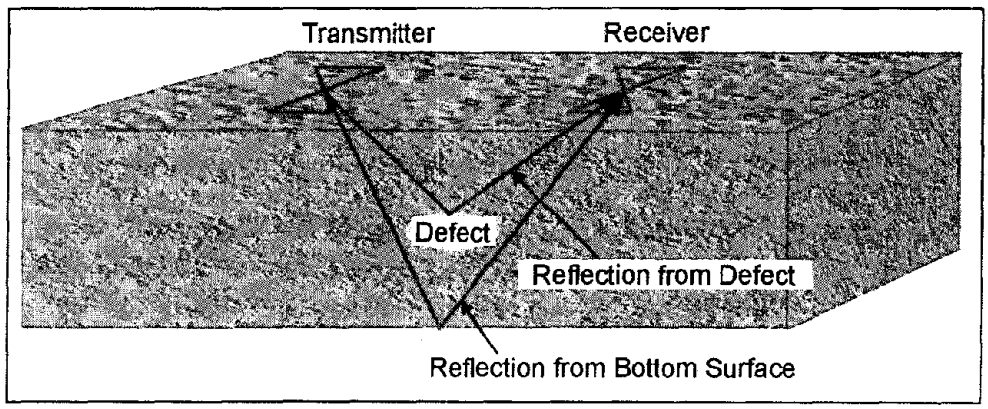

Figure 33. Ground Penetrating Radar system over a defect.

Data Acquisition: GPR surveys are conducted by moving an antenna over the surface of the object to be surveyed. The recorder stores the data and may also present a picture of the recorded data on a screen. As with all surface methods, source and receiver locations must be accurately surveyed.

Data Processing: It is possible to process the data much like the processing done on single channel reflection seismic data. However, this may not be necessary since the field records may be of sufficient quality that they satisfy the survey objectives without further processing.

Data Interpretation: GPR data are usually interpreted by visually inspecting the records and recognizing the events. Figure 34 shows GPR data from a post-tension tendon survey at two different times after the concrete pour. In this case, the penetration of the signals was to a depth of about 20 cm.

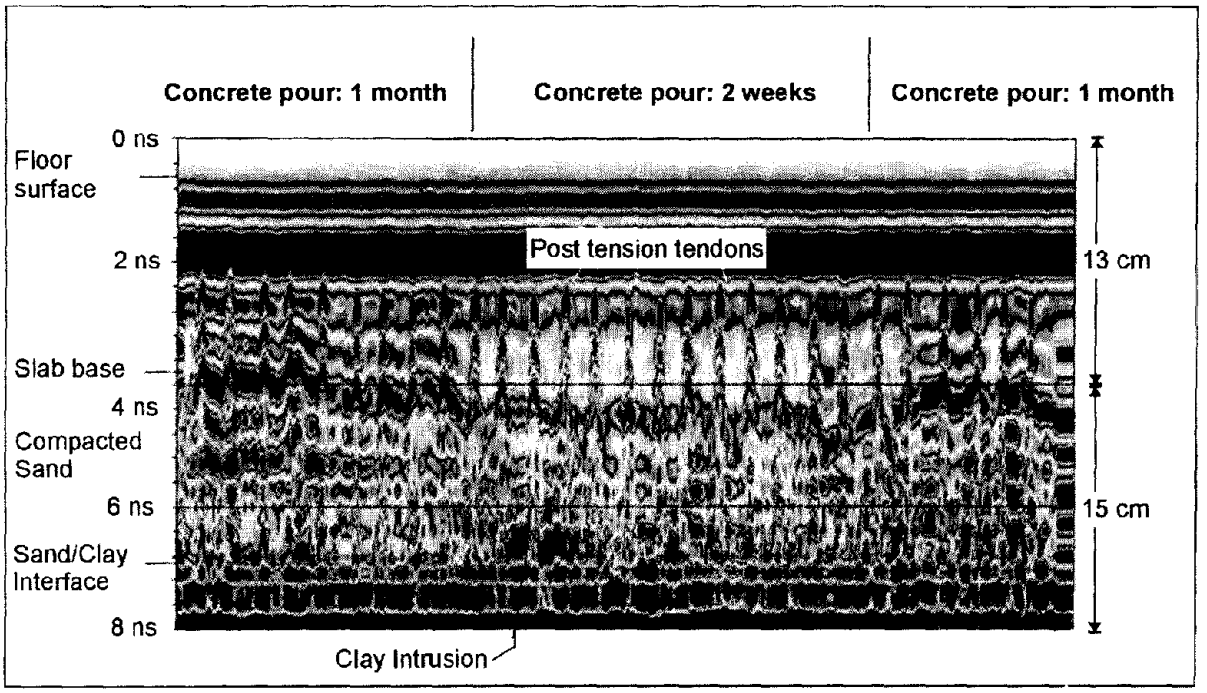

Figure 34. Plot of Ground Penetrating Radar data from a post-tension tendon survey.

Advantages: This is a quick and economical test method used for condition evaluation and high-resolution imaging inside or below structures. Only one-sided access is required for this method.

Limitations: The depth of penetration depends on the frequency of the GPR signal used and the resistivity (or its inverse, conductivity) of the material being investigated. Since the higher frequencies provide better resolution, the objective is to use a frequency as high as possible, consistent with the required depth of investigation.

Concrete may have resistivities that vary substantially depending on the amount of moisture it contains and the salt content of the moisture. Concrete that contains a significant amount of saline water will have much less penetration than dry concrete.

2.2.2.4 Spectral Analysis of Surface Waves (SASW)

SASW is a surface wave method used for determination of layer thickness, velocity (stiffness), and integrity of concrete, asphalt, timber and masonry structures.

Basic Concept: This method is based on the propagation of mechanically induced Rayleigh waves. By striking the concrete surface with a light hammer, a transient stress wave is created (surface or Rayleigh), which is registered by two transducers placed in line with the impact point on the ground surface at fixed separations. The transducers, which may be small accelerometers, register the passage of the waves. The receiver outputs are plots of the phase difference between the two transducers as a function of frequency. A profile of Rayleigh wave velocity versus wavelength, or so-called dispersion curve, is calculated from the phase plot. The ratio of Rayleigh wave velocity to shear wave velocity is approximately

0.9:1; thus, the shear wave velocity can be estimated. The shear stiffness (G) of the concrete can be calculated from the shear velocity if the material density is known, and a plot of ground stiffness as a function of depth from the surface can be obtained.

Rayleigh waves have velocities that depend on their wavelength, a phenomenon called dispersion. Waves having different wavelengths sample to different depths, with the longer wavelengths sampling to greater depths. Figure 35 illustrates the sampling depths and particle motion of two Rayleigh waves having different wavelengths.

This principle is used to measure the thickness of ground layers with different stiffness properties. It can also be used to locate and roughly delineate inhomogeneities such as voids.

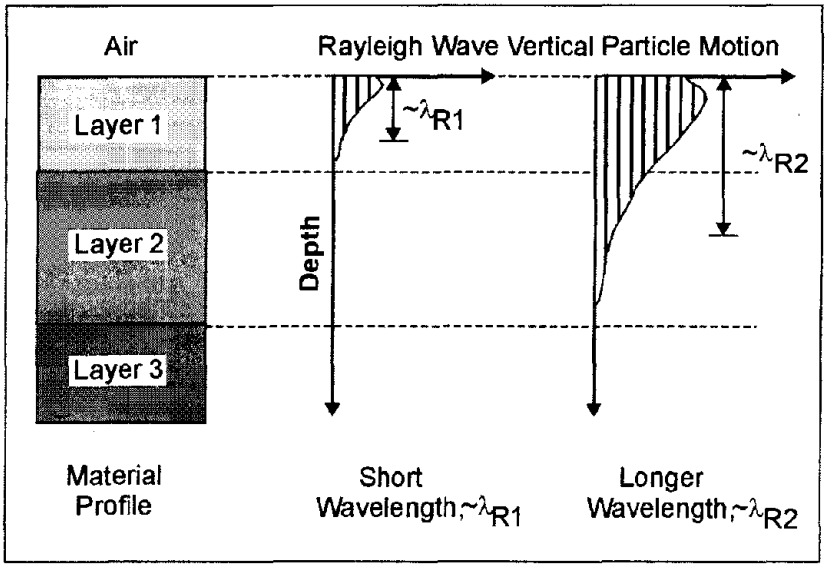

Figure 35. Schematic showing variation of Rayleigh wave partical motion with depth.

Data Acquisition: The surface wave dispersion curve can be measured using an active source and a linear array of receivers. The dispersion curve is then inverted to determine the corresponding shear wave velocity profile.

The two main methods used in surface wave exploration are SASW testing or array methods. The field setup is shown in figure 36. Either a transient or continuous point source is used to generate Rayleigh waves, which are monitored by in-line receivers. The data acquisition system calculates the phase difference between the receiver signals. These phase data are processed later into the dispersion curve, which is modeled analytically to determine a compatible shear wave velocity profile for the site. The data acquisition system is discussed in more detail below.

The source used depends on the desired profiling depth – heavier sources generate lower frequency waves that provide deeper interpretations. A combination of sources is commonly used to measure dispersion over a broad enough bandwidth to resolve both the near-surface and greater depth. Transient sources include sledgehammers (<15 m depth) and dropped weights. Continuous sources include the electromagnetic vibrator (< 40 m depth), eccentric

mass oscillator, heavy equipment such as a bulldozer (30 to 150-m depth), and the vibroseis truck (<120 m depth). A pair of vertical receivers monitors the seismic waves at the ground surface. For profile depths of approximately 100 m, 1 Hz geophones are required. Five or 10-Hz geophones can be used for surveys from 10 to 30 m deep. Theoretical, as well as practical, considerations, such as attenuation, necessitate the use of an expanding receiver spread. Data are recorded using sources on both sides of the geophone array, called the forward and reverse configuration (figure 36).

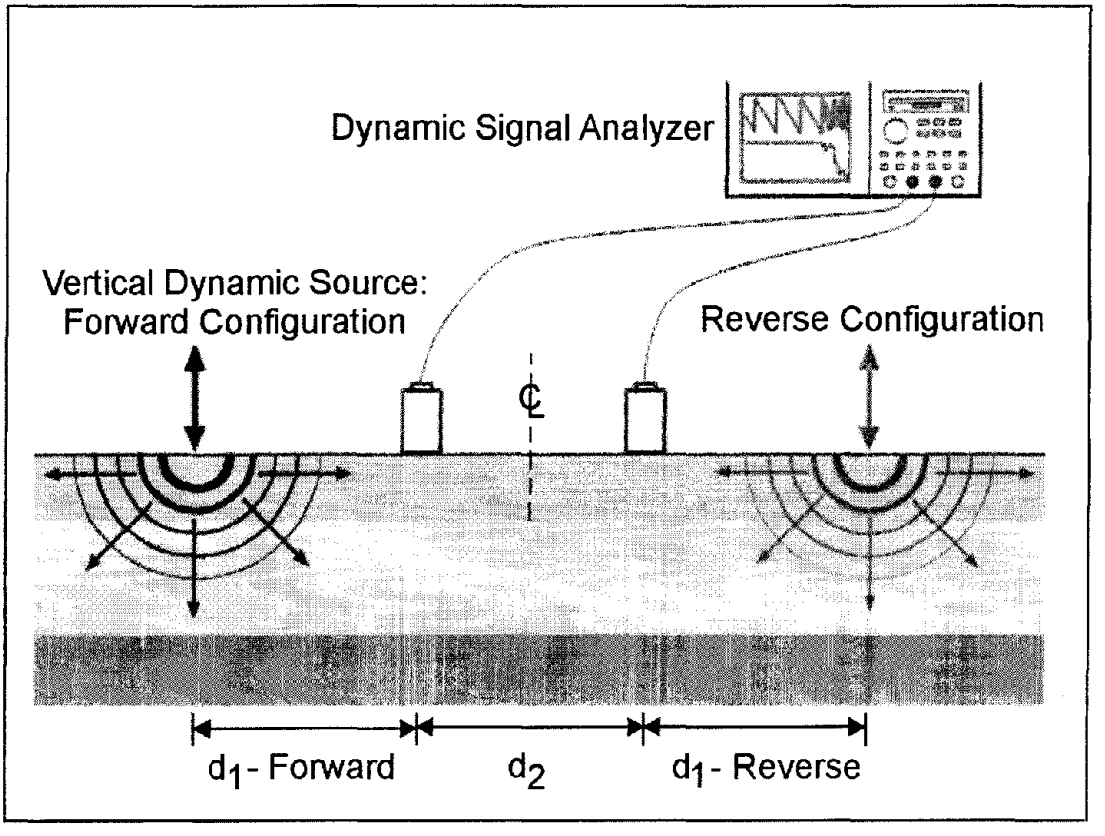

Figure 36. Basic configuration of Spectral Analysis Surface Waves measurements.

Data Processing: In the SASW method, a Fast Fourier Transform (FFT) analyzer or PC-based equivalent is used to calculate the phase data from the input time-voltage signals. Typically, only the cross power spectrum and coherence are recorded. Coherent signal averaging is used to improve the signal-to-noise ratio. The availability of either two- or four-channel analyzers has traditionally limited the number of receivers used. Because of the initial processing done by the analyzer in the field, the effectiveness of the survey can be assessed and modified if necessary. An initial estimate of the V_S profile can be made quickly.

Data Interpretation: Interpretation consists of modeling the surface wave dispersion to determine a layered V_S profile that is compatible. Interpretation can be done on a personal computer.

The acquisition and processing techniques of SASW methods do not separate motions from body wave, fundamental mode Rayleigh waves, and higher modes of Rayleigh waves. Most often, it is assumed that fundamental mode Rayleigh wave energy is dominant, and forward modeling is used to build a 1-D shear wave velocity (V_S) profile whose fundamental mode dispersion curve is a good fit to the data.

Advantages: This method provides for layer thickness profiles as well as stiffness. For slabs and pavements, velocity profiles including the surface layer, base and subgrade materials within 5% accuracy. Only one-sided access is required for this method.

Limitations: This method does not isolate fundamental mode Rayleigh waves in determining the velocity dispersion curves. The depth of penetration is determined by the longest wavelengths in the data and is site dependent. In modeling, there is a trade-off between resolution (layer thickness) and variance (change in V_S between layers). Data that are noisier must be smoothed and will have less resolution as a result. Whether a particular layer can be resolved depends on its depth and velocity contrast. The modeled V_S profile is insensitive to reasonable variations in density. V_P cannot be resolved from dispersion data, but has an effect on modeled V_S. The difference in V_P in saturated versus unsaturated conditions causes differences of 10% to 20% in surface wave phase velocities, which leads to differences in modeled V_S.

The depth of penetration is determined by the longest wavelengths that can be generated by the source, measured accurately in the field, and resolved in the modeling. Generally, heavier sources generate longer wavelengths, but site conditions are often the limiting factor. Available open space determines the offset from the source and aperture of the array, which determines the near-field wave filter criteria. Commonly, wavelengths are removed from the data that are longer than twice the distance from the source to the first receiver. Attenuation characteristics of the soil and overburden determine the signal level at the geophones. The cultural noise (traffic, rotating machinery, etc.) at a site may limit the signal-to-noise ratio at low frequencies. In SASW methods, the depth of resolution is usually one-half to one-third of the longest wavelength.

The field setup requires a distance between the source and most distant geophone of two to three times the resolution depth. However, forward modeling allows for subjective interpretation of the sensitivity of the dispersion curve to the layered V_S model. Resolution decreases with depth. A rule of thumb is that if a layer is to be resolved, then the layer thickness (resolution) should be at least approximately one-fifth of the layer depth.

For investigations of thin concrete structures, the presence of rebar will probably influence the data.

2.2.2.5 Acoustic Emissions (AE)

This method makes passive measurements of acoustic waves generated from cracks inside a concrete member that is undergoing stress.

Basic Concept: An acoustic emission (AE) is the stress wave that results from cracks and other dynamic sources within a material. These stress waves can be detected at the surface of

the structure, and can be analyzed to evaluate properties of the cracks that generated the event. Acoustic emissions (AE) have been shown to detect film cracking, gas evolution, and microcracking. It is also used to detect rebar corrosion. Field use of the AE method has been somewhat limited due to the highly attenuative nature of concrete.

The AE method measures the high-frequency acoustic energy that is emitted by an object that is under stress. Slow crack growth in ductile materials produces few events, whereas rapid crack growth in brittle materials produces a significant number of high amplitude events. Corrosion product buildup and subsequent microcracking of the concrete represents the latter phenomenon.

Data Acquisition: A typical AE monitoring system uses piezoelectric sensors acoustically coupled to the test object with a suitable acoustic coupling medium (grease or adhesive). A multi-channel transient sonic recorder with sampling rates of up to 10 MHz is added. The output of the sensors is amplified and filtered by pre-amplifiers and fed to the monitor via shielded coaxial cables. The monitor further filters and amplifies the AE signals, processes the data, and displays the results. Both results and raw data are typically recorded for archival purposes or for post-test analysis to determine location of the AE signal.

Data Processing and Interpretation: The evaluation of AE data has evolved from simply counting the acoustic emission events to the extraction of the signal parameters, like rise time or energy, to the use of several transducers to localize the event origin. Finally, geophysical algorithms are now being used to invert for crack types, orientation, and energy.

Advantages: Although the application of AE in concrete structures is relatively new, it is frequently applied in traditional NDT field for metals and compounds.

Limitations: Due to the complicated structure of the material, its application to concrete is not yet well established; although the progressive automation of the method will increase considerably its applicability and acceptance.

2.2.2.6 High Energy Radiography

The method involves producing high-energy X-ray beams to produce a high-resolution picture of the object that is imaged.

Basic Concept: Concrete coring and sawcutting can be risky, especially when the interior reinforcement structure is unknown. In many cases, the risks can be eliminated by using x-ray techniques prior to coring or sawcutting in order to locate rebar, post-tensioned cable, and conduit.

Data Acquisition: One particular instrument is called a Portable X-Ray Betatron (PXB) and produces X-Ray beams with an energy level of 7.5 Mev. With this energy level, the beams can penetrate thick concrete and reveal flaws inside the concrete structure. Figure 37 shows the instrument setup.

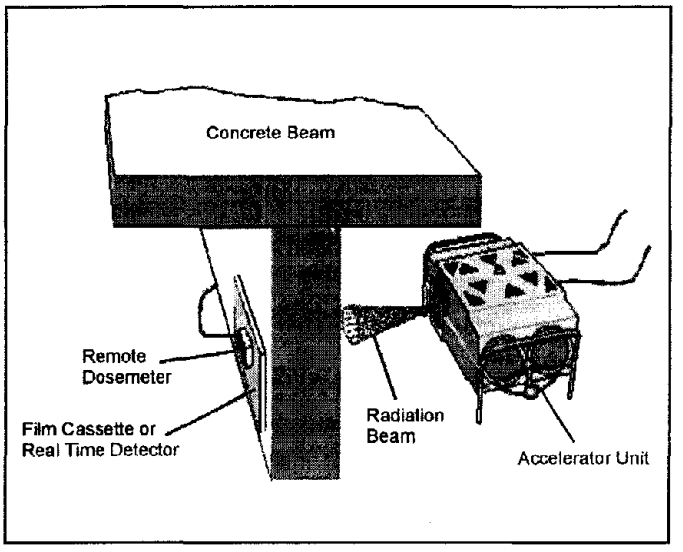

Figure 37. High Energy Radiography equipment and operation. (Force Technology)

Data Processing and Interpretation: Where the structure can be accessed on both sides, a 3.6 m x 4.3 m film is positioned on the opposite side of the structure to be examined to a depth up to 56 cm. X-ray computed tomography (CT) technique is now being used in concrete cylinders for a nondestructive visualizing of the aggregates used in the concrete. From a 3-D multi-aggregate image, individual particles can be extracted by this method.

Advantages: X-ray produces the highest quality NDT image of the interior structure of concrete.

Limitations: Special licensing is required by the State Radiological Health Department. For highly occupied sites such as hotels, hospitals, casinos, etc. where evacuating of two floors to perform x-ray inspections is impractical may require an alternate inspection method, such as GPR discussed in section 2.2.2.3. GPR is also the method of choice for slabs on grade, retaining walls, and other conditions where only one-side accessibility is available.

2.3 REBAR QUALITY AND BONDING TO CONCRETE WITHIN CONCRETE ELEMENTS

The steel reinforcement in concrete structures (rebar) is susceptible to corrosion when chloride ions enter into the concrete. If chlorides are present in sufficient quantity, they disrupt the passive film on the rebar resulting in corrosion. Oxygen content, moisture content, and temperature also affect the corrosion rate. Corroding rebar in concrete can weaken its structural strength, creating cracking, delamination, and spalling. Rebar corrosion may also affect bonding of the rebar to the surrounding concrete, caused by changes in the diameter of the rebar and from the friable iron oxide, which may accompany the corrosion.

A comprehensive search did not find any geophysical techniques that would indicate the amount of corrosion that had taken place and, hence, the quality of the rebar. However, there are numerous methods used to find if corrosion is currently active; these will be discussed in

this section. Presumably, if corrosion activity is monitored and found to be active for a significant period of time, then the "quality" of the rebar will become degraded.

One non-geophysical method was found for determining the degree of bonding of the rebar to the concrete. The test is done using an instrument called POWER, manufactured by Germann Instruments. POWER measures the pullout force of embedded anchors, either in situ or in the laboratory on specimens of rebar cast into concrete. Figures 38 a-b show the Power equipment.

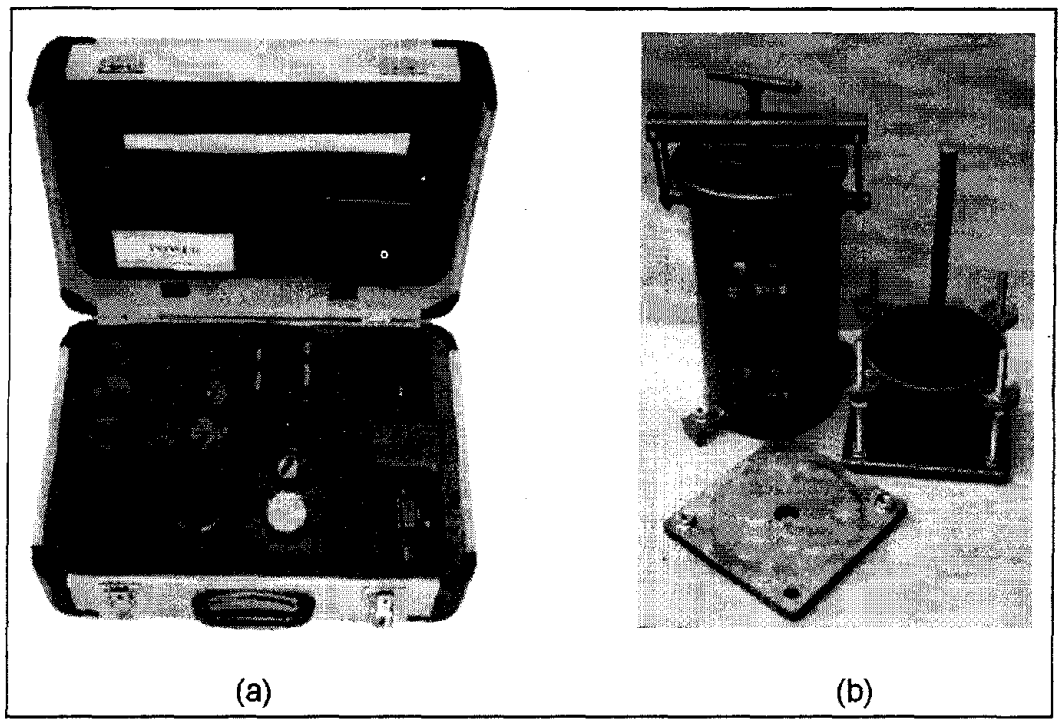

Figure 38. Power equipment to test rebar bonding: (a) Preparation Kit, and (b) Power equipment. (Germann Instruments)

The following section briefly describes the methods used to detect corroding rebar in concrete. These methods are classified as direct and indirect methods as listed below.

Direct Methods

These methods measure rebar corrosion directly from an exposed surface of a concrete structure, and include:

1. Half-cell Potential.
2. Linear Polarization Resistance.
3. Galvanostatic Pulse Technique.

4. Electrochemical Impedance Spectroscopy/Harmonic Analysis.

5. Acoustic Emissions.

Indirect Methods

These methods measure rebar corrsion using embedded probes in the concrete structure, and include:

1. Potentiodynamic Polarization Curves

2. Zero Voltage Ammetry/Zero Resistance Ammetry

3. Electrochemical Noise

Generally, there are two types of devices for measuring corrosion of steel in concrete. The first uses measurements on the surface of the concrete such as Rebar Potential Measurements (Half-cell Potential), and those that take measurements using embedded probes. Examples of methods using embedded probes include Electrochemical Impedance Spectroscopy (EIS) and Zero Resistance Ammetry.

The corrosion of steel in concrete is an electrochemical process that produces an electric current, similar to that of a battery. This electric current spreads out from the rebar into the surrounding concrete, and the resulting voltage is measurable at the surface of the concrete. A characteristic feature of rebar corrosion in concrete is the development of macrocells. These result from corroding areas of the rebar being adjacent to non-corroding areas. These sites may be macroscopically adjacent or they may be some distance apart. However, an electrically conductive path must exist between the sites. The metal rebar will conduct using electrons and ions through the electrolyte in the concrete. The corroding area is an anode and the non-corroding area is a cathode. These form a galvanic cell and can produce voltages between the anode and cathode of 0.5 volts or more, especially when chloride ions are present. The electrical resistance of the concrete and the anodic and cathodic reaction resistance determine the resulting current flow. The amount of current flow is directly proportional to the rate of loss of the steel mass.

Measurements of the rate of corrosion are usually made using sensors on the surface of the concrete. However, sensors are also available that can be attached to the rebar and can be used to measure the corrosion rate in the concrete environment using two electrodes on the sensor. Single corrosion rate readings have limited value, since the measurement is dependent on many factors, and rebar corrosion rates can change considerably with time. Such variations are the result of fluctuations in temperature, humidity, degree of aeration, microstructural changes in the concrete, and development of cracks. Much more value can be placed on corrosion readings taken over a period of time.

Listed below are three tables giving the steel corrosion rate in concrete (table 3), the relationship between corrosion rate and the remaining service life (table 4), and the likelihood of corrosion damage based on corrosion potential (table 5).

Table 3. Corrosion rates of steel in concrete.

Rate of Corrosion	Corrosion Current Density, (icorr) A/cm^2	Corrosion penetration, m/yr
High	10-100	100-1000
Medium	1-10	10-100
Low	0.1-1	1-10
Passive	<0.1	<1

Table 4. Proposed relationship between corrosion rate and remaining service life.

icorr (A/cm^2)	Severity of Damage
<0.5	No corrosion damage expected
0.5-2.7	Corrosion damage possible in 10 to 15 years
2.7-27	Corrosion damage expected in 2 to 10 years
>27	Corrosion damage expected in 2 years or less

Table 5. Likelihood of corrosion damage as a function of the corrosion potential.

Corrosion Potential (Volts vs. Cu/$CuSO_4$)	Probability of Corrosion
>-0.200	<10 %
-0.200 to -0.350	Uncertain
<-0.350	>90 %

2.3.1 Direct Measurement Methods

This section describes NDT methods used for measuring rebar corrosion directly from an exposed surface of a concrete structure.

2.3.1.1 Half-cell Potential

Basic Concept: This method is sometimes called the corrosion potential or rest potential method. The objective of this method is to measure the voltages that are present over rebar in concrete. The half-cell is a hollow tube containing a copper electrode and immersed in copper sulfate solution. The bottom of the tube is porous and is covered in a sponge material. The copper sulfate permeates this sponge that can then be placed on a concrete surface allowing an electrical potential (voltage) to be measured. The objective of the

method is to measure the voltage difference between the rebar and the concrete over the rebar. Large negative voltages (-350mV) indicate that corrosion may be taking place. Voltages smaller than about –200 mV generally mean corrosion is not taking place.

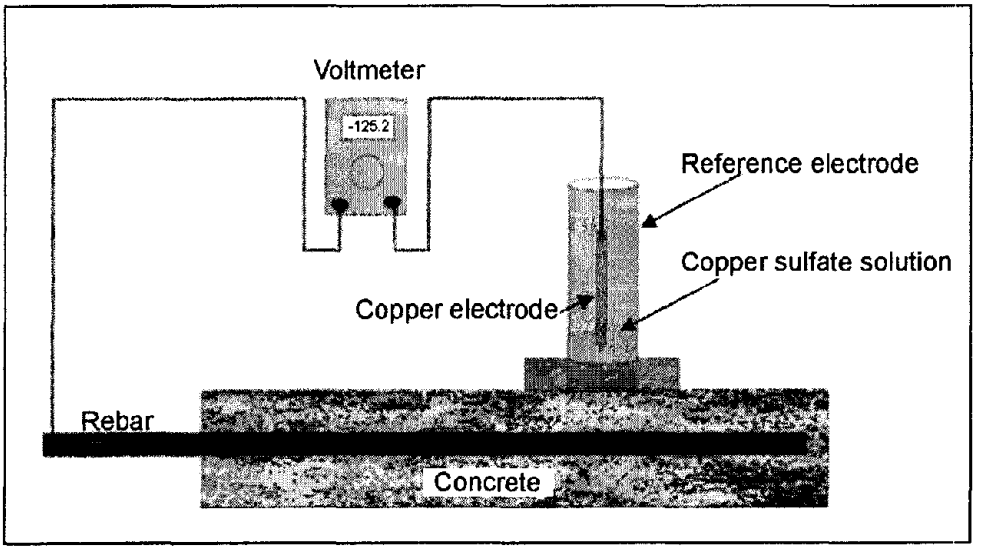

Figure 39. Half-cell measuring circuit for detecting rebar corrosion.

Figure 39 shows the circuit used and the concrete and rebar. The half-cell is the reference electrode.

Data Acquisition: Half-cell surveys simply require making an electrical connection to the rebar and then taking readings over the area of interest by pressing the sponge of the reference electrode against the concrete and observing the voltmeter reading. The readings are usually taken on some type of predetermined grid system. A device called a potential wheel is sometimes used. This provides a wheel for the tip of the half-cell and allows continuous readout of corrosion potentials, making the method quite rapid. To ensure that sufficient electrolyte is present at the surface, it is usual for all of the reading locations to be pre-wet using a fine spray of weak detergent mixture. A half-cell instrument is shown in figure 40.

Data Processing: Since the survey directly measures the quantity of interest (namely voltage), no data processing is required. The data may be plotted on a map and contoured for ease of interpretation and for presentation purposes.

Data Interpretation: Experience has shown that for potentials whose magnitude is greater than –350 mV, there is a 90% probability that corrosion is active. If the magnitude of the potential is less than –200 mV, then there is a 90% probability that corrosion is not active.

Figure 41 shows typical results from a half-cell survey. As can be seen, the voltages extend from about –50 mV to over –350 mV, suggesting that corrosion is taking place at these high negative voltage locations.

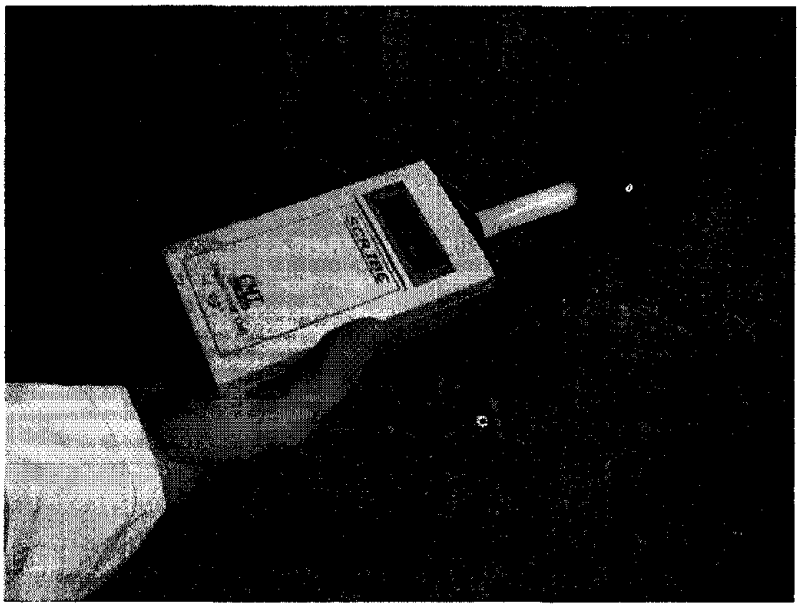

Figure 40. Half-cell instrument. (Hammond Concrete Testing)

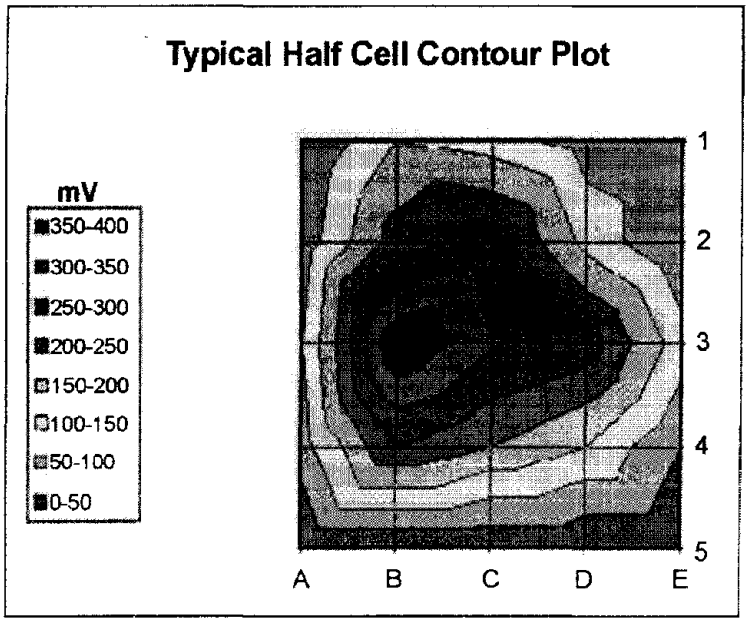

Figure 41. Example Half-cell Potential results. (Hammond Concrete Testing)

Limitations: Several factors must be kept in mind when conducting and interpreting half-cell measurements. It is important to consider the oxygen and chloride concentration and the resistivity of the concrete, all of which can influence the readings. Adding to these complications are the advances in concrete and repair technologies, such as dense material overlays, concrete sealers, corrosion inhibitors, chemical admixtures, and cathodic protection systems. It is important to understand and consider these complicating factors during a half-cell survey and to supplement the results with other nondestructive surveys. With most of the current equipment, an electrical connection has to be made with the rebar. However,

some recent developments involve the measurement of potential gradients using two reference electrodes, eliminating the need to make direct electrical contact with the rebar.

2.3.1.2 Linear Polarization Resistance (LPR)

Basic Concept: Linear Polarization Resistance (LPR) provides a relationship between the voltage (potential) and current density of a material. The polarization resistance of a material is defined as the slope of the potential-current density ($\Delta E/\Delta i$) curve at the free corrosion potential. Thus $R_p = \Delta E/\Delta i$ as ΔE tends to zero. There are a number of ways to carry out the LPR measurement. Perhaps the simplest is to use two nominally identical electrodes. A small potential difference (e.g., 20 mV) is applied to these electrodes, and the resulting current is measured. This current is proportional to the inverse of the polarization resistance and, hence, is directly proportional to the corrosion rate.

Data Acquisition: A more sophisticated approach is to use a potentiostat and a three-electrode arrangement. The test electrode is polarized by a small amount (10 to 20 mV) from its free corrosion potential, and the required current is measured. Again, this is directly proportional to the corrosion rate. Figure 42 shows a corrosion-monitoring sensor that can be installed at a site and measures the instantaneous corrosion rate of rebar in concrete using the LPR principles. This device, which is installed as a fixture at the site of interest, provides the instantaneous corrosion rate of the electrodes in the concrete environment. The probes are monitored frequently or continuously to track changes in the corrosion rate.

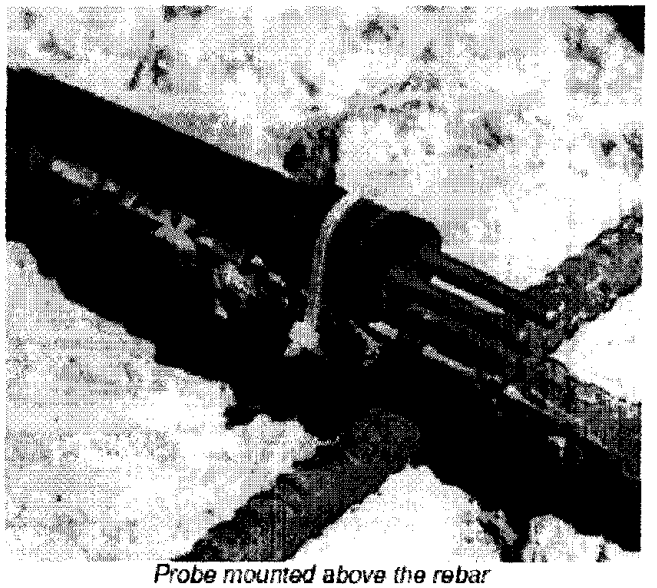

Figure 42. Linear Polarization Resistance probe. (Rohrback Cosasco Systems, Inc.)

The main challenge of applying well known corrosion rate measurement techniques such as the Linear Polarization Resistance (LPR) technique to actual rebars embedded in concrete has been confinement of the applied potential (or current) perturbation to a well-defined

rebar area to minimize measurement errors. The development of guard ring devices has addressed this issue.

The guard ring is maintained at the same potential as the counter electrode to prevent the current from the counter electrode from flowing beyond the confinement of the guard ring. The counter, reference, and guard ring electrodes can be conveniently located in a sensor placed directly above the rebar of interest (figure 43), necessitating only one electronic lead attachment to the rebar for corrosion rate measurements, as in the case of the simple potential measurements.

Guard ring devices will display a certain corrosion rate reading expressed as thickness loss per time unit (e.g., mm/year) after the polarization cycle is completed, but there are many simplifying assumptions in the derivation of this corrosion rate. Important limitations include the assumption of uniform corrosion over the rebar surface (this rarely applies to chloride- induced rebar corrosion), simplified models for the electrochemical reactions and charge transfer processes, assumed values for the Tafel constants, as well as possible inaccuracies in "IR" (voltage) drop resistance corrections.

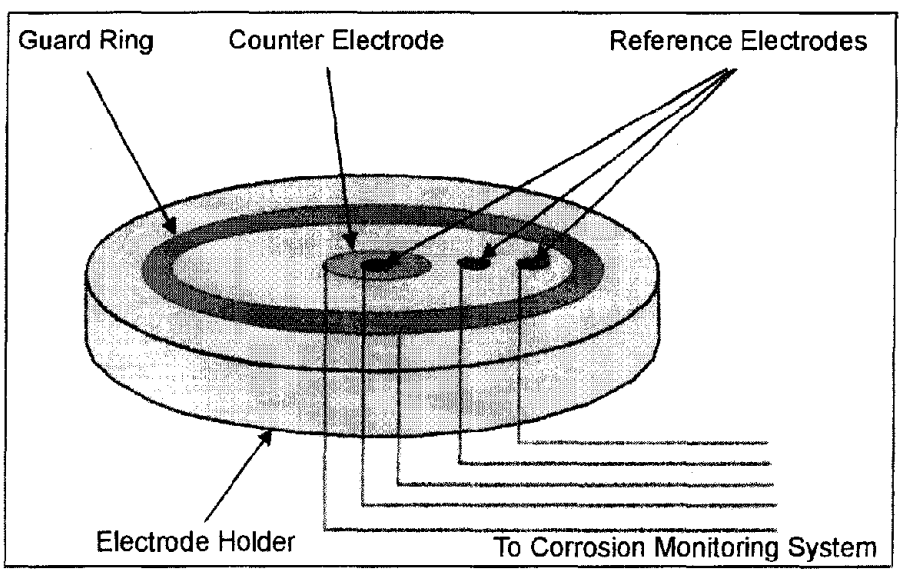

Figure 43. Guard ring setup for Linear Polarization Resistance measurements.

Data Interpretation: An example Tafel graph is shown as figure 44. This shows the voltage-current response of a corroding electrode, which tends to be linear over a small range of potential either side of the free corrosion potential. This is because both the anodic and cathodic currents are exponentially related to potential, and the difference between two such exponential curves is nearly linear over a small range of potential. Figure 44 shows the anodic and cathodic currents. A further fundamental source of inaccuracies is that no allowance is made for the effects of macrocell corrosion that are inherent to actual rebar grids. In addition, the applicability of these types of measurements to cracked concrete is presently not clear.

Limitations: For the steel in a concrete system, it is imperative that sufficient time is allowed for a current value to stabilize at a certain potential (or vice versa). For example, in the potentiostatic LPR technique, it will typically take several minutes for the current to reach a stable level after the polarizing voltage is applied. Shorter polarization could lead to significant measurement errors.

Unfortunately, the guard ring technology does not lend itself to quickly assessing large concrete surface areas. To reduce evaluation times to acceptable, practical levels, it may be advisable to map the corrosion potential values, followed by selective application of the guard ring device to critical areas.

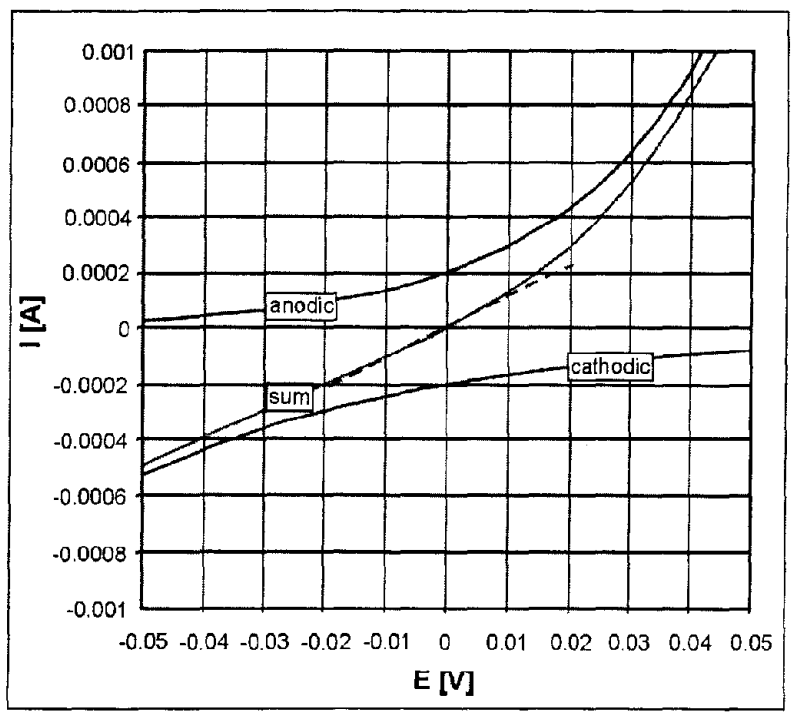

Figure 44. Example Tafel graph.

2.3.1.3 Galvanostatic Pulse Technique

Basic Concept: In this technique, an anodic current pulse is imposed onto the rebar for a short period of time, using a counter electrode positioned on the surface of the concrete. The resultant rebar potential change (E) is recorded by means of a reference electrode, also located on the concrete surface. Typical current pulse duration (t) and amplitude have been reported at 3s and 0.1 mA respectively.

Data Acquisition and Interpretation: The slope of the potential-vs-time curve (E/t) measured during the current pulse can be used to provide information on the rebar corrosion state. Passive rebar reportedly has a relatively high slope, whereas rebar undergoing localized

corrosion has a very small slope. In the latter case, the rebar potential only shifts by a few millivolts under the applied current pulse. It is also possible to use the potential data to obtain a measure of the concrete resistivity (for a given depth of cover). The technique is reportedly very rapid and may facilitate more unambiguous information on the rebar corrosion state than is possible by simple potential mapping. Figure 45 shows the GalvaPulse© instrument which is manufactured by Germann Instruments.

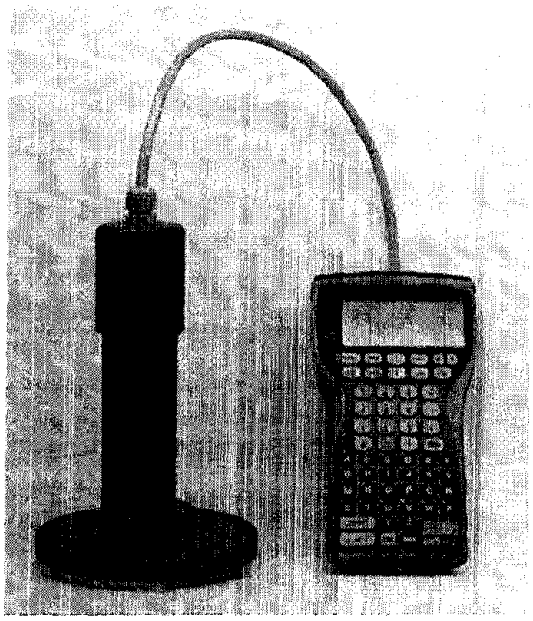

Figure 45. GalvaPulse© instrument. (Germann Instruments)

2.3.1.4 Electrochemical Noise

Basic Concept: Unlike other electrochemical techniques, noise measurements do not rely on any "artificial" signal imposed on the rebar probe elements. Rather, natural fluctuations in the corrosion potential and current are measured to characterize the severity and type of corrosive attack. For these measurements, three nominally identical rebar probe elements can be conveniently embedded in the concrete.

Data Acquisition: There may be some reluctance to using electrochemical noise for rebar corrosion measurements in the field due to a perceived "over sensitivity" of the equipment and fears of external signal interference. Although such concerns may be justified in certain cases, and this technology is relatively new to the rebar field, it has recently been used successfully in rebar corrosion measurements in the Vancouver harbor and in clarifier tanks of the paper and pulp industry in British Columbia. In these applications, the rebar noise probes were embedded in large (up to 4 meters long) concrete prisms. These prisms were partially submerged and exposed to seawater and to the effluent solution in the clarifiers.

Electrochemical noise data showed increased corrosion activity associated with the tidal cycle in the Vancouver harbor. In this case, the highest corrosion activity on the probe element, located in cracked concrete, occurred as the tide level approached that of the crack. Under these conditions, seawater is available to penetrate the concrete as corrosive

electrolyte, together with a high degree of aeration, a combination expected to stimulate electrochemical corrosion processes. Noise data from electrodes placed in cracked and uncracked concrete and exposed to pulp and paper effluent confirmed that, as expected, the presence of cracks facilitated more rapid diffusion of corrosive species to the rebar surface and led to higher electrochemical corrosion activity. To date, no significant interference or other problems have been encountered in the noise measurements of these two field exposure programs.

Data Processing and Interpretation: Apart from the interpretation of the "raw" noise data, it has become customary to conduct further statistical data processing, spectral analysis, and chaos theory analysis. Such data treatment serves to reduce the volume of data and to assist in distinguishing different forms of corrosion from one another.

Advantages: A distinct advantage of the electrochemical noise techniques is that the initiation and propagation of corrosion pits can be clearly identified. Distinct pit initiation transients, comprised of a sharp signal increase with passive film breakdown and a more gradual recovery of the signal to baseline levels as the passive film repairs itself, were observed for a carbon steel rebar probe exposed to chloride containing concrete pour solution. These distinct signatures of the initiation of corrosion pits were evident long before the attack was observable by visual means, indicating the "early warning" capabilities of this technology.

2.3.1.5 Acoustic Emissions

Basic Concept: Acoustic emissions (AE) monitoring of concrete has been used to detect rebar corrosion and has been shown to detect film cracking, gas evolution, and microcracking. Although attenuation of the AE signal in concrete has been a concern in the past, placement of the AE transducers on the reinforcing steel and using the steel as a sound propagation medium should allow the onset of steel corrosion to be detected. It is also possible to use the AE method to calculate the location where the steel corrosion is occurring. This appears to be a promising technique that can be used as a bridge inspection method to quantify the condition of steel-reinforced concrete where corrosion is occurring.

The AE method measures the high-frequency acoustic energy that is emitted by an object that is under stress. Slow crack growth in ductile materials produces few events, whereas rapid crack growth in brittle materials produces a significant number of high amplitude events. Corrosion product buildup and subsequent microcracking of the concrete represents the latter phenomenon.

Data Acquisition and Processing: A typical AE monitoring system uses piezoelectric sensors acoustically coupled to the test object with a suitable acoustic coupling medium, (grease or adhesive). The output of the sensors is amplified and filtered by pre-amplifiers and then fed to the monitor via shielded coaxial cables. The monitor further filters and amplifies the AE signals, processes the data, and displays the results. Both results and raw data are typically recorded for archival purposes or for post-test analysis, for instance, to determine location of the AE signal.

2.3.1.6 Magnetic Field Disturbance (MFD)

This technique can be used to detect flaws in steel, and, in particular, rebar.

Basic Concept: The method involves passing a strong magnetic field through a concrete structure to magnetize embedded steel. Sensors are used to measure the field produced by the metal in the structure. Anomalies are observed where flaws occur in the steel.

The flaws produce a distinctive anomaly depending on their size and the distance between the flaw and the sensor. The method can be used when the cables are encased in grout-filled ducts.

Advantages and Limitations: Laboratory experiments have shown that MFD can detect fractures and corrosion of reinforcing strands in air and concrete, as well as in filled plastic and metal ducts in concrete. Although there have been problems involving background structural disturbances, the MFD system has shown that it is one of the most feasible methods for detecting corrosion and failure of both strands and plain steel in pre-tensioned and post-tensioned structures.

2.3.2 Indirect Measurement Methods

This section describes NDT methods used for measuring rebar corrosion using embedded probes in the concrete structure.

2.3.2.1 Potentiodynamic Polarization Curves

Basic Concept: These well-known DC-type measurements can be performed on rebar steel in concrete using a three-electrode system. Typically, the working electrode is a small section of rebar, and stainless steel or graphite may be used for counter electrodes. Embedded reference electrodes need to be resistant to the highly alkaline concrete pour solution, such as manganese dioxide electrodes. External reference electrodes such as the $Cu/CuSO_4$ variety can also be used, but it is important to be aware of possible "IR" (voltage) drop errors.

The rebar potential and current density data can provide useful information such as:

1. Active or passive corrosion state of the rebar.
2. Corrosion rate estimates by the LPR or Tafel extrapolation techniques.
3. Risk of pit initiation from the pitting potential.
4. Tendency for pit repassivation from the size of the hysteresis loop in the reverse pitting scan.
5. Estimates of the Tafel constants for input into LPR analysis or for cathodic protection criteria.

6. Evaluation of the effectiveness of corrosion inhibitors and the effects of concrete composition variables.

7. Performance evaluation of alternative metallic rebar materials.

Limitations: A fundamental drawback of these measurements is that "artificial" corrosion damage and rebar surface changes can be induced at relatively high polarization levels. For steel in concrete, the potential scan rates used should be extremely low, making the tests time consuming. The data interpretation should be done by specialist personnel.

2.3.2.2 Electrochemical Impedance Spectroscopy (EIS) and Harmonic Analysis

Basic Concept: One method of obtaining corrosion rates from EIS data involves the use of equivalent circuit models. A number of different types of equivalent circuit models have been proposed for reinforcing steel in concrete. By accounting for the concrete "solution" resistance and the use of more sophisticated modeling, a more accurate corrosion rate value should theoretically be obtained compared with the more simplistic LPR analysis. However, EIS data generation and analysis generally require specialist electrochemical knowledge and can be rather lengthy, making it unsuitable for rapid evaluation of corrosion rates. To derive the corrosion rates, the Tafel constants also still have to be estimated or assumed.

Data Processing and Interpretation: A more recently evolving technique closely related to EIS measurements is harmonic analysis. One advantage of harmonic analysis is that mathematical data treatment facilitates direct computation of the Tafel constants and the corrosion rate. Since harmonic analysis is performed in a narrow frequency range, it can provide for practical and rapid rebar corrosion rate determination.

Limitations: A severe restriction of EIS and harmonic analysis is that, as in the LPR technique, the fundamental assumption of uniform rebar corrosion has to be made in the calculation of penetration rates. If localized corrosion damage is actually taking place, the data are, at best, of a qualitative nature, indicating the breakdown of passivity and the possibility of localized attack.

A number of initiatives have been launched aimed at applying EIS measurements directly to structural rebars, rather than small-scale embedded probes. These developments have involved guard ring concepts and modeling of signal transmission along the length of the rebar.

2.3.2.3 Zero Resistance Ammetry

Basic Concept: A Zero Resistance Ammeter (ZRA) is a current-to-voltage converter. This provides a voltage that is proportional to the current flowing between the input terminals while imposing a "zero" voltage drop to the external circuit. In the ZRA technique, a macrocell current is measured between two corrosion sensor elements.

Zero Resistance Ammetry is used to measure the galvanic coupling current between two dissimilar electrodes. An interesting application is when the coupling current between two nominally identical electrodes is measured. If both the electrodes were identical, then very

little coupling current would flow. However, in reality, the two electrodes will be slightly different, one being more anodic or cathodic than the other, and a small coupling current will exist. Perhaps the best way to visualize this is to think of a single electrode that supports distinct anodic and cathodic regions on its surface. Then imagine this electrode chopped in half, and the two parts connected via a ZRA. The ZRA will intercept some of the current flowing between the (now separated) anodic and cathodic regions.

Data Processing and Interpretation: The macro cell current measured between embedded rebar probes can serve as an indication of the severity of corrosion. This principle is used in the ASTM G102-92 corrosion test procedure, where the current flows between rebar embedded near the surface and rebar at greater depths of cover. A similar approach has been adopted in a rebar corrosion monitoring system, with currents being measured between strategically placed carbon steel rebar probe elements.

Interestingly, the concept of measuring a macro cell current as indicator of corrosion severity can also be applied to probe elements of identical materials and exposed to the same environment. It may be somewhat surprising that a significant current will flow between nominally identical probe elements, but this principle has been used in commercial corrosion monitoring and surveillance systems for many years. It can be argued that such measurements are mainly relevant to detecting the breakdown of passivity and the early stages of corrosion damage.

Limitations: If extensive corrosion damage is occurring on both the probe elements, the macro cell current measured will not accurately reflect the severity of attack.

2.3.3 General Discussion and Conclusions

A number of electrochemical rebar corrosion measurement techniques are available presently, each with certain advantages and limitations. The complexity and required specialist expertise in applying these techniques also varies significantly. To obtain maximum information about the corrosion state of rebar in a particular structure, a combination of measuring techniques is recommended. Furthermore, decisions should not be based on isolated corrosion readings.

Many measuring instruments will display a certain rate of corrosion penetration, but caution is required in interpreting these values, since they are often based on many simplifying (in some cases unrealistic) assumptions. Although the electrochemical corrosion measurements are usually qualitative, or at best semi quantitative, significant benefits can be derived from them.

2.4 BRIDGE FOUNDATION SCOUR

Scour has been linked to nearly 95% of all severely damaged and failed highway bridges constructed over waterways in the United States. There are two issues associated with such scour-induced damage to bridge pier footings. The first effect is the loss of foundation material, which exposes the footing and lowers its factor of safety with regard to sliding or lateral deformation. The greatest loss of sediment to scour occurs at high water velocities, such as during floods. Secondly, pier movement may occur because of material loss beside

and beneath the base of the footing, which produces undesired stresses in the bridge structure and ultimately results in structural collapse.

The various scour mechanisms are illustrated in figure 46. Total scour is comprised of long-term channel aggradation and degradation, contraction scour, and local scour. Local scour involves the removal of material from around underwater structures such as bridge piers, abutments, spurs and embankments; thus, it has the greatest impact on bridge integrity. Local scour results from acceleration of flow and subsequent development of vortices around obstructions. The action of both horseshoe and wake vortices is to displace material from the base of the obstruction. In this case, it is a cylindrical pier, which can result in undermining the structure.

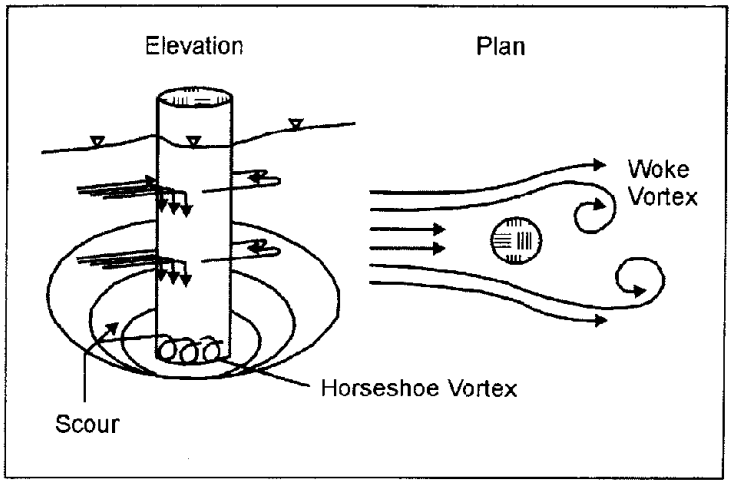

Figure 46. Scour mechanism. (Dowding, etal. 1994)

The most critical factors contributing to local scour are the velocity and depth of flow, both of which are significantly increased during heavy storms and floods. As the velocity and/or depth increase, the amount of scour increases. Other factors affecting bridge scour include the dimensions and orientation of piers, bed configuration and material size/gradation, and accumulation of ice and debris along the piers.

Current methods for measuring scour include visual underwater bridge inspection and various sonic devices such as sonar, sounding rods, and buried or driven rods, along with other buried devices. In these methods, measurements can be performed manually or can be integrated with real-time systems to monitor flood stage scour. Some of these devices are non-geophysical (i.e., sounding rods) and will not be discussed in this document.

Methods used to detect scour include Time Domain Reflectometry (TDR), Parallel Seismic, Ground Penetrating Radar (GPR), Continuous Seismic Profiling (CSP), and Fathometer. These methods are described below.

2.4.1 Time Domain Reflectrometry (TDR)

Basic Concept: In TDR, electrical pulses travel down the cable, and the reflected energy is recorded by the TDR instrument. Any impedance change, such as cable end or cable damage, will cause some energy to reflect back toward the TDR instrument where it is displayed. The method can also be used to detect bridge scour and monitor pier and abutment movement during flood events.

TDR is a relatively new method that appears to hold significant promise. However, it is not a typical geophysical method and is discussed here because of its apparent potential and importance in detecting scour.

TDR uses the same principle as radar. A pulse of energy is transmitted down a cable. When that pulse reaches the end of the cable, or a fault along the cable, part or all of the pulse energy is reflected back to the instrument. The TDR instrument measures the time it takes for the signal to travel down the cable, see the problem, and reflect back. The instrument then converts this time to distance and displays the information as a waveform and/or distance reading.

The TDR can display the information it receives in two ways. The first and more traditional method is to display the actual waveform or "signature" of the cable. The display, which is either a CRT or an LCD, will show the outgoing (transmitted) pulse generated by the TDR and any reflections that are caused by impedance discontinuities along the length of the cable. The second type of display is simply a numeric readout that supplies the distance indication in feet or meters to the first major reflection caused by an impedance change or discontinuity. Some instruments also display if the fault is an OPEN or SHORT indicating a HIGH IMPEDANCE change or a LOW IMPEDANCE change, respectively.

Any time two metallic conductors are placed close together, they form a cable impedance. A TDR instrument looks for a change in impedance, which can be caused by a variety of circumstances, including cable damage, water ingress, change in cable type, improper installation, and even manufacturing flaws.

The insulating material that keeps the conductors separated is called the cable dielectric. The impedance of the cable is determined by the spacing of the conductors from each other and the type of dielectric used.

Figure 47 shows two cable configurations that can be used with the TDR method. One configuration shows two cables close together, and the other shows one cable surrounded by an insulator, which is surrounded by a conductor. This cable is called a coaxial cable.

If the conductors are manufactured with exact spacing and the dielectric is exactly constant, then the cable impedance will be constant. If the conductors are unevenly spaced or the dielectric changes along the cable, then the impedance will also vary along the cable.

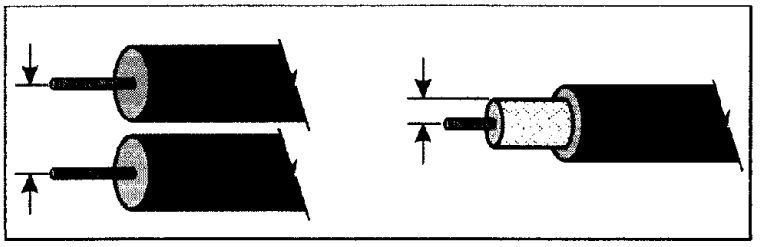

Figure 47. Cable configurations for use in the Time Domain Reflectometry method.

As mentioned above, any impedance change will cause some energy to reflect back toward the TDR instrument where it is displayed. How much the impedance changes will determine the amplitude of the reflection. Figure 48 shows the TDR signals from the ends of a cable as well as from a narrowing or pinching of the cable.

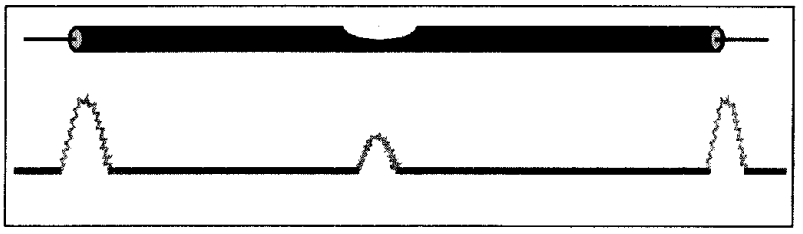

Figure 48. Time Domain Reflectometry signals from cable ends and a thinner section of the cable.

TDR instruments detect reflections and provide voltage readings that are proportional to transmission properties along the cable. These transmission properties change in proportion to the changes in the physical properties of the surrounding medium. TDR locates changes in transmission properties (capacitance) by pulsing known voltages along the cable and measuring the reflections resulting from these changes in transmission properties. Reflections are also observed from changes in the cross section of the TDR cable or from breaks in the cable. These reflections can be used to monitor rock joint shear, localized soil shear, structural cracking, and air-water interface and soil moisture.

Data Acquisition: For the TDR method, the survey design is essentially the design of the cable placement. Once the cable is in place, monitoring will begin, searching for TDR reflections that might indicate scour depth or pier movements in flood conditions.

Measurements of scour at bridges founded on shallow footings indicate maximum scour occurs around the upstream side of footings during floods. As scour progresses and soil deposits are eroded, footings may be exposed and eventually undermined, leading to intolerable pier movement. Optimal placement of TDR cables would, therefore, be through the footing section on the upstream side. Most importantly, the cable monitoring system must operate at high water flows when footing and pier displacement is most likely to occur as a result of scour.

Although bridge abutments may be less affected by scour, under certain circumstances they may need to be monitored for detrimental movements. Abutments and piers can be inspected

using the same system designed to measure very small structural movements (on the order of 2 mm) relative to their foundation materials. Detection of such small displacements should provide an early warning of progressive movements that may reduce the stability of the bridge.

Several cable installation schemes have been investigated for monitoring pier movement, but the most practical orientation of TDR cables is illustrated in figure 49.

A single cable is shown extending from an accessible location on or below the bridge deck, down along the pier, and into a hole drilled through the footing and foundation materials. The cable must be encased in grout through the hole to ensure direct transfer of soil-structure displacements. In addition, the cable should be enclosed by a protective pipe along the entire length of the pier to screen the cable from debris and weather. A more durable transmission line can be connected to the monitoring cable at the top of the pier and extended to the electronics.

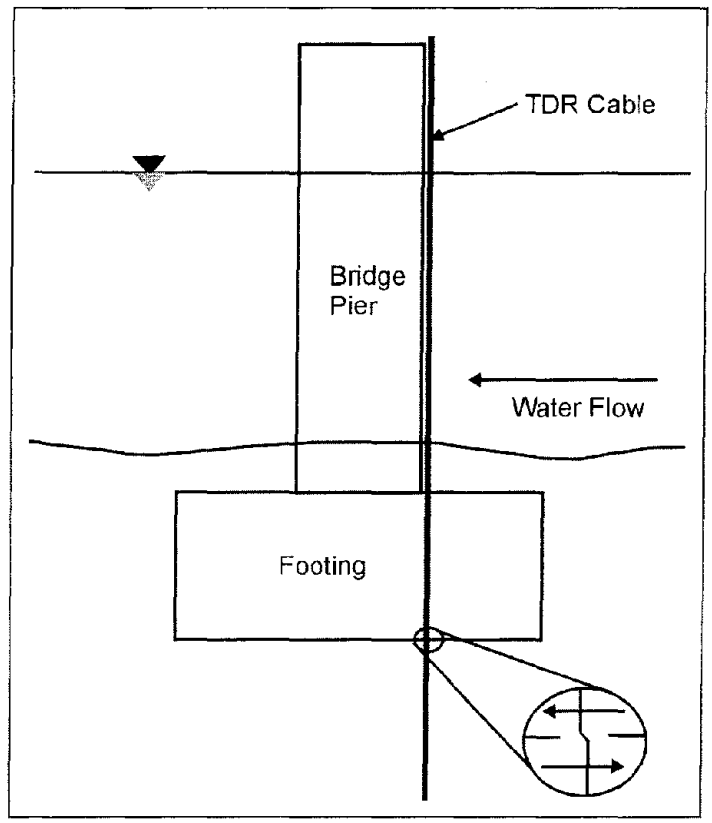

Figure 49. Cable installation for Time Domain Reflectrometry measurements at a pier. (Dowding, etal. 1995)

The number and arrangement of TDR cables installed on an individual bridge pier will depend on many factors, including the scour-critical classification, risk associated with structural collapse, and installation and monitoring costs, among others. It is expected that a TDR system can be installed on new bridges, since cables can be easily incorporated into

new construction. However, the complexity and cost of cable installation on existing bridges are significantly greater, and installation techniques to minimize these problems are currently being researched.

Data Interpretation: Pier footing movements can be detected from voltage reflections generated by local cable deformation. For instance, lateral translation or rotation of the footing would locally shear the cable-grout composite at the interface of the footing and foundation soils, as illustrated in figure 49. A minimum cable deformation of 2 mm produces a distinguishable voltage reflection in the TDR signal. Further footing displacement progressively shears the cable and produces increasingly larger voltage reflections at that point along the cable.

To accurately measure these structural displacements, the cable and grout must be sufficiently weak to deform under the applied loads. A special cable-grout system is currently being developed to measure localized soil deformation in earth structures. This development involves the design and production of an integrated cable and grout composite that exhibits low shear strength and compliance to deform uniformly with soft soils. In addition to embankments and excavations, this system can also be applied to monitor movements of footings or abutments founded on soft soils.

Advantages: A TDR measurement system provides several advantages for long-term monitoring of bridges. Previous deployment of TDR-based instrumentation suggests that it is robust enough to withstand emplacement during heavy construction and should perform during potentially damaging conditions such as floods and earthquakes. A miniaturized, low power, intelligent TDR pulser is currently being developed for remote monitoring. This signal pulsing and recording instrument is designed to reduce the size, complexity, and cost of current cable testing electronics. Remote access to multiplexed cables can be achieved with current electronics and existing telecommunication lines. These advantages would allow a survey of all bridge supports be performed remotely through one central unit, saving time and reducing costs.

Limitations: TDR cables are sometimes difficult to install, subject to damage, and accuracy of the TDR signal is reduced with increasing cable length.

2.4.2 Parallel Seismic (PS)

The Parallel Seismic (PS) method is a borehole test method primarily used to determine depths of foundations. However, it can also be used to measure the thickness of the scour zone when it has been filled with mud or soft sand after the flood surge has passed.

Parallel Seismic tests can be performed on concrete, wood, masonry, and steel foundations. Some portion of the structure that is connected to the foundation must be exposed for the hammer impacts. A borehole is also required. Typically, a 5- to 10-cm-diameter hole is drilled as close as possible to the foundation (within 150 cm preferred). The borehole should extend at least 3 to 4 m below the expected bottom of the foundation. In case of hydrophone use, the hole must be cased, capped at the bottom, and the casing and hole filled with water.

For geophone use, the hole must usually be cased and grouted to prevent the soil from caving in during testing.

Basic Concept: The PS method involves striking any part of the exposed structure that is connected to the foundation (or hitting the foundation itself, if accessible) and using a hydrophone or a three-component geophone to record compressional and/or shear waves traveling down the foundation. Analysis of the PS data is performed in the time domain. In PS tests, reliance is placed on identifying direct arrival times of compressional and shear waves at the receiver locations, as well as the wave amplitudes. The PS tests are performed at 30- to 60-cm vertical receiver intervals in a nearby borehole. Figure 50 shows the shaft and borehole configuration used for the test. Plotting the first arrival times as a function of depth and observing the depth where a change of slope occurs shows the depth to the bottom of the shaft and the scour depth. In addition, the foundation depth can be obtained by observing the depth where the signal amplitude of the first arrival energy is significantly reduced.

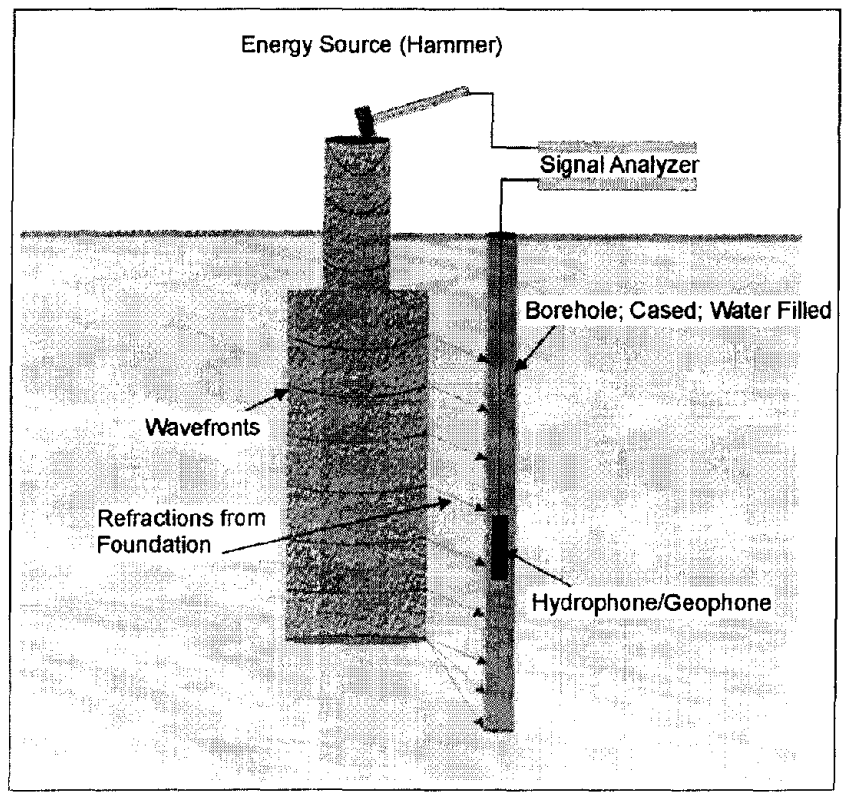

Figure 50. Parallel Seismic setup.

Data Acquisition: In a Parallel Seismic test, a hammer strikes the structure, and the response of the foundation is monitored by a hydrophone or a geophone receiver placed in the borehole. The hammer input and the receiver output are recorded by a signal analyzer and stored for further analysis. The receiver is first lowered to the bottom of the hole, and a measurement is taken. Then, the receiver is moved up 0.5 or 1 m, and the second measurement is made. This process is continued until the receiver has reached the top of the boring.

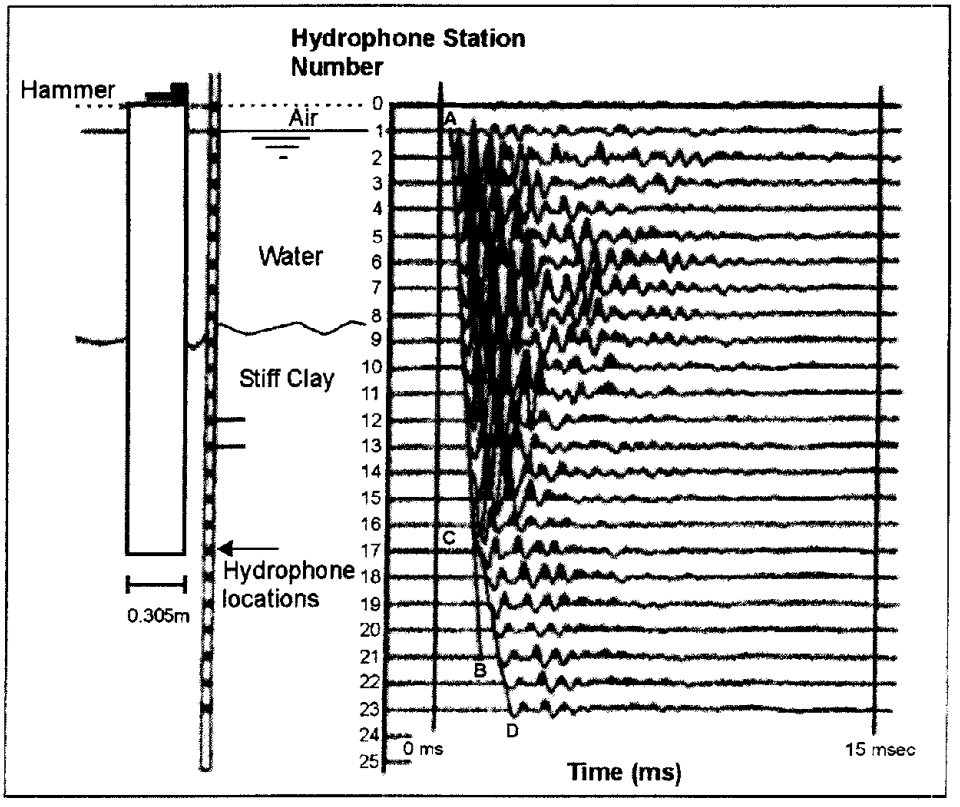

Figure 51. No scour case. Data not filtered. Note the uniform data amplitudes across the water-sediment interface. The linear refraction first-arrival pattern A-B changes to the hyperbolic first-break pattern C-D at C, which occurs at the base of the pier.

The following is an experimental example of the use of the parallel seismic method applied to a replica of a bridge with two cylindrical piers in a water-filled pond and shows the usefulness of the method along with some of the recorded data.

Two 60-cm-diameter, 5-m-long model piers were constructed. The depth of the pit before excavating the scour zone was 1.5 m. Adjacent to Pier 1 (60 cm away) a 10-cm-diameter, 8-m-deep hole was drilled and lined with PVC pipe. A refraction wave was generated in the pier by striking the top of the pier with a hammer. The refraction wave was recorded at 30-cm intervals in the PVC pipe. The pit was emptied, and a 1.2-m-deep scour zone was hand-dug around the pier and filled with soft mud created by liquefaction of the trench sides that slumped into the trench. This placed the bottom of the scour zone at a depth of 2.7 m. The refraction experiment was repeated, and the data were analyzed.

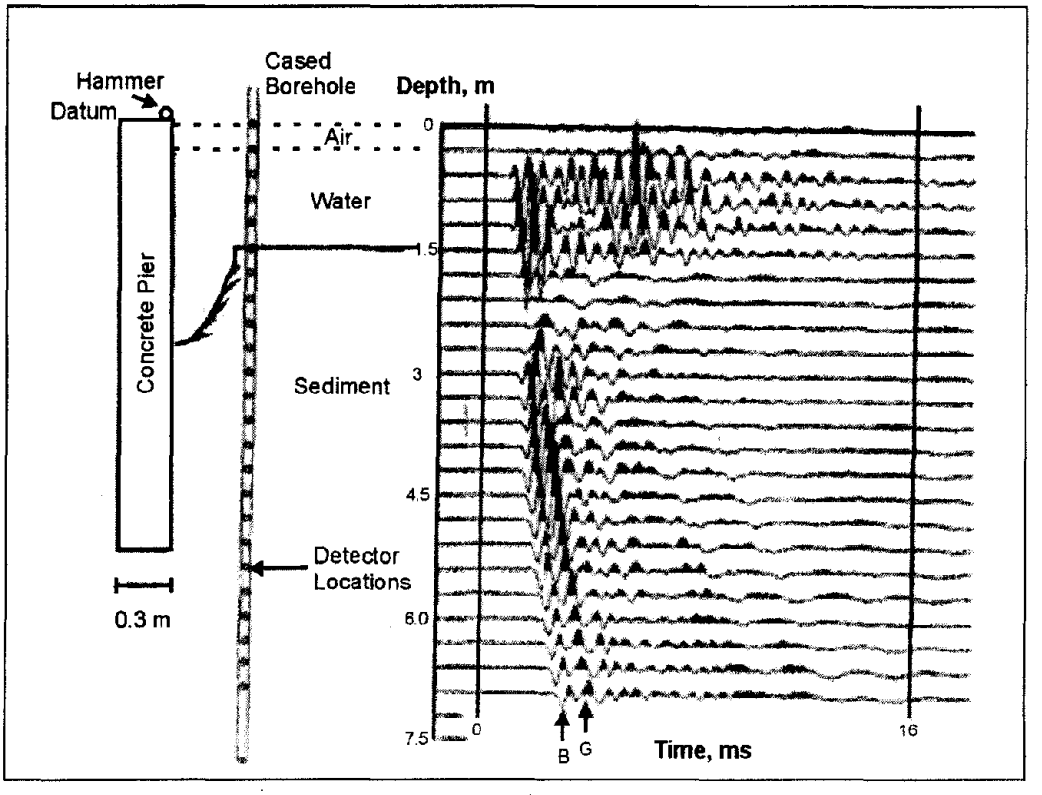

Figure 52. Scour case. Data not filtered. Note strong attenuation of data amplitudes where energy traverses the mud-filled scour zone.

Data Processing and Interpretation: Figure 51 shows the observed data from a Pier 1 test where the soft mud had been removed from the trench; thus, the water-soil interface is water over stiff competent clay. The seismic data show strong, continuous energy transmission across this interface, and the first breaks fall along the straight line A-B, corresponding to a refraction velocity of 4,730 m/s, which represents the P-wave velocity in the concrete pier. The acoustic characteristics of the mud are its strong energy attenuation as a function of frequency. The high frequencies are more strongly attenuated than the low frequencies, and much stronger than the attenuation characteristics of either water or competent soil.

Figure 52 shows the seismic data under the condition that the scour zone has been partially filled with soft mud that has slumped in from the sides of the trench. The anomalously low amplitude of the seismic data at recording depths 1.8 through 2.7 m is a consequence of the strong energy-attenuating nature of the mud compared to water above and competent soil below the mud-filled scour hole.

To take further advantage of this characteristic, the data were digitally filtered with a strong low-cut filter. The filtered data are shown in figure 53, the no-scour case, and figure 54, the scour case. The no-scour case, figure 53, shows uniform data amplitudes across the water-bottom interface. Figure 54, the scour case, shows virtually no high frequency in the mud-filled depth range 1.8 to 2.7 m.

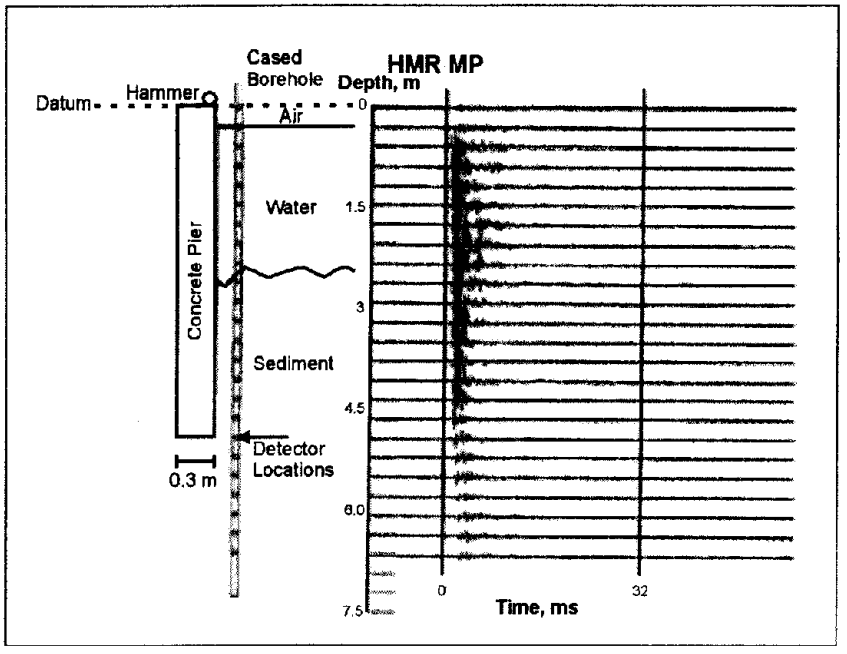

Figure 53. No scour case. Seismic data after digital filtering with a strong low-cut filter. Note the uniform amplitudes across the water-sediment interface.

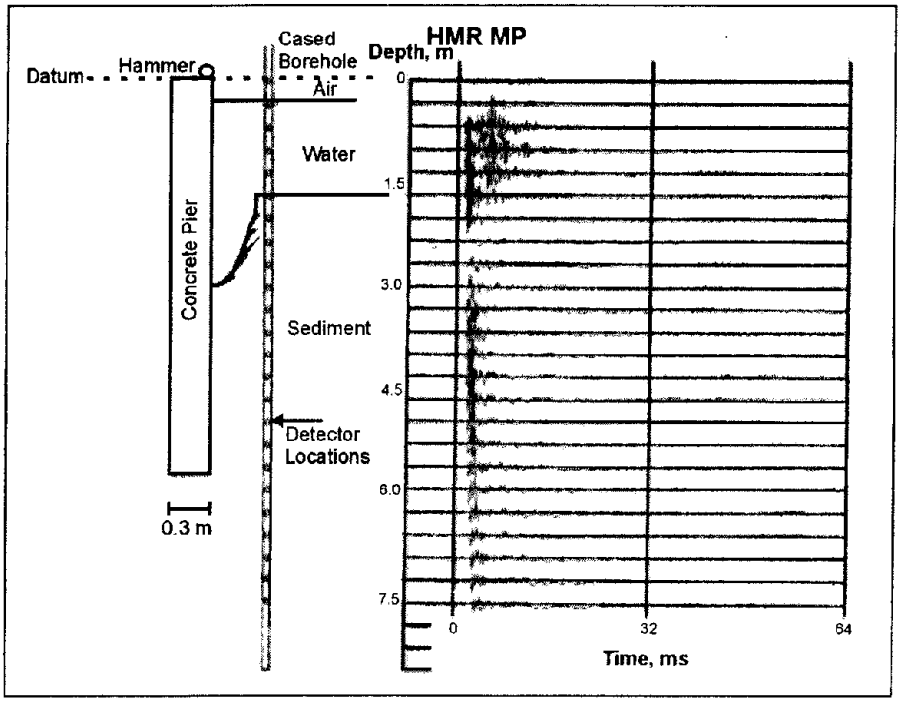

Figure 54. Scour case: Seismic data after digital filtering with a strong low-cut filter. Note the severe energy attenuation of data transmitted through the mud filled scour zone.

Advantages: The method can be used when the foundation tops are not available or when the piles are too long and slender (such as H piles or driven piles) to be tested by sonic echo techniques.

Limitations: Probably the biggest limitation is that a drill hole is needed close to the pier to measure the seismic travel times along the structure.

2.4.3 Ground-Penetrating Radar (GPR)

Ground-Penetrating Radar (GPR) transmits and records reflected electromagnetic energy. In bridge scour evaluations, the method can provide an essentially continuous image of the stream channel and the sub-bottom sediment, including the in-filled scour features.

Basic Concept: In the GPR method, a transmitter is used to send electromagnetic energy into the ground that then reflects from geologic interfaces where a dielectric contrast exists. The reflected energy is recorded by a receiver and produces a picture of the reflected waves. If the system is used over water, it will be placed on or immediately above the surface of the water. The transmitter produces short period (frequencies in megahertz range) pulsed electromagnetic signals at regular time or distance intervals as it towed across or above the surface of the water. Some of this pulsed electromagnetic (EM) energy is reflected from the water bottom and other prominent dielectric interfaces (facies contacts) and returned to the receiver. The arrival time and magnitude of the reflected energy are recorded at the surface by the receiver antenna. Traces from adjacent source locations are generally plotted side-by-side to form an essentially continuous time-depth profile of the stream bottom and shallow sub-strata (including in-filled scour features). Estimated EM velocities can be used to transform the time-depth profile into a depth profile. Velocities are a function of suspended sediment load and can vary appreciably. Figure 111 shows the GPR transmitter and receiver along with the transmitted and reflected waves.

GPR can be used with different antenna providing different frequencies, varying between 25 and 1500 MHz. A lower frequency antenna provides greater penetration depths but lower resolution. A higher frequency antenna provides less depth penetration but has better resolution. A GPR controller/data recorder and antenna are illustrated section 6.1.1.1.

Data Acquisition: In this application, the GPR system will have to be traversed over the water surface. Typically, a GPR system is placed in a small rubber boat that is towed with a motorized boat. The data recording equipment is placed in the towboat, and a GPS antenna could be attached to the rubber boat, providing its position. Care will be required close to the piers in case of debris, which may be caught around the pier along with the stronger current flow that may occur around the pier.

Unprocessed GPR data collected close to a pier is illustrated in figure 55.

Figure 56 shows the same data processed using digital filtering and migration.

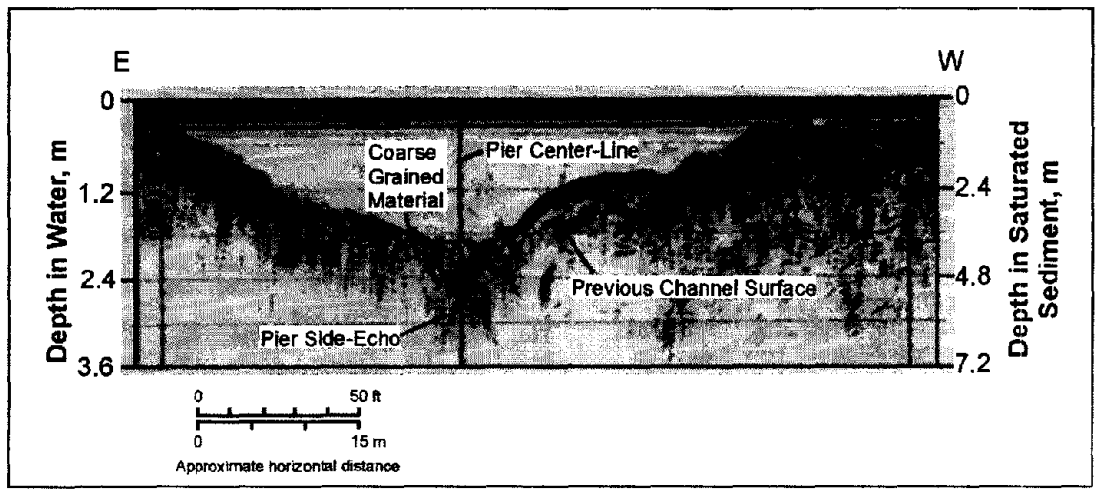

Figure 55. Unprocessed 300 MHz Ground Penetrating Radar data collected 2 feet upstream from a pier. (Placzek, et al. 1995, USGS Report 95-4009)

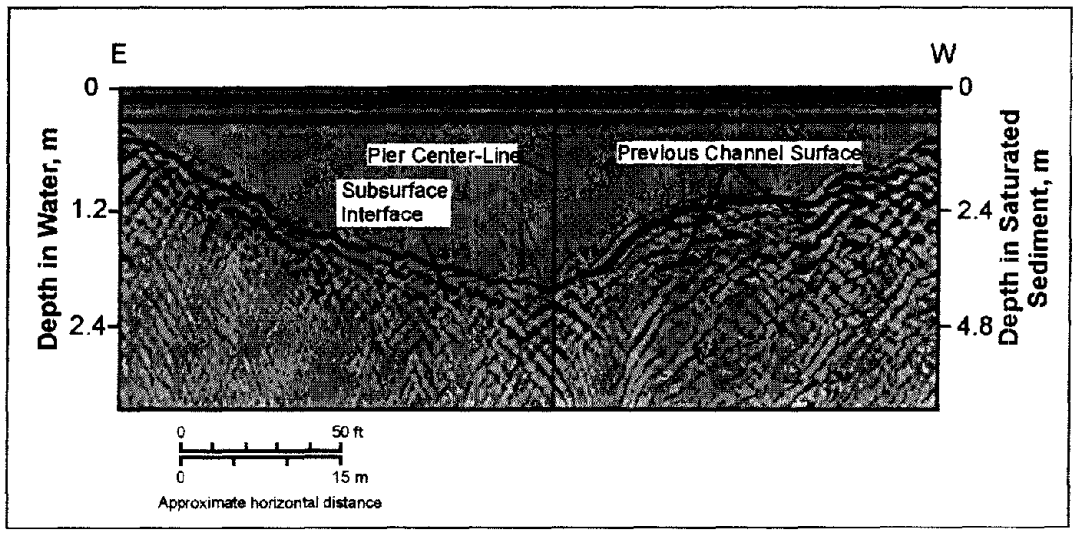

Figure 56. Digitally filtered and migrated 300 MHz Ground Penetrating Radar data. (Placzek, et al. 1995, USGS Report 95-4009)

Another example of GPR data is shown below in figure 57. In these data, a scour hole can be seen close to the upstream edge of the pier. On the downstream side, a pile of fill is seen.

Data Processing: GPR data can be viewed without any processing. However, some processing is often desirable. The common processing steps used are:

1. Distance normalization
2. Horizontal scaling (stacking)
3. Vertical frequency filtering

4. Horizontal filtering

5. Velocity corrections

6. Migration

7. Gain

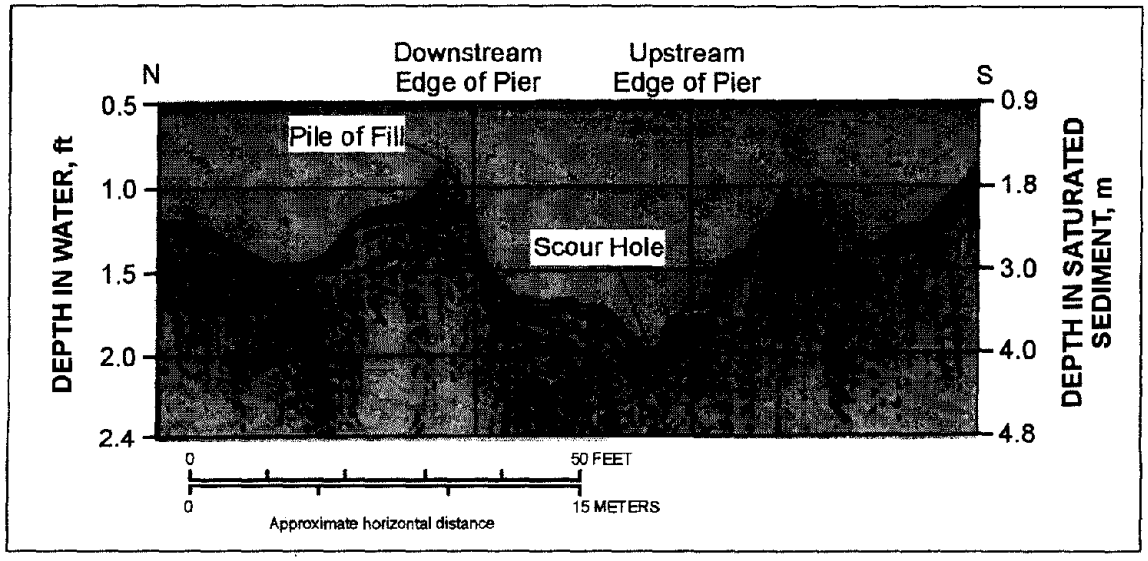

Figure 57. Unpositioned 300 MHz Ground Penetrating Radar data collected four feet from a central pier. (Placzek, et al. 1995, USGS Report 95-4009)

The above processing steps usually increase the interpretability of the GPR profiles by removing unwanted random noise and enhancing the amplitude events of interest. Figure 58 shows the changes in a GPR profile as these processing steps are applied.

Advantages: The main advantages of the GPR profiling tool are as follows:

1. The GPR antennae are non-invasive and can be moved rapidly across (or above) the surface of a stream at the discretion of the operator. The GPR tool does not need to be physically coupled to the water surface and can be operated remotely, ensuring that neither the operator nor equipment need be endangered by floodwaters. Profiles can be extended across emerged sand bars or onto the shore.

2. The tool can provide an accurate depth-structure model of the water bottom and sub-bottom sediments (to depths on the order of 9 m). Post acquisition processing (migration) can be applied.

3. Lithologic/facies units with thickness on the order of 0.1 m can be imaged with intermediate-frequency units (200 MHz).

Limitations: The main limitations of the GPR profiling tool are as follows:

1. The equipment is relatively expensive (hardware and software).

2. Data may be contaminated by noise (multiple reflections and echoes from pier footings).

3. Post-acquisition processing (migration) may be required in areas where significant structural relief is present.

4. GPR is not normally effective when water depths exceed 9 m.

5. GPR cannot be used in saline waters.

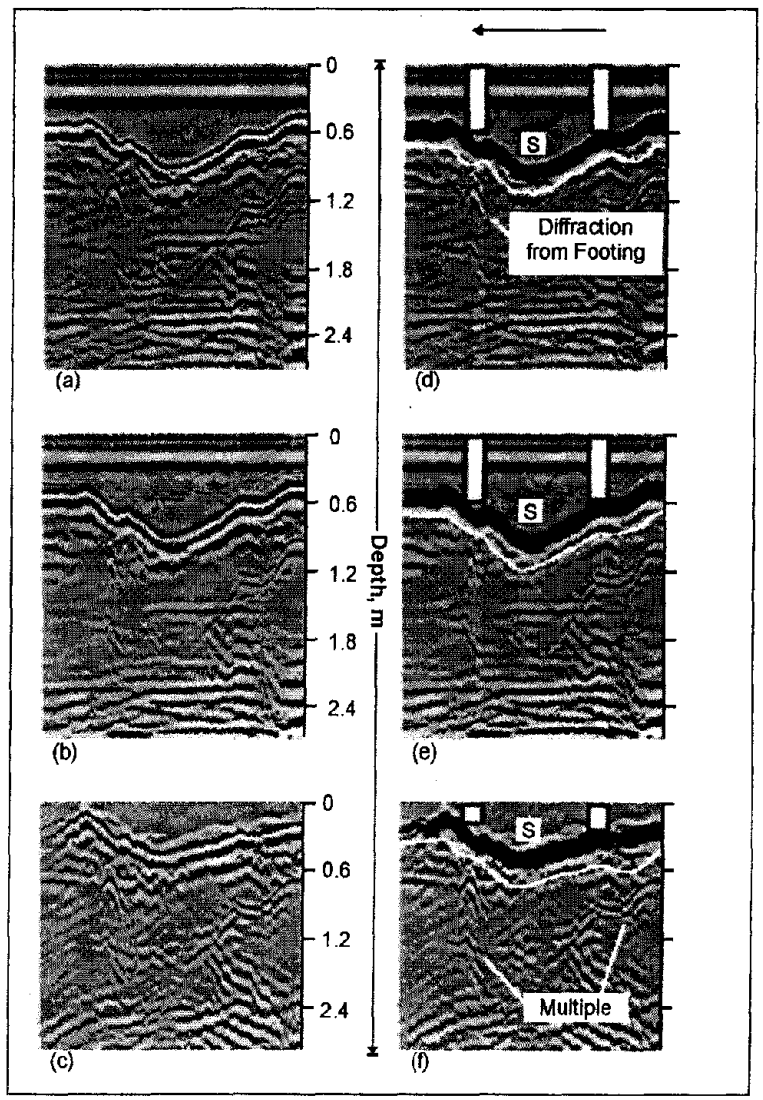

Figure 58. Ground Penetrating Radar data processed and interpreted to different stages: a) stacked, b) migrated, c) velocity corrected and interpreted. Interpreted sections d) stacked, e) migrated, f) velocity corrected. Grey and white lines identify water bottom and in-filled scour, respectively. (Webb, et al. 2000)

2.4.4 Continuous Seismic Reflection Profiling

Continuous seismic-reflection profiling (CSP), also known as Subbottom Profiling, transmits seismic energy from a transducer located just beneath the water surface. In bridge scour evaluations, the method can provide an essentially continuous image of the stream channel and the sub-bottom sediment, including the in-filled scour features.

Basic Concept: In the CSP method, a transducer element is used to generate seismic energy that passes through the water column and into the subbottom. Where a change in acoustic impedance occurs, such as at the water/bottom interface, part of the seismic energy is reflected back to the water surface. The remainder of the seismic energy is transmitted further into the material. The amount of energy that is reflected by an interface is determined by the reflection coefficient of that interface, which is dependent upon the acoustic impedance of the material above and below the interface. Acoustic impedance is defined as the product of the density of a material and the velocity of sound through the material.

Figure 59 shows the acoustic waves and their travel paths for two geophones. An acoustic impedance contrast exists between layers 1 (water) and 2 (bedrock), and between layers 2 and 3. At the boundary between layers 1 and 2, part of the seismic energy is reflected and part is transmitted and continues through layer 2 until it reaches the impedance contrast between layers 2 and 3. At this interface, part of the wave is again reflected and part is transmitted and continues into layer 3 (not shown). The two traces on the right hand side of the layer picture show the signals arriving at the two geophones. In conventional land seismic reflection surveys, many geophones are used that simultaneously record the reflected seismic waves. In addition, many shots are fired as the survey progresses along a line, thus building a series of seismic records that are later processed and assembled to form a seismic section.

A similar procedure is used for a CSP survey on water. However, in this case, the energy source automatically produces "shots" at regular intervals while being towed by a boat at a constant speed. The transducer that produces the "shots" is positioned just beneath the water surface. Single or multiple hydrophones record the reflected data. The energy passes through the water column and into the subbottom and is reflected at interfaces with an impedance contrast, the first of which is the water bottom.

The frequency of the seismic signal used by the CSP technique determines the maximum penetration depth and resolution. A high-frequency signal has a short wavelength and is attenuated by subbottom materials but provides high resolution of subbottom interfaces. A low-frequency signal has a longer wavelength and is attenuated less by subbottom materials but provides lower resolution. The fixed-frequency CSP technique uses a narrow bandwidth fixed-frequency signal usually centered at 3.5, 7.0, or 14 kHz. The CSP technique using a 14 kHz signal can be used in water as shallow as 1.2 m, can penetrate up to 6 m into the subbottom in certain materials, and can detect fill material as thin as 30 cm in a scour hole. The CSP technique using a 3.5 kHz signal can be used in water as shallow as 2 m, can penetrate up to 30 m into the subbottom in certain materials, and can detect fill material as thin as 75 cm in a scour hole. Swept-frequency (chirp) CSP techniques that sweep from 2 to 16 kHz can be used in water as shallow as 30 cm, and can penetrate 60 m into the subbottom

in silts and clays. Such signals can sometimes detect fill material as thin as 8 cm in a scour hole.

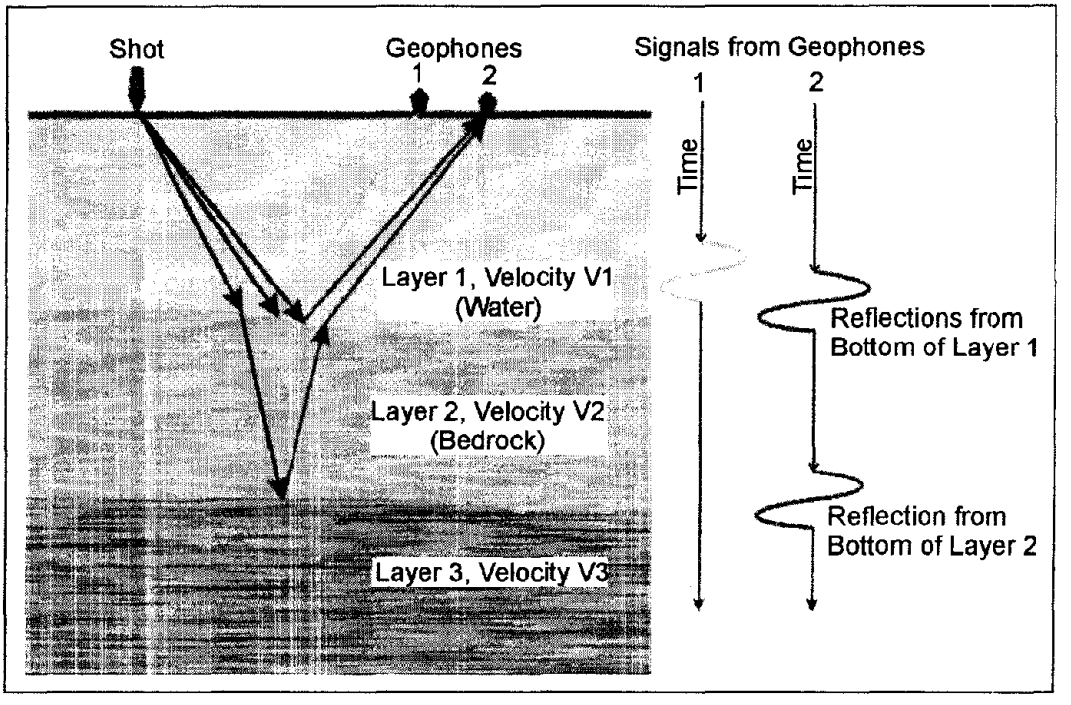

Figure 59. The Seismic Reflection method

The frequency of the seismic signal used also determines the size and weight of the transducer required to generate the signal. Generally, transducers that generate low-frequency signals are larger, heavier, and have wider beam angles than transducers that generate high-frequency signals. The beam angle of a transducer or antenna is the area beneath the device that contains most of the energy of the signal. A wide beam angle allows energy to be reflected by objects alongside as well as under the transducer such as the shoreline or the sides of piers. Echoes from the shoreline or from piers (side echoes) can interfere with the data.

Another source of interference in geophysical data is caused by multiple reflections. When a signal travels from the transducer to the water bottom, it is reflected by the bottom. When the signal returns to the surface it can be reflected at the air/water interface and transmitted back to the bottom. It is reflected by the bottom again and is received at the transducer a second time. This is called a second arrival or a water-bottom multiple. The energy may continue to ring in the water column causing more than one multiple reflection. Water-bottom multiples are most evident when the water-bottom reflection coefficient is large, as in rivers with hard bottoms.

Data Acquisition: CSP surveys are conducted over water using a boat with the equipment attached as described earlier. There are two types of CSP systems. One is a fixed-frequency

system, and the other is a swept-frequency system. Generally, a minimum water depth is needed to reduce reverberations from the water bottom "ringing" to acceptable levels. Often the water depth needs to be greater than a few feet deep. This interface is a strong reflector and produces high amplitude reflections. GPS can be used to position the data.

Data Processing: Often, unprocessed data contain sufficient information to satisfy the goals of many surveys. However, digital signal processing can be done and frequently improves the data making it more interpretable. Most of the processing routines are very similar to those utilized in the reflection seismic method used in hydrocarbon exploration. Processing can involve position data to correct for different speeds of the boat and to produce a geophysical profile with a horizontally corrected scale. Bandpass filtering can be applied along with deconvolution processes. Migration algorithms can be applied to the data correcting the geometry of the bottom of sinkholes and other features.

Data Interpretation: Interpretation of CSP data is mostly visual, looking for features of interest and locating reflections from known features. Two CSP sections are presented, one from a single- frequency system (figure 60) and the other from a swept-frequency system (figure 61).

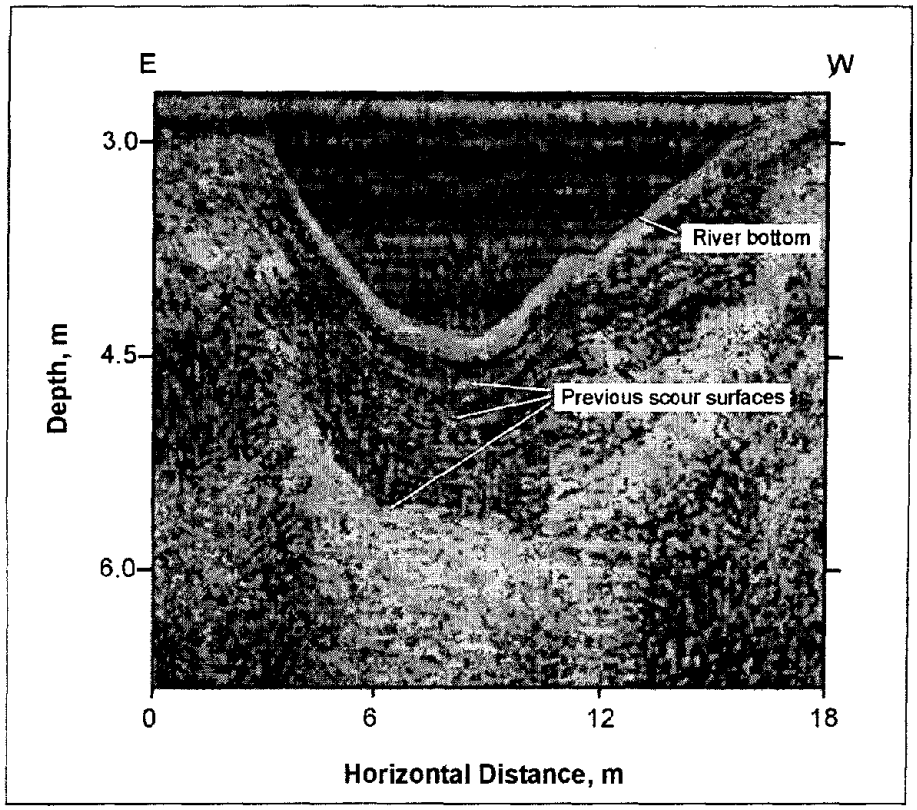

Figure 60. Continuous Seismic Profiling data recorded with a 14.4- kHz transducer. Data have been filtered, spatially corrected, and deconvolved. (Placzek, et al. 1995, USGS Report 95-4009)

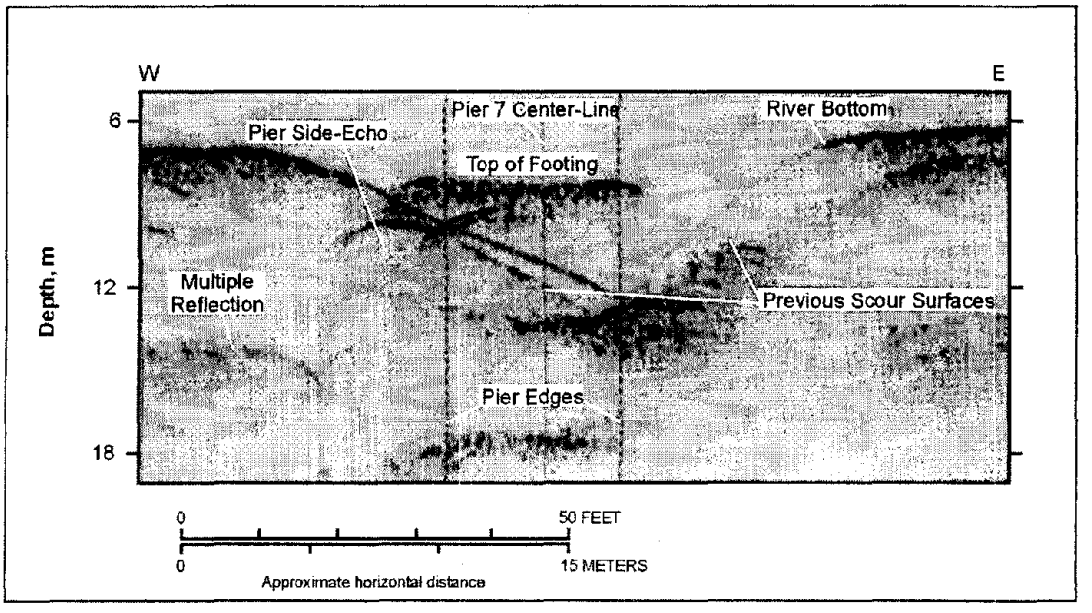

Figure 61. Continuous Seismic Profiling swept frequency data using two 16 kHz transducers. (Placzek, et al. 1995, USGS Report 95-4009)

Limitations: The water bottom interface is sometimes a very strong reflector and can limit the amount of energy being transmitted deeper. In addition, the reflected signal from the water bottom travels back to the water surface where it is reflected back to the water bottom again. This process may be repeated several times creating reverberations, often called multiples, which make the seismic record more difficult to interpret.

A very strong water bottom reflector makes the deeper reflectors faint and possibly unobservable, since little energy is available to be reflected from these deeper layers. Seismic signals are scattered by air bubbles, and the CSP method is not used in settings with gassing organic materials.

Generally, water bottom materials that are coarse-grained have a greater reflection coefficient than fine-grained sediments. Because of this, the depth of penetration of the method is less when coarse-grained sediments form the water bottom surface.

2.4.5 Fathometer

Fathometers surveys are used primarily for determining water depths.

Basic Concept: Fathometer surveys determine water depths by repeatedly transmitting seismic energy through the water column and recording the arrival time of the reflected energy from the water bottom. The instrument calculates the water depth from these data and prints a depth value as a continuous graphic profile. Most fathometers use a narrow bandwidth 200 kHz seismic signal. They provide accurate depth information, but very little information about the subbottom. Fathometers that use a lower frequency, e.g., 20 kHz, can detect reflections from subbottom interfaces such as the bottom of an infilled scour hole.

Fathometer systems come with black-and-white chart recording systems and in-color systems. Colors are often assigned according to the different amplitudes of the reflected signals. Color step sizes as low as four db are now available, allowing quite small changes in the reflected signals to be observed. An event marker button is often available, allowing vertical line marks to be placed on the records when specific locations are selected by the operator. Sometimes the data can be downloaded to a computer, allowing digital processing to be done along with data plots.

Data Acquisition and Data Processing: Fathometer surveys are conducted while traveling in a boat at a moderate speed. Typically, the transducer is mounted on the side of the boat and placed in the water. Data recording is essentially automatic with a chart recorder providing a hard copy of the data; a computer screen may also be used for the display. The data may be stored on magnetic tape for further processing and plotting. As with the CSP method, GPS can be used to position the data.

Data Interpretation: Interpretation is accomplished by viewing the plotted data. The response of specific objects may be used if these were noted on the records using a button marker.

Figure 62 shows Fathometer data recorded with a 200 kHz transducer. Note that only the water depth is observed in these data. Because of the high frequency, little energy is transmitted into the bottom sediments, and, thus, no reflections are observed from within the sediments.

Figure 63 presents fathometer data using a 3.5 kHz transducer. Because of the lower frequency, some of the energy is transmitted into the sediments, and reflections are seen.

Limitations: Most of the limitations have already been described and include limited penetration into the sub-bottom sediments with high-frequency fathometers, although low-frequency fathometers can provide some data about the sediments.

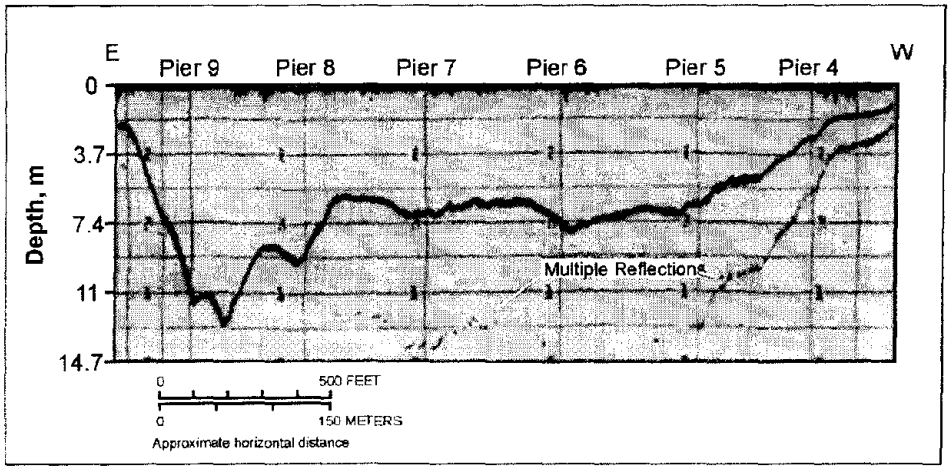

Figure 62. Fathometer data recorded with 200 kHz transducer

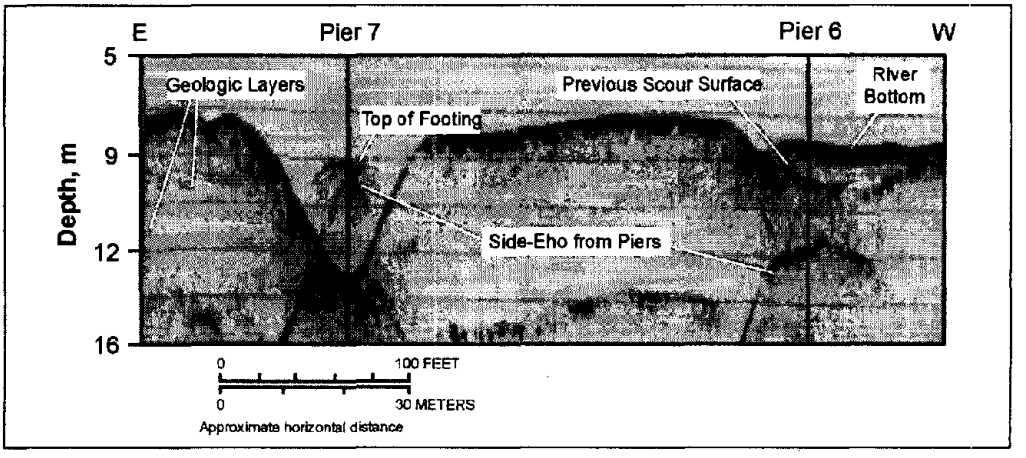

Figure 63. Fathometer data recorded using a 3.5 kHz transducer.

CHAPTER 3 BRIDGE SYSTEM – SUPERSTRUCTURE

In a bridge system, bridge superstructure is defined as all structure above bridge bearing elevation and bridge substructure is defined as everything below the superstructure. In this chapter, geophysical and nondestructive testing and evaluations (NDT&E) methods used mainly for evaluating bridge decks are discussed. This includes discussion of methods used for deck stability analysis in section 3.1, followed by discussion of condition evaluation of new and existing decks in sections 3.2 through 3.4.

Background

Most of the transportation infrastructure in the United States has aged to the point where serious repairs and rehabilitation, replacement, or upgrade of pavement and bridge deck systems have become necessary.

Upgrades are necessary primarily because increases in demand for access to transportation structures require that they handle more volume or increased loads. Design deficiencies and updated construction codes mandate upgrades or require retrofits to ensure public safety. However, diagnosis, repair, rehabilitation, and replacement decisions are generally not entered into because a structure has become functionally obsolete or unsafe because of its design. These decisions are based on the condition of a structure as it ages, through many years of exposure to loading, environment, and even other maintenance activities intended to increase public safety, such as de-icing activities on bridge decks and pavements.

Proper Role of Geophysics in Condition Assessment of New and Existing Structures

Bridge deck monitoring is an essential component of early stage deterioration detection, whether the deterioration manifests itself through material degradation or defect generation. One of the most common problems in concrete bridge decks is corrosion-induced deck delamination, where expansive corrosion products at the reinforcement level create internal stresses that result in cracking and detachment of the concrete from the reinforcement it is intended to protect.

Routine employment of geophysical surveys can yield good results when assessing deck conditions if the proper method(s) are selected. The more successful and/or promising methods are discussed in this document, in order of their current overall value toward solving a variety of bridge deck-related problems or characterizing the presence, pattern, and density of reinforcement. Not every geophysical or NDT method is mentioned, or given detailed discussion within the following text. Only those considered successful, promising, or widespread (even if widespread, but not highly recommended) are given due treatment so that recommended practices for nondestructive evaluations of deck structures and critical information (positive or negative) about commonly used methods can be better understood.

In this chapter, bridge deck evaluations are categorized as initial (QA verification) and baseline condition, as well as condition assessment of older, existing structures, with discussion emphasizing proactive, regularly scheduled diagnostic evaluation throughout the life of a deck. The major topics identified for discussions are decks stability analysis, deck

condition evaluation, rebar condition-corrosion, presence, pattern, density of rebar (PPD), and incipient spalling.

3.1 DECK STABILITY ANALYSIS

This section discusses periodic and permanent monitoring of bridge decks to assess their stability.

The stability of bridge decks has been of concern to designers and owners ever since the infamous destruction of the Tacoma Narrows Bridge in 1940 (figure 64) under moderate winds. Geophysical instruments, including accelerometers and tilt meters, as well as strain gages, are increasingly used for short- and long term monitoring of bridge decks. Issues regarding stability monitoring and methods used will be discussed here. There is additional information on vibration monitoring provided in this document under Chapter 7.0 -- Vibration Measurements.

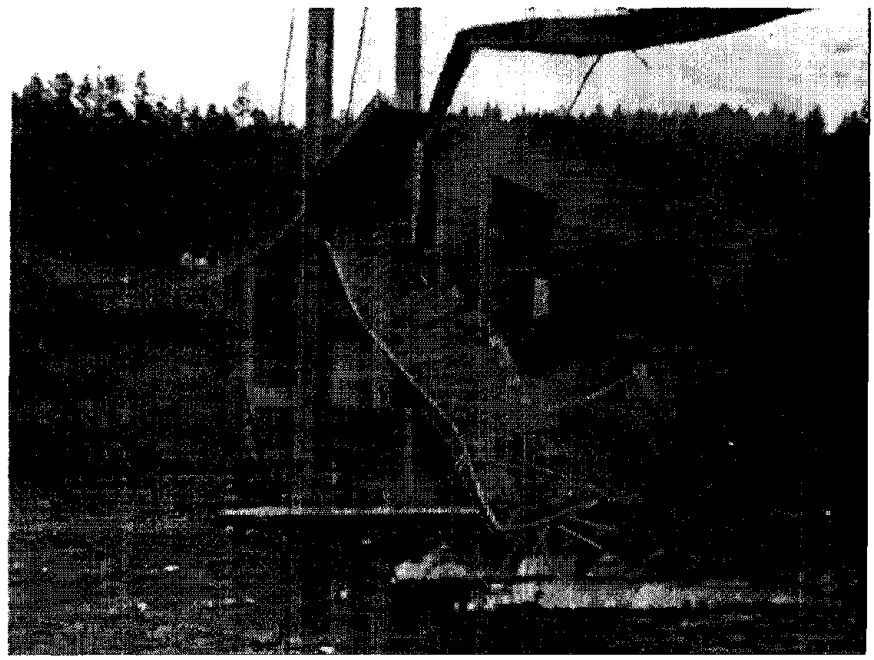

Figure 64. Collapse of Tacoma Narrows Bridge. (The Camera Shop, Tacoma WA)

The basic problems considered here are summarized briefly as follows:

1. The aerodynamic stability of bridge decks when subject to high winds.

2. The long-term stability of bridge decks due to fatigue caused by a variety of cyclic stresses including temperature, increased loading from traffic, and heavily loaded trucks. (See http://www.pubs.asce.org/ceonline/1098feat.html and http://www.kinemetrics.com/newprojects.html#newprojects.bangkok)

3. The stability of bridge decks during earthquakes. (See http://www.kinemetrics.com/halkis.html)

The primary method used to evaluate stability is to measure the baseline performance characteristics of a structure and then monitor the change in these characteristics with time. This can be done periodically, such as during an inspection cycle, or continuously using a permanent monitoring system.

The geophysical techniques applied to this problem are principally vibration monitoring, including strains, displacements, rotations, and accelerations, but also some environmental monitoring including wind and temperature, since these affect the response.

3.1.1 Initial Monitoring or Structural Verification

The purpose of initial monitoring is first to measure the as-built structural modal characteristics and use these data to evaluate the accuracy of the designer's model, and through this, the adequacy of the design. The second purpose is to measure the baseline performance to monitor stability over time. These data can also be used to assist in modeling older structures for the purpose of better retrofitting and upgrading.

Advantages: Better model accuracy means better predictions of performance under extreme loads and lower cost because structural upgrades can be planned more accurately.

Baseline performance is vital to long-term monitoring.

Limitations: None. This step is highly recommended for significant bridges.

Features: Two important questions are, "What characteristics should be monitored, and at how many locations?" For each bridge, this will depend on which structural elements the design engineer feels are most critical. Typical measurements include the following:

- Temperature and wind conditions during the study. Bridges are non-linear structures, and response characteristics can change under different conditions.
- Acceleration, both global movement, and individual elements. Sufficient channels are needed to measure simultaneous movements, with preferably at least 64 channels.
- Strains in critical structural elements under specific loads.
- Precise baseline locations (position or tilt) should be measured at critical locations.

The recording system should have the following minimum characteristics:

- Data should be recorded digitally with at least 16 bits of dynamic range.
- Sensors must be highly sensitive and capable of recording very small motions ($0.005 m/sec^2$ or less).
- Bandwidth will depend on the structure. For example, the fundamental mode of the Golden Gate Bridge has an 18-second period; therefore, sensors with DC (zero Hertz) response are required. Typically, DC to 50 Hz is recommended.

- The recording system must have sufficient capacity to record all 64 channels for many minutes. This will provide statistical redundancy when analyzing the data.

3.1.2 Periodic Monitoring

The purpose of periodic monitoring is to evaluate long-term behavioral and performance changes through intermittent measurements, separated by months or years.

Advantages: The primary advantage is cost. A temporary monitoring system can be mobilized for the survey at any time. Long-term monitoring systems are expensive and require maintenance to stay in optimal condition.

Another advantage is flexibility. New parameters can be added to or removed from the system as needed during each survey.

The third advantage is the potential for improvement. As new instruments and methods are developed, these can be deployed for better monitoring.

Limitations: The primary limitation to periodic monitoring is lack of availability. Usually, the system is not available during peak motions, such as an earthquake or windstorm.

Periodic monitoring can lead to inconsistency. It might be difficult to repeat the same measurements using the same instruments.

Features: Again, two important questions are, "What characteristics should be monitored, and at how many locations?" As with initial monitoring or structural verification, this will depend on which structural elements the design engineer feels are most critical. Typical measurements include the following:

- Temperature and wind conditions during each study. Bridges are non-linear structures, and response characteristics can change under different conditions.

- Strains in critical structural elements under specific loads. Even though measurements are temporary, permanent mounting locations should be established for periodic mounting of strain gages.

- Permanent displacements or rotations of piers and decks. These should be measured at critical locations.

3.1.3 Permanent Monitoring

The purpose of a permanent monitoring system is to monitor long-term behavioral and performance changes through continuous measurements. High-speed acquisition can be triggered by important events, such as an earthquake or high winds. Low-speed acquisition can be programmed for daily, weekly, or monthly measurements for long-term studies.

Advantages: The availability of the system is a primary advantage. The system is always available during peak motions, such as an earthquake or windstorm.

The consistency of the system is a second advantage. Measurements recorded today can be directly compared with measurements obtained 10 years ago.

Limitations: A critical limitation is cost. Long-term monitoring systems are expensive and require maintenance to stay in optimal condition.

As new instruments and methods are developed, the system may need to be upgraded to provide maximum utility.

Features: The same two important questions remain: "What characteristics should be monitored, and at how many locations?" Again, for each bridge this will depend on which structural elements the design engineer feels are most critical. Typical measurements include:

- Temperature and wind conditions. Bridges are non-linear structures, and response characteristics can change under different conditions.
- Strains in critical structural elements under specific loads.
- Permanent displacements or rotations of piers and decks. These should be measured at critical locations.
- Triggered event recording is an important benefit of a permanent monitoring system. This is particularly true if the bridge is located in a seismic zone. The system must be able to turn on automatically and record the event. The sample rate for these channels must be adequate to record full response, to at least 100Hz.

3.1.4 Recommendations

Table 6 summarizes the recommendations discussed above.

3.2 QA/QC OF NEW DECKS

Quality Control (QC) is the implementation, measurement, and enforcement of sound construction practices and jobsite inspections to ensure construction quality. Quality Assurance (QA) is the inspection and testing of the completed product, in accordance with specifications intended to verify the quality of the completed structure.

Table 6. Bridge deck monitoring.

Vibratory Motion	Frequency Range	Sensor Type (with link to example)	Motion Measured	Application (with link to example)
Tilt, or Rotations	0-1Hz	Tiltmeter http://www.geomechanics.com/products/tiltmeters.htm Inclinometer http://www.slopeindicator.com/instruments/inclin-intro.html	Rotation from vertical in degrees, sometimes expressed as the sine of the angle of tilt	Monitoring long term movement of bridge decks http://www.bridgetest.com/ http://www.kinemetrics.com/namhae.html
Motion due to earthquakes	0-200Hz	Accelerographs http://www.kinemetrics.com/etna.html http://www.kinemetrics.com/qdr.html Structural monitoring system http://www.kinemetrics.com/oasis.html	Absolute acceleration, m/sec^2	Monitor the performance of individual structures during earthquakes, such as piers, decks, and foundations http://www.kinemetrics.com/amoes.html Monitoring the performance of large structural systems http://www.kinemetrics.com/structural.html http://www.kinemetrics.com/namhae.html http://www.kinemetrics.com/halkis.html
Strains due to motions	0-100Hz	Strain gages Bonded http://www.vishay.com/brands/measurements_group/strain_gages/mm.htm http://www.geokon.com/straingages.htm http://www.jptechnologies.com/wsgages.html http://pages.prodigy.net/heatinc/ http://www.bridgetest.com/	Strain, mm/mm or in/in	Monitoring stresses in structural elements at critical location, steel and concrete Evaluate fatigue in structural elements
Motion due to ambient vibration to evaluate structural characteristics	1-100Hz	Vibration Monitoring http://www.kinemetrics.com/k2.html	Acceleration, m/sec^2 sometimes velocity, m/sec	Measure modal characteristics to "calibrate" the designers mathematical model ftp://ftp.kmi.com/pub/AppNotes/appnote44.pdf

QC programs intended to address construction quality of decks routinely include (a) visually inspecting the forms and deck reinforcement at regular intervals during construction (and carefully repairing nicks and scratches found in epoxy-coated bars within the reinforcing cage with fresh epoxy); (b) careful field and laboratory testing of the quality of materials used in its construction; and (c) testing and inspection activities, both in the field and laboratory, associated with placing and curing the concrete. Results are carefully measured and archived as a permanent part of the job record and/or used to modify field (construction and inspection) practices and take corrective action while construction is still underway.

Quality control of construction practices and materials selection contributes to a deck that can last at least as long as its design life, from meticulous construction and inspection of the reinforcing cage to care in designing, mixing, placing, finishing and curing the concrete, along with proper monitoring during each of these processes. This quality-control series of activities is consistently practiced, in general, throughout most of the industry.

However, the quality assurance component, particularly as it relates to inspection of the internal condition of the deck after construction, generally receives much less attention and care, because it seems to be physically more difficult to do. In addition, when accuracy or reliability of QA inspections come into doubt, QA can often be viewed as an added construction cost with low, or indeterminate, perceived value. Well-written QA verification specifications in terms of the desired inspection outcomes and consequences related to noncompliance often become seemingly meaningless when inspection capabilities appear to fall short of expected results. This statement is particularly true when the inspection methods cannot be effectively critiqued or corrected, resulting in an inherent ineffectiveness in their ability to be used for enforcement or improvement of QA policies.

Ultimately, it is not how well a deck appears to have adhered to standard practice prior to completion that matters in the end. More importantly, the design elements intended to be built into the structure must actually exist internally once it is finished. In other words, excellent QC is not much good without adequate QA. The only way to ensure compliance to construction requirements is to construct and adopt a meaningful, high-quality QA program that undeniably verifies the deck has been properly built. This includes development and implementation of good specifications, backed by selection of appropriate inspection methods that are accurate and repeatable for verifying compliance, to inspire confidence in both the construction community and the owners that the QA program is sound.

3.2.1 QA Using Geophysical Methods

Geophysical methods, such as ground penetrating radar and other electromagnetic or magnetic devices, are often employed to verify that the amount, size, layout, spacing, and depth of reinforcement meet design specifications. Often, the QA specifications or verification standards for the inspection process are more stringent than the capability (accuracy and/or repeatability of the selected method) to measure these properties.

An example of this statement is the preponderance of QA specifications related to verification of reinforcement layout and depth (concrete cover), specifications requiring

accurate measurement and reporting of these dimensions to within 0.25 to 0.635 cm of actual position in the deck. Yet, most of these specifications require that the measurements be made using a Pachometer or similar device. There is nothing wrong with the specifications requiring that a structure be properly built and verified, and the tolerances listed above are not unrealistic to achieve. Nor is there anything wrong (technically) in specifying a Pachometer for measurement of rebar position or depth. However, a Pachometer does not accurately or reliably measure these parameters, nor are the measurements repeatable, particularly within the stated measurement tolerances for accuracy and/or repeatability.

This problem has caused several DOT's to stop enforcing their QA verification inspections for cover or discontinued any attempt to measure it after the structure is built, relying solely on field inspections of the reinforcing cage, formwork, and placement operation—the QC component of their QC/QA program. Other states have dropped the cover verification specification altogether, or avoided adopting one because confidence in the reliability and accuracy of this instrument is not high.

Ground penetrating radar (GPR), only when used with a recently built, digital data acquisition system (post-1996) and a shielded 1.5 GHz ground-coupled antenna, has been proven by New Hampshire Department of Transportation (NHDOT) to accurately and routinely measure cover on a new bridge deck to within 0.25 cm. NHDOT's (Pachometer-based) specification was revised to allow only the Geophysical Survey Systems Model 5100, 1.5 GHz sensor (or a newer data acquisition unit that can provide as good, or better results) to be used for this purpose. NHDOT specifications, originally designed to reward contractors based on performance (mean cover depth and variability within specified tolerances to determine degree of compliance or non-compliance), are implemented in that fashion, and contractors can receive a pay factor on the portion of the contract covering deck construction (typically 40% of the bridge construction cost) as high as 1.05 (5% bonus). Overall contractor performance on the QC end in New Hampshire has also improved as a result. During the "non-enforcement" period, all contractors received a pay factor of 1.0, simply because no one could confidently determine the level of performance.

Problems exist in quality assurance (QA) verification of deck construction, even when stringent quality control (QC) initiatives are implemented and improved as part of a well-planned QC/QA strategy. Mostly, the inability to accurately and nondestructively verify reinforcement position (horizontally and vertically), layout, and quantity within a concrete deck, as well as to measure deck thickness to the degree specified or desired by most structure designers and/or owners as they develop and improve their QA methods, is systematically below acceptable standards in most areas of the country. QC/QA on new deck structures, by critically impacting how well they are constructed, are implemented so that future deck deterioration problems can be delayed and/or reduced, minimizing the quantity and cost of future maintenance on these decks during their service lives. The use of GPR as a primary evaluation tool for QA regarding placement (including cover), pattern and density of rebar is recommended, and should be seriously considered for verification purposes. Also, seismic methods should be used for concrete quality verification. Guidance for comparison of test methods, specification development, and implementation can be obtained by following New Hampshire DOT's lead in the area of GPR.

3.2.1.1 Ground Penetrating Radar (GPR)

For detailed description of GPR in this application, please refer to section 4.1.1, Chapter 4 – Pavements.

Data Acquisition: Vehicle mounted GPR systems, discussed in detail in section 3.4.5, can be used on bridge decks for overall assessment spotting areas of problems. However, vehicle mounted GPR systems are not generally the preferred method for accurate location of rebar. One of the portable systems with a 1.5 GHz antenna is more appropriate for that application.

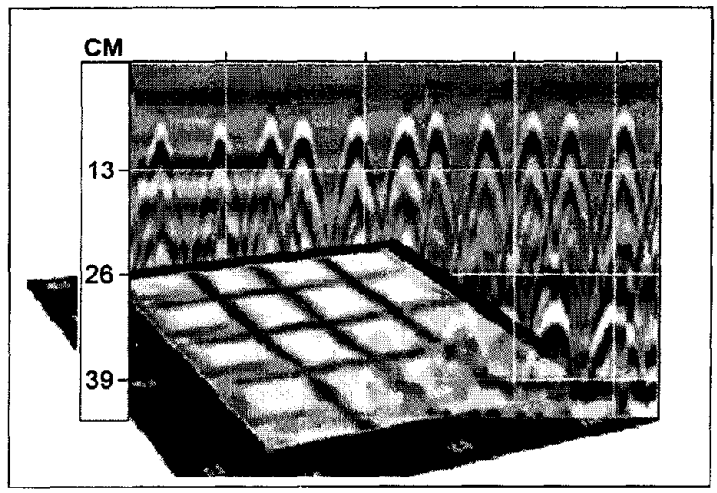

Figure 65. Ground Penetrating Radar image of rebar.

Interpretation: As indicated in figure 65, locating rebar is done by noting hyperbolic shapes in the GPR image. The apex of each hyperbola locates a rebar. Lateral separation can be determined to sub-centimeter accuracy as long as care is taken in the lateral location control of the instrument. Likewise, the rebar depths can be measured to a similar depth as long as local calibration of the EM wave velocity is carried out.

Advantages: This method is easy and inexpensive to run and can therefore be run over every meter of a bridge deck.

Limitations: On-site velocity calibration is necessary to get the best results.

3.2.1.2 Impact Echo (IE)

For detailed description of Impact Echo in this application, please refer to section 4.1.2, Chapter 4 – Pavements.

Interpretation: The best use of impact echo on a bridge deck is for overlay thickness. It is necessary to look for sites in between rebar to get the best depth measurement of the deck. Sites affected by the rebar will be readily in the data as a very shallow measurement (at the depth of the rebar).

Advantages: This method provides thickness with no coring.

Limitations: The user must make sure thickness measurements are made with interference of rebar.

3.2.1.3 Spectral Analysis of Surface Waves (SASW) and Ultrasonic Surface Waves Methods

For detailed description of these methods in this application, please refer to section 4.1.3, Chapter 4 – Pavements.

Interpretation: In bridge deck applications these methods are used to measure modulus just like in pavement applications. The purpose is to get a quality measurement of modulus without coring the new deck.

Advantages: This method gives concrete quality without coring.

Limitations: This method requires road and bridge closures.

3.2.1.4 Spectral Analysis of Surface Waves (SASW) and Impact Echo (IE) Combined

Ultrasonic Seismic (SASW) and Impact Echo (IE), particularly when applied together in an integrated instrument, such as the Portable Seismic Property Analyzer (PSPA), are high-frequency, acoustic (seismic) geophysical methods. Concrete condition assessment by integrated ultrasonic methods has recently been applied to a number of engineering problems associated with both new and aging concrete structures. Recent work on evaluating concrete integrity, particularly, looking for the formation of corrosion-induced delamination in early, moderate, and late stages of development, has demonstrated that these integrated methods show considerable promise in terms of current and potential capability.

See section 4.1.3 for further comments on this system.

3.3 BASELINE CONDITION ASSESSMENT

Baseline condition assessment is not a routinely practiced form of quality assurance; however, it is truly the only way to compare the overall as-built condition of a structure to its future condition at various stages during its life. One way to establish a baseline condition where "as-built factors" (variables in materials and workmanship that often hamper or adversely affect the accurate diagnosis of the condition of a structure) can be eliminated or minimized from consideration during a future evaluation is to perform measurements on a new structure identical to those that will be used for primary "screening" in the future to diagnose its overall condition.

To establish a baseline condition assessment, only nondestructive evaluations are of value, and only those that continuously sample the deck along every centimer or meter of its length and width in the manner highlighted above warrant consideration. That leaves only "full-coverage" methods, such as GPR, SASW and impact-echo, infrared (IR) thermography, or electrochemical analyses as candidates for this approach.

GPR will accurately measure initial presence, pattern, and density of the reinforcement layout, including cover (depth) of reinforcement and any overlay properties. Initial data can

very easily be collected in such a manner that it will be identical in scope to data collected during a future deterioration-mapping process. Additionally, it will provide repeatable and accurate condition assessment results in a more consistent fashion than any other NDT method at any stage of the life of a structure. Collecting the data is rapid, fully nondestructive, and straightforward once an established methodology is developed and adhered to; the data can be obtained on decks with or without overlays that protect the concrete surface to establish their effect on its initial and future condition states.

When factoring in economics, objective capability and repeatability of the measurement, effective deck coverage, and ability to collect the baseline data without the absolute need for other NDT or destructive sampling, GPR is the only sensible instrument to use for this screening process. It may be advantageous, however, to complement the GPR screening with diagnostic evaluations of a baseline nature in regions where the GPR or past experience reveals conditions (reinforcement depth, variations in depth and layout, or other heterogeneities not designed into the structure) typically indicative of potential problems in the future. Those targeted areas can be measured, and the data obtained can be compared with future information gathered from those precise locations to supplement, verify, or otherwise improve a future GPR-based condition assessment.

3.3.1 Baseline Condition Assessment Using Geophysical Methods

A geophysical survey method that provides useful, objective information about the relative condition of the various areas on a deck structure and samples the entire deck in a rapid and economic fashion is generally most valuable when it is used prior to making other important decisions. These include decisions on whether other NDT, destructive sampling, or laboratory testing and analyses are needed to provide a better evaluation, or choosing between complementary evaluation techniques, whether the deck structure is new or old. If approached in this manner, geophysical techniques can and will supplement any traditional bridge deck evaluation. They add little to the overall price of diagnosing the structure, and the information provided will minimize the overall inspection, maintenance, or replacement costs associated with the structure during its service life. Geophysics also helps to ensure that the appropriate maintenance and preventive maintenance measures are applied at the right time.

Methods used in bridge deck condition assessment should be accurate, rapid, and nondestructive whenever possible, whether QA verification testing or existing bridge deck evaluations are the desired goal. The current practice of deck inspection (existing structures) by chain dragging meets only the last two criteria, and is not any more rapid than some other, more objective, nondestructive geophysical evaluation techniques. The accuracy of chain dragging is significantly compromised by the fact that it can only be used to identify delaminations at stages where the deterioration has already progressed to such an extent that major rehabilitation or repair measures are needed.

Similarly, the Pachometer barely meets the last two criteria when it is used as a primary instrument for verifying that QA specifications are being achieved on new deck construction, because it cannot typically achieve requirements that mandate measurement accuracy within 0.25 to 0.635 cm, and the measurements are not repeatable.

Identifying the appropriate NDT method, or methods, prior to some verification ground-truth (limited coring—both older and new decks--and/or chemical, physical or optical analysis of deck samples on older decks) is always the best approach toward effective use of these geophysical methods.

When used as a primary investigative method, either as a baseline condition assessment tool early on in the life of a structure or as a deterioration-mapping instrument, geophysics is often beneficial if used as a "reconnaissance tool" in the early stages of an evaluation. The results of the geophysical survey can be used to help (a) select complementary inspection methods, destructive or nondestructive, that would best complete the analysis; (b) reduce the quantity of destructive testing or NDT investigations that are more time-consuming and require lane closures, even if they are essential to the overall evaluation; and (c) limit these other tests to much smaller areas on a given deck. Information obtained by these other techniques will generally complement, validate, and/or "calibrate" the initial geophysical survey method.

A competent bridge deck condition assessment professional will understand the following rationale. One should remain skeptical of any single geophysical method used alone with the promise of an all-purpose solution to deck condition assessments and is recommended without supplemental evaluation, testing, or ground truth. However, sometimes new applications or methodologies can produce results that are more accurate and reliable than traditional approaches that have been widely used. Improvements in analysis capabilities or new ways to use both newer and older instruments should not be ruled out because few people have used them. Similarly, one should not be overtly dismissive of geophysical techniques based on one, or even a few, less-than-satisfactory personal or anecdotal experiences, particularly if they occurred several years ago. Some data analysis and processing techniques were still somewhat experimental or in their developmental stages. Advancements in computing capabilities, analysis software, and survey methodologies over the last 3 to 5 years have contributed to significant gains in the value certain geophysical surveys add to bridge deck evaluations. Much of the subjectivity in interpretations has been reduced, minimized, or altogether eliminated.

3.3.1.1 Ground Penetrating Radar (GPR)

For detailed description of GPR (figure 66) in this application, please refer to section 3.4.5 and section 4.1.1, Chapter 4 – Pavements. GPR is regarded as the most promising nondestructive geophysical method available for assessing bridge deck condition on both new and old structures. For this reason, much attention is devoted to treatment of this method, and additional references to pavement applications (not covered in this section) are provided, because much of the information is inter-related.

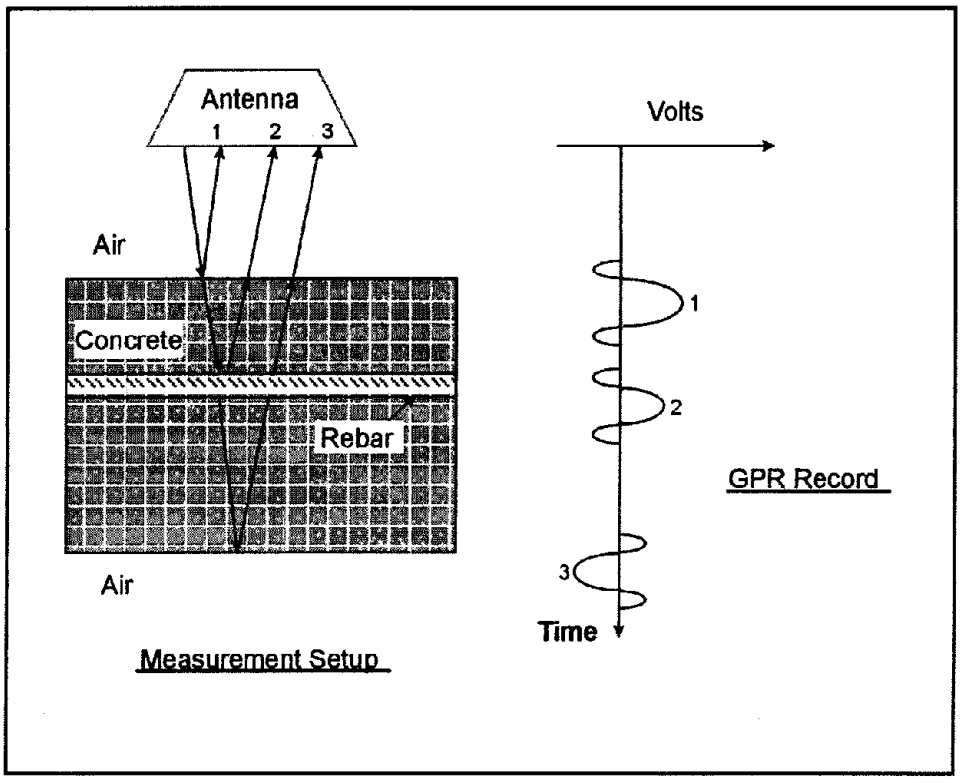

Figure 66. Horn antenna (air-coupled) setup and measurement: Basic horn antenna setup (single antenna) is used for bridge deck or pavement evaluation at high speed. Individual Ground Penetrating Radar methods.

After a GPR survey has been completed using sound methodology, appropriate analysis software, and the results contour-plotted, GPR should be used to provide guidance on where to use other NDT methods on decks (and/or where to sample using cores or other destructive means). Controversy exists regarding GPR and its abilities, partially because some methodologies used in bridge deck survey analysis (a) are not technically viable, from a theoretical or a methodological approach; (b) rely on subjective analysis (visual) of the raw data, based on evaluating amplitude with simple color-threshold levels applied, and conclusions based on these visual observations; (c) improperly characterize GPR as a tool that is used to identify and detect delaminations (it cannot); and (d) unrealistically assume that a GPR survey is best used as a stand-alone tool to compare directly against other "ground truth" such as chain-drag or hammer-sounding. The capabilities of GPR and the value of its contribution to a deck evaluation are considerable when the methods are fully understood and properly applied, and realistic expectations for results are defined. This awareness will significantly minimize the number of occurrences where incorrect or inconclusive results characterize GPR's success. A three-step approach is recommended: (1) GPR is used to specify locations that are candidates for other NDT testing and analysis; (2) NDT surveys completed; (3) limited and targeted ground truth (destructive testing).

Comparison of Pachometer w/GPR

A less-used, but decidedly better technology for approaching QA tasks often specified for Pachometer evaluation, one that can provide baseline as well as future condition assessment on bridge decks, is ground penetrating radar (GPR), another electromagnetic (EM) method based on generation and measurement of EM emissions in the radio-frequency spectrum. GPR is rapidly becoming the most useful geophysical (NDT) method for characterization of bridge deck condition or quality, whether the deck is newly constructed, or is in-service, as an existing deck that requires monitoring or extensive condition evaluation.

The Pachometer is not a recommended tool for QA verification of rebar PPD if accuracy and repeatability within 0.635 cm is consistently expected for quality assurance work. It should be used primarily for locating rebar in walls, floors, or decks prior to cutting and coring operations. Even then, it should be limited to uses where critical elements, such as conduits, post-tension steel, etc., are not present, or in situations where cutting through reinforcement does not pose a structural problem.

Because of these limitations, particularly when compared with more advanced and accurate instruments, discussion of Pachometers and similar instruments will be limited to this description and only few brief references within the text.

3.3.1.2 Electromagnetic (EM) Instruments Sensitive to Ferrous Content in Steel

A variety of nondestructive geophysical instruments can be used for these stated QA tasks. The most widely used instrument is the Pachometer, an electromagnetic (EM) instrument sensitive to ferrous content in steel and used to determine cover (depth to reinforcing steel from concrete surface), reinforcement quantity, and layout (spacing of bars and their lateral positions within the deck). However, the instrument is not accurate or repeatable enough to provide these measurements for verification purposes. Neither is it able to collect continuous data in a rapid fashion along the entire deck, while providing an initial (baseline) condition assessment of a deck for comparison to future evaluations.

This family of EM instruments is limited by its inability to differentiate between a single shallow reinforcing member and a closely spaced grouping of one or more bars. It is also limited in its ability to penetrate concrete more than 10 to 15 cm, in general. However, for quick verification of well-characterized structures (whose as-built drawings can be relied upon to provide accurate information about construction), Pachometers and other simple EM response instruments provide suitable accuracy for locating lateral placement and positioning of rebar and even determining depth. They are best used to locate reinforcement in (a) rehabilitation situations where cutting or coring into concrete does not involve the risk of damaging post-tensioned cables and ducts, electrical conduits, fiber-optic conduits, or other embedded utilities; and (b) structural analysis calculations where reinforcing is known to be spaced at fairly large and consistent intervals within the depth range that these instruments are suitably sensitive.

3.3.1.3 Ultrasonic-Seismic Techniques

It has been demonstrated that ultrasonic methods implemented in various forms of integrated ultrasonic seismic devices, such as the Portable Seismic Pavement Analyzer (PSPA), can be successfully used to assist in evaluating bridge deck condition, alone or in tandem with other geophysical and/or ground truth sampling. It is always recommended, however, to use a multiple-method approach.

Of special interest are three ultrasonic techniques: ultrasonic body wave (UBW), ultrasonic surface wave (USW), and impact echo (IE). These geophysical methods can be used separately or in combination. The first two are used in concrete characterization (concrete integrity and/or determination of mechanical properties using basic assumptions about the relationships between P-wave and S-wave velocities), and the IE method is the primary tool in delamination detection once a propagation velocity (speed) for travel of the seismic wave in the concrete is established. The primary advantage that the IE method has over the current practice of chain dragging is that it allows detection of delamination zones in various stages of deterioration, from initial, through moderate, to and fully developed (incipient spalling).

As demonstrated by finite element simulations of two probable scenarios of delamination progression, periodic monitoring of bridge decks by IE enables improved prediction of deterioration processes in bridge decks. Three-dimensional data visualization techniques constitute important components in condition assessment and delamination detection using the IE method. Results presented include three-dimensional translucent visualizations of a bridge deck section, horizontal cross sections through all distinctive zones (including a zone of delamination), and vertical cross sections along chosen test lines. Visualization techniques enable the PSPA to be used as a kind of bridge deck sonar device.

The combined ultrasonic seismic techniques, however, do require more sophisticated analysis than (a) the GPR and half-cell corrosion potential methods (condition assessment of existing decks), or (b) the GPR or Pachometer (new structure PPD of reinforcement). This statement is not necessarily true on some of the QA applications, however, such as determination of concrete integrity on new and fairly uniform structures, where use of the acoustic techniques can be straightforward and very simple. An example of a simple impact-echo device used to measure concrete thickness, for example, is a concrete thickness meter that can accurately determine thickness for QA verification purposes.

For detailed description of Spectral Analysis of Surface Waves (SASW) and Ultrasonic Surface Waves (USW) methods in this application, please refer to section 4.1.3, Chapter 4 – Pavements.

3.3.1.4 Ultrasonic Seismic and Impact Echo (Combined)

Ultrasonic Seismic and Impact-Echo, particularly when applied together in an integrated instrument such as a Seismic Pavement Analyzer (SPA) or Portable Seismic Pavement Analyzer (PSPA), are high-frequency, acoustic (seismic), geophysical methods. Concrete condition assessment by integrated ultrasonic methods has recently been applied to a number of engineering problems associated with both new and aging concrete structures, but

particularly in pavements. However, recent work on evaluating concrete integrity, particularly, looking for the formation of corrosion-induced delamination in early, moderate, and late stages of development, has demonstrated that these integrated methods show considerable promise, in terms of current and potential capability. Figure 67 shows a basic Ultrasonic Seismic and Impact Echo setup.

In the transportation sector, these integrated surveys can be used for quality assurance (QA) verification of new construction (thickness determination and homogeneity of concrete pour, even segregation of aggregates or suspected voids) and calculation of mechanical properties, both on bridge decks and pavements.

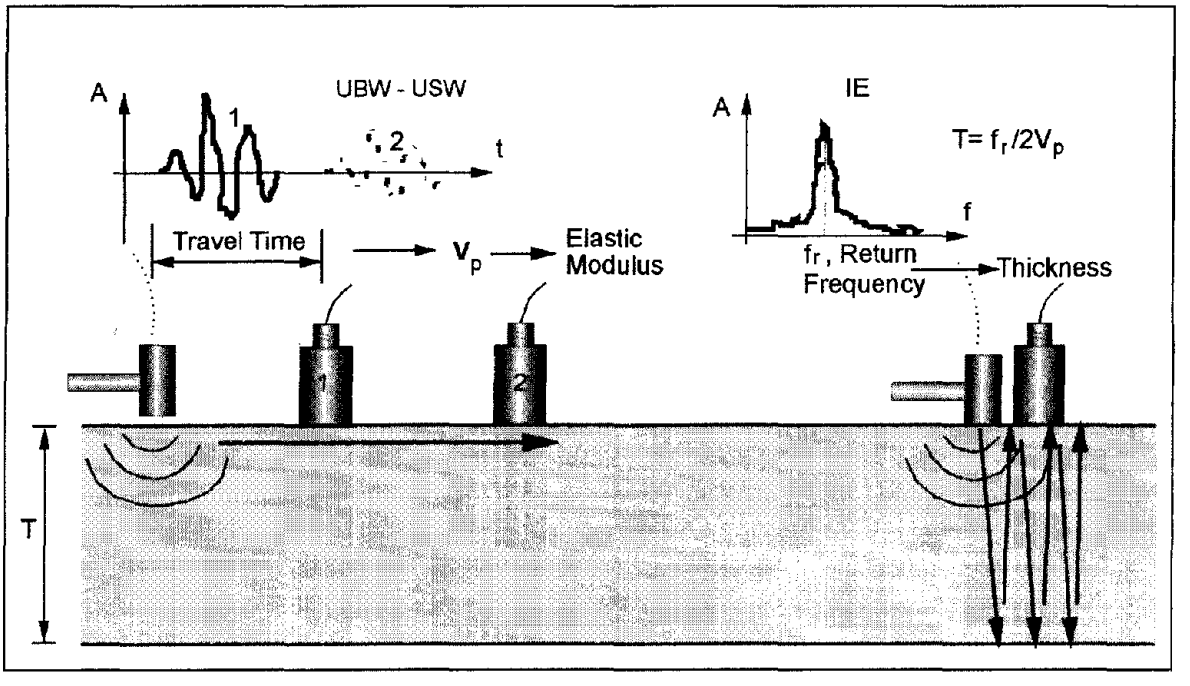

Figure 67. Ultrasonic Seismic and Impact Echo test methods (basic setup and measurement).

See section 4.1.3 for more details on the combined techniques. Also, see section 4.1.2 and the beginning of section 4.1.3 for detailed description of Impact Echo, SASW and USW in this application.

3.3.1.5 Half-Cell Corrosion Potential Mapping

The half-cell corrosion potential method is a geophysical method incorporating a semi-destructive (for the most part, nondestructive) electrical technique for assessing probability of corrosion in existing deck structures based on measuring voltage (electrical potential) between the anode (top mat reinforcing bars) and a reference electrode that is electrically coupled to the bridge deck surface.

The reference electrode is moved to discrete sampling intervals across the length and width of a deck at equal spacing (recommended at 1.52 m, but often applied at 3.05 m to reduce sampling time and lane closures by a factor of four). The voltage reading at each location, in

millivolts, is interpreted to signify an indication of the likelihood that corrosion activity is at or near pre-determined levels (or corrosion states); the data are typically represented in the form of a plan-view contour plot of the surface of the deck.

Half-cell corrosion potential testing (and contour-mapping) can be an effective way to characterize the onset of corrosion and/or corrosion state that most likely exists within a reinforced concrete deck. Figure 68 shows the setup for this testing method.

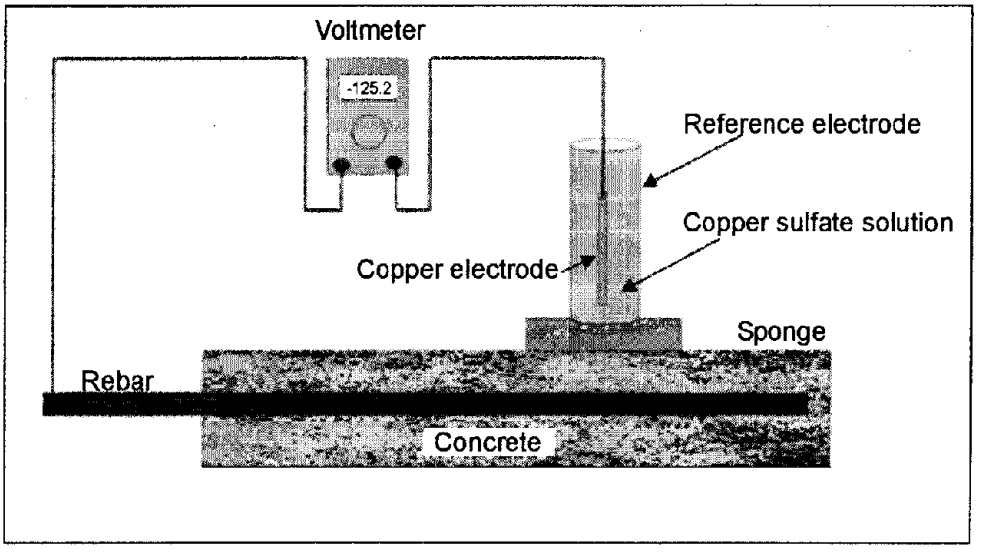

Figure 68. Half-Cell Corrosion Potential method (basic setup and measurement).

This method is applied, in practice, only to existing decks, so it is not considered of particular value in initial quality assurance. It could be included as a supplementary NDT method in a baseline condition survey, however, so that a higher confidence level can be maintained in future potential readings that predict corrosion activity states on regions of the deck.

3.3.1.6 Infrared (IR) Thermography

Imaging using infrared thermography is a nondestructive geophysical approach used with some degree of accuracy when evaluating the condition of existing bridge decks, specifically for detection of shallow delaminations in bare concrete decks or identification of de-bonded zones at an overlay/deck interface. If it is properly used under all the right conditions, it can be a useful supplement to other NDT evaluations, including GPR.

Typically, it is not suitable as a stand-alone method because there are many variables that affect its performance and objectivity. Because of this, IR thermography almost always has to accompany one or more other NDT techniques and ground truth. Often, it can be used successfully to complement a GPR survey; however, it must be analyzed and processed carefully by someone experienced with both its benefits and pitfalls so that the information is not over-analyzed, over-simplified or (often) over-emphasized. Over-emphasizing IE data, particularly if poor IR survey conditions exist, often results in either a serious over-estimation of defects in some areas and/or a large number of missed defects in others. Subjective engineering decisions, even if they are based on good knowledge of the method

and seem the right decisions to make, often over-ride objective ones that affect the outcome of the survey.

IR thermography identifies delaminations and de-bonded areas because it is sensitive to heat differences at the deck surface caused by the uneven rates of warming and cooling (accumulation and dissipation of thermal energy) between mass concrete, air-filled cavities (delaminations or de-bonded areas), and water-filled delaminations or de-bonded areas. Temperature differences on the surface can indicate the location of usually shallow delamination, but other factors affect surface temperature that will be discussed below. Although, in theory, this sounds like an excellent method, it is prone to several problems that reduce it more to a subjective than an objective analysis method.

Its primary advantage is complete deck coverage, along with visual interpretation of the results and isolation of delaminated/de-bonded zones by marking them directly on a map, taking into account distortion from low camera angle. Analysis is fairly straightforward, in principle, and can be reasonably reliable when ideal or very good conditions are present.

Its primary limitations are:

1. Unreliability of solar heating to provide even thermal energy input into all areas of the deck.

2. Speed of survey is limited to about 3 to 5 km/h, meaning that deck condition (thermal gradient) can change considerably from start to end of the survey, and a very slow-moving "mobile lane closure" is required.

3. Effect of shadows from trusses, cables, walls, jersey barriers, and/or overhead decks generally ensure that uneven thermal loading and dissipation are taking place, removing much of the objectivity of the analysis.

4. Dissipation of heat at a rapid rate by a mild breeze, particularly if the wind is sporadic with large variations in intensity; heat is removed temporarily at the surface on actual "hot-spots" that are missed as the survey progresses.

5. Problems with variations in reflectance from surface materials or surface conditions that can confuse or otherwise complicate the interpretation, such as pavement patches, surface staining from oil or burned pavement, surface 'polishing' of a concrete deck or asphalt overlay, light and dark areas on a deck caused by sunlight and shadow, pavement markings (paint), etc.

6. Time limitations brought about because surveys typically must be performed at limited times of the day when conditions are favorable, i.e., a few hours after initial warming of the deck when heat-retention differences at the surface reveal defects (morning hours) or immediately at or after sundown, when deck surfaces rapidly cool in some areas and more slowly cool in others.

Preferred methods to conduct an IR survey are (1) well-planned aerial surveys on selected decks with few of the uneven heating/cooling problems listed above, taken at appropriate

times of the day, when wind activity is low; or (2) survey behind a vehicle with an active heating source, which provides even heating to decks that cannot rely on solar-heating for uniform heat transfer. The survey, however, must be limited to single-passes that image only the width of the active heating array, and the vehicle with the IR camera must distance and pace itself accurately at constant distance and speed with the one heating the deck to objectively identify locations with cooling or heat-retention properties indicative of subsurface defects (delaminations or debonding). Clearly, this method is not extremely well suited for providing objective survey results on its own.

Infrared (IR) thermography should not be used as a stand-alone method, and, if considered as an added tool perhaps accompanying GPR, clients would be well-advised to learn as much as possible about the method and the service-provider recommending its use to determine if the combined interpretation weighs IR results too heavily. Because it is widely used in some areas and can be well implemented by some service providers, it is treated as an important geophysical (NDT) method; however, it is not discussed in any great detail, nor will it be recommended as a primary evaluation tool. Additionally, if a combined IR thermography/GPR survey is proposed, but one of the three preferred GPR survey methods is not incorporated with the IR survey, the entire proposal should be considered suspect.

Although the principles for each of the above methods are all fairly straightforward, skilled practitioners with considerable experience will almost always provide better results than those with less, provided they are employing the appropriate methods at the right time. Often, this requires a considerable investment in formal training of appropriate methodologies or techniques for each geophysical method.

Each of the above methods, depending on the desired quality of the investigation, the time required to obtain results, and cost has its merits. However, short-term diagnosis costs or equipment investment should be weighed against the long-term benefits of obtaining better information for deciding appropriate preventive maintenance and maintenance/replacement activities for existing decks, and for evaluating contractor compliance to specifications on new construction.

3.4 CONDITION EVALUATION OF EXISTING DECK

As a reinforced concrete bridge deck deteriorates with time and exposure, a proper diagnosis and preventive maintenance schedule, whereby smaller and less expensive repairs are made at properly timed intervals throughout the life of the structure, significantly extends its life and reduces the costs associated with its ownership. (See earlier discussions on baseline condition assessments and QA verification of construction related to this topic).

3.4.1 Presence, Pattern and Density (PPD) of Rebar

In older structures, it is sometimes necessary to construct "as-built" data to confirm existing design drawings, determine structural capacity of existing structures when no reliable information on the design of the structure or as-built construction are available, or create new replacement plans. Additionally, seismic retrofits or upgrades to existing structures, bridge deck widening, construction linking new ramps and elevated structures to existing ones, and

drilling or coring through existing decks to install or improve drains, lighting, or safety equipment, all require that deck reinforcement be quickly, accurately, and economically located before any of the proposed work can proceed. Critical reinforcing elements such as post-tension cables, embedded electrical and other conduits, or even superstructure elements that support the deck itself must be located prior to cutting, coring, and drilling so that they are not damaged.

When corrosion rate studies are being performed, or if corrosion activity levels within a reinforced concrete deck are being measured, detailed knowledge about the spatial location(s), depths, variability, and spacing of individual reinforcement elements (rebar) in a deck contribute tremendously to the ability to accurately characterize the severity of corrosion actually taking place. All electrochemical methods either require the presence, pattern, and density (PPD) of rebar to be known, whether on a local, regional, or global scale on the deck, so that confidence levels in the measurements being made can be established. Without sufficient knowledge about the PPD of rebar in a deck, many of the conclusions from these studies are suspect, particularly if they are not supplemented with chemical or petrographic analysis of the concrete, the construction materials, and methods that were used when the deck was built, or other NDT methods capable of verifying their accuracy.

Geophysics is useful for locating individual bars, measuring spatial distances between them, determining rebar depth (often for upper and lower mats) from single side, and quantifying the presence of rebar.

3.4.1.1 Ground Penetrating Radar (GPR)

GPR is the best method to identify presence, pattern, and density of rebar. As discussed above, applications include seismic retrofits/upgrades, bridge widening and tying into existing structure, cutting holes into deck to improve drainage and reduce ponding, particularly if de-icing chemical can cause acceleration of corrosion as they penetrate into deck or membrane, and determine structural load capacity based on PPD of rebar. See section 3.2.1.1 for a discussion of GPR for locating rebar. For vehicle mounted GPR systems, please refer to section 3.4.5.

3.4.2 Rebar Condition/Corrosion

Probably the most serious cause of accelerated degradation or deterioration of the integrity of a reinforced concrete bridge deck is corrosion of the reinforcing steel. It is common knowledge that when regular health monitoring and maintenance is delayed or eliminated on these structures, they inevitably deteriorate or fail prematurely. This makes any repair, rehabilitation or replacement decision more critical and costly, because deterioration is typically at an advanced stage.

Even a good visual inspection program alone does not uncover many early indications of distress that, if discovered, treated, or repaired early, can slow or effectively halt the rapid advance of deterioration. Many of the underlying factors contributing to deterioration cannot be seen. These factors include the variability in (a) rates, amounts, and locations of chloride intrusion into the protective alkaline coating that the concrete affords the steel; (b) concrete

depth from surface to top mat of reinforcing steel in small, localized areas and throughout the deck that contribute to accelerated corrosion or corrosion "hot-spots"; (c) shrinkage cracking "built into" the deck, often caused by high variability in cover and/or excessive cover, providing direct pathways for entry of chlorides through the protective concrete to the reinforcement; (d) quality of concrete materials and placement, as well as finishing, which can affect initial concrete integrity or permeability; and (e) condition of asphalt or other overlay and membrane, or presence of older repairs.

Geophysical methods, used properly, can be very effective to accurately measure some of these parameters, inferring others from the measurements made at or near the deck surface, and significantly enhancing traditional bridge deck evaluations. Unfortunately, geophysical methods are employed quite often when results obtained from other deck evaluations fall short of expectations, or seem inconclusive, i.e., either deterioration quantities are dramatically over- or under-estimated or are suspect, which can result in poor decision making. At such times, geophysics can be very useful, but often it is applied too late and at a time when budgets are already strained.

Geophysics provides its greatest potential benefit at the early stages of diagnosis. Very often, geophysics (NDT) is not employed because other nondestructive, highly subjective techniques, such as chain-drag and hammer-sounding used to identify delamination in decks, are used. They are also considered by many to be good tools for early diagnosis and timely treatment of concrete that has been damaged by corrosion simply because their results are straightforward. They do find damage in a deck when it is quite deteriorated, and they locate the worst surface damage quite well. However, they absolutely are not early-stage diagnosis methods, and are ineffective tools in early-stage diagnosis or detection of problems that should be addressed before deterioration becomes advanced. At that time, chain-drag and hammer-sounding can play a useful role in identifying severely damaged regions on the deck, or they can be used for comparative purposes to illustrate that late-stage damage is being detected by other means.

These two NDT (not geophysical) techniques cannot identify a deteriorated state in concrete that is indicative of early-stage, or onset of internal corrosion; rather, they reveal to some extent the regions within the deck where corrosion is so advanced that more extreme measures must be taken to repair, rehabilitate, or replace the deck, and they are extremely subjective and susceptible to influence from noisy conditions, such as nearby traffic. More realistic early-stage evaluation or screening methods are available, and should be employed at regular intervals.

Figure 69 shows the results of two geophysical surveys. Blue regions on GPR map indicate normal condition. Light blue indicates deterioration threshold with progressively increasing deterioration indications (green, yellow, red, etc.). On the half-cell map, bright orange indicates active corrosion, tan indicates approaching active, green is threshold, gray indicates approaching threshold, and white is normal. Sampling density on half-cell tests is approximately 30-cm spacing between samples. Chloride results support half-cell results and GPR, for the most part (too small to be seen on this image).
Many times, appropriate geophysical (NDT) methods, such as electrochemical methods, GPR, or ultrasonic-seismic tools, are used simply because they are specified in a given

project. By default, the geophysical "experience" is often less than desirable because it is likely to fall short of customer expectations, often because desired results are unrealistic and/or non-existent, or the evaluation is viewed as an unnecessary burden. This typically results in searching for the lowest cost NDT survey method available to meet the "requirement"; and even if a relevant NDT tool is selected, the scope of work is generally not well thought out or designed prior to solicitation of bids. When factors such as traffic control are considered, on top of the ineffectiveness or failing of a poorly selected or designed NDT program, the lowest cost often becomes more expensive than more effective techniques.

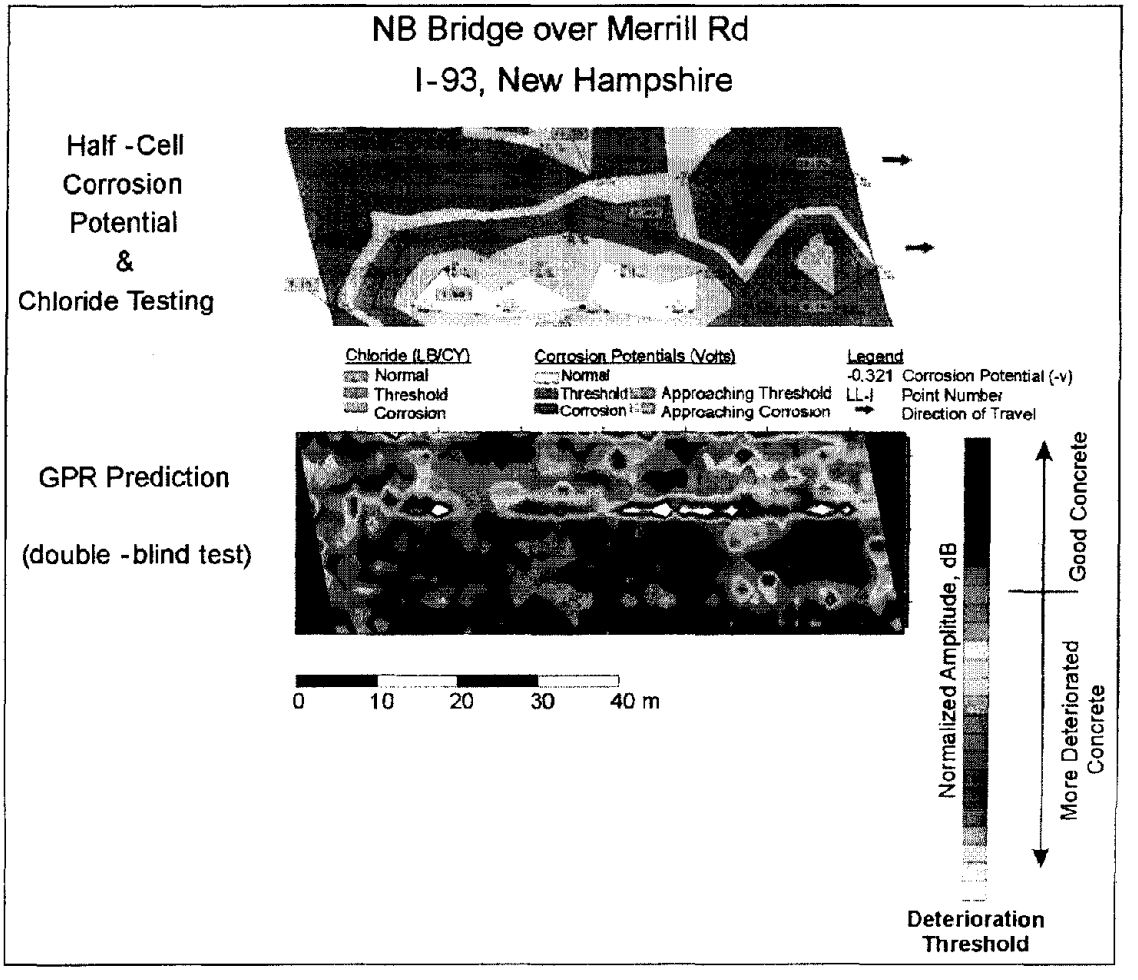

Figure 69. Geophysical method results (Ground Penetrating Radar and Half-Cell Corrosion Potential contour plots) from double-blind test.

3.4.2.1 Ground Penetrating Radar (GPR)

GPR systems are in regular use for mapping corrosion and debonding on bridge decks. See section 3.2.1.1 for further discussion. For vehicle mounted GPR systems, please refer to section 3.4.5.

In this application, GPR image character changes often correlate very well with areas of corrosion of rebar and debonding. It is important to note that GPR cannot identify or verify that corrosion is actually taking place, confirm that rebars within the deck are losing steel mass, or measure or predict the amount of cross-sectional loss in the steel at any given location. However, GPR has several strengths that lend itself to being used as the best method for initial screening for identification of the presence and/or degree of corrosion within a deck.

3.4.2.2 Half-Cell Corrosion Potential

A separate geophysical method includes a semi-destructive (for the most part, nondestructive) electrical technique for assessing potential for corrosion in existing deck structures, and is based on measuring voltage (electrical potential) between the anode (top mat reinforcing bars) and a reference electrode.

Galvanic cells form within regions of the deck that differ significantly in their level of corrosion activity. The half-cell potential method is based on the principle that variations in corrosion rate (activity) among these localized regions, or cells, cause electrical current to move through the deck and are proportional to the electrical potential between the reinforcing steel and the deck surface. This measured potential (mV) is thought to be proportional to the loss of steel mass from the reinforcing bars at any given location within the deck, and can be used as a reliable predictor of corrosion states that exist, particularly when PPD of rebar are well-established.

The anode connection is typically a direct one (electrical clamp) with a wire lead to the instrument, meaning a small hole has to be drilled into the concrete to secure to provide direct electrical contact to the reinforcing steel. The reference electrode is electrically coupled to the bridge deck surface using a copper-sulfate solution in which the other lead is suspended, and a sponge at the bottom of the container (holding the copper-sulfate and suspended reference electrode) allows copper sulfate solution to provide good electrical contact with a clean deck surface.

Measurements of electrical potential (voltage, mV) are obtained at discrete sampling intervals across the length and width of a deck, directly over rebar at known depth. Local variations in rebar depth near each sample location are desirable so that they can be factored into a more precise analysis, as a contour plot of the potential readings is prepared. These potential levels are used to characterize "activity" levels (corrosion states) existing beneath the surface of the deck. The voltage reading at each location, in mV, is interpreted to signify an indication of the likelihood that corrosion activity is at or near pre-determined levels, or corrosion states.

It is best used in combination with other methods, as summarized below, to obtain optimum results:

- GPR can be used to provide information about overall condition of the deck, indicating most likely locations (and severity levels) of deterioration—so that half-cell measurements can be focused to specific regions rather than used to characterize

an entire structure; this is a very economical approach to use, particularly when large decks or a multiple number of structures are to be characterized. GPR also provides complementary PPD information about the rebar in the deck, directly useful as input into the half-cell corrosion potential analysis.

Other electrochemical methods, e.g., acoustic emissions, etc., either estimate (and verify) corrosion activity level, or provide fairly good estimates about the corrosion rate of steel at specific areas within the deck.

3.4.3 Concrete Condition/Integrity

Concrete condition can be broadly defined as the following: (1) Concrete in good condition typically is free from, or has relatively minor indications of, internal corrosion-related problems as evidenced by visual inspection, mechanical testing, chemical sampling or petrography, acoustic (geophysical) methods, electrochemical testing and analysis, and/or investigations using ground penetrating radar. (2) Concrete is also relatively strong, mechanically, shows little evidence of damage or even cracking, appears very durable after considerable exposure to traffic and the environment, and is free from any significant defects in design, materials, and workmanship or loading. Again, this is evidenced by visual inspection, mechanical testing, chemical sampling or petrography, acoustic (ultrasonic-seismic) methods, or investigations using ground-penetrating radar.

Although corrosion can definitely be caused or exacerbated by the quality of construction, it is mostly a product of two mechanisms: corrosion induced by entry of chlorides into a concrete deck from the top surface because of application of de-icing chemicals, and corrosion induced by entry of carbon dioxide into warm, moist concrete, which forms carbonic acid and causes corrosion to accelerate due to a process known as carbonation. The end result is typically cracking, delamination, and spalling of concrete as it detaches from the reinforcement mat(s) within the deck and seriously affects the ability of a structure to reach its design life if measures are not taken to periodically monitor the internal, electrical, and chemical changes that have taken place.

Moisture entry into the concrete and its retention, moderate-to-high temperatures, and availability of oxygen provide the raw materials and conditions required to enhance corrosion activity. The complete lack of oxygen or moisture in a structure is enough to halt it, but this is typically not a realistic scenario.

Concrete that is well designed, contains high-quality materials, has a low water-cement ratio, and properly designed and entrained air content experiences relatively few problems when it is well maintained (preventively) and its condition is regularly monitored. Other factors that can determine the design life of concrete include whether the concrete was well placed, properly vibrated, finished, and cured in a structure where care was taken in fabricating the reinforcement in a uniform fashion according to specifications, and formwork was installed carefully as part of the construction process. Its initial condition—quality and integrity, strength and durability, appropriate and uniform cover—will ensure that the protective, alkaline concrete barrier surrounding the steel prevents early entry of chlorides, provides a difficult path for entry of water and oxygen into the concrete, and endures damage from

cyclic, flexural loading that induces cracks into the concrete surface or freeze-thaw damage caused by daily extremes in temperature above and below the freezing point of water. In short, its quality prevents excessive damage to the structure. Without initial quality assurance or baseline condition assessments using the appropriate full-coverage NDT method, however, initial quality is unknown.

Effective baseline condition evaluations include GPR and ultrasonic-seismic methods, properly designed so that they will duplicate future assessments used for diagnosing concrete condition/integrity as the structure ages. Once the structure is in-service for 5 to 10 years and before chloride intrusion has a chance to encounter the steel, a follow-up diagnosis, performed exactly like the first one, but perhaps including additional NDT and/or ground truth, must be performed to ensure early detection of any problems. If the initial baseline assessment indicated any structural defects, flaws, significant variation in concrete cover, or deviations in rebar PPD from design, earlier secondary diagnoses may be warranted.

Regardless of when serious NDT methods are employed on a regular basis for monitoring the health of a structure health as it degrades, the cost-effectiveness of early detection far outweighs the price paid in repairs, rehabilitation, or replacement during the life of any structure. The sooner the baseline and follow-up diagnostic schedule begins, the greater its impact and long-term, economic benefit will be.

Regular evaluations will also ensure that the structure is properly diagnosed each time a preventive maintenance measure is decided upon and implemented, removing almost all the concern about NDT evaluation limitations that exist when NDT is asked to diagnose a structure only when it is in a serious state of deterioration. These evaluations should always incorporate some degree of ground truth analysis, even if more limited at first.

Appropriate NDT never costs millions over the life of a structure; repairs and lost service life do. Ineffective diagnosis and timing are typical, not unusual, of current diagnostic practices, as well as the failure to use the best preventive NDT measures in the right manner during the life of a structure.

Two common nondestructive, acoustic, methods are widely used to assess the concrete integrity in existing decks and to determine the extent and quantity of deterioration. This information will be factored into an evaluation of its condition state and ultimately lead to a preventive or corrective maintenance decision. These two methods are chain dragging and hammer sounding, where either a heavy chain at the end of a hollow pipe is literally dragged across a bare concrete deck, or a rock-hammer or similarly designed hammer is used to repeatedly strike its surface. Both require the user to detect delaminations by the change in pitch or qualitative "thunk" that the instrument makes as it is used to test the integrity of the deck.

Both are highly subjective, vary from one operator to the next, and are subject to changes in environment (noise, like traffic). "Hollow-sounding" areas are marked on a deck with paint, and their respective sizes and locations are drawn onto a plan-view map representative of the surface area of the deck.

Unfortunately, however, because the "chain-drag method" is simple to use and understand, and it does identify definite serious damage on the deck, it is erroneously viewed as the "standard" by which to evaluate other methods that are typically more responsive to early-stage detection of deterioration. When another NDT method reports deterioration that the chain-drag does not confirm, the other method is considered flawed.

3.4.3.1 Ground Penetrating Radar (GPR)

The preferred method for identifying regions where deck deterioration is taking place, and using that information to guide evaluation is ground penetrating radar (GPR). For vehicle mounted GPR systems, please refer to section 3.4.5.

GPR should not be assumed to be directly sensitive to or even geared toward direct identification of delaminations, even though it is often misrepresented that way. Therefore, it is often deemed inappropriate for identifying the onset of deterioration even if it identifies larger areas of deteriorated concrete that include many individual delaminations.

In this case, GPR is said to "overestimate" delamination, when in reality it is helping identify areas that are already seriously degraded and will become either delaminated or otherwise deteriorated in due time. At other times, when a chain-drag or hammer sounding identifies a defect or delamination, GPR "misses" delaminations or spalls caused by means that are not corrosion-related (see discussion on incipient spalling in section 3.4.4). When it misses "delaminations," it is deemed unable to detect deterioration within the deck.

Not all delaminations are caused by electrochemical processes that GPR is sensitive to, and GPR is not suited toward identifying the symptom (delamination, crack, or spall) that results from these various deterioration mechanisms (refer to concrete condition in section 3.4.3.

GPR does not detect delaminations themselves in decks, unless they are extremely shallow, air-filled, and very thick (0.6 cm) or more. At that thickness, they would already be detectable by other means, loose, or reflect spalled areas that have simply not yet 'kicked out' of the deck surface. Even at 0.6 cm or thicker, these air-filled delaminations are not easy to identify as such. GPR will only measure delaminations directly at about 0.3 cm or thicker and completely water-filled. Water slows down the signal enough so that GPR is responsive to its presence, and it also causes the reflection from a thick enough delamination (water-filled) to be imaged or seen more directly in the data.

What GPR does do well, and why it is valuable in detecting both the onset of deterioration or advanced stages of it is respond to electrical changes in deteriorated or chloride-infiltrated concrete that result from (a) chemical changes in the concrete that cause its dielectric properties to vary from place to place, and (b) changes in electrical properties of the deck (electrical conductivity) that cause GPR to either reflect more energy back toward the surface at an abrupt, conductive interface, or disperse the signal (attenuate it) more rapidly so that little or none can return to the surface to be measured. Moisture variations in the deck associated with corrosive conditions, particularly when a conductive environment is present or electrically conductive agents (such as chlorides) have infiltrated, are also picked up by GPR.

Each of these variables within the deck that changes or affects how a GPR signal propagates through it and modifies how it reflects or penetrates at various material boundaries, contributes to signal variation that can be measured and compared at every location the GPR survey samples the deck. What makes GPR so valuable then is that it is an indicator that can identify quantities and locations of impending or advanced corrosion conditions that will cause the following: (a) reinforcement to corrode, (b) concrete integrity and chemistry to change, and (c) damage (such as cracking, delamination or spalling) to concrete.

The ability of GPR to detect cracking, delamination, or spalling directly is coincidental to its ability to identify impending and advanced corrosion-related conditions within the interior of a deck and identify where they most likely exist. If used properly, it can perform these tasks extremely well. However, it is best used in combination with other methods, particularly acoustic ones like ultrasonic-seismic geophysical methods (SASW/impact-echo), as part of a regular inspection process that diagnoses early stages of deterioration so that preventive measures and maintenance can be taken or applied at the appropriate times in service life of a deck.

The main tools for concrete condition evaluation are seismic methods and GPR. USW, SASW and IE methods can be used to measure modulus and stiffness of concrete. In some cases, it may be useful to employ GPR as a rapid reconnaissance to qualitatively find problem areas that can then be studied in more detail with seismic methods.

For detailed description of these methods in this application, please refer to sections 4.1.3 and 4.1.4, Chapter 4 – Pavements.

3.4.3.2 Impact Echo (IE)

For detailed description of Impact Echo in this application, please refer to section 4.1.2, Chapter 4 – Pavements.

Interpretation: Impact Echo data are interpreted for depth associated with the resonant frequency, just as in other applications. In the case of condition measurements, cracks or debonding within the concrete layer will show up as depths that are much too small to match the whole thickness of the structure.

Advantages: This method provides depth to the first break in the concrete. In the case of old concrete, identification of an impact echo break at less than the structure's original thickness indicates cracking, or some other problem.

Limitations: Interpretation of the breaks measured is not always straightforward. Also, this technique only identifies major problems such as cracks debonding.

3.4.3.3 Surface Wave Methods: SASW/MASW and USW Spectral Analysis of Surface Waves (SASW)/Multiple Channel Analysis of Surface Waves (MASW) and Ultrasonic Surface Waves (USW)

For detailed description of these methods in this application, please refer to section 4.1.3, Chapter 4 – Pavements.

Another grouping of geophysical techniques measures initial concrete condition (thickness and/or integrity) by integrated ultrasonic-seismic methods:

1. Spectral analysis of surface waves (SASW), where ultrasonic body-waves (UBW) and ultrasonic surface waves (USW) are used to determine mechanical properties of the concrete using an impact source and two sensors—so that propagation velocity of the sound energy can be determined—allows elastic and shear moduli to be calculated, assuming a value for Poisson's ratio and a relationship between the P- and S-wave velocities in concrete (reliable assumptions to make based on knowledge of the design strength). Stiffness (integrity) and strength can then be determined for deck structures, and can be verified by some destructive sampling, if required.

2. Together with Impact-Echo (IE) methods, an impact source and a single sensor can determine travel time between the top and bottom surfaces of a deck, or to and from an internal defect or around it to (a) measure deck thickness, and (b) establish deck integrity. These methods are useful during a QA evaluation on a new structure, as part of a baseline survey for comparison with future tests, or as part of a comprehensive condition assessment on an existing deck.

3. Utrasonic seismic devices, such as the Portable Seismic Pavement Analyzer (PSPA), can be successfully used to assist in evaluating bridge deck condition, alone or in tandem with other geophysical and/or ground truth sampling (see figures 79 and 80). It is always recommended, however, to use a multiple-method approach.

Ultrasonic-seismic methods, like impact-echo and SASW used in combination, are very useful at identifying already-damaged locations in the deck (see figure 70). Unlike chain dragging and hammer sounding, these geophysical methods identify this damage at early, moderate, and late stages of development. The common "NDT" methods of chain dragging and hammer sounding only detect those flaws that have developed to an advanced stage, and they finally become audible to the human ear. Effective preventive maintenance and/or treatments, such as cathodic protection, should already have been performed by the time these methods reveal problems.

Furthermore, localized repairs identified directly by hammer-sounding and chain-dragging are limited to application on smaller regions than the deteriorated zone(s) causing these defects, particularly when corrosion is what initiated the problem. Repeated maintenance at or near the same locations as previous maintenance applications indicates that the methods used to identify the deterioration are insufficient, and require a better ability to identify early-stage and moderate-stage development of mechanical failure.

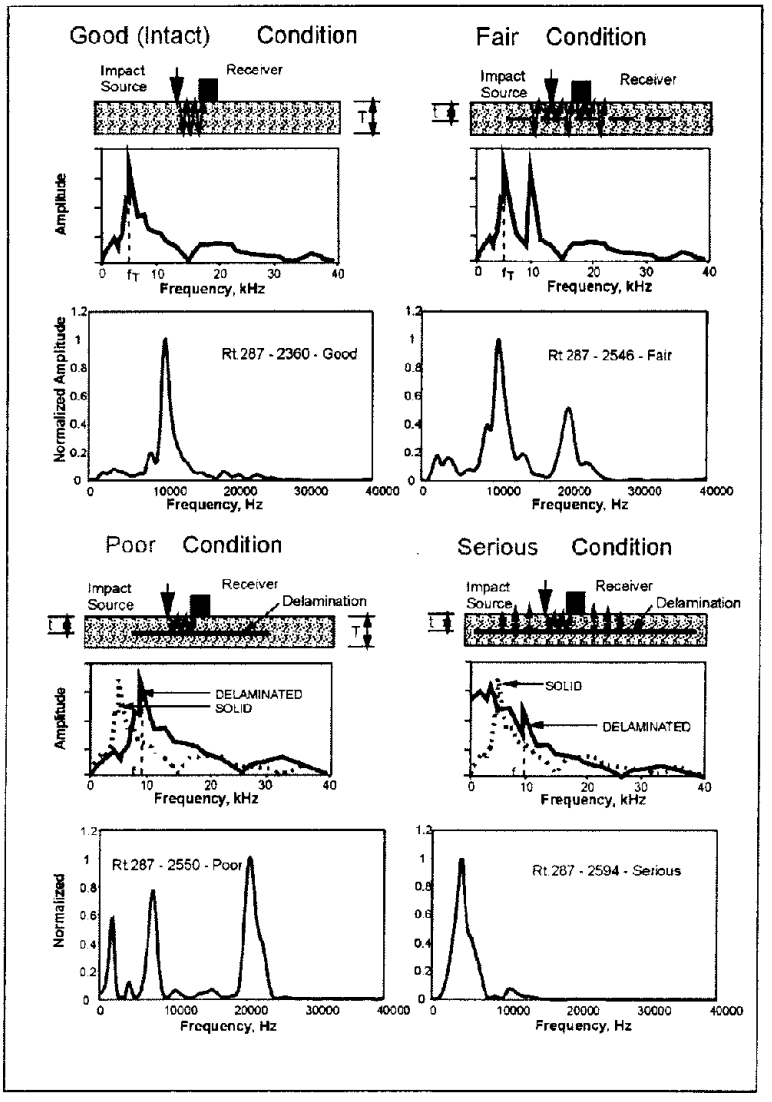

Figure 70. Portable Pavement Seismic Analyzer (PPSA) correlated to initial, moderate and severe delamination development (fair, poor, serious), respectively. Results plotted on plan-view map and compared with chain drag.

These ultrasonic-seismic techniques perform that task well; however, they do require lane closure as do chain dragging and hammer sounding. Sampling (although relatively speedy, considering the quality of the end-result) at lower speeds with any degree of efficiency or close proximity from sample-to-sample, can be a bit time-consuming when compared with a method like GPR. However, these methods can identify mechanical defects (like delaminations and incipient spalls) to confirm GPR-predicted deterioration interpretations, and they complement GPR in local regions where these defects may have been caused by mechanisms not related to corrosion.

A better approach is to survey the entire deck with GPR (preferably either Method One or Two), and focus on identifying locations on the deck where these ultrasonic-seismic methods can be applied. Characterizing a few, smaller regions using these acoustic methods will allow for a comparative analysis of the results (GPR and ultrasonic-seismic) to be performed.

It will also reveal the extent or degree of severity of mechanical damage that exists outside the regions identified by the GPR prediction.

This information can also be useful in identifying other deterioration mechanisms (perhaps alkali-silica reaction, defects caused by materials and workmanship, design flaws, mechanical damage due to a combination of the above, and repeated cycles of loading) that are likely causing some of these defects. This should prompt further discussion on how the deck condition should be investigated to uncover the root causes of other problems that are nearly as significant, or even more so, as any corrosion-based problems.

Interpretation: In bridge deck applications these methods are used to measure modulus just like in pavement applications. The purpose is to get a good quality measurement of modulus. Degraded concrete will give a lower modulus measurement. Problems can be identified early with these techniques since action can be taken before major failure occurs based on degrading modulus measurements, especially if periodic assessments are done for comparison over time.

Advantages: This method gives concrete quality without coring.

Limitations: None.

Combined Approach

The two methods mentioned previously can be used in much the same way that a combined GPR/coring or GPR/sounding evaluation is approached. The results of the localized sounding, performed in regions that represent the total degree of variability identified within GPR contour plots, but in a relatively small, localized area with respect to the total size of the deck, are used to verify and/or complement GPR interpretations of deterioration threshold levels on the deck. Initial, moderate, and advanced stages of delamination should correlate to some degree with the contour plots on a plan-view GPR presentation of the surface of the deck. By analyzing and comparing the two, appropriate deterioration threshold(s) can be selected from existing contour plots on the GPR map and be used to designate boundaries where relatively sound concrete meets locations that are undergoing either severe, moderate, or initial deterioration.

Incorporating the mechanical (acoustic) analysis into the results obtained by the full-coverage, electromagnetic one results in a very good-to-excellent, prediction tool (figure 71). This final interpretation can be used very effectively as a baseline condition assessment early in the life of a deck, a later investigation several years into the future whose purpose is to identify the onset of deterioration, or a condition assessment used to identify the degree and severity of corrosion already existing beneath the surface of a deck.

NDT surveys should be performed so that full-coverage, objective screening tools that best identify the predominant conditions existing when deterioration manifests itself (GPR) are followed by geophysical (NDT) methods best-equipped to identify defects that exist after this "condition state" is serious enough to cause damage (ultrasonic-seismic).

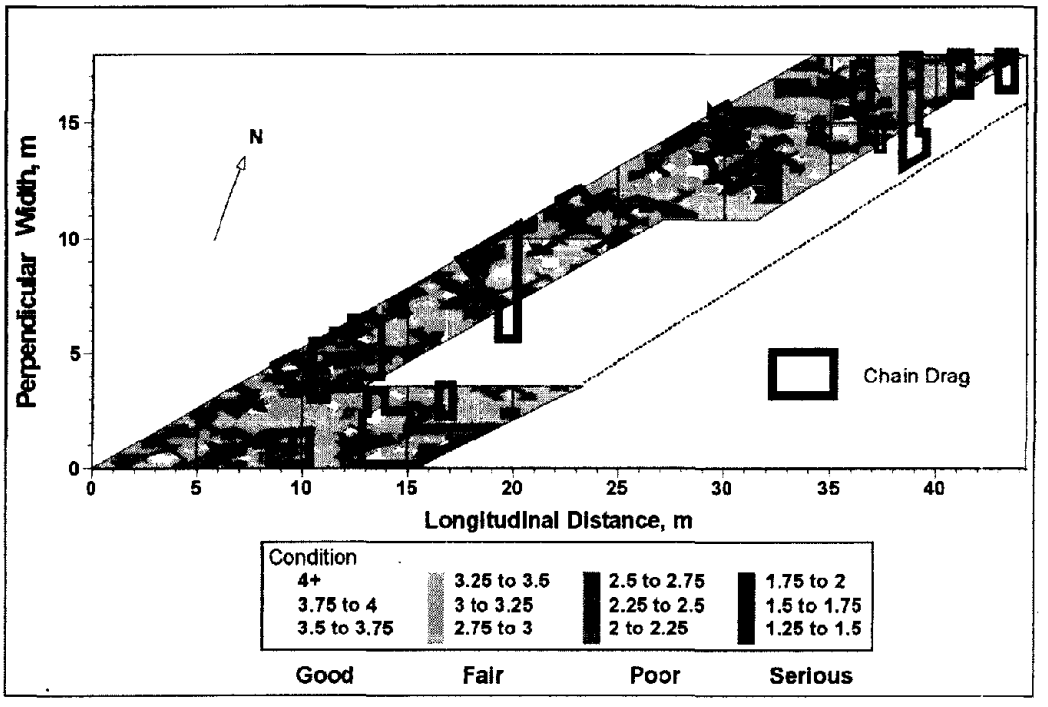

Figure 71. Condition levels obtained by using integrated Ultrasonic-Seismic method.

3.4.4 Incipient Spalling

Spalling is the actual separation of concrete from the reinforcement or from other concrete in a manner where separation is complete. Spalling occurs as a result of many different physical, chemical, or electrochemical processes that affect a deck (refer to sections 3.4.2 Rebar Condition/Corrosion, 3.4.3 Concrete Condition). Many times, flaws built into the deck or the nature of loading are more dominant in causing spalling than corrosion of the reinforcing steel. Generally, however, corrosion is the primary culprit. Most often, spalls detach and drop directly onto the pavement or ground surface beneath a deck, or they "pop-up" on the upper surface and reveal themselves as the potholes. Too often, however, they actually do cause serious accidents on highways beneath deck overpasses, result in safety concerns, or become costly repairs that cause the Government's liability insurance rates and taxes to increase. Beside these obvious negative impacts from detachments, spalling represents the final state of deterioration in any mechanical, chemical, or corrosion process that causes internal deck damage.

NDT methods are extremely valuable for early detection, as well as to diagnose a serious problem that may not be visually evident, but will ultimately result in spalling. By the time incipient spalling occurs, cumulative life-cycle maintenance costs are probably well beyond what they should be, particularly if this is a first attempt at NDT diagnosis prior to repair. Continued maintenance of this sort will undoubtedly reduce the long-term life and value of any structure. Unfortunately, our decks have deteriorated over the last 40 years to the point where a backlog in maintenance emergencies is increasing; however, use of appropriate NDT

in the recommended fashion will save considerable time and money in overall structure maintenance regardless of condition.

A proper evaluation methodology program based primarily on nondestructive geophysical methods and selective sampling leads to sound, economic engineering and decision making. The only strong argument against initiating a continued NDT-based diagnostic program is if the functional obsolescence of a structure is imminent, meaning it can no longer serve the purposes warranting its continued existence beyond a specific point in time. Designing a suitable maintenance program that will economically and safely extend a bridge's life to its predetermined end, without added burden or cost, is sound engineering practice.

Regardless of how well such a structure can be maintained or its service life economically extended, or whether it can be upgraded to design code or retrofit to meet current seismic standards, it may already be known the structure has to be replaced or eventually taken out of service entirely. When a structure has to be significantly enlarged or modified in a cost-prohibitive manner, or an alternative route more suitable to traffic needs is already being designed and built, often the costs related to the optimized life cycle of a structure for the sake of its existence pale cannot be justified. Optimal diagnostic and maintenance programs aimed at long-term economic benefit are obviously not required in this singular exception. However, NDT may judiciously be employed as part of a pro-active maintenance approach if the known life of the structure is 5 to 10 years distant, and short-term maintenance costs are considered beneficial prior to selecting a suitable maintenance regimen.

3.4.4.1 Ground Penetrating Radar (GPR)

Please refer to section 3.4.3.1 for detailed description of GPR in this application. For vehicle mounted GPR systems, please refer to section 3.4.5.

It is important to note that GPR docs not have inherent ability to image concrete delaminations. Rather, GPR is sensitive to the electrical and chemical changes that are present when an active corrosion environment exists within a deck. Interpretations of GPR data rely on knowledge about how these electrical and chemical changes will impact the characteristics and signal quality of a GPR wave as it propagates through the deteriorated (or sound) concrete, prior to its return to the sensor. Measurements of these signal characteristics are then used to make inferences about the condition or degree and extent of deterioration beneath the surface of a deck, which can be mapped on a contour plot representing the plan view of the deck.

3.4.4.2 Impact Echo (IE)

Please refer to section 3.4.3.2 for detailed description of IE in this application.

3.4.4.3 Surface Wave Methods: Spectral Analysis of Surface Waves (SASW)/Multiple Channel Analysis of Surface Waves (MASW) and Ultrasonic Surface Waves (USW)

Please refer to section 3.4.3.3 for detailed description of ultrasonic surface waves in this application.

3.4.5 Vehicle Mounted Ground Penetrating Radar (GPR) Systems

Basic Concept: Vehicle mounted GPR is a rapid, continuous data collection system that obtains highly accurate and repeatable data as it is moved over a pre-defined path. These GPR systems are used for condition evaluation of new and existing decks and pavements.

Data Acquisition: There are basically three primary GPR methods used for data collection and analysis:

3.4.5.1 GPR Method One: (High-Resolution, High-Speed Survey (48-72 km/h) Using Dual-Polarization of 1 GHz Horn Antennas

This method employs two 1.0 GHz air-coupled (horn) antennas (sensors), mounted behind the vehicle-in line, and in a manner where one antenna is responsive to signals influenced primarily by the longitudinal steel, and the other is responsive primarily to the transverse steel. In Method One, signals from both sensors are used, with their offset in longitudinal position along the same path accounted for, to simulate a higher resolution, ground-coupled antenna of Method Two used in the lower speed, high-resolution surveys.

- Method One can be applied at speeds between 48 and 72 km/h using a data acquisition unit, where both antennas collect data at rates between 400 and 500 scans/second simultaneously (pre-July 15, 2002 models only, in U.S.). These surveys can be collected using little or no traffic control (typically, an attenuator with a sign board). Using older, two-channel systems, survey speeds vary from 16 and 24 km/h, often requiring lane closures.

- Method One is an economic approach for all applications at both the project level and network level, particularly for QA verification inspections on new structures. An exception might be precisely locating reinforcement and measuring depth. It is the preferred approach for bridge deck condition assessments on existing structures because of a combination of its accuracy and speed.

Figure 72 shows the dual-polarization deployment of Method One (high speed, high-resolution), with the antennas mounted in-line. Currently, antennas are positioned for data collection in the right half of any given lane. Depending on current lateral location of the laser (or camera) positioning system, this survey line will be collected either 0.3 m, 0.9 m, or 1.5 m to the left of any given pavement stripe (lane marker) on which the laser (or camera) is focused. Lateral positioning of lines is within ±5 cm on any desired spacing interval.

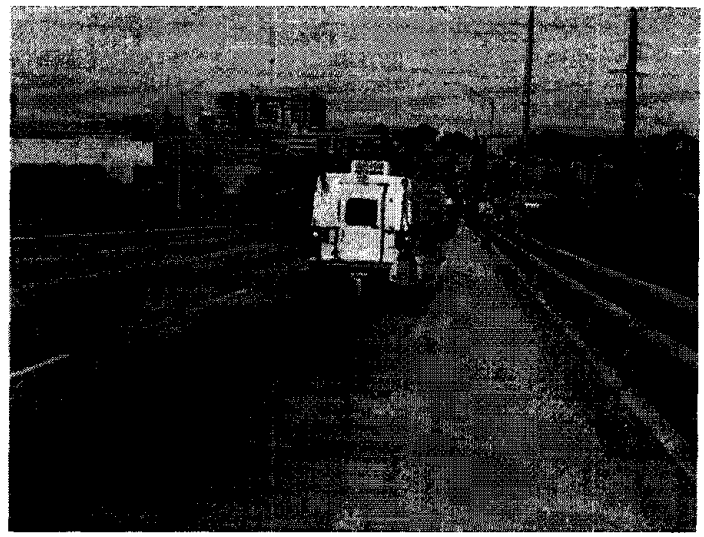

***Figure 72. Ground Penetrating Radar Method One: high-speed, high-resolution, Dual-Polarization Horn Antenna method.* (GEOVision Geophysical Services)**

3.4.5.2 GPR Method Two: (High-Resolution, Low-Speed Survey (8-16 km/h) Using One or More 1.5 GHz Antennas Each Collecting Data on Unique Scan Paths

This method uses a single 1.5 GHz antenna traveling along each survey line (although several can be placed beside each other at a maximum spacing of 60 cm) in a manner where the transverse steel in the top mat is crossed perpendicularly, and its reflection amplitude is accurately measured. It requires no signal modifications, and simulation of a higher frequency antenna is not needed because this antenna has been determined to be the most sensitive to conditions within a deck that are coincidental with corrosion-induced damage, and it easily discriminates between the signals generated from the desired transverse steel and signals generated from longitudinal steel (undesired) in the top mat of reinforcement.

1. Method Two is typically applied at speeds near 8 km/h, perhaps up to 16 km/h, depending on the surface condition of the deck and the number of antennas, and/or the number of data acquisition units used to sample the deck and control the sensor(s).

2. Method Two is useful primarily as a thorough, project-level evaluation tool, a QA verification tool (on new construction) or a baseline condition assessment instrument (early in the structure's life).

GPR Method Two is practical and/or economical only on relatively short bridge decks, and in rural locations or limited metropolitan areas where either light or moderate traffic volume and lane closures do not pose problems for transportation officials (figure 73). It provides highly accurate GPR survey results whose deterioration predictions for quantity, location, and extent cannot be exceeded. However, its slower data collection speed necessitates lane closures, making it less attractive in congested urban areas or on network-level projects where many decks have to be assessed in a short period of time, or at a lower cost. Survey speeds are limited to about 8 km/h on most bridge decks, but can be increased to about 16

km/h when deck surfaces are free of debris, potholes, or rough patches that might damage the antenna, or de-couple it from the deck surface. Also, this method requires the shallowest reinforcing bars in the upper steel mat be oriented perpendicular to the survey direction so that unbiased and accurate imaging of this layer and measurement of its properties can be performed. It is economically limited to those decks where transverse steel is tied above longitudinal steel in the upper reinforcing mat.

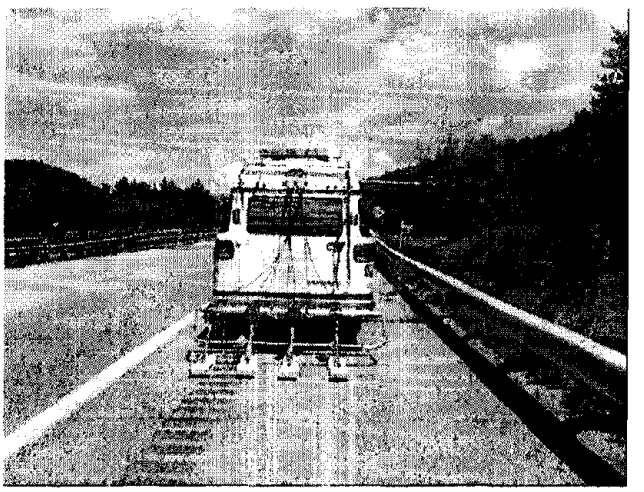

Figure 73. Ground Penetrating Radar Method Two: low-speed, high-resolution using four 1.5 GHz antennas spaced equal distance apart. **(Geophysical Survey Systems, Inc.)**

3.4.5.3 GPR Method Three: Lower-Resolution, High-Speed Survey (32-72 km/h) Using Single-Polarization 1 GHz Horn Antenna.

A distinctly separate high-speed GPR survey, using a single-polarization deployment of a single, 1.0 GHz horn antenna (or multiple antennas that are mounted on booms so that the sensors do not scan on the same paths), is probably the most common method of GPR evaluation. This method has been around the longest and provides good, overall results. It is used to rank a large number of decks based on a condition rating (good, fair, poor, etc.), and it provides fairly accurate deterioration quantity assessments that can be used to help decide among various maintenance/rehabilitation strategies on individual projects, or estimate project budgets.

Like the high-speed, high-resolution GPR survey that uses a dual-polarization deployment of two-horn antenna, a single-polarization deployment has the advantage of speed. More deck coverage, often several times as much (or many decks), can be surveyed in a single day even if the decks are open to traffic or separated by several kilometers of roadway. Unlike the dual-polarization method, however, accurately locating zones of deterioration with a high degree of confidence and pinpointing the boundaries between sound and poor concrete is not a reliable outcome of a single-polarization (high-speed) survey.

- This method is more traditional in terms of its longevity that uses only a single, in-line antenna, deployed at an orientation where it is sensitive to the reinforcing steel placed in either the longitudinal or transverse directions within the deck.

- This method is accurate for estimating deterioration quantities that can be used to (a) rank decks based on overall condition when many are being surveyed for comparison and future planning (network-level), or (b) estimate deterioration quantities at a level sufficient for planning overall budgets (project-level).

- It has been used to survey more decks than any other GPR method currently used; however, the other two methods cited above have been in existence (and under development) only for the past 5 years.

- It cannot be used reliably to plan daily maintenance activities or pinpoint deteriorated zones on the deck that may require additional evaluation, maintenance, or both.

- It can be used as an effective screening tool, in an economic fashion, for identifying candidates (decks) that should undergo further NDT and/or destructive evaluation.

All three methods are useful for different applications, with Method One being the most practical for all-purpose GPR work, although there are some variables affecting economic application of all methods that may impact why one method is selected over another. These will not be covered here. Some general applications are highlighted:

- A condition assessment survey can be performed using either GPR Method One or two, for the purpose of accurately predicting degree, extent, and location of deteriorated regions within the deck (preferable to GPR Method Three, which has limited value for isolating deterioration zones with accuracy and precision on a deck's plan view).

- GPR is sensitive to the electrical and chemical changes, even relative changes in moisture or intrusion of chlorides, that have occurred at all regions where the deck is surveyed.

- It can be used to accurately locate and establish presence, pattern, and density (PPD) of rebar (even depth) very simply and accurately, allowing better interpretations to be made from half-cell corrosion potential data (which identifies levels of potential corrosion activity within a deck, electrochemical analysis methods that estimate corrosion rate and mass loss, etc). Knowing local variability in PPD of rebar, including variability in cover or even depth to rebar at each sampling location using these methods, improves the confidence in the predictions made from these methods.

- The condition assessment described in item (1) on this listing (whose product is contour map) can be used to identify locations that can best confirm that (a) corrosion is taking place in predicted areas, and (b) rebar depth and position variations are accounted for in each region where these measurements are made. The condition assessment can also be used to make global corrections on any half-cell, electrochemical, or other test designed to identify and quantify the existence of corrosion of the deck steel.

Data Interpretation: GPR Method One yields nearly identical information to the Method Two 1.5 GHz ground-coupled sensor data, yet surveys can be carried out without the need for lane closures at speeds between 48 and 72 km/h. Typically, a chase vehicle following the GPR survey vehicle is the only traffic control requirement in most states. Figure 74 compares the two methods.

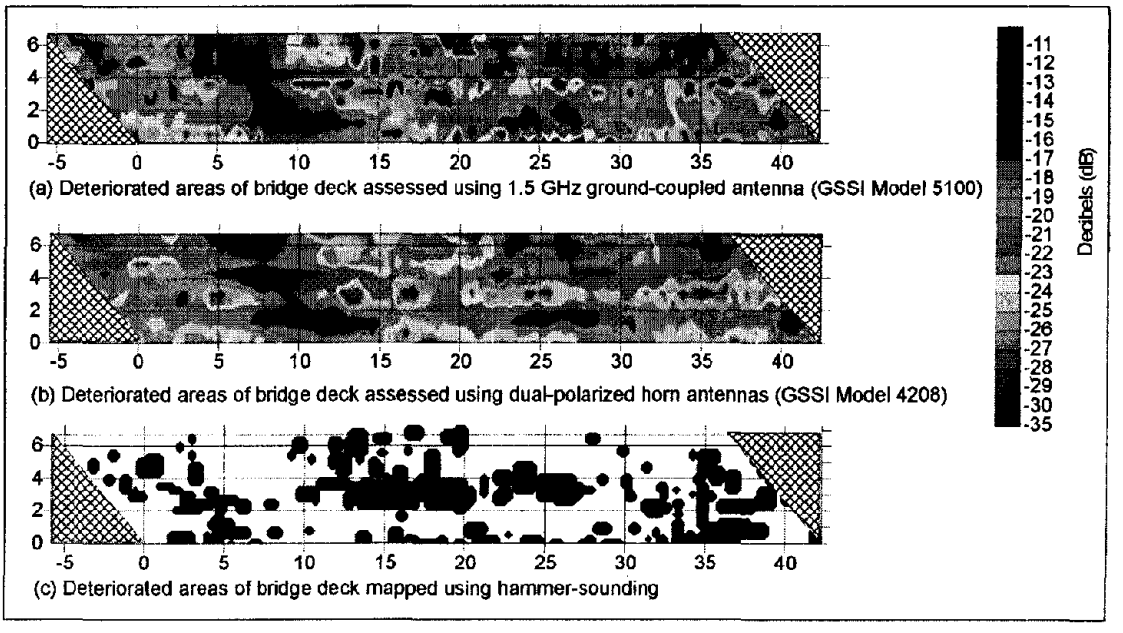

Figure 74. Comparison of Ground Penetrating Radar Methods with "ground truth": (a) method two (low speed, high-resolution, 1.5 GHz), (b) method one (high speed, high-resolution—dual polarization), and (c) delamination map produced from hammer-sounding the deck after overlay was removed. Both Ground Penetrating Radar data sets were collected and predicted prior to asphalt removal.

Advantages: Because of its unmatched imaging capabilities and speed of operation, GPR is the preferred method for condition evaluation of new and existing decks and pavements.

Limitations: FCC limitations restrict the use of the data acquisition units purchased after July 15, 2002, to 100 KHz; therefore no new vendors in the U. S. will have this capability until these regulations are relaxed. Also, it prevents the only manufacturer of the equipment and software for GPR Method One from selling data acquisition units (in the U. S.) that can function at the high data collection rates required to perform this survey (upwards of 400 scans/second/channel on a two-channel system that can operate two antennas simultaneously).

Understanding What a GPR Survey Cannot Do: Once this is understood, the basics behind what a well-designed survey can and will do are recognized, expectations will begin to match capabilities, and more confidence in the technology will begin to be established, as it should.

Although GPR can be very successful at identifying delaminated areas on a deck, or its results can correlate extremely well with half-cell corrosion potential tests, even maintenance

reports that validate the accuracy of its prediction capabilities, it cannot distinguish among any of the following symptoms of an active corrosion process:

a) Corroded reinforcement.

b) Delaminations, unless water-filled (and 0.3 cm (1/8-inch) thick or greater) at the time of the survey.

c) Spalling, unless water-filled and 0.3 cm (1/8 in) or thicker during the time of the survey.

d) Punky, deteriorated concrete that has lost much of its compressive, tensile and shear strength.

e) Otherwise moist, chloride-impregnated concrete.

It is important to make these distinctions, so that realistic expectations of survey results will predominate the current school of thought within the industry. Currently, most people accept that GPR is used to find delaminations, and that is an incorrect assumption. Rather, GPR is an ideal instrument for rapidly identifying that the environment for corrosion-induced damage exists within a deck, and the right methods can also be used to pinpoint and establish deterioration threshold levels and boundaries on a partially or almost fully deteriorated deck. When used as the primary NDT method in a comprehensive diagnosis, it provides important information that allows other NDT or destructive sampling to be utilized in a much more economic, efficient, and accurate manner, further improving the quality of the GPR results.

Proper Use of GPR Results With Other NDT Methods or Destructive Sampling

The value of all three GPR methods is significantly improved and should always be performed with additional "ground truth" (better called destructive examination) or nondestructive testing as supplementary information. A calibration of sorts can then be used to validate an initial interpretation and determine an accurate deterioration threshold, which will then be applied to the resulting relative deterioration map for an improved, final interpretation (contour map). Otherwise, expect the accuracy in the ability of GPR to estimate overall deterioration quantity on a deck and define locations of deteriorated zones and determine their physical boundaries to diminish, often significantly.

Typically, coring, half-cell corrosion potential testing (and contour-plotting of the results), or other destructive techniques, such as chloride ion content sampling, are performed in significantly limited quantities using guidance from the GPR results. Other NDT methods, and visual underside inspections of the deck, may also be used for this purpose, complementing the GPR data by providing information that supports or refines the initial GPR analysis. These geophysical methods may include ultrasonic seismic (SASW) techniques, such as ultrasonic body-wave (UBW), ultrasonic surface-wave (USW) and impact-echo (IE), alone or in combination. Although half-cell corrosion potential is typically thought of as a semi-destructive analysis technique because the lead at the anode is physically attached to the upper reinforcement mat for good electrical contact, it qualifies as a geophysical method because of the nature of its underlying principles. New equipment

under evaluation does not require drilling into the deck to attach the (anode) lead so that it truly becomes a nondestructive, geophysical technique.

IMPORTANT: Using previously obtained data from cores or other sampling/testing results generally does not enhance the GPR analysis much, if at all. Sometimes, depending on the data, a GPR analysis is better off without it. In order for these data to be useful, they must be obtained after the GPR survey takes place and must be sampled (a) in regions where GPR contour plots show relatively uniform contour levels (not steep contour gradients), (b) at several contour levels representing varying degrees of relative deck deterioration on these initial plots, (c) at control points where little or no deck deterioration is initially expected to exist based on the GPR data and the experience of the interpreter, and (d) redundant contour levels representing (a), (b) and (c) above.

CHAPTER 4 PAVEMENTS

In this chapter, geophysical or nondestructive test (NDT) methods used for condition evaluation of new and existing pavements are discussed.

Pavement condition monitoring is an essential component of pavement management, and geophysics has proven useful for objective, network-level pavement condition evaluation as well as early stage deterioration detection, whether the deterioration manifests itself through material degradation or defect generation. Geophysics is also beginning to play a more critical role in quality assurance verification of new construction and in project-level condition evaluations of existing pavements.

Geophysics can yield significant useful information for a pavement condition assessment, particularly if the proper method(s) are selected and implemented at the appropriate intervals. The more successful and/or promising methods are discussed here in order of their current overall value toward solving a variety of pavement-related problems.

A geophysical survey method that provides useful, objective information about the relative condition of the various areas on a pavement structure is generally most valuable when it is used prior to making other important decisions. These decisions include deciding whether other NDT, destructive sampling, and laboratory testing and analyses are needed to provide a better evaluation, or choosing between complementary evaluation techniques. If approached in this manner, geophysical techniques can and will supplement any traditional pavement structure evaluation. These techniques add little to the overall price of diagnosing the structure, and the information provided will help minimize the overall inspection, maintenance, or replacement costs associated with the structure during its service life. Geophysics also helps ensure that the appropriate maintenance and preventive maintenance measures are applied at the right time.

Methods used in pavement condition assessment should be accurate, rapid, and nondestructive whenever possible, whether QA verification testing or existing pavement evaluations are the desired goal.

The current practice of pavement condition inspection by chain dragging meets only the last two criteria, and it is not any more efficient than some other, more objective, nondestructive geophysical evaluation techniques. The accuracy of chain dragging is significantly compromised by the fact that it can only be used to identify delaminations at stages where the deterioration has already progressed to such an extent that major rehabilitation or repair measures are needed. Similarly, the pachometer barely meets the last two criteria when it is used as a primary instrument for verifying that QA specifications are being achieved, because it cannot typically achieve requirements that mandate measurement accuracy within 0.25 to 0.64 cm. In addition, this method does not provide repeatable results to the accuracy desired.

Identifying the appropriate NDT method, or methods, prior to some verification ground-truth is always the best approach toward effective use of these geophysical methods. When used as a primary investigative method, either as a baseline condition assessment tool early on in the life of a structure or as a deterioration-mapping instrument, geophysics often proves

beneficial if used as a "reconnaissance tool" in the early stages of an evaluation. The results of the geophysical survey can be used to help (a) select complementary inspection methods—destructive or nondestructive—that would best round out the analysis, (b) reduce the quantity of destructive testing or NDT investigations that are more time-consuming and require lane closures—even if they are essential to the overall evaluation, and (c) limit these other tests to much smaller areas. Information obtained by these other techniques will generally complement, validate, and/or "calibrate" the initial geophysical survey method.

4.1 QA/QC OF NEW PAVEMENTS

QA/QC testing newly constructed pavements with geophysical or NDT methods is desirable because in-situ testing is possible within hours after concrete roads are poured. The methods used are aimed at determining linear elastic modulus (Young's modulus) and thickness. These measurements can also be used for maturity analysis to aid in deciding when a new road can be opened.

Quality Control (QC) may be defined as the implementation, measurement and enforcement of sound construction practices and jobsite inspections to ensure construction quality. In contrast, Quality Assurance (QA) may be defined as the inspection and testing of the completed product, in accordance with specifications intended to verify the quality of the completed pavement. These two activities are inter-related, though distinct processes.

QC programs intended to address construction quality of pavements routinely include (a) visual inspection at regular intervals during construction, and (b) careful field and laboratory testing of the quality of materials used in its construction. Results are carefully measured and archived as a permanent part of the job record, and/or used to modify field (construction and inspection) practices and take corrective action while construction is still underway.

QA programs intended to verify the quality of newly constructed or repaired pavements can incorporate geophysics with excellent accuracy, and provide a needed tool for ensuring compliance with construction requirements.

Baseline Condition Assessment

Baseline condition assessment is not a routinely practiced form of quality assurance; however, it is truly the only way to compare the overall as-built condition of a pavement to its future condition at various stages during its life. One way to establish a baseline condition where "as-built factors" can be eliminated or minimized from consideration during a future evaluation is to perform measurements on a new structure identical in nature to those that will be used for primary "screening" in the future. To establish a baseline condition assessment, only nondestructive evaluations that continuously sample the pavement surface along every centimeter or meter of its length are of value and warrant consideration. These full-coverage methods, such as ground penetrating radar (GPR), profilometers, rutting, crack-mapping (using lasers and accelerometers), or other measurements that can effectively cover a pavement along its entire length, provide baseline condition data on roughness, degree of rutting, cracking, etc. These methods are followed by point-sampling techniques such as

integrated ultrasonic-seismic (SASW and impact-echo) to provide feedback about either initial quality of construction or condition as a pavement ages.

Other information about these additional methods in initial and future condition assessments is needed. Position, placement and density (PPD) of rebar or corrosion-related problems in pavements are secondary in nature to many other pavement problems. Providing a complete discourse on corrosion-induced deterioration is not appropriate to this topic.

4.1.1 Ground Penetrating Radar (GPR)

Ground penetrating radar (GPR) is a high-frequency electromagnetic method commonly applied to a number of engineering problems associated with both new and aging concrete structures. In the transportation sector, GPR surveys are routinely and successfully used for quality assurance (QA) verification of new construction. This includes periodic condition evaluations, beginning with a baseline survey. GPR is currently used to measure pavement thickness, determine pavement structure and condition, or categorize and inventory existing pavement types on roadways—for both hot-mix asphalt (HMA) and Portland cement concrete (PCC) pavements. It is also used in evaluating existing concrete bridge decks to determine extent of deterioration caused by corrosion.

Basic Concept: GPR is an electromagnetic (EM) method based on the rapid generation of well timed, "bursts" of wide-band radio emissions, with high-resolution signals being generated in the MHz to GHz frequency range. Impulse radar penetrates materials that are relatively resistive to electrical current, like asphalt and concrete.

The electromagnetic energy used by the GPR system depends primarily on two physical properties of the ground; the electrical conductivity and the dielectric constant. The dielectric constant determines the speed with which the wave travels and the electrical conductivity determines the attenuation of the electromagnetic signals. Through air, GPR travels at light speed; through another material, its speed is inversely proportional to the square root of its dielectric constant.

Most concrete in-service, has a dielectric of roughly 9 (GPR moves through the medium three times slower than the speed of light), and water slows GPR to only 1/9 its speed in air, because water has the highest dielectric constant (80) of any (dielectric) medium. Asphalt overlays typically have a dielectric constant of about 6 to 6.5. GPR moves faster in asphalt than in most concrete, except when concrete is extremely well cured and dry.

The dielectric contrast—absolute difference in magnitude between two adjacent materials through which a GPR signal will propagate—controls whether there will be a measurable reflection of energy transmitted from the antenna back to the receiver at the surface. The greater the dielectric contrast, the higher the amplitude of this reflection will be. Also, the polarity of the signal will depend on whether the GPR is propagating through a higher, then lower dielectric material or the reverse scenario exists. These and many other subtle GPR signal characteristics help determine accurate depth to rebar, concrete deterioration (condition), overlay thickness, deck thickness, and other structural properties of interest.

Electrical conductivity, the inverse of resistivity, is a property that measures how well a material transports or disperses an electrical current through that given medium. Highly conductive materials, such as metal or seawater, effectively impede all or most of a GPR signal from penetrating them. Similarly, conductive materials that do not fully impede signal penetration, but significantly impair the ability to penetrate them, typically attenuate or disperse the GPR signal so that very little of it can return to the receiver to be measured. Chloride-contaminated concrete is a relatively conductive medium, causing some relative increase in GPR signal amplitude to be measured at a wet surface where chlorides have intruded, and, more importantly, causing a marked decrease in amplitude at the top mat reinforcing level. Much of this amplitude decrease is attributed to greater signal attenuation of the GPR signal through the contaminated concrete, allowing less energy to return and be measured at the surface. These combined conditions are what allow GPR to be effective in identifying conditions that are dominant when rebar is corroding, corrosion products are causing cracking, delamination and spalling, and concrete is otherwise deteriorating.

Data Acquisition: GPR can be used as soon as the pavement is hard enough to drive on. Using the vehicle-mounted horn antenna scans of the pavement can be made in a very short time. Man portable units are more accurate for testing rebar locations since they move slower and get more accurate relative spatial data.

Data Processing: Standard geophysical processing as described in the earlier section is used to make the GPR image. Since the image gives signals as a function of travel in the pavement, velocity must be measured or assumed in order to obtain a depth image; therefore, local calibration of the velocity is recommended.

Data Interpretation: The combined effects of dielectric and conductive properties of subsurface materials, particularly at interfaces of dissimilar material, provide the basis for analyzing GPR data in the time domain, where two-way travel time and amplitude characteristics of the signal are used to make intuitive interpretations about concrete condition. GPR is very effective not only at QA assessments that verify uniformity of the concrete material to some degree and proper placement of the reinforcing elements in a structure, but also at investigations that contribute significantly toward identifying the degree and extent of deterioration beneath the surface of a pavement.

Advantages: Because it is the most rapid data collection technique among geophysical methods in terms of both wave propagation and sampling rates (scans/second), a GPR survey can be performed at walking or slow driving speeds (for QA assessments and condition assessments of concrete pavement). With more sophisticated sensors and data collection methods, a GPR survey can be performed at speeds requiring little or no traffic control, with essentially full coverage of the deck at extremely close spatial sampling.

Since data are collected to provide "real-time" images that can be quickly evaluated and processed in the field to provide some simple answers to problems, GPR is the most valuable geophysical instrument to accurately and quickly determine reinforcement position, placement, and density (PPD), which includes both layout and spatial position (including cover depth). Yet GPR data can also be processed in the office to obtain much more

sophisticated condition assessments on older concrete structures with a great deal of detail and accuracy in pinpointing deteriorated zones.

Limitations: Interpreted GPR thickness can sometimes be distorted by changes in conditions or calibration of velocities.

4.1.2 Impact Echo (IE)

Impact Echo (IE) test is used to determine pavement thickness as well as to evaluate pavement debonding and integrity.

Basic Concept: Impact Echo on pavements is done with small metal spheres or electronic solenoid sources. The impact, however it is made, sends acoustic energy into the pavement which resonates at a frequency whose wavelength is the thickness of the pavement.

Data Acquisition: Methods based on the original work by Sansalone use metal spheres of varying sizes to get a source impact of the proper strength and frequency, requiring a certain amount of experimentation in making the measurements. Systems that use electric solenoid sources rely signal processing techniques to determine the resonant frequency from a single source hit. Care must be taken when making these measurements that the true depth is being measured and not the depth to an inhomogeneity in the pavement.

Several companies manufacture instruments for IE; two sets of such equipment are illustrated below in figure 75.

Data Processing: Using frequency analysis techniques amplitudes of the frequencies in the data are computed. The velocity of the pavement must be measured (or assumed).

Data Interpretation: The frequency spectrum of the receiver is used to determine the depth of reflectors according to:

$$D = V_p / (2 \times f_r)$$

where D is the reflector depth, f_r is the large dominant frequency peak identified in the response, and V_p is the compressional wave velocity. If the velocity of the concrete is known or can be measured, then the depth of a reflector can be calculated from the reflection echo peak frequency. The wave speed V_p can be measured by observing the travel time of a compressional wave between two transducers held a fixed distance apart on the concrete surface or by performing a calibration test on a slab of known thickness and observing the dominant frequency.

The highest amplitude frequency peak is the main indicator of a reflector depth (thickness echo). The presence of additional echo peaks can also be significant, indicating the presence of possible defects or other interfaces in the concrete.

Advantages: This technique does not require coring.

Limitations: Impact Echo does not give accuracy to the level of 0.64 or 0.32 cm as is sometimes sought for certain engineering applications.

(a) (b)

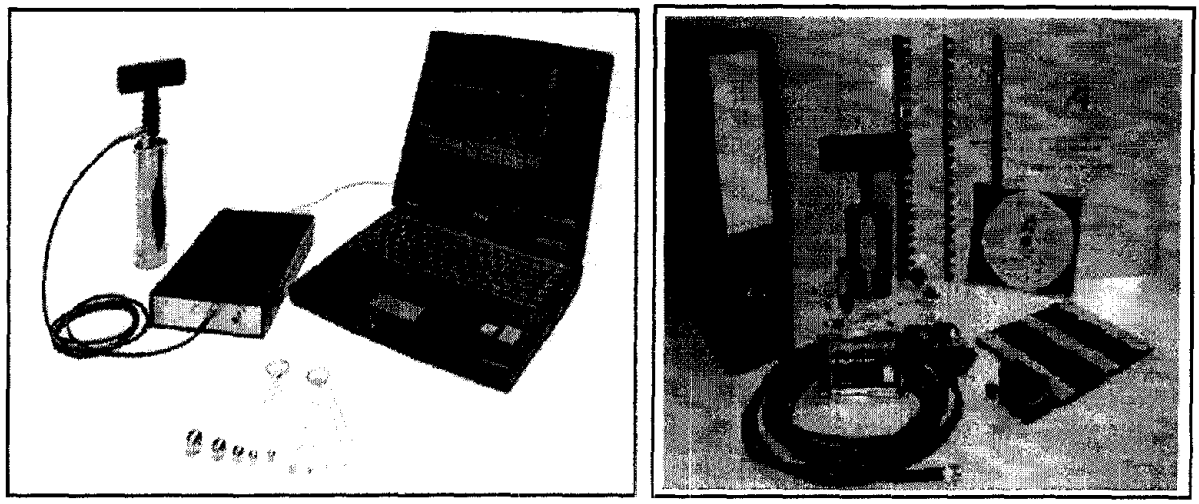

Figure 75. Example Impact Echo Systems: (a) Impact Echo Instruments, LLC, and (b) Germann Instruments A/S.

4.1.3 Spectral Analysis of Surface Waves (SASW) and Ultra Sonic Surface Wave (USW) Methods

SASW and USW are used to determine pavement thickness as well as to evaluate determine linear elastic modulus of pavement layers. The USW technique, and presumably the SASW and MASW techniques, can be used to measure modulus of base materials by adjusting the sensor spacing and frequency range of the instrument. Since the materials are not consolidated the velocities and moduli will be lower. This requires lower frequencies for the investigation.

Basic Concept: The surface wave methods including Spectral Analysis of Surface Waves (SASW), Multi-Channel Analysis of Surface Waves (MASW), or Ultra Sonic Surface Wave (USW) methods are used to determine linear elastic modulus of pavement layers. These methods operate by measuring surface seismic waves generated by an impulsive source (i.e. a hammer or electrically activated solenoid). As long as the wavelengths studied are smaller than the thickness of the exposed layer in question, the modulus computed will be indicative of that layer. The Ultra Sonic and SASW methods use this approach with two receivers to measure just the properties of the exposed layer. These methods measure in a few seconds and the instruments are easily portable. The MASW method uses more receivers (channels) to get information on all of the layers in a pavement system, as described in section 4.1.4.

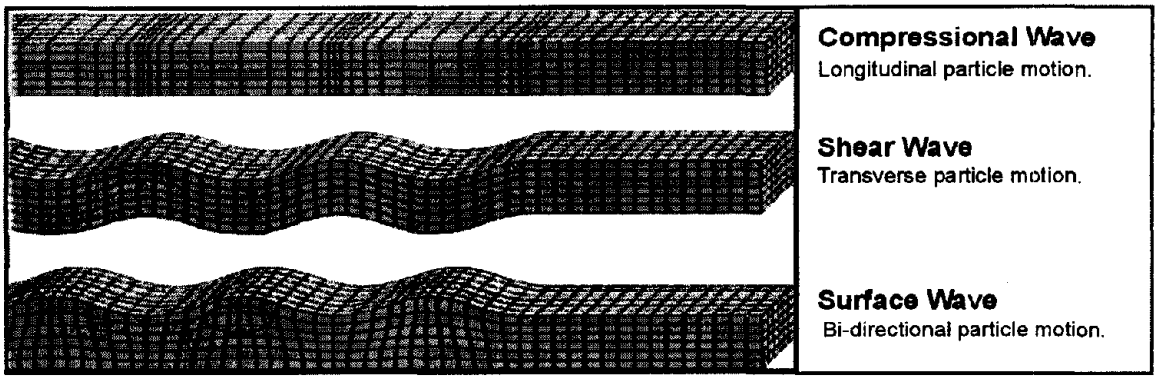

Figure 76. Seismic waves generated.

Data Acquisition: All of the systems to measure velocity and determine modulus use some method of deploying a source with two or more accelerometers located at known distances, usually inline, from the source. When the source is fired the short-duration pulse creates a packet of seismic waves that travel through the body and along the surface of the pavement. See figure 76.

Data Processing: In most systems, compressional waves arrive first at the receivers followed by shear waves and then surface waves. However, more than fifty percent of the energy in the wave train is in the surface waves, making them more easily studied. Figure 77 illustrates the relative arrival of the wave train at a near and far receiver. Figure 78 shows how two or more receivers can be used to measure the travel time between them using the recorded waves.

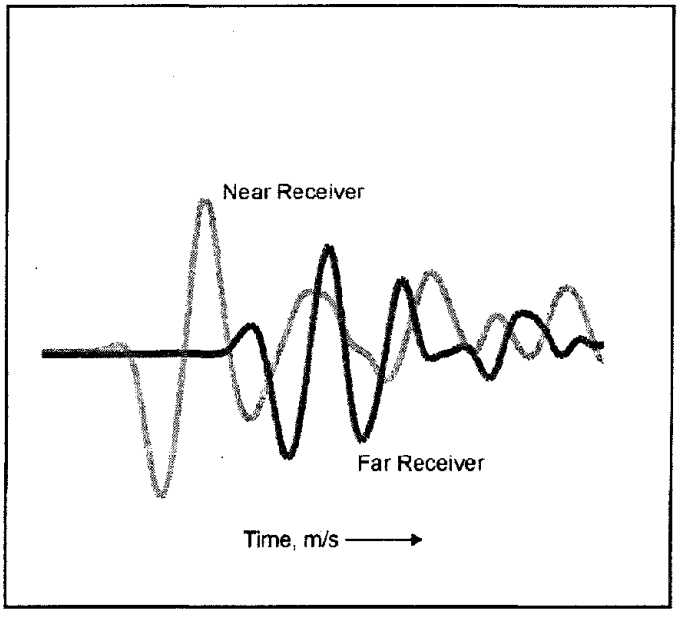

Figure 77. Recorded waveforms.

Several companies manufacture instruments for SASW; two sets of such equipment are illustrated below in figure 79.

Data Interpretation: It is easier to measure surface wave velocity, but shear wave velocity is required to compute Young's modulus. The conversion equation below is used.

Calculate Shear Wave Velocity (V_S) from Raleigh (or Surface) Wave Velocity (V_R)

$$V_S = V_R (1.13 - 0.16 \nu)$$

Following the conversion to shear wave velocity, the computation of Young's modulus is made with the formula below.

Calculate Young's Modulus (E)

$$E = 2 (\rho) V_S^2 (1 + \nu), \text{ where } \nu = \text{Poisson's Ratio}, \rho = \text{Mass Density}$$

The above computation is usually made for a number of frequencies in the surface wave data packet, using Fourier analysis. These values can be averaged over an appropriate number of frequencies (or wavelengths) to obtain an average modulus for a pavement of a certain thickness.

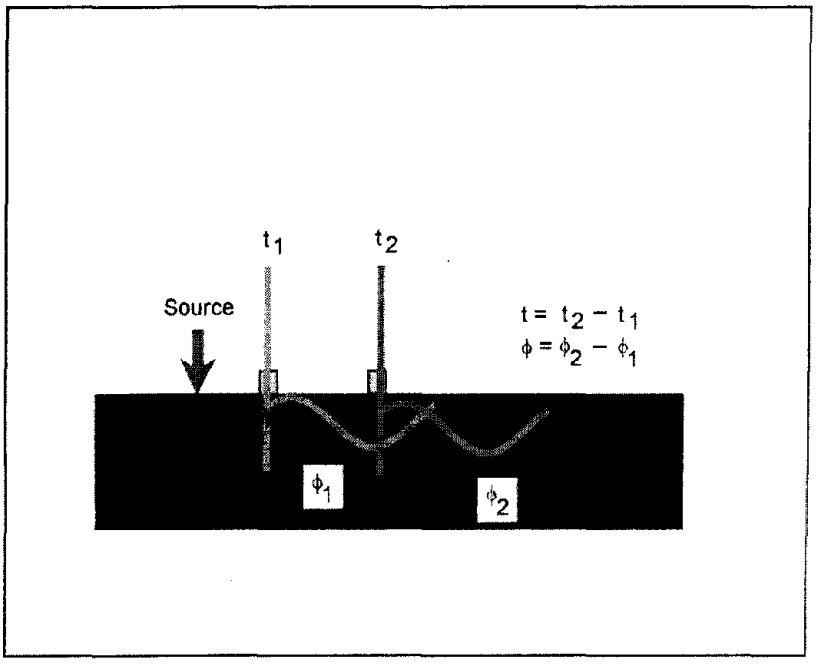

Figure 78. Velocity calculation.

Calculate Shear Wave Velocity (V_S) from Raleigh (or Surface) Wave Velocity (V_R)

$$V_S = V_R (1.13 - 0.16 \nu)$$

Following the conversion to shear wave velocity, the computation of Young's modulus is made with the formula below.

Calculate Young's Modulus (E)

$$E = 2\,(\rho)\,V_S^2\,(1 + \nu),$$

where

ν = Poisson's Ratio,

ρ = Mass Density

The above computation is usually made for a number of frequencies in the surface wave data packet, using Fourier analysis. These values can be averaged over an appropriate number of frequencies (or wavelengths) to obtain an average modulus for a pavement of a certain thickness.

The modulus of pavement can be specified before construction using techniques developed for Texas Department of Transportation (see Bibliography). Modulus standards are beginning to be set by AASHTO and other organizations.

Advantages: This is a test method that can take the place of lab testing of cores or cylinders. Test can be made within hours of construction.

Limitations: These measurement systems must occupy a particular location to be tested and remain stationary during the measurement process, with set and measurement time proportional to the number of receivers used. Therefore, road and bridge closures would be necessary for surveying existing pavements.

(a) (b)

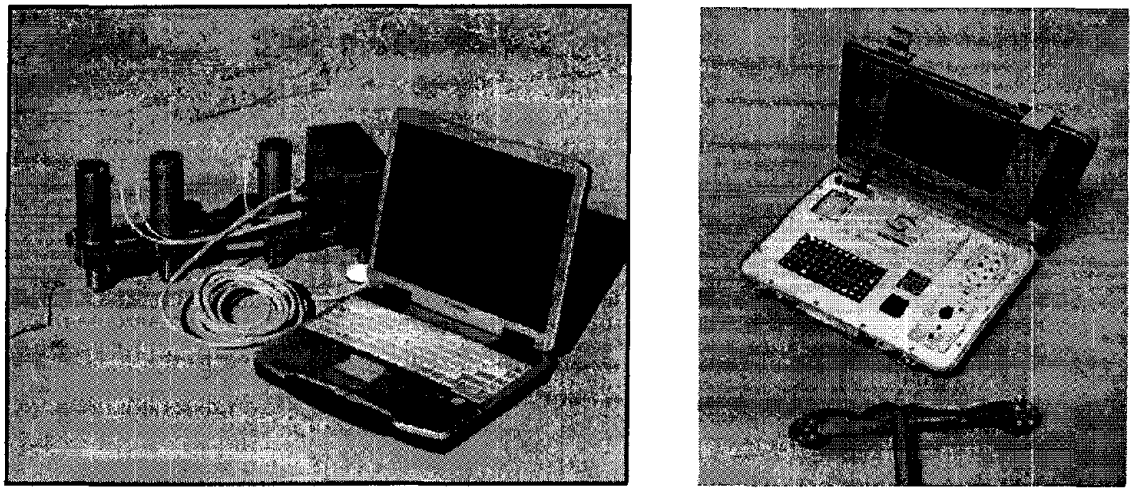

Figure 79. Spectral Analysis of Surface Waves Instruments (a) Portable Seismic Property Analyzer (PSPA) by Geomedia Research and Development, (b) SASW 1-S by Olson Instruments, Inc.

Spectral Analysis of Surface Waves and Impact-Echo Combined

Ultrasonic Seismic (SASW) and Impact Echo, particularly when applied together in an integrated instrument, such as the Portable Seismic Property Analyzer (PSPA), are high-frequency, acoustic (seismic) geophysical methods. Concrete condition assessment by integrated ultrasonic methods has recently been applied to a number of engineering problems associated with both new and aging concrete structures. Recent work on evaluating concrete integrity, particularly looking for the formation of corrosion-induced delamination in early, moderate, and late stages of development, has demonstrated that these integrated methods show considerable promise in terms of current and potential capability.

In the transportation sector, these integrated surveys can be used for quality assurance (QA) verification of new construction (thickness determination and homogeneity of concrete pour, even segregation of aggregates or suspected voids) and calculation of mechanical properties on bridge decks and pavements.

Ultrasonic methods implemented in various forms of integrated ultrasonic seismic devices, such as the Portable Seismic Property Analyzer (PSPA), can be successfully used to assist in evaluating concrete pavement structure condition, also alone (like GPR) or in tandem with other geophysical and/or ground truth sampling. However, it is always recommended to use a multiple-method approach.

Of special interest are three ultrasonic techniques: ultrasonic body-wave (UBW), ultrasonic surface-wave (USW), and impact echo (IE) geophysical methods that can be used separately or in combination. The first two are used in concrete characterization, and the IE method is used primarily in delamination detection once a propagation velocity of the seismic wave in the concrete is established. The primary advantage that the IE method has over the current practice of chain dragging is that it allows detection of delamination zones in various stages of deterioration.

Finite-element simulations of two probable scenarios of delamination progression, demonstrated that periodic monitoring of concrete pavement structures by IE enables improved prediction of the deterioration processes. Three-dimensional data visualization techniques constitute important components in condition assessment and delamination detection using the IE method. Results include three-dimensional translucent visualizations of a concrete pavement structure section, horizontal cross sections through all distinctive zones (including a zone of delamination), and vertical cross sections along chosen test lines. Visualization techniques enable the PSPA to be used as a kind of concrete pavement structure sonar device.

Combined ultrasonic seismic techniques, however, do require more sophisticated analysis than the GPR and half-cell corrosion potential methods or the GPR or pachometer. The pachometer is not a recommended tool for QA verification of rebar PPD if accuracy within 0.64 cm is consistently expected, and if high repeatability is desired. On some of the QA applications, however, such as determination of concrete integrity on new and fairly uniform structures, use of the acoustic techniques can be straightforward and very simple. A simple

impact-echo device used to measure concrete thickness, for example, is a concrete thickness meter that can accurately determine thickness for QA verification purposes.

Various methodologies are more fully explained chapter 3 on Bridge Decks.

4.1.4 Multichannel Analysis of Surface Waves (MASW) Method

The multichannel analysis of surface waves method (MASW) is a nondestructive seismic method to evaluate pavement thickness as well as to evaluate linear elastic modulus of ground and materials under pavement. It analyzes dispersion properties of certain types of seismic surface waves (fundamental-mode Rayleigh waves) propagating horizontally along the surface of measurement directly from impact point to receivers. It gives this shear-wave velocity (Vs) (or stiffness) information in either 1-D (depth) or 2-D (depth and surface location) format in a cost-effective and time-efficient manner. The main advantage with the MASW method is to take a full account of the complicated nature of seismic waves that always contain harmful noise waves such as higher modes of surface waves, body waves, scattered waves, traffic waves, etc. These noise waves may result in a significant portion of the recorded data being dubious if not properly accounted for. The fundamental framework of the MASW method is based on the multichannel recording and analysis approach long used in seismic exploration surveys. These techniques can discriminate useful signal against all other types of noise by utilizing pattern-recognition techniques.

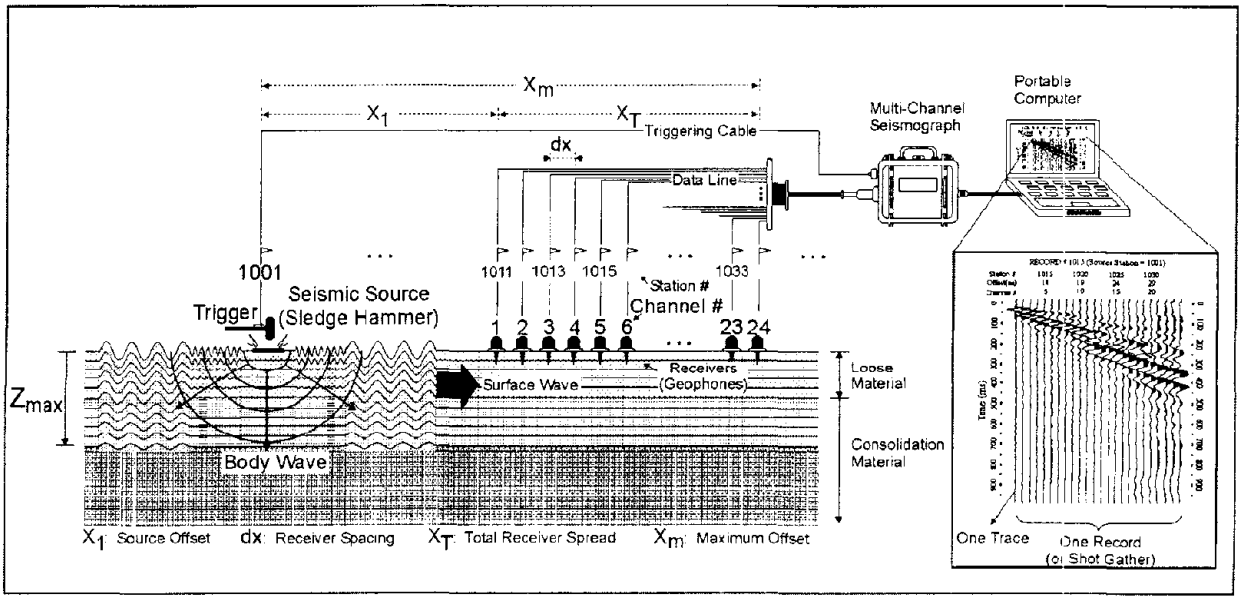

Figure 80. Schematic illustrating a typical Multichannel Analysis of Surface Waves survey setup. (Kansas Geological Survey)

Basic Concept: A multiple number of receivers (usually 24 or more) are deployed with even spacing along a linear survey line with receivers connected to a multichannel recording device (seismograph) (figure 80). Each channel is dedicated to recording vibrations from one receiver. One multichannel record (commonly called a shot gather) consists of a multiple number of time series (called traces) from all the receivers in an ordered manner. Data Acquisition: Unlike other types of seismic methods (e.g., reflection or refraction), acquisition parameters for MASW surveys have quite a wide range of tolerance. This is because the multichannel processing schemes employed in the wavefield transformation method have the capability to automatically account for such otherwise adverse effects as near-field, far-field, and spatial aliasing effects. Nevertheless, two types of parameters are considered to be most important: the source offset (x_1) and the receiver spacing (dx) (figure 80). The source offset (x_1) needs to change in proportion to the maximum investigation depth (z_{max}). A rule of thumb is $x_1 \approx z_{max}$. The receiver spacing (dx) may need to be slightly dependent on the average stiffness of near-surface materials. A rule of thumb is $dx \approx 1$ m. Table 7 summarizes optimum ranges of all the acquisition parameters.

Data Processing: Data processing consists of three steps (figure 81): 1) preliminary detection of surface waves, 2) constructing the dispersion image panel and extracting the signal dispersion curve, and 3) back-calculating Vs variation with depth. All these steps can be fully automated. The preliminary detection of surface waves examines recorded seismic waves in the most probable range of frequencies and phase velocities. Construction of the image panel is accomplished through a 2-D (time and space) wavefield transformation method that employs several pattern-recognition approaches. This transformation eliminates all the ambient noise from human activities as well as source-generated noise such as scattered waves from buried objects (building foundations, culverts, boulders, et.c). The image panel shows the relationship between phase velocity and frequency for those waves propagated horizontally directly from the impact point to the receiver line. These waves include fundamental and higher modes of surface waves as well as direct body (compressional) waves (figure 81). The necessary dispersion curve, such as that of fundamental-mode Rayleigh waves, is then extracted from the energy accumulation pattern in this image panel (figure 81). The extracted dispersion curve is finally used as a reference to back-calculate the Vs variation with depth below the surveyed area. This back-calculation is called inversion and the process can also be automated.

Table 7. Optimum acquisition parameters — rules of thumb.

Material Type* (V_s in m/sec)	x_1 (m)	dx (m)	x_M (m)	Optimum Geophone (Hz)	Optimum Source+ (Kg)	Recording Time (ms)	Sampling Interval (ms)
Very Soft ($V_s < 100$)	1 – 5	0.25 – 0.5	≤ 20	4.5	≥ 5.0	1000	1.0
Soft ($100 < V_s < 300$)	5 – 10	0.5 – 1.0	≤ 30	4.5	≥ 5.0	1000	1.0
Hard ($200 < V_s < 500$)	10 – 20	1.0 – 2.0	≤ 50	4.5 – 10.0	≥ 5.0	500	0.5
Very Hard ($500 < V_s$)	20 – 40	2.0 – 5.0	≤ 100	4.5 – 40.0	≥ 5.0	500	0.5

* Average properties within about 30-m depth range
+ Weight of sledge hammer

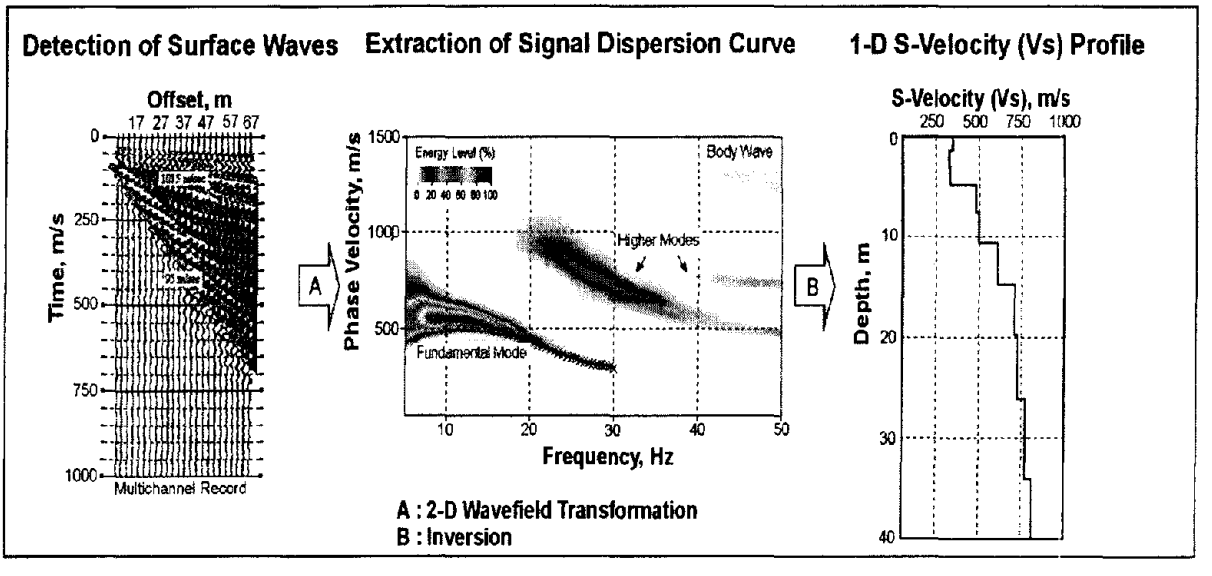

Figure 81. A 3-step processing scheme for Multichannel Analysis of Surface Waves data. Actual data set was acquired over a desert site near Yuma, Arizona.

Data Interpretation: A 2-D Vs map is constructed from the acquisition of multiple records (figure 82) with a fixed source-receiver configuration and a fixed increment (dC) of the

configuration (figure 83). A source-receiver configuration indicates a setup of given source offset (x_1), receiver spacing (dx), and total number of channels (N) used during a survey. The increment dC depends on the degree of horizontal variation in Vs along the entire survey line. A small increment would be necessary if a high degree of horizontal variation is expected. In most cases where total receiver spread length (x_T) is set in such a way that horizontal variation within x_T can be ignored, an increment of half the spread would be sufficient: $dC \approx 0.5\, x_T$. Therefore, determination of optimum x_T has to be made before optimum dC is determined. In theory, a shorter x_T would ensure a higher accuracy in handling the horizontal variation. However, on the other hand, it would impede the accurate assessment of dispersion curves. Therefore, it needs to be a trade-off. In most soil-site applications, x_T in the range of 10-30 m is most optimal and this gives the optimal dC in the range of 5-15 m.

Once a multiple number (> 5) of records are acquired by regularly moving the source-receiver configuration, one 1-D Vs profile is obtained from each record through surface wave processing. Each Vs profile also has the appropriate horizontal coordinate (i.e., station number) to represent the vertical Vs variation. Naturally, the midpoint of the receiver spread is used for this purpose. Multiple Vs profiles obtained are then used for a 2-D (x and z) interpolation to create the final map. The kriging method is usually used for the interpolation.

Advantages: The MASW technique is the best seismic technique for measuring the modulus of base materials and subgrade material.

Due to multichannel recording and processing schemes employed, results (Vs information) of the survey are highly reliable even under the presence of higher modes of surface waves and various types of cultural noise. For the same reason, the processing steps can be fully automated. Therefore, the method is extremely easy and fast to implement.

Limitations: Due to intrinsic properties of surface waves, resolution of the result is limited by the size of the anomaly. A rule of thumb is that the minimum size that can be resolved is about one tenth of depth.

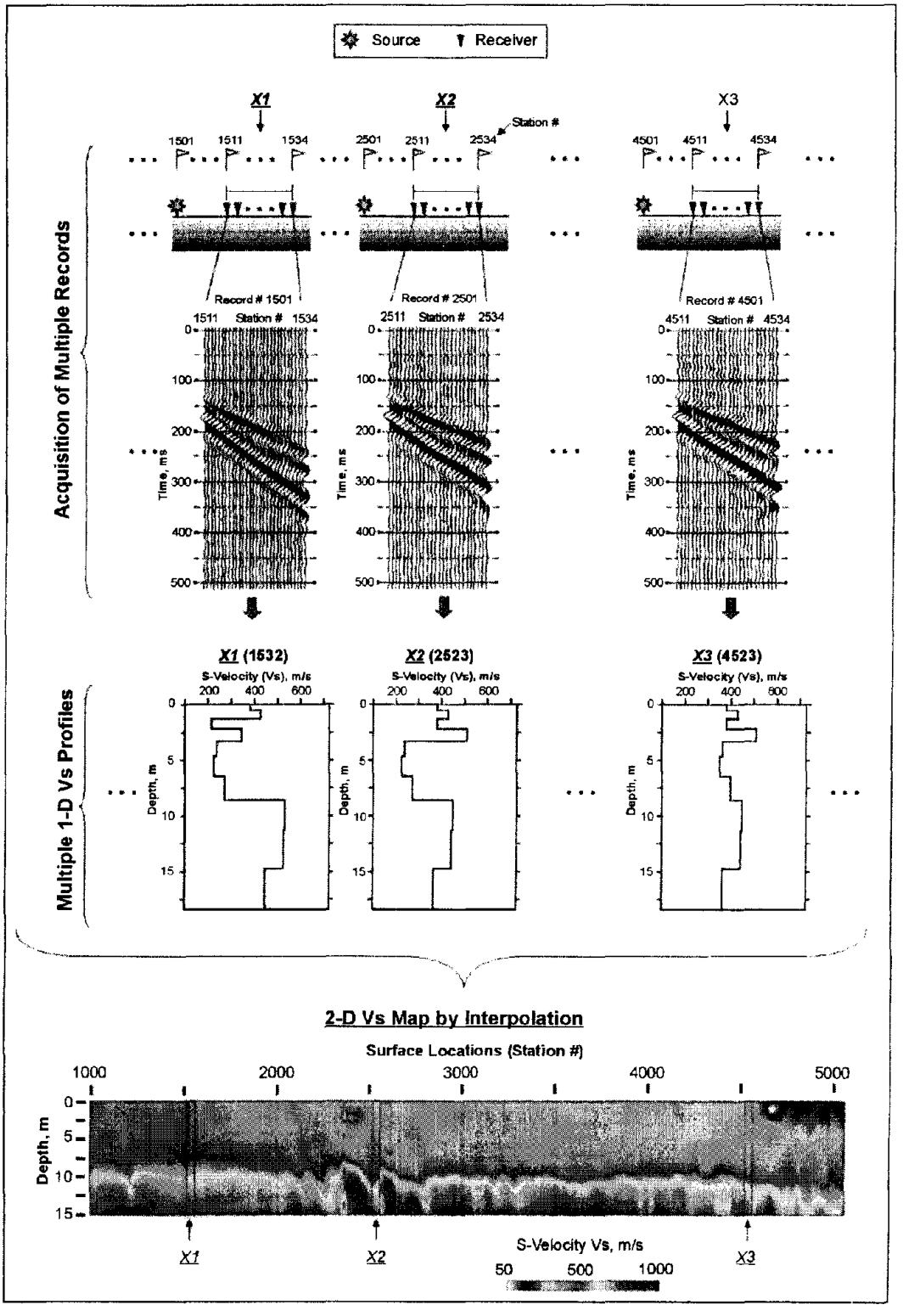

Figure 82. Overall procedure to construct a 2-D Vs map from an Multichannel Analysis of Surface Waves survey. (Kansas Geological Survey)

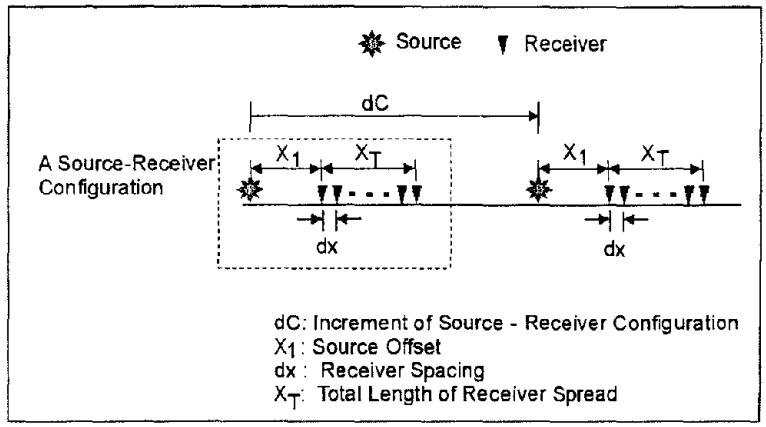

Figure 83. Definition of a source-receiver configuration and increment of the configuration.

4.2 CONDITION EVALUATION OF EXISTING PAVEMENTS

Pavement deteriorates with time, due to increases in loads and demand (loading cycles), variations in moisture within its base and subgrade that can damage its foundation, and exposure to the elements (freeze-thaw cycles or even de-icing chemical application). A proper diagnosis and preventive maintenance schedule—where smaller and less expensiverepairs are made at properly-timed intervals throughout the structure's life—significantly extends its life and reduces the costs associated with its ownership. (See earlier discussions on baseline condition assessments and QA verification of construction related to this topic.)

4.2.1 Segregation in Hot Mix Asphalt

A proper gradation of aggregate is essential for performance of a mix. Sometimes during plant mixing or placement of Hot Mix Asphalt (HMA), smaller aggregates are separated from larger aggregates leaving a fragmented mix. For example segregation occurs when a patch crew throws shovels of HMA in a hole rather than placing the HMA. Segregation reduces the performance of the mix by changing the stability of the product and compromising the air void content.

Somewhat related to segregation and evaluated with the same methodology is stripping in HMA. Stripping occurs when the asphalt covering the aggregate no longer adheres to the aggregate. This may happen with moisture and heat or be related to the aggregate. Observing the patterns from geophysical images, measuring them, and interpreting the results can often identify suspect stripping. GPR can often provide detailed screening, which can be followed up by other means, including geophysical NDT methods and destructive sampling.

Techniques Recommended

Surface NDT Methods:

- Ground penetrating radar (GPR).
- Spectral Analysis of Surface Waves (SASW) / MASW.
- Impact Echo.
- Acoustic-ultrasonic.
- Infrared Thermography.

A brief note on Infrared Thermography: It can successfully be applied to this application, particularly if variations in paving processes during initial construction are being identified. Variations in temperature within the asphalt as it is being unloaded from dump trucks, routed beneath the paving equipment and rolled, or "shoveled-in" HMA are areas that appear as thermal variations of significance in the infrared image. IR can be used very effectively for both QC and initial baseline condition assessment (QA of sorts). While other methods are available or under development, the ones listed provide cost-effective determination of pavement thickness.

4.2.2 Moisture Variation

Water enters a pavement structure from a variety of sources. This water may drain away from the pavement or pond in or under the pavement layers, weakening the pavement and causing premature failure. Tracking the presence of moisture or the variation of moisture within a pavement structure allows pavement engineers to correct the source of the water and/or repair the distressed area. Moisture variation is determined by first establishing a benchmark from the driest pavement. Geophysical methods will then locate changes from this benchmark, and they can also be useful in identifying where to look for an appropriate benchmark location, itself.

Techniques Recommended

Surface NDT Methods:

- Ground penetrating radar (GPR).
- Percometer (point data collection).

While other methods are available or under development, the ones listed above provide cost-effective ways to screen for locations with suspect moisture variation which can then be verified by other means, including in-situ sampling and laboratory testing—or instrumentation of suspect sites that are identified using a screening tool, such as GPR.

4.2.3 Rock Pockets

Rock pockets and other anomalies in a concrete pavement can be determined by skillful use of geophysical methods. Rock pockets occur when aggregate collects without a proper amount of binding cement. This may happen in placement or vibration of the concrete. The presence of rock pockets weakens the concrete structure. Rock pockets can be found with high frequency GPR and Impact Echo.

Techniques Recommended

Surface NDT Methods:

- Ground penetrating radar (GPR).
- Impact Echo.

While other methods are available or under development, the ones listed above provide cost-effective determination of pavement thickness.

4.2.4 Voids Beneath Pavements

Concrete pavements experience daily and seasonal variations in joints opening and closing. During the open periods, water may enter the base. The weakened base material may "pump" up through the joints with loading and therefore cause a void under the joint. Other sources of water such as springs and water main leaks may also erode the material under the slab. It is important to find and repair these voids before catastrophic failure leading to expensive repairs to the concrete slab. Deflection testing is sometimes used to locate the voids and determine load transfer efficiency. This method is not discussed here. Methods that have been found successful in locating voids under concrete are listed below.

Techniques Recommended

Surface NDT Methods:

- Ground penetrating radar (GPR)
- Impact Echo – other acoustic methods

While other methods are available or under development, the ones listed above provide cost-effective determination of pavement thickness.

4.2.5 Cracking

See Pavement Condition/Integrity (below).

Crack-mapping can be performed using lasers/accelerometers, and/or profilometers (IRI). High-resolution GPR (1.5 GHz ground-coupled and 1.0 GHz horn antennas) can be used as a screening tool to look for subsurface indications of cracking beneath pavements already

showing early signs of distress—in order to locate regions where more in-depth testing should be performed. However, these results are possible only if very high spatial sampling density (40 scans/meter using horn antenna to upwards of 100 scans/meter using the GC antenna) is used along each pass of the GPR antenna.

4.2.6 Pavement Condition/Integrity

Over time the forces such as freezing and thawing, exposure to sun, water and traffic combine to deteriorate a pavement structure. One measure of pavement integrity is strength (measured by physical methods such as Falling Weight Deflectometer (FWD). Another measure of integrity is the variance in homogeneity. Wave propagation techniques such as GPR, seismic, and Impact/Echo can be used to map integrity.

For concrete pavements, there is an excellent discussion of GPR and SASW/Impact Echo Methods discussed under Bridge Decks in a section under a similar title.

Techniques Recommended

Surface NDT Methods:

- Ground Penetrating Radar (GPR)-homogeneity
- Surface wave for modulus, stiffness and homogeneity
- Impact Echo-stiffness

While other methods are available or under development, the ones listed above provide cost-effective determination of pavement integrity.

4.2.7 Structural Changes

With repeated loading from traffic or weather, a pavement will fatigue. It is important to track the structural quality of a pavement in order to timely apply a corrective activity. Simply stated, the change in integrity over time is one measure of structural changes. Another measure is tracking the change in stiffness over time.

For concrete pavements, there is an excellent discussion of GPR and Surface Wave/Impact Echo Methods discussed under Bridge Decks. Although the discussion is directed toward a concrete structure, the same general approaches toward problem-solving and initial screening, followed up by point data collection (NDT or limited destructive sampling) at identified, or targeted, locations, should be used for all pavement types.

Techniques Recommended

Surface NDT Methods:

- Ground penetrating radar (GPR)

- Surface wave seismic methods
- Impact Echo

While other methods are available or under development, the ones listed above provide cost-effective determination of pavement structural changes.

4.3 TRANSPORTATION / GEOTECHNICAL METHODS

In this section, non-geophysical methods developed for pavement evaluations in the transportation and geotechnical fields are briefly discussed.

Falling Weight Deflectometer

The falling weight deflectometer is a nondestructive device that sends an impulse (with known magnitude and duration) to the pavement and/or base. The system response is measured using accelerometers and geophones. The recorded response is then related to design parameters including the sub-grade reaction and dynamic response of flexible and rigid pavement pavements (i.e., the in-situ resilient elastic moduli). These data are being used by state department of transportations to evaluate the structural health, aging, and use life of pavements.

There are deflectometers with impulse capacities that range from a few killograms force (for example the Keros) to several tons (for example, Dynatest FWD/HWD Test Systems). This wide range of impulses permits the use of deflectometers to monitor responses of systems with varying stiffnesses. For example, large deflectometers permit the evaluation of complete structural pavements, while lightweight deflectometers permit the evaluation of subsystems, such as bases and sub-bases.

Pavement Quality Indicators

The Pavement Quality Indicator (PQI) is an instrument available from TransTeck (http://www.transtechsys.com) and it is intended for the nondestructive measurement of in-situ mass density of asphalt/concrete mixtures. It measures the change in capacitive impedance of a toroid electric field and it relates the measured impedance to the dielectric permittivity. The measurement technique then correlates the dielectric permittivity of the pavement to the asphalt or concrete density using volumetric relationships.

However, the technique has some drawbacks including that the measurement is highly sensitive to moisture content, temperature, and aggregate mineral. In spite of these problems, the PQI system may provide a rapid indication of sudden changes and discontinuities in the mass density and quality of asphalt concrete pavement.

There are other similar types of instruments that use similar physical measurement concepts to evaluate in-situ pavement density. One of these instruments is the newly released Troxler's PaveTracker (non-nuclear device) used for the rapid measurements of segregation and overall pavement uniformity. The measurement results do not need to be corrected for changes in moisture or temperature.

Nuclear Densimeter

Nuclear densimeters are a set of devices that measure the decay of a radioactive source and they correlate this decay to the density and water content of soils. Their measurements are accurate and they have been used to monitor the quality of compaction in bases and sub-bases for the construction of dams, embankments, and roads. However because of their radioactive nature, they require special certifications and permits for their use and transport.

Troxler is a leading manufacturer of nuclear densimeters. Several systems are commercialized that can be used to monitor the density of soil, aggregates, asphalt, and concrete along with the moisture of soils and aggregates. The instrument makes counts of backscattered gamma rays from a cesium source in the instrument. That information is used to compute the average density of the material through which the gamma rays (photons) passed. Most instruments also have an americium source on board for making similar measurements from which moisture content can be determined. The instrument is simply placed on the surface to be tested and a measurement procedure of warm-up and counting time is followed for each station. Measurement takes a few seconds to a few minutes at each station.

Moisture Engineering Gauge

Commonly used moisture techniques relate the measurement of dielectric permittivity to the volumetric water content in granular materials. These techniques include coaxial transmission line, time domain reflectometry, and radio-frequency capacitance. These dielectric techniques have been applied to soil measurement and found wide applications in agricultural and soil science community. However, the geotechnical and transportation engineering communities have not widely adopted these techniques as they do not directly relate the volumetric water content to the engineering gravimetric water content.

In spite of this limitation, volumetric water content techniques can provide reliable measurements of point water content and help in the evaluation of homogeneity of bases and sub-bases. Furthermore, several correlations have been proposed to directly relate volumetric and gravimetric water contents.

Purdue Time Domain Reflectometry (TDR) Method

This method has been developed by Dr. V. Drenvich (Purdue University) and it is intended for the rapid determination of in-situ water content and density. Drnevich and co-workers rely in several independent sets of measurements for the evaluation of unit weight and water content:

- *In-situ soil unit weight*: the relative dielectric permittivity of the in-situ soil, the relative dielectric permittivity of the Proctor mold compacted soil, the Proctor mold compacted soil unit weight and the water content.

- *In-situ soil water content*: the relative dielectric permittivity of the in-situ soil, the soil dry unit weight, and experimentally determined correlation parameters.

In spite of depending on correlation parameters, this is a promising procedure and it is now being tested throughout the country to establish its applicability. The advantages of this methodology include its relative quick collection of results and its straightforward interpretation (once the correlation coefficients have been determined). An important drawback is that the technique yields unit weight measurements only at discrete points.

Humboldt Stiffness GeoGauge

This portable instrument is designed to rapidly determine the in-situ stiffness of bases and sub-bases, and to evaluate the engineering quality of the compacted soil. The instrument works by measuring the mechanical impedance/stiffness of soils under the annular footing of the instrument. This is done by monitoring the displacement of the soil under the action of a harmonic force.

The instrument was designed with the intent of replacing nuclear devices and other density measurement systems for the quality evaluation of compacted bases and sub-bases. However, the GeoGauge stiffness is not directly related to dry unit weight. As expected the stiffness values decrease with increasing water (due to the change of capillary forces. Therefore, the instrument cannot, at this time, replace traditional protocols to evaluate the quality control and acceptance of compacted soil for pavement constructions, but it can be used to nondestructively evaluate the homogeneity of the base and sub-base systems. New stiffness-based design practices and protocols are being proposed. These new protocols may take advantage of stiffness measurements of granular systems and their application in engineering design.

Infrared (IR) Thermography

Infrared thermography is increasingly being used in laboratories and in in-situ for the measurement of pavements properties. Infrared thermography (IRT) scanning can be used to evaluate delamination detection in rigid pavements, segregation in flexible pavements, and in general for the monitoring of deficient construction and quality of construction of buildings. Some researchers have used thermographic techniques to monitor subsurface anomalies in sewer lines and tunnels.

Thermographic techniques rely on the relative thermal emisivitty of the different components of the pavement system to render a thermal image that helps monitor possible structural problems. This technique can be used in rapidly moving vehicles and it can evaluate a large area in a few seconds. However, thermography can only capture information from the pavement surface; and, therefore, it is commonly combined with other nondestructive methods for the evaluation of pavement quality (e.g., GPR).

CHAPTER 5 ROADWAY SUBSIDENCE

In this chapter, the use of geophysics for condition evaluation of roadways (paved or unpaved) is discussed. This includes a discussion of roadway subsidence in section 5.1, followed by a discussion of mapping of expansive clays in section 5.2. Slope stability and subsurface characterization issues are covered in sections 6.1 and 6.2.

5.1 MAPPING VOIDS, SINKHOLES, ABANDONED MINES, AND OTHER CAVITIES

Detecting voids and other cavities is a problem often encountered in geophysics. Although this section mentions the use of Ground Penetrating Radar for locating voids under pavements, its focus is mostly on locating deeper voids. Locating voids under pavements is discussed in Chapter 4- Pavements.

The physical properties of the void and host rock and soils are an important consideration when deciding on the particular method to use. For example, when searching for cavities, the physical property of interest may be mass deficiency using the gravity method. However, if the cavity is filled with water or alluvium rather than air, it will be more difficult to locate. However, the water may assist in some seismic methods since compressional waves can travel through water but would not be observed if the cavity were filled with air. Often associated with a cavity are secondary structures that can aid in their delineation. Collapsed structures can occur above a cavity, bringing the low-density contrast nearer to the ground surface. Lateral fractures may also be present, making the width of the low-density region greater that that of the cavity itself.

Several methods can be used to locate cavities. These include gravity, resistivity (and conductivity), seismic methods, and Ground Penetrating Radar (GPR). The methods that should be used depend significantly on the host geology, as discussed previously, and the depth and configuration of the voids. Each of these methods is discussed below.

5.1.1 Gravity Method

Basic Concept. The gravity method measures small spatial differences in the gravitational pull of the earth. If the gravity field over an air-filled void is measured, and the void is close enough to the ground surface, then a decrease in the gravitational pull across the void will be measured. This concept is illustrated in figure 84, which shows an underground void and the gravity profile over this void.

The instrument that is used to measure the gravity pull is called a Gravimeter. This instrument does not measure the absolute value of the pull of gravity, but measures spatial differences in the gravity pull; essentially relative gravity.

Voids can produce reasonably sized anomalies when they are large and fairly near the ground surface, but only very small anomalies result from voids at depth. Clearly, the size of an anomaly depends on the size and depth of the void, and at some point it cannot be observed. Thus, it is important to be able to measure the gravity field with as much accuracy as possible.

Generally, for a spherical void to be detected, the depth to its top surface should be no greater than its diameter.

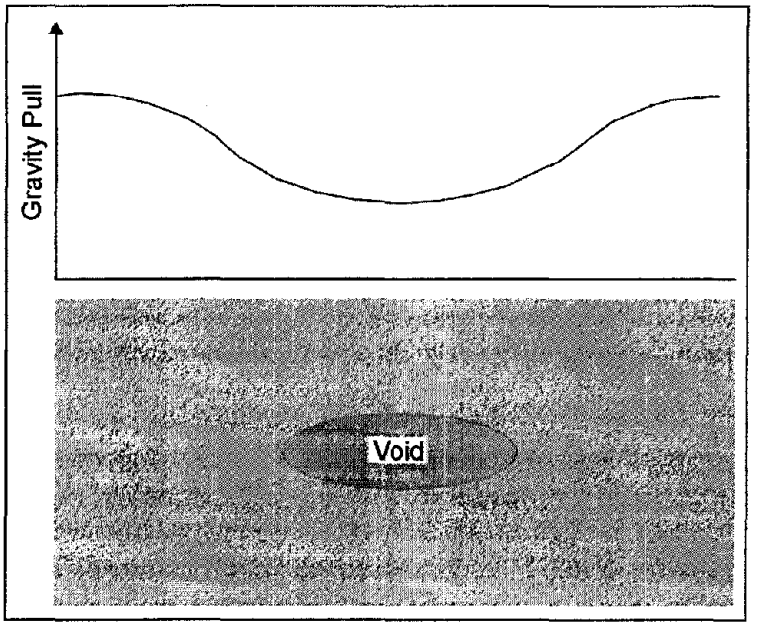

Figure 84. Gravity field over a void.

The Lacoste and Rhomberg model EG Gravity meter has an advertised repeatability of 3 microgals (980,000,000 microgals is the Earth's gravitational field) and is one of the preferred instruments for conducting gravity surveys (figure 85). Variations in gravity anomalies found when searching for cavities are typically a few tens to hundreds of microgals. These surveys are often called Microgravity surveys.

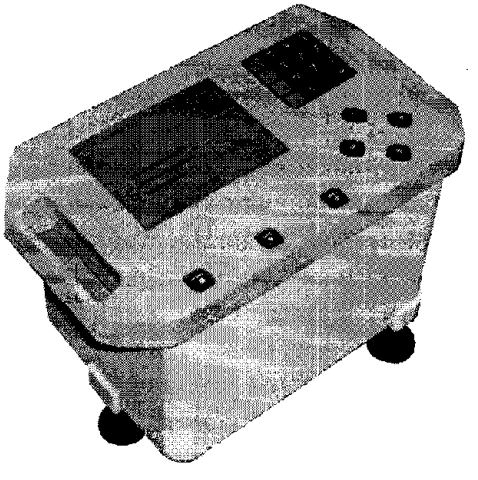

Figure 85. Graviton-EG gravity meter. (LaCoste & Romberg)

Data Acquisition: In order to detect a void, gravity readings must be taken along traverses that cross the location of the void. Its expected size will determine the distance between readings (station spacing), with larger station separations for large voids and small separations for small

voids. It is usually advisable to model the expected anomaly mathematically before conducting fieldwork. From this, along with the expected instrument accuracy, an estimate can be made of the anomaly size and the required station spacing.

Surveys are conducted by taking gravity readings at regular intervals along a traverse that crosses the expected location of the void. However, in order to take into account the expected drift of the instrument, one station (probably the first) has to be reoccupied every half hour or so (depending on the instrument drift characteristics) to obtain the natural drift of the instrument. Since gravity decreases as elevation increases, the elevation of each station has to be measured with an error of no more than about 3 cm. A more detailed description of the corrections to be applied to gravity data is described under Data Processing. Readings are taken by placing the instrument on the ground and leveling it. This may be automatic with some instruments, as it is with the Lacoste and Rhomberg model EG.

Data Processing: Several corrections have to be applied to the field gravity readings. Each reading has to be corrected for elevation, the influence of tides, latitude and, if significant local topography exists, a topographic correction. To understand the corrections, a gravity reading is first considered on the surface of a flat ground surface. Corrections are then applied to account for deviations from this condition. As the distance from the center of the earth increases, the pull of gravity decreases. The correction to account for this is called the elevation correction. If the gravity reading is taken on top of a hill, then there is a deficit of mass on either side of the hill, compared to a horizontal ground surface, as is illustrated in figure 86. This is corrected with a topographic correction. It is important to realize that mass higher than the reading site will also influence the data and has to be accounted for. This may occur in areas of significant topography or when surveys are conducted near large buildings. In a modern instrument such as the Lacoste and Rhomberg model EG, the meter may automatically apply the tidal and drift corrections.

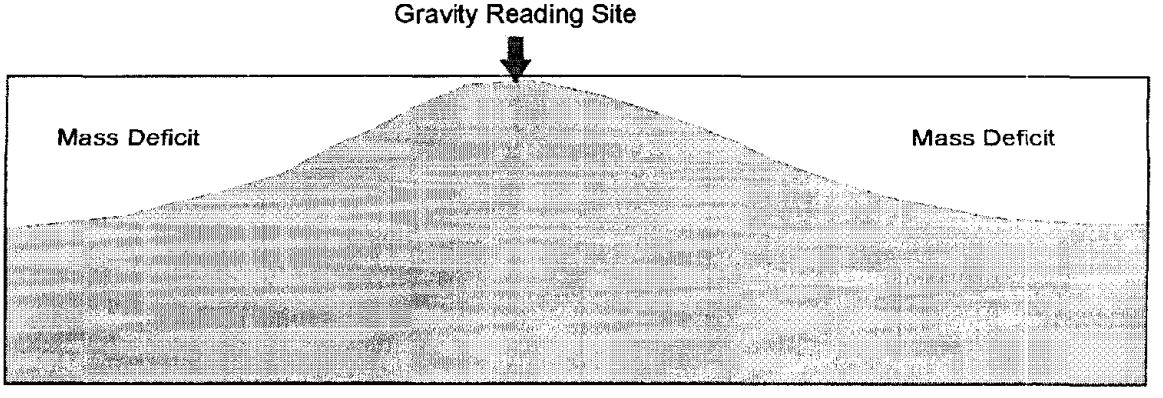

Figure 86. Correction for topography.

Data Interpretation: Gravity data are interpreted using software to calculate the gravity field of geologic features, input by the operator. The program will then change the parameters (shape, depth) of the body (in this case void) until the calculated gravity field matches the field gravity field. This process is called inversion and is commonly used in geophysical interpretation. If several lines of data, or data from a grid, have been acquired, then a map of the gravity field may be produced.

The interpretation involves searching for areas where the pull of gravity has decreased and then modeling these anomalies to find the depth to the source of the anomaly and the approximate size of the feature.

Advantages: The gravity method responds directly to the mass deficit created by a void. The method requires a relatively small amount of instrumentation and is an unobtrusive method able to be conducted in environmentally sensitive areas.

Limitations: Gravity surveying is a labor-intensive procedure requiring significant care by the instrument observer. Gravity instruments require careful leveling before a reading is taken. This may have to be done manually or it may be performed by the instrument itself. Once the reading has been taken, the gravity sensing mechanism must be clamped to stop excessive vibration that would influence the sensing mechanism and cause excessive drift, thereby affecting future readings. The instrument must be placed on solid ground (or a specially designed plate) so that it does not move (sink into the ground). All of the stations have to be accurately surveyed for elevation.

Because the anomaly from voids rapidly becomes smaller with void depth, void detectability rapidly decreases with void depth. Because of this, pre-survey modeling using as much geologic information as possible is important to establish the expected anomaly size, and to determine if a gravity survey is feasible.

If the cavity lies in bedrock beneath a layer of overburden, variations in the topography of the bedrock surface may be reflected in the gravity profile and need to be accounted for. These variations may occur because of fracturing above the void and preferential weathering causing a bedrock depression, or they may be simply part of the normal bedrock undulations. These variations will influence the gravity data, producing anomalies that could be misinterpreted as resulting from voids. Other geophysical methods may be needed to map the bedrock topography. If, as is likely, the velocity of the bedrock is greater than that of the overburden, then seismic refraction may be used to map the bedrock topography allowing the gravitational effects of bedrock surface elevation changes to be calculated. If the overburden and bedrock have different resistivities, then resistivity soundings or conductivity measurements can also be used to map the bedrock surface.

5.1.2 Ground Penetrating Radar

Basic Concept: Ground Penetrating Radar (GPR) can be used to locate shallow cavities. However, depth of penetration is very dependent on the site conditions, in particular on the resistivity of the ground and clay content. Best results will be obtained in unsaturated areas where no clay is present. For voids at depth, the most serious issue is penetration. Therefore, an antenna with a sufficiently low frequency to penetrate to the required depth is needed.

The GPR instrument consists of a recorder and a transmitting and receiving antenna, with different antennae being used to provide different frequencies. The transmitter provides the high-frequency (25 MHz to 1,500 MHz) electromagnetic signals that penetrate the ground and are reflected from objects and boundaries that have a different dielectric constant from their host material. The reflected waves are detected by the receiver and stored in memory. The

transmitter and receiver antenna and the GPR waves are illustrated in figure 87. An air-filled void will almost certainly provide a dielectric contrast with the host rocks. It is also possible that a water-filled void may provide a dielectric contrast with the host rocks.

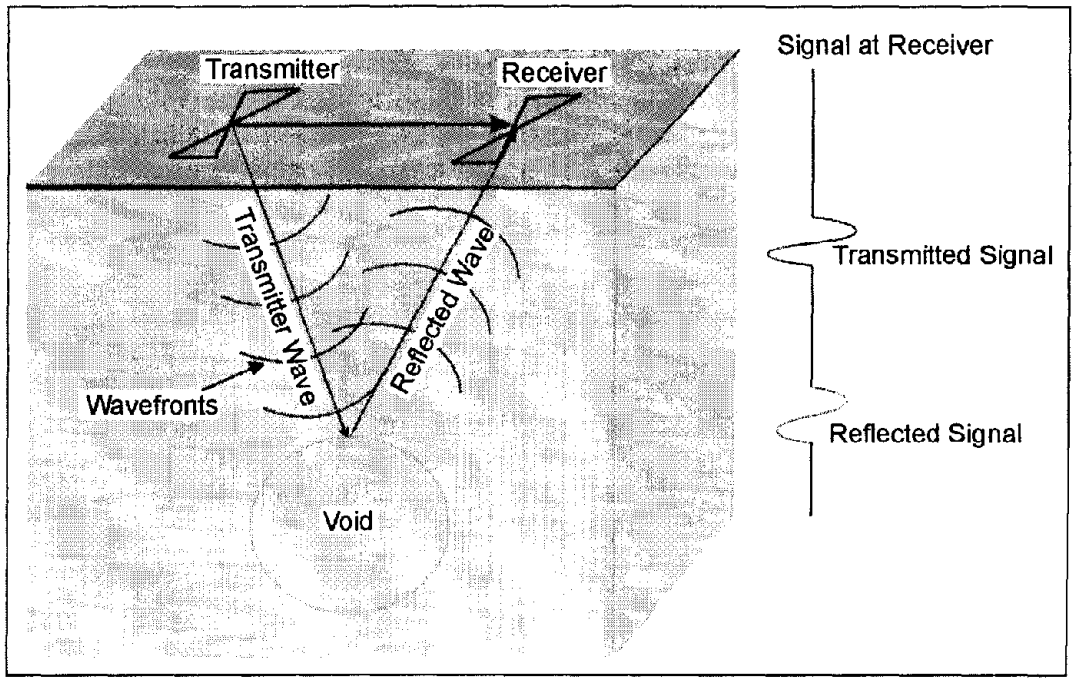

Figure 87. Ground Penetrating Radar system over a void.

Several companies manufacture GPR equipment, including Geophysical Survey Systems Inc, (GSSI), GeoRadar, Mala GeoScience, and Sensors and Software. Figure 112 shows a typical controller manufactured by GSSI and includes the data recorder and system control for a GPR system.

Any antenna supported by this instrument can be attached and used to collect data. Figure 113 shows a 100 MHz antenna that can be used with the above instrument. The 100 MHz antenna is suited for deeper applications to depths of about 20 m and could be used to locate cavities.

Data Acquisition: GPR surveys are conducted by pulling the antenna across the ground surface at a normal walking pace. The recorder stores the data as well as presenting a picture of the recorded data on a screen. When conducting GPR surveys, it is usually advisable to have a selection of antennae available and to perform tests to ascertain the most appropriate antenna to use for the survey.

Data Processing: It is possible to process the data, much like the processing done on single channel reflection seismic data. Processing might include distance normalization, horizontal scaling (stacking), vertical and horizontal filtering, velocity corrections, and migration. However, depending on the data quality, this may not be necessary since the field records may be all that is needed to observe the cavity.

Data Interpretation: To calculate the depth to the cavity, the speed of the GPR signal in the soil or rock at the site needs to be obtained. This can be estimated from charts showing speeds for typical soil/rock types or it can be obtained in the field by conducting a small traverse across a buried feature whose depth is known. A typical GPR record over voids (cavities) is shown in figure 88. The arrows show the reflectors thought to indicate voids.

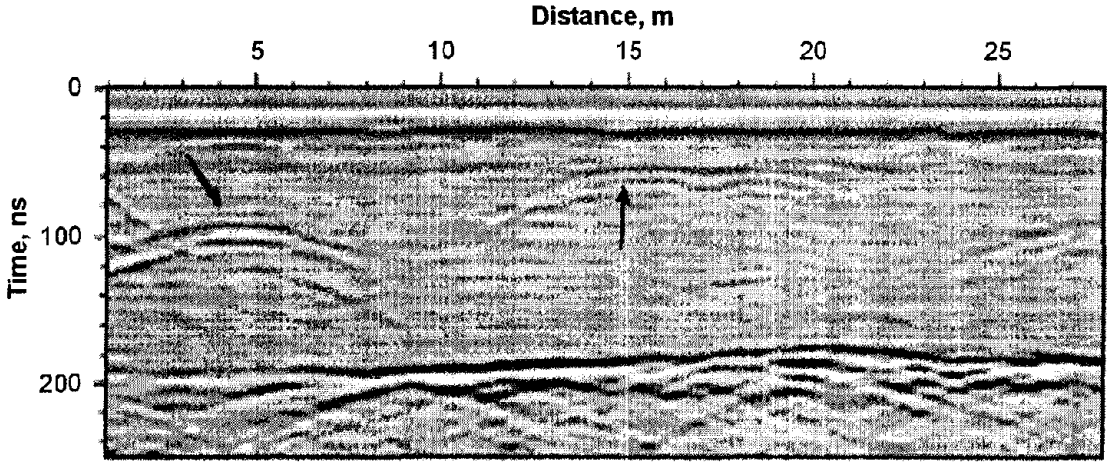

Figure 88. Ground Penetrating Radar data showing reflections thought to indicate voids.

Figure 89 shows GPR data from a pavement survey showing voids under the pavement, along with the geologic, structural interpretation.

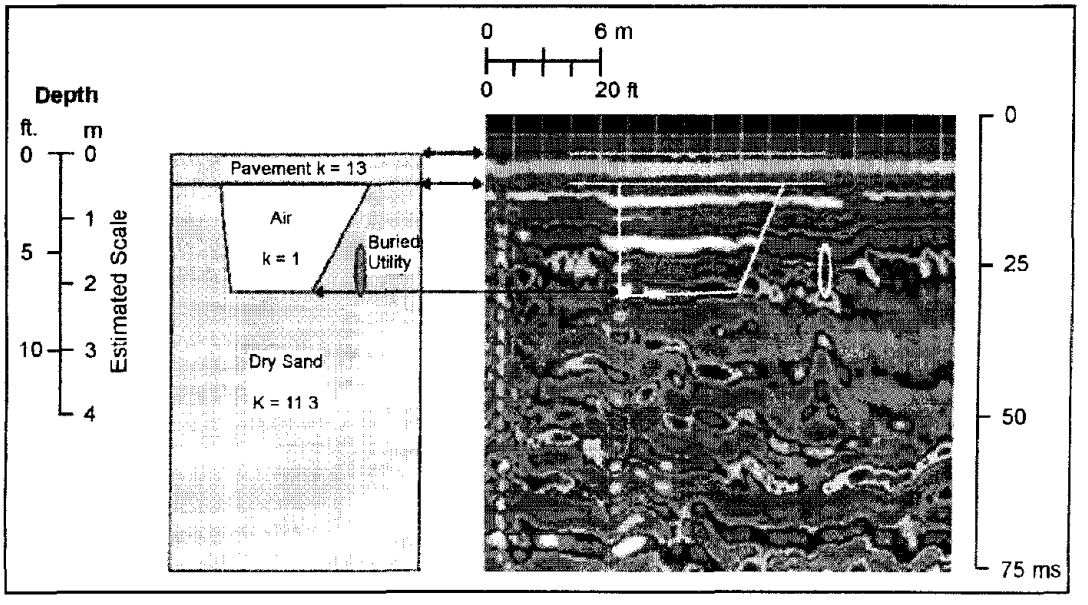

Figure 89. Ground Penetrating Radar data from a pavement survey showing its interpretation. (Hauser, et al. 2001

Advantages: GPR data can be recorded quickly and the data is presented on a screen during the survey allowing its quality to be evaluated. If the resolution or penetration depth are not appropriate then the antenna frequency can be changed.

Limitations: Probably the most limiting factor for GPR surveys is that their success is very site specific and depends on having a contrast in the dielectric properties of the target compared to the host overburden along with sufficient depth penetration to reach the target. Penetration of the GPR signal may be severely limited in saturated, electrically conductive ground containing clay. For shallow surveys along roads, saline conditions resulting from de-icer may produce conductive conditions. In addition, any metal reinforcement and other features, such as guardrails and power lines, may hinder a survey. However, it is likely that most cavities will provide the desired dielectric contrast needed; thus, depth of penetration is probably the most important factor. Dielectric contrasts will be greater with an air-filled void and least with a void filled with alluvium or water. Lower frequency GPR antennae are usually not shielded, allowing GPR energy to radiate in all directions. Thus, surveys under bridges or other structures using lower frequency antennae will produce reflections from these overhead features that may interfere with reflections for subsurface features. It may be possible to separate the reflection from the bridge deck or other overhead features from subsurface reflections, providing these two reflection times are significantly different.

5.1.3 Resistivity Methods

Basic Concept: Since an air-filled void usually presents a good resistivity contrast with the host rock, resistivity methods can sometimes be used to locate them. However, the voids have to be fairly shallow, maybe within 30 m of the ground surface. This is partly because the electrode array needed to investigate to greater depths becomes excessively long and cumbersome. In addition, being a long array, the resistivity results become influenced by other geological conditions, both along the traverse line and laterally. If the void is filled with water, then its resistivity contrast with the host rocks may be quite small, and may even provide a resistivity low, depending on the salinity or acidity of the water filling the void.

The measurement of resistivity, or more correctly apparent resistivity (since the value read may include several layers each with different resistivities), can be done using four electrodes placed into the ground. The electrodes are simply metal stakes about 0.3 m long that are hammered vertically into the ground. Resistivity readings can be conducted along lines using a constant electrode spacing, forming a traverse of resistivity values, or they can be conducted at one location, taking resistivity measurements using several electrode spacings to form a resistivity sounding. In order to locate cavities, resistivity traverses would be the most appropriate method, although soundings may be needed to find the depth to the cavity. However, instruments are now available that efficiently record resistivity data automatically, allowing resistivity values at several electrode spacings to be recorded along a traverse, thus combining sounding and traverse data. The use of these instruments provides the most appropriate method for locating cavities using resistivity measurements.

Several electrode arrays are used to measure resistivity, and most of the arrays used are illustrated in figure 90.

These arrays are used for different types of resistivity surveys. The Schlumberger array is often used for resistivity soundings, as is the Wenner array. The Pole pole array provides the best signal, but is cumbersome because of the long wires required for the remote electrodes, and it is rarely used. The Dipole dipole array was originally used mostly by the mining

industry for induced polarization surveys. Readings were taken using several different separations of the voltage and current dipoles, providing measurements of the variation of resistivity with depth. Long lines of data were recorded requiring many readings. This array has now become common for resistivity surveys using the automated resistivity systems. If more signal (voltage) is needed than can be provided with the dipole dipole array, then the pole dipole array can be used.

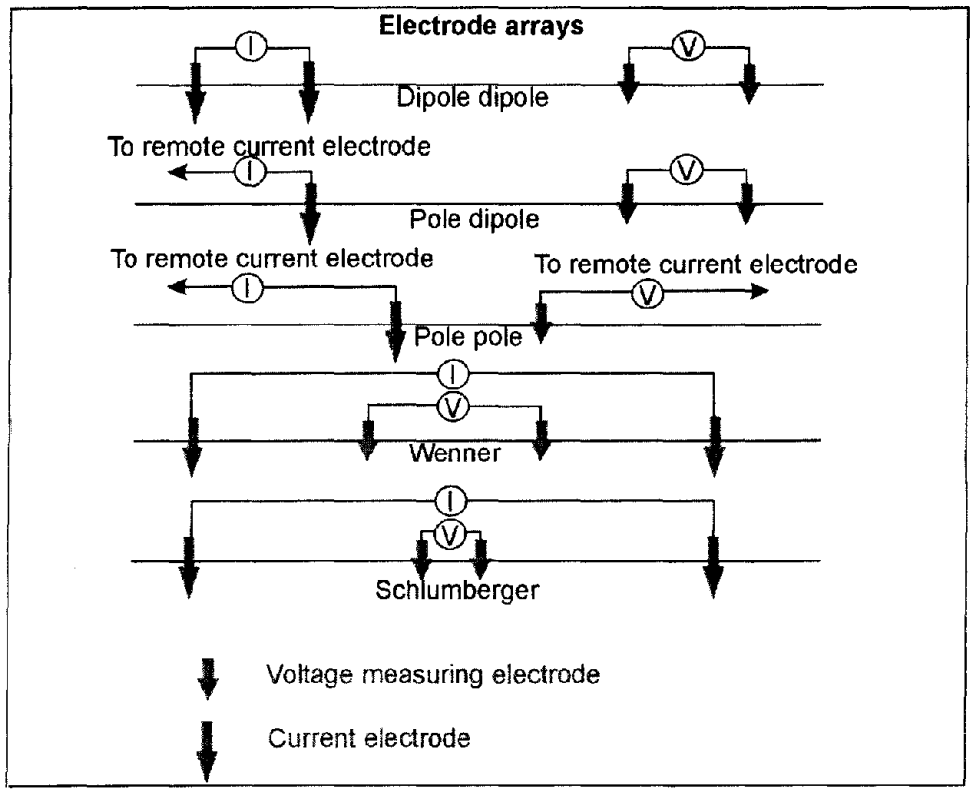

Figure 90. Electrode arrays used to measure resistivity.

The electrical current is passed into the ground using two electrodes, and the resulting voltage is measured using the other two electrodes. A geometric factor is calculated for each array and is used in the calculation of apparent resistivity. Resistivity soundings may be useful to find the depth of the bedrock, or to estimate depths to voids or collapse features, and are described here with that purpose in mind. Figure 91 shows the electrode array, the current flow lines (figure 91a), and the resulting sounding curve (figure 91b) over a resistive bedrock. Soundings are conducted by taking measurements at numerous electrode spacings while keeping the center of the array stationary. From these data, a sounding curve is produced (figure 91b).

One of the most commonly used electrode arrays for soundings is the Schlumberger array, which is described here. In this array, the two outer electrodes are used to pass switched current into the ground, and the resulting voltage is measured with the inner two electrodes.

When the electrode spacing (AB/2) is small, the measured resistivity approaches that of the upper layer (layer 1), and when the electrode spacing is large, the measured resistivity approaches that of the lower layer (layer 2, bedrock) (figure 91b). The sounding curve can be

interpreted to provide the depth and resistivities of the layers under the sounding site. Resistivity traverses are more commonly recorded using the dipole dipole array, although sounding information is obtained from this array if several dipole separations are used.

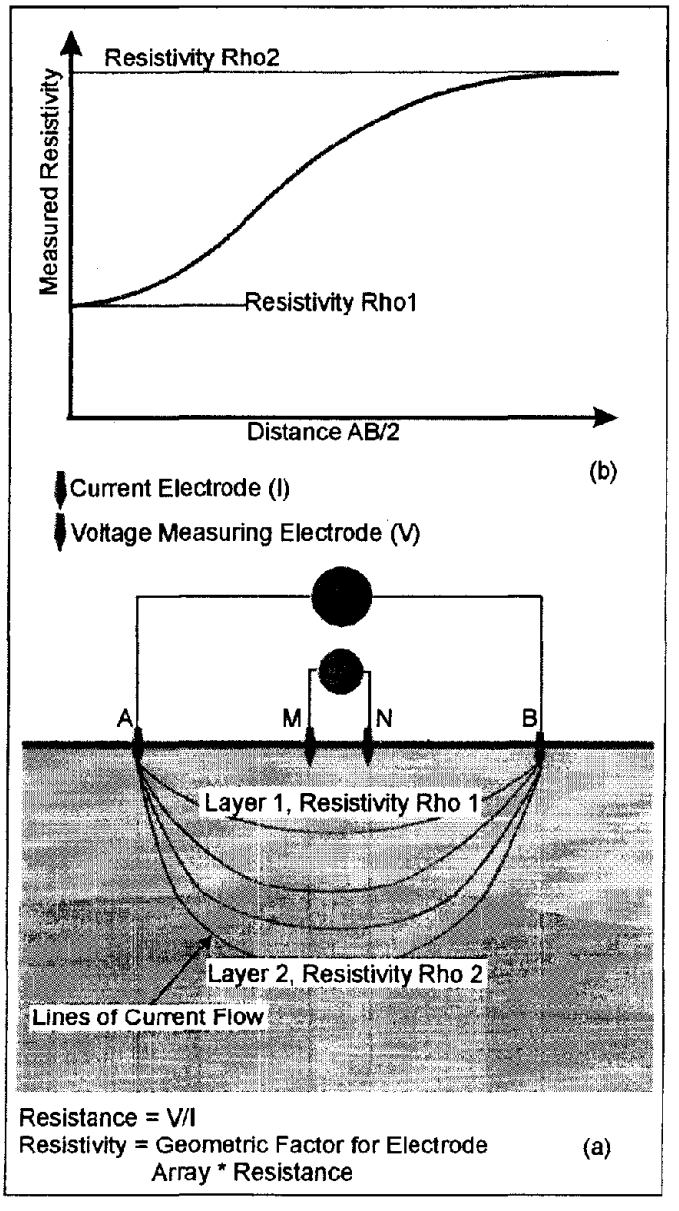

Figure 91. Electrode array for (a) measuring the resistivity of the ground, and (b) a resistivity-sounding curve.

Data Acquisition: Performing a resistivity survey is a moderately labor-intensive procedure, largely because four electrodes have to be inserted into the ground at each station. The first step is to decide the electrode array dimensions to use. This will depend on the depth of investigation and on the geologic section. A resistivity sounding involves taking resistivity readings at different electrode spacings, with the center of the array remaining fixed from which a sounding curve (figure 91b) can be plotted and interpreted. It is advisable to plot the resistivity-sounding curve in the field. If resistive bedrock is expected, then the sounding

curve will show increasing resistivities at larger electrode spacings. Before conducting a resistivity survey for cavities, modeling is advantageous to provide the required sensitivity of the method and the best data recording specifications.

If a resistivity traverse is to be recorded, then the dipole-dipole array will probably be used. If several dipole separations are proposed, allowing depth-sounding information to be obtained, then the dipole spacing and the separation of the dipoles need to be evaluated prior to field data recording. A small dipole spacing will provide the best anomaly resolution, but large dipole separations will be required for deep investigations. With small dipoles, only small voltages will be observed at large dipole separations. As with all electrical methods, the resolution of the target decreases with increasing depth.

There are instruments that allow the electrodes to be placed in the ground along a traverse prior to collecting any data. These systems have electrodes that are addressable by the control unit, which is able to automatically set the electrode function, either on/off or a current or voltage electrode. With these systems, a large number of electrodes are connected to the instrument prior to data recording. The electrode array to use, along with the data recording parameters, are entered into the instrument before data recording is initiated. Once data recording begins, the system automatically activates the necessary electrodes for each reading and then takes a reading. It does this for all of the electrodes, making data recording quite efficient. Thus, a large amount of data can be recorded, allowing a correspondingly better interpretation with more resolution. These systems are usually called Automated Resistivity systems. Unlike the resistivity sounding method discussed earlier, these systems are appropriate for the search for cavities. An example of the layout of electrodes for this type of system is shown in figure 92.

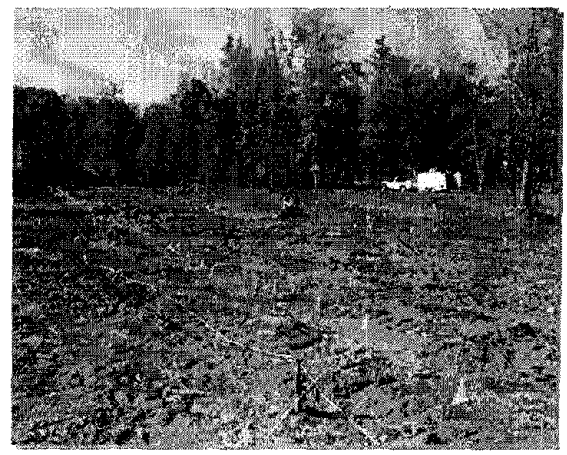

Figure 92. Electrode layout for a resistivity survey. (Bay Geophysical)

Data Processing: Usually no processing of the data is needed. The resistivity data are plotted to form a pseudosection (figure 93) in which data from small electrode spacings are plotted near the top of the plot (ground surface), and data from the large electrode spacings are plotted some distance vertically beneath the surface line, thus simulating a plot of resistivity against depth for the whole traverse.

Data Interpretation: Interpretation of the data is usually done with resistivity modeling software, which produces a plot of the interpreted resistivity against depth. The resistivity of the cavity and the host rocks determines the expected contrast. Usually, air-filled cavities will have a higher resistivity than the host rocks. However, if the cavity is water-filled, its resistivity may be similar to that of the host rocks, or if the host rocks are resistive or the water in the cavity is saline and, hence, has a low resistivity, the cavity may provide a low-resistivity target.

An example of data from an automated resistivity system is shown in figure 93, illustrating resistivity data across a sinkhole(s). Figure 93 presents three distinct resistivity lows consistent with voids or highly fractured rocks.

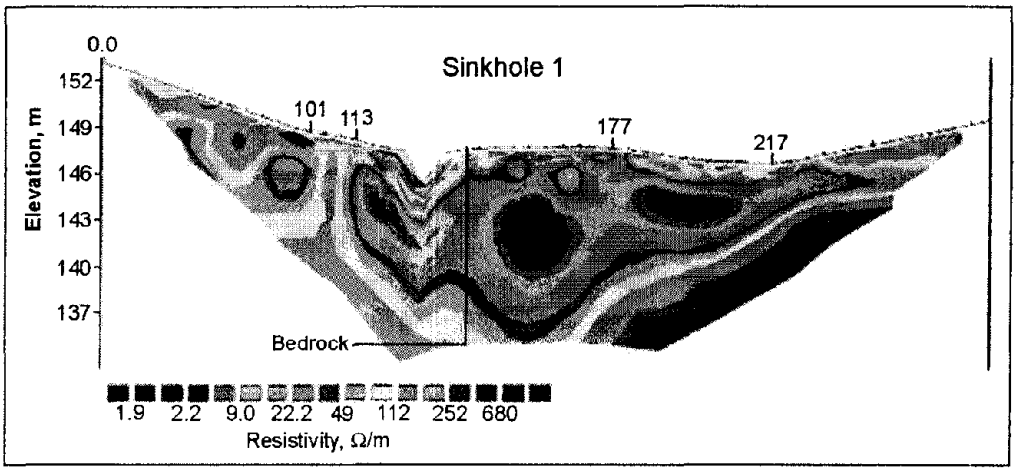

Figure 93. Data from a resistivity survey over a sinkhole plotted as a pseudosection. (Bay Geophysical)

Advantages: Since the resistivity of a cavity is very high, this method can be quite successful at locating cavities if they are large enough compared to their depth.

Limitations: The resistivity method is best suited for finding shallow voids, e.g., those no deeper than 20 or 30 m, depending on the size of the void and the host geology. This is because a long electrode array is needed to search deeper, and such an array is influenced by a large volume of rock and overburden. The influence of the void then becomes relatively quite small. If the host geology is electrically homogeneous, then its influence will be a constant and less of a problem, although the effect of the void is still diluted by larger electrode arrays.

The method is labor intensive in that electrodes have to be planted in the ground along the traverse. The automated resistivity system, in which the instrument automatically records the data while cycling through the required electrode settings, makes resistivity surveys more efficient, allows much more data to be obtained, and results in better interpretation. If the ground is hard, planting the electrodes can be difficult. If the ground is dry or stony, the electrical resistance of the electrode to ground will be very high. In this case, water may have to be poured on the electrodes to reduce this resistance and allow sufficient current to be put into the ground. Any grounded metal fences local to the measuring site will influence the data,

and may obscure the desired anomalies. Overhead power lines may induce 60 Hz noise into the data.

If data are obtained along a single line, lateral resistivity variations normal to the line are not accounted for and may introduce errors into the interpretation. However, this can be minimized by recording parallel lines or by recording a three-dimensional resistivity survey.

Seismic methods: Several seismic methods can be used to locate cavities, although some of these methods may only locate the cavity indirectly. For instance, seismic refraction can locate fractured bedrock that may occur above a cavity. Other methods, such as shear waves or Common Offset Surface Waves, attempt to locate cavities directly.

5.1.4 Seismic Refraction

Basic Concept: The seismic refraction method can be used to find fractures in the bedrock that might indicate voids beneath the fractures. The method involves looking at the amplitude and character of the refracted signals at each geophone. If a fracture, or more likely a fracture zone, is encountered, the amplitude of the refracted signal will be diminished. If a large open fracture is encountered, the signal may disappear completely. Figure 94 illustrates the concept, showing that traces 2 and 3 have diminished amplitudes over the fracture zone.

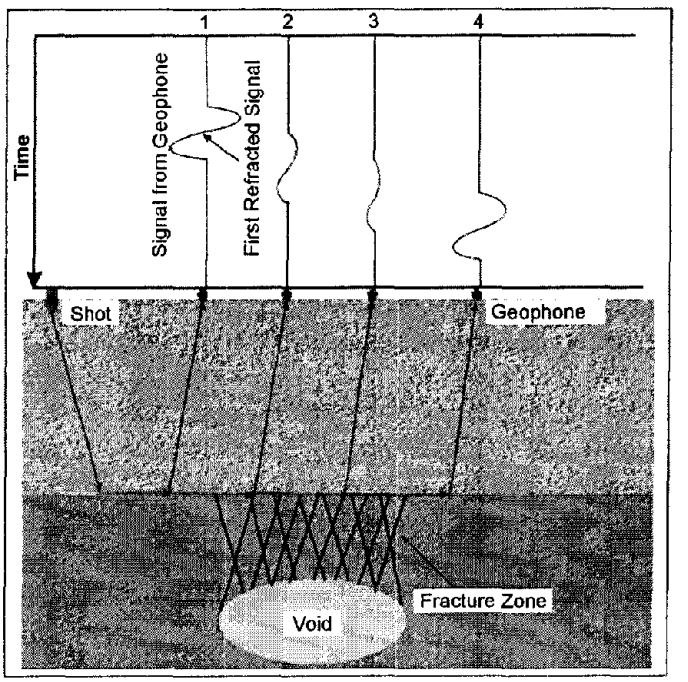

Figure 94. Seismic refraction across a fracture zone.

Data Acquisition: The design of the survey is the same as for any other seismic refraction survey. The length of the geophone spread should be sufficient to image the bedrock. Depending on the depth of investigation, an energy source of sufficient size is required. This may be a hammer and base plate or black powder charges in shallow (1 or 2 feet) holes. Other methods, such as weight drop techniques, are also available. Since the fracture zone may

attenuate the signals more than non-fractured bedrock, more energy may be needed than for an equivalent bedrock mapping survey.

Data Processing: Data processing is fairly simple and involves observing the seismic records for diminished amplitudes in the refraction arrival signals, as seen in figure 94.

Data Interpretation: The locations of diminished amplitude zones can be placed on a map of the area from which the fracture zone can be outlined.

Advantages: This application of the seismic refraction method is fairly rapid to apply in the field. The seismic records are displayed on the instrument allowing potential fractures to be recognized during the field survey.

Limitations: Probably the biggest limitation is that the method is indirect in that usually fracture zones are detected and not voids, although voids may be detected if they are not too far beneath the bedrock surface. The fractures may have some other origin and not be caused by voids. However, if voids are the cause of fractures, then by having small geophone spacings, sufficient data can be obtained over the fracture zone providing good lateral resolution. Any local source of seismic noise will reduce the quality of the data, and a larger seismic energy source may be required to overcome this noise. If the ground surface is hard (concrete or asphalt), it will be difficult to plant the geophones. Surveys conducted near roads or other industrial activity will also be subject to noise from these activities. Although shear waves can be used to locate fracture zones and are less influenced by traffic noise, creating impulsive shear waves with sufficient amplitude is more difficult than for compressional waves. The method is fairly labor intensive.

5.1.5 Shear Wave Reflection Surveys

Basic Concept: Voids can be detected using seismic shear wave reflection surveys. These surveys are conducted in much the same manner as compressional wave seismic reflection surveys, except that a shear wave source has to be used. One such source is called the Microvib and is shown in figure 95.

The seismic waves travel into the overburden and bedrock and are influenced by the void as is illustrated in figure 96.

Rays that encounter the upper surface of the void are reflected back to the ground surface. There is no transmission of the wave through the void because shear waves are not transmitted through air or water. Rays that do not encounter the void are reflected from the deeper layer as expected; however, rays that encounter the lower surface of the void are reflected back to the deeper reflector. Again, since air or water do not support shear waves, they are not transmitted through the expected void.

Figure 95. The Microvib shear wave generator. (Bay Geophysical)

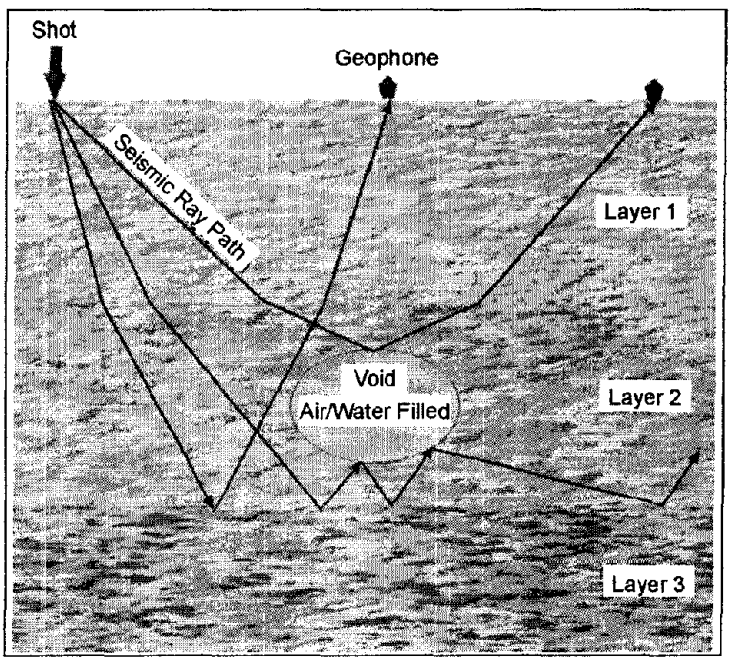

Figure 96. Ray paths for shear waves over a water/air-filled void.

Data Acquisition: Shear wave reflection surveys are conducted in much the same way as compressional wave surveys. Probably the most important difference is that the geophone spacing will be smaller for an equivalent depth of investigation, since the velocity of shear waves is only about 0.6 times that of compressional waves. The geophone spacing and spread length are also dependent on the expected depth and size of the void. Another important quantity to consider is the frequency, and, hence, wavelength, of the shear waves. The higher

the frequency, the smaller the voids that are be detected. However, higher frequencies also attenuate faster and have less depth penetration. A very rough estimate is to keep the wavelength no greater than about 0.25 times the dimensions of the void.

Data Processing: Data processing is essentially the same as for reflection seismic surveys. With vibrational sources, such as the Microvib, special processing techniques have to be applied to transform the data to that which would have been observed with a conventional impulse type seismic source. The records are then sorted to gathers with a common mid-point. Various kinds of filtering and other processes are then used to refine the data, after which the traces for each gather are summed to produce a single trace whose signal-to-noise ratio is much greater than the unprocessed traces. Once this procedure has been done for all of the traces, a plot can be produced showing the seismic reflectors. Additional processing, such as migration, can also be applied to this data.

Data Interpretation: Interpretation of the data requires some understanding of the influence of the ray paths, shown in figure 96, on the final seismic section. The rays that are reflected back to the lower layer do not reach the geophones on the ground surface and cause a lower amplitude signal to be recorded. Thus, voids produce a region in the seismic section where layer continuity decreases, and where amplitudes of the reflected waves are attenuated. Figures 97 and 98 show the results of two shear wave surveys for voids.

In figure 97, the continuity of the reflector, highlighted in red, is broken at about the center of the section. In addition, the area of reflectors above this main reflector becomes less coherent.

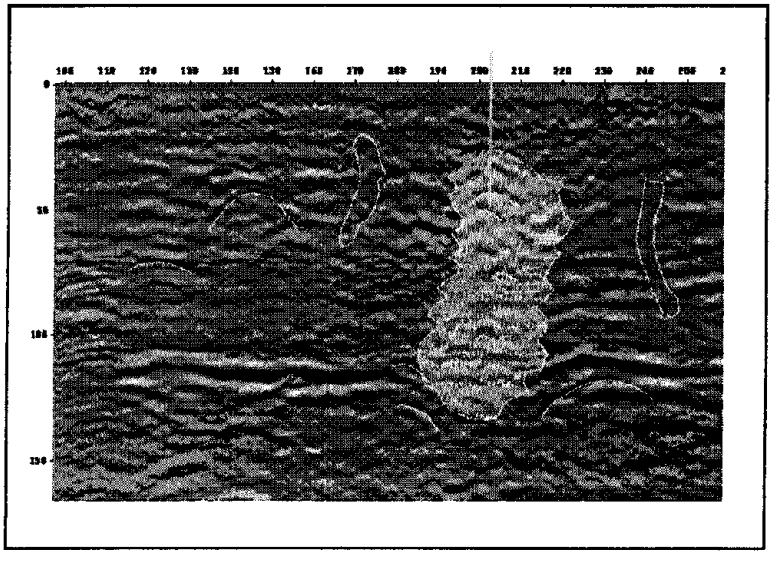

Figure 97. Results from a Microvib survey showing an interpreted void. (Bay Geophysical)

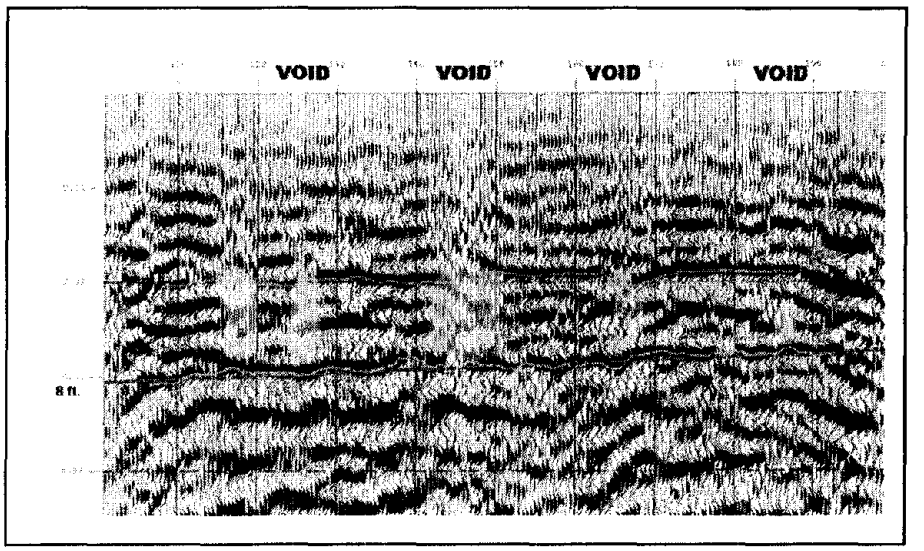

Figure 98. Voids interpreted from shear wave reflection data. (Bay Geophysical)

In figure 98, a similar situation occurs except there are more reflectors in this section than in the section shown in figure 97.

In figure 98, the voids are seen as a disappearance of coherence along the reflectors. As discussed above, this kind of response is expected when reflections from deeper layers are blocked (attenuated) by the void and do not reach the ground surface.

Advantages: The success of the method for locating voids depends on the frequency of the shear waves in the ground. If high frequencies can be generated then relatively small voids may be imaged. Probably one of the best sources in the Microvib since it can provide relatively high frequencies.

Limitations: The shear wave reflection method is quite labor intensive and requires significant processing. Besides the Microvib, there are few shear wave sources for the relatively shallow surveys for voids. There are larger truck-mounted shear wave sources if deeper investigation depths are needed.

5.1.6 Rayleigh Waves Recorded with a Common Offset Array

Basic Concept: This method uses Rayleigh waves to detect fracture zones and associated voids. Rayleigh waves, also known as surface waves, have a particle motion that is counterclockwise with respect to the direction of travel. Figure 99 illustrates the particle motion for Rayleigh waves traveling in the positive X direction. In addition, the particle displacement is greatest at the ground surface, near the Rayleigh wave source, and decreases with depth. Three shot points are shown, labeled A, B, and C. The particle motion and displacement are shown for five depths under each shot point. For shot B over the void, no Rayleigh waves are transmitted through the water/air-filled void. This affects the measured Rayleigh wave recorded by the geophones over the void. Four parameters are usually observed. The first is an increase in the travel time of the Rayleigh wave as the fracture zone above the void is crossed. The second parameter is a decrease in the amplitude of the

Rayleigh wave. The third parameter is reverberations (sometimes called ringing) as the void is crossed. The fourth parameter is a shift in the peak frequency toward lower frequencies. This is caused by trapped waves. The effective depth of penetration is approximately one-third to one-half of the wavelength of the Rayleigh wave.

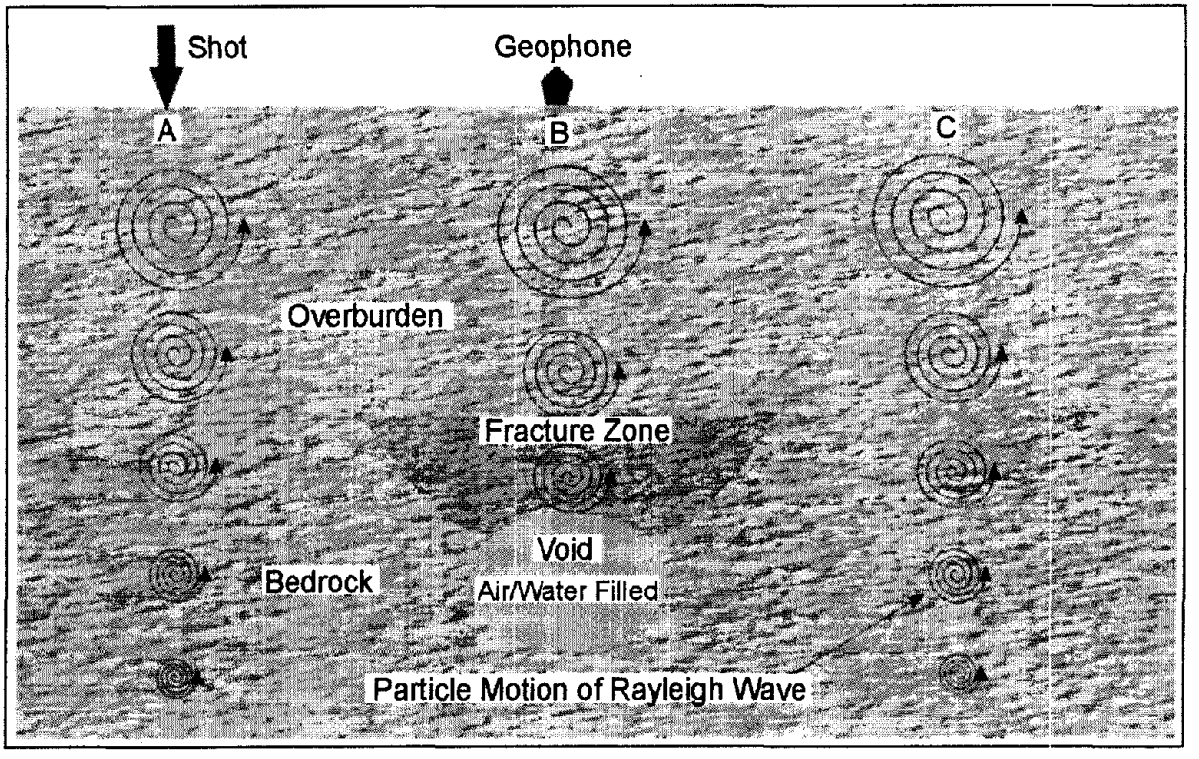

Figure 99. Rayleigh wave particle motion and displacement over a void.

Data Acquisition: Rayleigh waves are created by any impact source. For shallow investigations, a hammer is all that is needed. Data are recorded using one geophone and one shot point. The distance between the shot and geophone depends on the depth of investigation and is usually about twice the expected target depth. Data are recorded at regular intervals across the traverse while maintaining the same shot-geophone separation. The interval between stations depends on the expected size of the void/fracture zone and the desired resolution. Generally, in order to clearly see the void/fracture zone, it is desirable to have several stations that cross the area of interest. Figure 100 presents data from a common offset Rayleigh wave survey over a void/fracture zone in an alluvial basin.

The geophone traces are drawn horizontally with the vertical axis being distance (shot stations).

Data Processing: The data may be filtered to highlight the Rayleigh wave frequencies and is then plotted as shown on Figure 100.

Data Interpretation: If the frequency content of each trace is obtained then the tendency towards lower frequencies over a fracture/void can be observed. The data shown in Figure 100 illustrates many of the features expected over a void/fracture. The travel time to the first

arrival of the Rayleigh wave is greater across the void/fracture and is wider than the actual fractured zone. The amplitudes of the Rayleigh waves decrease as the zone is crossed. In addition, the wavelength of the signals over the void/fracture is longer than those over unfractured rock, showing that the high frequencies have been attenuated. Since the records are not long enough, the ringing effect is not observed in this data.

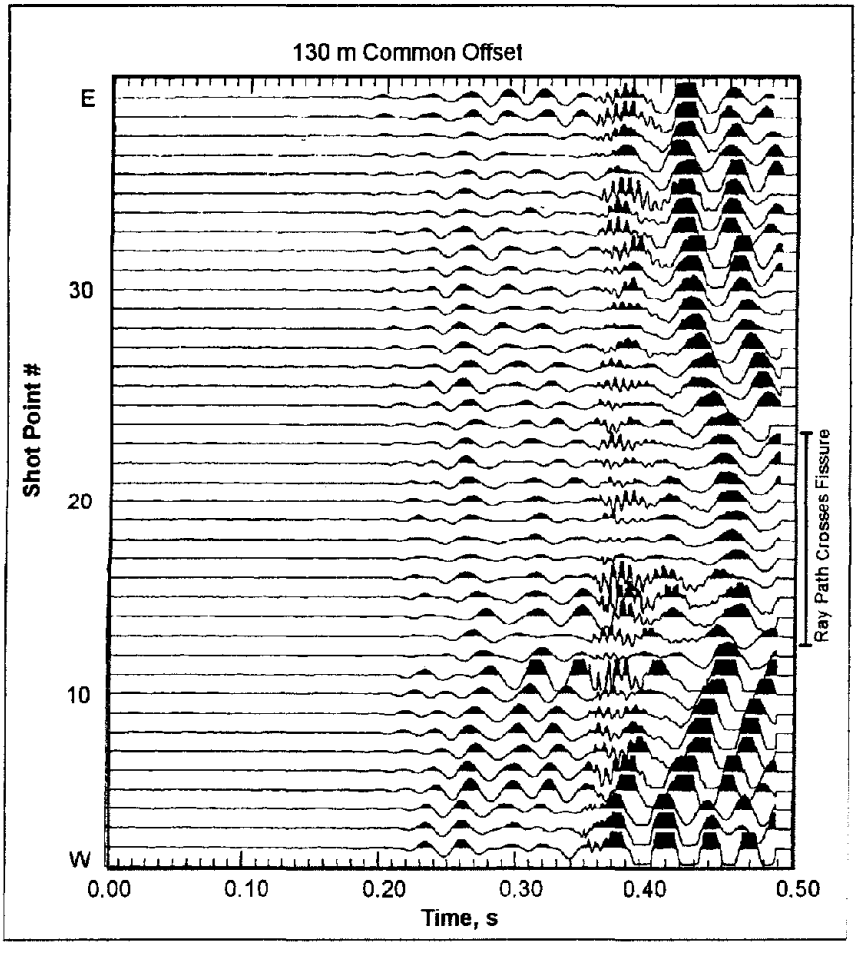

Figure 100. Data from a Rayleigh wave survey over a void/fracture zone.

Advantages: The field data recording is simple and requires much less effort for a given line length than the seismic refraction method.

Limitations: The method responds to the bulk seismic properties of the rocks and soil, which are influenced by factors other than voids. It has a limited depth of penetration and resolution. Penetration depth is limited by the wavelengths generated by the seismic source. However, this method is faster and less costly than most other seismic methods.

5.1.7 Cross-borehole Seismic Tomography

Two- and three-dimensional tomography is used for the high resolution imaging of the subsurface between boreholes.

Basic Concept: Tomography is an inversion procedure that provides for two- or three-dimensional (2-D and 3-D) velocity (and/or attenuation) images between boreholes from the observation of transmitted first arrival energy.

Data Acquisition: Tomography data collection involves scanning the region of interest with many combinations of source and receiver depth locations, similar to medical CATSCAN (figure 101). Typical field operation consists of holding a string of receivers (geophones or hydrophones) at the bottom of one borehole and moving the source systematically in the opposite borehole from bottom to top. The receiver string is then moved to the next depth location and the test procedure is repeated until all possible source-receiver combinations are incorporated.

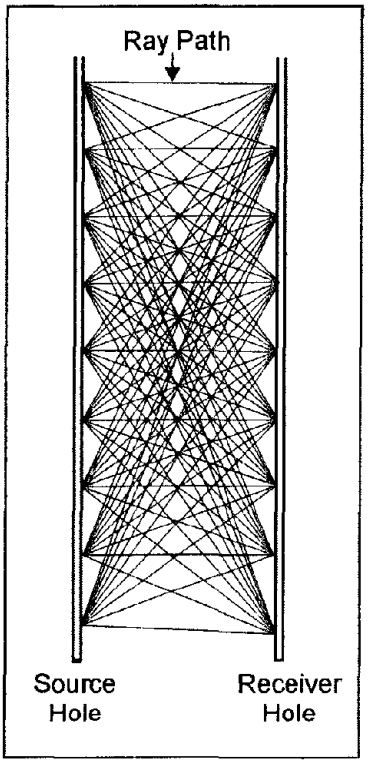

Figure 101. Source and receiver locations for a tomographic survey.

Data Processing: In the tomographic inversion technique, the acoustic wavefield is initially propagated through a presumed theoretical model and a set of travel times are obtained by ray-tracing (forward modeling). The travel time equations are then inverted iteratively in order to reduce the root mean square (RMS) error between the observed and computed travel times. The inversion results can be used for imaging the velocity (travel time tomography) and attenuation (amplitude tomography) distribution between boreholes.

Data Interpretation: An example of a cross borehole tomography survey to investigate an active sinkhole causing damage to property in a residential neighborhood in central Florida is shown below.

Figure 102 represents an isometric view of a low velocity zone defining the sinkhole. The surficial feature a approximately 8 meters depth is clearly visible. Also the "throat" of the sinkhole, at a depth of approximately 24 meters, indicates the presence of an opening in the confining layer. This is verified by the absence of a solid clay zone above the refusal material within a boring performed at the sinkhole.

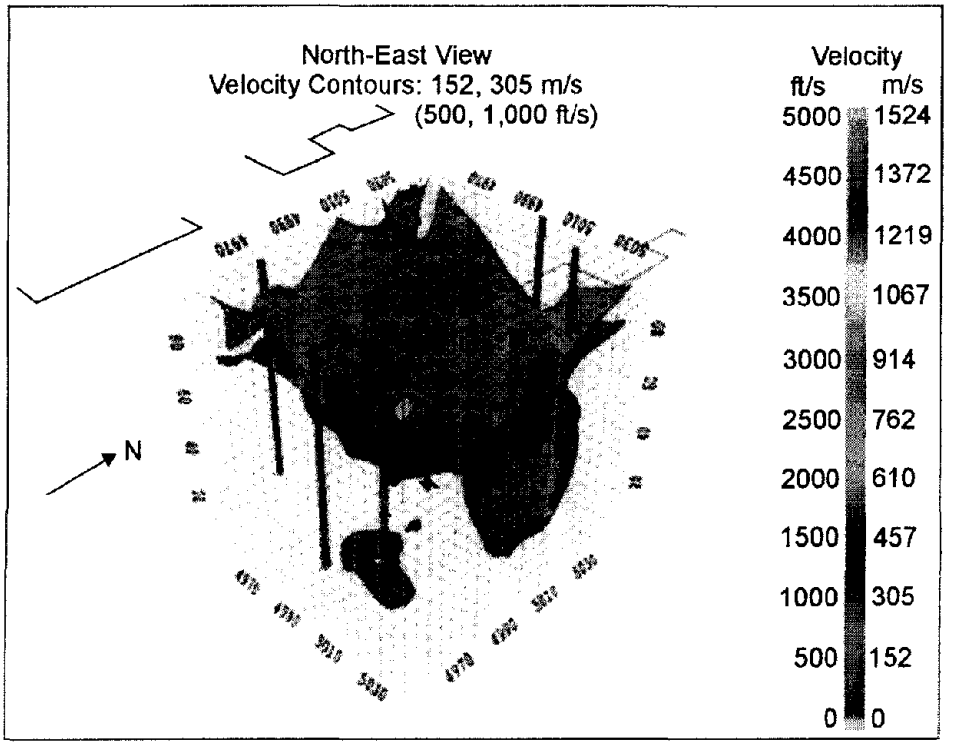

Figure 102. Isometric view of the low velocity zone. (NSA Geotechnical Services, Inc.)

Advantages: Tomography provides for a high-resolution two-dimensional area or three-dimensional volumetric imaging of target zones for immediate engineering remediation. Tomography can then be used in before and after surveys for monitoring effectiveness of remediation. Tomography can also be used in before and after surveys for monitoring fluid injections between test holes or for assessing the effectiveness of soil improvement techniques.

Attenuation tomography can be used for the delineating fracture zones. Wave equation processing can be used for a high-resolution imaging of the reflection events in the data including those outside and below the area between the boreholes.

Limitations: Tomography is data-intensive and specialized 3-D analyses software is required for true three-dimensional imaging. Artifacts can be present due to limited ray coverage near the image boundaries.

5.2 ROADBED CLAY PROBLEMS

In general, as described in section 5.2.1, estimating the clay content using geophysical methods is difficult. However, *mapping* clay underneath roadways can easily be performed as described in section 5.2.2.

5.2.1 Estimating Clay Content

Clays are very small-grained hydrous aluminosilicates with the phyllosilicate structure. Clays are classified as hydrosilicates, which means that they are formed from the chemical decomposition of pre-existing silicate minerals. Most clays result from the product of weathering and sedimentation, but they are also formed by hydrothermal activities. Clays can occur as part of a soil structure or as independent layers and lenses. They are also commonly found in glacial till, where glacial action has ground the rocks and boulders into fine particles.

Clay particle sizes range from 0.002 mm to 0.001 mm diameter for quartz, feldspar, mica, iron, and aluminum oxides. The finer parts (less than 0.001 mm in diameter) are colloidal and consist mainly of layer silicates with smaller amounts of iron and aluminum oxides. These consist of microscopically fine particles exhibiting a sheet-like structure. Their crystalline structure is such that, because of crystal imperfections, the surface appears negatively charged. During the formation of clay through weathering, positive charges (cations) are adsorbed to the surface. These cations are loosely held to the surface and can subsequently be exchanged for other cations or essentially go into solution if the clay is mixed with water. For this reason, they are called exchangeable ions, and the cation exchange capacity (CEC) of the soil is a measure of the number of cations that are required to neutralize the clay particle as a whole.

Any fine-grained mineral, including quartz, has a cation exchange capacity. However, clay particles are very small, and because the surface area per unit volume is very large, a large number of cations are adsorbed. These adsorbed cations can contribute significantly to the electrical conductivity of soil, which then becomes a function of the clay content. However, other factors influence the conductivity of soil, including the degree of saturation and the salinity of the pore fluid.

Because of their electrical structure, clay minerals often exhibit an effect called membrane polarization. This is a distribution of ions around the clay pores. When a DC potential is applied across the pore, negative ions accumulate at one end and leave the other end. Because of this polarization distribution, current flow is impeded. When the DC potential is switched off, the ions take a finite amount of time to return to their original positions.

From the above discussion, two basic parameters can be used to estimate the clay content of soils and other geologic layers. These are electrical conductivity and membrane polarization. Thus, the appropriate geophysical methods are conductivity measurements (or resistivity) and Induced Polarization to measure the membrane polarization.

The resistivities of soils and rocks vary from 1 to 30 ohm-m for some clays and shales to over 1,000 ohm-m for limestone, intrusive rocks such as granites, and some metamorphic rocks. However, in sedimentary soils and rocks, where resistivities generally range from 10 to 1,000

ohm-m, resistivity is also significantly influenced by the porosity and salinity of the water in the pore space.

In order to estimate clay content, the resistivity/conductivity of the layer/zone of interest has first to be determined. Then a relationship is needed to convert the conductivity to clay content. However, as mentioned previously, conductivity is strongly influenced by porosity and the salinity of the pore water, thus making the conversion from conductivity to clay content tenuous.

It is possible that the Induced Polarization method may be more successful since it is less influenced by the resistivity of the material. However, the method needs more research before production surveys are undertaken.

Methods

5.2.1.1 Conductivity Measurements

Basic Concept: Ground conductivity measurements are recorded using several instruments that use electromagnetic methods. The choice of which instrument to use generally depends on the depth of investigation desired. Instruments commonly used include the EM38, EM31, EM34, and the GEM2.

The EM38 is designed to measure soil conductivities and has a maximum depth of investigation of about 1.5 m. The EM31 has a depth of investigation to about 6 m, and the EM34 has a maximum depth of investigation to about 60 m. The depth of investigation of the GEM2 is advertised to be 30 to 50 m in resistive terrain (>1,000 ohm-m) and 20 to 30 m in conductive terrain (<100 ohm-m).

Electromagnetic instruments that measure ground conductivity use two coplanar coils, one for the transmitter and the other for the receiver. These instruments transmit sinusoidal electromagnetic fields oscillating between 330 Hz and 25 kHz (GEM2).

With the EM31 and EM34, the transmitter coil produces an electromagnetic field, oscillating at less than 10 kHz, that produces secondary currents in conductive material in the ground. The amplitude of these secondary currents depends on the conductivity of the material. These secondary currents then produce a secondary electromagnetic field that is recorded by the receiver coil.

These instruments can be used with the planes of the coils held parallel to the ground (vertical dipole mode) or perpendicular to the ground (horizontal dipole mode). The investigation depth is greatest in the vertical dipole mode and least in the horizontal dipole mode. In addition, in the vertical dipole mode, the conductivity readings are insensitive to near-surface conductivity changes, whereas in the horizontal dipole mode, the readings are significantly influenced by near-surface conductivity changes.

The EM38 instrument is shown in figure 103. This instrument is used for shallow surveys, usually measuring the conductivity of soil and has had a significant amount of use in agricultural areas, mapping areas of high salinity.

Figure 103. EM38 instrument being used in vertical dipole mode. (Geonics, Ltd.)

Figure 183 shows the EM31 instrument being used in vertical dipole mode, figure 197 shows the EM34 being used in horizontal dipole mode, and the GEM3 instrument is shown in figure 219.

Data measurements with the EM34 can be made using three different separations of the two coils, for each of the two modes, providing six different depths of investigation. However, as the depth of investigation increases, the lateral resolution decreases. The EM34 requires two people to operate. Data recording is also much slower than with the EM31. All of these instruments measure the bulk electrical conductivity of the ground. Since the conductivity of several different layers may be included in the measured conductivity, the correct technical term for the measured conductivity is apparent conductivity. When discussing data from these instruments in this document, conductivity is understood to mean apparent conductivity.

Data Acquisition: Surveys are conducted by taking readings along lines crossing the area of interest. These lines need to be surveyed to have spatial coordinates recorded. Readings are either taken at defined stations or on a timed basis, say every second (EM31). The mode in which the instruments are used (EM31 and EM34) depends on the target depth and the objectives. The instruments store the data in memory as they are recorded, allowing it to be downloaded to a computer later.

Data Processing: Data processing mostly involves assigning coordinates to each data point. These data are then gridded, contoured, and plotted, producing a map of the measured conductivity of the site.

Data Interpretation: Interpretation is done from this map. Generally, this will involve searching for areas of high electrical conductivity. These areas will be the most likely places to find clay.

A general relationship between clay content and conductivity when using the EM38 has been established during a survey in Denmark and is shown in figure 104. These data are for the EM38 used in the vertical dipole mode and is for shallow soils (less than 2 m). As can be seen, when the clay content increases, the soil conductivity also increases. The graph shows that when the conductivity is 10 mS/m, the clay content is 15%. When the soil conductivity is 15 mS/m, then the clay content is 20%.

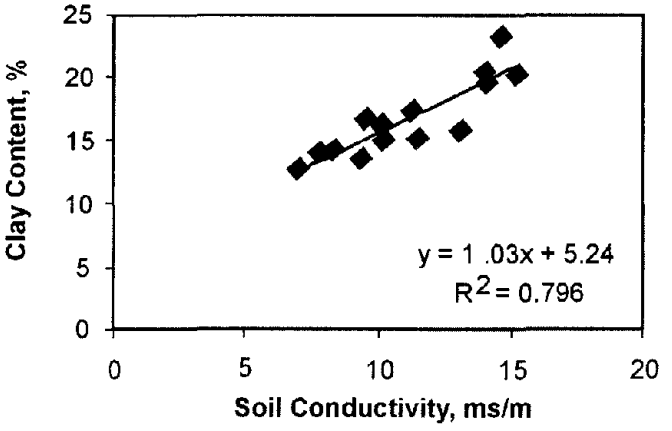

Figure 104. Relation between soil conductivity and clay content. (Dalgaard, et al.)

It is likely that this relationship is site specific, and a new relation will likely be required for each site surveyed. However, the data show that, at least in this case, a relationship was established between soil conductivity and clay content.

To establish this relationship with the EM31, where the depth of investigation may be up to about 6 m, the soil/overburden layer must have a depth greater than 6 m. If this is not the case, and the conductivity values are being influenced by bedrock, the measured conductivity will be a composite of the soil and bedrock conductivities. Therefore, the relationship shown in figure 104 probably cannot be established. In this case, areas of high conductivity may correspond to increased clay in the soil, an increase in the conductivity of the bedrock, or, if the conductivity of the soil or overburden is greater than that of the bedrock, possibly an increase in the thickness of the soil/overburden layer. In this case, areas of high conductivity will need to be investigated by other methods to establish the clay content.

If the EM34 is used in the horizontal dipole mode, the soil conductivity will influence the measured conductivity readings, depending on the thickness of the soil layer, since in this mode, the readings are sensitive to near-surface conductivity changes. If the vertical dipole mode is used, the influence of the soil conductivity on the measured conductivity values will probably be minimal. The interpretation of these data depends on the geology of the area. If geological layering exists, the conductivity changes may indicate overburden or layer thickness changes or lateral conductivity changes in one of the layers. Additional information about the layer thicknesses is needed to produce a more definitive interpretation. Seismic refraction or resistivity measurements may be able to provide this additional information.

Advantages: Conductivity data can be recorded with either then EM31 or EM34 fairly efficiently. The depth of investigation can be chosen by using the different modes of data

acquisition along with maximizing the depth of investigation (Vertical dipole mode) or the influence of near surface material (horizontal dipole mode).

Limitations: Clay is almost always electrically conductive, and areas of high conductivity have a reasonable chance that they will contain clay. However, estimating the amount of clay from conductivity measurements alone is generally not possible. This is because conductivity is influenced by many factors including the degree of saturation, porosity, and salinity of the pore fluids. In addition, the conductivity measurements taken with instruments that investigate to depths greater than the upper layer are also influenced by other layers. These layers can change in thickness and conductivity, making a definitive interpretation of the conductivity of any one of these layers difficult without additional information such as laboratory clay content analysis or soil boring results.

Conductivity measurements taken using electromagnetic instruments will be influenced by local above or below ground metal.

5.2.1.2 Resistivity Measurements

Basic Concept: Resistivity measurements, which are the inverse of conductivity measurements, can also be used to locate the occurrence of clay and possibly estimate the clay content.

Resistivity methods can be divided into three groups. The first two are resistivity soundings and traverses. The last group combines both resistivity sounding and traverse data to form a resistivity section. Since the data recording of conductivity along a traverse using the EM38/31/34 are much more efficient than resistivity measurements along a traverse, resistivity traverses are now rarely used. Resistivity soundings may be useful but only provide information on the vertical distribution of resistivity at the sounding location. It is, therefore, unlikely that resistivity soundings will be the primary tool for locating clay or attempting to obtain clay content, since lateral variations in resistivity are also important.

Since lateral resistivity measurements are efficiently taken using instruments that measure conductivity (the inverse of resistivity), resistivity traverses will not be discussed. Resistivity soundings may be appropriate in some cases and are discussed briefly. However, using one of the more recently developed resistivity systems, data can be efficiently recorded that combines both traverse and sounding results. These newer instruments use electrodes that are addressable by a central control system, and the term "automated resistivity" system is sometimes used to describe them.

Resistivity measurements are taken by passing electrical current into the ground using two electrodes and measuring the resulting voltage using two other electrodes. A number of different electrode arrays are used, some of which are shown in figure 90. The depth of investigation is determined by the electrode separation, with larger separations providing greater depths. The measured resistivity is calculated by dividing the measured voltage by the current and multiplying this by a geometric factor that accounts for the particular electrode array used.

These arrays are used for different types of resistivity surveys. The Schlumberger array is often used for resistivity soundings, as is the Wenner array. The Pole-pole array provides the best signal, but is cumbersome because of the long wires required for the remote electrodes, and it is rarely used. The Dipole-dipole array was originally used mostly by the mining industry for induced polarization surveys. Readings were taken using several different separations of the voltage and current dipoles providing measurements of the variation of resistivity with depth. Long lines of data were recorded requiring many readings. This array has now become common for resistivity surveys using the automated resistivity systems. If more signal (voltage) is needed than can be provided with the dipole Dipole-array, then the Pole-dipole array can be used.

Automated Resistivity Systems

Automated resistivity systems make recording resistivity data much more efficient, and by taking many measurements at different electrode spacings along a traverse, are able to build a comprehensive picture of the subsurface. Figure 201 shows one such system called the Sting/Swift automated resistivity measuring system.

Figure 105 shows a similar system called a Syscal Junior 72 system, which can access 72 electrodes.

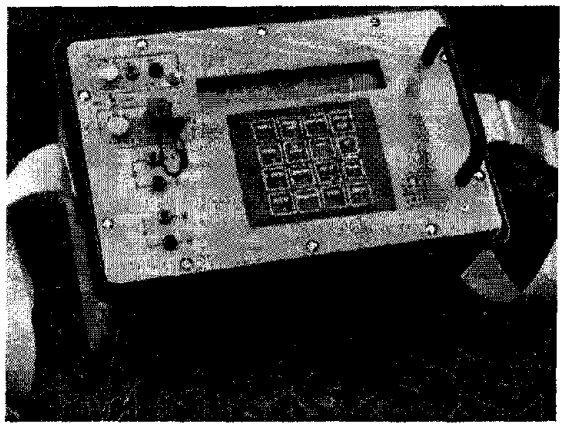

Figure 105. Syscal Junior automated resistivity system. (IRIS Instruments)

Data Processing: Usually little processing is done to the resistivity data obtained with this system. The data are plotted to form a "pseudosection" as shown in figure 152. Data from the smaller electrode spacings are plotted closer to the line representing the ground surface, and data from the larger electrode spacings are plotted more distant, vertically, from the top of the plot, thus simulating a plot of resistivity against depth along the traverse.

Data Interpretation: Data from the automated resistivity system are interpreted by software that calculates a pseudosection from a model and then alters the model until the calculated pseudosection matches that of the field data, a process called inversion. However, much information can be gained visually.

An example of the results from such a survey is presented in figure 149. The data have been inverted showing the resistivity variation, both laterally and vertically, against depth.

The data show low resistivity areas (less than 20 ohm-m) corresponding to silty clay layers and high resistivity zones (greater than 100 ohm-m) corresponding to sand and gravel lenses. Unlike the resistivity sounding method, this interpretation does not require that the ground be horizontally layered. Therefore, the interpreted resistivity values are probably better estimates of the true resistivities than those from the sounding method

Advantages: Automated resistivity systems record a large amount of data allowing relatively detailed interpretations.

Limitations: Since electrodes have to be inserted into the ground, the method is difficult to use in areas where the surface is hard, such as concrete or asphalt-covered areas. If the ground is dry, water may need to be poured on the electrodes to improve the electrical contact between the electrode and the ground. If the data are conducted along one line, resistivity changes normal to the line are not accounted for. However, recording lines parallel to each other can rectify this problem. Three-dimensional surveys can also be recorded.

Cultural features such as power lines, fences, and other metal features may provide false anomalies. These cultural features will have to be noted in the field and accounted for in the interpretation.

Resistivity Soundings

Resistivity soundings can be recorded using any of the electrode arrays shown in figure 90. However, the Schlumberger array is probably most commonly used for soundings and is discussed below. Figure 91 shows the Schlumberger electrode array being used to record resistivity data (figure 91a). Resistivity sounding data obtained using the Schlumberger array are often called Schlumberger soundings. Using data from several electrode spacings, a graph of measured resistivity against electrode spacing is plotted (figure 91b). This graph can be interpreted to provide the depths and resistivities of the layers indicated in the sounding curve. Although it may be possible to infer the rock type from the resistivity sounding interpretation, it is unlikely that the clay content can be estimated with reasonable accuracy from these data. In addition, the interpretation of the method assumes a horizontally layered geology exists with no lateral variations in resistivity. If this is not the case, then the interpreted resistivities and depths may be incorrect.

5.2.1.3 Time Domain Electromagnetic Soundings

Basic Concept: Time Domain Electromagnetic (TDEM) soundings are another method for obtaining the vertical distribution of the resistivity of the ground.

This method is particularly well suited to mapping conductive layers. To a significant degree, this method has now superseded the resistivity sounding method since it requires less work for a given investigation depth and generally provides more precise depth estimates. However, resistivity soundings are still useful for shallow investigations or when resistive targets are sought. Figure 120 provides a conceptual drawing of the TDEM method.

A square loop of wire is laid on the ground surface. The side length of this loop is about half of the desired depth of investigation. A receiver coil is placed in the center of the transmitter loop. Electrical current is passed through the transmitter loop and then quickly turned off. This sudden change in the transmitter current causes secondary currents to be generated in the ground. The currents in a conductive layer decay more slowly than those in a resistive layer. However, the relation between decay time, layer conductivity, and depth is complex, although, generally, longer decay times are related to greater depths. Thus, the conductive layer (shale) will generate currents that decay more slowly than those in the more resistive layer.

The voltage measured by the receiver coil does not decay instantly to zero when the current is turned off but continues to decay for some time caused by the decaying secondary electrical currents in the ground. The voltage measured by the receiver is then converted to resistivity. A plot is made of the measured resistivity against the time after the transmitter current is turned off (delay time), as illustrated in figure 121.

The resistivity sounding curve shown in figure 121 illustrates the curve that would be obtained over three-layered ground. The near-surface layer is fairly resistive. This is followed by a layer having a much lower resistivity (higher conductivity) and causes the measured resistivity values to decrease. The third layer is again resistive.

Data Acquisition: A transmitter loop and receiver coil are laid out as described earlier. Switched current, as described above, is passed through the transmitter loop, and the resulting voltage is measured by the receiver coil. The switching and measuring procedure is repeated many times, allowing the resulting voltages to be stacked and improving the signal-to-noise ratio. This procedure is repeated at different sounding locations until the area of interest has been covered. A sounding curve is plotted for each location showing the measured resistivity against delay time.

Data Processing: Probably the only processing required is the removal of bad data points.

Data Interpretation: This sounding curve is interpreted using computer software to provide a model showing the layer resistivities and thickness. The interpreter inputs a preliminary model into this software program that calculates the sounding curve for this model. It adjusts the model and calculates a new sounding curve that better fits the field data. This process is repeated until a satisfactory fit is obtained between the model and the field data, a process is called inversion. The sounding curve shown in figure 121 illustrates the type of curve expected over a conductive shale layer.

Advantages: The TDEM method is good at determining the resistivity of the ground for depths greater than about 10 meters, depending on the near surface resistivity. Interpreted depths to interfaces are generally more accurate than those for resistivity soundings, especially for conductive layers.

Limitations: TDEM soundings are an efficient method to investigate the vertical distribution of ground resistivity. Generally, the method is better suited to mapping conductive formations than resistive formations. However, since the desired targets in this section are clays, which are usually conductive, then this may not be a limitation.

Probably the most troublesome aspect of data recording is the influence of metal objects such as fences, power lines, and other "cultural" features at the survey site.

5.2.1.4 Induced Polarization

Basic Concept: Induced Polarization (IP) is an electrical method that measures the change in the measured resistivity of the ground with frequency. All of the electrode arrays used to measure resistivity (see figure 90) can also be used to measure IP. In fact, when measuring IP, resistivity is also measured. There are two methods used to record IP measurements: time domain and frequency domain. In time domain, a constant current is passed into the ground for a short time (seconds) using two of the four electrodes and then rapidly switched off. During this off time, the remaining two electrodes measure the resulting voltage. If an IP effect is present, the voltage across these electrodes will not suddenly return to zero as the current is turned off, but will decay to zero over a period of time, usually within a few seconds. Figure 110 illustrates the concept. Simple IP measurements usually integrate the IP voltage over a specified time, say T_1 and T_2 (figure 110), providing a single number that is a measure of the IP response, called chargeability with units of mV/V.

IP phenomena occur over clays, metallic minerals, and graphite zones. It is also observed near fences and other electrically grounded metallic features, either on the ground surface or buried, such as metal pipelines. The IP effect resulting from clay is discussed in the introduction to this section and involves Membrane Polarization.

Data Acquisition: Induced Polarization surveys are conducted much like resistivity surveys with readings taken at discrete stations to form lines of data crossing the area of interest.

The automated resistivity systems discussed previously can also be used to record IP data. Figure 151 illustrates one of the systems that can be used to record IP data using a multi-electrode system. If digital data are obtained at several frequencies, the variation of IP response with frequency is obtained. To get the frequency domain response in the time domain, the current and voltage waveforms have to be digitally recorded, and a Fourier analysis of the data performed providing the variation of resistivity with frequency, called Spectral Induced Polarization (SIP). This provides more interpretable information than the simple IP measure discussed above. However, this is still being researched and is rarely used as a production method

Data Processing: Both the resistivity and IP data are usually plotted to form a pseudosection. Figures 152 and 153 show a typical Chargeability pseudosection and the associated resistivity section, respectively.

Data Interpretation: Although these data are from a shallow survey using small electrode spacings, it does illustrate the method, presentation techniques, and the interpretation. Surveys to much greater depths can be performed using larger electrode spacings.

Although the literature often refers to the use of the IP method for locating clays, no references were found showing the correlation between clay content and the magnitude of either the simple or spectral IP response. This method appears to have promise for investigating clay content, and would probably benefit from additional research.

Since resistivity measurements are also obtained when recording IP data, these two parameters can be used to determine the occurrence of clay and possibly map the clay content.

Advantages: The IP method is reported to respond to clay providing a higher IP response in their presence. If this is so this may be the only method that, in the right environment, may provide a unique clay response.

Limitations: The IP method is fairly labor intensive and requires electrodes to be inserted into the ground. Generally, because the method requires more electrical current than the resistivity method, the contact resistance (resistance of the electrode to ground) of the electrodes usually has to be lower than that for an equivalent resistivity survey. Thus, the electrodes may have to be inserted to greater depths or saturated with water to improve the electrical contact between the electrode and the ground. If the ground surface is hard (concrete or asphalt), additional work has to be done to insert the electrodes. If Spectral IP measurements are required, additional care needs to be taken since the desired voltages may be very small, depending on the specifications of the recording parameters.

5.2.2 Identifying Roadbed Underlain by Expansive Clays (Determine Clay Content in Swelling Soils)

Roads constructed over areas of clay are subject to potential deformation due to volume changes of the clay. Such volume changes result from changes in the moisture content of the clay. Geophysical methods can be used to identify areas of clay.

Clays are very small-grained hydrous aluminosilicates with the phyllosilicate structure. Clays are classified as hydrosilicates, which means that they are formed from the chemical decomposition of pre-existing silicate minerals. Most clays result from the product of weathering and sedimentation, but they are also formed by hydrothermal activities. Clays can occur as part of a soil structure or as independent layers and lenses. They are also commonly found in glacial till, where glacial action has ground the rocks and boulders into fine particles.

Clay occurs in soil, shales, and as independent layers and is formed from weathered pre-existing minerals. It also occurs as weathered products from rocks such as granite, where the feldspars weather to form clay minerals. It is commonly found in glacial till, where glacial action has ground the rocks and boulders into fine particles.

Clay particle sizes range in size from 0.002 mm to 0.001 mm diameter for quartz, feldspar, mica, iron, and aluminum oxides. The finer parts (less than 0.001 mm in diameter) are colloidal and consist mainly of layer silicates with smaller amounts of iron and aluminum oxides. These consist of microscopically fine particles exhibiting a sheet-like structure. Their crystalline structure is such that, because of crystal imperfections, the surface appears negatively charged. During the formation of clay through weathering, positive charges (cations) are adsorbed to the surface. These cations are loosely held to the surface and can subsequently be exchanged for other cations or essentially go into solution if the clay is mixed with water. For this reason, they are called exchangeable ions, and the cation exchange capacity (CEC) of clay is a measure of the number of cations that are required to neutralize the clay particle as a whole.

Any fine-grained mineral, including quartz, has a cation exchange capacity. However, clay particles are very small, and because the surface area per unit volume is very large, a large number of cations are adsorbed. In addition to influencing the conductivity of clay, these adsorbed cations can also contribute significantly to the electrical conductivity in soils containing clay, which then becomes a function of the clay content. Cation Exchange Capacities of some common clay types are presented in Table 8.

Table 8. Cation Exchange Capacities (CEC) of common clay types.

Clay type	Cation Exchange Capacity
Kaolinite	3 - 15
Chlorite	10 - 40
Illite	10 - 40
Montmorillonite	80 - 150
Vermiculite	100 - 150

This table shows that kaolinite has the least influence on conductivity, and vermiculite has the greatest influence. However, other factors influence conductivity values, including the degree of saturation and the salinity of the saturating fluid.

Because of its electrical structure, clay minerals often exhibit an effect called membrane polarization. This is a distribution of ions around the clay pores. When a DC potential is applied across the pore, negative ions accumulate at one end and leave the other end. Because of this polarization distribution, current flow is impeded. When the DC potential is switched off, the ions take a finite amount of time to return to their original positions. This effect can be measured and may be used to help identify clays.

From the above discussion, two basic parameters can be used to map clays and possibly estimate the clay content of soils and other geologic layers–electrical conductivity and membrane polarization. The appropriate geophysical methods that can be used to measure these quantities are electrical conductivity (or resistivity) and Induced Polarization to measure membrane polarization.

The resistivities of rocks vary from 1 to 30 ohm-m for some clays and shales to over 1,000 ohm-m for limestone, intrusive rocks such as granites, and some metamorphic rocks. However, in sedimentary rocks, which often have much larger porosities than metamorphic and intrusive rocks, resistivities generally range from 10 to 1,000 ohm-m. In these rocks, the porosity and salinity of the water in the rock pores are also significant factors influencing resistivity. Although clay is specifically discussed in this document, other rock types such as shales may also be detrimental to roadbed stability. Since both clay and shale usually have low resistivities, this parameter may be an important predictor of potential roadbed problems.

Clays can swell as well as have low shear strength. Swelling is usually caused by moisture within the clay. Fine-grained material such as clay can hold a significant amount of water. Moisture can be acquired from surface runoff or, because of the small pores size in clays and the resulting strong capillary forces, moisture can be drawn from material beneath them. Shear strength of clays are significantly influenced by moisture content, decreasing with increased moisture. Furthermore, clays with high swelling potential are susceptible to extreme volume

changes as moisture content changes. Roads constructed over areas of soft clay will result in poorly performing pavement systems and often result in a subgrade failure. Subgrade failures may be visibly observed as pavement deformations over problem areas. Thus, there is a need to be able to identify where clays occur along roadways in order that remedial action may be taken before the problem becomes serious.

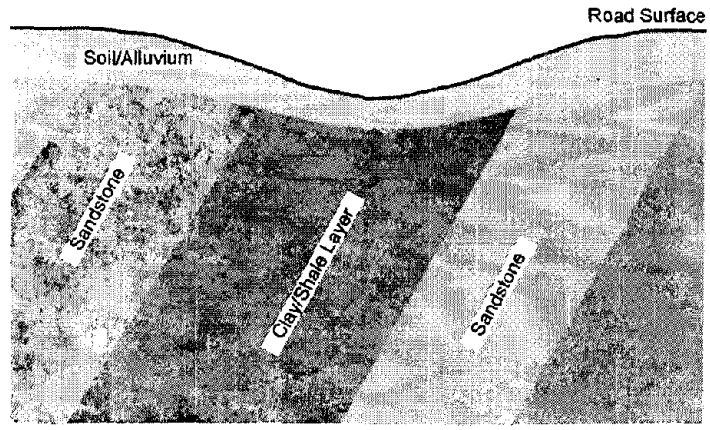

Figure 106. Dipping clay/shale layer.

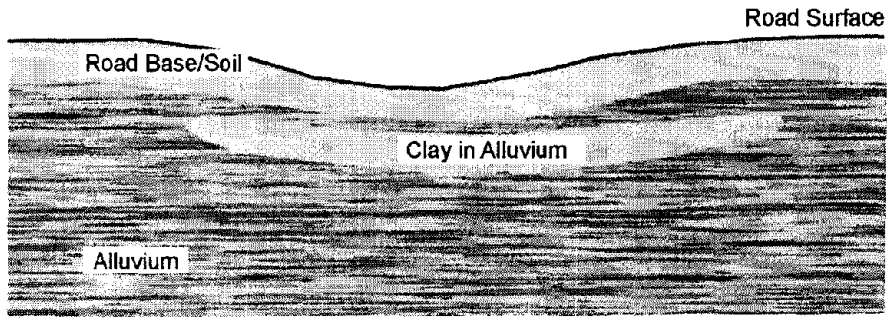

Figure 107. Clay in alluvium.

Clays may occur in many different geological contexts. Figures 106 and 107 show two common geologic conditions in which clay may occur.

In figure 106, the road is constructed over dipping strata. One of the stratum is a shale/clay layer that has caused the roadbed to deform. In figure 107, the clay layer is within the alluvium and has allowed the roadbed to become depressed. Geophysical methods can be used to help locate clay in both of these cases, although resistivity or conductivity soundings may be needed to distinguish between them.

Determining clay content from geophysical methods may be difficult. However, if this is to be attempted, then the true resistivity of the layer being imaged has to be obtained. Since the instruments measure the bulk resistivity of the ground, the true resistivity of any layer has to be determined by interpretation. To do this, it is also important to understand the geology and structural setting of the low resistivity occurrence. The use of different geophysical methods may be required, first to locate the conductive area, and second to evaluate its true conductivity (or resistivity) and geologic setting.

Methods

5.2.2.1 Conductivity Measurements

Basic Concept: Ground conductivity methods can rapidly locate conductive areas in the upper few meters of the ground surface. These measurements are recorded using several instruments that use electromagnetic methods. The choice of which instrument to use generally depends on the depth of investigation desired. Instruments commonly used include the EM38, EM31, EM34 (Geonics Ltd, Canada), and GEM2 (Geophex, USA). These instruments transmit sinusoidal electromagnetic waves at frequencies up to about 10 kHz (EM38, EM31, EM34) and between 330 Hz and 24 kHz for the GEM2.

The EM38 is designed to measure soil conductivities and has a maximum depth of investigation of about 1.5 m. The EM31 has a depth of investigation to about 6 m, and the EM34 has a maximum depth of investigation to about 60 m. The depth of investigation of the GEM2 is advertised to be 30 to 50 m in resistive terrain (>1000 ohm-m) and 20 to 30 m in conductive terrain (<100 ohm-m).

Electromagnetic instruments that measure ground conductivity use two coplanar coils, one for the transmitter and the other for the receiver. The transmitter coil produces an electromagnetic field, oscillating at several kHz, that produces secondary currents in conductive material in the ground. The amplitude of these secondary currents depends on the conductivity of the material. These secondary currents then produce secondary electromagnetic fields that are recorded by the receiver coil.

The EM34, EM31, and EM38 instruments can be used with the planes of the coils held parallel to the ground (vertical dipole mode) or perpendicular to the ground (horizontal dipole mode). The investigation depth is greatest in the vertical dipole mode and least in the horizontal dipole mode. In addition, in the vertical dipole mode, the conductivity readings are insensitive to near- surface conductivity changes, whereas in the horizontal dipole mode, the readings are significantly influenced by near-surface conductivity changes.

The EM38 instrument used for shallow surveys measures the conductivity of soil and is shown in figure 103. Figure 183 shows the EM31 instrument being used in vertical dipole mode. Figure 197 shows the EM34 being used in the horizontal dipole mode. The GEM2 instrument is shown in figure 191. This instrument uses a wide range of frequencies to obtain conductivities at different depths.

If conductivity values are required for depths beyond the 6 m available with the EM31, the EM34 can be used. This instrument provides three different separations of the two coils to provide six different depths of investigation (three coil separations and two modes for each separation). However, as the depth of investigation increases, the lateral resolution decreases. The EM34, unlike the EM31, requires two people to operate. Data recording is also much slower than with the EM31 since the automatic timed mode available with the EM31 is not available with the EM34. All of these instruments measure the bulk electrical conductivity of the ground. Since the conductivity of several different layers may be included in the conductivity measure, the correct technical term for the measured conductivity is apparent

conductivity. When discussing data from these instruments in this document, conductivity or measured conductivity is understood to mean apparent conductivity.

Data Acquisition: Surveys mapping roadbed clays are likely to require depths of investigation up to about 5 to 10 m and need to be performed over long distances. Ideally, the system should be towed by a vehicle traveling at reasonable speeds compatible with the data recording parameters of the instrument. Since the EM34 requires two people to operate and is not capable of automatic time based recording, this instrument is not generally suited to this application and will not be discussed further.

The EM38 and EM31 can record data on a time basis, usually taking readings every second or half second. Thus, they can be assembled on a trailer, coupled with GPS, and towed at a speed of a few kilometers per hour while recording data. Different depths of investigation can be obtained by using the vertical and horizontal dipole modes.

Data Processing: If conductivity readings are taken with both the EM38 and EM31 at each of the dipole modes top provide different investigation depths, the data can be inverted to produce a conductivity cross section along the traverse. The coordinates can be assigned to the conductivity data points using the GPS data.

Data Interpretation: The results of a conductivity survey along a road in New Mexico are shown in figure 108. The purpose of the survey was to see if conductivity data could be recorded along a road efficiently and to correlate the data with soil type and clay content. For this survey, data were recorded with one of the instruments mounted on a trailer constructed primarily from non-conductive materials. The trailer was towed by an All Terrain Vehicle (ATV). A GPS receiver was also mounted on the trailer to provide position information. Data were recorded automatically at half-second intervals with the EM31 and EM38, using both the vertical and horizontal dipole modes. In addition, data from the EM31 were recorded at two different instrument heights above the ground, giving two different penetration depths. Since data can be recorded from only one instrument using one configuration at a time, several passes along the road had to be made; one for each instrument and parameter (dipole mode and height). These procedures provided up to six conductivity values from different depths of investigation.

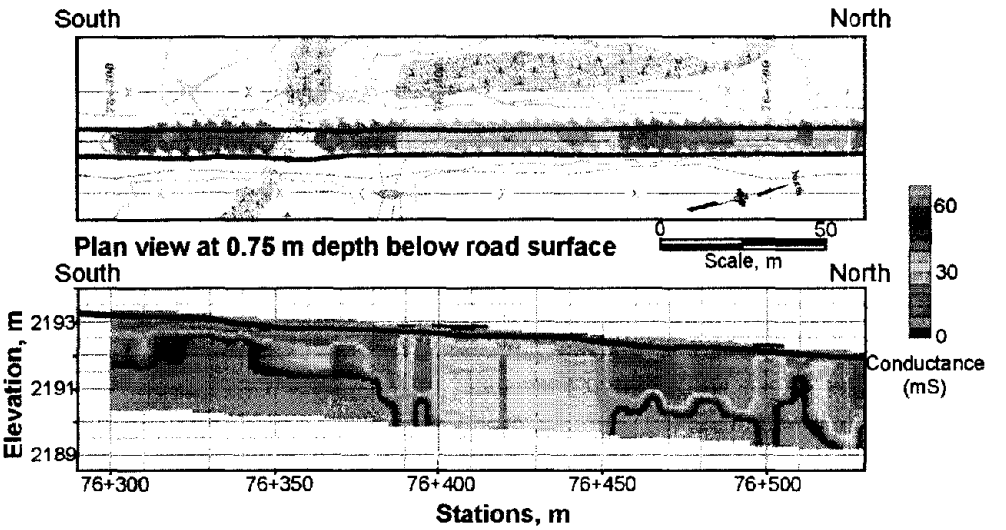

Figure 108. Conductivity data along a road and the interpretation. (Blackhawk GeoServices, Inc.)

Having obtained conductivity measurements at a number of different depths at each recording location, the data were modeled and provided the interpreted vertical distribution of conductivity with depth. This interpretation is shown in the lower plot in figure 108. The upper plot shows the ground conductivity measured with the EM38 at a depth of 0.75 m below the road surface.

Advantages: Conductivity data is fairly easy and efficient to record using the instruments described in the previous section. These instruments can be used in different modes providing different depths of investigation and can be tailored to focus on maximizing depth (Vertical dipole mode) or maximizing the influence of the near surface conductivity (horizontal dipole mode).

Limitations: Ground conductivity measurements are taken using a coil that transmits electromagnetic (EM) energy and induces electrical currents to flow in conductive objects. If metal objects are within the zone of influence of the transmitter, these will influence the data. Such objects might include any above-ground metal, including fences and buried objects such as pipelines, culverts, and utilities. If the instrument is being towed by a vehicle, it is important to make sure that the influence of the vehicle is minimal.

For the survey in New Mexico, several passes along the road had to be made to record the data with all of the desired recording parameters. This significantly reduced the overall productivity of the survey. However, there are newer instruments being developed that have three receiver coils placed at different distances from the transmitter coil that provide three different investigation depths at each reading location. The use of this instrument should significantly improve productivity.

5.2.2.2 Resistivity Methods

The EM38 and/or the EM31 can be used to map conductivity along roadways of interest and determine zones having high conductivities that may indicate clay. Although this may be

sufficient in order to locate areas of concern, if structural remediation is required, some understanding of the geological setting may be helpful. It is also not possible to estimate the clay content from these data without knowing the true conductivity of the zones of interest or correlation with laboratory analysis or drill results.

The true conductivity of a conductive zone may be determined using TDEM or resistivity sounding methods. In the case illustrated in figure 107, the sounding should indicate a thin clay layer with more resistive layers both above and below the clay layer. In the case shown in figure 106, the sounding should indicate high conductivity values for a considerable depth.

It may still be difficult to estimate absolute values of the clay content, although the relative clay content between different anomalies may be possible, with the higher conductivity layers suggesting higher clay content. If the absolute clay content at one anomaly location can be determined from drill results or other methods, it may be possible to estimate the clay content of other anomalies.

Resistivity Soundings

Basic Concept: Resistivity soundings are used to obtain the vertical distribution of resistivity in the ground. The result is an interpretation showing the depths and resistivities of the layers imaged by the sounding.

Resistivity soundings are recorded using a number of electrode arrays, some of which are illustrated in figure 90. These arrays are used for different types of resistivity surveys. The Schlumberger array is often used for resistivity soundings, as is the Wenner array. The Pole-pole array provides the best signal, but is cumbersome because of the long wires required for the remote electrodes and is rarely used. The Dipole-dipole array was originally used mostly by the mining industry for induced polarization surveys. Readings were taken using several different separations of the voltage and current dipoles, providing measurements of the variation of resistivity with depth. Long lines of data were recorded requiring many readings. This array has now become common for resistivity surveys using the automated resistivity systems. If more signal (voltage) is needed than can be provided with the Dipole-dipole array, the Pole-dipole array can be used.

Figure 91 shows the Schlumberger electrode array being used to record resistivity data (figure 91a). Resistivity sounding data obtained using the Schlumberger array are called Schlumberger soundings. Using data from several electrode spacings, a graph of measured resistivity against electrode spacing is plotted (figure 91b). This graph can be interpreted to provide the depths and resistivities of the layers indicated in the sounding curve. In the case illustrated, at small values of AB/2 (electrode spacings), the measured resistivity approaches that of the overburden (figure 91b). The measured resistivity values then fall as the conductive clay layer influences the data. Finally, the measured resistivity values begin to increase as the electrode spacings become large enough to allow current to penetrate beneath the clay layer into more resistive material.

Data Acquisition: Resistivity soundings are conducted by planting the electrodes in the ground, first at the smallest electrode spacing required, and taking a resistivity reading. The

electrode spacing is then increased, and the procedure is repeated. It is advisable to plot the measured resistivity values against electrode spacing in the field while recording the data, thereby producing a resistivity sounding curve. If a conductive clay layer is expected, measurements are taken until the measured resistivity first falls and then begins to increase, showing that the conductive layer has been fully imaged.

Data processing: Processing the data amounts to simply removing any obviously bad data points.

Data Interpretation: The data are then input to a computer program that produces a layered depth and resistivity model whose resistivity curve matches that of the field data. This process starts with the interpreter inputting a preliminary resistivity/depth model. The program calculates the resistivity curve from the model and evaluates the differences between the resistivity field data and the resistivity data from the model. It then adjusts the model and calculates a new resistivity curve. This process is repeated until the resistivity data from the model match that from the field data. This process is called inversion.

Advantages: Resistivity soundings are a good method for obtaining the vertical distribution of resistivity to depths of about 50 meters.

Limitations: The method is somewhat cumbersome in that four electrodes have to be inserted into the ground for each resistivity measurement. If the ground is hard or covered with concrete or asphalt, placing the electrodes can be quite time consuming. In addition, in dry ground, water may have to be poured onto the electrodes to improve the electrical contact between the electrode and the soil.

The interpretation assumes that the geological layers are homogeneous and horizontal and have a large lateral extent compared to their depth. In the case illustrated in figure 107, the clay layer has a limited lateral extent, and the interpreted depth and resistivity of the clay layer will not be correct.

Since this method uses electrodes to put current into the ground, any local metal objects above ground that provide a low resistance path between these objects and the ground, such as a fence, will also become influenced by the electrode array used to take the resistivity measurements. They will then produce voltages that will be detected by the electrode array and reduce the interpretability of the data.

Automated Resistivity Systems

Basic Concept: Resistivity measurements can be taken using recently developed instruments that use addressable electrodes and can be recognized by the control unit. These systems are called Automated Resistivity Systems. With these systems, the required electrodes are planted prior to any data recording, and the wires between all of the electrodes to the recorder are also connected. The recorder is then programmed with the electrode array and other data recording parameters and instructed to take the measurements. One such system is called a Sting/Swift system and is illustrated in figure 201.

Data Acquisition: This system is able to provide detailed resistivity data. However, because of the labor required to plant the electrodes and lay out the cables, this system is probably not suited for reconnaissance exploration of large areas. If large areas are to be explored, other methods should be used; this technique should be used for detailed analysis of interesting anomalies. Conductivity methods, discussed previously, may be appropriate for reconnaissance.

The automated resistivity instrument records data from a specified number of electrodes, depending on the instrument used. If longer lines of data are needed, the system is moved along the line as required, and the data recording process repeated.

Data Processing: Bad data points have to be removed. The data are then plotted as pseudosections, as illustrated in figure 153. These plots present data from the small electrode spacings near the ground surface line. Data from the larger electrode spacings are plotted some distance vertically beneath the ground surface line, simulating a plot of resistivity against depth along the traverse and creating a plot called pseudosection.

Figure 109 shows pseudosection data that have been interpreted to give a plot of resistivity versus interpreted depth along the traverse.

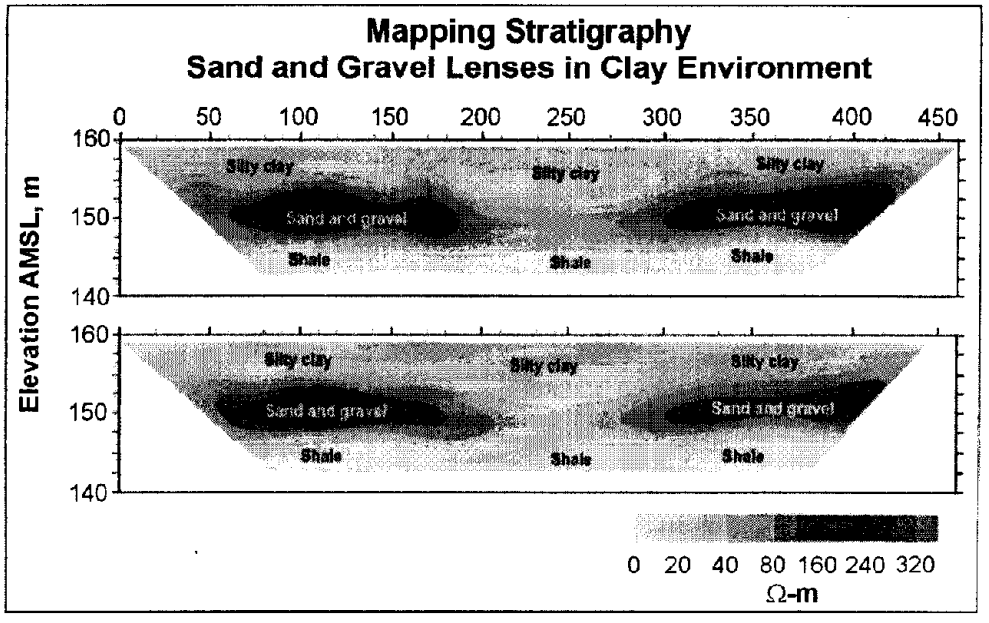

Figure 109. Resistivity data plotted to form a depth vs resitivity section. (Advanced Geosciences, Inc.)

Data Interpretation: Interpretation is done using inversion software. This software iteratively modifies a preliminary resistivity/depth model until the calculated model data fit the field data.

Advantages: The method records a significant amount of data, and since data recording is automated, this is done quite efficiently. Because of the amount of data, detailed interpretations are possible.

Limitations: Since electrodes have to be inserted into the ground, the method is difficult to use in areas where the surface of the ground is hard, such as concrete or asphalt- covered areas. Also, if the ground is dry, water may need to be poured on the electrodes to increase the electrical contact between the electrodes and ground. The data are taken along a line, and lateral variations in resistivity normal to the line are not accounted for. However, recording lines parallel to each other can rectify this problem, although this may not be feasible for some roadway surveys. In addition, three-dimensional surveys can also be recorded.

Cultural features such as power lines, fences, and other metal features may provide false anomalies. These cultural features will have to be noted in the field and accounted for in the interpretation.

5.2.2.3 Time Domain Electromagnetic Soundings

Basic Concept: Time Domain Electromagnetic (TDEM) soundings provide another method to obtain vertical distribution of the resistivity of the ground in addition to resistivity soundings. This method is particularly well suited to mapping conductive layers. To a significant degree, this method has now superseded the resistivity sounding method since it requires less work for a given investigation depth and generally provides more precise depth estimates. However, resistivity soundings are still useful for shallow investigations or when resistive targets are sought. Figure 120 provides a conceptual drawing of the TDEM method showing the transmitter and receiver and the current and voltage waveforms.

TDEM soundings are an electromagnetic method used to provide the vertical distribution of resistivity within the ground. A square loop of wire, whose side length is about half of the depth of investigation, is laid on the ground surface. This is the transmitter loop. A receiver coil is placed in the center of the transmitter loop. Electrical current is passed through the transmitter loop and then quickly turned off. This sudden change in the transmitter current causes secondary currents to be generated in the ground. Currents in conductive layers decay slower than those in resistive layers. The relation between the decay amplitude and time and layer conductivity and depth is quite complex. Generally, longer decay times relate to deeper depths.

The voltage measured by the receiver coil does not decay instantly to zero when the current is turned off but continues to decay for some time because of the decaying secondary electrical currents in the ground. The voltage measured by the receiver is then converted to resistivity. A plot is made of the measured resistivity against the time after the transmitter current has turned off (delay time), as illustrated in figure 121. At short delay times, the measured resistivity approaches that of the near-surface layer, whereas at longer delay times, the measured resistivity approaches that of the deeper layers.

Figure 121 illustrates the curve that would be obtained over three-layered ground where the near- surface layer is resistive. This is followed by a layer having a much lower resistivity (higher conductivity) and causes the measured resistivity values to decrease. The third layer is again resistive, as shown by the increasing measured resistivity values. This sounding curve illustrates the type of curve that may be expected over a clay layer between resistive layers.

Data Acquisition: The field layout for the equipment has been described previously. Switched current is passed through the transmitter loop, and the resulting voltage is measured by the receiver coil. The switching and measuring procedure is repeated many times, allowing the resulting voltages to be stacked and improving the signal-to-noise ratio. This procedure is repeated at different sounding locations until the area of interest has been covered.

Data Processing: Bad data points are removed and a sounding curve is plotted for each location showing the measured resistivity against decay time.

Data Interpretation: This sounding curve is interpreted using computer software to provide a model showing the layer resistivities and thickness. The interpreter inputs a preliminary model into this software program that calculates the sounding curve for this model. It then adjusts the model and calculates a new sounding curve that better fits the field data. This process is repeated until a satisfactory fit is obtained between the model and the field data. This process is called inversion.

Advantages: TDEM soundings are an efficient method for investigating the vertical distribution of ground resistivity. For conductive layers the interpretation is generally more accurate than that for resistivity soundings.

Limitations: Generally, the method is better suited to mapping conductive formations rather than resistive formations. However, since the desired target is clay, which is usually conductive, this is not a serious limitation.

The TDEM method is not suited to mapping targets at very shallow depths. This is particularly so when the resistivity of these layers is high. Generally, in a conductive environment, depths less than 2 m cannot be resolved.

The transmitter loop radiates electromagnetic fields in all directions. Metal objects on the ground surface are influenced by these fields and will influence the data. Such objects include fences, power lines, and other "cultural" features at the survey site. Since the transmitter loop has to have a side length about half of the investigation depth, surveys done along roadways may be constrained due to the limited space available.

5.2.2.4 Induced Polarization

Basic Concept: Induced Polarization (IP) is an electrical method that measures the change in the measured resistivity of the ground with frequency. All of the electrode arrays (figure 90) used to measure resistivity can also be used to measure IP. In fact, when measuring IP, resistivity is also measured.

Two methods are used to obtain IP data: time domain and frequency domain. In time domain, a constant current is passed into the ground for a short time (seconds) using two of the four electrodes and then rapidly switched off. During this off time, the remaining two electrodes measure the resulting voltage. If an IP effect is present, the voltage across these electrodes will not suddenly return to zero as the current is turned off, but will decay to zero over a period of time, usually within a few seconds. The electrode array, current and voltage

waveforms are illustrated in figure 110. Although any electrode array can be used, the Dipole-dipole array, as illustrated in figure 110, is probably the most commonly used array. Simple IP measurements usually integrate the IP voltage over a specified time, say T_1 and T_2 (figure 110), providing a single number that is a measure of the IP response, often called chargeability.

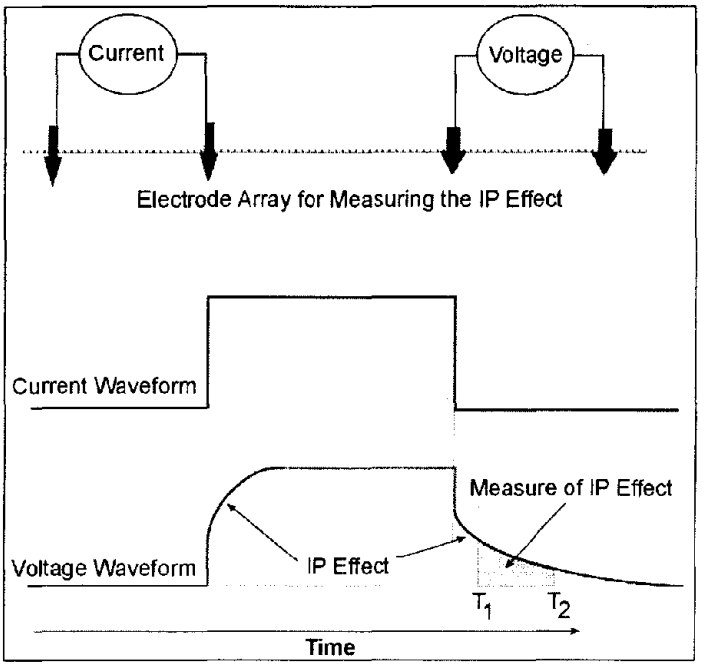

Figure 110. Induced Polarization waveform.

In frequency domain, the transmitter current waveform is sinusoidal. IP measurements are taken at different transmitter frequencies, producing a variation of the IP effect with frequency called Spectral IP (SIP) when more than two frequencies are measured. If spectral IP values are required from data obtained in time domain, the current and voltage signals have to be converted to frequency domain, which is done using the Fourier transform.

IP phenomena occur over clays, metallic minerals, and graphite zones. It is also observed near fences and other metallic surface features. The IP effect resulting from clay is discussed in the introduction to this section and involves Membrane Polarization.

Data Acquisition: Induced Polarization surveys are conducted much like resistivity surveys. Readings are taken at discrete stations to form lines of data crossing the area of interest. The automated resistivity systems discussed previously can also be used to record IP data. Figure 151 illustrates one of these systems, which can record up to 10 channels simultaneously.

Spectral IP data provide more interpretable information than the simple IP measurements discussed above and are reported to be more definitive for interpretation of clays. However, this is still being researched and is rarely used as a production method

Data Processing: Both the resistivity and IP data are usually plotted to form a pseudosection described previously. A typical chargeability pseudosection is shown in figure 152. Figure 153 shows the associated resistivity section.

Although these data are from a shallow survey using small electrode spacings, it does illustrate the method, presentation techniques, and the interpretation. Surveys to much greater depths can be performed using larger electrode spacings.

Data Interpretation: The data is interpreted using software that can produce a model that fits the field data. Although the literature often refers to the use of the IP method to locate clays, no published information was found showing a correlation between the magnitude of the IP or SIP response to clay type or content. The spectral IP response to clays may provide more interpretable information than the conventional IP response. Investigating clay content using the SIP method appears to have promise and would benefit from additional research.

Since resistivity measurements are also obtained when recording IP data, these two parameters can be used to determine the occurrence of clay and possibly map the clay content.

Advantages: The IP method is reported to respond to clay providing a higher IP response in their presence. If this is so, this may be the only method that, in the right environment, may provide a unique clay response.

Limitations: The IP method is quite labor intensive and requires electrodes to be inserted into the ground. Generally, because the method requires more electrical current than the resistivity method, the contact resistance (resistance of the electrode to ground) of the electrodes usually has to be lower than that for an equivalent resistivity survey. Thus, the electrodes may have to be inserted to greater depths or saturated with water to improve the electrical contact with the ground. If the ground surface is hard (concrete or asphalt), additional work has to be done to insert the electrodes. If spectral IP measurements are required, additional care must be taken since the desired voltages may be very small, depending on the specifications of the recording parameters.

Any grounded metal structures, for example metal fences, near the electrodes in use will influence the data, as will buried metal features such as pipelines.

CHAPTER 6 SUBSURFACE CHARACTERIZATION

6.1 SUBSURFACE GEOPHYSICAL MAPPING AND IMAGING

Geophysical techniques are commonly used to map subsurface properties of the ground. Numerous geophysical methods are used to map bedrock depths, locate fractures, map lithology and locate voids and other subsurface features. The following paragraphs illustrate some of the target for geophysical surveys and briefly describe the methods used. This section includes applying the various methods for both depth to bedrock and for locating fractures. Thus in some cases the techniques are discussed twice, each with the particular application in mind.

The methods most discussed are surface geophysical methods. However, for some problems in this, and the following Physical Properties section, logging methods are also important. The most important of these are presented in the relevant sections.

6.1.1 Determination of the Depth/Structure/Fractures of Bedrock

This section of the document discusses the determination of bedrock depths for materials source areas, foundations, mapping bedrock topography and mapping bedrock structure. The determination of bedrock depths is common to each of these topics, since bedrock topography is simply the lateral changes in bedrock depths. Bedrock structure is related more to fractures, faulting, and other features, although bedrock depth may also be important. The section is broadly divided into two parts with the first part describing the methods used to map bedrock depths. The second part concentrates on the methods that can be used to map fractures.

Unfortunately, no geophysical method, except possibly Ground Penetrating Radar under ideal conditions, can map fine/detailed structure internal to the bedrock. Generally, only successively deeper layers beneath the bedrock can be mapped geophysically. However, geophysical methods can be used to map fracturing, faulting, locate voids, and for other targets as described in other sections of this document.

Many of the methods used to map bedrock topography can also be used to locate fractures; hence, the basic theory of the method is common to both applications. It is, therefore, convenient to divide this section into two main parts. The first part discusses the basic theory of each method as well as presents its application to mapping bedrock topography and providing bedrock depths. The second part of this section will focus on the application of the techniques to locate fractures but will not describe the basic theory of each method, since these are described in the first section. Exceptions to this will be methods that are used only for detecting fractures but are not used to find bedrock depths and are not described in the first section. Finally, a brief discussion of the use of geophysical methods to map faults is given at the end of this section.

Methods to Map Bedrock Depths and Topography

Determining bedrock depths and topography is commonly done using geophysical methods. As with all geophysical methods, estimating the physical properties of the geologic section prior to conducting a survey is important in determining the best method to use. The estimated depth to the bedrock is also an important criterion, since some methods may not be able to penetrate to the required depths.

Determining bedrock depths and topography are somewhat different in that mapping the topography of the bedrock does not necessarily imply that its depth is known. However, usually, its depth can be found, and the topographic profile can be converted to a depth profile. There are several geophysical methods that are used to find depths to bedrock and map bedrock topography. These methods are listed below.

1. Ground Penetrating Radar (GPR).
2. Seismic Refraction.
3. Seismic Reflection.
4. Resistivity methods.
5. Time Domain Electromagnetic Soundings (TDEM).
6. Conductivity measurements using the EM31 and EM34.
7. Spectral Analysis of Surface Waves (SASW).
8. Analyzing acoustic noise using the SeisOpt software.
9. Gravity.

6.1.1.1 Ground Penetrating Radar (GPR)

Basic Concept: Ground-Penetrating Radar can be used where the bedrock is expected to be shallow, and the overburden is unsaturated and contains no clay or silt. If these conditions exist, then penetration depths may be a few meters. The GPR instrument consists of a recorder and a transmitting and receiving antenna. Different antennas provide different frequencies. Lower frequencies provide greater depth penetration but lower resolution. Figure 111 illustrates the GPR system. The transmitter provides the high-frequency electromagnetic signals that penetrate the ground and are reflected from objects and boundaries, providing a different dielectric constant exists from that of the overburden. The reflected waves are detected by the receiver and stored in memory.

Figure 112 shows typical GPR equipment that includes the display and controls for the equipment.

Figure 113 shows a 100 MHz antenna being pulled across the ground as the survey is conducted. This is a fairly low-frequency antenna and can provide penetration to about 20 m.

Data Acquisition: GPR surveys are conducted by pulling the antenna across the ground surface at a normal walking pace, as shown in figure 113. The recorder stores the data, as well as presenting a picture of the recorded data on a screen.

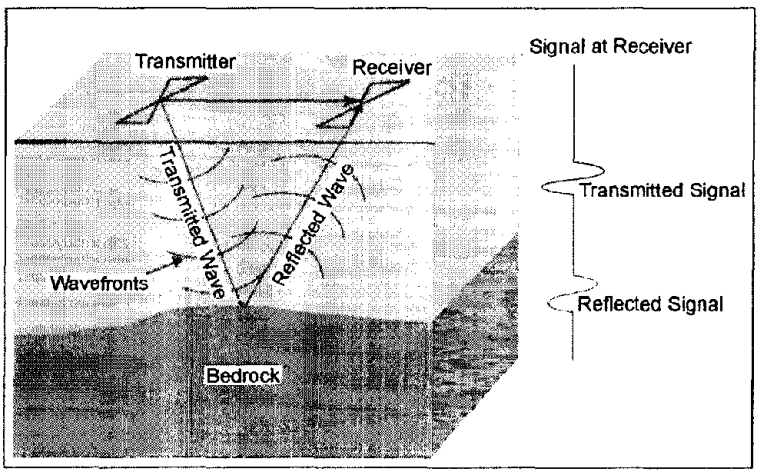

Figure 111. Ground Penetrating Radar system.

Figure 112. Ground Penetrating Radar instrument. (Geophysical Survey Systems, Inc.)

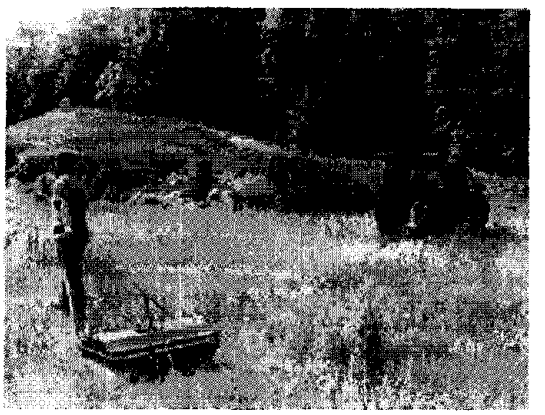

Figure 113. Ground Penetrating Radar antenna (100 MHz) used in a survey. (MALA GeoScience USA, Inc.)

Data Processing: The data are processed much like the processing done on single channel reflection seismic data. Processes such as distance normalization, horizontal scaling (stacking), vertical and horizontal filtering, velocity corrections, and migration can all be done. However, depending on the data quality, it may not be necessary to process the data since the field records may be all that is needed to observe the bedrock.

Data Interpretation: In order to calculate the depth to the bedrock, the speed of the GPR signal in the soil at the site needs to be obtained. This can be estimated from charts showing speeds for typical soil types or it can be obtained in the field by conducting a small traverse across a buried feature whose depth is known.

Advantages: GPR is a relative fast method and presents results as the survey progresses. Different antenna can easily be attached and tested if the resolution or depth penetration is insufficient.

Limitations: Probably the most limiting factor for GPR surveys is that their success is very site specific, and depends on having a contrast in the dielectric properties of the target compared to the host overburden. Clearly sufficient depth penetration to reach the target is needed. Penetration depends on the frequency of the antenna, the conductivity of the overburden, and whether clay is present in the overburden. Also, if a low-frequency antenna is used, then the resolution of targets is less than with a high-frequency antenna. In addition, with low-frequency antennas, which are usually not shielded, GPR energy radiates in all directions. Thus, reflections occur from local objects either on the ground surface or above the ground, such as power lines and buildings. For surveys under bridges, the bridge deck may provide a reflection. It may be possible to separate the reflection from the bridge deck from the reflection from the bedrock, providing these two reflection times are significantly different.

6.1.1.2 Seismic Refraction

Basic Concept: Seismic refraction is one of the most commonly used methods to determine bedrock depths, especially for depths of less than 30 m. The method requires a seismic energy source, usually a sledgehammer for depths of 15 m or less, and weight drop and black powder charges for depths to 30 m. The seismic waves produced by the energy source penetrate the

overburden and refract along the bedrock surface. While they are traveling along this surface, they continually radiate seismic waves back to the ground surface. These are detected by geophones placed on the ground surface. Both compressional waves (P-waves) and shear waves (S-waves) can be used in the seismic refraction method, although compressional waves are most commonly used. Figure 114a shows the layout of the instrument, the main seismic waves involved, and the resulting time distance graph. A typical seismic recorder is shown in figure 114b. The method can be used for up to about four layers. However, each layer has to have a higher velocity than the overlaying layer.

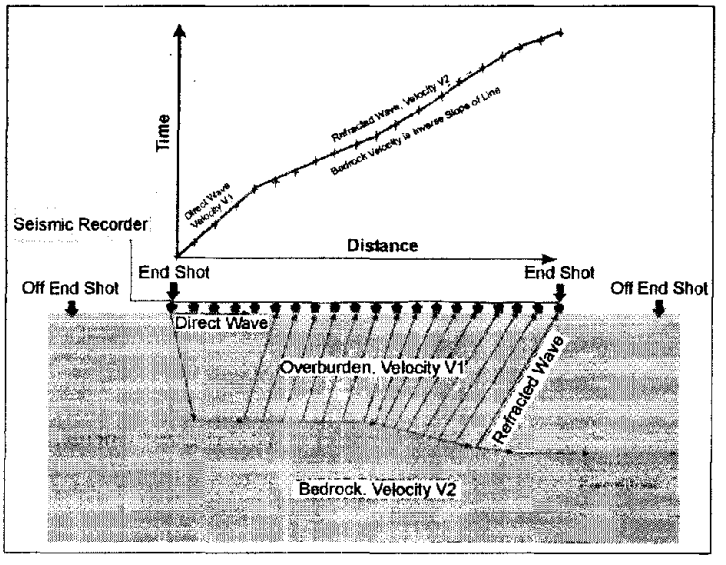

(a) Instrument layout, refracted waves, and time-distance plot.

(b) Seismograph data recorder. (Geometrics Inc.)

Figure 114. Seismic Refraction: field set up and data recorder.

Data Acquisition: The design of a seismic refraction survey requires a good understanding of the expected bedrock velocity and depth and overburden velocity. With this knowledge, velocities can be assigned to these features and a model developed that will show the parameters of the seismic spread best suited for a successful survey. These parameters include

the length of the geophone spread, the spacing between the geophones, the expected first break arrival times at each of the geophones, and the best locations for the off-end shots. Knowing the expected first break arrival times is also helpful in the field, where field arrival times that correspond fairly well to expected times help to confirm that the spread layout has been appropriately planned, and that the target layer is being imaged.

Data Processing: The first step in processing/interpreting refraction seismic data is to pick the arrival times of the signal, called first break picking. A plot is then made showing the arrival times against the distance between the shot and geophone. This is called a time-distance graph. An example of such a graph for two-layered ground (overburden and refractor) is shown in figure 117.

The red portion of the time distance plot shows the waves arriving at the geophones directly from the shot. These waves arrive before the refracted waves. The green portion of the graph shows the waves that arrive ahead of the direct arrivals. These waves have traveled a sufficient distance along the higher speed refractor (bedrock) to overtake the direct wave arrivals.

Data Interpretation: Several methods of refraction interpretation are used. One of the most common methods is the Generalized Reciprocal Method (GRM) that is described in detail in Part 2 Geophysical Methods, Theory and Discussion. A brief, and simplified, description of the GRM method is presented below. Figure 115 shows the basic rays used for this interpretation.

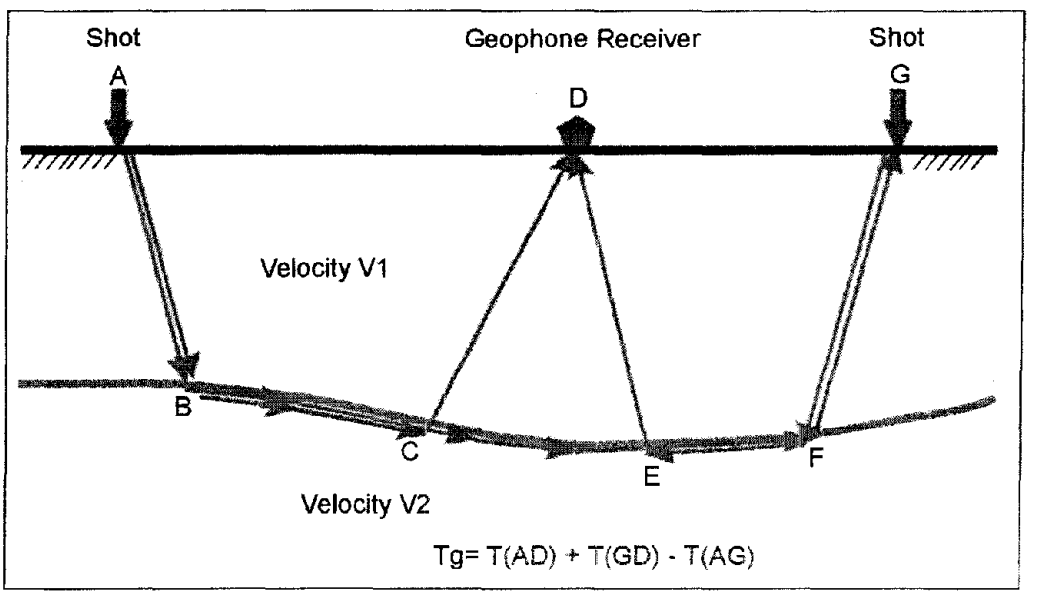

Figure 115. Basic Generalized Reciprocal method interpretation.

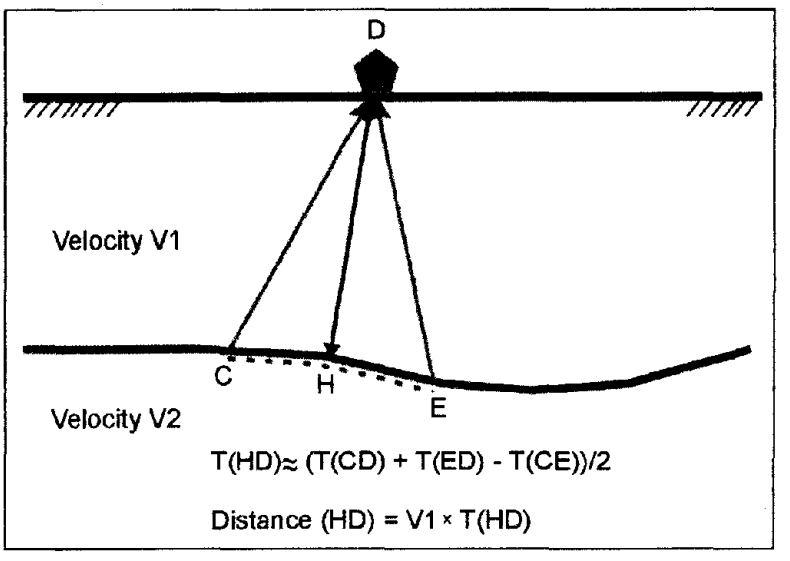

Figure 116. Generalized Reciprocal method interpretation.

The objective is to find the depth to the bedrock under the geophone at D. This is done using the following simple calculations. The travel times from the shots at A and G to the geophone at D are added together: T1= T(AD) + T(GD). The travel time from the shot at A to the geophone at G is then subtracted from T1. Figure 116 shows the remaining waves after the above calculations have been performed. These are the travel times from C to D added to the travel times from E to D subtracting the travel time from C to E. The sum of these travel times can be shown to be approximately the travel time from the bedrock at H to the geophone at D. Since the velocity of the overburden layer can be found from the time distance graph, the distance from H to D can be found giving the bedrock depth.

An example of the results from a seismic refraction survey is presented in figure 117. The upper figure shows the travel time graph, illustrating the time that the seismic waves take from the shot to each geophone. The second graph presents the interpreted seismic velocities, and the third graph shows the interpreted bedrock section.

Advantages: Refraction seismic is generally very effective at determining bedrock depths since bedrock usually has a higher velocity than the overburden. In addition, the method is able to provide fairly detailed lateral variations in depth since the depth beneath each geophone can also be found.

Limitations: Probably the most restrictive limitation is that each of the successively deeper refractors must have a higher velocity than the shallower refractor. However, for determining bedrock depths, this is probably not a significant limitation since, as mentioned above, the bedrock usually has a higher velocity than the overburden.

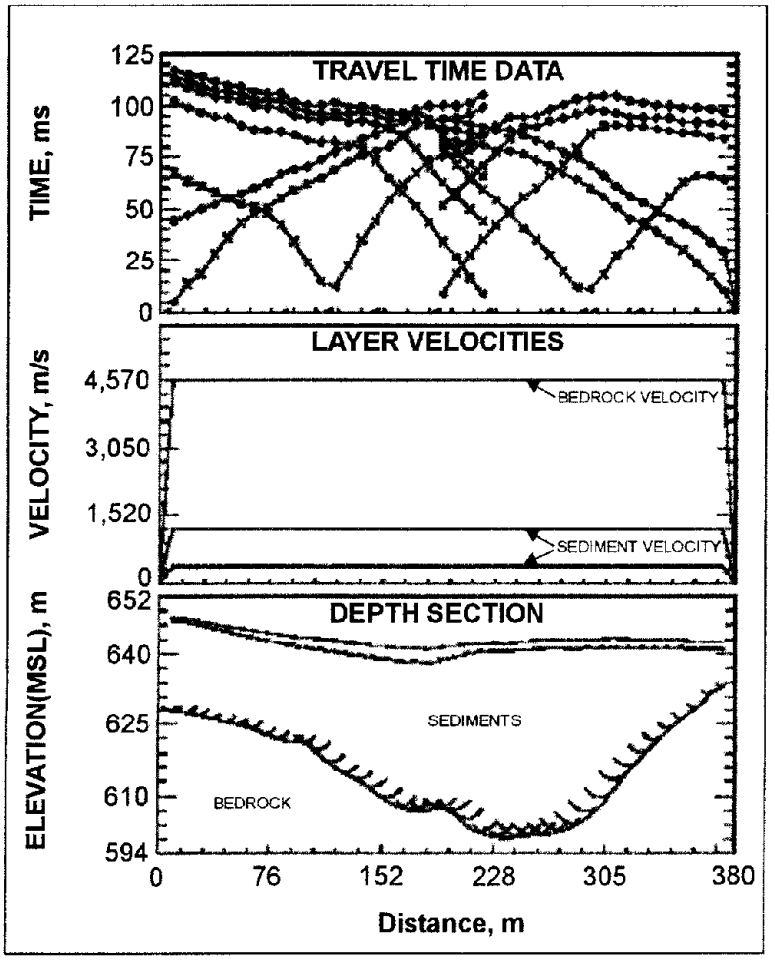

Figure 117. Example of a Seismic Refraction interpretation.

If the water table is in the overburden and close to the bedrock, this may obscure the bedrock arrivals since saturated soils have a higher velocity than unsaturated soils. This may result in a false interpretation of the bedrock depth.

Local noise, for example, traffic, may obscure the refractions from the bedrock. This can be overcome by using larger impact sources or by repeating the impact at a common shot point several times and stacking the received signals. If noise is still a problem, a larger energy source may be required. In addition, since some of the noise travels as airwaves, covering the geophones with sound absorbing material may also help to dampen the received noise.

6.1.1.3 Seismic Reflection

Basic Concept: Seismic reflection involves using a surface seismic source to create a seismic wave, which then travels into the subsurface. At interfaces that have an impedance contrast, (change in velocity and/or density) a portion of these waves is reflected back to the ground surface, and a portion is transmitted through the interface. These transmitted waves then reflect at the next impedance contrast and return to the ground surface. Geophones on the ground surface record these reflections. Figure 118 shows the seismic reflection method.

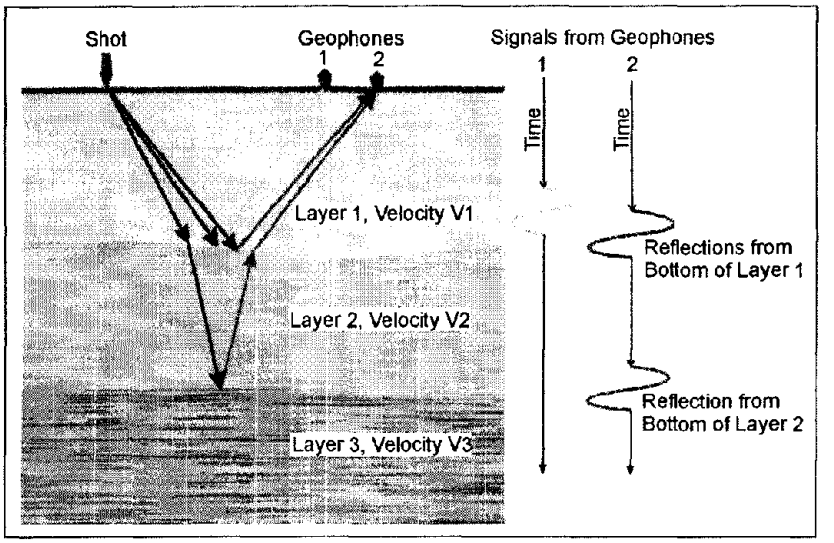

Figure 118. The Seismic Reflection method.

Data Acquisition: A line of geophones is placed on the ground surface. Shots (hammer or explosive sources) are initiated at regular intervals along the geophone spread and the resulting reflections are recorded by the geophones and stored in seismic recorder. Seismic reflection surveys require that the geophone and shot spacing are appropriate for the particular problem. The number of channels should be chosen so that the spread length is appropriate for the desired depth of investigation, and the geophone spacing needs to be such that the rugosity of the reflecting surface is imaged properly.

Data Processing: Many techniques are applied to process reflection seismic data. These include filtering, correcting for subsurface velocity effects, and stacking the traces that emanate from a common depth point (CDP) on the reflecting surface. The main objective of these techniques is to provide a gather (group) of seismic traces that can be stacked to image each reflection point as clearly as possible. The output from processing a line of seismic data is a seismic section showing the reflectors. This section can be presented as CDP location against record time, or when velocities are assigned to the different layers, as CDP against depth. More detail is provided in Part II Geophysical Methods, Theory and Discussion.

Data Interpretation: For reflection seismic surveys for bedrock depth determinations, a seismic section showing CDP against depth is most appropriate. Such a section should provide an immediate view of the depths to the bedrock.

Advantages: Seismic reflection generally requires a less intensive energy source for a given depth than the seismic refraction method. It is also better able to image greater depths than the refractions method.

Limitations: The seismic reflection method is usually fairly labor intensive and is often more expensive that other methods. In addition, when the bedrock depths are shallow, seismic refraction will usually be the more appropriate method. However, seismic reflection may be a more appropriate method when bedrock depths are more than 30 m.

6.1.1.4 Resistivity

Basic Concept: The resistivity method can be used to find bedrock depths if the overburden and bedrock have different resistivities, which is usually the case. There are two common resistivity methods: soundings and traverses. Figure 119 shows the resistivity sounding method. Resistivity traverses are used to map lateral variations in resistivity and are not usually used to provide bedrock depths.

Data Acquisition: Figure 119a shows the system used to measure the resistivity of the ground. Current is passed into the ground using the two electrodes labeled A and B. The voltage that results from this current is then measured using electrodes M and N. Using the amount of current passed into the ground along with the voltage and a geometric factor for the electrode layout, the resistivity of the ground is calculated. The electrode array is then expanded, making the current penetrate deeper into the ground and another reading is taken. This procedure is repeated for many electrode spacings, providing a set of resistivity values for different electrode spacings. These values are plotted on a graph of resistivity against electrode spacing, as illustrated in figure 119b. This graph shows that at small electrode spacings, the resistivity is that of the overburden. At large electrode spacings, the resistivity approaches that of the bedrock. The resistivity curve is interpreted using software that provides a resistivity model (depths and resistivities) whose resistivity calculations match the field data.

Advantages: Unlike the seismic refraction method, which requires that each successive layer have a higher velocity, the resistivity method works whether the deeper layers become more or less resistive. The field procedures are fairly simple and a sounding to depths of about 50 meters depth can be conducted in less than one hour.

Limitations: Because electrodes need to be placed in the ground, the method is difficult to use in areas where the surface of the ground is hard, such as concrete or asphalt-covered areas. In addition, if the ground is dry, water may need to be poured on the electrodes in order to improve the electrical contact between the electrode and the ground. Generally, the separation between the current electrodes will need to reach a maximum of about three times the investigation depth. Thus, if the bedrock is 15 m deep, the current electrodes will need to be spaced up to 45 m apart. Lateral variations in resistivity can affect the accuracy of the depth interpretation, or grounded metal objects near the sounding site may also influence the data.

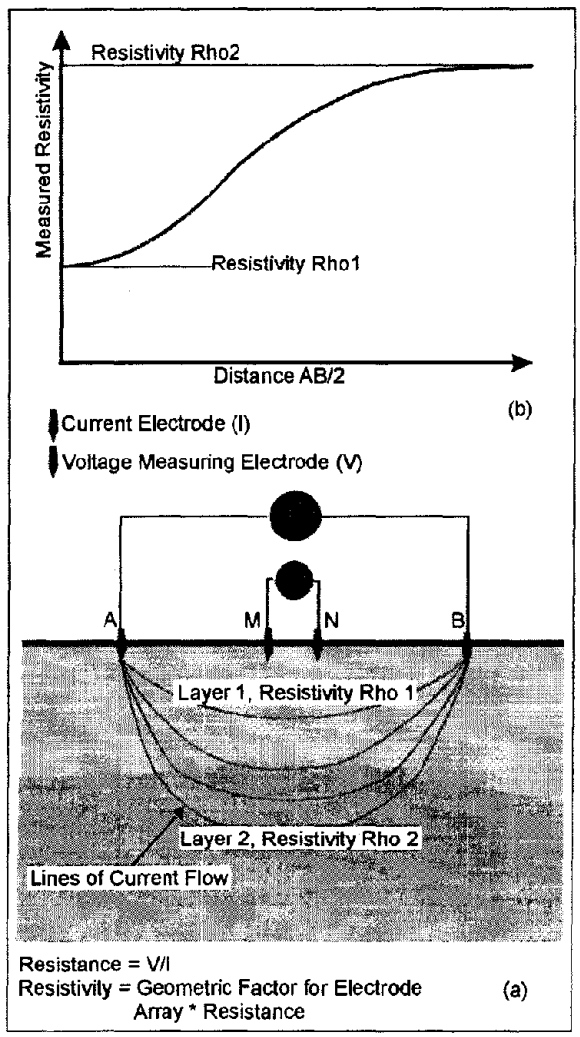

Figure 119. Resistivity Sounding (a) Data recording geometry, and (b) Sounding curve.

6.1.1.5 Time Domain Electromagnetic Soundings

Basic Concept: Time Domain Electromagnetic (TDEM) soundings are another method used to obtain the vertical distribution of the resistivity of the ground. This method is particularly well suited to mapping conductive layers, but can also be used to map resistive layers, which is likely to be the case for bedrock. To a significant degree, this method has now superseded the resistivity sounding method since it requires less work for a given investigation depth and generally provides more precise depth estimates. However, resistivity soundings are still useful for shallow investigations or when resistive targets are sought. Figure 120 provides a conceptual drawing of the TDEM method.

Data Acquisition: TDEM soundings are an electromagnetic method used to provide the vertical distribution of resistivity within the ground. A square loop of wire is laid on the ground surface. The side length of this loop is about half of the desired depth of investigation. A receiver coil is placed in the center of the transmitter loop. Electrical current is passed through the transmitter loop and then quickly turned off. This sudden

change in the transmitter current causes secondary currents to be generated in the ground. The amplitude of these currents is related to the conductivity of each of the layers in the ground. Thus, the conductive layer will generate stronger secondary currents than a less conductive layer. The voltage measured by the receiver coil does not decay instantly to zero when the current is turned off but continues to decay for some time. This decaying voltage is caused by the decaying secondary electrical currents in the ground. The voltage measured by the receiver is then converted to resistivity.

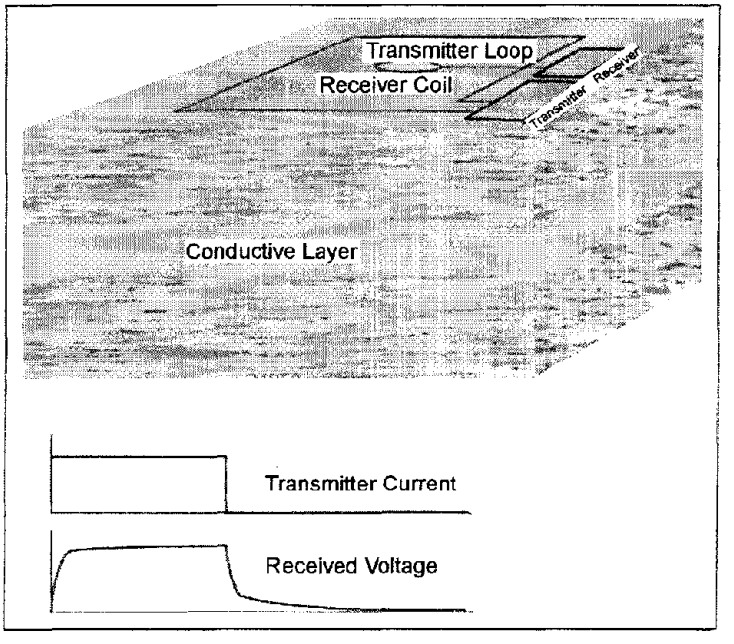

Figure 120. Time Domain Electromagnetic Sounding.

A plot is made of the measured resistivity against the decay time, as illustrated in figure 121.

The switching and measuring procedure is repeated many times, which allows the resulting voltages to be stacked, thereby improving the signal-to-noise ratio. This procedure is repeated at different sounding locations until the area of interest has been covered. A sounding curve is plotted for each location showing the measured resistivity against decay time.

The resistivity sounding curve shown in figure 121 illustrates the curve that would be obtained over three-layered ground. The near-surface layer is fairly resistive. This is followed by a layer having a much lower resistivity (higher conductivity) and causes the measured resistivity values to decrease. The third layer is again resistive.

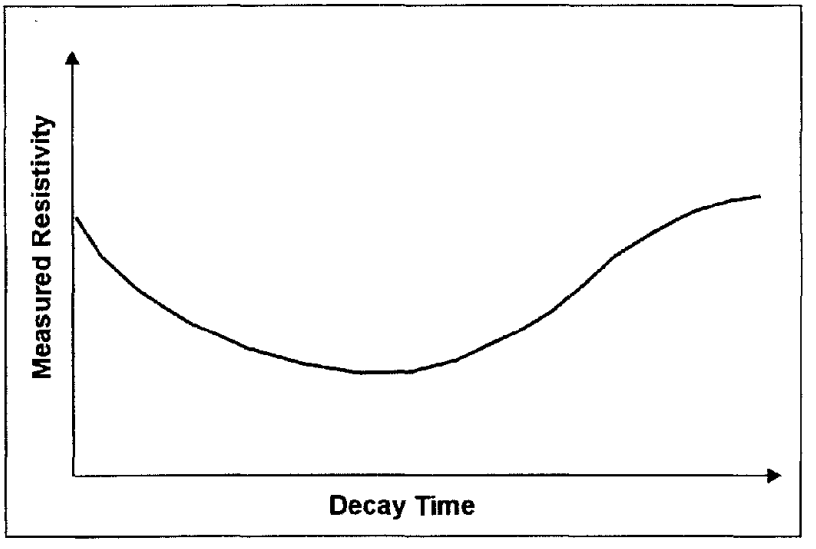

Figure 121. A Time Domain Electromagnetic Sounding curve.

Data Processing: The field data is transferred from the data recording instrument to a computer. The only processing required may be the removal of bad data. The data is then input to software that produces a sounding curve and facilitates interpretation.

Data Interpretation: The sounding curve is interpreted using computer software to provide a model showing the layer resistivities and thickness. The interpreter inputs a preliminary model into this software program, which then calculates the sounding curve for this model. It then adjusts the model and calculates a new sounding curve that better fits the field data. This process is repeated until a satisfactory fit is obtained between the model and the field data; this process is called inversion.

Advantages: Some of the advantages of the method have been mentioned under Basic Concept. Probably the most important of these is that the method is often more efficient than the resistivity method, especially if the target is at depth greater than about 50 meters. In addition, compared to the resistivity method, no electrodes have to be planted in the ground.

Limitations: TDEM soundings are an efficient method for investigating the vertical distribution of ground resistivity. Generally, the method is better suited to mapping conductive formations than resistive formations. However, it is also effective at mapping depths to resistive layers.

Probably the most troublesome aspect of data recording is the influence of fences, power lines, and other "cultural" features at the survey site. For surveys to find the depth to bedrock near bridges and other structures, the metal in these structures may prohibit the use of this method. However, if the bedrock is fairly horizontal and soundings can be conducted some distance from the site, then TDEM soundings may work.

6.1.1.6 Conductivity Measurements using the EM31 and EM34

Basic Concept: If the bedrock has a significantly higher or lower conductivity than the overburden, its topography can be mapped using conductivity measurements. The concept is illustrated in figure 122 where the bedrock has a higher conductivity than the overburden. When the conductive bedrock becomes deeper, then the measured conductivity decreases since it is more distant from the instrument. The reverse would occur if the bedrock had a lower conductivity than the overburden.

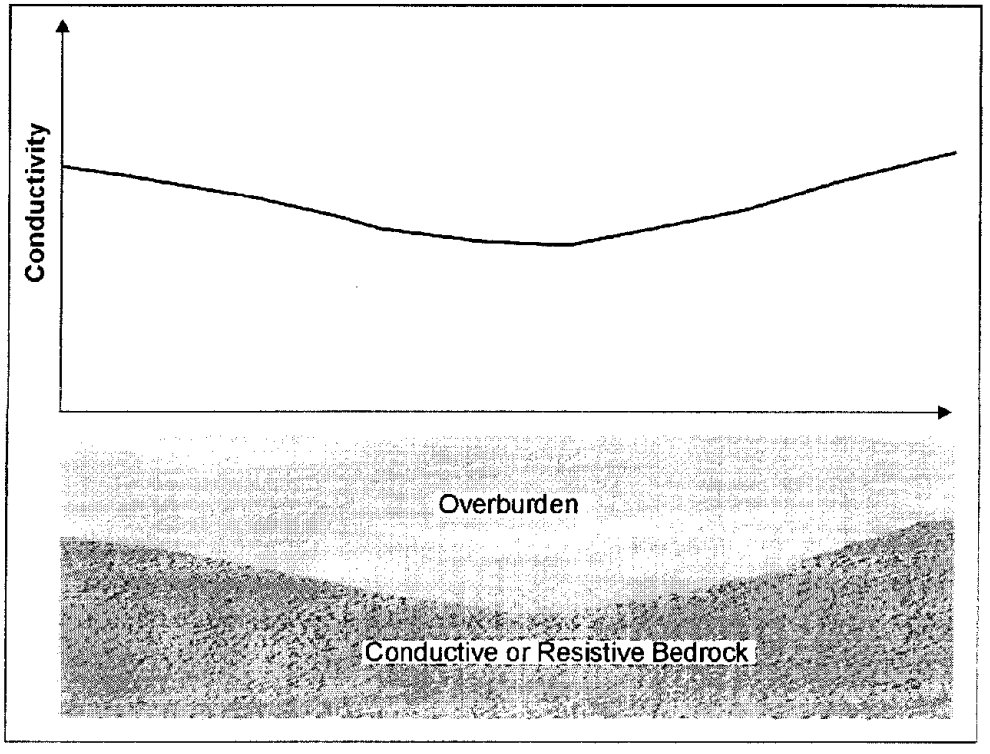

Figure 122. Model conductivity results over a conductive bedrock.

By mapping the conductivity of the ground to a depth sufficient to include the bedrock, the topography of the bedrock can be ascertained. However, this method does not give the depth to the top of the bedrock. If this is required, resistivity soundings can be performed at selected points along the conductivity traverses. Using these data, the conductivity values can be converted to bedrock depths.

Data Acquisition: Conductivity surveys designed to map the topography of a conductive, or resistive, unit at depth (bedrock) will normally be conducted along lines crossing the area of interest. Probably several lines will be surveyed and conductivity data recorded. These lines will need to have their spatial coordinates surveyed to draw a map of the final data.

Probably the most important parameter that has to be determined before conducting the conductivity survey is the depth of the bedrock and the configuration of the electromagnetic instrument to be used for the survey. The depth to the bedrock can be found from a resistivity sounding. This will also provide the electrical properties of the bedrock,

indicating whether it is conductive or resistive compared to the overburden. The next step is to find the parameters of the electromagnetic measuring instrument required to image this bedrock surface. The EM31 and EM34 both have a transmitter and receiver coil, which are coplanar. The transmitter produces sinusoidal electromagnetic waves oscillating at up to about 10 kHz, depending on the instrument, and, in the case of the EM34, the coil separation used. Measurements can be taken with the plane of these coils either parallel to the ground surface (vertical dipole mode) or normal to the ground surface (horizontal dipole mode). These two modes provide different depths of investigation and different responses to the geologic section. The vertical dipole mode provides the greater depth of investigation. In this mode, the conductivity readings are less sensitive to near-surface changes in conductivity. In the horizontal dipole mode, the depth of investigation is less than the vertical dipole mode, and the measured conductivity values are more sensitive to near-surface changes in conductivity.

The transmitter and receiver coils are mounted in a rigid boom in the EM31 and are, therefore, fixed (figure 183).

With the EM34, the coils are not mounted in a rigid structure, and the distance between them can be changed to provide increasing depths of investigation with increasing separation between the coils. Figure 197 shows the EM34 being used in the horizontal dipole mode.

In order to check whether the conductivity measurements are responding to a depth sufficient to image the bedrock, measurements can be taken with the EM34 using the two modes at each of the three coil spacings allowed. Since the contrast between the overburden and bedrock are known from the resistivity sounding, the EM34 measurement parameters needed to image the bedrock can be found. This then sets the EM34 data recording parameters to be used for the survey.

Data Processing: Usually little processing is done to the data although it may sometimes be necessary to remove bad data points.

Data Interpretation: Interpretation is often visual, looking for the conductivity lows for deeper sections of the conductor, or conductivity highs if the bedrock is more resistive than the overburden. If resistivity soundings have been recorded, the conductivity values can be converted to depth, as described earlier.

Advantages: The prime advantage of the method is that is can provide a rapid method of mapping bedrock topography.

Limitations: The bedrock layer has to be thick enough to have a significant influence on the conductivity readings. In addition, it has to be more conductive, or resistive, than the overburden. If shallower conductive layers occur, or possibly fade in and out spatially, this may obscure the interpretation of the deeper conductive layer. Any metal, either above or below the ground surface local to the instrument will influence the data.

6.1.1.7 Spectral Analysis of Surface Waves

Basic Concept: The Spectral Analysis of Surface Waves (SASW) method is used to measure the layer depth and shear wave velocity of the ground. Rather than responding to discrete layers, this method provides a more general (bulk) shear wave velocity along with the depth at which this velocity changes. The method may be used for investigating bedrock properties for foundation studies.

The method is based on the propagation of mechanically induced Rayleigh waves. By striking the ground surface with a hammer or other source, a transient stress wave is created, including surface or Rayleigh waves, which are registered by two transducers placed in line with the impact point on the ground surface at fixed separations. The transducers, which may be small accelerometers, register the passage of the waves. The receiver outputs are plots of the phase difference between the two transducers as a function of frequency. A profile of Rayleigh wave velocity versus wavelength, or so-called dispersion curve, is calculated from the phase plot. The ratio of Rayleigh wave velocity to shear wave velocity is approximately 0.9:1; thus, the shear wave velocity can be estimated. The shear stiffness (G) of the ground can be calculated from the shear velocity if the material density is known and a plot of ground stiffness as a function of depth from the surface can be obtained.

Rayleigh waves have velocities that depend on their wavelength, a phenomenon called dispersion. Waves having different wavelengths sample to different depths, with the longer wavelengths sampling to greater depths. Figure 35 illustrates the sampling depths and particle motion of two Rayleigh waves having different wavelengths.

This principle is used to measure the thickness of ground layers with different stiffness properties. It can also be used to locate and roughly delineate inhomogeneities such as voids.

Data Acquisition: The surface wave dispersion curve can be measured using an active source and a linear array of receivers. The dispersion curve is then inverted to determine the corresponding shear wave velocity profile.

There are two main methods used in surface wave exploration. The most common surface wave method in industry is called SASW testing. The other method uses an array of geophones and is generally called array methods (MASW). The field setup is shown in figure 36. Either a transient or continuous point source is used to generate Rayleigh waves, which are monitored by in-line receivers. The data acquisition system calculates the phase difference between the receiver signals. These phase data are processed later into the dispersion curve, which is modeled analytically to determine a compatible shear wave velocity profile for the site. The data acquisition system is discussed in more detail below.

The source used depends on the desired profiling depth. Heavier sources generating lower frequency waves provide deeper interpretations. A combination of sources is commonly used to measure dispersion over a broad enough bandwidth to resolve both the near-surface and greater depth. Transient sources include sledgehammers (<15 m depth) and dropped weights. Continuous sources include the electromagnetic vibrator (< 40 m depth), eccentric mass oscillator, heavy equipment such as a bulldozer (30 to 150 m depth), and the vibroseis

truck (<120 m depth). A pair of vertical receivers monitors the seismic waves at the ground surface. For profile depths of around 100 m, 1-Hz geophones are required. Five or 10-Hz geophones can be used for surveys from 10 to 30 m deep. Theoretical as well as practical considerations, such as attenuation, necessitate the use of an expanding receiver spread. Data are recorded from sources placed on both sides of the geophones, providing both the forward and reverse direction shots (figure 36).

Data Processing: In the SASW method, a Fast Fourier Transform (FFT) analyzer or PC-based equivalent is used to calculate the phase data from the input time-voltage signals. Typically, only the cross power spectrum and coherence are recorded. Coherent signal averaging is used to improve the signal-to-noise ratio, a process similar to stacking. Because of the initial processing done by the analyzer in the field, the effectiveness of the survey can be assessed and modified if necessary. An initial estimate of the shear wave velocity (V_S) profile can be made quickly.

Data Interpretation: Interpretation consists of modeling the surface wave dispersion to determine a layered V_S profile that is compatible. Interpretation can be done on a personal computer.

The acquisition and processing techniques of SASW methods do not separate motions from body wave, fundamental mode Rayleigh waves, and higher modes of Rayleigh waves. Usually it is assumed that fundamental mode Rayleigh wave energy is dominant, and forward modeling is used to build a 1-D shear wave velocity (V_S) profile whose fundamental mode dispersion curve is a good fit to the data.
Advantages: The major advantages of the SASW method are that it is non-invasive and non-destructive, and that a larger volume of the subsurface can be sampled than in borehole methods.

Limitations: The depth of penetration is determined by the longest wavelengths in the data. In modeling, there is a trade-off between resolution (layer thickness) and variance (change in V_S between layers). Data that are noisier must be smoothed and will have less resolution because of this. Whether a particular layer can be resolved depends on its depth and velocity contrast. The modeled shear wave velocity (V_S) profile is not sensitive to reasonable variations in density. The compressional wave velocity (V_P) cannot be resolved from dispersion data, but has an effect on modeled V_S. The difference in V_P in saturated versus unsaturated sediments causes differences of 10% to 20% in surface wave phase velocities, which leads to differences in modeled V_S.

The depth of penetration is determined by the longest wavelengths that can be generated by the source, measured accurately in the field and resolved in the modeling. Generally, heavier sources generate longer wavelengths, but site conditions are often the limiting factor. The available open space determines the offset from the source and aperture of the array, which determines the near-field wave filter criteria. Commonly, wavelengths are removed from the data that are longer than twice the distance from the source to the first receiver. Attenuation characteristics of the ground determine the signal level at the geophones. The cultural noise (traffic, rotating machinery) at a site may limit the signal-to-noise ratio at low frequencies. In SASW methods, the depth of resolution is usually one-half to one-third of the longest

wavelength. Surveys to depths of 100 m are reported using heavy equipment for the seismic source. With a hammer source, depths up to about 20 m may be expected. Exploration depths of 1 m, or maybe less, are possible.

The field setup requires a distance between the source and most distant geophone of two to three times the resolution depth. However, forward modeling allows for subjective interpretation of the sensitivity of the dispersion curve to the layered V_S model. Resolution decreases with depth. A rule of thumb is that if a layer is to be resolved, then the layer thickness (resolution) should be at least around one-fifth of the layer depth.

The SASW method is applicable for measuring the bulk shear and compressional wave velocities of the soil and overburden. It is used in earthquake-prone areas to evaluate the engineering properties of the soil/overburden to depths of about 30 m.

The SiesOpt Geophysical Method

The SeisOpt method is a seismic method that provides the velocity distribution within the subsurface. SeisOpt is the name given to the software that performs the calculations on the recorded seismic field data. The software was developed by a company called Optim LLC, based in Reno, Nevada.

Basic Concept: Using conventional seismic equipment, the ambient seismic noise is recorded. Such noise, sometimes called microtremors, is constantly being produced by cultural and natural noise. This data is then processed using the SeisOpt software to obtain a velocity model or using the SeisOpt ReMi method in order to produce shear wave velocity profiles. This latter method is reported to be able to determine shear wave profiles to depths of up to 100 meters.

Data Acquisition: As mentioned above, the ambient seismic noise is recorded using standard seismic equipment and geophones. The seismic equipment is laid out in an array very similar to that used in seismic refraction surveys. Geophones are usually set below loose surface material and buried under about 10 cm of tamped soil. If the ReMi method is to be used to shear wave profiles then the data acquisition procedure consists of recording three 15-second seismic noise records.

Data Processing and Interpretation: The data is processed using one of the several software packages offered by Optim. The SeisOpt software, which requires no prior assumptions about the subsurface structure, uses only the first arrival travel time data and array geometry. A velocity model is then produced as shown in figure 123. Optim is also able to process 3D data sets.

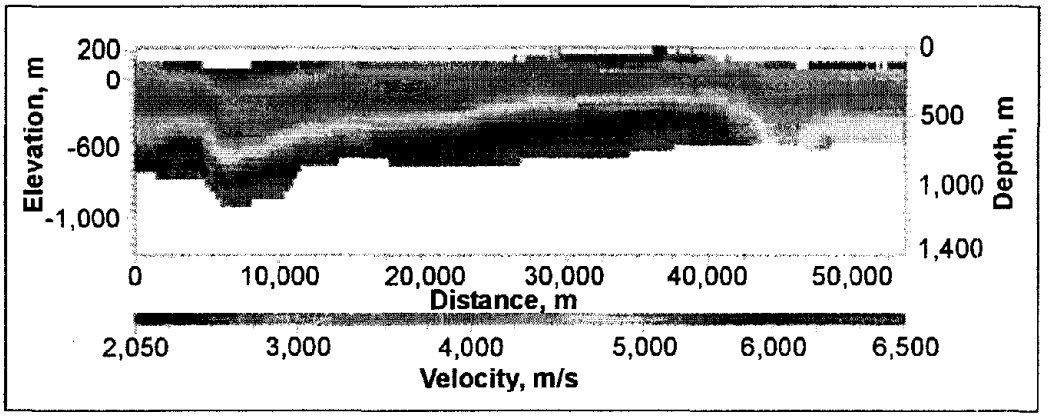

Figure 123. SeisOpt® 2D velocity in an area with strong lateral velocity gradient.

If a shear wave profile is required then the SeisOpt ReMi method can be used. Figure 124 shows a shear wave profile with the ReMi results being compared with a shear wave velocity log. Such results may be useful for several applications including soil compaction control, pavement evaluation, maping the subsurface and estimating the strength of subsurface materials and finding buried cultural features such as dumps and piers.

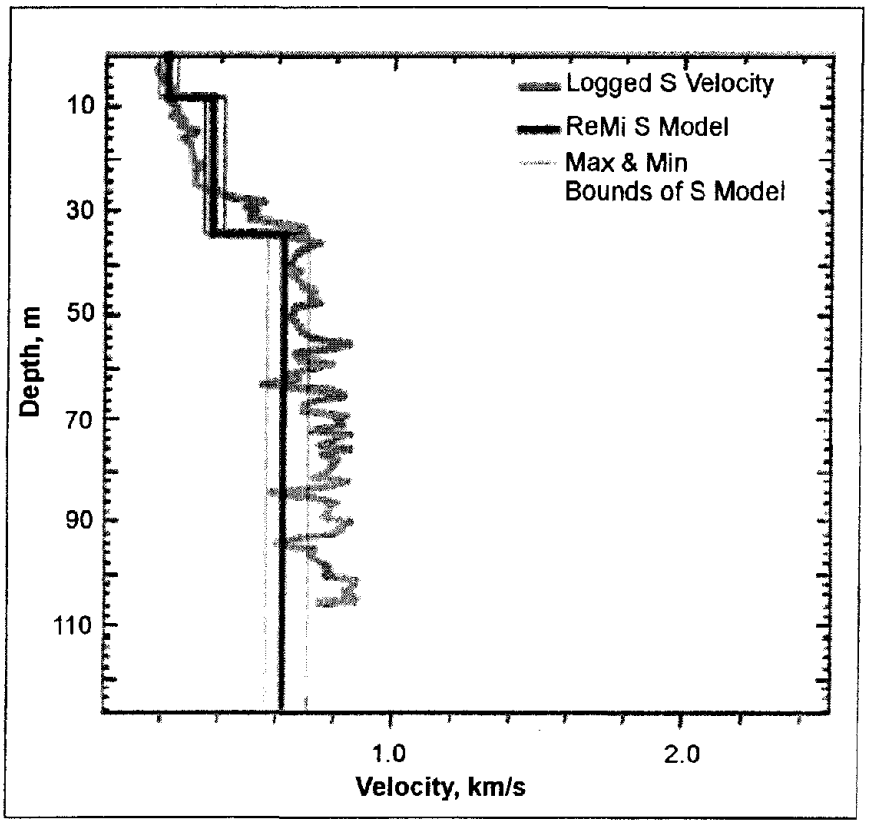

Figure 124. Shear-wave profile interpretation from a SeisOpt survey.

Advantages: The method is reported to have a wide range of applications, including rippability studies, void and utility detection, basement mapping and fault mapping. In addition, the ReMi

method, which determines shear wave velocities to depths of 100 meters, can be used to determine the NEHRP soil classification at a site.

Limitations: Since the method is relatively new, the limitations may not yet be apparent. However, since the method relies on ambient noise, it is possible that all of the frequencies required for a particular target may not be present at a particular site. At some sites, such as near a busy highway, the frequencies may be dominated by a small range of frequencies having a high amplitude.

6.1.1.8 Gravity

Basic Concept: The gravity method measures small spatial differences in the gravitational pull of the Earth. If the bedrock and overburden have different densities, the gravity pull will change over bedrock topographic features.

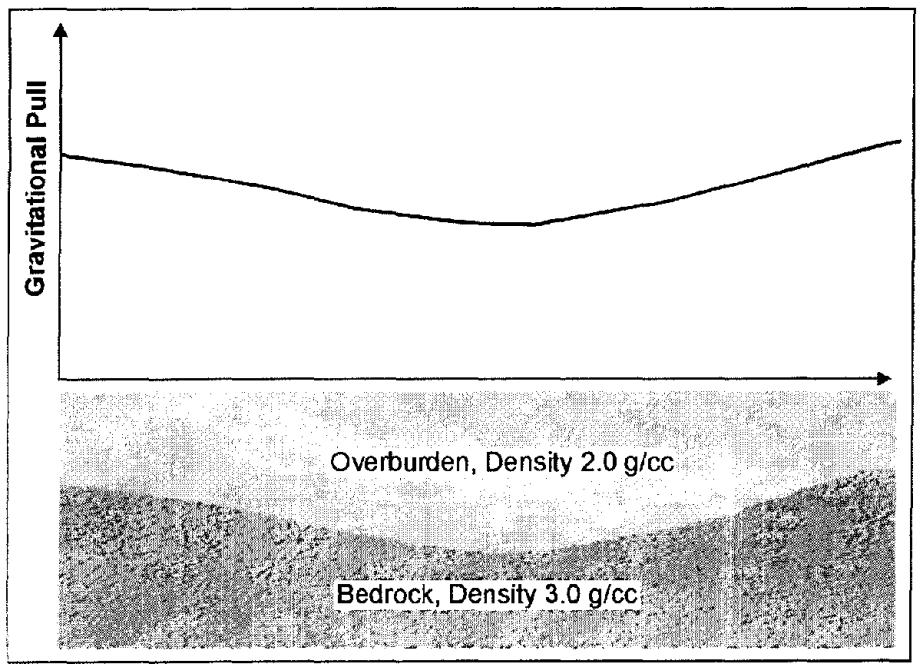

Figure 125. Gravitational pull over a bedrock depression.

In figure 125, the bedrock is assumed to have a density of 3.0 g/cc, and the overburden has a density of 2.0 g/cc. Since the bedrock density is greater than that of the overburden, the gravitational pull at the ground surface is higher when the bedrock is nearer the ground surface.

The instrument used to measure the gravity pull is called a Gravimeter. This instrument does not record the absolute value of the pull of gravity, but measures spatial differences in the gravity pull.

Figure 126. Model D1a gravity meter. (LaCoste & Romberg)

The anomalous gravitational field over a bedrock structure (depression or mound) depends on the amplitude of the depression, its width and depth, and the density contrast between the overburden and the bedrock. Significant bedrock topography with large density contrasts will produce large gravitational anomalies. Conversely, small amplitude structures at depth, even with large density contrasts, may produce only very small anomalies. Clearly, the size of an anomaly depends on the parameters of the structure and its depth, and, at some point, it cannot be observed. Thus, it is important to be able to measure the gravity field with as much accuracy as possible. The Lacoste and Rhomberg model D meter has an advertised accuracy of 10 microgals (980,000,000 microgals is the Earth's gravitational field). Variations in gravity anomalies found over topographic changes in bedrock vary from undetectable to hundreds of microgals. Figure 126 shows the Lacoste and Rhomberg model D1a gravity meter.

This is one of the preferred instruments for measuring small changes in the gravitational pull. If only very small anomalies are expected, the Lacoste and Rhomberg model EG can be used (figure 85). This instrument has an advertised repeatability of 3 microgals.

Data Acquisition: Surveys are usually conducted along lines crossing the area of interest. The expected size of the bedrock feature will determine the distance between readings (station spacing). A spatially small bedrock feature will require a smaller station spacing than that which would be required for a large bedrock feature. It is usually advisable to model the expected anomaly mathematically before conducting fieldwork. From this, along with the expected instrument accuracy, an estimate can be made of the anomaly size and the required station spacing.

Surveys are conducted by taking gravity readings at regular intervals along a traverse that crosses the expected location of the bedrock topography. However, in order to take into account the expected drift of the instrument, one station (probably the first) has to be reoccupied every half hour or so (depending on the instrument drift characteristics) in order to obtain a field graph of the instrument drift. Since gravity decreases with distance from the center of the earth, the elevation of each station has to be measured to an accuracy of about 3 cm.

Data Processing: Several corrections have to be applied to the field gravity readings. Each reading has to be corrected for elevation, the influence of tides, latitude, and, if significant local topography exists, a topographic correction. In a modern instrument such as the Lacoste and Rhomberg model D, the meter may do the tidal and drift corrections.

Data Interpretation: Gravity data are interpreted using software to calculate the gravity field of geologic features input by the operator. The program will then change the parameters (shape, depth) of the body (in this case, bedrock topography) until the calculated gravity field matches the observed gravity field. This process is called inversion and is commonly used in geophysical interpretation. If several lines of data have been acquired, a map of the gravity field may be produced.

Advantages: Gravity surveys require only a small amount of instrumentation (a gravity meter and instrument for elevation control). Gravity surveys are unobtrusive and can be conducted in environmentally sensitive areas.

Limitations: Gravity surveying is a labor-intensive procedure requiring significant care by the instrument observer. These instruments require careful leveling, although some of them are self-leveling, such as the Lacoste and Rhomberg EG. Once the reading has been taken, the gravity sensing mechanism must be clamped to stop excessive vibration, which would alter the readings. The instrument must be placed on solid ground (or a specially designed plate) so that it does not move (sink into the ground) while the reading is being taken. As mentioned above, all of the stations have to be surveyed for elevation.

The anomaly from bedrock topography rapidly becomes smaller with depth, and, therefore, detectability rapidly decreases with depth. Pre-survey modeling is important to establish the expected anomaly size and to determine if a gravity survey is feasible.

If other layers are present between the surface and bedrock, and these layers vary laterally in thickness or density, they will create gravity anomalies that may hinder an interpretation of the bedrock topography. In addition, fracture zones and voids may also create anomalies that may hinder an interpretation of bedrock depth.

Methods to Map Fractures

As with any geophysical method, fractures must present some physical property that can be detected from the ground surface to be detected. Generally, geophysical methods will not detect individual fractures unless they are large, but can detect fracture zones. Usually, fractures in the bedrock will contain more moisture than the host unfractured rock, and, therefore, will be more electrically conductive. They will also probably be areas of lower seismic velocity than unfractured bedrock. In some cases, since fractured areas are more subject to erosion, the fractured region may be topographically more depressed than the surrounding unfractured bedrock. Figure 127 presents a pictorial view of a fracture and the potentially useful attributes.

Several geophysical methods can be used to map bedrock fractures. The most commonly used methods are listed below:

1. Conductivity Measurements
2. Ground Penetrating Radar
3. Rayleigh waves recorded with a Common Offset Array (Common Offset Surface Waves)
4. Seismic Refraction
5. Shear Wave Seismic Reflection
6. Resistivity Measurements

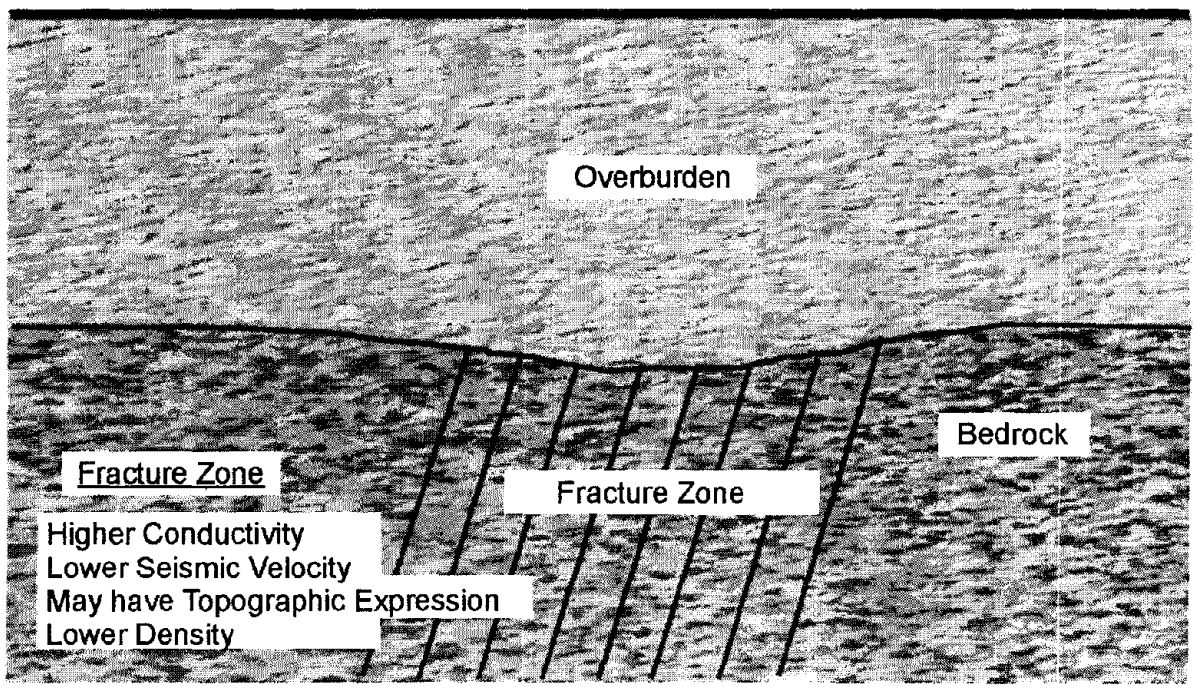

Figure 127. Bedrock fractures and potentially useful attributes.

The theory of all of these methods except Common Offset Surface Waves and Shear Wave Seismic Reflection has been described earlier and will not be presented in this section. However, there are some differences in the application of the above listed methods for locating fractures, which will be discussed where appropriate. The theory of Common Offset Surface Waves and Shear Wave Seismic Reflection will be briefly described

6.1.1.9 Conductivity Measurements to Map Fractures

Basic Concept: Conductivity measurements can be made with either the EM31 or EM34 in vertical dipole mode to locate conductive fracture zones. The anomaly measured in the vertical dipole mode is quite distinctive and is diagnostic of a vertical, or sub vertical, conductive feature. Figure 128 shows the anomaly over a conductive feature using an EM31 or EM34 in vertical dipole mode.

The measured conductivity increases as the conductive feature is approached. When the transmitter and receiver coils straddle the conductive zone the measured conductivity values decrease, reaching a minimum when they are equispaced about the conductive zone. This distinctive anomaly shape provides a good method for locating conductive fractures.

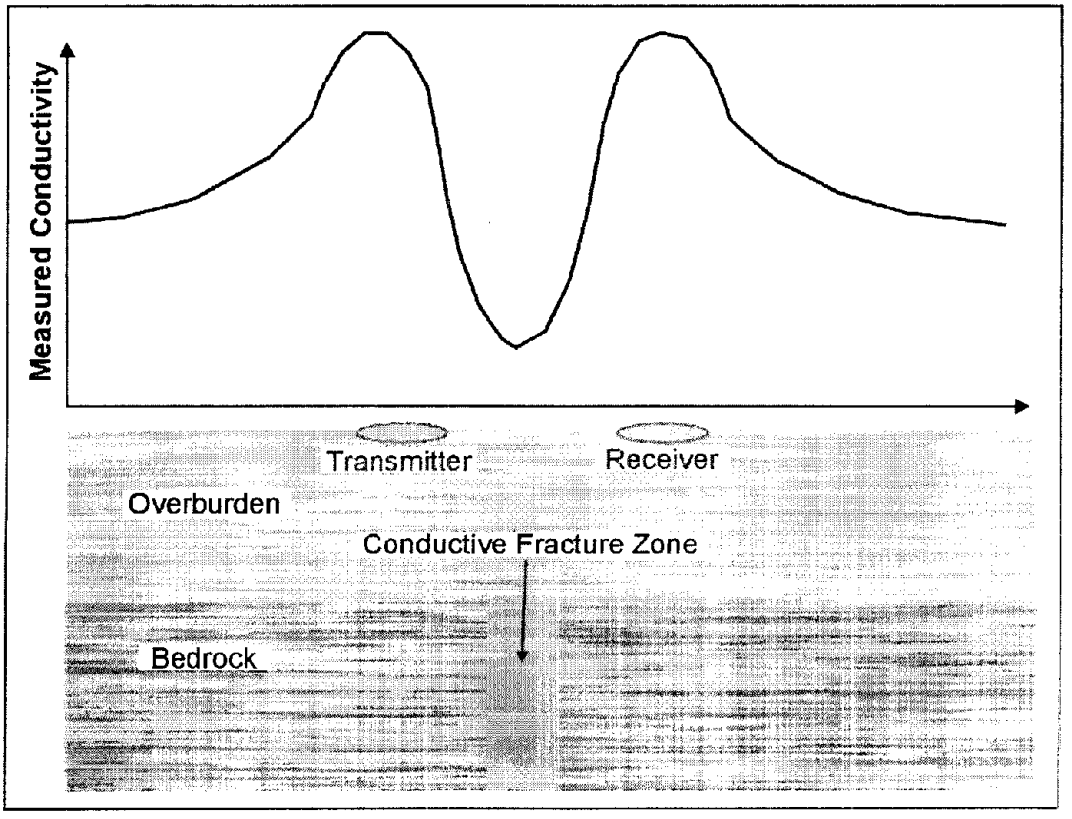

Figure 128. Anomaly from an EM31/34 used in vertical dipole mode over a conductive fracture zone.

6.1.1.10 Ground Penetrating Radar to Map Fractures

Ground Penetrating Radar (GPR) can be used to locate fractures and fracture zones. Reflections obtained over a fracture zone are more likely to be scattered that those emanating from the bedrock. This may allow fractured areas to be recognized. Figure 129 shows a GPR section over a fracture zone. In this case, the fracture is sub-horizontal and is seen as a reflector on the GPR section. Basic Concept, Data Acquisition, Data Processing, Data Interpretation, Advantages and Limitations have been discussed in a previous section.

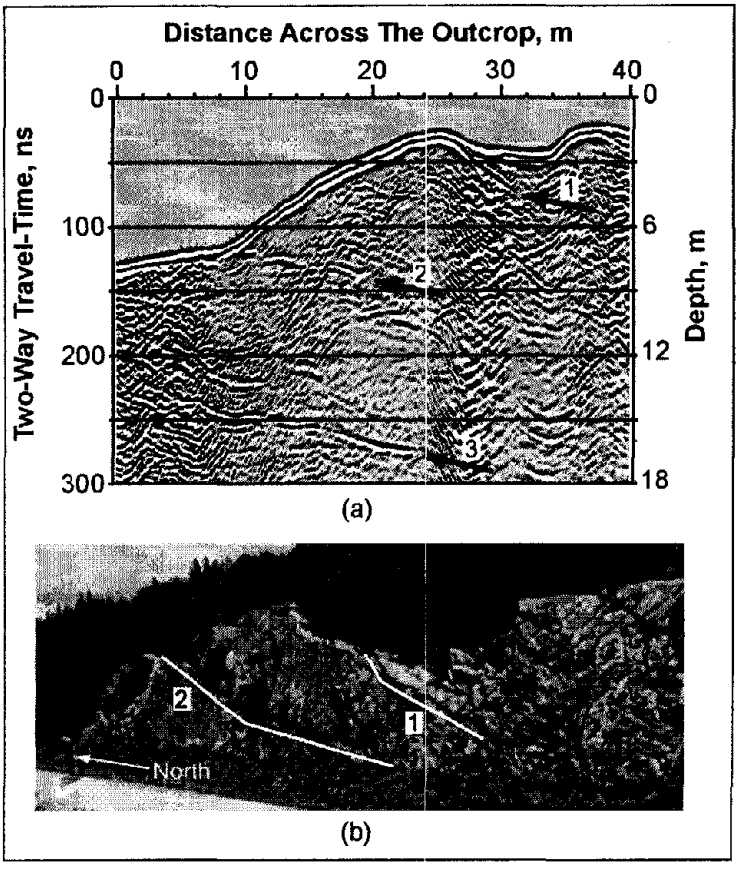

Figure 129. Ground Penetrating Radar data illustrating a section over a fracture zone. (Lane, 2000)

6.1.1.11 Rayleigh Waves Recorded with a Common Offset Array to Map Fractures

Basic Concept: This method uses Rayleigh waves (surface waves) to detect fracture zones. Rayleigh waves have a particle motion that is counterclockwise with respect to the direction of travel. Figure 130 illustrates the particle motion for Rayleigh waves traveling in the positive X direction. In addition, the particle displacement is greatest at the ground surface, near the Rayleigh wave source, and decreases with depth. Three shot points are shown, labeled A, B, and C. The particle motion and displacement are shown for five depths under each shot point. For shot B over the fracture zone, the amplitude of the Rayleigh waves is smaller than that for the other shots due to attenuation caused by the fractures. This affects the measured Rayleigh wave recorded by the geophones over the fracture zone. The effective depth of penetration is approximately one-third to one-half of the wavelength of the Rayleigh wave.

For interpretation, three parameters are usually observed. The first is an increase in the travel time of the Rayleigh wave as the fracture zone. The second parameter is a decrease in the amplitude of the Rayleigh wave. The third parameter is reverberations (sometimes called ringing) as the fracture zone is crossed. The data are recorded using a seismograph and geophone.

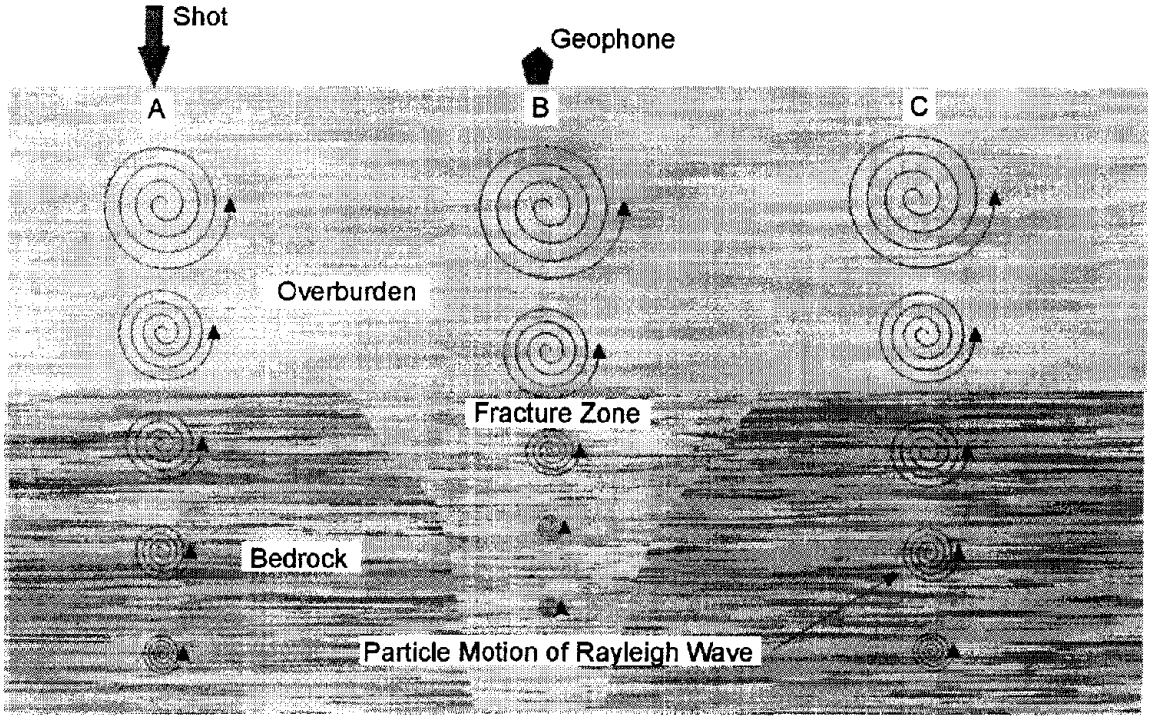

Figure 130. Rayleigh wave particle motion and displacement over a fracture zone.

Data Acquisition: Rayleigh waves are created by any impact source. For shallow investigations, a hammer is all that is needed. Data are recorded using one geophone and one shot point. The distance between the shot and geophone depends on the depth of investigation and is usually about twice the expected target depth. Data are recorded at regular intervals across the traverse while maintaining the same shot geophone separation. The interval between stations depends on the expected size of the fracture zone and the desired resolution. Generally, to clearly see the fracture zone, it is desirable to have at least several stations that cross this area. Figure 100 presents data from a common offset Rayleigh wave survey over a void/fracture zone in an alluvial basin. The geophone traces are drawn horizontally with the vertical axis being distance (shot stations).

Data Processing: The data may be filtered to highlight the Rayleigh wave frequencies and is then plotted as shown on figure 100. Spectral analysis can be performed on the individual traces and may show the lower frequencies over the fracture zone.

Data Interpretation: The data shown in figure 100 illustrates many of the features expected over a void/fracture. The travel time to the first arrival of the Rayleigh wave is greater across the void/fracture and is wider than the actual fractured zone. The amplitudes of the Rayleigh waves decrease as the zone is crossed. Since the records are not long enough, the ringing effect is not presented in these data.

Advantages: The field data recording is simple and efficient and requires much less effort for a given line length than seismic refraction.

Limitations: The method responds to the bulk seismic properties of the rocks and soil, which are influenced by factors other than voids. It has a limited depth of penetration and resolution. Penetration depth is limited by the wavelengths generated by the seismic source. However, this method is faster and less costly than most other seismic methods.

6.1.1.12 Seismic Refraction to Map Fractures

Basic Concept: The seismic refraction method can be used to locate fracture zones. Surveys for fracture zones are somewhat different from the more conventional application of the seismic refraction method described earlier, which is mapping bedrock topography. Bedrock fracture zones are recognized from the character of the first signal arrivals at the geophones, which can attenuate the signal and cause time shifts, as is illustrated in figure 131.

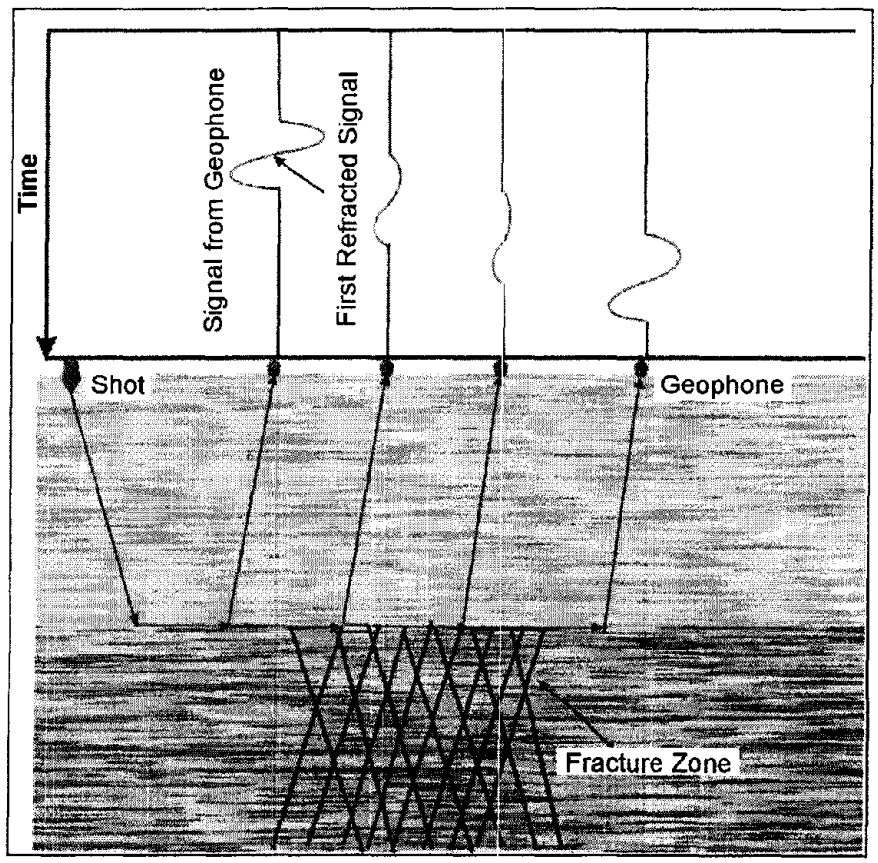

Figure 131. Seismic Refraction for locating fracture zones.

In addition to compressional wave surveys for fracture zones, shear waves can also be used. If a shear wave is oscillating at right angles to its direction of travel, it will be severely attenuated over a fracture zone. If, however, the shear wave is oscillating along the direction of travel, it will be relatively unaffected by the fracture zone.

For compressional wave surveys, surveys are conducted by traversing across the area of interest and evaluating the character of the first arrival waveform.

Data Acquisition: Data is recorded by placing a line of geophones across the area of interest and recording data from shots placed at the ends of the geophone spread.

Data Processing: No processing is usually required. The data is plotted so as to allow the character and amplitude of the first waves to arrive to be viewed.

Data Interpretation: The data is interpreted by viewing the first wave arrivals and looking for waves whose amplitude is diminished, indicating that a fracture zone has been crossed.

Advantages: Field recording for this method is quite fast and the data can usually be viewed on the recorder screen as the survey progresses.

Limitations: The velocity of the bedrock has to be greater than that of the overburden. If the water table is near the bedrock then this may also provide refractions. These refractions may interfere with refractions from the bedrock, or the bedrock refractions may not be visible.

6.1.1.13 Shear Wave Seismic Reflection to Map Fractures

Basic Concept: Fracture zones can be detected using seismic shear wave reflection surveys. These surveys are conducted in much the same manner as compressional wave seismic reflection surveys, except that a shear wave source has to be used. One such source is called the Microvib and is shown in figure 95. The data are recorded using a standard seismograph (figure 114b) using shear wave geophones.

Data Acquisition: Probably the most important difference between shear wave and compressional wave surveys is that, for shear wave surveys, the geophone spacing will be smaller for an equivalent depth of investigation, since the velocity of shear waves is only about 0.6 times that of compressional waves. The geophone spacing and spread length are also dependent on the expected depth and size of the fracture zone. Another important quantity to consider is the frequency and wavelength of the shear waves. Higher frequencies provide better resolution of the detected structures. However, higher frequencies also attenuate faster and therefore have less depth penetration.

Data Processing: Data processing is essentially the same as for reflection seismic surveys. Since the data are recorded in shot mode, the records are sorted to gathers with a common midpoint. Various kinds of filtering and other processes are then used to refine the data after which the traces for each gather are summed to produce a single trace whose signal-to-noise ratio is much greater than the unprocessed traces. Once this procedure has been done for all traces, a plot can be produced showing the seismic reflectors. Additional processing, such as migration, can also be applied to these data.

Data Interpretation: Data interpretation consists mostly of visual observation of the processed seismic records. Fracture zones produce scattering of the seismic energy, resulting in less energy being reflected back to the geophones on the ground surface. Areas where the amplitude of the bedrock reflector decreases or fades out will be of interest. In addition, an increase in travel time to the bedrock reflector may also occur. Figure 98 shows a shear wave seismic section, although in this case the target was voids. However, it does illustrate the presentation of the data.

Advantages: Providing the seismic source can produce high frequencies, the method can provide good resolution.

Limitations: As with compressional wave seismic reflection the method is quite labor intensive and can require significant data processing.

6.1.1.14 Resistivity Measurements to Map Fractures

Basic Concept: Resistivity measurements can also be used to locate fracture zones, since these areas often have a lower resistivity than unfractured bedrock. The method and instruments used are described earlier in this section and will not be described here.

Resistivity measurements can be taken with a simple four-electrode array or with the more sophisticated systems that use addressable electrodes, called Automated Resistivity systems. These systems provide an efficient method for measuring the lateral and vertical variations in resistivity and are the preferred system for locating fracture zones. Figure 201 shows the Sting/Swift instrument for taking these measurements.

Data Acquisition: With the automated resistivity system, the electrodes and wire connections are made before data recording begins. Once this is done, the data recording parameters and electrode array to be used are entered into the controller, which is then instructed to record the data. Since this system measures resistivity along the profile at a number of electrode spacings, it provides both lateral and vertical variations in resistivity. If long lines of data are recorded, the system is incrementally moved along the line as the survey progresses.

Fracture zones are also located using Azimuthal Resistivity measurements. With this method the electrode array is rotated about its center while taking resistivity readings. However, the method assumes that the bedrock surface is fairly flat and that no resistivity changes occur within the overburden.

Data Processing: The data is transferred from the field data recorder to a computer. Generally no processing is required and the data is loaded into interpretation software.

Data Interpretation: The data can be interpreted using computer software that provides a model whose calculated data fit the field data, thereby providing the variation of ground resistivity both laterally and vertically. A preliminary model is input by the interpreter, and the software then modifies this model until the resulting pseudosection matches that from the field data. The process of obtaining the model whose data fit the field data is called inversion.

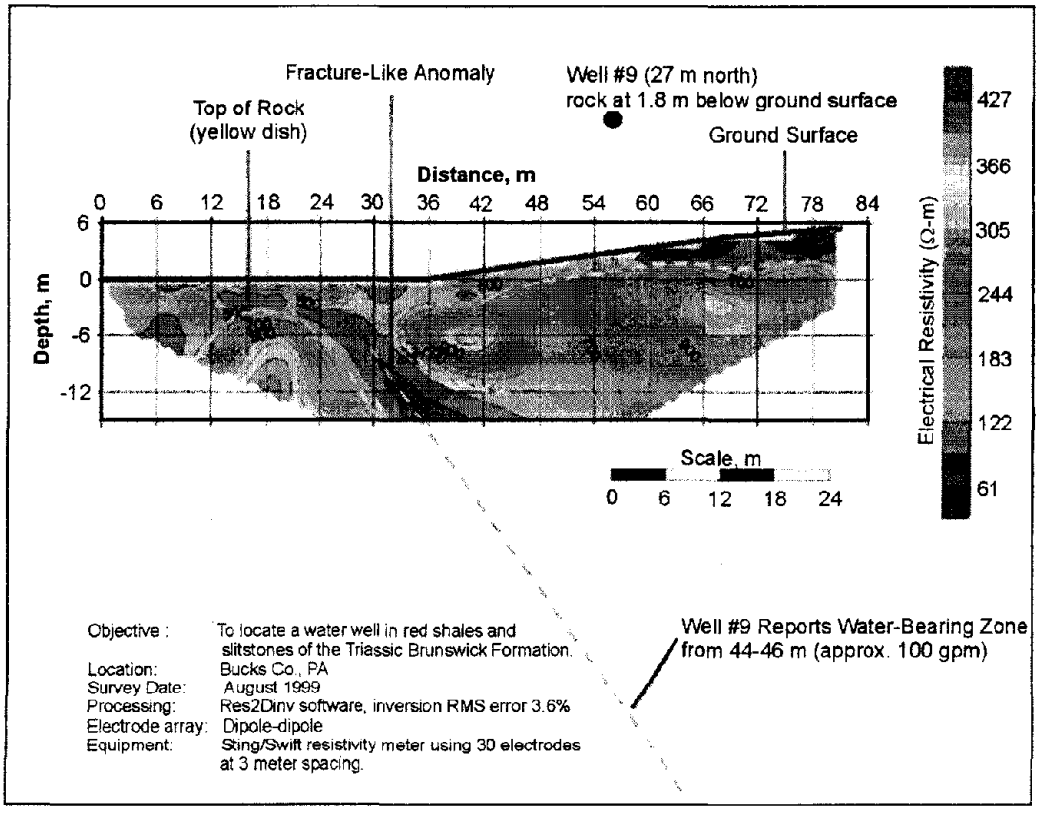

Figure 132. Resistivity measurements used for locating water-bearing fractures. (Quantum Geophysics, Inc.)

Figure 132 shows resistivity data obtained with the Sting/Swift resistivity system that has been inverted to provide a resistivity model showing a depth-versus-distance plot. As can be seen, the water-bearing fracture zone has a significantly lower resistivity than the host rocks.

Advantages: Compared to using a single electrode spacing to measure resistivity along a traverse the Automated Resistivity System provides much more data and allows for a much better interpretation.

Limitations: A resistivity contrast with the host rocks must exist at the fracture zone. Generally, because fracture zones have a higher porosity than unfractured rock, these areas will contain more moisture and have a lower resistivity then unfractured areas. Since electrodes have to be planted in the ground, areas with hard surfaces require more time to place these electrodes. Any grounded structure, e.g., metal fences, will influence the data if they are close to the electrode array. Likewise, buried metal features, e.g., pipes, will also create anomalies.

6.1.1.15 Geophysical Methods to Map Faults.

Since faults often do not often have clear ground or bedrock surface expressions, techniques used to map the locations of faults need to reach depths beyond the bedrock surface and, therefore, generally need to penetrate to depths greater than about 100 m.

For geophysical methods to be able to locate faults, there must, in general, be some difference in the physical properties of the rocks on either side of the fault. However, the seismic reflection method is able to map faults that do not have significant physical property differences on either side. This method provides detailed mapping of reflectors, and when a fault is present, the continuity of these reflectors is often disrupted. Figure 133 shows a seismic reflection section where faults are imaged.

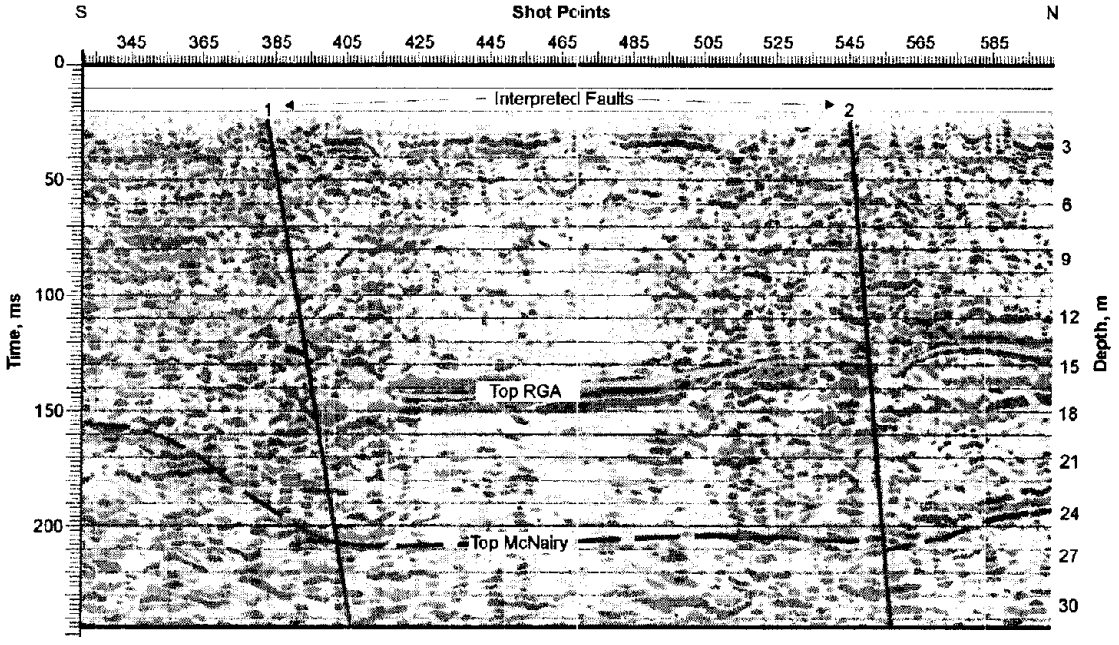

Figure 133. Seismic Reflection section showing faults.

If the fault has placed rocks having different densities next to each other, then the gravitational method may be useful.

A gravity profile across a faulted area will show higher values over more dense rocks and lower values over the rocks with lower densities. In addition to the rocks having different densities on either side of the fault, it is possible that they will also have different resistivities, in which case electrical soundings may be effective. Although resistivity soundings can be used, it is more likely that Time Domain Electromagnetic (TDEM) soundings will be conducted since the fieldwork for these soundings is more efficient than that for resistivity soundings. In addition, the TDEM method provides more depth penetration with less influence from lateral variations in resistivity.

6.1.2 Mapping Fractures and Identifying Weak Zones Within the Bedrock

Fractures in bedrock occur most often in competent rocks that are not able to adjust to the stresses placed upon them. Shales and clays are less likely to be fractured than harder rocks such as limestone and metamorphic rocks. Limestone may also develop solution cavities and fissures in addition to fractures. Since geophysical methods will rarely be able to detect individual fractures unless they are very large, regions of fracturing, called fracture zones, are

more likely to provide geophysical targets. Weak zones are regions or zones where the bedrock cannot tolerate significant compressive stress without deformation. They often have physical properties similar to those of fracture zones but may be more extensive. Weak zones may occur if the bedrock surface is a series of dipping layers with some layers being less competent than other layers. This may occur if one of the dipping layers is more prone to weathering than its host layers. Metamorphic rocks may exhibit weak zones due to differential weathering. In addition, shale or clay layers under a thin layer of more competent rocks may constitute a weak zone, as illustrated in figure 134a. In this case, stresses placed on the thin limestone layer may require more support from the deeper shale/clay layer than it can provide. Another example of a potential weak zone is presented in figure 134b.

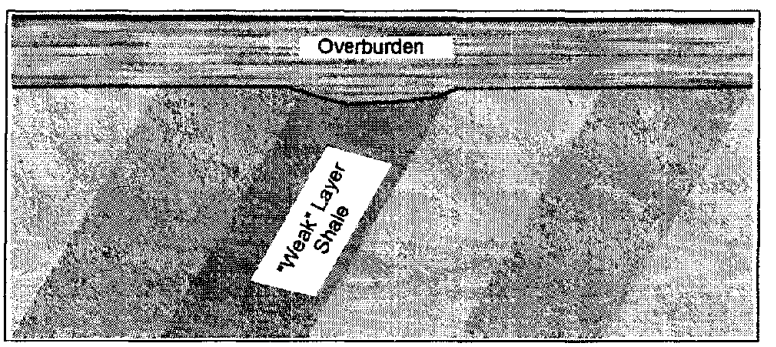

(a) Bedrock surface formed from a series of dipping layers.

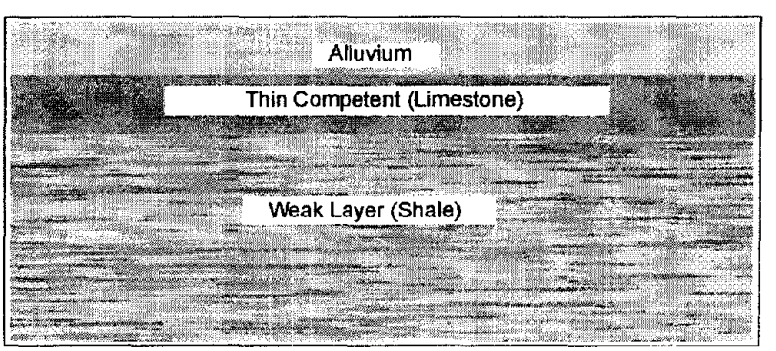

(b) Weak zone comprising a thin, competent limestone layer overlying a weak shale layer.

Figure 134. Two conceptual examples showing weak zones.

Geophysical methods are commonly used to find fractures in bedrock and can also be used to find weak zones. Generally, fracture zones are likely to contain more moisture than non-fractured bedrock, making them more electrically conductive, as well as having a lower seismic velocity. Fracture zones may provide the following physical parameter differences compared to the host rock:

1. Lower resistivity (higher conductivity).
2. Lower seismic velocity.
3. Bedrock topographic depressions due to fracturing and weathering.

In addition, the fracturing may cause scattering of seismic and Ground Penetrating Radar (GPR) waves. It is also possible that these areas will have lower densities that could theoretically produce gravity anomalies. However, many other interpretations of a gravity anomaly are possible and, because of this and the time-consuming nature of gravity surveys, these are not discussed further.

These parameters also generally apply to weak zones apart from the limestone/shale layering described above. In this case, the limestone will have a high resistivity and seismic velocity and the shale a low resistivity and seismic velocity. Mapping these layers requires the vertical distribution of resistivity, or velocity, rather than the horizontal distribution of these parameters as in the search for fracture zones. The methods used for detecting the limestone/shale layers will be described in the appropriate section below.

The physical parameters of weak zones that are useful for geophysical surveys are similar to those for locating fractures. In the case shown in figure 134a, these include a higher conductivity and a bedrock depression. However, depending on the complexity and thickness of the dipping layers, this weak zone may be more difficult to detect than fractures in horizontally layered bedrock. This is because the layering in the host bedrock may cause more varied physical parameters than those where the bedrock is horizontal and uniform. These variations may cause geophysical "noise" making it more difficult to observe the attributes of the weak zone.

There are many different geological conditions in which fractures and weak zones occur. The two weak zone cases and the fracture zone case are simple examples used to illustrate the application of geophysical methods. However, because of the complexity of geological conditions, for field surveys each case needs to be evaluated individually, and the appropriate geophysical method selected, since many factors influence the choice of geophysical method, or methods, to use.

The geophysical methods generally appropriate for locating fracture zones and weak zones are listed below.

1. Resistivity measurements (soundings and traverses).
2. Time Domain Electromagnetic Soundings.
3. Conductivity measurements.
4. Common offset surface (Rayleigh) waves.
5. Shear wave reflection surveys.
6. Seismic refraction surveys.

7. Ground Penetrating Radar surveys.

8. Very Low Frequency Electromagnetic surveys (VLF).

In the above list, resistivity and conductivity measurements are separated because they involve different instruments, and there are important differences in the application of the techniques.

Methods

Since all of these techniques, except VLF surveys, have been discussed in detail earlier in this section, only the important factors for locating fractures and weak zones will be discussed in this section.

6.1.2.1 Resistivity

Basic Concept: The resistivity method can be used to locate fracture zones and weak zones if they have a resistivity contrast with the host rocks. There are two common resistivity methods: soundings and traverses. Resistivity traverses are used to map changes in the bedrock and overburden resistivity. If the overburden resistivity does not change laterally, the method can be used to map variations in the elevation of the bedrock surface. Resistivity traverses are often done using only one electrode spacing and, therefore, do not provide the variation of resistivity with depth. Resistivity soundings provide the resistivities and depths of the layers under the sounding site. Lateral variations in resistivity, or conductivity, can be obtained much more efficiently using electromagnetic methods with instruments such as the EM31 and EM34. Hence, resistivity traverses using one electrode spacing are rarely used and will not be discussed further. However, automated resistivity systems are now available that record data from several different electrode spacings very efficiently, combining both traverse and sounding data.

These newer instruments, called automated resistivity systems, use electrodes that are addressable by a central control unit. This means that a large number of electrodes can be placed in the ground prior to starting the survey and connected to the central control unit. The data recording parameters and the electrode array to use are input to the central control unit. Once the electrodes are all connected, the measurements are automatically recorded by the central control unit. Resistivity soundings provide useful information and will be discussed in this section. Resistivity traverses have now largely been replaced by conductivity measurements, since these are much easier to acquire.

The resistivity of the ground is measured using a number of electrode arrangements, some of which are illustrated in figure 90. In all of these arrays, current is injected into the ground using two electrodes and the resulting voltage is measured using the remaining two electrodes.

The electrode arrays are used for different types of resistivity surveys. The Schlumberger array is often used for resistivity soundings, as is the Wenner array. The Pole-pole array provides the best signal, but is cumbersome because of the long wires required for the remote electrodes and is rarely used. The Dipole-dipole array was originally used mostly by the mining industry for

induced polarization surveys. Readings were taken using several different separations of the voltage and current dipoles providing measurements of the variation of resistivity with depth. Long lines of data were recorded requiring many readings. This array has now become common for resistivity surveys using the automated resistivity systems. If more signal (voltage) is needed than can be provided with the Dipole-dipole array, the Pole-dipole array can be used.

Resistivity Soundings

Figure 91 shows one of these electrode arrangements, called the Schlumberger array, and illustrates its use for obtaining a resistivity sounding.

Data Acquisition: In figure 91a, current is passed into the ground using the two electrodes labeled A and B. The voltage that results from this current is then measured using electrodes M and N. Using the amount of current passed into the ground along with the voltage and a geometric factor for the electrode layout, the resistivity of the ground is calculated. The electrode array is then expanded, making the current penetrate deeper into the ground, and another reading is taken. This procedure is repeated for many electrode spacings providing a set of resistivity values for each of these spacings. These values are plotted on a graph of resistivity against electrode spacing, as illustrated in figure 91b. This graph shows that, at small electrode spacings, the measured resistivity approaches that of the overburden, whereas at large electrode spacings, the measured resistivity approaches that of the bedrock. The resistivity curve is interpreted using software that provides a resistivity model (depths and resistivities) whose resistivity calculations match the field data.

Resistivity soundings are used to measure the vertical distribution of resistivity in the ground, and hence can be used to map the existence of a conductive shale layer that may occur beneath a more competent layer. Resistivity sounds alone are probably not a useful method for locating fractures. When conducting the survey, it is advisable to plot the measured resistivity versus electrode spacing in the field to ascertain that the deeper layers of interest have been observed.

Data Processing: Usually little processing is needed although bad data points may be removed.

Data Interpretation: Resistivity data are interpreted using software that calculates the sounding curve from a resistivity model. The interpreter inputs a preliminary model, and the computer calculates the sounding curve from this model and evaluates the fit of this model data to the field data. It then changes the model to provide an improved fit and recalculates the resistivity curve. The process, called inversion, is repeated until the curve from the model matches that from the field data.

Advantages: Resistivity soundings are probably more useful than seismic refraction method for locating weak zones, since weak zones are likely to have a lower velocity than the overlaying rocks and seismic refraction will not see the top of the lower velocity layer.

Limitations: Since electrodes have to be planted in the ground, this can be a problem is dry or rocky areas. In such conditions, water may need to be poured onto the electrodes in order to lower the resistance between the electrode and the ground.

Automated Resistivity Systems

Data Acquisition: As mentioned previously, newer resistivity systems are now available that make taking resistivity measurements much more efficient, and by taking many measurements at different electrode spacings along a traverse, these systems are able to build a comprehensive picture of the subsurface, combining both lateral and vertical variations in resistivity. Figure 201 shows the Sting/Swift automated resistivity measuring system. To take resistivity measurements, the electrodes along a traverse are inserted into the ground and connected to the wires leading the controller. The controller is programmed with the desired electrode array to use along with other factors and then instructed to take the measurements.

Data Processing: Usually little processing is applied to the data, apart from removing any bad data points.

Data Interpretation: Data from these systems are interpreted by using software that calculates the theoretical resistivity data from a resistivity/depth model, thus enabling a model to be developed that produces data that matches the field data, a process called inversion. However, much information can be gained visually. An example of the results from such a survey is presented in figure 135. These data show two low-resistivity zones, one of which was shown to be a water- filled fracture zone. The data have been inverted showing the resistivity variation, both laterally and vertically, against depth.

Fracture zones can also be located using a method called Azimuthal Resistivity surveys. In this method, resistivity is measured using an appropriate electrode array and spacing, say the Schlumberger array. The array is then rotated about its center a few degrees, and another reading taken. This process is repeated until readings have been taken as the array rotates through 360 degrees. Variations in resistivity as the array rotates are used to locate fracture zones. However, the method assumes that the bedrock surface is fairly flat, and that there are no resistivity changes in the overburden. Many azimuthal soundings will be required to adequately cover an area. Data recorded with the automated resistivity system probably provide data that offer a better interpretation, and the system is probably more efficient.

Advantages: Using the Automated Resistivity systems, fairly comprehensive data sets can be efficiently recorded and interpreted. Provided the geology is appropriate these systems can be used to locate fractures and weak zones.

Limitations: Three different methods (traverses, soundings, and automated resistivity systems) of using the resistivity method have been discussed above. All of them require electrodes be placed in the ground; thus, the method is difficult to use in areas where the surface of the ground is hard, such as concrete or asphalt-covered areas. In addition, if the ground is dry, water may need to be poured onto the electrodes to improve the electrical contact between the electrode and the ground.

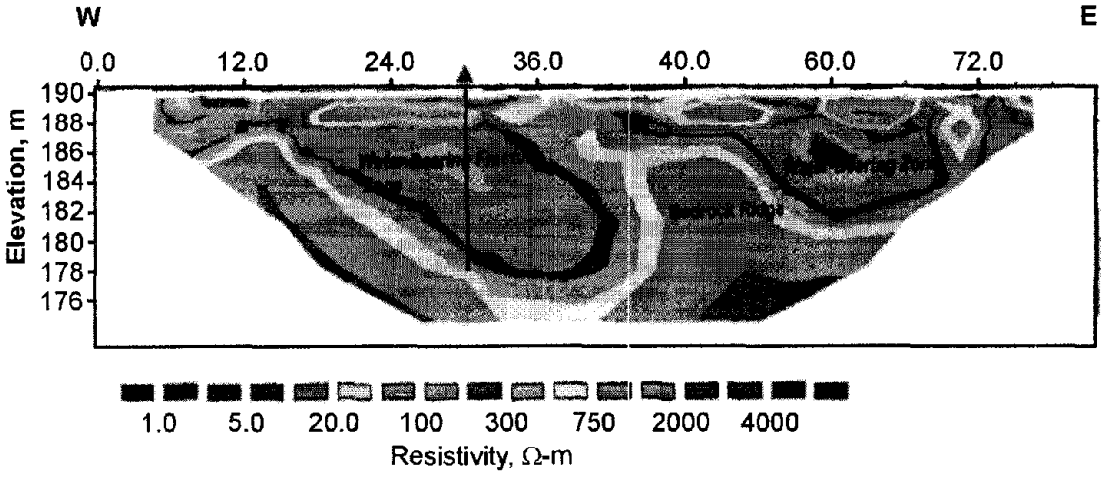

Figure 135. Resistivity data over a fracture zone. (Advanced Geosciences, Inc.)

Resistivity soundings are a useful tool and can provide the resistivities and depths of layers under the sounding site. However, the interpretation assumes horizontal layers with no lateral variations in resistivity. If this is not the case, the interpretation will be incorrect. Generally, with the Schlumberger array, the separation between the current electrodes will need to reach a maximum of about three times the investigation depth. If the bedrock is 15 m deep, the current electrodes will need to be spaced up to 45 m apart.

Clearly, the automated resistivity system provides the best interpretation, although it also requires the most effort. With this system, lateral variations in resistivity are recognized and resolved in the inversion process. Since the data are recorded along a line, the interpretation necessarily assumes that there are no variations in ground resistivity normal to the line, which is probably not true. Thus, errors in the interpretation will occur, depending on the resistivity variations normal to the survey line. This problem can be minimized by conducting parallel traverses or by conducting three-dimensional surveys.

6.1.2.2 Time Domain Electromagnetic Soundings

Basic Concept: Time Domain Electromagnetic soundings (TDEM) are used to obtain the vertical distribution of resistivity. This method is particularly well suited to mapping conductive layers. To a significant degree, this method has now superseded the resistivity sounding method since it requires less work for a given investigation depth and generally provides more precise depth estimates. However, resistivity soundings are still useful for shallow investigations or when resistive targets are sought.

TDEM soundings are an electromagnetic method used to provide the vertical distribution of resistivity within the ground. A square loop of wire is laid on the ground surface. The side length of this loop is about half of the desired depth of investigation. A receiver coil is placed in the center of the transmitter loop. Electrical current is passed through the transmitter loop and then quickly turned off. This sudden change in the transmitter current causes secondary currents to be generated in the ground. These decaying currents have associated decaying electromagnetic fields that produce a voltage in the receiver coil on the

ground surface. The TDEM field layout, transmitter current, and received voltage are illustrated in figure 120.

The currents in a conductive layer decay at a slower rate than those in a resistive layer. The relationship between the time after the current has turned off (delay time) and the depth and resistivity of the layers is complex, although longer delay times generally correspond to greater depths.

The voltage measured by the receiver coil does not decay instantly to zero when the current is turned off, but continues to decay for some time. This decaying voltage is caused by the decaying secondary electrical currents and the associated electromagnetic fields in the ground. The voltage measured by the receiver is then converted to resistivity. A plot is made of the measured resistivity against the delay time, as illustrated in figure 121.

The resistivity sounding curve illustrates the curve that would be obtained over three-layered ground. The near-surface layer has a higher resistivity than the middle layer. The final layer again has a higher resistivity. Figure 121 illustrates the type of curve expected over a resistive, competent limestone resting on a less competent shale.

The Protem receiver and transmitter, which are used to record TDEM data, are manufactured by Geonics Ltd of Canada and are illustrated in figure 136.

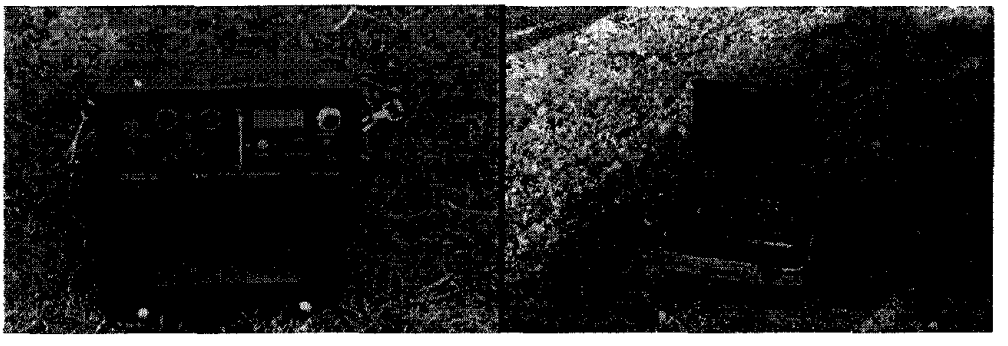

(a) **(b)**

Figure 136. Protem transmitter and receiver for Time Domain Electromagnetic sounding measurements: (a) Protem transmitter, and (b) Protem receiver. (Geonics, Ltd.)

Data Acquisition: The field layout of the system for TDEM soundings is described above and is shown in figure 120. Switched current is passed through the transmitter loop and the resulting voltage is measured by the receiver coil. The switching and measuring procedure is repeated many times allowing the resulting voltages to be stacked and improving the signal-to-noise ratio. Soundings are conducted at different locations until the area of interest has been covered. A sounding curve is plotted for each location showing the measured resistivity against delay time.

Data Processing: The only processing required is the possible removal of bad data points.

Data Interpretation: The sounding curves are interpreted using computer software that modifies a preliminary model input by the interpreter until the data from this model match that from the field. This process is called inversion.

Advantages: The TDEM method does not require electrodes to be inserted into the ground, as is the case with the resistivity method, and hence is an efficient method for obtaining resistivity soundings.

Limitations: Metal objects in the vicinity of the sounding site will create electromagnetic fields that will be detected by the receiver coil. This will distort the data from the ground and may produce data that are not interpretable. In addition, the interpretation assumes that the geologic layers are horizontal and have resistivities that do not change laterally. If this is not the case, the interpreted resistivities and depths may be incorrect.

6.1.2.3 Conductivity Measurements

Basic Concept: Conductivity methods can be used to map the lateral variations in bedrock conductivity (or its inverse, resistivity). Both the EM31 and EM34 can be used to record conductivity. They are designed to operate at particular frequencies and with defined transmitter and receiver coil separations such that the out-of-phase component of the received signal can be converted to apparent conductivity. These instruments use a transmitter and receiver coil, which are coplanar. Sinusoidal current, oscillating up to about 10 kHz (depending on the instrument) is passed through the transmitter coil, generating a sinusoidal electromagnetic field. This field then generates secondary sinusoidal currents in the ground, which, in turn, produce secondary electromagnetic fields that the receiver coil detects. Conductivity measurements can be recorded with the plane of the coils either parallel to the ground surface (vertical dipole mode) or orthogonal to the ground surface (horizontal dipole mode). The anomaly measured in the vertical dipole mode over a vertical, or sub-vertical conductive feature is quite distinctive and is diagnostic of that feature. Figure 128 shows the anomaly over a conductive feature (fracture zone) using an EM31 or EM34 in vertical dipole mode. In the horizontal dipole mode, only a weak anomaly would be observed, and this mode is not recommended for locating vertical conductive features.

As the conductive feature is approached, the measured conductivity increases. When the transmitter and receiver coils straddle the conductive zone, the measured conductivity values decrease, reaching a minimum when they are equispaced about the conductive zone. This distinctive anomaly shape provides a good method for locating conductive fractures. However, this method does not provide the depth to the bedrock, and a resistivity sounding will need to be done if this is required.

Figure 183 shows the EM31 being used in the vertical dipole mode, and figure 197 shows the EM34 being used in the horizontal dipole mode.

Since, with the EM34, a cable connects the transmitter and receiver coils, their separation can be changed, thereby altering the depth of investigation. Three separations are available, 10, 20, and 40 m, providing investigation depths in the vertical dipole mode of 15, 30and 60 m.

Data Acquisition: Conductivity measurements are taken along traverses crossing the area of interest. Probably the most important decision is the particular electromagnetic system to use, since this determines the depth of investigation. The EM31 has its coils mounted in a rigid boom, and its depth of investigation in the vertical dipole mode is about 6 m. However, the EM34, as discussed above, has three discrete depths of investigation in the vertical dipole mode.

The EM31 can record data either in timed mode, i.e., every second, or when a button is pressed on the instrument (discrete mode). In timed mode, readings are taken while walking at a moderate speed. With the EM34, readings are taken while the instrument is stationary. Both the EM31 and EM34 require the station spacing be sufficient to accurately portray the shape of the resistivity curve over a conductive feature. This generally means that the station spacing should be one-fourth to one-third of the coil spacing.

Data Processing: The data are usually plotted as conductivity values against distance, and usually no processing is required.

Data Interpretation: Interpretation is mostly visual, searching for the distinctive pattern shown in figure 128.

Advantages: Surveys with the EM31 and EM34 are generally efficient and large areas can be covered much more rapidly than with other methods, including resistivity systems.

Limitations: The EM31 provides a rapid method of measuring the ground conductivity, but only to a depth of about 6 m. The EM34 provides a much greater depth of investigation, but requires two people to operate and only takes discrete measurements. However, in spite of these limitations, the method still provides one of the most cost-effective methods of measuring the ground conductivity. Neither method provides much information regarding the depth of investigation, beyond the general depths estimated for the coil separations.

These instruments (EM31 and EM34) are also influenced by both buried and aboveground metal; thus, data collected near fences and other metal objects cannot be reliably interpreted.

6.1.2.4 Rayleigh Waves Recorded with a Common Offset Array

Basic Concept: This method uses Rayleigh waves (surface waves) to detect fracture zones. Rayleigh waves have a particle motion that is counterclockwise with respect to the direction of travel. Figure 99 illustrates the particle motion for Rayleigh waves traveling in the positive X direction. In addition, the particle displacement is greatest at the ground surface near the Rayleigh wave source and decreases with depth. The effective depth of penetration is approximately one-third to one-half of the wavelength of the Rayleigh wave.

Three shot points are shown in figure 99, labeled A, B, and C. The particle motion and displacement are shown for five depths under each shot point. For shot B, over the fracture zone, the amplitude of the Rayleigh waves is smaller than that for the other shots due to attenuation caused by the fractures and affects the measured Rayleigh waves recorded by the geophones over the fracture zone. Three parameters are usually observed. The first is an increase in the travel time of the Rayleigh waves at the fracture zone. The second is a

decrease in the amplitude of the Rayleigh waves. The third parameter is reverberations (sometimes called ringing) as the fracture zone is crossed. Rayleigh wave data are recorded using a standard seismograph and geophone system.

Data Acquisition: Rayleigh waves are created by any impact source. For shallow investigations, a hammer is all that is needed. Data are recorded at regular intervals along a traverse using one geophone and one shot point for each measurement, with the shot geophone distance remaining constant. The distance between the shot and geophone depends on the depth of investigation and is usually about twice the expected target depth. The interval between stations depends on the expected size of the fracture zone and the desired resolution. Generally, in order to clearly see the fracture zone, it is desirable to have at least several stations that cross this area. Data from a common offset Rayleigh wave survey over a void/fracture zone in an alluvial basin is presented in figure 100. The geophone traces are drawn horizontally with the vertical axis being distance (shot stations).

Data Processing: The data may be filtered to highlight the Rayleigh wave frequencies and are then plotted as shown on figure 100. Spectral analysis of the individual traces can be performed that may show the lower frequencies over the fracture zone.

Data Interpretation: The data shown in figure 100 illustrate many of the features expected over a void/fracture. The travel time to the first arrival of the Rayleigh waves is greater across the void/fracture and, in this case, is wider than the actual fractured zone. The amplitudes of the Rayleigh waves decrease as the zone is crossed. Since the records are not long enough, the ringing effect is not presented in this data.

Advantages: The field data recording is simple and efficient and requires much less effort for a given line length than seismic refraction.

Limitations: The method responds to the bulk seismic properties of the rocks and soil, which are influenced by other factors other than voids. It has a limited depth of penetration and resolution. Penetration depth is limited by the wavelengths generated by the seismic source. However, this method is faster and less costly than most other seismic methods.

6.1.2.5 Shear Wave Seismic Reflection

Basic Concept: Fracture zones can be detected using seismic shear wave reflection surveys. These surveys are conducted in much the same manner as compressional wave seismic reflection surveys, except that a shear wave source has to be used. One such source is called the Microvib shown in figure 95. The Microvib produces a shear wave vibration rather than an impact as with a hammer blow. Larger, truck-mounted shear wave sources are also available, one of which is called the Minivib. The Microvib is used for depths to about 100 m. Although impulse shear wave sources could be used, they have significant disadvantages compared to the Microvib source, including much lower frequencies. Shear wave impulse sources also simultaneously create some compressional waves (P-waves), which "contaminate" the shear wave data. Creating shear waves with an impulse source is much more time consuming than using the Microvib source.

Data Acquisition: Shear wave reflection surveys using the Microvib source are conducted much the same way as compressional wave reflection surveys using a vibroseis source. Probably the most important difference is that the geophone spacing will be smaller for an equivalent depth of investigation, since the velocity of shear waves is only about 0.6 times that of compressional waves. The geophone spacing and spread length are also dependent on the expected depth and size of the fracture zone. Another important quantity to consider is the frequency and wavelength of the shear waves. The higher the frequency, the better the resolution of detected structures. However, higher frequencies also attenuate faster and have less depth penetration.

Data Processing: The first process to be applied to shear wave data makes the data equivalent to that from an impulse source. Once this is done, standard seismic reflection processing techniques are applied. The records are sorted to gathers with a common mid-point, and various kinds of filtering and other processes are then used to refine the data. The traces for each gather are then summed to produce a single trace whose signal-to-noise ratio is much greater than the unprocessed traces. Once this procedure has been done for all of the traces, a plot is made showing the seismic traces plotted vertically against distance, called a seismic section. This plot shows the reflectors and other features imaged. Additional processing, such as migration, can also be applied to these data.

An example seismic section is shown in figure 137 showing interpreted faults. The vertical axis is time, and the horizontal axis is distance.

Data Interpretation: Data interpretation consists mostly of visual observation of the processed seismic records. Fracture zones produce scattering of the seismic energy, resulting in less energy being reflected back to the geophones on the ground surface. Areas where the amplitude of the bedrock reflector decreases or fades out will be of interest. In addition, an increase in travel time to the bedrock reflector may also occur.

The seismic reflection method can also be used to image the vertical succession of layers, such as the weak zone produced by the shale layer in figure 134b. Conventional data recording and processing techniques would be used, producing a seismic section showing the stratigraphy. The shale, if thick enough, would be recognized by its lower velocity. If more confirmation of the shale were required, a resistivity or TDEM sounding could be conducted. If both a low velocity and a high conductivity were obtained for the particular horizon, the chances of it being a shale layer would be substantially increased.

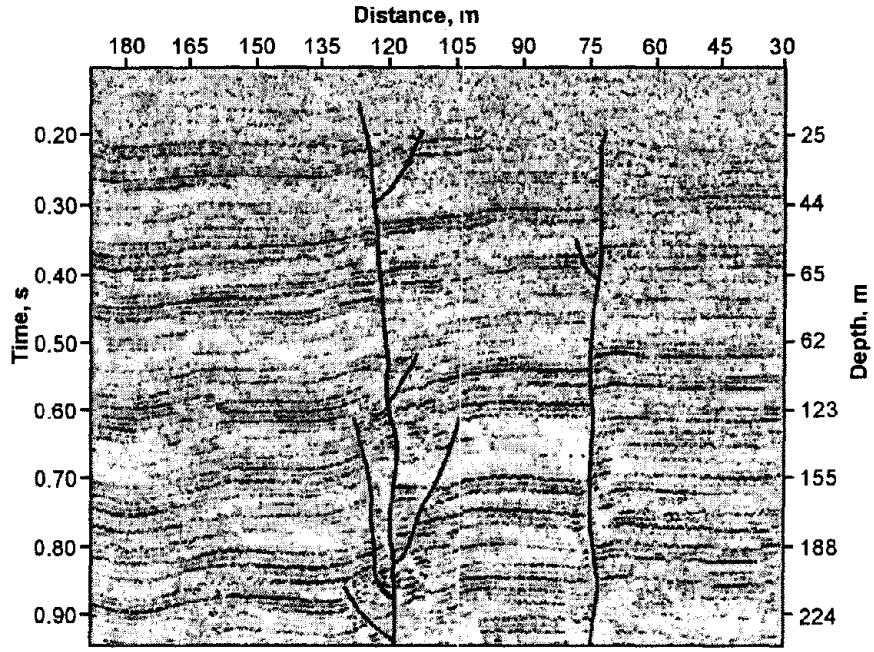

Figure 137. Example seismic section showing interpreted faults. (Bay Geophysical)

Advantages: The reflection seismic method generally proved the best resolution (except GPR) for structural information

Limitations: The seismic reflection method is quite labor intensive, and significant data processing is required. This is one of the more expensive geophysical methods. In addition, any local vibration source, including industrial areas and road traffic, may produce noisy data.

6.1.2.6 Seismic Refraction

Basic Concept: The seismic refraction method can be used to locate fractures and weak zones. The method requires a seismic energy source, usually a hammer for depths less than 15 m and black powder charges for depths to 30 m. The seismic waves then penetrate the overburden and refract along the bedrock surface. While they are traveling along this surface, they continually radiate seismic waves back to the ground surface. These are then detected by geophones placed on the ground surface. Both compressional waves and shear waves can be used in the seismic refraction method, although compressional waves are most commonly used. Figure 114a shows the layout of the instrument, the main seismic waves involved, and the resulting time-distance graph.

Surveys for fracture zones are somewhat different from the more conventional application of the seismic refraction method, which is mapping bedrock topography, as illustrated in figure 114. Bedrock fracture zones are recognized from the character of the first signal arrivals at the geophones. Fracture zones attenuate the signal and can cause time shifts as illustrated in figure 94. In this case, the amplitudes of the traces from geophones 2 and 3 are attenuated.

In addition to compressional wave surveys for fracture detection, shear wave surveys can also be used. If a shear wave is oscillating at right angles to its direction of travel, then its amplitude will be severely attenuated as it passes a fracture or fracture zone. However, if the shear wave is oscillating in the direction of travel, then the fracture zone has little effect.

Data Acquisition: The design of a compressional wave seismic refraction survey requires a good understanding of the expected bedrock and overburden. With this knowledge, velocities can be assigned to these features and a pre survey model developed that will show the parameters of the seismic spread best suited for a successful survey. These parameters include the length of the geophone spread, the spacing between the geophones, and the expected first break arrival times at each of the geophones. Knowing the expected first break arrival times is also helpful in the field, where field arrival times that correspond fairly well to expected times help to confirm that the spread layout has been appropriately planned, and that the target layer (bedrock) is being imaged. Surveys will be conducted by recording contiguous seismic spreads along traverses crossing the area of interest.

Data Processing: In order to interpret seismic refraction data for depths, the first arrival times of the refracted rays have to be picked. Once this is done these times are then input to interpretation software. If the data is to be used for locating fracture zones then it has to be plotted in order for the amplitudes of the first arrivals to be compared.

Data Interpretation: Interpretation of seismic refraction data for fracture or weak zones is mostly visual. The geophone traces have to be plotted for each seismic spread and viewed for areas of amplitude attenuation and possibly an increase in the time to the first arrival if the fracture zone is accompanied by a bedrock depression. The seismic refraction method could not be used to image the shale layer underlying the limestone illustrated in figure 134b. This is because the shale will probably have a lower velocity than the limestone and will not produce refractions, and would not, therefore, be observed by a seismic refraction survey.

Advantages: The seismic refraction method, using amplitude changes to locate fractures, usually provides good resolution for any observed fractures.

Limitations: It is clearly important that the seismic waves refract from the bedrock layer of interest. Usually this will be easily recognized. However, if refracting layers lie above the bedrock surface, these must be recognized. If the local geology is known from previous surveys or drill holes, a pre survey model will assist in identifying the travel times at which a seismic arrival from the bedrock is expected. If this is not known, a conventional seismic spread, as shown in figure 114a, should be applied and interpreted.

If the water table is in the overburden and close to the bedrock, this may obscure the bedrock arrivals, since saturated soils have a higher velocity than unsaturated soils. In some cases, water above the bedrock may remove the velocity contrast between the saturated overburden and the bedrock.

Local noise, for example traffic, may obscure the refractions from the bedrock. This can be overcome by using larger impact sources or by repeating the impact at a common shot point several times and stacking the received signals. If noise is still a problem, a larger energy

source may be required. In addition, since some of the noise travels as airwaves, covering the geophones with sound absorbing material may also help to dampen the received noise.

6.1.2.7 Ground Penetrating Radar

Basic Concept: Ground Penetrating Radar (GPR) can be used provided the conditions are appropriate for the method. For the method to work, the bedrock and fracture or weak zone must provide a contrast in dielectric properties from those of the overburden. Ideal conditions for this method are a dry sandy overburden. If clay occurs in the overburden, or if it is saturated, penetration may be limited. However, in ideal conditions, the method may penetrate to depths of 15 m.

The GPR instrument consists of a recorder and a transmitting and receiving antenna. Different antennae provide different frequencies. Lower frequencies provide greater depth penetration but lower resolution. Figure 111 provides a drawing illustrating the GPR system. The transmitter provides the high-frequency electromagnetic signals that penetrate the ground and are reflected from objects and boundaries providing a different dielectric constant from that of the overburden. The reflected waves are detected by the receiver and stored in memory.

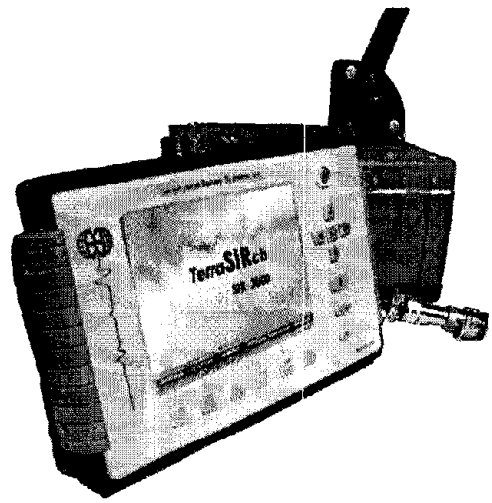

Figure 138. Ground Penetrating Radar equipment. (Geophysical Survey Systems, Inc.)

Figure 138 shows the data recording and system control for a GPR instrument. Any antenna supported by this instrument can be attached and used to collect data. Figure 139 shows a 250 MHz antenna being used in a field survey.

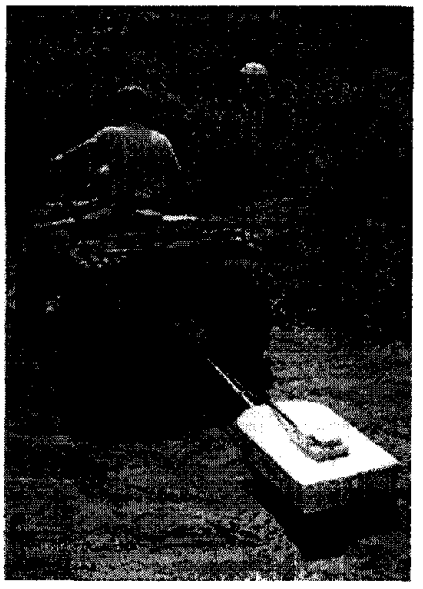

Figure 139. A 250 MHz antenna being used in a field survey. (MALA GeoSciences, Inc.)

Data Acquisition: GPR surveys are conducted by pulling the antenna across the ground surface at a normal walking pace. The recorder stores the data, as well as presenting a picture of the recorded data on a screen.

Data Processing: It is possible to process the data, much like the processing done on single-channel reflection seismic data. Techniques that can be applied include distance normalization, horizontal scaling (stacking), horizontal and vertical filtering, velocity corrections, and migration. However, depending on the data quality, this may not be necessary since the field records may be all that is needed to observe the fracture zone.

Data Interpretation: Interpretation of GPR data for fractures may involve searching for reflectors if the fractures are sub-horizontal to zones where the signal coherence is lost due to scattering of the waves caused by fracture zones. In addition, if the fracture zone is saturated, this may attenuate the GPR signal, causing decreased amplitudes over this zone.

To calculate the depth to the feature of interest, the speed of the GPR signal in the soil at the site needs to be obtained. This can be estimated from charts showing speeds for typical soil types, or it can be obtained in the field by conducting a small traverse across a buried feature whose depth is known.

Figure 129 presents a GPR profile over a fracture zone. In this case, the bedrock is quite shallow, and the fractures can be seen in a local roadcut. However, it does show the potential of the method if conditions are appropriate. In this case the fracture zone is sub-horizontal and is recognized as a reflector.

Advantages: The method is fairly rapid in the field and since the data is displayed in real time, fractures may be observed when the data is recorded. This may allow parallel lines to be surveyed in order to map the extent of the fracture.

Limitations: Probably the most limiting factor for GPR surveys is that their success is very site specific and depends on having a contrast in the dielectric properties of the target compared to the host overburden, along with sufficient depth penetration to reach the target. However, it is likely in many cases that the bedrock will provide a dielectric contrast with the overburden, making depth of penetration probably the most important factor.

6.1.2.8 Very Low Frequency Electromagnetic Surveys

Basic Concept: The Very Low Frequency (VLF) method is an electromagnetic technique that uses powerful military transmitters producing electromagnetic fields with frequencies between 15 and 30 kHz. The VLF method can be used to locate saturated (conductive) sub-vertical zones in which the primary field induces current flow. The field radiated from a VLF transmitter over a uniform or horizontally layered ground consists of a vertical electrical field component and a horizontal magnetic field component, each perpendicular to the direction of propagation. Because the source of the field is usually many kilometers from the survey area, the EM wave approximates a plane wave.

VLF is often used in two modes measuring tilt angle and resistivity. For tilt angle measurements, magnetic field coupling with the fracture zone is important. Therefore, the VLF transmitter should be located along the strike of the target. The depth of investigation depends on the frequency used and the resistivity of the host medium. It can vary from a few meters to over 100 m.

Measuring resistivity with the VLF equipment requires measuring the electric field with two electrodes connected to the control unit with a wire. For resistivity measurements, the electrical field coupling with the fracture zone is important. Therefore, the VLF transmitter should be located in a direction perpendicular to the target.

A VLF instrument is shown in figure 140. This instrument can also provide its own electromagnetic field source.

Data Acquisition: As mentioned above, it is preferable to have the transmitter located along strike when measuring tilt angles and perpendicular to strike when measuring resistivity. Measurements are made while traversing across the feature or area of interest. A conductive feature produces an anomaly similar to that shown in figure 141.

The data are plotted as a graph of magnetic field component against distance, similar to that shown in figure 141.

Data Processing: Usually minimal processing is done to the data, although various spatial filters can be applied to remove noise.

Data Interpretation: Interpretation is mostly visual searching for anomalies.

The conductive feature shown in figure 141 produces a tilt angle anomaly that looks similar to a sinusoid. The top of the fracture is centered at the inflection point of the anomaly.

Figure 140. Very Low Frequency instrument. (Geonics Ltd.)

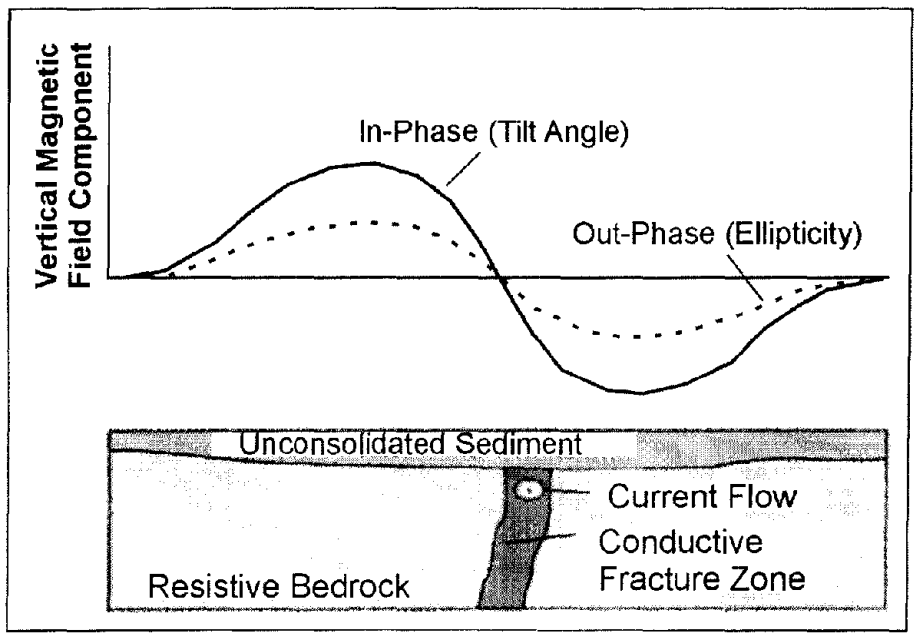

Figure 141. Very Low Frequency anomaly over a vertical conductor.

Advantages: The main advantage of the VLF method is that it is a rapid and inexpensive method.

Limitations: The VLF method is somewhat restrictive if the military VLF transmitters are to be used in that it works best for specific orientations of the fracture relative to the transmitter location, as discussed above. In addition, sometimes the VLF transmitter station desired is not broadcasting and cannot be used.

Exploration depths will be limited if the ground is electrically conductive. In addition, anomalies can be created by other geologic conditions unrelated to fractures such as changes in overburden thickness or conductivity.

Generally, methods using active sources (EM31, EM34) are preferred to the VLF method since these have no target orientation restrictions. Because these are active methods, they do not rely on other transmitters to produce the required electromagnetic field.

6.1.2.9 Borehole Televiewers (Optical & Acoustic)

Optical and acoustic televiewers are used for imaging stratigraphic and concrete features and for measuring fracture orientation and distribution (figure 142). Images are based on direct optical mapping or on the amplitude and travel time of an ultrasonic beam, reflected from the borehole wall. From televiewer imaging, fractures and bedding planes can be mapped over the length of the borehole. These planar features can be tabulated, analyzed, and expressed statistically in order to identify subsurface fracture zones, weak zones, and zones of subsurface flow.

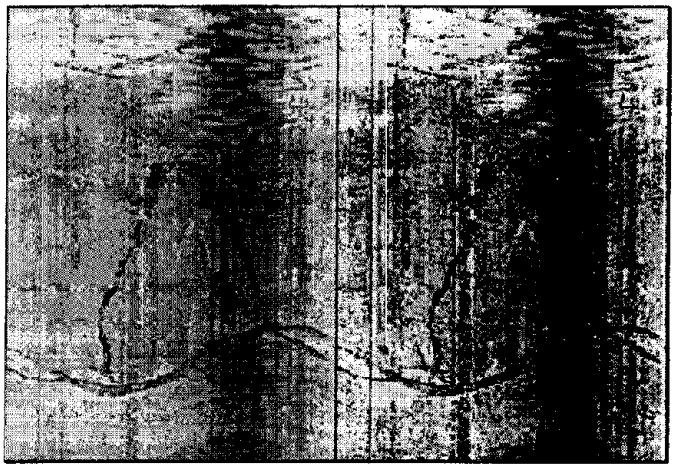

Figure 142. Examples of typical borehole images, optical and acoustic. (Layne Christensen, Colog)

Basic Concept: Televiewer probes provide images of the inside of boreholes by capturing a layer of several samples around the circumference of the hole and stacking the layers to reproduce a full, in-situ, oriented image of the borehole wall.

A televiewer log can be thought of as a cylinder that is opened along the north side. Planer features that intersect the borehole appear to be sinusoids on the unwrapped image (figure 143). Calculation of the dip direction and dip angle of a fracture requires the vertical intercept **h** and the direction of the dip from the televiewer log, and the diameter **d** of the

borehole from the caliper log or known bore diameter. The angle of dip is equal to the arc tangent of **h/d**, and the dip direction is picked at the trough of the sinusoid.

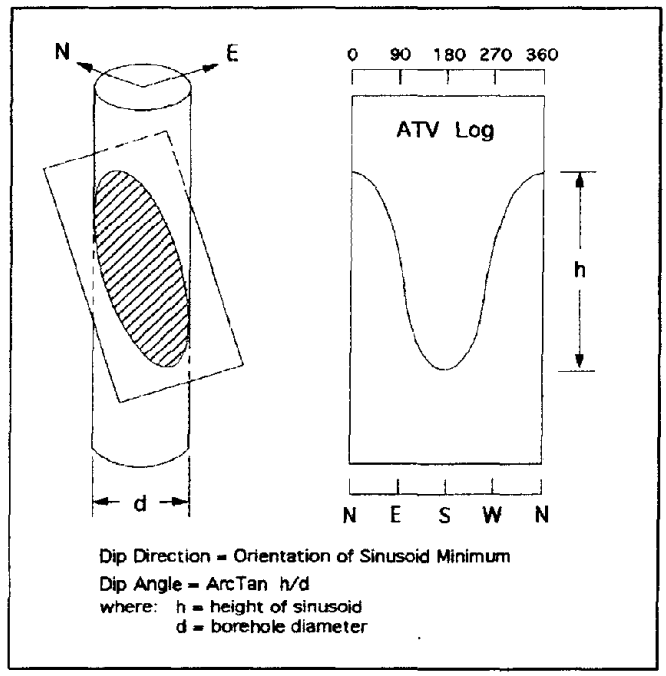

Figure 143. Projection of a planar intersection with a cylindrical borehole. (Layne Christensen, Colog)

Data Acquisition: To record a televiewer log, the appropriate probe is lowered slowly into a borehole, with depth being precisely recorded with regard to the data-conducting wireline. As the probe proceeds downhole, optical images or acoustic reflection parameters are digitized and displayed in real-time. Probes are carefully centralized within the borehole, and they record the azimuth and tilt of the borehole, along with image information. All data is recorded directly to a computer hard-drive. These data files and the relatively large but can be easily transferred via LAN, high-speed internet, or CD-ROM. The Optical televiewer is optimized when the borehole is air or clear-fluid filled, while acoustic televiewer requires the presence of fluid regardless of its clarity.

Data Processing: Oriented borehole images are picked manually, using software, searching for sinusoidal features. Such features correspond to planar intersections with the borehole (figure 143). By measuring the height, direction, and dip of each feature, statistical summaries such as stereonet and rose diagrams can be presented (figure 144).

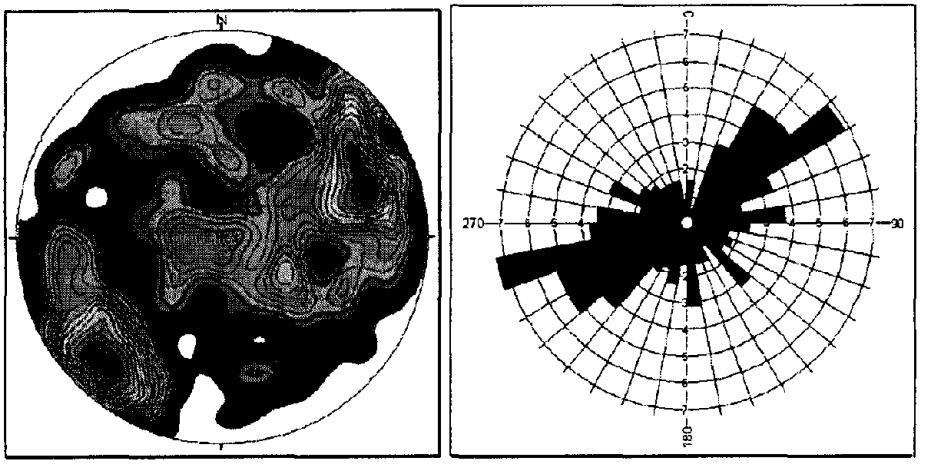

Figure 144. Statistical representations of fracture orientations. (Layne Christensen, Colog)

Data Interpretation: Dominant trends that present themselves in the orientation of planar features are directly related to fluid flow patterns, slope failure planes, and zones of weak or unstable subsurface. Depths to stable or unstable layers can be established.

Advantages: Borehole televiewer imaging provides information about the subsurface geology as it exists, in-situ, under natural temperature and pressure conditions. Unlike drilled core, imaging produces 100% recovery, with highly accurate depth and orientation control. Borehole televiewer imaging is rapid, and considerably less expensive than the recovery, transport, analysis, and storage of oriented core.

Limitations: Optical imaging required an optically transparent medium between the probe and the borehole wall, while acoustic imaging requires a liquid medium. Televiewer logs should be included in a suite of logs that can provide an array of subsurface information, and specific core samples may still be recovered for lab analysis. Image orientation can be affected by magnetic material, including rebar, within the near vicinity of the borehole.

6.1.3 Mapping Lithology

Lithology is a description of rocks, especially sedimentary rocks, mostly from hand specimens and outcrops. This description includes the color, structure, mineralogical composition, and grain size. Geophysical methods measure the physical properties of rocks, including seismic wave velocity, resistivity, induced polarization, magnetization, and, at shallow depths, dielectric properties. To use geophysical methods to map lithology, there has to be some relation between the lithological parameters and the physical properties of the rock.

The two lithological parameters that can be most readily correlated from geophysical measurements are structure and grain size. Color cannot be easily translated from geophysical methods to a physical property. Mineralogical composition is loosely related to seismic velocity, although this relationship is probably quite complex. The only minerals that can be detected directly using geophysical methods are magnetite and metallic sulfides, such as pyrite.

The distribution of grain size within a rock is related to porosity. Porosity is the ratio between the volume of pore space and the total volume of rock. A uniform wide grain size distribution usually results in a lower porosity than a narrow distribution, since the smaller grains can fill in the spaces between the larger grains. The critical grain size cannot generally be readily determined from porosity. Porosity can provide an indicator of the relative grain size distribution (wide or narrow) since materials with wide grain size distributions will typically have less pore space or lower porosity than materials with narrow distributions. Structure is probably related to seismic velocity and less to resistivity. Seismic velocity is strongly related to density, with denser rocks having a higher seismic velocity. However, since there is a considerable overlap of densities for different rock types, it is difficult to predict rock type, and hence lithology, from density. Likewise, the resistivity of any particular rock type varies over a wide range, and there is a large overlap of rock types having similar resistivities. Probably the most definitive relationship is between seismic velocity and porosity, although, as with density, there is a large overlap of different rock types with similar velocities. Figures 145 and 146 show the resistivities and seismic velocities of numerous rock types and illustrates the overlap in rock type for both resistivity and velocity.

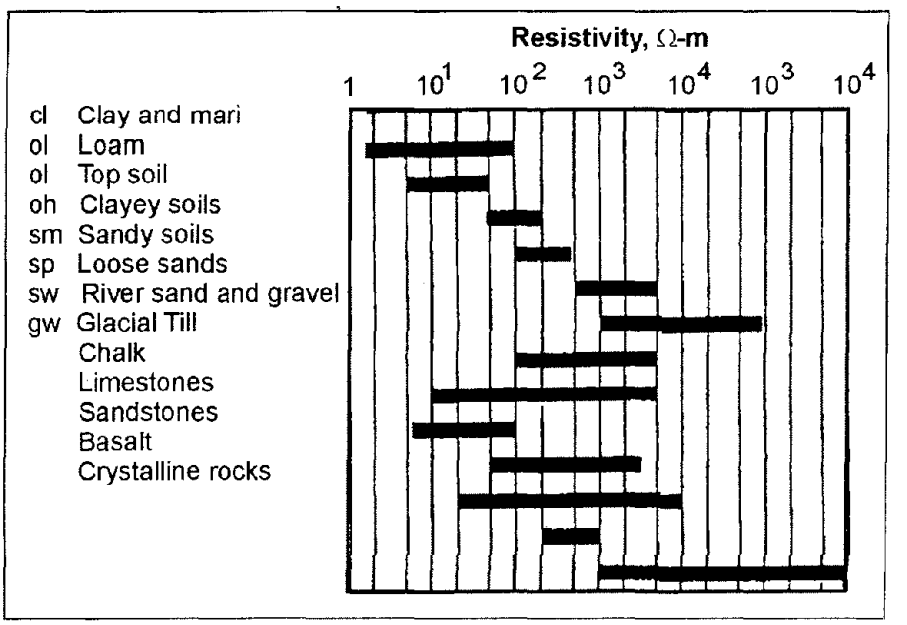

Figure 145. Resistivities of different rock types. (From TN5, Electrical Conductivity of Soils and Rocks, Geonics Ltd)

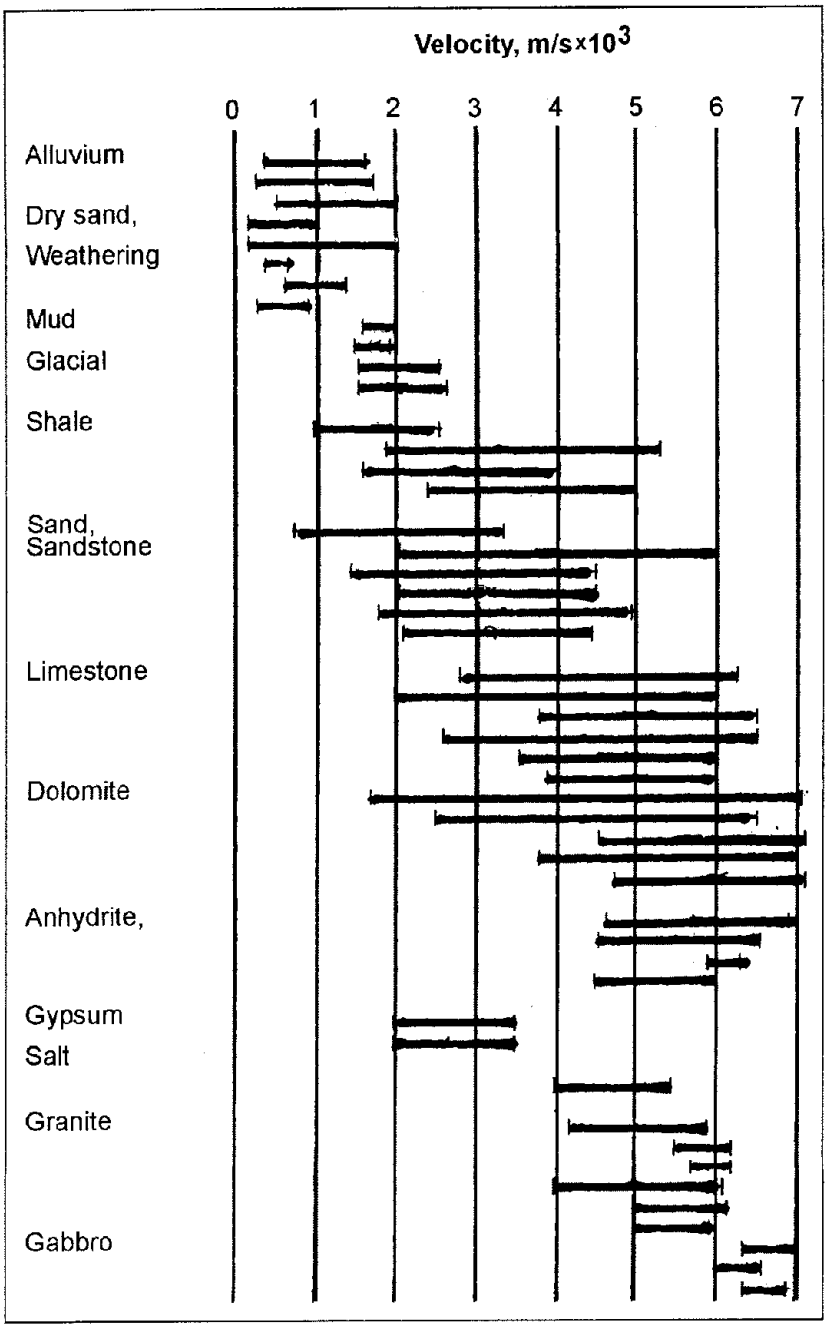

Figure 146. Seismic velocities of different rock types. (Modified from Exploration Seismology, R.E. Sheriff and L.P. Geldart)

The minerals comprising a rock are almost always electrical insulators. Thus, electrical conduction occurs because of the moisture contained within the pores of the rock or soil. The resistivity of soil or rocks depends on several parameters. These include the clay content, moisture salinity, degree of saturation of the pores, and the number, size, and shape of the interconnecting pores. For soils, the degree of compaction (influencing porosity) is also an important factor. Archie (1942) developed an empirical formulae relating resistivity to porosity, degree of saturation and resistivity of the saturating moisture, shown below.

$$\rho_e = a\phi^{-m}s^{-n}\rho_w, \qquad (5)$$

where ϕ is the fractional pore volume (porosity), s is the fraction of the pores containing water, ρ_w is the resistivity of the water, n is approximately 2, a and m are constants with a varying between 0.5 and 2.5 and m varying between 1.3 and 2.5.

Porosity determines the amount of water that a rock can contain, and this influences resistivity. However, because resistivity is also influenced by several other factors as described above, the absolute value of porosity can probably not be obtained from resistivity. However, changes in resistivity may possibly be used to indicate changes in porosity, assuming that the other factors influencing resistivity remain constant over the area of interest. In this case, resistivity changes may possibly be used to indicate changes in lithology.

It appears, therefore, that it is not easy to predict lithology from either seismic velocity or resistivity, although rock type is often interpreted from resistivity and seismic velocity data. As discussed above, these methods may be used to map changes in lithology and will be discussed within this context.

Magnetic methods will also be briefly described, since these can be used to estimate the magnetic susceptibility of a rock, which is related to the amount of magnetite it contains. Induced polarization is also described, since this technique is used to locate pyrite and other metallic sulfides.

Some of the methods discussed can be used for investigations to depths of hundreds of meters and beyond. These include the seismic reflection and magnetic methods. Seismic reflection methods are used extensively for hydrocarbon exploration surveys. Although the general techniques employed for hydrocarbon exploration are similar to those used for shallower surveys, this document concentrates only on techniques applicable to these shallower surveys. It is assumed that the primary depths of concern for this document are generally less than 100 m.

Methods

Six different geophysical methods will be discussed. These are listed below along with the observed or derived properties that are measured.

Method	Observed/Derived Property
Seismic Reflection	Layer stratigraphy and depth
Seismic Refraction	Rock velocity, layer depth
Time Domain Electromagnetic Methods	Resistivity, depth
Resistivity Methods	Resistivity, depth
Magnetic Methods	Magnetic susceptibility, magnetite content
Induced Polarization	Metallic sulfides, clay

Seismic Methods

Two seismic methods will be discussed. These are seismic refraction and seismic reflection. Seismic refraction can be used to obtain the velocity of up to four layers, along with the thickness of these layers. Seismic reflection can also be used to estimate the velocity and measure the thickness of rock layers, but is more commonly used to map the continuity of reflecting horizons to much greater depths than the seismic refraction method and is not restricted to four layers.

6.1.3.1 Seismic Refraction

Basic Concept: The seismic refraction method can be used to measure rock velocities and the depths to refractors. The method requires a seismic energy source, usually a hammer for depths less than 15 m and black powder charges for depths to 30 m. The seismic waves then penetrate the overburden and refract along the bedrock surface. While they are traveling along this surface, they continually refract seismic waves back to the ground surface. These are then detected by geophones placed on the ground surface. Both compressional waves and shear waves can be used in the seismic refraction method, although compressional waves are most commonly used.

Figure 114b shows the StrataVisor NZ instrument manufactured by Geometrics. This system can record 64 channels of data. In addition, the number of channels can be increased using attached secondary instrumentation. This instrument is used for both seismic refraction and seismic reflection surveys.

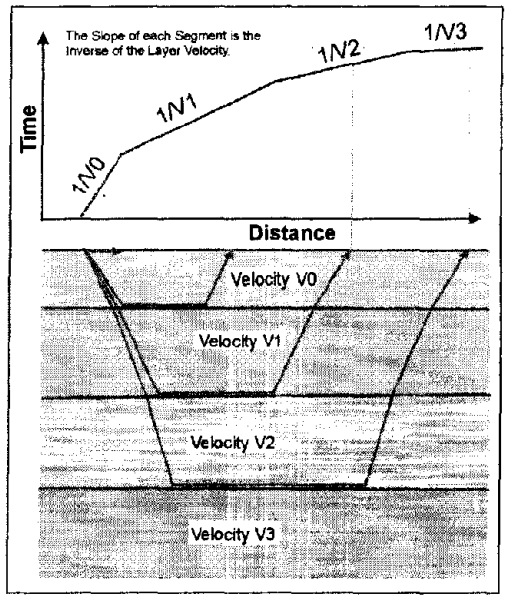

Figure 147. Seismic time-distance graph over four-layer ground.

The main seismic waves involved and the resulting time distance graph are shown in figure 114a. This figure shows the shot locations commonly used in seismic refraction surveys along

with the geophone layout. In addition to the shot locations shown, more shots internal to the geophone spread are sometimes used to better map the near surface velocities and stratigraphy.

The ray paths and time distance graph over four-layered ground are shown in figure 147. The inverse of the slopes of the line segments on the time-distance graph provide the velocities of the refractors.

Data Acquisition: The design of a seismic refraction survey requires a good understanding of the expected bedrock and overburden. With this knowledge, velocities can be assigned to these features and a model developed that will show the parameters of the seismic spread best suited for a successful survey. These parameters include the length of the geophone spread, the spacing between the geophones, and the expected first break arrival times at each of the geophones. Knowing the expected first break arrival times is helpful in the field, where field arrival times that correspond fairly well to expected times help to confirm that the spread layout has been appropriately planned, and that the target layers are being imaged. If lateral changes in velocity are required over a wide area, contiguous spreads will be used along traverses crossing the area of interest.

Data Processing: The first step in processing/interpreting refraction seismic data is to pick the arrival times of the signal, called first break picking. A plot is then made showing the arrival times against distance between the shot and geophone. This is called a time-distance graph. An example of such a graph for two-layered ground (overburden and refractor) is shown in figure 114a and that over four-layered ground is shown in figure 147. In figure 114a, the time-distance plot shows the waves arriving at the geophones directly from the shot (V1). These waves arrive before the refracted waves. The refracted waves arrive ahead of the direct arrivals (V2). These waves have traveled a sufficient distance along the higher speed refractor (bedrock) to overtake the direct wave arrivals. A similar argument is made for all of the waves shown in figure 147, where the first arrival waves from each successively faster refractor eventually arrive earlier than the first arrival waves from the slower refractors

Data Interpretation: There are several methods of refraction interpretation, the most common of which is the Generalized Reciprocal Method (GRM) that is described in detail in the Geophysical Methods section. A brief, and simplified, description of the GRM method is presented below. Figure 115 shows the basic rays used for this interpretation.

The objective is to find the depth to the bedrock under the geophone at D. This is done using the following simple calculations. The travel times from the shots at A and G to the geophone at D are added together (T1). The travel time from the shot at A to the geophone at G is then subtracted from T1. Figure 116 shows the remaining waves after the above calculations have been performed. These are the travel times from C to D added to the travel times from E to D subtracting the travel time from C to E. The sum of these travel times can be shown to be approximately the travel time from the bedrock at H to the geophone at D. Since the velocity of the overburden layer can be found from the time-distance graph, the distance from H to D can be found giving the bedrock depth. This process can be extended to apply to several layers.

Once the velocities of the layers are assigned, these should be interpreted to give appropriate geologic layers. For example, a layer with a velocity of 2,000 m/s suggests a soft rock such as shale, whereas a velocity of 4,000 m/s indicates a hard rock such as limestone. Lateral changes in the velocity of the layers may indicate changes in lithology.

Advantages: Seismic refraction is usually a good method to obtain the velocity of rocks, which one of the criteria for establishing lithology.

Limitations: Probably the most restrictive limitation is that each of the successively deeper refractors must have a higher velocity than the preceding shallower refractor. If this is not the case, errors in depth estimates of the deeper layers can occur, since a lower velocity layer beneath a higher velocity layer will not be observed in the data.

If the water table is in the overburden and close to the bedrock, this may obscure the bedrock arrivals since saturated soils have a higher velocity than unsaturated soils. This may also lower the velocity contrast between the saturated overburden and the bedrock.

Local noise, for example traffic, may obscure the refractions from the bedrock. This can be overcome by using larger impact sources or by repeating the impact at a common shot point several times and stacking the received signals. In addition, since some of the noise travels as airwaves, covering the geophones with sound-absorbing material may also help to dampen the received noise.

6.1.3.2 Seismic Reflection

Basic Concept: Geological layers can be mapped using the seismic reflection method. This can be done using either a shear wave source or a conventional compressional wave seismic source. One shear wave source is called the Microvib and is illustrated in figure 95. Compressional wave sources range from a simple hammer and base plate, to black powder and conventional explosive sources, to vibrators. For relatively shallow investigations, a hammer and base plate, weight drop, and black powder sources can be used. The actual depth of investigation depends on the geology and site conditions, but can be 50 m and deeper. For deeper investigations, a small vibrator can be used. Examples are the Microvib (figure 95) shear wave source and the Minivib source (figure 148), applicable for depths over 1,000 m.

Seismic sources, producing either vibrations or impulses can be used for seismic reflection surveys. Special processing techniques are applied to the vibrational sources to make the resulting data compatible with impulse sources.

Figure 148. The Minivib seismic source. (Industrial Vehicles, Inc.)

Seismic reflection involves using a surface seismic source to create a seismic wave, which then travels into the subsurface. At interfaces that have an impedance contrast (related to velocity and density), a portion of these waves is reflected back to the ground surface, and a portion is transmitted through the interface. Geophones on the ground surface record these reflections. Figure 118 shows the seismic ray paths for reflections from two layers. The signals at two geophones are illustrated to the right of the ray path diagram. The reflection from the interface between layers 1 and 2 arrives first at geophone 1. A short time after this arrival, the same interface provides a reflection that arrives at geophone 2. Some time later, the reflection from the boundary between layers 2 and 3 arrives at geophone 2.

Data Acquisition: In a seismic reflection survey, shots are positioned at regular intervals along the line to be surveyed, and the seismic reflections recorded by a series of geophones placed on the ground surface, called a geophone spread. The number of geophones varies from 12 to 60 or more for non-hydrocarbon seismic surveys. The data are stored in the seismic recorder and transferred to a computer for processing. The spacing between the geophones, the number of geophones used, and the shot spacing have to be determined before the survey begins, and depend on the exploration depth and the target resolution required. If long lines are to be recorded, a special switch box is needed, called a roll box, which allows the recording geophones to be advanced along the line as shooting progresses.

Data Processing: If a vibration source is used, such as the Microvib, then special processing techniques have to be applied to make the data compatible with an impulse source.

Many techniques are used to process reflection seismic data including filtering, correcting for velocity effects, and stacking the traces that emanate from a common depth point (CDP, sometimes called common mid point CMP) on the reflecting surface. The main objective of these techniques is to provide a gather of seismic traces that can be stacked to image each reflection point (CDP) as clearly as possible. The output from processing a line of seismic data is a seismic section showing the reflectors. This section can be presented as CDP location against record time or, when velocities are assigned to the different layers, as CDP against depth.

Data Interpretation: Reflection seismic surveys are usually used for stratigraphic exploration, and a seismic section showing CDP against depth is most appropriate. Such a section should provide an immediate view of the seismic stratigraphy, both vertically and laterally. The relation between the reflector stratigraphy and lithology will need to be constrained using other data such as a well log. This may enable the seismic reflectors to be associated to a particular rock type. Lateral changes in the character of the seismic reflector may indicate changes in the lithology.

Figure 133 presents a seismic reflection section showing several reflectors and interpreted faults. As can be seen, the character of some of the reflectors changes across the section. In particular, some of the reflectors are more pronounced and some are less pronounced between the faults. Presumably, at least some of these changes are related to lithological changes.

Advantages: The seismic reflection method provides a pictorial section that resembles the subsurface layers. The method is not restricted, as is the seismic refraction method, to a section in which the layer velocities successively increase.

Limitations: The main attribute of the seismic reflection method is that it provides a visual image of the continuity of the reflectors along the surveyed line. Layer velocities are also interpreted but are probably not as reliable as those found using the seismic refraction method. In addition, the method is best suited for investigation depths greater than 10 to 20 m, depending on the geology.

The seismic reflection method is one of the more expensive methods geophysical methods, and requires a significant amount of knowledge to process the data. In addition, any local vibrational noise will reduce the signal-to-noise ratio and make the resulting seismic section less definitive.

6.1.3.3 Time Domain Electromagnetic Soundings

Basic Concept: Time Domain Electromagnetic soundings (TDEM) are used to obtain the vertical distribution of resistivity. This method is particularly well suited to mapping conductive layers. To a significant degree, this method has now superseded the resistivity sounding method since it requires less work for a given investigation depth and generally provides more precise depth estimates. However, resistivity soundings are still useful for shallow investigations or when resistive targets are sought.

TDEM soundings are an electromagnetic method used to provide the vertical distribution of ground resistivity. The method uses pulses of electromagnetic energy rather than continuously oscillating electromagnetic sources. Figure 120 illustrates the system layout and the current and voltage waveforms.

A square loop of wire is laid on the ground surface. The side length of this loop is about half of the desired depth of investigation. A receiver coil is placed in the center of the transmitter loop. Electrical current is passed through the transmitter loop and then quickly turned off. This sudden change in the transmitter current causes secondary currents to be generated in the ground. The currents in conductive layers (shale) decrease more slowly than those in

resistive layers. The relation between the time after the current turns off (called delay time in this document) and layer depth and conductivity is complex. However, in general, longer decay times correspond to greater depths.

The voltage measured by the receiver coil does not decay instantly to zero when the current is turned off but continues to decay for some time. This decaying voltage is caused by the decaying secondary electrical currents in the ground. The voltage measured by the receiver coil is then converted to resistivity.

A plot is made of the measured resistivity against the delay time, as illustrated in figure 121. In this graph, the shallow layers are imaged at early decay times and the deeper layers at later decay times.

The resistivity sounding curve shown in figure 121 illustrates the curve that would be obtained over three-layered ground. The near-surface layer is fairly resistive. This is followed by a layer having a much lower resistivity (higher conductivity) and causes the measured resistivity values to decrease. The third layer is again resistive. This method can be used for up to four or five layers.

Data Acquisition: The transmitter loop and receiver coil are set up as described earlier. Switched current is passed through the transmitter loop, and the receiver coil measures the resulting voltage. The switching and measuring procedure is repeated many times allowing the resulting voltages to be stacked and improving the signal-to-noise ratio. Soundings are recorded at different sites until the area of interest has been covered. A sounding curve is plotted for each location showing the measured resistivity against decay time.

Data Processing: Usually the only processing required is the removal of bad data points.

Data Interpretation: The sounding curves are interpreted using computer software to provide a model showing the layer resistivities and thickness. The interpreter inputs a preliminary model into this software program that then calculates the sounding curve for the model. It then adjusts the model and calculates a new sounding curve that better fits the field data. This process is repeated until a satisfactory fit is obtained between the model and the field data. The process is called inversion.

If the TDEM soundings are conducted along a traverse, a section can be drawn showing the variation of resistivity with depth along the section, thus also providing the lateral variations of resistivity. The geologic interpretation then requires that the resistivities be assigned rock types. For example, a shale or clay layer will have a low resistivity, probably less than 30 ohm-m, whereas an impervious limestone may have a resistivity of over 1,000 ohm-m. If a well log is available, rock types can be assigned to the resistivity values with much greater confidence. Lateral changes in resistivity along a particular horizon will possibly indicate changes in lithology.

Advantages: For a given depth of investigation, the method is much more efficient in the field than the resistivity method. The TDEM method is particularly good at defining conductive layers, but less effective at defining resistive layers.

Limitations: Generally, the method is limited to four or five layers. Resistive layers usually have to be fairly thick in order to be resolved, with the thickness increasing with depth. Thin conductive layers can be detected, and, in fact, the method responds to the product of conductivity multiplied by the layer thickness. Thus, thin conductive layers may respond as well as thicker, but less conductive, layers. In these cases, it may not be possible to accurately determine either the thickness or conductivity of the layer.

Metal fences and other above or below ground metal features may prohibit recording interpretable data.

6.1.3.4 Resistivity

Resistivity methods can be divided into three groups. The first two are resistivity soundings and traverses. The last group combines both resistivity sounding and traverse data to form a resistivity section. Data for this latter group are recorded using relatively recently designed resistivity instruments. Resistivity soundings are useful if the depths and resistivities are needed, although resistivity traverses are now rarely used. This is partially because the ground conductivity can be more easily measured using electromagnetic methods, where no ground contact is required. In addition, resistivity measuring instruments are now available that automatically record data from several different electrode spacings very efficiently, combining traverse and sounding data.

These newer instruments, called automated resistivity systems, use electrodes that are addressable by a central control unit. This means that a large number of electrodes can be placed in the ground prior to starting the survey and connected to the central control unit. The data recording parameters and the electrode array to use are input to the central control unit. Once the electrodes are all connected, the measurements are automatically recorded by the central control unit. Because of the large amount of data obtained with these systems, a more detailed and reliable resistivity interpretation is obtained, making them the preferred instrument for lithology determination.

Resistivity is usually measured using one of the electrode arrays shown in figure 90. Electrical current is put into the ground using two electrodes, and the resulting voltage is measured using two other electrodes. Since the measured resistivity is a composite of the resistivities of several layers, the correct term is apparent resistivity. In this document, the term "measured resistivity" is understood to mean apparent resistivity.

These arrays are used for different types of resistivity surveys. The Schlumberger array is often used for resistivity soundings, as is the Wenner array. The Pole-pole array provides the best signal, but is cumbersome because of the long wires required for the remote electrodes, and it is rarely used. The Dipole-dipole array was originally used mostly by the mining industry for induced polarization surveys. Readings were taken using several different separations of the voltage and current dipoles providing measurements of the variation of resistivity with depth. Long lines of data were recorded requiring many readings. This array has now become common for resistivity surveys using the automated resistivity systems. If more signal (voltage) is needed than can be provided with the Dipole-dipole array, the Pole-dipole array can be used.

Automated Resistivity Systems

Basic Concept: As mentioned above, newer resistivity systems are now available that make taking resistivity measurements much more efficient. Figure 201 shows one such system called the Sting/Swift automated resistivity measuring system.

Data Acquisition: When using these automated resistivity systems, the electrodes for each spread are first placed in the ground and connected to the control unit. This is then programmed with the electrode array desired and other data recording parameters and then instructed to record the data.

Data Processing: Usually the only processing required is the removal of bad data points.

Data Interpretation: Data from the automated resistivity systems are interpreted by inversion software, although much information can be gained visually. An example of the results from such a survey is presented in figure 149, which shows two high-resistivity zones, each of which contains sand and gravel. The data have been inverted showing the resistivity variation, both laterally and vertically, against depth.

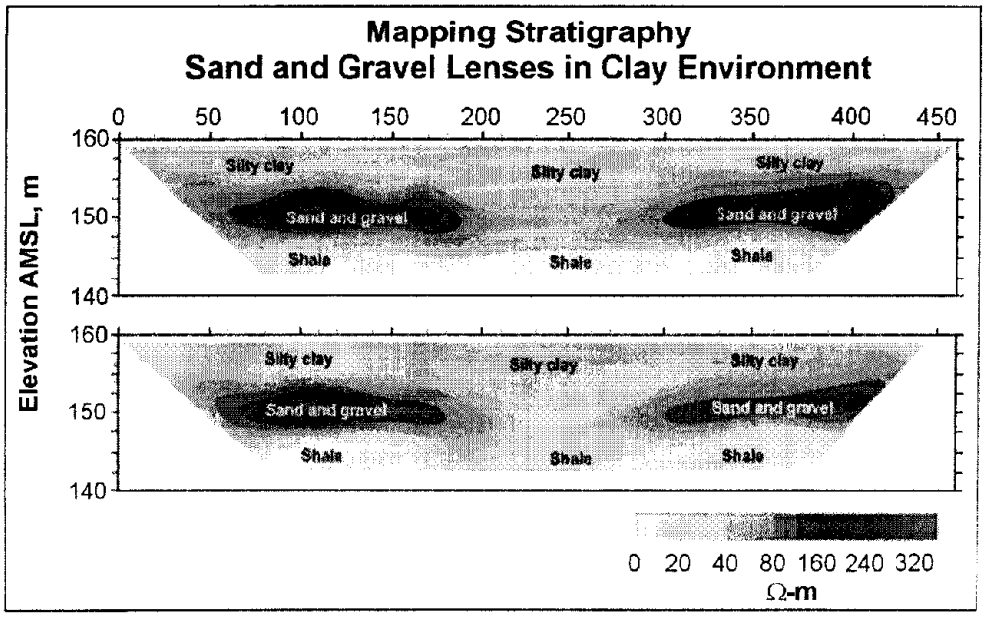

Figure 149. Resistivity data showing stratigraphic changes. (Advanced Geosciences, Inc.)

The low-resistivity areas (less than 20 ohm-m) correspond to clay layers and high-resistivity zones (greater than 100 ohm-m) correspond to sand and gravel lenses. Inasmuch as the change from clay to sand and gravel is clearly observed, and this likely corresponds to a change in grain size, the method has provided some information about changes in lithology.

Advantages: Automated resistivity systems obtain much more data than the simple resistivity systems and therefore are able to give a more detailed interpretation.

Limitations: Since electrodes have to be inserted into the ground, the method is difficult to use in areas where the surface of the ground is hard, such as concrete or asphalt-covered areas. If the ground is dry, water may need to be poured onto the electrodes to improve the electrical contact between the metal electrode and the soil.

If a survey is conducted along a single line, resistivity variations normal to this line are not accounted for in the interpretation. Recording lines parallel to each other, of course, can rectify this problem. In addition, three-dimensional resistivity surveys can now be recorded and interpreted.

6.1.3.5 Magnetic

Basic Concept: Magnetic methods can be used to estimate the magnetic susceptibility of rock formations, which is related to the amount of magnetite that the formations contain. To the extent that this is mapping mineral content, it can be considered as mapping one parameter related to lithology.

Magnetic data can be recorded using ground or airborne surveys. If large areas are to be covered, airborne surveys may be appropriate. Many considerations need to be evaluated before making a decision whether to use a ground or airborne survey, the most important being the size of the area to be surveyed. Other considerations include the density of data required, the comparative costs, and the expected depth of the target. Only ground surveys are discussed in this section of the document, since the theory of the method and interpretation are similar for both types of surveys.

Rock layers often contain small amounts of magnetite. This magnetite produces a secondary magnetic field that is superimposed on, and distorts, the Earth's magnetic field. Measurements of the magnetic field strength made on the ground surface can be used to determine the depth of the layer containing the magnetite and estimate its magnetic susceptibility. Estimating the susceptibility can only be done approximately, and only an estimate of the amount of magnetite can be given. However, lateral or vertical changes in susceptibility may be able to be used to assess relative magnetite content changes. The magnetic method is not well suited for interpretation of several successively deeper layers containing magnetite, since the magnetic anomaly from the shallowest layer dominates the measured magnetic field.

Several instruments are available for recording magnetic data, one of which is shown in figure 209. This instrument is also equipped with a GPS system allowing its location to be recorded at all times.

Data Acquisition: Magnetic surveys are conducted by recording data along a traverse crossing the area of interest. Data are normally recorded in time mode, usually at several readings per second. Positioning with the magnetometer illustrated in figure 209 is with the GPS system. If GPS is not used, other methods are required to position the data.

Because the magnitude of the Earth's magnetic field continuously changes in time, a base station is often set up to record these changes. Since these changes usually have a daily cycle, they are called diurnal effects. This station has to be time synchronized with the

magnetometer recording the spatial data. The effect of these magnetic variations can then be removed from the field data during processing provided the variations are not too severe. However, if the diurnal magnetic changes become significant, the survey should be stopped.

Data Processing: The magnetic data needs to have the diurnal drift removed, and the data spatial coordinates will have to be assigned. This can be done by obtaining the positions of the ends of each of the lines and using interpolation to assign coordinates to the other data points. However, magnetometers are now available with GPS allowing coordinates to be assigned to the data as they are being recorded (see figure 209). Various filtering routines can be applied to remove noise spikes and apply some smoothing if needed.

Data Interpretation: The kind of anomaly expected over a magnetite-rich zone is illustrated in figure 150. Because the direction of the Earth's magnetic field is not vertical (except at the magnetic poles), the anomaly has a positive and negative component and is not symmetrical about the source of the magnetite, which can make the interpretation of the source of the magnetic anomaly difficult. To make interpretation easier, the field strength data can be processed to produce a function that peaks over the top of the source. This is called the Analytic Signal, and is the sum of all of the spatial gradients of the magnetic field strength data. The width of the Analytic Signal at half of its amplitude is related to the depth to the magnetic source, and the amplitude of the Analytic Signal is related to the susceptibility of the magnetite source.

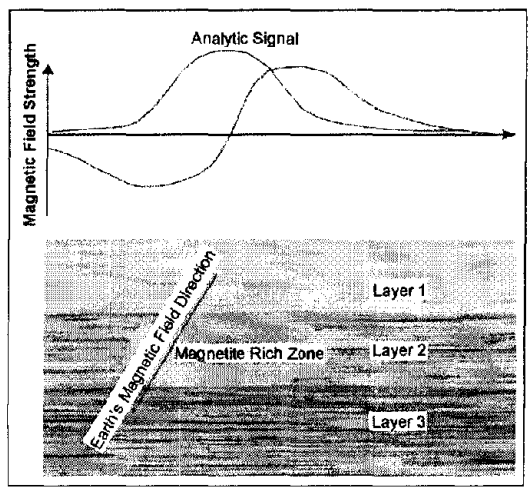

Figure 150. Magnetic anomaly over a magnetite rich zone.

Using the Analytic Signal data (or the magnetic field strength data), estimates can be made of the susceptibility of the magnetite source, which is related to the amount of magnetite in the rocks. The depth to the source can also be calculated. It may be possible using this method to map variations in magnetic susceptibility, which may indicate lithological changes.

Advantages: Magnetic data is relatively simple and efficient to record in the field.

Limitations: Since the source of the magnetic anomalies is a zone of magnetite whose edges are probably not well defined, depth calculations of its depth may have significant errors, since the calculations are based on well-defined source shapes.

If the diurnal variations in the Earth's magnetic field are large, then data recording should be stopped until the diurnal changes diminish. If areas of magnetite are in successively deeper layers, probably only the first layer will be recognized.

6.1.3.6 Induced Polarization

Basic Concept: Induced Polarization (IP) is commonly used in the mining industry to locate metallic sulfides such as pyrite, chalcopyrite, and other metallic minerals. It is discussed here only because, like the magnetic method, it provides data on the distribution of metallic minerals and could be regarded as mapping changes in lithology. Induced Polarization anomalies are found over metallic sulfides, graphite zones, and some clays.

Induced Polarization is an electrical method that measures the change in the measured resistivity of the ground with frequency. Numerous electrode arrays can be used to measure IP data, several of which are illustrated in figure 90.

For this section of the document, the Dipole-dipole array is used to illustrate the waveforms. This is probably the most commonly used array for measuring Induced Polarization. Two methods are used to obtain IP data: time domain and frequency domain. In time domain, a constant current is passed into the ground using two of the four electrodes. This current is then rapidly switched off. During this off time, the remaining two electrodes measure the resulting voltage. If an IP effect is present, the voltage across these electrodes will not suddenly return to zero as the current is turned off, but will decay to zero over a period of time, usually within a few seconds, as illustrated in figure 110. Simple IP measurements usually integrate the IP voltage over a specified time period, say T_1 and T_2 providing a single number that is a measure of the IP response. However, if a more detailed analysis is needed, the full voltage and current waveforms are recorded. The units used to measure the IP effect, called chargeability, are mV/V. Using the Fourier transform to convert the data to frequency domain, these data can then be converted to the variation of IP response with frequency, called Spectral IP (SIP). In frequency domain, the IP effect is measured at different current waveform frequencies. If more than two frequencies are used, SIP data are recorded.

Induced Polarization surveys require electrodes, a data recorder, current transmitter, and a power source for the transmitter. An example of an IP data recorder is shown in figure 151.

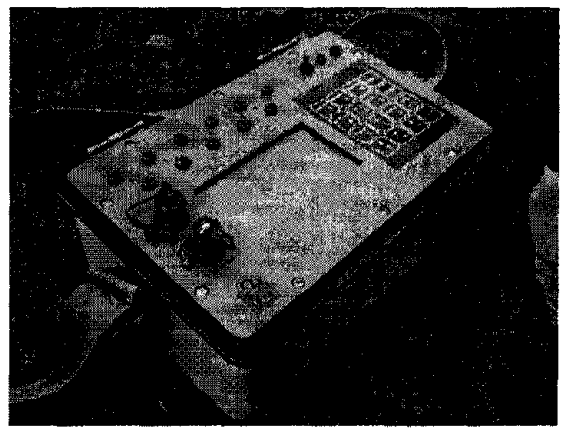

Figure 151. Induced Polarization instrument. (IRIS Instruments)

This particular instrument can record up to 10 channels of data simultaneously. It can also be configured with the automated data recording instrument systems, making data recording efficient.

Data Acquisition: Induced Polarization surveys are conducted much like resistivity surveys. Readings are taken at discrete stations to form lines of data crossing the area of interest. In frequency domain, the variation of IP response with frequency is obtained. In the time domain, if the current and voltage waveforms have been digitally recorded and a Fourier analysis performed, the variation of resistivity with frequency is measured producing SIP data. SIP data provide more interpretable information than the simple IP measure discussed above; however, this is still being researched and is rarely used as a production method. SIP data may be able to distinguish between the different minerals (metallic minerals, graphite, and clay) that produce IP anomalies. However, if the goal is to simply map the occurrence of metallic minerals, spectral IP methods are probably not required.

Data Processing: When recording IP data, resistivity data are also recorded. Both the resistivity and IP data are usually plotted in section form called a pseudosection. With this presentation, data from the smaller electrode separations are plotted near the top of the pseudosection (ground surface), and data from the largest electrode separations are plotted at the bottom of the pseudosection, thus simulating a plot showing resistivity and IP against depth for all values along the traverse. A typical chargeability pseudosection is shown in figure 152. The horizontal dimension is distance, and the vertical dimension is related to the electrode spacings used to take the measurements (n-value). Although these data are from a fairly shallow survey using small electrode spacings, it does illustrate the method, presentation techniques, and the interpretation. Surveys to much greater depths can be performed using larger electrode spacing.

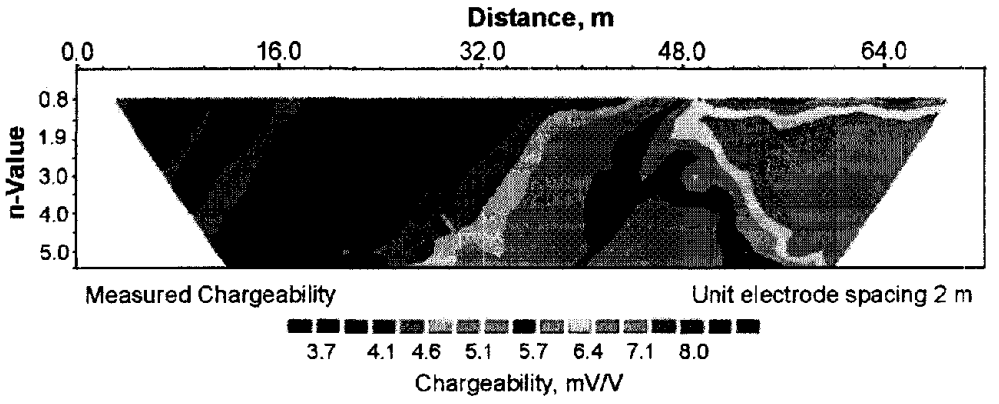

Figure 152. Chargeability pseudosection. (Terraplus, Inc.)

The corresponding resistivity pseudosection is shown in figure 153.

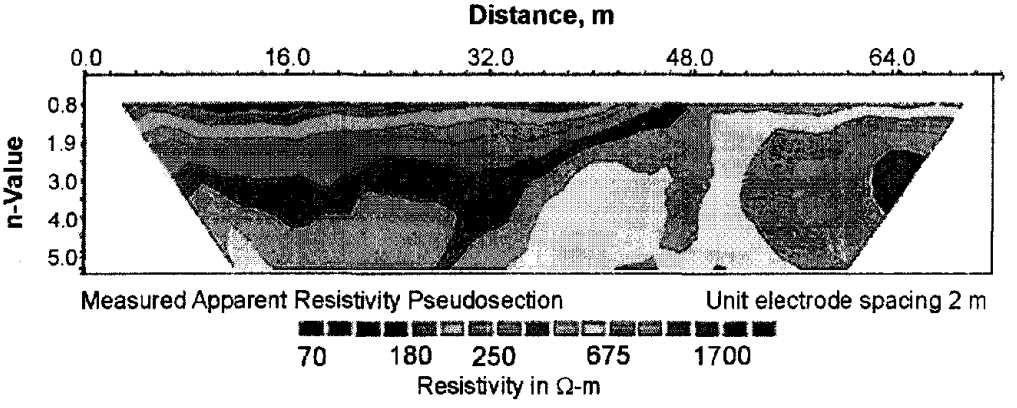

Figure 153. Measured (apparent) resistivity pseudosection. (Terraplus, Inc.)

Data Interpretation: The pseudosection data are usually interpreted by using inversion techniques, where initial model estimates are input to the program, which then calculates the pseudosection resulting from this model. It then determines the degree of fit of the calculated pseudosection with the field data, modifies the model accordingly, and a new pseudosection is then calculated. This process is repeated until the model provides a pseudosection that gives a good fit to the field data.

Figure 154 shows the interpretation of the data presented in figure 152. In this profile, the elevation of the ground surface has also been incorporated into the interpretation.

Since induced polarization phenomena also occur when clays are present in the subsurface, the method can possibly be used to estimate clay content. The survey techniques, processing, and interpretation are similar to those described above for metallic mineral detection.

Although IP anomalies are frequently observed over clays, and reports of its use to find clays are common, no published relationship was found showing a correlation between the magnitude of the IP response and the amount of clay.

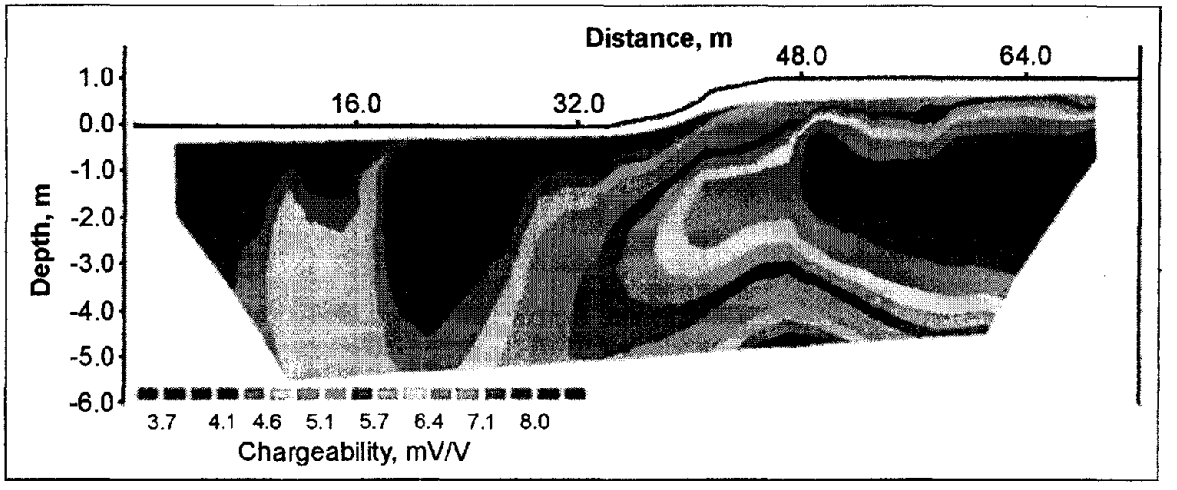

Figure 154. Interpreted Induced Polarization data shown in figure 153. (Terraplus, Inc.)

Advantages: IP measures the variation of resistivity with frequency and provides a unique interpretation showing polarizable material such as clays, graphite and metallic minerals.

Limitations: The induced polarization method, like the resistivity method, requires electrodes to be inserted into the ground. However, with the IP method, the polarization signals can be quite small, and it is important to put as much current into the ground as possible to increase the measured signals. If the ground surface is hard or dry, it may be difficult, not only to get the electrodes in the ground, but also to put electrical current in the ground. This can usually be solved by pouring water on the electrodes, thereby improving the electrical contact between the electrode and the surrounding soil.

6.1.3.7 Borehole Gamma Logs (Natural Gamma or Gamma Ray)

The gamma log (also known as natural gamma or gamma ray log) provides a measurement recorded in counts per second (CPS) that is proportional to the natural radioactivity of the formation. This log is used principally for lithologic identification and stratigraphic correlation. Because measured counts are proportional to the quantity of clay minerals present, the gamma log is an excellent indicator of clay layers, including swelling clays.

Basic Concept: Gamma radiation is measured, in counts per second, with scintillation NaI detectors. The gamma-emitting radioisotopes that naturally occur in geologic materials are Potassium^{40} and nuclides in the Uranium^{238} and Thorium^{232} decay series. Potassium^{40} occurs with all potassium minerals, including potassium feldspars. Uranium^{238} is typically associated with dark shales and uranium mineralization. Thorium^{232} is typically associated with biotite, sphene, zircon and other heavy minerals. The natural radioisotopes occur in exchange ions, which are attached to the clay particles.

Data Acquisition: To record a gamma log, the probe is lowered slowly into a borehole, as depth is precisely recorded with regard to the data-conducting wireline. As the probe proceeds up or downhole, CPS values are recorded at intervals, typically 0.3 cm, and plotted

and displayed in real-time (figure 155). All data is recorded directly to a computer hard-drive, and the data files can be easily transferred via LAN, internet, floppy disk, or CD-ROM.

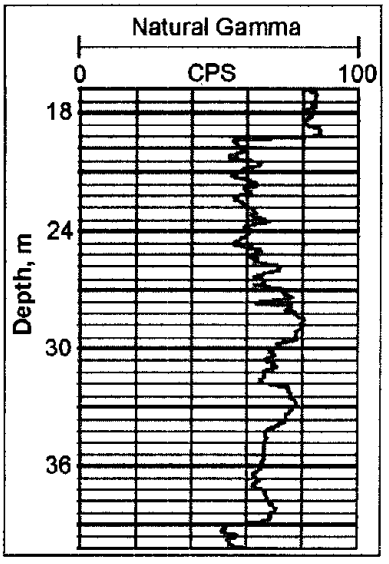

Figure 155. Example of gamma CPS vs. depth. (Layne Christensen, Colog.)

Data Processing: Gamma logs require minimal processing. Plots of CPS vs. depth can be created with raw values, or may be filtered slightly to reduce statistical noise.

Data Interpretation: The usual interpretation of the gamma log, for hydrogeology applications, is that measured counts are proportional to the quantity of clay minerals present. This assumes that the natural radioisotopes of potassium, uranium, and thorium occur in exchange ions, which are attached to the clay particles. Thus, the correlation is between gamma counts and the cation exchange capacity (CEC). Usually gamma logs show an inverse linear correlation between gamma counts and the average grain size (higher counts indicate smaller grain size, lower counts indicate larger grain size). With this simple correlation, depth and extent of layers containing clay particles can be established.

The assumption of a linear relationship between the clay mineral fraction in measured gamma activity can be used to produce a shale fraction calibration for a gamma log in the form:

$$\mu = \rho\beta^2, \tag{6}$$

Where $\mathbf{C_{sh}}$ is the shale volume fraction, **G** is the measured gamma activity; $\mathbf{G_{ss}}$ is the gamma activity in clean sandstone or limestone; $\mathbf{G_{sh}}$ is the gamma activity measured in shale.

Advantages: The gamma log provides information about the subsurface lithology with very little processing. Interpretation is simple and acquisition is rapid. Natural gamma rays travel through casing and pipe materials, such as PVC and steel. Thus, logs may be recorded within existing holes, including injection, extraction, or monitoring wells, cross-hole sonic tubes, or other borings that have been prepared for other reasons.

Limitations: This relation can become invalid if there are radioisotopes in the mineral grains themselves (immature sandstones or arkose), and if there are differences in the CEC of clay minerals in different parts of the formation. Both of these situations are possible in many environments. The former situation would most likely occur in basal conglomerates composed of granitic debris, and the latter where clay occurs as a primary sediment in shale and another as an authigenic mineral deposited in pore spaces during diagenesis. Gamma logs should be included in a suite of logs that can provide an array of subsurface information. Specific core samples may still be recovered for lab analysis.

6.1.4 Locating Shallow Sand and Gravel Deposits

Clastic rocks, including sand and gravel, are classified by geologists according to size, sorting, and distribution of particles, as well as chemical content of silica, feldspar, and calcite. It is often convenient for engineers to define clastic rocks such as sand and gravel by particle size. Sand is defined with particle diameters ranging from 0.0625 mm to 2 mm. Gravel is defined with diameters ranging from 2 mm to an excess of 256 mm. Sand and gravel are defined as continuously graded unconsolidated materials (sediments) formed as a result of the natural disintegration of rocks.

Sand and gravel can be found in numerous depositional environments including alluvial (mudflows and streams), fluviatile (river), aeolian (wind), Lacoustrine (lake), glacial, and beach/bar. Sand and gravel deposits can also occur without prior transportation in the form of residual (weathering) processes.

In the northern United States, many of the sand and gravel deposits were formed by glacial processes. Associated landforms include outwash plains, kames, eskers, and valley trains consisting of river terraces, flood plains, and channel deposits.

Alluvium is a broad term referring to all unconsolidated material formed in recent geological time under conditions other than subaqueous. Alluvial sand and gravel deposits are generally finer grained than glacial meltwater deposits, since present-day streams generally have less energy than meltwater streams and, therefore, less ability to transport large particles. In non-glaciated terrains, sand and gravel deposits are formed as sedimentary basins on talus slopes, and as alluvial deposits in flood plains and beds and terraces of rivers and streams.

The electrical properties and physical behavior of sand and gravel deposits will depend significantly on moisture content of the materials. Dry sand and gravel deposits will have a high electrical resistivity and a low seismic velocity. Saturated sand and gravel deposits will have a much lower resistivity and can be further influenced by the presence of salinity. Seismic velocity will probably be somewhat higher than that for water, which is about 1500 m/second.

The success of a geophysical survey will largely depend on the contrast in physical properties the sand and gravel deposit provides with its surroundings. The main methods used are resistivity methods. Seismic methods may be used to define the bedrock topography, but will probably not be used as an exploration technique for sand and gravel deposits. Likewise, Ground Penetrating Radar (GPR) methods may also be used if conditions permit, but should

only be used for detailed surveys of existing deposits. Both of these methods are somewhat labor intensive and not appropriate for regional surveys.

Geophysical methods are used to better define existing sand and gravel deposits and to search for new sand and gravel deposits. If the goal is to better define an existing deposit, detailed geophysical surveys will probably be appropriate. These may include any of the methods mentioned earlier. If the goal is to find new deposits, the area for the search will dictate the investigation method. If very large areas are of interest, then airborne geophysical methods, such as resistivity mapping, may be appropriate. In this case, a search is made for resistivity highs. A brief description of airborne surveys is described later in this section of the document.

Understanding the relationship of the sand and gravel deposits with the bedrock may be important. Figure 156 shows where sand and gravel is deposited in a simple geology on top of horizontal bedrock. In this case, the effect of the bedrock on the geophysical data is constant over the section and does not unduly complicate the interpretation.

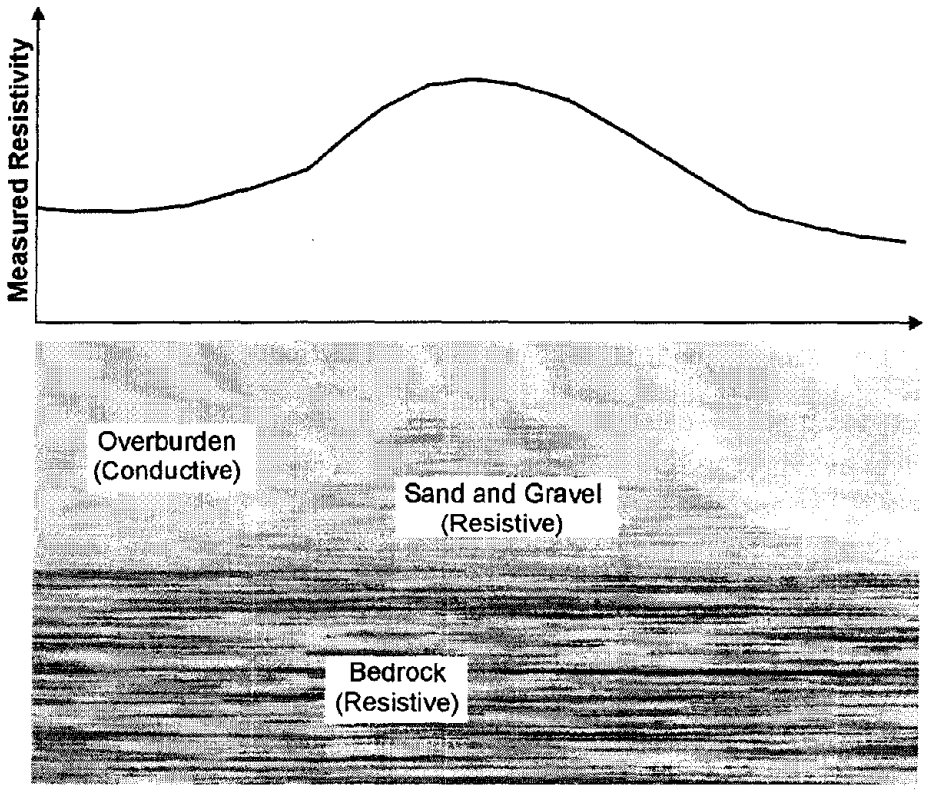

Figure 156. Sand and gravel - geological model.

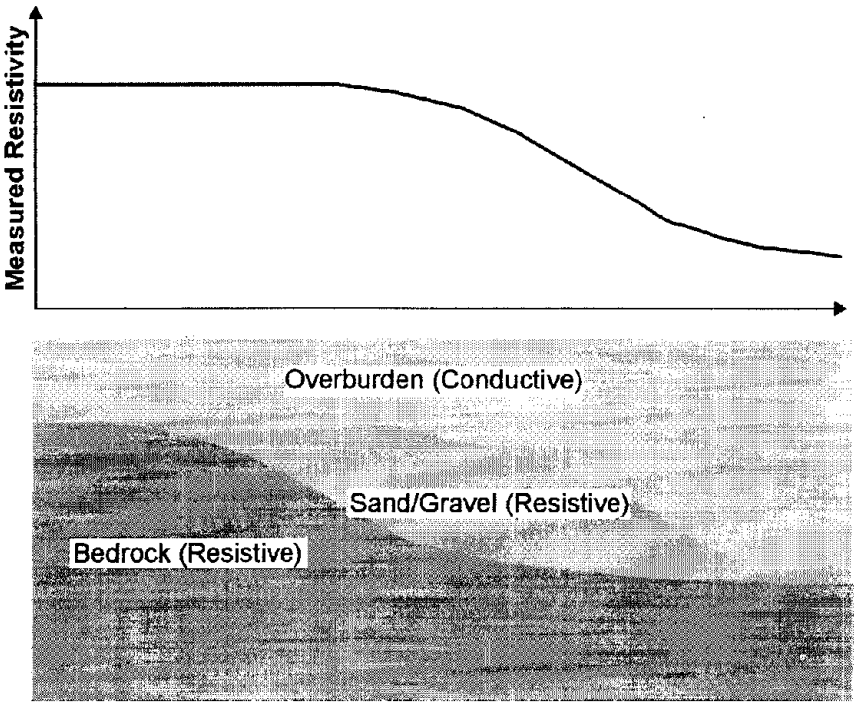

Figure 157. Sand and gravel deposit resting on bedrock slope.

However, figure 157 shows a more complex section where sand and gravel rests on a bedrock slope beneath an electrically conductive overburden. Both the sand and gravel and the bedrock are assumed to electrically resistive. Measurements of the electrical resistivity (or conductivity) over the sand and gravel deposit would not clearly define its position, since the bedrock and sand and gravel deposit are both electrically resistive. In fact, the resistivity measurements could be interpreted as simply indicating the bedrock topography. In this case, a different method is needed to define the bedrock surface. Since bedrock usually has a higher seismic velocity than either the sand and gravel or the overburden, resistivity measurements could be used to map the bedrock surface. Knowing the bedrock topography, along with the resistivity profile, should allow an interpretation of the extent of the sand and gravel deposit to be made.

Methods

6.1.4.1 Resistivity; Soundings, and Traverses

Basic Concept: The resistivity of the ground is usually measured using one of several four-electrode arrays. These arrays are shown in figure 90. Resistivity is measured by passing electrical current into the ground using two electrodes and measuring the resulting voltage using two other electrodes.

These arrays are used for different types of resistivity surveys. The Schlumberger array is often used for resistivity soundings, as is the Wenner array. The Pole-pole array provides the best signal, but is cumbersome because of the long wires required for the remote electrodes, and it is rarely used. The Dipole-dipole array was originally used mostly by the mining

industry for induced polarization surveys. Readings were taken using several different separations of the voltage and current dipoles providing measurements of the variation of resistivity with depth. Long lines of data were recorded requiring many readings. This array has now become common for resistivity surveys using the automated resistivity systems. If more signal (voltage) is needed than can be provided with the Dipole-dipole array, the Pole-dipole array can be used.

Resistivity measurements using the Schlumberger array are illustrated in figure 91. By enlarging the electrode spacing, deeper layers are imaged. If resistivity measurements from a number of electrode spacings are used, a plot of measured resistivity against electrode spacing can be drawn. This is called a resistivity sounding curve. At large electrode spacings, the measured resistivity is close to that of the bedrock, i.e. Rho2 (figure 91b). When the electrode spacings are small, the measured resistivity is close to that of the overburden, i.e. Rho1 (figure 91b).

Data Acquisition: Resistivity measurements can be made along traverses using one electrode spacing, thus providing the lateral variation of resistivity. However, this method is rarely used and will not be discussed further, since electromagnetic techniques are available to measure conductivity (inverse of resistivity) that do not require ground contact and are much more efficient. However, the resistivity method is still used to obtain the vertical distribution of resistivity, called resistivity soundings, as discussed previously.

Data Processing: The most important thing is to remove bad data points.

Data Interpretation: Resistivity soundings curves can be interpreted to give the resistivities and thickness of the layers imaged under the sounding site. This is done using software that modifies an initial model input by the interpreter such that the model data match the field data. The data are usually checked for bad data points before interpreting.

Resistivity soundings could be used to measure the vertical distribution of resistivity over an area of interest. If the method were used to search for unsaturated sand and gravel, the objective would probably be to search for electrically resistive regions. In addition, if the bedrock provided a good resistivity contrast with the overburden and was imaged by the resistivity soundings, then the bedrock depth could also be obtained. If the area was saturated, then the resistivity contrast with the host rocks will likely be smaller.

Advantages: Resistivity soundings prove an efficient and effective method of measuring the resistivity of the ground down to depths of 100 feet or more.

Limitations: The method is quite labor intensive since four electrodes have to be inserted into the ground for every resistivity reading. A sounding curve may have 15 measured resistivities, depending on the complexity of the geologic section.

The measured resistivity is influenced by nearby metal fences and other grounded metal objects. If the ground is hard then more effort is needed to place the electrodes and water may need to be poured on to the electrodes to improve the electrical contact between the electrode and ground.

Automated Resistivity Systems

Basic Concept: Resistivity measurements can be taken using recently developed instruments that use addressable electrodes, called Automated Resistivity systems. With these systems, the required electrodes are planted prior to recording data, and the wires between all of the electrodes and the recorder are also connected. The recorder is programmed with the electrode array to be used along with other data recording parameters and instructed to take the measurements. The system automatically records the data according to these preset instructions, automatically switching between electrodes as needed. One such system is called a Sting/Swift system illustrated in figure 201.

This system provides detailed resistivity data and is probably not suited to explore large areas. If large areas are to be explored, other methods should probably be used as reconnaissance techniques, and this technique used for detailed analysis of interesting areas. Conductivity methods, discussed in the next section, may be appropriate for reconnaissance.

Data Acquisition: As discussed previously, data are recorded automatically by the instrument. If long lines are required to be recorded, the system is moved along the line a specified distance and the data recording procedure repeated. The data are plotted as sections showing the variation of resistivity with depth, as illustrated in figure 202.

Data Processing: Little processing is applied to the measured resistivity data, although bad data points may need to be removed.

Data Interpretation: Interpretation is done using inversion software. The software iteratively modifies a preliminary model input by the interpreter until the calculated model data fit the field data, a process called inversion.

Advantages: Automated resistivity systems proved an efficient system for recording field data.

Limitations: The methods that require electrodes are difficult to use in areas where the surface of the ground is hard, such as concrete or asphalt-covered areas or frozen ground. In addition, if the contact between the electrode and ground is poor, as in rocky soil, water may need to be poured on the electrodes to lower the resistance to ground of the electrodes.

If data are only recorded along one line, lateral variations in resistivity normal to the line will not be accounted for. However, recording lines parallel to each other can rectify this problem. In addition, three-dimensional surveys can be recorded. Cultural features such as power lines, fences, and other metal features may provide false anomalies. These cultural features will have to be noted in the field and accounted for in the interpretation.

Another fairly recently developed instrument for measuring the resistivity is called the Ohm-Mapper, manufactured by Geometrics. This instrument has a series of electrodes on a cable that is dragged at a slow pace along the ground. Current is induced into the ground, and the resulting voltages measured. The electrodes are capacitively coupled to the ground and both transmit current into the ground and measure the resulting voltage. The Ohm-Mapper instrument being towed along the ground surface is shown in figure 200.

The instrument appears to provide the best results in resistive environments and is generally limited to fairly shallow surveys of less than about 10 m.

6.1.4.2 Conductivity Measurements

Basic Concept: Electrical conductivity measurements can be made over an area and a map produced showing the conductivity down to a particular depth. These data can be used to locate anomalous conductivity zones that may correspond to sand and gravel deposits.

Conductivity measurements can also be taken to map the vertical distribution of layers under the sounding site. The method used for this purpose is called Time Domain Electromagnetic Soundings (TDEM). However, this method is best suited to depths greater than 10 m in moderate-to-high conductivity sections and is less appropriate in resistive conditions. Thus, the method is unlikely to be frequently used for sand and gravel exploration unless thick deposits are expected. This method is probably more appropriate for mapping existing deposits than exploring large areas for new deposits.

Ground conductivity measurements are recorded using several instruments that use electromagnetic methods. The choice of which instrument to use generally depends on the depth of investigation desired. Instruments commonly used include the EM38, EM31, EM34, and GEM2. Since the EM38 has a maximum exploration depth of about 1.5 m, it is not appropriate for sand and gravel exploration and is not discussed in this section of the document.

The EM31 has a depth of investigation to about 6 m, and the EM34 has a maximum depth of investigation to about 60 m. The depth of investigation of the GEM2 is advertised to be 30 to 50 m in resistive terrain (>1,000 ohm-m) and 20 to 30 m in conductive terrain (<100 ohm-m).

Electromagnetic instruments that measure ground conductivity use two coplanar coils, one for the transmitter and the other for the receiver. The transmitter coil produces an electromagnetic field, oscillating at less than 10 kHz (EM31 and EM34) and from 330 Hz to 24 kHz for the GEM2. This oscillating electromagnetic field produces secondary currents in conductive materials in the ground. The amplitude of these secondary currents depends on the conductivity of the material. The secondary currents produce a secondary electromagnetic field that is recorded by the receiver coil.

These instruments can be used with the planes of the coils held parallel to the ground (vertical dipole mode) or perpendicular to the ground (horizontal dipole mode). The investigation depth is greatest in the vertical dipole mode and least in the horizontal dipole mode. In addition, in the vertical dipole mode, the conductivity readings are insensitive to near-surface conductivity changes, whereas in the horizontal dipole mode, the readings are significantly influenced by near-surface conductivity changes. Figure 183 shows the EM31 instrument being used in vertical dipole mode. Figure 197 shows the EM34 being used in horizontal dipole mode, and the GEM3 instrument is shown in figure 219.

The EM31 is effective to depths of about 6 m. If conductivity measurements are required to greater depths then the EM34 can be used. This instrument can be used to depths up to about

60 m. Three different separations of the two coils can be used providing six different depths of investigation (three coil separations and two modes for each separation). However, as the depth of investigation increases, the lateral resolution decreases. The EM34, unlike the EM31, requires two people to operate. Data recording is also much slower than with the EM31. All of these instruments measure the bulk electrical conductivity of the ground. Since the conductivity of several different layers may be included in the conductivity measure, the correct technical term for the measured conductivity is apparent conductivity. The term terrain conductivity is also often used to describe the conductivity values. When discussing data from these instruments in this document, conductivity or measured conductivity is understood to mean apparent (or terrain) conductivity.

Data Acquisition: Surveys are conducted by taking readings along lines crossing the area of interest. These lines need to be surveyed in order to have spatial coordinates recorded. Readings are taken either at defined stations or on a timed basis, e.g., every second (EM31). The mode in which the instruments are used depends on the target depth and the objectives. The instruments store the data in memory, allowing the data to be downloaded to a computer later. Surveys can be conducted using different coil spacings (EM34) and modes (EM31 and EM34, horizontal and vertical dipole modes) providing different investigation depths.

Data Processing: Data processing involves assigning coordinates to each data point. These data are then gridded, contoured, and plotted, producing a map of the measured conductivity of the site.

Data Interpretation: Interpretation is done from this map. Generally, this will involve searching for areas of low electrical conductivity (high resistivity). These areas will be the most likely places to find sand and gravel deposits.

In cases where data have been recorded with different modes and coil spacings, a layered model can be produced using inversion software.

Advantages: The EM31 and EM34 both provide efficient methods for mapping lateral changes in conductivity.

Limitations: The instruments transmit an electromagnetic field to produce secondary currents in conductive regions of the ground. However, currents are also generated in metal objects on the ground surface, such as fences and pipelines. The electromagnetic fields from these objects are detected by the receiver coil, in addition to fields from geological targets, making interpretation of the data difficult.

Measurements of conductivity simply map the conductivity of the ground to the depth of investigation of the instrument. Complex geological situations, such as that illustrated in figure 157, cannot be interpreted from these data alone. Conductivity or resistivity measurements along a traverse using a single coil (conductivity) or electrode (resistivity) spacing do not provide meaningful depth information beyond the broad investigation depth information provided by the coil or electrode spacing. Thus, the measurements could be responding to the bedrock geology as well as the overburden. Other methods, such as

electrical soundings or seismic refraction will typically be needed to map the bedrock depths, allowing a more comprehensive interpretation.

6.1.4.3 Time Domain Electromagnetic Soundings

Basic Concept: Time Domain Electromagnetic (TDEM) soundings are another method for obtaining the vertical distribution of the resistivity of the ground. This method is particularly well suited to mapping conductive layers. To a significant degree, this method has now superseded the resistivity sounding method since it requires less work for a given investigation depth and generally provides more precise depth estimates. However, resistivity soundings are still useful for shallow investigations or when resistive targets are sought. Figure 120 provides a conceptual drawing of the TDEM method.

TDEM soundings are an electromagnetic method used to provide the vertical distribution of resistivity within the ground. A square loop of wire is laid on the ground surface with a side length that is about half of the desired depth of investigation. A receiver coil is placed in the center of the transmitter loop. Electrical current is passed through the transmitter loop and then quickly turned off. This sudden change in the transmitter current causes secondary currents to be generated in the ground. These currents decay for longer times in more conductive rocks. The relationship between the time after the transmitter current has turned off (delay time), layer depth, and conductivity is quite complex, although generally, longer delay times are needed to investigate to greater depths.

The voltage measured by the receiver coil does not decay instantly to zero when the current is turned off, but continues to decay for some time. This decaying voltage is caused by the decaying secondary electrical currents in the ground. The receiver measures this voltage, which is then converted to measured resistivity. A plot is made of the measured resistivity against the delay time, as illustrated in figure 121.

The resistivity sounding curve shown in figure 121 illustrates the curve that would be obtained over three-layered ground. The near-surface layer is fairly resistive. This is followed by a layer having a much lower resistivity (higher conductivity) and causes the measured resistivity values to decrease. The third layer is again resistive.

Data Acquisition: The field layout for a TDEM survey is described previously. Switched current is passed through the transmitter loop, and the resulting voltage is measured by the receiver coil. The switching and measuring procedure is repeated many times, allowing the resulting voltages to be stacked and improving the signal-to-noise ratio. Soundings are conducted at additional locations until the area of interest has been covered. Sounding curves are plotted for each location showing the measured resistivity against decay time.

Data Processing: Little processing is applied to the data, although bad data points may sometimes be removed.

Data Interpretation: Sounding curves are interpreted using computer software to provide a model showing the layer resistivities and thickness. The interpreter inputs a preliminary model into this software program, which then calculates the sounding curve for this model. It adjusts the model and calculates a new sounding curve that better fits the field data. This

process, called inversion, is repeated until a satisfactory fit is obtained between the model and the field data. The sounding curve shown in figure 121 illustrates the type of curve expected over a conductive shale layer.

Advantages: TDEM soundings are an efficient method for investigating the vertical distribution of ground resistivity. Generally, the method is better suited to mapping conductive formations rather than resistive formations. However, bedrock is usually more resistive than the overburden, and, provided the bedrock is not too shallow or resistive, the TDEM method should be applicable.

Limitations: The interpretation of the TDEM method assumes that the layers are horizontal and homogeneous; incorrect interpreted resistivities and/or depths will result if this is not the case. However, this should not be a serious problem for mapping bedrock depths.

Probably the most troublesome aspect of data recording is the influence of fences, power lines, and other cultural features at the survey site.

6.1.4.4 Airborne Resistivity

Basic Concept: Airborne resistivity methods may be appropriate when large areas are to be explored for sand and gravel deposits. Airborne surveys can be conducted using either a fixed wing aircraft or a helicopter.

Figures 158 and 159 show fixed wing aircraft and helicopter conductivity (resistivity) measuring systems. In the fixed wing aircraft, the transmitter loop is the wire that can be seen encircling the aircraft and attached to the nose, wings, and tail. The electromagnetic instrumentation for the helicopter system is mounted in a cylindrical boom and attached to the helicopter using a long cable.

Specialized equipment mounted in small planes or helicopters is used to collect data on the magnetism or electromagnetic conductivity of rock over large areas.

Data Acquisition: Airborne geophysical surveys require very specialized knowledge and only a very brief discussion is presented in this document.

Most airborne surveys now use GPS for navigation. Lines are planned before surveying begins and transmitted to the pilot during flights using electronic instrumentation that guides him to the correct line to be surveyed.

Figure 158. Fixed wing airborne conductivity system. (Fugro Airborne Surveys)

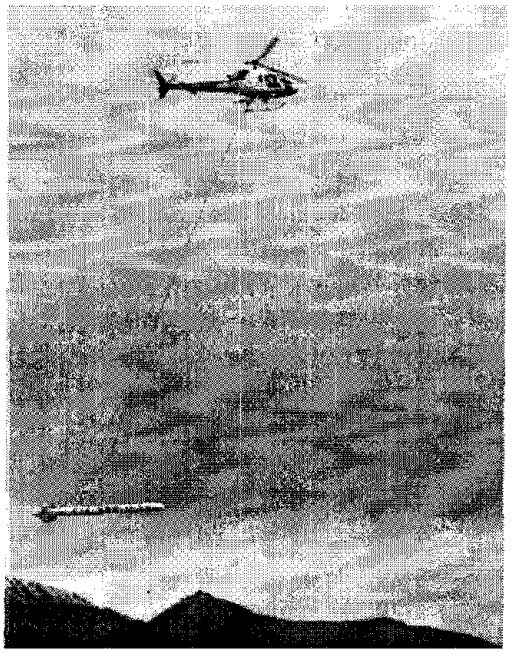

Figure 159 . Helicopter conductivity measuring system. (Fugro Airborne Surveys and John Holland, ERA Helicopters)

Data Processing: Depending on the type of survey conducted, a significant amount of processing may be required to correct for various factors. The final product is usually a map showing the conductivity (or resistivity) of the area surveyed.

Data Interpretation: The data is interpreted by observing the changes in resistivity and searching for more resistive areas. The results from an airborne survey for sand and gravel are illustrated in figures 160 and 161.

Figure 160 shows the high resistivity areas that were found to be sand and gravel deposits. A section across anomaly A has been drawn, showing the measured resistivity and the drill results and is presented in figure 161.

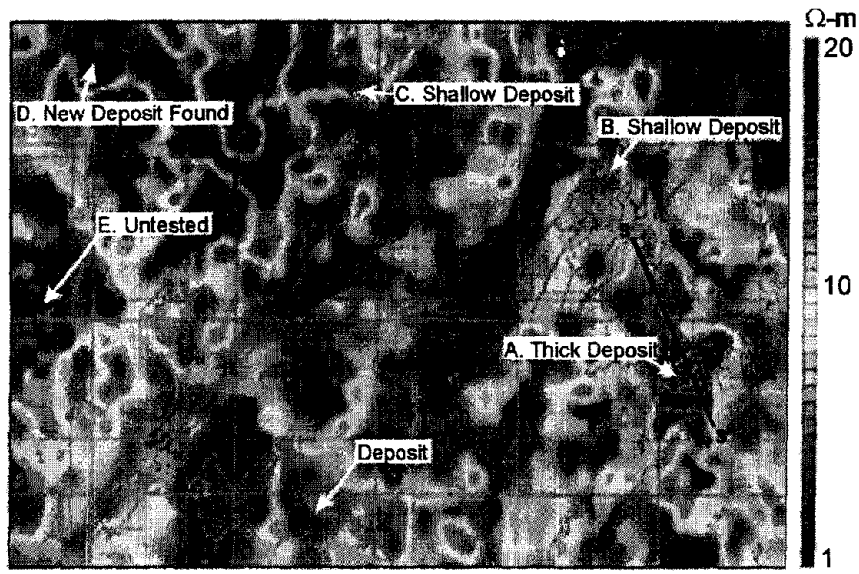

Figure 160. Results from an airborne survey for sand and gravel. (Fugro Airborne Surveys)

This survey was flown and processed by Fugro Airborne Surveys over an area in Saskatchewan, Canada.

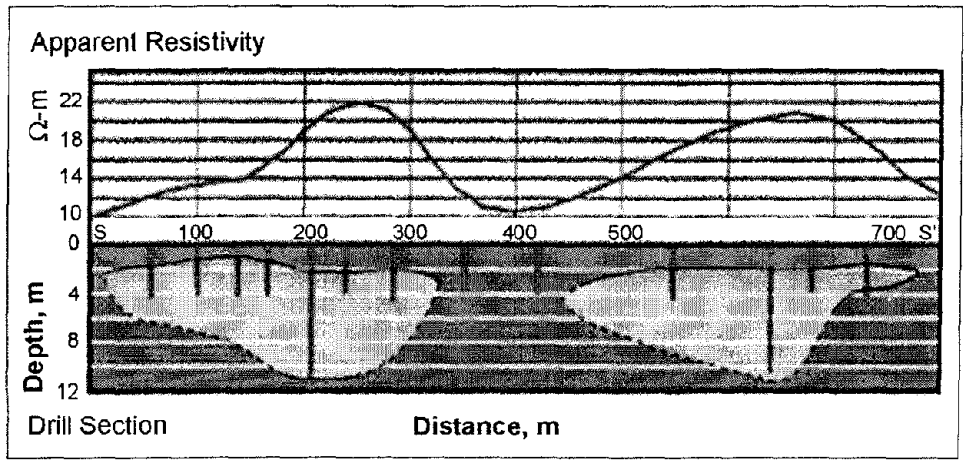

Figure 161. Section showing drill results and resistivity values over a sand and gravel deposit. (Fugro Airborne Surveys)

6.1.4.5 Seismic Refraction

Basic Concept: Seismic refraction methods will most likely be used to better define the boundaries of existing deposits. They may be used to map the bedrock depths over an area of interest for sand and gravel deposits. Areas where the bedrock is deepest will be of greatest interest. This method may be useful for geologic sections illustrated in figure 157.

Seismic refraction is one of the most commonly used methods for finding bedrock depths, especially for depths of less than 30 m. The method requires a seismic energy source,

usually a hammer for depths of less than 15 m and black powder charges for depths to 30 m. The seismic waves then penetrate the overburden and refract along the bedrock surface. While they are traveling along this surface, they continually refract seismic waves back to the ground surface. These are detected by geophones placed on the ground surface. Both compressional waves and shear waves can be used in the seismic refraction method, although compressional waves are most commonly used. Figure 114a shows the layout of the instrument, the main seismic waves involved, and the resulting time distance graph.

Data Acquisition: The design of a seismic refraction survey requires a good understanding of the expected bedrock and overburden. With this knowledge, velocities can be assigned to these features and a model developed that will show the parameters of the seismic spread best suited for a successful survey. These parameters include the length of the geophone spread, the spacing between the geophones, the expected first break arrival times at each of the geophones, and the best locations for the off-end shots. Knowing the expected first break arrival times is also helpful in the field, where field arrival times that correspond fairly well to expected times help to confirm that the spread layout has been appropriately planned, and that the target layer is being imaged.

Data Processing: The first step in processing/interpreting refraction seismic data is to pick the arrival times of the seismic signal, called first break picking. A plot is then made showing the arrival times against distance between the shot and geophone, called a time-distance graph. An example of such a graph for a two-layered ground (overburden and refractor) is shown in figure 114a.

The time distance plot shows the waves arriving at the geophones directly from the shot (V1) and the refracted waves that arrive ahead of the direct waves (V2). These refracted waves have traveled a sufficient distance along the higher speed refractor (bedrock) to overtake the direct wave arrivals.

Data Interpretation: One of the most common methods of refraction interpretation is Generalized Reciprocal Method (GRM) that is described in detail in the Geophysical Methods section. A brief, and simplified, description of the GRM method is presented below. Figure 115 shows the basic rays used for this interpretation.

The objective is to find the depth to the bedrock under the geophone at D. This is done using the following simple calculations. The travel times from the shots at A and G to the geophone at D are added together (T1). The travel time from the shot at A to the geophone at G is then subtracted from T1. Figure 116 shows the remaining waves after the above calculations have been performed. These are the travel times from C to D added to the travel times from E to D, subtracting the travel time from C to E. The sum of these travel times can be shown to be approximately the travel time from the bedrock at H to the geophone at D. Since the velocity of the overburden layer can be found from the time distance graph, the distance from H to D can be found giving the bedrock depth.

Advantages: The seismic refraction method may be useful to map the thickness of a sand and gravel deposit if the base has a higher velocity than the sand and gravel. In this can thee method provides reasonably accurate depth estimates.

Limitations: Probably the most restrictive limitation is that each of the successively deeper refractors must have a higher velocity than the shallower refractor. However, for determining bedrock depths, this is probably not a significant limitation since the bedrock usually has a higher velocity than the overburden.

If the water table is in the overburden and close to the bedrock, this may obscure the bedrock arrivals since saturated soils have a higher velocity than unsaturated soils. This could also limit the velocity difference between the bedrock and saturated overburden, making it difficult to observe the bedrock with the seismic refraction method.

Local noise, for example traffic, may obscure the refractions from the bedrock. This can be overcome by using larger impact sources or by repeating the impact at a common shot point several times and stacking the received signals. In addition, since some of the noise travels as airwaves, covering the geophones with sound absorbing material may also help to dampen the received noise.

6.1.4.6 Ground Penetrating Radar

Basic Concept: The Ground Penetrating Radar (GPR) method is not expected to be commonly used for exploration of sand and gravel deposits. However, there may be occasions where its use is justified, and it is described here for that reason. If the method is used, it seems likely that the target will be the bedrock depth.

GPR can be used where the bedrock is expected to be shallow, and the overburden is unsaturated and contains no clay or silt. If these conditions exist, penetration depths may be a few meters. The GPR instrument consists of a recorder and a transmitting and receiving antenna. Different antennas provide different frequencies, which vary between 25 MHz to 1500 MHz. Lower frequencies provide greater depth penetration but lower resolution. Figure 111 provides a drawing illustrating the GPR system. The transmitter provides the high frequency electromagnetic signals, which penetrate the ground and are reflected from objects and boundaries providing a different dielectric constant from that of the overburden. The reflected waves are detected by the receiver and stored in memory.

Figure 112 shows typical GPR equipment. This picture shows the display and the controls for the equipment.

Figure 113 shows a 100 MHz antenna being pulled across the ground as the survey is conducted. This is a fairly low-frequency antenna and can provide penetration to about 20 m, depending on the ground conditions.

Data Acquisition: GPR surveys are conducted by pulling the antenna across the ground surface at a normal walking pace, as shown in figure 113. The recorder stores the data as well as presenting a picture of the recorded data on a screen. Surveys for sand and gravel are likely to be done using the lower frequency antenna since depth of penetration is more important than resolution.

Data Processing: It is possible to process the data, much like the processing done on single-channel reflection seismic data. Processes that may be applied include distance

normalization, horizontal scaling (stacking), vertical and horizontal filtering, velocity corrections, and migration. However, depending on the data quality, this may not be done since the field records may be all that is needed to observe the bedrock.

Data Interpretation: The data are usually interpreted visually. If the target is the bedrock, a horizontal, or sub horizontal, reflector would be observed at the expected depth. To calculate the depth to the bedrock, the speed of the GPR signal in the soil at the site needs to be obtained. This can be estimated from charts showing speeds for typical soil types, or it can be obtained in the field by conducting a small traverse across a buried feature whose depth is known.

Advantages: The method is easy to use and provides a visual display of the results as the survey progresses. Different antenna, providing different penetration depths and resolution, can easily be tested.

Limitations: Probably the most limiting factor for GPR surveys is that their success is very site specific and depends on having a contrast in the dielectric properties of the target compared to the host overburden along with sufficient depth penetration to reach the target. The method is slow compared to recording conductivity data with the EM31 or EM34. It is more suited to defining the extent of existing sand and gravel deposits and will probably find little use in exploring new areas.

If the sand and gravel deposit contains a significant amount of cobbles, these may reflect and scatter the GPR signal, resulting in only a small amount of energy reaching the bedrock surface. In this case, the bedrock surface may not be observed with this method.

*6.*1.5 Mapping Groundwater Surface and Flow

The groundwater surface lies at depths ranging from the ground surface to many hundreds of feet. The exact configuration of this surface depends on the geology of the area, topography, and precipitation. In sedimentary areas, the configuration depends on the type of sediments and their grain size. In hard-rock areas, the groundwater surface may exist in the alluvium above the bedrock. If this is not the case, then groundwater may exist in fractures within the rocks, and a well-defined water table may not exist.

The groundwater surface is usually related to the topographic surface, although with smaller elevation changes. Thus the depth to the water table on top of a hill is usually greater than the depth in a valley. Streams and lakes occur where the water table reaches the topographic surface. Figure 162a shows several important features about groundwater and the water table.

If the bedrock is impervious, such as granite and other igneous and/or metamorphic rocks, groundwater can rest in hollows on top of the bedrock, as is illustrated in figure 162b. The situation shown in figure 162b is much less common than that illustrated in figure 162a.

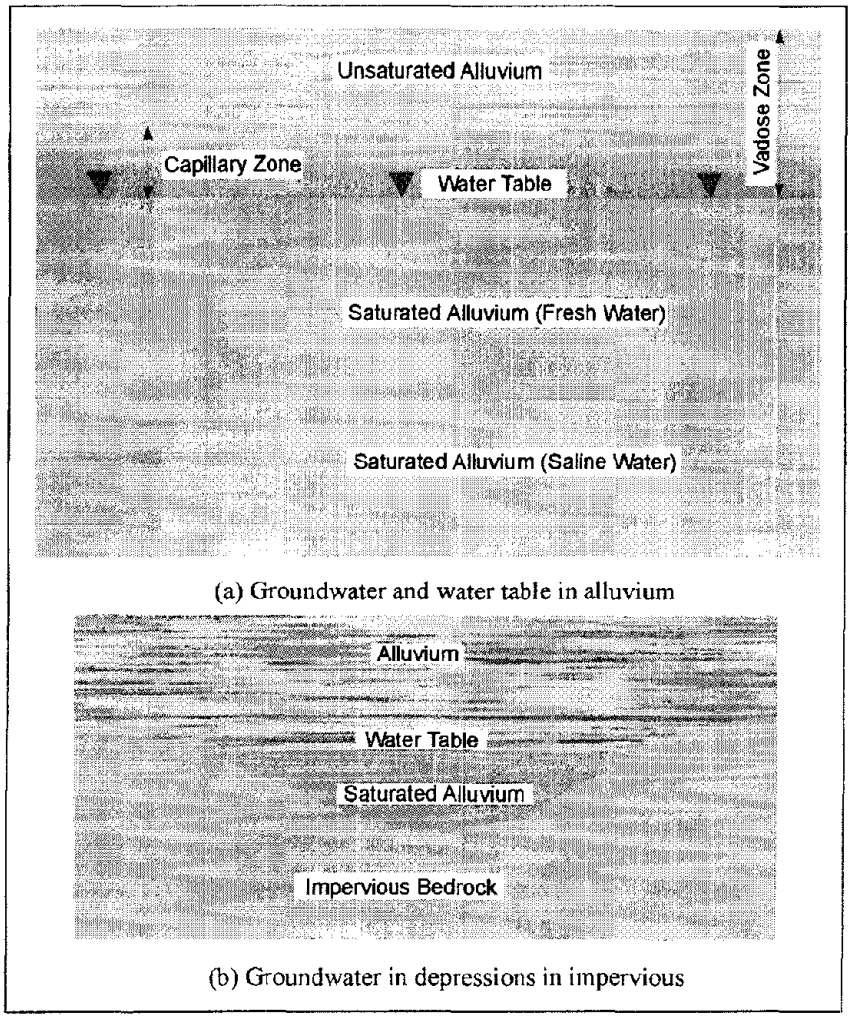

Figure 162. Two common groundwater occurrences.

Groundwater occurs in aquifers, which can be classified as unconfined or confined. In an unconfined aquifer, the water only partially fills the aquifer, and the upper surface is free to rise and decline. Unconfined aquifers are also known as water table aquifers. In a confined aquifer, water completely fills the aquifer, which is overlain by a confining bed, called an aquitard. Aquifers can also be perched, in which an aquitard restricts the downward movement of the water.

Geophysical methods are most applicable to mapping the surface of the water table aquifer, although saturated fracture zones can also be detected. Perched aquifers will probably be difficult to detect because the contrast in physical properties with the surrounding rocks will probably be small. Therefore, the following discussions refer to groundwater and the water table in alluvial geology. Figure 162a shows unsaturated alluvium that transitions into saturated alluvium at depth. The transitional nature of the change from unsaturated to saturated alluvium is caused by capillary action, which draws water from the saturated zone into the unsaturated zone. The height of the capillary zone depends significantly on the grain size of the alluvium. If the alluvium were mostly cobbles, which could be classified as very

large grain sizes, there would be very little capillary action, and the capillary zone would be very small. In this case, the water table is well defined and is the best case for detection by geophysical means.

If, however, the alluvium is fine grained, then the height of the capillary zone can be quite large. In this case, the water table is very poorly defined, making its surface more difficult to map. Eventually, at some depth, the fresh water usually becomes more saline. The thickness of the fresh water layer varies considerably from a few meters to many hundreds of meters.

The physical properties that may be used to map the top of the water table are resistivity and seismic velocity. Ground Penetrating Radar (GPR) may also be useful for some locations. One new method that has been investigated is called Nuclear Magnetization Resonance (NMR), which will be briefly discussed along with a method called the Electroseismic method that is said to provide hydraulic conductivity values.

As discussed previously, when there is a large capillary zone, the measurable physical properties change gradually from the unsaturated zone to the saturated zone. Thus, resistivity changes gradually from being resistive to conductive; this is the same for seismic velocity.

Methods

Groundwater Surface

6.1.5.1 Resistivity Soundings

Basic Concept: Mapping the groundwater surface will usually require sounding methods. Resistivity, or conductivity, soundings may be appropriate since there may be a significant resistivity contrast between the unsaturated soil and the saturated alluvium. Generally, the contrast will be greater for coarse-grained alluvium than for fine-grained alluvium. This is because fine-grained unsaturated alluvium can hold and retain more moisture than coarse-grained alluvium.

Ground resistivity is measured using four electrodes inserted into the ground. Two of the electrodes are used to pass electrical current into the ground, and the other two are used to measure the resulting voltage. A number of different electrode arrays are used and are illustrated in figure 90. The Schlumberger array is often used for resistivity soundings, as is the Wenner array. The Pole-pole array provides the best signal but is cumbersome because of the long wires required for the remote electrodes, and it is rarely used. The Dipole-dipole array was originally used mostly by the mining industry for induced polarization surveys. Readings were taken using several different separations of the voltage and current dipoles providing measurements of the variation of resistivity with depth. Long lines of data were recorded requiring many readings. This array has now become common for resistivity surveys using the automated resistivity systems. If more signal (voltage) is needed than can be provided with the Dipole-dipole array, the Pole-dipole array can be used.

Resistivity data can be recorded using one electrode spacing and taking readings along a traverse or by taking readings using a number of different electrode spacings while keeping the location of the center of the array fixed. When the center of the array remains fixed, it is

called a resistivity sounding. To map water table depths only, resistivity soundings are likely to be used since resistivity traverses would only provide lateral changes in resistivity and not depths. However, for detailed surveys, automated resistivity systems, which record data using many electrode spacings, may be used. These are described later in this section.

Figure 91 shows resistivity measured with the Schlumberger electrode array (figure 91a) and the sounding curve (figure 91b) over an unsaturated resistive near-surface layer and conductive saturated layer. In this figure, the current is injected into the ground using the two outer electrodes, and the resulting voltage is measured using the two inner electrodes. Figure 91b is a plot of the measured resistivities against the current electrode spacing. As figure 91b shows, at small electrode spacings the measured resistivity approaches that of the near-surface unsaturated layer, whereas at large electrode spacings, the measured resistivity approaches that of the saturated layer.

Since the measured resistivity is usually a composite of the resistivity of several layers, the term "Apparent Resistivity" is usually used. In this document, the term Apparent Resistivity is usually named simply as "measured resistivity." Apparent Resistivity is calculated using the equations shown at the bottom of figure 91.

To conduct a resistivity sounding, resistivity data are recorded at a number of electrode spacings, since electrode spacing determines the depth of investigation. These resistivity values are then plotted against the electrode spacing used to obtain the measurements to produce a resistivity sounding curve, illustrated in figure 91b. Figure 163 shows an instrument used to measure the resistivity of the ground.

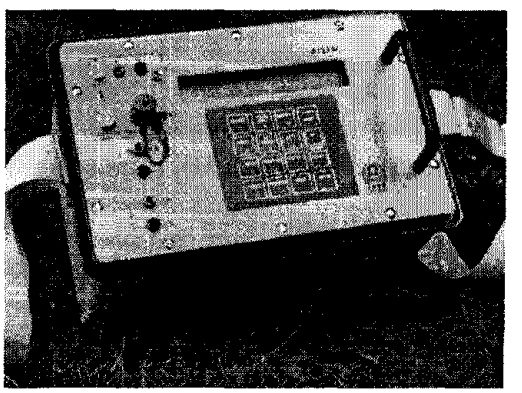

Figure 163. Resistivity instrument. (IRIS Instruments)

Data Acquisition: Resistivity soundings are conducted by initially planting the electrodes in the ground using a fairly small electrode spacing (a few meters) and taking a reading. This process is repeated using larger electrode spacings while keeping the center of the array fixed until the desired layer is imaged. It is usually advisable to plot the resistivity sounding curve in the field in order to evaluate the data. Where the groundwater surface is desired, data will be recorded from successively larger electrode spacings until the measured resistivity values are clearly decreasing, showing that a conductive layer has been imaged.

Data Processing: Bad data points need to be removed after which the measured resistivity data are plotted against electrode spacing, and a preliminary interpretation made.

Data Interpretation: The resistivity sounding data and the model are input to a computer program that inverts the data to produce a layer depth and resistivity model whose sounding curve matches that of the field data. Inversion is a process whereby the computer program calculates the sounding curve from the model and then compares this with the field data. It appropriately modifies the model and calculates another sounding curve, repeating this process until the sounding curve from the model matches that from the field data.

Advantages: Resistivity soundings are fairly easy to record and are an effective sounding technique down to depths of 50 meters, depending on the geology. A sounding curve can be plotted in the field and can be visually interpreted to provide very approximate estimates of the subsurface resistivities and depths.

Limitations: Resistivity soundings require electrodes to be placed in the ground. If the ground surface is hard, placing the electrodes may be difficult. The interpretation of resistivity soundings assumes that the geological layers under the sounding site are horizontal and homogeneous, with no lateral changes in resistivity. If these conditions are not met, the interpretation will not be correct. Errors in the field data can occur if soundings are recorded close to grounded metallic features such as fences.

Generally, the separation between the current electrodes will need to reach a maximum of about three times the investigation depth. Thus, if the bedrock is 15 m deep, the current electrodes will need to be spaced up to 46 m apart.

Automated Resistivity Systems

Basic Concept: Resistivity systems are available that make taking resistivity measurements much more efficient, automatically taking many measurements at different electrode spacings along a traverse. These systems are able to build a comprehensive picture of the subsurface, combining both lateral and vertical variations in resistivity. Figure 201 shows an example of automated resistivity measuring system called the Sting/Swift system.

Data Acquisition: With these systems, many electrodes are planted and connected to the central recorder before taking any data. When this is done, the recording parameters for the survey are entered into the instrument, and data recording is initiated. The instrument automatically records all of the required data, selecting the electrodes as needed.

Data Processing: Probably the only processing which needs to be done is the removal of bad data points.

Data Interpretation: Data from the automated resistivity system are interpreted by inversion software, although much information can be gained visually. An example of the results from such a survey is presented in figure 135. These data show a low resistivity zone, which was later shown to be a water-bearing fracture. The data have been inverted showing the resistivity variation, both laterally and vertically, against depth. Software to interpret three dimensional resistivity surveys is now available.

Advantages: The Automated Resistivity system allows a considerable amount of data to be recorded quite efficiently. Fairly detailed interpretations are possible with this data.

Limitations: Three different methods (traverses, soundings, and automated resistivity system) of using the resistivity method have been discussed above. All of them require electrodes be placed in the ground; thus, the resistivity method is difficult to use in areas where the surface of the ground is hard, such as concrete or asphalt-covered areas. If the ground is dry, water may need to be poured on the electrodes to improve the electrical contact between the electrode and ground.

Clearly the automated resistivity system provides the best interpretation, although it also requires the most effort. With this system, lateral variations in resistivity are recognized and solved for in the inversion process. If data are recorded along a single line, lateral variations in resistivity normal to the line are not accounted for. However, additional parallel lines can be recorded to minimize this potential problem, or a three-dimensional survey can be conducted.

6.1.5.2 Time Domain Electromagnetic Soundings

Basic Concept: Time Domain Electromagnetic (TDEM) soundings are used to obtain the vertical distribution of resistivity. This method is particularly well suited to mapping conductive layers. To a significant degree, this method has now superseded the resistivity sounding method since it requires less work for a given investigation depth and generally provides more precise depth estimates. However, resistivity soundings are still useful for shallow investigations or when resistive targets are sought.

Data Acquisition: To perform TDEM soundings, a square loop of wire is laid on the ground surface. The side length of this loop is about half of the desired depth of investigation. A receiver coil is placed in the center of the transmitter loop (figure 120). Electrical current is passed through the transmitter loop and then quickly turned off. This sudden change in the transmitter current causes secondary currents to be generated in the ground. The currents in a conductive layer decay at a slower rate than those in a resistive layer. However, the relationship between the voltage at a particular time after the current is turned off (delay time) and the conductivity and depth of layers under the sounding site is complex, although, longer delay times generally correspond to greater depths.

The voltage measured by the receiver coil does not decay instantly to zero when the current is turned off but continues to decay for some time. This decaying voltage is caused by the decaying secondary electrical currents in the ground. The voltage measured by the receiver is then converted to resistivity. A plot is made of the measured resistivity against the time after the transmitter current is turned off (delay time), as illustrated in figure 121.

The resistivity sounding curve shown in figure 121 illustrates the curve that would be obtained over three-layered ground. The near-surface layer is fairly resistive. This is followed by a layer having a much lower resistivity (higher conductivity) and causes the measured resistivity values to decrease. The third layer is again resistive.

The field layout for TDEM soundings is described earlier. Switched current, as described earlier, is passed through the transmitter loop, and the resulting voltage is measured by the receiver coil. The switching and measuring procedure is repeated many times, allowing the resulting voltages to be stacked, thereby improving the signal-to-noise ratio. This procedure is repeated at different sounding locations until the area of interest has been covered. A sounding curve is plotted for each location showing the measured resistivity against decay time.

Data Processing: Little processing is applied to the data, apart from possibly the removal of bad data points.

Data Interpretation: Interpretation is usually done by inverting the TDEM sounding curves to give interpretations of the resistivity and depths of the layers under the sounding site.

Advantages: The TDEM method is an efficient method for obtaining the subsurface layer resistivities and thicknesses. It should provide an effective method for mapping the groundwater surface providing a resistivity contrast exist with the host materials. It is a more efficient method to use than resistivity soundings when the depths of investigation exceed about 50 meters.

Limitations: The TDEM method is best suited for mapping conductive layers. Groundwater usually increases the conductivity of the rocks and, hence, mapping of conductive layers is needed. If metallic objects (i.e., pipelines), are close to the transmitter loop, electrical currents are induced into these objects by the transmitter loop, and they generate secondary currents and fields. These fields interfere with the electromagnetic fields from the ground and may significantly reduce the interpretability of the data. This method is probably not suitable if the groundwater is less than about 3 meters deep.

At the present time, only one-dimensional interpretation software is available. Therefore, the interpretation assumes that the subsurface layers are horizontal and homogeneous.

6.1.5.3 Seismic Refraction

Basic Concept: The seismic refraction method can be used to map the water table surface under certain conditions. If the alluvial sediments are fine grained, then the seismic refraction method will probably not be effective because the capillary zone destroys a well-defined seismic velocity contrast between the unsaturated and saturated alluvium. In addition, there may not be a significant velocity contrast between the unsaturated and saturated alluvium. However, if the alluvium is composed of coarse gravels, there will be only a very limited capillary zone. In addition, there will usually be a reasonable velocity contrast between the unsaturated alluvium, which will have a low velocity, and the saturated alluvium, which will have a velocity somewhat greater than that of water, which is about 1,400 m/sec.

The method requires a seismic energy source, usually a hammer for depths less than 15 meters and black powder charges for depths to 30 meters. The seismic waves then penetrate the overburden and refract along the water table surface. While they are traveling along this surface, they continually refract seismic waves back to the ground surface. These are then

detected by geophones placed on the ground surface. Figure 114b shows a seismic recorder instrument, and figure 114a shows the layout of the instrument, the main seismic waves involved and the resulting time distance graph.

Data Acquisition: The design of a seismic refraction survey requires a good understanding of the expected depth to the saturated layer. With this knowledge, velocities can be assigned to these features, and a model developed that will show the parameters of the seismic spread best suited for a successful survey. These parameters include the length of the geophone spread, the spacing between the geophones, the expected first break arrival times at each of the geophones, and the best locations for the off-end shots. Knowing the expected first break arrival times is also helpful in the field, where field arrival times that correspond fairly well to expected times help to confirm that the spread layout has been appropriately planned, and that the target layer is being imaged.

Data Processing: The first step in processing/interpreting refraction seismic data is to pick the arrival times of the signal, called first break picking. A plot is then made showing the arrival times against distance between the shot and geophone, called a time-distance graph. An example of such a graph for a two-layered ground (overburden and refractor) is shown in figure 114a.

The red portion of the time-distance plot shows the waves arriving at the geophones directly from the shot. These waves arrive before the refracted waves. The green portion of the graph shows the waves that arrive ahead of the direct arrivals. These waves have traveled a sufficient distance along the higher speed refractor (water table) to overtake the direct wave arrivals.

Data Interpretation: One of the most common methods of refraction interpretation is called the Generalized Reciprocal Method (GRM) that is described in detail in the Geophysical Methods section. A brief, and simplified, description of the GRM method is presented below. Figure 115 shows the basic rays used for this interpretation.

The objective is to find the depth to the bedrock under the geophone at D. This is done using the following simple calculations. The travel times from the shots at A and G to the geophone at D are added together (T1). The travel time from the shot at A to the geophone at G is then subtracted from T1. Figure 116 shows the remaining waves after the above calculations have been performed. These are the travel times from C to D added to the travel times from E to D subtracting the travel time from C to E. The sum of these travel times can be shown to be approximately the travel time from the bedrock at H to the geophone at D. Since the velocity of the overburden layer can be found from the time-distance graph, the distance from H to D can be found giving the bedrock depth.

Advantages: The seismic refraction method can provides reliable estimates of the water table depths if a velocity contrast exists between the water table and the overlying sediments.

Limitations: It is clearly important that the seismic waves refract from the water table. Usually this will be easily recognized from the field data, assuming the water table provides a refracting surface. However, if refracting layers lie above the water table, these must be

recognized if a reliable depth estimate is to be made. If the water table is in the overburden and close to the bedrock, this may obscure the bedrock arrivals since saturated soils have a higher velocity than unsaturated soils.

Local noise, for example traffic, may obscure the refractions from the bedrock. This can be overcome by using larger impact sources or by repeating the impact at a common shot point several times and stacking the received signals. If noise is still a problem, a larger energy source may be required. In addition, since some of the noise travels as airwaves, covering the geophones with sound absorbing material may also help to dampen the received noise.

6.1.5.4 Ground Penetrating Radar

Basic Concept: Ground Penetrating Radar (GPR) can be used provided the conditions are appropriate for the method. In order for the method to work, the saturated alluvium must provide a contrast in dielectric properties from those of the unsaturated alluvium. In addition, any clay in the alluvium will significantly attenuate the GPR signal and limit the depth of investigation. Ideal conditions for this method are a dry, sandy overburden. In ideal conditions, the method may penetrate to depths of 15 meters.

The GPR instrument consists of a recorder and a transmitting and receiving antenna. Different antennae provide different frequencies. Lower frequencies provide greater depth penetration but lower resolution. Figure 111 provides a drawing illustrating the GPR system. The transmitter provides the electromagnetic signals that penetrate the ground and are reflected from objects and boundaries, providing a different dielectric constant from that of the alluvium. The reflected waves are detected by the receiver and stored in memory.

Several companies manufacture GPR equipment including Geophysical Survey Systems (GSSI), GeoRadar, Mala GeoScience, and Sensors and Software. Figure 112 shows a typical instrument.

Any antenna supported by this instrument can be attached and used to collect data. Figure 113 shows a 100 MHz antenna that can be used with the above instrument. The 100 MHz antenna is suited for deeper applications to depths of 15 to 20 m in ideal conditions. This antenna could be used to map the water table depth.

Data Acquisition: GPR surveys are conducted by pulling the antenna across the ground surface at a normal walking pace. The recorder stores the data as well as presenting a picture of the recorded data on a screen.

Data Processing: It is possible to process the data, much like the processing done on single-channel reflection seismic data. Processes may include distance normalization, horizontal scaling (stacking), vertical and horizontal filtering, velocity corrections, and migration. However, depending on the data quality, this may not be necessary since the field records may be all that is needed to observe the water table.

Data Interpretation: To calculate the depth to the water table, the speed of the GPR signal in the alluvium at the site needs to be obtained. This can be estimated from charts showing speeds for typical soil types, or it can be obtained in the field by conducting a small traverse

across a buried feature whose depth is known. Once this is known, the depth to the water table can be found from the travel time to the reflector that images the water table and the speed of the GPR signal.

Advantages: GPR data is recorded simply by pulling the system across the area of interest. Data can be viewed in the field allowing recording parameter, such as antenna frequency, changes to be made if needed.

Limitations: Probably the most limiting factor for GPR surveys is that their success is very site specific and depends on having a contrast in the dielectric properties of the target compared to the host overburden, along with sufficient depth penetration to reach the target. However, it is likely that in many cases the water table will provide a dielectric contrast with the unsaturated overburden, and depth of penetration is probably the most important factor. Clay in the overburden will usually severely limit the depth penetration of the GPR signals.

6.1.5.5 Nuclear Magnetic Resonance

Basic Concept: The Nuclear Magnetic Resonance (NMR) method is also known as the Proton Magnetic Resonance (PMR) method. In this document, the term NMR will be used. This method is still being developed, although commercial equipment for taking NMR measurements is currently available. The NMR method is based on the excitation of protons in the subsurface water in the presence of the Earth's magnetic field. Because the method is essentially experimental, only a brief discussion is presented below.

The instrument consists of a transmitter and receiver. The transmitter drives alternating current at the proton resonance frequency through a loop of wire laid on the ground. The current is abruptly terminated, and the NMR signal is then measured using the transmitter wire loop as a receiving antenna. This procedure is repeated several tens to a few hundreds of times, during which the NMR signal is recorded and averaged to improve the signal-to-noise ratio. The signal is interpreted in terms of hydrological parameters as a function of depth. Figure 164 shows the basic physics of the NMR (or PMR) method.

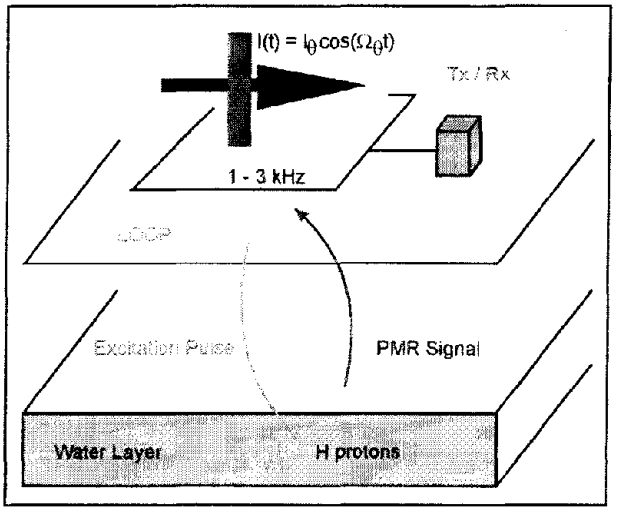

Figure 164. Schematic of the Nuclear Magnetic Resonance method. (IRIS Instruments)

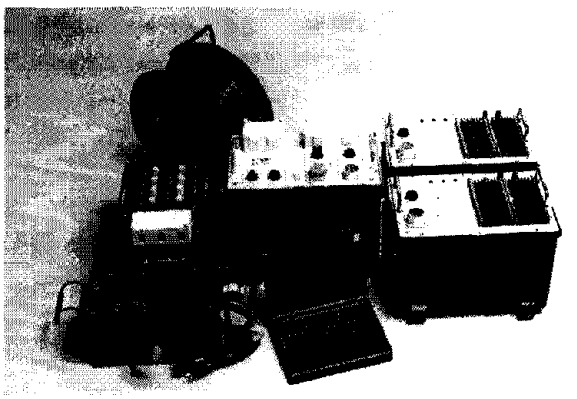

Figure 165. Instrument for measuring Nuclear Magnetic Resonance. (IRIS Instruments)

The transmitter/receiver loop provides the electromagnetic pulses that excite the protons in groundwater. These protons then decay during the transmitter current off time, and the field from this decay is detected by the same loop of wire now acting as a receiver. The data are stored in the control transmitter/receiver (Tx/Rx) box. Figure 165 shows the instruments for measuring NMR.

Data Acquisition: NMR surveys are conducted by laying a loop of wire on the ground. The size of the loop depends on the Pulse Moment (current multiplied by time while current is transmitted) during the measurement, which determines the depth of investigation. A typical loop size for investigation depths to 100 m might be 100 m side length. Rectangular pulses of alternating current are passed through the wire with a frequency equal to that of the proton resonance in the Earth's magnetic field, as illustrated in figure 164. Signals are received by the wire loop while the current is off.

Six basic steps define the general procedure for carrying out NMR soundings.

1. Measure the strength of the Earth's magnetic field. From this, the frequency of the signal to transmit can be found.
2. Transmit a pulse of current using the wire loop at the frequency found in step 1.
3. Measure the amplitude of the water NMR signal.
4. Measure the time constant of the signal
5. Change the pulse intensity to modify the depth of investigation.
6. Interpret the data using an inversion program.

Data Interpretation: An example of the field data and interpretation is shown in figure 166. The figure shows the field data from a sounding, along with the interpretation. The field data curve (left plot) shows the noise level (blue circles), the measured field data (black squares) and the interpretation fit (red line).

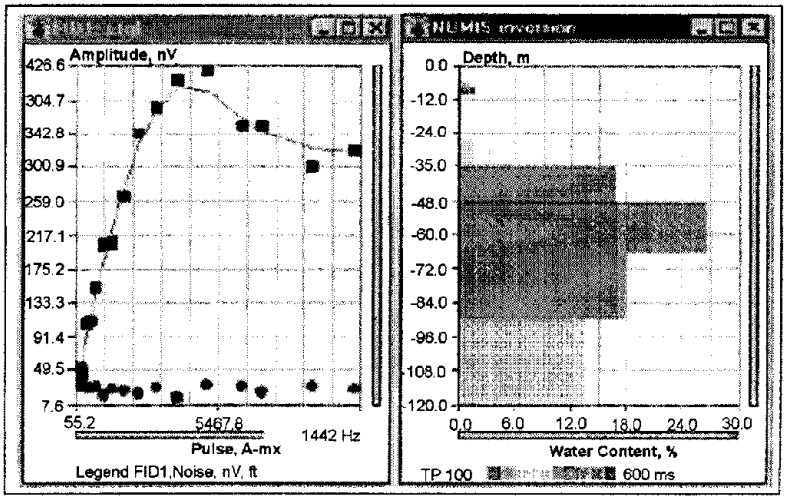

Figure 166. Field data and interpretation of a Nuclear Magnetic Resonance survey. (IRIS Instruments)

There are four important items concerning the interpretation of the results.

1. The method detects water. No signal is observed if no water is present.
2. The amplitude of the NMR signal is related to the variation in water content with depth.
3. The decay time constant of the NMR signal is related to the variation in mean pore size against depth.
4. The phase shift between the NMR signal and the current is related to the layer resistivity variation with depth.

The right-hand graph shows the interpretation, presenting a plot of porosity versus depth. Since water within the rock pores is required for the method to work, this plot shows the water content of the rock layers.

Advantages: The main advantage of the NMR method is that it responds only to the protons within water.

Limitations: The method requires large currents to be used when transmitting, necessitating large-diameter wire. Therefore, the wire is heavy and can be difficult to lay out in any area with bush or significant topography. Probably the biggest limitation is the influence of electrical noise, such as power line noise. Generally, soundings need to be at least 1,000 m from any power line. If magnetic minerals are present in the subsurface, these destroy the uniform magnetic field required, normally the Earth's field, to initialize the proton oscillations in the groundwater. When these magnetic minerals are present, the NMR method is ineffective.

Groundwater Flow

6.1.5.6 Self Potential

Basic Concept: The only geophysical method used to detect groundwater flow is the Self Potential (SP) method. This method measures naturally occurring electrical potentials on the ground surface, some of which may result from the flow of groundwater.

Self Potential voltages have a number of causes. The largest potential probably results from mineralization where negative SP anomalies of hundreds of millivolts can occur. Natural electrical potentials can also occur due to telluric currents. These are large currents flowing in the earth that result from electrical activity in the earth's atmosphere and beyond.

Figures 167 and 168 show the SP potentials over a fracture zone when water is flowing into and out of the fracture zone. When water flows into a fracture (figure 167) a negative SP anomaly is observed above the flowing water. Conversely, when water flows out of the fracture zone (figure 168), there is a positive SP anomaly.

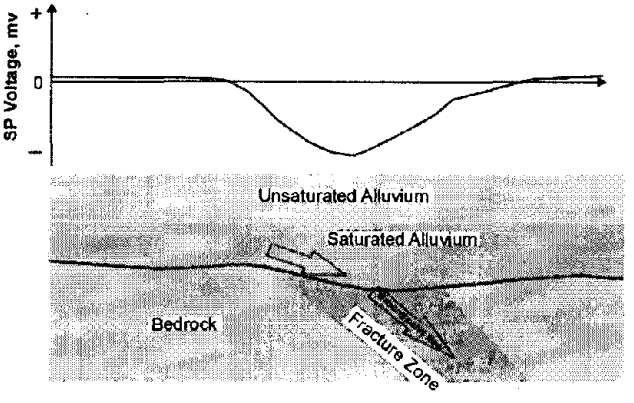

Figure 167. Self Potential anomaly expected over water flowing into fracture zone.

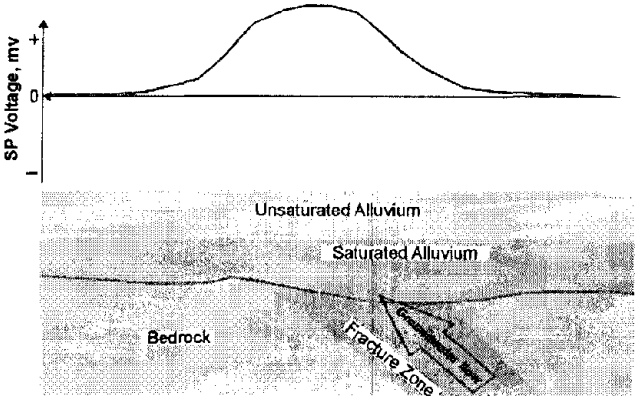

Figure 168. Self Potential anomaly expected over water flowing out of a fracture zone.

Data Acquisition: There are two techniques for recording SP data. These are illustrated in figure 169. One requires an electrode (normally a porous pot or stainless steel spike) at a

permanent reference point, called the remote electrode in figure 169. Long wires are required to connect a second electrode to the reference electrode. The second electrode is then moved along the desired traverse while taking voltage readings between the two electrodes. This system is called the remote electrode system in figure 169. This provides the SP voltage at each station with reference to the reference electrode. The second technique is much easier to use in the field. There is a fixed distance between the two electrodes, and the electrode system is moved in increments along the traverse. This system is called the dipole system in figure 169.

Data Processing: The measured voltages usually require little processing.

Data Processing: Interpretation is usually done from profiles of the measured voltage against distance, searching for the anomalies shown in figures 167 and 168. Some modeling is also available for a more quantitative interpretation.

Advantages: The Self Potential method is very simply to perform in the field and uses inexpensive equipment.

Limitations: Self Potential anomalies can result from several other factors, some of which give larger anomalies than those due to water flow. However, the method is simple and easy to apply. The method will not work near grounded structures or near grounded metal features such as fences since these may generate potentials due to corrosion. In addition, surveys near electrical groundings will probably be ineffective.

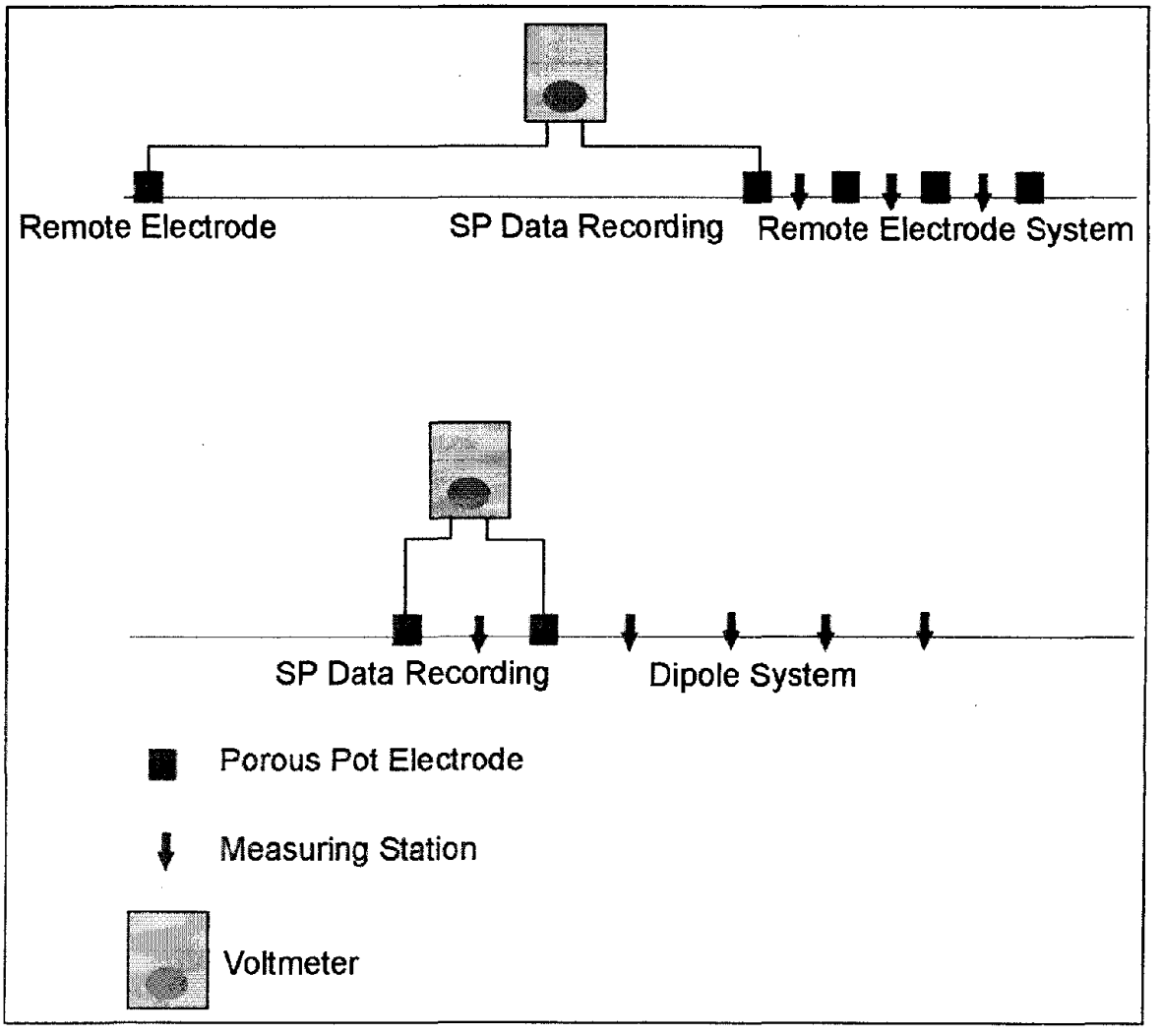

Figure 169. Methods of recording Self Potential data.

6.1.5.7 The Electroseismic

Basic Concept: The Electroseismic method (also called the Seismoelectrical method) is based on the generation of electromagnetic fields in soils and rocks by seismic waves. Although the method is not reported to detect groundwater flow, it is reported to measure permeability and, therefore, to detect the potential for groundwater flow.

As the seismic (P or compression) waves stress earth materials, four geophysical phenomena occur:

1. The resistivity of the earth materials is modulated by the seismic wave.

2. Electrokinetic effects analogous to streaming potentials are created by the seismic wave.

3. Piezoelectric effects are created by the seismic wave.

High-frequency audio and high-frequency radio frequency impulsive responses are generated in sulfide minerals (sometimes referred to as RPE).

The dominant application of the Electroseismic method is to measure the Electrokinetic effect or streaming potential (item 2, above). Electrokinetic effects are initiated by sound waves (typically P-waves) passing through a porous rock inducing relative motion of the rock matrix and fluid. Motion of the ionic fluid through the capillaries in the rock occurs with cations (or less commonly, anions) preferentially adhering to the capillary walls, so that applied pressure and resulting fluid flow relative to the rock matrix produces an electric dipole. In a non-homogeneous formation, the seismic wave generates an oscillating flow of fluid and a corresponding oscillating electrical and EM field. The resulting EM wave can be detected by electrode pairs placed on the ground surface.

Surface seismic sources and measurement electrode pairs are generally used to measure the Electrokinetic effect. Borehole systems also have recently been developed. A hammer blow or small explosive (black powder charge) are typically used for the seismic source. Two short (few meters) electrode pairs are typically located collinear and symmetric to the seismic source. Stacking of repeat seismic "shots" is often used to improve signal to noise.

Only one company was found that produces a commercially available Electroseismic prospecting system, GroundFlow Ltd. in the UK. This system has been used mainly for field demonstration purposes and research and development studies. Very few detailed case histories are available to document the performance of the system. The Electroseismic system made by GroundFlow is called "GroundFlow 1500." The main equipment components are a combined computer-receiver, antenna cables and electrodes, and the trigger cable. The Groundflow 1500 instrument is shown in figure 170.

Figure 170. The GroundFlow 2500 instrument. (Groundflow, Ltd., Northwest Aquifer Surveying, Inc.)

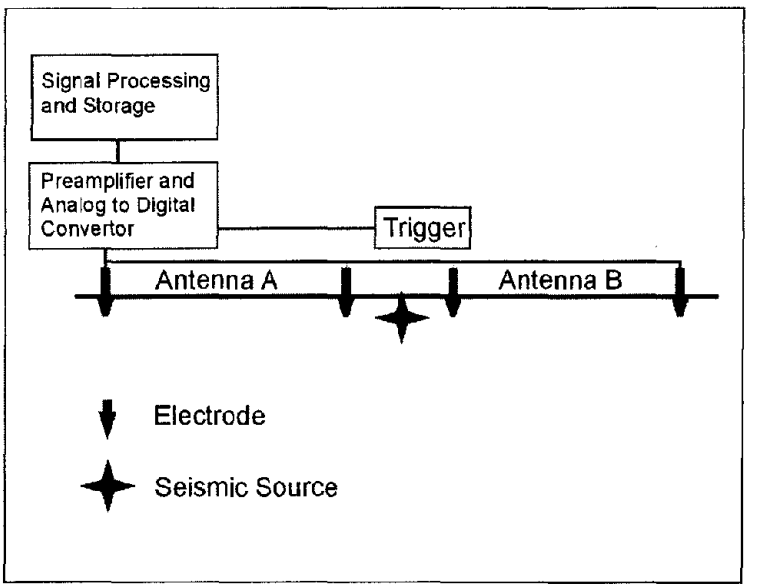

Figure 171. System layout for Electroseismic surveys.

The computer-receiver contains a preamplifier, analog to digital converter and power supply system to measure the voltages induced in the grounded dipoles. The system layout used by GroundFlow is shown in figure 171.

The hammer and plate seismic source is used along with two pairs of electrodes arranged in a straight line with electrodes offset (from the center of the array) by 0.25 and 2.25 m. The seismic source is positioned in the center of the array. Larger electrode spacings can be used; however, they are typically centered in pairs around the shot point and are generally less than about 10 m in length. Timing of the measurement is achieved by a hammer trigger (or other mechanical trigger). The signal is acquired with the instrument shown in figure 170. Measurements are made for a period of 400 ms after triggering. The last 200 ms of the record is used as a sample of background noise and is subtracted from the first 200 ms of signal to remove the first, third, and fifth harmonics of the background noise at the receivers. This noise is typically from power lines.

Data Acquistion: Measurements are recorded using the instrument and system setup described above. Data processing consists of stacking repetitive hammer (or explosive) shots and removing power line and other noise. This processing is conducted on the computer-receiver while in the field. Depending upon field conditions, up to 20 soundings can be conducted in a day. It is expected that measurement time will increase proportionally with stacking times, and that long stacking times would be needed in the vicinity of power lines.

Data Processing: The signal files are processed to give a sounding plot of permeability and porosity against one-way seismic travel time. Values for a simple seismic velocity model are required to allow time to depth conversion. The resulting logs against depth are displayed in the field.

Output from the Electroseismic inversion is typically a plot showing hydraulic conductivity versus depth. This interpretation assumes a one-dimensional layered earth. In theory, the

inversion also can derive fluid conductivity and fluid viscosity from the rise time of the signal. Where many soundings are measured in close vicinity, a pseudo 2-D cross section can be generated.

The maximum depth of penetration of Electroseismic measurements is stated to be about 500 m depending upon ambient noise and water content. Lateral resolution is not stated in the literature, but is expected to be on the order of the depth of exploration. No information was found regarding the vertical resolution of the method.

Advantages: Since this method is primarily used by only one contractor, and little independent data is available about the results, it is not known what the advantages of the method are.

Limitations: The Electroseismic method is apparently susceptible to electrical noise from nearby power lines. Typical Electroseismic signals are at the microvolt level. The Electroseismic signal is proportional to the pressure of the seismic wave. Thus, it would seem possible to increase the signal by using stronger seismic sources. This is not mentioned in the literature. Although Electroseismic soundings are reported to have a maximum exploration depth of about 500 m, no examples have been shown with results from deeper than about 150 m.

6.1.5.8 Borehole HydroPhysical™ Logging

HydroPhysical™ logging is a technology used for evaluating the vertical distribution of permeability and water quality in wells. Using this procedure, interval-specific contaminant concentrations, hydraulic conductivity, and flow rates are assessed with great accuracy and sensitivity. Cross-hole flow evaluations are also possible with this method.

Basic Concept: Borehole fluids are replaced or diluted with deionized (DI) water. During this process, profiles of the changes in fluid electrical conductivity (FEC) of the fluid column are repeatedly recorded using a highly sensitive FEC/temperature logging probe. These changes occur when electrically contrasting formation water is drawn back into the borehole by pumping or by native formation pressures (figure 172). A downhole wireline simultaneously measures FEC and temperature of the emplaced fluid.

Data Acquisition: Truck mounted pumping, logging, and deionization equipment is rigged up on the screened or open borehole. FEC logs are recorded before, during, and after emplacement of deionized water. Formation water recovery may be monitored during native (ambient) or pumping (stressed) conditions. Natural borehole fluid is extracted and stored, as the DI water is injected.

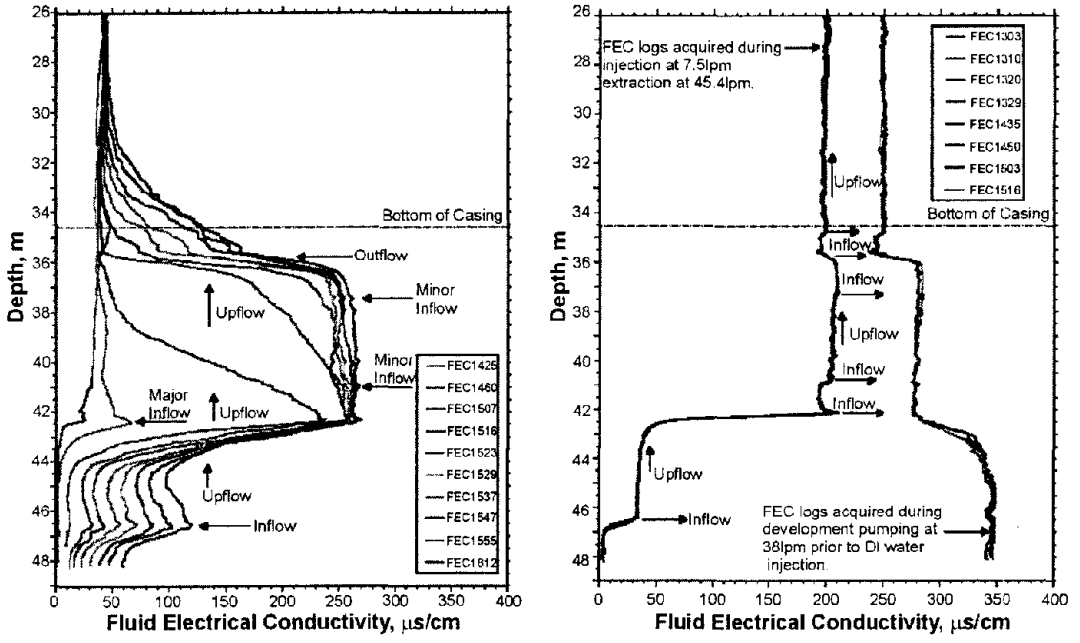

Figure 172. Examples of ambient flow characterization and 10 gpm production test, respectively. (Layne Christensen, Colog)

Data Processing and Interpretation: Software developed in conjunction with Lawrence Berkley laboratory is used to perform modeling showing upflow, downflow, ambient horizontal flow, outflow and inflow quantities of formation fluid for specific intervals. Using the mass-balance equation, and numerical modeling of FEC logs, interval-specific flow rates and the hydrochemistry of the water-bearing intervals can be determined.

Advantages: HydroPhysical™ logging provides a wide range of interval-specific flow rates that can be quantified from 0.01 to 2,000+ gpm. The technology is more cost effective than packer testing, and it is applicable in low and high yield bedrock, alluvial settings, karst, and volcanic acquifers. HydroPhysical™ logging allows the identification and evaluation of ambient horizontal and vertical flows, and ambient horizontal velocities can be converted into Darcian velocities for the acquifer.
Limitations: Concerns about fluid discharge are continuing to mount as environmental responsibility moves to the forefront. Fluid extracted during DI emplacement must be disposed of. Disposal may require permission for ground or stream discharge from the local water authority, or it can require storage, and removal for processing, if the presence of contaminants is possible.

6.2 GEOPHYSICAL METHODS TO DETERMINE PHYSICAL PROPERTIES

6.2.1 Determining Engineering Properties of the Subsurface

Geophysical methods can be used to measure engineering properties of rocks. These include the Bulk Modulus, Young's Modulus, Shear Modulus, and Poisson's ratio, called the elastic constants of a rock. The density of rocks can be estimated from seismic velocity. Porosity and permeability are more difficult to determine, although a relatively new method called Nuclear Magnetic Resonance (NMR) has provided some promising results. Degree of

saturation, or percent of the pore space filled with water is mentioned in the literature for soil surveys using the Ground Penetrating Radar (GPR) method.

To determine the elastic constants, the shear wave and compressional wave velocities have to be measured. The elastic constants can be calculated using the equations given below.

$$\rho = a\alpha^{0.25}, \tag{7}$$

where

$$a = 0.31 \text{ if } \alpha \text{ is in } \frac{\text{m}}{\text{sec}},$$

$$a = 0.23 \text{ if } \alpha \text{ is in } \frac{\text{ft}}{\text{sec}},$$

$$\sigma = \frac{(p^2 - 0.5)}{(p^2 - 1)}, \tag{8}$$

or

$$\sigma = \frac{(a^2 - 2\beta^2)}{2(a^2 - \beta^2)}, \tag{9}$$

$$E = \rho\beta^2 \frac{(3\alpha^2 - 4\beta^2)}{(\alpha^2 - \beta^2)}, \tag{10}$$

$$K = \rho(a^2 - \frac{4}{3}\beta^2), \tag{11}$$

where

α = commressional wave (P) velocity,

β = shear wave (S) velocity,

$p = \frac{\beta}{\alpha}$,

σ = Poisson's ratio,

K = Bulk modulus,

E = Young's Modulus

μ = shear modulus,

ρ = density.

Shear and Compressional Wave Velocities

To calculate the above quantities, the shear (S) and compressional (P) wave velocities have to be measured. For relatively shallow surveys, say less than 30 m deep, seismic refraction surveys can be used to measure these quantities. The data recording for the two surveys is very similar, the only difference being the source for the seismic energy.

Compressional wave sources include a hammer and base plate, black powder or other explosive charge, or a vibrator truck that puts energy into the ground using a base plate that vibrates at specified frequencies. Shear wave energy is more difficult to produce. One method of putting shear wave energy into the ground is to put a long piece of wood on the ground and hold it to the ground by placing the wheels of a vehicle on top of the wood. Shear waves are then created by using a hammer to impact the sides of the wood. Various other shear wave sources are available. One of these devices is the Microvib (figure 95). This is a small portable shear wave generator that uses vibration rather than impact techniques. Shear waves can also be created using conventional truck vibrators. However, these are usually used only when deep investigations are required.

The data are recorded using a seismic recorder with geophones that detect the vibrations. A typical seismic recorder is shown in figure 114b.

Determining Porosity and Permeability

Porosity influences many physical properties of rocks, including seismic velocity and resistivity. However, these parameters are also influenced by many other factors, such as degree of saturation and the mechanical properties of the rock. Equations are presented describing the relationship between the compressional and shear wave velocities and porosity. However, other factors also influence the velocity of seismic waves in a rock, including the structure of the rock matrix, the connectivity of the pores, cementation, and past history. The resistivity of a rock is significantly influenced by the amount of water in the rock pores as well as the salinity of the water. However, clays also influence the resistivity. Thus, measurements of resistivity generally cannot be used to reliably estimate the porosity of soil or rocks. However, the relationship between resistivity and porosity, established by Archie in 1942, is presented since there may be instances where the factors other than porosity remain constant, and variations in porosity can be estimated.

Permeability is even more difficult to determine, since this is related to the degree of connectedness of the rock pores and has no direct physical property. However, a relatively new method called Nuclear Magnetic Resonance (NMR) is reported to be able, in the right conditions, to be able to determine the mean pore size and provide an estimate of the permeability.

Relationships between Seismic Velocities and Porosity

Relationships have been developed between the porosity of a rock and its seismic velocity, since porosity is an important factor in determining rock velocity. The equation presented below relates the transit time of a seismic wave to the porosity and transit times of the seismic wave in the pore fluid and rock matrix.

$$\Delta t = \varphi.\Delta tf + (1-\varphi)\Delta tm, \qquad (12)$$

where

Δt = specific transit time (slowness),

Δtf and Δtm = specific transit times of the pore fluid and rock matrix,

φ = porosity.

where Δt is the specific transit time (slowness), Δtf and Δtm are the specific transit times of the pore fluid and rock matrix, and φ is the porosity.

This is an empirical equation and makes no allowance for the structure of the rock matrix and other factors that influence the velocity. In addition, this equation does not take into account pores occupied by other constituents other than water, e.g., clay. The equations presented below relate the velocity of the seismic waves to porosity and include a clay content term (C).

$$\alpha = 5.59 - 6.93\phi - 2.1C\left(\frac{\text{km}}{\text{sec}}\right), \tag{13}$$

$$\beta = 3.52 - 4.91\phi - 1.89C\left(\frac{\text{km}}{\text{sec}}\right), \tag{14}$$

where

α = commressional wave (P) velocity,

β = shear wave (S) velocity,

ϕ = porosity (in volume fraction),

C = clay content volume fraction.

where α is the compressional wave velocity, β is the shear wave velocity, ϕ is the porosity (in volume fraction), and C is the clay content volume fraction.

Although these equations are used in well logging, especially for hydrocarbons, no literature was found showing their use for measuring porosity from surface geophysical methods.

Relationships between Resistivity and Porosity

The minerals comprising a rock are almost always electrical insulators. Thus, electrical conduction occurs because of the moisture contained within the pores of the rock or soil. The resistivity of soil or rocks depends on several parameters including the clay content, moisture salinity, degree of saturation of the pores, and the number, size, and shape of the interconnecting pores. For soils, the degree of compaction (influencing porosity) is also an important factor. Archie (1942) developed an empirical formula relating resistivity to porosity, degree of saturation, and resistivity of the saturating moisture, shown below.

$$\rho = a\phi^{-m}S^{-n}\rho_w, \tag{15}$$

where

ϕ = porosity (in fractional pore volume),

S = fraction of pores containing water,

ρ_w = resistivity of the water,

$n \approx 2$,

$0.5 \leq a \leq 2.5$,

$1.3 \leq m \leq 2.5$.

where ϕ is the fractional pore volume (porosity), s is the fraction of the pores containing water, ρ is the resistivity of the water, n is approximately 2, a and m are constants, with a varying between 0.5 and 2.5, and m varying between 1.3 and 2.5.

Under fairly restrictive conditions, this equation may be used to estimate porosity changes. It will be necessary to assume that the values of a and m remain constant for the area of interest. If the true resistivity of the formation or soil has been obtained, the pores are assumed to be saturated, and the resistivity of the pore fluid remains constant, variations in the measured resistivity can be attributed to variations in porosity. It seems likely that the variables a, m, s, n, and ρ_w will remain constant over limited areas.

Methods

6.2.1.1 Seismic Refraction

Basic Concept: The following description of the seismic refraction method applies to data recorded with either compressional or shear waves.

Seismic refraction can be used to find rock velocities, especially for depths less than 30 m. The method requires a seismic energy source, as discussed above, producing either compressional or shear waves. The seismic waves penetrate the overburden and refract along the bedrock surface. While they are traveling along this surface, they continually refract seismic waves back to the ground surface. If deeper refractors are present and are imaged by the refraction spread, they will also refract seismic waves back to the geophones on the ground surface. Figure 114a shows the layout of the instrument, the main seismic waves involved, and the resulting time-distance graph for a single layer, which is the bedrock surface.

Data Acquisition: The design of a seismic refraction survey requires a good understanding of the expected refractor layers and overburden. With this knowledge, velocities can be assigned to these features and a model developed that will show the parameters of the seismic spread best suited for a successful survey. These parameters include the length of the geophone spread, the spacing between the geophones, the expected first break arrival times at each of the geophones, and the best locations for the off-end shots. Knowing the expected first break arrival times is also helpful in the field, where field arrival times that correspond fairly well to expected times helps to confirm that the spread layout has been appropriately planned and that the target layer is being imaged.

Data Processing: The first step in processing/interpreting refraction seismic data is to pick the arrival times of the signal, called first break picking. A plot is then made showing the arrival times against distance between the shot and geophone. This is called a time-distance graph. An example of such a graph for a two-layered ground (overburden and refractor) is shown in figure 114a.

The red portion of the time-distance plot shows the waves arriving at the geophones directly from the shot. These waves arrive before the refracted waves. The green portion of the graph shows the waves that arrive ahead of the direct arrivals. These waves have traveled a sufficient distance along the higher speed refractor (bedrock) to overtake the direct wave arrivals. Rock velocities are obtained from the slope of the time-distance graph when the layers are horizontal. When this is not the case, other methods have to be used.

Data Interpretation: There are several methods of refraction interpretation. One of the most common methods is called the Generalized Reciprocal Method (GRM) that is described in detail in the Geophysical Methods section. A brief and simplified description of the GRM method is presented below. Figure 115 shows the basic rays used for this interpretation.

The depth to the bedrock under the geophone at D can be found using the following simple calculations. The travel times from the shots at A and G to the geophone at D are added together (T1). The travel time from the shot at A to the geophone at G is then subtracted from T1. Figure 116 shows the remaining waves after the above calculations have been performed. These are the travel times from C to D added to the travel times from E to D subtracting the travel time from C to E. The sum of these travel times can be shown to be approximately the travel time from the bedrock at H to the geophone at D. Since the velocity of the overburden layer can be found from the time-distance graph, the distance from H to D can be found giving the bedrock depth.

The velocity of the refracting layer is found by calculating the function $T=(T(AD) - T(GD) + T(AB))/2$ and plotting this function against distance. The inverse slope of this line is the velocity of the refractor. A more comprehensive interpretation is available with the full GRM method and is described in the section on Geophysics.

Once the compressional and shear wave velocities are obtained from a common layer, the elastic moduli can be calculated by substituting these velocities in the relevant equations given above. Thus, Poisson's Ratio, Young's Modulus, Bulk Modulus, Rock Density, and Shear Modulus can all be found.

Advantages: The seismic refraction method provides a reliable technique for determining the shear and compressional wave velocity in the bedrock.

Limitations: Probably the most restrictive limitation is that each successively deeper refractor must have a higher velocity than the shallower refractor. However, if only the bedrock velocity is required, then this should not be a serious limitation since the bedrock usually has a higher velocity than the overburden. If the weathered layer (overburden) velocity is laterally variable, a greater density of shots will be needed to measure this

velocity. These data can then be used in the interpretation to provide more accurate bedrock depths.

If the water table is in the overburden and close to the bedrock, this may obscure the bedrock arrivals since saturated soils have a higher velocity than unsaturated soils.

Local noise, for example traffic, may obscure the refractions from the bedrock. This can be overcome by using larger impact sources or by repeating the impact at a common shot point several times and stacking the received signals. If noise is still a problem, a larger energy source may be required. In addition, since some of the noise travels as airwaves, covering the geophones with sound absorbing material may also help to dampen the received noise.

6.2.1.2 Nuclear Magnetic Resonance

Basic Concept: The Nuclear Magnetic Resonance (NMR) method is also known as the Proton Magnetic Resonance (PMR) method. In this document, the term "NMR" will be used. This method is still being developed, although commercial equipment for taking NMR measurements is currently available. The NMR method is based on the excitation of protons in the subsurface water in the presence of the Earth's magnetic field. Because the method is essentially experimental, only a brief discussion is presented below.

The instrument consists of a transmitter and receiver. The transmitter drives alternating current at the proton resonance frequency through a loop of wire laid on the ground. The current is abruptly terminated, and the NMR signal is measured using the transmitter wire loop as a receiving antenna. This procedure is repeated several tens to a few hundreds of times, during which the NMR signal is recorded and averaged to improve the signal-to-noise ratio. The signal is interpreted in terms of hydrological parameters as a function of depth. Figure 164 shows the basic physics of the NMR method.

The transmitter/receiver loop provides the electromagnetic pulses that excite the protons in groundwater. These protons decay during the transmitter current off time, and the field from this decay is detected by the same loop of wire now acting as a receiver. The data are stored in the control transmitter/receiver (Tx/Rx) box. Figure 165 shows the instruments for measuring NMR.

Data Acquisition: NMR surveys are conducted by laying a loop of wire on the ground. The size of the loop depends on the Pulse Moment (current multiplied by time while current is transmitted) during the measurement, which determines the depth of investigation. A typical loop size for investigation depths to 100 m might be 100 m side length. Rectangular pulses of alternating current are passed through the wire with a frequency equal to that of the proton resonance in the Earth's magnetic field, as illustrated in figure 164. Signals are received by the wire loop while the current is off.

Six basic steps define the general procedure for carrying out NMR soundings:

1. Measure the strength of the Earth's magnetic field. From this, the frequency of the signal to transmit can be found.

2. Transmit a pulse of current using the wire loop at the frequency found in step1.

3. Measure the amplitude of the water NMR signal.

4. Measure the time constant of the signal.

5. Change the pulse intensity to modify the depth of investigation.

6. Interpret the data using an inversion program to get porosity versus depth.

Data Interpretation: Figure 166 shows the field data from an NMR sounding along with the interpretation. The field data curve (left plot) shows the noise level (blue circles), the measured field data (black squares), and the interpretation fit (red line). The right-hand graph shows the interpretation, presenting a plot of porosity versus depth. Since the method detects water, in order to obtain porosity, it is assumed that the layers are saturated. The method is also reported to be able to provide mean pore size along with permeability estimates. There are four important facts concerning the interpretation of the results.

- The method detects water. No signal is observed if no water is present.
- The amplitude of the NMR signal is related to the variation in water content with depth.
- The decay time constant of the NMR signal is related to the variation in mean pore size against depth.
- The phase shift between the NMR signal and the current is related to the layer resistivity variation with depth.

Advantages: The main advantage of the NMR method is that it responds only to the protons within water.

Limitations: The method requires large currents to be used when transmitting, necessitating large-diameter wire. Therefore, the wire is heavy and can be difficult to lay out in any area with bush or significant topography. Probably the biggest limitation is the influence of electrical noise, such as power line noise. Generally, soundings need to be at least 1,000 m from any power line.

If magnetic minerals are present in the subsurface, these destroy the uniform magnetic field required, normally the Earth's field, to initialize the proton oscillations in the groundwater. When these magnetic minerals are present, the NMR method is ineffective.

6.2.1.3 Ground Penetrating Radar

Basic Concept: Ground Penetrating Radar (GPR) is used to measure the moisture content of soils. Water has a dielectric constant of about 80, whereas air is 1. Dry sand has a value varying between 3 and 5, and saturated sand has a value between 20 and 30. Therefore, since the GPR signals respond to variations in the dielectric constant, water content is one of the most important factors. This, along with the velocity of the GPR signals in the soil, can be used to estimate soil moisture content.

Ground Penetrating Radar (GPR) can be used providing the conditions are appropriate for the method. Clay in the soil will attenuate the GPR signal and severely limit depth penetration. The GPR signal is severely attenuated if the ground is electrically conductive. Ideal conditions are dry, sandy soils, although good results should be obtained in soils saturated with fresh (resistive) water. In ideal conditions, the method may penetrate to depths of 15 m.

The GPR instrument consists of a recorder and a transmitting and receiving antenna. Different antennae provide different frequencies. Lower frequencies provide greater depth penetration, but lower resolution. Figure 111 provides a drawing illustrating the GPR system. The transmitter provides the electromagnetic signals that penetrate the ground and are reflected from objects and boundaries that have a different dielectric constant from that of the overburden. The reflected waves are detected by the receiver and stored in memory.

Several companies manufacture GPR equipment. These include Geophysical Survey Systems Inc (GSSI), GeoRadar, Mala GeoScience, and Sensors and Software.

Figure 112 shows the data recording and system control for a GPR instrument. Any antenna supported by this instrument can be attached and used to collect data. Figure 113 shows a 100 MHz antenna that can be used with the above instrument. The 100 MHz antenna is suited for deeper applications to depths of 15 to 20 m. Different antennas are available each with a different frequency. Higher frequencies provide better resolution, but less depth penetration. The choice of antenna is important in GPR surveys. However, the most important parameter is to provide sufficient penetration depth.

Data Acquisition: GPR surveys are conducted by pulling the antenna across the ground surface at a normal walking pace. The recorder stores the data, as well as presenting a picture of the recorded data on a screen.

Data Processing: It is possible to process the data, much like the processing done on single-channel reflection seismic data. Processing might include distance normalization, horizontal scaling (stacking), vertical and horizontal filtering, velocity corrections- and migration.

Data Interpretation: Changes in the electrical properties of the soil are usually related to changes in the soil moisture content. Soil moisture content can be derived from the velocity of electromagnetic waves in the soil using a conversion from velocity to dielectric constant. The prediction of soil moisture content is still being researched.

Advantages: The GPR method is easy to use in the field and the data is presented on a screen as is being recorded. This allows changes in the data recording parameters to be made during

the survey. Thus, if the depth of penetration is insufficient then a lower frequency antenna can be tested.

Limitations: In determining the moisture content of soils, probably the most limiting factor is the amount of clay that the soil contains, since this will attenuate the GPR signal and limit penetration. In addition, determining soil moisture content requires fairly uniform soils. If the soil is not homogeneous, other factors may influence velocity changes and give false moisture content values.

6.2.1.4 Spectral Analysis of Surface Waves

Basic Concept: The velocity of shear waves can be obtained from the Spectral Analysis of Surface Waves (SASW) method. This method has an advantage over the seismic refraction method in that data can be recorded in areas where the velocity of deeper material is less than the overlaying material, called a velocity inversion. In addition, the method gives bulk estimates of the subsurface velocities, which may sometimes be more appropriate than the more defined values given by the seismic refraction method.

This method is based on the propagation of mechanically induced Rayleigh waves. By striking the ground surface with a light hammer, a transient stress wave is created, including surface or Rayleigh waves, which are registered by two transducers placed in line with the impact point on the ground surface at fixed separations. The transducers, which may be small accelerometers, register the passage of the waves. The receiver outputs are plots of the phase difference between the two transducers as a function of frequency. A profile of Rayleigh wave velocity versus wavelength, or so-called dispersion curve, is calculated from the phase plot. The ratio of Rayleigh wave velocity to shear wave velocity is approximately 0.9:1; thus, the shear wave velocity can be estimated. The shear stiffness (G) of the ground can be calculated from the shear velocity if the material density is known. Thus, we obtain a plot of ground stiffness as a function of depth from the surface.

Rayleigh waves have velocities that depend on their wavelength, a phenomenon called dispersion. Waves having different wavelengths sample to different depths, with the longer wavelengths sampling to greater depths. Figure 35 illustrates the sampling depths and particle motion of two Rayleigh waves having different wavelengths.

This principle is used to measure the thickness of ground layers with different stiffness properties. It can also be used to locate and roughly delineate inhomogeneities such as voids.

The major advantages of the SASW method are that it is non-invasive and non-destructive, and that a larger volume of the subsurface can be sampled than in borehole methods.

Data Acquisition: The surface wave dispersion curve can be measured using an active source and a linear array of receivers. The dispersion curve is then inverted to determine the corresponding shear wave velocity profile.

There are two main methods used in surface wave exploration. The most common surface wave method in industry is called SASW testing. The other method, which uses an array of geophones, is generally called array methods. The field setup is shown in figure 36. Either a

transient or continuous point source is used to generate Rayleigh waves, which are monitored by in-line receivers. The data acquisition system calculates the phase difference between the receiver signals. These phase data are processed later into the dispersion curve, which is modeled analytically to determine a compatible shear wave velocity profile for the site. The data acquisition system is discussed in more detail below.

The source used depends on the desired profiling depth. Heavier sources generating lower frequency waves provide deeper interpretations. A combination of sources is commonly used to measure dispersion over a broad enough bandwidth to resolve both the near-surface and greater depth. Transient sources include sledgehammers (<15 m depth) and dropped weights. Continuous sources include the electromagnetic vibrator (< 40 m depth), eccentric mass oscillator, heavy equipment such as a bulldozer (30 to 150 m depth), and the vibroseis truck (<120 m depth). A pair of vertical receivers monitors the seismic waves at the ground surface. For profile depths of around 100 m, 1-Hz geophones are required. Five or 10-Hz geophones can be used for surveys from 10 to 30 m depth. Theoretical as well as practical considerations, such as attenuation, necessitate the use of an expanding receiver spread. Data are recorded using sources on both sides of the geophones, called the forward and reverse directions (figure 36).

Data Processing: In the SASW method, a Fast Fourier Transform (FFT) analyzer or PC-based equivalent is used to calculate the phase data from the input time-voltage signals. Typically, only the cross power spectrum and coherence are recorded. Coherent signal averaging is used to improve the signal-to-noise ratio, a process similar to stacking of seismic records.

Because of the initial processing done by the analyzer in the field, the effectiveness of the survey can be assessed and modified if necessary. An initial estimate of the shear wave velocity (V_S) profile can be made quickly.

Data Interpretation: Interpretation consists of modeling the surface wave dispersion to determine a layered V_S profile that is compatible. The acquisition and processing techniques of SASW methods do not separate motions from body wave, fundamental mode Rayleigh waves, and higher modes of Rayleigh waves. Usually it is assumed that fundamental mode Rayleigh wave energy is dominant, and forward modeling is used to build a 1-D shear wave velocity (V_S) profile whose fundamental mode dispersion curve is a good fit to the data.

Advantages: The major advantages of the SASW method are that it is non-invasive and non-destructive, and that a larger volume of the subsurface can be sampled than in borehole methods.

Limitations: The depth of penetration and resolution of surface wave methods have not been thoroughly studied. This is due, in part, to the widespread use of forward modeling rather than formal inversion. The depth of penetration and resolution are also heavily site and profile dependent.

The depth of penetration is determined by the longest wavelengths in the data. In modeling, there is a trade-off between resolution (layer thickness) and variance (change in V_S between

layers). Data that are noisier must be smoothed and will have less resolution because of this. Whether a particular layer can be resolved depends on its depth and velocity contrast. The modeled V_S profile is insensitive to reasonable variations in density. The compressional wave velocity (V_P) cannot be resolved from dispersion data, but has an effect on modeled V_S. The difference in V_P in saturated versus unsaturated sediments causes differences of 10% to 20% in surface wave phase velocities, which lead to differences in modeled V_S.

The depth of penetration is determined by the longest wavelengths that can be generated by the source, measured accurately in the field, and resolved in the modeling. Generally, heavier sources generate longer wavelengths, but site conditions are often the limiting factor. Attenuation characteristics of the ground determine the signal level at the geophones. Cultural noise (traffic, rotating machinery) at a site may limit the signal-to-noise ratio at low frequencies. In SASW methods, the depth of resolution is usually one-half to one-third of the longest wavelength.

The field setup requires a distance between the source and most distant geophone of two to three times the resolution depth. However, forward modeling allows for subjective interpretation of the sensitivity of the dispersion curve to the layered V_S model. Resolution decreases with depth. A rule of thumb is that if a layer is to be resolved, the layer thickness (resolution) should be at least around one-fifth of the layer depth.

Data recording and processing are more difficult than with the seismic refraction method.

6.2.2 Borehole Logging

This section includes three important logging methods for obtaining the physical properties of rocks. These are a typical suspension logging method, an integrated logging system and Crosshole shear logging.

Borehole engineering logging surveys are performed to accurately acquire rock properties, structural stress-strain relationships, fracture statistics, and other in-situ properties for major tunneling and engineering projects. Wireline logging methods have been shown to dramatically reduce costs of rock quality analysis by reducing the number of core samples required for laboratory analysis.

6.2.2.5 Suspension logging

Basic Concept: Suspension P-S velocity logging, or suspension logging for short, is a method for determining shear (V_S) compressional (V_P) wave velocity profiles. Measurements are made in a single, uncased, fluid-filled borehole. It is similar to full-waveform sonic logging, but is optimized for low frequency measurements in soil.

A diagram of the suspension logging setup is shown in figure 173, showing the OYO PS 170 system. A solenoid source generates an acoustic wave in the borehole fluid, which impacts the borehole wall. Both P- and SV-waves are generated, which travel radially away from the borehole wall. A portion of the energy travels along the formation as a head wave and radiates energy back into the fluid. These waves are sensed by two geophones on the probe.

The geophone separation (distance) divided by the difference in travel time is equal to the average velocity of the formation over that interval.

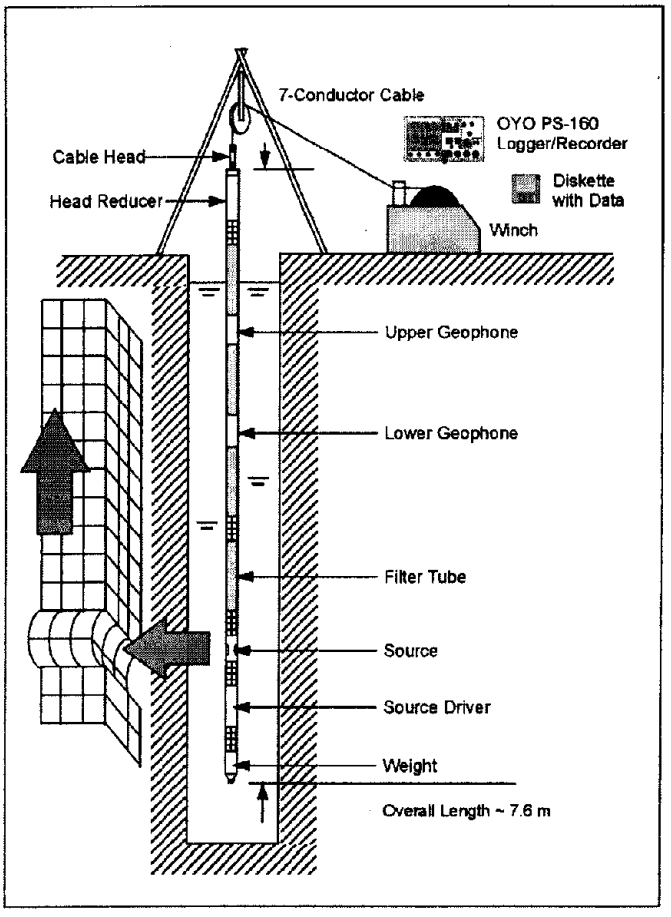

Figure 173. Schematic showing suspension logging system. (GEOVision Geophysical Services)

Commonly, measurements are made at 0.5 to 1-m intervals, although the data can be processed for higher resolution. The method has been proven at depths up to 2 km.

Data Acquisition: A typical suspension P-S Logging system, one of which is manufactured by OYO Corporation, consists of a borehole probe, cable, winch, and control/recording instrument. The probe length is approximately 7 meters.

The probe consists of a source and two biaxial geophones, separated by flexible isolation sections. It is centered in the borehole via the attached nylon whiskers. The solenoid source is reversible and produces energy between 500 and 5000 Hz. In practice, the maximum spectral amplitudes is stiff soil or soft rock are around 1000 Hz for shear waves and 3000 Hz for compressional waves. The corresponding wavelengths are tens of centimeters.

The separation between geophones is one meter. The vertical axis of the geophone corresponds to P-wave energy and the horizontal to S-wave energy. The probe is connected to the recorder on the surface by an armored 7-conducter cable. The cable serves both to

support the probe, to transmit activation signals to the source, and to transmit the geophone signals back to the recorder. The depth is measured by the rotary encoder on the winch.

The electronics system activates the source, and records the geophone signals on different channels. Modern loggers have up to 8 channels. Filters may be used in acquisition, but data are usually recorded unfiltered and digitally filtered later during processing.

The measurement procedure is as follows. The probe is lowered to the bottom of the borehole to verify total depth and then raised slightly to the first measurement point. The source is activated in one direction and the output from the two horizontal geophones (SH-wave) is recorded. The source is then activated in the reverse direction, producing a reverse polarity SH-wave. Finally, the source is activated in the first direction again and the vertical geophone signal recorded, which represents the P-wave.

After the data is stored, the probe is raised to the next level and the measurement sequence repeated. Gains, record length, filters, and stacking can be adjusted during acquisition.

Data processing: The stored data are transferred from floppy disk to a personal computer for processing. PS Log, Dos-based software provided with the suspension logging system, is used to pick the wave arrivals and compute the velocities. A complete record for one depth is shown in figure 174.

Commonly, the first break or first peak is picked on each waveform. If the data are noisy, they can be filtered digitally first. The time differences between horizontal and vertical receivers (R1-R2) are used to calculate the interval S- and P-wave velocities, respectively, over the 1-m interval. These values are compared with source to receiver (S-R1) travel times and velocities.

Ideally, the shear wave signal on the horizontal geophones should be a mirror image for normal and reverse source activation. This aids in identifying the first arrival of the shear wave. The velocities calculated from normal and reverse polarity are averaged.

Data interpretation: The processed suspension logging results consist of the V_S and V_P profile, sampled at the measurement interval. Commonly no further interpretation is done. If desired, constant velocity layers can be fit to the discrete velocity points, by averaging travel time (or 1/V) over the layer depths. Interfaces, such as the depth to water table in sediments, and the soil/rock transition, can usually be identified.

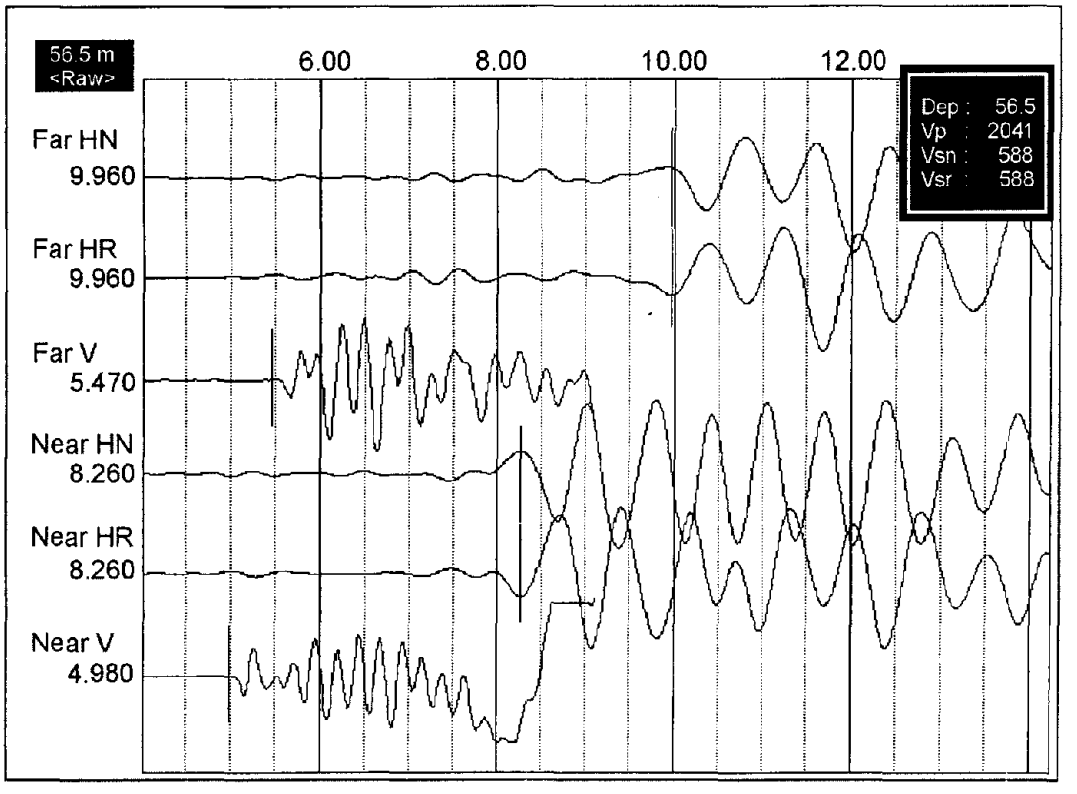

Figure 174. Sample suspension logging waveform record. (GEOVision Geophysical Services)

Limitations: Interpretation of clean suspension logging data is relatively straightforward, but poor data is often ambiguous. The data quality is heavily influenced by the borehole conditions. The best borehole conditions are achieved by drilling with the mud-rotary wash method. Borehole quality deteriorates with time after drilling. If another drilling method is used that results in a rough borehole surface, the hole is usually grouted and cased. Care must be taken to use grout that is comparable in stiffness with the native material so that good coupling between the casing, grout, and native material is achieved. PVC casing is acceptable but steel is not. Logging cased holes eliminates standby time but may result in lower quality data.

Changes to the suspension logging processing method could improve the processing of noisy data. Cross correlation could be used to determine the time lag at which the waveforms from the near and far receivers match best.

Suspension logging does not always provide excellent results in the near surface (< ~5 m depth). This is because it is difficult to generate waveforms in the surrounding soil under low confining stress. Steel conductor casing may also be present in the top of the borehole.

6.2.2.6 Integrated Logging System

Basic Concept: The integration of acoustic or optical televiewer, full waveform sonic, calibrated formation density, borehole caliper, natural gamma, and relative neutron porosity logs (figure 175) allows the geotechnical engineer to obtain dynamic soil and rock dynamic

properties and geological information. These properties include bulk density, bulk modulus, Young's modulus, shear modulus, Poisson's ratio, fracture density, dominant bedding and fracturing trends, stress-strain relationships, and rock rippability.

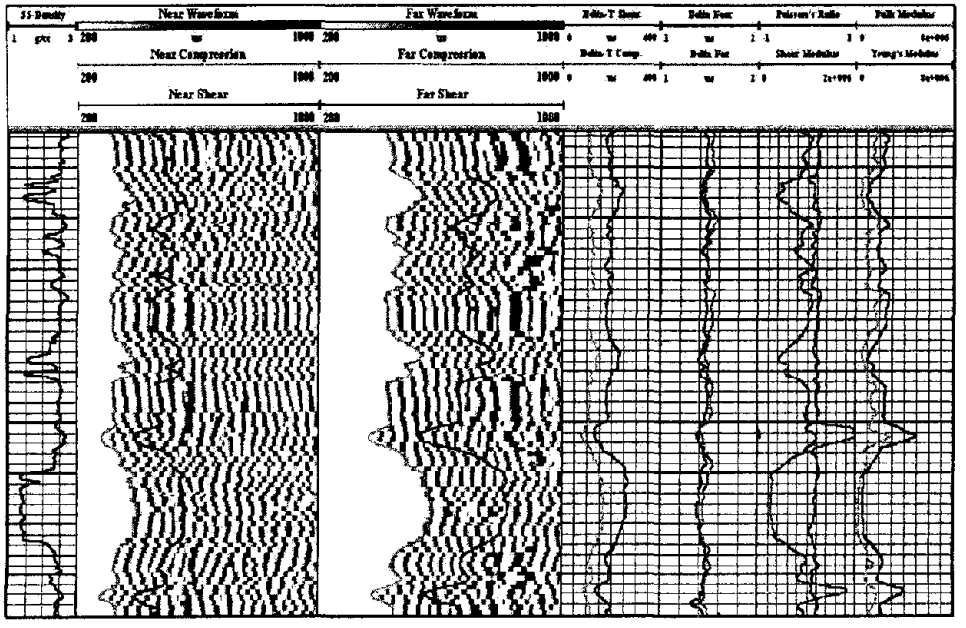

Figure 175. Examples of engineering rock property traces as calculated from density and sonic logs. (Layne Christensen, Colog)

Data Acquisition: In wireline logging operations, a truck mounted logging system is used to obtain borehole geophysical logs. In engineering rock properties applications, a minimum of calibrated multi-detector density and multi-receiver full waveform sonic logs are acquired.

Data Processing and Interpretation: In this application, sonic waveforms are initially picked for compressional and shear wave arrival times. Specialized algorithms are then applied to the density logs to compensate for borehole effects such as mud or fluid invasion, mud cake, and rugosity. Finally, P and S travel times and compensated density values are combined in obtaining bulk density, bulk modulus, Young's modulus, shear modulus, and Poisson's ratios.

Advantages: Borehole logging significantly reduces the need for core sampling and laboratory analysis by providing a continuous borehole geophysical log of in-situ properties. When combined with the fracture analysis of imaging televiewer logs, inferences can be made regarding fracture density, dominant bedding, fracturing trends, stress-strain relationships, and rock rippability.

Limitations: In rock properties applications, an open, stable borehole is required. Sonic logging requires a fluid-filled borehole. Density logging requires special handling of radioactive cesium sources.

6.2.2.7 Crosshole Shear logging

Basic Concept: The primary purpose of obtaining crosshole data is to obtain the most detailed in situ seismic wave velocity profile for site-specific investigations and material characterization. Crosshole velocity data are valuable for assessing man-made materials, soil deposits, or rock formations.

The seismic technique determines the compressional (P-) and/or shear (S-) wave velocity of materials at depths of engineering and environmental concern where the data can be used in problems related to soil mechanics, rock mechanics, foundation studies, and earthquake engineering. Crosshole geophysical testing is generally conducted in the near surface (upper hundred meters) for site-specific engineering applications. All of the dynamic elastic moduli of a material can be determined from knowledge of the in situ density, P-, and S-wave velocity. Therefore, since procedures to determine material densities are standardized, acquiring detailed seismic data yields the required information to analytically assess a site. Low-strain material damping and inelastic attenuation values can also be obtained from crosshole surveys. However, the most robust application of crosshole testing is the ability to define in situ shear-wave velocity profiles for engineering investigations associated with earthquake engineering.

Data Acquisition: Crosshole testing takes advantage of generating and recording (seismic) body waves, both the P- and S-waves, at selected depth intervals where the source and receiver(s) are maintained at equal elevations for each measurement. Figure 176 illustrates a general field setup for the crosshole seismic test method. Using source-receiver systems with preferential orientations in tandem (i.e., axial orientations, which complement the generated and received wave type/signal) allows maximum efficiency for measurement of in situ P- or S-wave velocity depending on the axial orientation. Due to the different particle motions along the seismic ray path, it is crucial to use optimal source-receiver systems in order to best record crosshole P- or S-waves. Because only body waves are generated in the source borehole during crosshole tests, surface waves (ground roll) are not generated and do not interfere with the recorded body-wave seismic signals. Crosshole testing are three-directional in nature. Therefore, three-component geophones with orthogonal orientations yield optimal results when acquiring crosshole P- and/or S-wave seismic signals. With three-component geophones, there is one vertically oriented geophone and two horizontal geophones. For crosshole tests, one horizontal geophone remains oriented parallel to the axis between the boreholes (radial orientation), and the other one remains oriented perpendicular to the borehole axis (transverse orientation). In this case, the two horizontal axis geophones must remain oriented, radially and transversely, throughout the survey. This is accomplished with loading poles or with geophones that can be electronically oriented.

Data Processing: Utilizing digital recording equipment affords the operator the ability to store the data on magnetic media for analysis at a later date; but more importantly, digital data can be filtered, smoothed, and time-shifted during analysis. Also, digital signal processing may be directly performed for coherence, frequency-dependent attenuation, and spectral analysis.

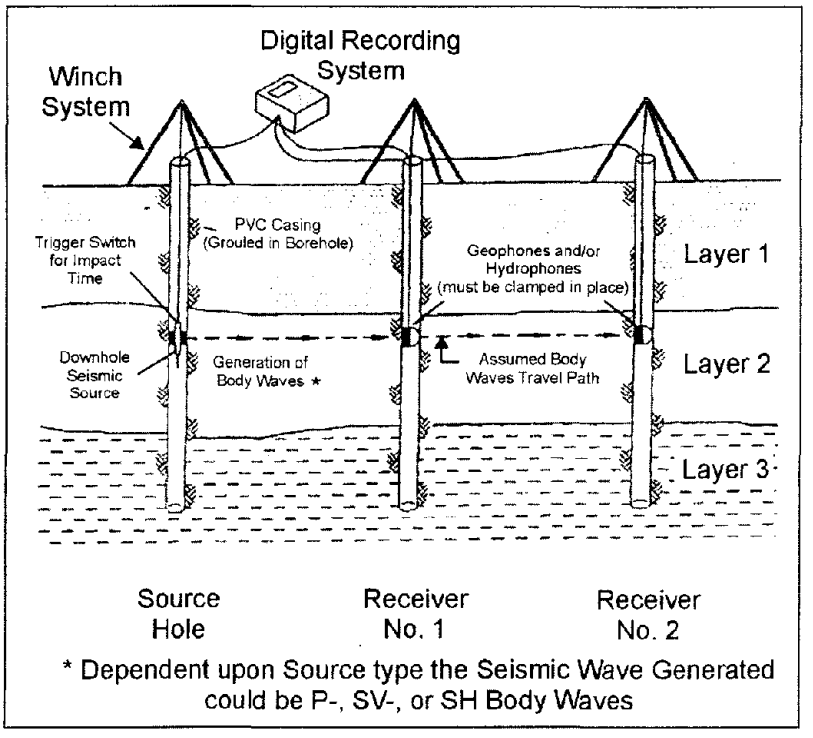

Figure 176. Schematic of crosshole method.

Data Interpretation: For interpretation of direct ray path travel times between two or three boreholes, the Bureau of Reclamation has published a computer program that is designed specifically for reducing crosshole seismic data. Furthermore, the program was fashioned around the ASTM conventions and test procedures outlined for crosshole seismic testing. The program CROSSIT (Version 2.0) is intended to be a step-by-step program that allows the user to:

a) Input lithologic information obtained from geologic drill hole logs.

b) Input deviation survey for each drill hole.

c) Input travel times for P- and/or S-wave arrivals at one or two receiver holes.

d) Enter site-specific information (location, surface elevation, etc.).

e) Map each borehole using deviation survey information.

f) Determine corrected crosshole distances between respective drill shot pairs:

g) source/receiver 1, source/receiver 2 and receiver1/receiver2.

h) Compute direct P- and S-wave velocities from travel time data.

i) Tabulate and/or graph (to hard copy or disk file).

j) Borehole directional survey data and plots.

k) P- and S-wave velocity depth profiles from each drill hole pair.

l) i)Interactively edit input or graphical files and combine data sets.

m) Post-process seismic data and/or plots for alternative uses.

CROSSIT is built for compatibility with laptop or desktop computers and dot matrix or laser-jet printers such that data reduction could be performed in the field as geophysical data are being acquired. The logic and flowchart for this interpretation and data presentation program are designed to follow the typical field data acquisition process (i.e., geologic information, borehole information, travel-time information) to permit interactive computer analysis during data collection. This technique of reducing data in the field has proven its value because of the ability to determine optimal testing intervals and adjust the program as necessary to address the site-specific problem.

Data Processing: There are a number of digital signal processing techniques useful for determining material properties other than P- or S-wave velocity, as well as confirming the computed crosshole velocity profile, such as:

1. Spectral analysis for determination of inelastic constants (attenuation and/or material damping).

2. Frequency analysis for correlation of phase and group velocity.

3. Cross-correlation of recorded seismic signals from one receiver to another receiver borehole, or source to receiver coupling for signal coherence.

Sophisticated processing is rarely required in (engineering) crosshole testing, and the straightforward distance/travel time relationship for velocity computations is considered functional and effective.

Advantages: Crosshole seismic testing has the unique advantage of sampling a limited volume of material at each test depth. Thus, the final result is a significantly more detailed and accurate in situ seismic (P- and/or S-wave) velocity profile. Because boreholes are required, there is the opportunity to obtain more site-specific geotechnical information, which, when integrated with the seismic data, yields the best assessment for the engineering application (liquefaction, deformation, or strong motion characterization). .

Crosshole seismic testing has the definitive advantage of assessing a complex layered velocity structure with alternating high and low relative velocities. Other surface techniques such as spectral analysis of surface waves can theoretically evaluate the high/low layered velocity structure, but due to a number of inherent assumptions associated with surface geophysical methods, several non-unique velocity profiles may be derived (from inverse modeling) without specific information about the subsurface layering at the site. Since considerable confidence can be placed on engineering scale crosshole seismic data, computation of in situ low-strain elastic constants (Shear and Young's modulus, Poisson's

ratio, etc.) permits dependable assessment of geotechnical parameters for the site-specific evaluation.

Limitations: The primary detriments or obstacles encountered during crosshole testing are typically related to the placement and completion of multiple drill holes. Sites where noninvasive techniques are required due to hazardous subsurface conditions, crosshole seismic tests are not applicable because of tight regulatory procedures regarding drilling, sampling, and decontamination. However, at sites where detailed in situ P- and S-wave velocities are required, drill hole completion must follow ASTM procedures, and when unusual conditions exist (e.g., open-work gravels), specialized techniques for borehole completion should be employed. The U.S. Bureau of Reclamation has encountered numerous sites in the western United States where loose, liquefiable sand and gravel deposits needed to be investigated, and crosshole testing effectively evaluated the in situ material density and stiffness with P- and S-wave velocities, respectively; however, considerable care and caution were used for completion of each borehole.

Seismic data for crosshole testing needs considerably more waveform interpretation because refraction events from high-velocity layers either *above or below* a low-velocity layer must be identified and the first-arrival velocity corrected. Direct-wave arrivals are easily recognized (even with low-amplitude refracted arrivals) as long as the previously described field equipment is utilized for preferential generation of P-waves or polarized SV or SH-waves. The ASTM requirement of three drill holes seems costly to a project budget; however, the necessary source/receiver configurations and borehole separation allow optimal correction and evaluation of in situ P- and S-wave velocities for each material layer at depth.

6.2.3 Determining the Rippability of Rocks

Rippability is the ease with which soil or rock can be mechanically excavated. According to Bieniawski, rippability of rock is assessed by numerous parameters including uniaxial strength, degree of weathering, abrasiveness, and spacing of discontinuities. Nevertheless, seismic refraction has historically been the geophysical method utilized to indirectly predetermine the degree of rippability.

Ripping is typically performed by tractor-mounted equipment. The size of the tractor (dozer) is determined by the ripping assessment of the rock. The hardness and competency of each individual material will determine the ease of rippability. Rock that is too hard to be ripped is fragmented with explosives.

Rocks can be classified into three categories: igneous, sedimentary, and metamorphic. Igneous rocks, formed by cooling of molten masses originating within the earth, are the most difficult to rip. This is partly because they lack lines of weakness such as stratification or cleavage planes. Metamorphic rocks are generally defined as any rocks derived from pre-existing rocks by mineralogical, chemical, and/or structural changes, in response to marked changes in temperature, pressure, shearing stress, and chemical environment. Common metamorphic rocks are gneiss, quartzite, schist, and slate. These rocks vary in rippability, depending on their degree of stratification or foliation.

Sedimentary rocks consist of material derived from the destruction of preexisting rocks. Water action is responsible for the largest percentage of sedimentary rocks, although some are formed by wind or glacial ice. Sedimentary rocks are generally the most rippable.

Few or no problems are found with hardpan, clays, shales, or sandstones. Likewise, any highly stratified or laminated rocks, and rocks with extensive fracturing are usually rippable.

The physical characteristics that are favorable for ripping are given below:

1. Frequent planes of weakness such as fractures, faults, and laminations.
2. Weathered rocks.
3. Rocks with moisture permeating the formations.
4. Highly stratified rocks.
5. Brittle rocks.
6. Rocks with low "shear strength."
7. Rocks with low seismic velocities.

Conditions that make ripping difficult are as follows:

1. Massive rocks.
2. Rocks with no planes of weakness.
3. Crystalline rocks.
4. Non-brittle energy absorbing rock fabrics.
5. Rocks with high "shear strengths."
6. Rocks with a high seismic velocity.

The above rippability criteria are presented by The Caterpillar Company in a book titled Handbook of Ripping.

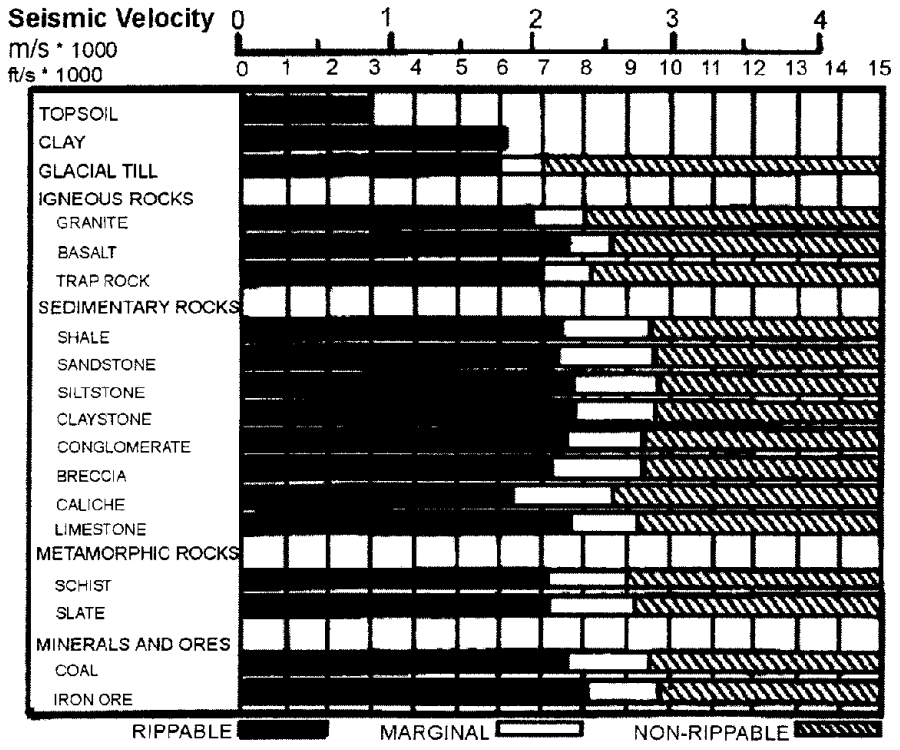

Figure 177. Rippability versus seismic velocity. (Caterpillar. Handbook of Ripping, 8th Edition)

Figure 177 shows the rippability of various rock types for different seismic velocities using a D9 Caterpillar tractor. As can be seen, when the seismic velocity is more than 2,000 m/s, the D9 tractor is insufficient, and a larger tractor will be required. A D11 tractor can rip some rocks with velocities of almost 3,000 m/s.

6.2.3.1 Seismic Refraction

Basic Concept: The seismic refraction method can be used to find rock velocities. The method requires a seismic energy source, usually a hammer for depths of less than 15 meters and explosives for depths to 30 meters. The seismic waves then propagate through the overburden and refract along the bedrock surface. While they are traveling along this surface, they continually refract seismic waves back to the ground surface. These refractions are then detected by geophones placed on the ground surface. Figure 114a shows the layout of the instrument, the geometry of the seismic refraction procedure, and the corresponding time-distance graph that is used in data processing.

Data Acquisition: The design of a seismic refraction survey involves (1) location of survey, (2) geophone spacing, and (3) the spread (cable length). Surveys should be recorded on days with little wind, away from traffic and other sources of noise and vibrations. If unwanted energy received on site is minimal, the true waveform may be captured employing larger energy sources and filtering and/or stacking the received signals. In addition, since some of the noise travels as airwaves, covering the geophones with sound- absorbing material (partially filled sandbag) may help dampen unwanted noise and enhance coupling of the geophones to the ground.

In general, refraction spreads need to have a length at least three times the desired depth of investigation, which, if investigating to depths of 20 meters, will be 60 meters. If a 24 channel seismic system is used, a geophone spacing of 3 meters, giving a spread length of about 70 meters, will be sufficient, and will also provide velocities for shallower bedrock layers. Both refractor depth and velocity can be obtained from the seismic data. Generally, geophones having a natural frequency of less than about 10 Hz will be used.

Data Processing: The first step in processing/interpreting refraction seismic data is to pick the arrival times of the signal, called first break picking. A plot is then made showing the arrival times against distance between the shot and geophone. This is called a time-distance graph. An example of such a graph for two-layered ground (overburden and refractor) is shown in figure 114a.

The red portion of the time distance plot shows the waves arriving at the geophones directly from the shot. These waves arrive before the refracted waves. The green portion of the graph shows the waves that arrive ahead of the direct arrivals. These waves have traveled a sufficient distance along the higher speed refractor (bedrock) to overtake the direct wave arrivals.

Data Interpretation: The velocity of the refractor and overburden are immediately available from the slope of the time-distance lines. The depth to the refractor can be obtained using several methods. One of the most common methods is called the Generalized Reciprocal Method (GRM) that is described in detail in the Geophysical Methods section. A brief, and simplified, description of the GRM method is presented below. Figure 115 shows the basic rays used for this interpretation. A full GRM interpretation can also provide more detail about the velocity of the refractor, or refractors.

The objective is to find the depth to the bedrock under the geophone at D. This is done using the following simple calculations. The travel times from the shots at A and G to the geophone at D are added together (T1). The travel time from the shot at A to the geophone at G is then subtracted from T1. Figure 116 shows the remaining waves after the above calculations have been performed. These are the travel times from C to D added to the travel times from E to D subtracting the travel time from C to E. The sum of these travel times can be shown to be approximately the travel time from the bedrock at H to the geophone at D. Since the velocity of the overburden layer can be found from the time-distance graph, the distance from H to D can be found giving the bedrock depth.

Advantages: The refraction seismic method is probably the best and most field efficient method for determining the velocity of the bedrock.

Limitations: The seismic refraction method takes advantage of a common occurrence; seismic velocities increase as a function of depth. In other words, the underlying strata, represented by V2 in figure 114a, is assumed to provide a higher seismic velocity than the overlaying layer, represented by V1. This is an important assumption when utilizing the seismic refraction method because "first arrivals," the fastest seismic velocity measured at each geophone, are the only ones considered when data are processed.

If this assumption is false, then no critical refraction occurs at the V1 – V2 interface. This would lead to an overestimate of the thickness of the V1 layer by including the thickness of the V2 layer as "part" of the V1 layer thickness. This dilemma is known as the "hidden layer" problem. Since the velocity of the overburden and refractor are obtained from the slope of the line on the time-distance plot, geological investigations (i.e., borings from wells) would be required to detect the hidden zone.

If seismic velocities do not increase with depth, as in weathered zones where hard lenses may occur, then problems may occur. This will depend on the thickness and extent of the hard lens, along with its velocity contrast with the surrounding material. The thickness of the hard lens will have to be greater at greater depths in order to be a problem. The thickness of a layer depends on the seismic wavelength to influence the seismic refraction data. However, a one-meter-thick hard lens 10 meters deep will probably not be observed. For localized lenses, these may be recognized during the interpretation since, if refractions are emanating from the hard lens, the bedrock may suddenly appear shallow. In addition, the rock velocity may change.

6.3 GEOPHYSICAL METHODS TO IMAGE BURIED MANMADE FEATURES

6.3.1 Detecting Subsurface Utilities

Utilities are usually pipes and cables and include electric, natural gas, telephone, fuel, water, and sewer lines. The ability of geophysical methods to detect utilities depends on the material from which the utility is made, its size, depth, and proximity to other sources of "noise" that may mask the signal from the detection equipment.

The main methods used to locate utilities are magnetic, electromagnetic, and Ground Penetrating Radar (GPR). In addition, if a direct electrical connection to a utility made from conductive material can be made, the utility can be energized with an oscillating electrical field. Another method of energizing a buried metal pipe is to use inductive methods, in which a coil is placed above the pipe and oscillating current made to flow through the coil creating an oscillating magnetic field. This field then creates an oscillating current in the pipe. The resulting magnetic field from the utility can then be located and used to trace its path. Electrical cables with alternating electrical current flowing through (usually 60 Hz) them can be located by detecting the alternating magnetic field associated with the alternating electrical current. A more recent method is the development of an Acoustic Pipe Tracer that detects a sonic frequency transmitted through a plastic pipe.

If the utility is made from metal, electromagnetic methods can then be used. If the metal is ferromagnetic, magnetic methods can also be used. Non-metallic utilities, such as plastic, clay, and concrete cannot be detected with electromagnetic of magnetic methods. However, these, along with metal utilities, can be found using Ground Penetrating Radar (GPR) providing the conditions are appropriate; GPR is significantly influenced by the local soil conditions and may not be appropriate where clay rich soils are present.

6.3.1.1 Magnetic

Basic Concept: To be able to use magnetic methods, the utility must be constructed from, or have included in its construction, some ferromagnetic material. Ferromagnetic materials become magnetized by the earth's magnetic field, which then produce a secondary magnetic field. The resulting field at the ground surface is a combination of the earth's magnetic field and the secondary field from the utility. This creates an anomaly in the resultant magnetic field that can be detected by the instrument. A secondary magnetic field occurs when the small magnetic domains within the ferromagnetic material become predominantly aligned in one direction. If the object is a pipe, in the center of the pipe the magnetic fields from the domains cancel each other out and there is no resultant magnetic field. Thus, with ferromagnetic pipes, the strongest magnetic fields are produced at joints and the ends of the pipe.

Two kinds of magnetic detection instruments are used. One detects the strength of the magnetic field using one sensor, and the other detects the gradient of the magnetic field using two sensors. This instrument is called a Gradiometer. The magnetic field from a ferromagnetic object is illustrated in figure 178, and shows both the total magnetic field strength and the vertical gradient of the magnetic field for an object in the northern hemisphere. Since the inclination of the Earth's field changes with location, this will affect the magnetic field anomaly at that location.

In the United States, the Earth's magnetic field is dipping to the north at a moderately steep angle. The total magnetic field strength shows high values to the south of the object and negative values to the north. This is because the Earth's field induces north poles (positive values) as it enters the object and south poles (negative values) as it leaves the object. The vertical gradient of the magnetic field peaks over the top of the object and is flanked by negative values on either side. As can be seen from this diagram, the peak positive anomaly using the total magnetic field is not over the top of the object whereas the vertical gradient does peak over the top of the object. Thus, instruments that measure the vertical (or something close to vertical) magnetic gradient are better able to more accurately locate the top of the object.

A magnetic locator, manufactured by the Schonstedt Instrument Company, is illustrated in figure 179. These instruments have two magnetic sensors and therefore respond to the gradient of the magnetic field.

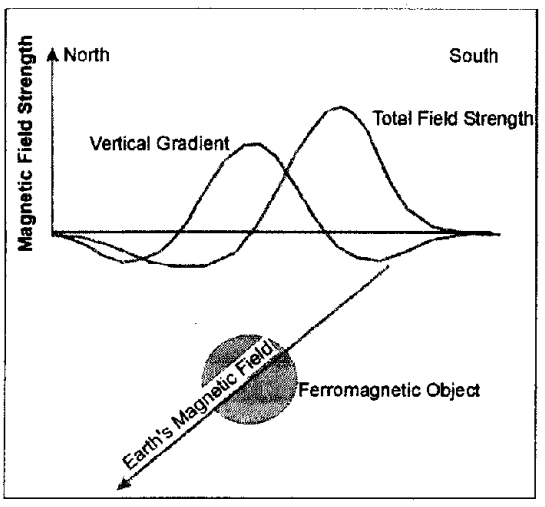

Figure 178. Magnetic field from a cylindrical object.

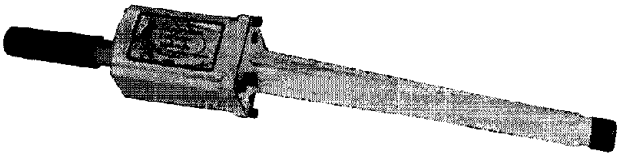

Figure 179. Magnetic locating instrument. (Schonstedt Instrument Company)

If the instrument is held vertically, then the vertical gradient of the magnetic field is measured. Figure 180 illustrates a magnetic detector (Gradiometer) showing the two sensors and the magnetic field from a ferromagnetic object.

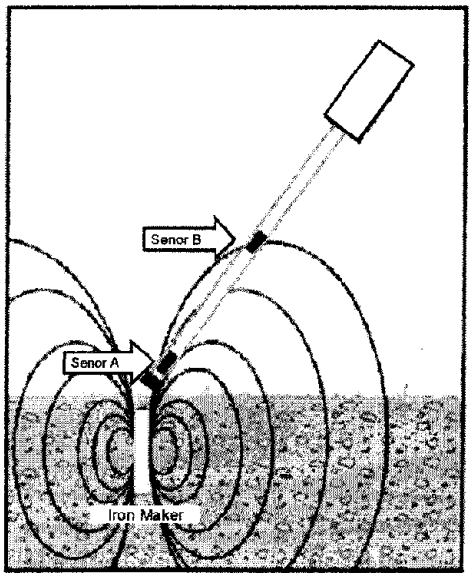

Figure 180. Magnetic locator using two sensors to measure the gradient.

Data Acquisition: Surveys are conducted by sweeping the instrument back and forth while walking at a slow pace. When using a gradiometer to measure the vertical gradient, the instrument should be held in a vertical position. Usually, these instruments have both a display and an audible sound when anomalies are found. No data processing can be done, or is needed, and no data are output from these instruments.

Data interpretation: Data interpretation is not required since only the maximum signal (or maximum audible sound) is observed. Usually, spray paint marks will be placed on the ground where pipes are indicated by the instrument. These will typically be colored according to the American Public Works Standard, which are shown below:

Conductor	**Color**
Electric power lines, cables or conduits	Red
Communication lines, cables or conduits	Orange
Gas, oil, petroleum or other gaseous material	Yellow
Storm and sanitary sewers; drain lines	Green
Water, irrigation or slurry lines	Blue

Advantages: Magnetic locators are simple to operate and provide a field readout or signal when an anomaly is detected.

Limitations: Magnetic locators will only respond to metal that is ferromagnetic. Metals such as copper, aluminum, and stainless steel are not magnetized by the Earth's field and, therefore, do not produce a magnetic anomaly. The method will also not detect plastic, clay, or concrete pipes.

6.3.1.2 Electromagnetic

Basic Concept: Electromagnetic instruments for detecting utilities produce and sense electromagnetic fields. These instruments will only work if the utility is made from an electrically conductive material. The instruments produce the electromagnetic fields using a coil through which oscillating current is made to flow, thus producing an oscillating electromagnetic field. Another coil is used to sense this oscillating electromagnetic field. When a coil senses a changing electromagnetic field, a voltage is produced that can be displayed or activate a sound. If a utility is not made from metal, sometimes a metal tracer wire is placed along with the utility, thereby allowing electromagnetic instruments to be used to locate the utility.

This discussion of the instruments is divided into two parts. This is because there are a number of conventional utility-locating instruments that are commonly used, an example of

which is presented above. In addition, geophysical instruments can be used for utility location. These instruments are mostly used by geophysical companies, and less so by utility-locating companies.

The first section discusses the conventional utility-locating instruments and is titled Conventional Electromagnetic Utility Equipment. The second section is titled Geophysical Electromagnetic Utility Instruments.

Conventional Electromagnetic Utility-Locating Instruments

A utility detection instrument, manufactured by Metrotech Inc. that uses electromagnetic fields, is illustrated in figure 181.

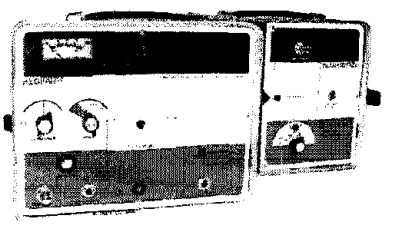

Figure 181. Utility-locating instrument. (Metrotech, Inc.)

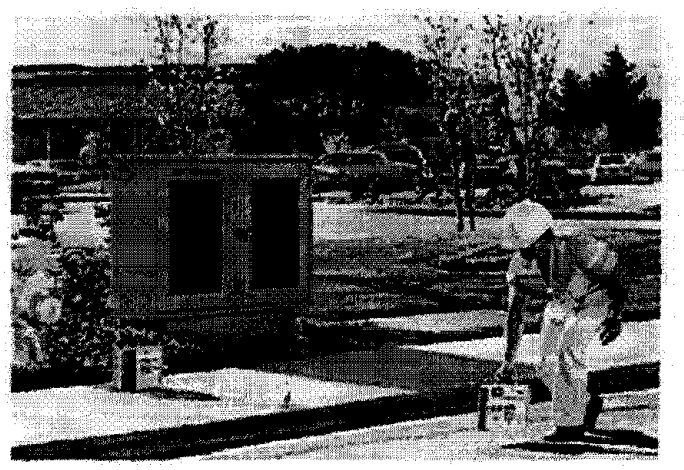

Figure 182. Utility-locating instrument in use. (Metrotech, Inc.)

This instrument has several modes of operation and can do both inductive and conductive pipe and cable locating. It also has a passive mode in which it responds to the electromagnetic fields from 50/60 Hz signals. It provides the ability to directly connect to a metal pipe, thus allowing the pipe to be energized. In addition, a clamp can be used to connect to a pipe where no direct connection is available. This clamp then inductively energizes the pipe and allows it to be located. Figure 182 shows the instrument being used. In this picture, the pipe is being energized inductively, and the operator then searches for anomalies using the receiver.

Data Acquisition: The design of a survey depends on the method of use. If a direct or inductive clamp can be made to the pipe, the detector portion of the instrument is used to trace the location of the pipe. If the location of some part of the pipe is known, the instrument can be used to inductively energize the pipe by placing a transmitting coil on the ground surface over the top of the pipe. If the location of the pipe is not known, and the investigation is to see if a pipe exists in a particular area, a system has to be devised to survey the area using numerous locations for the transmitting coil.

Data Processing: No data are output from the instrument, and no data processing is needed.

Data Interpretation: Interpretation is done by the operator who marks the ground with surveyor's spray paint where anomalies are observed. To locate a power line, the instrument is used in passive mode during which it detects 50/60 Hz magnetic field oscillations.

Advantages: The instruments are simple to use and provide anomaly indications while the survey is being conducted.

Limitations: The limitations are generally the depth of the utility, size of the utility (amount of metal), proximity to other local surface or buried metal, and local power line noise. Generally, these instruments are not significantly influenced by power line noise unless the power line is very close.

Geophysical Electromagnetic Utility Instruments.

Basic Concept: Two instruments are commonly used by geophysical companies for utility locating. One is called the EM31, manufactured by Geonics Ltd. in Canada, and the other instrument, also manufactured by Geonics Ltd., is called an EM61. In order for electromagnetic methods to work, the utility must be electrically conductive.

EM31 Instrument

The EM31 instrument is shown in figure 183 and illustrates the most common method of use. This instrument uses two coils, one of which transmits electromagnetic energy at about 9.8 kHz, and the other coil receives the resulting signal. The coils are located at the ends of the boom. Because the instrument uses oscillating electromagnetic fields, this instrument is said to operate in the frequency domain. The newer EM31-MK2 model, shown in figure 183, incorporates the data logger into the control console.

Figure 183. The EM31-MK2 instrument. (Geonics, Ltd.)

The EM 31 can be used to locate buried pipes. It is particularly effective when a long pipe is to be located, since it produces a large response when a length of buried pipe extends on either side of the instrument. The instrument can be used in various modes. Its boom can be held parallel to the direction of travel or perpendicular. It can be used in a normal operating orientation (vertical dipole mode) or turned 90 degrees about its long axis (horizontal dipole mode). In the figure, the instrument is being used with its boom parallel to the direction of travel and in vertical dipole mode. This is the mode most often used for utility search surveys. The EM31 has a maximum depth of penetration of about 6 m. The depth at which it can detect a metal pipe will depend on the conductivity of the soil, local electromagnetic interference, and the amount of metal that the pipe contains. Thus, the diameter and wall thickness of the pipe each influence the data.

Data Acquisition: Surveys are conducted by walking at a slow pace normal to the expected utility orientation. Data can be observed on a meter or it can be setup to be stored on a data logger.

Data Interpretation: The data can be interpreted in the field by evaluating the shape of the anomalies. Just before a metal pipe is crossed, the readings increase, and then rapidly drop to a low value over the top of the pipe. Once the pipe has been crossed, the readings increase again before finally descending to non-anomalous values. Interpretation involves locating the anomaly described above on as many traverses as possible and then positioning a line through them to position the pipe.

Advantages: The EM31 is simple to use and provides a readout on the instrument allowing field evaluations of the anomalies. This instrument will generally find metal utilities to depths up to about 3 meters.

Limitations: Probably the largest limitation is that the electromagnetic fields generated by the instrument produce secondary fields, not only in utilities, but also in any other local metal objects, which then radiate their own field that is also detected by the instrument. The instrument is quite long and may be difficult to use in spatially restrictive areas.

EM61 Instrument

The EM61 transmits pulses of electromagnetic energy, rather than a continuous frequency as with the EM31, and as discussed above, is called a time domain instrument. Figure 184 shows the EM61 recording data as it is being pulled by the operator.

Figure 184. The EM61-MK2 instrument. (Geonics, Ltd.)

Two square-shaped coils are used. The lower coil transmits the electromagnetic energy, and both the lower and upper coils receive the resulting signals. In general, this instrument is not as proficient at detecting pipes as is the EM31. The EM61 also has a hand-held version for surveys where the conventional EM61 may be too bulky and for shallower surveys. This instrument is shown in figure 185.

Figure 185. The EM61-HH2 hand held instrument. (Geonics, Ltd.)

Data acquisition: As with the EM31, surveys are conducted by traversing across the area where buried pipes are thought to occur. The data can be observed using the display on a data logger and also stored in memory. The readings are presented in millivolts. Anomalies are simply higher millivolt values. Using the two coils, it is possible to minimize the influence of near-surface metal. This is because the lower coil has a greater response to surface metal than the upper coil. To evaluate whether the anomaly results from surface (or

near- surface) metal, the amplitude of the signal from the upper coil is increased to what would be expected were it positioned at the level of the lower coil. If the anomaly observed results from surface metal, then the two amplitudes (amplified top and bottom coils) will be similar.

Advantages: The EM61 is an excellent instrument for locating metal in the top 2 meters of the ground surface.

Limitations: As with the EM31, the instrument produces electromagnetic fields and can energize local metal. However, this is a much less serious problem with this instrument than with the EM31. Because of its size, the EM61 may be difficult to use in confined areas. If that is the case, the hand-held EM61 can be used.

6.3.1.3 Ground Penetrating Radar

Basic Concept: Ground Penetrating Radar (GPR) is a technique that uses high frequency radar waves to image the subsurface. The GPR instrument consists of a recorder and a transmitting and receiving antenna. Different antennas provide different frequencies, which usually vary between 25 and 1,500 MHz. Lower frequencies provide greater depth penetration but lower resolution. A schematic showing the transmitter and receiver along with the transmitted waves is illustrated in figure 111. The technique can be used where the overburden contains little clay or silt. An unsaturated overburden will provide the best penetration depths. If these conditions exist, then penetration depths may be a few meters.

Several companies manufacture GPR equipment, including Geophysical Survey Systems, Inc. (GSSI), GeoRadar, Mala GeoScience, and Sensors and Software.

Figure 112 shows the data recording and system control for a GPR system. Any antenna supported by this instrument can be attached and used to collect data. A 400 MHz antenna that can be used with the above instrument is illustrated in figure 186.

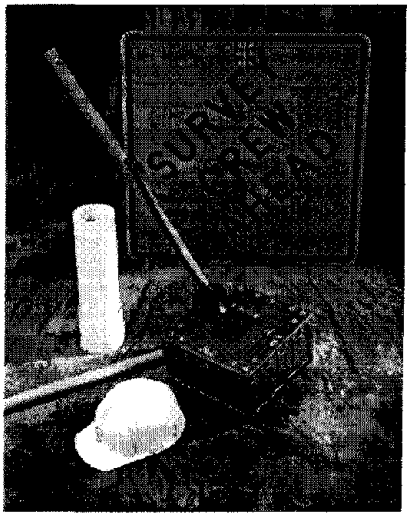

Figure 186. 400 MHz Ground Penetrating Radar antenna. (Geophysical Survey Systems, Inc.)

This antenna is suited for fairly shallow applications to depths of about 3 meters and can be used to locate buried utilities.

Data Acquisition: GPR surveys are conducted by pulling the antenna across the ground surface at a normal walking pace. The recorder stores the data as well as presenting a picture of the recorded data on a screen. A typical GPR record searching for utilities is shown in figure 187 and illustrates anomalies from rebar and the utilities.

As can be seen, the rebar is seen as large numbers of small anomalies whereas the utilities are larger anomalies. It is worth noting that the GPR signal was able to penetrate through the rebar and present clear anomalies of the utilities.

Data Processing: It is possible to process the data, much like the processing done on single-channel reflection seismic data. Routines such as distance normalization, horizontal and vertical scaling, along with frequency filtering, can be performed. However, depending on the data quality, this may not be necessary since the field records may be all that is needed to observe the utility.

Data Interpretation: To calculate the depth to the utility, the speed of the GPR signal in the soil at the site needs to be obtained. This can be estimated from charts showing speeds for typical soil types, or it can be obtained in the field by conducting a small traverse across a buried feature whose depth is known.

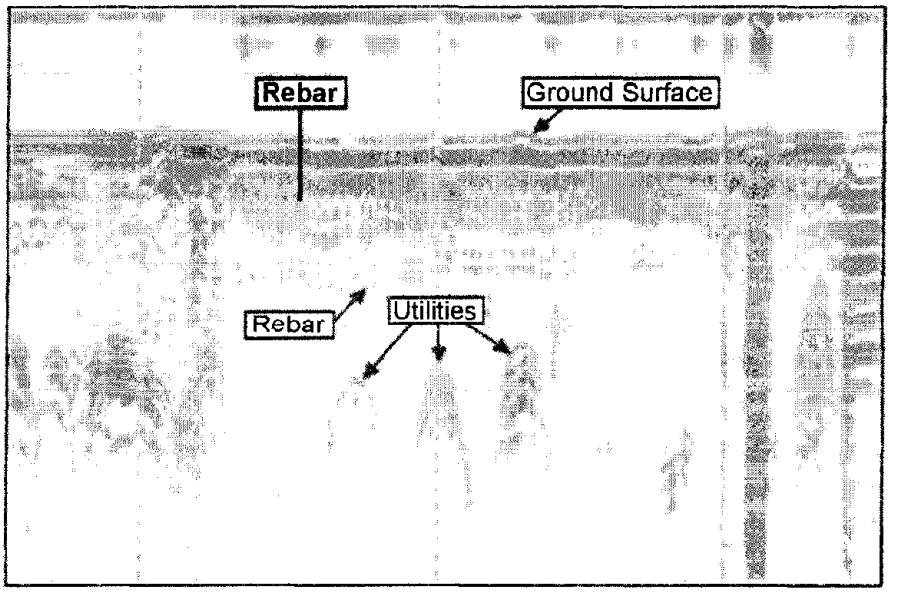

Figure 187. Ground Penetrating Radar data from a utility trench. (Golder, Associates, Inc.)

Advantages: The GPR method provides a rapid technique for locating utilities. Since the data is viewed on a screen on the instrument, the data can be viewed in the field and the locations of anomalies marked on the ground.

Limitations: Probably the most limiting factor for GPR surveys is that their success is very site specific, and depends on having a contrast in the dielectric properties of the target compared to the host overburden, along with sufficient depth penetration to reach the target. However, it is likely that most utilities will provide the desired dielectric contrast needed, thus depth of penetration is probably the most important factor. Penetration depends on the frequency of the antenna, the conductivity of the overburden, and whether clay is present in the overburden. In addition, for lower frequencies, where the antenna is not shielded, reflections can occur from other objects. Generally, this should not be a problem for utility searches since most of the higher frequency antennas are shielded and are the ones used for buried utility surveys. For surveys under bridges, the bridge deck may provide a reflection. It may be possible to separate the reflection from the bridge deck from the reflection from the bedrock, providing these two reflection times are significantly different.

6.3.1.4 Acoustic Pipe Tracer

This instrument is able to locate buried plastic pipe and is used to locate buried plastic natural gas lines. An identifiable acoustic signal is introduced into the pipe. The receiver detects the sound waves that radiate from the pipe. An acoustic driver is used to put the signal into the pipe, and the sound is detected by sensors attached to a portable receiver.

6.3.2 Detecting Underground Storage Tanks

Underground storage tanks (UST) are made from steel, fiberglass, and other materials. They range in size from fairly small tanks with capacities of less than a few hundred gallons to those with capacities of many thousands of gallons. Tanks are usually buried with their tops a few feet beneath the ground surface. Pipes and other facilities may be connected to the tanks. They are also often buried in industrial areas where a significant amount of other metal is present.

Different geophysical methods are applicable to tanks composed of different materials. For example, metal tanks (made from ferromagnetic material) can be found with magnetic, electromagnetic, and Ground Penetrating Radar (GPR) methods. Non-metal tanks can usually only be found with GPR, although electromagnetic methods may work in some cases.

6.3.2.1 Magnetic Methods

Basic Concept: A metal tank is magnetized by the Earth's magnetic field. It then produces a secondary field. The resultant field contains both the Earth's magnetic field and the field from the tank and results in a distortion of the Earth's magnetic field. A magnetometer can be used to survey an area where metal tanks are expected and should be able to locate the tanks. In addition to measuring the Earth's total magnetic field, magnetic instruments are produced with two sensors and are able to measure the gradient of the Earth's magnetic field. The gradient of the field is usually less sensitive to local interferences and may be the best method in industrial sites with significant cultural features. It may also be easier to interpret since the peak of the anomaly is over the center of the magnetic source (a tank). The total field data peaks to the south of the magnetic source and has a negative amplitude to the north

of the source. Almost all magnetometers can record data to memory during the survey. This can then be downloaded to a computer for further processing if needed.

Data Acquisition: Magnetometer surveys are usually conducted along straight lines covering the area of interest. Readings are often taken at regular time intervals (say one second or faster) while walking at a reasonable pace. To position the data, either the ends of the lines will have to be surveyed or a Global Positioning System (GPS) is used. Figure 188 shows a gradiometer system measuring the horizontal gradient of the earth's magnetic field. This equipment has two gradiometers, one on either side of the operator, allowing more efficient field surveying.

Figure 189 shows a magnetometer system with a GPS unit attached to give the coordinates of the survey.

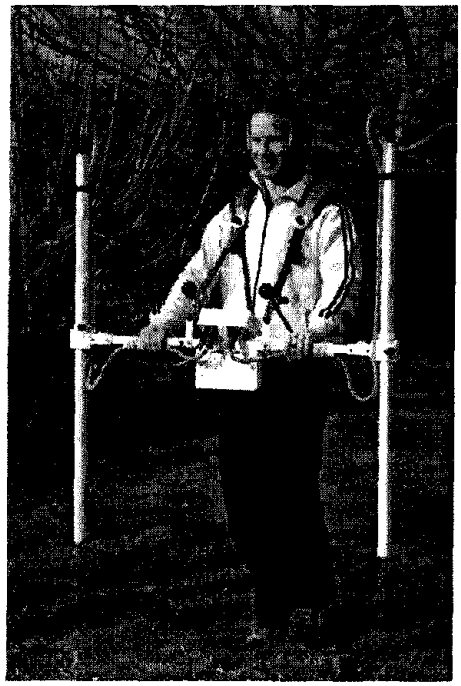

Figure 188. Grad-601 magnetic gradiometer system. (Bartington Instruments)

Figure 189. Magnetometer with Global Positioning System. (Geometrics, Inc.)

The Earth's magnetic field continuously changes strength and has a daily cycle, called the diurnal variation. If the survey takes more than a few hours, or significant magnetic field changes are occurring, a base station should be used. The base station is set up at a location close to the investigation site where no magnetic anomalies are present. The base station records the magnetic field strength at regular intervals along with the time of the reading. The instrument used to conduct the survey also records the time that each reading is taken. Thus, it is possible to remove the influence of diurnal changes from the field data. Removal of the diurnal effect is not required with gradient magnetic data, since the diurnal changes affect both sensors simultaneously. However, surveys for UST's are likely to be completed fairly quickly, and moderate to large anomalies are often encountered; thus, the base station corrections will not usually significantly influence the data.

Data Processing: As mentioned above, probably the most important item is to remove the influence of diurnal changes in the Earth's magnetic field. Coordinates have to be assigned to the data so that maps can be drawn. This requires that the ends of the traverse lines are surveyed or a GPS system is used. The data can be filtered if needed, although little processing is usually required.

Data Interpretation: Interpretation of magnetic data for tanks usually involves visual inspection of the data for anomalies that suggest tanks. These are then located on a map of the area. Since magnetometer surveys are very simple, they can be used as a rapid screening tool. Magnetic data can be interpreted using modeling software providing estimates of the size and depths to the sources of the magnetic anomalies.

Advantages: The magnetic method provides a simple way to locate metallic underground storage tanks. Since the data is observed while conducting the field survey, anomalies can be located and marked on the ground at the time of the field survey.

Limitations: The method requires the tank be constructed of ferromagnetic metal. If a significant amount of local surface metal exists, it may be difficult to separate anomalies from the surface metal from those emanating from buried tanks. This can be a significant problem in some industrial areas. Magnetic data should not be recorded if the diurnal magnetic field variations are large, depending on the expected size of the anomaly and the duration of the survey. However, since the target for these surveys are tanks made from ferromagnetic material, which should produce large anomalies, and the surveys will generally be completed in a short amount of time, this should not be a serious limitation.

6.3.2.2 Electromagnetic

Basic Concept: Electromagnetic (EM) methods are commonly used to locate buried tanks. They use a transmitter (coil) to produce an electromagnetic field, which then induces electrical currents in electrically conductive material. The amount of current induced depends on the electrical conductivity of the material. Since metal is highly conductive, relatively large currents are induced in metal objects. These currents then generate a secondary electromagnetic field that can be detected at the ground surface using a receiver coil. The final output from the receiver coil is a voltage related to the conductivity of the material influenced by the electromagnetic field from the transmitter. Electromagnetic instruments can locate both ferrous and non-ferrous objects.

There are two kinds of electrical signals used by electromagnetic equipment. One is called Frequency Domain, and the other is called Time Domain. Frequency domain signals are sinusoidal electromagnetic signals, and for geophysical equipment, usually have frequencies below 10 kHz. Time domain signals occur when the transmitter current is switched on for a short time and then switched off. This procedure is repeated continuously. When the current switches on or off, the rapid change in the transmitter current and corresponding electromagnetic field produces currents in local conductive material. As with frequency domain signals, the amount of current induced depends on the conductivity of the material. These currents then generate a secondary electromagnetic field, which is detected by the receiver coil during the time that the transmitter current is off.

Figure 190 presents a conceptual drawing showing the different current and electromagnetic fields involved.

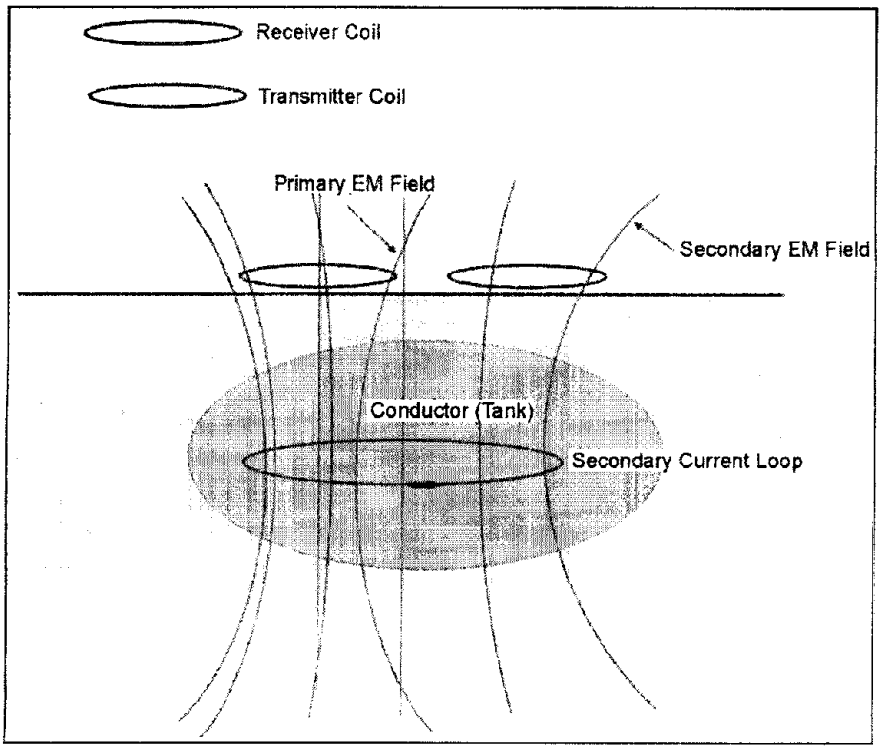

Figure 190. Concept diagram for electromagnetic methods.

In the above diagram, the transmitter generates an electromagnetic field using electrical current in the transmitter coil (shown in red). This electromagnetic field then creates currents in conductors (shown in green). These conductors then generate secondary magnetic fields (shown in green) that are detected by the receiver coil. The receiver coil then outputs a voltage that indicates the conductivity of the object.

Several electromagnetic instruments can be used to find buried tanks. These include the EM31 and the EM61, manufactured by Geonics Ltd. of Canada, and the GEM2 manufactured by Geophex USA. The EM31 and GEM2 are frequency domain instruments, whereas the EM61 is a time domain instrument. Generally, these instruments have a depth of investigation of 4 m or more, depending on the target size and the local conditions. Figure 191 shows the GEM2 instrument.

Figure 184 shows the EM61 in use. The lower coil is the transmitter and data is recorded using both the lower and upper coils. Since surface metal influences the lower receiver coil more than the upper receiver coil, having two receiver coils allows the influence of surface metal to be minimized.

Figure 191. The GEM2 electromagnetic instrument. (Geophex Inc.)

A hand-held EM61, shown in figure 185, is also available and is useful when the larger EM61 is too cumbersome for use in the area to be surveyed.

Data Acquisition: Electromagnetic surveys for tanks are conducted in much the same manner as magnetic surveys for tanks. Lines are laid out crossing the area of interest and data are recorded along these lines.

Data Processing: Some metal detectors record data to memory and some do not. The EM instruments (EM31, EM61, GEM2) all record data to solid-state memory. This can then be downloaded to a computer, and maps produced of the data. The data can be filtered if needed, but this is probably not common. The data can have coordinates assigned if the magnetic traverses have been surveyed or a GPS system was used.

Data Interpretation: If the instrument does not record the field data to memory then the locations of the anomalies are marked on the ground while conducting the field survey. If the data is stored in memory then this can be downloaded to a computer and maps produced showing the anomalies. These can then be interpreted.

Advantages: The instruments described above provide a good method for locating underground storage tanks. If the geophysical instruments are used then the data can be downloaded to a computer and plotted to provide a record of the survey.

Limitations: Probably the most significant limitation of the EM31, EM61, and GEM2 instruments is the influence of local metal at the site. In addition, highly conductive soils may limit the effective penetration of these instruments. Of these instruments, the EM61 is least influenced by local metal. By using data from the two receiver coils, this influence can be minimized.

6.3.2.3 Metal Detectors

Basic Concept: Metal detectors use the same principles as do the geophysical instruments described above. However, they are generally smaller instruments and are easier to use,

although their investigation depths will often be smaller. Some metal detectors use magnetic sensors and others use electromagnetic waves. The magnetic metal detectors often use two sensors and measure the gradient of the magnetic field. Figure 192 shows a drawing of two sensors and the magnetic field lines from a buried object.

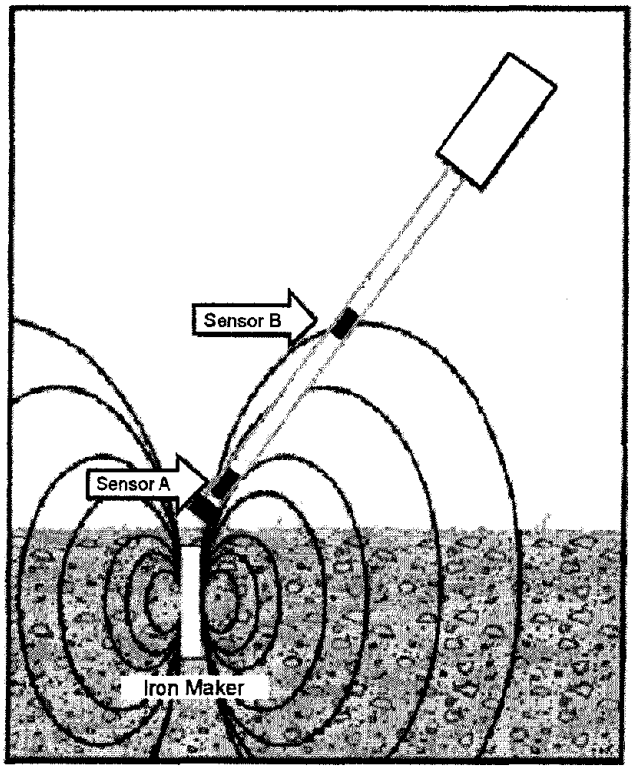

Figure 192. Metal detector using two magnetic sensors.

Metal detectors that use electromagnetic methods use a wide range of frequencies (500 Hz to over 80 kHz) producing sinusoidal electromagnetic waves to produce secondary electrical currents in the targets. These secondary currents then produce secondary electromagnetic fields that are sensed by the metal detector.

Metal detectors, also called pipe and cable detectors, are widely used at UST sites for locating buried metal objects. The depth of investigation of metal detectors is dependent primarily on the surface area and depth of the object. However, the response of an object decreases rapidly as depth increases. However, metal detectors can detect a 55-gallon drum to depths of 3 m and a 10,000-gallon tank up to 6 m. Metal detectors are particularly useful for tracing pipes and cables at UST sites. These detectors are less sensitive to surface and subsurface interferences than the larger geophysical EM instruments, although care must be taken to minimize noise from fences, vehicles, buildings, and buried pipes. In addition, these instruments are less influenced by the conductivity of the soil than EM instruments. However, mineralized soils and iron-bearing minerals can provide significant natural interference.

Data Acquisition: Surveys are conducted by sweeping an area and listening (for those with audio signals) or observing the signal magnitude for anomalies. These locations are then marked on the ground as the survey progresses.

Data Processing: Usually no processing of the data can be done with a metal detector.

Data Interpretation: Metal detectors provide visual or audio display that is viewed in the field. Anomalies are usually marked on the ground as they are observed.

Advantages: Metal detectors are usually easy to use and provide anomaly information as the survey progresses.

Limitations: Since metal detectors do not usually store field data in memory, no record of the results, and anomalies, can be made.

6.3.2.4 Ground Penetrating Radar

Basic Concept: Ground Penetrating Radar (GPR) is a technique that uses high frequency radar waves to image the subsurface. Ground Penetrating Radar (GPR) can be used to locate buried tanks and utilities. The depth of investigation of GPR depends on the soil conditions. A saturated soil with significant clay will severely limit the penetration of the method. Ideal conditions are unsaturated, clay-free soils. Depth of penetration also depends on the frequency of the signal. Different antennas provide different frequencies, which range from about 25 MHz to 1500 MHz. A low-frequency antenna (signal) will provide the best penetration depth. Since resolution, which is better with a high-frequency antenna, is usually not a serious issue for UST's, a low-frequency antenna is probably sufficient.

The GPR instrument consists of a recorder and a transmitting and receiving antenna (see figure 193). The transmitter provides the high-frequency sinusoidal electromagnetic signals that penetrate the ground and are reflected from objects and boundaries providing a different dielectric constant from that of the overburden. The reflected waves are detected by the receiver and stored in memory.

This figure shows the GPR signal being transmitted into the ground. In this figure the tank is reflecting the GPR signal.

Several companies manufacture GPR equipment. These include Geophysical Survey Systems, Inc (GSSI), GeoRadar, Inc, Mala GeoScience, and Sensors and Software Inc. Figure 194 shows a GPR system manufactured by GeoRadar.

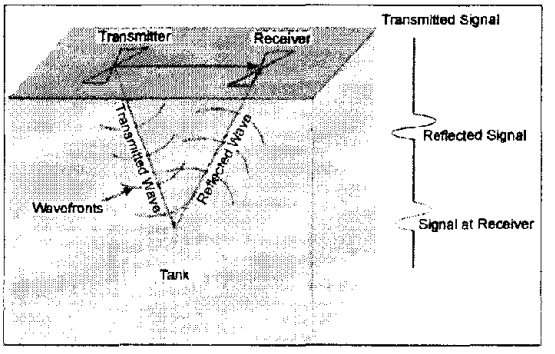

Figure 193. Ground Penetrating Radar over a tank.

Figure 113 shows a 100 MHz antenna being used during a survey. This antenna is manufactured by GSSI and requires one of their control units for use. The 100 MHz antenna is suited for deeper applications to depths of about 20 m and may be appropriate for locating UST's.

Data Acquisition: GPR surveys are conducted by pulling the antenna across the ground surface at a normal walking pace. The recorder stores the data as well as presents a picture of the recorded data on a screen. If maps are to be produced, the coordinates of the ends of the lines need to be surveyed.

Figure 194. Ground Penetrating Radar instrument. (GeoRadar, Inc)

Data Processing: It is possible to process the data, much like the processing done on single-channel reflection seismic data. Processes that can be applied include distance normalization, horizontal scaling (stacking), horizontal and vertical filtering, velocity corrections and migration. However, depending on the data quality, this may not be necessary since the field records may be all that is needed to observe the target.

Data Interpretation: If the depth to an anomaly is required, the speed of the GPR signal in the soil at the site has to be obtained. This can be estimated from charts showing speeds for

typical soil types or it can be obtained in the field by conducting a small traverse across a buried feature whose depth is known. Figure 195 shows three fiberglass tanks found using the GeoRadar instrument.

Figure 195. Ground Penetrating Radar images over three Underground Storage Tanks (UST). (GeoRadar, Inc.)

This image provides much more information than simply the location of the underground storage tanks (UST). The darker images on either side of the tanks represent undisturbed soil. As can be seen, the excavation into which the tanks were placed has vertical sides. A concrete slab has been placed on the ground surface above the tanks. This slab has rebar reinforcing, which is clearly seen as the regular vertical dark lines above the image of the tanks. The dark areas near the top of the tanks may represent air above the liquid in the tanks. Metal tanks provide an even clearer signal since they provide a large dielectric contrast with the surrounding soil. Figure 196 shows the GPR image from three tanks.

Advantages: GPR surveys are fairly easy to conduct and provide the results during the field survey. Different antenna can be used providing different frequencies if better anomaly resolution or greater penetration depth is needed.

Limitations: Probably the most limiting factor for GPR surveys is that their success is very site specific and depends on having a contrast in the dielectric properties of the target compared to the host overburden along with sufficient depth penetration to reach the target. However, it is likely that most UST's will provide the desired dielectric contrast needed; thus, depth of penetration is probably the most important factor. Tanks are usually buried with their tops a few feet beneath the ground surface. Unless there are significant amounts of clay in the soil above the tank, or heavy reinforcing metal bar, penetration to at least the top of the tank should be possible in most cases.

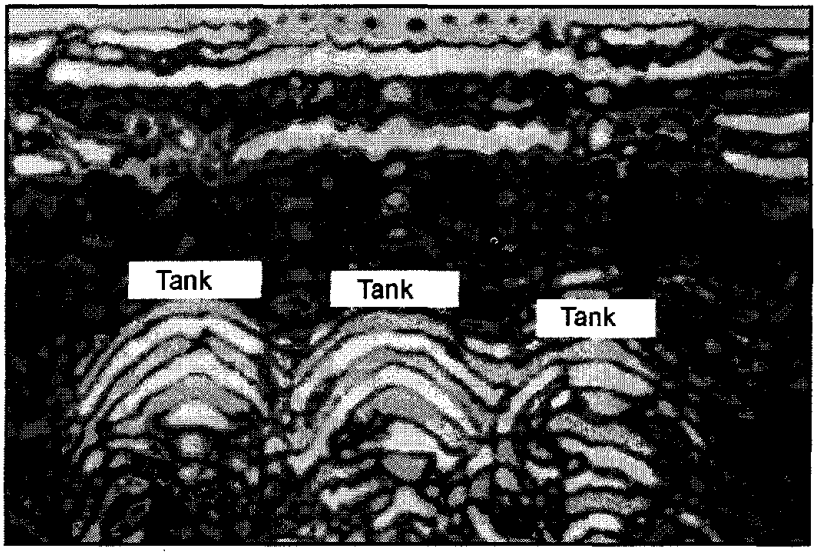

Figure 196. Ground Penetrating Radar signal from three Underground Storage Tanks. (GeoModel, Inc.)

Low-frequency antennas are usually not shielded. Thus, they radiate electromagnetic fields in all directions. If these fields encounter aboveground objects, they will produce reflections in addition to those resulting from buried objects. Sometimes the combination of reflections from above ground and subsurface objects makes the interpretation of the data difficult.

*6.*3.3 Mapping Contaminant Plumes

Contamination plumes usually refer to plumes in groundwater. These can arise because of point sources, such as direct discharge of effluent from a pipe or from non-point sources such as the application of pesticides over a wide area, which then seep into the groundwater over time. Plumes can vary in size from quite small to those covering many hectares. In addition to contaminant plumes, geophysical methods are used to find buried trenches, landfill boundaries, and solve other environmental problems.

Often, the original source of contamination contains a suite of chemicals, of which only a small number are contaminants. Because the concentration of contaminants is usually quite small, often measured in parts per million, geophysical surveys can rarely directly detect contaminants. An exception to this might be severe hydrocarbon contamination, where Ground Penetrating Radar (GPR) is sometimes successful. For geophysical methods to be used to detect contamination, other factors must be involved. Some of these are listed below.

The suite of chemicals making up the contamination may be electrically conductive, either because it is acidic or because it contains salts. In this case, the plume is also electrically conductive and can often be detected using electromagnetic methods. If the contaminants are heavier than water, such as dense non-aqueous phase liquids (DNAPL), these chemicals will sink to the bottom of an aquifer. In this case, mapping the topography of the top of the aquitard (maybe a clay layer) that impedes the downward movement of the DNAPL may be valuable. Depending on the geologic conditions, this can be done using several geophysical methods such as electromagnetic, resistivity, refraction seismic, and possibly GPR. It is also

possible that the suite of chemicals reacts with clay layers, altering their electrical properties. If that is the case, Spectral Induced Polarization (SIP) may be used. However, this application of the IP method is still being researched and should be considered experimental. Another method that can sometimes be used to detect chemically altered soils and overburden is GPR, since such changes can sometimes affect the dielectric properties of the overburden.

Methods

6.3.3.1 Electromagnetic

Basic Concept: Electromagnetic methods are used to measure the electrical conductivity of the ground. Several instruments are available to do this including the EM31, EM34, and GEM2. If the vertical distribution of conductivity is needed (or its inverse resistivity), then time domain electromagnetic or resistivity sounding methods can be used. However, usually the most important component in mapping contaminant plumes is to find the aerial extent of the plume. The EM31 instrument is shown in figure 183.

Electromagnetic instruments designed to measure the ground conductivity use sinusoidal waveform oscillating between 50 and about 20 kHz. The EM31 oscillates just below 10 kHz. This instrument is effective to depths of about 6 m. If conductivity measurements are required to greater depths then the EM34, shown in figure 197, can be used. This instrument can be used to depths greater than 50 m. Three different separations of the two coils can be used providing three different depths of investigation. However, as the depth of investigation increases, the lateral resolution decreases. The EM34, unlike the EM31, cannot be used with one person; two people are required. Data recording is much slower than with the EM31.

All of these instruments measure the bulk electrical conductivity of the ground. Since the conductivity of several different layers may be included in the conductivity measure, the correct technical term for the measured conductivity is apparent conductivity. When discussing EM31 and EM34 data in this document, conductivity is understood to mean apparent conductivity.

Both the EM31 and EM34 use a transmitter and receiver coil, usually used with the coils coplanar. These instruments can be used in two different modes: one is called the vertical dipole mode, and the other is called the horizontal dipole mode. In this mode, the plane of the coils is vertical. In the vertical dipole mode the plane of the coils is horizontal. These two different modes provide different ground responses. In the vertical dipole mode, the instrument is less sensitive to near-surface effects and has the deepest penetration. In the horizontal dipole mode, the near surface ground conductivity has most effect, with deeper layers having much less influence.

Figure 197. The EM34 being used in horizontal dipole mode. (Geonics, Ltd.)

Data Acquisition: Surveys are conducted by taking readings along lines crossing the area of interest. These lines need to be surveyed to provide spatial coordinates. Readings either are taken at defined stations, or with the EM31, on a timed basis, say every second. The mode (vertical or horizontal dipole) in which the instruments are used depends on the target depth and the objectives. The instruments store the data in memory as it is recorded, allowing it to be downloaded to a computer at a later time.

Example data from an EM survey around a landfill in Oklahoma is presented in figures 198 and 199. Figure 198 shows EM31 data and figure 199 shows EM34 data. Both show conductivity increasing significantly near the landfill boundary.

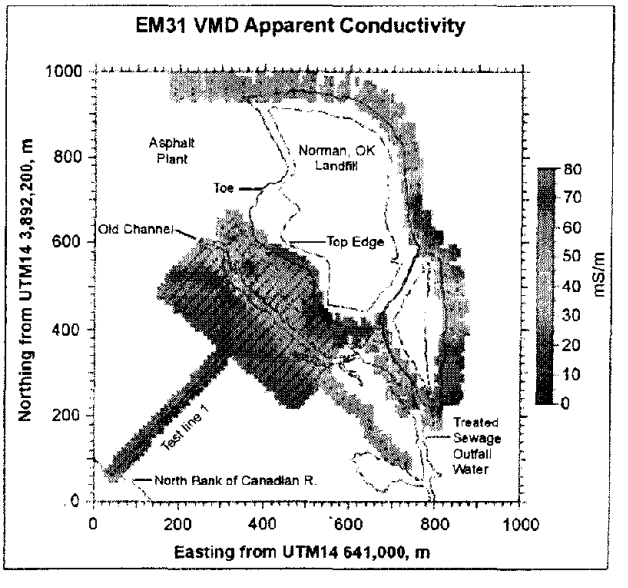

Figure 198. EM31 conductivity data - vertical dipole mode. (USGS)

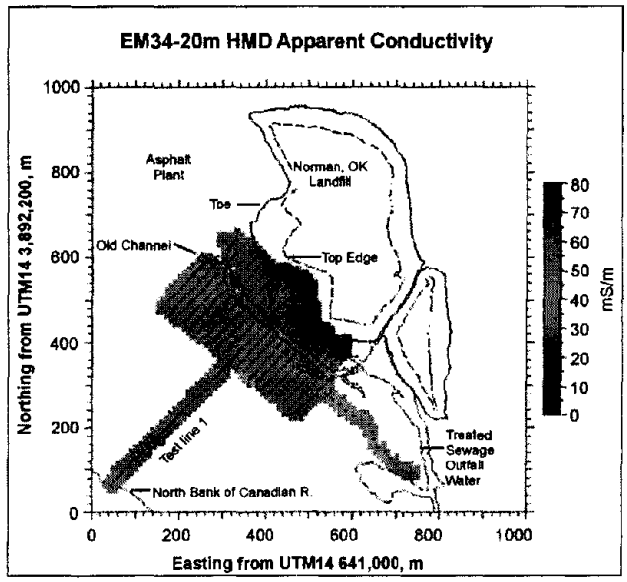

Figure 199. EM34 conductivity data – horizontal dipole mode. (USGS)

The EM31 data were recorded with the instrument in vertical dipole mode (VMD). In this mode, the instrument has a depth of investigation of about 6 m. As can be seen, the conductivity increases from less than 20 mS/m some distance from the landfill to 80 mS/m or more near the landfill boundary. It is likely that the effluent from the landfill has contaminated the groundwater, making it more electrically conductive.

The EM34 data were recorded in horizontal dipole mode using a coil separation of 20 m, giving it an exploration depth of about 15 m, nearly twice the exploration depth of the EM31 data shown in figure 198. The EM34 data show conductivities near the landfill of over 70 mS/m, decreasing to about 30 mS/m some distance from the landfill.

Data Processing: Data processing mostly involves assigning coordinates to each data point. The data are then gridded, contoured, and plotted, producing a map of the measured conductivity at the site.

Data Interpretation: Interpretation is done from this map. Generally, when investigating conductive plumes, this will involve searching for areas of high electrical conductivity. With the EM31, these areas will be fairly well defined since the instrument has a fairly limited area of influence. However, with the EM34, which has a much greater depth of investigation, the lateral resolution is less well defined.

When both the EM31 and EM34 have been used at a site to provide different depths of investigation, more information can be obtained about the site. In the case shown above in figures 198 and 199, the EM34 data, where the depth of investigation was about twice that of the EM31 data, show higher conductivities some distance from the landfill, with values being about 30 mS/m. The EM31 data at this location show values of about 10 mS/m. Clearly, the conductivities are increasing with depth. In addition, the region of high conductivity near the landfill shows a greater aerial extent with the EM34 data. This suggests some of the

contaminant plume extends to depths beyond the reach of the EM31 and is, therefore, deeper than about 6 m.

Advantages: The conductivity instruments described above are easy to use and provide efficient field surveys. Although the data is usually plotted and then interpreted, the instruments display the measured conductivity and approximate anomaly locations can be observed during the field survey.

Limitations: Clearly, a conductivity contrast has to occur for the method to be effective. Probably the largest limitation is the influence of surface metal, fences, power lines, and other cultural features. However, if the plume is expected to have a significant aerial extent, local metal interferences will probably be easily recognized from the long wavelength conductivity anomaly from a plume. The EM34 is considerably more cumbersome to use and slower than the EM31. Since it requires two people to operate, the field cost is also much greater.

6.3.3.2 Resistivity

Basic Concepts: Resistivity methods can also be used to map the spatial and vertical extent of plumes, providing they have a resistivity contrast. Resistivity measurements can be obtained using four electrodes placed in the ground. A number of different electrode arrays can be used, several of which are shown in figure 90.

These arrays are used for different types of resistivity surveys. The Schlumberger array is often used for resistivity soundings, as is the Wenner array. The Pole-pole array provides the best signal but is cumbersome because of the long wires required for the remote electrodes, and it is rarely used. The Dipole-dipole array was originally used mostly by the mining industry for Induced Polarization surveys. Readings were taken using several different separations of the voltage and current dipoles providing measurements of the variation of resistivity with depth. Long lines of data were recorded requiring many readings. This array has now become common for resistivity surveys using the automated resistivity systems. If more signal (voltage) is needed than can be provided with the dipole dipole array, the pole dipole array can be used. Resistivity is measured by passing electrical current into the ground using two electrodes and measuring the resulting voltage using the other two electrodes. The apparent resistivity is calculated by multiplying a geometric factor for the array by the measured resistance (voltage divided by current).

These arrays are used for different types of resistivity surveys. The Schlumberger array is often used for resistivity soundings, as is the Wenner array. The Pole-pole array provides the best signal but is cumbersome because of the long wires required for the remote electrodes and it is rarely used. The Dipole-dipole array was originally mostly used by the mining industry for Induced polarization surveys. Readings were taken using several different separations of the voltage and current dipoles providing measurements of the variation of resistivity with depth. Long lines of data were recorded requiring many readings. This array has now become common for resistivity surveys using the automated resistivity systems. If more signal (voltage) is needed than can be provided with the Dipole-dipole array, then the Pole-dipole array can be used.

Data Acquisition: Resistivity traverses can be obtained by taking readings using one electrode spacing at regular stations forming a line of data. In this case, the spatial variation of resistivity is obtained. Resistivity data can also be taken keeping the center of the array fixed and expanding the electrode array, thus obtaining data from different depths and forming a resistivity sounding. If the depth to the aquitard is needed, the electrical soundings can be used. An electrode arrangement, lines of current flow, and a resistivity sounding curve are shown in figure 91a.

In figure 91b, the measured resistivity in influenced by both layer 1 and layer 2. When the electrode spacings are small, the measured resistivity approaches that of layer 1. Likewise, when the electrode spacing is large, the measured resistivity approaches that of layer. By measuring resistivity at a number of electrode spacings, a graph of apparent resistivity against electrode spacing can be drawn. The data can then be interpreted to give the depth to the top of layer 2.

Resistivity traverses using one electrode spacing are rarely used since EM methods can provide very similar results with much greater efficiency. If resistivity traverse measurements are made with many electrode spacings, as is usually the case with the Automated Resistivity systems discussed below, the variation of resistivity with depth can also be obtained.

Data Processing: Usually little processing is required apart from removing bad data points.

Data Interpretation: Resistivity soundings are interpreted by using software that calculates the expected field curve from a resistivity model. The program then modifies this model until the calculated field data matches the actual field data. This process is called inversion.

Advantages: Resistivity soundings will mostly be used to find the vertical extent of a contaminant plume, providing there is a resistivity contrast associated with the plume.

Limitations: As stated under Advantages, the plume must have a resistivity contrast in order to be detected.

Another fairly recently developed instrument for measuring the resistivity of the ground is called the Ohm-Mapper, manufactured by Geometrics in California. This instrument has a series of electrodes on a cable that is dragged at a slow pace along the ground. Current is induced into the ground, and the resulting voltages measured. The electrodes are capacitively coupled to the ground, and both transmit current into the ground and measure the resulting voltage. The Ohm-Mapper instrument being towed along the ground surface is shown in figure 200.

Figure 200. The Ohm-Mapper. (Geometrics, Inc.)

Automated Resistivity Systems

Basic Concept: Taking resistivity readings using many electrode spacings can be done using instruments that use automated resistivity recording, making resistivity data collection quite efficient. These systems allow the electrodes to be placed in the ground and connected to the data recorder prior to recording data. When setup is complete, the recorder is programmed with the data recording parameters to use and then automatically collects the data according to a pre-programmed schedule. One system that does this is illustrated in figure 201.

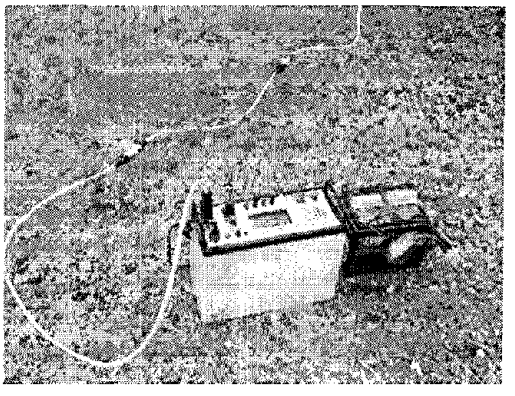

Figure 201. SuperSting R1 IP resistivity meter. (Advanced Geosciences, Inc.)

An example of data recorded using this system is shown in figure 202.

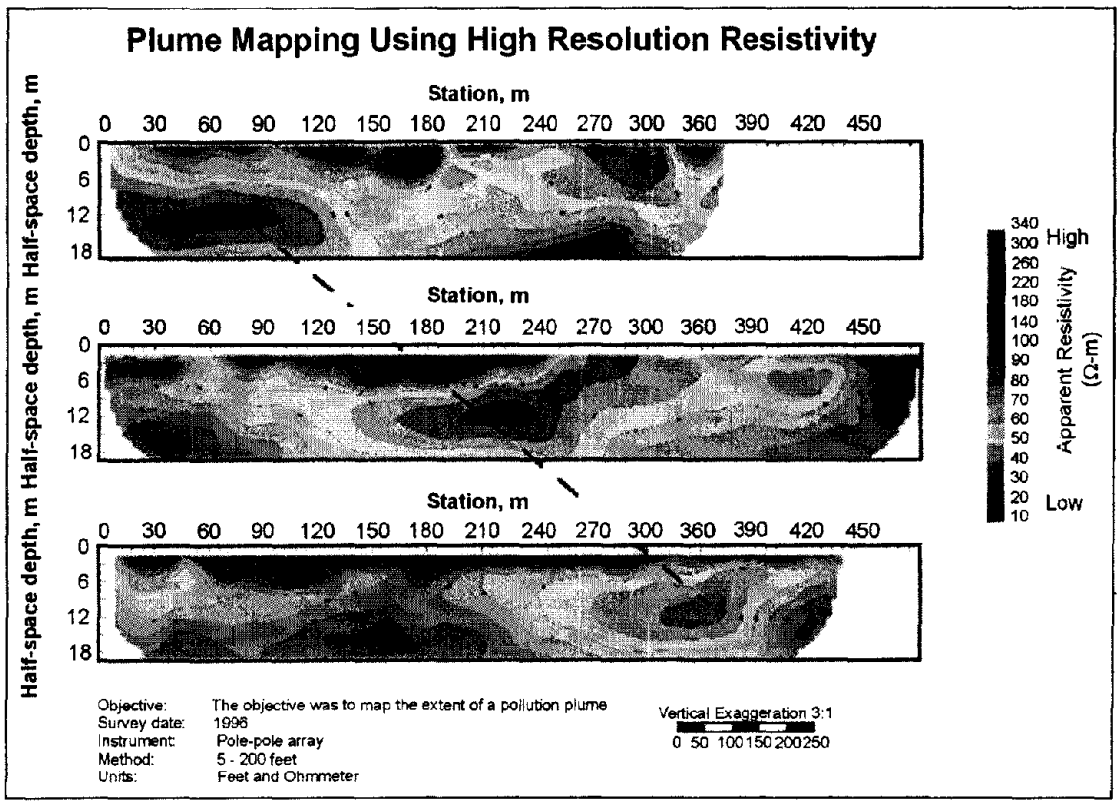

Figure 202. Example data recorded with the Sting-Swift System. (Advanced Geosciences, Inc.)

Data Acquisition: The electrodes are laid out along a straight line and connected to the data recorder. This is then programmed with the particular electrode array to use and instructed to take the data. Figure 202 illustrates the detail that can be obtained when resistivity measurements are taken using several electrode spacings along a traverse. The data are plotted in the form of a pseudosection, in which the data from small electrode spacings are plotted near the ground surface line, and those from large electrode spacings are plotted at greater distances vertically beneath the ground surface line, thus simulating depth. In this case, a low resistivity region on each of the three lines marks the occurrence of a contamination plume. The data can also be modeled to give the depth of the source of the resistivity anomalies.

Data Processing: Resistivity data require little processing although bad data points may be removed.

Data Interpretation: Interpretation may be visual, or modeling can be done to provide the spatial distribution of the source of the anomaly along with its depth. This is usually done using software that modifies a preliminary resistivity/depth model until the output data from the model matches the field data, a process called inversion.

Advantages: The Automated Resistivity System records a significant amount of data quite efficiently. Fairly detailed interpretations can be done using this data.

Limitations: Resistivity methods can be used to spatially map contaminant plumes. They rely on the plume having a different resistivity (or conductivity) to that of the surrounding, uncontaminated areas. Essentially, if electromagnetic methods can be used to map a plume, then resistivity methods can probably also be used.

If a single electrode spacing is used, the resistivity measuring system is rather slow, and EM methods are a better choice. However, if an automated resistivity system is used, much more data are obtained, and a better interpretation can be produced. Clearly, the resistivity method will be difficult if the ground is hard or if there are areas of concrete or asphalt, making electrode placement difficult.

If grounded metal objects, such as metal fences, are close to the electrode array being used, the data will be influenced by these metal features. Below ground, metal objects such as metal pipes will also influence the data.

6.3.3.3 Ground Penetrating Radar

Basic Concept: Ground Penetrating Radar (GPR) can be used to map contaminant plumes. However, the method is fairly site specific, and care needs to be taken that the site conditions are appropriate for the GPR method.

The depth of investigation of GPR depends on the soil conditions. A saturated soil with significant clay will severely limit the penetration of the method. Ideal conditions are unsaturated, clay-free soils. Depth of penetration also depends on the frequency of the signal. Different antennas provide different frequencies, which range from about 25 MHz to 1500 MHz. A low-frequency antenna (signal) will provide the best penetration depth but has the lowest resolution.

The GPR instrument consists of a recorder and a transmitting and receiving antenna (see figure 112).

When the GPR signal reaches an object, or interface, with different dielectric properties, part of the wave is reflected back to the ground surface, where it is recorded by the receiving antenna. Several companies manufacture GPR equipment. These include Geophysical Survey Systems, Inc (GSSI), GeoRadar, Inc, Mala GeoScience, and Sensors and Software Inc.

The 100 MHz antenna (figure 113) is suited for deeper applications to depths of about 20 m. This antenna can be used to locate contaminant plumes.

Data Acquisition: GPR surveys are conducted by pulling the antenna across the ground surface at a normal walking pace. The recorder stores the data as well as presenting a picture of the recorded data on a screen.

Data Processing: It is possible to process the data, much like the processing done on single-channel reflection seismic data. Processes that can be applied include distance normalization, horizontal scaling (stacking), vertical and horizontal filtering, velocity

corrections, and migration. However, depending on the data quality, processing may not be done since the field records may be all that is needed to observe the contamination plume.

Data Interpretation: Data interpretation is mostly visual. If the depth to an anomaly is required, then the speed of the GPR signal in the soil at the site has to be obtained. This can be estimated from charts showing speeds for typical soil types or it can be obtained in the field by conducting a small traverse across a buried feature whose depth is known.

Figure 203 shows the results of a GPR survey over a hydrocarbon plume. The plume is easily observed from the signal attenuation and lack of spatial coherence caused by the plume.

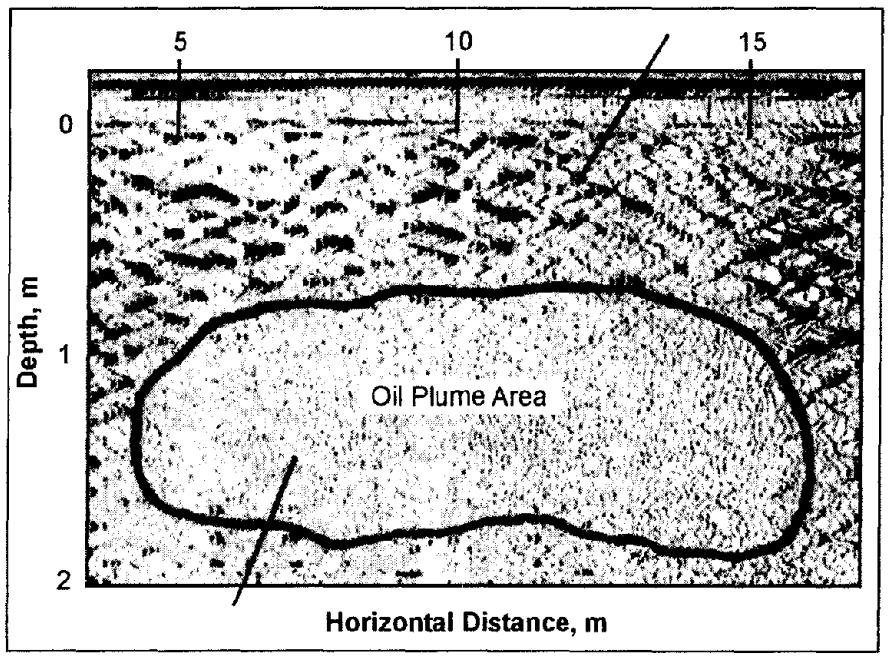

Figure 203. Ground Penetrating Radar data over a hydrocarbon plume. (Geosurvey)

Advantages: GPR surveys are fairly easy to conduct and different antenna can be tested if the anomaly resolution of depth penetration are insufficient.

Limitations: Probably the most limiting factor for GPR surveys is that their success is very site specific and depends on having a contrast in the dielectric properties of the target compared to the host overburden, along with sufficient depth penetration to reach the target. Surveys near high-powered radio frequency antenna may also inhibit subsurface data collection.

6.3.3.4 Induced Polarization

Basic Concept: Induced Polarization (IP) is an electrical method that measures the change in the measured resistivity of the ground with frequency. All of the electrode arrays used to measure resistivity (see figure 90) can also be used to measure IP. In fact, when measuring IP, resistivity is also measured. There are two methods used to obtain IP data: one called

time domain, and the other called frequency domain. In time domain, a constant current is passed into the ground using two of the four electrodes. This current is then rapidly switched off. During this off time, the remaining two electrodes measure the resulting voltage. If an IP effect is present, the voltage across these electrodes will not suddenly return to zero as the current is turned off, but will decay to zero over a period of time, usually within a few seconds. In frequency domain the resistivity of the ground is measured at different current/voltage frequencies.

Figure 110 illustrates the electrode array and the current and voltage waveforms showing the voltage decay after the current is turned off. Simple IP measurements usually integrate the IP voltage over a specified time period, say T_1 and T_2 (see figure 110), providing a single number, called chargeability that is a measure of the IP response. However, if the current and voltage waveforms are recorded, a Fourier transform can be applied to the data, and the variation of resistivity with frequency obtained, called Spectral Induced Polarization (SIP).

The use of the IP method for mapping contamination and plumes is essentially still being researched. This is especially true for the SIP method. The method relies extensively on the influence that chemical contaminants have on clay. Clay often has a natural IP response, and this is sometimes changed by the chemicals comprising the plume.

Data Acquisition: Induced Polarization surveys are conducted much like resistivity surveys. Readings are taken at discrete stations to form lines of data crossing the area of interest. The automated recording system discussed previously for resistivity measurements can also be used to record IP data. Generally, the dipole dipole electrode array is used.

Data Processing: If digital data are obtained at several frequencies, the variation of IP response with frequency is obtained. In the time domain, the current and voltage waveforms have to be digitally recorded and a Fourier analysis of the data be performed providing the variation of resistivity with frequency. The variation of IP response with frequency is called Spectral Induced Polarization and provides more interpretable information than the simple IP measure discussed above. However, this is still being researched and is rarely used as a production method.

IP data field is usually plotted in the form of a pseudosection where data from the smallest dipole spacing are plotted near the ground surface line and those from the larger dipole spacings are plotted at a greater vertical distance from the ground surface line, thus simulating a plot of data against depth. Both the resistivity data and the IP data (chargeability) are plotted on pseudosections.

Data Interpretation: Often the pseudosection data is interpreted visually, using standard model curves of specific geologic structures. However, it is also possible to use software to invert the data, thereby providing a geologic model whose calculated values (resistivity and chargeability) that fit the field data.

Advantages: This method is not commonly used to map contaminant plumes although it may provide some useful information in some cases.

Limitations: The IP method is quite labor intensive and requires electrodes be inserted into the ground. Generally, more current is needed than for a resistivity survey to the same depth since the IP voltages can be quite small; hence, the resistance of the electrodes to ground (contact resistance) needs to be as low as possible. This may require watering the electrodes to improve the electrical contact between the electrodes and ground (reduce the contact resistance). If the ground surface is hard, then inserting the electrodes may be difficult.

Grounded metal structures such as fences that are local to the measuring site can significantly influence the data, possibly making the data uninterpretable.

6.3.3.5 Electromagnetic Methods to Map Aquitard Topography

Basic Concept: The EM31 and EM34 can be used to map variations in the depth to the top of an electrically conductive aquitard. This may be useful when DNAPL's are the contaminant, and it is suspected they may have pooled in a depression on top of an aquitard. The EM31 and EM34 instruments are shown in figures 183 and 197, respectively, and their mode of use is described previously. If depths to the aquitard are needed, and the aquitard is less than about 30-m deep, then resistivity soundings can be used to convert the conductivity data to depth data. This can be done by performing soundings at regular intervals along the traverse and using the interpreted depths to convert the conductivity values from the EM31 or EM34 data to depths.

Figure 204 presents a diagram showing the DNAPL resting in a depression on top of an aquitard. In this case, a relatively low conductivity overburden rests on a conductive aquitard, with DNAPL resting in the depression on top of the aquitard. Providing the EM instrument used penetrates well into the aquitard, the measured conductivity will be significantly influenced by the conductivity of the aquitard. Conductivity measurements taken when the aquitard is near the ground surface will show high values, whereas those taken when the aquitard is deep will show low values. Thus, a traverse across the depression in the aquitard will image the depression, as shown in the illustration. The DNAPL's probably have a low electrical conductivity and will therefore have little influence on the data.

Data Acquisition: Conductivity surveys designed to map the topography of a conductive unit at depth (an aquitard) will normally be conducted along lines crossing the area of interest. Probably several lines will be surveyed and conductivity data recorded. These lines will need to be surveyed in order to draw a map of the final data.

Data Processing: Usually, little processing is done to the data, although bad data points may be removed.

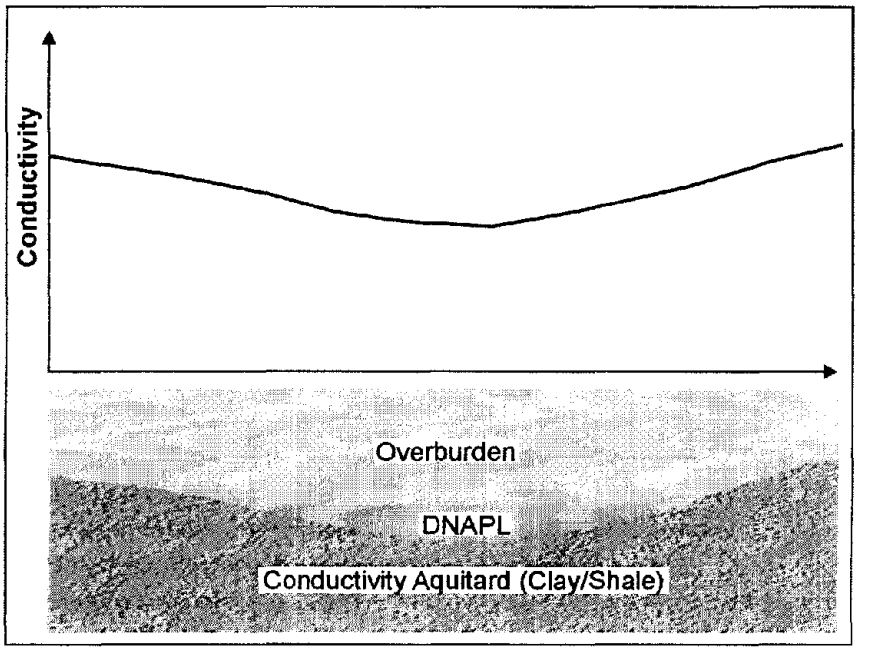

Figure 204. Using conductivity to map aquitard topography.

Data Interpretation: Interpretation is often visual, looking for the conductivity lows for deeper sections of the conductor. If resistivity soundings have been recorded, the conductivity values can be converted to conductivity versus depth.

Advantages: Measuring the ground electrical conductivity with the instruments described above is easy and field production is quite fast.

Limitations: The aquitard layer has to be thick enough to have a significant influence on the conductivity readings. In addition, it has to be more conductive than the overburden, which should usually be the case. If shallower conductive layers occur, or possibly fade in and out spatially, this may obscure the interpretation of the deeper conductive layer. Local metal, either above or below the ground surface, will influence the measured conductivity data.

The method provides lateral variations in conductivity, but only very limited depth determinations. If these are needed, then other methods will have to be used.

6.3.3.6 Seismic Refraction to Map Aquitard Topography

Basic Concept: The seismic refraction method can be used to map the top of the aquitard if it has a velocity greater than that of the overburden.

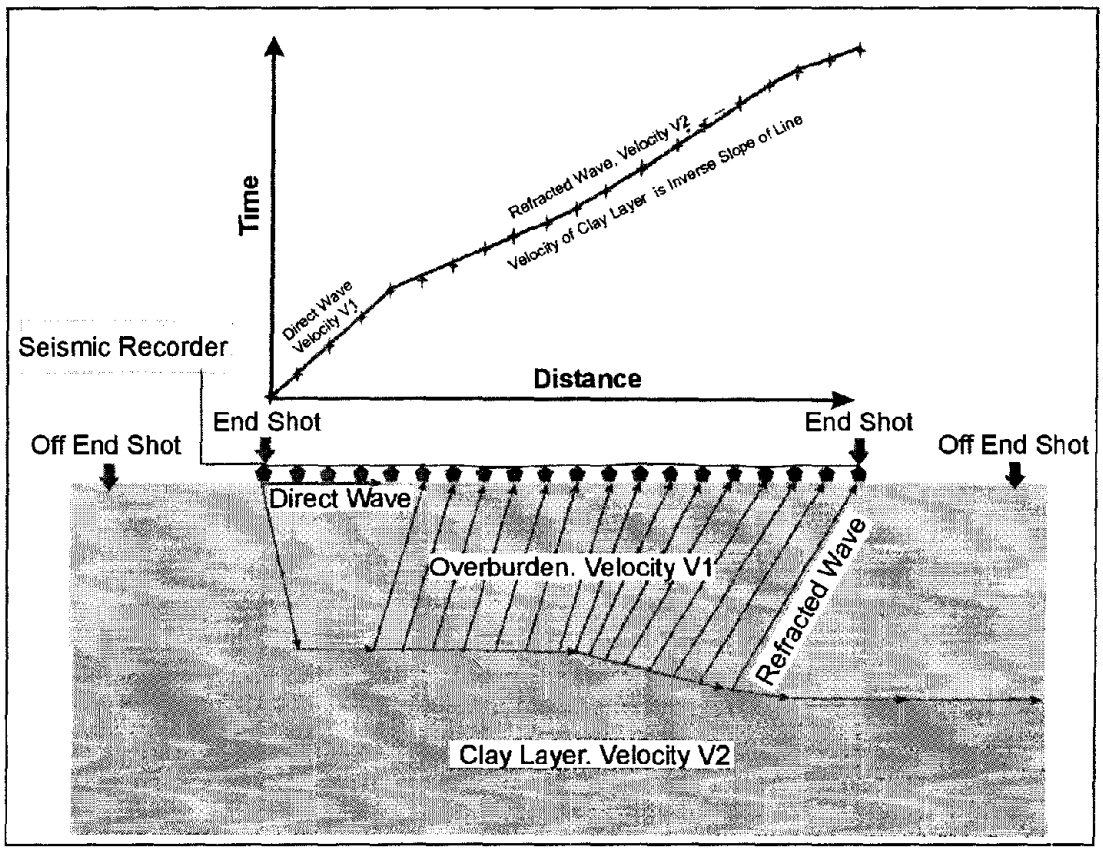

Figure 205. Seismic refraction principles.

In this method, illustrated in figure 205, a seismic wave is created (hammer blow to the ground or explosive shot), and the wave travels into the ground until it reaches a higher velocity layer. At this boundary, part of the energy travels along the boundary and some is transmitted through the boundary to greater depths. The wave traveling along the boundary continually refracts energy back to the ground surface where it is detected by geophones. The seismic recorder records these geophone signals. Several shots are recorded at different distances along the geophone spread. A time-distance graph is constructed from these data, as shown in figure 205, and is interpreted to give the depth to the refractor. The depth of investigation depends on the seismic source used. A hammer and base plate may be able to penetrate to 15 m, whereas a black powder charge buried at a depth of about 0.75 m may provide penetration to about 30 m. Both compressional and shear waves can be recorded with this method, although compressional waves are mostly used for mapping bedrock topography.

Data Acquisition: The design of a seismic refraction survey requires a good understanding of the expected bedrock and overburden. With this knowledge, velocities can be assigned to these features and a model developed that will show the parameters of the seismic spread best suited for a successful survey. These parameters include the length of the geophone spread, the spacing between the geophones, the expected first break arrival times at each of the geophones, and the best locations for the off end shots. Knowing the expected first break arrival times is also helpful in the field, where field arrival times that correspond fairly well

to expected times helps confirm that the spread layout has been appropriately planned and that the target layer is being imaged.

Data Processing: The first step in processing/interpreting refraction seismic data is to pick the arrival times of the signal, called first break picking. A plot is then made showing the arrival times against distance between the shot and geophone. This is called a time-distance graph, as shown in figure 205 for two-layered ground (overburden and refractor).

The red portion of the time-distance plot shows the waves arriving at the geophones directly from the shot. These waves arrive before the refracted waves. The green portion of the graph shows the waves that arrive ahead of the direct arrivals. These waves have traveled a sufficient distance along the higher speed refractor (bedrock) to overtake the direct wave arrivals.

Data Interpretation: There are several methods of refraction interpretation. One of the most common methods is called the Generalized Reciprocal Method (GRM) that is described in detail in the Geophysical Methods section. A brief and simplified description of the GRM method is presented below. Figure 206 shows the basic rays used for this interpretation.

The objective is to find the depth to the bedrock under the geophone at D. This is done using the following simple calculations. The travel times from the shots at A and G to the geophone at D are added together (T1). The travel time from the shot at A to the geophone at G is then subtracted from T1. Figure 207 shows the remaining waves after the above calculations have been performed. These are the travel times from C to D added to the travel times from E to D subtracting the travel time from C to E. The sum of these travel times can be shown to be approximately the travel time from the bedrock at H to the geophone at D. Since the velocity of the overburden layer can be found from the time distance graph, the distance from H to D can be found giving the bedrock depth.

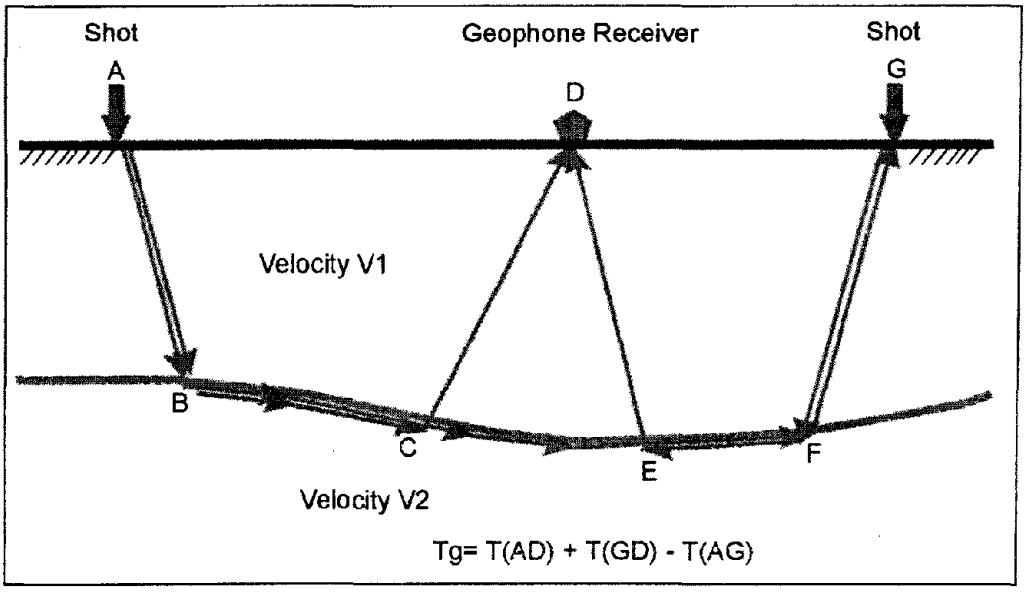

Figure 206. Basic Generalized Reciprocal Methods interpretation.

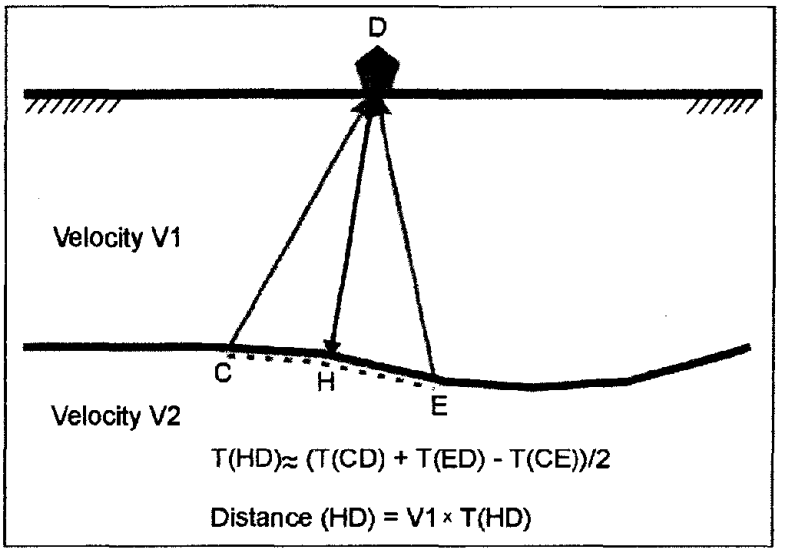

Figure 207. Generalized Reciprocal Methods interpretation.

An example of the results from a seismic refraction survey is presented in Figure 208. Although this example does not map aquitard topography, it does show the field data and results from a seismic refraction survey. The upper figure shows the travel time graph, illustrating the time that the seismic waves take from the shot to each geophone. The second graph presents the interpreted seismic velocities and the third graph shows the interpreted bedrock section.

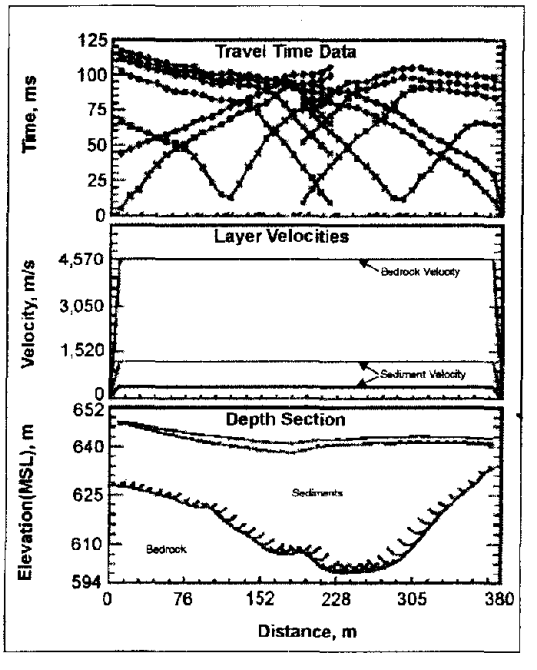

Figure 208. Example of a seismic refraction interpretation.

Advantages: Providing the velocity of the bedrock is greater than that of the overburden, the refraction seismic method can provide good estimates of the bedrock depth, and hence topography.

Limitations: Probably the most restrictive limitation is that each of the successively deeper refractors must have a higher velocity than the shallower refractor. However, for determining the topography of a fairly shallow (less than 15 m deep) clay layer, this is probably not a significant limitation, providing the clay layer has a higher velocity than the overburden. If the water table is in the overburden and close to the bedrock, this may obscure the bedrock arrivals since saturated soils have a higher velocity than unsaturated soils.

Local noise, for example traffic, may obscure the refractions from the bedrock. This can be overcome by using larger impact sources or by repeating the impact at a common shot point several times and stacking the received signals. If noise is still a problem, then a larger energy source may be required. In addition, since some of the noise travels as airwaves, covering the geophones with sound-absorbing material may also help to dampen the received noise.

6.3.4 Detecting Unexploded Ordnance (UXO)

Unexploded ordnance exists at current and former sites where the military has used an area for target practice or other activities. The ordnance range from 20 mm projectiles to air-dropped bombs having weights of 454 or 907 kg. Depths of burial range from a few centimeters to a several meters for the air-dropped bombs. However, the vast majority of items are found to lie within a meter of the ground surface.

These areas are usually large and require a sustained and methodical approach to adequately cover the area. If the area is spatially fairly small, then a different approach may be warranted. The techniques used to search for UXO are mostly magnetic and electromagnetic methods. Both ground and airborne magnetic and electromagnetic systems are used. Other techniques used on a more limited extent include Ground Penetrating Radar (GPR) and airborne Synthetic Aperture Radar (SAR).

Positioning of the data is very important for UXO surveys, especially where a survey is completed and then an excavation teams return later to excavate and remove the ordnance. Positioning is usually done using high precision Global Positioning System (GPS) where centimeter-level accuracy can be obtained under ideal conditions.

Table 9 shows the depths for various ordnance at which electromagnetic and magnetic methods can detect them.

In addition to the geophysical methods mentioned above, there are other techniques based more on physics than geophysics. These methods will be mentioned for completeness but will not be discussed in detail. Each of the geophysical methods used for UXO exploration will be discussed below.

Table 9. Ordnance penetration and detection using magnetic and electromagnetic methods.

Ordnance Penetration Detection

Ordnance Item	Depth Penetration[1,2] (ft)			Typical Max Detection Depth[4] (ft)	
	Sand	Loam	Clay	Magnetometry	TDEM[5]
14.5 mm Trainer/Spotter, M1813A1	0.2	0.3	0.4	0.3	0.5
20mm, M56A4	2.3	3	4.6	0.4	0.7
22 mm Subcal for 81 mm mortar	1.4	1.9	2.8	0.5	0.8
35 mm Subcal M73	0.5	0.7	1	0.9	1.3
37 mm, M63	3.9	5.2	7.9	1	1.3
40 mm, M822 (AA)	2.3	3	4.5	1.1	1.4
40 mm, M677 (Mk 19)	0.2	0.3	0.4	1.1	1.4
40 mm, M381 (M203/M79)	0.2	0.3	0.4	1.1	1.4
Mk 118 Bomblet	1.9	2.4	3.7	1.5	1.8
Mk 23 3 lb. Practice Bomb	2.7	3.5	5.4	1.7	2
57 mm, M306A1	2.7	3.6	5.5	1.7	2
M9 Rifle Grenade	0.1	0.2	0.2	1.7	2
2.25" Rocket, Mk 4	4	5.2	8	1.7	2
60 mm, M49A1 (charge 4)	1.1	1.5	2.3	1.9	2.2
2.36" Rocket, M6A1	0.4	0.5	0.8	1.9	2.2
66 mm, M72 LAW	0.9	1.2	1.8	2.1	2.4
66 mm TPA, M74	0.7	0.9	1.4	2.1	2.4
BLU-3/B,-27/B,-28/B	2.2	2.9	4.4	2.3	2.5
2.75" Rocket, Practice	8.1	10.7	16.3	2.3	2.5
6 lb. Incendiary Bomb	3.4	4.4	6.7	2.4	2.6
75 mm, M48	4.9	6.4	9.8	2.5	2.7
75 mm, M310	3.9	5.1	7.8	2.5	2.7
81 mm, M43A1 (charge 8)	2.7	3.5	5.4	2.8	2.9
83 mm SMAW Mk 3	2.8	3.6	5.6	2.9	3
84 mm, M136 (AT4)	2.5	3.7	5	2.9	3
3.5" Rocket, M28	0.8	1.1	1.7	3.2	3.2
90 mm, M371A1	2	2.7	4.1	3.2	3.2
25 lb. Frag Bomb[3]	2.1	2.8	4.3	3.2	3.2
AN-M41A1 20 lb. Practice Bomb	5	6.6	10	3.3	3.3
105 mm, M1 (charge 7)	7.7	10.1	15.4	4	3.8
106 mm, M344A1	6.5	8.5	13	4	3.8
4.2" Mortar, M3 (max charge)	4.1	5.4	8.3	4.1	3.9
Dragon Guided Missile	0.9	1.1	1.7	4.3	4
155 mm, M107	14	16.4	28	6.7	5.6
8", M106 (charge 8)	16.4	24.2	36.9	9.7	7.3
M38A2 100 lb. Practice Bomb	8.6	11.3	15.2	9.9	7.4

[1]Penetration depths include the following "worst case" conditions assumptions: impact velocity is equal to maximum velocity of round; impact is perpendicular to ground surface; munition decelerates subsurface in a straight line, munition does not deform upon impact. Typical penetration depth for any individual usually be significantly less.

[2]Maximum depth of penetration assuming a velocity of 500 fps.

[3]All bombs are assumed to have an impact velocity of 1135 fps.

[4]Actual detection depth may vary based on field conditions and be either lower or deeper.

[5]Time Domain Electromagnetics Methods

6.3.4.1 Magnetic

Basic Concept: Magnetic methods are appropriate for UXO composed of or including ferromagnetic materials. The Earth's magnetic field induces a secondary magnetic field in ferromagnetic objects. This secondary field distorts the Earth's magnetic field around the object. Magnetometers measure the intensity of the total magnetic field, which is about 35,000 nT (nano Tesla) at the equator and 60,000 nT at the magnetic poles. Distortions to this field may be only fractions of one nT for small ordnance to tens or hundreds of nT for

large ordnance. The anomaly magnitude decreases with distance from its source. The decrease depends on the size of the object relative to the height of the sensor, but for a small object, will decrease as the inverse square of the distance from the source (ordnance). Thus, the amplitude of an anomaly decreases rapidly with distance from the source. The Earth's magnetic field intensity is continuously changing, usually by only a few nT per hour, often called the Diurnal (daily) drift. However, sometimes the field intensity can change by tens or hundreds of nT per hour during magnetic storms. This effect has to be accounted for during processing of the magnetic data.

There are numerous kinds of magnetometers including cesium, potassium, proton precession, fluxgate, fiber optic, and Superconducting Quantum Interference Device (SQUID). Probably the most common types in use for UXO search are the cesium and potassium magnetometers. Figure 209 shows a cesium magnetometer with a GPS system for positioning.

Figure 209. Cesium magnetometer with GPS. (Geometrics, Inc.)

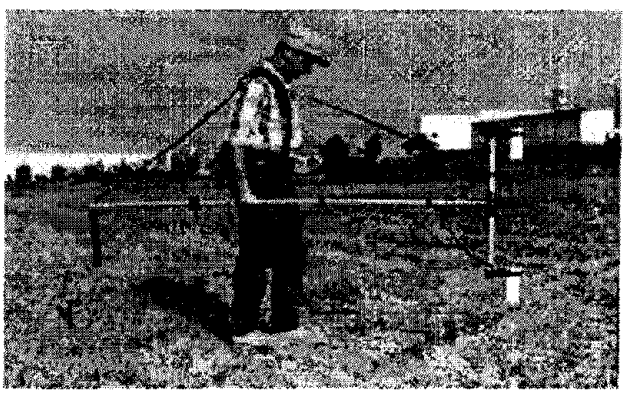

Figure 210. Gradiometer using two cesium sensors. (Geometrics, Inc.)

In addition to measuring the total magnetic field strength using one sensor, the gradient of the magnetic field is also measured using two sensors spaced a nominal distance apart. This instrument is called a gradiometer. Figure 210 shows a gradiometer using two cesium magnetometer heads. Since the sensors are arranged one above the other vertically, the instrument would measure the vertical gradient if used as illustrated.

Measuring the vertical magnetic gradient has two advantages. The first is that the output data are much less affected by diurnal drift, and the second is that the vertical gradient peaks over the top of a magnetic source whereas the total magnetic field anomaly does not. Figure 211 shows the total magnetic field and vertical gradient from a spherical object magnetized by the Earth's field. However, the depth of investigation of the vertical gradient method is less than that with the total magnetic field.

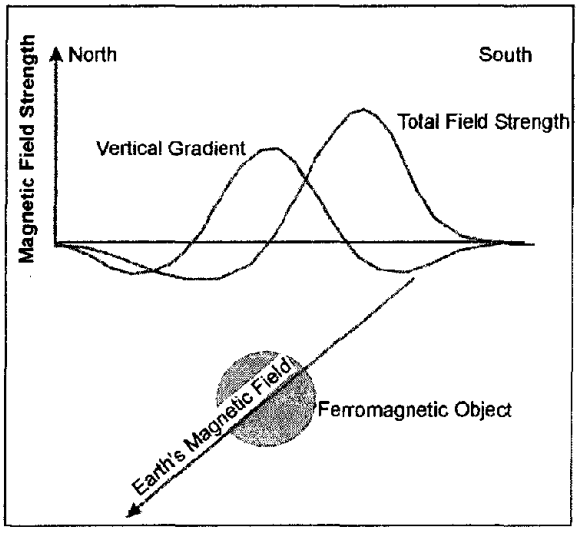

Figure 211. Total magnetic field strength and vertical gradient anomalies.

In addition to hand-held magnetometers, such as those discussed above, magnetic sensors are now assembled on frames with wheels. One such system is shown in figure 212.

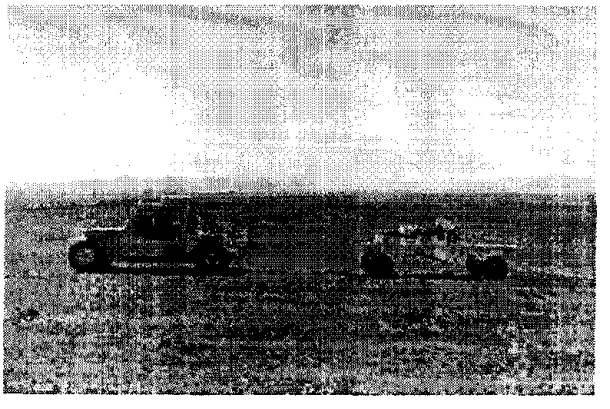

Figure 212. The MTADS UXO detection system. (Blackhawk GeoServices, Inc.)

MTADS is an acronym for Multi sensor Towed Array Detection System. The sensor array is mounted on a non-magnetic structure and is towed by a special vehicle constructed to minimize its magnetic field. The system includes GPS allowing positioning to within a few centimeters. The system can be configured to measure either the magnetic field, the vertical magnetic gradient or with electromagnetic sensors. An on board computer controls the data acquisition and stores the data in memory. A similar system is called Surface Towed Ordnance Locator System (STOLS) and is shown in figure 213.

Figure 213. STOLS UXO detection system. (GEO-CENTERS, Inc.)

In addition to the above equipment, all of which stores data in memory for later downloading and processing, there are hand-held instruments that do not store the data and are used to locate anomalies that are marked in the field during the survey. One of these instruments is called a Schonstedt gradiometer. One gradiometer manufactured by the Schonstedt is shown in figure 179.

Data Acquisition: Magnetometer surveys for UXO must provide coverage of the area of interest with as near to 100% subsurface coverage as possible. Data is normally recorded along lines crossing the area. Surveyors paint markings are sometimes used to mark the lines that have been surveyed.

Prior to data recording, the instruments are checked each morning to ascertain that they are functioning properly. In addition, the GPS system is checked. Tests are conducted to determine the amount of time between the GPS sensor taking a reading and the reading being logged with a time stamp in the computer, called the latency of the system. Latency also takes into account the time interval between GPS readings. With the MTADS system, when recording data traveling a few kilometers per hour and attempting to position anomalies to within a few centimeters, latency is an important correction to apply. Latency is less of a problem for hand-held magnetic surveys, where data are recorded at walking speed.

A magnetic base station must also be set up to record the diurnal variation in the Earth's magnetic field. This instrument and the magnetometer recording the field data must be time synchronized so that the time when the diurnal field is measured by the base station corresponds to the time the data are recorded by the field magnetometer. Magnetic data are also collected using airborne surveys. Figure 214 shows a helicopter-mounted magnetometer system.

Helicopter surveys require special navigation aids so that the area of interest is covered. Lines are pre-planned, and the navigation system then informs the pilot of the correct course to take.

Figure 214. Helicopter-mounted magnetometer system. (Fugro Airborne Surveys)

Data Processing: Data processing involves assigning the correct spatial coordinates to each magnetic field reading and correcting the magnetic field data for diurnal variations.

Data Interpretation: Anomalies from magnetic field data consist of a magnetic high to the south of the magnetic source and a magnetic low to the north of the source. Neither the magnetic high nor the low are positioned over the top of the source, making determination of the spatial coordinates of the source difficult to locate accurately. Additional processing can be done to make the anomaly peak over the top of the source. This process is called calculation of the analytic signal and is routinely done for many magnetic surveys. The analytic signal and total magnetic field are shown in figure 215.

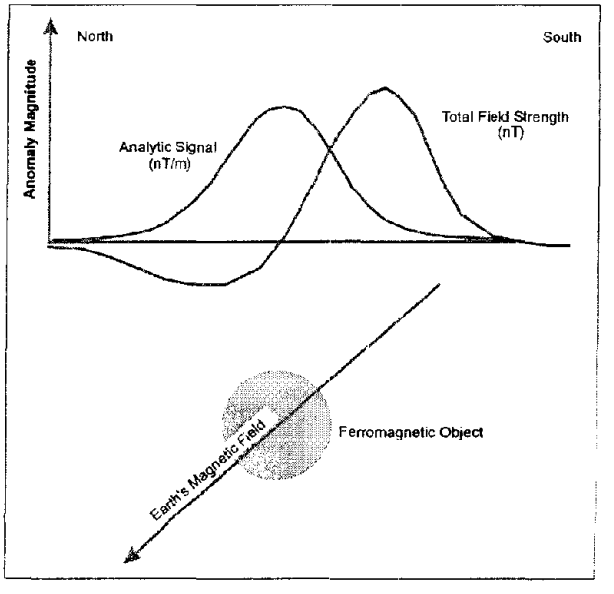

Figure 215. Analytic Signal

Figures 216 and 217 present the total magnetic field for an airborne helicopter magnetic survey (figure 216) and the analytic signal calculated using the same data. These data were acquired while flying at a height of a few meters above the vegetation, with some of the data being obtained at elevations of about 6 meters above the ground surface, over an area where earlier military activity had occurred.

Figure 216 shows the positive (red) and negative (blue) magnetic field values associated with each magnetic source. In figure 217, showing the Analytic Signal, only positive anomalies are seen. The peak of these anomalies is positioned over the source of the anomaly. Depths to the source of the magnetic anomalies can be found from the analytic signal.

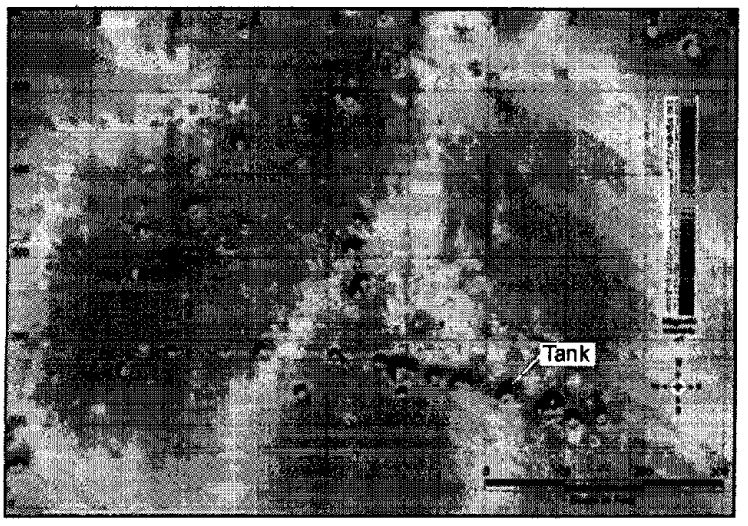

Figure 216. Total magnetic field data from a helicopter magnetic survey

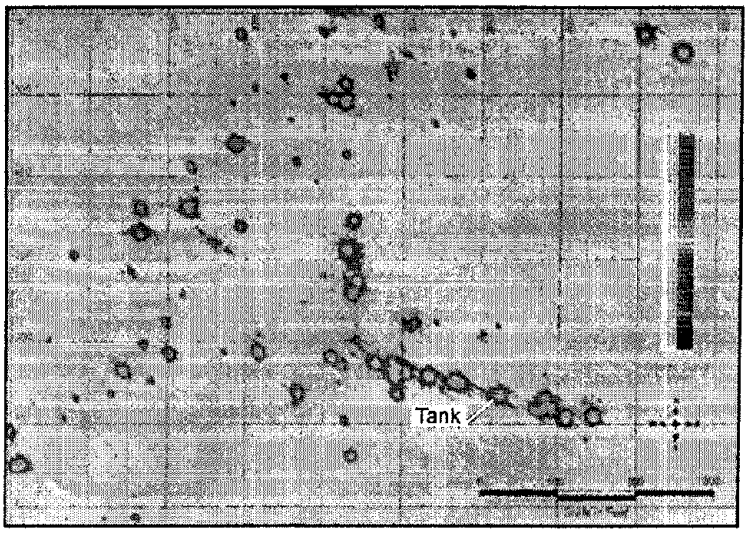

Figure 217. Analytic signal for data shown in figure 216.

Advantages: The magnetic method is fairly easy to use and provides and anomalies from both near surface UXO and those buried at some depth, depending on their size.

Limitations: The magnetic method detects anomalies only from ferromagnetic sources. Objects made from stainless steel, copper, or aluminum will not provide a magnetic anomaly. If the diurnal variations in the Earth's magnetic field are high, it may be difficult to remove its influence completely from the data. Interpretation of the data for detailed analysis of the source of the anomalies is difficult. Thus, it is usually not possible to obtain any of the parameters (length, diameter) of the source of the anomaly.

6.3.4.2 Electromagnetic

Basic Concept: Electromagnetic methods use actively created electromagnetic fields to excite metal objects. These objects then radiate their own electromagnetic field that can be detected.

Two kinds of electromagnetic instruments are available. One operates in the frequency domain, and the other operates in the time domain. These instruments have a transmitter and receiver coil. The transmitter coil generates the electromagnetic field, and the receiver coil measures the resulting signal. Instruments that operate in the frequency domain transmit an electromagnetic field whose amplitude is sinusoidal at one or several frequencies from 30 Hz to over 20 kHz. Instruments that operate in the time domain generate electromagnetic pulses having a square wave shape for the signal. Electromagnetic systems can be used on the ground or they can be attached to aircraft and used for airborne surveys. Airborne EM systems have been used for mineral exploration and environmental surveys for many years. However, although one company (Fugro) advertises airborne EM systems for UXO, no data could be found regarding this system. Geonics Ltd. and the U.S. Army Corps of Engineers are designing another system.

There are several ground EM systems that are being used for UXO exploration. These include the EM61 (Geonics Ltd.) and GSM3 (Geophex, Inc.), all of which record data to memory. Systems that do not record data to memory include the Fisher and a metal detector manufactured by Minelab of South Australia and marketed by Geometrics under the name Metal Mapper.

The EM31 (figure 183) is primarily designed to measure the electrical conductivity of the ground. It does record an in-phase component reported to be appropriate for detecting metal, and tests have been conducted to find its usefulness for UXO exploration. As might be expected, the results were not encouraging since only large pieces of metal can be detected, and the instrument is rarely, if ever, used for UXO detection.

Probably the most commonly used instrument for UXO exploration is the EM61. This instrument is used as a single instrument, or it can be configured as a set of three, allowing greater ground coverage along each traverse.

Figure 184 shows a single EM61 being manually towed. The backpack contains controls and batteries. This system uses two coils, one placed vertically over the other with their planes parallel. The lower coil contains both a transmitter and a receiver coil and the upper coil is just a receiver coil. Data are recorded using both the lower and upper receiver coils. Since

the lower coil is more influenced by surface metal than the upper coil, data from these two coils can be used to reduce the influence of surface metal on the data.

Figure 218 shows a system with an assembly of two EM61 instruments being towed by an All Terrain Vehicle. A GPS antenna is placed over the central EM61 to position the data.

Figure 218. An array of two EM61 instruments. (Blackhawk GeoServices, Inc.)

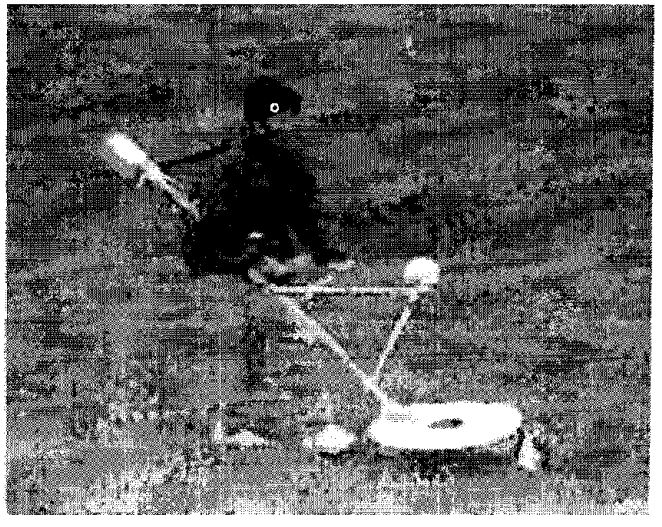

Figure 219. The GEM-3 electromagnetic instrument. (Geophex Inc.)

Hand-held instruments include the Metal Mapper (Geometrics), the GEM3 (Geophex), the EM61 hand-held version, and the Fisher electromagnetic metal detector. Figure 219 shows the GEM3; Figure 185 shows the hand-held version of the EM61.

The GEM3 shown above has a GPS system attached allowing the position of the sensor coils to be determined at all times.

Data Acquisition: Surveys conducted with the towed systems are done along lines crossing the area of interest. Surveyor's spray paint may be used to show which lines have been recorded. At the start of each day, the equipment is tested over a known target to check that it is functioning properly. As with the magnetic surveys, latency tests with the GPS systems are required.

Hand-held instruments are usually used for "real time" surveys where the anomalies are located and marked at the same time.

Data Processing: Data from a towed array system, where a GPS positioning system is used, has to be processed and then applied to the electromagnetic data so as to provide the coordinates of the recorded data. The EM61 data can be processed using data from the two receiver coils. This allows a "differential" channel to be produced. This procedure involves amplifying the data from the upper coil so that anomalies from near-surface metal are seen as anomalies with similar amplitudes on both coils. The difference is then found between the data from the two coils, allowing the near-surface metal to be screened out of the data. During processing, the depth to the source of the anomaly is also calculated.

Data Interpretation: Electromagnetic data from UXO anomalies can theoretically be modeled to provide information regarding the shape of the source. Although this is not commonly done at the current time, it does have the potential to assist in preliminary discrimination since long objects, which might be more likely to be UXO than round objects, can be identified.

Advantages: The electromagnetic method reliably detects buried UXO and is not influences by diurnal variations as is magnetic data.

Limitations: The resolution for the location of the source of any anomaly is diluted slightly by the area of the transmitter and receiver coils. This may be somewhat more significant with the EM61, which has coils with quite a large surface area, compared to the hand held EM61, which uses a much smaller coil. However, the size of the coil and the electrical current passing through it and used to produce the electromagnetic field are strongly related to the depth of investigation of the instrument. Exploration depths with the EM61 are limited to about 3 m.

6.3.4.3 Ground Penetrating Radar

Basic Concept: Ground Penetrating Radar (GPR) can be used to locate UXO. However, generally the method is slow and rather cumbersome compared to the magnetic and electromagnetic methods. It is primarily used for surveys covering small areas.

The depth of investigation of GPR depends on the soil conditions. A saturated soil with significant clay will severely limit the penetration of the method. Ideal conditions are unsaturated, clay free soils. Depth of penetration also depends on the frequency of the signal. Different antennae provide different frequencies, which range from about 25 MHz to 1500 MHz. A low-frequency antenna (signal) will provide the best penetration depth. For UXO detection, a high-frequency antenna will be needed to locate small ordnance. A lower frequency antenna can be used for larger ordnance.

The GPR instrument consists of a recorder and a transmitting and receiving antenna. Figure 111 provides a drawing illustrating the GPR system.

This figure shows the GPR signal being transmitted into the ground. When it reaches an object, or interface with different dielectric properties, part of the wave is reflected back to the ground surface, where it is recorded by the receiving antenna.

Several companies manufacture GPR equipment. These include Geophysical Survey Systems, Inc (GSSI), GeoRadar, Inc, Mala GeoScience, and Sensors and Software Inc.

The 100 MHz antenna is suited for deeper applications to depths of about 20 m. This antenna can be used to locate larger ordnance at depth.

Data Acquisition: GPR surveys are conducted by pulling the antenna across the ground surface at a normal walking pace. The recorder stores the data as well as presenting a picture of the recorded data on a screen.

Data processing: It is possible to process the data, much like the processing done on single channel reflection seismic data. Processing can include distance normalization, vertical and horizontal filtering, velocity corrections, and migration. However, depending on the data quality, this may not be done since the field records may be all that is needed to detect the ordnance.

Data Interpretation: If the depth to an anomaly is required, the speed of the GPR signal in the soil at the site has to be obtained. This can be estimated from charts showing speeds for typical soil types, or it can be obtained in the field by conducting a small traverse across a buried feature whose depth is known. Probably the most important feature of GPR is its ability to detect both metal and plastic UXO. Neither magnetic nor electromagnetic methods can detect plastic objects.

An example of GPR data from a site in Arizona is shown in figure 220, illustrating anomalies from both metal and plastic targets.

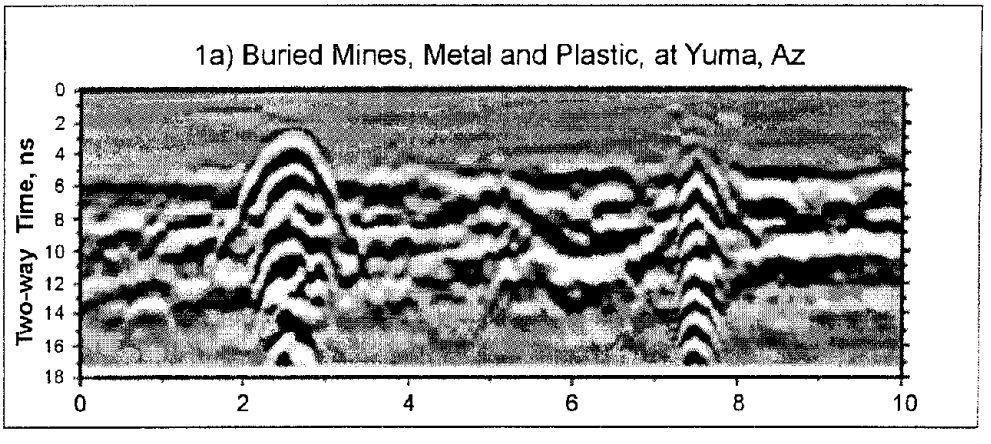

Figure 220. Ground Penetrating Radar data across buried metal and plastic mines. (Powers, et al. 1996)

Advantages: Probably the biggest advantage is that this method can detect both metal and plastic (non metal) buried UXO.

Limitations: Probably the most limiting factor for GPR surveys is that their success is very site specific and depends on having a contrast in the dielectric properties of the target compared to the host overburden, along with sufficient depth penetration to reach the target. However, it is likely that most ordnance will provide the desired dielectric contrast needed. Thus, depth of penetration and the resolution required are probably the most important factors. In soils containing many cobbles, reflections may be obtained from these cobbles making it difficult to distinguish cobbles from UXO. Another disadvantage of GPR systems is that the electromagnetic field transmitted could potentially detonate ordnance with electric fuses; therefore, its use is prohibited in areas where these fuses may exist.

Synthetic Aperture Radar

Two basic radar systems are used for various applications: real aperture radar and Synthetic Aperture Radar (SAR). The difference between these two systems is that SAR uses extensive processing to increase the effective size of the antenna. This results in higher resolution in the "along track" direction. SAR is predominantly used as an airborne system.

Other Methods

The following is a partial list of other methods used to locate UXO. These are either borderline geophysical methods or are physics-based rather than geophysics-based.

- Airborne GPR
- Infrared Radiometry
- Light Detect and Ranging (LIDAR)
- Acoustics. This technique is probably best suited to underwater detection.

CHAPTER 7 VIBRATION MEASUREMENTS

7.1 VIBRATIONS CAUSED BY TRAFFIC, CONSTRUCTION, AND BLASTING

This section covers Traffic Vibrations, Blasting Vibrations and Construction Vibrations. In addition, Vibration Recommendations are also included along with references.

Vibrations are found everywhere in nature and are generated by a wide variety of sources, both natural and manmade. They can propagate through air, ground, and water. Vibrations are used in geophysics to develop a better understanding of the subsurface, whereby vibrations are generated under planned and controlled conditions to gain specific objectives. The vibrations generated during geophysical data acquisition are normally imperceptible to humans and quickly attenuate once the surveys are completed. However, vibrations generated from other sources and for other reasons can be very perceptible and unwanted. The following discussion examines various options for measuring/monitoring, evaluating, and responding to unwanted ground vibrations from construction, blasting, pile driving, and other highway/transportation-related sources.

Many unwanted ground vibrations originate from natural sources such as volcanoes, earthquakes, and landslides. Since these events can be unpredictable and cause significant damage, they are considered in structural designs and building codes. An application of geophysics that addresses structural issues is seismic engineering observations, or the measurement of earthquake motions for comparison with structural design levels. Seismic engineering observations are real-time, continuous monitoring systems and have been installed on many critical bridges around the world. This is addressed in this document under Bridge Deck Structures – Stability.

Generally, vibration issues can be broken down into three broad areas: human perception, deleterious effects on critical processes, and physical damage, all of which can be important. For example, human perception becomes important in critical areas, such as near hospitals or residential neighborhoods. Vibrations can harmfully diminish the quality of Magnetic Resonance (MRI) images in a nearby hospital, or affect crystal growth in a semiconductor factory. Higher amplitude vibrations can cause physical damage to structures. Unfortunately, the procedures for measuring effects on human perception can be quite different from those used to measure effects on critical processes, or potential damage.

7.1.1 Traffic Vibrations

Many of the problems caused by traffic vibrations are more related to human perception and harmful effects than actual physical damage. These are often addressed in Environmental Impact Statements in which future effects are predicted and evaluated and compared to recommended threshold criteria. They are outlined in the FTA Guidance Manual Transit Noise and Vibration Impact Assessment http://www.hmmh.com/rail05.html. Although this reference focuses primarily on Rail Transit issues, the concepts and procedures are usually applicable to roads, highways, and bridges.

Traffic vibrations are addressed either during the planning stage, prior to construction when engineers anticipate potential problems, or during the operating stage, usually in response to a complaint. Engineers are not generally concerned about the impact of vibrations directly on the highway structure, with the notable exception of bridges.

Human Perception

Of all vibration effects, human perception is the most difficult to quantify, since it varies according to many independent factors, such as the following:

- The sensitivity of an individual.
- The structure the individual is in or on.
- The setting (a factory, or a surgical operating room).
- The position of the individual (standing or sitting).
- The axis of orientation.
- The time of day (people notice vibrations more at night, in their homes).
- The duration of each event.
- The amplitude of each event.
- The frequency of the motions.
- The frequency of events.
- The sound associated with the event, and its magnitude.

There have been many attempts recorded in literature to label human sensitivities, and descriptions have ranged from barely perceptible to annoying, and the units used have included acceleration, velocity, and displacement. There are now international conventions for measuring and evaluating these vibrations, and for most highway applications, the more simple evaluations suffice. People are similar enough that if a vibration is characterized in literature as "annoying," most people will find it annoying.

Procedures for measurement

The FTA Manual (Ch. 11) offers general guidelines. Griffin (1990, p.453) describes methods for evaluating whole-body exposure to vibrations that are basically the same as the ANSI Standards. These procedures can be quite complicated and are, in most cases, unnecessary unless litigation is anticipated. Moreover, some of the procedural aspects are outdated by modern digital instrumentation. One important difference is that the ANSI Guidelines require measurement of acceleration, but the FTA guideline suggests velocity. There is sufficient research to support both, but perhaps the more modern data are in acceleration. Included in

this section is an example generalized procedure entitled Ambient Ground Vibration Measurement borrowed from GEOVision that can be helpful. Bruel & Kjaer have published an on-line document that is a primer on vibration measurement at http://www.bksv.com/pdf/Measuring%20Vibration.pdf. A generalized approach that will work in most applications is presented below. Table 10 defines the strength of perception of various magnitudes of vibration.

Table 10. Approximate strength of perception for various magnitudes of weighted vibration. (M.J. Griffin, 1990, p. 262)

Semantic label	r.m.s. weighted acceleration (m/sec)	Semantic label
Very strong perception	0.315 0.25 0.20 0.16	
	0.16 0.125 0.10 0.08	Strong perception
Very clear perception	0.08 0.063 0.05 0.04	
	0.04 0.0315 0.025 0.020	Clear perception
Perception probable	0.020 0.016 0.0125 0.01	
	0.01 0.008 0.0063 0.005	Perception improbable

It should be noted that human perception sensitivity is most sensitive below 2 Hz horizontally, between 5 and 15Hz vertically, and decreases at higher frequencies. It cannot be overemphasized that merely measuring the vibration levels and interpreting them in terms of human perception only partly addresses the problem. There are many factors that contribute to vibrations as perceived by humans, and cannot be addressed using only geophysics.

The most important axis of measurement for human perception vibrations is vertical, since people are generally more sensitive to vertical motions than horizontal motions. The general Ambient Ground Vibration Measurement methodology below should also be followed. However, there are some key differences:

1. Measurements should be made using an accelerometer.

2. Triaxial measurements are best, but the vertical axis is the minimum required.

3. Minimum resolution should be 0.001m/sec^2 (0.039in/sec^2).

4. Digital recordings should be made either directly in the frequency domain (such as with a spectrum analyzer), or anticipating analysis in the frequency domain.

5. Sufficient data should be collected for at least 20 averages to achieve some statistical benefit.

6. The bandwidth of interest is generally 1 to 100 Hz; the sampling rate should be at least 250 Hz.

7. Data should be recorded at the location and time period the subject claims is the "worst."

8. Careful consideration should be given to the location of the complaint, the hours during which the vibration is perceived, the duration, the frequency, and whether the vibration events are associated with sound. Each factor can contribute to weighting factors that could elevate or reduce the evaluated motion. For example, the same vibration measured in a factory setting will be much more tolerable than in a doctor's office.

Harmful Effects

Having addressed harmful effects on people, this section discusses harmful effects on critical processes. It is not the role of this document to discuss all the possible processes that can be affected by vibrations, but it is important to have some idea of the types of processes that can be affected. This will allow engineers to understand why some types of vibration measurement programs are necessary, and when they should be used.

Usually, critical processes involve imaging (both medical and graphical), medical procedures, delicate manufacturing, or assembly operations. Some examples of these include the following:

- Electronic imaging for high resolution photography, such as an electron-scanning microscope or high-resolution printing operations

- Magnetic resonance imaging (MRI) for medical research

- Semiconductor crystal growth.

(http://microgravity.msfc.nasa.gov/snell/vibration.html and
http://www.vibemaven.com/SUCCESS-STORIES.HTML)

In most cases, hospitals and manufacturing plants will evaluate and design their facilities to mitigate the effects of vibrations. To do this, they measure the existing ambient conditions and design foundations or, under worst-case conditions, full floating foundations. These are

expensive, but do an excellent job. In summary, if the highway is already in existence, facilities will make appropriate accommodations.

Sometimes, however, it will be necessary to route a highway or build a bridge near such a facility, and the potential harmful effects must be evaluated and addressed. The best approach, as outlined in the FTA Manual (1995, ch. 11), is as follows:

1. Obtain from the facility or equipment manufacturer the threshold of tolerance for vibration. Make sure this is the threshold at the input to the foundation, and not at the input to the machine or instrument itself. Some analysis may be required to make this conversion.

2. Evaluate the vibration propagation/attenuation characteristics of the soils between the proposed highway or bridge, and the critical process.

3. Predict what the vibration amplitude and frequency characteristics will be emanating from the source.

4. Combine 1, 2, and 3 to predict and compare what the motions will be at the equipment foundation.

The general measurement procedures outlined under Human Perception above will be equally useful here.

There are no known cases in which traffic vibrations have actually caused structural damage. However, in such a case, the approach and procedures outlined under Construction Vibrations below will apply.

Example Procedure for Ambient Ground Vibration Measurements (Used with Permission from GEOVision Geophysical Services)

Accurate characterization of ground vibrations is often needed for siting of vibration-sensitive facilities or for diagnosis of existing vibration-related problems. Due to the small amplitudes of these vibrations, special instrumentation and special care is needed to obtain meaningful data.

The objective of ground vibration measurements is to accurately obtain site vibration data in terms of time histories, spectra (Power Spectral Density (PSD) or response), or statistical parameters; obtain data over time to determine the statistical variability of ground vibrations; and obtain data with sufficient quality to assist in identification of the major contributors to the site vibrations.

The objective of this procedure is to provide a formal framework for a skilled, experienced engineer to accomplish high-quality, consistent ground vibration measurements. This procedure covers equipment, measurements, and basic data analysis, but does not include advanced analyses or reporting.

Equipment

1. Kinemetrics ES-T Episensor Broadband Accelerometer or equivalent (figure 221). All three channels (X, Y, and Z) or any subset may be used for a specific project. Multiple sensors are good if available.

2. Portable digital recorder with very-low-noise preamplifier and digital resolution of a least 16 bits. The Kinemetrics K2 Seismograph or SSR-1 Digital Recorder are specified in this procedure, but others may be used if equivalent or better.

3. Laptop computer with recorder control software (Kinemetrics Quicktalk, Quicklook, and PSD) and communications cable.

4. Power/signal cable from recorder to sensor.

5. Batteries to operate system.

6. Solar panel (if required) for long-term unattended measurements.

7. GPS antenna (if needed) for precision timing.

8. Field enclosure (if needed) for environmental protection.

9. Tape measure for accurate location of measurements. DGPS may be used if available.

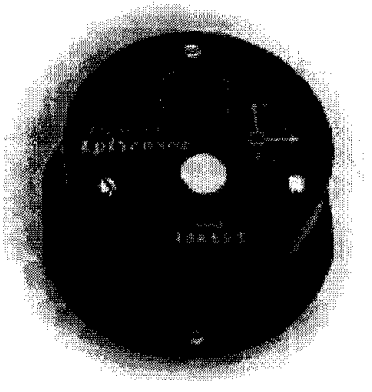

Figure 221. High resolution sensor for ambient vibration monitoring. (Kinemetrics)

The measurement site should be selected to be representative of "average" site conditions. Measurement site or general site conditions that could affect vibrations (proximity of roads, mechanical equipment, construction, etc.) should be carefully documented in a field notebook.

If the site is under construction, the construction activities should be documented (type, location, durations) in a field notebook. Unless construction vibrations are the subject of the investigation, efforts should be made to avoid measurements during times of construction activities.

Other environmental conditions that could affect vibrations should be documented in a field notebook. These may include wind, temperature, humidity, rain, noise, or others.

The sensor(s) and recorder(s) should have been calibrated within 12 months of the vibration measurements. A copy of these calibration data should accompany the instrumentation. Calibration constants important to the measurements (sensor sensitivities, sensor natural frequencies, and recorder gains) should be recorded in the field notebook.

Immediately prior to the field measurements, the sensor-recorder sensitivity should be checked by tilting each sensor through its full-scale range (90 degrees for a 1g accelerometer, 14.5 degrees for a 1/4g accelerometer), and the output measured using the voltmeter function on the recorder. These data should be recorded in the field notebook. Although not a calibration, results of this sensitivity check should be within ±5% of the formal calibration data.

Measurement Procedure

The general field procedures (for 5 minute/hour survey) are as follows:

1. Install the recording station. This should be at least 3 m from the sensor. For multiple-day measurements, provide adequate power and environmental protection.

2. Connect the sensor to the recorder and turn on the recorder. Connect to the computer and turn on computer.

3. Set up recorder parameters. Include the setting of sensor calibration data where appropriate. Document recorder parameters in field notebook. Depending on the recorder, download the parameter file and save it to diskette for the project file.

4. Check sensor zero settings. If greater than 500 mv, manually adjust sensor zero.

5. Record a functional test. Download file. View the file with QL16 or other appropriate file viewer. Make sure response is normal.

6. Mark location of each measurement/Run numbers on the Site Map.

7. Proceed with measurement. Manually record the first event (typically 5 minutes) using the keyboard trigger. Download the file and check with QUICKLOOK.

8. Set up the recorder for event recording. For 7-day ambient tests, set instrument to record 5 minutes of data every hour. Start acquisition.

9. Wait on site until the next measurement period. Check the recorder to verify that it has correctly performed the automatic data collection. If not, troubleshoot and repeat

10. Leave the site if desired. For multiple-day measurement programs, site inspection once per day is required (twice per day is recommended). Data should be downloaded and memory cleared if more than 75% of available recorder memory is used.

11. Site conditions should be noted for each site visit. If possible, ask site personnel about unusual conditions that may have occurred while the engineer was not present. Examples would be the passage of large, heavy vehicles.

12. Daily, or upon completion of the measurement period, download data to the PC and check all data using QUICKLOOK.

13. If there is more than one site, repeat these steps for each additional site.

Required Field Records

a) Field log for each vibration measurement describing:

b) Location of each measurement..

c) Date and time of test.

d) Tester or data recorder.

e) Description of source (ambient, heel-drop, etc.).

f) Any gain or filtering by channel during recording.

g) Any deviations from test plan and action taken as a result.

h) File name as recorded on disk.

i) QA Review.

Much of the above information will be automatically recorded in the seismograph header at the time of recording (gains, filtering, date and time) and need not be recorded on the paper log:

1. Site Map showing to scale the locations of measurements referenced to physical objects.

2. Diskettes with backup copies of data on hard disk, labeled with measurement designation, record ID numbers, date, and tester name.

Basic Analysis and Interpretation

Following completion of fieldwork, the recorded digital records are processed by computer and analyzed by an experienced engineer to produce plots and tables of transient motion (time histories) and steady-state motion (converted from PSD's).

Again, the specific procedure varies according to the project requirements. The following steps are for projects using the K2 recorder only.

1. Retrieve K2 files and transfer to PC for analysis. NOTE: K2 file names are randomly assigned by the recorder, and will differ from Measurement ID numbers. Save the original *.evt files, and then copy to new files with logical, project-based names.

2. Run QUICKLOOK on all *.evt files. Visually review all time-series data for quality. Note any unusual data aspects in the field notebook.

3. Using the print command, print the QUICKLOOK screen for each data file. This will act as a "road map" for future data analyses. Mark (in ink) any notes or observations on the paper plots.

4. Run Kinemetrics' PSD program. For each channel, calculate and plot the PSD. Use the default window, overlap, and gains.

5. Using the print command, print the PSD plot for each channel. Mark any notes or observations on the paper plots.

6. Export the PSD data for each channel to ASCII using the "print to file" function.

7. After each of the data channels is completed, import the ASCII PSD data to an EXCEL spreadsheet. Make a single plot containing all channels of PSD data. Print this plot and include with the field files.

Documentation

A "Field File" should be made for each distinct measurement project. If a project contains distinct sites, separate field files shall be made.

The field file should contain:

- Calibration data.
- Copies of field notebook pages.
- Completed logs and forms as appropriate.
- Original time history plots.
- Original PSD spectra plots.
- Original EXCEL composite spectra plot(s).
- Any other notes, maps, etc., as appropriate.

Although the scope of this procedure does not include reporting, the material contained in the field file is appropriate for inclusion as an appendix or in the main body of a project report.

7.1.2 Blasting Vibrations

Blasting vibrations can impact all three areas of concern: human perception, harmful effects, and structural damage, and special care must be taken to mitigate their effects. Fortunately, blasting operations are normally discontinuous, short-duration events, and for most construction operations, can be handled as an isolated problem. More importantly, blasting can be planned to minimize impacts and stay within local and federal guidelines and limits.

Human Perception

The general issues involving human perception are similar to those outlined under Traffic Vibrations. The important difference for blast vibrations is that they are normally discontinuous, short-duration events. It is well known that humans will tolerate much higher transient vibrations, particularly if they have been warned and notified, than continuous steady state, or even intermittent but often recurring vibrations. Federal guidelines require an analysis predicting the ground motions at a distance. If these motions are below 0.01m/sec^2 (0.4in/sec^2), most people will not notice the vibrations, being more distracted by the massive dust cloud rising in the sky. If required, a well-designed leaflet, distributed to the neighborhood, announcing an upcoming daytime blast, and describing the probable minimal effects will eliminate any surprises.

Procedures for Measurement

Blast monitoring procedures are perhaps the best developed of all vibration monitoring procedures. This is mostly due to the fact that officially recognized guidelines for monitoring have not changed significantly since 1987 as described in the Blasting Guidance Manual, 1987. In fact, many instrument companies have incorporated most of the required elements in their digital seismographs (figure 222). These are portable, battery operated devices that incorporate triaxial seismometers, are self-triggering, and record and store motions in the required format, and provide direct comparison with the OSMRE limits either on site or via software provided. Table 11 provides some links to these manufacturers. Following the manufacturer's instructions is generally all that is necessary. There is one caution, however. It is vital that the instrument be placed in a location where the sensor can be firmly coupled to soil. This is often accomplished by using spikes on the bottom of the instrument, but sometimes it is necessary to dig down to remove loose soil. Also, from the standpoint of the overburden pressure measurement (sound), it is important not to locate the sensor directly in front of a building or wall. Sound waves bouncing off the wall will add to the sound coming from the blast.

It is interesting to note that throughout the history of blasting and continuing to this day, blast monitoring has been conducted using seismometers, recording velocity. The research in this industry is all in terms of velocity.

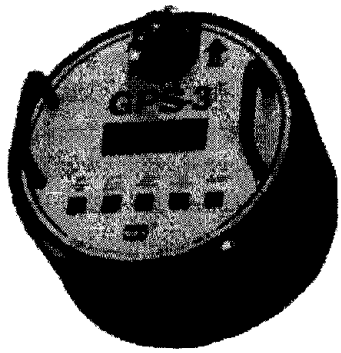

Figure 222. GPS-3™ general purpose seismograph. (OZA Inspections)

General Interpretation

Table 10 applies to blasting vibration concerns as well.

According to Siskind (2000) "Where people can be assured that damage is not going to occur, they will tolerate up to 0.5in/sec, at least during the day when ambient vibrations are also high. However, when their fears are not allayed, any perceptible rattling is a potential problem. Complaints would then be expected from some persons whenever the impacting vibration (outside-measured vibration) exceeds perceptibility, about 0.01in/sec (or 0.01m/sec^2)."

Harmful Effects

The general issues involving harmful effects are the same as outlined under Traffic Vibrations. The important difference for blast vibrations is that they are normally discontinuous, short-duration events. Contacting operators of critical facilities and notifying them of upcoming events (a schedule is best) are vitally important to minimizing complaints. Most operations can be delayed or rescheduled to avoid problems.

Damage to Structures

Of all the potential vibration sources discussed in this document, blast vibrations have the greatest potential for damaging structures. It is for this reason that Federal guidelines for this industry are so well developed. Blasting contractors are typically well aware of their responsibilities, and meticulous care is taken in the planning and design of all blast operations to minimize the damage potential.

Nevertheless, special procedures are recommended to mitigate or minimize the potential for litigation. These are well documented in Dowding (1996), and include the following:

- Calculations of probable motions (peak particle velocity) at the nearest structure using empirical formula.
- Preblast tests, to directly measure attenuation characteristics.
- Preblast crack surveys, to document the existing status of nearby homes.

- Monitoring, using more than one instrument, preferably one next to the closest structure or residence in each direction.

- Control of blasting, using instrument data, i.e., evaluate predictions in the light of actual data and make adjustments during the blasting program.

- Careful documentation of all facts and events.

It should be noted that potential damage is not limited to stress caused by motions, but can also occur in sands due to densification. In other words, foundation settlement can be caused by blasting vibrations (Dowding, 1996).

Procedures for Measurement

As discussed above, blast monitoring procedures are perhaps the best developed of all vibration monitoring procedures as described in Rosenthal and Morlock, 1987. Table 11 provides links to manufacturers. Following the manufacturer's instructions is generally all that is necessary. Again, it is vital that the instrument be placed in a location where the sensor can be firmly coupled to soil. This is often accomplished by using spikes on the bottom of the instrument, but sometimes it is necessary to dig down to remove loose soil.

General Interpretation

Modern blast monitoring seismographs automatically provide analysis according to requirements, and compare this analysis to the OSMRE guidelines. The graph in figure 223 shows the criteria:

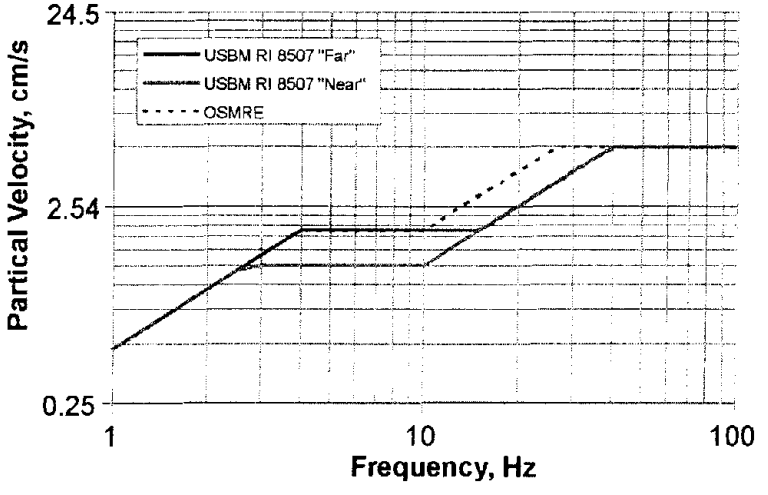

Figure 223. Safe level blasting criteria from OSMRE.

7.1.3 Construction Vibrations

Construction vibrations can impact all three areas of concern: human perception, harmful effects, and structural damage, and special care must be taken to mitigate their effects,

particularly for pile driving or other vibratory impact operations. Dowding (1996) provides an excellent resource for understanding the issues surrounding construction vibration monitoring.

Human Perception

The general issues involving human perception are the same as outlined under Traffic Vibrations.

Procedures for measurement

The guidelines and procedures outlined under Traffic Vibrations above are entirely applicable here.

General Interpretation

Table 10 applies for construction vibration concerns as well.

Harmful Effects

The general issues involving harmful effects are the same as outlined under Traffic Vibrations.

Damage to Structures

Besides blasting operations, construction vibrations also have potential for damaging structures. This is particularly true for pile-driving operations, pipe pulling/driving, tunneling, and other methods that require high vibratory energy.

Figure 224. CVM-2 continuous vibration monitor. (OZA Inspections)

As with blasting, special procedures are recommended to mitigate or minimize the potential for litigation (Dowding, 1996). These include the following:

- Calculations of probable motions (peak particle velocity) at the nearest structure using empirical formula.

- Preconstruction tests, to directly measure attenuation characteristics.
- Preconstruction crack surveys, to document the existing status of nearby homes.
- Monitoring, using more than one instrument, preferably one next to the closest structure or residence in each direction.
- Control of construction operations, using instrument data, i.e., evaluate predictions in the light of actual data and make adjustments.
- Careful and thorough documentation.

Procedures for Measurement

Most blast monitoring seismograph manufacturers have begun to supply instruments capable of also recording construction vibrations, and particularly vibrations from pile-driving operations. However, there are differences. A blast seismograph is designed to record a single, short-duration blast event, and in the presence of a pile-driving operation, its memory capacity will be rapidly exhausted. Manufacturers have modified these instruments so that once the memory is filled, new events will be evaluated, and if the amplitudes exceed the stored data, the instrument will overwrite the data. This means that when a day's recording is completed, only the maximum events are stored in memory. Table 11 provides links to these manufacturers. Following the manufacturers instructions is generally all that is necessary.

It is vital that the instrument be placed in a location where the sensor can be firmly coupled to soil. This is often accomplished by using spikes on the bottom of the instrument, but sometimes it is necessary to dig down to remove loose soil.

General Interpretation

Modern construction vibration monitoring seismographs (figure 224) automatically provide analysis according to requirements, and compare this analysis to the Office of Surface Mining and Reclamation and Enforcement (OSMRE) guidelines. This is appropriate, even though these are not blast vibration events, because the OSMRE guidelines are essentially response spectra. The limitation of using the OSMRE curve for construction vibrations is that response spectra do not properly represent energy. Obviously, there may be a greater impact from a pile-driving operation that lasts for weeks, than a single blast.

7.1.4 Vibration Recommendations

Table 11 summarizes the recommendations discussed above

Table 11. Summary of vibration recommendations.

Vibratory Motion	Frcq. Range	Sensor Type (with link to example)	Motion Measured	Application (with link to example)
Tilt, or Rotations	0-1Hz	Tiltmeter, http://www.geomechanics.com /products/tiltmeters.htm Inclinometer http://www.slopeindicator.com/instruments/inclin-intro.html	Rotation from vertical in degrees, sometimes expressed as the sine of the angle of tilt	• Monitoring slopes and landslides to detect zones of movement and establish whether movement is constant, accelerating, or responding to remedial measures. • Monitoring diaphragm walls and sheet piles to check that deflections are within design limits, that struts and anchors are performing as expected, and that adjacent buildings are not affected by ground movements. • Monitoring the effects of tunneling operations to ensure that adjacent structures are not damaged by ground movements. • Providing settlement profiles of embankments, foundations, and other structures. • Monitoring deformation of the concrete face of a retaining wall (From Slope Indicator)
Settlement	0-1Hz	Settlement cells http://www.slopeindicator.com/instruments/settlementcell.html	Changes in elevation, mm or inches	• Monitoring settlement or heave in embankments and embankment foundations. • Monitoring subsidence due to tunneling. • Monitoring consolidation under structures. • Monitoring settlement due to dewatering or preloading. • Monitoring settlement in marine fills (From Slope Indicator)
Motion due to earthquakes	0-200Hz	Accelerographs http://www.kinemetrics.com/etna.html http://www.kinemetrics.com/qdr.html Structural monitoring system http://www.kinemetrics.com/oasis.html	Absolute acceleration, m/sec^2	• Monitor the performance of individual structures during earthquakes, such as piers, large retaining walls, and foundations http://www.kinemetrics.com/amoes.html • Monitoring the performance of large structural systems during earthquakes, such as bridges http://www.kinemetrics.com/structural.html http://www.kinemetrics.com/namhae.html http://www.kinemetrics.com/halkis.html
Motion due	1-200Hz	Blast seismograph	Particle velocity, m/sec	• Monitoring ground motion during blasting • http://www.geovision.com/PDF/A_Blast Monitoring.PDF

Table 11. Summary of vibration recommendations continued.

Vibratory Motion	Freq. Range	Sensor Type (with link to example)	Motion Measured	Application (with link to example)
to blasting		http://www.instantel.com/ http://vibra-tech-inc.com/products/ http://www.driller.com/vms2000.html		
Strains due to motions	0-100Hz	Strain gages Bonded http://www.vishay.com/brands/measurements_group/strain_gages/mm.htm Weldable http://www.geokon.com/straingages.htm http://www.jptechnologies.com/wsgages.html http://pages.prodigy.net/heatinc/	Strain, mm/mm or in/in	• Monitoring stresses in structural elements at critical location, both steel and concrete • Evaluate fatigue in structural elements
Motion due to construction	1-200Hz	Construction seismograph http://vibra-tech-inc.com/products/ http://www.the-oza-group.com/ozahome.asp	Particle velocity, m/sec	• Monitoring ground motion during construction operations, like pile driving http://www.geovision.com/PDF/A_Vibration_Monitoring.PDF
Motion due to ambient vibration, used to evaluate human perception, structural	1-100Hz	Vibration Monitoring	Acceleration, m/sec^2	• Monitor construction vibrations to evaluate potential for damage to nearby structures • Monitor effects of roadway deterioration (such as potholes) on nearby critical processes http://www.geovision.com/PDF/A_MRI_

Table 11. Summary of vibration recommendations continued.

Vibratory Motion	Freq. Range	Sensor Type (with link to example)	Motion Measured	Application (with link to example)
characteristics		Human http://www.bksv.com/2506.htm	sometimes velocity, m/sec	Vibration.PDF ftp://ftp.kmi.com/pub/AppNotes/appnote44.pdf

GEOPHYSICAL METHODS, THEORY, AND DISCUSSION – PART II

This part provides more detailed descriptions of the geophysical methods discussed in the applications section of the report. However, the intent of the descriptions is to give a conceptual understanding of the methods, using equations only when needed. The text is written for readers who are not familiar with geophysics but require a deeper understanding without being burdened by excessive theory. Bibliographies are provided at the end of the Geophysical Methods section for those readers who want a more rigorous description of the methods along with more theory and mathematical treatment. In addition, bibliographies are provided at the end of the Geophysical Quantities chapter.

The geophysical methods presented in Part II are listed below. In addition to surface methods, the most commonly used borehole methods are also briefly presented.

Surface Geophysical Methods

Potential Field Methods

Gravity Methods
Magnetic Methods

Seismic Methods

Seismic Refraction
Shallow Seismic Reflection
Surface Wave Methods (SASW)
Rayleigh Waves Recorded with a Common Offset Array
Sub Bottom Profiling
Fathometer

Electrical Methods

Self Potential (SP) method
Equipotential and Mise-a-la-Masse Methods
Resistivity methods
Induced Polarization (IP), Spectral IP

Electromagnetic Methods

Frequency Domain Electromagnetic Methods
Time Domain Electromagnetic Methods
Ground Penetrating Radar (GPR)
Very Low Frequency (VLF) method
Seismoelectrical Method
Metal Detectors

Nuclear Methods

Nuclear Magnetic Resonance (NMR)

Borehole Geophysical Methods

Electrical Methods

Self Potential logging
Single Point Resistance logging
Normal Resistivity logging
Lateral Resistivity logging
Focused Resistivity logging
Microresistivity logging
Dipmeter logging
Induction Logging

Nuclear Methods

Gamma logging
Gamma-gamma logging
Neutron logging
Acoustic logging
Acoustic velocity logging
Acoustic waveform logging
Cement Bond logging
Acoustic Televiewer logging
Acoustic Caliper logging

Flow Logging

Impellar Flowmeter logging
Heat pulse Flowmeter logging

Well Completion Logging

Casing Logging
Logging Annual Materials logging
Borehole Deviation logging

Hole to Hole Logging

Crosshole Sonic Logging (CSL)
CSL Tomography (CSLT)

CHAPTER 8 GEOPHYSICAL QUANTITIES

This chapter is substantially based on a report produced by the Environmental and Engineering Geophysical Society titled Applications of Geophysics in Geotechnical and Environmental Engineering, 1998.

Many physical properties and quantities are involved in an understanding of geophysics and geophysical methods. In this section, the units of measurement are defined and some relationships established such as saturated porosity vs. dielectric constant. In addition, some of the physical properties of earth materials are presented.

8.1 ELECTRICAL CONDUCTIVITY (σ) AND RESISTIVITY (ρ)

Electrical conductivity is the proportionality factor relating the current that flows in a medium to the electric force field that is applied. It is a measure of the ability of electrical charge to move through that material. Resistivity is the reciprocal of conductivity. The units of conductivity are Siemens per meter (S/m). The practical unit is milliSiemens per meter (mS/m). Because Siemen, the unit of conductance, is the reciprocal of the Ohm, the unit of resistance, the units of conductivity are sometimes given as mhos/meter or millimhos/meter. . Resistivity is the inverse of conductivity ($\rho = 1 / \sigma$). The units of resistivity are Ohm meters (Ωm).

8.1.1. Factors Influencing Electrical Conductivity

Electrical conductivity of earth materials is influenced by the metal content (sulfides) in the rock, porosity, clay content, permeability, and degree of pore saturation.

8.1.1.1 .Metal Content

All metal objects of interest in contaminated site assessments have a very large conductivity contrast with their surroundings and can usually be readily detected with electrical and electromagnetic methods. Quantitative estimates of the metal content are not easily obtained. Nelson and Van Voorhis (1982) show the resistivities of a large number of sulfide-bearing rocks (from 0.5 to 15 weight percent). A version of their figure is reproduced from Hearst and Nelson (1985) in figure 225. As Hearst and Nelson point out, below 2% there is not much correlation, whereas between 2% and 10%, there is a steady decrease in electrical resistivity The slope of resistivity vs. percent sulfides decreases (i.e. conductivity increases) noticeably beyond ten percent sulfides. This decrease quickens beyond 10%, suggesting that small veins are forming exceptionally conductive pathways. Note that IP effects are much more pronounced than resistivity anomalies at the low metal content.

8.1.1.2 Porosity

In the absence of metals, which conduct electronically, formation conductivity is related to the volume and conductivity of the water in earth materials. The groundwater conducts through its ions, and its conductivity, therefore, depends strongly on the total dissolved solids. Within a porous, clay-free medium whose matrix is non-conducting, a relationship known as Archie's Law is widely used and reasonably valid:

$$\frac{\sigma_w}{\sigma_f} = F = a\phi^{-m}, \tag{16}$$

where

σ_w = conductivity of the water,

σ_f = conductivity of the formation as a whole,

a = empirical constant, typically 1 for unconsolidated sediments,

m = empirical constant, typically 2 for unconsolidated sediments,

ϕ = effective porosity, the fraction of interconnected pore space,

F = "formation factor," related to the volume and tortuaosity of the pore space.

As Hearst and Nelson point out, it is amazing that the conductivity of so many geological formations is well represented by this simple function of porosity. It holds true even to the very low porosities found in crystalline rocks.

For a simple three-component system of air, water, and matrix, the relation

$$\frac{\sigma_\varpi}{\sigma_\phi} = FS^n, \tag{17}$$

where

S = fractional saturation of the pore volume,

n = an empirical constant.

Therefore, if the formation factor and groundwater conductivities of a saturated formation can be measured (say by geophysics and sampling, respectively), the porosity can be approximately estimated. If F is known, then S can be estimated in a partially saturated medium.

8.1.1.3 Clay Content

Clays and shales are hydrated minerals with high porosities and low permeabilities. The minerals themselves may not be very conductive, but their surface charge causes an excess of cations in the pore fluid immediately adjacent to the clay surfaces. The result is high conductivity near the clay surfaces, which can dominate the overall conductance if the pore water conductivity is low. A commonly quoted relationship (Waxman and Smits, 1968) is:

$$\sigma_\phi = F^{-1}(\sigma_\varpi + \sigma_\chi), \tag{18}$$

where σ_χ = conductivity of the exchangeable cations. σ_χ can be estimated from its cation exchange capacity. However, there are several problems in applying this apparently simple equation.

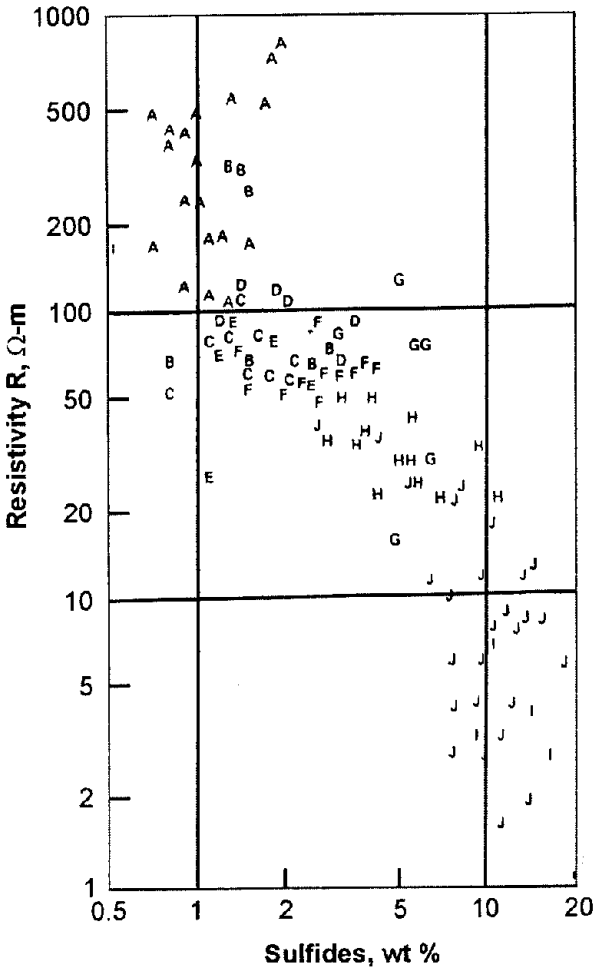

Figure 225. Electrical resistivity of rocks with various wt % of sulfide. Samples each average over several cubic meters.

8.1.1.4 Permeability

Archie's relationship notwithstanding, a rock with a non-conducting matrix must be permeable as well as porous to conduct electricity. There is a clear symmetry between the laws of Darcy and Ohm, which predict electrical current and fluid flow, respectively.

Darcy's Law:

$$q = -k\frac{dV}{dh}, \tag{19}$$

Ohm's Law:

$$j = -\sigma\frac{dV}{dh}, \tag{20}$$

where

q = fluid density,

j = current density,

$\frac{dV}{dh}$ = head or voltage gradient, respectively.

Nonetheless, relationships between electrical conductivity and permeability are tricky and site specific.

These relationships are sought at both the material (sample) level and on aquifer scales. An excellent summary is given by Mazac, et al. (1985). At the aquifer level, the resistivity, transverse resistance, and horizontal conductance, as measured by surface resistivity and EM soundings or well logs, are compared to average hydraulic conductivity, transmissivity, and leakance. These parameters are illustrated in figure 226 and table 12.

Table 12. Comparison of electric and hydraulic properties.

Electrical	Hydraulic
Transverse resistance: $T = \Sigma h_i\rho_i = H\rho_l$	Transmissivity: $T_h = \Sigma h_i k_i = K_l H$
Longitudinal conductance: $S = \Sigma h_i/\rho_i = H/\rho_l$	Leakance: $L_h = \Sigma k_i/h_i = K_t/H$
Average aquifer resistivities: ρ_l, ρ_t	Average hydraulic conductivities: K_l, K_t

Depending on the resistivity structure, surface resistivity soundings can often estimate either T or S for an aquifer sequence, but not H or ρ_t or ρ_l independently. If $H = \Sigma h_i$ can be estimated from other data, then the average resistivities can be obtained.

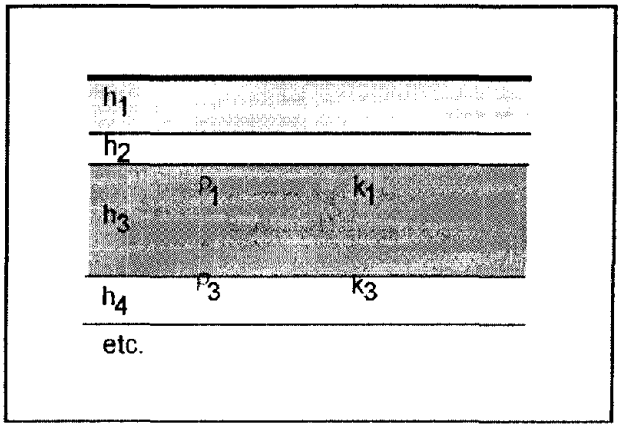

Figure 226. A layered aquifer model.

Also, it is useful to be able to correct for known changes in the water quality between sites since these will affect ρ but not K. At the material level, both direct and inverse relationships between resistivity and hydraulic conductivity are quite possible.

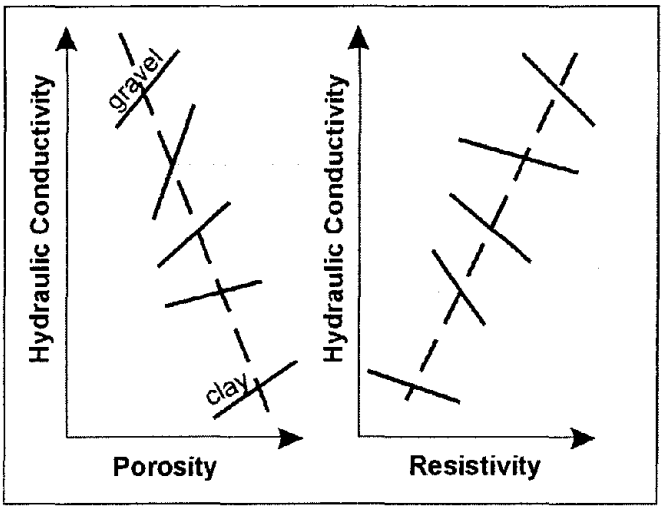

Figure 227. Schematic relationship between hydraulic conductivity, porosity and resistivity (Mazac et al., 1985).

For a clean aquifer, where Archie's Law predicts an inverse relationship between resistivity and (effective) porosity, effective porosity determines hydraulic conductivity, and an inverse relationship with hydraulic conductivity can be expected.

For different materials, however, hydraulic conductivity increases and porosity decreases with grain size, leading to a direct relationship between ρ and k. In situations where clay content dominates the resistivity of a material, again a direct relationship between ρ and k can be expected (as in the example above). Mazac, et al., (1985) shows a generic trend between different materials (clay to gravel) with an inverse k vs. ϕ and a direct ρ vs. k relationship. Superimposed, for any given material, they show opposite trends. This is shown schematically in figure 227.

8.1.1.5 Skin Depth

In electromagnetic methods, the electrical conductivity of the earth plays a pivotal role in the penetration that can be obtained. Conductivity removes (attenuates) energy from the EM wave through the work done by moving charge. Higher frequency EM waves lose energy more quickly than low frequency waves because, conceptually at least, they move more charge in a given time. The depth at which a plane electromagnetic wave will be attenuated to $\frac{1}{e}$ (0.37) of its surface amplitude is called the skin depth, δ. The usefulness of the skin depth concept is that it represents the maximum penetration of an EM method operating at frequency f in a medium of conductivity σ. The actual exploration depth may well be much less than a skin depth owing to other factors, notably the geometry of the prospecting system. Skin depth is related to conductivity as:

$$\delta = (\pi\phi\mu\sigma)^{-1/2} = 503.4(\sigma\phi)^{-1/2}, \tag{21}$$

where

f = frequency in Hz,

σ = conductivity in $\frac{\text{Seimens}}{\text{m}}$,

μ = magnetic permeability.

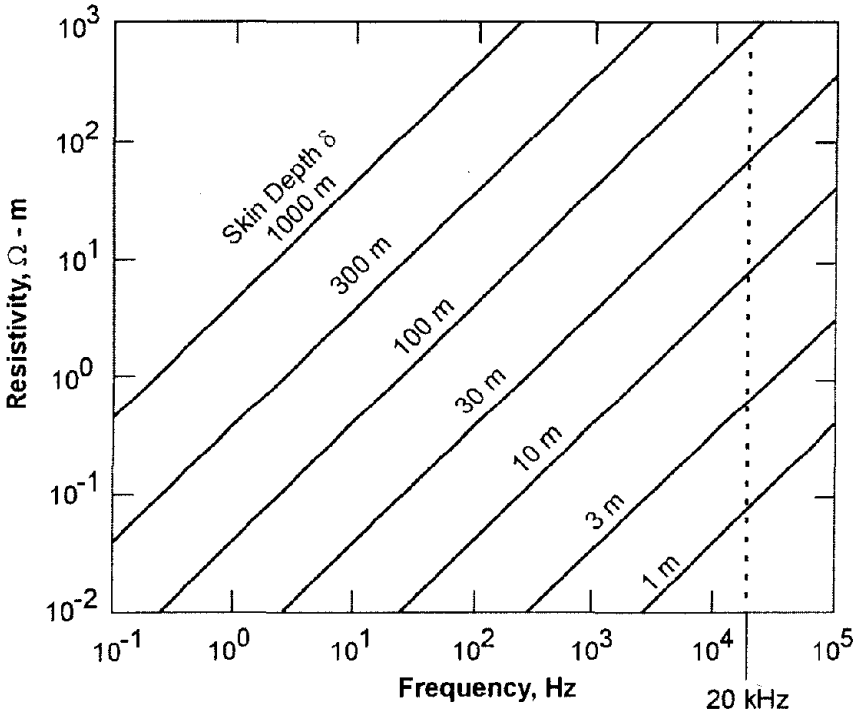

Figure 228. Skin depth as a function of resistivity and frequency.

The second formulation assumes a free space permeability of $4\pi.10^{-7}$. A chart of skin depth versus frequency is shown in figure 228.

8.1.2 Ground Penetrating Radar Attenuation

An issue related to conductivity is the attenuation (α) of radar signals by conductive soils and overburden. This is usually quoted in decibels per meter and in the frequency range 100 to 1000 MHz is approximated as (Annan, 1991):

$$\alpha = 1.69\frac{\sigma}{K^{1/2}}\left(\frac{\text{dB}}{\text{m}}\right), \tag{22}$$

where

K = relative dielectric constant,

σ = conductivity in $\frac{\text{mS}}{\text{m}}$.

For example, over ground having a conductivity of 30 mS/m and K of 25, a typical GPR signal would be attenuated at $\alpha = 10.1$ decibels/meter. A good radar system might have 100 dB of sensitivity to use in ground transmission. In this environment, its penetration would be limited to 5 meters (of two-way travel).

8.1.3 Induced Polarization (Ip) And Complex Resistivity

These properties are not widely used in environmental or engineering surveys but have interesting applications to the detection of clay and organics.

As previously defined, electrical resistivity, ρ, is the constant of proportionality between the electrical current and the applied electric field (Ohm's Law). If the applied field varies in time, the current behaves similarly. For example, if the applied field is a sinusoid with a zero crossing at time t_1, then the current will be similar. The implication is that ρ is independent of the frequency or time behavior of the applied field. In fact, the resistivity (or conductivity) will almost always be frequency dependent to some degree, and is also complex. The resistivity then has the form $\rho(f) = \rho'(f) + i\rho''(f)$. In this case, the current is still linearly proportional to the applied electrical field at each frequency, but it will have a phase shift in its response. In the diagram (figure 229), a complex ρ has shifted the current sinusoid with respect to the applied field. An equivalent representation of the effects of a complex resistivity is the result of a sharp turn-off of the applied voltage. Normally, the current in the ground would also cease immediately. When the resistivity is complex, the current will continue to flow for a period of microseconds to as much as several seconds in some cases.

Methods known as induced polarization (I P), spectral I P, and complex resistivity (CR) exploit these more general properties of the resistivity (conductivity) parameter. The process of shifting implies delay between cause and effect, and this, in turn, requires that the energy in the applied field be stored for an instant before being converted into current flow. In an electrical circuit, this storage could be depicted as a capacitor.

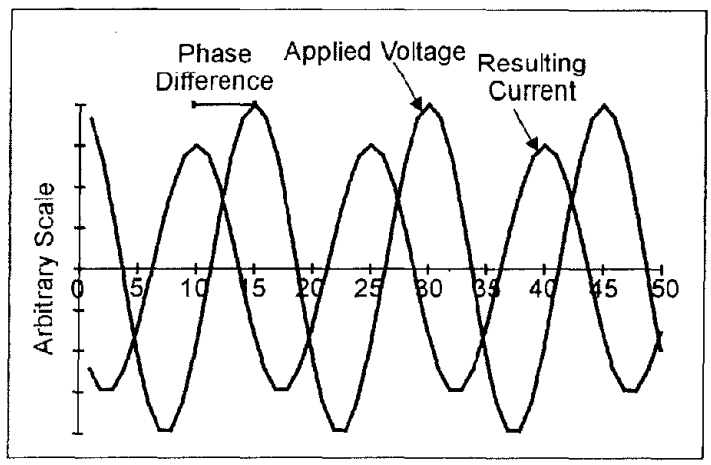

Figure 229. Schematic of the phase shift between an applied voltage and the resulting current when ρ is complex.

There are several mechanisms in the earth that enhance this complex, frequency- dependent behavior of resistivity. Disseminated metal ores are by far the most (commercially) important target of I P surveys. The mechanism for storage/delay is at least conceptually related to the blocking of pores by metallic grains. Pore water ions build up on either side of the grain, giving the effect of a capacitor. A similar effect can be observed in some garbage dumps containing a lot of scrap metal. The disseminated metal may not increase the average resistivity substantially but are charged by an applied electric field. Their presence can be recognized by the slow voltage discharge after the applied field is turned off. These effects are most pronounced at frequencies below 1,000 Hz. IP effects arising from metallic sources are generally most pronounced at fairly low frequencies (below 100 Hz). However, in conductive terrain, maximum anomalies can occur at higher frequencies. Conductivity ranges of some materials are shown in figure 230.

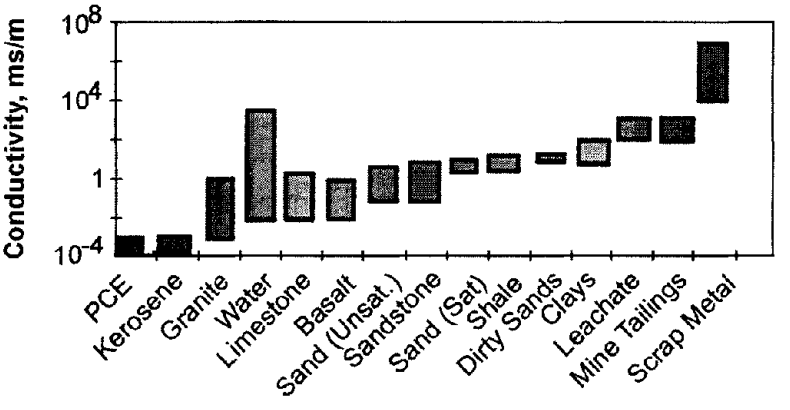

Figure 230. Conductivity ranges of some materials. Note this is a very variable parameter, and the ranges are approximate.

Olhoeft (1986) describes three other active chemical processes that produce smaller but, in some circumstances, important IP and CR anomalies. In clays, ion exchange processes effectively create different mobilities for cations and anions within the pores. This separates or polarizes charge and is usually known as membrane polarization. This effect is much smaller than is observed for disseminated metals, but can be exploited in some cases to distinguish clay and contaminated aquifers, both of which will have a low direct current (DC) resistivity. Olhoeft (1986) also describes some poorly understood polarization effects that occur when organics react with clay minerals. The most promising aspect of this, from the standpoint of detecting organic wastes, is that measurable reduction of the IP response of clays following organic contamination has been recorded. The effect, however, is subtle.

It is usual to talk of complex resistivity instead of complex conductivity, although this is an arbitrary choice. The simplest of complex resistivity units are ohm meters, but measured as a real (ρ') and imaginary (ρ'') part and as a function of frequency. Alternatively, it is convenient to consider the resistivity as having a magnitude $|\rho| = (\rho'^2 + \rho''^2)^{1/2}$ [ohm•meters] and a phase lag or lead $\phi = \tan^{-1}(\rho''/\rho')$ [radians or, more practically, milli-radians].

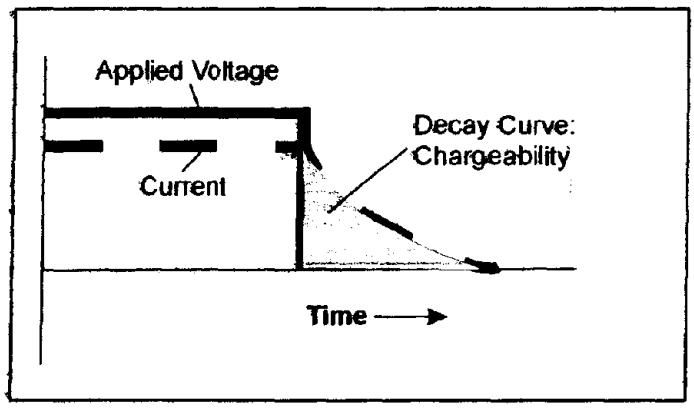

Figure 231. Schematic of decay time associated with complex resistivity, IP.

In IP surveys, the percentage frequency effect PFE is defined as the normalized difference between the resistivity measured at two different frequencies (typically 0.1Hz and 10Hz). A related parameter, the chargeability(m), is measured by systems that record the time delay in current flow following an abrupt interruption or onset of the applied voltage. Chargeability is a measure of the area under the decay curve in figure 231.

Figure 232 shows the CR response of a montmorillonite (clay) soil from the EPA Pittman site near Henderson, Nevada, taken from Olhoeft (1986). One of the two samples (triangles) is contaminated by waste that includes organics. Note the decrease in resistivity with frequency and the presence of a phase peak for both samples, consistent with the theoretical response of Figure 231. The contamination has lowered the resistivity of the second sample - clearly inorganic contaminants dominate - but the shift of the phase peak to lower frequencies is stated by the author to represent peptization, a process whereby organic molecules preferentially attach themselves to the clay surfaces, inhibiting cation exchange.

8.1.4 Dielectric Permittivity ε

Permittivity is conceptually similar to electrical conductivity. It relates charge separation, rather than current, to the applied electric field. Materials that have no free charge carriers such as ions or electrons may still appear to pass current when a voltage is applied. That is, energy will be drawn from the voltage source to move charge.

The charge that moves is bound to the molecules of the material, for example the positive charge on the nucleus and the negative charges of the electron shells. An applied field polarizes the charge distribution with the positive charges moving in one direction and the negative charges moving in the opposite direction. Figure 233 shows a schematic result of applying an electric field to a molecule.

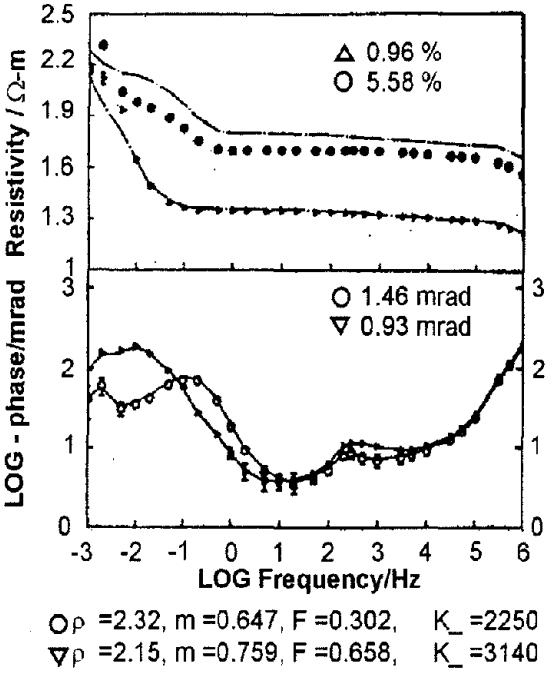

Figure 232. Variation of resistivity (upper) and phase as function of frequency for some montmorillonite clays (from Olhoeft, 1986).

Intrinsic polarization, p, has units of charge•distance per meter^3, or coulombs/m^2. The dielectric permittivity relates polarization to the applied field:

$$p = \varepsilon E, \tag{23}$$

The permittivity is often expressed in terms of the permittivity of free space, ε_0, in terms of the dielectric constant K.

$$\varepsilon = K\varepsilon_0, \tag{24}$$

As the figure 235 shows, K varies from its free space value of 1 to a maximum of 80 for water. K is strongly frequency dependent in parts of the frequency spectrum, and should more properly be portrayed as complex. For our purposes, these aspects can be ignored. For this report, K is considered only at ground penetrating radar (GPR) frequencies, in the range 100 to 1,000 MHz.

Permittivity is the primary factor influencing the speed of electromagnetic radiation in earth materials at GPR frequencies. Contrasts in velocity, in turn, produce reflections of electromagnetic energy within the Earth. Thus, K is the major influence on ground penetrating radar measurements. From equation 23, ε has units of coulombs/(volt-meter) or farads/m. From equation 23, K is dimensionless.

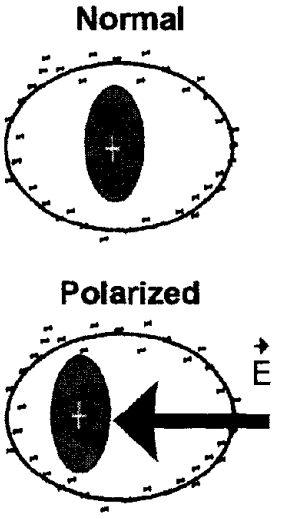

Figure 233. Schematic displacement of charge within a molecule by an electric field E.

8.1.4.1 Velocity of EM Radiation

The speed **V** of electromagnetic waves through a medium of permittivity **ε** and magnetic permeability (see next section) **μ** is:

$$V = (\mu\varepsilon)^{-1/2}, \tag{25}$$

8.1.4.2 Reflection Coefficient

The ratio R of the reflected to incident signal amplitude for an EM signal traveling from medium 1 towards medium 2 is:

$$R = \frac{(K_1^{1/2} - K_2^{1/2})}{(K_1^{1/2} + K_2^{1/2})}, \tag{26}$$

8.1.4.3 Water Content

With a dielectric constant of 80, water dominates the permittivity of rock water mixtures. There does not appear to be one widely accepted model for water-saturated rocks. One model, proposed by Calvert (1987), is:

$$K_f = (1-\phi^2)K_m + \phi^2 K_w, \tag{27}$$

This relationship is plotted in figure 234.

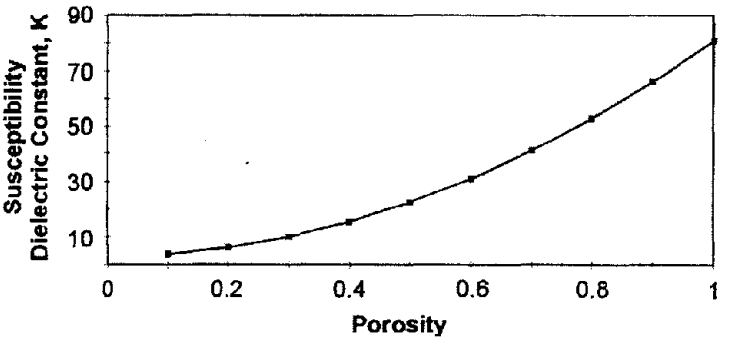

Figure 234. Dielectric constant of a water-saturated rock as a function of porosity ($K_w = 81$; $K_m = 3$).

8.2 MAGNETIC SUSCEPTIBILITY (K)

Magnetic susceptibility is a measure of the ability of a material to be magnetized. The proportional constant links magnetization to the applied magnetic field intensity (at levels below which saturation and hysteresis are important). Magnetic susceptibility, k, is related to magnetic permeability (μ) by:

$$\mu = \mu_0 (1 + k), \tag{28}$$

where μ_0 is the magnetic permeability of free space, which is $4\pi \cdot 10^{-7}$. The most magnetically susceptible materials are called ferromagnetic materials which contain iron, nickel, cobalt and many alloys of these materials. Of the several ferromagnetic minerals, magnetite predominates in the applications addressed here. In waste sites, iron and steel are the major sources of magnetic anomalies.

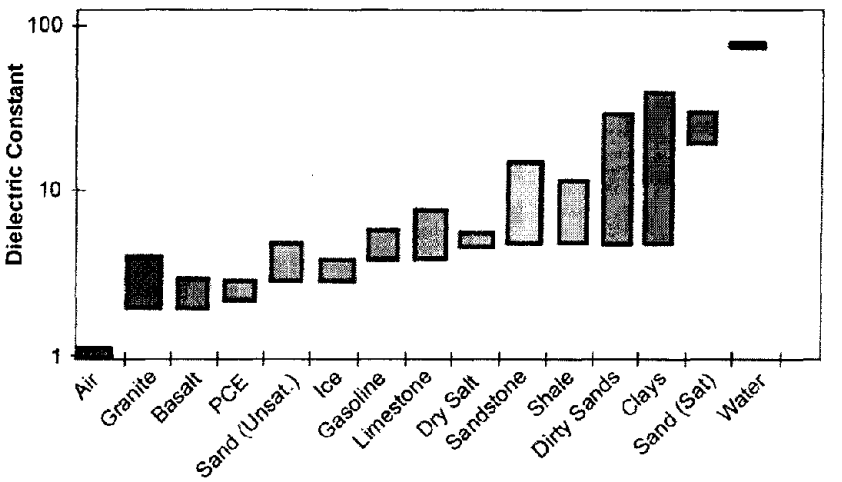

Figure 235. Dielectric constant range for some common materials.

There are several other magnetic quantities, and their relationship is sometimes confusing. The basic magnetic object is the magnetic pole, equivalent to the north end of a magnet.

Magnetic poles (a) do not exist as discrete particles, and (b) always appear to come in pairs, and are, therefore, a dipole. A dipole is the result of electric charge in motion; one is made by passing a current I (amperes) around a circuit of area A (meters). Hence, the dipole strength or magnetic dipole moment, M is a vector perpendicular to the plane of that coil with units of ampere-meter^2.

All matter consists of charge in motion, but for most materials, the resulting dipoles are randomly aligned and cancel. For certain materials, this cancellation is incomplete, and they become magnetic. Magnetization, J, is the density of aligned dipoles per cubic meter, with units (ampere/m).

The earth's geomagnetic field, B, is the origin of most of the magnetization, J, found in rocks, that is, the magnetization is induced by the present Earth's magnetic field. The relationship is:

$$J = B \cdot \left(\frac{k\mu_0}{(1+k)} \right), \tag{29}$$

The exceptions are materials that have a permanent or remnant magnetization, acquired elsewhere in a strong local magnetic field.

We detect magnetic objects in the subsurface by the way their magnetic fields distort the earth's geomagnetic field. These distortions are termed anomalies. It is generally safe to assume that sediments are non-magnetic. Igneous or metamorphic rocks can have appreciable and locally variable susceptibility.

The magnetic moment M of an object, assuming it is uniformly magnetized, can be estimated as:

$$M = JV, \tag{30}$$

where V is the volume of the object.

The unit of magnetic susceptibility, k, in the SI system is dimensionless. Magnetic permeability (μ) has units of Henrys per meter. The geomagnetic field (B) has units of force per magnetic pole or Teslas. The practical unit of geomagnetism is the nano-Tesla, or gamma.

8.2.1 Geomagnetic Field

The geomagnetic field of the earth is very similar to that of a large bar magnet placed at the center of the Earth, with its south end oriented toward the north magnetic pole. The field is dipolar, vertically downward at the north magnetic pole, vertically upward at the south magnetic pole, and horizontal at the (magnetic) equator. It has a strength of roughly 30,000 gammas at the equator, 70,000 gammas at the poles. In the United States, it is acceptable for the purposes of simple modeling to assume that a field declination of about 60 degrees has a strength of 55,000 gammas.

8.2.1.1 Susceptibility and Magnetite

The susceptibility of most rocks can be related to magnetite content reasonably well as follows:

$$k = 12.2 f^{1.2}, \tag{31}$$

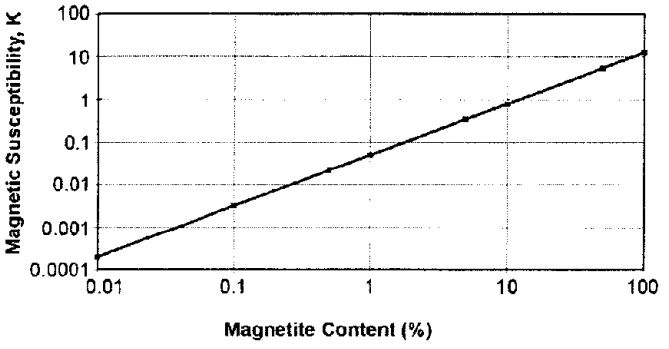

Figure 236. Susceptibility as a function of magnetite content.

where f is the volume percent of magnetite (Grant and West, 1965). A plot of this empirical relationship is shown in figure 236.

8.2.1.2 Magnetization of Soils

Breiner (1973) points out that soils reflect their parentage, and that some, as a result, will be considerably more magnetic than others. Because magnetite tends to concentrate in sediments where streams carrying heavy metals lose velocity, concentrations can be expected in distributing streams, in alluvial fans, in glaciated terrain (particularly eskers, outwash, and beach deposits). In highly organic soils, maghemite, a relatively magnetic form of hematite, can be produced. As a result, the magnetic susceptibility of soils can be laterally variable and, because they are close to the magnetometer, give rise to very localized anomalies of significant magnitude. Figure 237 presents the susceptibility range of common materials.

8.3 DENISTY

Density, σ, is the intrinsic unit mass of a material, defined as the mass of one cubic meter with units of kilograms per cubic meter (kg/m^3). However, the old cgs units of grams-per-cubic-centimeter are still widely used. One gm/cc is equivalent to1,000 kg/m^3.

8.4 POROSITY

Porosity, saturation, and density are related as a function of porosity Φ as:

$$\sigma_f = \sigma_m(1-\phi) + 1000S\phi, \tag{32}$$

in which subscripts f and m refer to the formation and the matrix, respectively, and S is the fractional water saturation. A water density of 1,000 kg/m^3 is assumed. Figure 238 shows the density ranges of common materials.

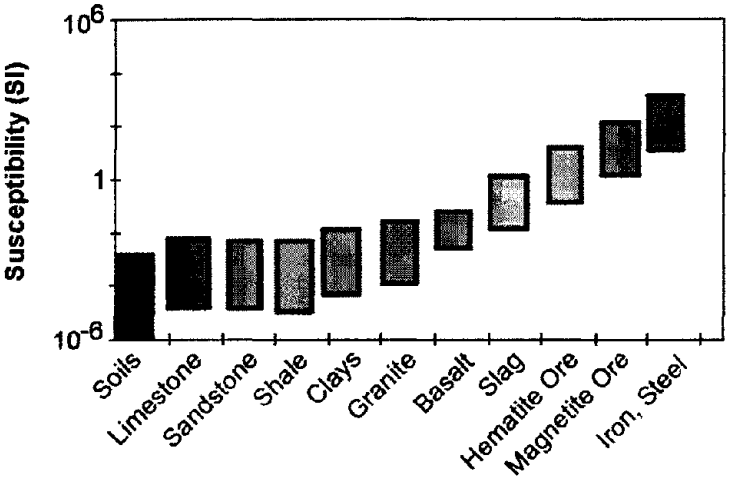

Figure 237. Susceptibility range of common materials.

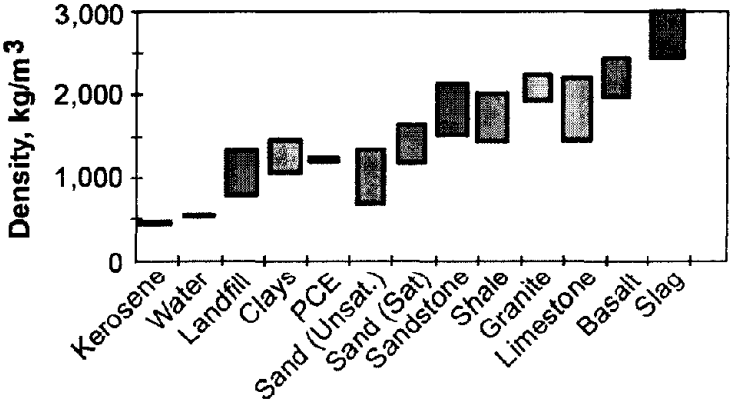

Figure 238. Density ranges in common materials.

8.5 SEISMIC VELOCITIES (VS, VP)

If the ground is stressed by an explosion or a hammer blow, it generates three fundamental types of elastic waves: **P** (primary, push-pull) waves; **S** (secondary, shear) waves, and **surface** waves. The P and S waves propagate through the body of the earth; the surface waves can exist only close to the free surface.

Only P and S are discussed in this section. P waves are characterized by having a particle motion in the direction of propagation, whereas S waves have particle motion transverse to

the direction of propagation. P waves are the faster of the two, with velocities typically 50% higher than those for associated S waves. The wave velocities $\mathbf{V_p}$ and $\mathbf{V_s}$ are related to the elastic moduli (Young's modulus (E), Poisson's ratio (ν), and Bulk modulus (k)) and the density ρ as follows.

$$V_p^2 = (1.331 + m)/s, \quad Vs^2 = m/s \tag{33}$$

Since liquids have no shear rigidity, shear waves cannot propagate through them. Velocities have SI units of meters per second, sometimes also expressed as kilometers per second or meters per millisecond.

The P-wave velocity of a water/competent rock mixture obeys the following relationship (Wyllie's Equation) reasonably well up to porosities of 0.35.

$$S_f = \phi S_w + (1-\phi) S_m, \tag{34}$$

where S is the slowness (1/V), and subscripts f ,w, and m stand for formation, water, and matrix, respectively. Assuming a matrix Vp of 5,950 m/sec for sandstone, and a water velocity of 1,500 m/sec we get the porosity dependence shown in figure 239.

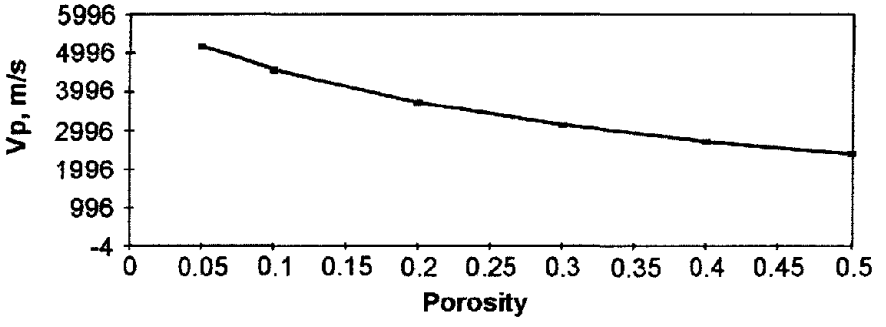

Figure 239. P-wave velocities as a function of porosity. Valid for competent rock only. Overestimates velocity for soft sediments.

8.6 REFLECTIVITY

The cause of seismic reflections is contrasts in the seismic impedance (**ρV**) across a boundary (ρ is the density of the rock). In particular, for waves at normal incidence, the ratio R of reflected-to-incident amplitude is given by:

$$R = \frac{(\rho_2 V_2 - \rho_1 V_1)}{(\rho_2 V_2 + \rho_1 V_1)}, \tag{35}$$

8.7 GEOMECHANICAL (ENGINEERING) PROPERTIES

Seismic velocities can be related to standard geotechnical properties. For example, Poisson's ratio ν can be found from:

$$\left(\frac{V_s}{V_p}\right)^2 = \frac{(0.5-\nu)}{(1-\nu)}, \tag{36}$$

Figures 240 and 241 show the S and P wave velocities of seismic waves for a number of different rock types.

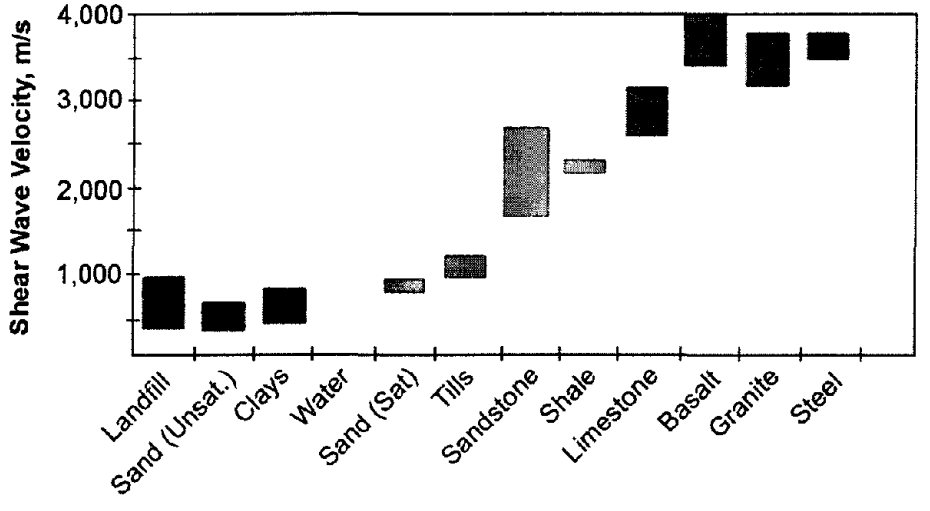

Figure 240. S-wave velocity ranges for common materials.

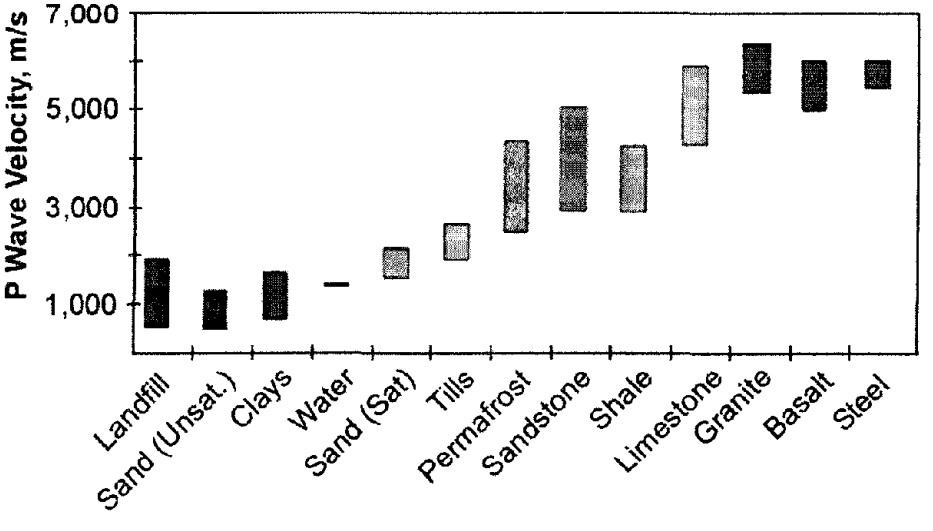

Figure 241. P wave velocity ranges for common materials.

CHAPTER 9 SURFACE GEOPHYSICAL METHODS

This chapter is substantially based on a report produced by the US Army Corps of Engineers titled Geophysical Exploration for Engineering and Environmental Investigations, 1995, Report number EM1110-1-1802.

9.1 POTENTIAL FIELD METHODS

9.1.1 Magnetic Methods

Basic Concepts

The Earth possesses a magnetic field caused primarily by sources in the core. The form of the field is roughly the same as would be caused by a dipole or bar magnet located near the Earth's center and aligned sub parallel to the geographic axis. The intensity of the Earth's field is customarily expressed in S.I. units as nanoteslas (nT) or in an older unit, gamma (γ): $1\ \gamma = 1\ \text{nT} = 10^{-3}\ \mu\text{T}$. Except for local perturbations, the intensity of the Earth's field varies between about 25 and 80 μT over the conterminous United States.

Many rocks and minerals are weakly magnetic or are magnetized by induction in the Earth's field, and cause spatial perturbations or "anomalies" in the Earth's main field. Man-made objects containing iron or steel are often highly magnetized and locally can cause large anomalies up to several thousands of nT. Magnetic methods are generally used to map the location and size of ferrous objects. Determination of the applicability of the magnetics method should be done by an experienced engineering geophysicist. Modeling and incorporation of auxiliary information may be necessary to produce an adequate work plan.

Theory

The Earth's magnetic field dominates most magnetic measurements made at or near the surface of the Earth. The Earth's total field intensity varies considerably by location over the surface of the Earth. Most materials except for permanent magnets, exhibit an induced magnetic field due to the behavior of the material when the material is in a strong field such as the Earth's. Induced magnetization (sometimes called magnetic polarization) refers to the action of the field on the material wherein the ambient field is enhanced causing the material itself to act as a magnet. The field caused by such a material is directly proportional to the intensity of the ambient field and to the ability of the material to enhance the local field--a property called magnetic susceptibility. The induced magnetization is equal to the product of the volume magnetic susceptibility and the inducing field of the Earth:

$$I = kF, \tag{37}$$

where

k = volume magnetic susceptibility (unitless),

I = induced magnetization per unit volume,

F = field intensity in tesla (T).

For most materials, k is much less than 1 and, in fact, is usually of the order of 10^{-6} for most rock materials. The most important exception is magnetite whose susceptibility is about 0.3. From a geologic standpoint, magnetite and its distribution determine the magnetic properties of most rocks. There are other important magnetic minerals in mining prospecting, but the amount and form of magnetite within a rock determines how most rocks respond to an inducing field. Iron, steel, and other ferromagnetic alloys have susceptibilities one to several orders of magnitude larger than magnetite. The exception is stainless steel, which has a small susceptibility.

The importance of magnetite cannot be exaggerated. Some tests on rock materials have shown that a rock containing 1% magnetite may have a susceptibility as large as 10^{-3}, or 1,000 times larger than most rock materials. Table 13 provides some typical values for rock materials. Note that the range of values given for each sample generally depends on the amount of magnetite in the rock.

Table 13. Approximate magnetic susceptibility of representative rock types.

Rock Type	Susceptibility (k)
Altered ultra basics	10^{-4} to 10^{-2}
Basalt	10^{-4}
Gabbro	10^{-4} to 10^{-3}
Granite	10^{-5} to 10^{-3}
Andesite	10^{-4}
Rhyolite	10^{-5} to 10^{-4}
Metamorphic rocks	10^{-4} to 10^{-6}
Most sedimentary rocks	10^{-6} to 10^{-5}
Limestone and chert	10^{-6}
Shale	10^{-5} to 10^{-4}

Thus, it can be seen that in most engineering and environmental scale investigations, the sedimentary and alluvial sections will not show sufficient contrast such that magnetic measurements will be of use in mapping the geology. However, the presence of ferrous materials in ordinary municipal trash and in most industrial waste does allow the magnetometer to be effective in direct detection of landfills. Other ferrous objects, which may be detected, include pipelines, underground storage tanks, and some ordnance.

Data Acquisition

Ground magnetic measurements are usually made with portable instruments at regular intervals along more or less straight and parallel lines that cover the survey area. Often the interval between measurement locations (stations) along the lines is less than the spacing between lines.

The magnetometer is a sensitive instrument that is used to map spatial variations in the Earth's magnetic field. In the proton magnetometer, a magnetic field that is not parallel to the Earth's field is applied to a fluid rich in protons causing them to partly align with this artificial field. When the controlled field is removed, the protons tend to return to its original

direction in the earth's magnetic field by precessing around the Earth's field at a frequency depending on the intensity of the Earth's field. By measuring this precession frequency, the total intensity of the field can be determined. The physical basis for several other magnetometers, such as the cesium or rubidium-vapor magnetometers, is similarly founded in a fundamental physical constant. The optically pumped magnetometers have increased sensitivity and shorter cycle times (as small as 0.04 s), making them particularly useful in airborne applications.

The incorporation of computers and non-volatile memory in magnetometers has greatly increased their ease of use and data handling capability. The instruments typically will keep track of position, prompt for inputs, and internally store the data for an entire day of work. Downloading the information to a personal computer is straightforward, and plots of the day's work can be prepared each night.

To make accurate anomaly maps, temporal changes in the Earth's field during the period of the survey must be considered. Normal changes during a day, sometimes called diurnal drift, are a few tens of nT, but changes of hundreds or thousands of nT may occur over a few hours during magnetic storms. During severe magnetic storms, which occur infrequently, magnetic surveys should not be made. The correction for diurnal drift can be made by repeat measurements of a base station at frequent intervals. The measurements at field stations are then corrected for temporal variations by assuming a linear change of the field between repeat base station readings. Continuously recording magnetometers can also be used at fixed base sites to monitor the temporal changes. If time is accurately recorded at both base site and field location, the field data can be corrected by subtraction of the variations at the base site.

The base-station memory magnetometer, when used, is set up every day prior to collection of the magnetic data. Ideally the base station is placed at least 100 m from any large metal objects or traveled roads and at least 500 m from any power lines when feasible. The base station location must be very well described in the field book, as others may have to later locate it based on the written description.

Some QC/QA procedures require that several field-type stations be occupied at the start and end of each day's work. This procedure indicates that the instrument is operating consistently. Where it is important to be able to reproduce the actual measurements on a site exactly (such as in certain forensic matters), an additional procedure is required. The value of the magnetic field at the base station must be asserted (usually a value close to its reading on the first day) and each day's data corrected for the difference between the asserted value and the base value read at the beginning of the day. As the base may vary by 10 to 25 nT or more from day to day, this correction ensures that another person using the same base station and the same asserted value will get the same readings at a field point to within the accuracy of the instrument. This procedure is always good technique but is often neglected by persons interested in only very large anomalies (> 500 nT, etc.).

Intense fields from man-made electromagnetic sources can be a problem in magnetic surveys. Most magnetometers are designed to operate in fairly intense 60-Hz and radio frequency fields. However, extremely low frequency fields caused by equipment using direct

current or the switching of large alternating currents can be a problem. Pipelines carrying direct current for cathodic protection can be particularly troublesome. Although some modern ground magnetometers have a sensitivity of 0.1 nT, sources of cultural and geologic noise usually prevent full use of this sensitivity in ground measurements.

After all corrections have been made, magnetic survey data are usually displayed as individual profiles or as contour maps. Identification of anomalies caused by cultural features, such as railroads, pipelines, and bridges is commonly made using field observations and maps showing such features. For some purposes, a close approximation of the gradient of the field is determined by measuring the difference in the total field between two closely spaced sensors. The quantity measured most commonly is the vertical gradient of the total field.

The magnetometer is operated by a single person. However, grid layout, surveying, or the buddy system may require the use of another technician. If two magnetometers are available, production is usually doubled as the ordinary operation of the instrument itself is straightforward.

Distortion

Steel and other ferrous metals in the vicinity of a magnetometer can distort the data. Large belt buckles, etc., must be removed when operating the unit. A compass should be more than 3 m away from the magnetometer when measuring the field. A final test is to immobilize the magnetometer and take readings while the operator moves around the sensor. If the readings do not change by more than 1 or 2 nT, the operator is "magnetically clean." Zippers, watches, eyeglass frames, boot grommets, room keys, and mechanical pencils can all contain steel or iron. On very precise surveys, the operator effect must be held under 1 nT.

To obtain a representative reading, the sensor should be operated well above the ground. This procedure is done because of the probability of collections of soil magnetite disturbing the reading near the ground. In rocky terrain where the rocks have some percentage of magnetite, sensor heights of up to 4 m have been used to remove near-surface effects. One obvious exception to this is some types of ordnance detection where the objective is to detect near-surface objects. Often a rapid-reading magnetometer is used (cycle time less than 1/4 s) and the magnetometer is used to sweep across an area near the ground. Small ferrous objects can be detected, and spurious collections of soil magnetite can be recognized by their lower amplitude and dispersion. Ordnance detection requires not only training in the recognition of dangerous objects, but also experience in separating small, intense, and interesting anomalies from more dispersed geologic noise.

Data recording methods will vary with the purpose of the survey and the amount of noise present. Methods include taking three readings and averaging the results, taking three readings within a meter of the station and either recording each or recording the average. Some magnetometers can apply either of these methods and even do the averaging internally. An experienced field geophysicist will specify which technique is required for a given survey. In either case, the time of the reading is also recorded unless the magnetometer stores the readings and times internally.

Sheet-metal barns, power lines, and other potentially magnetic objects will occasionally be encountered during a magnetic survey. When taking a magnetic reading in the vicinity of such items, describe the interfering object and note the distance from it to the magnetic station in your field book.

Items to be recorded in the field book for magnetics include:

a) Station location, including locations of lines with respect to permanent landmarks or surveyed points.

b) Magnetic field and/or gradient reading.

c) Time.

d) Nearby sources of potential interference.

The experienced magnetics operator will be alert for the possible occurrence of the following:

1. Excessive gradients may be beyond the magnetometer's ability to make a stable measurement. Modern magnetometers give a quality factor for the reading. Multiple measurements at a station, minor adjustments of the station location and other adjustments of technique may be necessary to produce repeatable, representative data.

2. Nearby metal objects may cause interference. Some items, such as automobiles, are obvious, but some subtle interference will be recognized only by the imaginative and observant magnetics operator. Old buried curbs and foundations, buried cans and bottles, power lines, fences, and other hidden factors can greatly affect magnetic readings.

Data Processing and Interpretation

Total magnetic disturbances or anomalies are highly variable in shape and amplitude; they are almost always asymmetrical, sometimes appear complex even from simple sources, and usually portray the combined effects of several sources. An infinite number of possible sources can produce a given anomaly, giving rise to the term ambiguity.

One confusing issue is the fact that most magnetometers used measure the total field of the Earth: no oriented system is recorded for the total field amplitude. The consequence of this fact is that only the component of an anomalous field in the direction of Earth's main field is measured. Figure 242 illustrates this consequence of the measurement system. Anomalous fields that are approximately perpendicular to the Earth's field are undetectable.

Additionally, the induced nature of the measured field makes even large bodies act as dipoles, that is, like a large bar magnet. If the (usual) dipolar nature of the anomalous field is combined with the measurement system that measures only the component in the direction of the Earth's field, the confusing nature of most magnetic interpretations can be appreciated.

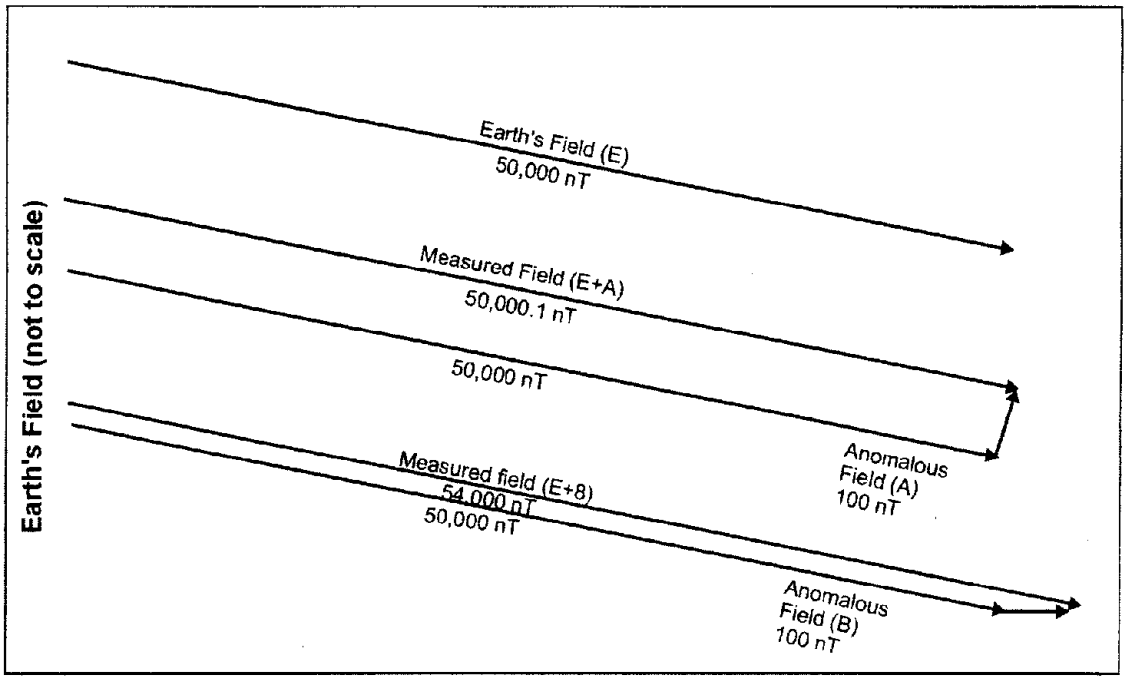

Figure 242. Magnetic field vector examples for two anomalous fields.

To achieve a qualitative understanding of what is occurring, consider figure 243. Within the contiguous United States, the magnetic inclination, that is the angle the main field makes with the surface, varies from 55 to 70 degrees. The figure illustrates the field associated with the main field, the anomalous field induced in a narrow body oriented parallel to that field, and the combined field that will be measured by the total-field magnetometer. The scalar values that would be measured on the surface above the body are listed. From this figure, one can see how the total-field magnetometer records only the components of the anomalous field.

9.1.2 Gravity Methods

Basic Concept

Lateral density changes in the subsurface cause a change in the force of gravity at the surface. The intensity of the force of gravity due to a buried mass difference (concentration or void) is superimposed on the larger force of gravity due to the total mass of the earth. Thus, two components of gravity forces are measured at the Earth's surface: first, a general and relatively uniform component due to the total earth, and second, a component of much smaller size that varies due to lateral density changes (the gravity anomaly). By very precise measurement of gravity and by careful correction for variations in the larger component due to the whole Earth, a gravity survey can sometimes detect natural or man-made voids, variations in the depth to bedrock, and geologic structures of engineering interest.

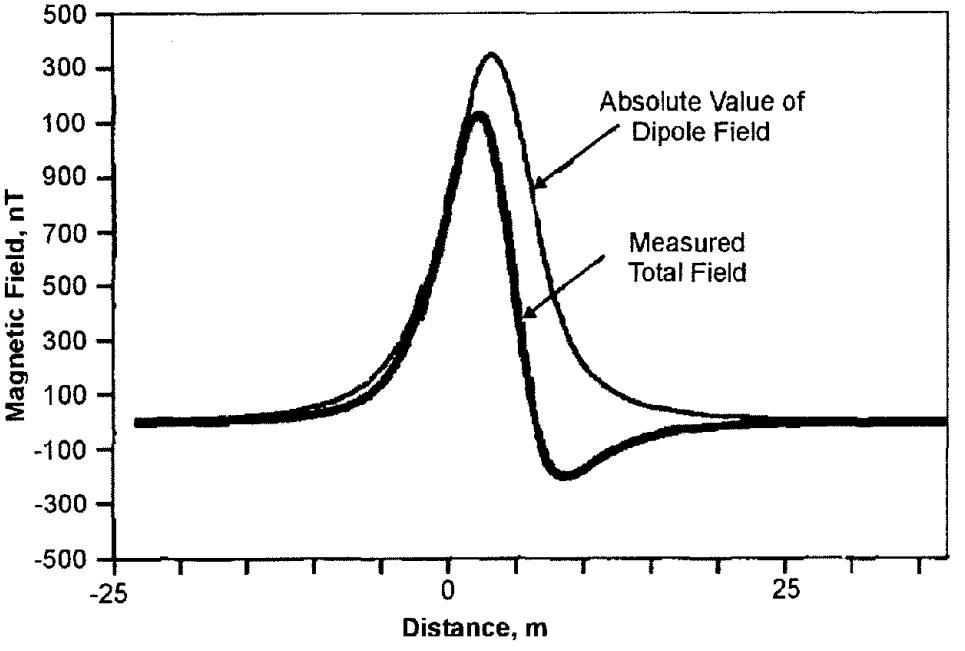

Figure 243. Actual and measured fields due to magnetic inclination.

For engineering and environmental applications, the scale of the problem is generally small (targets are often from 1 to 10 m in size). Therefore, conventional gravity measurements, such as those made in petroleum exploration, are inadequate. Station spacings are typically in the range of 1 to 10 m. Even a new name, microgravity, was invented to describe the work. Microgravity requires preserving all of the precision possible in the measurements and analysis so that small objects can be detected.

The interpretation of a gravity survey is limited by ambiguity and the assumption of homogeneity. A distribution of small masses at a shallow depth can produce the same effect as a large mass at depth. External control of the density contrast or the specific geometry is required to resolve ambiguity questions. This external control may be in the form of geologic plausibility, drill-hole information, or measured densities.

The first question to ask when considering a gravity survey is for the current subsurface model, can the resultant gravity anomaly be detected? To answer this question the information required are the probable geometry of the anomalous region, its depth of burial, and its density contrast. A general rule of thumb is that a body must be almost as big as it is deep. To explore this question, figure 244 was prepared. The body under consideration is a sphere. The vertical axis is normalized to the attraction of a sphere whose center is at a depth equal to its diameter. For illustration, the plotted values give the actual gravity values for a sphere 10 m in diameter with a 1,000 kg/m^3 (1.0 g/cc) density contrast. The horizontal axis is the ratio of depth to diameter. The rapid decrease in value with depth of burial is evident. At a ratio of depth to diameter greater than 2.0, the example sphere falls below the practical noise level for most surveys as will be discussed below.

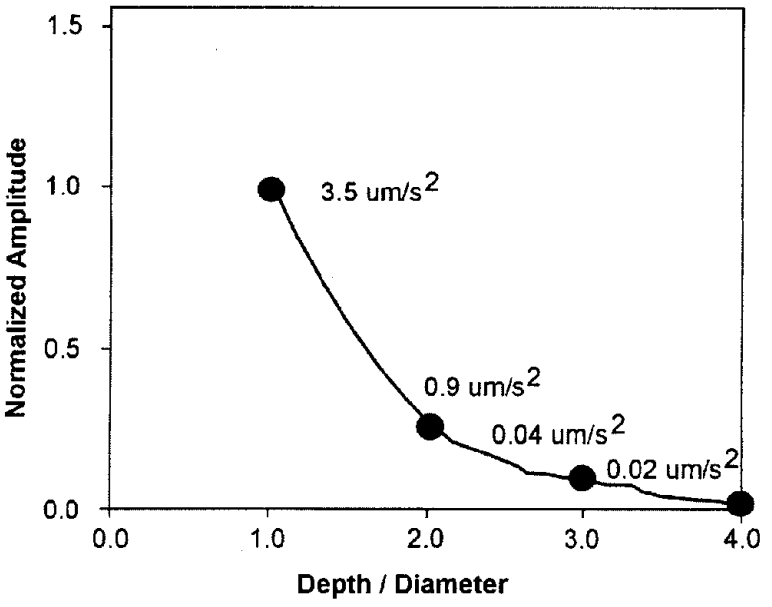

Figure 244. Normalized peak vertical attraction versus depth to diameter for a spherical body. Values are for a 10-m sphere with a 1.0 g/cc density contrast.

A second rule of thumb is that unless you are very close to the body, its exact shape is not important. Thus, a rectangular-shaped horizontal tunnel sometimes can be modeled by a horizontal circular cylinder, and a horizontal cylinder sometimes can be modeled by a horizontal line source. Odd-shaped volumes can be modeled by disks, and where close to the surface, even infinite or semi-infinite slabs.

Among the many useful nomograms and charts that are available, Figure 245 (which is adapted from Arzi, 1975) is very practical. The gravity anomaly is linear with density contrast so other density contrasts can be evaluated by scaling the given curves. For cylinders of finite length, very little correction is needed unless the cylinder length is less than four times its width. Nettleton (1971) gives the correction formula for finite length of cylinders. Another useful simple formula is the one for an infinite slab. This formula is:

$$A_z = 2\pi G t \Delta p_b, \tag{38}$$

where

A_z = vertical attraction, $\frac{\mu m}{s^2}\left(1\frac{\mu m}{s^2} = 10^{-6}\frac{m}{s^2} = 10^{-4}\frac{cm}{s^2} = 10^{-4}\,gal = 10^{2}\,\mu gal\right)$,

G = gravitational constant, $0.668x10^{-4}\left(\frac{m^3}{kg - s^2}\right)10^{-6}$,

T = thickness, m,

Δp_b = density contrast, $\frac{kg}{m}$.

As an example, consider a 1-m-thick sheet with a density contrast with its surroundings twice that of water. From equation 38, the calculation would be $Az = 2\pi\ (0.668x10^{-4})(1.0)(2{,}000)$ $\mu m/s^2 = 0.84\ \mu m/s^2$.

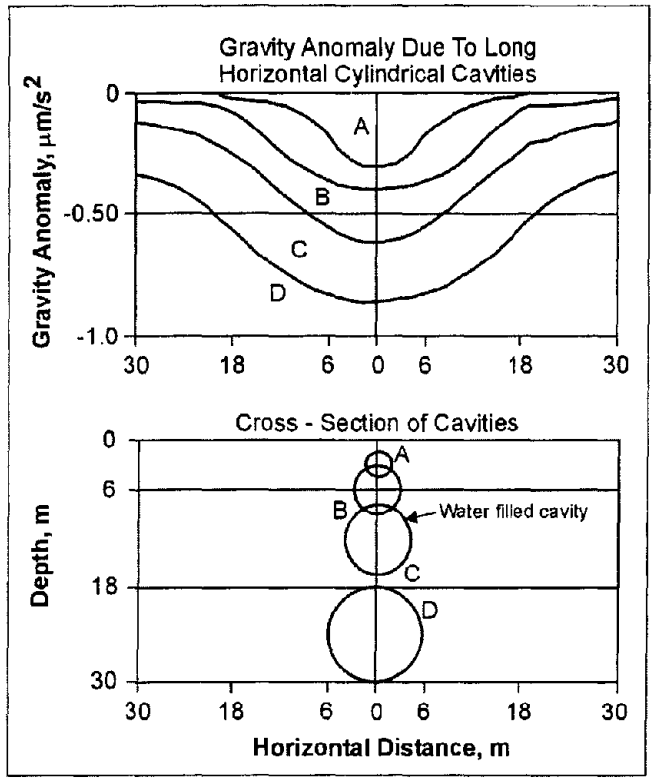

Figure 245. Gravity anomalies for long horizontal cylindrical cavities as a function of depth, size, and distance from peak.

A surprising result from potential theory is that there is no distance term in this formula. The intuitive objections can be quelled by focusing on the fact that the slab is infinite in all directions. The usefulness of this formula increases if one recognizes that the attraction of a semi-infinite slab is given by one-half of the above formula at the edge of the slab. Thus, near the edge of a fault or slab-like body, the anomaly will change from zero far away from the body to ($2\pi G t \Delta p_b$) at a point over the body and far away from the edge (above the edge the value is $G\pi t \Delta p_b$). This simple formula can be used to quickly estimate the maximum response from a slab-type anomaly. If the maximum due to the infinite sheet is not detectable, then complicated calculations with finite bodies are not justified. Nettleton (1971) is a good source of formulas that can be used to approximate actual mass distributions.

Items that should not be overlooked in estimating the probable density contrast are:

1. Variability (1,000 to 3,500 kg/m^3) of the density of rocks and soils.
2. Possibility of fractures and weathering in rocks.
3. Probability of water filling in voids.

Each of these items should be individually considered before a density contrast is set. The effects of upward-propagating fractures, which can move a mass deficiency nearer the surface, and the presence or absence of air pockets usually cannot be evaluated if one is after subsurface mass deficiencies. However, these effects will increase the amplitude of the anomaly, sometimes by a factor of two or more.

Data Acquisition

Usually more important in a feasibility study than the anomaly evaluation is the estimation of the noise sources expected. This section will discuss the larger contributions to noise and evaluate each.

Modern gravimeters have a least-significant scale reading of 0.01 $\mu m/s^2$. However, repeated readings including moving the meter, releveling, and unclamping the beam several times indicate an irreducible meter reading error of about 0.05 $\mu m/s^2$. New electronically augmented versions of these gravimeters consistently repeat to 0.02 to 0.03 $\mu m/s^2$. Some surveys may do slightly better, but one should be prepared to do worse. Factors that may significantly increase this type of error are soft footing for the gravimeter plate (surveys have been done on snow), wind, and ground movement (trucks, etc.) in the frequency range of the gravimeter. Again, the special versions of these gravimeters that filter the data appropriately can compensate for some of these effects. A pessimist, with all of the above factors in action, may allow 0.08 to 0.1 $\mu m/s^2$ for reading error.

Gravity measurements, even at a single location, change with time due to Earth tides, meter drift, and tares. These time variations can be dealt with by good field procedure. The Earth tide may cause changes of 2.4 $\mu m/s^2$ in the worst case, but it has period of about 12.5 hours; it is well approximated as a straight line over intervals of 1 to 2 hours, or it can be calculated and removed. Drift is also well eliminated by linear correction. Detection of tares and blunders (human inattention) is also a matter of good field technique and repeated readings. One might ascribe 10 to 20 nm/s^2 to these error sources.

Up to 50% of the work in a microgravity survey is consumed by the survey. For the very precise work described above, relative elevations for all stations need to be established to +/- 1 to 2 cm. A firmly fixed stake or mark should be used to allow the gravity meter reader to recover the exact elevation. Position in plan is less critical, but relative position to 50-100 cm or 10 percent of the station spacing (whichever is smaller) is usually sufficient. Satellite surveying, GPS, can achieve the required accuracy, especially the vertical accuracy, only with the best equipment under ideal conditions.

High station densities are often required. It is not unusual for intervals of 1-3 m to be required to map anomalous masses whose maximum dimension is 10 m. Because the number of stations in a grid goes up as the square of the number of stations on one side, profiles are often used where the attitude of the longest dimension of the sought body can be established before the survey begins.

After elevation and position surveying, actual measurement of the gravity readings is often accomplished by one person in areas where solo work is allowed. Because of short-term variations in gravimeter readings caused by less than perfect elasticity of the moving parts of

the suspension, by uncompensated environmental effects, and by the human operator, it is necessary to improve the precision of the station readings by repetition. The most commonly used survey technique is to choose one of the stations as a base and to reoccupy that base periodically throughout the working day. The observed base station gravity readings are then plotted versus time, and a line is fitted to them to provide time rates of drift for the correction of the remainder of the observations. Typically, eight to ten measurements can be made between base station occupations; the time between base readings should be on the order of 1-2 hr. Where higher precision is required, each station must be reoccupied at least once during the survey.

If even higher precision is desired or if instrumental drift is large in comparison with the expected gravity anomaly, then a leapfrogging of stations can be used. For example, if the stations are in an order given by a,b,c,d,e,f,. then the station occupations might be in the sequence ab, abc, abcd, bcde, cdef, defg, etc. In this way, each station would be occupied four times. Numerical adjustments, such as least squares minimization of deviations, may be applied to reoccupation data sets. This procedure allows data quality to be monitored and controlled and distributes any systematic errors throughout the grid.

If base reoccupations are done approximately every hour, known errors such as the earth tide are well approximated by the removal of a drift correction that is linear with time. Even if the theoretical earth tide is calculated and removed, any residual effects are removed along with instrumental drift by frequent base station reoccupation.

Data Processing

Four main corrections are made to gravity data:

1. International Gravity formula accounts for the variation of gravity with latitude.

2. The Free Air correction accounts for the change of gravity for the distance of the station above a datum (sea level) and the station at an elevation Δh.

3. The Bouguer correction accounts for the attraction of the rock material between a datum level and the station at an elevation Δh.

4. Topographic corrections account for all the materialshigher than the gravity stations and removes the effect of the material needed to fill in any hollow below the station.

Details of the free air, Bouguer slab, and terrain corrections will not be expressed here (see Blizkovsky, 1979), but the formula will be given.

The International Gravity formula or variation of gravity with latitude is given by:

$$g = 9.780318\frac{\mathrm{m}}{\mathrm{s}^2}(1 + 0.0053024\sin^2\phi - 0.0000059\sin^2\phi), \qquad (39)$$

where

g = acceleration of gravity in m/s^2,
ϕ = latitude in degrees.

Calculations show that if the stations at which gravity are collected are located with less than 0.5 to 1.0 m of error, the error in the latitude variation is negligible. In fact, for surveys of less than 100 m north to south, this variation is often considered part of the regional and removed in the interpretation step. Where larger surveys are considered, the above formula gives the appropriate correction.

The free-air and the Bouguer slab are corrected to a datum by the following formula (the datum is an arbitrary plane of constant elevation to which all the measurements are referenced):

$$G_s = G_{obs}[1 + (3.086 - 0.000421\Delta p_b)\Delta h], \quad (40)$$

where

G_s = simple Bouguer corrected gravity value measured in $\mu m/s^2$,
G_{OBS} = observed gravity value in $\mu m/s^2$,
Δp_b = near-surface density of the rock in kg/m^3,
Δh = elevation difference between the station and datum in meters.

If these formulas were analyzed, see that the elevation correction is about 20 nm/s^2 per cm. It is impractical in the field to require better than ≅1 to 1.5 cm leveling across a large site, so 30 to 40 nm/s^2 of error is possible due to uncertainty in the relative height of the stations and the meter at each station.

The formula for free air and Bouguer corrections contains a surface density value in the formulas. If this value is uncertain by ±10 percent, its multiplication times Δh can lead to error. Obviously, the size of the error depends on Δh, the amount of altitude change necessary to bring all stations to a common level. The size of the Δh for each station is dependent on surface topography. For a topographic variation of 1 m (a very flat site!), the 10% error in the near-surface density corresponds to ±60 nm/s^2. For a ±10-m site, the error is ±0.6 $\mu m/s^2$. All of these estimates are based on a mistaken estimate of the near-surface-density, not the point-to-point variability in density, which also may add to the error term.

The terrain effect (basically due to undulations in the surface near the station) has two components of error. One error is based on the estimate of the amount of material present above and absent below an assumed flat surface through the station. This estimate must be made quite accurately near the station; farther away some approximation is possible. In addition to the creation of the geometric model, a density estimate is also necessary for terrain correction. The general size of the terrain corrections for stations on a near flat (±3-m) site, the size of tens of acres might be 1 $\mu m/s^2$. A 10% error in the density and the terrain model might produce ±0.1 $\mu m/s^2$ of error. This estimate does not include terrain density variations. Even if known, such variations are difficult to apply as corrections.

To summarize, a site unsuited for microgravity work (which contains variable surface topography and variable near-surface densities) might produce 0.25 to 0.86 $\mu m/s^2$ of difficult-to-reduce error.

Rock Properties. Values for the density of shallow materials are determined from laboratory tests of boring and bag samples. Density estimates may also be obtained from geophysical well logging. Table 14 lists the densities of representative rocks. Densities of a specific rock type on a specific site will not have more than a few percent variability as a rule (vuggy limestones being one exception). However, unconsolidated materials such as alluvium and stream channel materials may have significant variation in density.

Once the basic latitude, free-air, Bouguer and terrain corrections are made, an important step in the analysis remains. This step, called regional-residual separation, is one of the most critical. In most surveys, and in particular those engineering applications in which very small anomalies are of greatest interest, there are gravity anomaly trends of many sizes. The larger sized anomalies will tend to behave as regional variations, and the desired smaller magnitude local anomalies will be superimposed on them. A simple method of separating residual anomalies from microregional variations is simply to visually smooth contour lines or profiles and subtract this smoother representation from the reduced data. The remainder will be a residual anomaly representation. However, this method can sometimes produce misleading or erroneous results.

Several automatic versions of this smoothing procedure are available including polynomial surface fitting and band-pass filtering. The process requires considerable judgment and, whichever method is used, should be applied by an experienced interpreter.

Note that certain unavoidable errors in the reduction steps may be removed by this process. Any error that is slowly varying over the entire site, such a distant terrain or erroneous density estimates, may be partially compensated by this step. The objective is to isolate the anomalies of interest. Small wavelength (about 10 m) anomalies may be riding on equally anomalous measurements with wavelengths of 100 or 1,000 m. The scale of the problem guides the regional-residual separation.

Data Interpretation

Software packages for the interpretation of gravity data are plentiful and powerful. The ease of use as determined by the user interface may be the most important part of any package. The usual inputs are the residual gravity values along a profile or traverse. The traverse may be selected from a grid of values along an orientation perpendicular to the strike of the suspected anomalous body. Some of the programs allow one additional chance for residual isolation. The interpreter then constructs a subsurface polygonal-shaped model and assigns a density contrast to it. When the trial body has been drawn, the computer calculates the gravity effect of the trial body and shows a graphical display of the observed data, the calculated data due to the trial body, and often the difference. The geophysicist can then begin varying parameters in order to bring the calculated and observed values closer together.

Table 14. Density approximations for representative rock types.

Rock Type	Number of Samples	Density	
		Mean (kg/m^3)	Range (kg/m^3)
Igneous Rocks			
Granite	155	2,667	2,516-2,509
Gramodlortle	11	2,716	2,665-2785
Syenite	24	2,757	2,630-2,599
Quartz Diorite	21	2,805	2,680-2,960
Diorite	13	2,839	2,721-2,960
Gabbra (olvine)	27	2,976	2,850-3,120
Diabase	40	2,965	2,804-3,110
Peridotite	3	3,234	3,152-3,276
Dunite	15	3,277	3,204-3,314
Pyroxente	8	3,231	3,100-3,318
Amorthosite	12	2,734	2,640-2,920
Rhyolite obsidian	15	2,370	2,330-2,413
Basalt glass	11	2,772	2,704-2,851
Sedimentary Rock			
Sandstone			
St. Peter	12	2,500	
Bradford	297	2,400	
Berea	18	2,390	
Cretanceous, Wyo	38	2,320	
Limestone			
Glen Rose	10	2,370	
Black River	11	2,720	
Ellenberger	57	2,750	
Dolomite			
Beckrnantown	56	2,800	
Niagara	14	2,770	
Marl (Green River)	11	2,260	
Shale			
Pennsylvania		2,420	
Cretanceous	9	2,170	
Silt (loess)	3	1,610	
Sand			
Fine	54	1,930	
Very fine	15	1,920	
Silt-sand-clay			
Hudson River	3	1,440	
Metamorphic Rocks			
Gneiss (Vermont)	7	2,690	2,880-2,730
Granite Gneiss			
Austria	19	2,610	2,590-2,630
Gneiss (New York)	25	2,540	2,700-3,060
Schists			
Quartz-mica	76	2,820	2,700-2,960
Muscovite-blotite	32	2,760	
Chlorite-sericite	50	2,820	2,730-3,030
Slate (Taconic)	17	2,810	2,710-2,840
Amphibolite	13	2,990	2,790-3,140

Parameters usually available for variation are the vertices of the polygon, the length of the body perpendicular to the traverse, and the density contrast. Most programs also allow multiple bodies.

Because recalculation is done quickly (many programs work instantaneously as far as humans are concerned), the interpreter can rapidly vary the parameters until an acceptable fit is achieved. Additionally, the effects of density variations can be explored and the impact of ambiguity evaluated.

Case Study

Two examples were prepared to illustrate the practical results of the above theoretical evaluations. The geologic section modeled is a coal bed of density 2,000 kg/m^3 and 2 m thickness. This bed, 9 m below the surface, is surrounded by country rock of density 2,200 kg/m^3. A water-filled cutout 25 m long and an air-filled cutout 12 m long are present. The cutouts are assumed infinite perpendicular to the cross-section shown at the bottom of figure 246. The top of figure 246 illustrates the theoretical gravity curve over this geologic section. The middle curve is a simulation of a measured field curve. Twenty-two hundredths of a $\mu m/s^2$ of random noise have been added to the values from the top curve as an illustration of the effect of various error sources. The anomalies are visible, but quantitative separation from the noise might be difficult.

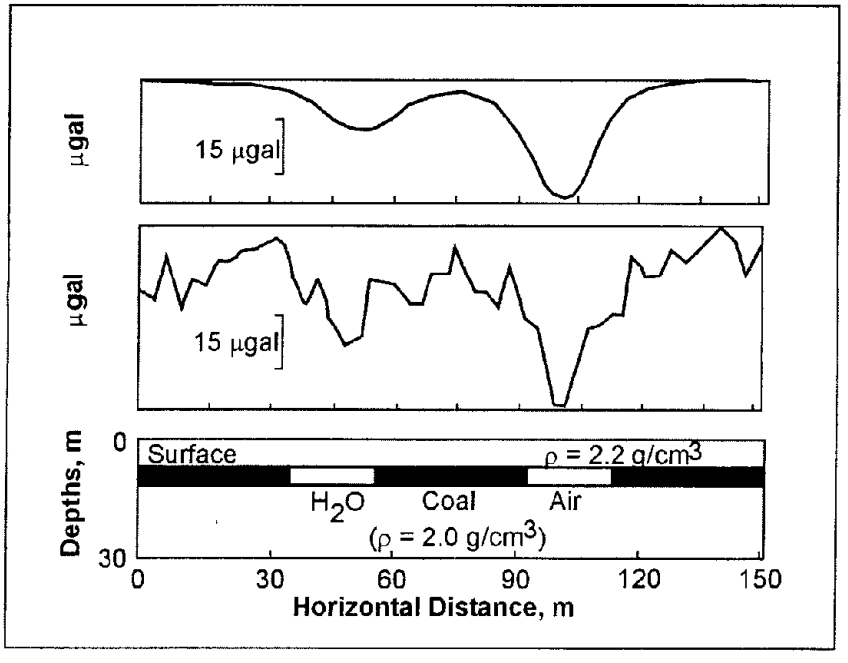

Figure 246. Geologic model (bottom) including water- and air-filled voids; theoretical gravity anomaly (top) due to model; and possible observed gravity (middle), if 22 microgals (0.22 $\mu m/s^2$) of noise is present. Depth of layer is 10 m.

Figure 247 is the same geologic section, but the depth of the coal workings is 31 m. The anomalies are far more subtle (note scale change) and, when the noise is added, the anomalies disappear. For the two cases given, figure 247 represents a clearly marginal case. Several points need to be discussed. The noise added represents a compromise value. In a hilly eastern coalfield on a rainy day, 0.22 $\mu m/s^2$ of error is optimistic. On a paved parking lot or level tank bottom, the same error estimate is too high. Note that the example uses random noise, whereas the errors discussed above (soil thickness variations, etc.) will be correlated over short distances.

Another point is the idea of fracture migration or halo effect. Some subsidence usually occurs over voids, or, in the natural case, the rock near caves may be reduced in density (Butler 1984). The closer to the gravimeter these effects occur, the more likely is detection.

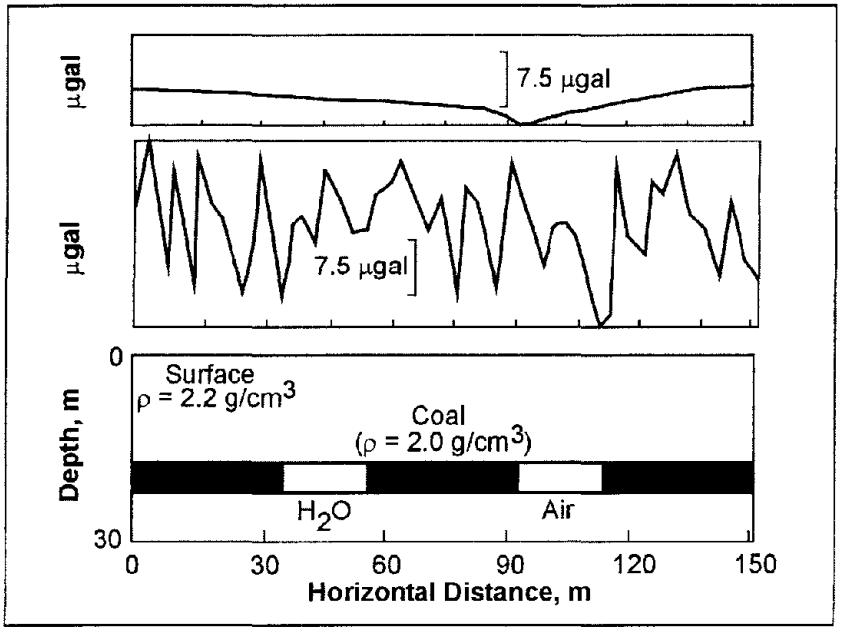

Figure 247. Geologic model (bottom) including water and air filled voids, theoretical gravity anomaly (top) due to model; and possible observed gravity (middle), if 22 microgals of noise is present. Depth of layer is 31 m.

Figure 248 illustrates a high precision survey over a proposed reservoir site. The large size of the fault and its proximity to the surface made the anomaly large enough to be detected without the more rigorous approach of microgravity. The area to the east is shown to be free of faulting (at least at the scale of tens of meters of throw) and potentially suitable as a reservoir site.

As a conclusion, in addition to anomaly evaluation, the source and size of the irreducible field errors must be considered. Under the proper conditions of large enough anomalies, good surface conditions, and some knowledge of densities, microgravity can be an effective tool for engineering investigations.

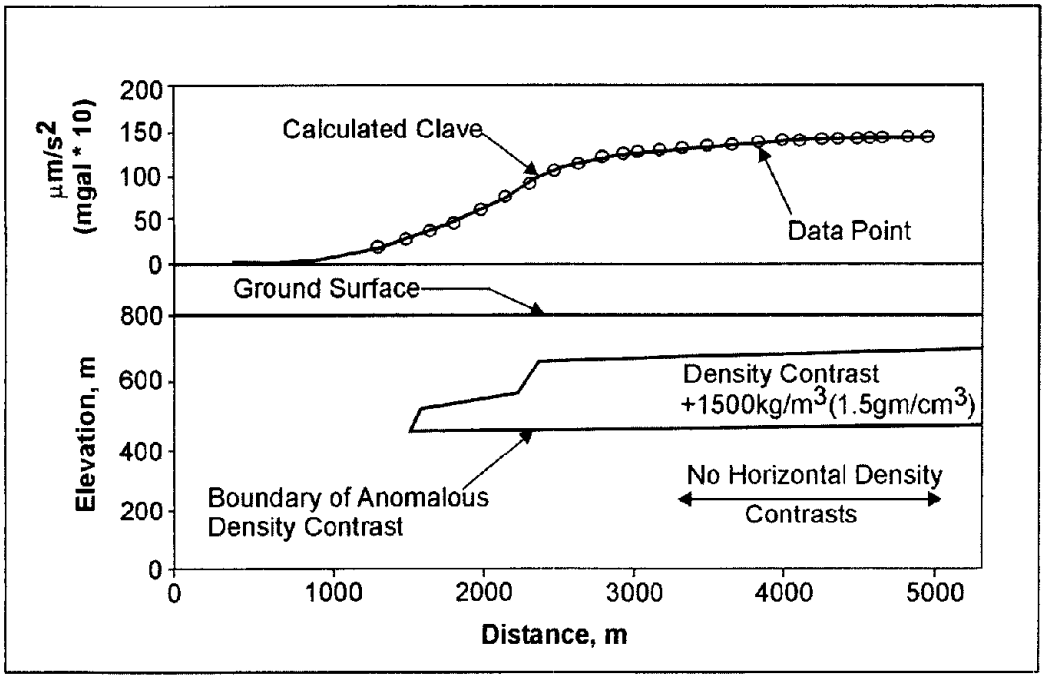

Figure 248. Gravity traverse and interpreted model

9.2 SEISMIC METHODS

Introduction.

Seismic methods are the most commonly conducted geophysical surveys for engineering investigations. Seismic refraction provides engineers and geologists with the most basic of geologic data via simple procedures with common equipment.

Any mechanical vibration is initiated by a source and travels to the location where the vibration is noted. These vibrations are seismic waves. The vibration is merely a change in the stress state due to a disturbance. The vibration emanates in all directions that support displacement. The vibration readily passes from one medium to another and from solids to liquids or gasses and in reverse. A vacuum cannot support mechanical vibratory waves, while electromagnetic waves can be transmitted through a vacuum. The direction of travel is called the ray, ray vector, or ray path. Since a source produces motion in all directions the locus of first disturbances will form a spherical shell or wave front in a uniform material. There are two major classes of seismic waves: body waves, which pass through the volume of a material; and, surface waves, that exist only near a boundary.

Body waves. These are the fastest traveling of all seismic waves and are called compressional or pressure or primary wave (P-wave). The particle motion of P-waves is extension (dilation) and compression along the propagating direction. P-waves travel through all media that support seismic waves; air waves or noise in gasses, including the atmosphere. Compressional waves in fluids, e.g., water and air, are commonly referred to as acoustic waves.

The second wave type is the secondary or transverse or shear wave (S-wave). S-waves travel slightly slower than P-waves in solids. S-waves have particle motion perpendicular to the propagating direction, like the obvious movement of a rope as a displacement speeds along its length. These transverse waves can only transit material that has shear strength. S-waves therefore do not exist in liquids and gasses, as these media have no shear strength.

S-waves may be produced by a traction source or by conversion of P-waves at boundaries. The dominant particle displacement is vertical for SV-waves traveling in a horizontal plane. Dominant particle displacements are horizontal for SH-waves traveling in the vertical plane. SH-waves are often generated for S-wave refraction evaluations of engineering sites.

Elastic body waves passing through homogeneous, isotropic media have well-defined equations of motion. Most geophysical texts, including Grant and West (1965), include displacement potential and wave equations. Utilizing these equations, computations for the wave speed may be uniquely determined. Field surveys can readily obtain wave velocities, V_P and V_S; velocities are in units of length per time, usually meters/second (m/s). A homogeneous, isotropic medium's engineering properties of Young's or elastic modulus (E) and shear modulus (G) and either density (p_b) or Poisson's ratio (ν) can be determined if V_P and V_S are known. The units of these measures are: moduli in pressure, usually pascals (Pa); density in mass per volume, grams/cubic meter (g/m^3 = 10-6 mg/m^3); and Poisson's ratio, ν, is dimensionless. Manipulation of equations from Grant and West (1965) yields

$$\nu = \left[\frac{\left(V_p / V_s\right)^2 - 2}{\left\{2\left[\left(V_p / V_s\right)^2 - 1\right]\right\}} \right], \tag{41}$$

$$E = \frac{p_b V_p^2 (1-2\nu)(1+\nu)}{(1-\nu)}, \tag{42}$$

$$G = \frac{E}{[2(1+\nu)]}, \tag{43}$$

$$p_b = \frac{G}{V_s^2}, \tag{44}$$

Note that these are not independent equa tions. Knowing two velocities uniquely determines only two unknowns of p_b, ν, or E. Shear modulus is dependent on two other values. Poisson's ratio, ν, varies from 0.0 to a value less than 0.5 from Equations 41 and 42. For units at the surface, p_b , the density, can be determined from samples or for the subsurface from bore hole samples or downhole logging. Estimates may be assumed for ν by material type. Usually the possible range of p_b is approximated, and ν is estimated. Equations 41 through 44 may be compared to the approximate values with some judgment applied. Table 15 provides some typical values selected from Hempen and Hatheway (1992) for V_P; Das (1994) for dry p_b of soils; Blake (1975) for $p_{b,dry}$ of rock; and Prakash (1981) for ν. Other

estimates of p_b are contained in the section on gravity methods. Blake (1975) offers laboratory values of all these parameters, but field values will vary considerably from the lab estimates.

Surface waves. Two recognized vubrations, which exist only at "surfaces" or interfaces, are Love and Rayleigh waves. Traveling along a surface, these waves attenuate rapidly with distance from the surface. Surface waves travel slower than body waves. Love waves travel along the surfaces of layered media, and are most often faster than Rayleigh waves. Love waves have particle displacement similar to SH-waves. A point in the path of a Rayleigh wave moves back, down, forward, and up repetitively in an ellipse like ocean waves. Surface waves are produced by surface impacts, explosions, and waveform changes at boundaries. Love and Rayleigh waves are also portions of the surface wave train in earthquakes. These surface waves may carry greater energy content than body waves. These wave types arrive last, following the body waves, but can produce larger displacements in surface structures. Therefore, surface waves may cause more damage from earthquake vibrations.

Table 15. Typical/representative field values of V_p, p_b and v for various materials.

Material	V_p (m/s)	$p_{b,dry}$ (mg/m^3)	v
Air	330		
Damp loam	300-750		
Dry sand	450-900	1.6-2.0	0.3-0.35
Clay	900-1,800	1.3-1.8	0.5
Fresh, shallow water	1,430-1,490	1.0	
Saturated, loose sand	1,500		
Basal/lodgement till	1,700-2,300	2.3	
Rock			0.15-0.25
Weathered igneous sand	450-3,700		
Weathered sedimentary	600-3,000		
Shale	800-3,700		
Sandstone	2,200-4,000	1.9-2.7	
Metamorphic rock	2,400-6,000		
Unweathered basalt	2,600-4,300	2.2-3.0	
Dolostone and limestone	4,300-6,700	2.5-3.0	
Unweathered granite	4,800-6,700	2.6-3.1	
Steel	6,000		

Wave theory. A seismic disturbance moves away from a source location; the locus of points defining the expanding disturbance is termed the wavefront. Any point on a wavefront acts as a new source and causes displacements in surrounding positions. The vector normal to the wavefront is the ray path through that point, and is the direction of propagation. Upon striking a boundary between differing material properties, wave energy is transmitted,

reflected, and converted. The properties of the two media and the angle at which the incident ray path strikes will determine the amount of energy reflected off the surface, refracted into the adjoining material, lost as heat, and changed to other wave types.

An S-wave in rock approaching a boundary of a lake will have an S-wave reflection, a P-wave reflection, and a likely P-wave refraction into the lake water (depending on the properties and incident angle). Since the rock-water boundary will displace, energy will pass into the lake, but the water cannot support an S-wave. The reflected S-wave departs from the boundary at the same angle normal to the boundary as the arriving S-wave struck. In the case of a P-wave incident on a boundary between two rock types (of differing elastic properties), there may be little conversion to S-waves. Snell's Law provides the angles of reflection and refraction for both the P- and S-waves. [Zoeppritz's equations provide the energy conversion for the body wave forms.] In the rock on the source side (No. 1), the velocities are V_{P1} and V_{S1}; the second rock material (No. 2) has properties of V_{P2} and V_{S2}. Then for the incident P-wave ($P_1 i$), Snell's Law provides the angles of reflections in rock No. 1 and refraction in rock No. 2 as:

$$\frac{\sin \alpha_{P1i}}{V_{P1i}} = \frac{\sin \alpha_{P1}}{V_{P1}} = \frac{\sin \alpha_{S1}}{V_{S1}} = \frac{\sin \alpha_{P2}}{V_{P2}} = \frac{\sin \alpha_{S2}}{V_{S2}}, \qquad (45)$$

The second and third terms of equation 45 are reflections within material No. 1; the fourth and fifth terms are refractions into medium No. 2. Note that none of the angles can exceed 90 degrees, since none of the sin terms can be over 1.0, and $\alpha_{P1i} = \alpha_{P1}$.

Two important considerations develop from understanding equation 45. First is the concept of critical refraction. If rock No. 1 has a lower velocity than rock No. 2 or $V_{P1} < V_{P2}$, then from Equation 45, sin α_{P2} > sin α_{P1i} and the refracted $\alpha_{P2} > \alpha_{P1i}$, the incident angle. Yet sin α_{P2} cannot exceed 1.00. The critical incident angle causes the refraction to occur right along the boundary at 90° from the normal to the surface. The critical angle is that particular incident angle such that sine α_{P2} = 1.0 and α_{P2} = 90 deg, or $\alpha(_{P1i})_{cr}$ = sin-1(V_{P1}/V_{P2}). Secondly, any incident angle > $\alpha(_{P1i})_{cr}$ from the normal will cause total reflection back into the source-side material, since sin α_{P2} ⇑ 1.0. For the latter case, all the P-wave energy will be retained in medium No. 1.

Other wave phenomena occur in the subsurface. Diffractions develop at the end of sharp boundaries. Scattering occurs due to inhomogeneities within the medium. As individual objects shrink in size, their effect on scatter is reduced. Objects with mean dimensions smaller than one- fourth of the wavelength will have little effect on the wave. Losses of energy or attenuation occur with distance of wave passage. Higher frequency waves lose energy more rapidly than waves of lower frequencies, in general.

The wave travels outward from the source in all directions supporting displacements. Energy dissipation is a function of the distance traveled, as the wave propagates away from the source. At boundaries, the disturbance passes into other media. If a wave can pass from a particular point A to another point B, Fermat's principle states that the ray path taken is the one requiring the minimum amount of time. In crossing boundaries of media with different properties, the path will <u>not</u> be the shortest distance (a straight line) due to refraction. The

actual ray path will have the shortest travel time. Since every point on a wavefront is a new source, azimuths other than that of the fastest arrival will follow paths to other locations for the ever-expanding wave.

Data Acquisition

Digital electronics have continued to allow the production of better seismic equipment. Newer equipment is hardier, more productive, and able to store greater amounts of data. The choice of seismograph, sensors(geophones), storage medium, and source of the seismic wave depend on the survey being undertaken. The sophistication of the survey, in part, governs the choice of the equipment and the field crew size necessary to obtain the measurements. Costs rise as more elaborate equipment is used. However, there are efficiencies to be gained in proper choice of source, number of geophone emplacements for each line, crew size, channel capacity of the seismograph, and requirements of the field in terrain type and cultural noise.

Sources. The seismic source may be a hammer striking the ground or an aluminum plate or weighted plank, drop weights of varying sizes, rifle shot, a harmonic oscillator, waterborne mechanisms, or explosives. The energy disturbance for seismic work is most often called the "shot," an archaic term from petroleum seismic exploration. Reference to the "shot" does not necessarily mean an explosive or rifle source was used. The type of survey dictates some source parameters. Smaller mass, higher frequency sources are preferable. Higher frequencies give shorter wavelengths and more precision in choosing arrivals and estimating depths. Yet, sufficient energy needs to be transmitted to obtain a strong return at the end of the survey line. The type of source for a particular survey is usually known prior to going into the field. A geophysical contractor normally should be given latitude in selecting or changing the source necessary for the task. The client should not hesitate in placing limits on the contractor's indiscriminate use of some sources. In residential or industrial areas, perhaps the maximum explosive charge should be limited. The depth of drilling shot holes for explosives or rifle shots may need to be limited; contractors should be cautious not to exceed requirements of permits, utility easements, and contract agreements.

Geophones. The sensor receiving seismic energy is the geophone (hydrophone in waterborne surveys) or phone. These sensors are either accelerometers or velocity transducers, and convert ground movement into a voltage. Typically, the amplification of the ground is many orders of magnitude, but accomplished on a relative basis. The absolute value of particle acceleration cannot be determined, unless the geophones are calibrated.

Most geophones have vertical, single-axis response to receive the incoming waveform from beneath the surface. Some geophones have horizontal-axis response for S-wave or surface wave assessments. Triaxial phones, capable of measuring absolute response, are used in specialized surveys. Geophones are chosen for their frequency band response.

The line, spread, or string of phones may contain one to scores of sensors depending on the type of survey. The individual channel of recording normally will have a single phone. Multiple phones per channel may aid in reducing wind noise or air blast or in amplifying deep reflections.

Seismographs. The equipment that records input geophone voltages in a timed sequence is the seismograph. Current practice uses seismographs that store the channels' signals as digital data at discrete time. Earlier seismographs would record directly to paper or photographic film. Stacking, inputting, and processing the vast volumes of data and archiving the information for the client virtually require digital seismographs. The seismograph system may be an claborate amalgam of equipment to trigger or sense the source, digitize geophone signals, store multichannel data, and provide some level of processing display. Sophisticated seismograph equipment is not normally required for engineering and environmental surveys. One major exception is the equipment for sub-bottom surveys or nondestructive testing of pavements.

Data processing of seismic information can be as simple as tabular equations for seismic refraction. Processing is normally the most substantial matter the geophysicists will resolve, except for the interpretation.

A portion of the seismic energy striking an interface between two differing materials will be reflected from the interface. The ratio of the reflected energy to incident energy is called the reflection coefficient. The reflection coefficient is defined in terms of the densities and seismic velocities of the two materials as:

$$R = \frac{(p_{b2}V_2 - p_{b1}V_1)}{(p_{b2}V_2 + p_{b1}V_1)}, \tag{46}$$

where

R = reflection coefficient,
p_{b1}, p_{b2} = densities of the first and second layers, respectively,
V_1, V_2 = seismic velocities of the first and second layers, respectively.

Modern reflection methods can ordinarily detect isolated interfaces whose reflection coefficients are as small as 0.02.

9.2.1 Seismic Reflection Methods

The physical process of reflection is illustrated in Figure 249, where the raypaths through successive layers are shown. There are commonly several layers beneath the earth's surface that contribute reflections to a single seismogram. The unique advantage of seismic reflection data is that it permits mapping of many horizon or layers with each shot.. At later times in the record, more noise is present in the record making the reflections difficult to extract from the unprocessed data.

Figure 250 indicates the paths of arrivals that would be recorded on a multichannel seismograph. Note that the subsurface coverage is exactly one-half of the surface distance across the geophone spread. The subsurface sampling interval is one-half of the distance between geophones on the surface. Another important feature of modern reflection-data acquisition is illustrated by figure 251. If multiple shots, S1 and S2, are recorded by multiple

receivers, R1 and R2, and the geometry is as shown in the figure, the reflection point for both raypaths is the same. However, the ray paths are not the same length, thus the reflection will occur at different times on the two traces. This time delay, whose magnitude is indicative of the subsurface velocities, is called normal-moveout. With an appropriate time shift, called the normal-moveout correction, the two traces (S1 to R2 and S2 to R1) can be summed, greatly enhancing the reflected energy and canceling spurious noise.

This method is called the common reflection point, common midpoint, or common depth point (CDP) method. If all receiver locations are used as shot points, the multiplicity of data on one subsurface point (called CDP fold) is equal to one-half of the number of recording channels. Thus, a 24-channel seismograph will record 12-fold data if a shot corresponding to every receiver position is shot into a full spread. Thus, for 12-fold data, every subsurface point will have 12 separate traces added, after appropriate time shifting, to represent that point.

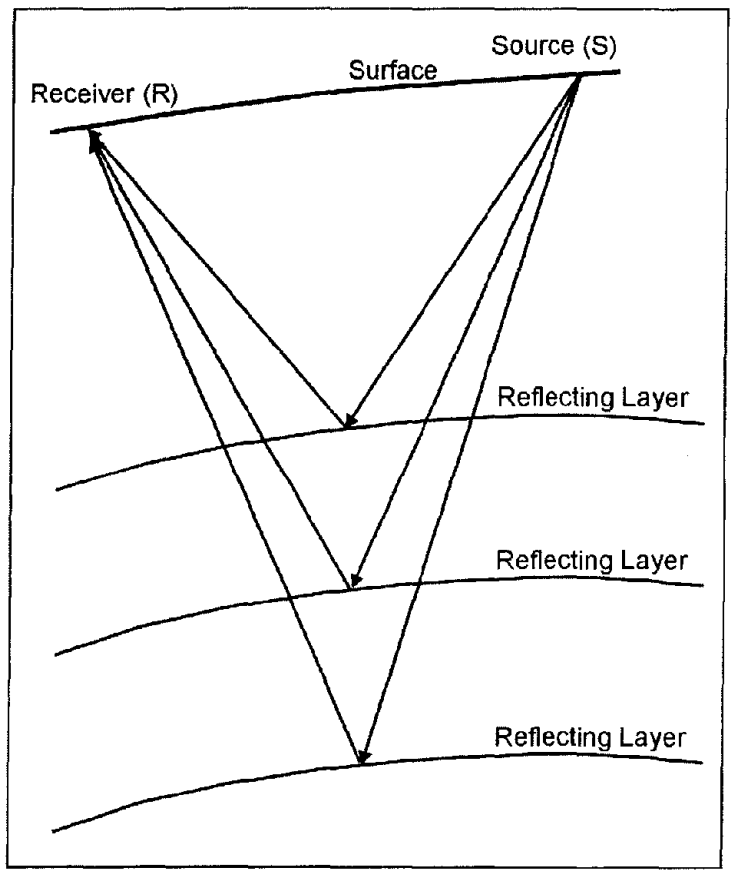

Figure 249. Schematic of the seismic reflection method.

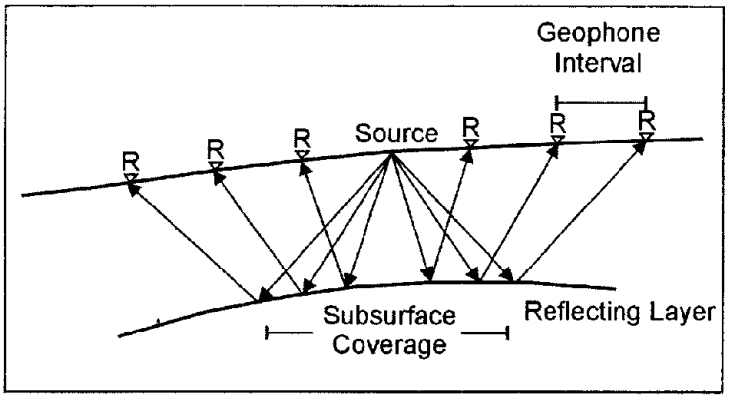

Figure 250. Multichannel recordings for seismic reflection.

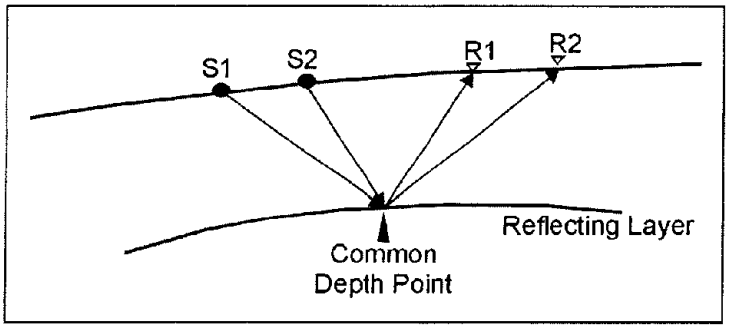

Figure 251. Illustration of common depth point (often called common mid point).

Arrivals on a seismic reflection record can be seen in figure 252. The receivers are arranged to one side of a shot, which is 15 m from the first geophone. Various arrivals are identified on figure 252. Note that the gain is increased down the trace to maintain the signals at about the same size by a process known as automatic gain control (AGC). One side of the traces is shaded to enhance the continuity between traces.

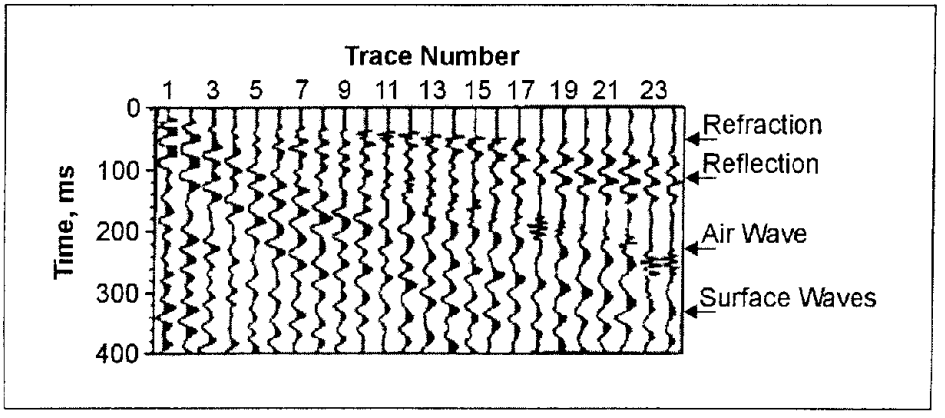

Figure 252. Simple seismic reflection record.

The ultimate product of a seismic reflection survey is a corrected cross section of the earth with reflection events in their true subsurface positions. This section does not present every detail of the acquisition and processing of shallow seismic reflection data. Thus, the difference between deep petroleum-oriented reflection and shallow reflection work suitable for engineering and environmental applications will be stressed.

Cost and frequency bandwidth are the principal differences between the two applications of seismic reflection. One measure of the nominal frequency content of a pulse is the inverse of the time between successive peaks. In the shallow subsurface, the exploration objectives are often at depths of 15 to 45 m. At 450 m/s, a wave with 10 ms peak-to-peak (nominal frequency of 100 Hz) is 45 m long. To detect (much less differentiate between) shallow, closely spaced layers, pulses with nominal frequencies at or above 200 Hz may be required. A value of 1,500 m/s is used as a representative velocity corresponding to saturated, unconsolidated materials because, without saturated sediments, both attenuation and lateral variability make reflection generally difficult.

9.2.1.1 Common-Offset Seismic Reflection Method

A technique for obtaining one-fold reflection data is called the common-offset method or common-offset gather (COG). It is instructive to review the method, but it has fallen into disuse because of the decreased cost of CDP surveys and the difficulty of quantitative interpretation in most cases. Figure 253 illustrates time-distance curves for the seismic waves that can be recorded. In the optimum offset distance range, the reflected and refracted arrivals will be isolated in time. Note that no quantitative scales are shown as the distances or velocities, and wave modes are distinct at each site. Thus, testing is necessary to establish the existence and location of the optimum offset window. Figure 254 illustrates the COG method. After the optimum offset distance is selected, the source and receiver are moved across the surface. Note that the subsurface coverage is one-fold, and there is no provision for noise cancellation. Figure 255 is a set of data presented as common offset data. The offset between geophone and shot is 14 m. Note that the acoustic wave (visible as an arrival near 40 ms) is attenuated (the shot was buried for this record). Note the prominent reflection near 225 ms that splits into two arrivals near line distance 610 m. Such qualitative changes are the usual interpretative result of a common offset survey. No depth scale is furnished.

Data Acquisition.

A shallow seismic reflection crew consists of three to five persons. The equipment used allows two to three times the number of active receivers to be distributed along the line. A switch (called a roll-along switch) allows the seismograph operator to select the particular set of geophones required for a particular shot from a much larger set of geophones that have been previously laid out. The operator can then switch the active array down the line as the position of the shot progresses. Often the time for a repeat cycle of the source and the archiving time of the seismograph are the determining factors in the production rates. With enough equipment, one or two persons can be continually moving equipment forward on the line while a shooter and an observer are sequencing through the available equipment.

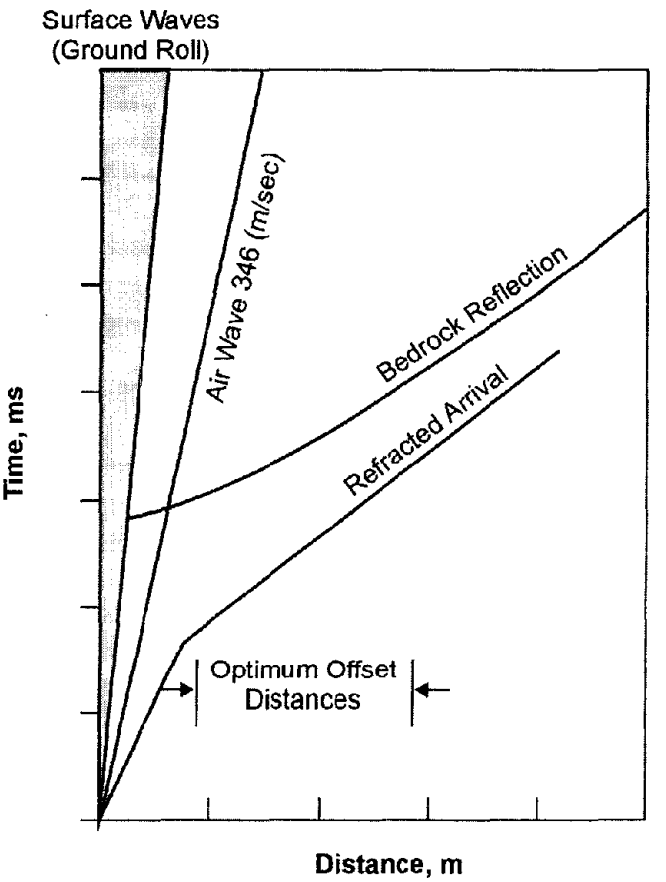

Figure 253. Optimum offset distance determination for the common offset method.

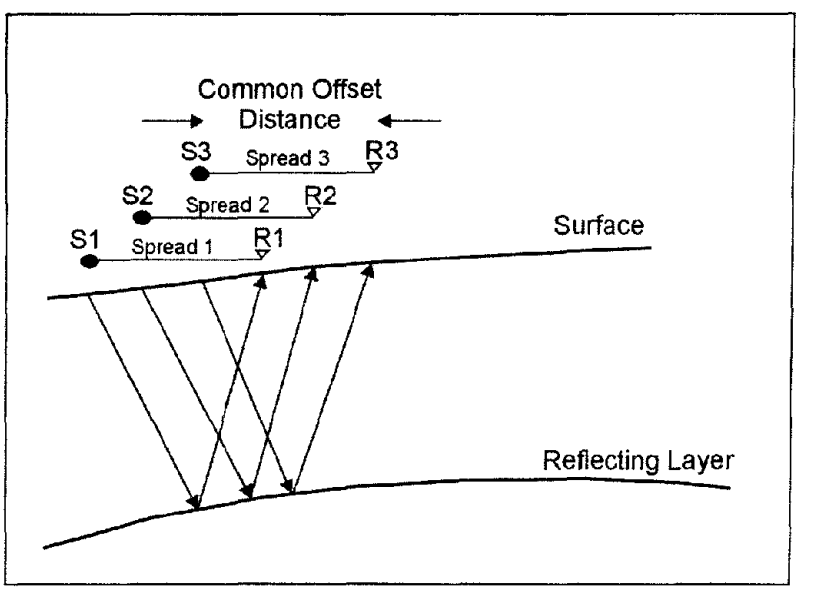

Figure 254. Common offset method schematic.

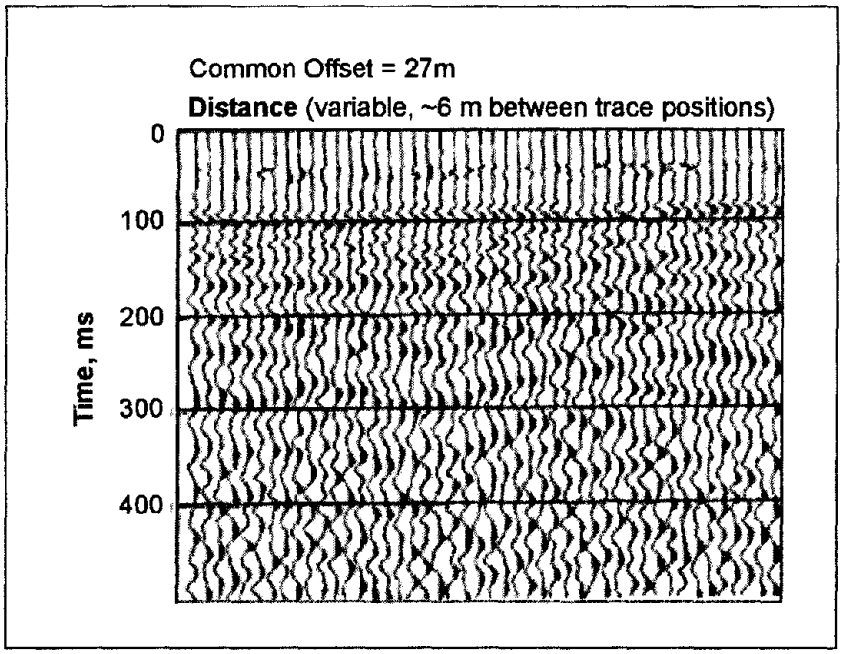

Figure 255. Sample common offset record.

If the requirements for relative and absolute surveying are taken care of at a separate time, excellent production rates, in terms of number of shot points per day, can be achieved. Rates of 1/min or 400 to 500 normal shots can be recorded in a field day. Note that the spacing of these shot points may be only 0.6 to 1.2 m, so the linear progress may be only about 300 m of line for very shallow surveys. Also, note that the amount of data acquired is enormous. A 24-channel record sampled every 1/8 ms that is 200 ms long consists of nearly 60,000 32-bit numbers, or upwards of 240 KB/record. Three hundred records may represent more than 75 MB of data for 1 day of shooting.

Field data acquisition parameters are highly site specific. Up to a full day of testing with a knowledgeable consultant experienced in shallow seismic work may be required. The objective of these tests is identifiable, demonstrable reflections on the raw records. If arrivals consistent with reflections from the zone of interest cannot be seen, the chances that processing will recover useful data are slim. One useful testing technique is the walkaway noise test. A closely spaced set of receivers is set out with a geophone interval equal to 1% or 2% of the depth of interest - often as little as 30 or 60 cm for engineering applications. By firing shots at different distances from this spread, a well-sampled long-offset spread can be generated. Variables can include geophone arrays, shot patterns, high and low-cut filters, and AGC windows, among others.

Because one objective is to preserve frequency content, table 15 is offered as a comparison between petroleum-oriented and engineering-oriented data acquisition. The remarks column indicates the reason for the differences.

Table 16. Seismic reflection use differences by methodology.

	Petroleum	Engineering	Remarks
Explosive seismic source	10-25 kg or more in a distributed pattern in deep holes	20 to 50 g, single shot	To increase frequency content
Mechanical seismic source	1-7 vibrators 5-15,000 kg peak force 10-100 Hz sweep	Hammer and Plate, guns	Cost, increased frequency
Geophones	Arrays of 12-48 phones; 25-40 Hz fundamental frequency; 3-20 m spacing	Single or 3-5 geophones 50-100 Hz fundamental frequency; 1-3 m spacing	To preserve frequency content
Recorders	Instantaneous floating point, 48-1,000 channels	Instantaneous floating point, 24-96 channels	Cost
Passband analog filters	10-110 Hz	100-500 Hz	To increase frequency content
Sample interval	1-2 ms	1/4-1/8 ms	Higher frequencies

Data Processing

Processing is typically done by professionals using special purpose computers. These techniques are expensive but technically robust and excellent results can be achieved. A complete discussion of all the processing variables is well beyond the scope of this manual. However a close association of the geophysicist, the processor and the consumer is absolutely essential if the results are to be useful. Well logs, known depths, results from ancillary methods, and the expected results should be furnished to the processor. At least one iteration of the results should be used to ensure that the final outcome is successful.

One important conclusion of the processing is a true depth section. The production of depth sections requires conversion of the times of the reflections to depths by derivation of a velocity profile. Well logs and check shots are often necessary to confirm the accuracy of this conversion.

Advantages and Limitations

It is possible to obtain seismic reflections from very shallow depths, perhaps as shallow as 3 to 5 m.

1. Variations in field techniques are required depending on depth.

2. Containment of the air-blast is essential in shallow reflection work.

3. Success is greatly increased if shots and phones are near or in the saturated zone.

4. Severe low-cut filters and arrays of a small number (1-5) of geophones are required.

5. Generally, reflections should be visible on the field records after all recording parameters are optimized.

6. Data processing should be guided by the appearance of the field records and extreme care should be used not to stack refractions or other unwanted artifacts as reflections.

9.2.1.2 Subbottom Profiling

A variant of seismic reflection used at the surface of water bodies is subbottom profiling or imaging. The advantage of this technique is the ability to tow the seismic source on a sled or catamaran and to tow the line of hydrophones. This procedure makes rapid, continuous reflection soundings of the units below the bottom of the water body, in other words, the subbottom. This method and significant processing requirements have been recently developed by Ballard, et al., (1993) of the U.S. Army Engineer Waterways Experiment Station (WES). The equipment, acquisition, and processing system reduce the need for over-water boring programs. The developed WES imaging procedure resolves material type, density, and thickness (Ballard, et al., 1993).

Basic Concepts

The acoustic impedance method may be used to determine parameters of the soft aqueous materials. The acoustic impedance z for a unit is the product of its p_b and V_P. The reflection coefficient R from a particular horizon is

$$R = \left(\frac{E_{ref}}{E_{inc}}\right)^{1/2} = \left[\frac{(z_i - z_j)}{(z_i + z_j)}\right], \tag{47}$$

where

E_{refl} = energy reflected at the i-j unit boundary

E_{inc} = incident energy at the i-j unit boundary

z_i = acoustic impedance of the i (lower) material

z_j = acoustic impedance of the j (upper) medium

At the highest boundary, the water-bottom interface, z_j,water is known to be $1.5 * 10^9$ g/(m^{2}s). Since the $E_{refl,1\text{-}2}$ can be determined, and $E_{inc,1\text{-}2}$ and z_1,water are known, $z_{i,2}$ may be determined. $V_{P,2}$ may be assessed from the depth of the 2-3 boundary, and thus $\rho_{i,2}$ may be resolved. The material properties of lower units can be found in succession from the reflections of deeper layers.

Data Acquisition

A variety of different strength sources are available for waterborne use. By increasing strength, these sources are: pingers, boomers, sparkers, and airguns. Although there is some

strength overlap among these sources, in general, as energy increases, the dominant period of the wave increases. For the larger source strength, therefore, the ability to resolve detail is impaired as period and wavelength become larger. The resolving accuracy of the system may change by more than an order of magnitude from <0.2 m for a pinger to >1.0 m for an airgun.

The conflicting impact of energy sources is the energy available for penetration and deeper reflections. The greater energy content and broad spectrum of the boomer allow significantly greater depth returns. Some near-bottom sediments contain organic material that readily absorbs energy. Higher energy sources may allow penetration of these materials.

Data collection is enormous with a towed subbottoming system. Graphic displays print real-time reflector returns to the hydrophone set. Recording systems retrieve the data for later processing. The field recorders graph time of source firing versus time of arrival returns. Figure 256 provides the field print for Oakland Harbor (Ballard, McGee, and Whalin, 1992).

Data Processing

Office processing of the field data determines the subbottoming properties empirically. The empiricisms are reduced when more sampling (boring) data are available to assess unit ρ and loss parameters for modeling. The processing imposes the Global Positioning System (GPS) locations upon the time of firing records to approximately locate the individual shot along the towed boat path. The seismic evaluation resolves the layer V_P and unit depths. From the firing surface locations and unit depths, the field graphs are correlated to tow path distance versus reflector depths. Figure 257 shows cross sections of the Gulfport Ship Channel, Mississippi. These are fence diagrams of depth and material types once all parallel and crossing surveys are resolved.

Advantages and Limitations

The subbottoming technique can be applied to a large variety of water bodies. Saltwater harbors, shipping channels, and river waterways were the original objective for the technique. The method is now used on locks, dams, reservoirs, and engineering projects such as the location of pipelines.

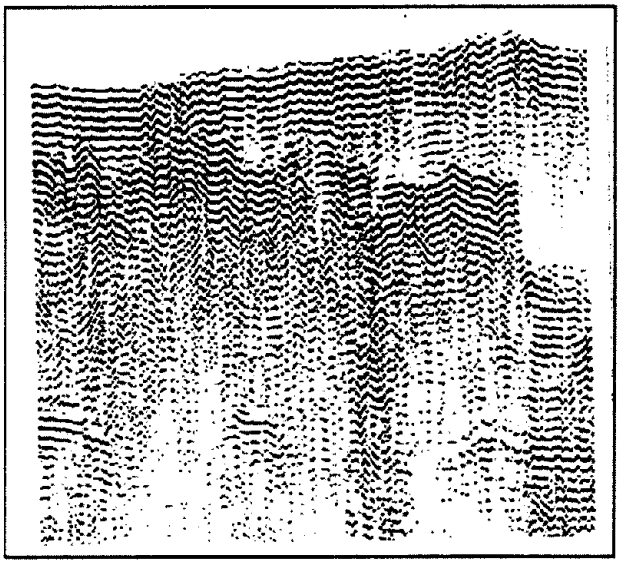

Figure 256. Reflected subbottoming signal amplitude cross section, 3.5 kHz in Oakland Harbor, California (Ballard, McGee and Whalin, 1992).

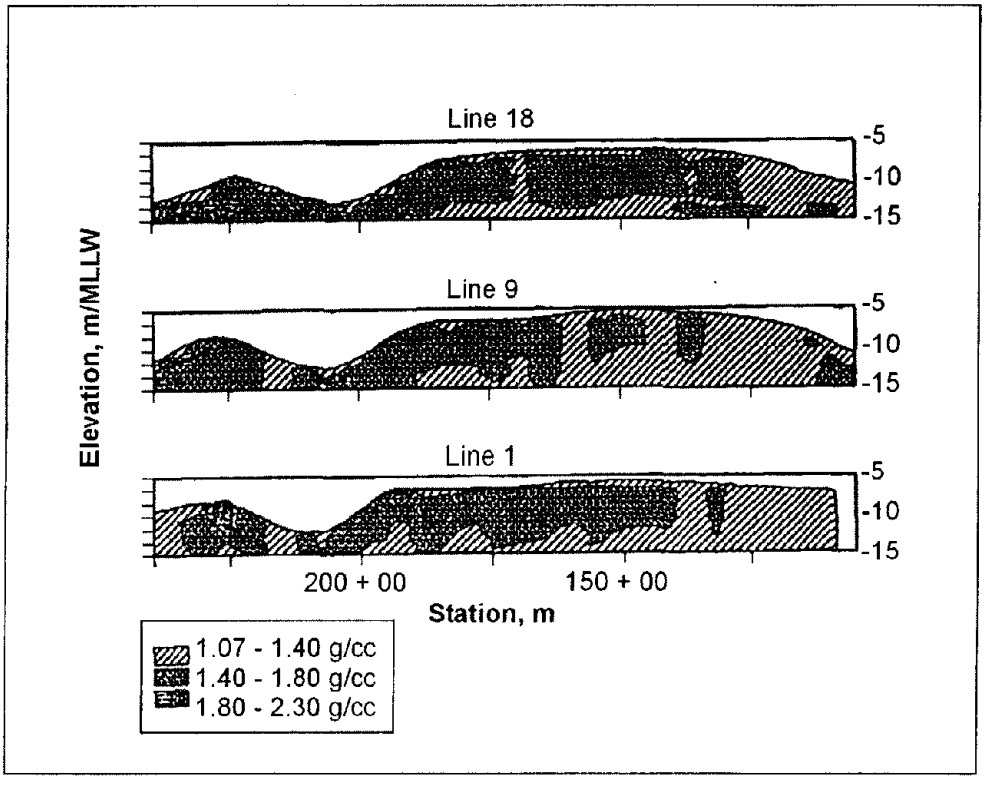

Figure 257. Density cross section in Gulfport ship canal, Mississippi. (Ballard. McGee and Whalin 1992).

9.2.1.3 Fathometer Surveys

Basic Concepts

Fathometers are also called Echo Sounders and are similar to reflection seismic profilers in that they also employ an acoustic source and receiver placed immediately beneath the surface of the water. However, fathometers differ from reflection seismic profilers in that they use higher frequency acoustic source pulses varying from less than 10 kHz up to about 200 kHz. Some of this energy transmitted by the source is reflected from the sediments at the water bottom, and the reflections are recorded by the receiver and stored digitally.

Data Acquisition

Fathometers determine water depth by repeatedly transmitting seismic energy through the water column and recording the arrival time of the reflected energy from the water bottom. The time required for the seismic signal to travel from its source to a reflector and back is known as the two-way travel time, and it is measured in milliseconds (ms) (equal to 1×10^{-3} seconds). The Fathometer calculates the depth to a water bottom by dividing the two-way travel time by two and multiplying the result by the velocity of sound through water:

$$D = V\frac{t}{2}, \tag{48}$$

where

D= depth to the water bottom (m),
V= velocity of sound through water (m/s), and
t= two-way travel time (s).

Fathometer surveys are conducted while traveling at a moderate speed in a boat. Typically, the transducer is mounted on the side of the boat and placed in the water. Data recording is essentially automatic with a chart recorder plotting providing a hard copy of the data or a computer screen may be used for the display. The data may also be stored on magnetic tape for further processing and plotting. As with the CSP method, GPS can be used to position the data.

Data Processing

The depth value is printed as a continuous graphic profile and/or displayed as a numeric value by the Fathometer. Fathometers are calibrated by adjusting the value of V, which may vary slightly depending on water type. Most Fathometers use a narrow-bandwidth 200 kHz seismic signal. These Fathometers provide accurate depth data, but little or no information about the subbottom. Fathometers that use a lower frequency signal, such as 20 kHz, can detect reflected energy from subbottom interfaces, such as the bottom of an infilled scour hole.

Fathometer systems come with black and white chart recording systems and in color systems. Colors are often assigned according to the different amplitudes of the reflected signals.

Fathometers color step sizes as low as four dB are now available, allowing quite small changes in the reflected signals to be observed. An event marker button is often available allowing vertical line marks to be placed on the records when specific locations are selected by the operator. Sometimes the data can be downloaded to a computer allowing digital processing to be done along with data plots.

A color Fathometer can be calibrated to measure and display in color the amplitude of the reflected signal, which, in constant water depths, can be related to characteristics of the bottom material.

Data Interpretation

Traces from adjacent source/receiver locations are plotted side-by-side to form an essentially continuous time-depth profile of the stream bottom. Estimated seismic interval velocities can be used to transform the time-depth profile into a depth profile. However, water velocities are a function of suspended sediment load, and can vary appreciably.

The data are interpreted by viewing the plotted data. The response of specific objects may be used if these were noted on the records using a button marker.

Figure 258 shows Fathometer data recorded with a 200 kHz transducer. Note that only the water depth is observed in these data. Because of the high frequency, little energy is transmitted into the bottom sediments, and thus no reflections are observed from within the sediments.

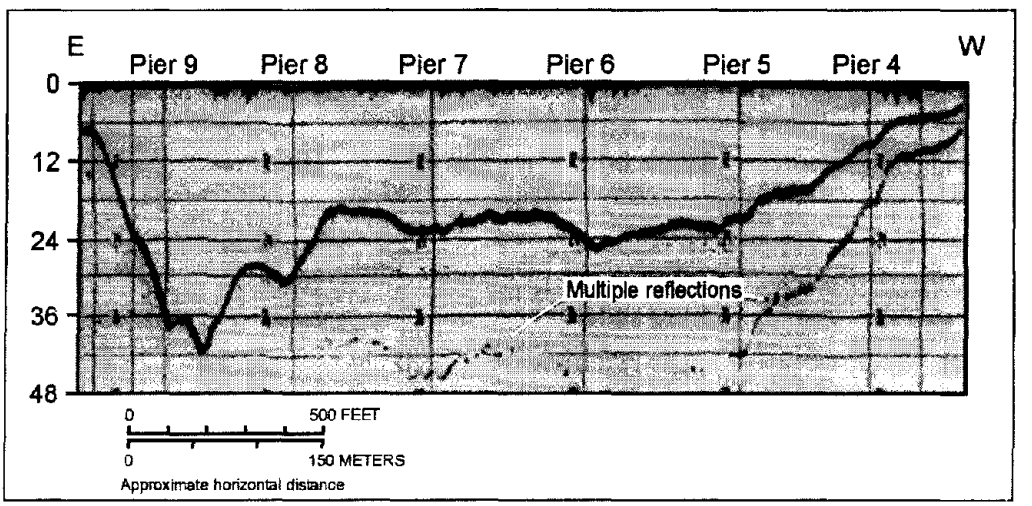

Figure 258. Fathometer data recorded with 200 kHz transducer. (Placzek, et al. 1995, USGS Report 95-4009)

Figure 259 presents fathometer data using a 3.5 kHz transducer. Because of the lower frequency, some of the energy is transmitted into the sediments and reflections are seen.

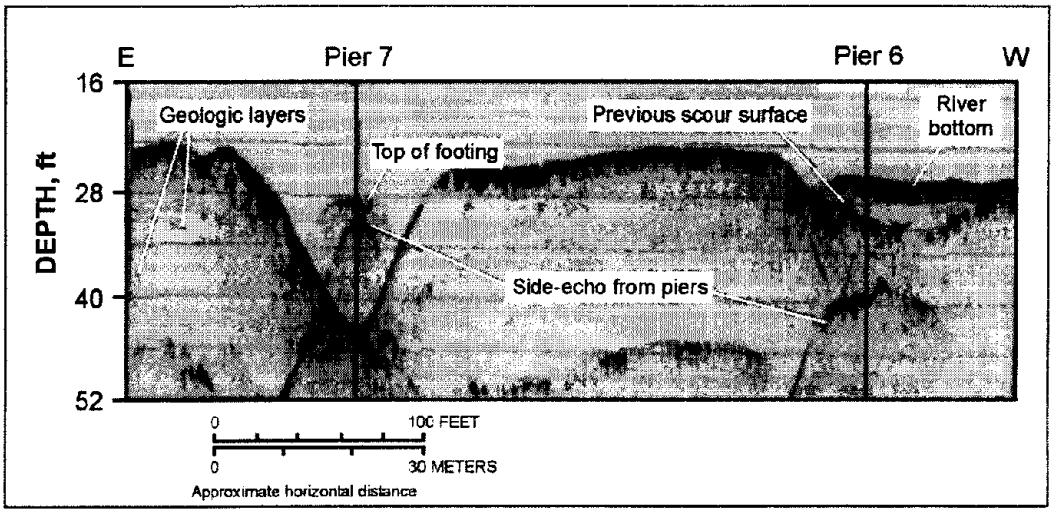

Figure 259. Fathometer data recorded using a 3.5 kHz transducer. (Placzek, et al. 1995, USGS Report 95-4009)

Advantages and Limitations

The main advantages of Fathometers (in continuous mode) are as follows:

1. The tool can provide an accurate depth-structure model of the water bottom (if acoustic velocities are known).

2. Post acquisition processing (migration) can be applied.

The main disadvantages of Fathometers (in continuous mode) are as follows:

1. The source and receiver need to be submerged. Profiles cannot be extended across emerged sand bars or onto the shore.

2. The equipment is relatively expensive (hardware and software).

3. Data may be contaminated by noise (multiple reflections, and echoes from the shoreline, water bottom, and/or piers).

4. Post acquisition processing (migration) may be required in areas where significant structural relief is present.

Fathometers are also employed in a spot survey mode. In this type of survey, sounding data (single reflection traces) are acquired at irregularly (or uniformly) spaced intervals (typically on the order of meters) at the water surface. The first high-amplitude reflected event is usually interpreted to be the water bottom reflection. Note, that spot data usually cannot be accurately migrated because of aliasing problems.

9.2.2 Surface Wave Methods

Introduction

A wide variety of seismic waves propagate along the surface of the earth. They are called surface waves because their amplitude decreases exponentially with increasing depth. The Rayleigh wave is important in engineering studies because of its simplicity and because of the close relationship of its velocity to the shear-wave velocity for earth materials. As most earth materials have Poisson's ratios in the range of 0.25 to 0.48, the approximation of Rayleigh wave velocities as shear-wave velocities causes less than a 10% error. Rayleigh wave studies for engineering purposes have most often been made in the past by direct observation of the Rayleigh wave velocities. One method consists of excitation of a monochromatic wave train and the direct observation of the travel time of this wave train between two points. As the frequency is known, the wavelength is determined by dividing the velocity by the frequency.

The assumption that the depth of investigation is equal to one-half of the wavelength can be used to generate a velocity profile with depth. This last assumption is somewhat supported by surface wave theory, but more modern and comprehensive methods are available for inversion of Rayleigh-wave observations. Similar data can be obtained from impulsive sources if the recording is made at sufficient distance such that the surface wave train has separated into its separate frequency components.

9.2.2.1 Spectral Analysis of Surface Waves (SASW)

The promise, both theoretical and observational, of surface wave methods has resulted in significant applications of technology to their exploitation. The problem is twofold:

To determine, as a function of frequency, the velocity of surface waves traveling along the surface (this curve, often presented as wavelength versus phase velocity, is called a dispersion curve).

From the dispersion curve, determine an earth structure that would exhibit such dispersion. This inversion, which is ordinarily done by forward modeling, has been automated with varying degrees of success.

Basic Concept

Spectral analysis, via the Fourier transform, can convert any time-domain function into its constituent frequencies. Cross-spectral analysis yields two valuable outputs from the simultaneous spectral analysis of two time functions. One output is the phase difference between the two time functions as a function of frequency. This phase difference spectrum can be converted to a time difference (as a function of frequency) by use of the relationship:

$$\Delta t(f) = \frac{\Phi(f)}{2\pi f}, \tag{49}$$

where

$\Delta t(f)$ = frequency-dependent time difference,
$\Phi(f)$ = cross-spectral phase at frequency f,
f = frequency to which the time difference applies.

If the two time functions analyzed are the seismic signals recorded at two geophones a distance d apart, then the velocity, as a function of frequency, is given by:

$$V(f) = \frac{d}{t(f)}, \tag{50}$$

where

d = distance between geophones,
$t(f)$ = term determined from the cross-spectral phase.

If the wavelength (λ) is required, it is given by:

$$\lambda(f) = \frac{V(f)}{f}, \tag{51}$$

As these mathematical operations are carried at for a variety of frequencies, an extensive dispersion curve is generated. The second output of the cross-spectral analysis that is useful in this work is the coherence function. This output measures the similarity of the two inputs as a function of frequency. Normalized to lie between 0 and 1, a coherency of greater than 0.9 is often required for effective phase difference estimates. Once the dispersion curve is in hand, the calculation-intensive inversion process can proceed. Although the assumption given above of depth equal to one-half the wavelength may be adequate if relatively few data are available, the direct calculation of a sample dispersion curve from a layered model is necessary to account for the abundance of data that can be recorded by a modern seismic system. Whether or not the inversion is automated, the requirements for a good geophysical inversion should be followed, and more observations than parameters should be selected.

Calculation methods for the inversion are beyond the scope of this manual. The model used is a set of flat-lying layers made up of thicknesses and shear-wave velocities. More layers are typically used than are suspected to be present, and one useful iteration is to consolidate the model layers into a geologically consistent model and repeat the inversion for the velocities only.

The advantages of this method are:

a) High frequencies (1-300 Hz) can be used, resulting in definition of very thin layers.

b) The refraction requirement of increasing velocities with depth is not present; thus, velocities that decrease with depth are detectable.

By using both of these advantages, this method has been used to investigate pavement substrate strength. An example of typical data obtained by an SASW experiment is shown in figure 260. The scatter of these data is smaller than typical SASW data. Models obtained by two different inversion schemes are shown in figure 261 along with some crosshole data for comparison. Note that the agreement is excellent above 20 m of depth.

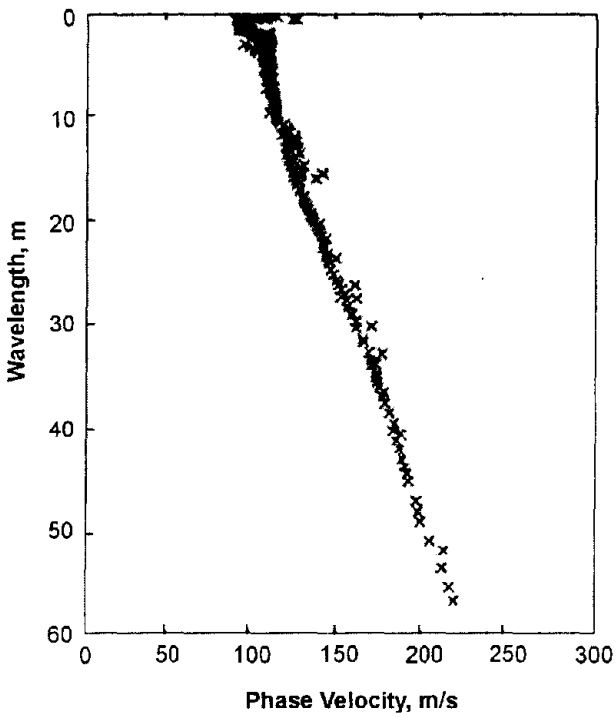

Figure 260. Typical Spectral Analysis of Surface Waves data.

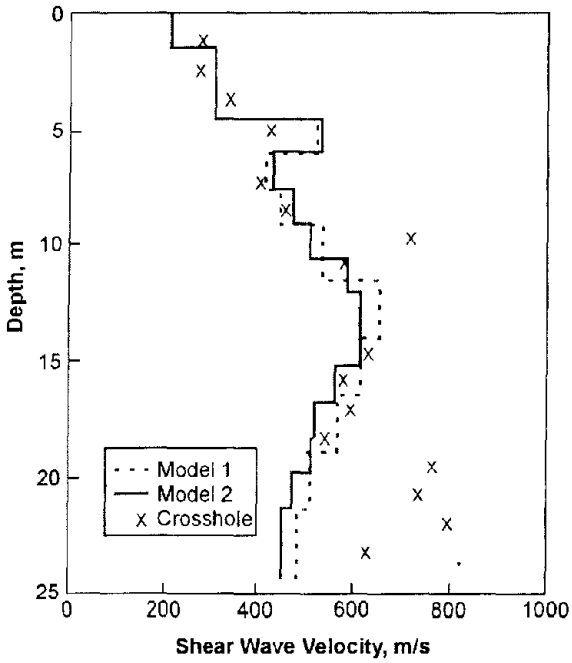

Figure 261. Inversion results of typical Spectral Analysis of Surface Waves data.

Data Acquisition

Most crews are equipped with a two- or four-channel spectrum analyzer, which provides the cross-spectral phase and coherence information. The degree of automation of the subsequent processing varies widely from laborious manual entry of the phase velocities into an analysis program to automated acquisition and preliminary processing. The inversion process similarly can be based on forward modeling with lots of human interaction or true inversion by computer after some manual smoothing.

A typical SASW crew consists of two persons, one to operate and coordinate the source and one to monitor the quality of the results. Typical field procedures are to place two (or four) geophones or accelerometers close together and to turn on the source. The source may be any mechanical source of high-frequency energy; moving bulldozers, dirt whackers, hammer blows, and vibrators have been used. Some discretion is advised as the source must operate for long periods of time, and the physics of what is happening are important. Rayleigh waves have predominantly vertical motion; thus, a source whose impedance is matched to the soil and whose energy is concentrated in the direction and frequency band of interest will be more successful.

Phase velocities are determined for waves with wavelength from 0.5 to 3 times the distance between the geophones. Then the phones are moved apart, usually increasing the separation by a factor of two. Thus, overlapping data are acquired, and the validity of the process is checked. This process continues until the wavelength being measured is equal to the required depth of investigation. Then the apparatus is moved to the next station where a sounding is required. After processing, a vertical profile of the shear-wave velocities is produced.

Advantages and Limitations

1. The assumption of plane layers from the source to the recording point may not be accurate.

2. Higher modes of the Rayleigh wave may be recorded. The usual processing assumption is that the fundamental mode has been measured.

3. Spreading the geophones across a lateral inhomogeneity will produce complications beyond the scope of the method.

4. Very high frequencies may be difficult to generate and record.

9.2.2.2 Common-Offset Rayleigh Wave Method

This method is also called Common-Offset Surface Waves. The method is quite effective at mapping inhomogeneities in the near surface, although it is not a frequently used method. The field techniques are easy to apply, and compared to other seismic methods, it is a rapid technique.

This method uses Rayleigh waves to detect fracture zones and associated voids. Rayleigh waves, also known as surface waves, have a particle motion that is counterclockwise with respect to the direction of travel. Figure 262 illustrates the particle motion for Rayleigh waves traveling in the positive X direction. In addition, the particle displacement is greatest at the ground surface, near the Rayleigh wave source, and decreases with depth. Three shot points are shown, labeled A, B, and C. The particle motion and displacement are shown for five depths under each shot point. For shot B, over the void, no Rayleigh waves are transmitted through the water/air filled void. This affects the measured Rayleigh wave recorded by the geophones over the void. Four parameters are usually observed. The first is an increase in the travel time of the Rayleigh wave as the fracture zone above the void is crossed. The second parameter is a decrease in the amplitude of the Rayleigh wave. The third parameter is reverberations (sometimes called ringing) as the void is crossed. The fourth parameter is a shift in the peak frequency toward lower frequencies. This is caused by trapped waves, similar to a tube wave in a borehole. The effective depth of penetration is approximately one-third to one-half of the wavelength of the Rayleigh wave.

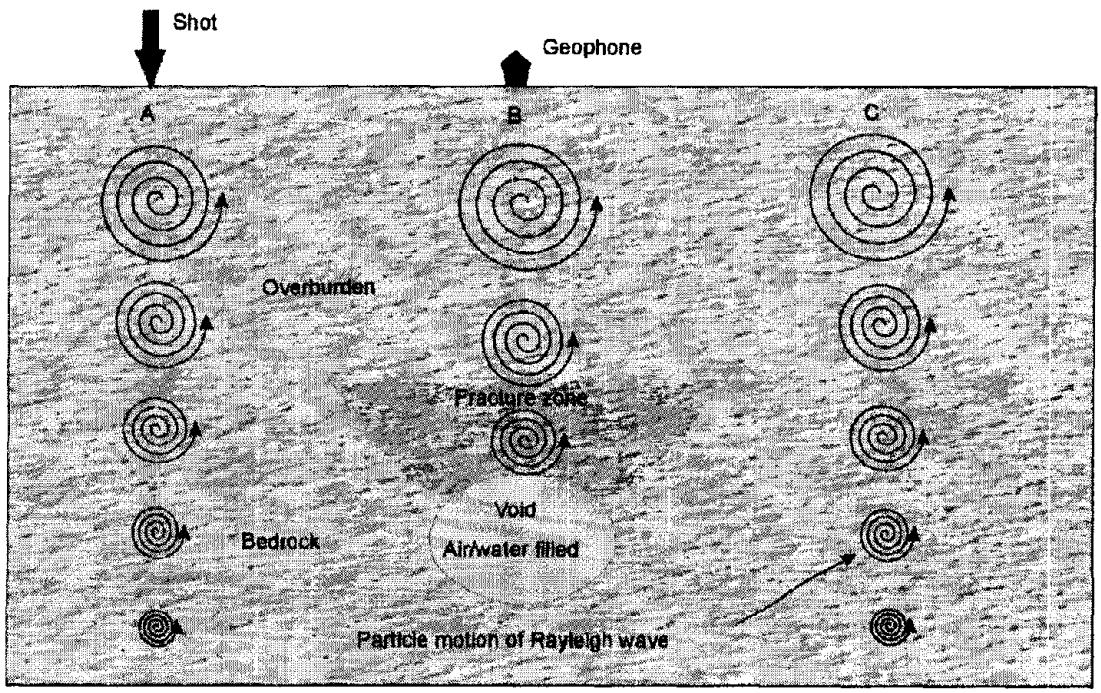

Figure 262. Rayleigh wave particle motion and displacement.

Rayleigh waves are created by any impact source. For shallow investigations, a hammer is all that is needed. Data are recorded using one geophone and one shot point. The distance between the shot and geophone depends on the depth of investigation and is usually about twice the expected target depth. Data are recorded at regular intervals across the traverse while maintaining the same shot geophone separation. The interval between stations depends on the expected size of the void/fracture zone and the desired resolution. Generally, in order to clearly see the void/fracture zone, it is desirable to have several stations that cross the area of interest. Figure 263 presents data from a common offset Rayleigh wave survey over a

void/fracture zone in an alluvial basin. The geophone traces are drawn horizontally with the vertical axis being distance (shot stations).

The data may be filtered to highlight the Rayleigh wave frequencies and is then plotted as shown on figure 263. Because the peak frequency of the seismic signal decreases over a void/fracture zone, a spectral analysis of the traces can assist in the interpretation of the data by highlighting the traces with lower frequencies. The data shown in figure 263 illustrate many of the features expected over a void/fracture zone. The travel time to the first arrival of the Rayleigh wave is greater across the void/fracture and is wider than the actual fractured zone. The amplitudes of the Rayleigh waves decrease as the zone is crossed. In addition, the wavelength of the signals over the fracture/void is longer than those over unfractured rock, showing that the high frequencies have been attenuated. Since the records are not long enough, the ringing effect is not presented in these data.

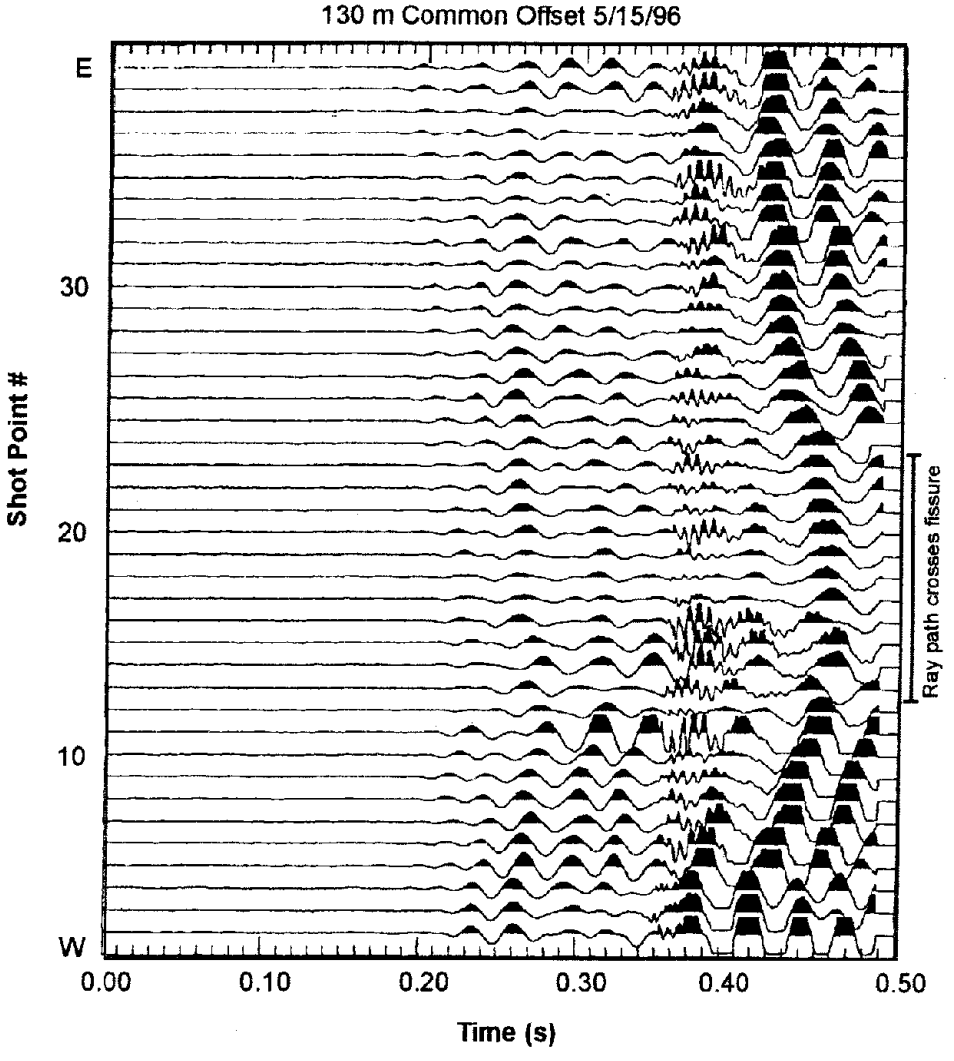

Figure 263. Data from a Rayleigh wave survey over a void/fracture zone.

Rayleigh waves are influenced by the shear strength of the rocks as well as fractures and voids, and changes in shear strength can cause anomalies similar to those obtained over these

features. The depth of penetration and target resolution are influenced by the wavelengths generated by the seismic source. Since longer wavelengths, which have lower resolution, are needed to investigate to greater depths, fractures and voids at depth need to be increasingly larger in order to be observed. However, this method is faster and less costly than most other seismic methods.

9.3 ELECTRICAL METHODS

Electrical geophysical prospecting methods detect the surface effects produced by electric current flow in the ground. Using electrical methods, one may measure potentials, currents, and electromagnetic fields that occur naturally or are introduced artificially in the ground. In addition, the measurements can be made in a variety of ways to determine a variety of results. There is a much greater variety of electrical and electromagnetic techniques available than in the other prospecting methods, where only a single field of force or anomalous property is used. Basically, however, it is the enormous variation in electrical resistivity found in different rocks and minerals that makes these techniques possible (Telford, et al., 1976).

Electrical Properties of Rocks

All materials, including soil and rock, have an intrinsic property, resistivity, that governs the relation between the current density and the gradient of the electrical potential. Variations in the resistivity of earth materials, either vertically or laterally, produce variations in the relations between the applied current and the potential distribution as measured on the surface, and thereby reveal something about the composition, extent, and physical properties of the subsurface materials. The various electrical geophysical techniques distinguish materials through whatever contrast exists in their electrical properties. Materials that differ geologically, such as described in a lithologic log from a drill hole, may or may not differ electrically and, therefore, may or may not be distinguished by an electrical resistivity survey. Properties that affect the resistivity of a soil or rock include porosity, water content, composition (clay mineral and metal content), salinity of the pore water, and grain size distribution.

In an electrically conductive body that lends itself to description as a one-dimensional body, such as an ordinary wire, the relationship between the current and potential distribution is described by Ohm's law:

$$V = IR \tag{52}$$

Where:

V = voltage,

I = current,

R = resistance.

The resistance (R) of a length of wire is given by

$$R = \rho \frac{L}{A}, \tag{53}$$

where

ρ = resistivity of the medium composing the wire,
L = length,
A = area of the conducting cross section.

Note that if R is expressed in ohms (Ω), the resistivity has the dimensions of ohms multiplied by a unit of length. It is commonly expressed in Ωm but may be given in Ω-cm or Ω-ft. The conductivity (σ) of a material is defined as the reciprocal of its resistivity (ρ). Resistivity is thus seen to be an intrinsic property of a material, in the same sense that density and elastic moduli are intrinsic properties.

In most earth materials, the conduction of electric current takes place virtually entirely in the water occupying the pore spaces or joint openings, since most soil- and rock-forming minerals are essentially nonconductive. Clays and a few other minerals, notably magnetite, specular hematite, carbon, pyrite, and other metallic sulfides, may be found in sufficient concentration to contribute measurably to the conductivity of the soil or rock.

Water, in a pure state, is virtually nonconductive but forms a conductive electrolyte with the presence of chemical salts in solution, and the conductivity is proportional to the salinity. The effect of increasing temperature is to increase the conductivity of the electrolyte. When the pore water freezes, there is an increase in resistivity, perhaps by a factor of 104 or 105, depending on the salinity. However, in soil or rock, this effect is diminished by the fact that the pore water does not all freeze at the same time, and there is usually some unfrozen water present even at temperatures considerably below freezing. The presence of dissolved salts and the adsorption of water on grain surfaces act to reduce the freezing temperature. Even so, electrical resistivity surveys made on frozen ground are likely to encounter difficulties because of the high resistivity of the frozen surface layer and high contact resistance at the electrodes. On the other hand, the effect of freezing on resistivity makes the resistivity method very useful in determining the depth of the frozen layer. It is very helpful in the interpretation of such surveys to have comparison data obtained when the ground is unfrozen.

Since the conduction of current in soil and rock is through the electrolyte contained in the pores, resistivity is governed largely by the porosity, or void ratio, of the material and the geometry of the pores. Pore space may be in the form of intergranular voids, joint or fracture openings, and blind pores, such as bubbles or vugs. Only the interconnected pores effectively contribute to conductivity, and the geometry of the interconnections, or the tortuosity of current pathways, further affects it. The resistivity ρ of a saturated porous material can be expressed as

$$\rho = F\rho_w, \tag{54}$$

where

F = formation factor,

ρ_W = resistivity of pore water.

The formation factor is a function only of the properties of the porous medium, primarily the porosity and pore geometry. An empirical relation, Archie's Law, is sometimes used to describe this relationship:

$$F = a\phi^{-m}, \tag{55}$$

where

a and m = empirical constants that depend on the geometry of the pores,

φ = porosity of the material.

Values of a in the range of 0.47 to 2.3 can be found in the literature. The value of m is generally considered to be a function of the kind of cementation present and is reported to vary from 1.3 for completely uncemented soils or sediments to 2.6 for highly cemented rocks, such as dense limestones. Equations 54 and 55 are not usually useful for quantitative interpretation of data from surface electrical surveys but are offered here to help clarify the role of the pore spaces in controlling resistivity.

Bodies of clay or shale generally have lower resistivity than soils or rocks composed of bulky mineral grains. Although the clay particles themselves are nonconductive when dry, the conductivity of pore water in clays is increased by the desorption of exchangeable cations from the clay particle surfaces.

Table 17 shows some typical ranges of resistivity values for manmade materials and natural minerals and rocks, similar to numerous tables found in the literature (van Blaricon 1980; Telford et al. 1976; Keller and Frischknecht 1966). The ranges of values shown are those commonly encountered but do not represent extreme values. It may be inferred from the values listed that the user would expect to find in a typical resistivity survey low resistivities for the soil layers, with underlying bedrock producing higher resistivities. Usually, this will be the case, but the particular conditions of a site may change the resistivity relationships. For example, coarse sand or gravel, if it is dry, may have a resistivity like that of igneous rocks, whereas a layer of weathered rock may be more conductive than the soil overlying it. In any attempt to interpret resistivities in terms of soil types or lithology, consideration should be given to the various factors that affect resistivity.

Table 17. Typical electrical resistivities of earth materials.

Material	Resistivity (Ωm)
Clay	1-20
Sand, wet to moist	20-200
Shale	1-500
Porous limestone	100-1,000
Dense limestone	1,000-1,000,000
Metamorphic rocks	50-1,000,000
Igneous rocks	100-1,000,000

Classification of Electrical Methods

The number of electrical methods used since the first application around 1830 (Parasnis 1962) is truly large; they include self-potential (SP), telluric currents and magnetotellurics, resistivity, equipotential and mise-à-la-masse, electromagnetic (EM), and induced polarization (IP). Because of the large number of methods, there are many ways of classifying them for discussion. One common method is by the type of energy source involved, that is, natural or artificial. Of the methods listed above, the first two are grouped under natural sources and the rest as artificial. Another classification, which will be used here, is to group by whether the data are measured in the time domain or the frequency domain. Only techniques in common use today for solving engineering, geotechnical, and environmental problems will be treated in this discussion, thus omitting telluric current techniques, magnetotellurics, and many of the EM methods.

Time domain methods (often abbreviated as TDEM or TEM) are those in which the magnitude only or magnitude and shape of the received signal is measured. The techniques in this class are discussed under the headings DC resistivity, induced polarization, time-domain electromagnetics, and self-potential. Frequency domain methods (often abbreviated as FDEM or FEM) are those in which the frequency content of the received signal is measured. Generally FDEM methods are continuous source methods, and measurements are made while the source is on. The measurement is of magnitude at a given frequency. Techniques in this class are discussed under the headings of VLF, terrain conductivity, and metal detectors.

Resistivity Methods Versus Electromagnetic Methods

Before discussing the individual methods, it is useful to outline the main differences between the resistivity (including induced polarization) methods and the electromagnetic methods. With resistivity methods, the source consists of electrical current injected into the ground through two electrodes. The transmitted current waveform may be DC, low- frequency sinusoidal (up to about 20 Hz), or rectangular, as in induced polarization surveys with a frequency of about 0.1 Hz. The energizer, therefore, is the electrical current injected into the ground through current electrodes.

With electromagnetic methods, the source most commonly consists of a closed loop of wire in which AC current flows. It can be a small, portable transmitter coil up to 1 m in diameter,

in which case there are many turns of wire. Alternately, the source can be a large transmitter loop on the ground, as large as 1 km in diameter. The frequency of the transmitter current can range from about 0.1 to about 10,000 Hz. Instruments commonly used for engineering applications (such as the EM-31, EM-34, and EM-38) use the small, multitum type of coil and frequencies above 2,500 Hz. Electric current in the transmitter loop generates a magnetic field. The magnetic field is the energizer in electromagnetic methods as compared with electric current in resistivity methods.

In terms of response, with resistivity methods, anomalies result from resistivity contrasts. For example, if a target with a resistivity of 10 Ωm is in a host rock with a resistivity of 100 Ωm, the same anomaly results as if the target had a resistivity of 100 Ωm in a host rock with a resistivity of 1,000 Ωm. In both cases, there is a resistivity contrast of 10. This example holds as long as the transmitter frequency is low enough that there is no appreciable electromagnetic induction in the rocks. With electromagnetic methods, anomalies are due more to absolute resistivity rather than resistivity contrasts. The two examples mentioned previously for resistivity methods would not produce the same anomalies with electromagnetic methods (Klein and Lajoie, 1980).

9.3.1 Self-Potential (SP) Method

Basic Concept

Various potentials are produced in native ground or within the subsurface altered by our actions. Natural potentials occur about dissimilar materials, near varying concentrations of electrolytic solutions, and due to the flow of fluids. Sulfide ore bodies have been sought by the self potential generated by ore bodies acting as batteries. Other occurrences produce spontaneous potentials, which may be mapped to determine the information about the subsurface. Spontaneous potentials can be produced by mineralization differences, electro-chemical action, geothermal activity, and bioelectric generation of vegetation.

Four different electrical potentials are recognized. Electrokinetic, or streaming, potential is due to the flow of a fluid with certain electrical properties passing through a pipe or porous medium with different electrical properties (figure 264). Liquid-junction, or diffusion, potential is caused by the displacement of ionic solutions of dissimilar concentrations. Mineralization, or electrolytic contact, potential is produced at the surface of a conductor with another medium. Nernst, or shale, potential occurs when similar conductors have a solution of differing concentrations about them. Telford, Geldart and Sheriff (1990) provide equations for differing potentials. Generally, the SP method is qualitative and does not attempt to quantify the anomalous volume size, owing to the unknown volumetric shapes, concentration/density of various masses, and electrical properties of the sought causative media.

Recognition of different spontaneous-potential sources is important to eliminate noise, the low background voltages. Some engineering and environmental occurrences may be mapped by contouring surficial voltages between base/reference electrode(s) and the mobile electrodes. Flow of gasses and fluids in pipes, leakage of a reservoir within the foundation or abutment of a dam, movement of ionic fluids to or within the groundwater, flow of

geothermal fluids, and movement of water into or through a karst system can be the origin of streaming potentials. These potentials may exceed the background voltage variation of a site.

Data Acquisition

A simple SP survey consists of a base electrode position and a roving electrode to determine potential differences on a gridded survey or along profile lines. The required equipment merely includes electrodes, wire, and a precise millivolt meter.

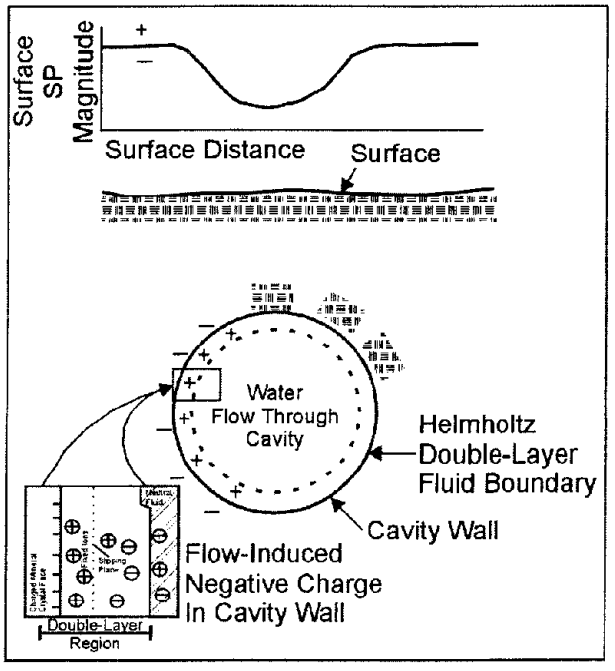

Figure 264. Schematic of flow-induced negative streaming potentials (Erchul and Slifer, 1989)

The electrodes in contact with the ground surface should be the nonpolarizing type, also called porous pots. Porous pots are metal electrodes suspended in a supersaturated solution of their own salts (such as a copper electrode suspended in copper sulfate) within a porous container. These pots produce very low electrolytic contact potential, such that the background voltage is as small as possible. Tinker and Rasor manufacture models of porcelain nonpolarizing electrodes that are reliable and sealed to avoid evaporation of the salt solution. Sealed pots can keep their supersaturated solutions for more than a week, even in arid locales. Refilling the pot with solution must occur before a day's work due to the possible contact potential change while performing a measurement set. A useful procedure is to mix remaining fluids from pots in a single container, add new solution to the mixture in the pot, and use the mixed solution to fill the pots. Then all pots contain the same solution mix.

Multiple pots are purchased such that breakage and cleaning may be accomplished readily in the field. Only one set of a base and mobile electrode are used at any one measurement loop/grid. Base station pots are usually larger in size to assure constant electrical contact through the time of use of that station. Mobile or traveling pots are often smaller in volume of salt solution and size.

Copper-clad steel electrodes are used in a variety of electrical surveys. Steel electrodes should be avoided in SP investigations. Contact potential of these electrodes is quite high and variable in the soil at various stations of the survey.

Survey Wire. The wire used in SP surveys must be strong, hardy, and of low resistance. Wire needs to have sufficient tensile strength to be able to withstand long-term pulls of survey work for multiple sites. For some field use, heavy twine or light rope may need to be twisted and knotted to long lengths of wire to add strength. Survey wire must have abrasion-resistant insulator wrapping. Pulling the wire over roadway surfaces can expose bare wire. Usually random bare wire positions will not fully ground to the soil, and the effects will be variable as differing lengths of wire are unreeled and occupy differing positions for the survey. This error will only modify the signal by a few to tens of millivolts (mV). Twisted two-conductor, 18-gauge, multistrand (not solid conductor) copper wire has been found to be strong and abrasion resistant.

Resistance will be constant for survey wire between stations if the wire for a reading set is not permanently stretched in length, does not develop insulator leaks, and is not repaired. Repairs to wire should be made when needed because of bare wire or severe plastic stretching of the wire. Repairs and addition of wire to lengthen the survey use should only be made between measurement loops/grids. No changes to the wire may be made during a loop or grid of readings without reoccupation of those positions. Wire accidentally severed requires a remeasurement of that complete set of circuit stations.

Millivolt Meter. An inexpensive, high-input-impedance voltmeter is used to read the potential in the millivolt range. Actual field voltage will be in error when the source potential is within an order of magnitude of the input impedance of the meter. The meter uses a bias current to measure the desired potential. The input impedance should exceed 50 MΩ. Higher input impedances are desirable due to the impedance reduction of air's moisture. The resolution of the meter should be 0.1 or 1.0 mV.

Several useful options on meters are available. Digital voltmeters are more easily read. Water-resistant or sealed meters are extremely beneficial in field use. Notch filters about 60 Hz will reduce stray alternating current (AC) potentials in industrial areas or near power lines.

Field Deployment. Background potentials for these surveys may be at a level of a few tens of millivolts. Source self-potentials must exceed the background to be apparent. Potentials exceeding 1.0 *V* have occurred for shallow or downhole measurements of large sources. When large potentials are expected or have been found at the site with nonpolarizing electrodes, the easier to use copper-clad steel electrodes have been substituted for porous pots, but steel electrodes are not recommended. Contact potentials of the steel electrodes and reversing electrode positions are required systematically for steel electrodes. Large errors may develop from the use of steel electrodes (Corwin 1989).

Measurements with the electrodes may require a system of reversing the electrode position to resolve contact potentials at the electrodes. Previously measured locations may need to be remeasured on a systematic or periodic basis. Reoccupation of stations is necessary when

very accurate surveys are being conducted and for sites with temporal potential changes or spatial variations of electrode potential. Changes temporally in the electrodes or due to the self potential of the field require the survey to be conducted in a gridded or loop array. Loops should have closure voltages of zero or only a few millivolts. High closure potential requires remeasuring several to all of the loop stations. Station reoccupation should be in the same exact position of the earlier reading(s). Unclosed lines should be avoided. Reoccupation of particular station intervals should be made when closed loops are not possible.

The traveling electrode should periodically remeasure the base location to observe contact potential, dirty electrodes, or other system changes. Reversing the survey electrodes or changing the wire polarity should only change the voltage polarity.

Electrodes may have contact differences due to varying soil types, chemical variations, or soil moisture. Temporal and temperature variations are also possible, which may require the reoccupation of some of the survey positions on some arranged loop configuration. Electrode potentials have minor shifts with temperature changes (Ewing 1939). Variation in the flow of fluid due to rainfall, reservoir elevation changes, channelization of flow, or change of surface elevation where measurements are obtained are sources of variation of streaming potential. Self potentials may have temporal or spatial changes due to thunderstorm cloud passage, dissemination of mineralization or electrolytic concentration, and in the groundwater flow conduits and location. High telluric potential variations may require the SP survey to be delayed for a day.

Some simple procedures are required to perform accurate and precise SP surveys. Good maintenance of porous pots, wires, and voltmeters must be observed through the survey. The traveling pot needs to be kept clean of soil with each position. Contact with moist soil, or more elaborate measures for good electrical contact with roadways or rock, must be assured. A water vessel may be carried to moisten the soil hole and clean the porcelain surface. Wire reels speed the pulling of cable and wire recovery for changing loops, and lessen wear on the cable. Reversing the wire polarity for some measurements and reoccupation of adjacent stations assures the cable has not been grounded or stripped. Repair and checking of the wire must be made between loops and is easily done when rewinding the cable reel.

Quality assurance in the field is conducted by reoccupation of loop closure points with the same base position. Repeated and reversed readings of particular loop-end stations and checking base locations provide statistics for the assessment of measurement quality.

Grid surveys offer some advantages in planning SP surveys. Changes in elevation (changing the distance to the potential source) and cognizance of cultural effects can be minimized with planning survey grids or loops. AC power lines, metal fences, and underground utilities are cultural features that affect the potential field extraneous to the normal sources of interest.

Data Interpretation

Most SP investigations use a qualitative evaluation of the profile amplitudes or grid contours to evaluate self- and streaming-potential anomalies. Flow sources produce potentials in the

direction of flow. Fluid inflow produces negative relative potentials, as would greater distance from the flow tube; outflow of the fluid results in positive potentials.

Quantitative interpretations for a dam embankment with possible underseepage would be determined from the profiles across the crest. Negative anomalies may be indicative of flow from the reservoir at some depth. The width of the half-amplitude provides a depth estimate. Outflow at the toe of an embankment or at shallow depths beneath the toe would produce positive, narrow anomalies. Mineral or cultural utilities produce varying surface potentials depending on the source. Semiquantitative, forward solutions may be estimated by equations or programs (Corwin, 1989; Wilt and Butler, 1990) for sphere, line, and plate potential configurations. These solutions of potential configurations aid in evaluation of the corrected field readings, but are solutions of the data set taken.

Sample Field Surveys

Geothermal use of the SP method is documented in Corwin and Hoover (1979). Erchul and Slifer (1989) provide the included example for karst surveys. The leakage of water from a reservoir (Butler, et al., 1989, Llopis and Butler, 1988) through an abutment and the movement of rainfall into and through a karst system produce streaming potentials. High reservoir leakage through rock or soil forms the greatest streaming potential when confined flow conduits develop instead of diffuse flow through pore space. SP surveys have been recommended for grouting location, split spacing and effectiveness. The self-potential due to water flow is a direct parameter for the grouting remediation of reservoir leakage.

SP methods can be very useful for karst groundwater regimes in quick surveys of a site or in long-term surveys during a rainy season. Sinkholes can be pathways of surface water flow. The subsurface flow in karst can be erratic. Figure 265 shows the ability of an SP survey to resolve groundwater flow. Note the grid approach used in the survey for this site. There can be a qualitative evaluation of the flow volume in different subsurface routes if the ground surface may be assumed parallel to the surface through the irregular flow paths.

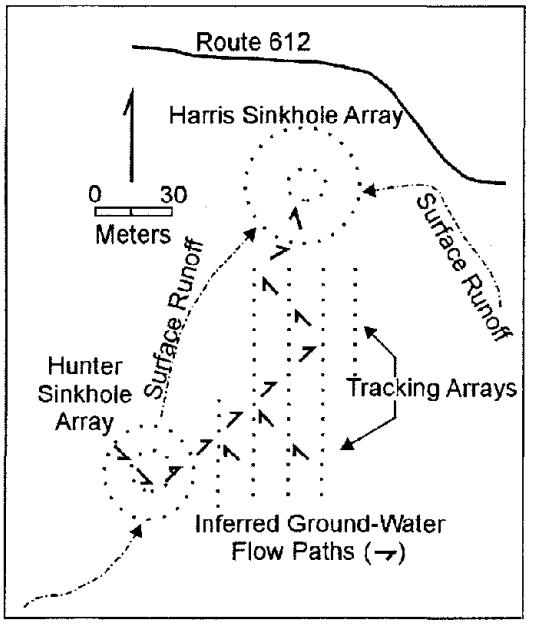

Figure 265. Electrode configurations at the Harris-Hunter sinkhole site, showing groundwater flowpaths inferred by SP anomalies. (Erchul and Slifer, 1989)

9.3.2 Equipotential and Mise-a-la-Masse Methods

Basic Concept

According to Parasnis (1973), the equipotential method was one of the first electrical methods and was used as far back as 1912 by Schlumberger. As explained elsewhere in this volume, when electric energy is applied to two points at the ground surface, an electric current will flow between them because of their difference in potential. If the medium between the two electrodes is homogeneous, the current and potential distribution is regular and may be calculated. When good or poor conductors are imbedded in this homogeneous medium, a distortion of the electrical field occurs. Good conductors have a tendency to attract the current lines toward them, whereas poor conductors force current flow away. Theoretically, it should be possible to detect bodies of different conductivity by measuring the geometric pattern of these current lines. In practice, this cannot be done with sufficient accuracy; it is necessary to determine the direction in which no current flows by locating points that have no potential difference (Heiland, 1940). The lines of identical potential, called equipotential lines, are at right angles to the current lines. The equipotentials are circles in the immediate vicinity of the electrodes.

In the past, equipotentials were traced individually in the field by using a null galvanometer, but such a procedure was tedious and time-consuming. The modern practice is to measure the electric voltage at each observation point with respect to a fixed point, plot the results, and draw contours. The equipotential method was used extensively in the early days of geophysics, but has been almost completely replaced by modern resistivity and electromagnetic methods. When the method is used, it is usually in a reconnaissance mode, and quantitative interpretation of equipotential surveys is rarely attempted.

Mise-a-la-masse

One variant of the method, called mise-a-la-masse, is still used in mining exploration and occasionally in geotechnical applications. The name, which may be translated as "excitation of the mass," describes an electrode array, which uses the conductive mass under investigation as one of the current electrodes. In mining, the conductive mass is a mineral body exposed in a pit or drill hole. In geotechnical applications, the object under investigation might be one end of an abandoned metal waste pipe. The second current electrode is placed a large distance away. "Large" usually means five or ten times the size of the mass being investigated. The potential distribution from these two current electrodes will, to some extent, reflect the geometry of the conductive mass and would be expected to yield some information concerning the shape and extent of the body. The left-hand part of figure 266 (Parasnis, 1973) shows the equipotentials around a subsurface point electrode in a homogeneous isotropic earth. The right-hand part shows (schematically) the distribution of potentials such as might be expected when the point current electrode is placed in a conducting body situated in an otherwise homogeneous earth of lesser conductivity. In this case, the equipotentials tend to follow the ore body, and on the ground surface, the centroid of the equipotential map does not coincide with the point on the ground vertically above the electrode in the borehole.

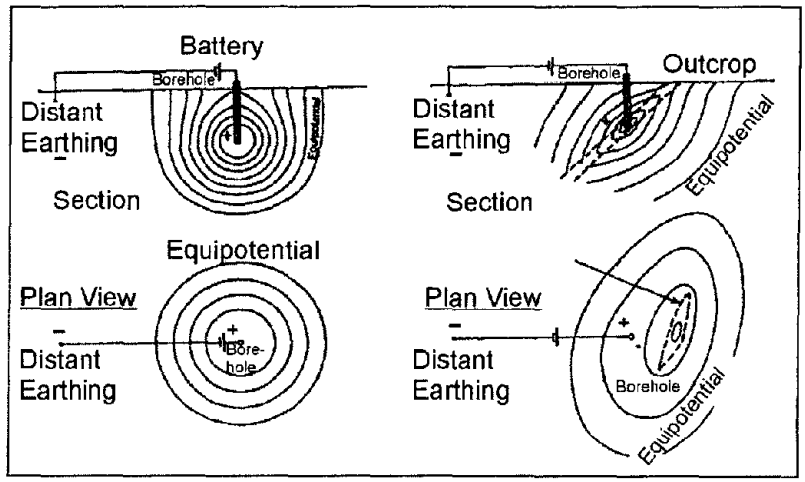

Figure 266. Principle of the mise-a-la-masse method. Right side of figure shows distortion of the equipotential lines due to conductive ore body. (Parasnis, 1973; Copyright permission granted by Elsevier Science)

Example 1 - Buried Ammunition Magazine. Although equipotential surveys have all but been replaced by the mise-a-la-masse variant, there are occasions when passing an electric current directly through the mass under investigation might be ill advised. Such a case is shown in figure 267, in which Heiland (1940) shows the results of a classic equipotential survey over an abandoned ammunition magazine. Distortion of the equipotential lines clearly outlines the magazine, and shows that expensive and/or sophisticated techniques are not always necessary.

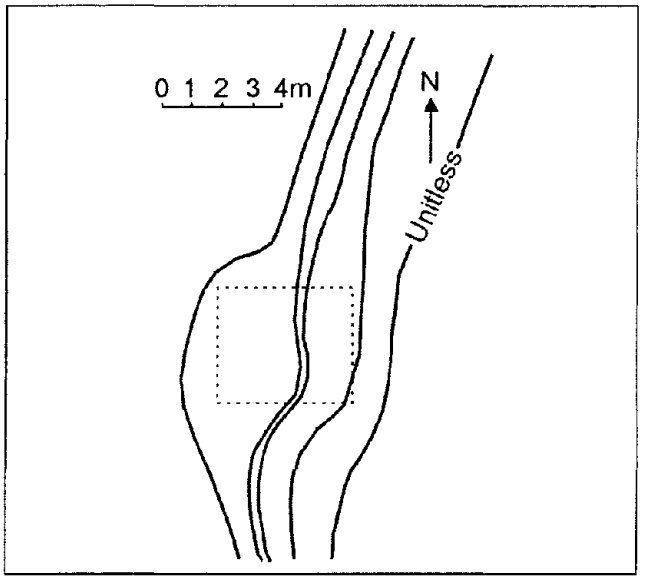

Figure 267. Location of a buried ammunition magazine by equipotential methods. (Heiland 1940)

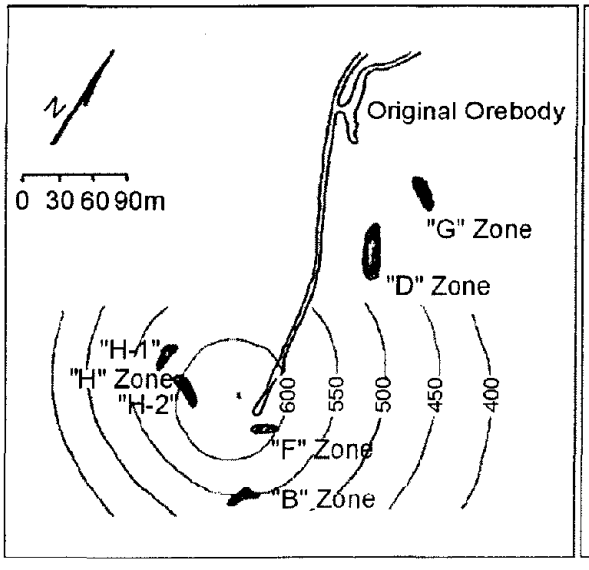

Figure 268. Potential pattern from current source in test position. (Modified from Hallof, 1980)

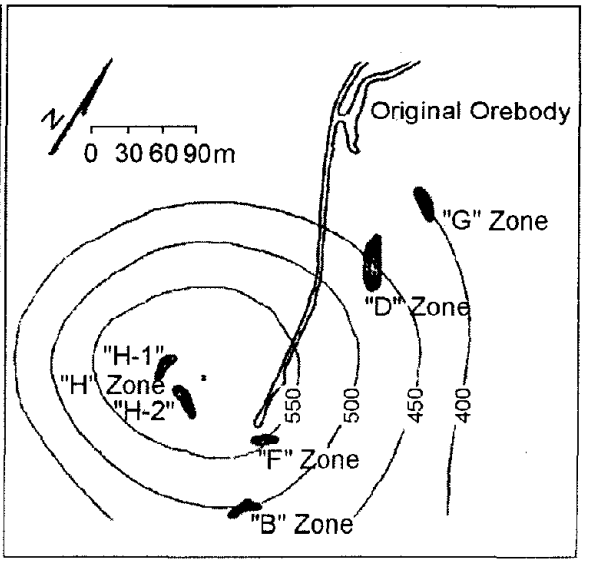

Figure 269. Potential pattern from current source in H-1 zone (Modified from Hallof, 1980)

Example 2 - Advance of Groundwater from an Infiltration Pit. Only one example of mise-a-la-masse used for groundwater investigations was found in the literature. Cahyna, Mazac, and Vendhodova (1990) claim a mise-a-la-masse survey was successfully used to determine the prevailing direction of groundwater leaving an infiltration pit, but unfortunately no figures are included.

Example 3 - Partially Exposed Buried Conductors. The need sometimes arises in hazardous-waste site restoration to trace the extent of buried metal objects such as pipes, cables, and

tanks. Often electromagnetic and/or magnetic methods are used to trace these objects, but a special opportunity arises for surveying by mise-a-la-masse when part of the object under investigation has been partially exposed at the surface or in a drill hole. Although no geotechnical examples were found in the literature, one of the numerous mining examples will be used, as the results should be similar. Hallof (1980) shows the results of a mise-a-la-masse survey at York Harbour, Newfoundland, where sulfides were exposed in underground workings. The objective was to find where the ore most closely approached the surface, and if the H-1 zone and the H-2 zone were the lower portions of a single zone near the surface. Figure 268 shows the equipotential pattern for the near current electrode located at depth but NOT in one of the ore zones. The pattern is nearly circular, and its center is immediately above the current electrode at depth. This was not the case when the current electrode was placed first in the H-1 zone (figure 269) and then in the H-2 zone (not shown). In both cases the center of the surface potential distribution is considerably to the east of the underground position of the mineralization. Further, since almost exactly the same potential distribution was measured for both locations for the current electrode at depth, both zone H-1 and zone H-2 are probably part of a single mineralization that has its most shallow position beneath the center of the surface potential pattern.

9.3.3 Resistivity Methods

Introduction

Surface electrical resistivity surveying is based on the principle that the distribution of electrical potential in the ground around a current-carrying electrode depends on the electrical resistivities and distribution of the surrounding soils and rocks. The usual practice in the field is to apply an electrical direct current (DC) between two electrodes implanted in the ground and to measure the difference of potential between two additional electrodes that do not carry current. Usually, the potential electrodes are in line between the current electrodes, but in principle, they can be located anywhere. The current used is either direct current, commutated direct current (i.e., a square-wave alternating current), or AC of low frequency (typically about 20 Hz). All analysis and interpretation are done on the basis of direct currents. The distribution of potential can be related theoretically to ground resistivities and their distribution for some simple cases, notably, the case of a horizontally stratified ground and the case of homogeneous masses separated by vertical planes (e.g., a vertical fault with a large throw or a vertical dike). For other kinds of resistivity distributions, interpretation is usually done by qualitative comparison of observed response with that of idealized hypothetical models or on the basis of empirical methods.

Mineral grains comprised of soils and rocks are essentially nonconductive, except in some exotic materials such as metallic ores, so the resistivity of soils and rocks is governed primarily by the amount of pore water, its resistivity, and the arrangement of the pores. To the extent that differences of lithology are accompanied by differences of resistivity, resistivity surveys can be useful in detecting bodies of anomalous materials or in estimating the depths of bedrock surfaces. In coarse, granular soils, the groundwater surface is generally marked by an abrupt change in water saturation and thus by a change of resistivity. In fine-grained soils, however, there may be no such resistivity change coinciding with a piezometric surface. Generally, since the resistivity of a soil or rock is controlled primarily

by the pore water conditions, there are wide ranges in resistivity for any particular soil or rock type, and resistivity values cannot be directly interpreted in terms of soil type or lithology. Commonly, however, zones of distinctive resistivity can be associated with specific soil or rock units on the basis of local field or drill hole information, and resistivity surveys can be used profitably to extend field investigations into areas with very limited or nonexistent data. Also, resistivity surveys may be used as a reconnaissance method, to detect anomalies that can be further investigated by complementary geophysical methods and/or drill holes.

The electrical resistivity method has some inherent limitations that affect the resolution and accuracy that may be expected from it. Like all methods using measurements of a potential field, the value of a measurement obtained at any location represents a weighted average of the effects produced over a large volume of material, with the nearby portions contributing most heavily. This tends to produce smooth curves, which do not lend themselves to high resolution for interpretations. Another feature common to all potential field geophysical methods is that a particular distribution of potential at the ground surface does not generally have a unique interpretation. Although these limitations should be recognized, the non-uniqueness or ambiguity of the resistivity method is scarcely less than with the other geophysical methods. For these reasons, it is always advisable to use several complementary geophysical methods in an integrated exploration program rather than relying on a single exploration method.

Theory

Data from resistivity surveys are customarily presented and interpreted in the form of values of apparent resistivity ρ_a. Apparent resistivity is defined as the resistivity of an electrically homogeneous and isotropic half-space that would yield the measured relationship between the applied current and the potential difference for a particular arrangement and spacing of electrodes. An equation giving the apparent resistivity in terms of applied current, distribution of potential, and arrangement of electrodes can be arrived at through an examination of the potential distribution due to a single current electrode. The effect of an electrode pair (or any other combination) can be found by superposition. Consider a single point electrode, located on the boundary of a semi-infinite, electrically homogeneous medium, which represents a fictitious homogeneous earth. If the electrode carries a current I, measured in amperes (a), the potential at any point in the medium or on the boundary is given by:

$$U = \rho \frac{I}{2\pi r}, \tag{56}$$

where

U = potential, in V,

ρ = resistivity of the medium,

r = distance from the electrode.

The mathematical demonstration for the derivation of the equation may be found in textbooks on geophysics, such as Keller and Frischknecht (1966).

For an electrode pair with current I at electrode A, and -I at electrode B (figure 270), the potential at a point is given by the algebraic sum of the individual contributions:

$$U = \frac{\rho I}{2\pi r_A} - \frac{\rho I}{2\pi r_B} = \frac{\rho I}{2\pi}\left[\frac{1}{r_A} - \frac{1}{r_B}\right], \tag{57}$$

where

r_A and r_B = distances from the point to electrodes *A* and *B*

Figure 270 illustrates the electric field around the two electrodes in terms of equipotentials and current lines. The equipotentials represent imagery shells, or bowls, surrounding the current electrodes, and on any one of which the electrical potential is everywhere equal. The current lines represent a sampling of the infinitely many paths followed by the current, paths that are defined by the condition that they must be everywhere normal to the equipotential surfaces.

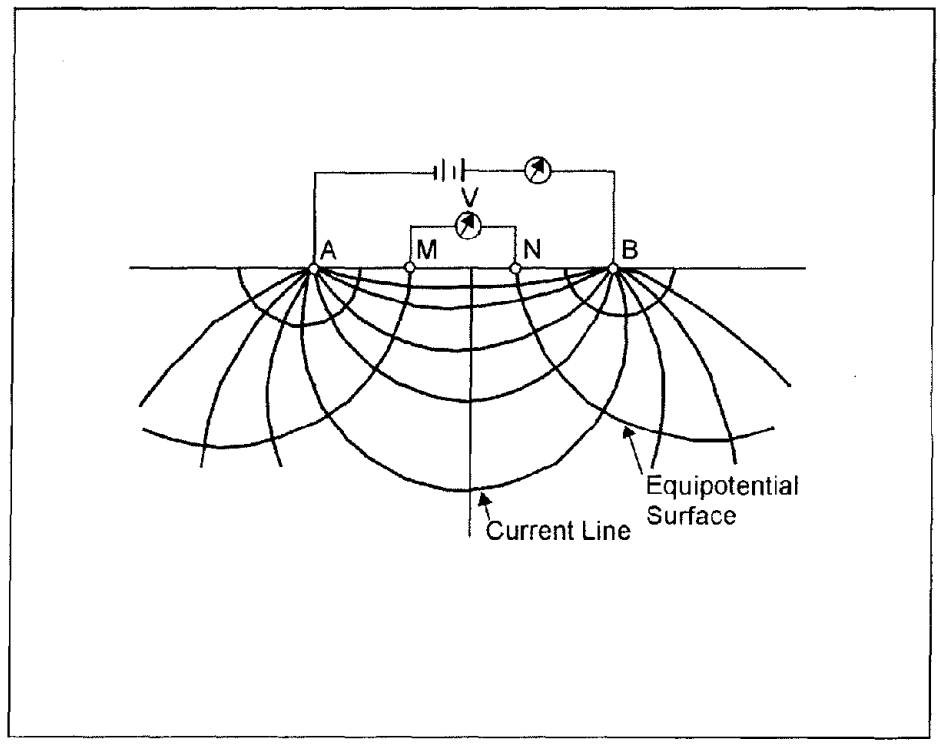

Figure 270. Equipotentials and current lines for a pair of current electrodes A and B on a homogeneous half-space.

In addition to current electrodes A and B, figure 270 shows a pair of electrodes M and N, which carry no current, but between which the potential difference V may be measured. Following the previous equation, the potential difference *V* may be written

$$V = U_M - U_N = \frac{\rho I}{2\pi}\left[\frac{1}{\overline{AM}} - \frac{1}{\overline{BM}} + \frac{1}{\overline{BN}} - \frac{1}{\overline{AN}}\right], \tag{58}$$

where

U_M and U_N = potentials at M and N,

AM = distance between electrodes A and M, etc.

These distances are always the actual distances between the respective electrodes, whether or not they lie on a line. The quantity inside the brackets is a function only of the various electrode spacings. The quantity is denoted $1/K$, which allows rewriting the equation as:

$$V = \frac{\rho I}{2\pi}\frac{1}{K}, \tag{59}$$

where

K = array geometric factor.

Equation 58 can be solved for ρ to obtain:

$$\rho = 2\pi K\frac{V}{I}, \tag{60}$$

The resistivity of the medium can be found from measured values of V, I, and K, the geometric factor. K is a function only of the geometry of the electrode arrangement.

Apparent Resistivity

Wherever these measurements are made over a real heterogeneous earth, as distinguished from the fictitious homogeneous half-space, the symbol ρ is replaced by ρ_a for apparent resistivity. The resistivity surveying problem is, reduced to its essence, the use of apparent resistivity values from field observations at various locations and with various electrode configurations to estimate the true resistivities of the several earth materials present at a site and to locate their boundaries spatially below the surface of the site.

An electrode array with constant spacing is used to investigate lateral changes in apparent resistivity reflecting lateral geologic variability or localized anomalous features. To investigate changes in resistivity with depth, the size of the electrode array is varied. The apparent resistivity is affected by material at increasingly greater depths (hence larger volume) as the electrode spacing is increased. Because of this effect, a plot of apparent resistivity against electrode spacing can be used to indicate vertical variations in resistivity.

The types of electrode arrays that are most commonly used (Schlumberger, Wenner, and dipole-dipole) are illustrated in figure 271. There are other electrode configurations that are used experimentally or for non-geotechnical problems or are not in wide popularity today. Some of these include the Lee, half-Schlumberger, polar dipole, bipole dipole, and gradient arrays. In any case, the geometric factor for any four-electrode system can be found from

equation 58 and can be developed for more complicated systems by using the rule illustrated by equation 57. It can also be seen from equation 58 that the current and potential electrodes can be interchanged without affecting the results; this property is called reciprocity.

Schlumberger Array

For this array (figure 271a), in the limit as a approaches zero, the quantity V/a approaches the value of the potential gradient at the midpoint of the array. In practice, the sensitivity of the instruments limits the ratio of s to a and usually keeps it within the limits of about 3 to 30. Therefore, it is typical practice to use a finite electrode spacing and equation 57 to compute the geometric factor (Keller and Frischknecht, 1966). The apparent resistivity (ρ) is:

$$\rho_a = \pi\left[\frac{s^2}{a} - \frac{a}{4}\right]\frac{V}{I} = \pi a\left[\left(\frac{s}{a}\right)^2 - \frac{1}{4}\right]\frac{V}{I}, \tag{61}$$

In usual field operations, the inner (potential) electrodes remain fixed, while the outer (current) electrodes are adjusted to vary the distance s. The spacing a is adjusted when it is needed because of decreasing sensitivity of measurement. The spacing a must never be larger than $0.4s$ or the potential gradient assumption is no longer valid. Also, the a spacing may sometimes be adjusted with s held constant in order to detect the presence of local inhomogeneities or lateral changes in the neighborhood of the potential electrodes.

Wenner Array

This array (figure 271b) consists of four electrodes in line, separated by equal intervals, denoted a. Applying equation 57, the user will find that the geometric factor K is equal to a, so the apparent resistivity is given by:

$$\rho_a = 2\pi a\frac{V}{I}, \tag{62}$$

Although the Schlumberger array has always been the favored array in Europe, until recently, the Wenner array was used more extensively than the Schlumberger array in the United States. In a survey with varying electrode spacing, field operations with the Schlumberger array are faster, because all four electrodes of the Wenner array are moved between successive observations, but with the Schlumberger array, only the outer ones need to be moved. The Schlumberger array also is said to be superior in distinguishing lateral from vertical variations in resistivity. On the other hand, the Wenner array demands less instrument sensitivity, and reduction of data is marginally easier.

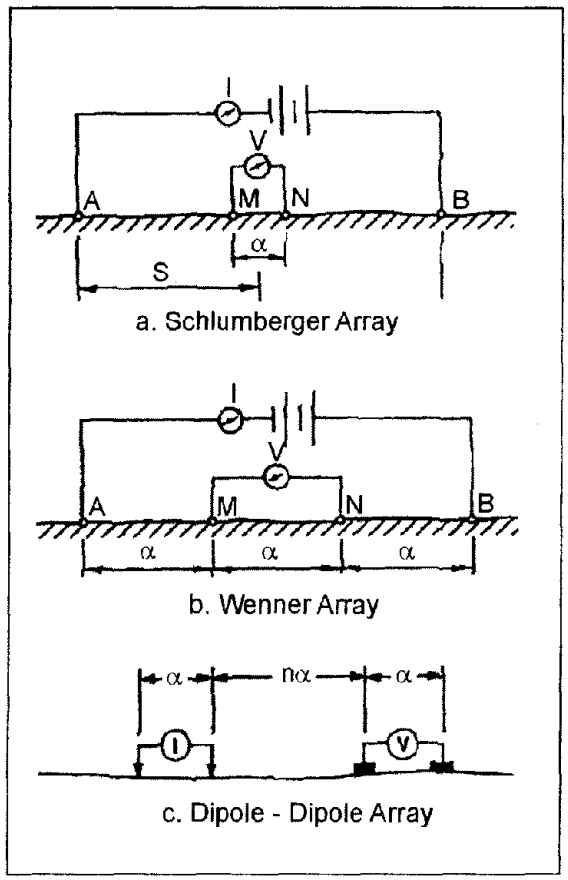

Figure 271. Electrode array configurations for resistivity measurements.

Dipole-dipole Array

The dipole-dipole array (figure 271c) is one member of a family of arrays using dipoles (closely spaced electrode pairs) to measure the curvature of the potential field. If the separation between both pairs of electrodes is the same *a,* and the separation between the centers of the dipoles is restricted to *a(n+1)*, the apparent resistivity is given by:

$$\rho_a = \pi an(n+1)(n+2)\frac{V}{I}, \tag{63}$$

This array is especially useful for measuring lateral resistivity changes and has been increasingly used in geotechnical applications.

Depth of Investigation

To illustrate the major features of the relationship between apparent resistivity and electrode spacing, figure 272 shows a hypothetical earth model and some hypothetical apparent resistivity curves. The earth model has a surface layer of resistivity ρ1 and a basement layer of resistivity ρn that extends downward to infinity (figure 272a). There may be intermediate layers of arbitrary thicknesses and resistivities. The electrode spacing may be either the

Wenner spacing *a* or the Schlumberger spacing *a*; curves of apparent resistivity versus spacing will have the same general shape for both arrays, although they will not generally coincide.

For small electrode spacings, the apparent resistivity is close to the surface layer resistivity, whereas at large electrode spacings, it approaches the resistivity of the basement layer. Every apparent resistivity curve thus has two asymptotes, the horizontal lines $\rho_a = \rho_1$ and $\rho_a = \rho_n$, that it approaches at extreme values of electrode spacing. This is true whether ρ_n is greater than ρ_1, as shown in figure 272b, or the reverse. The behavior of the curve between the regions where it approaches the asymptotes depends on the distribution of resistivities in the intermediate layers. Curve A represents a case in which there is an intermediate layer with a resistivity greater than ρ_n. The behavior of curve B resembles that for the two-layer case or a case where resistivities increase from the surface down to the basement. The curve might look like curve C if there were an intermediate layer with resistivity lower than ρ_1. Unfortunately for the interpreter, neither the maximum of curve A nor the minimum of curve C reach the true resistivity values for the intermediate layers, though they may be close if the layers are very thick.

There is no simple relationship between the electrode spacing at which features of the apparent resistivity curve are located and the depths to the interfaces between layers. The depth of investigation will ALWAYS be less than the electrode spacing. Typically, a maximum electrode spacing of three or more times the depth of interest is necessary to assure that sufficient data have been obtained. The best general guide to use in the field is to plot the apparent resistivity curve (figure 272b) as the survey progresses, so that it can be judged whether the asymptotic phase of the curve has been reached.

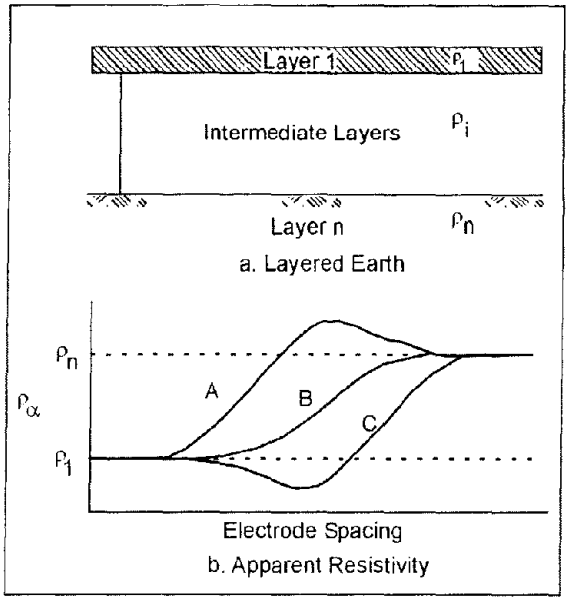

Figure 272. Asymptotic behavior of the apparent resistivity curves at very small and very large electrode spacings.

Instruments and Measurements

The theory and field methods used for resistivity surveys are based on the use of direct current, because it allows greater depth of investigation than alternating current and because it avoids the complexities caused by effects of ground inductance and capacitance and resulting frequency dependence of resistivity. However, in practice, actual direct current is infrequently used for two reasons: (1) direct current electrodes produce polarized ionization fields in the electrolytes around them, and these fields produce additional electromotive forces that cause the current and potentials in the ground to be different from those in the electrodes; and (2) natural Earth currents (telluric currents) and spontaneous potentials, which are essentially unidirectional or slowly time-varying, induce potentials in addition to those caused by the applied current. The effects of these phenomena, as well as any others that produce unidirectional components of current or potential gradients, are reduced by the use of alternating current, because the polarized ionization fields do not have sufficient time to develop in a half-cycle, and the alternating component of the response can be measured independently of any superimposed direct currents. The frequencies used are very low, typically below 20 Hz, so that the measured resistivity is essentially the same as the direct current resistivity.

In concept, a direct current (I), or an alternating current of low frequency, is applied to the current electrodes, and the current is measured with an ammeter. Independently, a potential difference V is measured across the potential electrodes, and, ideally, there should be no current flowing between the potential electrodes. This is accomplished either with a null-balancing galvanometer (old technology) or very high input impedance operational amplifiers. A few resistivity instruments have separate "sending" and "receiving" units for current and potential; but in usual practice, the potential measuring circuit is derived from the same source as the potential across the current electrodes, so that variations in the supply voltage affect both equally and do not affect the balance point.

Power is usually supplied by dry cell batteries in the smaller instruments and motor generators in the larger instruments. From 90 V up to several hundred volts may be used across the current electrodes in surveys for engineering purposes. In the battery-powered units, the current usually is small and is applied only for very short times while the potential is being measured, so battery consumption is low. Care should be taken to NEVER energize the electrodes while they are being handled, because with applied potentials of hundreds of volts, DANGEROUS AND POTENTIALLY LETHAL shocks could be caused.

Current electrodes used with alternating current (or commutated direct current) instruments commonly are stakes of bronze, copper, steel with bronze jackets, or, less desirably, steel, about 50 cm in length. They must be driven into the ground far enough to make good electrical contact. If there is difficulty because of high contact resistance between electrodes and soil, it can sometimes be alleviated by pouring salt water around the electrodes. Many resistivity instruments include an ammeter to verify that the current between the current electrodes is at an acceptable level, a desirable feature. Other instruments simply output the required potential difference to drive a selected current into the current electrodes. Typical currents in instruments used for engineering applications range from 2 mA to 500 mA. If the current is too small, the sensitivity of measurement is degraded. The problem may be

corrected by improving the electrical contacts at the electrodes. However, if the problem is due to a combination of high earth resistivity and large electrode spacing, the remedy is to increase the voltage across the current electrodes. Where the ground is too hard or rocky to drive stakes, a common alternative is sheets of aluminum foil buried in shallow depressions or within small mounds of earth and wetted.

One advantage of the four-electrode method is that measurements are not sensitive to contact resistance at the potential electrodes so long as it is low enough that a measurement can be made, because observations are made with the system adjusted so that there is no current in the potential electrodes. With zero current, the actual value of contact resistance is immaterial, since it does not affect the potential. On the current electrodes also, the actual value of contact resistance does not affect the measurement, so long as it is small enough that a satisfactory current is obtained, and so long as there is no gross difference between the two electrodes. Contact resistance affects the relationship between the current and the potentials on the electrodes, but because only the measured value of current is used, the potentials on these electrodes do not figure in the theory or interpretation.

When direct current is used, special provisions must be made to eliminate the effects of electrode polarization and telluric currents. A nonpolarizing electrode is available in the form of a porous, unglazed ceramic pot, which contains a central metallic electrode, usually copper, and is filled with a liquid electrolyte that is a saturated solution of a salt of the same metal (copper sulphate is used with copper). The central electrode is connected to the instrument, and electrical contact with the ground is made through the electrolyte in the pores of the ceramic pot. This type of electrode may be advantageous for use on rock surfaces where driving rod-type electrodes is difficult. Good contact of the pot with the ground can be aided by clearing away grass and leaves beneath it, embedding it slightly in the soil, and if the ground is dry, pouring a small amount of water on the surface before placing the pot. The pots must be filled with electrolyte several hours before they are used to allow the electrolyte to penetrate the fine pores of the ceramic. The porous pot electrodes should be checked every several hours during the field day to verify the electrolyte level and the presence of the solid salt to maintain the saturated solution.

Telluric currents are naturally occurring electric fields that are widespread, some being of global scale. They are usually of small magnitude, but may be very large during solar flares or if supplemented by currents of artificial origin. Spontaneous potentials in the earth may be generated by galvanic phenomena around electrochemically active materials, such as pipes, conduits, buried scrap materials, cinders, and ore deposits. They may also occur as streaming potentials generated by groundwater movement. (Electric fields associated with groundwater movement will have the greatest amplitude where groundwater flow rates are high, such as through subsurface open-channel flow. Groundwater movement in karst areas can exhibit rapid flow through dissolved channels within the rock. Springs and subsurface flow may be the cause of telluric sources, which may obscure resistivity measurements.) Telluric currents and spontaneous potential effects can be compensated by applying a bias potential to balance the potential electrodes before energizing the current electrodes. Because telluric currents generally vary with time, frequent adjustments to the bias potential may be necessary in the course of making an observation. If the instrument lacks a provision for applying a bias potential, a less satisfactory alternative is to use a polarity-reversing switch to make readings

with alternately reversed current directions in the current electrodes. The average values of V and I for the forward and reverse current directions are then used to compute the apparent resistivity.

Layout of electrodes should be done with nonconducting measuring tapes, since tapes of conducting materials, if left on the ground during measurement, can influence apparent resistivity values. Resistivity measurements can also be affected by metallic fences, rails, pipes, or other conductors, which may induce spontaneous potentials and provide short-circuit paths for the current. The effects of such linear conductors as these can be minimized, but not eliminated, by laying out the electrode array on a line perpendicular to the conductor; but in some locations, such as some urban areas, there may be so many conductive bodies in the vicinity that this cannot be done. Also, electrical noise from power lines, cables, or other sources may interfere with measurements. Because of the nearly ubiquitous noise from 60-Hz power sources in the United States, the use of 60 Hz or its harmonics in resistivity instruments is not advisable. In some cases, the quality of data affected by electrical noise can be improved by averaging values obtained from a number of observations; sometimes electrical noise comes from temporary sources, so better measurements can be obtained by waiting until conditions improve. Occasionally, ambient electrical noise and other disturbing factors at a site may make resistivity surveying infeasible. Modern resistivity instruments have capability for data averaging or stacking; this allows resistivity surveys to proceed in spite of most noisy site conditions and to improve signal-to-noise ratio for weak signals.

Data Acquisition

Resistivity surveys are made to satisfy the needs of two distinctly different kinds of interpretation problems: (1) the variation of resistivity with depth, reflecting more or less horizontal stratification of earth materials; and (2) lateral variations in resistivity that may indicate soil lenses, isolated ore bodies, faults, or cavities. For the first kind of problem, measurements of apparent resistivity are made at a single location (or around a single center point) with systematically varying electrode spacings. This procedure is sometimes called vertical electrical sounding (VES), or vertical profiling. Surveys of lateral variations may be made at spot or grid locations or along definite lines of traverse, a procedure sometimes called horizontal profiling.

Vertical Electrical Sounding (VES)

Either the Schlumberger or, less effectively, the Wenner array is used for sounding, since all commonly available interpretation methods and interpretation aids for sounding are based on these two arrays. In the use of either method, the center point of the array is kept at a fixed location, while the electrode locations are varied around it. The apparent resistivity values, and layer depths interpreted from them, are referred to the center point.

In the Wenner array, the electrodes are located at distances of a/2 and 3a/2 from the center point. The most convenient way to locate the electrode stations is to use two measuring tapes, pinned with their zero ends at the center point and extending away from the center in opposite directions. After each reading, each potential electrode is moved out by half the increment in electrode spacing, and each current electrode is moved out by 1.5 times the increment. The increment to be used depends on the interpretation methods that will be

applied. In most interpretation methods, the curves are sampled at logarithmically spaced points. The ratio between successive spacings can be obtained from the relation

$$\frac{a_i}{a_{i-1}} = 10^{1/n}, \tag{64}$$

where

n = number of points to be plotted in each logarithmic cycle.

For example, if six points are wanted for each cycle of the logarithmic plot, then each spacing a will be equal to 1.47 times the previous spacing. The sequence starting at 10 m would then be 10, 14.7, 21.5, 31.6, 46.4, 68.2, which, for convenience in layout and plotting, could be rounded to 10, 15, 20, 30, 45, 70. In the next cycle, the spacings would be 100, 150, 200, and so on. Six points per cycle is the minimum recommended; 10, 12, or even more per cycle may be necessary in noisy areas.

VES surveys with the Schlumberger array are also made with a fixed center point. An initial spacing s (the distance from the center of the array to either of the current electrodes) is chosen, and the current electrodes are moved outward with the potential electrodes fixed. According to Van Nostrand and Cook (1966), errors in apparent resistivity are within 2 to 3 percent if the distance between the potential electrodes does not exceed $2s/5$. Potential electrode spacing is, therefore, determined by the minimum value of s. As s is increased, the sensitivity of the potential measurement decreases; therefore, at some point, if s becomes large enough, it will be necessary to increase the potential electrode spacing. The increments in s should normally be logarithmic and can be chosen in the same way as described for the Wenner array.

For either type of electrode array, minimum and maximum spacings are governed by the need to define the asymptotic phases of the apparent resistivity curve and the needed depth of investigation. Frequently, the maximum useful electrode spacing is limited by available time, site topography, or lateral variations in resistivity. For the purpose of planning the survey, a maximum electrode spacing of at least three times the depth of interest may be used, but the apparent resistivity curve should be plotted as the survey progresses in order to judge whether sufficient data have been obtained. Also, the progressive plot can be used to detect errors in readings or spurious resistivity values due to local effects. Sample field data sheets are shown in figures 273 through 275.

SCHLUMBERGER ELECTRICAL RESISTIVITY DATA SHEET

STATION NO._____DIRECTION_____DATE_____

PROJECT_____LOCATION_____

OPERATOR_____EQUIP_____

REMARKS_____

$$\rho_a = \pi b\left[\left(\frac{a}{b}\right) - \frac{1}{4}\right]\frac{V}{I}$$

a (AB/2 (m)	b MN (m)	v (mv)	I (ma)	R=V/I (ohms)	ρ_a (ohm-m)	remarks

Figure 273. Example data sheet for Schlumberger vertical sounding.

WENNER ELECTRICAL RESISTIVITY DATA SHEET

STATION N_____DIRECTION_____DATE_____

PROJECT_____LOCATION_____

OPERATOR_____EQUIP_____

REMARKS_____

$$\rho_a = 2\pi a\frac{V}{I}$$

a (m)	V (mv)	I (ma)	R=V/I (ohms	ρ_a (ohm-m)	remarks

Figure 274. Example data sheet for Wenner array.

DIPOLE-DIPOLE ELECTRICAL RESISTIVITY DATA SHEET

STATIONNO._____DIRECTION_____DATE_____

PROJECT_____LOCATION_____

OPERATOR_____EQUIP_____

REMARKS_____DIPOLELENGTH____m

$$\rho_a = \pi a n(n+1)(n+2)\frac{V}{I}$$

TX	RX	n	V (mv)	I (ma)	R=V/I (ohms)	ρ_a (ohms)	remarks

Figure 275. Example data sheet for dipole-dipole array.

In a normal series of observations, the total resistance, $R = V/I$, decreases with increasing electrode spacing. Occasionally, the normal relationship may be reversed for one or a few readings. If these reversals are not a result of errors in reading, they are caused by some type of lateral or local changes in resistivity of the soil or rock. Such an effect can be caused by one current electrode being placed in a material of much higher resistivity than that around the other, for instance, in a pocket of dry gravel in contact with a boulder of highly resistive rock or close to an empty cavity. Systematic reversals might be caused by thinning of a surface conductive stratum where an underlying resistant stratum approaches the surface because it dips steeply or because of surface topography. In hilly terrains, the line of electrodes should be laid out along a contour if possible. Where beds are known to dip steeply (more than about 10 deg), the line should be laid out along the strike. Electrodes should not be placed in close proximity to boulders, so it may sometimes be necessary to displace individual electrodes away from the line. The theoretically correct method of displacing one electrode, e.g., the current electrode A, would be to place it at a new position A' such that the geometric factor K is unchanged. This condition would be satisfied (see Equation 65) if

$$\frac{1}{AM} - \frac{1}{AN} = \frac{1}{A'M} - \frac{1}{A'N} \tag{65}$$

If the electrode spacing is large as compared with the amount of shift, it is satisfactory to shift the electrode on a line perpendicular to the array. For large shifts, a reasonable approximation is to move the electrode along an arc centered on the nearest potential electrode, so long as it is not moved more than about 45° off the line.

The plot of apparent resistivity versus spacing is always a smooth curve where it is governed only by vertical variation in resistivity. Reversals in resistance and irregularities in the apparent resistivity curve, if not due to errors, both indicate lateral changes and should be further investigated. With the Wenner array, the Lee modification may be used to detect differences from one side of the array to the other, and a further check can be made by taking a second set of readings at the same location but on a perpendicular line. Where the Schlumberger array is used, changing the spacing of the potential electrodes may produce an offset in the apparent resistivity curve as a result of lateral inhomogeneity. Such an offset may occur as an overall shift of the curve without much change in its shape (Zohdy, 1968). Under such conditions, the cause of the offset can often be determined by repeating portions of the sounding with different potential electrode spacing.

Horizontal Profiling

Surveys of lateral variations in resistivity can be useful for the investigation of any geological features that can be expected to offer resistivity contrasts with their surroundings. Deposits of gravel, particularly if unsaturated, have high resistivity and have been successfully prospected for by resistivity methods. Steeply dipping faults may be located by resistivity traverses crossing the suspected fault line, if there is sufficient resistivity contrast between the rocks on the two sides of the fault. Solution cavities or joint openings may be detected as a high resistivity anomaly, if they are open, or low resistivity anomaly if they are filled with soil or water.

Resistivity surveys for the investigation of aerial geology are made with a fixed electrode spacing, by moving the array between successive measurements. Horizontal profiling, per se, means moving the array along a line of traverse, although horizontal variations may also be investigated by individual measurements made at the points of a grid. If a symmetrical array, such as the Schlumberger or Wenner array, is used, the resistivity value obtained is associated with the location of the center of the array. Normally, a vertical survey would be made first to determine the best electrode spacing. Any available geological information, such as the depth of the features of interest, should also be considered in making this decision, which governs the effective depth of investigation. The spacing of adjacent resistivity stations, or the fineness of the grid, governs the resolution of detail that may be obtained. This is very much influenced by the depths of the features, and the achievable resolution diminishes with depth. As a general rule, the spacing between resistivity stations should be smaller than the width of the smallest feature to be detected, or smaller than the required resolution in the location of lateral boundaries.

Field data may be plotted in the form of profiles or as contours on a map of the surveyed area. For a contour map, resistivity data obtained at grid points are preferable to those obtained from profile lines, unless the lines are closely spaced, because the alignment of data along profiles tends to distort the contour map and gives it an artificial grain that is distracting and interferes with interpretation of the map. The best method of data collection for a contour map is to use a square grid, or at least a set of stations with uniform coverage of the area, and without directional bias.

Occasionally, a combination of vertical and horizontal methods may be used. Where mapping of the depth to bedrock is desired, a vertical sounding may be done at each of a set

of grid points. However, before a commitment is made to a comprehensive survey of this type, the results of resistivity surveys at a few stations should be compared with the drill hole logs. If the comparison indicates that reliable quantitative interpretation of the resistivity can be made, the survey can be extended over the area of interest.

When profiling is done with the Wenner array, it is convenient to use a spacing between stations equal to the electrode spacing, if this is compatible with the spacing requirements of the problem and the site conditions. In moving the array, the rearmost electrode need only be moved a step ahead of the forward electrode, by a distance equal to the electrode spacing. The cables are then reconnected to the proper electrodes, and the next reading is made. With the Schlumberger array, however, the whole set of electrodes must be moved between stations.

Detection of Cavities

Subsurface cavities most commonly occur as solution cavities in carbonate rocks. They may be empty or filled with soil or water. In favorable circumstances, either type may offer a good resistivity contrast with the surrounding rock since carbonate rocks, unless porous and saturated, usually have high resistivities, whereas soil or water fillings are usually conductive, and the air in an empty cavity is essentially nonconductive. Wenner or Schlumberger arrays may be used with horizontal profiling to detect the resistivity anomalies produced by cavities, although reports in the literature indicate mixed success. The probability of success by this method depends on the site conditions and on the use of the optimum combination of electrode spacing and interval between successive stations. Many of the unsuccessful surveys are done with an interval too large to resolve the anomalies sought.

Interpretation of Vertical Electrical Sounding Data

The interpretation problem for VES data is to use the curve of apparent resistivity versus electrode spacing, plotted from field measurements, to obtain the parameters of the geoelectrical section: the layer resistivities and thicknesses. From a given set of layer parameters, it is always possible to compute the apparent resistivity as a function of electrode spacing (the VES curve). Unfortunately, for the converse of that problem, it is not generally possible to obtain a unique solution. There is an interplay between thickness and resistivity; there may be anisotropy of resistivity in some strata; large differences in geoelectrical section, particularly at depth, produce small differences in apparent resistivity; and accuracy of field measurements is limited by the natural variability of surface soil and rock and by instrument capabilities. As a result, different sections may be electrically equivalent within the practical accuracy limits of the field measurements.

To deal with the problem of ambiguity, the interpreter should check all interpretations by computing the theoretical VES curve for the interpreted section and comparing it with the field curve. The test of geological reasonableness should be applied. In particular, interpreted thin beds with unreasonably high resistivity contrasts are likely to be artifacts of interpretation rather than real features. Adjustments to the interpreted values may be made on the basis of the computed VES curves and checked by computing the new curves. Because of the accuracy limitations caused by instrumental and geological factors, effort

should not be wasted on excessive refinement of the interpretation. As an example, suppose a set of field data and a three-layer theoretical curve agree within 10 percent. Adding several thin layers to achieve a fit of 2 percent is rarely a better geologic fit.

All of the direct interpretation methods, except some empirical and semi-empirical methods such as the Moore cumulative method and the Barnes layer method, which should be avoided, rely on curve matching in some form to obtain the layer parameters. Because the theoretical curves are always smooth, the field curves should be smoothed before their interpretation is begun to remove obvious observational errors and effects of lateral variability. Isolated one-point spikes in resistivity are removed rather than interpolated. The curves should be inspected for apparent distortion due to effects of lateral variations.

Comparison with theoretical multilayer curves is helpful in detecting such distortion. The site conditions should be considered; excessive dip of subsurface strata along the survey line (more than about 10 percent), unfavorable topography, or known high lateral variability in soil or rock properties may be reasons to reject field data as unsuitable for interpretation in terms of simple vertical variation of resistivity.

The simplest multilayer case is that of a single layer of finite thickness overlying a homogeneous half-space of different resistivity. The VES curves for this case vary in a relatively simple way, and a complete set of reference curves can be plotted on a single sheet of paper. Standard two-layer curves for the Schlumberger array are included in figure 276. The curves are plotted on a logarithmic scale, both horizontally and vertically, and are normalized by plotting the ratio of apparent resistivity to the first layer resistivity ($\rho a/\rho 1$) against the ratio of electrode spacing to the first layer thickness (a/d1). Each curve of the family represents one value of the parameter k, which is defined by

$$k = \frac{\rho_2 - \rho_1}{\rho_2 + \rho_1} \tag{66}$$

The apparent resistivity for small electrode spacings approaches ρ_1 and for large spacings approaches ρ_2; these curves begin at $\rho_a/\rho_1 = 1$, and asymptotically approach $\rho_a/\rho_1 = \rho_2/\rho_1$.

Any two-layer curve for a particular value of k, or for a particular ratio of layer resistivities, must have the same shape on the logarithmic plot as the corresponding standard curve. It differs only by horizontal and vertical shifts, which are equal to the logarithms of the thickness and resistivity of the first layer. The early (i.e., corresponding to the smaller electrode spacings) portion of more complex multiple-layer curves can also be fitted to two-layer curves to obtain the first layer parameters $\rho 1$ and d1 and the resistivity $\rho 2$ of layer 2. The extreme curves in figure 276 correspond to values of k equal to 1.0 and -1.0; these values represent infinitely great resistivity contrasts between the upper and lower layers. The first case represents a layer 2 that is a perfect insulator; the second, a layer 2 that is a perfect conductor. The next nearest curves in both cases represent a ratio of 19 in the layer resistivities. Evidently, where the resistivity contrast is more than about 20 to 1, fine resolution of the layer 2 resistivity cannot be expected. Loss of resolution is not merely an effect of the way the curves are plotted, but is representative of the basic physics of the problem and leads to ambiguity in the interpretation of VES curves.

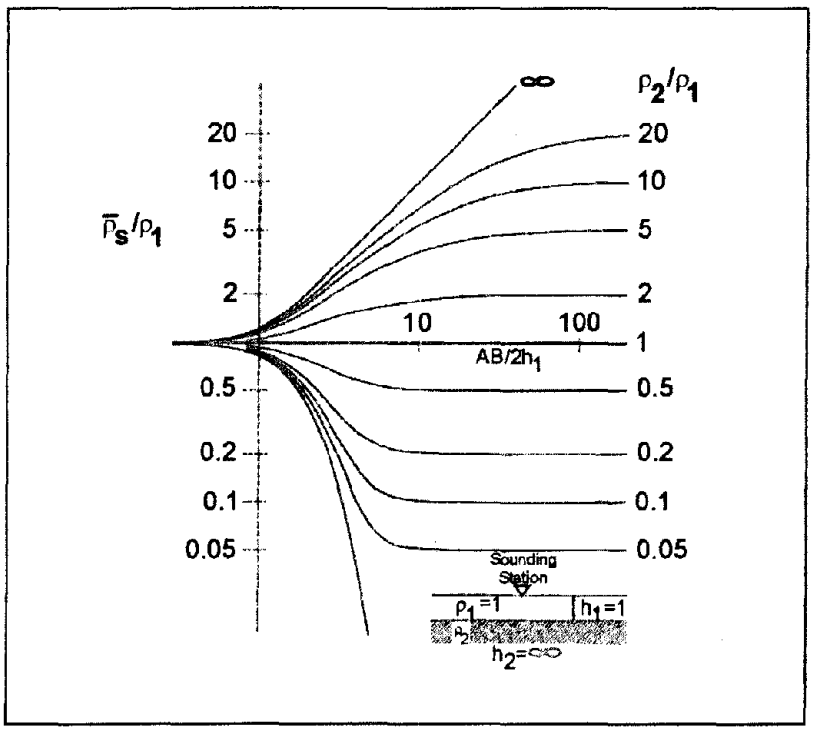

Figure 276. Two-layer master set of sounding curves for the Schlumberger array. (Zohdy 1974a, 1974b)

Where three or more strata of contrasting resistivity are present, the VES curves are more complex than the two-layer curves. For three layers, there are four possible types of VES curves, as shown in figure 277, depending on the nature of the successive resistivity contrasts. The classification of these curves is found in the literature with the notations H, K, A, and Q. These symbols correspond respectively to bowl-type curves, which occur with an intermediate layer of lower resistivity than layers 1 or 3; bell-type curves, where the intermediate layer is of higher resistivity; ascending curves, where resistivities successively increase; and descending curves, where resistivities successively decrease. With four layers, another curve segment is present, so that 16 curve types can be identified: HK for a bowl-bell curve, AA for a monotonically ascending curve, and so on.

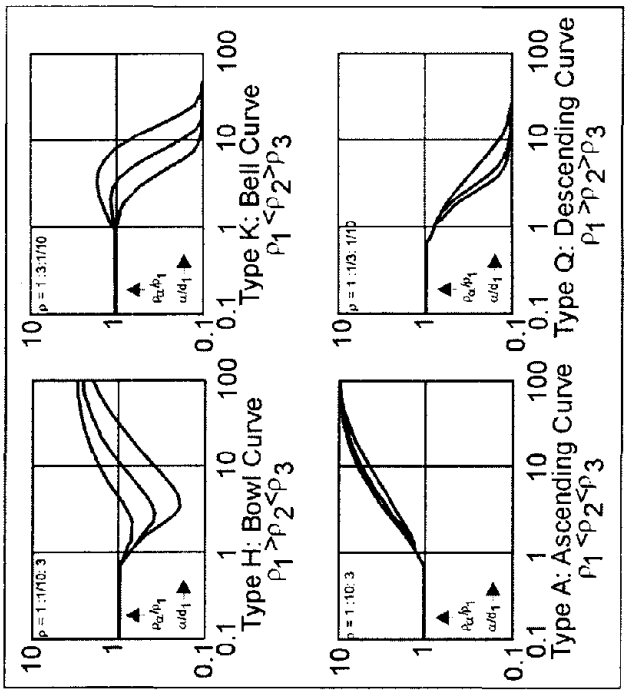

Figure 277. Four types of three-layer VES curves; the three sample curves for each of the four types represent values of d2/d1= 1/3, 1 and 3.

Before the availability of personal computers, the curve-matching process was done graphically by plotting the field data plotted on transparent log-log graph paper at the same scale of catalogs of two- and three-layer standard curves. The use of standard curves requires an identification of the curve type followed by a comparison with standard curves of that type to obtain the best match. Two-layer and three-layer curves can be used for complete interpretation of VES curves of more layers by the Auxiliary Point Method, which requires the use of a small set of auxiliary curves and some constructions. Discussions and step-by-step examples of this method are given by Zohdy (1965), Orellana and Mooney (1966), and Keller and Frischknecht (1966). Sets of standard curves have been developed by several workers. Orellana and Mooney (1966) published a set of 1,417 two-, three-, and four-layer Schlumberger curves, accompanied by a set of auxiliary curves, and tabulated values for both Schlumberger and Wenner curves. Apparent resistivity values for 102 three-layer Wenner curves were published by Wetzel and McMurray (1937). A collection of 2,400 two-, three-, and four-layer curves was published by Mooney and Wetzel (1956). Most, if not all, of these publications are out of print, but copies may be available in libraries.

Ghosh (1971a, 1971b) and Johansen (1975) used linear filter theory to develop a fast numerical method for computing apparent resistivity values from the resistivity transforms, and vice versa. With these methods, new standard curves or trial VES curves can be computed as needed, with a digital computer or a calculator, either to match the curves or to check the validity of an interpretation of the field data. Thus, trial-and-error interpretation of VES data is feasible. Trial values of the layer parameters can be guessed, checked with a computed apparent resistivity curve, and adjusted to make the field and computed curves agree. The process will be much faster, of course, if the initial guess is guided by a

semiquantitative comparison with two- and three-layer curves. Computer programs have been written by Zohdy (1973, 1974a, 1975), Zohdy and Bisdorf (1975), and several commercial software companies for the use of this method to obtain the layer parameters automatically by iteration, starting with an initial estimate obtained by an approximate method. Most computer programs require a user-supplied initial estimate (model), whereas some programs can optionally generate the initial mode. After a suite of sounding curves have been individually interpreted in this manner, a second pass can be made where certain layer thicknesses and/or resistivities can be fixed to give a more consistent project-wide interpretation.

Interpretation of Horizontal Profiling Data

Data obtained from horizontal profiling for engineering applications are normally interpreted qualitatively. Apparent resistivity values are plotted and contoured on maps, or plotted as profiles, and areas displaying anomalously high or low values or anomalous patterns are identified. Interpretation of the data, as well as the planning of the survey, must be guided by the available knowledge of the local geology. The interpreter normally knows what he is looking for in terms of geological features and their expected influence on apparent resistivity, because the resistivity survey is motivated by geological evidence of a particular kind of exploration problem (e.g., karst terrain). The survey is then executed in a way that is expected to be most responsive to the kinds of geological or hydrogeological features sought. A pitfall inherent in this approach is that the interpreter may be misled by his preconceptions if he is not sufficiently alert to the possibility of the unexpected occurring. Alternative interpretations should be considered, and evidence from as many independent sources as possible should be applied to the interpretation. One way to help plan the survey is to construct model VES sounding curves for the expected models, vary each model parameter separately by say 20%, and then choose electrode separations that will best resolve the expected resistivity/depth variations. Most investigators then perform a number of VES soundings to verify and refine the model results before commencing horizontal profiling.

The construction of theoretical profiles is feasible for certain kinds of idealized models, and the study of such profiles is very helpful in understanding the significance of field profiles. Van Nostrand and Cook (1966) give a comprehensive discussion of the theory of electrical resistivity interpretation and numerous examples of resistivity profiles over idealized models of faults, dikes, filled sinks, and cavities.

Figure 278 illustrates a theoretical Wenner profile crossing a fault, a situation that can be thought of more generally as a survey line crossing any kind of abrupt transition between areas of different resistivity. The figure compares a theoretical curve, representing continuous variation of apparent resistivity with location of the center of the electrode array, and a theoretical field curve that would be obtained with an interval of $a/2$ between stations. More commonly, an interval equal to the electrode spacing would be used; various theoretical field curves for that case can be drawn by connecting points on the continuous curve at intervals of a. These curves would fail to reveal much of the detail of the continuous curve and could look quite different from one another. Figure 279 illustrates a profile across a shale-filled sink (i.e., a body of relatively low resistivity) and compares it with the theoretical continuous curve and a theoretical field curve. The theoretical curves are for a

conductive body exposed at the surface, while the field case has a thin cover of alluvium, but the curves are very similar. Figure 280a shows a number of theoretical continuous profiles across buried perfectly insulating cylinders. This model would closely approximate a subsurface tunnel and less closely an elongated cavern. A spherical cavern would produce a similar response but with less pronounced maxima and minima. Figure 280b shows a set of similar curves for cylinders of various resistivity contrasts.

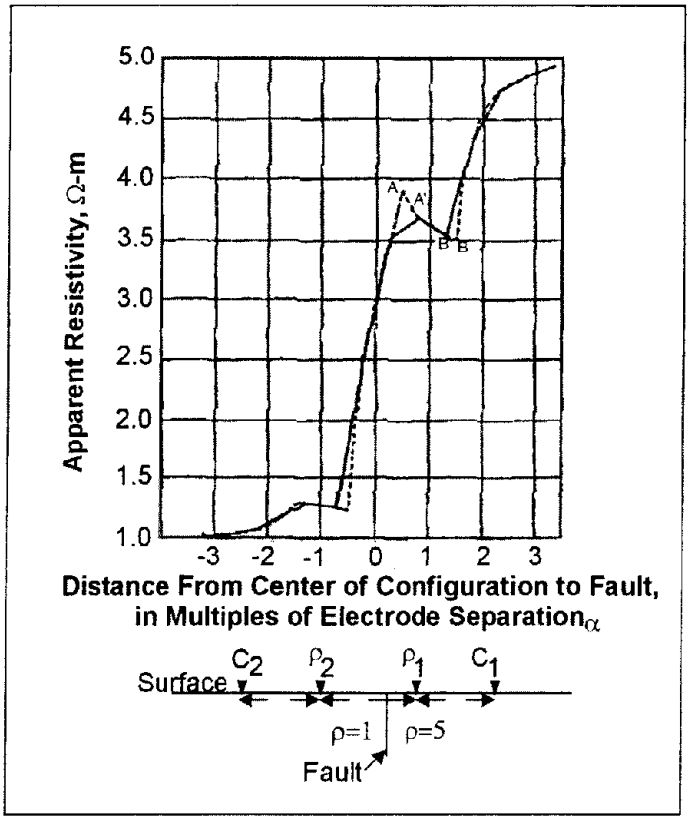

Figure 278. Wenner horizontal resistivity profile over a vertical fault; typical field curve (solid line), theoretical curve (dashed line). (Van Nostrand and Cook 1966)

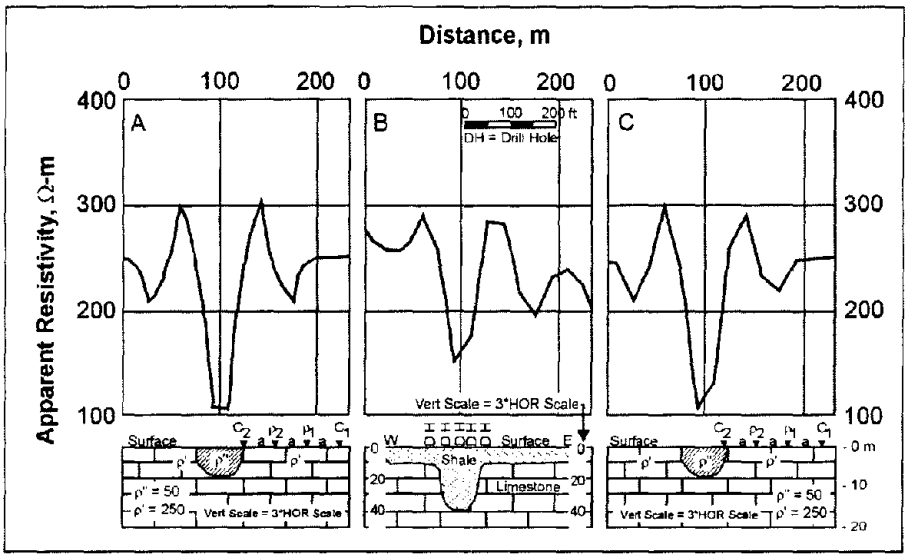

Figure 279. Wenner horizontal resistivity profiles over a filled sink: A) continuous theoretical curve over hemispherical sink, b) observed field curve with geologic cross section, c) theoretical field plot over hemispherical sink (Van Nostrand and Cook 1966).

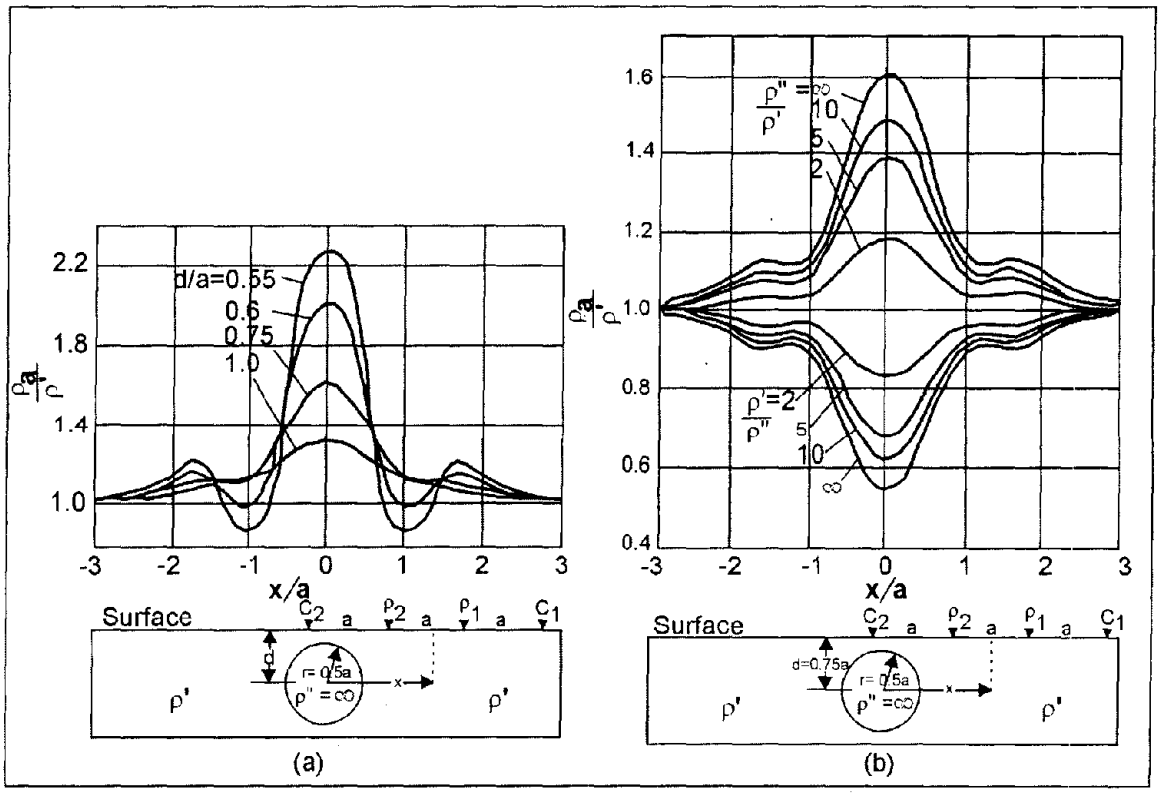

Figure 280. Theoretical Wenner profiles across a circular cylinder; a) perfectly insulating cylinders at different depths, b) cylinders of different resistivity contrasts. (Van Nostrand and Cook 1966)

9.3.4 Induced Polarization

Introduction

Conrad Schlumberger (Dobrin 1960) probably was first to report the induced polarization phenomenon, which he called "provoked polarization." While making conventional resistivity measurements, he noted that the potential difference, measured between the potential electrodes, often did not drop instantaneously to zero when the current was turned off. Instead, the potential difference dropped sharply at first, then gradually decayed to zero after a given interval of time. Certain layers in the ground can become electrically polarized, forming a battery when energized with an electric current. Upon turning off the polarizing current, the ground gradually discharges and returns to equilibrium.

The study of the decaying potential difference as a function of time is now known as the study of induced polarization (IP) in the time domain. In this method the geophysicist looks for portions of the earth where current flow is maintained for a short time after the applied current is terminated. Another technique is to study the effect of alternating currents on the measured value of resistivity, which is called IP in the "frequency domain." In this method the geophysicist tries to locate portions of the earth where resistivity decreases as the frequency of applied current is increased. The induced electrical polarization method is widely used in exploration for ore bodies, principally of disseminated sulfides. Use of IP in geotechnical and engineering applications has been limited, and has been used mainly for groundwater exploration. Groundwater IP studies generally have been made with time-domain IP.

General Theory of the IP Effect

The origin of induced electrical polarization is complex and is not well understood. This is primarily because several physio-chemical phenomena and conditions are likely responsible for its occurrence. Only a fairly simple discussion will be given here. According to Seigel (1970), when a metal electrode is immersed in a solution of ions of a certain concentration and valence, a potential difference is established between the metal and the solution sides of the interface. This difference in potential is an explicit function of the ion concentration, valence, etc. When an external voltage is applied across the interface, a current is caused to flow, and the potential drop across the interface changes from its initial value. The change in interface voltage is called the "overvoltage" or "polarization" potential of the electrode. Overvoltages are due to an accumulation of ions on the electrolyte side of the interface waiting to be discharged. The time constant of buildup and decay is typically several tenths of a second.

Overvoltage is therefore established whenever current is caused to flow across an interface between ionic and electronic conduction. In normal rocks, the current that flows under the action of an applied emf does so by ionic conduction in the electrolyte in the pores of the rock. There are, however, certain minerals that have a measure of electronic conduction (almost all the metallic sulfides (except sphalerite) such as pyrite, graphite, some coals, magnetite, pyrolusite, native metals, some arsenides, and other minerals with a metallic lustre). Figure 281 is a simplified representation of how overvoltages are formed on an electronic conducting particle in an electrolyte under the influence of current flow.

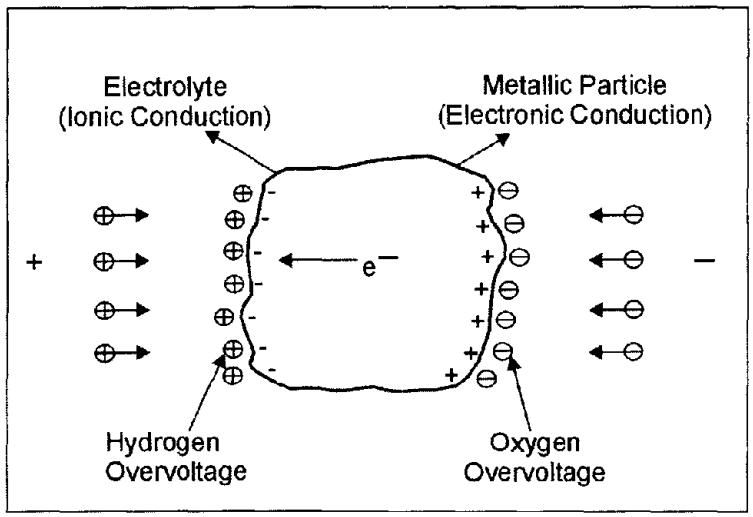

Figure 281. Overvoltage on a metallic particle in electrolyte. (Seigel 1970; copyright permission granted by Geological Survey of Canada)

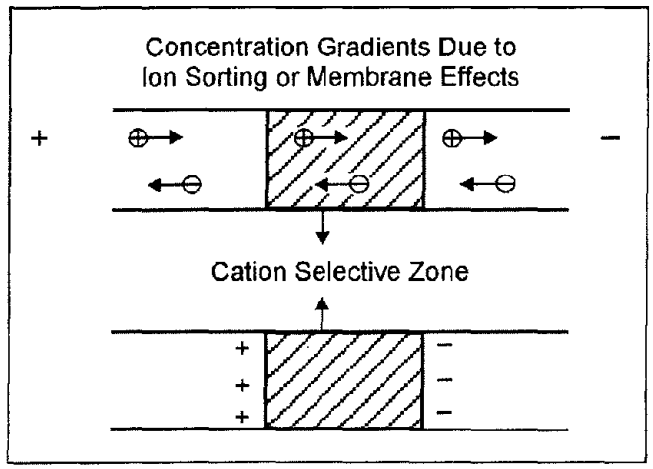

Figure 282. Nonmetallic induced polarization agent. (Seigel 1970; copyright permission granted by Geological Survey of Canada)

The most important sources of nonmetallic IP in rocks are certain types of clay minerals (Vacquier 1957, Seigel 1970). These effects are believed to be related to electrodialysis of the clay particles. This is only one type of phenomenon that can cause "ion-sorting" or "membrane effects." For example, figure 282 shows a cation-selective membrane zone in which the mobility of the cation is increased relative to that of the anion, causing ionic concentration gradients and therefore polarization. A second group of phenomena includes electrokinetic effects that produce voltage gradients through the `streaming potential' phenomenon. These voltage gradients will have the same external appearance as polarization effects due to separation of charge. Electrokinetic effects seem less important than membrane effects in the overall polarization picture.

In time-domain IP, several indices have been used to define the polarizability of the medium. Seigel (1959) defined "chargeability" (in seconds) as the ratio of the area under the decay curve (in millivolt-seconds, mV-s) to the potential difference (in mV) measured before switching the current off. Komarov, et al., (1966) defined "polarizability" as the ratio of the potential difference after a given time from switching the current off to the potential difference before switching the current off. Polarizability is expressed as a percentage.

Seigel (1959) showed that over a heterogeneous medium comprised of n different materials, apparent chargeability η_a is approximately related to apparent resistivity by

$$\eta_a = \sum_{i=1}^{n} \eta_i \frac{\partial \log \rho_a}{\partial \log \rho_i}, \tag{67}$$

where

η_i = chargeability of the ith material,

ρ_i = resistivity of the ith material.

Seigel provided the validity of

$$\sum_{i=1}^{n} \frac{\partial \log \rho_a}{\partial \log \rho_i} = 1 \tag{68}$$

Equations 67 and 68 yield the useful formula for $\eta a/\eta 1$:

$$\frac{\eta_a}{\eta_1} = 1 + \sum_{i=2}^{n} \frac{\partial \log \rho_a}{\partial \log \rho_i} \left[\frac{\eta_i}{\eta_1} - 1 \right], \tag{69}$$

If the theoretical expression for apparent resistivity ρ_a is known, then the corresponding expression for the reduced apparent chargeability η_a/η_i can be derived.

Spectral Induced Polarization

Spectral Induced Polarization (SIP) measures the variation of resistivity with frequency. The method, therefore, requires several resistivity measurements at different frequencies. These can be recorded in the frequency domain or in the time domain. In the time domain, where voltage measurements are recorded after the transmitting current has been turned off, the decaying voltage is sampled several times as it decays. Using the Fourier Transform, these data can be transformed into the frequency domain providing resistivity values at different frequencies.

SIP measurements are occasionally used in mineral exploration to assist in identifying graphite and clay from sulfide mineralization. In addition, some information about the habit of the polarizable minerals could be obtained. It can also be used to map clay and, in some cases, contamination.

Sounding and Profiling

The techniques of sounding and profiling, used in resistivity measurements, are also used in the IP method. IP soundings are most commonly made using the Schlumberger array, pole-dipole array, or Wenner array, and usually in the time domain. The apparent chargeability η_a versus the electrode spacing a is plotted on logarithmic coordinates. The IP sounding curve is an interpreted curve matching procedures, either graphically, using sets of IP sounding master curves, or by computer. At present, only a few two-layer master curves (for the Wenner array) have been published in the United States (Seigel, 1959; Frische and von Buttlar, 1957). Three- and four-layer curves have been published in the Soviet Union.

An IP sounding curve can be of significant value in complementing a resistivity sounding curve. For example, the resistivity and IP sounding curves for the following four-layer geoelectric section are shown in figure 283:

Layer No.	Thickness (m)	Resistivity (Ωm)	Chargeability (s)
1.....	10	10	1
2.....	10	160	1
3.....	5	40	10
4.....	infinity	infinity	1

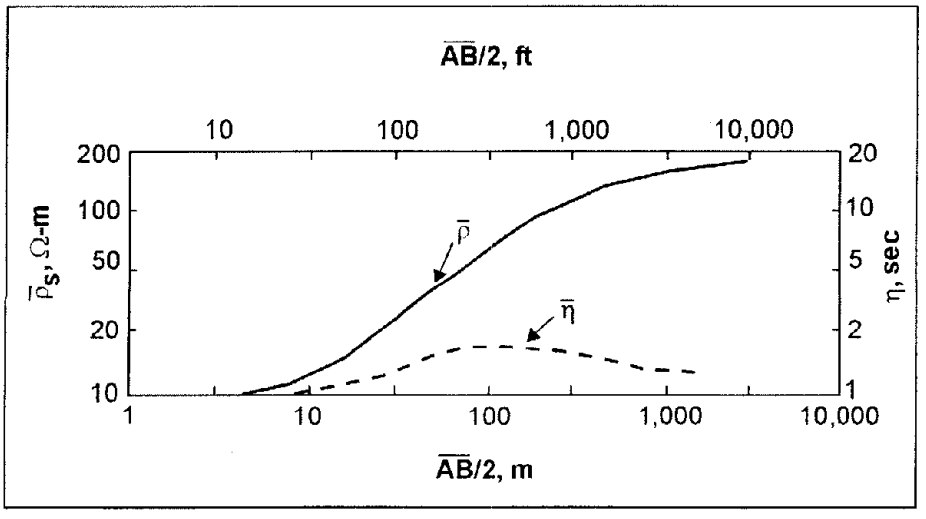

Figure 283. Apparent resistivity and apparent chargeability (IP) sounding curves for a four-layer model. (Zohdy 1974a, 1974b)

It is obvious that layer 3 cannot be distinguished on the four-layer resistivity curve (which resembles a two- or three-layer curve). But layer 3 is characterized by a different chargeability from the surrounding layers, and its presence is indicated clearly by the IP sounding curve.

When profiling, the pole-dipole or dipole-dipole (see figure 284) arrays are used almost exclusively. It can be easily employed in the field using short lengths of wire or multi-conductor cables allowing several values of the spacing multiplier (n) to be measured from one current dipole location. For one or two values of n, the IP and resistivity results are plotted as profiles. For more than two values of n, the profile method of presentation becomes confusing. A two-dimensional (usually called pseudosection) format has been developed to present the data (figure 284). This form of presentation helps the interpreter separate the effects of IP and resistivity variations along the line from vertical variations. The 45° angle used to plot the data is entirely arbitrary. The pseudosection plots are contoured, and the resulting anomalous patterns can be recognized as being caused by a particular source geometry and/or correlated from line to line. However, the contoured data are not meant to represent sections of the electrical parameters of the subsurface (Hallof, 1980). The pseudosection data plots are merely a convenient method for showing all of the data along one given line in one presentation.

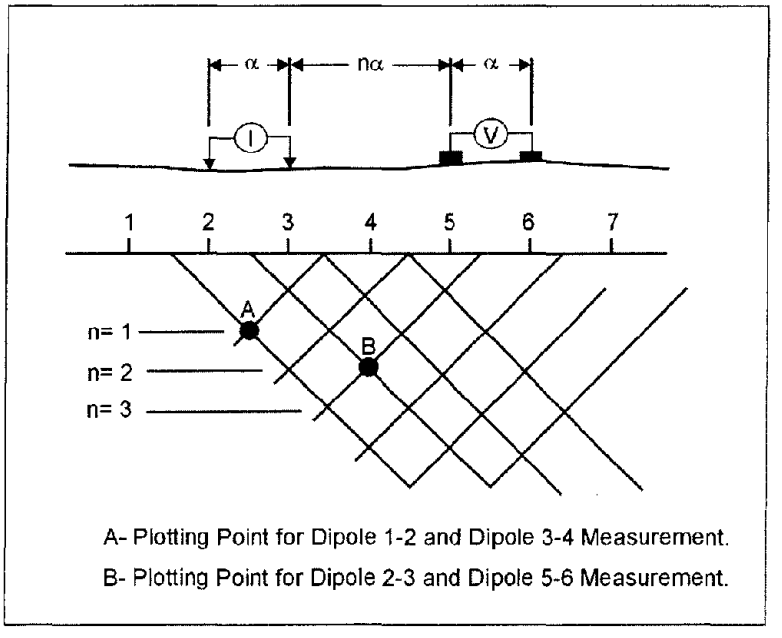

Figure 284. Dipole-dipole plotting method.

Examples

Example 1 - Groundwater exploration. The majority of published case histories using IP surveys have been for mining exploration, but those treating groundwater exploration is growing: Vacquier, et al. (1957), Kuzmina and Ogil'vi (1965), Bodmer, et al. (1968), and Sternberg, et al. (1990). Kuzmina and Ogil'vi reported on work done near the Sauk-Soo River in Crimea and in the Kalinino region of Armenia. In Crimea, the IP work consisted essentially of IP sounding (time domain) using the Wenner array. The alluvial deposits in the studied area were poorly differentiated by their resistivities, but three horizons were clearly distinguished by their polarizabilities (figure 285). The section consisted of a top layer of weak polarizability (h1 = 2-4 m; η1 = 0.8-1.5%), which represents a dry loamy layer; a second layer of strong polarizability (h2 = 18-20 m; η2 = 3-5%), which represented a clayey

sand layer saturated with fresh water; and a third layer of weak polarizability (h3 very thick; $\eta 3 = 1\%$), which represents impervious siltstones. The survey in this area demonstrates that the IP work provided more complete information about the groundwater occurrence than did the resistivity soundings alone.

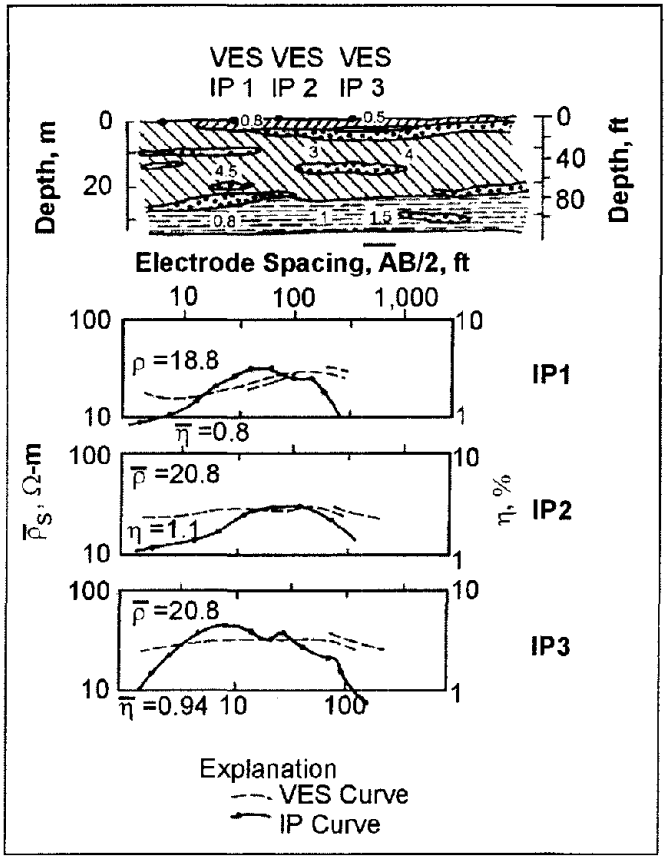

Figure 285. Geoelectric section, VES and IP sounding curves at alluvial deposits. (Zohdy, 1974b).

Example 2 - Detection of metal pipes and cables. Zhang and Luo (1990) show model experiments and analytical results that show that, in certain circumstances, a buried metal pipe or armored cable can introduce anomalies in IP (and apparent resistivity) with large amplitude and wide range. These results are important for two reasons. The first is that such man-made features have the potential to cause "noise" or errors in electrical surveys. The general rule of thumb when planning a survey is to orient soundings and profiles as nearly perpendicular to any known buried pipes or cables as the field conditions allow. The obvious second reason for the importance of this paper is that the IP may be used to locate a pipe or cable. Figure 286 (Zhang and Luo, 1990) shows results of an IP survey using the gradient array in Baima, China. An η_a anomaly of 10% to 3% with a width of more than 200 m was obtained near the road (the dot-and-dash lines on the figure). This anomaly can be traced for 4 km along the road. The trend of the anomalies is basically consistent with road and independent of the stratum strike or structural direction within the prospect area. Apparently, it results from a buried communication cable along the highway rather than geological features. The apparent resistivity profiles (the dot-and-double-dash lines on the figure) also appear to correlate with the cable, but with much less consistency or amplitude.

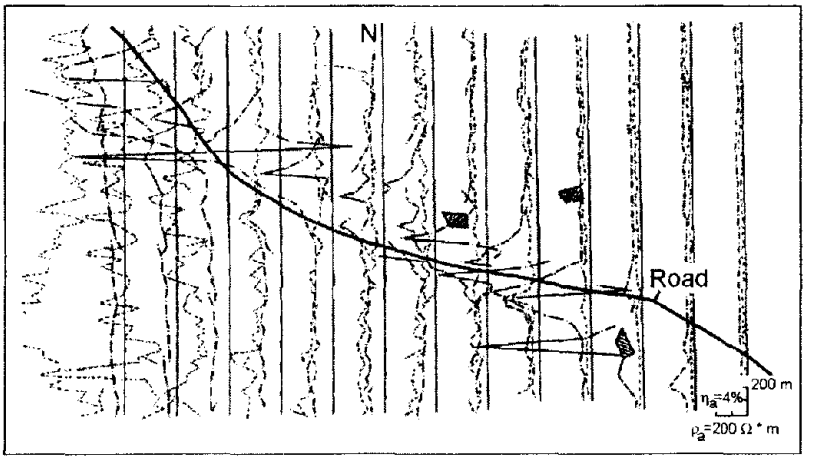

Figure 286. Plan profiles for η_a and ρ_a using the gradient array in Baima, China, over a buried cable (Zhang and Luo 1990; copyright permission granted by Society of Exploration Geophysicists).

Example 3 - Mapping soil and groundwater contamination. Cahyna, Mazac, and Vendhodova (1990) show a valuable IP example used to determine the slag-type material containing cyanide complexes that have contaminated groundwater in Czechoslovakia. Figure 287 shows contours of η_a (percent) obtained from a 10-m grid of profiles. The largest IP anomaly (ηa = 2.44%) directly adjoined the area of the outcrop of the contaminant (labeled A). The hatched region exhibits polarizability over 1.5% and probably represents the maximum concentration of the contaminant. The region exhibiting polarizability of less than 0.75% was interpreted as ground free of any slag-type contaminant.

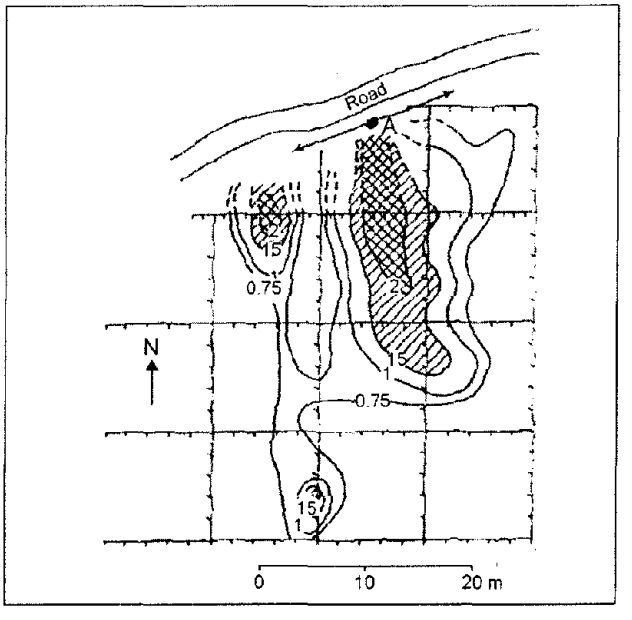

Figure 287. Network of SRP-IP profiles with contours of IP vs ηa (%) and extent of contaminant interpreted on the basis of the geophysical survey. (Cahyna, Mazac and Vendhodova 1990; copyright permission granted by Society of Exploration Geophysicists).

9.4 ELECTROMAGNETIC METHODS

Electromagnetic Induction Process

The electromagnetic induction process is conceptually summarized in figure 288 from Klein and Lajoie (1980). An EM transmitter outputs a time-varying electric current into a transmitter coil. The current in the transmitter coil generates a magnetic field of the same frequency and phase. Lines of force of this magnetic field penetrate the earth and may penetrate a conductive body. When this occurs, an electromotive force or voltage is set up within the conductor, according to Faraday's Law:

$$EMF_C = M_{TC} \frac{dI_T}{dt}, \tag{70}$$

where

EMF_C = electromotive force or voltage in the conductor,

M_{TC} = mutual inductance between the transmitter and the conductive body in the ground (a complex number),

dI_T/dt = time rate of change (derivative) of the current (I_T) in the transmitter loop.

Current will flow in the conductor in response to the induced electromotive force. These currents will usually flow through the conductor in planes perpendicular to lines of magnetic field of force from the transmitter, unless restricted by the conductor's geometry. Current flow within the conductor generates a secondary magnetic field whose lines of force, at the conductor, are such that they oppose those of the primary magnetic field. The receiver coil, at some distance from the transmitter coil, is therefore energized by two fields: from the transmitter and from the induced currents in the ground.

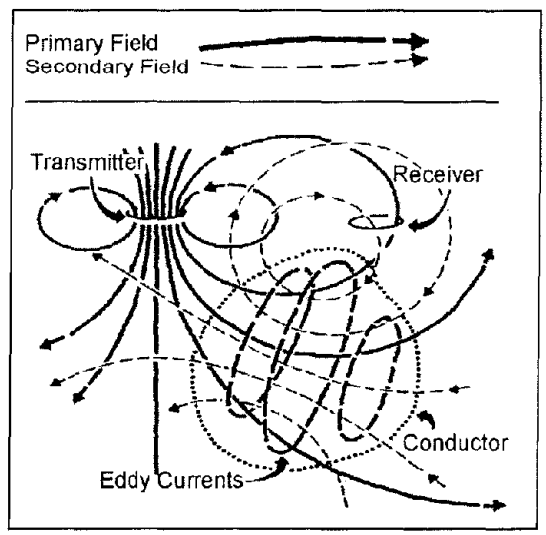

Figure 288. Generalized picture of electromagnetic induction prospecting. (Klein and Lajoie 1980; copyright permission granted by Northwest Mining Association and Klein)

From Faraday's Law, the EMF induced in the receiver may be expressed as

$$EMF_R = M_{RT}\frac{dI_T}{dt} + M_{RC}\frac{dI_C}{dt}, \tag{71}$$

where

EMF_R	= *EMF* induced in the receiver,
M_{RT}	= mutual inductance between the receiver (R) and transmitter (T)
M_{RC}	= mutual inductance between the receiver (R) and conductor (C) in the ground, a complex number,
dI_C/dt or dI_T/dt	= time derivative of the current induced in the conductor (C) or transmitter (T),
I_T or I_C	= current induced in the conductor (C) or transmitter (T).

Note that induced currents occur throughout the subsurface, and that the magnitude and distribution are functions of the transmitter frequency, power, and geometry and the distribution of all "electrical properties" in the subsurface, i.e., everything (not just an isolated "conductor"). The above discussion simplifies the problem by assuming the presence of only one conductor embedded in a much less conducting medium.

9.4.1 Frequency Domain Electromagnetic Methods

In the frequency domain method, the transmitter emits a sinusoidally varying current at a specific frequency. For example, at a frequency of 100 Hz, the magnetic field amplitude at the receiver will be that shown in the top part of figure 289. Because the mutual inductance between the transmitter and conductor is a complex quantity, the electromagnetic force induced in the conductor will be shifted in phase with respect to the primary field, similar to the illustration in the lower part of figure 289. At the receiver, the secondary field generated by the currents in the conductor will also be shifted in phase by the same amount. There are three methods of measuring and describing the secondary field.

Amplitude and Phase

The amplitude of the secondary field can be measured and is usually expressed as a percentage of the theoretical primary field at the receiver. Phase shift, the time delay in the received field by a fraction of the period, can also be measured and displayed.

In Phase and Out-of-Phase Components

The second method of presentation is to electronically separate the received field into two components, as shown in the lower part of figure 289.

The first component is in phase with the transmitted field whereas the second component is exactly 90° out-of-phase with the transmitted field. The in-phase component is sometimes called the real component, and the out-of-phase component is sometimes called the"quadrature" or "imaginary" component. Both of the above measurements require some

kind of phase link between transmitter and receiver to establish a time or phase reference. This is commonly done with a direct wire link, sometimes with a radio link, or through the use of highly accurate, synchronized crystal clocks in both transmitter and receiver.

9.4.1.1 Tilt Angle Method

The simpler frequency domain EM systems are tilt angle systems that have no reference link between the transmitter and receiver coils. The receiver simply measures the total field irrespective of phase, and the receiver coil is tilted to find the direction of maximum or minimum magnetic field strength. As shown conceptually in figure 288, at any point the secondary magnetic field may be in a direction different from the primary field. With tilt angle systems, therefore, the objective is to measure deviations from the normal in-field direction and to interpret these in terms of geological conductors.

The response parameter of a conductor is defined as the product of conductivity-thickness (σt), permeability (μ), angular frequency ($\omega = 2\pi f$), and the square of some mean dimension of the target (a^2). The response parameter is a dimensionless quantity. In MKS units, a poor conductor will have a response parameter of less than about 1, whereas an excellent conductor will have a response value greater than 1,000. The relative amplitudes of in-phase and quadrature components as a function of response parameter are given in figure 290 for the particular case of the sphere model in a uniform alternating magnetic field. For low values of the response parameter (< 1), the sphere will generally produce a low-amplitude out-of-phase anomaly; at moderate values of the response parameter (10-100), the response will be a moderate-amplitude in-phase and out-of-phase anomaly, whereas for high values of the response parameter (>1,000), the response will usually be in the in-phase component. Although figure 290 shows the response only for the particular case of a sphere in a uniform field, the response functions for other models are similar.

In frequency domain EM, depth and size of the conductor primarily affect the amplitude of the secondary field. The quality of the conductor (higher conductivity means higher quality) mainly affects the ratio of in-phase to out-of-phase amplitudes (A_R/A_I), a good conductor having a higher ratio (left side of figure 290) and a poorer conductor having a lower ratio (right side of figure 290).

Of the large number of electrical methods, many of them are in the frequency domain electromagnetic (FDEM) category and are not often used in geotechnical and environmental problems. Most used for these problems are the so-called terrain conductivity methods, VLF (very low frequency EM method), and a case of instruments called metal detectors.

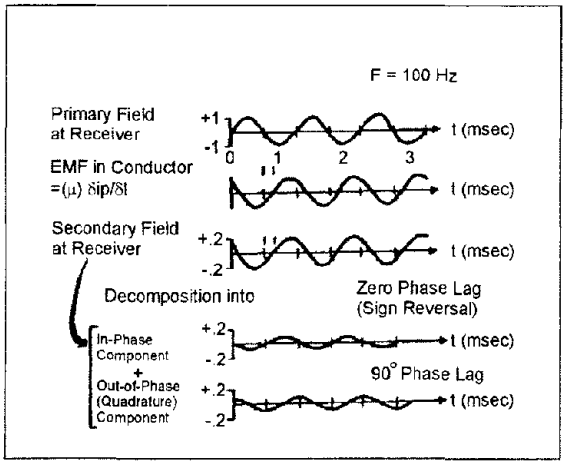

Figure 289. Generalized picture of the frequency domain EM method. (Klein and Lajoie 1980; copyright permission granted by Northwest Mining Association and Klein)

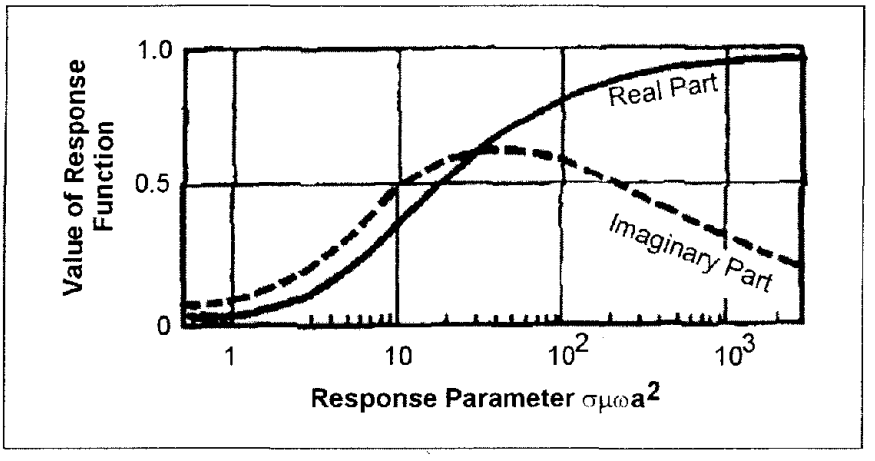

Figure 290. In-phase and out-of-phase response of a sphere in a uniform alternating magnetic field. (Klein and Lajoie 1980; copyright permission granted by Northwest Mining Association and Klein)

Data Interpretation

Interpretation of electromagnetic surveys follows basic steps. Most of the common EM systems have nomograms associated with them. Nomograms are diagrams on which the measured parameters, e.g., in-phase and out-of-phase components, are plotted for varying model conductivity and one or more geometrical factors, e.g., depth to top, thickness, etc. The model responses available for most electromagnetic methods are those of the long, thin dike (to model thin tabular bodies), a homogeneous earth, and a horizontal layer for simulating conductive overburden.

The first step is to attempt to determine from the shape of the anomaly a simple model geometry that can be thought to approximate the cause of the anomaly. The second step is to measure characteristics of the anomaly such as in-phase and out-of-phase amplitudes, and to plot these at the scale of the appropriate nomograms. From the nomogram and the shape of

the anomaly, estimates generally can be made for quality of the conductor, depth to top of the conductor, conductor thickness, dip, strike, and strike length.

9.4.1.2 Terrain Conductivity Method

Introduction

Terrain conductivity EM systems are frequency domain electromagnetic instruments, which use two loops or coils. To perform a survey, one person generally carries a small transmitter coil, while a second person carries a second coil, which receives the primary and secondary magnetic fields. Such devices can allow a rapid determination of the average conductivity of the ground because they do not require electrical contact with the ground as is required with DC resistivity techniques. The disadvantage is that unless several (usually three) intercoil spacings for at least two coil geometries are measured at each location, minimal vertical-sounding information is obtained. If the geology to the depth being explored is fairly homogeneous or slowly varying, then the lack of information about vertical variations may not be a problem, and horizontal profiling with one coil orientation and spacing is often useful. This technique is usually calibrated with a limited number of DC resistivity soundings. Horizontal profiling with the terrain conductivity meter is then used to effectively extend the resistivity information away from the DC sounding locations.

McNeill (1990) gives an excellent review and tutorial of electromagnetic methods, and much of his discussion on the terrain conductivity meter is excerpted here (see also Butler (1986)). He lists three significant differences between terrain conductivity meters and the traditional HLEM (horizontal loop electromagnetic) method usually used in mining applications. Perhaps the most important is that the operating frequency is low enough at each of the intercoil spacings that the electrical skin depth in the ground is always significantly greater than the intercoil spacing. Under this condition (known as operating at low induction numbers), virtually all response from the ground is in the quadrature phase component of the received signal. With these constraints, the secondary magnetic field can be represented as

$$\frac{H_s}{H_p} = \frac{i\omega\mu_0\sigma s^2}{4}, \tag{72}$$

where

H_S = secondary magnetic field at the receiver coil

H_P = primary magnetic field at the receiver coil

Ω = $2\pi f$

f = frequency in Hz

μ_0 = permeability of free space

σ = ground conductivity in S/m (mho/m)

s = intercoil spacing in m

I = (-1)1/2, denoting that the secondary field is 90° out of phase with the primary field

Thus, for low and moderate conductivities, the quadrature phase component is linearly proportional to ground conductivity, so the instruments read conductivity directly (McNeill 1980). Given H_S/H_P, the apparent conductivity indicated by the instrument is defined as

$$\sigma_a = 4\frac{\left(H_S/H_P\right)}{\mu_0 \omega s^2}, \tag{73}$$

The low induction number condition also implies that the measured signals are of extremely low amplitude. Because of the low amplitude signals, terrain conductivity meters must have detection electronics that are an order of magnitude more sensitive than conventional HLEM systems.

The second difference is that terrain conductivity instruments are designed so that the quadrature phase zero level stays constant with time, temperature, etc., to within about 1 millisiemen/meter (mS/m). The stability of this zero level means that at moderate ground conductivity, these devices give an accurate measurement of bulk conductivity of the ground. These devices, like the conventional HLEM system, do not indicate conductivity accurately in high resistivity ground, because the zero error becomes significant at low values of conductivity.

The third difference is that operation at low induction numbers means that changing the frequency proportionately changes the quadrature phase response. In principle and in general, either intercoil spacing or frequency can be varied to determine variation of conductivity with depth. However, in the EM-31, EM-34, and EM-38 systems, frequency is varied as the intercoil spacing is varied. Terrain conductivity meters are operated in both the horizontal and vertical dipole modes. These terms describe the orientation of the transmitter and receiver coils to each other and the ground, and each mode gives a significantly different response with depth as shown in figure 291. Figure 292 shows the cumulative response curves for both vertical dipoles and horizontal dipoles. These curves show the relative contribution to the secondary magnetic field (and hence apparent conductivity) from all material below a given depth. As an example, this figure shows that for vertical dipoles, all material below a depth of two intercoil spacings yields a relative contribution of

approximately 0.25 (25%) to the response, i.e., the conductivity measurement. Thus, effective exploration depth in a layered earth geometry is approximately 0.25 to 0.75 times the intercoil spacing for the horizontal dipole mode and 0.5 to 1.5 for the vertical dipole mode. The commonly used systems use intercoil spacings of 1 m, 3.66 m, 10 m, 20 m, and 40 m.

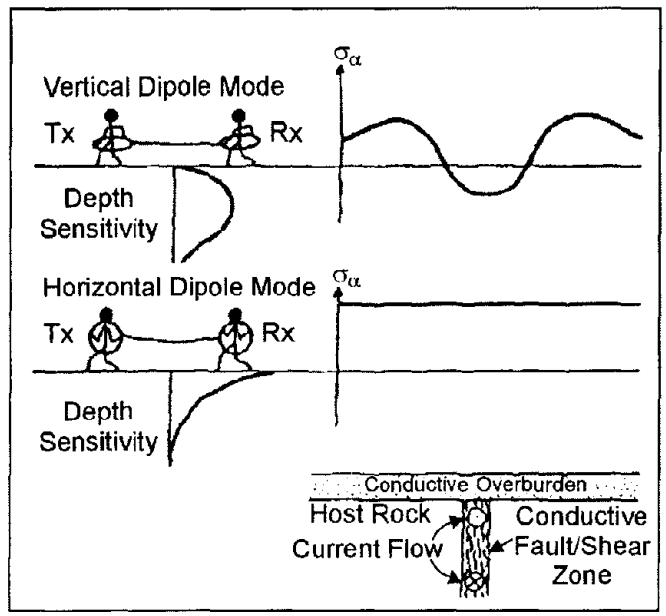

Figure 291. Terrain conductivity meter response over conductive dike. (McNeill 1990; copyright permission granted by Society of Exploration Geophysicists)

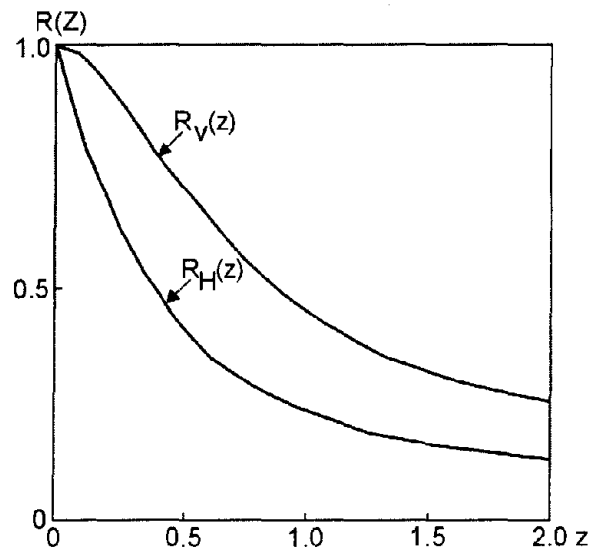

Figure 292. Cumulative response curves for both vertical coplanar and horizontal coplanar dipoles. Z is actually depth/intercoil spacing. (McNeill 1980; copyright permission granted by Geonics Ltd)

Terrain conductivity meters have shallower exploration depths than conventional HLEM, because maximum intercoil spacing is 40 m for the commonly used instruments. However, terrain conductivity meters are being widely used in geotechnical and environmental investigations. Of particular interest is the fact that when used in the vertical dipole mode, the instruments are more sensitive to the presence of relatively conductive, steeply dipping structures, whereas in the horizontal dipole mode the instruments are quite insensitive to this type of structure and can give accurate measurement of ground conductivity in close proximity to them.

Phase and other information are obtained in real time by linking the transmitter and receiver with a connecting cable. The intercoil spacing is determined by measuring the primary magnetic field with the receiver coil and adjusting the intercoil spacing so that it is the correct value for the appropriate distance. In the vertical dipole mode, the instruments are relatively sensitive to intercoil alignment, but much less so in the horizontal dipole mode. Terrain conductivity is displayed on the instrument in mS/m. (A conductivity of 1 mS/m corresponds to a resistivity of 1 kΩm or 1,000 Ωm.)

Data Interpretation

Because terrain conductivity meters read directly in apparent conductivity and most surveys using the instrument are done in the profile mode, interpretation is usually qualitative and of the "anomaly finding" nature. That is, the area of interest is surveyed with a series of profiles with a station spacing dictated by the required resolution and time/economics consideration. Typical station spacings are one-third to one-half the intercoil spacing. Any anomalous areas are investigated further with one or more of the following: other types of EM, resistivity sounding, other geophysical techniques, and drilling. Limited information about the variation of conductivity with depth can be obtained by measuring two or more coil orientations and/or intercoil separations and using one of several commercially available computer programs. The maximum number of geoelectric parameters, such as layer thicknesses and resistivities, which can be determined, is less than the number of independent observations. The most common instrument uses three standard intercoil distances (10, 20, and 40 m) and two intercoil orientations, which results in a maximum of six observations. Without other constraints, a two-layer model is the optimum.

Example 1 - Mapping Industrial Groundwater Contamination. Non-organic (ionic) groundwater contamination usually results in an increase in the conductivity of the groundwater. For example, in a sandy soil, the addition of 25 ppm of ionic material to groundwater increases ground conductivity by approximately 1 mS/m. The problem is to detect and map the extent of the contamination in the presence of conductivity variations caused by other parameters such as changing lithology. Organic contaminants are generally insulators and thus tend to reduce the ground conductivity, although with much less effect than an equivalent percentage of ionic contaminant. Fortunately, in many cases where toxic organic substances are present, there are ionic materials as well, and the plume is mapped on the theory that the spatial distribution of both organic and ionic substances is essentially the same, a fact that must be verified by subsequent sampling from monitoring wells installed on the basis of the conductivity map.

McNeill (1990) summarizes a case history by Ladwig (1982) that uses a terrain conductivity meter to map the extent of acid mine drainage in a rehabilitated surface coal mine in Appalachia. Measurements were taken with an EM ground conductivity meter in the horizontal dipole mode at both 10- and 20-m intercoil spacings (10-m data are shown in figure 293). Ten survey lines, at a spacing of 25 m, resulted in 200 data points for each spacing; the survey took 2 days to complete. In general, conductivity values of the order of 6 to 10 mS/m are consistent with a porous granular material reasonably well-drained or containing nonmineralized groundwater. Superimposed on this background are two steep peaks (one complex) where conductivities rise above 20 mS/m.

Wells F, G, and X were the only wells to encounter buried refuse (well W was not completed), and all three are at or near the center of the high conductivity zones. The water surface at well F is about 3 m below the surface, and at well X is 16.2 m below the surface. In fact, the only region where the water surface is within 10 m of the surface is at the southern end of the area; the small lobe near well D corresponds to the direction of groundwater flow to the seep (as the result of placement of a permeability barrier just to the west of the well). It thus appears that in the area of wells X and W, where depth to water surface is large, the shape and values of apparent conductivity highs are due to vertically draining areas of acidity. Further to the south, the conductivity high is probably reflecting both increased acidity and proximity of the water surface.

Examples 2 And 3 - Mapping Soil And Groundwater Salinity. EM techniques are well suited for mapping soil salinity to depths useful for the agriculturalist (the root zone, approximately 1 m), and many salinity surveys have been carried out with EM ground conductivity meters (McNeill 1990). In arid areas where the water surface is near the surface (within a meter or so), rapid transport of water to the surface as a result of capillary action and evaporation takes place, with the consequence that dissolved salts are left behind to hinder plant growth (McNeill 1986).

An EM terrain conductivity meter with short intercoil spacing (a few meters or less) is necessary to measure shallow salinity. Fortunately, the values of conductivity, which result from agriculturally damaging salinity levels, are relatively high, and interfering effects from varying soil structure, clay content, etc., can usually be ignored. Equally important, because salt is hygroscopic, those areas that are highly salinized seem to retain enough soil moisture to keep the conductivity at measurable levels even when the soil itself is relatively dry.

McNeill (1990) summarizes the results of a high-resolution survey of soil salinity carried out by Wood (1987) over dry farm land in Alberta, Canada (figure 294). For this survey, an EM terrain conductivity meter with an intercoil spacing of 3.7 m was mounted in the vertical dipole mode on a trailer, which was, in turn, towed behind a small four-wheeled, all-terrain vehicle. The surveyed area is 1,600 m long by 750 m wide. The 16 survey lines were spaced 50 m apart resulting in a total survey of 25 line km, which was surveyed in about 7 hr at an average speed of 3.5 km/hour. Data were collected automatically every 5.5 m by triggering a digital data logger from a magnet mounted on one of the trailer wheels.

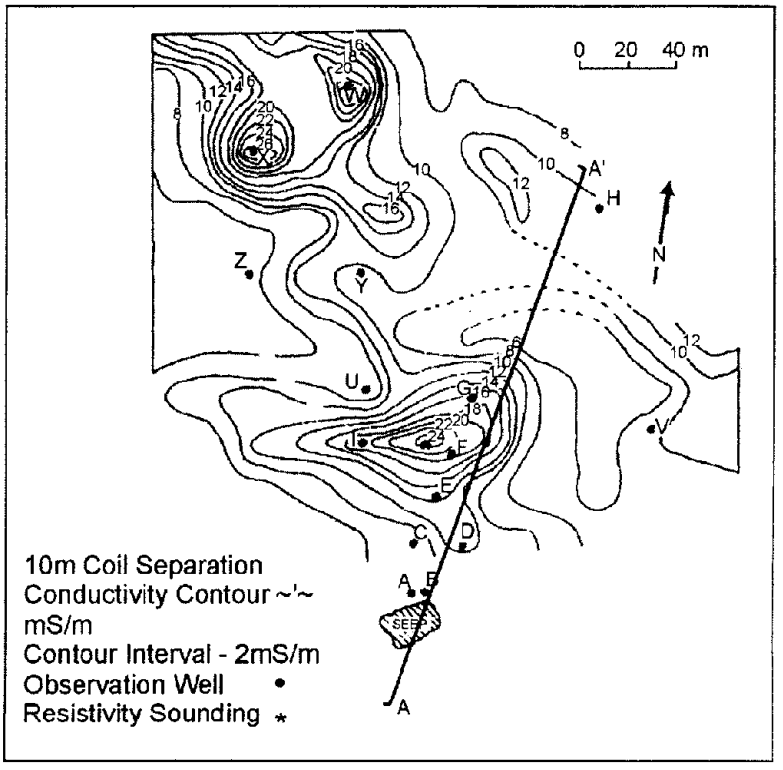

Figure 293. Contours of apparent conductivity for an acid mine dump site in Appalachia from terrain conductivity meter. (Ladwig (1982) and McNeill (1990); copyright permission granted by Society of Exploration Geophysicists)

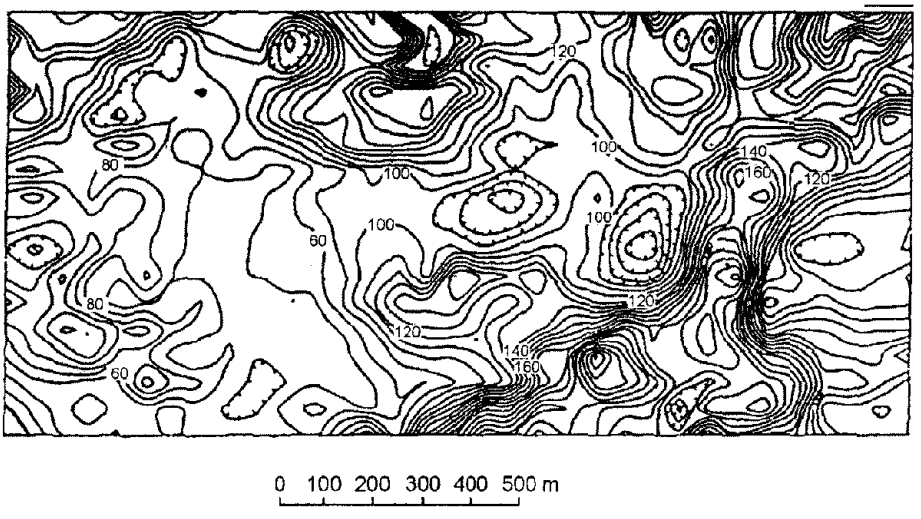

Figure 294. Contours of apparent conductivity measured with ground conductivity meter over dry farm land. Alberta, Canada. (Wood (1987) in McNeill (1990); copyright permission granted by Society of Exploration Geophysicists)

Survey data are contoured directly in apparent conductivity at a contour interval of 20 mS/m. The complexity and serious extent of the salinity is quite obvious. The apparent conductivity ranges from a low of 58 mS/m, typical of unsalinized Prairie soils, up to 300 mS/m, a value indicating extreme salinity. Approximately 25% of the area is over 160 mS/m, a value indicating a high level of salinity. The survey revealed and mapped extensive sub-surface salinity, not apparent by surface expression, and identified the areas most immediately threatened.

An example of a deeper penetrating survey to measure groundwater salinity was conducted by Barker (1990). The survey illustrates the cost-effective use of electromagnetic techniques in the delineation of the lateral extent of areas of coastal saltwater intrusion near Dungeness, England. As with most EM profiling surveys, a number of resistivity soundings were first made at the sites of several drill holes to help design the EM survey. In figure 295, a typical sounding and interpretation shows a three-layer case in which the low resistivity third layer appears to correlate with the conductivity of water samples from the drill holes and the clay/ sand lithology. To achieve adequate depth of investigation so that changes in water conductivity within the sands would be clearly identified, large coil spacings of 20 and 40 m were employed. The area is easily accessible and measurements can be made rapidly, but to reduce errors of coil alignment over some undulating gravel ridges, a vertical coil configuration was employed. This configuration is also preferred as the assumption of low induction numbers for horizontal coils breaks down quickly in areas of high conductivity. The extent of saline groundwater is best seen on figure 296, which shows the contoured ground conductivity in mS/m for the 40-m coil spacing. This map is smoother and less affected by near-surface features than measurements made with the 20-m coil spacing, and shows that the saline intrusion generally occurs along a coastal strip about 0.5 km wide. Flooding of inland gravel pits by the sea has allowed marine incursion in the west, leaving an isolated body of fresh water below Dungeness.

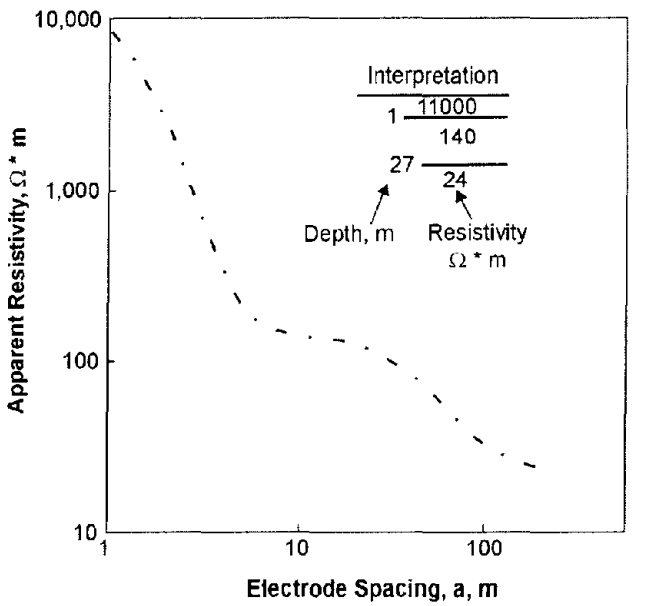

Figure 295. Typical resistivity sounding and interpretation, Dungeness, England. (Barker 1990; copyright permission granted by Society of Exploration Geophysicists)

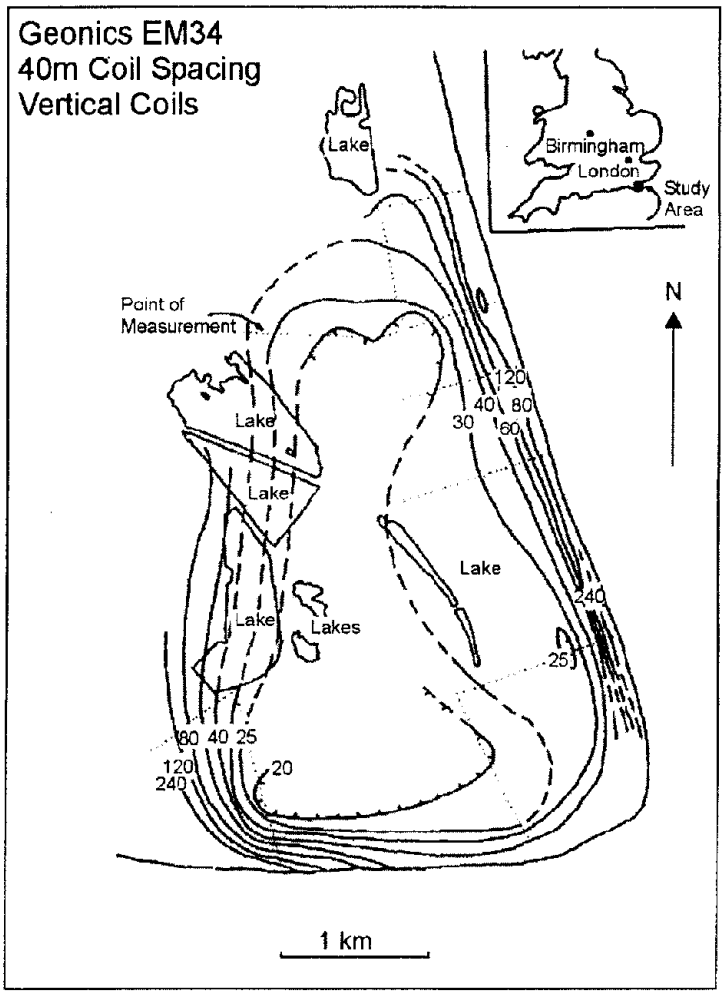

Figure 296. Contours of ground conductivity in mS/m, Dungeness, England. (Baker 1990; copyright permission granted by Society of Exploration Geophysicists)

Example 4 - Subsurface Structure. Dodds and Ivic (1990) describe a terrain conductivity meter survey to investigate the depth to basement in southeast Australia. During the first part of the survey, time domain EM and resistivity soundings were used to detect a basement high, which impedes the flow of saline groundwater. In the second part of the survey, a terrain conductivity meter was used to map the extent of the basement high as far and as economically as possible. The largest coil separation available with the instrument, 40 m, was used to get the deepest penetration with horizontal coil orientation. A very limited amount of surveying, using short traverses, successfully mapped out a high-resistivity feature (figure 297). This zone is confirmed by the plotted drilling results.

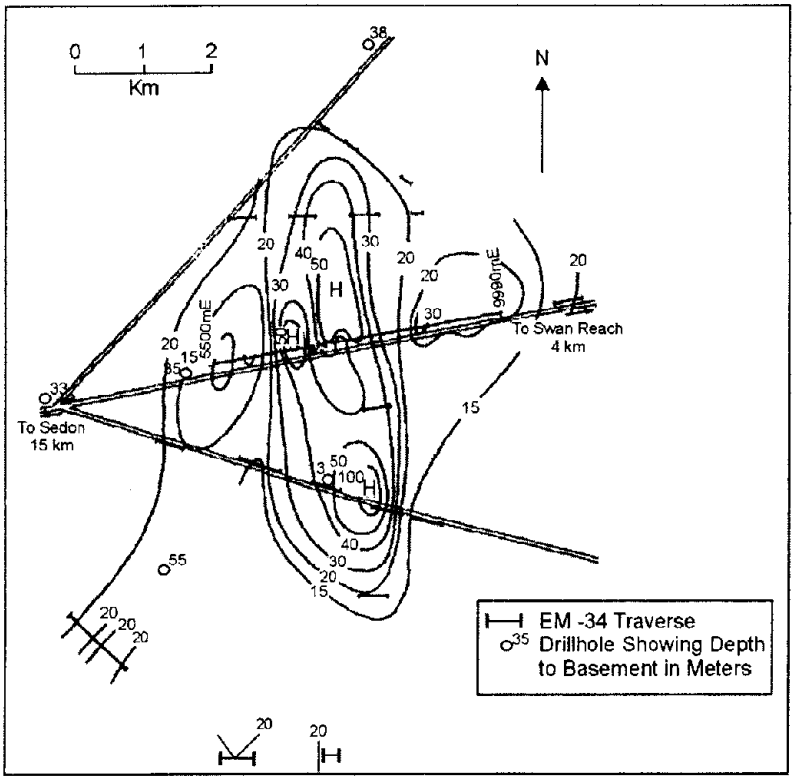

Figure 297. Apparent conductivity contours in ohm-m from a terrain conductivity meter Survey in southern Australia. (Dodds and Ivic 1990; copyright permission granted by Society of Exploration Geophysicists)

9.4.2 Time-Domain Electromagnetic Methods

Basic Concept

Conventional DC resistivity techniques have been applied for many years to a variety of geotechnical applications. More recently, electromagnetic techniques, with different advantages (and disadvantages) compared with conventional DC, have been used effectively to measure the resistivity (or its reciprocal, the conductivity) of the Earth.

Electromagnetic techniques can be broadly divided into two groups. In frequency-domain instrumentation (FDEM), the transmitter current varies sinusoidally with time at a fixed frequency that is selected on the basis of the desired depth of exploration of the measurement (high frequencies result in shallower depths). In most time-domain (TDEM) instrumentation, on the other hand, the transmitter current, although still periodic, is a modified symmetrical square wave, as shown in figure 298. It is seen that after every second quarter-period, the transmitter current is abruptly reduced to zero for one quarter period, whereupon it flows in the opposite direction.

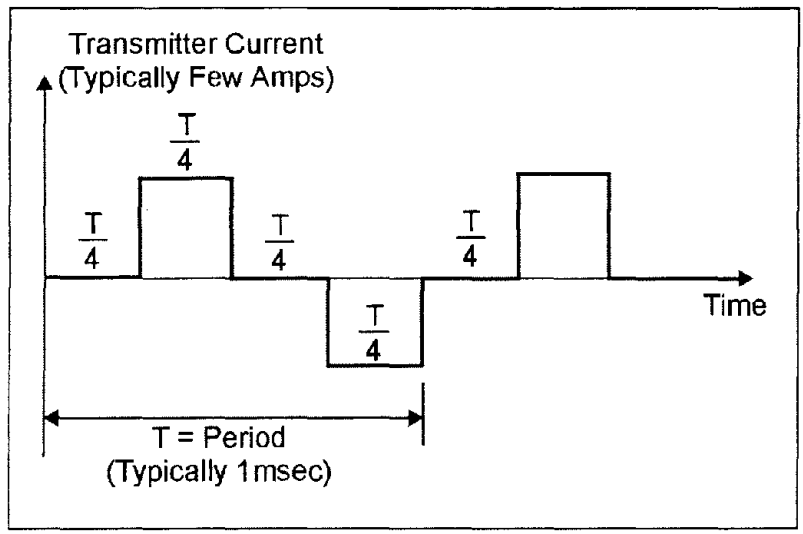

Figure 298. Transmitter current wave form.

A typical TDEM resistivity sounding survey configuration is shown in figure 299, where it is seen that the transmitter is connected to a square (usually single turn) loop of wire laid on the ground. The side length of the loop is approximately equal to the desired depth of exploration, except that for shallow depths (less than 40 m), the length can be as small as 5 to 10 m in relatively resistive ground. A multi-turn receiver coil, located at the center of the transmitter loop, is connected to the receiver through a short length of cable.

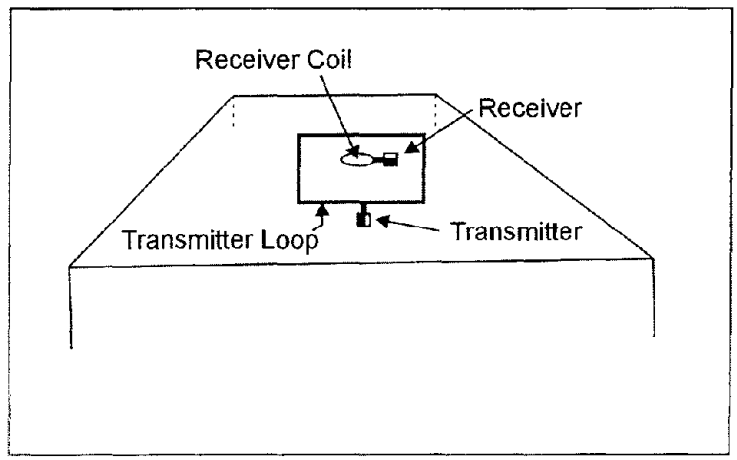

Figure 299. Central loop sounding configuration.

The principles of TDEM resistivity sounding are relatively easily understood. The process of abruptly reducing the transmitter current to zero induces, in accord with Faraday's law, a short-duration voltage pulse in the ground, which causes a loop of current to flow in the immediate vicinity of the transmitter wire, as shown in figure 300. In fact, immediately after transmitter current is turned off, the current loop can be thought of as an image in the ground of the transmitter loop. However, because of finite ground resistivity, the amplitude of the current starts to decay immediately. This decaying current similarly induces a voltage pulse that causes more current to flow, but now at a larger distance from the transmitter loop, and

also at greater depth, as shown in figure 300. This deeper current flow also decays due to finite resistivity of the ground, inducing even deeper current flow and so on. The amplitude of the current flow as a function of time is measured by measuring its decaying magnetic field using a small multi-turn receiver coil usually located at the center of the transmitter loop. From the above, it is evident that, by making measurement of the voltage out of the receiver coil at successively later times, measurement is made of the current flow and thus also of the electrical resistivity of the earth at successively greater depths. This process forms the basis of central loop resistivity sounding in the time domain.

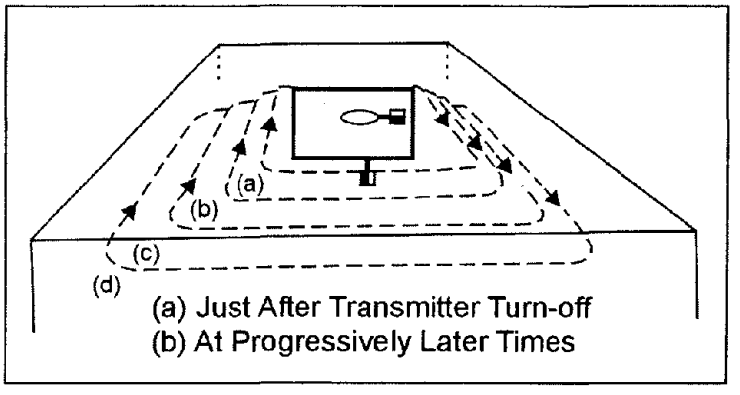

Figure 300. Transient current flow in the ground.

The output voltage of the receiver coil is shown schematically (along with the transmitter current) in figure 301. To accurately measure the decay characteristics of this voltage, the receiver contains 20 narrow time gates (indicated in figure 302), each opening sequentially to measure (and record) the amplitude of the decaying voltage at 20 successive times. Note that to minimize distortion in measurement of the transient voltage, the early time gates, which are located where the transient voltage is changing rapidly with time, are very narrow, whereas the later gates, situated where the transient is varying more slowly, are much broader. This technique is desirable since wider gates enhance the signal-to-noise ratio, which becomes smaller as the amplitude of the transient decays at later times. It will be noted from figure 301 that there are four receiver voltage transients generated during each complete period (one positive pulse plus one negative pulse) of transmitter current flow. However, measurement is made only of those two transients that occur when the transmitter current has just been shut off, since in this case, accuracy of the measurement is not affected by small errors in location of the receiver coil. This feature offers a very significant advantage over FDEM measurements, which are generally very sensitive to variations in the transmitter coil/receiver coil spacing since the FDEM receiver measures while the transmitter current is flowing. Finally, particularly for shallower sounding, where it is not necessary to measure the transient characteristics out to very late times, the period is typically of the order of 1 msec or less, which means that in a total measurement time of a few seconds, measurement can be made and stacked on several thousand transient responses. This is important since the transient response from one pulse is exceedingly small, and it is necessary to improve the signal-to-noise ratio by adding the responses from a large number of pulses.

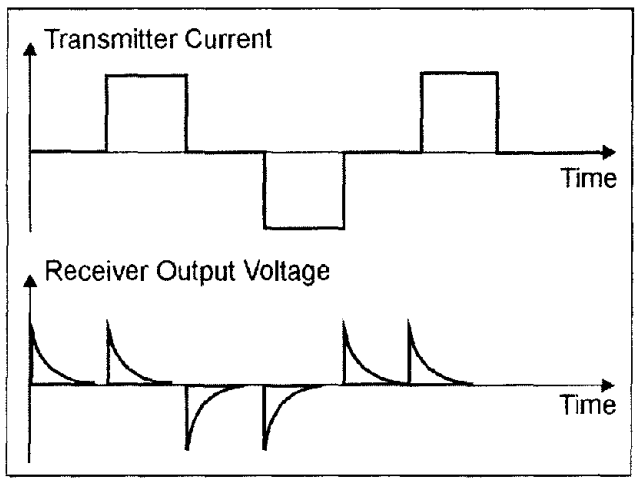

Figure 301. Receiver output wave form.

Apparent Resistivity In TDEM Soundings

Figure 302 shows, schematically, a linear plot of typical transient response from the earth. It is useful to examine this response when plotted logarithmically against the logarithm of time, particularly if the earth is homogeneous (i.e. the resistivity does not vary with either lateral distance or depth). Such a plot is shown in figure 303, which suggests that the response can be divided into an early stage (where the response is constant with time), an intermediate stage (response shape continually varying with time), and a late stage (response is now a straight line on the log-log plot). The response is generally a mathematically complex function of conductivity and time; however, during the late stage, the mathematics simplifies considerably, and it can be shown that during this time the response varies quite simply with time and conductivity as

$$e(t) = \frac{k_1 M \sigma^{3/2}}{t^{5/2}}, \tag{74}$$

where

$e(t)$= output voltage from a single-turn receiver coilof area 1 m2
k_1 = a constant
M = product of Tx current x area (a-m2)
σ = terrain conductivity (siemens/m = S/m = 1/Ωm)
t = time (s)

Unlike the case for conventional resistivity measurement, where the measured voltage varies linearly with terrain resistivity, for TDEM, the measured voltage e(t) varies as $\sigma^{3/2}$, so it is intrinsically more sensitive to small variations in the conductivity than conventional resistivity. Note that during the late stage, the measured voltage is decaying at the rate $t^{-5/2}$, which is very rapidly with time. Eventually the signal disappears into the system noise, and further measurement is impossible. This is the maximum depth of exploration for the particular system.

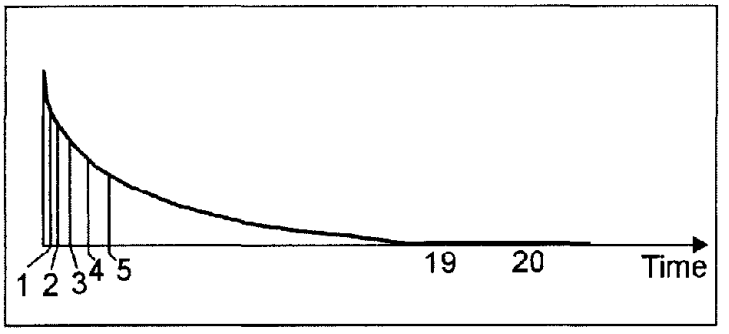

Figure 302. Receiver gate locations.

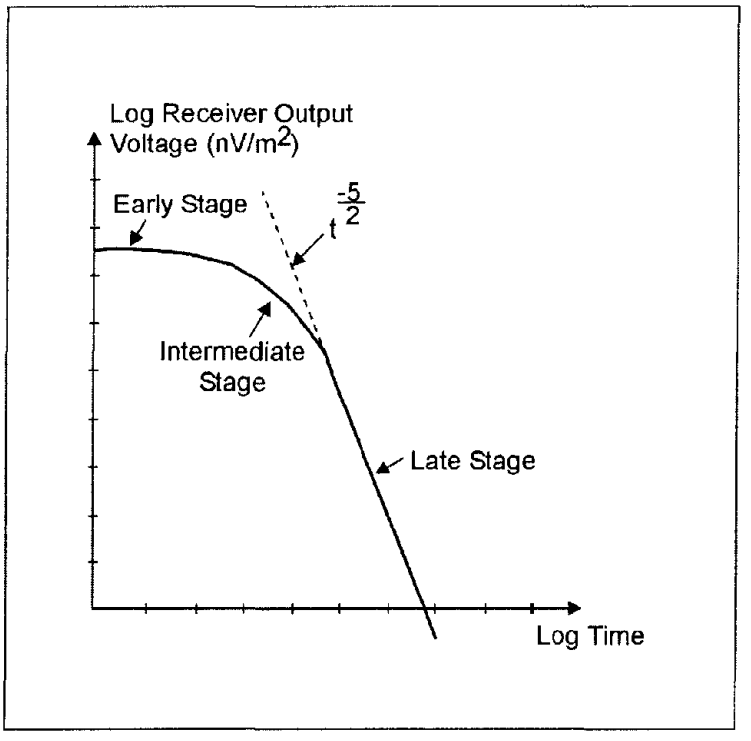

Figure 303. Log plot-receiver output voltage versus time (one transient).

With conventional DC resistivity methods, for example the commonly used Wenner array, the measured voltage over a uniform earth can be shown to be

$$V(a) = \frac{\rho I}{2\pi a} \tag{75a}$$

where

a = interelectrode spacing (m)
ρ = terrain resistivity (Ωm)
I = current into the outer electrodes
$V(a)$ = voltage measured across the inner electrodes for the specific value of a

In order to obtain the resistivity of the ground, equation 75a is rearranged (inverted) to give equation 75b:

$$\rho = 2\pi a \frac{V(a)}{I} \tag{75b}$$

If ground resistivity is uniform as the interelectrode spacing (a) is increased, the measured voltage increases directly with a so that the right-hand side of equation 75b stays constant, and the equation gives the true resistivity. Suppose now that the ground is horizontally layered (i.e., that the resistivity varies with depth); for example, it might consist of an upper layer of thickness h and resistivity $\rho 1$, overlying a more resistive basement of resistivity $\rho 2 > \rho 1$, (this is called a two-layered earth). At very short interelectrode spacing ($a<<h$), virtually no current penetrates into the more resistive basement, and resistivity calculation from equation 75b will give the value $\rho 1$. As interelectrode spacing is increased, the current (I) is forced to flow to greater and greater depths. Suppose that, at large values of a ($a>>h$), the effect of the near-surface material of resistivity $\rho 1$ will be negligible, and resistivity calculated from equation 75b will give the value $\rho 2$, which is indeed what happens. At intermediate values of a ($a.h$), the resistivity given by equation 75b will lie somewhere between $\rho 1$ and $\rho 2$.

Equation 75b is, in the general case, used to define an apparent resistivity $\rho a(a)$, which is a function of a. The variation of a $\rho_a(a)$ with a

$$\rho_a(a) = 2\pi a \frac{V(a)}{I} \tag{76}$$

is descriptive of the variation of resistivity with depth. The behavior of the apparent resistivity $\rho_a(a)$ for a Wenner array for the two-layered earth above is shown schematically in figure 304. It is clear that in conventional resistivity sounding, to increase the depth of exploration, the interelectrode spacing must be increased. In the case of TDEM soundings, on the other hand, it was observed earlier that as time increased, the depth to the current loops increased, and this phenomenon is used to perform the sounding of resistivity with depth. Thus, in analogy with equation 76, equation 74 is inverted to read (since $\rho = 1/\sigma$)

$$\rho_a(t) = \frac{k_2 M^{2/3}}{e(t)^{2/3} t^{5/3}}. \tag{77}$$

Suppose once again that terrain resistivity does not vary with depth (i.e. a uniform half-space) and is of resistivity $\rho 1$. For this case, a plot of $\rho_a(t)$ against time would be as shown in figure 305. Note that at late time the apparent resistivity $\rho_a(t)$ is equal to $\rho 1$, but at early time $\rho_a(t)$ is much larger than $\rho 1$. The reason for this is that the definition of apparent resistivity is based (as seen from figure 303) on the time behavior of the receiver coil output voltage at late time when it decays as $t^{-5/2}$. At earlier and intermediate time, figure 303 shows that the

receiver voltage is too low (the dashed line indicates the voltage given by the late stage approximation) and thus, from equation 77, the apparent resistivity will be too high. For this reason, there will always be, as shown on figure 305, a "descending branch" at early time where the apparent resistivity is higher than the half-space resistivity (or, as will be seen later, is higher than the upper layer resistivity in a horizontally layered earth). This is not a problem, but it is an artifact of which we must be aware.

If we let the earth be two-layered of upper layer resistivity $\rho 1$, and thickness h, and basement resistivity $\rho 2$ ($>\rho 1$), at early time when the currents are entirely in the upper layer of resistivity $\rho 1$ the decay curve will look like that of figure 303, and the apparent resistivity curve will look like figure 304. However, later on the currents will lie in both layers, and at much later time, they will be located entirely in the basement, of resistivity $\rho 2$. Since $\rho 2>\rho 1$, equation 77 shows that, as indicated in figure 306a, the measured voltage will now be less than it should have been for the homogeneous half-space of resistivity $\rho 1$. The effect on the apparent resistivity curve is shown in figure 307a. Since at late times all the currents are in the basement, the apparent resistivity $\rho_a(t)$ becomes equal to $\rho 2$, completely in analogy for figure 304 for conventional resistivity measurements. In the event that $\rho 2<\rho 1$, the inverse behavior is also as expected, i.e., at late times the measured voltage response, shown in figure 306b, is greater than that from a homogeneous half-space of resistivity $\rho 1$, and the apparent resistivity curve correspondingly becomes that of figure 307b, becoming equal to the new value of $\rho 2$ at late time. Note that for the case of a (relatively) conductive basement, there is a region of intermediate time (shown as t^*), where the voltage response temporarily falls before continuing on to adopt the value appropriate to $\rho 2$. This behavior, which is a characteristic of TDEM, is again not a problem, as long as it is recognized. The resultant influence of the anomalous behavior on the apparent resistivity is also shown on figure 307b at t^*.

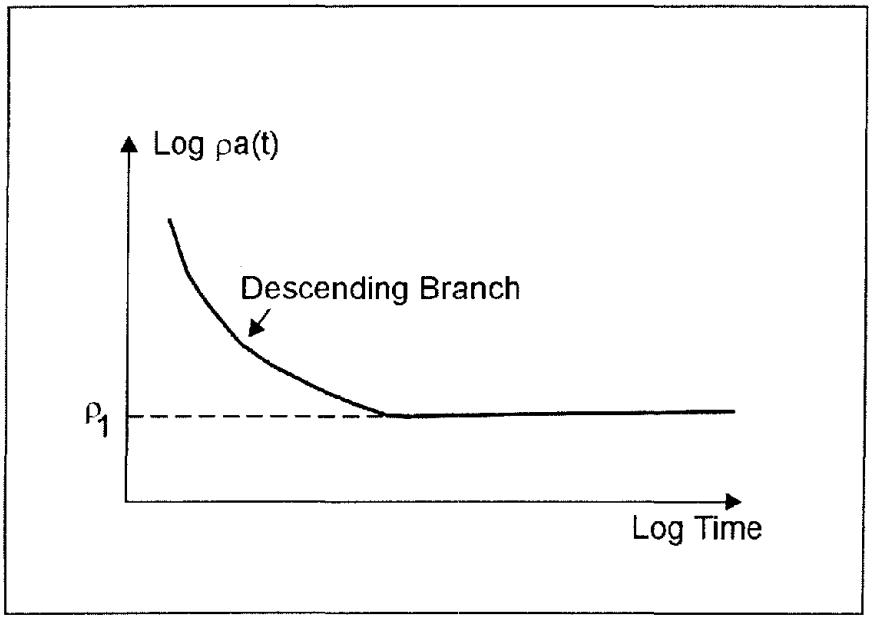

Figure 304. Wenner array: apparent resistivity, two layer curve

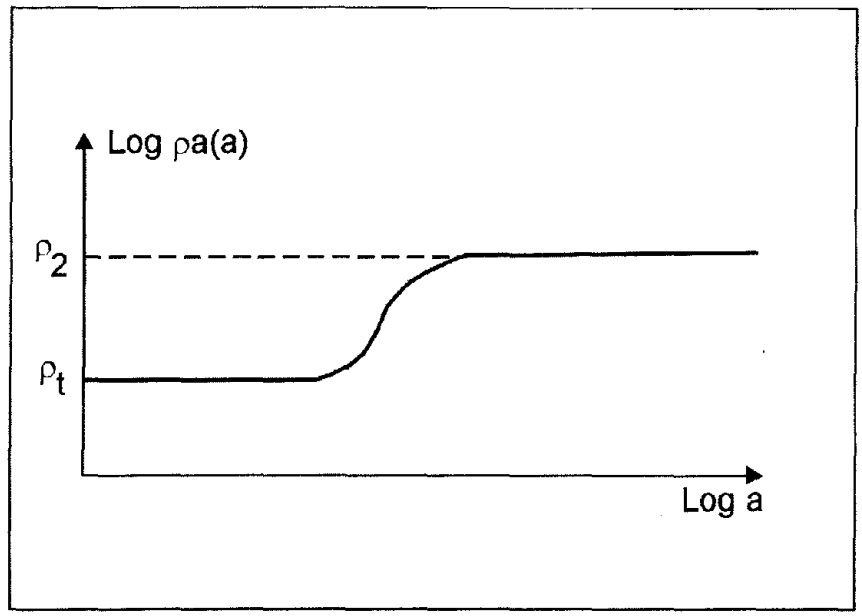

Figure 305. Time Domain Electromagnetic (TDEM): apparent resistivity, homogeneous half space.

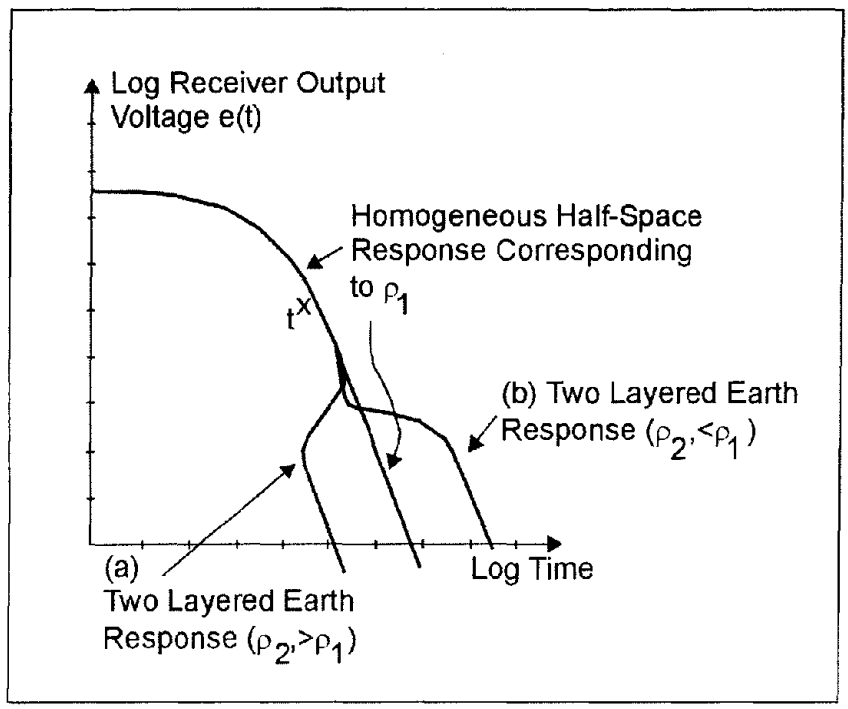

Figure 306. Time Domain Electromagnetic (TDEM): receiver output voltage, two layer earth.

To summarize, except for the early-time descending branch and the intermediate-time anomalous region described above, the sounding behavior of TDEM is analogous to that of conventional DC resistivity if the passage of time is allowed to achieve the increasing depth of exploration rather than increasing interelectrode spacing.

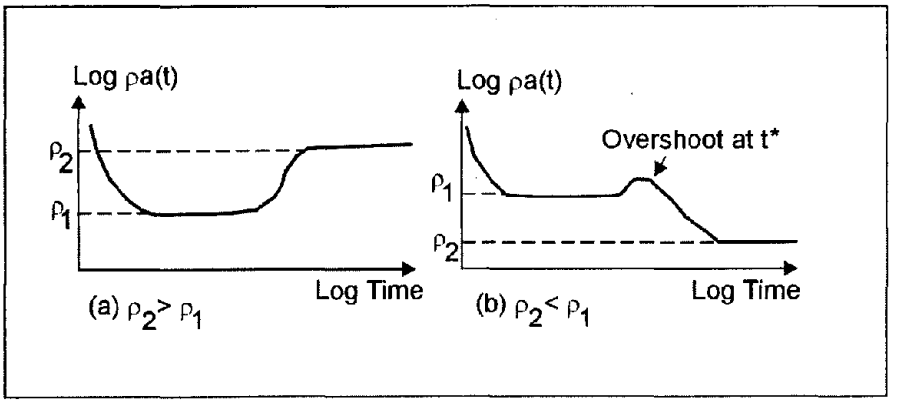

Figure 307. Time Domain Electromagnetic (TDEM): apparent resistivity, two layered earth.

Curves of apparent resistivity such as figure 307 tend to disguise the fact, that, at very late times, there is simply no signal, as is evident from figure 306. In fact, in the TDEM central loop sounding method, it is unusual to see, in practical data, the curve of apparent resistivity actually asymptote to the basement resistivity due to loss of measurable signal. Fortunately, both theoretically and in practice, the information about the behavior of the apparent resistivity curve at early time and in the transition region is generally sufficient to allow the interpretation to determine relatively accurately the resistivity of the basement without use of the full resistivity-sounding curve.

Data Acquisition

A common survey configuration consists of a square single turn loop with a horizontal receiver coil located at the center. Data from a resistivity sounding consist of a series of values of receiver output voltage at each of a succession of gate times. These gates are located in time typically from a few microseconds up to tens or even hundreds of milliseconds after the transmitter current has been turned off, depending on the desired depth of exploration. The receiver coil measures the time rate of change of the magnetic field $e(t)_2$=dB/dt, as a function of time during the transient. Properly calibrated, the units of e(t) are V/m^2 of receiver coil area; however, since the measured signals are extremely small, it is common to use nV/m^2, and measured decays typically range from many thousands of nV/m^2 at early times to less than 0.1 nV/m^2 at late times. Modern receivers are calibrated in nV/m^2 or V/m^2. To check the calibration, a "Q-coil," which is a small short-circuited multi-turn coil laid on the ground at an accurate distance from the receiver coil, is often used so as to provide a transient signal of known amplitude.

The two main questions in carrying out a resistivity sounding are (a) how large should the side lengths of the (usually single-turn) transmitter be, and (b) how much current should the loop carry? Both questions are easily answered by using one of the commercially available forward layered-earth computer modeling programs. A reasonable guess as to the possible geoelectric section (i.e., the number of layers, and the resistivity and thickness of each) is made. These data are then fed into the program, along with the proposed loop size and current, and the transient voltage is calculated as a function of time. For example, assume that it is suspected that a clay aquitard may exist at a depth of 20 m in an otherwise clay-free sand. Resistivity of the sand might be 100 Ωm, and that of the clay layer 15 Ωm. Desired

information includes the minimum thickness of the clay layer that is detectable, and the accuracy with which this thickness can be measured. The depth of exploration is of the order of the loop edge size, so 10 m by 10 m represents a reasonable guess for model calculation, along with a loop current of 3 A, which is characteristic of a low-power, shallow-depth transmitter. Before doing the calculations, one feature regarding the use of small (i.e., less than 60 m by 60 m) transmitter loops for shallow sounding should be noted. In these small loops, the inducing primary magnetic field at the center of the loop is very high, and the presence of any metal, such as the receiver box, or indeed the shielding on the receiver coil itself, can cause sufficient transient response to seriously distort the measured signal from the ground. This effect is greatly reduced by placing the receiver coil (and receiver) a distance of about 10 m outside the nearest transmitter edge. As shown later, the consequence of this on the data is relatively small.

The first task is to attempt to resolve the difference between, for example, a clay layer 0 m thick (no clay) and 1 m thick. Results of the forward layered-earth calculation, shown in figure 308, indicate that the apparent resistivity curves from these two cases are well separated (difference in calculated apparent resistivity is about 10%) over the time range from about 8 μs to 100 μs, as would be expected from the relatively shallow depths. Note that to use this early time information, a receiver is required that has many narrow early time gates in order to resolve the curve, and also has a wide bandwidth so as not to distort the early portions of the transient decay. Note from the figure that resolving thicknesses from 1 to 4 m and greater will present no problem.

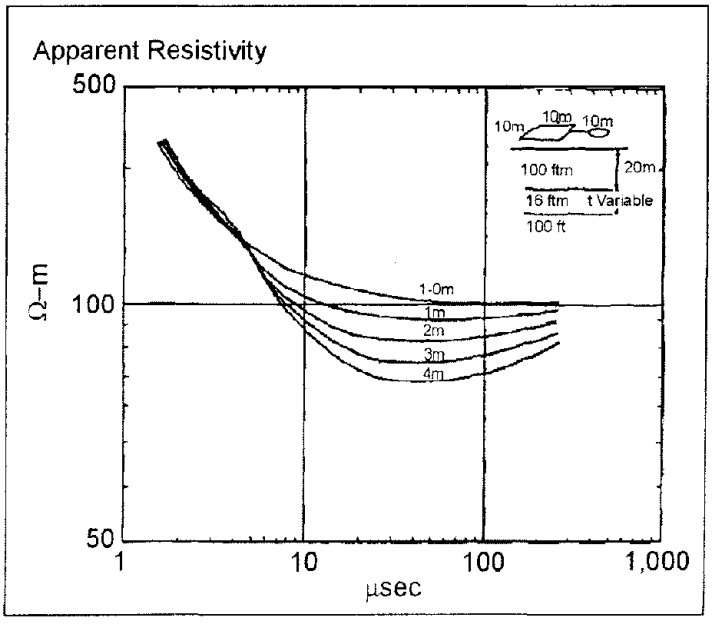

Figure 308. Forward layered-earth calculations

Having ascertained that the physics of TDEM sounding will allow detection of this thin layer, the next test is to make sure that the 10- by 10-m transmitter running at 3 A will provide sufficient signal-to-noise over the time range of interest (8 to 100 μs). The same forward layered-earth calculation also outputs the actual measured voltages that would be measured from the receiver coil. These are listed (for the case of thickness of 0 m, which

will produce the lowest voltage at late times) in table 15. Focus attention on the first column (which gives the time, in seconds) and the third column (which gives the receiver output as a function of time, in V/m^2). The typical system noise level (almost invariably caused by external noise sources) for gates around 100 to 1,000 μs is about 0.5 nV/m^2, or 5 x $10^{-10} V/m^2$. From columns 1 and 3 see that, for the model chosen, the signal falls to 5 x $10^{-10} V/m^2$ at a time of about 630 μs and is much greater than this for the early times when the apparent resistivity curves are well-resolved, so it is learned that the 10- by 10-m transmitter at 3 A is entirely adequate. In fact, if a 5- by 5-m transmitter was used, the dipole moment (product of transmitter current and area) would fall by 4, as would the measured signals, and the signal-to-noise ratio would still be excellent over the time range of interest. Thus assured, assuming that the model realistically represents the actual conditions of resistivity, the procedure will be able to detect the thin clay layer. Before proceeding with the actual measurement, it would be wise to vary some of the model parameters, such as the matrixand clay resistivities, to see under what other conditions the clay will be detectable. The importance of carrying out such calculations cannot be overstated. The theory of TDEM resistivity sounding is well understood, and the value of such modeling, which is inexpensive and fast, is very high.

It was stated above that offsetting the receiver coil from the center of the transmitter loop would not greatly affect the shape of the apparent resistivity curves. The reason for this is that the vertical magnetic field arising from a large loop of current (such as that shown in the ground at late time in figure 300) changes very slowly in moving around the loop center. Thus, at late time, when the current loop radius is significantly larger than the transmitter loop radius, it would be expected that moving the receiver from the center of the transmitter loop to outside the loop would not produce a large difference, whereas at earlier times, when the current loop radius is approximately the same as the transmitter radius, such offset will have a larger effect. This behavior is illustrated in figure 309, which shows the apparent resistivity curves for the receiver at the center and offset by 15 m from the center of the 10- by 10-m transmitter loop. At late time, the curves are virtually identical.

One of the big advantages of TDEM geoelectric sounding over conventional DC sounding is that for TDEM, the overall width of the measuring array is usually much less than the depth of exploration, whereas for conventional DC sounding, the array dimension is typically (Wenner array) of the order of three times the exploration depth. Thus, in the usual event that the terrain resistivity is varying laterally, TDEM sounding will generally indicate those variations much more accurately. If the variations are very closely spaced, one might even take measurements at a station spacing of every transmitter loop length. It should be noted that most of the time spent doing a sounding (especially deeper ones where the transmitter loop is large) is utilized in laying out the transmitter loop. In this case, it can be much more efficient to have one or even two groups laying out loops in advance of the survey party, who then follow along with the actual transmitter, receiver, and receiver coil to make the sounding in a matter of minutes, again very favorable compared with DC sounding. A further advantage of TDEM geoelectric sounding is that, if a geoelectric interface is not horizontal, but is dipping, the TDEM still gives a reasonably accurate average depth to the interface. Similarly, TDEM sounding is much less sensitive (especially at later times) to varying surface topography.

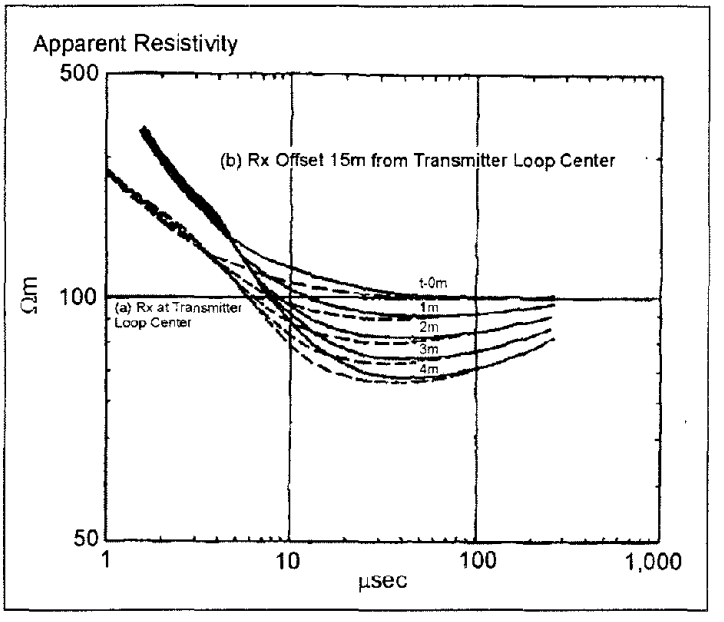

Figure 309. Forward layered earth calculations, a) central loop sounding, b) offset sounding.

It was explained above that, particularly at later times, the shape of the apparent resistivity curve is relatively insensitive to the location of the receiver coil. This feature is rather useful when the ground might be sufficiently inhomogeneous to invalidate a sounding (in the worst case, for example, due to a buried metallic pipe). In this case, a useful and quick procedure is to take several measurements at different receiver locations, as shown in figure 310. Curve 5 is obviously anomalous, and must be rejected. Curves 1-4 can all be used in the inversion process, which handles both central and offset receiver coils. Another useful way to ensure, especially for deep soundings, that the measurement is free from errors caused by lateral inhomogeneities (perhaps a nearby fault structure) is to use a three- component receiver coil, which measures, in addition to the usual vertical component of the decaying magnetic field, both horizontal components. When the ground is uniform or horizontally layered, the two horizontal components are both essentially equal to zero, as long as the measurement is made near the transmitter loop center (which is why the technique is particularly relative to deep sounding). Departures from zero are a sure indication of lateral inhomogeneities that might invalidate the sounding.

Most receivers, particularly those designed for shallower sounding, have an adjustable base frequency to permit changing the length of the measurement time. With reference to figures 298 and 301, changing the base frequency f_b will change the period T ($T=1/f_b$), and thus the measurement duration T/4. For transients that decay quickly, such as shallow sounding, the measurement period, which should be of the order of duration of the transient, should be short, and thus the base frequency high. This has the advantage that, for a given total integration time of, say 5 s, more transient responses will be stacked, to improve the signal-to-noise ratio and allow the use of smaller, more mobile, transmitter loops, increasing survey speed. On the other hand, for deep sounding, where the response must be measured out to very long time, it is clear that the measurement period must be greatly extended so that the transient response does not run on to the next primary field cycle or indeed the next transient response, and thus the base frequency must be significantly reduced. The signal-to-noise

ratio will deteriorate due to fewer transients being stacked, and must be increased by either using a larger transmitter loop and transmitter current (to increase the transmitter dipole) and/or integrating the data for a longer stacking time, perhaps for 30 s or even a minute. It should be noted that should such run-on occur because too high a base frequency was employed, it can still be corrected for in modern data inversion programs; however, in extreme cases, accuracy and resolution of the inversion will start to deteriorate.

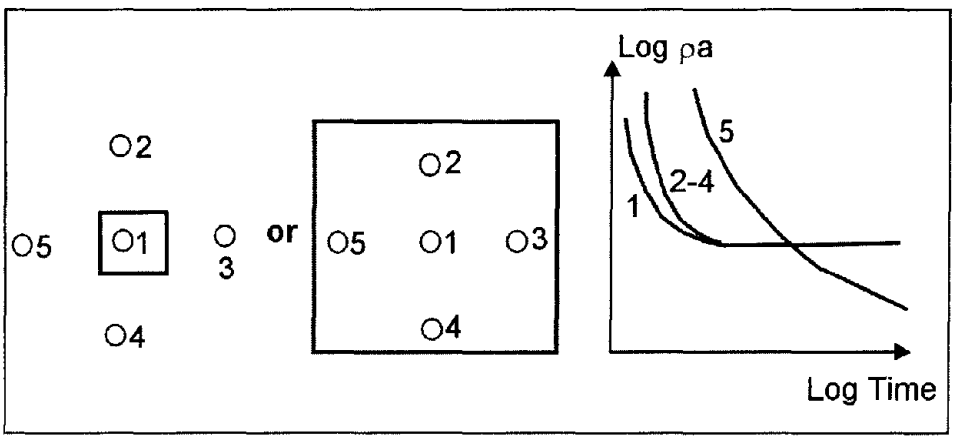

Figure 310. Offset Rx locations to check lateral homogeneity; position 5 is near lateral inhomogeneity.

In figure 301 and in this discussion, it was assumed that the transmitter current is turned off instantaneously. To actually accomplish this with a large loop of transmitter wire is impossible, and modern transmitters shut the current down using a very fast linear ramp. The duration of this ramp is maintained as short as possible (it can be shown to have an effect similar to that of broadening the measurement gate widths) particularly for shallow sounding where the transient decays very rapidly at early times. The duration of the transmitter turn-off ramp (which can also be included in modern inversion programs) is usually controlled by transmitter loop size and/or loop current.

Sources of Noise

Noise sources for TDEM soundings can be divided into four categories:

a) Circuit noise (usually so low in modern receivers as to rarely cause a problem).

b) Radiated and induced noise.

c) Presence of nearby metallic structures.

d) Soil electrochemical effects (induced polarization).

Radiated noise consists of signals generated by radio and radar transmitters and also from thunderstorm lightning activity. The first two are not usually a problem; however, on summer days when there is extensive local thunderstorm activity, the electrical noise from lightning strikes (similar to the noise heard on AM car radios) can cause problems, and it may be necessary to increase the integration (stacking) time or, in severe cases, to discontinue the survey until the storms have passed by or abated.

The most important source of induced noise consists of the intense magnetic fields from 50- to 60-Hz power lines. The large signals induced in the receiver from these fields (which fall off more or less linearly with distance from the power line) can overload the receiver if the receiver gain is set to be too high, and thus cause serious errors. The remedy is to reduce the receiver gain so that overload does not occur, although in some cases, this may result in less accurate measurement of the transient since the available dynamic range of the receiver is not being fully utilized. Another alternative is to move the measurement array further from the power line.

The response from metallic structures can be very large compared with the response from the ground. Interestingly, the power lines referred to above can often also be detected as metallic structures, as well as sources of induced noise. In this case, they exhibit an oscillating response (the response from all other targets, including the earth, decays monotonically to zero). Since the frequency of oscillation is unrelated to the receiver base frequency, the effect of power line structural response is to render the transient "noisy" as shown in figure 311. Since these oscillations arise from response to eddy currents actually induced in the power line by the TDEM transmitter, repeating the measurement will produce an identical response, which is one way that these oscillators are identified. Another way is to take a measurement with the transmitter turned off. If the "noise" disappears, it is a good indication that power-line response is the problem. The only remedy is to move the transmitter farther from the power line. Other metallic responses, such as those from buried metallic trash or pipes, can also present a problem, a solution for which was discussed in the previous section (multiple receiver sites, as shown in figure 310). If the response is very large, another sounding site must be selected. Application of another instrument such as a metal detector or ground conductivity meter to quickly survey the site for pipes can often prove useful.

A rather rare effect, but one which can occur, particularly in clayey soils, is that of induced polarization. Rapid termination of the transmitter current can charge up the minute electrical capacitors in the soil interfaces (induced polarization). These capacitors subsequently discharge, producing current flow similar to that shown in figure 300, but in the opposite direction. The net effect is to reduce the amplitude of the transient response (thus increasing the apparent resistivity) or even, where the effect is very severe, to cause the transient response to become negative over some range of the measurement time. Since these sources of reverse current are localized near the transmitter loop, using the offset configuration usually reduces the errors caused by them to small values.

In summary, it should be noted that in TDEM soundings, the signal-to-noise ratio is usually very good over most of the time range. However, in general, the transient response is decaying extremely rapidly (of the order of $t^{-5/2}$, or by a factor of about 300 for a factor of 10 increase in time). The result is that toward the end of the transient, the signal-to-noise ratio suddenly deteriorates completely, and the data become exceedingly noisy. The transient is over!

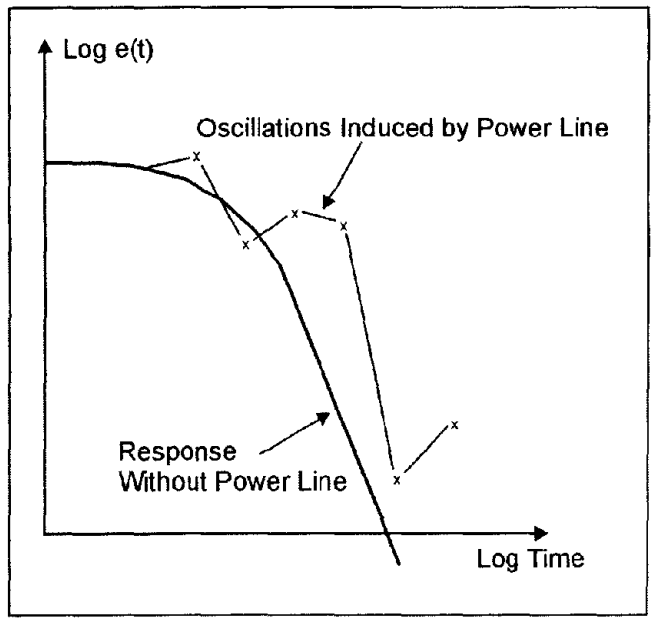

Figure 311. Oscillations induced in receiver response by power line.

Data Processing and Interpretation

In the early days of TDEM sounding, particularly in Russia where the technique was developed (Kaufman and Keller 1983), extensive use was made of numerically calculated apparent resistivity curves for a variety of layered earth geometrics. Field data would be compared with a selection of curves, from which the actual geoelectric section would be determined. More recently, the advent of relatively fast computer inversion programs allows field transient data to be automatically inverted to a layered earth geometry in a matter of minutes. An inversion program offers an additional significant advantage. All electrical sounding techniques (conventional DC, magneto-telluric, TDEM) suffer to a greater or less extent from equivalence, which basically states that, to within a given signal-to-noise ratio in the measured data, more than one specific geoelectric model will fit the measured data. This problem, which is seldom addressed in conventional DC soundings, is one of which the interpreter must be aware, and the advantage of the inversion program is that, given an estimate of the signal-to-noise ratio in the measured data, the program could calculate a selection of equivalent geoelectric sections that will also fit the measured data, immediately allowing the interpreter to decide exactly how unique his solution really is. Equivalence is a fact of life, and must be included in any interpretation.

Advantages and Limitations

The advantages of TDEM geoelectric sounding over conventional DC resistivity sounding are significant. They include the following:

1. Improved speed of operation.

2. Improved lateral resolution.

3. Improved resolution of conductive electrical equivalence.

4. No problems injecting current into a resistive surface layer.

The limitations of TDEM techniques are as follows:

1. Do not work well in very resistive material.

2. Interpretational material for TDEM on, for example, 3D structures is still under development.

3. TDEM equipment tends to be somewhat more costly due to its greater complexity.

As mentioned above, the advantages are significant, and TDEM is becoming a widely used tool for geoelectrical sounding.

9.4.3 Ground-Penetrating Radar

Basic Concept

Ground-penetrating radar (GPR) uses a high-frequency (80 to 1,500 MHz) EM pulse transmitted from a radar antenna to probe the earth. The transmitted radar pulses are reflected from various interfaces within the ground, and this return is detected by the radar receiver. Reflecting interfaces may be soil horizons, the groundwater surface, soil/rock interfaces, man-made objects, or any other interface possessing a contrast in dielectric properties. The dielectric properties of materials correlate with many of the mechanical and geologic parameters of materials.

The radar signal is imparted to the ground by an antenna that is in close proximity to the ground. The reflected signals can be detected by the transmitting antenna or by a second, separate receiving antenna. The received signals are processed and displayed on a graphic recorder. As the antenna (or antenna pair) is moved along the surface, the graphic recorder displays results in a cross-section record or radar image of the earth. As GPR has short wavelengths in most earth materials, resolution of interfaces and discrete objects is very good. However, the attenuation of the signals in earth materials is high, and depths of penetration seldom exceed 10 m. Water and clay soils increase the attenuation, decreasing penetration.

The objective of GPR surveys is to map near-surface interfaces. For many surveys, the location of objects such as tanks or pipes in the subsurface is the objective. Dielectric properties of materials are not measured directly. The method is most useful for detecting changes in the geometry of subsurface interfaces.

Geologic problems conducive to solution by GPR methods are numerous and include the following: bedrock configuration, location of pipes and tanks, location of the groundwater surface, borrow investigations, and others. Geologic and geophysical objectives determine the specific field parameters and techniques. Delineation of the objectives and the envelope of acceptable parameters are specified in advance. However, as the results cannot be

foreseen from the office, considerable latitude is given to the field geophysicist to incorporate changes in methods and techniques.

The following questions are important considerations in advance of a GPR survey.

What is the target depth? Though target detection has been reported under unusually favorable circumstances at depths of 100 m or more, a careful feasibility evaluation is necessary if the investigation depths need to exceed 10 m.

What is the target geometry? Size, orientation, and composition are important.

a) What are the electrical properties of the target? As with all geophysical methods, a contrast in physical properties must be present. Dielectric constant and electrical conductivity are the important parameters. Conductivity is most likely to be known or easily estimated.

b) What are the electrical properties of the host material? Both the electrical properties and homogeneity of the host must be evaluated. Attenuation of the signal is dependent on the electrical properties and on the number of minor interfaces that will scatter the signal.

c) Are there any possible interfering effects? Radio frequency transmitters, extensive metal structures (including cars) and power poles are probable interfering effects for GPR.

The physics of electromagnetic wave propagation are beyond the scope of this manual. However, there are two physical parameters of materials that are important in wave propagation at GPR frequencies. One property is conductivity (σ), the inverse of electrical resistivity (ρ). The relationships of earth material properties to conductivity, measured in mS/m (1/1,000 Ωm), are given in the section on electrical methods.

The other physical property of importance at GPR frequencies is the dielectric constant (ε), which is dimensionless. This property is related to how a material reacts to a steady-state electric field; that is, conditions where a potential difference exists but no charge is flowing. Such a condition exists between the plates of a charged capacitor. A vacuum has the lowest ε, and the performance of other materials is related to that of a vacuum. Materials made up of polar molecules, such as water, have a high ε. Physically, a great deal of the energy in an EM field is consumed in interaction with the molecules of water or other polarizable materials. Thus, waves propagating through such a material both go slower and are subject to more attenuation. To complicate matters, water, of course, plays a large role in determining the conductivity (resistivity) of earth materials.

Earth Material Properties

The roles of two earth materials that cause important variations in the EM response in a GPR survey need to be appreciated. The ubiquitous component of earth materials is water; the

other material is clay. At GPR frequencies, the polar nature of the water molecule causes it to contribute disproportionately to the displacement currents that dominate the current flow at GPR frequencies. Thus, if significant amounts of water are present, the ε will be high, and the velocity of propagation of the electromagnetic wave will be lowered. Clay materials with their trapped ions behave similarly. Additionally, many clay minerals also retain water.

The physical parameters in table 18 are typical for the characterization of earth materials. The range for each parameter is large; thus, the application of these parameters for field use is not elementary.

Simplified equations for attenuation and velocity (at low loss) are:

$$V = \frac{(3\times10^8)}{\varepsilon^{1/2}}, \tag{78}$$

$$a = 1.69\frac{\sigma}{\varepsilon^{1/2}}, \tag{79}$$

where

V = velocity in m/s,

ε = dielectric constant (dimensionless),

a = attenuation in decibels/m (db/m),

σ = electrical conductivity in mS/m.

A common evaluation parameter is dynamic range or performance figure for the specific GPR system. The performance figure represents the total attenuation loss during the two-way transit of the EM wave that allows reception; greater losses will not be recorded. As sample calculations, consider a conductive material (σ = 100 mS/m) with some water content (ε=20). The above equations indicate a velocity of 0.07 m per nanosecond (m/ns) and an attenuation of 38 dB/m. A GPR system with 100 dB of dynamic range used for this material will cause the signal to become undetectable in 2.6 m of travel.

The transit time for 2.6 m of travel would be 37 to 38 ns. This case might correspond geologically to a clay material with some water saturation. Alternatively, consider a dry material (ε=5) with low conductivity (σ = 5 mS/m). The calculated velocity is 0.13 m/ns and the attenuation is 3.8 dB/m, corresponding to a distance of 26-27 m for 100 dB of attenuation and a travel time of 200 ns or more. This example might correspond to dry sedimentary rocks.

These large variations in velocity and especially attenuation are the cause of success (target detection) and failure (insufficient penetration) for surveys in apparently similar geologic settings. As exhaustive catalogs of the properties of specific earth materials are not readily available, most GPR work is based on trial and error and empirical findings.

Table 18. Electromagnetic properties of earth materials.

Material	E	Conductivity, (mS/m)	Velocity, (m/ns)	Attenuation, (dB/m)
Air	1	0	0.3	0
Distilled Water	80	0.01	0.033	0.002
Fresh Water	80	0.5	0.033	0.1
Sea Water	80	3,000	0.01	1,000
Dry Sand	3-5	0.01	0.15	0.01
Wet Sand	20-30	0.1-1	0.06	0.03-0.3
Limestone	4-8	0.5-2	0.12	0.4-1
Shales	5-15	1-100	0.09	1-100
Silts	5-30	1-100	0.07	1-100
Clays	5-40	2-1,000	0.06	1-300
Granite	4-6	0.01-1	0.13	0.01-1
Dry Salt	5-6	0.01-1	0.13	0.01-1
Ice	3-4	0.01	0.16	0.01
Metals				

Modes of Operation

The useful item of interest recorded by the GPR receiver is the train of reflected pulses. The seismic reflection analogy is appropriate. The two reflection methods used in seismic reflection (common offset and common midpoint) are also used in GPR. Figure 312 illustrates these two modes. A transillumination mode is also illustrated in the figure, which is useful in certain types of nondestructive testing. The typical mode of operation is the common-offset mode where the receiver and transmitter are maintained at a fixed distance and moved along a line to produce a profile (figure 313). Note that as in seismic reflection, the energy does not necessarily propagate only downwards, and a reflection will be received from objects off to the side. An added complication with GPR is the fact that some of the energy is radiated into the air and, if reflected off nearby objects like buildings or support vehicles, will appear on the record as arrivals.

GPR records can be recorded digitally and reproduced as wiggle trace or variable area record sections. Figure 314 illustrates the presentation used when a graphic recorder is used to record analog data. Both negative and positive excursions in excess of the threshold appear as blackened portions of the record. This presentation is adequate for most tasks where target detection is the object, and post-survey processing is not anticipated. Wide variations in the appearance of the record are possible, depending on the gain settings used.

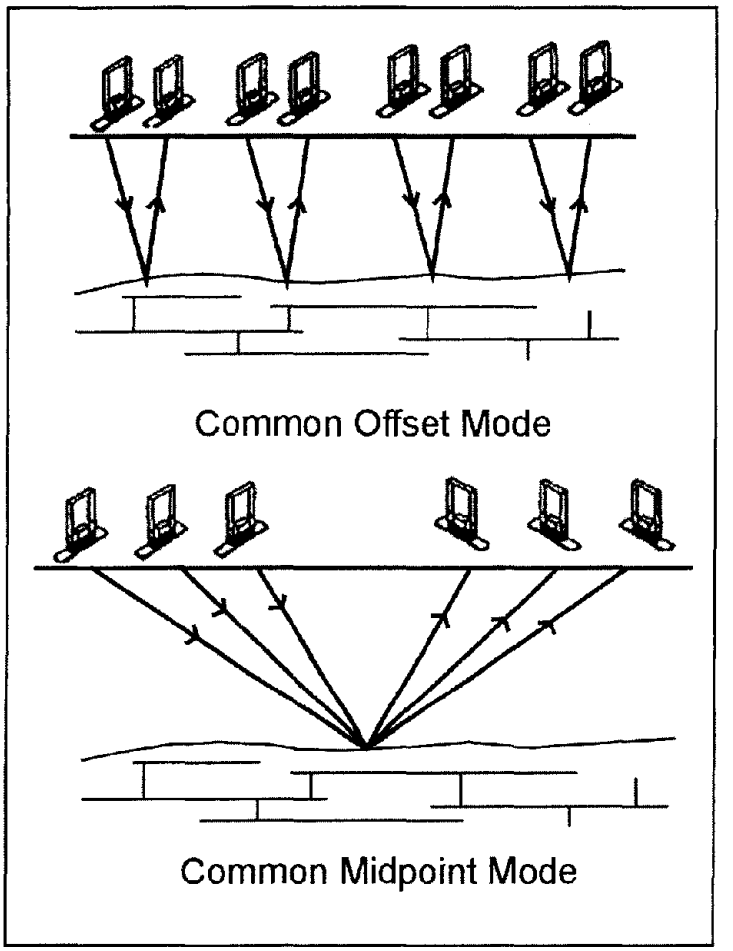

Figure 312. Common offset and common midpoint acquisition modes. (Annan, 1992)

Data Acquisition

A GPR crew consists nominally of two persons. One crew person moves the antenna or antenna pair along the profiles, and the other operates the recorder and annotates the record so that the antenna position or midpoint can be recovered.

The site-to-site variation in velocity, attenuation, and surface conditions is so large that seldom can the results be predicted before fieldwork begins. Additionally, the instrument operation is a matter of empirical trial and error in manipulating the appearance of the record. Thus, the following steps are recommended for most fieldwork:

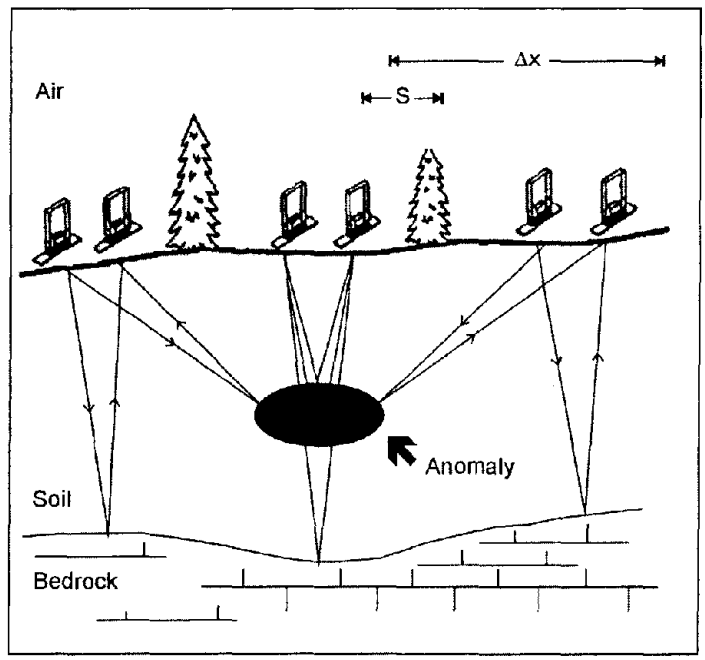

Figure 313. Schematic illustration of common offset single-fold profiling.

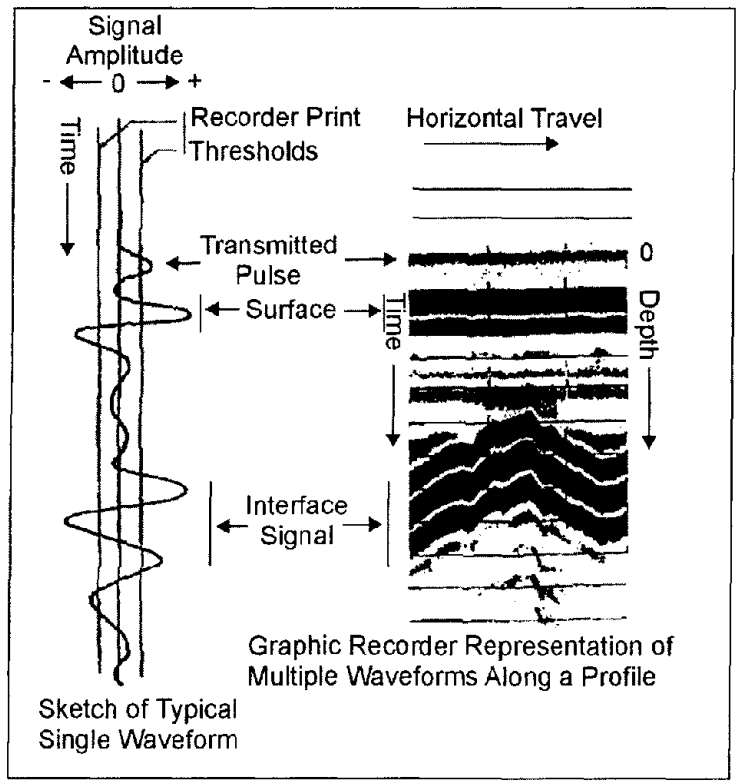

Figure 314. GPR received signal and graphic profile display. (Benson, Glaccum, and Noel, 1983)

1. Unpack and set up the instrument and verify internal operation.

2. Verify external operation (one method is to point the antenna at a car or wall and slowly walk toward it. The reflection pattern should be evident on the record).

3. Calibrate the internal timing by use of a calibrator.

4. Calibrate the performance by surveying over a known target at a depth and configuration similar to the objective of the survey (considerable adjustment of the parameters may be necessary to enhance the appearance of the known target on the record).

5. Begin surveying the area of unknown targets with careful attention to surface conditions, position recovery, and changes in record character.

Often a line will be done twice to be sure that all the features on the record are caused by the subsurface.

Data Interpretation

Because of the strong analogy between seismic reflection and GPR, the application of seismic processing methods to GPR data is a fertile field of current research. Such investigations are beyond the scope of this manual. The focus herein is on the most frequent type of GPR survey, i.e., location of specific targets.

GPR surveys will not achieve the desired results without careful evaluation of site conditions for both geologic or stratigraphic tasks and target-specific interests. If the objectives of a survey are poorly drawn, often the results of the GPR survey will be excellent records that do not have any straightforward interpretation. It is possible to tune a GPR system such that exceptional subsurface detail is visible on the record. The geologic evaluation problem is that, except in special circumstances (like the foreset beds inside of sand dunes), there is no ready interpretation. The record reveals very detailed stratigraphy, but there is no way to verify which piece of the record corresponds to which thin interbedding of alluvium or small moisture variation. GPR surveys are much more successful when a calibration target is available. GPR can be useful in stratigraphic studies; however, a calibrated response (determined perhaps from backhoe trenching) is required for geologic work.

Figure 315 indicates that localized objects will produce a hyperbola on the record. The hyperbolic shape is due to reflection returns of the EM pulse before and after the antenna system is vertically above the target. The shortest two-way travel distance is when the antenna (or center of the antennae pair) is on the ground surface directly above the object. All other arrivals are at greater distances along a different hypotenuse with each varying horizontal antenna location.

Figure 316 is the schematic of a set of targets surveyed by GPR. The record section of figure 317 indicates the excellent detection of the targets.

GPR Case Histories

GPR has been widely used, and reports on its effectiveness are available both in government and professional documents. Some useful references are:

Butler (1992), which is the proceedings of a GPR workshop and includes a tutorial and a collection of case histories.

Butler, Simms, and Cook (1994), which provides an archaeological site evaluation.

Sharp, Yule, and Butler (1990), which reports the GPR assessment of an HTRW site.

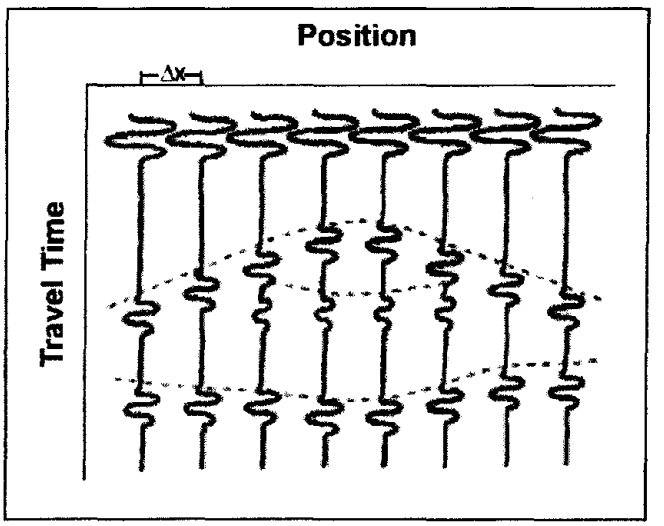

Figure 315. Format of a Ground Penetrating Radar reflection section with radar events shown for features depicted in figure 313.

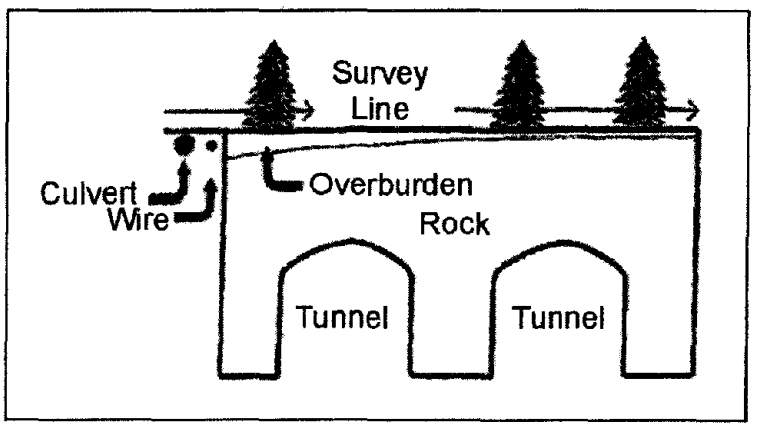

Figure 316. Schematic of a set of targets surveyed by Ground Penetrating Radar.

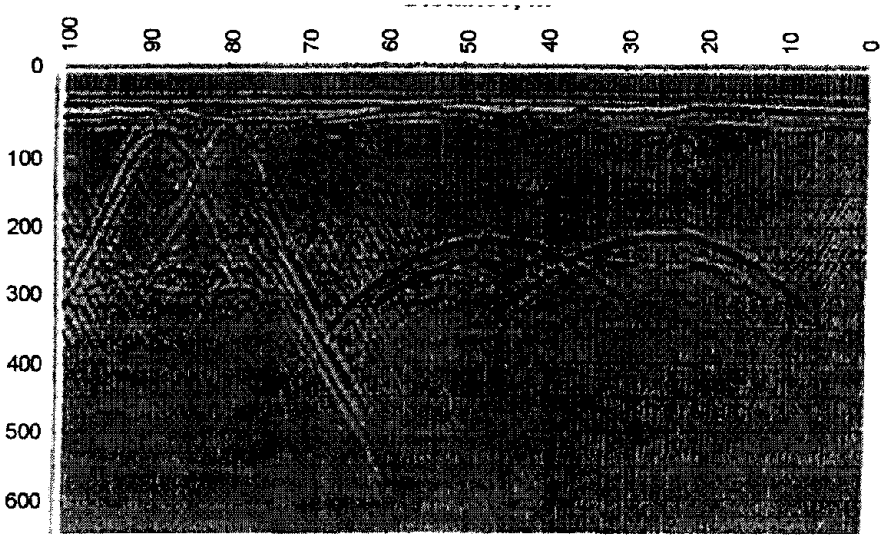

Figure 317. Actual GPR record over a culvert, pipe, and two tunnels showing the hyperbolic shape of the reflected/diffracted energy. (Annan, 1992)

9.4.4 Very Low-Frequency (VLF) Method

Basic Concept

The VLF method uses powerful remote radio transmitters set up in different parts of the world for military communications (Klein and Lajoie, 1980). In radio communications terminology, VLF means very low frequency, about 15 to 25 kHz. Relative to frequencies generally used in geophysical exploration, these are actually very high frequencies. The radiated field from a remote VLF transmitter, propagating over a uniform or horizontally layered earth and measured on the earth's surface, consists of a vertical electric field component and a horizontal magnetic field component each perpendicular to the direction of propagation.

These radio transmitters are very powerful and induce electric currents in conductive bodies thousands of kilometers away. Under normal conditions, the fields produced are relatively uniform in the far field at a large distance (hundreds of kilometers) from the transmitters. The induced currents produce secondary magnetic fields that can be detected at the surface through deviation of the normal radiated field.

The VLF method uses relatively simple instruments and can be a useful reconnaissance tool. Potential targets include tabular conductors in a resistive host rock such as faults in limestone or igneous terrain. The depth of exploration is limited to about 60% to 70% of the skin depth of the surrounding rock or soil. Therefore, the high frequency of the VLF transmitters means that in more conductive environments, the exploration depth is quite shallow; for example, the depth of exploration might be 10 to 12 m in 25-Ωm material. Additionally, the presence of conductive overburden seriously suppresses response from basement conductors, and relatively small variations in overburden conductivity or thickness can themselves generate significant VLF anomalies. For this reason, VLF is more effective in areas where the host rock is resistive and the overburden is thin.

Case Histories

VLF response is a maximum when the target strikes in the direction of the transmitter, falling off roughly as the cosine of the strike angle for other directions. However, there are a number of transmitters worldwide and seldom is the selection of an appropriate transmitter a problem. Because of the rudimentary nature of VLF measurements, simple interpretational techniques suffice for most practical purposes. The conductor is located horizontally at the inflection point marking the crossover from positive tilt to negative tilt and the maximum in field strength. A rule-of-thumb depth estimate can be made from the distance between the positive and negative peaks in the tilt angle profile.

One cannot make reliable estimates of conductor quality, however. Finally, the major disadvantage of the VLF method is that the high frequency results in a multitude of anomalies from unwanted sources such as swamp edges, creeks, and topographic highs. A VLF receiver measures the field tilt and hence the tilt profile shown in figure 318 (Klein and Lajoie, 1980). Figure 318 also shows schematically how the secondary field from the conductor is added to the primary field vector so that the resultant field is tilted up on one side of the conductor and down on the other side. Some receivers measure other parameters such as the relative amplitude of the total field or any component and the phase between any two components. Figure 319 (Klein and Lajoie, 1980) shows a comparison of the main types of measurements made with different VLF receivers. A variant of VLF measures the electric field with a pair of electrodes simultaneously with the tilt measurement.

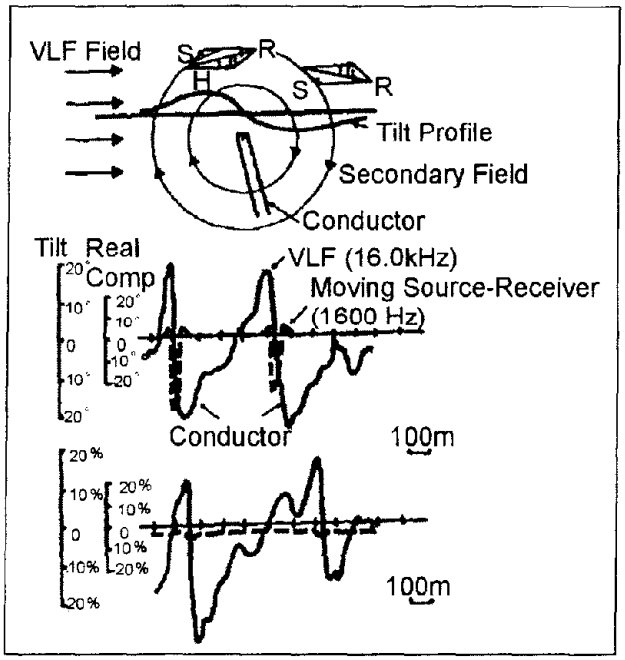

Figure 318. Tilt of the VLF field vector over a conductor. (Klein and Lajoie, 1980; copyright permission granted by Northwest Mining Association and Klein)

Case History

Groundwater. Figure 320 presents VLF results taken over granite terrain in Burkina Faso, Africa (Wright, 1988, after Palacky, Ritsema, and De Jong, 1981). The objective of the survey was to locate depressions in the granite bedrock, which could serve as catchments for groundwater. Depressions in the very resistive bedrock beneath poorly conductive overburden (100 to 300 Ωm at this site) likely produce VLF responses as a result of galvanic current flow. That is, the large current sheet flowing in the overburden, as a result of the primary electric field, is channeled along these bedrock depressions and appears as a line of anomalous current. The conductor axis is centered near station 70 to 75. A water well was drilled at station 70 and encountered bedrock beneath approximately 20 m of overburden and flowed at a rate of 1.0 m^3/hour.

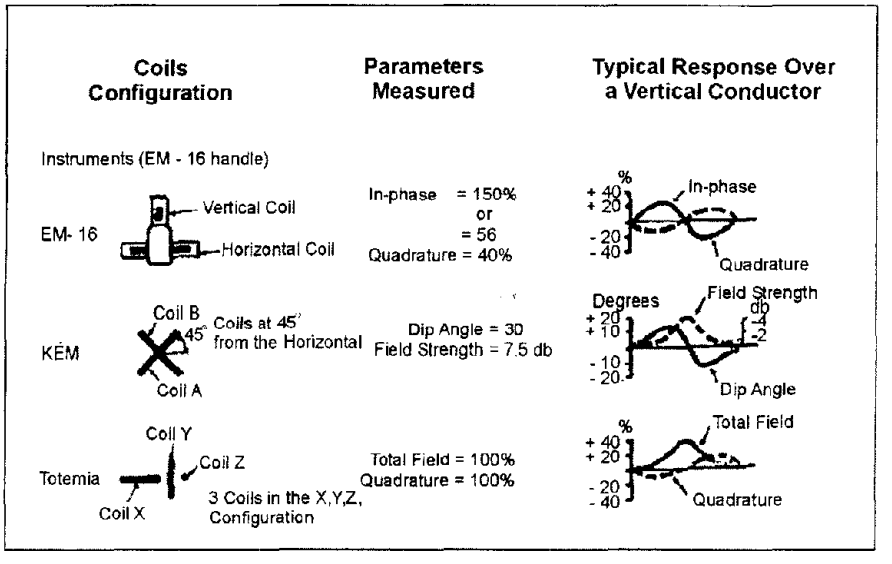

Figure 319. Comparison of VLF instruments. (Klein and Lajoie, 1980; copyright permission granted by Northwest Mining Association and Klein)

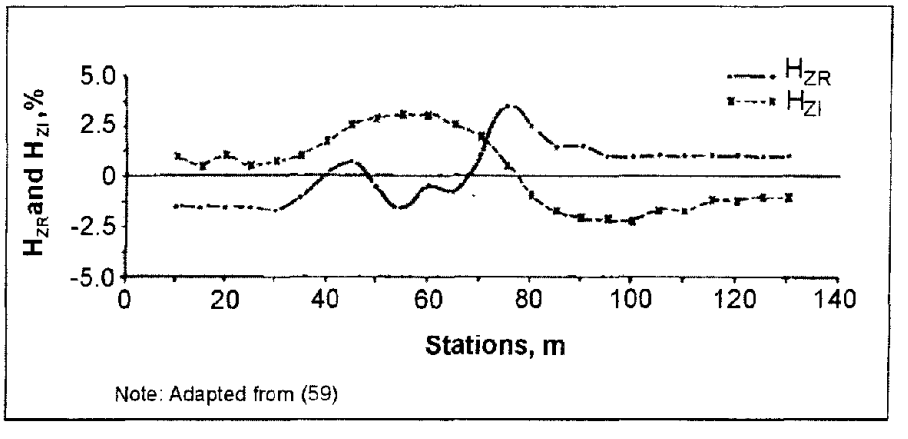

Figure 320. VLF profile, Burkina Faso, Africa. (Wright, 1988; copyright permission granted by Scintrex)

Buried Cables. Figure 321 presents VLF measurements along a profile crossing a buried telephone line (Wright, 1988). A classic crossover is observed that places the line beneath station -2.5. However, this curve is a good example of a poorly sampled response, because the exact peaks on the profile are probably not determined. One possible model is presented on figure 321 for a line current at a depth of 1.25 m and station -2.5. The fit is only fair, which could be the result of poor station control, inapplicability of the line current model, or distortion of the measured profile by adjacent responses.

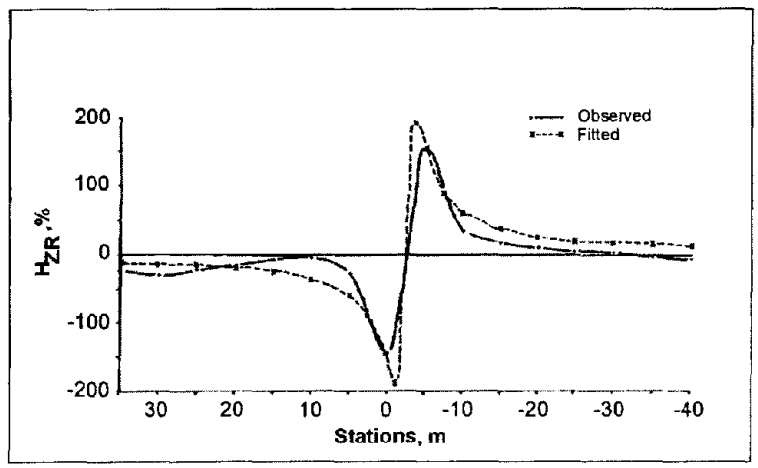

Figure 321. VLF profile over buried telephone line. (Wright, 1988;copyright permission granted by Scintrex)

9.4.5 Seismoelectrical Method

Basic Concept

The Seismoelectrical method (also called the Electroseismic method) is based on the generation of electromagnetic fields in soils and rocks by seismic waves. Although the method is not reported to detect groundwater flow, it does measure the hydraulic conductivity, which is related to permeability and, therefore, to the potential for groundwater flow.

The phenomenon is illustrated by figures 322 and 323.

When a seismic wave encounters an interface, it creates a charge separation at the interface forming an electrical dipole. This dipole radiates an electromagnetic wave that can be detected by antennae on the ground surface.

As in the case shown in figure 322, an antenna on the ground surface is used to detect the electric field. In the case illustrated in figure 323, a seismic head wave traveling along an interface creates a charge separation across the interface, which induces an electric field.

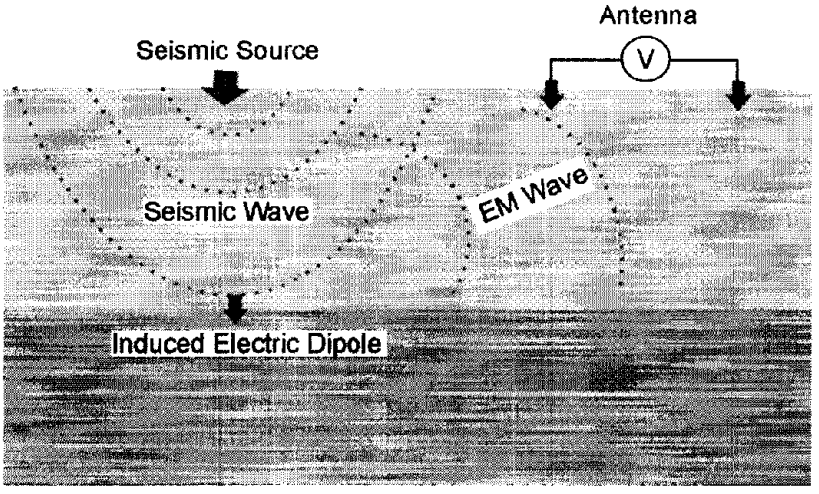

Figure 322. Seismoelectrical conversion at an interface.

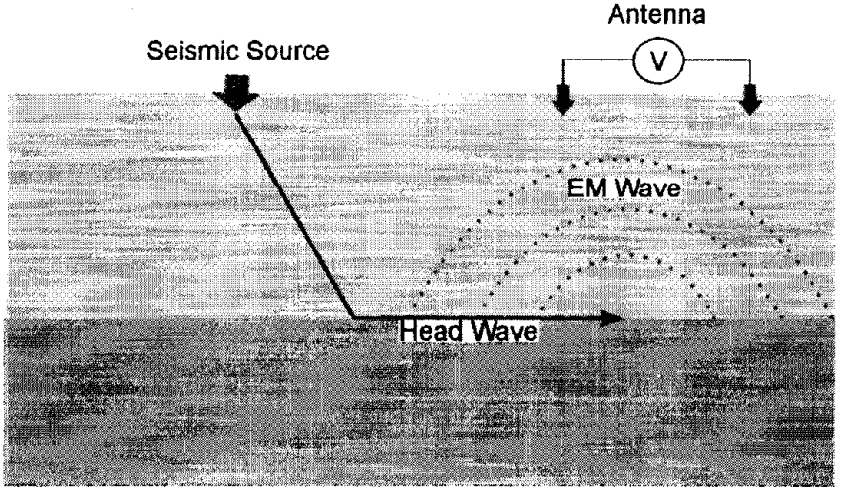

Figure 323. Generation of an electric field by a head wave.

As the seismic (P or compression) waves stress earth materials, four geophysical phenomenon occur:

1. The resistivity of the earth materials is modulated by the seismic wave;

2. Electrokinetic effects analogous to streaming potentials are created by the seismic wave;

3. Piezoelectric effects are created by the seismic wave; and

4. High-frequency, audio- and high-frequency radio frequency impulsive responses are generated in sulfide minerals (sometimes referred to as RPE).

The dominant application of the electroseismic method is to measure the electrokinetic effect or streaming potential (item 2, above). Electrokinetic effects are initiated by sound waves

(typically P-waves) passing through a porous rock inducing relative motion of the rock matrix and fluid. Motion of the ionic fluid through the capillaries in the rock occurs with cations (or less commonly, anions) preferentially adhering to the capillary walls, so that applied pressure and resulting fluid flow relative to the rock matrix produces an electric dipole. In a non-homogeneous formation, the seismic wave generates an oscillating flow of fluid and a corresponding oscillating electrical and EM field. The resulting EM wave can be detected by electrode pairs placed on the ground surface.

Surface seismic sources and measurement electrode pairs are generally used to measure the electrokinetic effect. Borehole systems also have been recently developed. A hammer blow or small explosive (black powder charge) are typically used for the seismic source. Two, short (few meters) electrode pairs are typically located collinear and symmetric to the seismic source. Stacking of repeat seismic "shots" is often used to improve signal to noise.

The only company found that produces a commercially available electroseismic prospecting system is GroundFlow Ltd. in the UK. This system has been mainly used for field demonstration purposes and research and development studies. Very few detailed case histories are available to document the performance of the system. The electroseismic system made by GroundFlow is called "GroundFlow 1500" and the main equipment components are:

1. A combined computer-receiver
2. Antenna cables and electrodes,
3. Trigger cable

The Groundflow 1500 instrument is shown in figure 324.

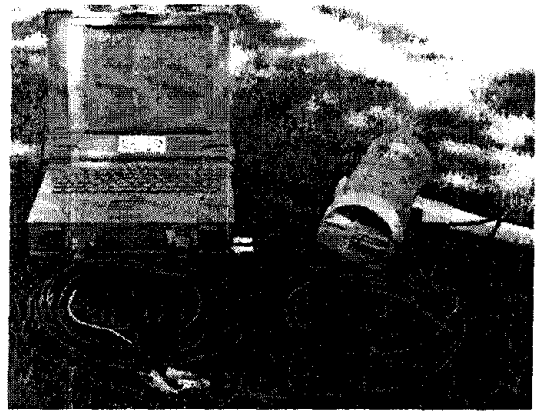

Figure 324. Ground Flow 1500 instrument. (Groundflow Ltd.)

The computer-receiver contains a preamplifier, analog to digital converter and power supply system to measure the voltages induced in the grounded dipoles. One system layout used to measure the electroseismic effect is shown in figure 325.

The hammer and plate seismic source is used along with two pairs of electrodes arranged in a straight line with electrodes offset (from the center of the array) by 0.25 and 2.25 m. The seismic source is positioned in the center of the array. Larger electrode spacing can be used; however, they are typically centered in pairs around the shot point and are generally less than about 10 m in length. Timing of the measurement is achieved by a hammer trigger (or other mechanical trigger). The signal is acquired with the instrument shown in figure 324. Measurements are made for a period of 400 ms after triggering. The last 200 ms of the record is used as a sample of background noise and is subtracted from the first 200 ms of signal in order to remove the first, third, and fifth harmonics of the background noise at the receivers. This noise is typically from power lines.

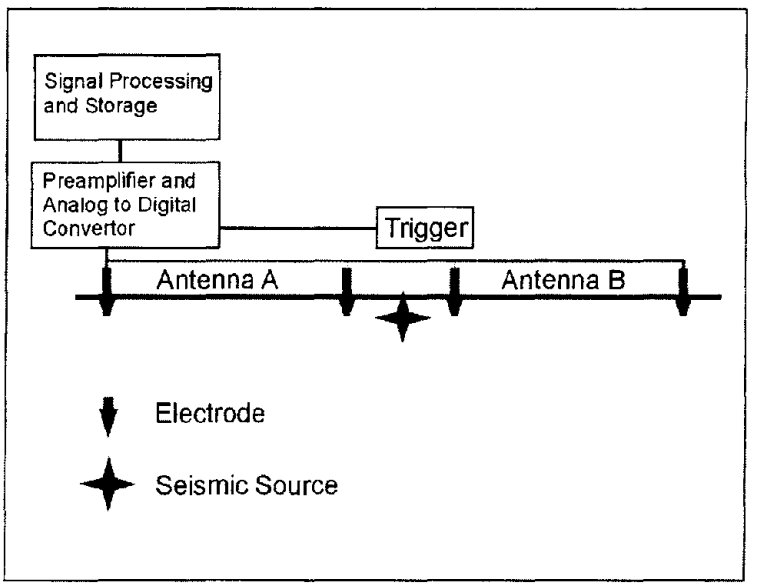

Figure 325. System layout for electroseismic surveys.

Data Acquisition, Processing, and Interpretation

Measurements are recorded using the instrument and system setup described above. Data processing consists of stacking repetitive hammer (or explosive) shots and removal of power line and other noise as described above. This processing is conducted on the computer-receiver while in the field. Depending upon field conditions, up to 20 soundings can be conducted in a day. It is expected that measurement time will increase proportionally with stacking times, and that long stacking times would be needed in the vicinity of power lines.

The signal files are processed to give a sounding plot of permeability and porosity against one-way seismic travel time. Values for a simple seismic velocity model are required to allow time- to-depth conversion. The resulting logs against depth are displayed in the field.

Output from the electroseismic inversion is typically a plot showing hydraulic conductivity versus depth. This interpretation assumes a one-dimensional layered earth. In theory, the inversion also can derive fluid conductivity and fluid viscosity from the rise time of the

signal. Where many soundings are measured in close vicinity, a pseudo 2-D cross section can be generated.

The maximum depth of penetration of electroseismic measurements is stated to be about 500 m depending upon ambient noise and water content. Lateral resolution is not stated in the literature but is expected to be on the order of the depth of exploration. No information was found regarding the vertical resolution of the method.

Limitations

The electroseismic method is apparently susceptible to electrical noise from nearby power lines. Typical electroseismic signals are at the microvolt level. The electroseismic signal is proportional to the pressure of the seismic wave. Thus, it would seem possible to increase the signal by using stronger seismic sources. This is not mentioned in the literature. Electroseismic soundings have a maximum exploration depth of about 500 m in the reported literature, although no examples have been shown with results from deeper that about 150 m.

9.4.6 Metal Detectors

The term "metal detector" (MD) generally refers to some type of electromagnetic induction instrument, although traditional magnetometers are often used to find buried metal. The disadvantage of magnetometers is that they can be used only for locating ferrous metals. MD instruments in geotechnical and hazardous-waste site investigations have several uses:

a) Location of shallow metal drums, canisters, cables, and pipes.

b) Progress assessment during metal object removal and location of additional objects.

c) Avoidance of old buried metal objects during new construction, remediation, or well placement.

Basic Concept

In the smaller terrain conductivity meters, the transmitter and receiver coils are rigidly connected, allowing the in-phase response to be measured in addition to the quadrature response (McNeill, 1990). Some basic equations are given in the section on Frequency-Domain EM Methods. This feature allows systems such as the EM-31 and EM-38 to function as MD's. Several coil arrangements are favored by different commercial manufacturers. The smallest units have coil diameters of as little as 0.2 m and use a vertical-axis, concentric coil arrangement. These instruments are the coin and jewelry treasure finders used on every tourist beach in the world; they have very limited depth of investigation for geotechnical targets (figure 326). One of the newest and most sophisticated MD uses three vertical-axis, 1-m^2 coils: one transmitter coil, one main receiving coil coincident with the transmitter, and one focusing coil 0.4 m above the main coil. This instrument continuously records the data and has sophisticated computer software, which can yield depth of the object and other properties. In a third arrangement, the transmitter loop is horizontal, and the receiver loop is perpendicular in the vertical plane (figure 327).

Another method of classifying MD instruments is by typical application: hobby and treasure finding equipment, sensitive to very shallow and smaller surface area targets; utility-location and military instruments, sensitive to deeper and larger objects, but usually without data recording and post-processing provisions; and, specialized instruments with large coils, possibly vehicle-mounted with continuous data recording and postprocessing.

The two most important target properties that increase the secondary field (and thus optimize detection) are increased surface area within the target mass and decreased depth of burial. Overall target mass is relatively unimportant; response is proportional to surface area cubed (Hempen and Hatheway, 1992). Signal response is proportional to depth; therefore, depths of detection rarely exceed 10 to 15 m, even for sizable conductors. Often of great importance, and unlike magnetometers, MD produces a response from nonferrous objects such as aluminum, copper, brass, or conductive foil.

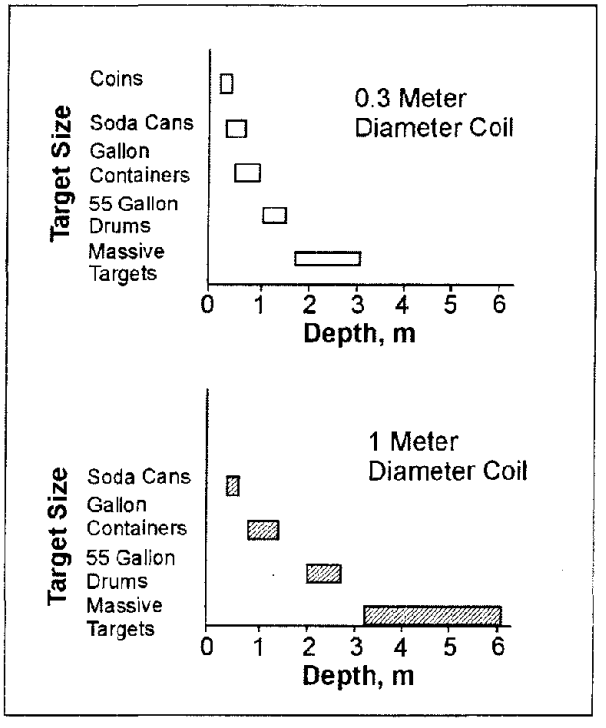

Figure 326. Approximate metal detector (MD) detection depths for various targets with two coil sizes. **(Benson, Glaccum, and Noel, 1983)**

The main advantages of MD instruments are that both ferrous and nonferrous metals may be detected; the surface area of the target is more important that its mass; and surveys are rapid, detailed, and inexpensive. The main disadvantages are that the depth of investigation is very limited with most instruments, and metallic litter and urban noise can severely disrupt MD at some sites.

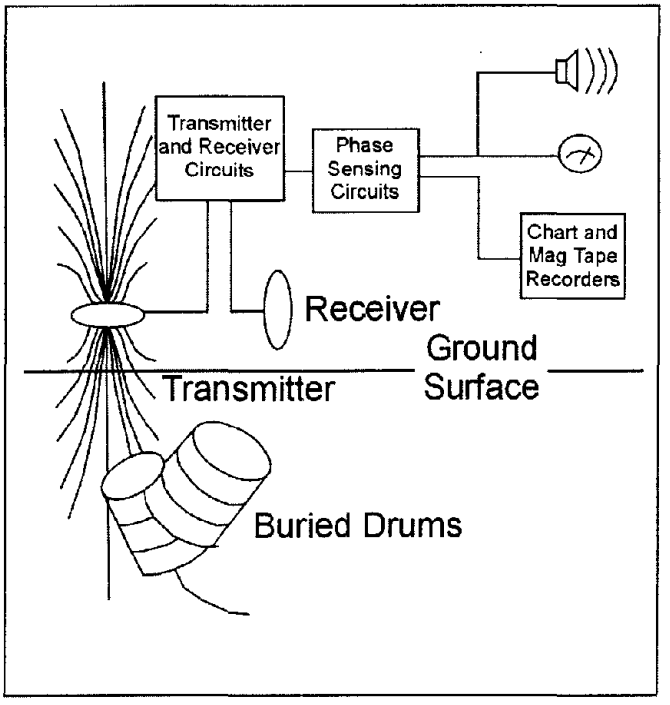

Figure 327. Block diagram of one MD coil arrangement and associated electronics. (Benson, Glaccum, and Noel, 1983)

Example Problem

Figure 328 shows a test survey made with one of the new generation of sophisticated MD over a variety of buried metal objects and compared with a magnetic gradiometer (Geonics, 1993). Both instruments appear to have "detected" all of the buried objects, but the quality of spatial resolution is quite different. Spatial resolution is judged by how tightly the response of an instrument fits the target. The magnetometer resolves the single barrels very well. Spurious dipolar-lows become evident for the barrel clusters, and complex responses are recorded around the pipes and sheets. The MD responses fit all the targets very well, regardless of shape, orientation, or depth. This particular MD also shows the value of a second receiver coil to help distinguish between near- surface and deeper targets.

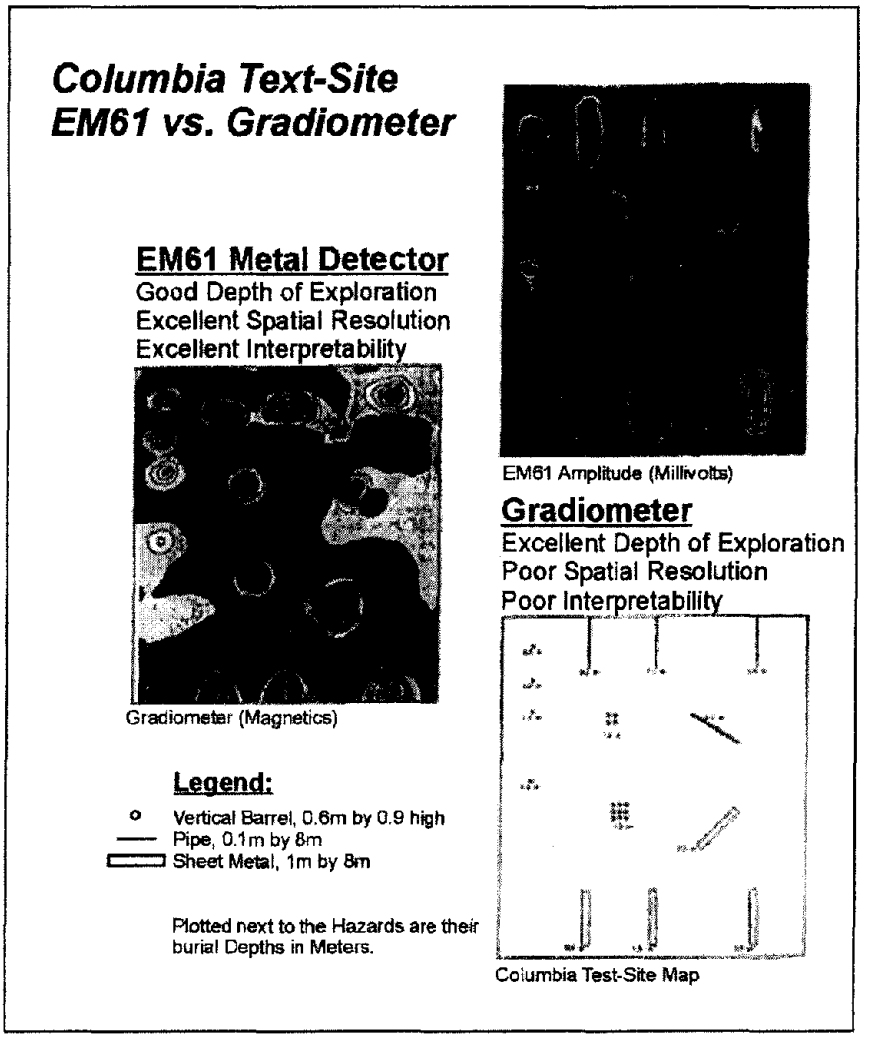

Figure 328. Test survey using a metal detector and a magnetic gradiometer. (Geonics, 1983; copyright permission granted by Geonics Ltd)

9.5 NUCLEAR METHODS

9.5.1 Nuclear Magnetic Resonance (NMR) Method

Basic Concept

The Nuclear Magnetic Resonance (NMR) method is also known as the Proton Magnetic Resonance (PMR) method. NMR is a method of measuring the quantity of free water in soils and rocks. The method is based on the fact that a hydrogen proton has a magnetic moment and an angular momentum. The hydrogen atoms produce a magnetic field when they are excited by an alternating field (from a transmitter loop) in the presence of a static magnetic field (the Earth's magnetic field). In the NMR methods, three magnetic fields have to be considered:

1. The Earth's field, the amplitude of which determines the precession frequency of the protons.

2. The excitation field, produced by a current into a loop laid on the ground surface, at a frequency equal to the precession frequency (called the Larmor frequency).

3. The relaxation field produced by the protons excited by the excitation field. The amplitude of the relaxation field measured at the ground surface, after the excitation is turned off, is directly related to the number of protons that have been excited and, thus, to the water content.

Figure 329 shows the basic physics of the NMR method.

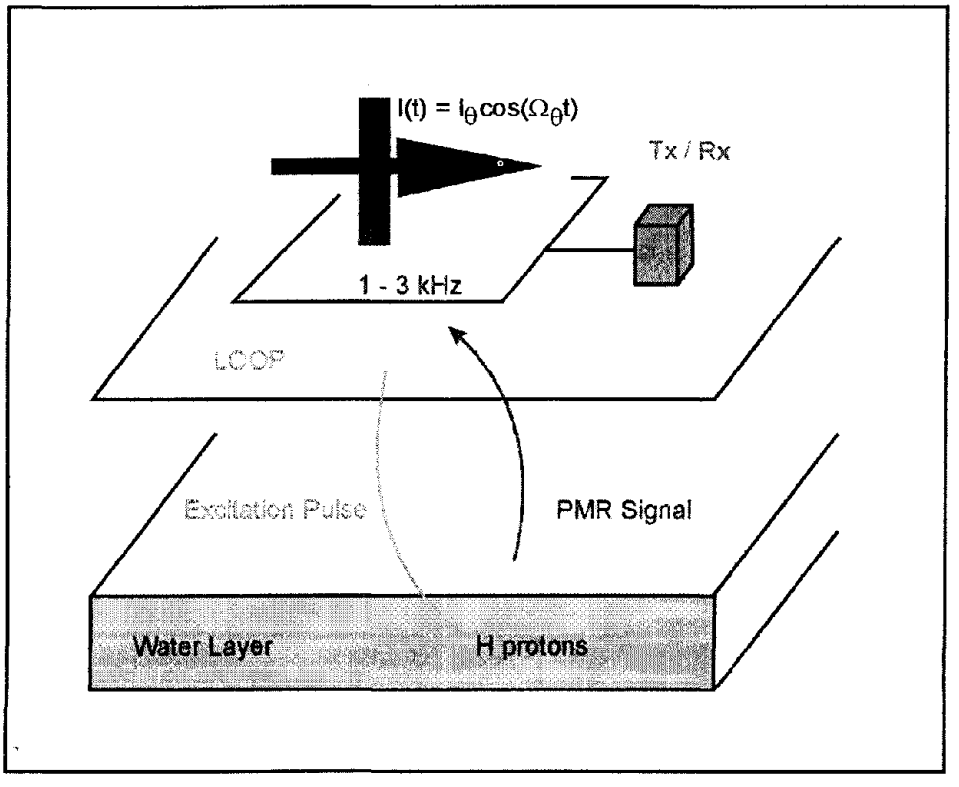

Figure 329. Schematic of the Nuclear Magnetic Resonance methods. (IRIS Intruments)

The transmitter/receiver loop provides the electromagnetic pulses that excite the protons in groundwater. These protons then decay during the transmitter current off time, and the field from this decay is detected by the same loop of wire now acting as a receiver. The data are stored in the control transmitter/receiver (Tx/Rx) box.

Data Acquisition

To our knowledge, only one company produces a commercially available NMR system, IRIS Instruments in France. This system has been used for field demonstration purposes and research and development studies. The IRIS Instruments, NMR system is called NUMIS, and the equipment consists of:

- A converter unit powered by two 12V batteries,
- A transmitter-receiver unit for pulse generation and signal measurement,
- A wire loop used both as a transmitting and a receiving antenna, and
- A portable computer for control of the system and for data recording.

The transmitter loop typically consists of a 100-m-diameter loop laid out on the ground. Other loop configurations can also be used (i.e., loop shaped like a figure 8, multi-turn 50-m loops, etc.). The excitation frequency of the transmitted pulse is typically between 1.5 and 3 kHz depending upon the amplitude of the local Earth's magnetic field. The excitation current in the loop is up to 300 amps.

Data processing consists of stacking repetitive decays at various pulse moments. To derive water content as a function of depth, measurements must be made over a range of pulse moments since the depth from which maximum signal contribution is derived increases with pulse moment. Typically, measurements are made at 16 pulse moments that may be varied from 200 ampere-milliseconds to 9,000 ampere-milliseconds. A cycle of measurements from one stack consists of the following steps:

- Charging capacitors
- Noise measurement before stack
- Current Pulse generation
- Delay time for switching from transmitter to receiver
- Signal measurement
- Data transmission

These steps require approximately 8 seconds per stack, so that measurement time for 32 stacks for 16 pulse moments requires about 75 minutes. During the acquisition process, diagnostic information is available about data quality and progress of the acquisition process.

Depending upon field conditions, a complete NMR measurement may take from 2 to 8 hours. The NMR equipment is heavy and bulky, and moving the equipment can be time consuming, especially if this is done by hand carrying. Measurement time increases proportionally with stacking times. Extremely long stacking times are sometimes needed in the vicinity of power lines.

Data Interpretation

The data mainly used in inversion and interpretation is signal amplitude as a function of pulse moment. These data contain the information about water content distribution versus depth. Inversion of the data into water content versus depth proceeds along the following steps:

- Computing the component of the magnetic field perpendicular to the local Earth's magnetic field caused by the transmitter loop, as a function of depth. This magnetic field can be computed for ground stratified in resistivity with depth.

- Computing the voltage induced in the receiver, caused by the decay of the Larmor processing component of the nuclear magnetization, after termination of the applied dynamic field. This computation for different pulse moments contains the water distribution in the ground.

- Output from the NMR inversion is a one-dimensional layered earth graphical presentation of water content (in percent) versus depth. The number of layers in the inversion can be specified or a smooth model interpretation can be selected. The inversion also derives a decay time for each layer. The decay time is an indicator of the average pore size.

An example of the field data and their interpretation is shown in figure 330.

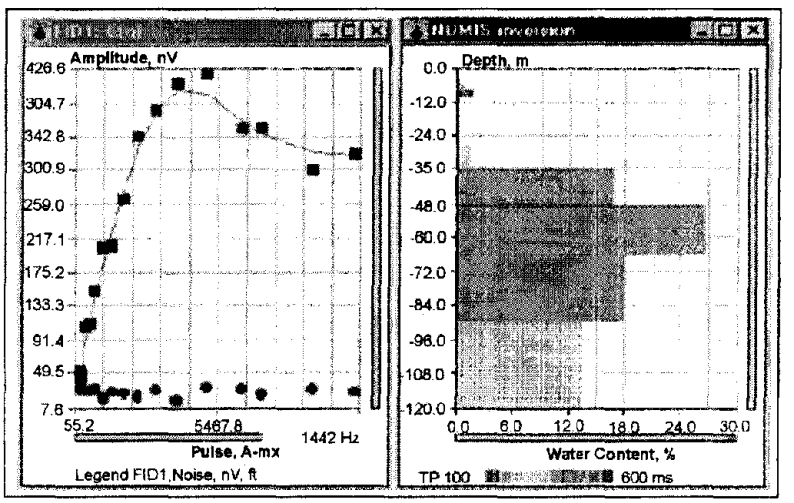

Figure 330. Field data and interpretation of a Nuclear Magnetic Resonance survey. (IRIS Intruments)

Figure 330 shows the field data from a sounding along with the interpretation. The field data curve (left plot) shows the noise level (blue circles), the measured field data (black squares), and the interpretation fit (red). The right hand graph shows the interpretation, presenting a plot of porosity vs. depth. Since water within the rock pores is required for the method to work, this plot shows the water content of the rock layers.

Depth of Penetration and Resolution of Method

The maximum depth of penetration of NMR measurements is typically about 100 to 150 m depending upon ambient noise and water content. Lateral resolution is on the order of the loop size (100 m) or better. Vertical resolution is dependent upon the product of the water content and thickness of the water-bearing layer.

Numerical modeling reveals that, for a 100-m circular antenna, a one-m-thick layer of water (water content 100%) can be detected down to 120 m when the geomagnetic field is vertical and only 100 m when it is horizontal. The layers can be discriminated down to a maximum depth of about 70 m in the case of a horizontal field and 60 m in the case of a vertical field.

Limitations

The NMR method is extremely susceptible to electrical noise from nearby power lines. Typical NMR signals are at the nanovolt level, and as mentioned above, to derive this signal in the presence of high ambient electrical noise may require up to 8 hours, or may not be possible. The NMR signal is proportional to the ambient (static) magnetic field. Thus, it is not possible to boost the signal from the groundwater protons by increasing transmitter power. In geologic environments with a high percentage of magnetic minerals, the signal from the groundwater can be screened out. In these cases, NMR measurements will not work. NMR soundings have a maximum exploration depth of about 100 to 150 m with present equipment.

CHAPTER 10 BOREHOLE GEOPHYSICAL METHODS

10.1 GENERAL IN-HOLE PROCEDURES

Introduction

Borehole geophysics, as defined here, is the science of recording and analyzing measurements in boreholes or wells, for determining physical and chemical properties of soils and rocks. The purpose of this chapter is to provide the basic information necessary to apply the most useful geophysical well logs for the solution of problems in groundwater, the environmental field, and for engineering applications. Some of the objectives of geophysical well logging are:

1. Identification of lithology and stratigraphic correlation.
2. Measuring porosity, permeability, bulk density, and elastic properties.
3. Characterizing fractures and secondary porosity.
4. Determining water quality.
5. Identifying contaminant plumes.
6. Verifying well construction.

Although the U.S. Government and some private industry have been converting to the metric system for logging equipment and log measuring units, the inch-pound (IP) system is still standard in the United States. In this manual, the IP system is used where IP is the standard for presently used equipment.

Benefits

The main objective of borehole geophysics is to obtain more information about the subsurface than can be obtained from drilling, sampling, and testing. Although drilling a test hole or well is an expensive procedure, it provides access to the subsurface where vertical profiles or records of many different kinds of data can be acquired.

Geophysical logs provide continuous analog or digital records of in situ properties of soils and rocks, their contained fluids, and well construction. Logs may be interpreted in terms of lithology, thickness, and continuity of aquifers and confining beds; permeability, porosity, bulk density, resistivity, moisture content, and specific yield; and the source, movement, chemical and physical characteristics of groundwater and the integrity of well construction. Log data are repeatable over a long period of time, and comparable, even when measured with different equipment. Repeatability and comparability provide the basis for measuring changes in a groundwater system with time. Changes in an aquifer matrix, such as in porosity by plugging, or changes in water quality, such as in salinity or temperature, may be recorded. Thus, logs may be used to establish baseline aquifer characteristics to determine how substantial future changes may be or what degradation may have already occurred. Logs that are digitized in the field or later in the office may be corrected rapidly, collated, and analyzed with computers.

Some borehole geophysical tools sample or investigate a volume of rock many times larger than core or cuttings that may have been extracted from the borehole. Some probes record data from rock beyond that disturbed by the drilling process. Samples provide point data from laboratory analysis. In contrast, borehole logs usually are continuous data, and can be analyzed in real time at the well site to guide completion or testing procedures. Unlike descriptive logs written by a driller or geologist that are limited by the authors' experience and purpose and are highly subjective, geophysical logs may provide information on some characteristic not recognized at the time of geophysical logging. Data from geophysical logs are useful in the development of digital models of aquifers and in the design of groundwater supply, recharge, or disposal systems. A log analyst with the proper background data on the area being studied can provide reasonable estimates of hydraulic properties needed for these purposes. Stratigraphic correlation is a common use of geophysical logs; logs also permit the lateral extrapolation of quantitative data from test or core holes. Using logs, a data point in a well can be extended in three dimensions to increase its value greatly. Many techniques used in surface geophysics are related closely to techniques in borehole geophysics, and the two are considered together when setting up comprehensive groundwater, environmental, or engineering investigations. Geophysical logs, such as acoustic-velocity and resistivity, can provide detailed profiles of data that are useful in interpreting surface surveys, such as seismic and resistivity surveys.

Limitations

Geophysical logging cannot replace sampling completely, because some information is needed on each new area to aid log analysis. A log analyst cannot evaluate a suite of logs properly without information on the local geology. Logs do not have a unique response; for example, high gamma radiation from shale is indistinguishable from that produced by granite. To maximize results from logs, at least one core hole should be drilled in each depositional basin or unique aquifer system. If coring the entire interval of interest is too expensive, then intervals for coring and laboratory analysis can be selected on the basis of geophysical logs of a nearby hole. Laboratory analysis of core is essential either for direct calibration of logs or for checking calibration carried out by other means. Calibration of logs carried out in one rock type may not be valid in other rock types because of the effect of chemical composition of the rock matrix.

In spite of the existence of many equations for log interpretation and charts that provide values like porosity, log analysis still is affected by many variables that are not completely understood. Correct interpretation of logs is based on a thorough understanding of the principles of each technique. For this reason, interpretation of logs in the petroleum industry largely is done by professional log analysts. In contrast, very few log analysts are working in the environmental and engineering fields, so interpretation of logs for these applications often is carried out by those conducting the investigation.

A thorough understanding of the theory and principles of operation of logging equipment is essential for both logging operators and log analysts. An equipment operator needs to know enough about how each system works to be able to recognize and correct problems in the field and to select the proper equipment configuration for each new logging environment. A log analyst needs to be able to recognize malfunctions on logs and logs that were not run

properly. The maximum benefit is usually derived from a logging operation where operators and analysts work together in the truck to select the most effective adjustments for each log.

Cost

The cost of logging can be reduced significantly by running only those logs that offer the best possibility of providing the answers sought. Further reductions in cost can be achieved by logging only those wells that are properly located and constructed to maximize results from logging. In contrast, more money needs to be spent on log analysis. More time may be required to analyze a suite of logs for maximum return than to run the logs. Too often, this time is not budgeted when the project is planned.

Planning a Logging Program

A logging program must be properly planned to be of maximum benefit. Borehole geophysics is frequently applied to environmental investigations, such as hydrogeology to aid site selection, monitoring, determining well construction, and planning remediation. In planning a logging program for environmental applications, one of the most difficult questions to answer is what geophysical logs will provide the most information for the funds available. There are several important questions in the decision-making process.

a) What are the project objectives?

b) What is the hydrogeology of the site?

c) How will test holes be drilled and wells constructed?

d) Who will do the logging and log analysis?

e) What are the financial limitations, and how else might some of these data be obtained?

The log selection process needs to start at the time of the initial work plan.

In addition to selecting the general types of logs to be run, many varieties of some logging tools exist (e.g., resistivity, flowmeter, and caliper). The basic information needed to simplify the selection process among the more commonly used logs is provided in a chart in figure 331 (Keys, Crowder, and Henrich, 1993). Decisions on what logs to be run should not be based on this table alone. The chart should only be used to select logs that should be investigated further. The logs selected should meet specific project objectives, provide the necessary information in the rock units to be drilled, and consider the planned well construction.

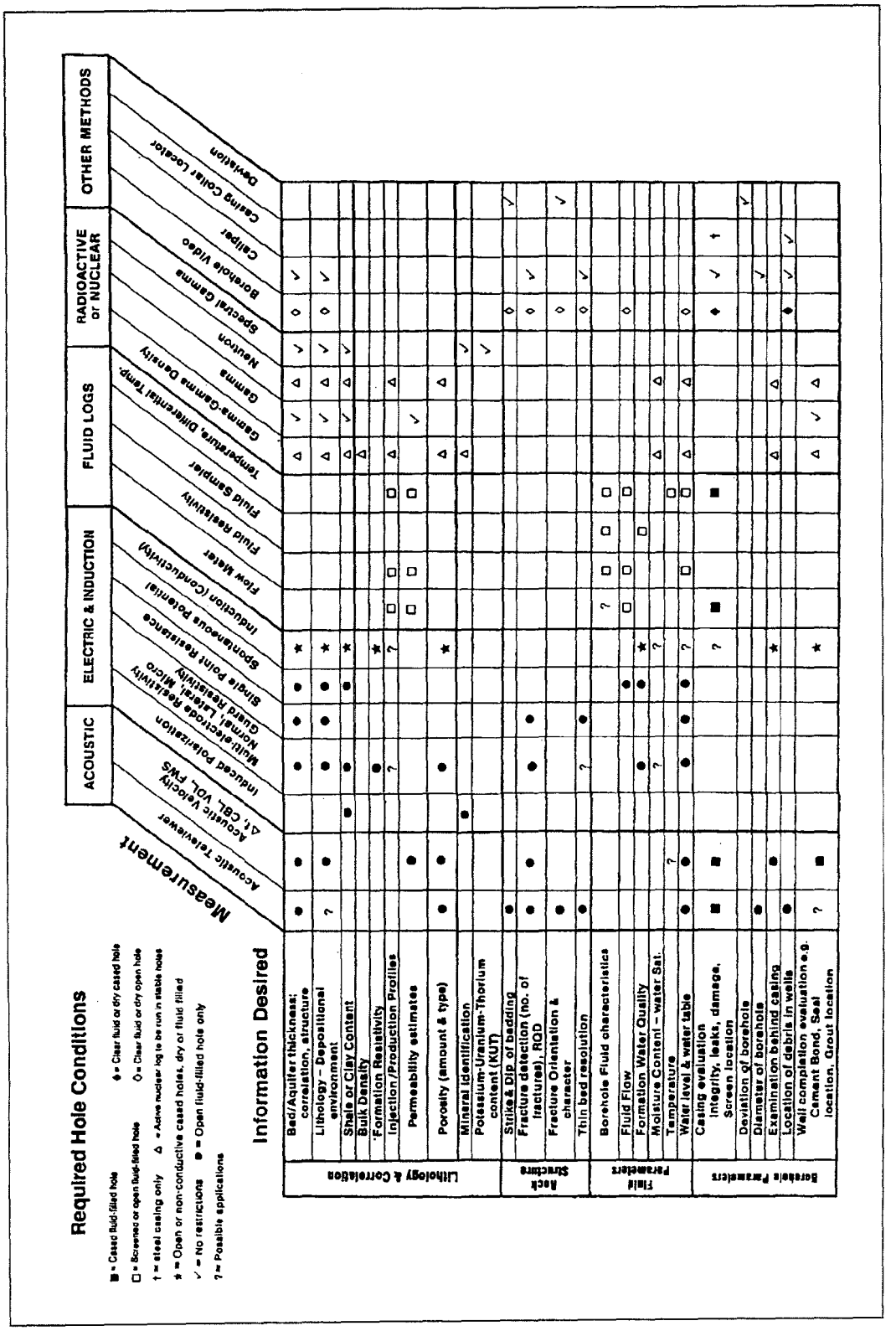

Figure 331. Log selection chart.

Log Analysis

In recent years, computer techniques have dominated log analysis; however, this development has not changed the basic requirements for getting the most information from logs. First, background information on each new hydrogeologic environment is essential where logs are to be used. The amount and kind of background data needed are functions of the objectives of the program. Second, the suite of logs to be run should not only be based on project objectives but also on knowledge of the synergistic nature of logs. Two logs may provide answers that may not be possible with either log separately, and each additional log may add much more to a total understanding of the system. Third, logs need to be selected, run, and analyzed on the basis of a thorough understanding of the principles of each log, even if the final results come out of a computer. The process of log analysis can be simplified into several steps, as follows:

a) Data processing, which includes depth matching, merging all logs and other data from a single well, and editing and smoothing the data set.

b) Correction of borehole effects and other errors.

c) Conversion of log measurements to hydrogeologic and engineering parameters of interest, such as porosity.

d) Combining logs and other data from all wells on a project so the data can be extrapolated laterally in sections or on maps.

Qualitative Analysis

Logs were first used for the identification of rock and fluid types, their lateral correlation, and the selection of likely producing intervals for well completion; these uses are still vital today in many fields. Qualitative log analysis is based mostly on knowledge of the local geology and hydrology, rather than on log-response charts or computer plots. Examination of outcrops, core, and cuttings, coupled with an understanding of log response, will permit the identification and correlation of known aquifers and confining beds.

Lithologic interpretation of logs needs to be checked against data from other sources, because geophysical logs do not have a unique response. This requirement is also true of stratigraphic correlation, where gross errors can be made by just matching the wiggles. Correlation by matching log character can be done without understanding the response to lithology, but this approach can lead to erroneous results. Even within one depositional basin, the response of one type of log may shift from lateral facies changes.

For example, the feldspar content of a sandstone may increase toward a granitic source area, which probably would cause an increase in the radioactivity measured by gamma logs. This measurement might be interpreted mistakenly as an increase in clay content unless other logs or data were available. For this reason, the synergism of composite log interpretation is stressed in this manual. Logs should be interpreted as an assemblage of data, not singly, to increase the accuracy of analysis.

Accuracy of qualitative interpretation usually improves with an increase in the number of wells that are logged in an area and the amount of available sample data. A gradual change in log response across a depositional basin may indicate a facies change. One anomalous log caused by unusual hole conditions may be identifiable when compared with a number of logs with consistent response; such errors are not likely to repeat. Continuous core or a large number of core samples from one test hole is more useful than a few nonrepresentative samples scattered throughout the section. If continuous coring of one hole cannot be funded, then geophysical logs of a nearby hole can be used to select representative intervals for coring.

Quantitative Analysis

Obtaining quantitative data on aquifers or rocks under dam sites is an important objective of many environmental and engineering logging programs; however, the proper steps to ensure reasonable accuracy of the data often are not followed. The scales on logs in physical units, such as percent porosity and bulk density, in grams per cubic centimeter (g/cc), or resistivity, in Ωm, must be determined. Even if the procedures described under log calibration and standardization are followed carefully, corroborating data for the particular rocks and wells logged are needed. Repeatability is ensured by logging selected depth intervals a second time; equipment drift is indicated by changes in response as a function of time or temperature. Because of the effect of rock matrix or specific rock type, calibration in one rock type may not ensure accurate parameter scales in another rock type. For this reason, if the rocks being logged are not the same as those in which the equipment was calibrated, core analyses are needed to check values on the logs. Before any log data are used quantitatively, they must be checked for extraneous effects, such as hole diameter or bed thickness.

Data are of questionable value where hole diameter is significantly greater than bit size, or from intervals where bed thickness is equal to or less than the vertical dimension of the volume of investigation for the probe. The volume of investigation is defined for the purposes of this manual as that part of the borehole and surrounding rocks that contributes 90% of the signal that is recorded as a log. The radius of investigation is the distance from the sensor out to the 90% boundary. These terms do not mean that the volume of investigation is spherical or that the boundary is a sharp cutoff. Instead, a gradual decrease in contribution to the signal occurs with increasing distance from the borehole. The size and shape of the volume of investigation changes in response to varying borehole conditions, the physical properties, and geometry of boundaries in the rock matrix and the source-to-detector spacing. Bed-thickness effects on log response can be best explained using the concept of volume of investigation and its relation to source-to-detector spacing. If a bed is thinner than the vertical dimension of the volume of investigation or thinner than the spacing, the log seldom provides accurate measurement of the thickness or physical properties of that bed because, under these conditions, the volume of investigation includes some of the adjacent beds. From the standpoint of quantitative log analysis, the best procedure is to eliminate from consideration those depth intervals that demonstrate diameter changes that are significant with respect to the hole diameter response of the logging tool.

Both vertical and horizontal scales on logs need to be selected on the basis of the resolution and accuracy of the data required. Logs obtained by large commercial logging service

companies generally have vertical scales of 20 or 50 ft/in., which is not adequate for the detail required in many engineering and environmental studies, where the wells may be only about 100 m deep. Similarly, the horizontal scales on many service company logs are compressed to avoid off-scale deflections. Logs digitized in the field will overcome many of these problems, and this subject is discussed in detail later. Some logs may be run too fast for the accuracy and thin bed resolution required. When the detector is centered on the contact between two beds of sufficient thickness, half the signal will be derived from one unit, and half from the other; selection of contacts at half amplitude for nuclear logs is based on this fact. If a nuclear or other slow-responding log is run too fast, contacts will be hard to pick and will be displaced vertically.

Few logs measure the quantity shown on the horizontal scale directly. For example, the neutron log does not measure porosity; it responds chiefly to hydrogen content. The difference between porosity and hydrogen content can lead to a large porosity error where bound water or hydrocarbons are present. Thus, a knowledge of the principles of log-measuring systems is prerequisite to the accurate quantitative analysis of logs.

Synergistic Analysis

Multiple log analysis takes advantage of the synergistic nature of many logs; usually much more can be learned from a suite of logs than from the sum of the logs individually. For example, gypsum cannot be distinguished from anhydrite with either gamma or neutron logs alone, but the two logs together are diagnostic in areas where gypsum and anhydrite are known to exist. They are both very low in radioactive elements, but gypsum has a significant amount of water of crystallization, so it appears as high porosity on the neutron log. In contrast, anhydrite appears as very low porosity on neutron logs. Both minerals will be logged as high resistivity. Computer analysis of logs can be very helpful in identifying such relationships because shading to emphasize differences between logs is easily accomplished.

Examining a suite of logs from a distance is good practice so that significant trends and shifts in response become more obvious in contrast to the detail seen up close. Thus, replotting logs at different vertical or horizontal scales, using a computer, may bring out features not previously obvious. The suite of logs needs to be examined for similarities and differences, and explanations need to be sought for log response that departs from that anticipated, based on the available background geologic data. When searching for explanations for anomalous log response, first examine the caliper log to determine if an increase in borehole diameter offers a possible reason. Although many logs are titled borehole-compensated or borehole-corrected, almost all logs are affected to some degree by significant changes in borehole diameter. All drill holes, except those drilled in very hard rocks like granite, have thin intervals where hole diameter exceeds bit size sufficiently to cause anomalous log response. Logs usually can be corrected for average borehole diameter, but thin zones of different diameter spanned by the logging tool are difficult to correct. Drilling technique can have a major effect on variations in borehole diameter.

Well construction information also may explain anomalous response, as may information on the mineral or chemical composition of the rock. Casing, cement, and gravel pack have substantial effects on log character. Some logs are designed specifically to provide

information on the location and character of casing and cement. These logs are described in the section on well-completion logging.

Computer Analysis

Computer analysis of geophysical well logs is now widely used, and if done properly, can contribute significantly to results from log interpretation. The very large amount of data in a suite of well logs cannot easily be collated or condensed in the human mind so that all interrelations can be isolated and used; computer analysis makes this possible. All of the major commercial well-logging service companies offer digitized logs and computer interpretation. Software packages for log editing and analysis are available that will run on microcomputers with sufficient memory, data storage, and graphics capability. Although the spreadsheet was not designed for log analysis, someone who understands logs can manipulate the data and plot the results (Keys, 1986). They do not, however, offer all of the features and flexibility of a program written specifically for log analysis. Programs written for the analysis of oil well logs have many features not needed for environmental and engineering applications and are often more expensive.

Computer analysis of logs offers a number of advantages over other methods used in the past: a large mass of data can be collated and displayed; logs can be corrected and replotted; scales can be changed; smoothing and filtering operations can be carried out; cross-plots can be made between different kinds of logs, and between logs and core data; calibration curves, correlation functions, and ratios can be plotted, as well as cross-section and isopach maps. Finally, these results can be plotted as publication-quality figures at a cost lower than hand plotting. Although all of these manipulations can be carried out by hand, the large quantity of data present in a suite of logs, or in the logs of all wells penetrating an aquifer system, is ideally suited for computer analysis. Figure 332 is a computer-generated cross section of three test holes in the Chicago area. The lithology was entered with key terms capitalized so that a column with lithologic symbols could be automatically generated. The correlation lines were sketched using the program, and shading between logs can also be added, as in figure 333.

Changing the vertical and horizontal scales of logs independently was almost impossible before computer processing was available; now replotting to produce scales best suited for the intended purpose is a simple matter. Correcting for nonlinear response or changing from a linear to a logarithmic scale are also relatively simple procedures. Most probes output a pulse frequency or a voltage that is related to the desired parameter by an equation that can easily be solved using a computer. Data from probe calibration can be entered in the computer to produce a log in the appropriate environmental units. For example, most neutron logs are recorded in pulses per second, which can be converted to porosity if proper calibration and standardization data are available. Other logs that might be computed from raw digital data are differential temperature, acoustic velocity from transit time, and acoustic reflectivity or acoustic caliper.

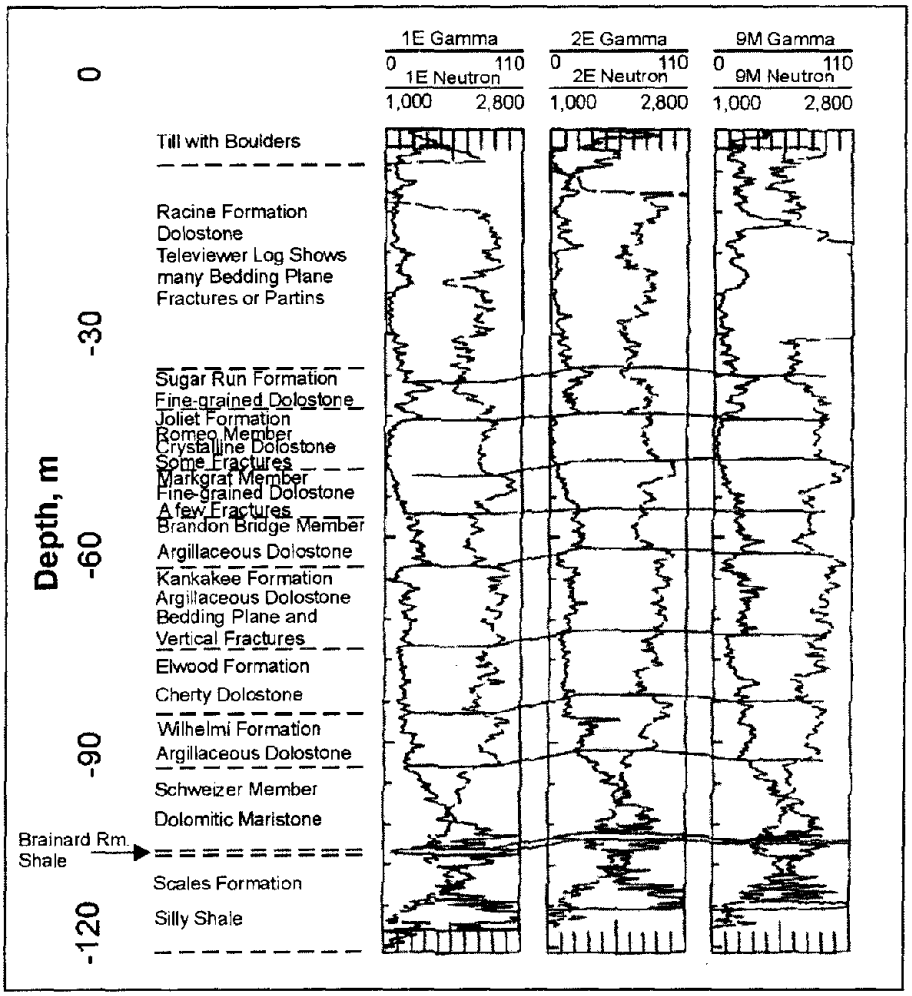

Figure 332. Computer plot of gamma and neutron logs of three test holes in the Chicago area, showing stratigraphic correction based on logs and lithology.

A computer is ideally suited for correcting logs and plotting them with calibrated scales. Depth correction is required on a large number of logs, and it can be carried out at the same time the computer is being used to make the first plot of digitized data. The most common correction needed is a consistent depth shift for the entire log to make it correlate with other logs of the same well or with core data, but stretching of part of a log can also be carried out.

Another important technique for log analysis is the computer plotting of data obtained from logs against data from other logs, core analyses, or tests. The technique most used is the cross plot, which compares the response of two different logs. A cross plot of transit time from the acoustic-velocity log versus porosity from the neutron log, calibrated for limestone, is given in figure 334. Data were plotted from digitized commercial logs of Madison test well No. 1 drilled by the U.S. Geological Survey in Wyoming. The calibration lines labeled sandstone, limestone, and dolomite were obtained from a plot in a book of log interpretation charts provided by the company that did the logging. These two logs indicate that two major rock types are in the interval plotted: limestone and dolomite. The group of points to the right of the dolomite line indicates secondary porosity in the dolomite. Another kind of

cross-plot that can be made using a computer is illustrated in figure 335. The plot shows a third log variable plotted on the Z-axis as a function of the neutron log response. This is the same rock sequence shown in figures 332 and 333. When the figure is plotted in color or displayed on a color monitor, the bars in the center track are the same color as the areas on the cross plot representing various lithologic units, and the neutron log response is shown by colors. The numerical values in the plot represent the neutron log values.

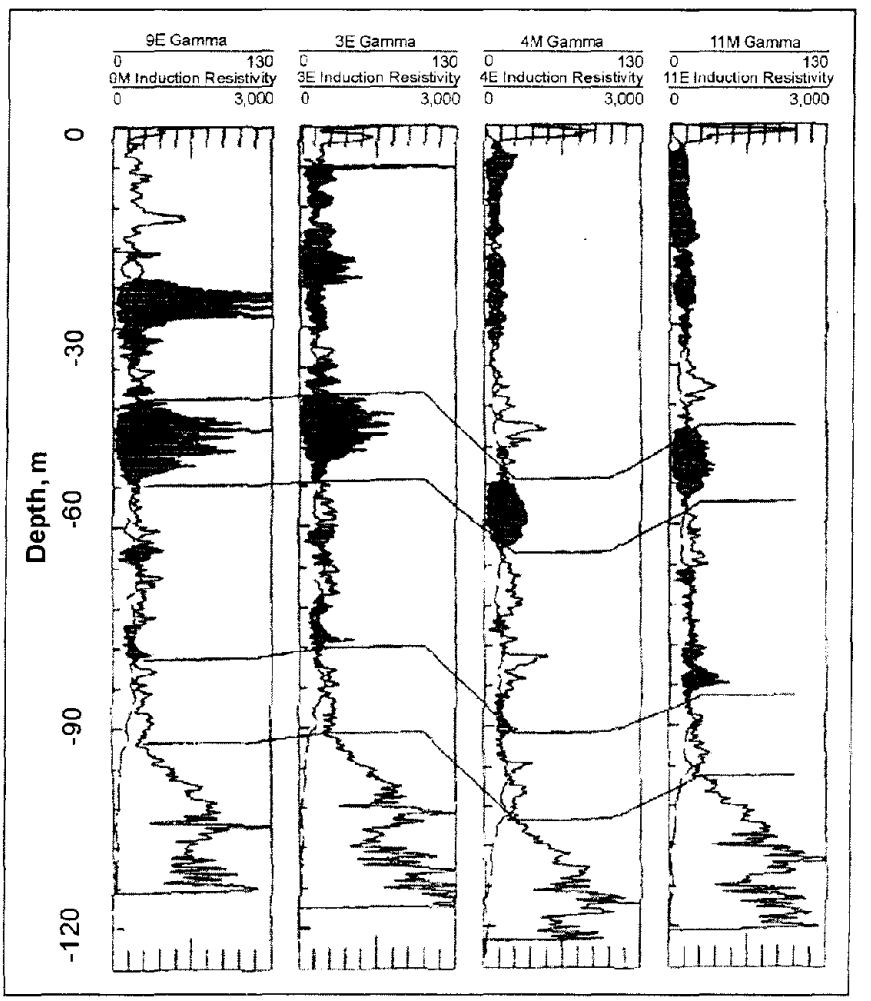

Figure 333. Cross section of four test holes in the Chicago area showing correlation enhanced by computer shading between gamma and induction logs.

Digitizing Logs

Geophysical logs may be digitized at the well while they are being run or subsequently from the analog record. Onsite digitizing is the most accurate and least expensive; with computers now on some logging trucks, real-time processing of the data may be carried out. Onsite digitizing also provides backup for recovery of data that are lost on the analog recorder because of incorrect selection of scales. Off-scale deflections lost from the analog recorder will be available from the digital record. Some systems permit immediate playback of the digital record to the analog recorder with adjustment of both horizontal and vertical scales.

Some probes transmit digital information to the surface and others transmit analog data that are digitized at the surface. There are advantages and disadvantages to both systems but regardless of which is used, logs should be digitized while being run. For most logs, it is recommended that the data files be made available to the user in ASCII format because it can be read and reformatted easily by most computers. Some log data, such as acoustic waveforms and televiewer logs, are digitized in other formats.

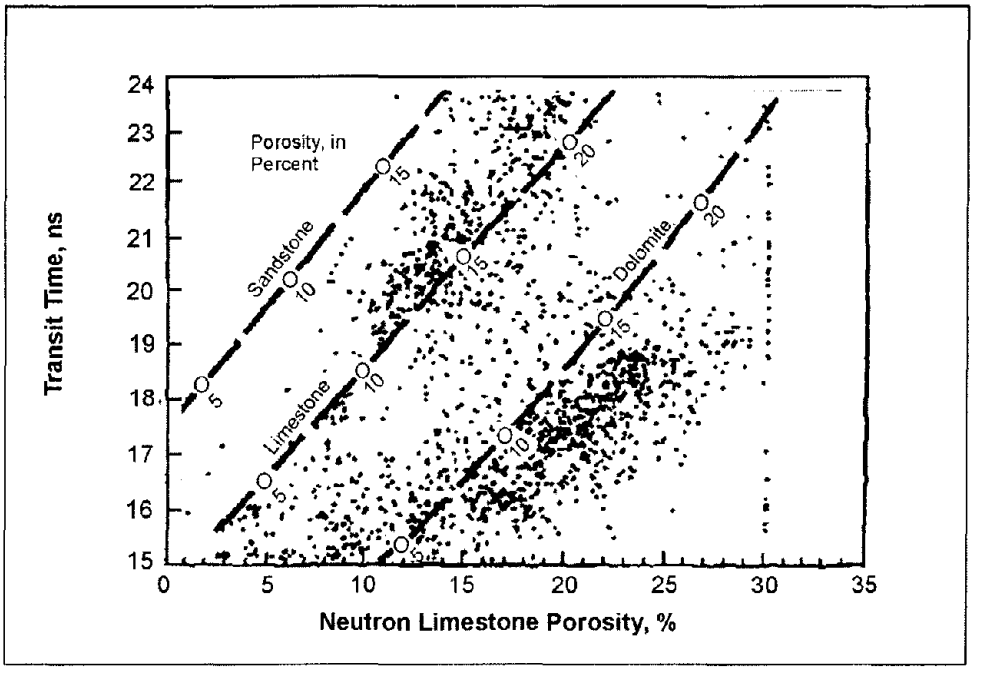

Figure 334. Cross plot of acoustic transit time versus neutron porosity, Madison limestone test well No. 1, Wyoming.

Sample interval and sample time need to be correctly selected for onsite digitizing of logs. Sample intervals of 0.15 m are used widely in both the petroleum industry and in groundwater hydrology; however, for detailed engineering and environmental investigations, intervals as small as 0.03 m are often used. If too many samples of the data are recorded, some samples can later be erased, and they can be averaged or smoothed; if not enough samples are recorded, needed information may be lost. Sample time is the duration of time over which a single sample is reorded. Sample time may be milliseconds (ms) or less for analog voltages, but may be 1 s or longer for pulse signals from a nuclear-logging probe. Digital data may be printed, plotted, or displayed on a computer monitor while the log is being run. An analog display in real time is needed because watching a log develop is one of the best ways to avoid major errors in logging and to optimize probe and data output configuration.

Information on the digital record should be listed on the log heading of the analog plot. This information includes the label on the recording medium, file number, sample interval, time, depth interval recorded, and any calibration information pertinent to the digital record.

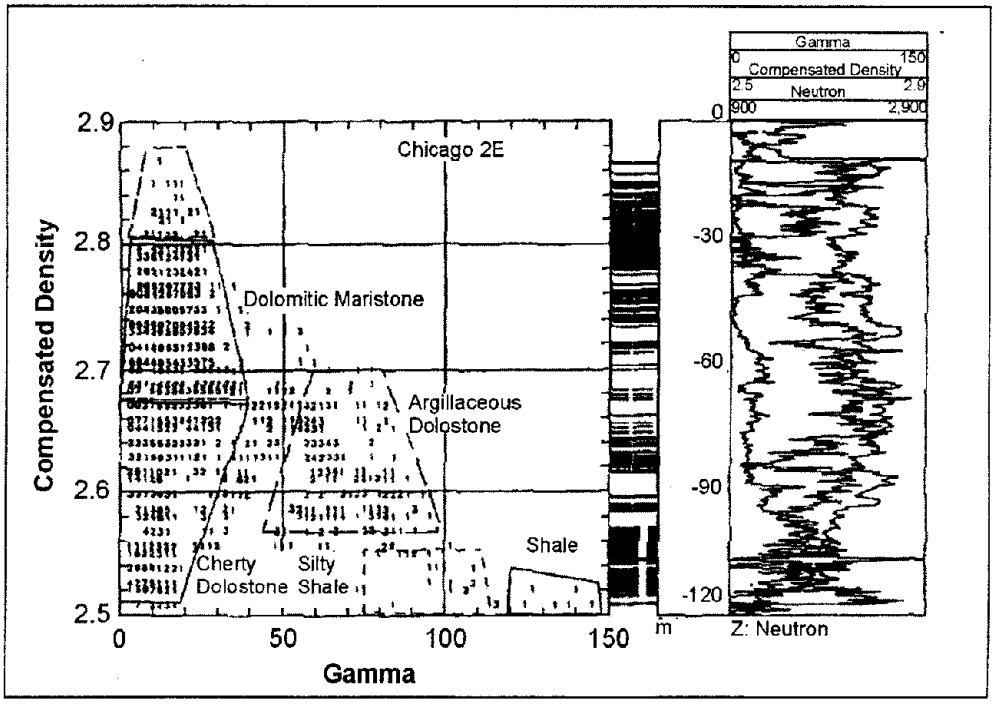

Figure 335. Three-dimensional "Z-plot" of gamma, density, and neutron log response of a test hole in the Chicago area.

Although office digitizing of analog records is expensive and time-consuming, no other choice may exist for old logs. Because of the training needed to digitize logs correctly, particularly multicurve commercial logs, better and less expensive results usually are obtained from a company specializing in digitizing geophysical logs. To have logs digitized commercially, certain specifications or instructions must be provided to the company with the purchase order. The types of logs to be digitized must be listed, along with the specific curve on each log, the depth interval, the sample interval, and vertical and horizontal scales. If editing of logs is to be done, it must be specified, but usually this should be done by the user. In addition to specifying the computer-compatible recording medium, the user can request a printout of all digital data and check plots of the logs. If the check plots are on the same scale as the original, they can be overlaid to verify the accuracy of digitizing.

Borehole Effects

The manner in which a test hole or well is drilled, completed, and tested has a significant effect on geophysical logs made in that well (Hodges and Teasdale, 1991). One of the objectives of logging is to obtain undisturbed values for such rock properties as porosity, bulk density, acoustic velocity, and resistivity, but the drilling process disturbs the rock near the drill hole to varying degrees. Although a number of different types of logging probes are called borehole compensated or borehole corrected, all probes are affected by the borehole to some degree. Borehole effects on geophysical logs can be divided into those produced by the drilling fluids, mud cake, borehole diameter, and well construction techniques. All procedures can be controlled to produce better logs. In some situations, it may be cost effective to drill two holes close together, the first designed to optimize logging, and the

second cored in the depth intervals suggested by those logs. Even if drilling and completion techniques are beyond control, their effect on log response can be reduced by proper probe selection and an understanding of borehole effects.

All drill holes, except those drilled in very hard rocks like granite, have thin intervals where hole diameter exceeds bit size sufficiently to cause anomalous log response. From the standpoint of log analysis, the best procedure is to not consider those depth intervals that demonstrate diameter changes that are significant with respect to the hole diameter response of the logging tool.

The difference between a rotary-drilled hole and a nearby core hole in an area where the sedimentary rocks change very little over great distances is shown in figure 336. The core hole was drilled very slowly, with considerable circulation of drilling mud to maximize core recovery. Core recovery was close to 100% in these well-cemented mudstones, sandstones, anhydrite, and dolomite. The coring procedure caused significant variations in borehole diameter, partly because of solution of halite cement and veins during the lengthy drilling process, which included numerous trips with the core barrel. The core hole produced some very poor quality logs. The rotary hole was drilled very rapidly to minimize hole diameter changes. Although increases in hole diameter occurred at the same depths in both holes, the range of diameter was much greater in the core hole. Stratigraphic correlation can be done with caliper logs in this area because hole diameter changes are closely related to rock type. The very sharp deflections just above 60 m are the result of the solution of halite veins. The very rugose interval below 90 m probably is the result of thin-bedded layers of anhydrite and mudstone.

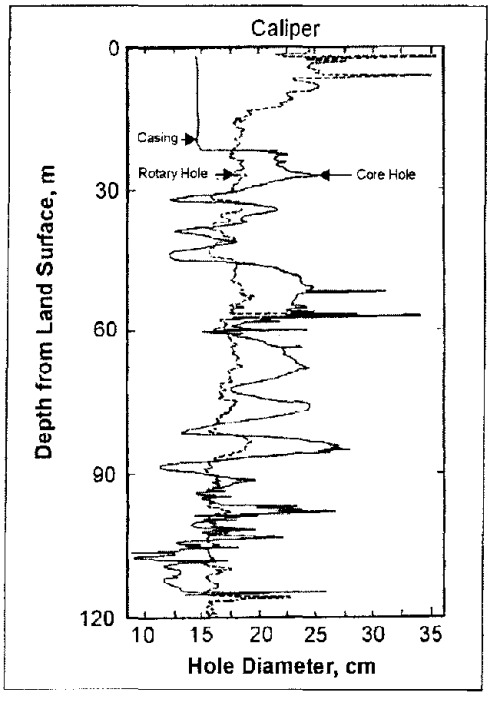

Figure 336. Effect of drilling technique on hole diameter. Holes are close together in an area of persistent lithology, Upper Brazos River basin, Texas.

The hydrostatic pressure of the fluid column is an important factor in preventing caving in poorly consolidated materials. This same pressure can cause invasion of an aquifer by the mud filtrate and the development of a filter cake or mud cake on the wall of the hole. Mud cake may reduce permeability and, thus, change results obtained from various flow logging devices. The thickness of mud cake often is related to the permeability and porosity of the rocks penetrated. Invasion by drilling fluids may change the conductivity of the pore water and reduce porosity and permeability in the vicinity of the drill hole. Hydraulic fractures can be induced in hard rocks by overpressure during drilling. One technique that is available for determining the extent of alteration of rock and fluid properties adjacent to the borehole is the use of different spacing between source and detector in acoustic or nuclear probes or between electrodes in resistivity probes. Longer spacing usually increases the volume of investigation or increases the percentage of the signal that is derived from material farther from the drill hole. The casing, cement, and gravel pack also have substantial effects on log character. Well completion logs are designed specifically to provide information on the location and character of casing and annular materials.

Operation of Equipment

If maximum benefit is to be obtained from an in-house logger that is purchased or rented on a long-term basis, an operator needs to be trained and assigned sole responsibility for the maintenance and repair of that unit. Logging equipment used by a number of people without adequate training and experience will have higher repair costs and more downtime than equipment assigned to one experienced person.

The larger logging service companies are based almost entirely on oil well operations; smaller companies rely mostly on environmental, engineering, water wells, or mineral exploration holes. Oil well logging equipment is larger and, therefore, more expensive, so that the costs-per-meter of log are much higher. Oil well logging probes may be too large for some environmental or engineering test holes, and a large drill rig is needed on the hole to suspend the upper logging sheave. A number of smaller local companies specialize in logging shallower, smaller diameter test holes or wells; some drillers own their own logging equipment. The smaller equipment owned by these companies may not include all the logging techniques available from the commercial service companies. Depth charges, standby time, and mileage costs will be lower for these small companies, but they may not have the calibration facilities common to the larger companies. The low bidder may not provide quality data, so proof of ability to perform should be required, and a written quality assurance and quality control program should be followed.

The total cost of commercial logging may be difficult for the inexperienced to calculate from price lists, because of the various unit costs involved. Depth and operation charges usually are listed per foot, and a minimum depth is specified. Mileage charges usually prevail over 250 km (150 miles) per round trip. The price of logging on environmental projects may be based on the following daily service charge:

a) Footage charges.

b) Mobilization.

c) Need for special health and safety measures or training.

d) Equipment decontamination.

e) Probe and cable loss insurance.

f) Crew per diem.

g) Any reports, special processing, or data processing required.

The well needs to be ready for logging when the equipment arrives because standby charges are relatively high. The customer is required to sign an agreement before any logging is done, stating that he assumes full responsibility for the cost of any probes that are lost, the cost of all fishing operations for lost probes, and the cost of any damage to the well. If a radioactive source is lost, fishing is required by law, and the well must be cemented up if the source is not recovered. The use of radioactive sources requires a written agreement, which must be addressed in the logging contract.

Quality Control

Control of the quality of geophysical logs recorded at the well site is the responsibility of all concerned, from the organization providing the logs to the analyst interpreting them; the ultimate responsibility lies with the professional who ordered and accepted the logs. No widely accepted standard or guidelines for log quality control exist at present; however, ASTM is presently working on a set of guidelines. Neither private logging companies nor government logging organizations accept responsibility for the accuracy of the data recorded. Agreements signed prior to logging by commercial companies usually include a disclaimer regarding the accuracy of the log data; therefore, the customer needs to assure that the best practices are followed. To obtain the most useful data, the logging program needs to be discussed early in the planning process with a local representative of the organization that will do the logging.

A geoscientist who understands the project objectives and the local geohydrology needs to be in the logging truck during the entire operation. The observer first will specify the order in which the logs will be run. Usually fluid logs will be run first, if the fluid in the well has had time to reach equilibrium. Nuclear logs always will be run last, or through drill stem if necessary, to reduce the possibility of losing a radioactive source. The observer usually makes preliminary interpretations of the logs as they come off the recorder. Based on immediate analysis, reruns can be requested if problems on the logs can be demonstrated. So many factors must be remembered by the observer to help control the quality of logs that many major oil companies provide a quality control checklist. Log headings that have blanks for a complete set of well and log data also can serve as partial quality control checklists. Incomplete log headings may prevent quantitative analysis of logs and make qualitative analysis much more difficult. Copies of digital data and field prints of all logs, including repeat runs, and field calibration or standardization should be left with the project manager before the logging equipment leaves the site. These data should be checked by a qualified person to determine if it is complete and without obvious problems before the logging equipment leaves.

Log headings may be divided into two basic sections: information on the well, and data pertaining to the logging equipment and operations. The completed heading needs to be attached to the analog record in the field. A short reference to the log heading information entered on the digital recording of each log enables the two records to be related. This reference will include the following information, as a minimum: hole number, date, log type, and run number. The format of a log heading is not important; the information is essential.

The well information section of the heading must contain all of the following, if available:

a) Well name and number.

b) Location - township, range, section, distance from nearest town, etc.

c) Owner.

d) Driller, when drilled, drilling technique, and drilled depth.

e) Elevation of land surface.

f) Height of casing above land surface.

g) Depth reference.

h) Complete description of all casing, type, size, and depth intervals.

i) Location of cement, bentonite, perforations, and screens.

j) Drilled size(s) (or bit size) and depth intervals.

k) Fluid type, level, resistivity, and temperature.

The log information section of a heading will contain different information for each type of log, although the same heading can be used for similar logs. The following information is needed on the heading for each log:

a) Type of log, run (___ of ___), date.

b) Number or description of logging truck.

c) Logging operator(s), observers.

d) Probe number and description -- including diameter, type, detector(s), spacing, centralized or decentralized, source type and size, etc.

e) Logging speed.

f) Logging scales - vertical (depth) and horizontal, including all changes and depths at which they were made.

g) Recorder scales - millivolts (span) and positioning.

h) Module or panel settings - scale, span, position, time constant, discrimination.

i) Power supply - voltage, current.

j) Calibration and standardization data - pre- and post-log digital values recorded on heading and analog positions on logs.

k) List all other logs of the well run on the same date. Also briefly describe all problems or any unusual response during logging; mark at the appropriate depth on the log.

Calibration and Standardization

Logs need to be properly calibrated and standardized if logs are to be used for any type of quantitative analysis or used to measure changes in a groundwater system with time. Calibration is considered to be the process of establishing environmental values for log response in a semi-infinite model that closely simulates natural conditions. Environmental units are related to the physical properties of the rock, such as porosity or acoustic velocity. Probe output may be recorded in units, such as pulses per second, which can be converted to environmental units with calibration data. Calibration pits or models are maintained by the larger commercial service companies; these are not readily available for use by other groups. The American Petroleum Institute maintains a limestone calibration pit for neutron probes, a simulated shale pit for calibrating gamma probes, and a pit for calibrating gamma spectral probes at the University of Houston; these have been accepted internationally as the standards for oil well logging. Boreholes that have been carefully cored, where the cores have been analyzed quantitatively, also may be used to calibrate logging probes. To reduce depth errors, core recovery in calibration holes needs to approach 100% for the intervals cored, and log response can be used to elect samples for laboratory analyses. Because of the possibility of depth errors in both core and logs, and of bed-thickness errors, samples need to be selected in thicker units, where log response does not vary much. It is advisable to have a well for periodic logging to determine if log response is consistent. A core hole is excellent for this purpose.

Standardization is the process of checking response of the logging probes in the field, usually before and after logging. Standardization uses some type of a portable field standard that usually is not infinite and may not simulate environmental conditions. Frequent standardization of probes provides the basis for correcting for system drift in output with time and for recognizing other equipment problems. The frequency of log standardization should be related to project objectives. If accurate data are needed, standardization should be more frequent.

10.2 GENERAL CROSSHOLE PROCEDURES

Introduction

The primary purpose of obtaining crosshole data is to obtain the most detailed in situ seismic wave velocity profile for site-specific investigations and material characterization. Crosshole velocity data are valuable for assessing man-made materials, soil deposits, or rock formations.

The seismic technique determines the compressional (P-) and/or shear (S-) wave velocity of materials at depths of engineering and environmental concern where the data can be used in problems related to soil mechanics, rock mechanics, foundation studies, and earthquake engineering. Crosshole geophysical testing is generally conducted in the near surface (upper hundred meters) for site-specific engineering applications (Sirles and Viksne, 1990). All of the dynamic elastic moduli of a material can be determined from knowledge of the in situ density, P-, and S-wave velocity. Therefore, since procedures to determine material densities are standardized, acquiring detailed seismic data yields the required information to analytically assess a site. Low-strain material damping and inelastic attenuation values can also be obtained from crosshole surveys. However, the most robust application of crosshole testing is the ability to define in situ shear-wave velocity profiles for engineering investigations associated with earthquake engineering (Mooney, 1984).

The objective of acquiring crosshole data can be multipurpose; that is, the seismic velocity results obtained may be used for evaluation of lateral and vertical material continuity, liquefaction analyses, deformation studies, or investigations concerning amplification or attenuation of strong ground motion. Typically, crosshole surveys are a geophysical tool for performing explorations during what are considered phase two field investigations (where phase one field investigations include surface geophysical surveys, follow-up drilling, trenching, and sampling of the in situ materials). During phase two field exploration, the information gathered is more critical to the analytical site-specific characterization. Although both phase one and phase two results are important, the two independent sets of data must be integrated into the final analysis.

Crosshole techniques are most useful when phase one site explorations indicate horizontal and particularly vertical variability of material properties. When layers of alternating density or stiffness are either known to exist or are encountered during phase one field investigations, crosshole seismic tests are recommended to define the in situ velocities within each layer. Acquiring crosshole seismic data resolves hidden layer velocity anomalies that cannot be detected with conventional surface methods, allows both final interpretation of other surface geophysical data (seismic or electrical), and permits both empirical and theoretical correlation with other geotechnical material parameters.

In order to have quantitative and quality assured results, crosshole tests performed for either engineering or environmental problems should be conducted in accordance with procedures established by the American Society for Testing and Materials (ASTM). Crosshole seismic test procedures are outlined in ASTM test designation D4428 M-84 (1984). The ASTM procedures provide specific guidelines for borehole preparation, data acquisition, and data

reduction/ interpretation. Based on 10 years of experience, since the inception of the ASTM standard in 1984, crosshole geophysical surveys have become more widely used and accepted for engineering as well as environmental applications. Coupling detailed site information obtained from the crosshole tests with the overall acceptance of the validity of the velocity data, these standards use both empirical correlations for liquefaction and specific input parameters for deformation or ground motion analyses (U.S. Bureau of Reclamation, 1989).

Theory

Crosshole testing takes advantage of generating and recording (seismic) body waves, both the P- and S-waves, at selected depth intervals where the source and receiver(s) are maintained at equal elevations for each measurement. Figure 337 illustrates a general field setup for the crosshole seismic test method. Using source-receiver systems with preferential orientations in tandem (i.e., axial orientations, which complement the generated and received wave type/signal) allows maximum efficiency for measurement of in situ P- or S-wave velocity depending on the axial orientation. Due to the different particle motions along the seismic ray path, it is crucial to use optimal source-receiver systems in order to best record crosshole P- or S-waves (Hoar, 1982). Because only body waves are generated in the source borehole during crosshole tests, surface waves (ground roll) are not generated and do not interfere with the recorded body-wave seismic signals.

Stokoe (1980) demonstrated that particle motions generated with different seismic source types used during crosshole testing are three-directional. Therefore, three-component geophones with orthogonal orientations yield optimal results when acquiring crosshole P- and/or S-wave seismic signals. With three-component geophones, there is one vertically oriented geophone and two horizontal geophones. For crosshole tests, one horizontal geophone remains oriented parallel to the axis between the boreholes (radial orientation), and the other one remains oriented perpendicular to the borehole axis (transverse orientation). In this case, the two horizontal axis geophones must remain oriented, radially and transversely, throughout the survey. This is accomplished with loading poles or with geophones that can be electronically oriented.

P-waves are generated with a sparker or small explosive device (one that will not damage the PVC casing) such that along the assumed straight-ray propagation path the seismic impulse compresses and rarefies the materials radially toward the receiver borehole(s). Experience has proven that for optimal measurement of the P-wave signal, a hydrophone has the greatest pressure-pulse sensitivity for compressional-wave energy. Also, hydrophones do not need to be clamped against the borehole wall; however, water must be present in the receiver borehole in order to couple the hydrophone to the casing/formation.

For either surface or crosshole seismic testing in unconsolidated materials, P-wave velocity measurements are greatly affected by the moisture content or percent saturation (Allen, Richart, and Woods, 1980). In crosshole testing, the seismic measurements encroach closer to the water surface with each successive depth interval. As the vadose zone and water surface are encountered, P-wave velocities become dependent upon the percent saturation, and the Poisson's ratio is no longer a valid representation of the formation characteristics

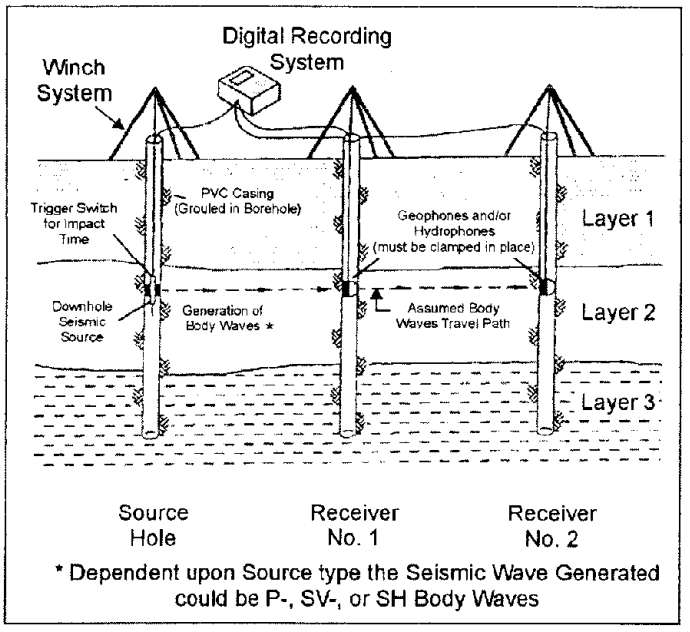

Figure 337. Schematic of crosshole method.

(e.g., Poisson's ratio increases to 0.48-0.49 in 100% saturated soils). Hence, below the water surface, the P-wave is commonly termed the fluid wave, because its propagation velocity is governed by the pore fluid(s), not the formation density. Fluid-wave velocities in fresh water range from 1,400 to 1,700 m/s, depending upon water temperature and salt content.

S-waves generated in crosshole testing may be split into two wave types, each with different particle motions--SV- and SH-waves, vertical or horizontal particle motions, respectively. Shear waves have the unique capability of polarization, which means that impacting the material to be tested in two directions (up or down, left or right) yields S-wave signals that are 180° out of phase. A seismic source with reversible impact directions is the key factor for quality crosshole S-wave data acquisition and interpretation. Figure 338 shows a series of crosshole SV-waves with reversed polarity (note the low amplitude of the P-wave energy compared to the S-wave energy) received at both receiver boreholes.

Typically, the S-wave generated in most crosshole testing is the SV-wave, which is a vertically polarized horizontally propagating shear wave. That is, the ray path is horizontal but the (shear) particle motion along the ray path is in the vertical plane. These SV-waves are easiest to generate because of commercially available borehole impact hammers that have reversible impact directions (up or down), and they are also the easiest to record because only one vertically oriented geophone is required in each receiver borehole. Alternatively, SH-waves can be generated and recorded in crosshole testing. SH-waves also propagate horizontally, but their (shear) particle motion is in the horizontal plane (i.e., horizontally polarized horizontally propagating S-waves). Therefore, in order to generate and record SH-wave signals, horizontal impacts and geophones are required; also, the orientation of the source and receiver must be parallel while their respective orientation remains perpendicular to the axis of the boreholes (transverse orientation).

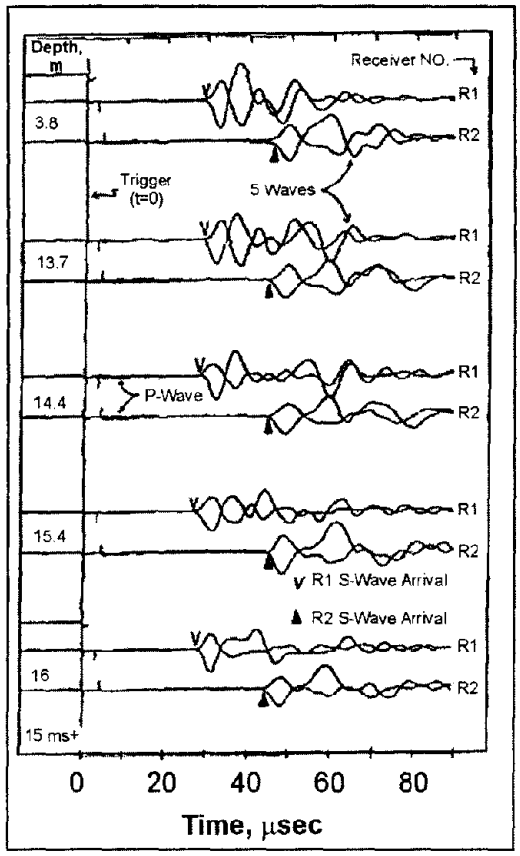

Figure 338. Crosshole SV-wave paired borehole records at five depths.

Theoretically, there is no difference in the body wave velocity for SV- and SH-waves, which justifies use of the uncomplicated vertical source for generation of SV-waves, and vertically oriented geophones for signal detection. There are studies, however, which indicate significant velocity dependence of the SV- and SH-waves due to anisotropic states of stress in either the horizontal or vertical stress field (particularly in soil deposits; (Redpath, et al., 1982) or fractured rock formations (White, 1983).

The requirement for multiple drill holes in crosshole testing means that care must be taken when completing each borehole with casing and grout. ASTM procedures call for PVC casing and a grout mix that closely matches the formation density. Basically, borehole preparation and completion procedures are the success or failure of crosshole seismic testing. Poor coupling between the casing and the formation yields delayed arrival times and attenuated signal amplitudes, particularly for (higher frequency) P-waves. Matching the formation density with a grout mix is not too difficult, but in open coarse-grained soils, problems arise during grout completion with losses into the formation. Even small grout takes begin to affect the velocity measured between two closely spaced drill holes. Several techniques to plug the porosity of the surrounding formation are commercially available (e.g., cotton-seed hulls, crushed walnut shells, or increased bentonite concentration in the grout mix). It should be recognized that increasing the ratio of bentonite/cement within the

grout mix does affect density, but so long as the mix sets and hardens between the casing and in situ formation, quality crosshole seismic signals will be obtained..

Another critical element of crosshole testing, which is often ignored, is the requirement for borehole directional surveys. There are several very good directional survey tools available that yield detailed deviation logs of each borehole used at a crosshole site. Borehole verticality and direction (azimuth) measurements should be performed at every depth interval that seismic data are acquired. With the deviation logs, corrected crosshole distances between each borehole may be computed and used in the velocity analysis. Since seismic wave travel times should be measured to the nearest tenth of a millisecond, relative borehole positions should be known to within a tenth of a foot. Assuming that the boreholes are vertical and plumb leads to computational inaccuracies and ultimately to data that cannot be quality assured.

Data Acquisition

Recording instruments used in crosshole testing vary considerably, but there are no standard requirements other than exact synchronization of the source pulse and instrument trigger for each recording. Crosshole measurements rely considerably on the premise that the trigger time is precisely known as well as recorded. The recorded trigger signal from zero-time geophones or accelerometers mounted on the downhole impact hammer allows accurate timing for the first arrival at each drill hole. This becomes uniquely critical when only two drill holes are used (i.e., source and one receiver) because there is no capability of using interval travel times; in this case, the velocity is simply determined through distance traveled divided by direct travel time. Utilizing digital recording equipment affords the operator the ability to store the data on magnetic media for analysis at a later date; but more importantly, digital data can be filtered, smoothed, and time-shifted during analysis. Also, digital signal processing may be directly performed for coherence, frequency-dependent attenuation, and spectral analysis.

Numerous studies have shown that the effects on crosshole measurements by the choice of geophone are not critical to the results (e.g., Hoar, 1982). There are only two requirements for the receivers: the receiver (velocity transducer) must have a flat or uniform output response over the frequency range of crosshole seismic waves (25 to 300 Hz); and, a clamping device must force the receiver against the borehole wall such that it is not free-hanging. The clamping device should not affect the mechanical response of the geophone (i.e., resonance), nor should the uphole signal wire. If an SH-wave source is selected, then horizontal geophones must be used and oriented as previously described to detect the SH-wave arrivals. It is paramount that the polarity of each geophone be known prior to data acquisition because the direct arrivals of S-waves with reversed polarity can be easily misinterpreted. Hoar (1982) provides an excellent description of picking P- and S-wave arrivals off recorded crosshole signals. Hoar's dissertation shows that with proper borehole completion, digital recording equipment, and a preferential source-receiver system, clean reversed polarized and interpretable S-wave signals are relatively easy to acquire.

Data Interpretation

For interpretation of direct ray path travel times between two or three boreholes, the Bureau of Reclamation (Sirles, Custer, and McKisson, 1993) has published a computer program that is designed specifically for reducing crosshole seismic data. Furthermore, the program was fashioned around the ASTM conventions and test procedures outlined for crosshole seismic testing. The program CROSSIT (Version 2.0) is intended to be a step-by-step program that allows the user to:

a) Input lithologic information obtained from geologic drill hole logs.

b) Input deviation survey for each drill hole.

c) Input travel times for P- and/or S-wave arrivals at one or two receiver holes.

d) Enter site-specific information (location, surface elevation, etc.).

e) Map each borehole using deviation survey information.

f) Determine corrected crosshole distances between respective drill shot pairs: source/receiver 1, source/receiver 2 and receiver1/receiver2.

g) Compute direct P- and S-wave velocities from travel time data.

h) Tabulate and/or graph (to hard copy or disk file).

i) Borehole directional survey data and plots.

j) P- and S-wave velocity depth profiles from each drill hole pair.

k) Interactively edit input or graphical files and combine data sets.

l) Post-process seismic data and/or plots for alternative uses.

CROSSIT is built for compatibility with laptop or desktop computers and dot matrix or laser-jet printers such that data reduction could be performed in the field as geophysical data are being acquired. The logic and flowchart for this interpretation and data presentation program are designed to follow the typical field data acquisition process (i.e., geologic information, borehole information, travel-time information) to permit interactive computer analysis during data collection. This technique of reducing data in the field has proven its value because of the ability to determine optimal testing intervals and adjust the program as necessary to address the site-specific problem.

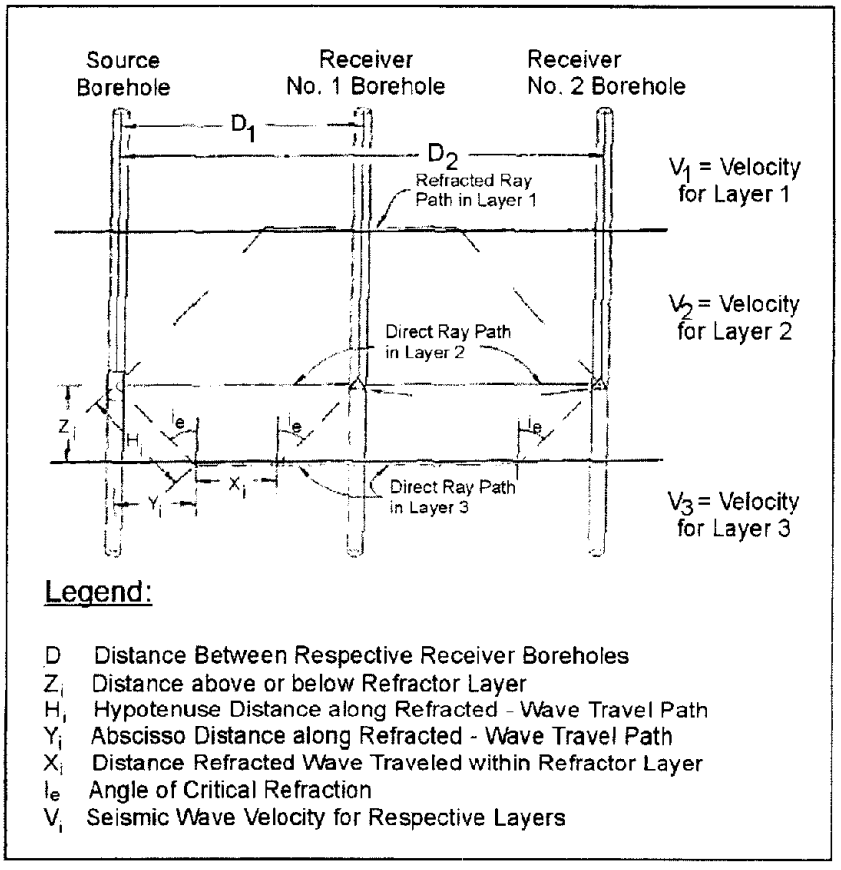

Figure 339. Illustration of refracted ray path geometries in crosshole seismic tests where $V_1 > V_2 < V_3$ and $V_1 < V_3$.

Unlike surface seismic techniques, crosshole testing requires a more careful interpretation of the waveforms acquired at each depth. For example, in crosshole testing, the first arrival is not always the time of arrival of the direct ray path. As illustrated schematically in figure 339, when the source and receivers are located within a layer that has a lower velocity than either the layer above or below it (this is termed a hidden layer in refraction testing), refracted waves can be the first arrivals. Both the source/receiver distance above or below the high-velocity layer and the velocity contrast (V1 : V2) across the seismic interface determine if the refracted wave will arrive before the direct wave. Due to the effect refracted waves have on crosshole data sets, ASTM procedures require a three-borehole array because velocity corrections can be made for refracted arrivals. Also, depending upon the velocity contrast across layer boundaries, direct arrivals through low-velocity layers are generally larger amplitude and thereby recognizable. This permits timing direct arrivals directly off the waveform. Figure 340 shows an example of (SV-) direct-wave arrivals and refracted-wave arrivals where the arrival time of the direct wave (slower) can be picked later in the waveform behind the low-amplitude refracted-wave arrival. In this example, refractions occur in a situation similar to that depicted in figure 339; that is, refractions occur from high-velocity materials either above or below the low-velocity layer.

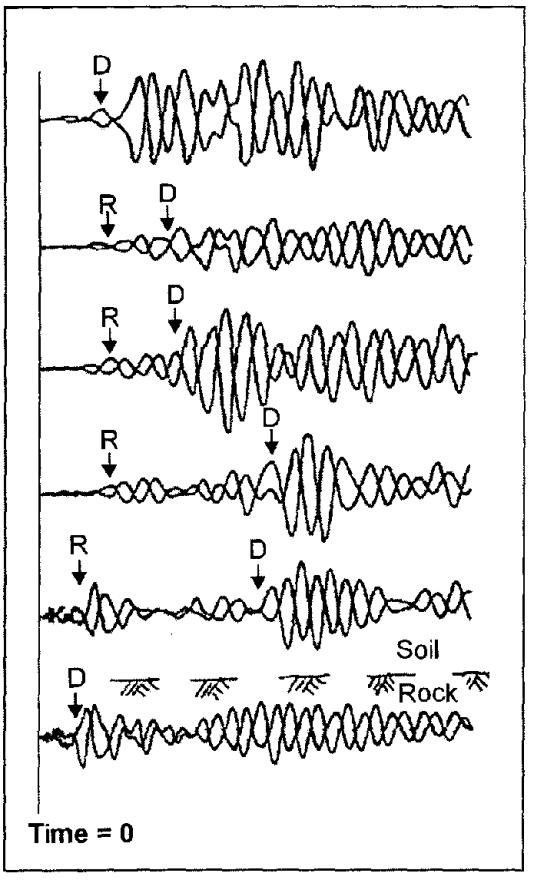

Figure 340. Crosshole SV-waves showing direct (D) and refracted (R) arrivals.

When approaching seismic interfaces, refracted-wave arrivals begin to be timed as the first arrival, which could (easily) be misinterpreted as direct-wave arrival. Therefore, the following sequence of eight steps (equations) will confirm detection of refracted-wave travel time or direct-wave travel time at each recording depth (ASTM 1984):

Compute i_c: $\sin i_c = V_1/V_2$

Compute hypotenuse distance H_i: $H_1 = H_2 = H_3 = Z/\cos i_c$

Compute abscissa distance Y_i: $Y_1 = Y_2 = Y_3 = Z\tan i_c$

Compute travel times through both materials:

$t_{V1} = 2H_1 / V_1$

$t_{V2} = (D1 - 2Y_1) / V_2$

[V_1 and V_2 are known from measurement above and below the seismic interface.]

Compute total refracted travel time: $T_{rfr} = t_{V1} + t_{V2}$

Compute total direct travel time: $T_{dir} = D_1 / V_1$

Retrieve measured crosshole travel time: T_{meas}

Compare T_{rfr} with T_{dir} *and* T_{meas}

IF: $T_{rfr} \leq T_{dir} \approx T_{meas}$ THEN: True V_1

IF: $T_{rfr} \geq T_{meas} < T_{dir}$ THEN: Apparent V_1 (refracted velocity)

Comparing both sets of direct wave velocities, that is, source to receiver No. 1 ($V_{(R1)}$) and source to receiver No. 2 ($V_{(R2)}$), with the interval velocity (V_I) computed from

Internal velocity $\equiv V_1 = (D2 - D1)/(T_{meas(R2)} - T_{meas(R1)})$,

allows easy identification of boundaries with velocity contrasts. When V_I is much greater than the two computed direct-wave velocities, then refracted-wave arrivals are being timed as first arrivals at the second receiver borehole. Therefore, a systematic comparison of measured travel times, computed direct velocities, and interval velocities at each recording depth enables interpretation of true in situ velocity at all measurement depths. For crosshole tests, Butler, et al. (1978) developed a computer program that performs this comparison of the respective computed velocities determined at every depth. Based on this discussion, to ensure that true in situ velocities are presented, crosshole measurements should be performed a minimum of four measurement intervals *below* the zone of concern to adequately define the velocity profile.

The comparative technique for defining the refractor velocities outlined above assumes that the velocities are constant within each layer; however, occasionally this is an oversimplification. Some deposits have linearly increasing velocity with depth, primarily due to vertical pressures, where the apparent velocity for each depth can be computed with

$$V_{app}(z) = V_i + Kz$$

In these cases, V_{app} is a function of depth (z), V_i is the initial velocity at zero depth, and K is the increase in velocity per unit depth. Direct-wave velocities computed for the far receiver (R2) at each depth will always be slightly higher than the near receiver (R1); hence, the interval velocity will be even higher. Increasing velocity with depth implies the seismic ray path is nearly circular between source and receiver, thereby sensing deeper (higher velocity) material as the source-receiver separation increases. The effect of increasing velocity with depth is greatest within thick homogeneous soil deposits. In these soil conditions, computing an average velocity from the two direct velocities (i.e., $V_{ave} = (V_{(R1)} + V_{(R2)})/2$) is often the best estimate for presenting the in situ velocity profile.

Modeling and Data Processing

Typically, either forward or inverse modeling for cross-borehole seismic investigations consists of computing synthetic travel times to test the ray path coverage and resolution of either unknown or identified velocity anomalies, respectively. For engineering applications, there is not much advantage in determining (via modeling) the ray coverage or residual velocity resolution because crosshole testing at the engineering scale utilizes a simple horizontal, straight-ray path geometry to determine average velocity. Also, lithologic information such as stratigraphy and material type are determined from the drilling and sampling program prior to seismic data acquisition; this allows reliable constraints, or

boundary conditions, to be placed on the field data along the boundaries of the material between the boreholes.

For engineering applications, digital signal processing in crosshole seismic tests is, similar to modeling, of minimal value. This, of course, assumes field data are acquired properly and no analog filtering or digital aliasing was performed prior to recording seismic data from each depth. There are a number of digital signal processing techniques useful for determining material properties other than P- or S-wave velocity, as well as confirming the computed crosshole velocity profile, such as:

a) Spectral analysis for determination of inelastic constants (attenuation and/or material damping).

b) Frequency analysis for correlation of phase and group velocity.

c) Cross-correlation of recorded seismic signals from one receiver to another receiver borehole, or source to receiver coupling for signal coherence.

Sophisticated processing is rarely required in (engineering) crosshole testing, and the straightforward distance/travel time relationship for velocity computations is considered functional and effective

Advantages and Limitations

Crosshole seismic testing has the unique advantage of sampling a limited volume of material at each test depth. Thus, the final result is a significantly more detailed and accurate in situ seismic (P- and/or S-wave) velocity profile. Crosshole tests are not unique in the use of preferential source/receiver configurations; however, there is the distinctive opportunity to generate and record only body wave energy, as well as preferentially excite particle motion in three directions with respect to the vertical borehole wall. Because of this, the crosshole test permits much easier interpretation of direct arrivals in the recorded waveforms. Because boreholes are required, there is the opportunity to obtain more site-specific geotechnical information, which, when integrated with the seismic data, yields the best assessment for the engineering application (liquefaction, deformation, or strong motion characterization). Also, because each drill hole was cased for the crosshole tests, additional geophysical surveys should be conducted. Typically, geophysical borehole logging will be conducted in each drill hole for the purpose of defining lithologic and stratigraphic continuity of the deposits.

Crosshole seismic testing has the definitive advantage of assessing a complex layered velocity structure with alternating high and low relative velocities. Other surface techniques such as spectral analysis of surface waves can theoretically evaluate the high/low layered velocity structure, but due to a number of inherent assumptions associated with surface geophysical methods, several non-unique velocity profiles may be derived (from inverse modeling) without specific information about the subsurface layering at the site. Since considerable confidence can be placed on engineering scale crosshole seismic data, computation of in situ low-strain elastic constants (Shear and Young's modulus, Poisson's ratio, etc.) permits dependable assessment of geotechnical parameters for the site-specific evaluation. Recently, sites of particular concern for obtaining P- and S-wave velocities are

liquefaction studies where the subsurface contains considerable unconsolidated coarse-grained material, and standard geotechnical test procedures (blow counts and material sampling) cannot effectively evaluate in situ properties. For successful engineering analysis of coarse-grained materials, crosshole testing is one of the most acceptable geophysical techniques available.

The primary detriments or obstacles encountered during crosshole testing are typically related to the placement and completion of multiple drill holes. Sites where noninvasive techniques are required due to hazardous subsurface conditions, crosshole seismic tests are not applicable because of tight regulatory procedures regarding drilling, sampling, and decontamination. However, at sites where detailed in situ P- and S-wave velocities are required, drill hole completion must follow ASTM procedures, and when unusual conditions exist (e.g., open-work gravels), specialized techniques for borehole completion should be employed. The U.S. Bureau of Reclamation has encountered numerous sites in the western United States where loose, liquefiable sand and gravel deposits needed to be investigated, and crosshole testing effectively evaluated the in situ material density and stiffness with P- and S-wave velocities, respectively; however, considerable care and caution were used for completion of each borehole (U.S. Bureau of Reclamation, 1992).

Seismic data for crosshole testing need considerably more waveform interpretation because refraction events from high-velocity layers either *above or below* a low-velocity layer must be identified and the first-arrival velocity corrected. Direct-wave arrivals are easily recognized (even with low-amplitude refracted arrivals) as long as the previously described field equipment is utilized for preferential generation of P-waves or polarized SV or SH-waves. The ASTM requirement of three drill holes seems costly to a project budget; however, the necessary source/receiver configurations and borehole separation allow optimal correction and evaluation of in situ P- and S-wave velocities for each material layer at depth.

Example Problem

To illustrate the effect of a high S-wave velocity layer overlying a low S-wave velocity layer on crosshole waveforms, the following sample problem is presented using data acquired at a site in central Utah. Figure 341 shows a portion of the waveforms collected over the depth interval 17.5 to 32.0 m, as well as the entire S-wave velocity profile obtained at this site. Only one polarity of the S-waves obtained is plotted over this depth interval (unlike the opposite polarity data shown in figure 340), but the arrival of the S-wave is clearly distinguished from the lower-amplitude and higher-frequency P-wave arrival.

The objective of this investigation was to determine if a low-velocity alluvial layer exists beneath the embankment, which was constructed in 1943. Data are then used to determine the liquefaction potential of the foundation alluvial deposits. As clearly shown on the sample problem figure, directly beneath the embankment the velocities decrease to less than 240 m/s in a layer of lean clay, which is not considered liquefiable; however, within the silty sand alluvial deposits, the wave forms show considerable increase in the S-wave travel times, and the computed velocities indicate potentially liquefiable deposits with S-wave velocities less than 180 m/s. Beneath approximately 30 m, the S-wave velocities gradually increase to greater than 240 m/s.

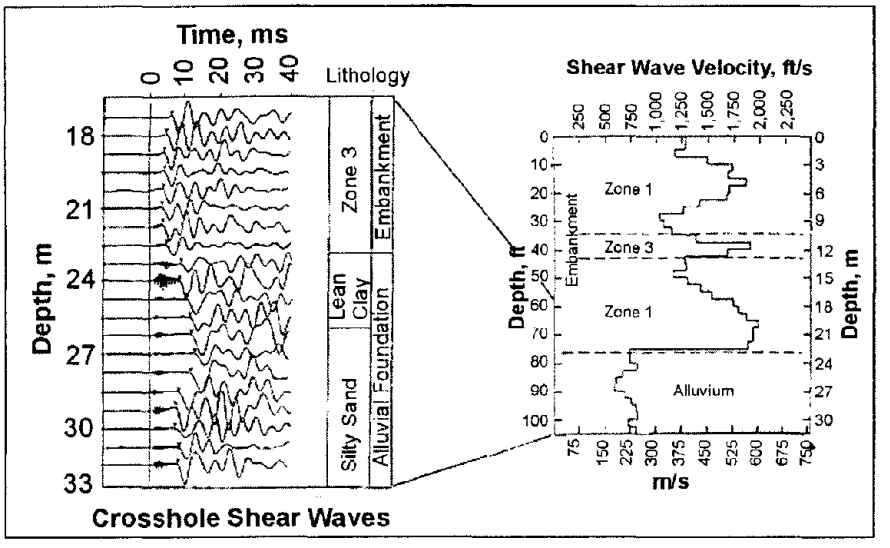

Figure 341. Example problem.

This sample problem, or example data set, illustrates three distinct advantages that crosshole testing has over conventional surface geophysical testing for these types of investigations:

a) Ease of identification of direct arrival S-waves.

b) Ability to determine the presence of low-velocity materials (alluvium) directly beneath high-velocity materials (embankment).

c) Direct and fairly straightforward computation of the S-wave velocity profile, which is correlated with the liquefaction potential of both the materials and depth intervals of engineering concern for the safety of the structure.

10.3 SURFACE TO BOREHOLE PROCEDURES

10.3.1. Overview of Borehole Seismic Methods

There are fundamental physical reasons why borehole seismic techniques can provide potentially better answers than conventional surface seismic techniques. There is a progression in both complexity and benefits from check shot and synthetic seismogram to vertical seismic profiles (VSP), three-component VSP, offset VSP, and extrapolation and description of lithologic parameters into the geologic formations surrounding the borehole. Presently VSP's are run in wells to aid in the correlation of surface seismic data. Borehole velocity surveys, commonly called *check shot surveys*, are often expanded into VSP's since additional acquisition costs are relatively small.

Synthetic Seismograms

Synthetic seismograms have traditionally been used to correlate surface seismic sections. Like all theoretical models, synthetic seismograms suffer from the simplifying assumptions that go into the model. An approximate fit to surface seismic lines is often obtainable. However, synthetic seismograms offer an important link in trying to understand the seismic tie to the well log. An example of a synthetic seismogram is shown in figure 342.

Velocity Surveys

Velocity or check shot surveys are well established in the geophysical community. Sources and receivers are distributed to obtain vertical travel paths through the formation of interest. Receivers are placed at or near geological horizons of interest. On the recorded seismic trace, only the information from the first arrival is used. A velocity survey field setup and recorded field data are illustrated in figure 343.

Time-depth Plots

Seismic first arrivals are converted to vertical travel times and plotted on time-depth graphs. The time-depth information is used to calculate average, root-mean-square, and interval velocities.

Sonic Log Calibration

Sonic log calibration is one of the applications of velocity surveys. Velocity obtained from sonic logs can be affected by a variety of borehole effects. Integrated sonic logs are subsequently distorted by these borehole effects. The resultant discrepancy between seismic and sonic measurements, called drift, must be corrected prior to the construction of synthetic seismograms to prevent the shifting in time of the seismic reflections or the introduction of pseudoevents.

Vertical Seismic Profiles

In vertical seismic profiling, full use is made of the entire recorded seismic trace, in addition to the first break. Receivers are spaced at close intervals throughout most of the well bore in order to obtain a seismic section of the well bore. The seismic wave itself and the effects on it as it propagates through the earth are measured as a function of depth. Receivers are now close to reflectors. In addition, both upgoing and downgoing wave fields are recorded at each receiver. The downgoing wavelet with its reverberant wave train is observed as a function of depth and can be used to design deconvolution filters. Signal changes in terms of bandwidth and energy loss can be measured. In general, the VSP also provides better satial and temporal resolution. Figure 343 illustrates the generation and travel paths of direct arrivals, reflected primaries, and examples of upgoing and downgoing multiples.

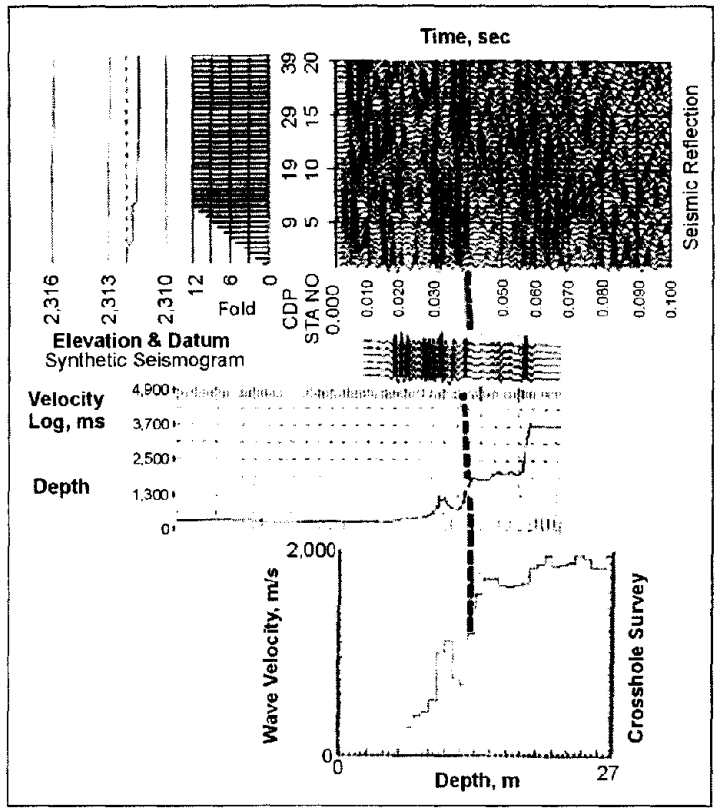

Figure 342. Correlation between crosshole survey, velocity log synthetic seismogram, and surface seismic reflection section.

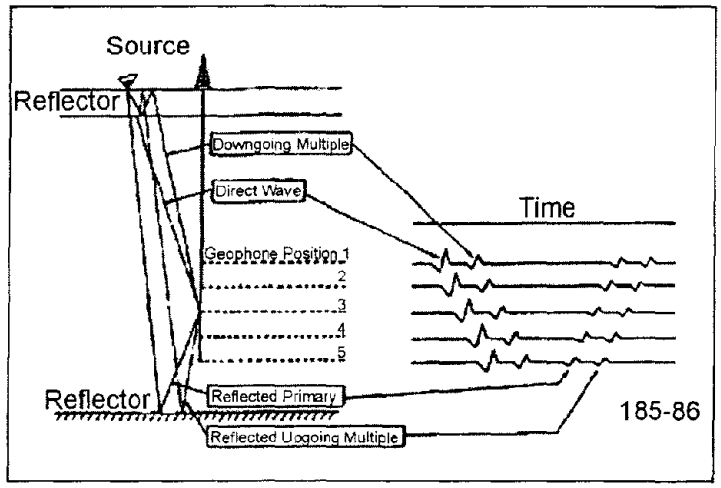

Figure 343. Recording of a vertical seismic profile; direct arrivals, reflected primaries, and examples of downgoing and upgoing multiples.

Vertical seismic profiling permits correlation of the actual seismic event inclusive of all the changes it undergoes (multiples, attenuation, etc.) at the actual recorded depth. This leads to

a great deal more confidence in correlating surface seismic profiling. An example of correlation between VSP and surface seismic profiling is shown in figure 344.

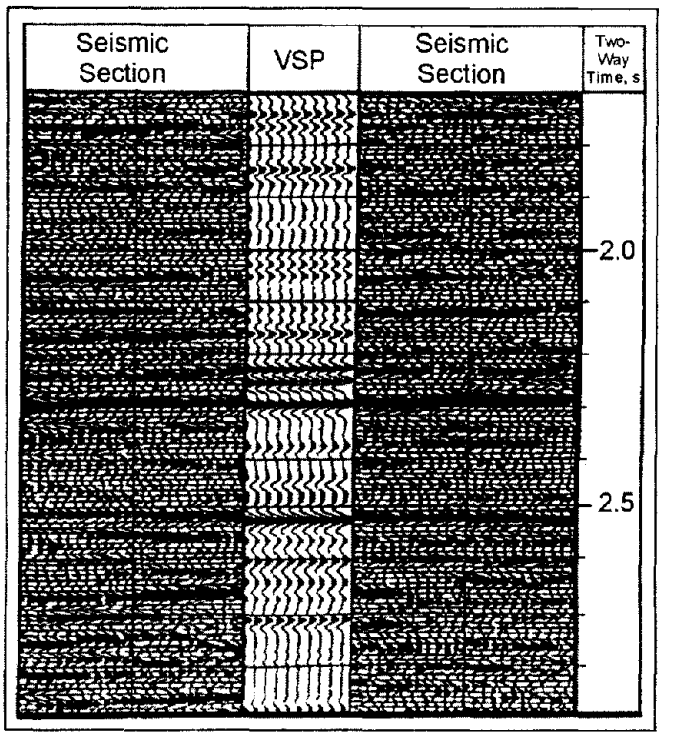

Figure 344. Example of correlation between Vertical Seismic Profiling and surface seismic profiling; the Vertical Seismic Profiling data stack is shown at the proper well location with respect to the seismic section.

Resolution in vertical seismic profiling is generally much improved over that obtainable with conventional surface seismic profiling. This is largely the result of the shorter travel path. With VSP's, high-resolution mapping of, for example, a reservoir can be accomplished. Better estimates of rock properties, including below the bit, can be obtained. The information from the VSP about multiples and signature attenuation can be used to upgrade the processing of surface seismic profiling. In fact, it is anticipated that reprocessing of surface seismic profiling will be done routinely when good VSP data are available.

The inversion of seismic traces from VSP data to predict impedance changes below the drill bit has been demonstrated with remarkable success. This is largely because careful matching of impedances in the known portion of the drillhole has led to increased reliability when predicting below the bit. A popular application is that of predicting overpressure zones. Details of the technique will be discussed under VSP applications.

Offset VSP's were developed to illuminate structure away from the well bore. Applications are primarily to find faults and pinchouts. An example of an offset VSP is shown in figure 345. The figure shows a fault model (figure 345a), and a synthetic VSP with the typical break in the upgoing primary (figure 345b).

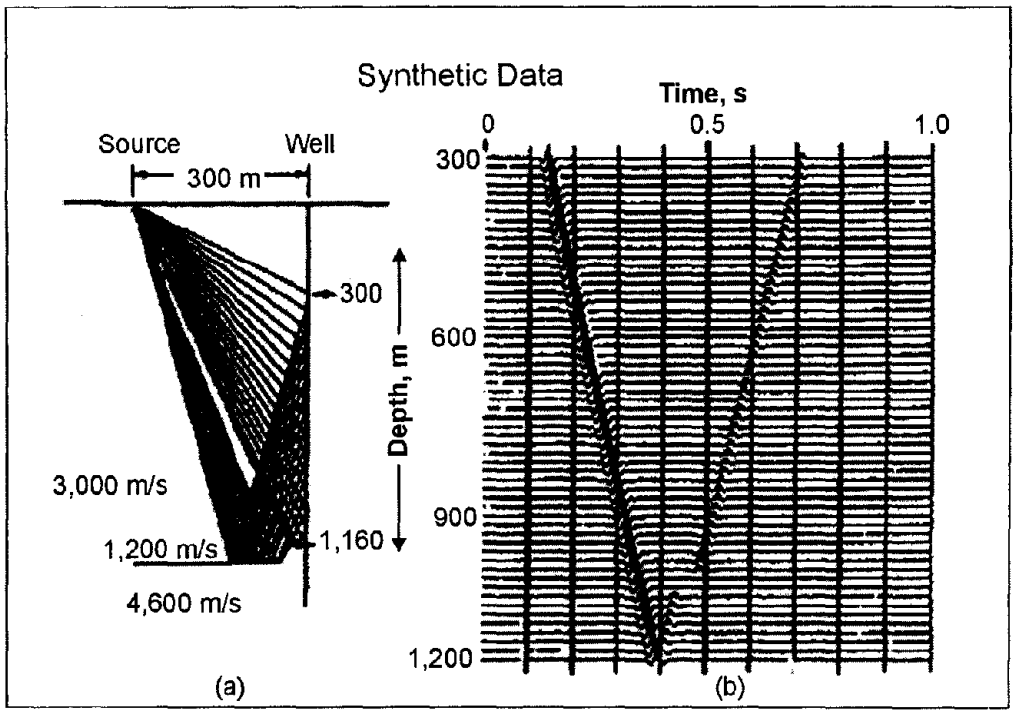

Figure 345. Model of a fault structure.

Multiple offset or walkaway VSP's were developed to supply high-resolution seismic structural detail or provide seismic data in areas where interference from shallow layers all but renders surface seismic profiling useless. Notable improvements have been observed in some no-record seismic areas. Lateral extension of structural and stratigraphic detail around the well bore is made possible with this type of survey.

VSP's can be obtained around each well in a multiwell project to help map the geology. Careful correlation can be accomplished with existing 2-D and 3-D surface seismic profiling. Finally, the entire sequence of formations of interest may be mapped in terms of porosity, saturation, permeability, etc., by carefully calibrating VSP data with well log data.

Downhole Sources

Downhole sources such as explosives, implosive devices, airguns, and sparkers are economically desirable, and a great deal of research has gone into making them successful. Downhole sources suffer from a bad reputation concerning well bore damage. Data from a number of experiments show that borehole-generated events associated with downhole sources tend to overwhelm data quality to the point of turning this technology into an interpretational problem.

Downhole Receiver Arrays

Downhole receiver arrays of only a few geophone receiver elements have been used successfully and have greatly reduced acquisition costs in borehole seismics. Downhole hydrophone arrays have been used commercially to measure permafrost thickness. An

interesting application of hydrophone arrays was the successful measurement of tube waves generated by permeable fracture zones in granite.

10.3.2 Velocity Surveys

As discussed previously, velocity surveys in well bores are a well-established technology in the geophysical industry. An accurate measurement of the travel time and depth location, in combination with a knowledge of travel path, will provide the geophysicist with the necessary velocities to convert the seismic time sections to depth and also to migrate the data properly.

Sonic logs provide these data also; however, sonic logs are usually run only to the surface casing. Tying the information from the sonic log to the surface requires a velocity or check shot survey. Usually, enough levels are obtained in the well bore to provide sufficient detail to forego the data obtained from the sonic log.

Some problems that can affect sonic log data accuracy were discussed briefly in the section on overview of borehole seismic techniques. Seismic travel times are considered accurate within the limitations of sample rate and first break picking accuracy, and sonic times must be adjusted to fit seismic data.

Data Acquisition

Sources for data acquisition must be carefully chosen for the given desired depth penetration. These sources may include explosives, airguns or water guns in containers, or vibrators. Source and acquisition parameters often tend to match those used during acquisition of surface seismic data. Receivers are downhole geophones. A more detailed discussion of source and receiver characteristics will follow in the section on vertical seismic profiling.

In locating the source, an attempt is made to obtain a travel path that minimizes refractive bending through the formations. For the case of horizontal layering and a vertical well, that would imply placing the source close to the well bore. For a deviated well, the source is frequently moved above the receiver in the well. This, of course, requires information from a well deviation survey prior to the check shot survey. Dipping layers can also introduce sizeable changes in travel time because of refraction along bed boundaries.

When working with surface sources such as vibrators, it is advisable to obtain some shallow levels in order to get some information on velocities in the weathered zone. The limitation in this case is the source location, since the drilling platform itself may take up a sizeable space. In addition, refracted arrivals from the top of the subweathering zone or casing may interfere with direct arrival through weathering.

When working with explosives, an uphole high-velocity geophone is needed to obtain the uphole times. A proper shot depth geophone is needed to obtain the uphole times. Proper shot depth with the uphole time can provide the information on weathering velocities. Shot holes are generally located some distance from the well bore to prevent well bore damage. Therefore, in this case, shallow levels in the borehole may not add much to the survey.

Concerning the placement of geophones in the borehole, the geologists often pick recording depths corresponding to formation tops obtained from logs. If acoustic boundaries of sufficient contrast are in that vicinity, interference between direct and reflected arrivals may lead to errors in first arrival times. Better receiver locations can sometimes be picked below the horizon of interest from existing sonic logs. Another effect may include the gradual polarity reversal of the first break

If receiver spacing is too close, there may be errors in computed interval velocities. In this case, the picking of the first break is rarely more accurate than 1 ms. With a receiver spacing of, for example, 30 m and a velocity of 3,000 m/s, a 1-ms error would amount to a 10% error in the computation of velocities.

Data Processing

When converting travel times to vertical travel times, a straight-line path is normally assumed, as shown in figure 346. Refinement of the results can be obtained by modeling and using the initial straight ray path as a first guess. For a vertical well, the horizontal distance from the source to the well and the vertical distance from the source to the geophone in the well are used. For the deviated well, the horizontal distance from the energy source to the geophone is used in addition to the vertical distance. The azimuth of the energy source is required when corrections for deviations are required. For offset or walk-away shooting, where the source is moved, the coordinates must be known for every shot.

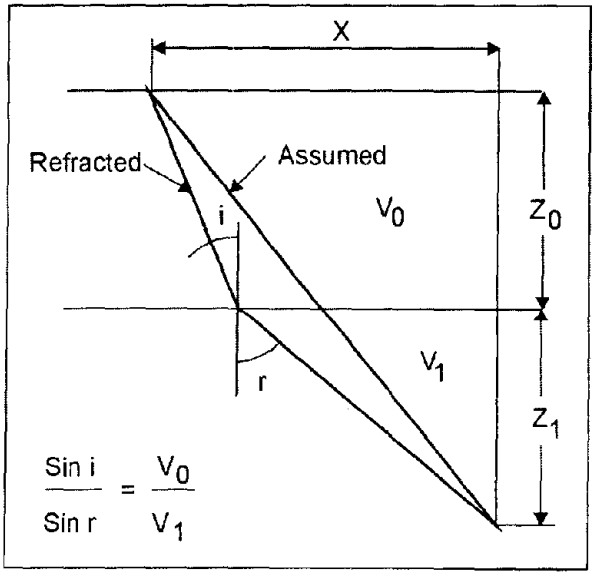

Figure 346. Travel path used for converting total travel time to vertical travel time.

All computations are corrected to the seismic reference datum (SRD). These corrections are summarized in figure 347. Finally, the corrected computations are displayed in the familiar time-depth plot shown in figure 348. This graph also provides an opportunity for quality control. Points deviating greatly from the trend may require a more detailed evaluation.

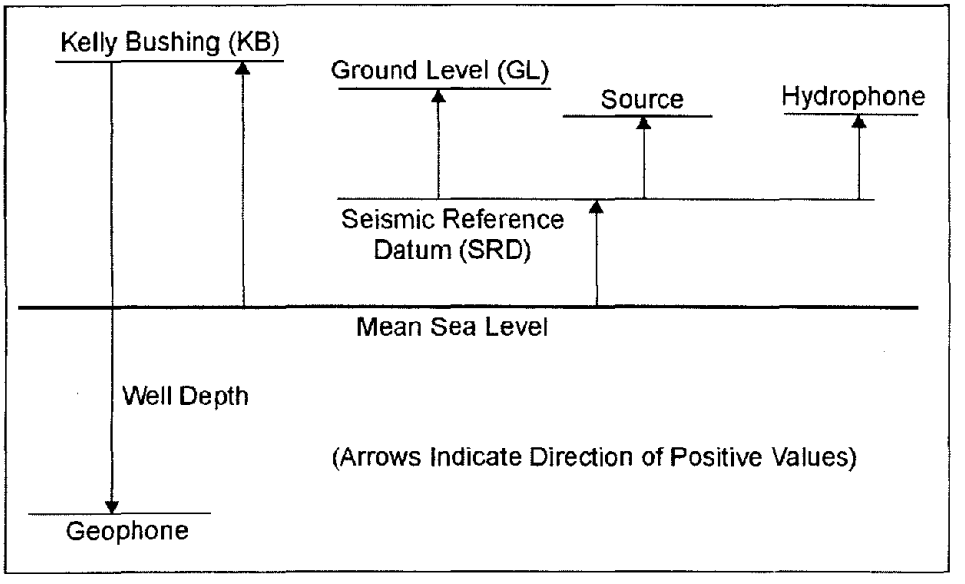

Figure 347. Summary of possible corrections to tie velocity survey to surface seismic data.

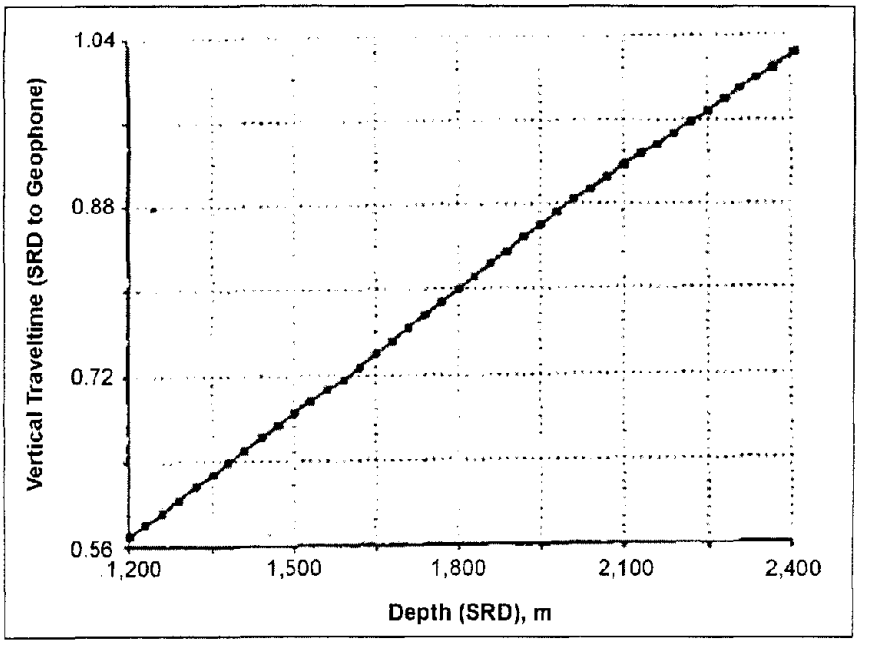

Figure 348. Vertical time depth plot corrected to Seismic Reference Datum.

Results of the survey or check shot survey are used to tie time to depth and calculate average, interval, and RMS velocities (see figure 349). These velocities are used to study normal moveout (NMO) in data migration and are often used to correct sonic logs prior to the computation of a synthetic seismogram.

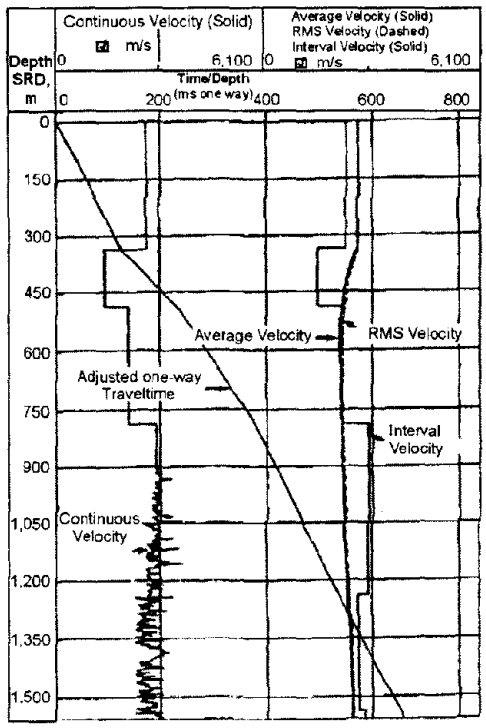

Figure 349. Example of final display from velocity survey with sonic log.

10.3.3 Vertical Incidence VSP

Vertical seismic profiling has been one of the more rapidly developing technologies in geophysics in recent years. It is perhaps surprising that the information following the first breaks on the seismic trace routinely recorded in velocity surveys was simply disregarded. Acquisition in the field for VSP's consisted then merely of the addition of a sufficient number of geophone depth levels in a routine velocity survey. The additional rig time was perhaps the major deterrent to the widespread use of VSP's in the industry.

The geophysicist had also settled for the use of check shot surveys and synthetic seismograms to provide him with a more or less accurate nexus between surface seismic profiling and the well bore. This meant accepting all the assumptions of plane acoustic waves striking a horizontally layered medium at normal incidence to obtain a model of a seismic trace arriving at the surface. Another shortcoming was the lack of knowledge of the makeup of the seismic wavelet.

The VSP permits the actual measurement of seismic energy as a function of depth. The surface geophone measures only the upgoing wave. The downhole geophone measures the downgoing wave field in addition to the upgoing wave field. Effects of reflection, transmission, multiples, and attenuation can be traced as a function of depth. The increase in resolution resulting from retention of higher frequencies (due to the decrease in travel path to the downhole geophone compared to a surface geophone) permits more confident measurement of lithological effects than ever before from surface seismic profiling. The advent of shear-wave seismic technology has brought with it the difficulty of resolving both

P- and S-waves to the same lithologic boundary. Again, the VSP can provide an accurate tie between these two events. Finally, the VSP is one of the more effective means to provide quality control for both surface seismic profiling and the generation of a reasonable synthetic seismogram. As the geophysicist gains experience with VSP acquisition, processing, and interpretation, this relatively new technology will become an integral part of exploration technology.

Principles

Simultaneous recording of both upgoing and downgoing wave fields by the downhole geophone requires some discussion of the principles involved. In figure 350(b), examples of some possible upgoing and downgoing events are displayed. For convenience and clarity, upgoing events are to the left of the well, downgoing are to the right. Furthermore, only two geophone locations are shown, again separated for convenience in illustrating the concept. In reality, more events than those shown are possible. Figure 350(a) is the simple impedance model for this hypothetical well. Figure 350(c) shows the VSP generated from this model as a function of the depth of the well versus one-way time.

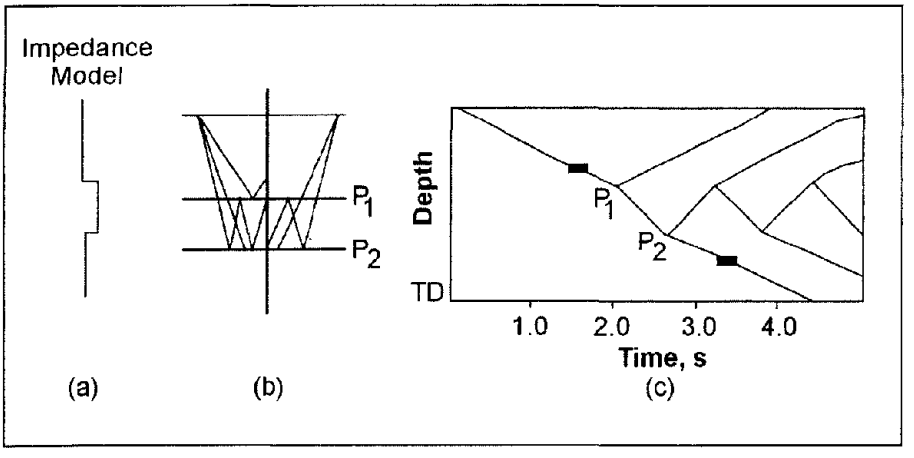

Figure 350. Basic concept of upgoing and downgoing wave fields; (a) impedance model, (b) ray geometry, (c) Vertical Seismic Profiling.

The upgoing events shown consist of two simple primary reflections and one multiple. The downgoing events shown consist of the direct arrival and one downgoing multiple. In Figure 350(c), the first arrivals are on the left-most line increasing in time with depth; i.e., from upper left to lower right. Changes in slope on this line indicate changes in velocity in the subsurface. Primary upgoing events (P1, P2 in figure 350(b)) intersect this line of first arrivals and proceed toward the upper right on the graph.

In zero-offset VSP's, the primary events are symmetric to the first arrivals, and together with the first arrivals, have typically a "V" shape. Primary reflection P1 illustrates the time-depth tie necessary for correlation.

The diagram shows the important fact that upward-traveling multiple events cease as soon as the geophone is located below the last reflector involved in its generation. The primary

reflection and all the multiples in its tail have their last bounce on that reflector; thus, when the geophone is below that reflector, primary and upgoing multiple reflections in the tail can no longer be recorded. This multiple, or reverberant, is henceforth only present in the downgoing wave below this point. Upgoing events that terminate within the data permit the recognition of the origin of a multiple.

Figure 351 shows a real VSP with data corrected for amplitude losses. The traces are arranged with depth increasing from top to bottom and time increasing to the right; thus, longer travel times to the first arrival are seen with increasing depth. One should note the sparsity of strong upgoing events and the usual predominance of downgoing multiple events from near-surface highly reverberant systems. When lowering the geophone, a downgoing multiple event will be delayed by the same additional amount as the primary event. As a result, in the case of horizontal layering, the whole family of multiples follows but remains parallel to the first arrival alignment. This fact will subsequently be exploited in the processing of the vertical incidence VSP. The first arrivals then draw the time-depth curve. As the geophone moves farther from the source, it moves closer to the reflector. The additional delay from source to receiver, therefore, is equivalent to an identical loss in travel time from reflector to receiver in horizontal layering. As a result, reflected arrivals slope in the opposite direction from first arrivals.

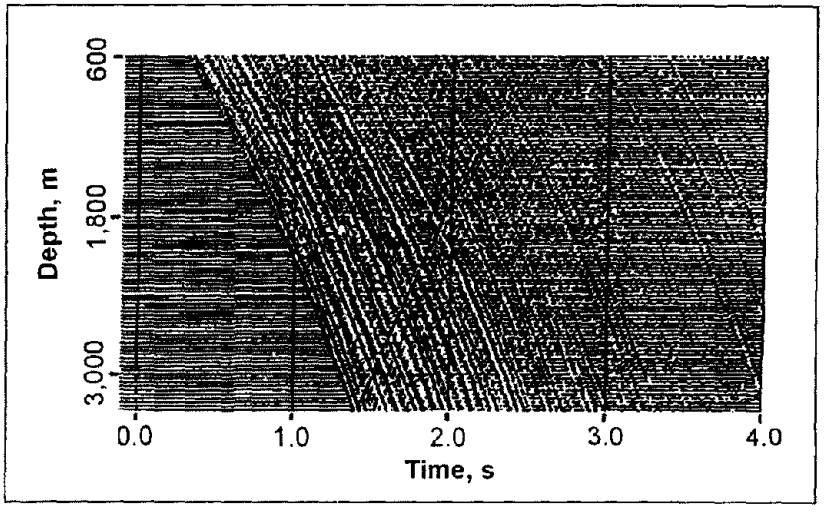

Figure 351. Example of a Vertical Seismic Profiling recording in one-way time with gain correction applied.

Synthetic VSP's

The synthetic VSP is rapidly becoming a valuable aid in studying the behavior of upgoing and downgoing wave fields with acoustic impedances obtained from borehole logging. Whereas the synthetic seismogram models a layered earth as seen from the surface, the synthetic VSP is a study of seismic events as a function of depth. It also allows the interpreter of VSP's to gain a better understanding of the complexities of interacting wave fields and gives more confidence in interpretations.

In calculating synthetic VSP's, one should incorporate the various multiple events. Upward-traveling multiples are reflected an odd number of times, downward-traveling multiples are reflected an even number of times (figure 350). For upward-traveling multiples, a so-called first- order multiple would have been reflected three times, a second order multiple five times, etc. By analogy, a first-order multiple for downgoing waves has been reflected twice, etc. (see figure 350).

For a synthetic VSP, the earth model is divided into equal travel time layers. The total seismic response for the layered system can be computed from the individual contributions of upgoing and downgoing waves at the individual interfaces for all the layers in the model. Multiples up to a given order can be included with overall attenuation as a function of reflection losses. The proper choice of input wavelet again becomes important if one attempts to match a synthetic with a real VSP. It is noted that the real VSP may be contaminated by random and coherent noise, difficult to reproduce with a synthetic. In order to illustrate the principles and the effects illustrated above, a simple model and the synthetic VSP calculated from it are shown in figure 352 (Wyatt, 1981). The velocity contrasts in the model are rather large to accentuate the effects discussed above. Velocities are seen to range from 1,500 to 6,100 m/s. Density was held constant.

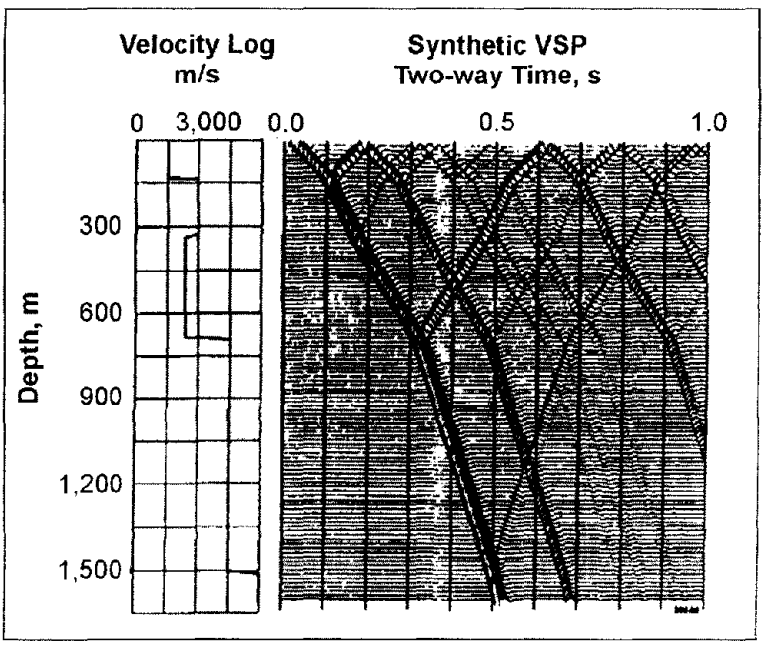

Figure 352. Simple synthetic Vertical Seismic Profiling illustrating effects of multiples.

Real VSP's rarely show multiple events that clearly. The first arrival slopes in this model show the velocity changes clearly. Amplitudes of primary events give a good indication of the impedance contrast at the boundaries. Amplitudes also show how a shallow reverberant system gives rise to many strong multiples. The origin of multiples is also clearly visible on this synthetic VSP. An excellent example of a comparison between a synthetic and a real VSP is shown in figure 353. Coherent noise interference for the example is seen between 1676 and 1828 m on the real VSP. Differences in primary and multiple amplitudes are also

very much apparent. Synthetics then become a valuable aid (but not a replacement) for measuring true waveforms in the earth.

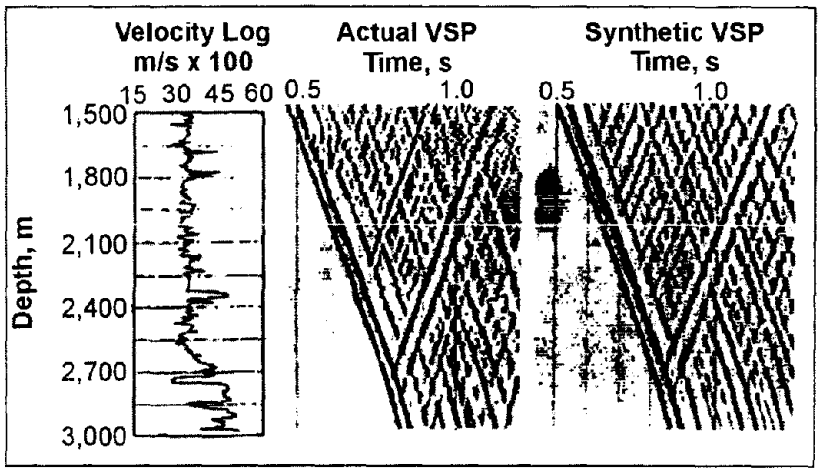

Figure 353. Comparison of real and synthetic Vertical Seismic Profiles.

Survey sources and equipment.

Selecting a source for a VSP survey is largely a function of what was used in obtaining surface seismic data. For improved matching of VSP and surface seismic data, the same sources are desirable for both surveys. To date the majority of seismic data are collected with vibrators, airguns, and explosives. However, a number of other devices have appeared on the market and some familiarity with signal strengths and source characteristics is desirable. A great deal of care must go into the choice of sensors and recording equipment. In VSP work, demands on recording equipment and the number of sensors employed are much smaller than in surface seismic operations. Recording equipment may have as few as two channels for single-axis tools. Downhole sensors may have only a single geophone per axis with three-axis tools. Downhole geophone tools require a clamping mechanism. Data for VSP's and check shots have been collected both with geophones and hydrophones in the downhole environment for specific applications.

State-of-the-Art Technology

State-of-the-art geophones may be used in downhole seismic data acquisition. A variety of choices are available in the marketplace. As a starting point in downhole tool evaluation, the geophysicist should know the amplitude and phase response of each type of geophone used in the tool. This is of increased importance when considering the differing response characteristics of vertical and horizontal geophones used in the three-axis tools.

Additional complications are introduced by geophone-to-ground or formation coupling. Seismic phase and amplitude are highly distorted upon approaching resonant frequencies. The useable seismic frequency band must then remain well below the frequency peaks introduced by coupling to the formation. These formation-coupling effects do exist in the borehole. Here the geophone becomes part of the larger downhole tool, which, in combination with the formation, can give rise to formation coupling resonances. In practice,

this is mostly experienced with horizontally oriented geophones. With presently available commercial tool designs, coupling resonances have been observed to fall into a frequency range as low as 18 to 30 Hz.

Borehole seismic operations

For borehole seismic operations, conventional surface seismic systems are more than adequate for most applications. The requirement of only a few channels simplifies the field acquisition. Adjustable fixed downhole gain is most certainly desirable to prevent overdriving of the surface amplifiers by direct arrival.

With continued interest in shear-wave data from three-axis VSP's and large S-wave sources, shear-wave attenuation rates amount to twice the decibel loss of that experienced by compressional waves. Adding attenuation losses from spherical divergence, scattering, and transmission losses would quickly tax the dynamic range of most recording equipment except for low frequencies.

Planning

It has become apparent from the preceding sections that more than casual job planning is required to obtain good field data. A variety of additional field parameters are to be determined prior to venturing out into the field. Rig time and source expense often lead to a series of compromises concerning sources, and number of levels obtained in the well. Source offset may be a function of desirable noise suppression of tube waves. Shallow levels are often noisy.

Quality Control

Quality control must extend to the borehole environment. Poor tool coupling may lead to tool creep or slippage. Improved clamping pressure, or perhaps installation of clamping arms or a more suitable length for a given borehole, will usually solve creep and slippage problems with their attendant noise bursts. Slacking off the cable eliminates cable waves in addition to reducing surface noises traveling down the cable. Tool resonance associated with poor coupling at a given location is solved by moving the tool to a different location. Both caliper and sonic logs may become helpful in relocating the tool.

The effects of casing may lead to additional phenomena in VSP acquisition. Refracted casing arrivals may precede direct arrivals. Unbonded casing may lead to casing ring. Cased hole VSP's can be obtained after the rig has moved off the site. This leads to a sizable savings in rig time during acquisition.

The effect of tube waves in VSP recording is coherent noise. Tube waves can be generated by body waves impinging on the borehole or by surface waves crossing the borehole. Tube wave velocities typically arrive at velocities of about 1,450 m/s. There are a number of field approaches to reduce tube waves such as improved clamping. Another approach is source offset from the borehole shown in figure 354. Different sources give rise to sizeable differences in tube wave energy.

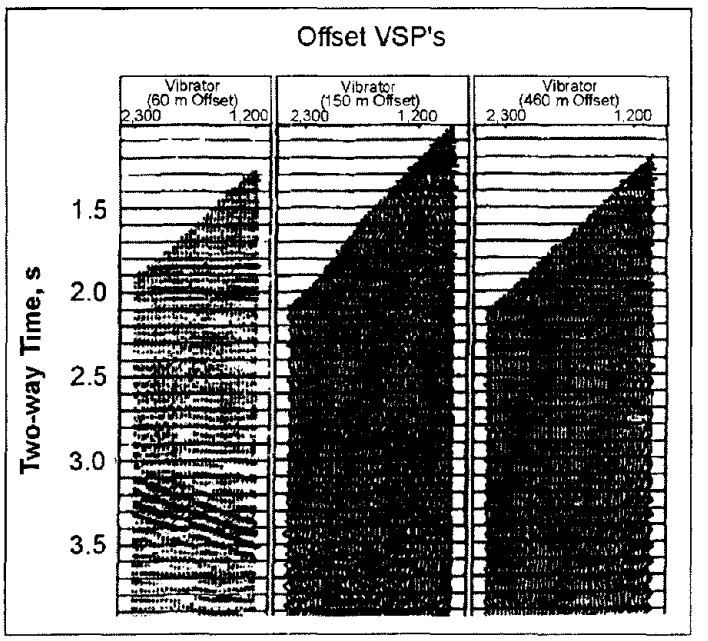

Figure 354. Tube wave amplitudes as a function of source offset.

With increasing experience in both data acquisition and processing, VSP can supply the additional refinements in seismic exploration that heretofore were elusive with surface methods. Data from the VSP can now help to solve a number of exploration problems and give the additional confidence needed to solve interpretational ambiguities.

In the past, direct correlation of synthetic seismograms with surface seismic profiling, however successful in some areas, led to a great number of unresolvable errors between well logs and surface seismic profiling. The synthetic seismogram, after all, is a theoretically calculated response based on some rather simple assumptions and, as applied to logging data, is subject to all the various restrictions discussed in earlier sections. With the VSP, one finally has a measured response of the Earth to the actual source wave field as it progresses with depth. A connection can now be established directly between seismic analysis and well bore information. The synthetic then becomes a means to model and study seismic signal interaction with the details of formations rather than serving explicitly as a link to the well. A synthetic log is then relegated to serve to some degree as quality control in the design of VSP data acquisition in conjunction with ray trace modeling and synthetic VSP computations. A well tie that serves both the geologist and the geophysicist will typically include the display of time-scaled logs, synthetic log, corridor or sum stack, the VSP itself, and the surface seismic section. In addition, a VSP converted to an equivalent section by summing corridors of traces along equal offset distances from the well bore may be included. A variety of displays can now aid the interpreter. Figure 355 shows the correlation from time-scaled logs to VSP to surface seismic. Shown from left to right are caliper, gamma ray, bulk density, sonic, reflectivity, synthetic log, corridor stack, VSP-CDP, and surface seismic data.

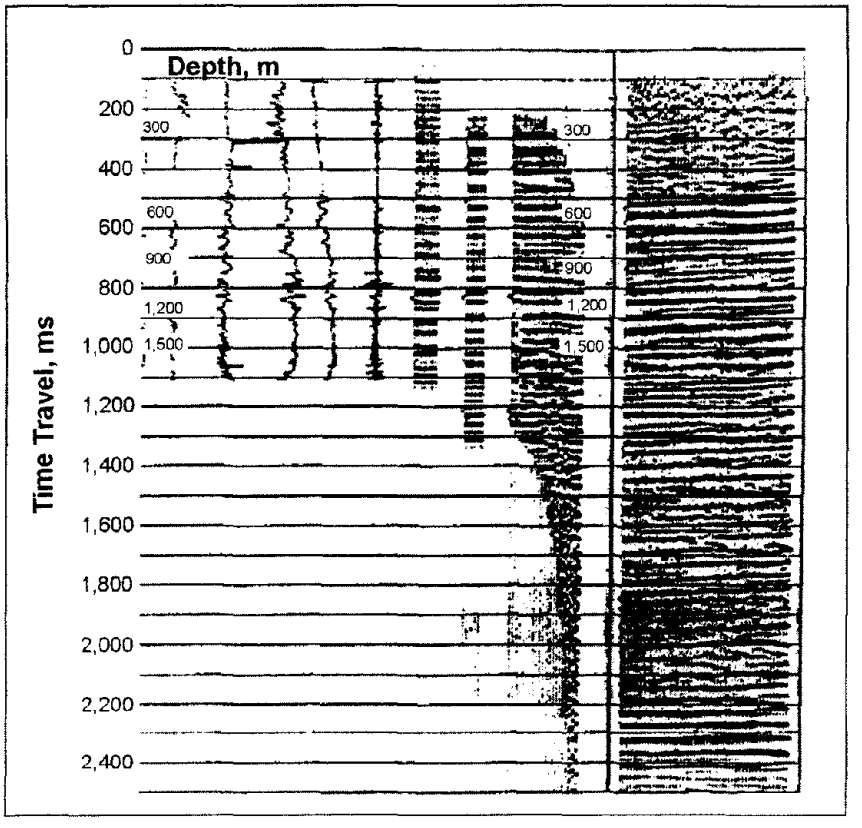

Figure 355. Correlation of time-scaled logs with Vertical Seismic Profile and surface seismic section. From left to right: caliper, gamma ray, bulk density, sonic, reflectivity, synthetic seismogram, sum stack of near traces of VSP-CDP, VSP-CDP, surface seismic section.

Conclusions and Examples

Many benefits can be obtained as noted in previous discussions on vertical VSP applications. Careful calibration of logs with VSP's and calibration of VSP's with surface seismic profiling can lead to better refinement in the interpretive process. Correlation of log-derived lithologic facies can be directly correlated with the results of seismic studies. To establish better communication between geologist, log analyst, and geophysicist, displays such as that shown in figure 356 were developed. Additional calibration with logs and seismic profiling can be achieved by comparing data from seismic events to those obtained from logs. Amplitudes of reflection coefficients and seismic events may be correlated with more confidence to porosity, pore fluids, saturation, and lithology after proper calibration with logs.

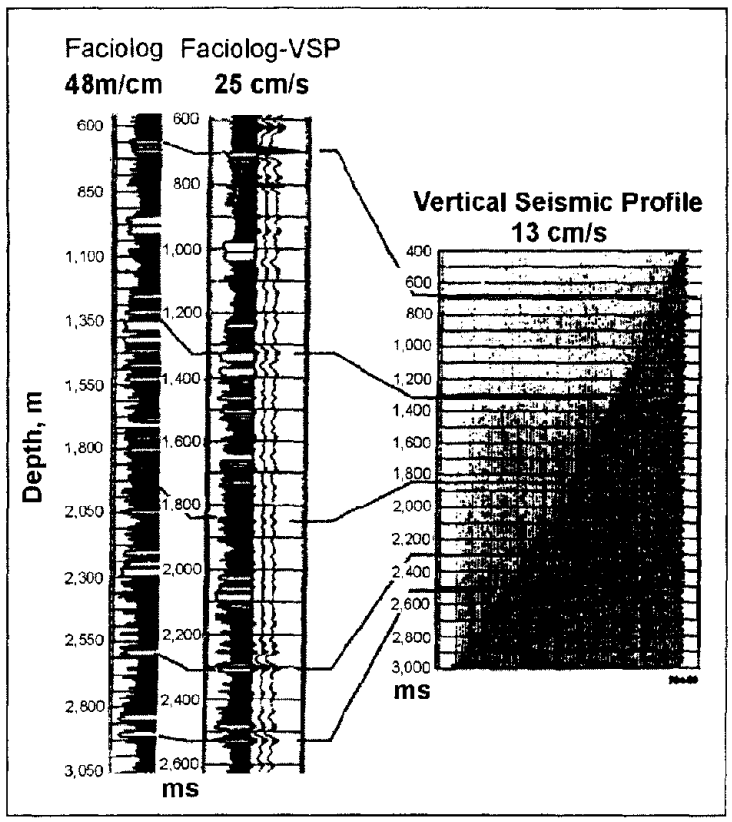

Figure 356. Example of tying a Vertical Seismic Profiling to a log derived from lithiofacies analysis.

An example of how a VSP is correlated with existing log information is shown in figure 357. In this example from the petroleum industry, the repeated sum stack trace is correlated to a time-scaled, log-derived section of the borehole showing lithology, porosity, and hydrocarbon saturation. The lithologic column indicates the volumetric percentage of the major constituent lithologies of the formation. Note that the peak of the seismic reflector yields an excellent fit with the top of the carbonate section (top of the reservoir). Hydrocarbon saturation, shown on the far left, is seen to increase at the top of the reservoir.

10.4 LOGGING TECHNIQUES AND TOOLS

10.4.1 Electrical Methods

10.4.1.1 Spontaneous Potential Log

Basic Concept

Spontaneous potential (SP) is one of the oldest logging techniques. It employs very simple equipment to produce a log whose interpretation may be quite complex, particularly in freshwater aquifers. This complexity has led to misuse and misinterpretation of spontaneous potential (SP) logs for groundwater applications. The spontaneous potential log (incorrectly called self potential) is a record of potentials or voltages that develop at the contacts between

shale or clay beds and a sand aquifer, where they are penetrated by a drill hole. The natural flow of current and the SP curve or log that would be produced under the salinity conditions given are shown in Figure 358.

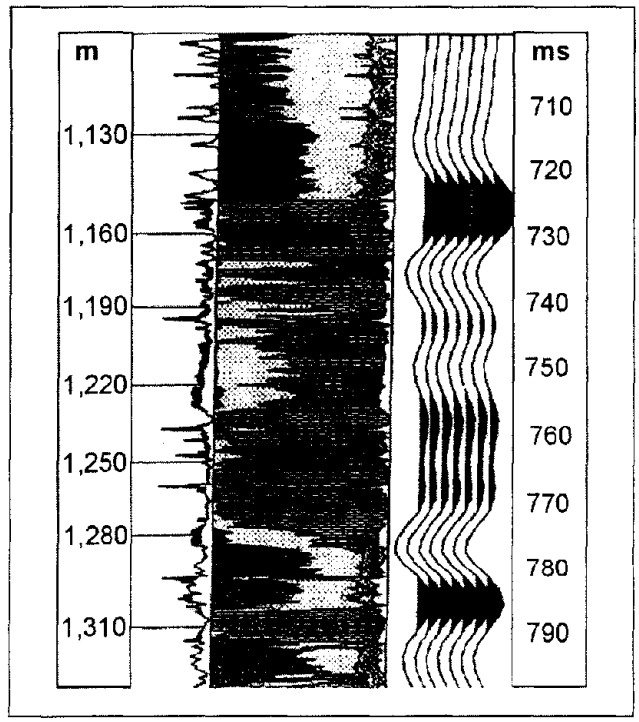

Figure 357. Tying the sum stack to log-derived volumetric analysis of lithology, porosity, and hydrocarbon saturation.

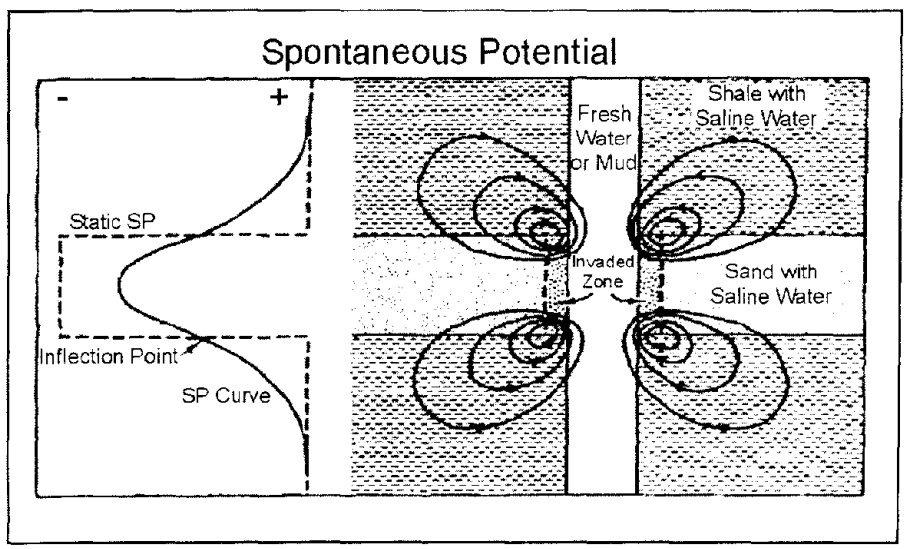

Figure 358. Flow of current at typical bed contacts and the resulting spontaneous potential curve and static values.

Data Acquisition

The SP measuring equipment consists of a lead or stainless steel electrode in the well connected through a millivolt meter or comparably sensitive recorder channel to a second electrode that is grounded at the surface (Figure 359). The SP electrode usually is incorporated in a probe that makes other types of electric logs simultaneously so it is usually recorded at no additional cost. Spontaneous potential is a function of the chemical activities of fluids in the borehole and adjacent rocks, the temperature, and the type and amount of clay present; it is not directly related to porosity and permeability. The chief sources of spontaneous potential in a drill hole are electrochemical, electrokinetic, or streaming potentials and redox effects. When the fluid column is fresher than the formation water, current flow and the SP log are as illustrated in Figure 358; if the fluid column is more saline than water in the aquifer, current flow and the log will be reversed. Streaming potentials are caused by the movement of an electrolyte through permeable media. In water wells, streaming potential may be significant at depth intervals where water is moving in or out of the hole. These permeable intervals frequently are indicated by rapid oscillations on an otherwise smooth curve. Spontaneous potential logs are recorded in millivolts per unit of chart paper or full scale on the recorder. Any type of accurate millivolt source may be connected across the SP electrodes to provide calibration or standardization at the well. The volume of investigation of an SP sonde is highly variable, because it depends on the resistivity and cross-sectional area of beds intersected by the borehole. Spontaneous potential logs are more affected by stray electrical currents and equipment problems than most other logs. These extraneous effects produce both noise and anomalous deflections on the logs. An increase in borehole diameter or depth of invasion decreases the magnitude of the SP recorded. Obviously, changes in depth of invasion with time will cause changes in periodic SP logs. Because the SP is largely a function of the relation between the salinity of the borehole fluid and the formation water, any changes in either will cause the log to change.

Data Interpretation

Spontaneous potential logs have been used widely in the petroleum industry for determining lithology, bed thickness, and the salinity of formation water. SP is one of the oldest types of logs, and is still a standard curve included in the left track of most electric logs. The chief limitation that has reduced the application of SP logs to groundwater studies has been the wide range of response characteristics in freshwater environments. As shown in Figure 358, if the borehole fluid is fresher than the native interstitial water, a negative SP occurs opposite sand beds; this is the so-called standard response typically found in oil wells. If the salinities are reversed, then the SP response also will be reversed, which will produce a positive SP opposite sand beds. Thus, the range of response possibilities is very large and includes zero SP (straight line), when the salinity of the borehole and interstitial fluids are the same. Lithologic contacts are located on SP logs at the point of curve inflection, where current density is maximum. When the response is typical, a line can be drawn through the positive SP-curve values recorded in shale beds, and a parallel line may be drawn through negative values that represent intervals of clean sand.

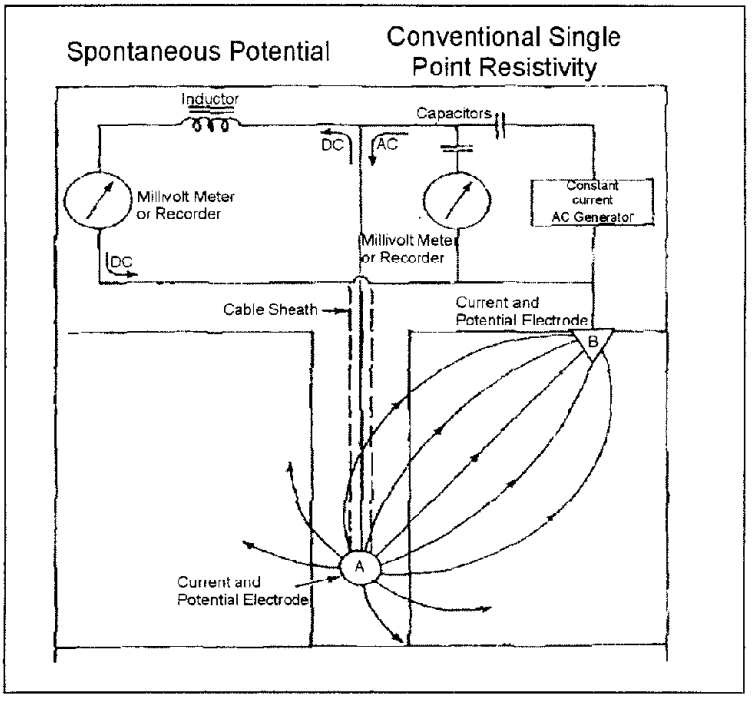

Figure 359. System used to make conventional single-point resistance spontaneous potential logs.

A typical response of an SP log in a shallow-water well, where the drilling mud was fresher than the water in the aquifers, is shown in Figure 360. The maximum positive SP deflections represent intervals of fine-grained material, mostly clay and silt; the maximum negative SP deflections represent coarser sediments. The gradational change from silty clay to fine sand near the bottom of the well is shown by a gradual change on the SP log. The similarity in the character of an SP log and a gamma log under the right salinity conditions also is shown in this figure. Under these conditions, the two types of logs can be used interchangeably for stratigraphic correlation between wells where either the gamma or the SP might not be available in some wells. The similarity between SP and gamma logs also can be used to identify wells where salinity relationships are different from those shown in Figure 360. Spontaneous-potential logs have been used widely for determining formation-water resistivity (R_w) in oil wells, but this application is limited in fresh groundwater systems. In sodium chloride type saline water, the following relation is used to calculate R_w:

$$SP = -K \log\left(\frac{R_m}{R_w}\right), \tag{80}$$

where

SP = log deflection in mV,
K = $60 + 0.133T$,
T = borehole temperature, in degrees Fahrenheit (metric and IP units are mixed for equation validity),
R_m = resistivity of borehole fluid, in Ohm-m,
R_w = resistivity of formation water, in ohm-m.

The SP deflection is read from a log at a thick sand bed; R_m is measured with a mud-cell or fluid-conductivity log. Temperature may be obtained from a log, but it also can be estimated, particularly if bottom-hole temperature is available. The unreliability of determining R_w of fresh water using the SP equation has been discussed by Patten and Bennett (1963) and Guyod (1966). Several conditions must be met if the equation is to be used for groundwater investigations. These conditions are not satisfied in most freshwater wells. Both borehole fluids and formation water need to be sodium chloride solutions. The borehole fluid needs to be quite fresh, with a much higher resistivity than the combined resistivity of the sand and shale; this requirement usually means that the formation or interstitial water must be quite saline. The shales need to be ideal ion-selective membranes, and the sands need to be relatively free of clay. No contribution can be made to the SP from such sources as streaming potential.

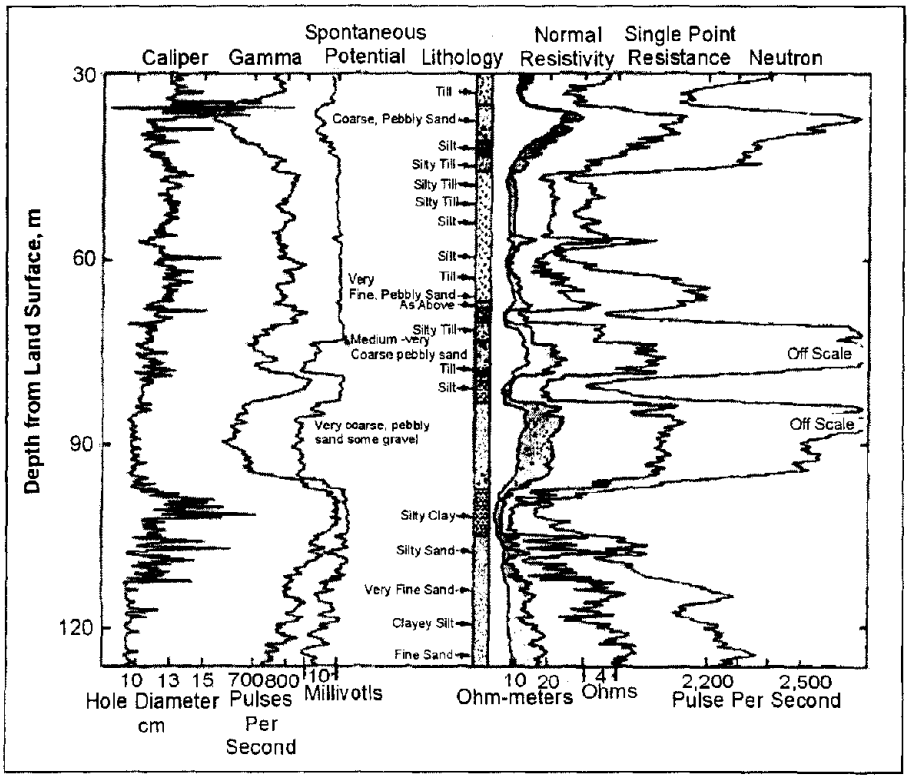

Figure 360. Caliper, gamma, spontaneous potential, normal resistivity, single point resistance and neutron logs compared to lithology; Kipling, Saskatchewan, Canda.

10.4.1.2 Single-Point Resistance Log

Basic Concept

The single-point resistance log has been one of the most widely used in non-petroleum logging in the past; it is still useful, in spite of the increased application of more sophisticated techniques. Single-point logs cannot be used for quantitative interpretation, but they are excellent for lithologic information. The equipment to make single-point logs usually is available on most small water-well loggers, but it is almost never available on the larger units

used for oil-well logging. The resistance of any medium depends not only on its composition, but also on the cross-sectional area and length of the path through that medium. Single-point resistance systems measure the resistance, in Ω, between an electrode in the well and an electrode at the surface or between two electrodes in the well. Because no provision exists for determining the length or cross-sectional area of the travel path of the current, the measurement is not an intrinsic characteristic of the material between the electrodes. Therefore, single-point resistance logs cannot be related quantitatively to porosity, or to the salinity of water in those pore spaces, even though these two parameters do control the flow of electric current.

Data Acquisition

A schematic diagram of the equipment used to make conventional single-point resistance and spontaneous potential logs is shown in Figure 359. The two curves can be recorded simultaneously if a two-channel recorder is available. The same ground and down-hole electrodes (A and B) are used for both logs. Each electrode serves as a current and as a potential sensing electrode for single-point logs. The single-point equipment on the right side of the figure actually measures a potential in volts (V) or mV, which can be converted to resistance by use of Ohm's law, because a constant current is maintained in the system. For the best single-point logs, the electrode in the well needs to have a relatively large diameter, with respect to the hole diameter, because the radius of investigation is a function of electrode diameter. The differential system, with both current and potential electrodes in the probe, which are separated by a thin insulating section, provides much higher resolution logs than the conventional system but is not available on many loggers. Scales on single-point resistance logs are calibrated in Ω per inch of span on the recorder. The volume of investigation of single-point resistance sonde is small, approximately 5 to 10 times the electrode diameter. Single-point logs are greatly affected by changes in well diameter, partly because of the relatively small volume of investigation.

Data Interpretation

Single-point resistance logs are useful for obtaining information on lithology; the interpretation is straightforward, with the exception of the extraneous effects described previously. Single-point logs have a significant advantage over multi-electrode logs; they do not exhibit reversals as a result of bed-thickness effects. Single-point logs deflect in the proper direction in response to the resistivity of materials adjacent to the electrode, regardless of bed thickness; thus, they have a very high vertical resolution. The response of both differential and conventional single-point logs to fractures is illustrated in figure 361. In this figure, at least one of the logging systems was not properly calibrated, because the scales differ by an order of magnitude. Hole enlargements shown on the caliper log are almost entirely caused by fractures in the crystalline rocks penetrated by this hole. The differential single-point log defines the fractures with much greater resolution than the log made with the conventional system.

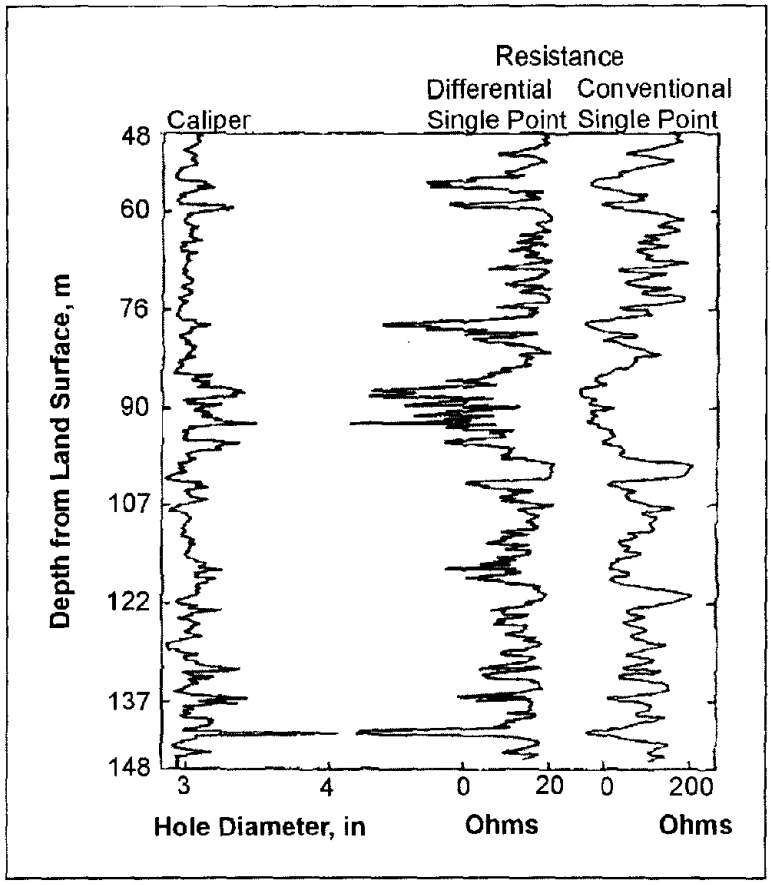

Figure 361. Caliper, differential and conventional single-point resistance logs in a well in fractured crystalline rocks.

10.4.1.3 Normal Resistivity Log

Basic Concept

Among the various multi-electrode resistivity-logging techniques, normal resistivity is probably the most widely used in groundwater hydrology, even though the long normal log has become rather obsolete in the oil industry. Normal-resistivity logs can be interpreted quantitatively when they are properly calibrated in terms of Ωm. Log measurements are converted to apparent resistivity, which may need to be corrected for mud resistivity, bed thickness, borehole diameter, mudcake, and invasion, to arrive at true resistivity. Charts for making these corrections are available in old logging manuals. Figure 362 is an example of one of these charts that is used to correct 40-cm (16-cm) in normal curves for borehole diameter and mud resistivity. The arrows on this chart show examples of corrections for borehole size and mud resistivity (R_m). If the resistivity from a 40-cm (16-in) normal curve divided by the mud resistivity is 50 in a 25-cm (10-in) borehole, the ratio will be 60 in an 20cm (8-in) borehole. If the apparent resistivity on a 40-cm (16-in) normal log is 60 Ωm and the R_m is 0.5 Ωm in a 23-cm (9-in) well, the ratio on the X-axis is 195. The corrected log value is 97.5 Ωm at formation temperature. Temperature corrections and conversion to conductivity and to equivalent sodium chloride concentrations can be made using figure 363.

To make corrections, the user should follow along isosalinity lines because only resistivity or conductivity change as a function of temperature, not ionic concentrations.

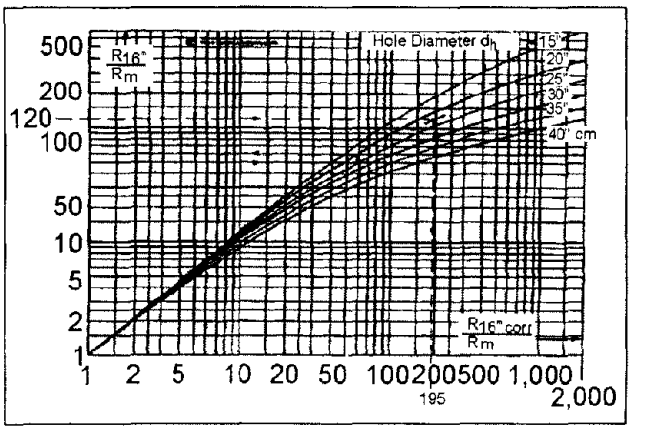

Figure 362. Borehole correction chart for 16-in normal resistivity log. (copyright permission granted by Schlumberger)

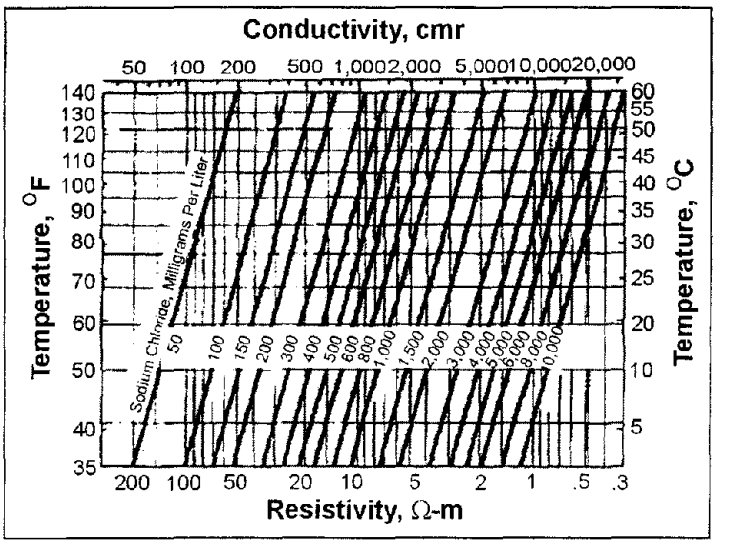

Figure 363. Electrically equivalent sodium chloride solution plotted as a function of conductivity or resistance and temperature.

Definition

By definition, resistivity is a function of the dimensions of the material being measured; therefore, it is an intrinsic property of that material. Resistivity is defined by the formula:

$$R = \frac{rS}{L}, \tag{81}$$

where

R = resitivity in Ωm,

r = resistance in Ω,

S = cross section in m^2,

L = length in m.

The principles of measuring resistivity are illustrated in figure 364. If 1 amp of current from a 10-V battery is passed through a 1-m^3 block of material, and the drop in potential is 10 V, the resistivity of that material is 10 Ωm. The current is passed between electrodes A and B, and the voltage drop is measured between potential electrodes M and N, which, in the example, are located 0.1 m apart-, so that 1 V is measured rather than 10 V. The current is maintained constant, so that the higher the resistivity between M and N, the greater the voltage drop will be. A commutated DC current is used to avoid polarization of the electrodes that would be caused by the use of direct current.

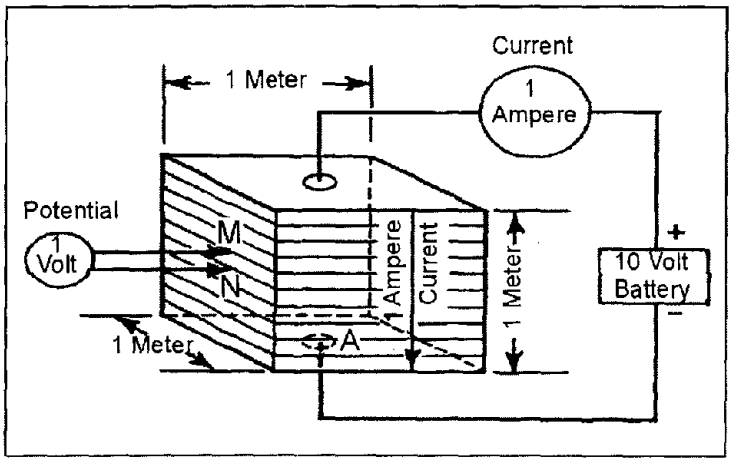

Figure 364. Principles of measuring resistivity in Ohm-meter. Example is 10 Ohm-meter.

Data Acquisition for Normal Resistivity Logs

AM spacing. For normal-resistivity logging, electrodes A and M are located in the well relatively close together, and electrodes B and N are distant from AM and from each other, as shown in figure 364. Electrode configuration may vary in equipment produced by different manufacturers. The electrode spacing, from which the normal curves derive their name, is the distance between A and M, and the depth reference is at the midpoint of this distance. The most common AM spacings are 40 and 162 cm (16 and 64 in); however, some loggers have other spacings available, such as 10, 20, 40 and 81 cm (4, 8, 16, and 32 in). The distance to the B electrode, which is usually on the cable, is approximately 15 m; it is separated from the AM pair by an insulated section of cable. The N electrode usually is located at the surface, but in some equipment, the locations of the B and N electrodes may be reversed. Constant current is maintained between an electrode at the bottom of the sonde and a remote-current electrode. The voltage for the long normal (162 cm (64 in)) and the short normal (40 cm (16 in)) is measured between a potential electrode for each, located on the sonde, and a remote potential electrode. The SP electrode is located between the short normal electrodes. The relative difference between the volumes of material investigated by

the two normal systems also is illustrated in figure 365. The volume of investigation of the normal resistivity devices is considered to be a sphere, with a radius approximately twice the AM spacing. This volume changes as a function of the resistivity, so that its size and shape are changing as the well is being logged.

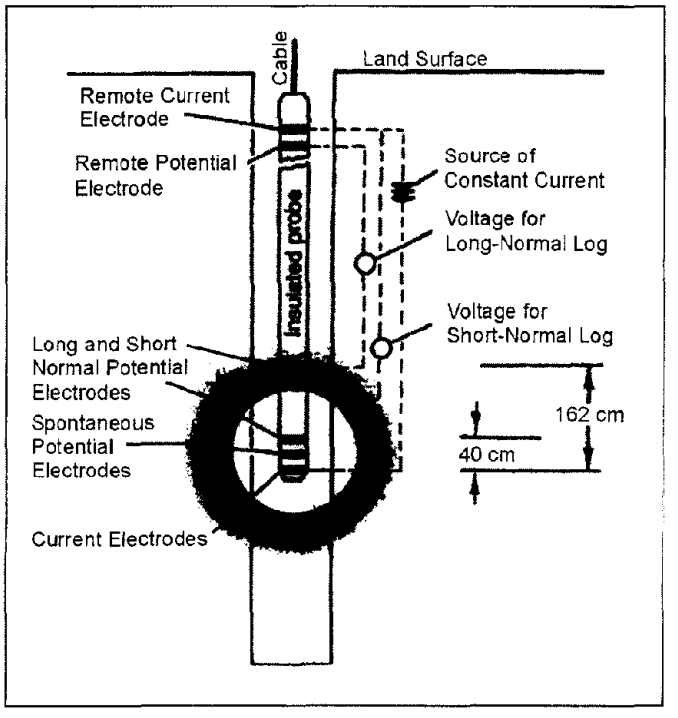

Figure 365. System used to make 40- and 162 cm (16- and 64-in) normal resistivity logs. Shaded areas indicate relative size volumes of investigation.

Depth of Invasion. Although the depth of invasion is a factor, short normal (40 cm (16 in or less)) devices are considered to investigate only the invaded zone, and long normal (162 cm (64 in)) devices are considered to investigate both the invaded zone and the zone where native formation water is found. These phenomena are illustrated in figure 360 . In this figure, the area between a 81 cm (32-in) curve on the left and a 10-cm (4-in) curve on the right is shaded. The longer spaced curve indicates a lower resistivity farther back in the aquifers than in the invaded zone near the borehole wall, which suggests that the formation water is relatively saline with respect to the borehole fluid.

Calibration. Normal-resistivity logging systems may be calibrated at the surface by placing fixed resistors between the electrodes. The formula used to calculate the resistor values to be substituted in the calibration network shown in figure 366 is given in Keys (1990).

Data Interpretation

Long normal response is affected significantly by bed thickness; this problem can make the logs quite difficult to interpret. The bed thickness effect is a function of electrode spacing, as illustrated in figure 367. The theoretical resistivity curve (solid line) and the actual log (dashed line) for a resistive bed, with a thickness six times the AM spacing, is shown in the

top part of the figure. Resistivity of the limestone is assumed to be six times that of the shale, which is of infinite thickness. With a bed thickness six times AM, the recorded resistivity approaches, but does not reach, the true resistivity (R_t); the bed is logged as being one AM spacing thinner than it actually is. The actual logged curve is a rounded version of the theoretical curve, in part because of the effects of the borehole. The log response when the bed thickness is equal to or less than the AM spacing is illustrated in the lower half of figure 367. The curve reverses, and the high-resistivity bed actually appears to have a lower value than the surrounding material. The log does not indicate the correct bed thickness, and high-resistivity anomalies occur both above and below the limestone. Although increasing the spacing to achieve a greater volume of investigation would be desirable, bed-thickness effects would reduce the usefulness of the logs except in very thick lithologic units.

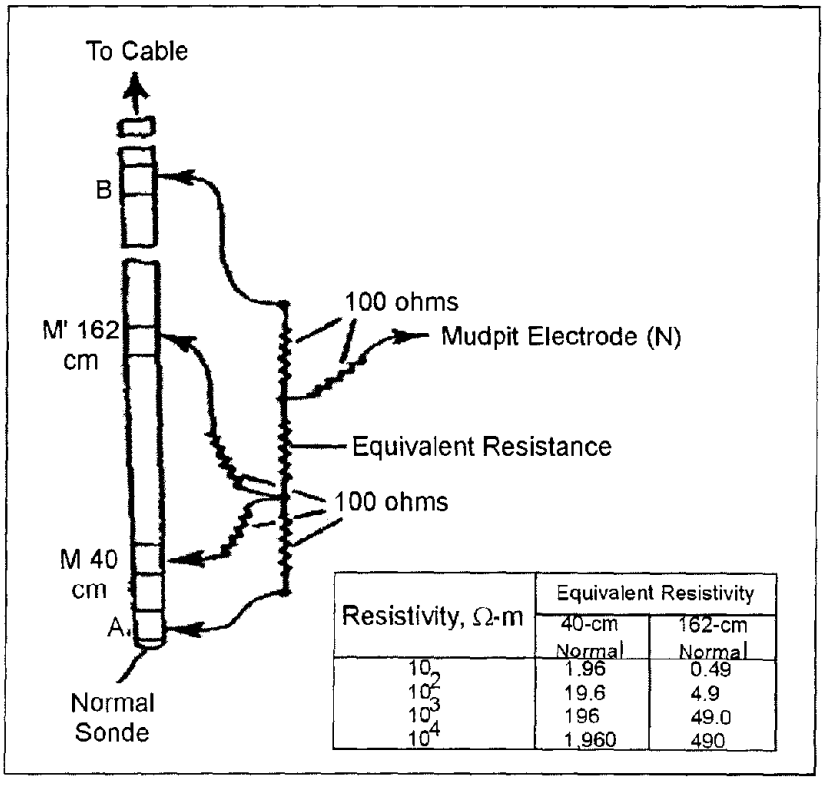

Resistivity, Ω-m	Equivalent Resistivity	
	40-cm Normal	162-cm Normal
10^2	1.96	0.49
10^2	19.6	4.9
10^3	196	49.0
10^4	1,960	490

Figure 366. System for calibrating normal resistivity equipment.

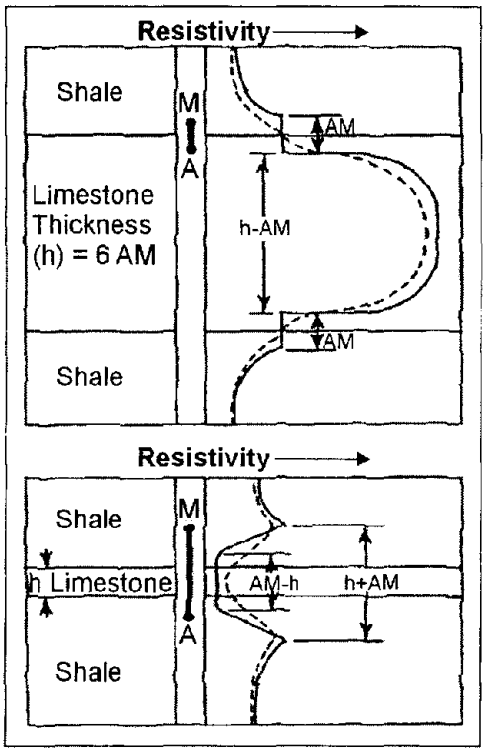

Figure 367. Relation of bed thickness to electrode spacing for normal devices at two thicknesses.

Applications

Water Quality. An important application of normal resistivity logs and other multi-electrode logs is to determine water quality. Normal logs measure apparent resistivity; if true resistivity is to be obtained from these logs, they must be corrected with the appropriate charts or departure curves. A summary of these techniques is found in "The Art of Ancient Log Analysis," compiled by the Society of Professional Well Log Analysts (1979). A practical method is based on establishing field-formation resistivity factors (F) for aquifers within a limited area, using electric logs and water analyses. After a consistent formation factor is established, the long normal curve, or any other resistivity log that provides a reasonably correct R_t can be used to calculate R_w from the relationship: $F = R_o/R_w$. Under these conditions, Ro, the resistivity of a rock 100% saturated with water, is assumed to approximate R_t, after the appropriate corrections have been made. Resistivities from logs can be converted to standard temperature using figure 362, and the factors listed in Keys (1990) can be used to convert water containing other ions to the electrically equivalent sodium chloride solution.

The formation resistivity factor (F) also defines the relation between porosity ($\emptyset$) and resistivity as follows: $F = a/\emptyset^m = R_o/R_w$, where m is the cementation exponent (Archie's formula). See Jorgensen (1989) for a more complete description of these relations. Using porosity derived from a neutron, gamma-gamma, or acoustic velocity log, and R_o from a deep investigating resistivity log, one can determine the resistivity of the formation water in granular sediments. The relation between resistivity from normal logs and the concentration of dissolved solids in groundwater is only valid if the porosity and clay content are relatively

uniform. The method does not apply to rocks with a high clay content or with randomly distributed solution openings or fractures. Surface conduction in clay also tends to reduce the resistivity measured. The resistivity logs in figure 360 were used to calculate the quality of the water in aquifers at the Kipling well site in Saskatchewan, Canada. The left trace of the two normal resistivity logs shown is the 81-cm (32-in) normal, which was used to calculate Rw for three of the shallower aquifers intersected. These aquifers are described as coarse, pebbly sand based on side-wall core samples. The 81-cm (32-in) normal was selected because many of the beds in this area are too thin for longer spacing. Wyllie (1963) describes a method for estimating F from the ratio Ri/Rm, where Ri is the resistivity of the invaded zone from a short normal log like the 10-cm (4-in), and Rm is the measured resistivity of the drilling mud. On the basis of the 10-cm (4-in) curve, F was estimated to be 2.5 for the upper aquifer and 1.8 for the lower two. The true resistivities for the three aquifers obtained from departure curves are 30, 20, and 17 Ω*m* at depths of 40, 76, and 90 m (130, 250, and 295 ft), respectively. A formation factor of 3.2 provided good agreement with water quality calculated from SP logs and from laboratory analyses. Using an F of 3.2, Rw was calculated to be 9.4, 6.2, and 5.3 Ω*m* at 4° C for the three aquifers. The drilling mud measured 13 Ω*m* at borehole temperature. The separation of the two normal curves and the SP log response substantiated the fact that the water in the aquifers was more saline than the drilling mud.

10.4.1.4 Lateral Resistivity Log

Lateral logs are made with four electrodes like the normal logs but with a different configuration of the electrodes. The potential electrodes M and N are located 0.8 m apart; the current electrode A is located 5.7 m above the center (*O*) of the MN spacing in the most common petroleum tool, and 1.8 m in tools used in groundwater. Lateral logs are designed to measure resistivity beyond the invaded zone, which is achieved by using a long electrode spacing. They have several limitations that have restricted their use in environmental and engineering applications. Best results are obtained when bed thickness is greater than twice AO, or more than 12 m for the standard spacing. Although correction charts are available, the logs are difficult to interpret. Anomalies are asymmetrical about a bed, and the amount of distortion is related to bed thickness and the effect of adjacent beds. For these reasons, the lateral log is not recommended for most engineering and environmental applications.

10.4.1.5 Focused Resistivity Log

Focused resistivity systems were designed to measure the resistivity of thin beds or high-resistivity rocks in wells containing highly conductive fluids. A number of different types of focused resistivity systems are used commercially such as "guard" or "laterolog." Focused or guard logs can provide high resolution and great penetration under conditions where other resistivity systems may fail. Focused-resistivity devices use guard electrodes above and below the current electrode to force the current to flow out into the rocks surrounding the well. The depth of investigation is considered to be about three times the length of one guard, so a 1.8 m guard should investigate material as far as 5.5 m from the borehole. The sheetlike current pattern of the focused devices increases the resolution and decreases the effect of adjacent beds in comparison with the normal devices.

Microfocused devices include all the focusing and measuring electrodes on a small pad; they have a depth of investigation of only several centimeters. Because the geometric factor, which is related to the electrode spacing, is difficult to calculate for focused devices, calibration usually is carried out in a test well or pit where resistivities are known. When this is done, the voltage recorded can be calibrated directly in terms of resistivity. Zero resistivity can be checked when the entire electrode assembly is within a steel-cased interval of a well that is filled with water.

Correction for bed thickness (h) is only required if h is less than the length of M, which is 6 in. on some common tools. Resistivities on guard logs will approach R_t, and corrections usually will not be required if the following conditions are met: $Rm/Rw < 5$, $Rt/Rm > 50$, and invasion is shallow. If these conditions are not met, correction charts and empirical equations are available for obtaining R_t (Pirson, 1963).

10.4.1.6 Microresistivity Log

A large number of microresistivity devices exist, but all employ short electrode spacing so that they have a shallow depth of investigation. They can be divided into two general groups: focused and non-focused. Both groups employ pads or some kind of contact electrodes to reduce the effect of the borehole fluid. Non-focused sondes are designed mainly to determine the presence or absence of mud cake, but they also can provide very high-resolution lithologic detail. Names used for these logs include microlog, minilog, contact log, and micro-survey log. Focused microresistivity devices also use small electrodes mounted on a rubber-covered pad forced to contact the wall of the hole hydraulically or with heavy spring pressure. The electrodes are a series of concentric rings less than 2.5 cm apart that function in a manner analogous to a laterolog system. The radius of investigation is from 76 to 127 mm, which provides excellent lithologic detail beyond the mudcake, but probably is still within the invaded zone.

10.4.1.7 Dipmeter Log

The dipmeter includes a variety of wall-contact microresistivity devices that are widely used in oil exploration to provide data on the strike and dip of bedding planes. The most advanced dipmeters employ four pads located 90° apart, oriented with respect to magnetic north by a magnetometer in the sonde. Older dipmeters used three pads 120° apart. The modern dipmeter provides a large amount of information from a complex tool, so it is an expensive log to run. Furthermore, because of the amount and complexity of the data, the maximum benefit is derived from computer analysis and plotting of the results. Interpretation is based on the correlation of resistivity anomalies detected by the individual arms, and the calculation of the true depth at which those anomalies occur. The log from a four-arm tool has four resistivity curves and two caliper traces, which are recorded between opposite arms, so that the ellipticity of the hole can be determined. The Formation Microscanner is related to the dipmeter. It uses arrays of small electrodes to provide oriented conductance images of segments of the borehole wall scanned by the pads. These images are similar to an acoustic televiewer log, but they do not include the entire borehole wall. The microscanner may be preferable in heavy muds or deviated holes.

Although strike and dip can be determined from the analog record at the well using a stereo net, complete analysis is only possible with a computer. A computer program can make all necessary orientation and depth corrections and search for correlation between curves with a selected search interval. Computer output usually consists of a graphic plot and a listing of results. The graphic plot displays the depth, true dip angle, and direction of dip by means of a symbol called a "tadpole" or an arrow. The angle and direction of the tool also is displayed. Linear polar plots and cylindrical plots of the data also are available. A printout that lists all the interpreted data points, as well as the quality of the correlation between curves, also is provided.

The dipmeter is a good source of information on the location and orientation of primary sedimentary structures over a wide variety of hole conditions. The acoustic televiewer can provide similar information under the proper conditions. The dipmeter also has been advertised widely as a fracture finder; however, it has some of the same limitations as the single-point resistance log when used for this purpose. Computer programs used to derive fracture locations and orientations from dipmeter logs are not as successful as those designed for bedding. Fractures usually are more irregular, with many intersections, and may have a wider range of dip angles within a short depth interval. The acoustic televiewer provides more accurate fracture information under most conditions.

10.4.1.8 Induction Logging

Basic Concept

Induction logging devices originally were designed to make resistivity measurements in oil-based drilling mud, where no conductive medium occurred between the tool and the formation. The basic induction logging system is shown in figure 368. A simple version of an induction probe contains two coils: one for transmitting an AC current, typically 20 to 40 kHz, into the surrounding rocks, and a second for receiving the returning signal. The transmitted AC generates a time-varying primary magnetic field, which induces a flow of eddy currents in conductive rocks penetrated by the drill hole. These eddy currents set up secondary magnetic fields, which induce a voltage in the receiving coil. That signal is amplified and converted to DC before being transmitted up the cable. Magnitude of the received current is proportional to the electrical conductivity of the rocks. Induction logs measure conductivity, which is the reciprocal of resistivity. Additional coils usually are included to focus the current in a manner similar to that used in guard systems. Induction devices provide resistivity measurements regardless of whether the fluid in the well is air, mud, or water, and excellent results are obtained through plastic casing. The measurement of conductivity usually is inverted to provide curves of both resistivity and conductivity. The unit of measurement for conductivity is usually milliSiemens per meter (mS/m), but millimhos per meter and micromhos per centimeter are also used. One mS/m is equal to 1,000 Ωm. Calibration is checked by suspending the sonde in air, where the humidity is low, in order to obtain a zero conductivity. A copper hoop is suspended around the sonde while it is in the air to simulate known resistivity values. The volume of investigation is a function of coil spacing, which varies among the sondes provided by different service companies. For most tools, the diameter of material investigated is 1.0 to 1.5 m; for some tools, the signal produced by material closer to the probe is minimized. Figure 369 shows the relative

response of a small-diameter, high-frequency induction tool as a function of distance from the borehole axis. These smaller diameter tools, used for monitoring in the environmental field, can measure resistivities up to 1,000 Ωm.

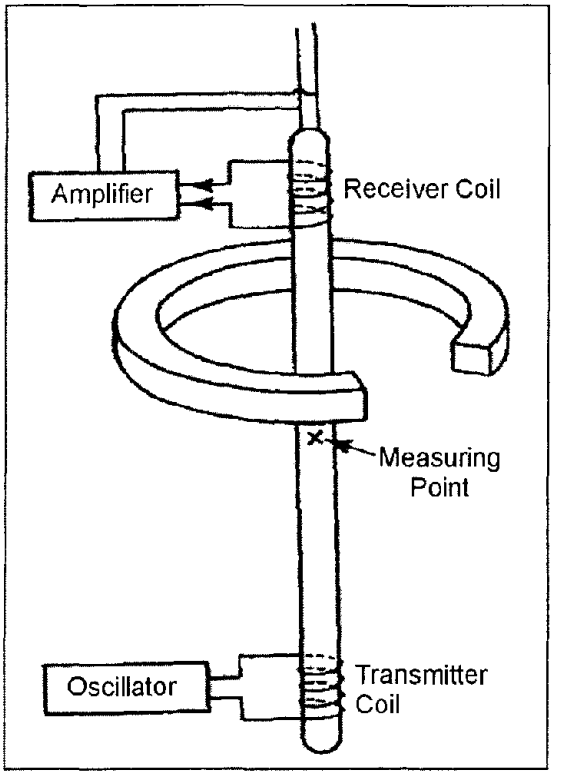

Figure 368. System used to make induction logs.

Data Interpretation

Induction logs are becoming widely used on environmental projects for monitoring saline contaminant plumes by logging small-diameter, PVC- or fiberglass-cased wells. They also provide high-resolution information on lithology through casing and are excellent for this purpose when combined with gamma logs. The response curve in figure 369 is for a tool that can be used in 5-cm diam (2-in) casing. Figure 370 is a comparison of induction resistivity logs in an open and cased well with a 40-cm (16-in) normal resistivity log. The open hole was 23 cm (9 in) and drilled with a mud rotary system. The well was completed to a depth of 56 m with 20-cm (4-in) Schedule 80 PVC casing and neat cement, bentonite seal, and gravel pack. Even in such a large- diameter well with varying completion materials, the differences in resistivity are not significant.

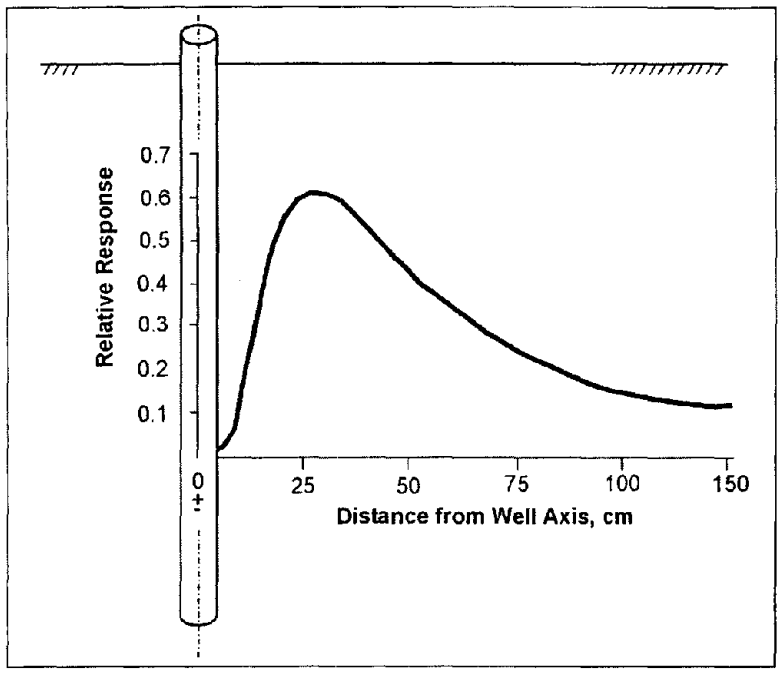

Figure 369. Relative response of an induction probe with radial distance from borehole axis. (copyright permission granted by Geonics Ltd.)

10.4.2 Nuclear Logging

Principles

Nuclear logging includes all techniques that either detect the presence of unstable isotopes, or that create such isotopes in the vicinity of a borehole. Nuclear logs are unique because the penetrating capability of the particles and photons permits their detection through casing and annular materials, and they can be used regardless of the type of fluid in the borehole. Nuclear-logging techniques described in this manual include gamma, gamma spectrometry, gamma-gamma, and several different kinds of neutron logs. Radioactivity is measured by converting the particles or photons to electronic pulses, which then can be counted and sorted as a function of their energy. The detection of radiation is based on ionization that is directly or indirectly produced in the medium through which it passes. Three types of detectors presently are used for nuclear logging: scintillation crystals, Geiger-Mueller tubes, and proportional counters. Scintillation detectors are laboratory-grown crystals that produce a flash of light or scintillation when traversed by radiation. The scintillations are amplified in a photomultiplier tube to which the crystal is optically coupled, and the output is a pulse with amplitude proportional to that of the impinging radiation. This output can be used for spectral logging. The pulse output from a photomultiplier tube IS small enough that it requires additional amplification before it can be transmitted to the surface and counted. The number of pulses detected in a given radiation field is approximately proportional to the volume of the crystal, so probe sensitivity can be varied by changing crystal size. Scintillation crystals probably are the most widely used detectors for nuclear well logging. Sodium-iodide crystals are used for gamma logging, and lithium-iodide crystals and Helium 3 gas-filled tubes are used for many types of neutron logs.

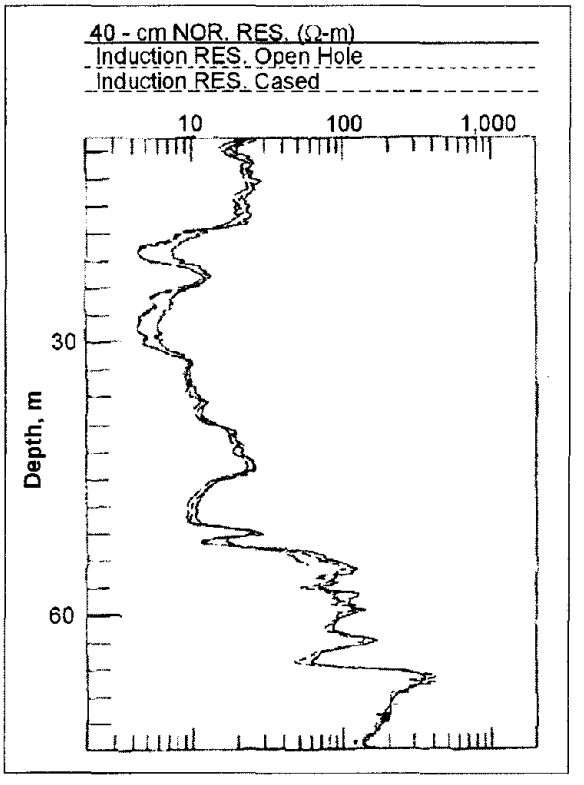

Figure 370. Comparison of open hole induction log with 16-in normal log and induction log made after casing was installed. (copyright permission granted by Colog, Inc.)

Data Interpretation

The statistical nature of radioactive decay must be considered when running or interpreting nuclear logs. Half-life is the amount of time required for one-half the atoms in a radioactive source to decay to a lower energy state. Half-life of different radioisotopes varies from fractions of a second to millions of years, and it has been accurately measured. In contrast, it is impossible to predict how many atoms will decay or gamma photons will be emitted within the short periods of time in the range of seconds that commonly are used for logging measurements. Photon emission follows a Poisson distribution; the standard deviation is equal to the square root of the number of disintegrations recorded. The accuracy of measurement is greater at high count rates and for a long measuring period. Time constant is an important adjustment on all analog nuclear-recording equipment. Time constant is the time, in seconds, over which the pulses are averaged. Time constant (t_c) is defined as the time for the recorded signal level to rise to 63% of the total increase that occurred, or to fall to 37% of the total decrease that occurred. The true value in any radiation field is approached after five time constants, if the probe is still in the same bed that long. If the probe is moving too fast, or if the time constant is too long in thin-bedded materials, the true value never will be recorded before the probe moves out of the layer of interest. The logging speed, count rate being measured, vertical resolution required, and equipment variations have a significant effect on the selection of time constant, so specific values cannot be recommended.

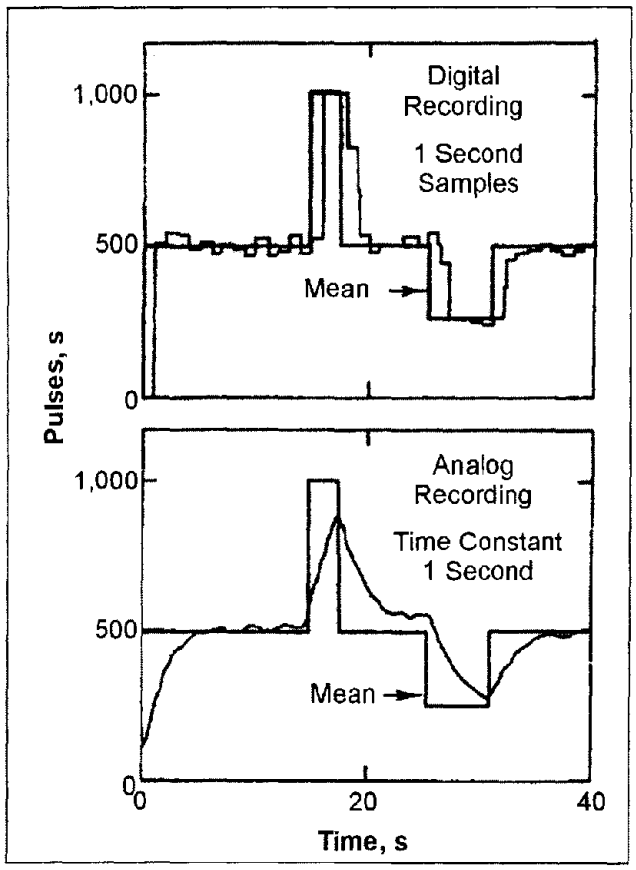

Figure 371. Comparison of a digital recording of a gamma signal with 1-s samples to an analog recording with 1-s time constant.

Analog versus digital recording. The difference between an analog recording with a time constant of 1 sec and a digital recording with a sample time of 1 sec is shown in figure 371. Digital recording is gradually replacing analog, but some systems that digitize at the surface still use a time constant circuit to drive an analog recorder. Average or mean radioactivity is shown as the heavier line in figure 371. Note that the digital system changes more rapidly because the time window used does not have a memory like the RC circuit used for time constant in analog measurements. Note also that the analog measurement did not reach the mean value for short time periods. Some commercial logs are recorded at a low sensitivity, long time constant, and high logging speed, so that real changes are small. This results in a smoother curve, and thin beds may not be detected. Bed thickness and lag are additional factors related to the speed at which nuclear logs are run. Lag (L), in feet, is defined as the distance the detector moves during one time constant:

$$L = \frac{St_c}{60}, \tag{82}$$

where

L = lag in feet,

S = logging speed in $\frac{\text{feet}}{\text{sec.}}$,

t_c = time constant, seconds.

Lithologic Contacts. The contacts between lithologic units on a nuclear log are shifted approximately the amount of lag. Furthermore, beds that are thinner than L are not defined. The general practice for locating lithologic contacts on nuclear logs is to place them at one-half of the maximum log amplitude for a given bed. Thus, if the average count rate for a gamma log in a sandstone was 100 pulses per second (PPS), and the average count rate for a shale was 200 PPS, the contact would be placed at 150 PPS, using the half-amplitude rule. The true depth of the contact would be deeper by the amount of lag. See figure 372 for an illustration of the relation of bed thickness, volume of investigation, and location of contacts for a neutron log. The principles are the same for other types of nuclear logs.

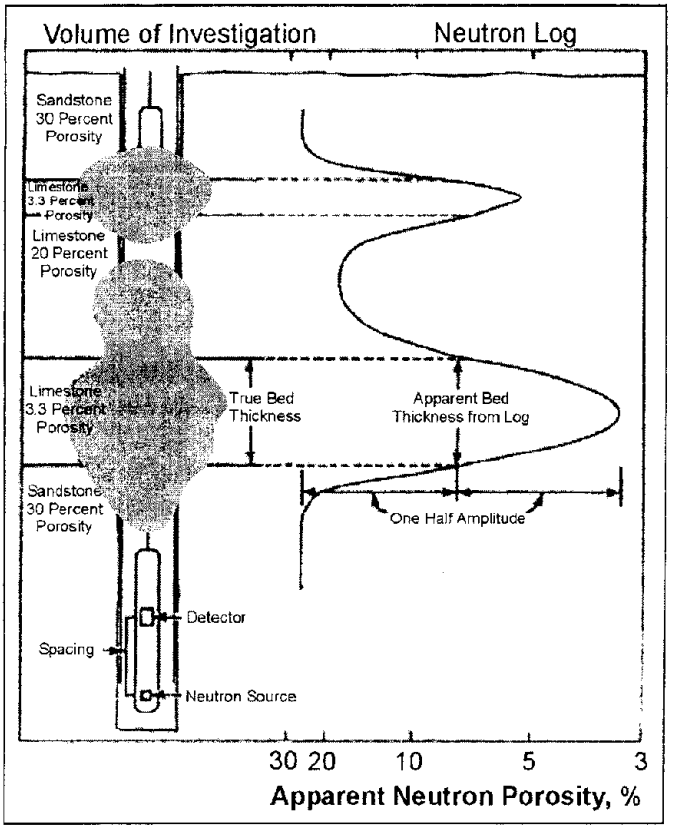

Figure 372. Theoretical response of a neutron probe to changes in porosity and bed thickness. The shaded area represents the volume of investigation at different probe positions.

Regulation. Use and transportation of radioactive materials is regulated by both Federal and State government agencies. Because of the numerous agencies involved and the frequent changes in regulations, specific information on the subject cannot be provided in this manual. A potential user must consult the appropriate government agency for regulations that apply to the specific type and area of use. The loss of most probes can be prevented if the proper

logging procedures are followed. Probes containing radioactive sources need to be the last to be run in an uncased well; they never are run if other probes encounter problems.

10.4.2.1 Gamma logging

Basic Concept

Gamma logs, also called gamma ray logs or natural-gamma logs, are the most widely used nuclear logs for most applications. The most common use is for identification of lithology and stratigraphic correlation, and for this reason, gamma detectors are often included in multi-parameter logging tools. Gamma logs provide a record of total gamma radiation detected in a borehole and are useful over a very wide range of borehole conditions. The petroleum industry has adopted the American Petroleum Institute (API) gamma ray unit as the standard for scales on gamma logs. The API gamma-ray unit is defined as 1/200 of the difference in deflection of a gamma log between an interval of very low activity in the calibration pit and the interval that contains the same relative concentrations of radioisotopes as an average shale, but approximately twice the total activity. The API gamma calibration pit is located at the University of Houston. The API values of field standards can be determined when that pit is used so that reference values are available when logging. The volume of material investigated by a gamma probe is related to the energy of the radiation measured, the density of the material through which that radiation must pass, and the design of the probe. Under most conditions, 90% of the gamma radiation detected probably originates from material within 150 to 300 mm of the borehole wall.

Data Interpretation

In rocks that are not contaminated by artificial radioisotopes, the most significant naturally occurring gamma-emitting radioisotopes are potassium-40 and daughter products of the uranium- and thorium-decay series. If gamma-emitting artificial radioisotopes have been introduced by man into the groundwater system, they will produce part of the radiation measured, but they cannot be identified unless gamma spectral-logging equipment is used. Average concentrations in 200 shale samples from different locations in the United States indicate that 19% of the radioactivity of shale comes from Potassium-40, 47% from the Uranium series, and 34% from the Thorium series, but these ratios can vary significantly. Only gamma spectral logging can provide the identification and relative concentrations of the natural and man-made radioisotopes that produce the total radioactivity measured by a gamma log. Borehole-gamma spectrometry has considerable application to the monitoring of radioactive waste migration, and it also can provide more diagnostic information on lithology, particularly the identification of clay minerals. Uranium and thorium are concentrated in clay by the processes of adsorption and ion exchange. Some clays are rich in potassium. Fine-grained detrital sediments that contain abundant clay tend to be more radioactive than quartz sands and carbonates, although numerous exceptions to this norm occur. Rocks can be characterized according to their usual gamma intensity, but knowledge of the local geology is needed to identify the numerous exceptions to the classification shown in figure 373. Coal, limestone, and dolomite usually are less radioactive than shale; however,

all these rocks can contain deposits of uranium and can be quite radioactive. Basic igneous rocks usually are less radioactive than silicic igneous rocks, but exceptions are known. Several reasons exist for the considerable variability in the radioactivity of rocks. Uranium and thorium are trace elements and are not important in the genesis of rocks. Uranium also is soluble in groundwater under some conditions, so solution, migration, and precipitation may cause redistribution at any time.

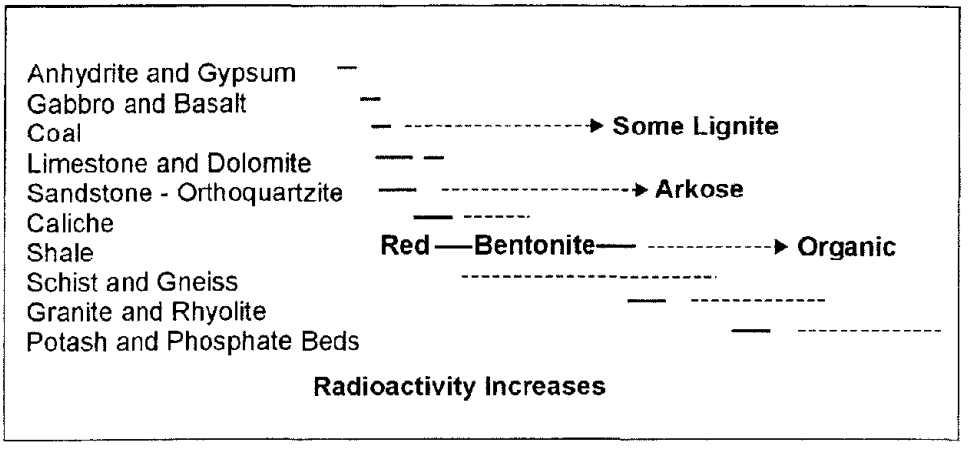

Figure 373. Relative radioactivity of common rocks.

Background Information. Because of frequent variations from the typical response of gamma logs to lithology, some background information on each new area is needed to reduce the possibility of errors in interpretation. Gamma logs are used for correlation of rock units; however, this approach can lead to significant errors without an understanding of their response within the area being studied. For example, gradual lateral change in grain size or increase in arkosic materials in a sandstone may change the response of gamma logs. In igneous rocks, gamma intensity is greater in the silicic rocks, such as granite, than in basic rocks, such as andesite. Orthoclase and biotite are two minerals that contain radioisotopes in igneous rocks; they can contribute to the radioactivity of sedimentary rocks if chemical decomposition has not been too great. Gamma logs are used widely in the petroleum industry to establish the clay or shale content of reservoir rocks. This application also is valid in groundwater studies where laboratory data support such a relation.

Amplitude. The amplitude of gamma-log deflections is changed by any borehole conditions that alter the density of the material through which the gamma photons must pass or the length of the travel path. Thus, casing and cement will reduce the recorded radiation, as will large-diameter wells. The correction factor for water in a borehole as compared to the same borehole filled with air is 1.024 for a 5.72-cm diameter (2.25-in) hole and 1.115, 1.205, and 1.296 for 11.4-, 16.5-, and 21.6-cm (4.5-, 6.5-, and 8.5-in) boreholes, respectively. Correction for steel casing wall thickness varies almost linearly from 1.141 for 0.159 cm (0.0625 in) thickness to 1.891 for 0.953 cm (0.375 in) thickness. The type of borehole fluid has a very minor effect, unless the hole is very large in diameter or the mud contains radioactive clay or sylvite.

Probe Position. The position of a probe in the borehole can have an effect on a gamma log. Most probes are naturally decentralized or running along the borehole wall because of

borehole deviation, but if the probe moves to a centralized position, an error is introduced. Changes in gamma-log response over a period of time are not rare. Changes in gamma response in 1 year that apparently were caused by migration of uranium daughter products along fractures have been reported (Keys, 1984).

10.4.2.2 Gamma-Gamma Logging

Basic Concept

Gamma-gamma logs, also called density logs, are records of the radiation from a gamma source in the probe after it is attenuated and backscattered in the borehole and surrounding rocks. The logs can be calibrated in terms of bulk density under the proper conditions and converted to porosity if grain and fluid density are known. Gamma-gamma probes contain a source of gamma radiation, usually cesium-137 in newer probes, and one or two gamma detectors. Detectors in a gamma-gamma probe are shielded from direct radiation from the source by heavy metal, often lead or a tungsten alloy. Single detector probes, termed "4 pi," are not focused and thus are more affected by borehole parameters. Modern gamma-gamma probes are decentralized and side-collimated with two detectors. Side collimation with heavy metal tends to focus the radiation from the source and to limit the detected radiation to that part of the wall of the hole in contact with the source and detectors. The decentralizing caliper arm also provides a log of hole diameter. Modern tools are called borehole-compensated or borehole-corrected, but they still exhibit some borehole diameter effects. The ratio of the count rates for the near and far detectors is plotted against bulk density, either in the logging equipment, or preferably later so that algorithms can be changed (Scott, 1977). This ratio reduces borehole diameter effects because the near detector has a smaller radius of investigation than the far detector and is thus more affected by changes in diameter. Gamma-gamma logging is based on the principle that the attenuation of gamma radiation, as it passes through the borehole and surrounding rocks, is related to the electron density of those rocks. If a probe detects only radiation resulting from Compton scattering, the count rate will be inversely proportional to the electron density of the material through which the radiation passes. Electron density is approximately proportional to bulk density for most materials that are logged. A correction for the "Z To A" ratio needs to be applied for any minerals that do not have the same ratio of atomic number to atomic mass as the calibration environment. The electron density of water is 1.11 g/cc versus a bulk density of 1 g/cc, and some companies may make this correction. Like other logging systems, calibration of gamma-gamma response is best done in pits designed for that purpose. Calibration can be done in porosity pits like the American Petroleum Institute neutron pit in Houston or in pits maintained by commercial service companies. A set of bulk-density pits is available for free use by anyone at the Denver Federal Center, Denver, CO. Onsite standardization of probe response usually is done with large blocks of aluminum, magnesium, or lucite that are machined with a groove that tightly fits the source and detector section of the probe. The blocks need to be large enough that effects of the environment are minimized, and they need to be located off the ground and away from a logging truck that may contain radioactive sources.

Volume of Investigation. The volume of investigation of a gamma-gamma probe probably has an average radius of 127 to 152 mm; 90% of the pulses recorded originate from within

this distance. However, the volume of investigation is a function of many factors. The density of the material being logged and any casing, cement, or mud through which the radiation must pass have a significant effect on the distance gamma photons will travel before being stopped. Within limits, the greater the spacing between source and detector, the larger the volume of investigation. Standoff error is caused when a side-collimated, decentralized probe or skid is separated from the borehole wall by mudcake or wall roughness. According to Scott (1977), standoff errors of 10 mm or more may be corrected accurately using the algorithms he developed.

Data Interpretation

Gamma-gamma logs may be used to distinguish lithologic units and to determine well construction, in addition to determining bulk density, porosity, and moisture content when properly calibrated. The chief use of gamma-gamma logs has been for determining bulk density that can be converted to porosity. Gamma-gamma logs conventionally are recorded with bulk density increasing to the right, which means that porosity increases to the left as it does on conventionally plotted neutron and acoustic velocity logs. Although commercial gamma-gamma logs often have a scale in porosity, the log response is related directly to electron density, which may be related to bulk density by calibration and correction for Z-A errors. The accuracy of bulk-density determinations with these logs is reported by various authors to be from 0.03 to 0.05 g/cc. Figure 374 is a plot of bulk density from laboratory analyses of core versus density log values from a study in Canada (Hoffman, Fenton, and Pawlowica, 1991). It shows how accurate density logs can be under the right conditions. The best results are obtained with gamma-gamma logs in rocks of low bulk density or high porosity. Bulk density can be converted to porosity by the following equation: porosity = grain density minus bulk density divided by grain density minus fluid density. Bulk density may be derived from a calibrated and corrected log. Fluid density is 1 g/cc for most non-petroleum applications, where the rock is saturated. Grain or mineral density may be obtained from most mineralogy texts; grain density is 2.65 g/cc for quartz; 2.71 g/cc commonly is used for limestone, and 2.87 g/cc commonly is used for dolomite. At many sites, gamma-gamma logs provide more accurate porosity data than neutron and acoustic velocity logs. Figure 375 is an example of a comparison of data from the three types of porosity sensing logs versus core data at a Superfund site in Oklahoma (Keys, 1993). Because moisture content affects the bulk density of rocks, gamma-gamma logs can be used to record changes in moisture above the water surface. Thus they can be used in the same way as neutron logs to monitor the downward migration of water from waste disposal or artificial recharge ponds.

Well Construction

Gamma-gamma logs can be used to locate cement tops, gravel pack fill-up, or one string of casing outside of another. Gamma-gamma logs for this application are discussed in the section on well completion logs.

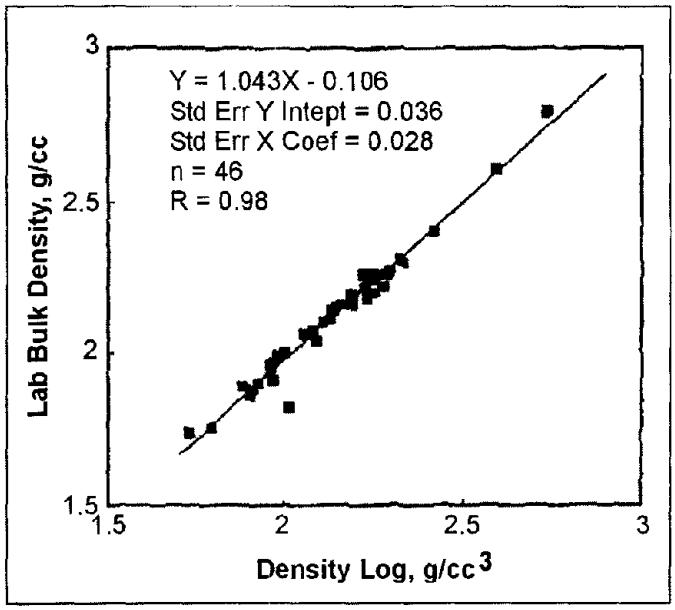

Figure 374. Plot of laboratory measurements of bulk density versus gamma-gamma log response in the same borehole. (Hoffman, Fenton, and Pawlowicz, 1991; copyright permission granted by Alberta Research Council)

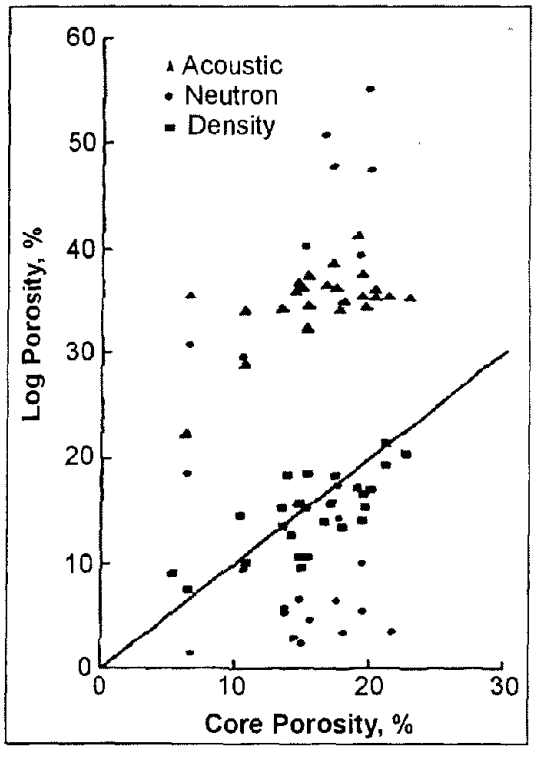

Figure 375. Comparison of laboratory measurements of porosity versus acoustic, neutron and density log response in the same borehole.

10.4.2.3 Neutron Logging

Basic Concept

Neutron logs are made with a source of neutrons in the probe and detectors that provide a record of the interactions that occur in the vicinity of the borehole. Most of these neutron interactions are related to the amount of hydrogen present, which, in groundwater environments, is largely a function of the water content of the rocks penetrated by the drill hole. Neutron probes contain a source that emits high-energy neutrons. The most common neutron source used in porosity logging tools is americium-beryllium, in sizes that range from approximately 1 to 25 Curies. Moisture tools may use a source as small as 100 millicuries. Two different neutron-logging techniques are used in groundwater studies: Neutron probes with a large source and long spacing are used for measuring saturated porosity and moisture content in a wide range of borehole diameters; probes with a small source and short spacing are used for measuring moisture content in small-diameter monitoring wells. Three general types of neutron-porosity logs exist: neutron-epithermal neutron, neutron-thermal neutron, and neutron-gamma. Cadmium foil may be used to shield crystal or Helium-3 detectors from thermal neutrons. Neutron-epithermal neutron logs are least affected by the chemical composition of the rocks logged. Two or more detectors are used in modern neutron tools, and they may be collimated and decentralized by a caliper arm. The ratio of the near to the far detector provides logs that are less affected by borehole parameters than single-detector logs.

Moderating Neutrons. Fast neutrons, emitted by a source, undergo three basic types of reactions with matter in and adjacent to the borehole as they lose energy and ultimately are captured: inelastic scatter, elastic scatter, and absorption or capture. In elastic scatter, the mass of the scattering element controls the loss of energy by the neutron. Light elements are most effective in moderating, or slowing neutrons, whereas heavy elements have little effect on neutron velocity or energy. Hydrogen is the element most effective in moderating neutrons because it has the same mass as a neutron. Because hydrogen is the most effective moderating element, the cloud of epithermal and thermal neutrons occurs closer to the source in rocks with a large hydrogen content than in rocks with a small hydrogen or water content. The moderating and capture processes result in the number of epithermal and thermal neutrons and capture gamma photons being inversely related to the hydrogen content of the rocks, at source-to-detector spacing greater than approximately 300 mm. If detectors are located closer than 300 mm from the source, as in moisture probes, the number of moderated and captured neutrons increases with increasing hydrogen content.

Volume of Investigation. The volume of investigation of a neutron probe is related closely to the content of hydrogen or other strong neutron absorbers in the material surrounding the probe, the spacing between the source and detector, and the energy of the neutrons. In sand with a saturated porosity of 35%, three different types of neutron probes received 90% of the recorded signal within 170, 236, and 262 mm of the borehole wall. In dry rocks, the radius of investigation may be several meters. The reference depth, or point of measurement, on a probe may change somewhat if significant differences in water content are logged. Increasing the source-to-detector spacing increases the volume of investigation in the vertical direction as well as in the horizontal direction, into the rock. This increased volume

decreases thin-bed resolution as demonstrated in figure 372. The hypothetical volume of investigation is shown by shading in the figure. Note that size and shape of this volume are shown to change as a function of the porosity as the probe moves up the hole. The log only gives an approximately correct value for porosity and thickness when the volume of investigation is entirely within the bed being logged. Thus, in figure 372, the upper thin limestone bed with 3.3% porosity is indicated by the log to have a much higher porosity and greater apparent thickness than the lower bed with a porosity of 3.3%. The usual technique for determining bed thickness from any type of nuclear log is to make the measurement at one-half the maximum amplitude of the deflection that represents that bed, as shown on the figure.

Data Acquisition

Calibration of all neutron-logging systems used in the petroleum industry is based on the API calibration pit in Houston, Texas. The pit contains quarried limestone blocks that have average porosities of 1.884%, 19.23%, and 26.63%. These values have been rounded by the American Petroleum Institute to 1.9%, 19%, and 26%, and the 19% block has been assigned the value of 1,000 API neutron units (Belknap, et al., 1959). Figure 376 shows calibration data for a compensated neutron probe in the API pit (Keys, 1990). Although the API pit is the widely accepted primary standard, it is only valid for limestone, so that most large logging companies maintain their own calibration facilities for other rock types, like dolomite and sandstone. Careful evaluation of laboratory analyses of core samples may lead to a valid calibration, but scatter of data points is to be expected. Regardless of how primary calibration is carried out, field standardization must be done at the time of calibration and frequently during logging operations. The most practical field standards permit the checking of probe response with the source installed in a reproducible environment that has a high hydrogen content. Although a plastic sleeve may be used, it must be quite heavy to be large enough to cover both source and detectors and thick enough to reduce outside effects.

Data Interpretation

In many rocks, the hydrogen content is related to the amount of water in the pore spaces. This relation is affected by the chemical composition of the water, hydrogen in some minerals and bound water in shales. Neutron logs are affected by many of the same borehole parameters that affect gamma-gamma logs, although usually to a lesser degree. These extraneous effects include borehole diameter, mud cake or stand off, salinity of the borehole and interstitial fluids, mud weight, thickness of casing and cement, temperature and pressure, and elemental composition of the rock matrix. Matrix effects are considered part of the interpretation process and may be analyzed by cross-plotting techniques, as illustrated in the General In-hole Logging Procedures section. Casing does not cause a major shift on most neutron logs, as it typically does on a gamma-gamma log. Neutron logs run through drill stem do not show the location of collars as a gamma-gamma log does. Plastic pipe of constant thickness merely causes a shift in log response similar to, but of lower magnitude than that caused by the water level in a small-diameter well. The short spacing used in moisture probes reduces the volume of investigation, so that borehole effects are increased. For this reason, boreholes to be used for logging with a moisture probe need to be drilled as small as possible. The annular space between casing and borehole wall also needs to be

small, and the probe needs to fit the casing tightly. Neutron logs are most suitable for detecting small changes in porosity at low porosities; gamma-gamma logs are more sensitive to small changes at high porosities. Although the interpretation of neutron logs for porosity and moisture content are stressed as primary applications, much use has been made of the logs for determining lithology. Like gamma logs, they can be used for lithology and stratigraphic correlation over a wide range of borehole conditions.

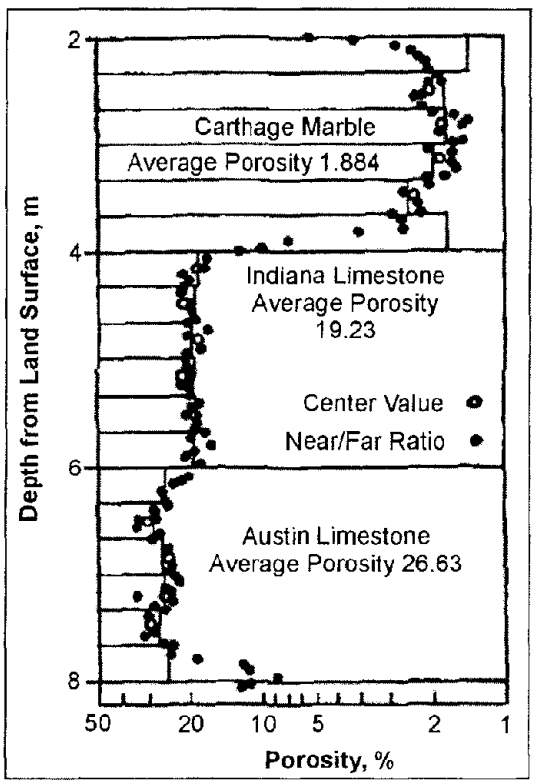

Figure 376. Calibration data for a compensated neutron-porosity probe in the API limestone pit.

Applications

Neutron-activation logging has potential for application to groundwater quality problems, because this technique permits the remote identification of elements present in the borehole and adjacent rocks under a wide variety of borehole conditions. Neutron activation produces radioisotopes from stable isotopes; the parent or stable isotope may be identified by the energy of the gamma radiation emitted and its half-life, using a gamma spectral probe (Keys and Boulogne, 1969).

10.4.3 Acoustic Logging

Acoustic logging includes those techniques that use a transducer to transmit an acoustic wave through the fluid in the well and surrounding elastic materials. Several different types of acoustic logs are used, based on the frequencies used, the way the signal is recorded, and the purpose of the log. All these logs require fluid in the well to couple the signal to the surrounding rocks. Four types will be described here: acoustic velocity, acoustic waveform, cement bond, and acoustic televiewer.

10.4.3.1 Acoustic-Velocity Logs

Basic Concept

Acoustic-velocity logs, also called sonic logs or transit-time logs, are a record of the travel time of an acoustic wave from one or more transmitters to receivers in the probe. Acoustic energy travels through the fluid in the well and through surrounding materials at a velocity that is related to the lithology and porosity of the rocks. Most acoustic-velocity probes employ magnetorestrictive or piezoelectric transducers that convert electrical energy to acoustic energy. Most of the transducers are pulsed from 2 to 10 or more times per second, and the acoustic energy emitted has a frequency in the range of 20 to 35 kHz. Probes are constructed of low-velocity materials, producing the shortest travel path for the acoustic pulse through the borehole fluid and the adjacent rocks, which have a velocity faster than that of the fluid. Acoustic probes are centralized with bow springs or rubber fingers so the travel path to and from the rock will be of consistent length. Some of the energy moving through the rock is refracted back to the receivers. The receivers reconvert the acoustic energy to an electrical signal, which is transmitted up the cable. At the surface, the entire signal may be recorded digitally for acoustic waveform logging, or the transit time between two receivers may be recorded for velocity logging. Amplitude of portions of the acoustic wave also may be recorded; that technique is described later under waveform logging.

Acoustic Energy Components

Acoustic energy transmitted in the borehole and adjacent rocks is divided into several components. The most important for this discussion are compressional (P) and shear wave (S) components. Standard acoustic-velocity logs are based on the arrival of the compressional wave. Compressional and shear waves at near and far receivers, along with the fluid waves that are transmitted through the borehole, are shown in figure 377 (Paillet and White, 1982). Most acoustic-velocity probes have paired receivers located a foot apart; some probes have several pairs of receivers with different spacing that may be selected from the surface. P-waves have a higher velocity and lower amplitude than shear waves, or S-waves. S-waves have a velocity about one- half that of P-waves and are characterized by particle movement perpendicular to the direction of wave propagation.

Data Acquisition

Tracking Circuits. Acoustic-velocity logging modules contain a tracking circuit that detects the arrival of the P-wave using a threshold amplitude or algorithm selected by the operator. If the waveform is digitized in the field, it is frequently possible to improve acoustic velocity logs by modifying the technique used to pick the first arrival. Amplitude of the transmitted signal and the received signal may be controlled from the surface, along with the height of the detection threshold. A circuit is employed to convert the difference in time of arrival at the two detectors to transit time (t) in μs/ft. Acoustic-velocity logs are recorded with interval transit time increasing from right to left; porosity also will increase to the left, as it does on conventionally plotted neutron and gamma-gamma logs.

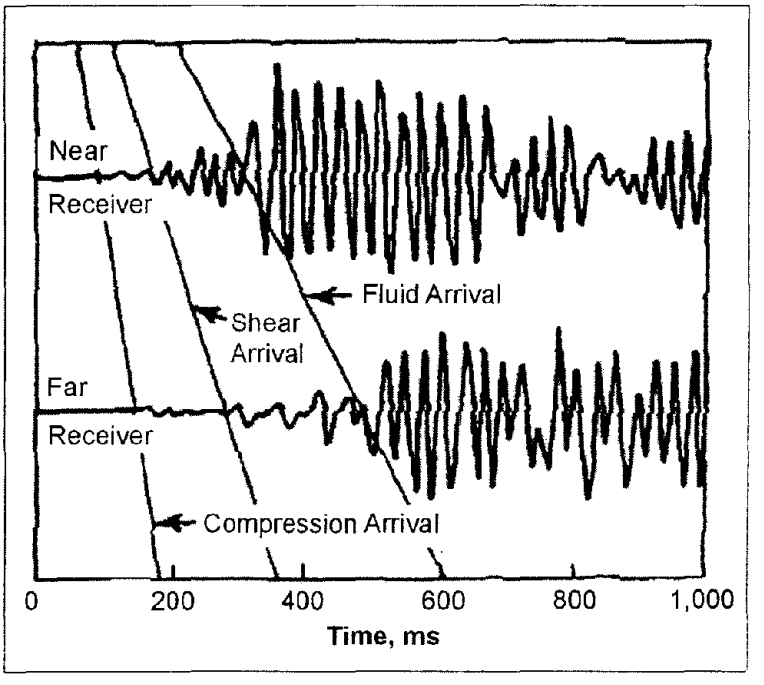

Figure 377. Acoustic waveforms for a two-receiver system.

Data Interpretation

For rocks with uniformly distributed, intergranular pore spaces, porosity usually is derived from the Wyllie time-average equation. This equation is based on the theory that the path of an acoustic wave through saturated rock consists of two velocities in series, the velocity in the fluid V_f, and the velocity in the rock matrix V_m. The length of the path in the fluid is equal to the porosity (Φ); the length of the path in the rock matrix is equal to 1-Φ. The time-average equation can be expressed as:

$$\frac{1}{V_L} = t = \frac{\Phi}{V_f} + \frac{(1-\Phi)}{V_m}, \tag{83}$$

where

V_L = velocity of the rock from a log.

For calculation of porosity, the time-average equation is converted to the form:

$$\Phi = \frac{(t_L - t_m)}{(t_f - t_m)}, \tag{84}$$

where

t_L = transit time from the log,

t_m = transit time of the wave in the matrix,

t_f = transit time in the fluid.

Velocities and transit times for some common rocks and fluids are provided in table 19. Note that the range can be very large, so laboratory measurements or background experience in specific rocks may be needed to calculate accurate porosities. The interval transit-time scale usually is accurate within 1 μs/ft on most acoustic-velocity logs; however, it should be checked, if possible. The difference in arrival of the P-wave at two receivers can be read directly from a calibrated oscilloscope, which is an essential part of any acoustic-logging system unless the waveform is digitized in the tool. In this case, a computer can be used to observe the waveforms. Calibration also can be accomplished using core samples analyzed in the laboratory for acoustic velocity and porosity. The response of a velocity probe can be checked onsite with a piece of steel pipe cut in half lengthwise. The tool can be laid in the pipe, and dams made at both ends with flexible caulking, so that half of the transmitters and receivers can be covered with water. Steel has a velocity ranging from 5,180 to 6,100 m/s (17,000 to 20,000 ft/s), which can be used to check the calibration of the sonde. It is possible to make the same check in a drill hole that contains free, hanging steel pipe.

Radius of Investigation. The radius of investigation of an acoustic-velocity probe is reported to be approximately three times the wavelength (Pirson, 1963). The wavelength is equal to the velocity divided by the frequency. At a frequency of 20,000 Hz, the radius of investigation theoretically is about 0.23 m for unconsolidated rocks with a velocity of 1,500 m/s, and 1.1 m for very hard rocks with a velocity of 7,600 m/s. A lower transmitter frequency will increase the volume of investigation, but it will decrease the resolution of small features, such as fractures.

Cycle Skipping. One of the most obvious problems on acoustic-velocity logs is cycle skipping, caused by the amplitude of the first compressional cycle being too low for detection, or by pre-arrival noise of sufficient amplitude to be detected. If the first cycle is detected at the near receiver, and the second cycle is detected at the far receiver, the resulting transit time will be much too long, and the log will show a very sharp deflection. Often signal amplitude will vary above and below detection level causing rapid fluctuations in the log trace, which can be recognized as cycle skips. Cycle skipping frequently is blamed on gas in the well; however, any condition that causes the compressional wave to drop below detection level will produce cycle skipping on the log. Causes include improper adjustment of signal or detection level, fractures or washouts, high-attenuation rocks, and gas in the fluid. Cycle skipping can be used to locate fractures in some wells, but corroborating evidence is necessary.

Lithologic Factors. Acoustic velocity in porous media is dependent on such lithologic factors as the type of matrix, density, size, distribution, and type of grains and pore spaces, degree of cementation, and the elastic properties of the interstitial fluids. The widely used time-average equation does not account for most of these factors, but it has been found to produce reasonably correct porosity values under most conditions. Figure 378 is a plot of porosity values measured on core versus transit time from an acoustic-velocity log for a sequence of basin-fill sedimentary and volcanic rocks in Idaho. The correlation coefficient

for the core and log data from this well is 0.87, even though a wide range of rock types with different matrix velocities were logged. Acoustic-velocity logs are very useful for providing information on lithology and porosity under a fairly wide range of conditions. They usually are limited to consolidated materials penetrated by uncased, fluid-filled wells; however, lithologic information can be obtained when casing is well bonded to the rocks. Resolution of thin beds is good when 1-ft receiver spacing is used; contacts usually are marked by sharp deflections.

Table 19. Compressional-wave velocity and transit time in common rocks and fluids (single values are averages).

	Velocity		
Rock or Fluid Type	**(m/s)**	**(ft/s)**	**Transit time (us/ft)**
Fresh Water	1,500	5,000	200.0
Brine	1,600	5,300	189.0
Sandstone			
Unconsolidated	4,600-5,200	15,000-17,000	58.8-66.7
Consolidated	5,800	19,000	52.6
Shale	1,800-4,900	6,000-16,000	62.5-167.0
Limestone	5,800-6,400	19,000-21,000+	47.6-52.6
Dolomite	6,400-7,300	21,000-24,000	42.0-47.6
Anhydrite	6,100	20,000	50.0
Granite	5,800-6,100	19,000-20,000	50.0-52.5
Gabbro	7,200	23,600	42.4

Secondary Porosity. In some geohydrologic environments, such as carbonates, porosity from an acoustic-velocity log and from a neutron log or core can be cross-plotted to identify intervals of secondary porosity. Acoustic-velocity logs do not detect most nonuniformly distributed secondary porosity, whereas neutron logs respond to all water-filled pore spaces.

10.4.3.2 Acoustic Waveform Logging

Basic Concept

Considerable information on lithology and structure is available through analyses of the various components of a received acoustic signal. Analyses may include amplitude changes, ratios of the velocities of various components of the wave train, and frequency-dependent effects. Hearst and Nelson (1985) present a broad discussion on acoustic logging and the propagation of waves in geologic media. There are two main categories of waves in a borehole: refracted waves and guided waves. Refracted waves travel from the transmitter through the fluid and are refracted at the borehole wall, where they travel through the rock until refracted again through the fluid to the receivers. Guided waves travel in the borehole fluid or at the borehole wall/fluid interface. Cement-bond logs are included in this section,

because waveform data are needed to increase the accuracy of interpretation of these logs. Acoustic waveforms can be recorded digitally, pictures can be made of the display on an oscilloscope, or a variable-density log can be made. The variable-density log (VDL) or three-dimensional (3-D) velocity log is recorded photographically, so that variations in darkness of the record are related to changes in amplitude of cycles in the waveform. Figure 379 includes a VDL display. The banded display on the right is the VDL, which is a representation of the wave train in time from transmitter pulse. Frequency of the waves is related to the width of the black and white or gray bands. The gray scale scheme in this VDL is such that white represents high-amplitude negative wave pulses, gray the low-amplitude waves, and black represents high-amplitude positive pulses. A digitized waveform log is the most useful type of record, because data can be analyzed quantitatively. Velocities and amplitudes of all parts of the recorded waveform can be measured from a digital record. Furthermore, digitized waveform data enable acoustic velocity or transit time logs to be corrected later where the algorithm that detected the first arrival was not functioning properly.

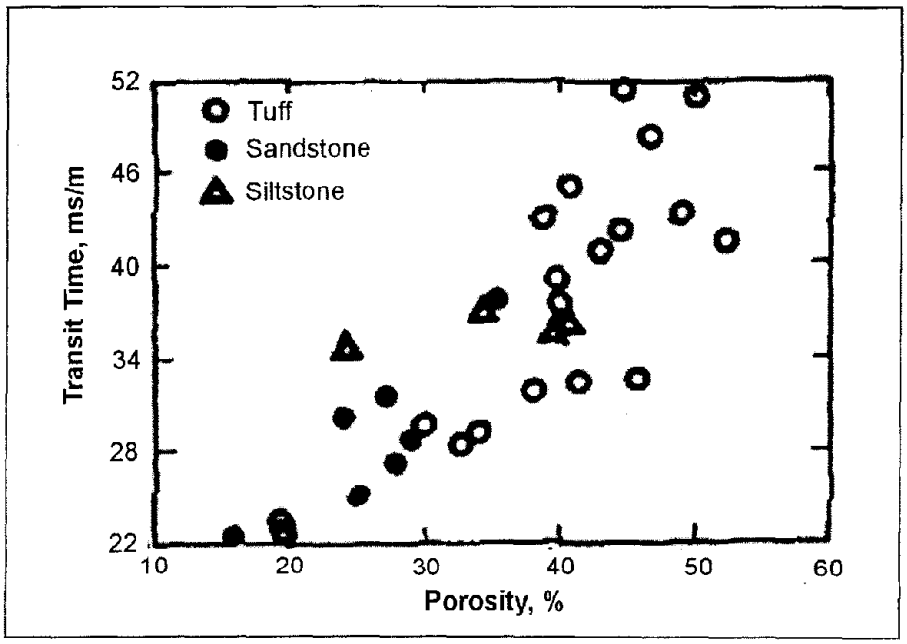

Figure 378. Relation of acoustic-transit time to porosity for a tuff, sandstone and siltstone, Raft River geothermal reservoir, Idaho.

Data Interpretation

Elastic properties of rocks can be calculated from the velocities of P- and S-waves and from corrected bulk density from a gamma-gamma log. The elastic properties or constants that can be determined are shear modulus, Poisson's ratio, Young's modulus, and bulk modulus (Yearsley and Crowder, 1990). The shear modulus is defined in terms of density and S-wave velocity, as given in the following equation:

$$G = p_b V_s^2,$$

(85)

where

G = shear modulus,

p_b = bulk, mass density,

V_s = shear-wave velocity.

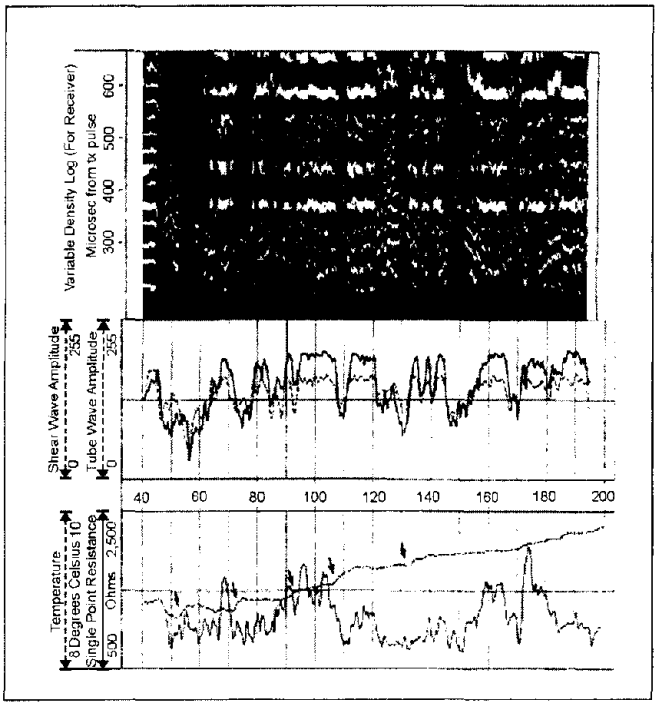

Figure 379. Composite of logs showing the location of permeable fractures indicated by the arrows at changes in temperature gradient and by low tube and shear wave amplitude. (Yearsley and Crowder, 1990; copyright permission granted by Colog, Inc)

Poisson's ratio ν is the ratio between strain in the direction of principal stress and strain in either transverse direction, and is defined in terms of P- and S-wave velocities by the following:

$$v = \frac{(a^2 - 2)}{2(a^2 - 1)},$$

(86)

where

ν = Poisson's ratio,

a = V_p/V_s,

V_p = P-wave velocity.

Young's modulus is the factor of proportionality between stress and strain and is fundamentally related to the material constants given above by the following equation:

$$E = 2G(1+\nu), \tag{87}$$

where

E = Young's modulus.

It should be noted that the above relationships were derived for homogeneous, isotropic conditions, which do not exist in the geologic environment. Still, in practice, these expressions provide useful engineering estimates for the elastic properties of rocks, and an analytical overview of the interrelationships among density, velocity, and moduli. For example, equation 85 reveals that the shear modulus varies directly with density, but with the square of shear velocity, indicating the strong dependency of the shear modulus on transverse velocity. It is interesting to note from equation 85 that Poisson's ratio is not physically meaningful for compression/shear velocity (V_p/V_s) ratios less than 1.42 (Poisson's ratio becomes negative). In general, higher Poisson's ratios indicate less competent rock. Ice, which is more deformable than most rock, has a V_p/V_s ratio of approximately 2.0, which corresponds to a Poisson's ratio of 0.33. The result of this type of analysis is the engineering properties log shown in figure 380. Competent rock below 44 m stands out clearly in figure 380, with moduli of nearly twice the weathered rock and five times the fractured rock. However, note the minor fracture zones in evidence in the competent rock mass, indicated by excursions to the left on both the moduli curves and velocity curve. The major fracture zones in the overlying rock are shown by extremely low shear moduli of less than 14 GPa (two million psi). The core-derived rock quality determination plotted in figure 380 grossly indicates the difference between the competent rock mass and the overlying weathered and fractured rock in this core hole.

Tube Waves. Paillet (1980 and 1981) describes the characterization of fractures by various acoustic techniques. A significant finding was that a semiquantitative correlation exists between the attenuation of tube-wave amplitude in small-diameter drill holes in crystalline rocks and the permeability of fractures determined by packer-isolation tests. Thus, tube-wave amplitude logging has the potential for predicting the relative flow through fractures in hard rocks. The tube wave is part of the fluid wave propagated along the borehole wall under certain conditions; it apparently is attenuated where water in the borehole is free to move in and out of fractures. Figure 381 shows the correlation between a tube wave amplitude log calculated from digitized acoustic waveform data and fracture aperture or permeability from straddle packer tests (Davison, Keys, and Paillet, 1982). Figure 379 is a composite log including shear and tube wave amplitude, temperature, single point resistance, and VDL. VDL indicates fractures as the low-velocity zones. The single point resistance is primarily controlled by the presence or absence of fractures. Natural flow in or out of the borehole through fractures affects the thermal gradient of the borehole fluid so that changes noted on the temperature log by arrows indicate natural fracture flow. The amplitude logs in figure 379 were computed by calculating the root mean square amplitude within specified time windows. Two additional fracture zones evident on the VDL, and as low-amplitude excursions on the amplitude logs at 44.5 - 45 and 52 m are not obvious on the temperature log.

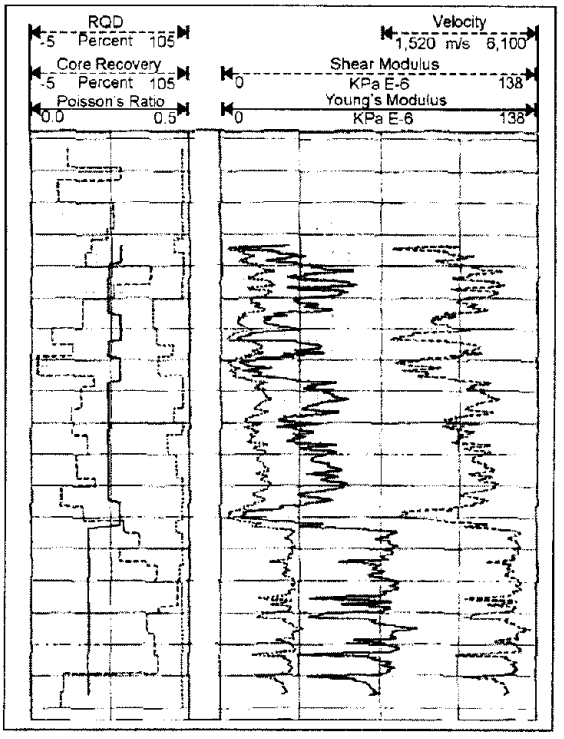

Figure 380. Engineering properties calculated from geophysical logs of a core hole compared with rock quality determination (RQD) from the core. (Yearsley and Crowder, 1990; copyright granted by Colog, Inc)

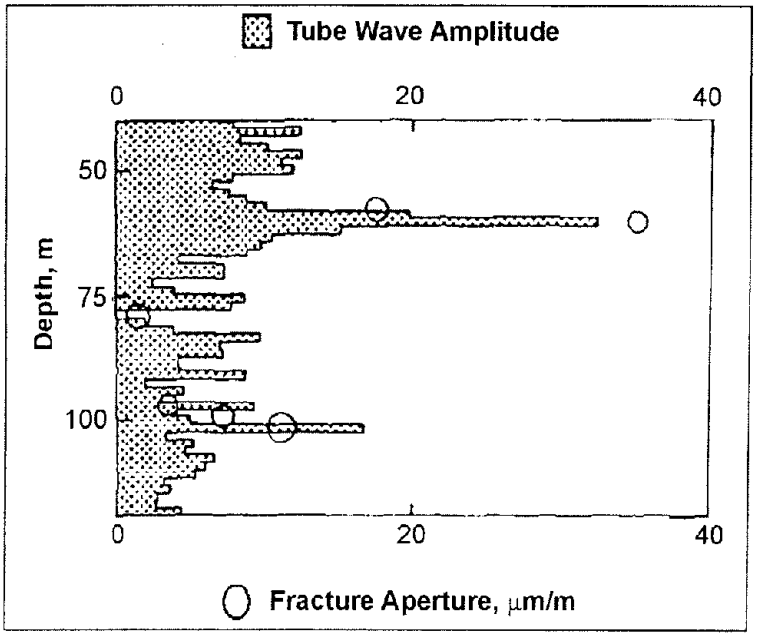

Figure 381. Plot showing a comparison of a tube wave amplitude calculated from acoustic waveform data and hydraulic fracture aperture calculated from straddle packer tests.

10.4.3.3 Cement-Bond Logging

Cement-bond logging usually employs a single receiver to obtain information on the quality of the bond between casing and cement and between cement and borehole wall. Most cement-bond logs are a measurement only of the amplitude of the early arriving casing signal, but to improve the accuracy of interpretation, the full acoustic wave form is needed for study. Although a small amount of the total acoustic energy may be received from the rock when the casing is free to vibrate, the formation signal usually is not detectable. The detection of channeling through cement in the annular space is one of the main objectives of cement-bond logging; yet, even an expert in the analysis of cement-bond logs probably will not locate all channels accurately.

10.4.3.4 AcousticTeleviewer

Basic Concept

An acoustic televiewer (ATV) is a logging device that can provide high-resolution information on the location and character of secondary porosity, such as fractures and solution openings. It also can provide the strike and dip of planar features, such as fractures and bedding planes. An ATV also is called the borehole televiewer, but this term occasionally causes it to be confused with borehole television. An ATV employs a rotating high-frequency transducer that functions as both transmitter and receiver (Zemanek, et al., 1969). The piezoelectric transducer is rotated at three or more revolutions per second and is pulsed approximately 1,200 times per second. High-frequency acoustic energy is reflected from, but does not penetrate, the borehole wall. A trigger pulse is transmitted to the surface equipment from a flux-gate magnetometer each time the transducer rotates past magnetic north. This pulse triggers the sweep of an oscilloscope or graphic recorder, so that each sweep represents a 360° scan of the borehole wall. The brightness of the oscilloscope trace is proportional to the amplitude of the reflected acoustic signal, somewhat analogous to a rotating depth finder in a boat.

Data Acquisition

The probe must be centralized accurately with bow springs so the signal path will be the same length in all directions. As the probe moves up the hole, a signal is generated that moves the sweeps across the oscilloscope or other type of graphic recorder to produce a continuous record of the acoustic reflectivity of the borehole wall. The received signal may also be recorded in analog format on standard VHS tape for later playback and enhancement of the graphic record. The signal from the ATV probe may be digitized in new generation probes or subsequently from the VHS analog tape from older systems. The digital data file may then be enhanced, analyzed, and displayed in various color formats using a computer program. This program, and similar programs developed by logging companies, produces three-dimensional plots, calculates the aperture and strike and dip of fractures, the orientation of breakouts, borehole diameter, acoustic reflectivity, stress field, etc. The ATV log is a cylinder that has been opened along the north side and flattened, as illustrated in figure 382. In this figure, an open fracture dipping to magnetic south is shown intersecting a drill hole in a three-dimensional drawing on the left. The hypothetical televiewer log on the right shows the fracture as it might appear, as a dark sinusoid, with the low point oriented toward

magnetic south. The transducer rotates clockwise, as viewed looking down the well; thus, compass directions are in the order shown at the bottom of the log. Fractures and other openings in the borehole wall or in casing appear as dark areas for several reasons. Increasing well diameter means the acoustic signal must travel farther, and that it will be more attenuated by the fluid in the borehole. In addition, part of the surface of fractures and other openings is not at right angles to the incident acoustic signal, so that it is not reflected back to the transducer.

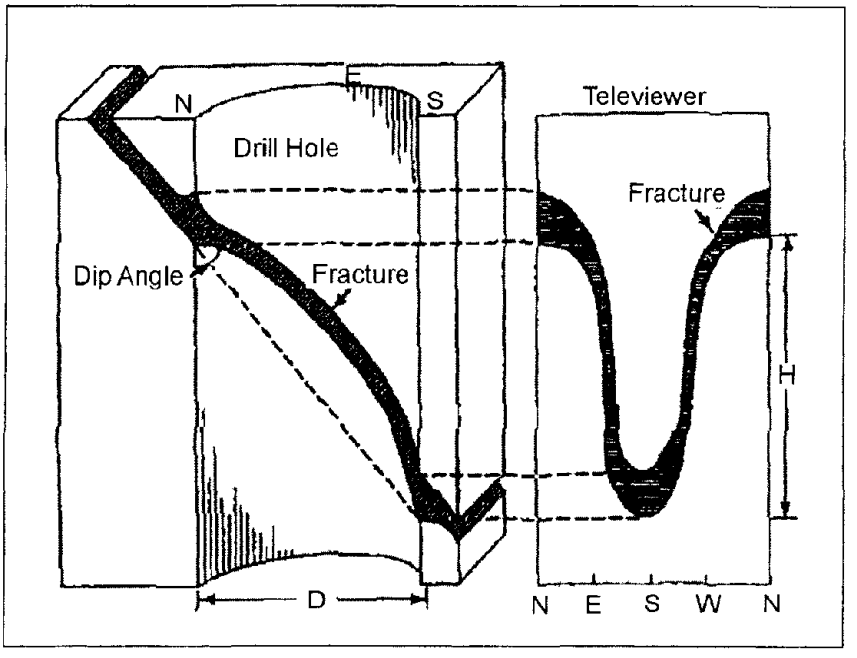

Figure 382. Three-dimensional view of a fracture and appearance of the same fracture on an acoustic televiewer log. D is borehole diameter and h is the length of the fracture intercept in the borehole.

Acoustic Caliper Log. Modifications to ATV equipment permit recording an acoustic-caliper log, which consists of four high-resolution traces. Use of a lower frequency transducer provides better penetration of casing, and the tool can be used to examine cement in the annular space. Broding (1984) demonstrated the ability of a lower frequency probe to locate voids and channels in cement that were not detected by other logging methods. Acoustic televiewer logs, made in steel casing or in the presence of large concentrations of magnetic minerals, are not oriented, because the magnetometer will not work under these conditions. A switch in the tool can be used for triggering the sweep instead of the magnetometer; as a result, compass orientation of the edge of the log will rotate as the tool is brought up the hole.

Quantitative Output. Two quantitative outputs of the acoustic televiewer occur that may require calibration and occasional standardization onsite. The magnetometer needs to be checked with a compass to determine if it triggers on magnetic north within a degree, if possible; this can be accomplished by using a narrow reflective object in a plastic bucket filled with water. The lower set of centralizers usually is removed for this procedure. If an acoustic-caliper log is to be run, hole-diameter response needs to be checked.

Volume of Investigation. The concept of volume of investigation does not apply to the televiewer in a strict sense because, with the typical high-frequency transducer, most of the signal is received from the wall of the borehole. Even if the frequency is reduced to half the usual value, rock penetration is small. However, acoustic-televiewer probes have mechanical and electronic limits to the diameter of the well that can be logged. The operating range of borehole diameter for most tools is from 76 to 400 mm.

Data Interpretation

An acoustic televiewer provides a record of the location, character, and orientation of any features in the casing or borehole wall that alter the reflectivity of the acoustic signal. These include diameter and shape of the drill hole, wall roughness that may be caused by drilling procedures or lithology, differences in rock hardness, and structural features like bedding, fractures, and solution openings. The smallest feature that can be resolved on an ATV log depends on a number of factors such as hole diameter and wall roughness. Under the right conditions, features as small as 1 mm, or possibly even smaller, can be identified. Figure 383 is a comparison of fractures detected by borehole television, detailed core description, and by the acoustic televiewer at a reactor site in Canada (Davison, Keys, and Paillet, 1982). The first two are diagrammatic reconstructions of the fractures, and the ATV log is a copy of the field log. The ATV shows all of the open fractures that are likely to be capable of transmitting water. Borehole television or video missed some of these fractures, and some of the fractures shown as dashed on the core log are actually only visible with a hand lens. Paillet (1994) discusses the televiewer and other techniques used to characterize flow in fractured rocks.

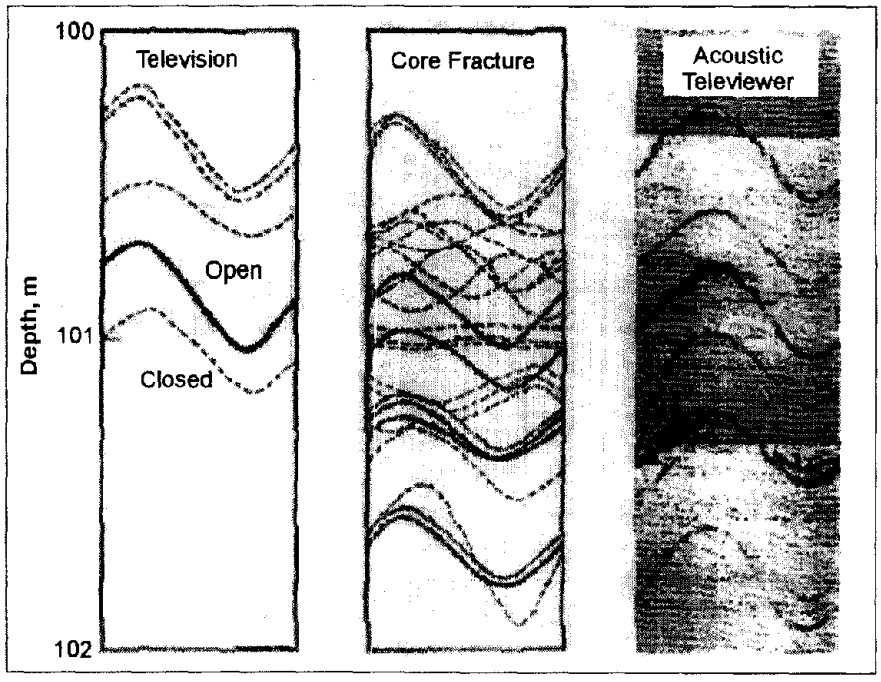

Figure 383. Diagram showing comparison of reconstructed fracture data from borehole television, and a detailed core log, with a copy of an acoustic televiewer log.

Acoustic Televiewer Applications

A televiewer log of a fracture-producing zone in a geothermal well at Roosevelt Hot Springs, Utah, is shown in figure 384. Acoustic- and mechanical-caliper logs of this zone are shown in figure 385. These logs were made at temperatures as high as 260°C (Keys, 1979). The fracture-producing interval shown in figure 383 is approximately 1.2 m thick; it apparently is the result of alteration and solution along a series of subparallel fractures seen as black sinusoids in the figure. The fracture at the top of the interval appears to be about 150 mm wide, based on the log; it is probably much less. Fractures tend to be broken out during drilling, and the broken edges further increase the apparent thickness on the log by refracting the acoustic signal. This is particularly evident at the top and bottom of the sinusoid on steeply dipping fractures, as illustrated in figure 382. The open fracture in the fracture-producing zone is paralleled by one relatively tight fracture above, and probably six fractures below, which produced a brecciated, and probably altered, permeable zone. The effect of drilling technique and lithology on the interpretation of fracture character from ATV logs is discussed by Paillet, Keys, and Hess (1985). Log quality generally is not as good where the wall of the hole is rough, or where rocks are soft.

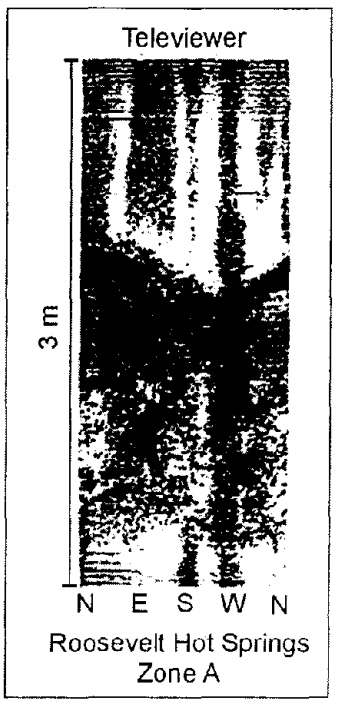

Figure 384. Acoustic-televiewer log of fracture-producing zone A in a geothermal well, Roosevelt Hot Springs, Utah.

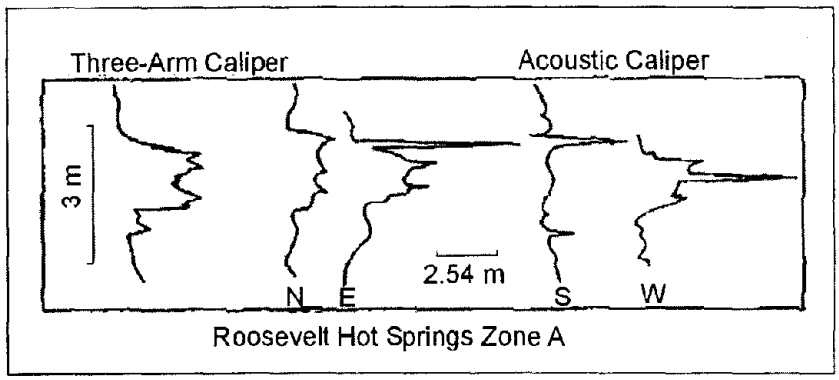

Figure 385. Mechanical and acoustic-caliper logs of fracture-producing zone A in a geothermal well, Roosevelt Hot Springs, Utah.

Strike and Dip. To calculate the strike and dip of fractures or bedding, the following information is needed: the vertical intercept distance on the ATV log H as shown in figure 382; the direction of dip from the ATV log; and, the hole diameter D from a caliper log. The same measuring units must be used for H and D. The angle of dip, in degrees, is equal to the arc tangent of H/D. If the average H for the fractures in figure 382 is 12 in, and the hole diameter is 6 in, the dip would be 63°; if the hole diameter is 12 in, the dip would be 45°. Direction of dip usually can be measured to the nearest 5°, using a 360° scale constructed to fit the width of the ATV log. The average direction of dip of the fractures in figure 384 is slightly south of west.

Orientation of the Stress Field. Orientation of the stress field may be determined from an analysis of ATV logs made in wells where fractures have been induced hydraulically, either intentionally or accidentally, by drilling (Wolff, et al., 1974; Keys, et al., 1979). Hydraulic fractures are oriented perpendicular to the direction of least principal stress. Hydraulic fractures accidentally induced during drilling may provide permeable pathways for waste migration at environmental sites. Breakouts are increases in borehole diameter oriented at right angles to the maximum, principal, horizontal stress. They are easily recognized on ATV logs and have been discussed in detail by Paillet and Kim (1985). Breakouts appear as two vertical dark bands with irregular margins located approximately 180° apart on the log.

Casing Examination. The acoustic televiewer can also be used to examine casing for holes and to locate joints in pipe and well screens; borehole television might be better for these purposes if the water is clear and the walls are clean. Above the water level, television needs to be used, because the ATV will not operate.

Extraneous Effects. Interpretation of televiewer logs is complicated by a number of extraneous effects. Most significant are poor centralization, incorrect gain settings, errors from borehole deviation, and aberrations in the magnetic field. Significant deviation from

vertical is common in deep drill holes, which introduces several errors on ATV logs. In addition to the obvious error in the measured vertical depth, corrections must be made to dip and strike calculated from ATV logs in deviated holes. Boreholes are not usually round, and this produces vertical black bands on ATV logs. Poor tool centralization in deviated wells produces similar features on the logs. Choosing the proper gain setting for the tool is a matter of operator experience and is quite important in producing high- quality logs.

10.4.4 Other Methods of Logging

10.4.4.1 Caliper Logging

Basic Concept

Caliper logs provide a continuous record of borehole diameter and are used widely for groundwater applications. Changes in borehole diameter may be related to both drilling technique and lithology. Caliper logs are essential to guide the interpretation of other logs, because most of them are affected by changes in well diameter. They also are useful in providing information on well construction, lithology, and secondary porosity, such as fractures and solution openings. Many different types of caliper probes are described in detail by Hilchie (1968). The most common type of probe used for logging water wells has three arms approximately the diameter of a pencil, spaced 120° apart. Arms of different lengths can be attached to this type of tool to optimize sensitivity over the hole-diameter range expected. Mechanical caliper probes have been used that will measure to a maximum hole diameter of 1 m. The typical water-well caliper employs arms that are connected to move a linear potentiometer, so changes in resistance transmitted to the surface as voltage changes are proportional to average hole diameter. Single-arm calipers commonly are used to provide a record of hole diameter while running another type of log. The single arm also may be used to decentralize a probe, such as a side-collimated gamma-gamma tool, but logs made with this type of probe are usually not high resolution. High-resolution caliper-logging devices usually employ three or four independent arms, and they are compass oriented in some tools. The difference in resolution between logs made with a four-arm device and the more common types is shown in figure 386. The high-resolution logs on the left were made with four independent arms. The three-arm averaging tool is typical of that used in engineering and environmental applications, and the single-arm log on the right was recorded during the running of a compensated gamma-gamma log. The apparent erratic response on the four-arm caliper logs in part of the well is repeatable and is caused by solution openings in the carbonate rock. Digital sample interval should be close spaced, such as 0.03 m if high-resolution logs are desired. Acoustic calipers may use the time-of-travel data from an acoustic televiewer to provide compass-oriented, high-resolution traces.

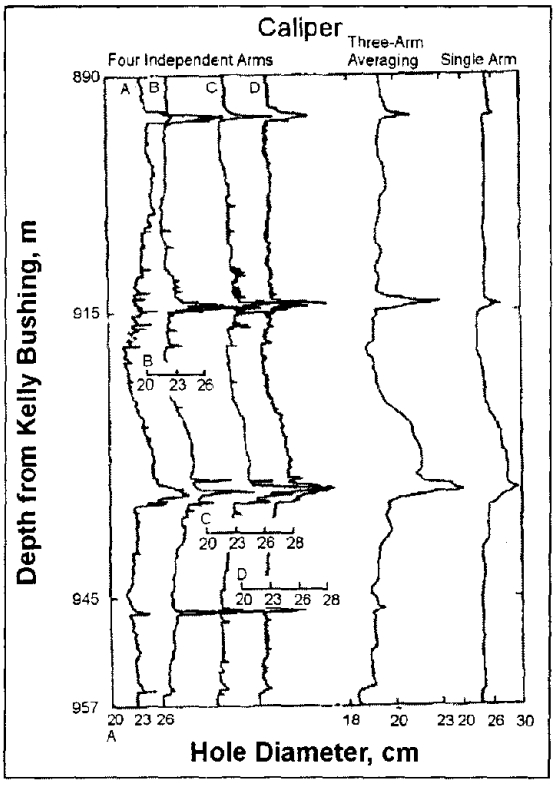

Figure 386. Caliper logs from probes having four independent arms, three averaging arms, and a single arm. Madison limestone test well No 1, Wyoming.

Data Acquisition

Calibration. Calibration of calipers is carried out most accurately in cylinders of different diameters. Large cylinders occupy a considerable amount of room in a logging truck, so it is common practice to use a metal plate for onsite standardization of three-arm averaging or single-arm probes. The plate is drilled and marked every inch or two and machined to fit over the body of the probe and accept one caliper arm in the holes. Because values obtained with a calibration plate are not as accurate as those obtained with a cylinder, usually log scale is checked using casing of known diameter in the well.

Data Interpretation

A valid caliper log is essential to guide the interpretation of the many different types of logs that are affected by changes in hole diameter, even those that are labeled borehole compensated. Differences in hole diameter are related to drilling technique and lithology and structure of the rocks penetrated. The shallower part of a hole is usually larger diameter than the deeper part, because it has been exposed to more drilling activities. Couplings, welds, and screens may be located on a high-resolution caliper log.

Applications. Caliper logs have been used to correlate major producing aquifers in the Snake River Plain in Idaho (Jones, 1961). Vesicular and scoriaceous tops of basalt flows, cinder beds, and caving sediments were identified with three-arm caliper logs. In the Snake River, basalt caliper logs also were used to locate the optimum depth for cementing monitoring

wells and to estimate the volume of cement that might be required to achieve fill of the annulus to a pre-selected depth (Keys, 1963). Similarly, a caliper log can be used to calculate the volume of gravel pack needed and to determine the size of casing that can be set to a selected depth. Caliper logs are particularly useful for selecting the depths for inflating packers. Packers can be set only over a narrow specified range of hole diameters and may be damaged if they are set in rough or irregular parts of a well. Packers set under these conditions may explode; if they are set on a fracture, they may implode or be bypassed by flow. Caliper logs are useful for determining what other logs can be run and what range of diameters will be accepted by centralizers or decentralizers. Hole diameter information is essential for the calculation of volumetric rate from many types of flowmeter logs. Because of the usefulness of a caliper log to the interpretation of other logs, it needs to be run before casing is installed in a hole that is in danger of caving. When hole conditions are questionable, the first log run is usually the single-point resistance log, because it will provide some lithologic information; if it is lost, the tool is relatively inexpensive to replace. If no serious caving problems are detected during the single-point log, a caliper log needs to be run before casing is installed so it can be used to aid the analysis of nuclear logs made through the casing. Very rough intervals of a drill hole, with changes in hole diameter of several inches, cannot be corrected based on caliper logs, and they need to be eliminated from quantitative analysis.

Lithology and Secondary Porosity. Caliper logs can provide information on lithology and secondary porosity. Hard rocks such as limestone will show on the log as a smaller diameter than adjacent shales. Shales may produce an irregular caliper trace, caused by thin bedding. Secondary porosity, such as fractures and solution openings, may be obvious on a caliper log, although the character will not be uniquely defined, as it would be on an acoustic-televiewer log. Open fractures are detected readily by three-arm averaging calipers, but the true character of the fractures may not be correctly interpreted from a caliper log. If an open fracture is dipping at a sufficient angle so that the three arms enter the opening at different depths, the separate anomalies produced will indicate three fractures rather than one.

10.4.4.2 Fluid

Fluid logging includes those techniques that measure characteristics of the fluid column in the well; no direct signal is derived from the surrounding rocks and their contained fluids. The fluid logs that are described here are temperature, electrical conductivity, and flow. Fluid logs are unique in that the recorded characteristics of the fluid column may change rapidly with time and may be altered by the logging process.

10.4.4.3 Temperature Logging

Basic Concept

Temperature probes used in groundwater and environmental studies employ a glass-bead thermistor, solid-state IC device, or platinum sensor mounted in a tube that is open at both ends to protect it from damage and to channel water flow past the sensor. The sensor may be enclosed in a protective cover, but it must be made of materials with a high thermal conductivity and small mass to permit fast response time. Thermistor probes used by the U.S. Geological Survey have an accuracy, repeatability, and sensitivity on the order of

0.02°C. They also are very stable over long periods of time, but they have the disadvantage of a nonlinear temperature response. For high-temperature logging in geothermal wells, platinum sensors may be used that have an accurate, stable, and linear response. Two general types of temperature logs are in common use: the standard log is a record of temperature versus depth, and the differential-temperature log is a record of the rate of change in temperature versus depth. The differential-temperature log, which can afford greater sensitivity in locating changes in gradient, can be considered to be the first derivative of the temperature. It can be obtained with a probe with two sensors located from 0.3 to 1.0 m apart or by computer calculation from a temperature log. A differential log has no scale, and log deflections indicate changes from a reference gradient.

Calibration. Calibration of temperature probes needs to be carried out in a constant temperature bath, using highly accurate mercury thermometers. The bath and probe need to reach equilibrium before a calibration value is established. Onsite standardization cannot be carried out with great accuracy because no portable substitute exists for a constant-temperature bath. The only temperature that can be achieved and maintained for sufficient time to permit a valid calibration is 0°C in an ice bath.

Data interpretation

Temperature logs can provide very useful information on the movement of water through a well, including the location of depth intervals that produce or accept water; thus, they provide information related to permeability. Temperature logs can be used to trace the movement of injected water or waste and to locate cement behind casing. Although the temperature sensor only responds to water or air in the immediate vicinity, recorded temperatures may indicate the temperatures of adjacent rocks and their contained fluids if no flow exists in the well.

Applications. Temperature logs can aid in the solution of a number of groundwater problems if they are properly run under suitable conditions, and if interpretation is not oversimplified. If there is no flow in, or adjacent to a well, the temperature gradually will increase with depth, as a function of the geothermal gradient. Typical geothermal gradients range between 0.47 and 0.6°C per 30 m of depth; they are related to the thermal conductivity or resistivity of the rocks adjacent to the borehole and the heat flow from below. The geothermal gradient may be steeper in rocks with low intrinsic permeability than in rocks with high intrinsic permeability.

Thermal Gradient. The sensor in a temperature probe only responds to the fluid in its immediate vicinity. Therefore, in a flowing interval, measured temperature may be different from the temperature in adjacent rocks. Under these conditions, a thermal gradient will exist from the well outward. Only in a well where no flow has occurred for sufficient time to permit thermal equilibrium to be established does a temperature log reflect the geothermal gradient in the rocks. If vertical flow occurs in a well at a high rate, the temperature log through that interval will show little change. Vertical flow, up or down, is very common in wells that are completed through several aquifers or fractures that have different hydraulic head, although the flow rate is seldom high enough to produce an isothermal log. Movement

of a logging probe disturbs the thermal profile in the fluid column. Unless rapid flow is occurring, each temperature log will be different. High logging speed and large-diameter probes will cause the greatest disturbance. The most accurate temperature log is made before any other log, and it is recorded while moving slowly down the hole. Convection is a major problem in the interpretation of temperature logs, particularly in large-diameter wells and in areas of high thermal gradient. Convective cells in large-diameter wells can cause major temperature anomalies unrelated to groundwater movement (Krige, 1939).

Example. Identification of fractures producing groundwater from Triassic sedimentary rocks is illustrated in figure 387. The temperature log on the left shows several changes in gradient that are clearly defined by the computer-derived differential-temperature log. The caliper log suggests that water production may come from fractures; this interpretation is substantiated by the acoustic-televiewer logs on the right.

Movement of Injected Water

Temperature logs can be used to trace the movement of injected water (Keys and Brown, 1978). A sampling of several hundred temperature logs run during a 7--day recharge test in the high plains of Texas is shown in figure 388. Water from a playa lake was injected into an irrigation well, and logging was used to determine the movement of the recharge water and the extent of plugging of the Ogallala aquifer. Several monitoring holes were drilled and completed with 2-in steel pipe, capped on the bottom, and filled with water. The logs in figure 388 were of a monitoring hole located 12 m from the injection well. Most of the time, the water in the playa lake was warmer than the groundwater, and the lake temperature fluctuated several degrees each day. The passing of a cold front caused a marked decrease in temperature of the lake water. The first warm water was detected in the monitoring hole less than 4 hours after recharge started. The temperature logs indicated that the interval of highest permeability was located at a depth of approximately 50 m. Water did not arrive at a depth of 55 m until the third day. Diurnal temperature fluctuations and buildup of a recharge cone can be observed in figure 388. Data plotted in figure 389 were calculated from temperature logs of the same borehole; however, logs from other holes gave similar results. The solid line in the upper half of figure 389 shows the diurnal temperature fluctuations of the recharge water obtained from a continuous recorder on the recharge line. The other three lines represent fluctuations at three depths in the monitoring well, as obtained from temperature logs. The points shown by symbols represent the calculated center of the thermal waves. Travel times of the centers of the waves did not decrease during the life of the test, except possibly at the end. Test results show that the aquifer was not plugged by recharging water with a high content of suspended solids and entrained air, and the well yield was greatly increased.

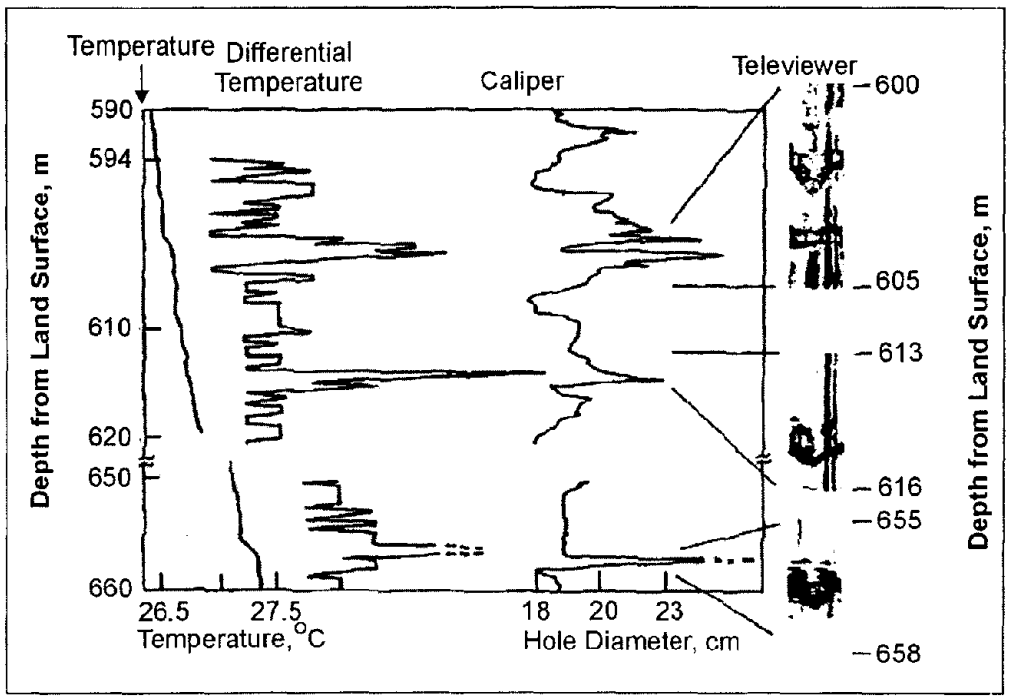

Figure 387. Temperature, differential temperature, caliper, and acoustic televiewer logs of Sears test well No 1, near Raleigh, NC.

Temperature logs can be used to trace the movement of water that has been injected from a tank that has been allowed to heat in the sun. In a similar fashion, temperature logs can be used to locate plumes of wastewater that result from injection if sufficiently different from the groundwater. Temperature logs also can be used to determine the location of cement grout outside of casing. The casing is filled with water, and the log usually is run within 24 hours of grout injection; however, anomalous temperatures may persist for several days.

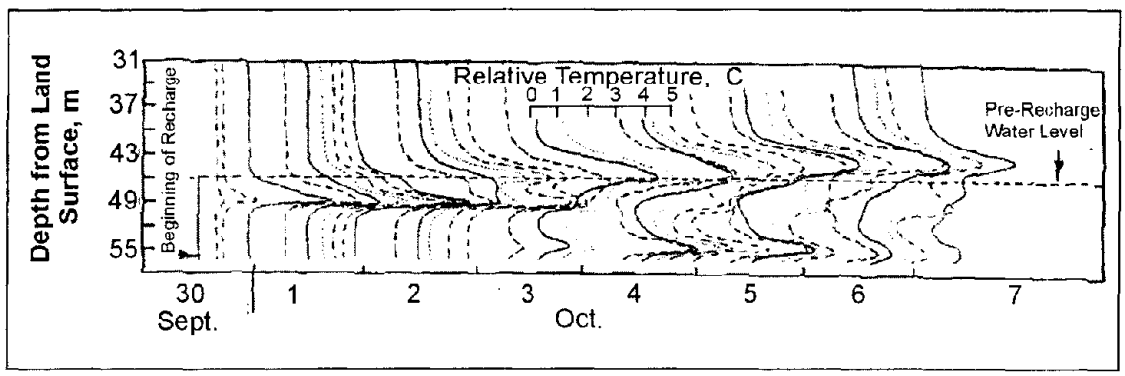

Figure 388. Selected temperature logs of a monitoring hole 12 m from a recharge well, high plains, Texas.

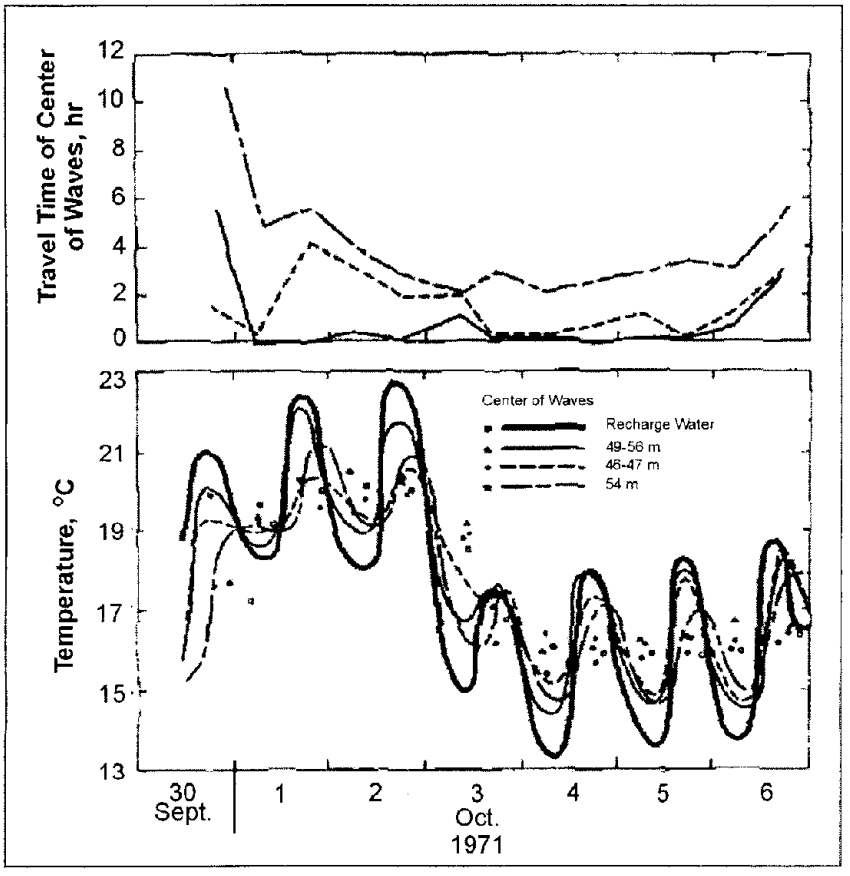

Figure 389. Diurnal temperature cycles and travel times, based on temperature logs of a monitoring hole 12 m from a recharge well.

10.4.4.4 Conductivity Logging

Basic Concept

Logs of fluid electrical conductivity, which is the reciprocal of fluid resistivity, provide data related to the concentration of dissolved solids in the fluid column. Although the fluid column may not reflect the quality of adjacent interstitial fluids, the information can be useful when combined with other logs. Fluid-conductivity or resistivity logs are records of the capacity of the borehole fluid that enters the probe to transmit electrical current. The probe should not be affected by changes in the conductivity of adjacent fluids or solid materials because it is constructed with the electrodes inside a housing. Ring electrodes are installed on the inside of a steel tube that is open at both ends, so water will flow through as the probe moves down the well. The electrodes are usually gold or silver to reduce changes in contact resistance caused by chemical reactions, and they are insulated from the steel housing. Conductivity is recorded in μmho/cm or μS/cm, which is equal to 10,000 divided by the resistivity in Ωm. Specific conductance is measured at the standard temperature of 25°C. Calibration usually is done empirically in solutions of known sodium chloride concentration, because most charts are based on this salt, and conversion factors are available to correct for the presence of other ions. The salinity of the calibration solution may be calculated by adding a known amount of salt to distilled water and converting to

conductivity, or by measuring with an accurate laboratory conductivity meter. Temperature of the calibration solution is recorded while the measurement is being made, and it needs to be uniform and stable. Onsite standardization may be carried out using several fluids of known concentration in plastic bottles sufficiently large to allow submersion of all electrodes in the probe. A laboratory conductivity cell or a less accurate mud resistivity kit also can be used. Disturbance of the fluid column in the borehole can make fluid-conductivity logs difficult to interpret. Disturbance of an equilibrium-salinity profile can be caused by the movement of logging probes or by convective flow cells. Because of the possibility of disturbance by logging, the most accurate fluid-conductivity log is made on the first trip down the well. This recommendation also pertains to temperature logs, so an ideal probe is capable of making simultaneous fluid-conductivity and temperature logs.

Data Interpretation

The interpretation of fluid-conductivity logs is complicated by the flow regime in a well. Unless the flow system is understood, analysis of the conductivity profile is subject to considerable error. Information on the construction of the well, flowmeter logs, and temperature logs are useful in the interpretation of conductivity logs. When both fluid conductivity and temperature are known, the sodium chloride concentration can be determined. Water samples must be analyzed to determine the concentrations of the various ions so corrections can be made.

Applications. Regional patterns of groundwater flow and recharge areas may be recognized from fluid-conductivity logs of the wells in an area. Fluid-conductivity data can be used to map and monitor areas of saltwater encroachment. Similarly, the logs can be used to monitor plumes of contaminated groundwater from waste-disposal operations. Commonly, chemical waste or leachate from solid-waste-disposal operations produces groundwater with a higher than normal conductivity. Conductivity logs provide the basis for selecting depths from which to collect water samples for chemical analyses. Fluid-conductivity logging equipment can be used to trace the movement of groundwater by injecting saline water or deionized water as a tracer. Small amounts of saline water may be injected at selected depths, and conductivity logs may be used to measure vertical flow in a single well, or larger amounts may be detected in nearby wells. Another important use for fluid-conductivity logs is to aid in the interpretation of electric logs. Spontaneous potential, single-point resistance, and many types of multi-electrode-resistivity logs are affected by the salinity of the fluid in the well.

10.4.5 Flow Logging

Basic Concept

The measurement of flow within and between wells is one of the most useful well-logging methods available to interpret the movement of groundwater and contaminants. Flow measurement with logging probes includes mechanical methods, such as impellers, chemical and radioactive tracer methods, and thermal methods (Crowder, Paillet, and Hess, 1994). Their primary application is to measure vertical flow within a single well, but lateral flow through a single well or flow between wells also may be recorded by borehole-geophysical methods.

10.4.5.1 Impeller Flowmeter

The most common logging probe used at the present time for measuring vertical fluid movement in water wells is the impeller flowmeter, which is a relatively inexpensive and reliable instrument. Most impeller flowmeters incorporate a lightweight three- or four-bladed impeller that rotates a magnet mounted on the same shaft. The magnet actuates a sealed microswitch, so that one or more pulses are impressed on low-voltage direct current that is connected across the switch. The impeller is protected from damage by a basket or housing, and the probe is centralized with bow springs, or similar devices, for best results. Baskets and impellers of different diameters are available and are easily changed, so the maximum size for a well can be used to increase sensitivity. Continuous logs of flow rate may be made at a constant logging speed and supplemented by more accurate stationary measurements at selected depths. The main shortcoming of impeller-type flowmeters is the lack of sensitivity to low-velocity flow. The most commonly used impeller flowmeters usually stall at vertical velocities of 1.2 to 1.5 m/min, although it is possible to measure velocities as low as one-half those velocities under some conditions. The addition of a packer or other flange-like device to divert most of the flow through the basket will improve sensitivity to low velocity, particularly in large-diameter wells.

Tracer Techniques

Tracer methods have been used in groundwater for many years, but only those that employ logging equipment are described here. Tracer techniques are useful at much lower velocities than impeller flowmeters; rates of about 1 m/day may be detected. The most commonly employed methods use a probe to follow the vertical movement of a chemical or radioactive tracer injected at selected depths in a well. An extension of this method may permit the detection of arrival of the tracer by logging adjacent wells. Radioactive tracers can be detected at lower concentrations than chemical tracers; most of them can be detected through casing. The difficulties in obtaining the permits necessary for using radioactive tracers have restricted their application. Temperature and fluid conductivity logs can also be used to measure flow rates between wells.

10.4.5.2 Heat-Pulse Flowmeters

A heat-pulse flowmeter originally was developed in England (Dudgeon, Green, and Smedmor, 1975). Its design was modified extensively, and a new probe was built by A. E. Hess of the U.S. Geological Survey (Hess, 1982). The modified version works reliably and has been used in wells to measure very low velocities. The logging system is shown schematically in figure 390, modified from Hess (1982). The wire heat grid, located between two thermistors, is heated by a 1-ms pulse of electric current, which is triggered from the surface. The heated sheet of water moves toward one of the thermistors under the influence of the vertical component of flow in the well. The arrival of the heat pulse is plotted on a chart recorder running on time drive, as illustrated in figure 391. A deflection of the recorder trace to the right indicates upward flow, and to the left, downward flow. The system is calibrated in flow columns of various sizes for flow in each direction, because the tendency for heated water to rise and the asymmetry of the probe produce slightly different calibration curves in the two directions. The USGS heat-pulse flowmeter can be used to measure vertical water velocities from 30 mm/min or less to 12 m/min or greater, and it has

advantages over both impeller flowmeters and tracer logging. An inflatable packer or flexible diverter can be attached to a flowmeter to force all flow through the probe and, thus, improve the performance of the heat-pulse flowmeter. A similar heat pulse flowmeter is now available commercially. A number of techniques have been tried for measuring horizontal flow in wells without much success or wide use. The technique may not provide an accurate estimate of average direction and velocity of flow in the aquifer because of the perturbations in the flow system caused by the well. A heat-pulse logging system has been developed for measuring horizontal flow (Kerfoot, 1982); it employs a series of paired thermistors located circumferentially around a heat emitter, and it is based on thermal transmission through an enclosing porous matrix of glass beads.

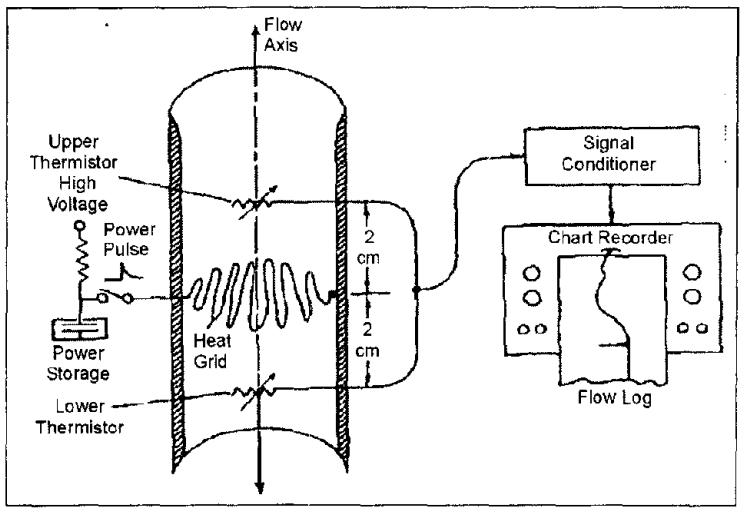

Figure 390. Equipment for making heat pulse flow meter logs. (Hess, 1982)

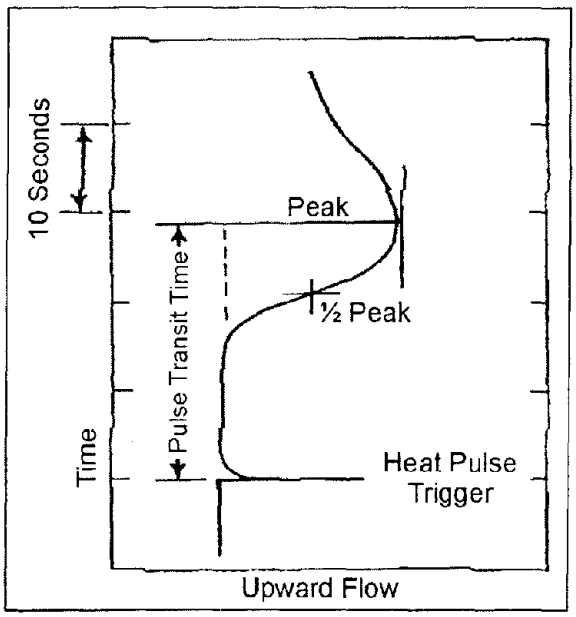

Figure 391. Analog record of a heat pulse from a thermal flowmeter. (Hess, 1982)

Data Acquisition

Calibration. Calibration of flow-measuring probes is done best in laboratory facilities designed for this purpose. Subsequent calibration checks and standardization may be carried out in a well under the proper conditions. The U.S. Geological Survey has designed and built a facility that is used for calibrating their flow-measuring probes (Hess, 1982). The test facility consists of clear plastic columns with inside diameters of 5, 10 and 15 cm (2, 4, and 6 in) connected to a pump that can circulate water in either direction at velocities from 21 mm/min to 15 m/min, depending on column size. Onsite standardization or calibration can be performed by moving the flowmeter up or down a cased portion of a well at carefully controlled logging speeds. Calibration by this method is only valid at the casing diameter logged. An example of this type of calibration is shown in figure 392, where the pulses per unit time are plotted against the logging speed. The two lines with different slopes represent opposite directions of impeller rotation. The range of tool speeds near this intersection represents the stall zone where the velocity is too low to turn the impeller. Theoretically, this intersection represents the velocity at which water was flowing up the well.

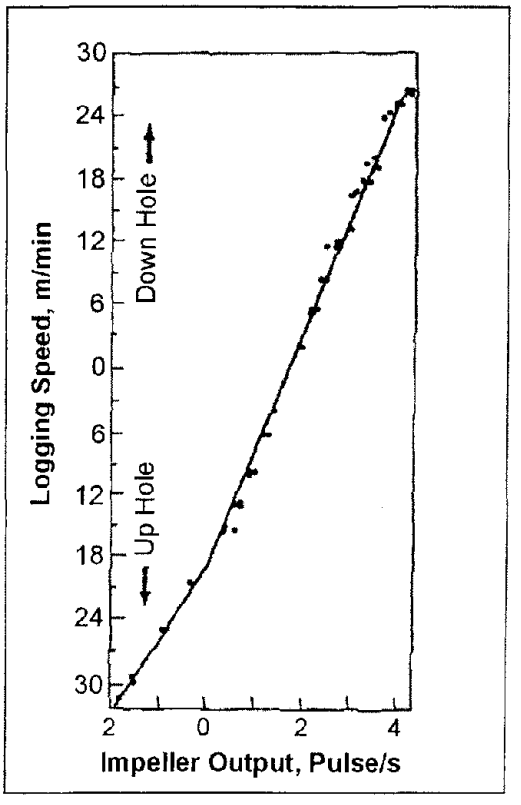

Figure 392. Calibration data for an impeller flowmeter.

10.4.6 Hydrophysical Logging

Fluid replacement and fluid-column conductivity logging, or "Hydrophysical" logging (Pedler, et al., 1990; Pedler, Head, and Williams, 1992; Tsang, Hufschmied, and Hale, 1990) involves fluid-column conductivity logging over time after the fluid column has been diluted or replaced with environmentally safe deionized water. Hydrophysical logging results are

independent of borehole diameter, and the method does not require a flow concentrating diverter or packer. The logging probe involves relatively simple and readily available technology and has a small diameter allowing it to be run through an access pipe below a pump. Hydrophysical logging is used to determine flow magnitude and direction during pumping and under ambient conditions, and to identify hydraulically conductive intervals to within one well bore diameter. Figure 393 is a schematic drawing of the equipment used to replace the borehole fluid with deionized water and to subsequently run a series of fluid conductivity logs to record the inflow of formation fluids.

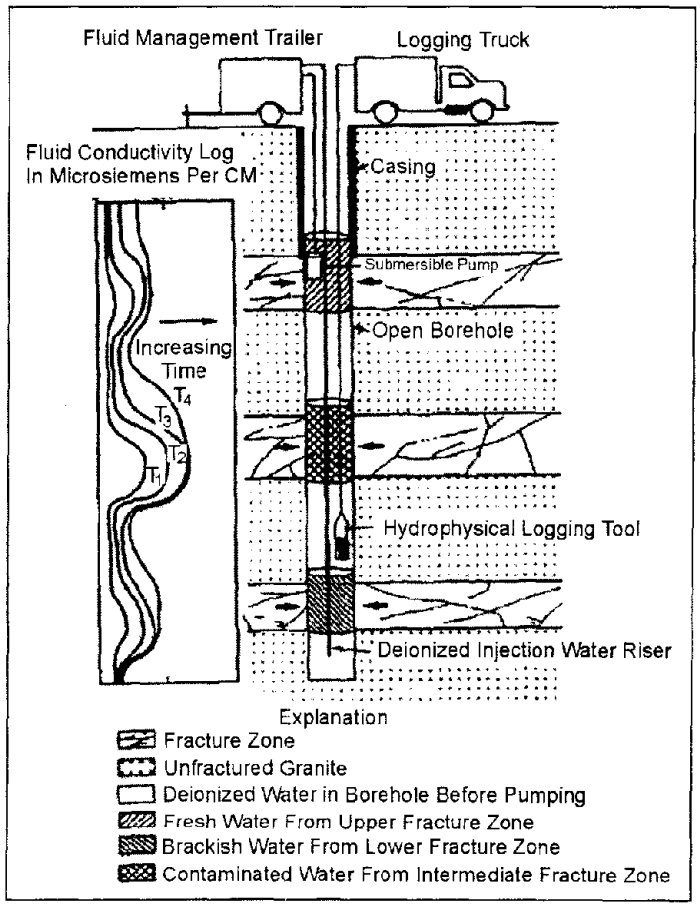

Figure 393. Schematic drawing of equipment used for hydrophysical logging after injection of deionized water; and time series of fluid conductivity logs. (Vernon, et al., 1993; copyright permission granted by Colog, Inc.)

Data Interpretation

Interpretation of flowmeter logs is simple if the probe has been properly calibrated and if all the essential information on hole diameter and construction is available. Vertical flow is common in most wells that are open to more than one aquifer, and flow can be induced by pumping or injecting water. The heat-pulse flowmeter developed by Hess (1982) was used first in the field to identify fractures producing and accepting water in granitic rocks (Keys, 1984). A caliper log and data from the heat-pulse flowmeter are shown in figure 394. Data from the heat-pulse flowmeter were quite reproducible over a period of 2 weeks, even

though pumping and injection tests being conducted in a well approximately 300 m from the logged well caused short-term changes. The flowmeter logs and acoustic-televiewer logs at this site enabled the characterization of permeable fractures. In figure 394, the upper fracture zone, at a depth of approximately 90 m, and the lower zone, at a depth of approximately 290 m, both contain thin, discrete fractures that are transmitting much of the water, rather than thicker, complex fractures within each zone. Note that slightly less than half of the flow from the upper zone originates in the fracture at a depth of 94 m, although that fracture appears to be the widest on the caliper log. Similarly, the fracture that appears to be the largest in the lower zone is accepting only a small percentage of the flow. Acoustic-televiewer logs indicated that the same two fracture zones were intersected in other wells in the area and appear to constitute major aquifers. Paillet, Crowder, and Hess (1994) present a detailed description of how the heat-pulse flowmeter, in combination with acoustic-televiewer logs, can be used to characterize the hydraulic properties of fracture systems that intersect multiple drill holes.

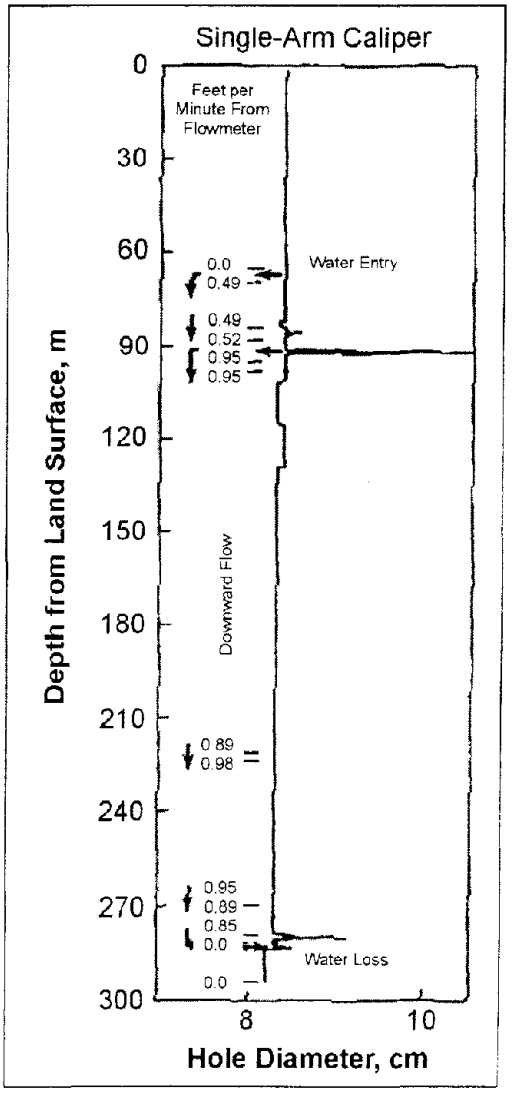

Figure 394. Single arm caliper log on the right and data from heat pulse flowmeter showing zones of water entry and exit.

Data Interpretation

Finite Difference Modeling Software. A critical element in the application of hydrophysical logging compared to established conductive tracer technology is the development of finite difference modeling software routines to simulate the data obtained in the field. This software also permits the calculation of permeability. The method can also be expanded to measure other properties such as water temperature and pH, to determine the properties of the formation water entering the borehole. Therefore, fluid replacement logging can indicate the quality and physical properties of water entering the borehole along with the magnitude and direction of flow. In theory, there are no upper or lower limits to the magnitude of flow that can be detected. Published field studies demonstrate that the technique has achieved better low-flow resolution than that reported with other flow measurement techniques (Vernon, et al., 1993).

10.4.7 Well-Completion Logging

Logging to determine the construction of a well is useful to plan for cementing operations, installation of casing and screens, hydraulic testing, and guiding the interpretation of other logs. Most of the logs described in other sections of this manual can provide information on well construction under some conditions. They will be listed briefly here so the reader can refer to the detailed descriptions of these logs in the appropriate sections of this manual.

10.4.7.1 Casing Logging

A number of different types of logs can be used to locate cased intervals in wells. Most electric logs will show a sharp deflection at the bottom of a string of steel casing. Resistivity-logging systems that are operating properly will record zero resistivity when all the electrodes are in the casing. Gamma-gamma logs commonly demonstrate a sharp deflection at the bottom of the casing and may shift at depths where a second string of casing is located outside the first; however, such shifts may be difficult to distinguish from changes in hole diameter. High-resolution caliper logs are excellent for locating the bottom of the inside string of casing and threaded couplings. If small arms are used, they also may provide data on casing corrosion and the location of screens and perforations. Care must be taken to assure that the arms do not get caught in screens or perforations.

The acoustic-televiewer is one of the highest resolution devices for obtaining information on casing and screens, but it may be too expensive for some operations. The televiewer must be operated on the mark switch in steel casing, rather than magnetometer, to avoid distortion of the log caused by random triggering. Televiewer logs can provide clear images and accurate locations of screens, perforations, couplings, and damaged casing. Features as small as 1 mm can be resolved under the right conditions. Borehole television can provide some of the same data, but a hard copy of the log is not available for examination at any time. The water in the well also must be clear to allow light transmission.

The casing-collar locator (CCL) is a useful and relatively inexpensive device that can be operated on any logging equipment. The simplest CCL probe contains a permanent magnet wrapped with a coil of wire. Changes in the magnetic properties of material cutting the magnetic lines of flux cause a small DC current to flow, which can be used to drive a

recorder channel. The standard mode of operation is to record event marks along the margin of other logs to represent the location of collars in the casing. The event marker is adjusted so that it is triggered when the DC voltage exceeds a certain level. A continuous-collar log can be interpreted in terms of the location of perforations and screens. Corroded casing sometimes can be located by a high-resolution caliper log; spontaneous-potential logs have been used to locate depth intervals where active corrosion is taking place (Kendall, 1965). Commercial logging services are available for detecting corroded casing. An electromagnetic casing inspection log measures changes in the mass of metal between two coils; loss of mass may be due to corrosion (Edwards and Stroud, 1964). A pipe-analysis survey is run with a centralized probe that employs several coils (Bradshaw, 1976). This survey is reported to provide information on the thickness of casing penetrated by corrosion, whether the damage is internal or external, and isolated or circumferential. The electromagnetic-thickness survey measures the average casing thickness over an interval of about 0.6 m and can be used to monitor changes in thickness with time. Casing-inspection logging methods are summarized by Nielsen and Aller (1984).

10.4.7.2 Logging Annular Materials

The location of cement, bentonite, and gravel pack in the annular space outside of casing can be accomplished with several logs, but the interpretation may be ambiguous. A caliper log made before the casing is installed is important to planning cementing or installation of gravel pack. Caliper logs also are useful in interpreting logs run for the purpose of locating annular material, because they indicate the thickness that would be present.

Temperature logs can be used to locate cement grout while it is still warm from setup reactions. Cement-bond logs can be used to locate cement after it has cured, and they may provide information on the quality of the bond between casing and cement and between cement and rock. Uncompensated, short-spaced gamma-gamma logs can indicate the location of cured cement or gravel pack, if a gamma-gamma log was run after installing the casing and prior to filling the annular space; the difference between the two logs may show the filled interval clearly. The pre-cementing gamma-gamma log may resemble the reversed caliper log made prior to installation of the casing. The location of bentonite often is indicated by an increase in radioactivity on gamma logs; however, all bentonite is not more radioactive than the various background materials that might be present.

Acoustic cement bond logging was developed for annular cement evaluation in oil and gas production wells (Bateman, 1985). The interpretation of cement bond logs involves the analysis of the amplitude of the compression wave arrival, and the full waveform display. Where pipe, cement, and formation are well bonded, the full waveform display indicates that the acoustic energy from the logging probe is being transmitted to the formation (a formation response is evident). Furthermore, for the case of continuous cement in the annular space with no voids or channels, the compression wave amplitude is a minimum, increasing where the cement is discontinuous.

A quantitative method employing gamma-gamma density logs calibrated for backfill materials is shown in figure 395 (Yearsley, Crowder, and Irons, 1991). Below the water surface, the saturated sand pack is indicated by a far detector measurement of 1.9 g/cc, and a near detector measurement of 1.7 g/cc, values that were confirmed by physical modeling.

The difference in densities between the near and far detectors is due to the greater effect of the low-density PVC on the near detector. The bentonite slurry seal is less dense than the sand pack, and is readily recognized on the geophysical log, but appears to be 3-2/3 m thick rather than the 1-1/2 m specified on the completion schedule. The water surface is identified by an increase in the 4π count rate above a depth of 40 m. Also, note at the water surface, the low densities registered by the near and far detectors and high count rate anomaly on the 4π log, which indicate a washout at that depth. The cement/bentonite grout below the water surface may be indicated by far detector densities greater than 2.0 g/cc, and near detector densities of approximately 1.8 g/cc. The distinct density contrasts above the water surface in figure 395 result from the density differences among grout, unsaturated alluvium, and air voids. Air voids behind the pipe on this log are identified by densities of approximately 1.0 g/cc for both the near and far detectors. Grout above the groundwater surface is interpreted for far detector densities ranging between 1.6 and 2.0 g/cc. The range in density is due primarily to variations in grout thickness. Unsaturated alluvium is indicated by far detector densities between 1.4 and 1.6 g/cc. On the left of figure 395 is a "4π grout line," which indicates the expected 4π count rate in a 10 cm (4-in) PVC air-filled pipe with 6:2 cement:bentonite grout behind the pipe.

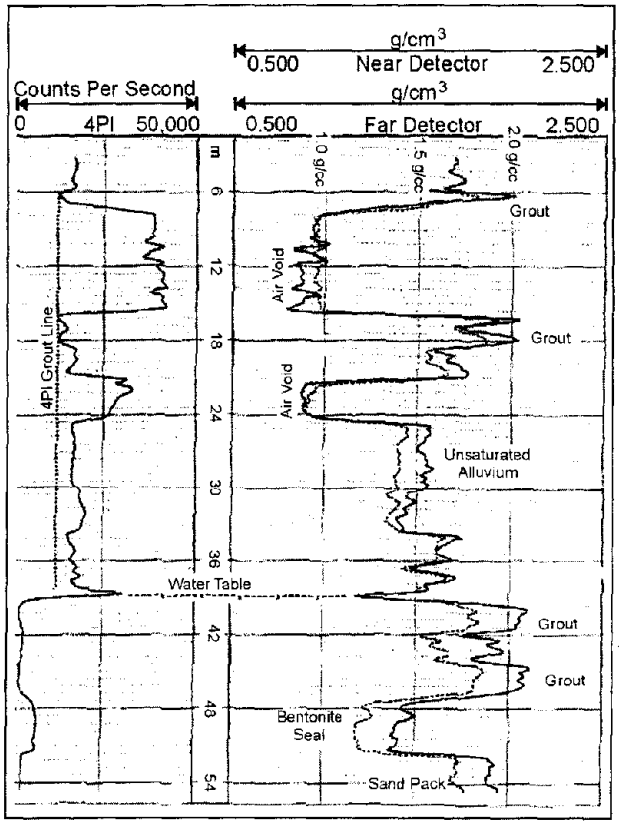

Figure 395. Dual spaced and 4π density logs in a cased monitoring well showing completion as interpreted from the logs. (Yearsley, Crowder, and Irons, 1991; copyright permission granted by Colog, Inc.)

10.4.7.3 Borehole-Deviation

Deviation of drill holes and wells from the vertical is common; it affects proper completion of the well for its intended use, and it may prevent testing and logging. Casing and pumps may be impossible to install in a well that is highly deviated, and centralized logging probes may not function properly in such a well. The deviation seldom is consistent, so that both the angle from the vertical and direction may change rapidly along the borehole. Even auger holes less than 30 m deep have deviated enough that transmittance logs between the holes are adversely affected. Information on borehole deviation is needed to calculate the true vertical depth to features of interest and to correct the strike and dip of fractures or bedding obtained from such logs as the acoustic televiewer.

Continuous logs of hole deviation usually are run by companies that specialize in this technique. Hole-deviation data usually are not recorded by standard logging equipment, except modern dipmeters, which rarely are included on small loggers. A dipmeter log usually includes a continuous record in the left track of the azimuth (magnetic north) and the amount of deviation. Some hole-deviation services provide a printout of azimuth and deviation at predetermined depth intervals, and there are several methods to mathematically describe the path of the deviated hole from these measurements (Craig and Randall, 1976).

10.4.8 Hole-to-Hole Logging

10.4.8.1 Crosshole Seismic/Sonic Logging Survey

Basic Concept

Crosshole Sonic Logging (CSL) uses compressional seismic waves as the energy source. Seismic waves passing through concrete are influenced by the density and elastic modulus of the concrete. Fractured or "weak" concrete zones lower the velocity of the seismic waves and can, therefore, be detected. In addition, the amplitude of a seismic pulse is affected by these defects although this is not extensively used at the present time. The frequency content of the seismic energy pulse determines the resolution and penetration of the signal. High frequencies have high-amplitude attenuation but can image small targets. Conversely, lower frequencies have less attenuation but image larger targets. The seismic source produces an impulse whose frequency content is usually 30 to 40 kHz.

The CSL method is a "derivative" of the ultrasonic pulse velocity (UPV) test. The basic principle of the CSL test is that ultrasonic pulse velocity through concrete varies proportionally with the material density and elastic modulus. A known relationship between fractured or weak zones and measured pulse velocity and signal attenuation is fundamental for these tests. Research has shown that weak zones reduce velocities and increase attenuations. During the CSL measurements, the apparent signal travel time between transmitter and receiver are measured and recorded. By measuring the travel times of a pulse along a known distance (between transmitter and receiver), the velocity can be calculated as a function of distance over time. If a number of such measurements are made and compared at different points along the concrete structure, the overall integrity of the concrete can be

assessed. The first-arrival travel times (FAT) recorded during CSL testing are known as compressional, primary, longitudinal, or P-wave arrivals. The P-wave is the wave having discrete particle motion in the same direction as the wave is moving. The surface of the constant phase, or the surface on which particles are moving together at a given moment in time, is called the wavefront. An imaginary line perpendicular to the wavefront is called a ray path. It is often assumed that a beam of produced ultrasonic energy travels along the ray path (Robert E. Sheriff and Lloyd P. Geldart, 1995). Basic elements of the emitted wave during CSL testing are presented in figure 396.

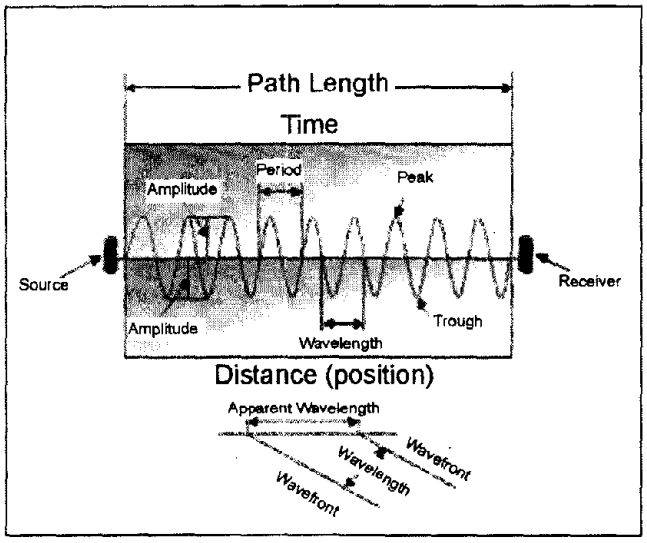

Figure 396. Basic wave elements.

The following are definitions of terminology used with CSL analyses (Robert E. Sheriff, 1978):

- *wavelength* (l) - distance between successive repetitions of a wavefront,
- *amplitude* (A) - maximum displacement from equilibrium,
- *period* (T) - time between successive repetitions of a wavefront,
- *frequency* (f) - number of waves per unit time,
- *velocity* (V) - speed at which a seismic wave travels, proportional to the frequency and wavelength ($V=f\lambda$),
- *apparent wavelength* - distance between successive similar points on a wave measured at an angle to the wavefront,
- *apparent velocity* - product of frequency and apparent wavelength.

Velocity of the P-wave in homogenous "isotropic" media is related to the modulus and density of the medium through which the wave travels and is given as:

$$V_p = \sqrt{\frac{\left(4/3\right)\mu + k}{\rho}}, \tag{88}$$

where

V_p = velocity of the P - wave,

ρ = density of the medium through which the wave travels,

$k = \frac{E}{3(1-2\nu)}$, bulk modulus of the medium through which the wave travels,

$\mu = \frac{E}{2(1+\nu)}$, shear modulus of the medium through which the wave travels,

ν = Poisson's ration of the medium.

The P-wave velocity can then be written as:

$$V_p = \sqrt{\frac{E(1-\nu)}{(1-\nu)(1-2\nu)}}, \tag{89}$$

where

E = dynamic elastic modulus or Young's modulus.

During CSL analysis, the first arrival times of the P-wave are picked using an automated picker within the CSL software, and the pulse velocity can be calculated as follows:

$$Pulse\ Velocity = \frac{Path\ Length}{Transit\ Time}. \tag{90}$$

For accurate results, it is recommended that the path lengths and transit times be measured with a precision greater than 1%. Although pulse velocity varies with different concrete mixes, the average pulse velocity of typical concrete is approximately 3,600 m/s. Knowing the linear distance between transmitter and receiver (path length), and the pulse transit time (first arrival time of the P-wave), the pulse velocity can then be calculated. If the CSL access tubes are not installed in a near-vertical position and/or the distance between them varies significantly along the length of the shaft, errors in velocity calculations may occur, and the results may be misleading.

The seismic wavelength can be calculated based on the known frequency of the transmitted signal and the calculated pulse velocity as shown in table 20.

Table 20 suggests that the higher the transmitted frequencies used during CSL testing, the shorter the wavelength, allowing for the detection of smaller defects. However, the tradeoff is that the higher the source signal frequency, the greater the signal absorption and the shorter the wavelength. This implies that if higher frequencies are used during the CSL testing, more accurate detection of small defects is permitted, but signal absorption will also be high, limiting the penetration range of the method. Frequencies in the range between 30 kHz and 40 kHz are commonly used for CSL tests.

Table 20. Numerical relationship between path length, transit time,frequency, period, velocity, and wavelength.

Path length, m	Transit time, s	Frequency, kHz	Period (1/frequency), s	Velocity (path length/ Transit time), m/s	Wave length (velocity/ frequency), m
0.6 m	0.00016 s	35 kHz	0.000028 s	3750 m/s	0.1 m
0.6 m	0.00016 s	50 kHz	0.00002 s	3750 m/s	0.075 m
0.6 m	0.00024 s	35 kHz	0.000028 s	2500 m/s	0.071 m
0.6 m	0.00024 s	50 kHz	0.00002 s	2500 m/s	0.05 m

The energy of an ultrasonic wave is a measure of the motion of the medium as the wave passes through it. Energy per unit volume is called energy density (Robert E. Sheriff and Lloyd P. Geldart, 1995). A wave passing through a medium possesses both kinetic and potential energy. Because the medium oscillates as the wave passes through it, energy is converted back and forth from kinetic to potential forms, but the total energy remains fixed. When the particle has zero displacement, the kinetic energy is maximum, and potential energy is zero. Conversely, when maximum displacement of the particle occurs, the kinetic energy is zero, and the total energy is all potential energy. When the total energy equals the maximum value of the kinetic energy, the energy density for a harmonic wave is proportional to the first power of the density of the medium and to the second power of the frequency and amplitude as shown in the following equation:

$$E = 2\pi^2 \rho f^2 A^2, \tag{91}$$

where

E = total energy,

ρ = density,

f = transmitted frequency,

A = wave amplitude.

Data Acquisition

Figure 397 illustrates the CSL method. At least two drill holes, usually having a diameter of 50 mm, are required. The number of access tubes depends on the diameter of the shaft, and is shown in table 21.

Table 21. Required number of access tubes versus shaft diameter.

Shaft Diameter (D)	Recommended Number of Tubes	Tube Spacing, deg.
D < 2.5ft (0.76 m)	2	180
2.5 (0.76 m) < D < 3.5ft (1.07m)	3	120
3.5 ft (1.07 m) < D < 5.0 ft (4.52 m)	4	90
5.0 (1.52 m) < D < 8.0 ft (2.43 m)	6	60
8.0 (2.43 m) < D	8	45

For existing shafts, coreholes must be drilled to allow access for the CSL transmitter and receiver.

The access tubes are cased with either steel or schedule 40 PVC, and are securely tied to the rebar cage in a nearly vertical orientation before construction. Special care must be taken when installing access tubes to avoid debonding between the concrete and the tubes. Poor bonding between access tubes and concrete, or delamination, can cause complete signal loss. Since defects can also cause complete signal loss, poor bonding can be misinterpreted as a defect. The tubes must be filled with water before the survey is conducted. One of the tubes is used for the seismic transmitter and the other for the seismic receiver. These can be oriented such that the path between them is horizontal (zero offset, as seen in figure 399) or with some offset. Zero offset logging is called Crosshole Sonic Logging. Readings are taken at regular intervals down the shaft while maintaining the same offset. Defects are observed as a reduction in the travel time of the seismic wave from the transmitter to the receiver. It is important that the tubes are vertical and that the distance between them is constant for their entire length. If this is not the case, then the seismic travel time differences may result from these distance differences rather than defects in the concrete. In addition, unrecognized distance differences in the distance between tubes may result in false interpretations of defects.

Other variations in the geometric configuration are also used. These include the source and receiver lowered into the same tube, a source and multiple receivers lowered into separate holes, and a single source and single receiver lowered into adjacent holes, as described above. The most commonly used configuration is the later one.

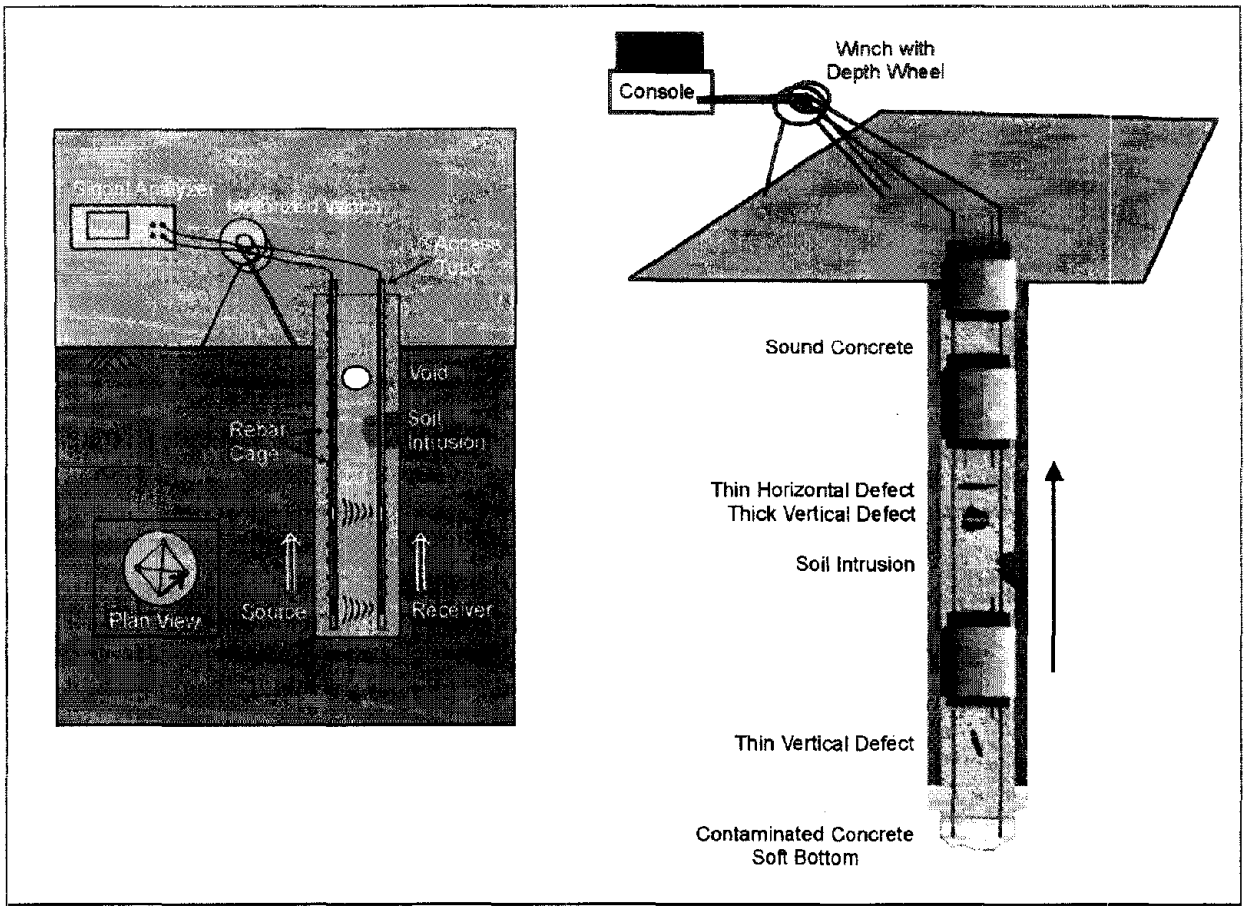

Figure 397. Crosshole Sonic Logging method with various kinds of defects/anomalies. (Blackhawk GeoServices, Inc.)

Figure 397 shows the CSL method and the ray paths. Common defects are also shown, illustrating their influence on the seismic wave travel times.

Data Processing

The received data have to be plotted and presented such that any defects in the shaft are clearly observed. Figure 398 shows a typical CSL travel time plot. If only two access tubes are available and only one offset between the transmitter and receiver is used, then any anomalies may exist anywhere between the two tubes, and it is difficult to determine the geometry and exact location of the anomaly with respect to the tube location. However, if data are collected with several different offsets between the transmitter and receiver, then a more definitive location can be given for any anomalies.

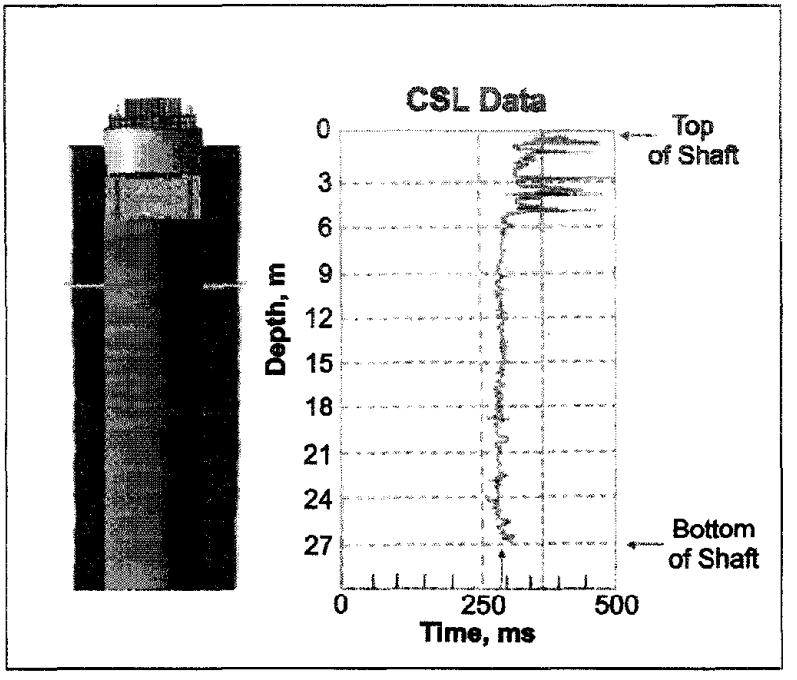

Figure 398. Travel time plot for a Crosshole Sonic Logging log. (Blackhawk GeoServices, Inc.)

10.4.8.2 Crosshole Seismic/Sonic Tomography Survey

Basic Concept

If more drilled holes are available in the shaft, then CSL can be conducted using these holes, producing a better definition of the location of the defects. Recording readings from a number of offsets also helps to define the location of an anomaly. Data recording with two holes and a constant source-receiver offset is called CSL. If a number of offsets between the source and receiver are used, then tomographic calculations can be done and the method is called CSL Tomography (CSLT). The probes (source (S) and receiver (R)) are lowered to the bottom of a tube pair. Before the logging begins, one of the probes (e.g., the receiver) is lifted or lowered a specific offset distance (or angle) above or below the source level (respectively). Both probes are then pulled simultaneously up to maintain that offset distance. When the receiver is above the source, the records are defined as "positive" offset data. Conversely, when the receiver probe is lower than the source level, the records are defined as "negative" offset data. The offset, either positive or negative, is maintained during that logging run.

Use of multiple tubes and these multiple vertical offsets creates the ability to produce true 3-D tomographic images of an entire shaft. Figure 399 illustrates the different data recording geometries for CSL and CSLT. Tomographic calculations can also be done when more than one pair of holes is logged.

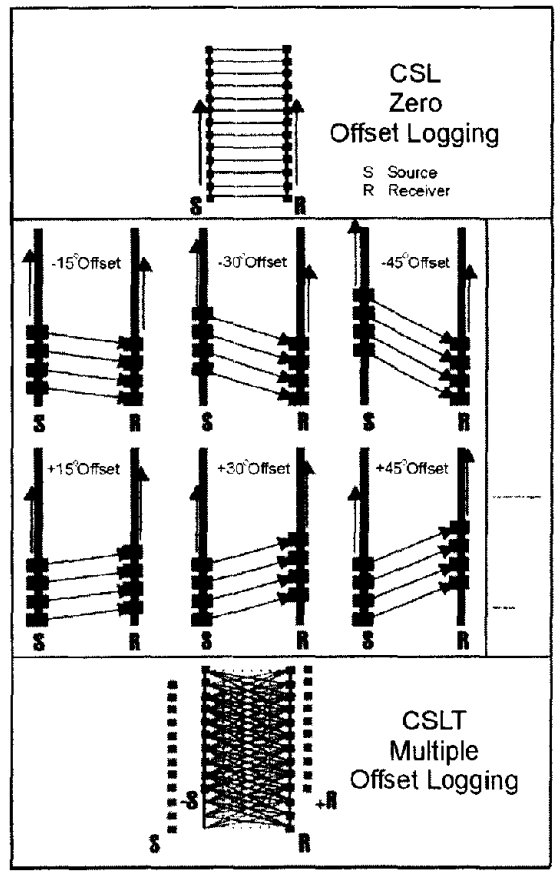

Figure 399. Ray paths for Crosshole Sonic Logging and Crosshole Sonic Logging Tomography; S-source, R-receiver. (Blackhawk GeoServices, Inc.)

Figure 400 illustrates the results of a CSL survey compared to a CSLT survey. The two drawings on the left side of the figure show the ray paths for the CSL and CSLT systems. The third drawing shows the location of the defects in the shaft, and the fourth drawing illustrates the results of the CSL survey. As can be seen, the top and bottom of the defect are observed. However, it is not possible to identify the exact location of the source of the anomaly from the CSL data. However, with the CSLT data, it is possible to identify to a much greater extent, the location of the source of the anomaly.

Limitations

Probably the most important item is to make sure that the access tubes are vertical and bonded to the concrete. The seismic source must be capable of generating the high frequencies required to provide detailed images of any defects.

Currently this method cannot be used to image defects between the access tubes and the edge of the concrete shaft. However, research is currently being done to rectify this problem using CSLT.

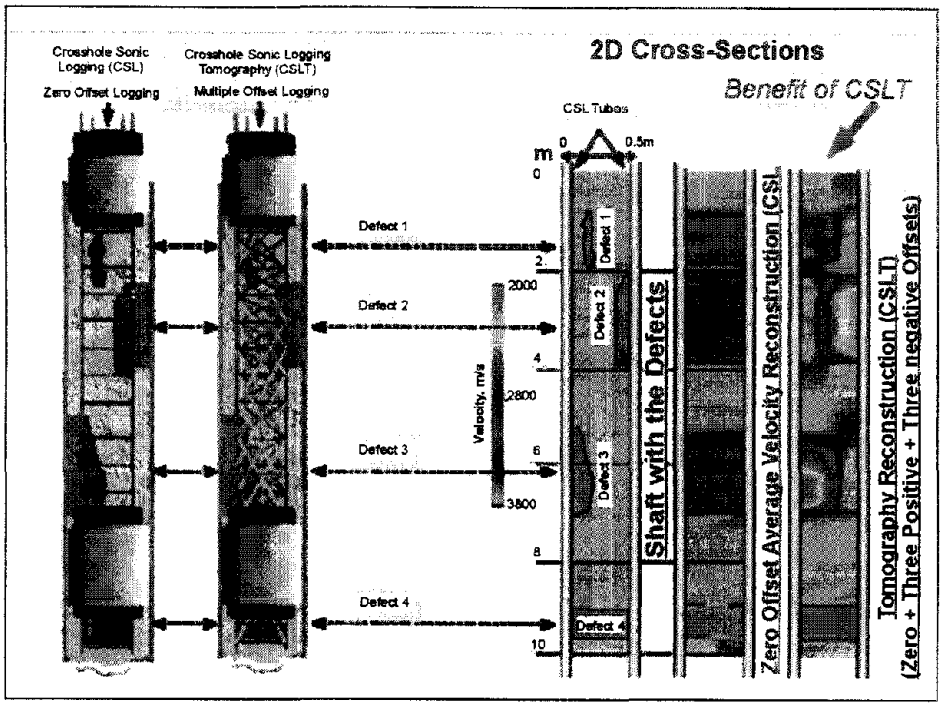

Figure 400. Comparison of Crosshole Sonic Logging and Crosshole Sonic Logging Tomography results. (Blackhawk GeoServices, Inc.)

BIBLIOGRAPHY

PART I

CHAPTER 2

Depth of Foundations

Anthony, R., and Pandy, A., 1996. Determining the Length of Timber Piles in Transportation Structures." Engineering Data Management, Inc.
www.fpl.fs.fed.us/documnts/PDF1996/Antho96a.pdf

Dix, G., Dynamic Analysis in Geotechnical Engineering. Course Notes -CEE6442,Georgia Institute of Technology.
www.courses.ce.gatech.edu/200202/CEE6442A/Course_Notes/Nondestructive%20Testing.pdf

FDH Website. www.fdh-inc.com/FDH_inc/FDH_Pile_Testing.pdf

Finno, R.J., 1997. Parallel Seismic Evaluation of the NDE Test Section at the National Geotechnical Experimentation Site at Northwestern University. Final Report to the Infrastructure Technology Institute.
http://iti.acns.nwu.edu/projects/NDE/pse_index.html#contents

Finno, R.J., and Prommer, P.J., 1994. Evaluation of Inaccessible Drilled Shafts Using the Impulse Response Method. www.iti.northwestern.edu/pubs/tr3.html

Infraseis, Inc. Web Site. Parallel Seismic. http://www.infraseis.com

Infraseis, Inc. Web Site. Ultraseismic Test Methods, http://www.infraseis.com/ust.htm

Infraseis, Inc. Web Site. Borehole Radar. www.infraseis.com/radar0.htm

Mercado, E., and J. McDonald, 2002. Two New Non-destructive Methods to Measure Scour Depth and the Depth of Unknown Foundations. Paper in Proceedings of Geophysics 2002, American Society of Civil Engineers, Los Angeles, CA.

Morgano, C.M., 1996, Determining Embedment Depth of Deep Foundations using Non-destructive Methods. www.web.pile.com/Education/698/default.asp?company=PDI

Nazarian, S., and J. Diehl, 2000. Use of Geophysical Methods in Construction. Paper in Proceedings of GEO-DENVER 2000, American Society of Civil Engineers, Denver, CO.

New York State Department of Transportation, Geotechnical Engineering Bureau, 2000. Drilled Shaft Inspector's Guidelines. GEM-18.
www.dot.state.ny.us/tech_serv/geo/dsiman1a.pdf

Olson Engineering Web Site. Sonic Echo/ Impulse Response. www.olsonengineering.com/SEIR.html

Olson, L., Jalinoos, F., Aouad M. Determination of Unknown Subsurface Bridge Foundations, Transportation Research Board, National Cooperative Highway Research Program (NCHRP) Project 21-5, Final Report, August 1995.

Rausche, F., G. Likins, and Shen Ren Kung, 1992. Pile Integrity Testing and Analysis. Proceedings of the Fourth International Conference on the Application of Stress-Wave Theory to Piles, The Netherlands. http://web.pile.com/Education/645/default.asp?company=GRL

Stegman Engineering Web Site. Length Determination or Integrity Testing. http://www.stegmanengineering.com/geotech.htm#Pile/Caisson

Socketing

Dong-Soo Kim, Hyung-Woo Kim, 2000. Impact Echo Response of Rock Socketed Drilled Shafts. Paper in Proceedings of First International Conference on the Application of Geophysical Methodologies & NDT to Transportation Facilities and Infrastructure, St. Louis, MO. www.modot.state.mo.us/g2000/PAPERS/CAT4/GEOPH38.PDF

Finno, R.J., 1997. Parallel Seismic Evaluation of the NDE Test Section at the National Geotechnical Experimentation Site at Northwestern University. Final Report to the Infrastructure Technology Institute. http://iti.acns.nwu.edu/projects/NDE/pse_index.html#contents

Oklahoma Department of Transportation, 2000. Design of Rock Socketed Drilled Shafts. http://www.dot.state.oh.us/divplan/research/FY03ProblemStatements/DrilledShafts.pdfm

Integrity Testing

Amir, J., 2002. Single-tube Ultrasonic Testing of Pile Integrity. http://www.piletest.com/papers/shut/Orlando2002.htm

Electrical and Magnetic Methods of Nondestructive Testing. 2nd edition, Book, http://www.normas.com/ASNT/pages/447.htm

Finno, R.J., 1997. Parallel Seismic Evaluation of the NDE Test Section at the National Geotechnical Experimentation Site at Northwestern University. Final Report to the Infrastructure Technology Institute. http://iti.acns.nwu.edu/projects/NDE/pse_index.html#contents

Finno, R.J., and P. Champy, 1997. Cross-hole Sonic Logging Evaluation of Drilled Shafts at the Northwestern University National GeoTechnical Experimentation Site. Final Report to the Infrastructure Technology Institute. http://www.iti.northwestern.edu/projects/NDE/

Hanna, K., K. Haramy, A. Rock, and B. Hoekstra, 2000. Three-Dimensional Tomographic Imaging for Deep Foundation Integrity Testing. Paper in Proceedings of First International Conference on the Application of Geophysical Methodologies & NDT to Transportation Facilities and Infrastructure, St. Louis, MO.
http://www.modot.state.mo.us/g2000/PAPERS/CAT4/GEOPH54.PDF

Haramy, K.Y, and N. Mekic-Stall, 2000. Cross-hole Sonic Logging and Tomographic Imaging Surveys to Evaluate the Integrity of Deep Foundations – Case Studies. FHWA.
www.cflhd.gov/CSL-Tomo.

Haramy, K.Y, and N. Mekic-Stall, 2000. Evaluation of Drilled Shafts at Piney Creek Bridge using Cross-hole Sonic Logging Data and 3D Tomographic Imaging Method. Paper in Proceedings of First International Conference on the Application of Geophysical Methodologies & NDT to Transportation Facilities and Infrastructure, St. Louis, MO.
www.modot.state.mo.us/g2000/PAPERS/CAT4/GEOPH49.PDF
Impact-Echo Instruments, LLC. Web Site. www.impact-echo.com
InfraSeis, Inc. Web Site. www.infraseis.com/ust.htm

Innovative Technology Summary Report, DOE/EM-0538. Electrical Resistance Tomography for Subsurface Imaging. http://apps.em.doe.gov/ost/pubs/itsrs/itsr17.pdfm

Iskander, M., D. Roy, 2001. Class-A Prediction of Construction Defects in Drilled Shafts. Transportation Research Board, Session on Drilled Shaft Capacity & Defects in Varved Clay.

Jalinoos, F., 1995 Ultrasonic Cross-hole and Crossmedium Tomography for the Detection of Defects in Structural Concrete. Paper in Proceedings of SAGEEP '95, Orlando, FL.

Natural Resources Canada, 2002. Spectral Gamma-Gamma, Geological Interpretation of Density and Spectral Gamma-Gamma (SGG) Logs. http://borehole.gsc.nrcan.gc.ca/sgg_e.html

Olson Engineering, Inc. Web Site. Cross-hole Sonic Logging.
http://www.olsonengineering.com/CSL.html

Olson Engineering, Web Site. Sonic Echo/ Impulse Response.
www.olsonengineering.com/SEIR.html

Olson Instruments, Inc Web Site. Single Hole Sonic Logging.
http://www.olsoninstruments.com/site/csl.html

Research and Technology Transporter, Federal Highway Administration, 2001. New CSL Method Makes Process More Accurate. K. Y. Haramy.
http://www.tfhrc.gov/trnsptr/jan01/jan01.pdf
Rucker, M., M. Verquer, 2002. Gamma Density Logging of Drilled Shafts - Some Observations and Interpretations. Paper in Proceedings of Geophysics 2002, Los Angeles, CA.

Sample Specifications for Crosshole Sonic Logging (CSL).
www.web.pile.com/download/docs/csl.rtf

Test Method Review- A Comparison of Gamma-gamma and Cross-hole Sonic Logging.
http://members.aol.com/ndtman1/papers/gammacsl.zip

Rebar Quality

ACI Committee 222, 1996. Corrosion of Metals in Concrete. Publication ACI 222.R-96,
http://www.civil.uwaterloo.ca/soudki/222r-96.pdf

Berke, M., 2000. Nondestructive Materials Testing with Ultrasonics, Introduction to Basic Principles. NDT.net, September 2000, Vol. 5, No. 09.
http://www.ndt.net/article/v05n09/berke/berke1.htm

Branagan and Associates Inc., Nondestructive Testing Service for Assessing Cast-in-Place Concrete Columns, www.branagan.com/pdf_files/B&A_CSL%20Services.pdf,

Corrosion Doctors Website, http://www.corrosion-doctors.org

Corvib Web Site, http://www.corvib.com/concrete/canin.htm

Electrochemical Impedance Spectroscopy Theory: A Primer.
www.gamry.com/G2/Appnotes/Reference/EISTheory/Theory/EIS_Theory.htm

Gannon, E. and Cady, P., 1992, Condition Evaluation of Concrete Bridges Relative to Reinforcement Corrosion, Strategic Highway Research Program; SHRP_S/FR-92-103.
http://gulliver.trb.org/publications/shrp/SHRP-S-330.pdf

Germann Website. http://www.germann.org/products/power.htm

Halfcell Potential Testing. MGA web site, www.mg-assoc.co.uk/halfcell.htm

Introduction to Corrosion Monitoring. http://www.alspi.com/corrosion(intro).pdf

KH Design and Development Web site. www.khdesign.co.uk/techniquesindex.htm

Klinghoffer, O., 1995, In situ Monitoring of Reinforcement Corrosion by Means of Electrochemical Methods. Nordic Mini Seminar; Lund.
http://www.germann.org/download/nordic_concrete_95.pdf

Lamtenzan, D., Washer, G., and Lozev, M., 2000, Detection and Sizing of Cracks in Structural Steel using the Eddy Current Method. FHWA-RD-00-018, Federal Highways Administration.
http://www.tfhrc.gov/hnr20/pubs/0018.pdf

Measurement of Corrosion in Steel. www.khdesign.co.uk/bgb/concrete.htm

Model 800- LPR Corrosion Rate Monitoring in Concrete. Rohrback Cosesco Systems, Inc., www.corrpro.com/rcs/datasheets/catalog/800.PDF

Nazarian, S., and Diehl, J., 2000. Use of Geophysical Methods in Construction. Proceedings of GEO-DENVER 2000, American Society of Civil Engineers.

Obtaining Effective Half Cell Potential Measurements in Reinforced Concrete Structures. http://www.nrc.ca/irc/ctus/18.html

Reinforcement Electropotentials - Half Cell Potential Measurements. www.techno.users.netlink.co.uk/half1.html

Tullmin, M, Hansson,C., Roberge,P., 1996. Electrochemical Techniques for Measuring Reinforcing Steel Corrosion. www.corrosionsource.com/events/intercorr/techsess/papers/session1/abstracts/tullmin.html

Zdunek, A., Prine D., 1995. Early Detection of Steel Rebar Corrosion by Acoustic Emission Monitoring. Proceedings of Corrosion 1995 Conference, Paper 547. http://www.iti.northwestern.edu/publications/technical_reports/tr16.html

Zero Resistance Ammetry. www.corrosion-club.com/zra.htm

Concrete Condition

ACI Committee 201, 1992. Guide for Making a Condition Survey of Concrete in Service. Publication ACI 201.1R-92. http://www.civil.uwaterloo.ca/soudki/222r-96.pdf

ACI Committee 224, 1993. Causes, Evaluation and Repair of Cracks in Concrete Structures. Publication ACI 224.1R. http://www.civil.uwaterloo.ca/soudki/224-1r93.pdf,

Advanced Geological Services Web site, Concrete Evaluation/Imaging Services. www.advancedgeo.com/concreteservices.html

Branagan and Associates Inc. Nondestructive Testing Service for Assessing Cast-in-Place Concrete Columns. www.branagan.com/pdf_files/B&A_CSL%20Services.pdf,

Cardimona, S, B. Willeford, D. Webb, J. Wenzlick, and N. Anderson. Ground Penetrating Radar Survey of Interstate 70 Across Missouri. http://www.utc.umr.edu/Project/Completed/seq2.pdf
Density of In Place Unhardened and Hardened Concrete by Nuclear methods. http://manuals.dot.state.tx.us:80/dynaweb/colmates/mtp/@Generic__BookTextView/107611;pt=107299

Evaluation and Repair of Concrete Structures, 2002. Army Corps of Engineers Pub. 1110-2-2002. http://www.civil.uwaterloo.ca/soudki/em11110.pdf

Forbis, J., 2001. Radiography for Building Renovation. The American Society for Nondestructive Testing, Inc. www.asnt.org/publications/materialseval/basics/jun01basics/jun01basics.htm]

Gannon, E. and Cady, P., 1992. Condition Evaluation of Concrete Bridges Relative to Reinforcement Corrosion. Strategic Highway Research Program; SHRP_S/FR-92-103. http://gulliver.trb.org/publications/shrp/SHRP-S-330.pdf

High Energy X-Ray Radiography-Force Institute. www.force-institute.com/ciad/her.htm,

Impact-echo Device Gives Quick, Reliable Information on Concrete Condition. Pub. FHWA-SA-96-045 (CS048), 1996. www.fhwa.dot.gov/winter/roadsvr/CS048.htm

Kim, W., Cardimona, S., and J. Lambert. Concrete Road Inspection Using Ground Penetrating Radar. www.utc.umr.edu/Project/Completed/Seq54.pdf

Landis, E., Peterson, M. et al, 1994. Developments in NDE of Concrete. Northwestern University Center for Advanced Cement-Based Materials. http://www.iti.northwestern.edu/publications/landis.html

Liu, L. and Guo, T., 2000. Seismic Non-destructive Tests on Reinforced Concrete Column of the Longton Highway Bridge, Guangxi, China. Proceedings of The First International Conference on the Application of Geophysical Methodologies and NDT to Transportation Facilities and Infrastructure, St Louis, Missouri. http://www.modot.state.mo.us/g2000/PAPERS/CAT4/GEOPH23.PDF,

Neutron Radiography and Neutron and X-Ray Radiographs of a Concrete Core Sample Cross Section. www.osp.cornell.edu/vpr/ward/Nray.html

Non-destructive Testing Solutions for Roads and Bridges-Aggregates and Road Building. http://rocktoroad.com/non.html

Reinhart, H., 2001. Material Characterization of Steel Fiber Reinforced Concrete using Neutron CT, Ultrasound and Quantitative Acoustic Emission Techniques. University of Stuttgart, http://iwb.unistuttgart.de/grosse/papers/Nondestructive%20testing%20of%20steel%20fibre%20reinforced%20concrete.htm

Rosch, A. et al, 2002. Air Voids, Poor Compaction and Areas of Low Concrete Strength Detection by Pulse Velocity Measurement. Technische Universität Berlin, http://beta.bv.tu-berlin.de/forsch/roesch/column.htm

Shaw, P., T. Petersen, 2000. High Energy Radiography Combined with the Agfa Strukturix DPS-Imaging System and Comparison with other NDE-methods for Inspection of Thick Reinforced Concrete Structures. Proceedings of 2nd Intl Conference on NDE in Relation to

Structural Integrity for Nuclear and Pressurized Components, New Orleans. http://www.ndt.net/article/v05n08/shaw/shaw.htm

Scour

Bridgetest Web site. Evaluating Scour at Bridges. FWHA Pub. HI-96-031, Edition 3, 1995, http://www.fhwa.dot.gov/bridge/hec18SI.pdf

Dowding H.Charles et al. Time Domain Reflectometry Monitoring of Bridge Integrity and Performance. http://www.iti.northwestern.edu/publications/dowding/ndt.html

Dowding, C. and C. Pierce, 1994. Use of Time Domain Reflectometry to Detect Bridge Scour and Monitor Pier Movement. Northwestern University Center for Advanced Cement-Based Materials. http://www.iti.northwestern.edu/publications/dowding/dowding.html,

Dowding, C. Geophysical Applications of Time-Domain Reflectometry. Northwestern University. http://iti.acns.nwu.edu/publications/dowding/book/chap1.pdf

Finno, R.J., and P.J. Prommer, 1994. Evaluation of Inaccessible Drilled Shafts Using the Granite Island Group, Introduction to TDR. www.tscm.freeservers.com/riprcop.html,

Heinrichs, Thomas et al. Methodology and Estimates of Scour at Selected Bridge Site in Alaska. http://water.usgs.gov/pubs/wri/wri004151/pdf/WRIR00_4151.pdf
Impulse Response Method. www.iti.northwestern.edu/pubs/tr3.html

Kutrubes, D., and K. Maser, K., 1998. Use of GPR in 2D and 3D Imaging of Bridge Footings and Scour Studies. Proceedings of Symposium for the Applications of Geophysics to Environmental and Engineering Problems, March 1998, Chicago, IL, pp. 893-902.

Mercado, E., and J. McDonald, 2002. Two New Non-Destructive Methods to Measure Scour Depth and the Depth of Unknown Foundations. Proceedings of Geophysics 2002, Los Angeles, CA.

O'Conner, K., C. Dowding, 2000. Real Time Monitoring of Infrastructure Using TDR Technology Principles. Proceedings of The First International Conference on the Application of Geophysical Methodologies & NDT to Transportation Facilities and Infrastructure, December 2000, St Louis, Missouri.
www.modot.state.mo.us/g2000/PAPERS/CAT1/GEOPH28.PDF

Placzek, G. and Haeni. Surface-Geophysical Techniques used to Detect Existing and Infilled Scour Holes Near Bridge Piers. USGS Water-Resources Investigations Report 95-4009. http://water.usgs.gov/ogw/bgas/scour/

Webb J. D., and T. Newton, 2002. Ground Penetrating Radar (GPR): A tool for Monitoring Bridge Scour. Proceedingss from Geophysics 2002, Los Angeles, CA.

Webb, D., N. Anderson, et al, 2000. Bridge Scour: Application of Ground Penetrating Radar. Proceedings First International Conference on the Application of Geophysical Methodologies & NDT to Transportation Facilities and Infrastructure. December 2000, St. Louis, MO. www.modot.state.mo.us/g2000/PAPERS/CAT4/GEOPH48.PDF

CHAPTER 3

Deck Stability

A Study of Wind Action on the Weirton-Steubenville Cable Stayed Bridge. Boundary Layer Wind Tunnel Report BLWT-SS1-77, 1977.
A Study of Wind Effects for the Sunshine Skyway Bridge, Tampa, Florida - Concrete Alternate. Boundary Layer Wind Tunnel Report, BLWT-SS24-82. (see also - Steel Alternate, BLWT-SS25-82).
Abdel-Ghaffar, A., S. Masri, R. Nigbor, A. Abouhashish, and A. Nazmy, 1996. Issues on Structural Dynamic Monitoring, Integrity, and Control of Cable-Supported Bridges. Proceedings of 2nd International Workshop on Structural Control, Hong Kong.

Design Procedures for Dynamically Loaded Structures (Ch. 10), Prentice-Hall Inc, Englewood Cliffs, NJ 1970.

Diehl, J.G. and Ahmed Abdel-Ghaffar, 1985. Analysis of the Dynamic Characteristics of the Golden Gate Bridge by Ambient Vibration Measurements. Report No. 85-SM-1, Dept. of Civil Engineering, Priceton University.

Diehl, J.G., and W.D. Iwan, 1992. A Technical Review of Modern Strong Motion Accelerographs. Proceedings of 10th World Conference on Earthquake Engineering, Madrid, Spain.

Nigbor, R., 1996. State-of-the-Practice in Structural Monitoring. Proceedings of 2nd International Workshop on Structural Control, Hong Kong.

Nigbor, R., 1999. Some New Developments in Real-Time Monitoring of Civil Structures. Proceedings of NATO Advanced Research Workshop on Strong Motion Instrumentation for Civil Engineering Structures, Istanbul.

Nigbor, R., 2000. Instrumentation Systems for Dynamic Monitoring of Bridges. Proceedings of Workshop on Instrumental Diagnostics of Seismic Response of Bridges and Dams, UCB/PEER.
Nigbor, R., 2000. Practical Issues in Health Monitoring for Civil Structures. Proceedings 2nd Workshop on Advanced Technologies in Urban Earthquake Disaster Mitigation, Kyoto, Japan.

Nigbor, R., 2001. Advanced Sensors for Building Monitoring. COSMOS Workshop on Strong Motion Instrumentation of Buildings, Oakland, CA.

Nigbor, R., 2001. New Developments in Health Monitoring for Civil Structures. in Strong Motion Instrumentation for Civil Engineering Structures, M. Erdik, ed., Kluwer, 2001.
Nigbor, R., and J. Swift, 2001. Quality Assurance Issues with Geotechnical Databases. COSMOS Workshop on Geotechnical Databases, Richmond, CA.

Nigbor, R., and O. Viengkhou, 2000. OASIS – A Real-Time Monitoring System. Proceedings of 17th International Symposium on Automation and Robotics in Construction (ISARC17), Taipei.

Nigbor, R., et al., 2001. Feasibility of Detecting Known Structural Changes from Ambient Vibration Data. Proceedings of 3rd International Workshop on Structural Health Monitoring, Stanford Univ.

Nigbor, R.L. 1991. Measurement Techniques for Structural Vibration Problems. Proceedings of ASCE So. Carolina Section Meeting, Columbia, SC.

Nigbor, R.L., 1984. Full-Scale Ambient Vibration Measurements of the Golden Gate Suspension Bridge - Instrumentation and Data Acquisition. Proceedings of Eighth World Conference on Earthquake Engineering, San Francisco.

Nigbor, R.L., 1990. Applied Seismic Instrumentation for Long-Span Bridges. Proceedings of Second Workshop on Bridge Engineering Research in Progress, Reno.

Nigbor, R.L., 1990. Instrumentation Concepts for Post-Earthquake Assessment. Proceedings of 6th U.S.-Japan Bridge Engineering Workshop, Lake Tahoe.

Nigbor, R.L., 1991. Dynamic Monitoring of Suspension Bridges. Proceedings of International Workshop on Technology for Hong Kong's Infrastructure Development, Hong Kong.

Nigbor, R.L., 1993. Experimental Techniques for Structural Performance. ACI 1993 Convention, Vancouver, BC.

Nigbor, R.L., 1995. Seismic Refraction Maps Soil/Rock Layers. International Groundwater Technology.

Nigbor, R.L., A. Cakmak, R. Mark, R., 1992. Measured to the Max. Civil Engineering.
Nigbor, R.L., J. Diehl, M. Higazy, 1996. OASIS: A New Real-Time Structural Monitoring System. Proceedings of 2nd International Conference in Civil Engineering on Computer Applications, Bahrain.
Nigbor, R.L., J.G. Diehl, 1996. Real-Time Remote Condition Monitoring of a Cable-Stayed Bridge in Bangkok, Thailand. 4th National Workshop on Bridge Research in Progress.

Predicting Wind-Induced Response in Hurricane Zones. J. Str. Div., ASCE 1976.
Smyth, A., S. Masri, A. Abdel-Ghaffar, and Nigbor, R., 2000. Development of a Nonlinear MultipInput/Multi-Output Model for the Vincent Thomas Bridge under Earthquake Excitations. Proc. 12WCEE, New Zealand.

Vibration of Buildings – Guidelines for the Measurement of Vibrations and Evaluation of their Effects on Buildings, American National Standard Institute (ANSI) S2.47-1990 (R1997) http://webstore.ansi.org/ansidocstore/default.asp.
Wind Induced Response of Suspension Bridges - Wind Tunnel Model and Full Scale Observations, 1979. Proceedings of 5th International Conference on Wind Engineering, C.S.U., Fort Collins, Colorado.

Condition Evaluation

Barnes, C., L., J. Trottier, 2000. Ground-Penetrating Radar for Network-Level Concrete Deck Repair Management. ASCE Journal of Transportation Engineering, Vol. 126, No.3. May/June 2000. pp. 257-262.

Barnes, C. L., and J. Trottier. 2003. Effectiveness of GPR in Predicting Deck Repair Quantities. ASCE Journal of Infrastructure Systems, (accepted; submitted in December 2002 for peer review prior to publication).

Cardimona, S. 2000. Ground Penetrating Radar. Proceedings of Geophysics 2000-The First Annual Conference on the Application of Geophysical and NDT Methodologies to Transportation Facilities and Infrastructure. Missouri Department of Transportation—publishers, Jefferson, Missouri.

Gucunski, N., S. Antoljak, and A. Maher, 2000. Seismic Methods in Post Construction Condition Monitoring of Bridge Decks. Use of Geophysical Methods in Construction, Geotechnical Special Publication No. 108, Soheil Nazarian and John Diehl, Editors, Geo Institute, ASCE, pp. 35-51.

Gucunski, N. G. Consolazio, and A. Maher, 2002. Concrete Bridge Deck Delamination Detection by Integrated Ultrasonic Methods. American Concrete Institute (recently accepted for publication in an ACI Journal).

Gucunski, N., and A. Maher, 1998. Bridge Deck Condition Monitoring by Impact Echo Method. Proceedings of International Conference MATEST '98 - Life Extension, Brijuni, Croatia, October 1-2, 1998, pp. 39-45.

Hickman, S., and S. Cardimona, 2000. Ground Penetrating Radar Survey of Interstate 70 Across Missouri. Proceedings of Geophysics 2000- The First Annual Conference on the Application of Geophysical and NDT Methodologies to Transportation Facilities and Infrastructure, Missouri Department of Transportation—publishers, Jefferson, Missouri, 2001.

Maser, K. R., 2002. Use of Ground Penetrating Radar Data for Rehabilitation of Composite Pavements on High Volume Roads. Proceedings of Pavement Evaluation 2002, Roanoake, VA.

Maser, K. R., and M. Bernhardt, 2000. Statewide Bridge Deck Survey Using Ground Penetrating Radar. Proceedings of 2000 Structural Materials Technology IV: An NDT Conference, Atlantic City, NJ, Technomic Publishing Company, Inc., pp. 23 – 30.

Maser, K. R.; T. Holland, R. L. Roberts, J. Popovics, and A. Heinz, 2003. Technology for Quality Assurance of New Pavement Thickness. TRB-Paper #03-3850, Transportation Research Board.

Nazarian, S., and D. Yuan, 1997. Evaluation and Improvement of Seismic Pavement Analyzer. Research Project 7-2936, The Center for Highway Materials Research, The University of Texas at El Paso, El Paso, TX.

Perkins, A. D., J. J. Amrol, F. A. Romero, R. L. Roberts, 2000. DOT Specification Development Based on Evaluation of Ground-Penetrating Radar System Performance in Measuring Concrete Cover (Reinforcement Depth) on New Bridge Deck Construction. Proceedings of Structural Materials Technology IV: An NDT Conference, Feb. 28 – Mar. 3, 2000, Technomic Publishing Company, Inc., pp. 53 – 60.

Roberts, G. E.. and J. J. Amrol, 1999. Concrete Cover Determination Using Ground Penetrating Radar (GPR). United States Department of Transportation (Federal Highway Administration—FHWA) Priority Technology Program, Project No. NH1997-01, State of New Hampshire Department of Transportation, Bureau of Materials & Research Final Report.

Roberts, R., 2000. Effect of Antenna-Surface Distance on the Radiation of a GPR Antenna. Proceedings of the Eighth International Conference on GPR, Gold Coast Australia, Noon, D., Stickley, G., and Longstaff, D., Editors, SPIE Vol. 4084, p. 702-707.

Roberts, R., and D. Cist, 2002. Enhanced Target Imaging in 3D Using GPR Data from Orthogonal Profile Lines. Proceedings of the Ninth International Conference on GPR, April 29-May 2, 2002, Santa Barbara, CA., Koppenjan and Lee Editors., SPIE Vol. 4758, p. 256-261.

Roberts, R. L., F. A. Romero, 1998. High-Resolution GPR Bridge Deck Evaluation Surveys. Proceedings of the International Conference on Corrosion and Rehabilitation of Reinforced Concrete Structures, Dec. 7-11, 1998, FHWA-SA-99-014.

Romero, F. A., D. Allen, R. L. Roberts, and J. Fleckenstein, 2000. Ground-Penetrating Radar Investigation of an Interstate Concrete Pavement for Evidence of Segregation Caused by Poor Consolidation During Construction. Proceedings of Geophysics 2000- The First Annual Conference on the Application of Geophysical and NDT Methodologies to Transportation Facilities and Infrastructure, Paper 4-21, Dec. 2000, Missouri Department of Transportation, publishers, Jefferson, Missouri.

Romero, F. A., G. E. Roberts, and R. L. Roberts, 2000. Evaluation of GPR Bridge Deck Survey Results Used for Delineation of Removal/Maintenance Quantity Boundaries on

Asphalt-Overlaid, Reinforced Concrete Deck. Proceedings of 2000 Structural Materials Technology IV: An NDT Conference, Technomic Publishing Company, Inc., Feb. 28-Mar. 3, 2000, Atlantic City, NJ, pp. 23 – 30.

Romero, F. A., and R. L. Roberts, 2002. Mapping Concrete Deterioration: High-Speed Ground Penetrating Radar Surveys on Bridge Decks Using New Analysis Method Based on Dual-Polarization Deployment of Horn Antennae. Proceedings of the 2002 International Bridge Conference, Pittsburgh, PA, June 10-12, 2002, Paper IBC-02-12.

Romero, F. A., and R. L. Roberts, 2002. The Evolution in High-Resolution Ground Penetrating Radar Surveys from Ground-Coupled to High-Speed, Air-Coupled Evaluations. Proceedings of the Structural Materials Technology V: An NDT Conference, Cincinnati, OH.

Saarenketo, T. 1997. Using Ground Penetrating Radar and Dielectric Probe Measurements in Pavement Density Quality Control. Transportation Research Record, pp. 34-41.

Saarenketo, T., and P. Roimela, 1998. Ground Penetrating Radar Technique in Asphalt Pavement Density Quality Control. Proceedings of the Seventh International Conference on Ground Penetrating Radar, Lawrence, KS. Volume 2, pp. 461-466.

Saarenketo, T., and T. Scullion, 2002. Implementation of Ground Penetrating Radar Technology in Asphalt Pavement Testing. Proceedings of the Ninth International Conference on Asphalt Pavements, International Society for Asphalt Pavements (ISAP), Kopenhagen, Denmark.

Saarenketo, T., and T. Scullion, 2000. Road Evaluation with Ground Penetrating Radar. Journal of Applied Geophysics, Vol. 43, pp. 119 –138.

Scullion, T., T. Saarenketo, 1998. Applications of Ground Penetrating Radar Technology for Network and Project Level Pavement Management Survey Systems. Proceedings of the 4th International Conference on Managing Pavements, Durban, South Africa.

Wenzlick, J. D., S. Cardimona, 2000. Investigation of Bridge Decks Utilizing Ground Penetrating Radar. Proceedings of Geophysics 2000- The First Annual Conference on the Application of Geophysical and NDT Methodologies to Transportation Facilities and Infrastructure. St. Louis, Missouri.

CHAPTER 4

Pavements, Condition Evaluation

Evaluation of Ground-Penetrating Radar and Infrared Thermography Prepared by Materials and Research Division of Highways, Delaware Department of Transportation, for Federal Highway Administration Experimental Project No. 11, FHWA-EP-11-002, May 1989

Baker, M.R., Crain, K., and Nazarian, S., 1995. Determination of Pavement Thickness with a New Ultrasonic Device, Research Report 1966-1, Center for Highway Materials Research, The University of Texas as El Paso.
Barnes, Christopher. L.;Trottier, Jean-Francois. 2003. "Effectiveness of GPR in Predicting Deck Repair Quantities", *ASCE Journal of Infrastructure Systems* (accepted; submitted in December 2002 for peer review prior to publication).
Cardimona, Steve. 2000. Ground Penetrating Radar, Geophysics 2000- The First Annual Conference on the Application of Geophysical and NDT Methodologies to Transportation Facilities and Infrastructure, St. Louis, Missouri.

Chung, T and C.R. Carter, Pavement Determination and Detection of Pavement Cavities Using Radar, Ontario Ministry of Transportation, Research & Development Branch Project 21187, MAT-91-03, Downsview, Ontario, Canada.

Geomedia Research and Development. Company Web Site: www.Geomedia.US

German Instruments A/S. Company Web Site. www.germann.org

Hauser, E.C. , and Howell, M.J., 2001. Ground Penetrating Radar Survey to Evaluate Roadway Collapse in Northern Ohio. 2001 Symposium on Application of Geophysics to Environmental and Engineering Problems (SAGEEP), 2001 CD Publication RBA-2, 7p.

Hickman, Shane; Cardimona, Steve, 2000. Ground Penetrating Radar Survey of Interstate 70 Across Missouri. Geophysics 2000. The First Annual Conference on the Application of Geophysical and NDT Methodologies to Transportation Facilities and Infrastructure, December 2000, Missouri Department of Transportation—publishers, Jefferson, Missouri.

Impact-Echo Instruments, LLC. Company Web Site: www. Impact-echo.com

Mary J. Sansalone and William B. Streett,1997. Impact-Echo: Nondestructive Evaluation of Concrete and Masonry, Bullbrier Press, 339 pp.
Maser, K. Radar Pavement Thickness Evaluation: Case Studies at 13 WES Sites:, report prepared for the US Army Waterways Experiment Station, Vicksburg, Miss., December 1991
Maser, K. Use of Radar Technology for Pavement Layer Evaluation. Report 930-5F, Texas Transportation Institute, Texas A&M University, College Station, TX February 1991

Maser, Kenneth R. 2002. Use of Ground Penetrating Radar Data for Rehabilitation of Composite Pavements on High Volume Roads. *Conference Proceedings—Pavement Evaluation 2002*, Roanoake, VA.
Maser, Kenneth R.; Bernhardt, M. 2000. Statewide Bridge Deck Survey Using Ground Penetrating Radar. *2000 Structural Materials Technology IV: An NDT Conference*, Technomic Publishing Company, Inc., Atlantic City, New Jersey, pp. 23 – 30.

Maser, Kenneth R.; Holland, T. Joe; Roberts, Roger L.; Popovics, John; Heinz, Ariadna. 2003. "Technology for Quality Assurance of New Pavement Thickness", TRB—Paper #03-3850, *Transportation Research Board.*

Nazarian, S., Baker, M.R., and Crain, K., 1997. Assessing Quality of Concrete with Wave Propagation Techniques. Materials Journal, American Concrete Institute, Vol. 94, No. 4, Farmington Hills, MI, pp 296-306.

Nazarian, S., Yuan, D., and Baker, M.R., 1995. Rapid Determination of Pavement Moduli with Spectral-Analysis-of-Surface-Waves Method. Research Report 1243-1, Center for Highway Materials Research, The University of Texas as El Paso.

Olson Instruments, Inc. Company Web Site: www.olsoninstruments.com
Research Report 4188-2

Roberts, Roger L., Romero; Francisco A. 1998. High Resolution GPR Bridge Deck Evaluation Surveys. *Highway Applications of Engineering Geophysics with an Emphasis on Previously Mined Ground,* pp. 249 – 54. Missouri Department of Transportation—publishers, Jefferson City, Missouri.

Roddis, W.M., Maser, K., and Gisi, A., 1992 Radar Pavement Thickness Evaluations for Varying Base Conditions. TRB—Paper #92-0682, *Transportation Research Board*, January.

Romero, Francisco A., Allen, David, Roberts, Roger L., Fleckenstein, John. 2000. Ground-Penetrating Radar Investigation of an Interstate Concrete Pavement for Evidence of Segregation Caused by Poor Consolidation During Construction. *Geophysics 2000- The First Annual Conference on the Application of Geophysical and NDT Methodologies to Transportation Facilities and Infrastructure*, Paper 4-21, St. Louis, Missouri.

Romero, Francisco A.; Roberts, Glenn E.; Roberts, Roger L. 2000. Evaluation of GPR Bridge Deck Survey Results Used for Delineation of Removal/Maintenance Quantity Boundaries on Asphalt-Overlaid, Reinforced Concrete Deck. *2000 Structural Materials Technology IV: An NDT Conference,* Technomic Publishing Company, Inc., Atlantic City, New Jersey, pp. 23 – 30.

Romero, Francisco A.; Roberts, Roger L. 2002. Mapping Concrete Deterioration: High-Speed Ground Penetrating Radar Surveys on Bridge Decks Using New Analysis Method Based on Dual-Polarization Deployment of Horn Antennae, 2002. *International Bridge Conference Paper IBC-02-12,* Proceedings International Bridge Conference, Pittsburgh, PA.

Romero, Francisco A.; Roberts, Roger L. 2002. The Evolution in High-Resolution Ground Penetrating Radar Surveys from Ground-Coupled to High-Speed, Air-Coupled Evaluations. *Proceedings from Structural Materials Technology V: An NDT Conference*, Cincinnati, OH.
Saarenketo, Timo 1997. Using Ground Penetrating Radar and Dielectric Probe Measurements in Pavement Density Quality Control. Transportation Research Record. pp. 34-41.

Saarenketo, Timo,. 1997. Using Ground Penetrating Radar and Dielectric Probe Measurements in Pavement Density Quality Control. *Transportation Research Record.* pp. 34-41.

Saarenketo, Timo; Roimela, Petri, 1998. Ground Penetrating Radar Technique in Asphalt Pavement Density Quality Control. *Proceedings from Seventh International Conference on Ground Penetrating Radar, Lawrence, Kansas.* Volume 2, pp. 461-466.

Saarenketo, Timo; Scullion, Tom 2002. "Implementation of Ground Penetrating Radar Technology in Asphalt Pavement Testing", *Proceedings of the Ninth International Conference on Asphalt Pavements, International Society for Asphalt Pavements (ISAP),* Kopenhagen, Denmark.

Saarenketo, Timo; Scullion, Tom, 2000. Road Evaluation with Ground Penetrating Radar. *Journal of Applied Geophysics* 43 119 –138.
Sansalone, M., Carino, N.J., 1986, Impact Echo: A Method for Flaw Detection in Concrete Using Transient Stress Waves, NBSIR 86-3452, National Technical Information Service, Springfield.

Scullion, Tom; Saarenketo, Timo. 1998. Applications of Ground Penetrating Radar Technology for Network and Project Level Pavement Management Survey Systems. *Proceedings of the 4th International Conference on Managing Pavements*, Durban, South Africa.

Wenzlick, John D; Cardimona, Steve. 2000. Investigation of Bridge Decks Utilizing Ground Penetrating Radar. Geophysics 2000- The First Annual Conference on the Application of Geophysical and NDT Methodologies to Transportation Facilities and Infrastructure, St. Louis, Missouri.

Yuan, Deren, Nazarian, Soheil and Medichetti, Anitha, 2002, A Methodology for Optimizing Opening of PCC Pavements to Traffic, Texas Department of Transportation

Transportation/Geotechnical Methods

Drnevich, V.P., Yu, X., and Lovell, J., 2003. Time Domain Reflectometry for Water Content and Density of Soils: Test Procedures and Typical Results. TRB 2003 Annual Meeting CD-ROM.

Evaluation of Ground-Penetrating Radar and Infrared Thermography. Prepared by Materials and Research Division of Highways, Delaware Department of Transportation, for Federal Highway Administration Experimental Project No. 11, FHWA-EP-11-002, May 1989.
Hanna, K., and Haramy, K, 2000. Y2K Ground Imaging Technology for Geotechnical Performance Evaluation Proceedings. Amherst 2K Conference, Amherst, Massachusetts.
Kaya, A. 2002 Evaluation of Soil Porosity Using a Low MHz Range Dielectric Constant. Turkish Journal of Engineering Environmental Science. Vol. 26. No. 301-307.

Lenke, L. R., McKeen, R. G., and Grush, M. P. 2003. Laboratory Evaluation of the GeoGauge for Compaction Control. TRB 2003 Annual Meeting CD-ROM.

Lin, C.-P., Drnevich, V. P., Feng, W., and Deschamps, R. J. 2000. Time Domain Reflectometry for Compaction Quality Control. Use of Geophysical Methods in Construction, Edited by S. Nazarian and J. Diehl. Geophysical Special Publication 108. ASCE Press. pp. 15-34.

Look, B. G. and Reeves, I. N. (1992). The Application of Time Domain Reflectometry in Geotechnical Instrumentation. Geotechnical Testing Journal. Vol. 15. No. 3. pp. 277-283.
Ooi, P. S. K and Pu, J. (2003). Use of Stiffness for Evaluating Compactness of Cohesive Pavement Geomaterials. TRB 2003 Annual Meeting CD-ROM.

Romero, P. 2000. Laboratory Evaluation of the PQI-Model 300. Report to FHWA as part of Pooled-Fund Study.

Sebesta, S. and Scullion. T. 2003. Application of Infrared Imaging and Ground-Penetrating Radar for Detecting Segregation in Hot-Mix Asphalt Overlays. TRB 2003 Annual Meeting CD-ROM.

Siddiqui, S. I., Drnevish, V. P., and Deschamps, R. J. 2000. Time Domain Reflectometry Development for Use in Geotechnical Engineering. Geotechnical Testing Journal. Vol. 23. No. 1. pp. 9-20.

Topp, G. C., Davis, J. L., and Annan, A. P. 1980. Electromagnetic Determination of Soil Water Content: Measurements in Coaxial Transmission Lines. Water Resources Journal. Vol. 16. No. 3. pp. 574-582.

Troxler 2003. Company Web Site. http://www.troxlerlabs.com.

TransTeck (2003). Company Web Site. http://www.transtechsys.com. Corporate Headquarters. 1594 State Street. Schenectady, NY 12304.

CHAPTER 5
Voids

Adams, G., N. Anderson, J. Baker, M. Shoemaker, A. Shaw, and A. Hatheway, A., 1998. GPR and High Resolution Reflection Seismic Used to Map Subsidence under HW 44, Missouri. Proceedings of SAGEEP '98, Chicago, IL.

Anderson, N., G. Adams, G. Goesmann, T. Newton, A. Hatheway, and S. Cardimona, 1997. Ground-Penetrating Radar and Shallow Reflection Seismic Study of Karstic Damage to I-44 Embankment, West Springfield Area, Missouri.
www.utc.umr.edu/Project/Completed/Seq50.pdf

Army Corps of Engineers. Difficult Problems Require Geophysical Solutions. http://geoscience.wes.army.mil/GeophysicalSolutions.PDF

Earth Resources Laboratory. Environmental Applications. http://www-eaps.mit.edu/erl/research/environment.html

Geo Model Web Site. Sinkhole and Subsidence. www.groundpenetratingradar.com/sinkholes

Geo-Radar and No-Dig Technologies-Some Applications. www.malags.se/case/Geo_Radar_and_NoDig_Technologies.pdf

Gucunski, N., V. Krstic, and A. Maher, 1997. Field Implementation of the Surface Waves for Obstacle Detection (SWOD) Method. www.ndt.net/article/wcndt00/papers/idn097/idn097.htm

Haeni, F.P., 2002. Detection and Mapping of Fractures and Cavities Using Borehole Radar. Fractured Rock. www.water.usgs.gov/ogw/bgas/publications/FracRock02_haeni/FracRock02_haeni.pdf,

Hanna, K., Strid, J., and Hanson, D., 2001. Imaging Old Mine Works. Proceedings of National Association of Abandoned Mine Land Programs, Athens, Ohio.

Keele University Web Site. Microgravity Surveying. www.esci.keele.ac.uk/geophysics/html/microgravity_surveying.html

Microgravity Survey for Cavity Detection. www.oyo.co.jp/english/geo_e/mgcavity/mgcavity.html

Miller, R.D., J. Xia, 2002. High Resolution Seismic Reflection Investigation of a Subsidence Feature on HW50, Kansas. Proceedings of SAGEEP '02, Las Vegas, NV.

Munk, J., and R. A. Sheets, 1997. Detection of Underground Voids in Ohio by Use of Geophysical Methods. USGS Water-Resources Investigations Report 97-4221. http://www-oh.er.gov/reports/Abstracts/wrir.97-4221.html

Park, C., R. Miller, et al., 2000. Multichannel Seismic Surface Wave Methods for Geotechnical Applications. Proceedings First International Conference on the Application of Geophysical Methodologies & NDT to Transportation Facilities and Infrastructure. www.modot.state.mo.us/g2000/PAPERS/CAT4/GEOPH4.PDF

Phillips, C., G. Casante, D. Hutchinson, 2002. The Innovative Use of Seismic Surface Waves for Void Detection and Material Characterization. Proceedings of SAGEEP '02, Las Vegas, NV. Potential Field Techniques. www.geophysics.co.uk/mets4.html

Pyrak-Nolte, L., 2002. Seismic Imaging of Fractured Media. http://www.liv.ac.uk/seismic/news/narms/fulltextpyrak.pdf
Road Radar and Micro-Seismic Surveys. www.geophysicsgpr.com/Qualification/road_4.htm

Rosch, A. et al., 2002. Air Voids, Poor Compaction and Areas of Low Concrete Strength Detection by Pulse Velocity Measurement. Technische Universität Berlin. http://beta.bv.tu-berlin.de/forsch/roesch/column.htm

Roubal, M., 2000. Evaluating & Locating Engineering Structures Using Non-destructive Testing Technology. Proceedings First International Conference on the Application of Geophysical Methodologies & NDT to Transportation Facilities and Infrastructure. www.modot.state.mo.us/g2000/PAPERS/CAT2/GEOPH51.PDF

Shear Waves-Techniques and Systems. www.georentals.co.uk/Shearwaves.pdf
Shoemaker, M., N. Anderson, J. Baker, A. Hatheway, M. Roark, T. Newton, S. Cardimona, and S. Oppert, 1998. High Resolution Seismic Reflection Survey of Abandoned Mines along a Proposed Interstate Route, Missouri. Proceedings of SAGEEP '98, Chicago, IL.

Stahl, B. A., J. L. Leberfinger, and J. J. Warren. Electrical Imaging: a Method for Identifying Potential Collapse and Other Karst Features Near Roadways. www.quality-geophysic.com-50th1.pdf

Technos Inc. Web Site. Surface Geophysics. www.technos-inc.com/Surface.html

Terradat Geophysical. Ground Penetrating Radar Surveying. www.terradat.co.uk/gpr.html

The MicroVib. www.baygeo.com/html/the_micovib.html

Void and Utility Detection. http://optimsoftware.com/studies/geotechnical/void

Wolfe, P.J., B. H. Richard, E. C. Hauser, and J. D. Hicks, 2000. Identifying Potential Collapse Zones under Highways. Proceedings of SAGEEP '00, Arlington, VA.

Clay Content

Dalgaard, M., H. Nehmdahl, and H. Have. Soil Clay Mapping from Measurements of Electromagnetic Conductivity. KVL Precision Farming. http://www.cpf.kvl.dk/posters/EM38poster.pdf

Morrison, F., and J. Yang. Near Surface Mapping of Induced Polarization. http://appliedgeophysics.berkeley.edu:7057/geoengineering/appliedgeophysics/research/nearsurfaceIP.html

Palacky, C., 1987. Clay Mapping using Electromagnetic methods. First Break, Vol 5, No. 8, August 1987, pp. 295-306.

Slater, L., and D. Lesmes, 2000. The Induced Polarization Method. Proceedings of the First International Conference on the Application of Geophysical Methodologies & NDT to Transportation Facilities and Infrastructure.
www.modot.state.mo.us/g2000/PAPERS/CAT1/GEOPH10.PDF

Roadbed Clay

Pfeiffer, J., 2001. EM Survey over Road to Detect the Presence of Clays. Blackhawk GeoServices Report.

Slater, L., and D. Lesmes, 2000. The Induced Polarization Method. Proceedings of the First International Conference on the Application of Geophysical Methodologies & NDT to Transportation Facilities and Infrastructure.
www.modot.state.mo.us/g2000/PAPERS/CAT1/GEOPH10.PDF

CHAPTER 6

Bedrock Depth/Structure/Fractures For Materials Source Areas And Foundations

Barker, R.D., 2001. Imaging fractures in hardrock terrain.
http://www.earthsciences.bham.ac.uk/downloads/Resnote2.pdf

FHWA Web Site. Proper Use of Surface Geophysical Equipment.
www.fhwa.dot.gov/programadmin/equip.htm

Fugro Airborne Surveys Web Site. Airborne Magnetics Used to Map Bedrock Structure.
http://www.fugroairborne.com/ProductsServices/airborne/oilandgas.shtml

Gettings, M., and B. Houser. Depth to Bedrock in the Upper San Pedro Valley, Cochise County, Southeastern Arizona. http://wrgis.wr.usgs.gov/open-file/of00-138/

Hager, J. L., and M. C. Hager, M.C. GPR as a Cost Effective Bedrock Mapping Tool for Large Areas. http://www.hagergeoscience.com/pdf_files/gpr.pdf
Hayward, C., and T. Goforth, "Seismic Reflection Investigations of a Bedrock Surface Buried under Alluvium. http://geology.heroy.smu.edu/~hayward/Acrobat/Brazos.pdf

Hickman, S. et al., 2000. Geophysical Site Characterization in Support of Highway Expansion Project. International Conference on the Application of Geophysical Technologies to Planning, Design, Construction, and Maintenance of Transportation Facilities, St. Louis, MO.
www.utc.umr.edu/Publications/Proceedings/2000/Geophysical_Site_Characterization.pdf

Kick, J. Depth of Bedrock Using Gravimetry.
http://www.science.ubc.ca/~eoswr/geop/appgeop/gravity/gravmc1.html

Met Geophysics Web Site. Bedrock Profiling Using Resistivity and GPR. http://www.metgeo.com/cases/bedrock.htm

Naeva Geophysics Inc. Web Site. Seismic Reflection and Refraction Used for Bedrock Imaging. http://www.naevageophysics.com/seismics.html

Pinelli, G, et.al., 1999. A Dedicated Radar System for Preliminary No-Dig Investigation. http://georadar.ids-spa.it/download/papers/no_dig_conf_99.pdf

Roubal, M., 2000. Evaluating & Locating Engineering Structures Using Non-destructive Testing Technology. Proceedings First International Conference on the Application of Geophysical Methodologies & NDT to Transportation Facilities and Infrastructure. www.modot.state.mo.us/g2000/PAPERS/CAT2/GEOPH51.PDF

Sterling, R. Utility Locating Technologies: A Summary of Responses to a Statement of Need. Distributed by the Federal Laboratory Consortium for Technology Transfer. http://flc2.federallabs.org/utilities/Presentations/Utility_Locating_Technologies_Report.pdf

Fractures and Weak Zones

Advanced Geosciences Inc. 2-D Resistivity Structure. http://www.agiusa.com/tunnel.shtml, Advanced Geosciences Inc. Web Site. 2-D Resistivity Mapping. http://www.agiusa.com/sections.shtml

Barker, R., 2001. Imaging Fractures in Hardrock Terrain. http://www.earthsciences.bham.ac.uk/downloads/Resnotc2.pdf

Buursink, M., and J. Lane. Characterizing Fractures in a Bedrock Outcrop Using Ground-penetrating Radar at Mirro Lake, Grafton County.
Cosma, C., and N. Enescu, 2002. Multi-azimuth VSP Methods for Fractured Rock Characterization. Proceedings of he 5th International Workshop on the Application of Geophysics in Rock Engineering, Toronto, Canada
http://www.liv.ac.uk/seismic/news/narms/fulltextcosma.pdf

Crampin, S., J. Queen, and W. Rizer. The Need for Underground Research Laboratories in Sedimentary Basins NS2.1, Near-Surface Seismic Reflection Studies. http://www.eap.bgs.ac.uk/PUBLICATIONS/ABSTRACTS/SEG93/s1993scjq.pdf

Goupil, F. New in Geophysics. Tunnel Canada Web Site. http://www.tunnelcanada.ca/News/1998_12/geophysi.htm

Haeni, F., et al., 2002. Detection and Mapping of Fractures and Cavities Using Borehole Radar. Fractured Rock.
water.usgs.gov/ogw/bgas/publications/FracRock02_haeni/FracRock02_haeni.pdf

Haeni, F.P., L. Halleux, C. Johnson, J. Lane. Detection and Mapping of Fractures and Cavities Using Borehole Radar. USGS Web Site. http://water.usgs.gov/ogw/bgas/publications/FracRock02_haeni/

Leberfinger, J., 2000. Three Dimensional Electrical Imaging. Proceedings First International Conference on the Application of Geophysical Methodologies & NDT to Transportation Facilities and Infrastructure. www.modot.state.mo.us/g2000/PAPERS/CAT4/GEOPH41.PDF

Rock Quality Assessment Using Borehole Seismic. http://www.kolumbus.fi/vibrometric/page10.htm

Rock Solid Images Web Site. Seismic Fracture Detection, Exploiting the Range of Seismic Signatures. http://www.rocksolidimages.com/pdf/fracture_detection.pdf

Singha, K., et al., 2000. Borehole Radar Methods: Tools for Characterization of Fractured Rock. EPA Fact Sheet 054-00. www.water.usgs.gov/ogw/bgas/publications/FS-054-00/FS-054-00.pdf

USGS Web Site. New Hampshire. http://water.usgs.gov/ogw/bgas/outcrop/

Lithology

Advanced Geosciences, Inc. Resistivity Imaging. http://www.agiusa.com/sections.shtml,

Bayless, E., D. Westjohn, and L. Watson. Use of Surface and Borehole Geophysics to Delineate the Glacial-drift Stratigraphy of Northeastern St. Joseph County, Indiana. U.S. Geological Survey, Water-Resources Investigations Report 95-4041. http://in.water.usgs.gov/newreports/baylessbh/baylessbh.pdf

Cardimona, S., D. Webb, and T. Lippincott, 2000. Ground Penetrating Radar": Proceedings of the First International Conference on the Application of Geophysical Methodologies & NDT to Transportation Facilities and Infrastructure. www.modot.state.mo.us/g2000/PAPERS/CAT1/GEOPH17.PDF

Clark, R., G. Swayze, and A. Gallaher, A. Mapping the Mineralogy and Lithology of Canyonlands, Utah with Imaging Spectrometer Data and Multiple Spectral Feature Mapping Algorithm. USGS Web Site. http://speclab.cr.usgs.gov/PAPERS.arches.92/arches.geology.92.html

Ellefsen, K., J. Lucius, and D. Fitterman. TEM and DC Resistivity. USGS Web Site. http://rockyweb.cr.usgs.gov/frontrange/aggregate/geophysics/geophysics.htm

Fugro Airborne Surveys. DIGHEM Airborne Resistivity Mapping of Sand and Gravel. http://www.fugroairborne.com/CaseStudies/t_sand.shtml

Kilner, M., L. West, and T. Murray. Identifying Spatial Variability in Glacial Sediment Using Electrical Methods. http://www.esci.keele.ac.uk/gisse/Kilner-etal.pdf

Natural Resources Canada. Induced Polarization. http://borehole.gsc.nrcan.gc.ca/ip_e.htm,

Slater,L., and D. Lesmes, 2000. The Induced Polarization Method. Proceedings of the First International Conference on the Application of Geophysical Methodologies & NDT to Transportation Facilities and Infrastructure. www.modot.state.mo.us/g2000/PAPERS/CAT1/GEOPH10.PDF

Applied Geophysics for Groundwater Studies.http://www.st-andrews.ac.uk/~www_sgg/personal/crblink/web/GWATER1.pdf

Bernard, J., 1997. The Proton Magnetic Resonance Method for Groundwater Investigations. IRIS Document.

Butler, K., R. Russell, A. Kepic, and M. Maxwell, M., 1996. Measurement of the Seismoelectric Response from a Shallow Boundary. Geophysics, Vol. 61, No. 06, pp. 1769-1778.

Connor, C., S. Sandberg, R. Green, and D. Farrell. Transient Electromagnetic Mapping and Monitoring of the Edwards Aquifer. 20-9212. http://www.swri.edu/3pubs/IRD2001/20-9212.htm

GEO ENG Web Site. Groundwater Geophysics Solutions. http://www.geo-eng.com.au/mine_resource/download/Geo-Eng_gwater_geophys_brochure2.pdf

Goldman, G., M. Rabinovich, and I. Rabinovich, 1996. Detection of the Water Level in Fractured Phreatic Aquifers Using NMR Geophysical Measurements. Journal of Applied Geophysics.

Goldman, M., B. Rabinovich, M. Rabinovich, D. Gilad, I. Gev, and M. Schirov, 1994. Application of the Integrated NMR-TDEM Method in Groundwater Exploration in Israel. Journal of Applied Geophysics.

Groundwater Surface and Flow

Haartsen, M., and R. Pride, 1994. Modeling of Coupled Electroseismic Wave Propagation from Point Sources in Layered Media. Annual Meeting Abstracts, Society Of Exploration Geophysicists, pp. 1155-1158.

Haartsen, M., Z. Zhu, and M. Toksoz, 1995. Seismoelectric Experimental Data and Modeling in Porous Layer Models at Ultrasonic Frequencies. Annual Meeting Abstracts, Society Of Exploration Geophysicists, pp. 696-699.

Hatch, M., B. Barrett B. et al. Improved Near Surface Mapping in Groundwater Studies: Application of Fast-sampling Time-domain EM Survey Methods. http://www.aseg.org.au/publications/full/Prev96-pp25-29.pdf

Kindij, E., 1960. Discussion of the Electroseismic Effect by Martner, S. T., et al. GEO-24-02-0297-0308, Geophysics, 25, No. 01, p. 325.

Legchenko, A., 1996. Some Aspects of the Performance of the Surface NMR Method. SEG, Denver.

Legchenko, A., 1996. "A Practical Accuracy of the Surface NMR Measurements. EAGE, Amsterdam.

Legchenko, A., A. Beauce, A. Guillen, P. Valla, and J. Bernard, J, 1996. Capability of the NMR Applied to Aquifers Investigation from the Surface. EEGS, Nantes.

Legchenko, A., A. Beauce, P. Valla, J. Bernard, and G. Pierrat, 1997. Development of a Proton Magnetic Resonance Equipment for Groundwater Investigations. High Resolution Geophysics.

Legchenko, A., O. Shushakov, J. Perrin, and A. Portselan, 1995. Non-invasive NMR Study of Subsurface Aquifers in France. SEG, Houston, Texas.

Lieblich, D., A. Legchenko, F. Haeni, and A. Portselan, 1994. Surface Nuclear Magnetic Resonance Experiments to Detect Subsurface Water at Haddam Meadows, Connecticut. SAGEEP, Boston, Massachusetts.

Long, L., and W. Rivers, 1975. Field Measurement of the Electroseismic Response. Geophysics, 40, No. 02, pp. 233-245.

Martner, S., and N. Sparks, 1959. The Electroseismic Effect. Geophysics, 24, No. 02, pp. 297-308. (* Discussion in GEO-25-01-0325-0325)

Mikhailov, O., J. Queen, and N. Toksoz, 1997a. Using Borehole Electroseismic Measurements to Detect and Characterize Fractured (Permeable) Zones. Annual Meeting Abstracts, Society Of Exploration Geophysicists, pp. 1981-1984.

Mikhailov, O., M. Haartsen, and M. Toksoz, 1997b. Electroseismic Investigation of the Shallow Subsurface: Field Measurements and Numerical Modeling. Geophysics, 62, No. 01, pp. 97-105.

Millar, J, and R. Clarke. Electrokinetic Techniques for Measurement of Rock Permeability. Company Brochure from GroundFlow Ltd.

Murthy, Y., 1985. First Results on the Direct Detection of Groundwater by Seismoelectric Effect - A Field Experiment. ASEG 13th Geophysical Conference, Australian Society Of Exploration Geophysicists, 16, pp. 254-256.

Pride, S., and Morgan, F., 1991. Electrokinetic Dissipation Induced by Seismic Waves. Geophysics, 56, No. 07, pp. 914-925.

Pride, S., and W. Haartsen, 1993. Modelling Electroseismic Wave Phenomena in Layered Media. 61st Meeting. European Association of Exploration Geophysicists, Extended Abstracts, European Association Of Geophysical Exploration, Session:D017.

Pride, S., T. Madden, and N. Toksoz, 1992. Theoretical Modeling of the Electroseismic Effect. 61st Meeting European Association of Exploration Geophysicists, Extended Abstracts, European Association Of Geophysical Exploration, pp. 348-349.

Ramboll Web Site. New Seismic Method for Mapping of Groundwater. http://www.ramboll.dk/other/uk/geotechnology/pulled_array_seismic.htm

Russell, R., K. Butler, A, Kepic, and M. Maxwell, M., 1997. Seismoelectric Exploration. The Leading Edge, 16, No. 11, pp. 1611-1615.

Schirov, M., and A. Legchenko, 1991. A New Direct Non-invasive Groundwater Detection Technology for Australia. Exploration Geophysics.

Shankar, R. Groundwater Exploration. 20th WEDC Conference. http://www.lboro.ac.uk/departments/cv/wedc/papers/20/sessiong/ravi.pdf

Shushakov, O., 1996. Groundwater NMR in Conductive Water. Geophysics.

Sorensen, K., E. Auken, and P. Thomsen. TDEM in Groundwater Mapping – A Continuous Approach. http://www.geofysiksamarbejdet.au.dk/media/soerensen2000c.pdf

Thompson, A., and G. Gist, 1991. Electroseismic Prospecting. Annual Meeting Abstracts, Society of Exploration Geophysicists, pp. 425-427.

Thompson, A., and G. Gist, 1993. Geophysical Applications of Electrokinetic Conversion. The Leading Edge, 12, No. 12, pp. 1169-1173.

Trinks, I., D. Wachsmuth, and H. Stumpel. Monitoring Water Flow in the Unsaturated Zone Using Georadar. First Break. Vol. 19, December 12, 2001. http://www.geo.cornell.edu/eas/education/course/descr/EAS101/PaperDownloads4/MapWaterflowGPR.pdf

Trushkin, D., O. Shushakov, and A. Legchenko, 1994. The Potential of a Noise-reducing Antenna for Surface NMR Groundwater Surveys in the Earth's Magnetic Field. Geophysical Prospecting.

Trushkin, D., O. Shushakov, and A. Legchenko, 1995. Surface NMR Applied to an Electroconductive Medium. Geophysical Prospecting.

University of New South Wales. Geophysical Methods (Electrical) in Groundwater Investigation. http://www.wrl.unsw.edu.au/groundwater/research/electrical.html

Van Overmeeren, R., 1981. A Combination of Electrical Resistivity, Seismic Refraction, and Gravity Measurements for Groundwater Exploration in Sudan. Geophysics, Vol 46, # 9, pg 1304-1313. http://www.science.ubc.ca/~eoswr/geop/appgeop/stucases/instruct/vano.html

Zhu, Z., and D. Toksoz, 1999. Seismoelectric and Seismomagnetic Measurements in Fractured Borehole Models. Annual Meeting Abstracts, Society Of Exploration Geophysicists, pp. 144-147.

Engineering Properties

Bigelow, E. Investigating Rock Mechanical and Fluid Flow Properties. http://www.mgls.org/95Sym/Papers/Bigelow/

Dunn, T., 1997. UNB Geology 1001 Lecture 8-Geophysics I. http://www.unb.ca/courses/geol1001a/lec-8.htm

Gray, D., B. Goodway, and T. Chen. Amplitude Versus Offset, Bridging the Gap: Using AVO to Detect Changes in Fundamental Elastic Constants. http://www.cseg.org/events/meetings/abstracts/1999/avo_ch2.pdf

High Resolution Geotomography and 3D-GPR Techniques to Characterize Quarternary Gravel Deposits and Their Hydraulic Properties http://www.uni-tuebingen.de/geo/gpi/geophys/projects/shallow.html

Hoar, J. H., 1982. Field Measurement of Seismic Wave Velocity and Attenuation for Dynamic Analyses. Ph.D. dissertation, University of Texas at Austin.

Mooney, H. M., 1984. Handbook of Engineering Geophysics; Volume 1: Seismic. Bison Instruments Inc., Minneapolis, MN, (612/926-1846).

Natural Resources Canada. Full Waveform Acoustic, Geologic Interpretation of Full Waveform Acoustic Logs. http://borehole.gsc.nrcan.gc.ca/acst_e.htm

Nigbor, R.L., and T. Imai, 1994, The suspension P-S velocity logging method Proceedings XIII ICSMFE, New Delhi, India.

Remediation Requires a Knowledge of Subsurface Porosity, Permeability, and Fluid Saturation. November, 2001. http://geosciences.llnl.gov/esd/expgeoph/berge/emsp/intro.html

Seismic Services International Corporation, Engineering Properties. http://www.quality-geophysics.com/seismic.pdf

Sheriff, R., and L. Geldart, 1995. Exploration Seismology. Cambridge University Press.

Sirles, P. C., and A. Viksne, 1990. Site-Specific Shear Wave Velocity Determinations for Geotechnical Engineering Applications. Geotechnical and Environmental Geophysics,

Investigations in Geophysics No. 5, Society of Exploration Geophysicists, Tulsa, OK, pp 121-131.

Sirles, P. C., D. Custer, and D. McKisson, 1993. CROSSIT Version 2, (computer program for data reduction and presentation of crosshole seismic measurements), US Bureau of Reclamation, Denver, CO.

Stokoe, K. H., 1980. Field Measurement of Dynamic Soil Properties. Specialty Conference on Civil Engineering and Nuclear Power, ASCE, Sept. 15-17, Knoxville, TN.

U.S. Bureau of Reclamation, 1992. Geophysical Investigations at Tabor Dam, Unpublished report D-3611, Seismotectonics and Geophysics Section, US Bureau of Reclamation, Denver, CO.

Rippability

Caterpillar, 1988. Handbook of Ripping. 8th Edition.

Hasbrouck Geophysics, Inc., Rippability (refraction seismic). http://www.oilsurvey.com/php/link.php3?CoId=7035&path=refrac.htm&PHPSESSID=a8744e535ce2fb5f285d5828e09650d1

Natural Resources. Seismic Exploration with a General Relation of Wave Velocity to Rippability. http://www.tcd.ie/Natural_Resources/Geoscience/prog/seism.htm

Rucker, M., 2000. Applying the Seismic Refraction Technique to Exploration for Transportation Facilities. www.modot.state.mo.us/g2000/PAPERS/CAT1/GEOPH52.PDF,

Utilities Detection

Cist, D., and A. Schutz, 2001. State of the Art for Pipe and Leak Detection DE-FC26-01NT41317 A Low Cost GPR Gas and Pipe and Leak Detector. Geophysical Survey Systems, Inc. www.netl.doe.gov/scng/publications/t&d/tsa/pipe_leak.pdf

Ditchwitch Web Site. Utility Detection. www.ditchwitch.com

Duffy, D., 2001, Finding Buried Utilities Before They Find You. www.forester.net/gx_0103_finding.html

FHWA Web site. Proper Use of Surface Geophysical Equipment. www.fhwa.dot.gov/programadmin/equip.htm.

G.P.R. Geophysical Services. Ground Penetrating Radar. www.geosurvey.co.nz/cases.htm

Geometrics. OhmMapper-Resistivity Mapping. www.iris-instruments.com/Pdf%20file/Mapper_Gb.pdf

Geovision Web Site. Geophysical Techniques for Shallow Environmental Investigations.

Hertlein, B., 1998. Geophysics for Utility Location: When it Works-When it Won't. Presented at the American Gas Association 1998 Operations Conference. http://members.aol.com/ndtman1/papers/papmenu.html

Locating Buried Utilities (using GPR). www.geophysicalsurveys.com/utility.htm,

Park, C., R. Miller, et al., 2000. Multichannel Seismic Surface Wave Methods for Geotechnical Applications: Proceedings First International Conference on the Application of Geophysical Methodologies & NDT to Transportation Facilities and Infrastructure. www.modot.state.mo.us/g2000/PAPERS/CAT4/GEOPH4.PDF

Pinelli, G, G. DePasquale, G. Manacorda, and P. Papeschi, 1999. A Dedicated Radar System for Preliminary No-Dig Investigation. http://georadar.ids-spa.it/download/papers/no_dig_conf_99.pdf

Roubal, M., 2000. Evaluating & Locating Engineering Structures Using Non-destructive Testing Technology. Proceedings First International Conference on the Application of Geophysical Methodologies & NDT to Transportation Facilities and Infrastructure. www.modot.state.mo.us/g2000/PAPERS/CAT2/GEOPH51.PDF

Sterling, R., 2000. Utility Locating Technologies: A Summary of Responses to a Statement of Need. Distributed by the Federal Laboratory Consortium for Technology Transfer. http://flc2.federallabs.org/utilities/Presentations/Utility_Locating_Technologies_Report.pdf

Utility Detection. Rycom 8875 Pipe and Cable Locator. www.pollardwater.com/Emarket/Pages/P884%208875%20Pipe&CableLocator.asp

Utility Detection. RD 590 APT. www.radiodetection.com/products/html/rd590apt.cfm

Utility Detection. Risor-bond 1205. www.omnitest.co.uk/tdr.html

Utility Detection. Sensors & Software-Noggin. www.sensoft.ca/pmds/nn_br.pdf

Utility Detection. Subsite 75R/75T-action. www.ricona.de/produkte/dw/75r75t/start.shtml

www.geovision.com/PDF/M_Environmental.PDF

Tanks

Expedited Site Assessment Tools for Underground Storage Tank Sites-A Guide for Regulators. EPA 510-B-97-001;March 1997, www.epa.gov/swerust1/pubs/esa-ch3.pdf,

NWGLED Web Site. List of Leak Detection Evaluations for Underground Storage Tank (UST) Systems. www.nwglde.org/downloads.html

Soule, R. Survey Over a UST Using Combined Magnetometer/EM61. www.terraplus.com/papers/soule.htm

Plumes

Anderson, J., and J. Peltola, 1996. Ground Penetrating Radar as a Tool for Detecting Contaminated Areas. http://www.cee.vt.edu/program_areas/environmental/teach/gwprimer/gprjp/gprjp.html,

Berryman, J.G. Surface and Borehole Electromagnetic Imaging of Conduction Contaminant Plumes. http://math.stanford.edu/~dorn/elmag/report1/firstyear.html,

BYU Web Site. GPR Used to Assess Natural Hydrogeologic Conditions. http://emrl.byu.edu/chris/gpr.htm

Cist, D., and A. Schutz, 2001. State of the Art for Pipe and Leak Detection DE-FC26-01NT41317 A Low Cost GPR Gas and Pipe and Leak Detector. Geophysical Survey Systems, Inc. www.netl.doe.gov/scng/publications/t&d/tsa/pipe_leak.pdf,

Digistar Web Site. EM Mapping of Plumes. http://www.digistar.mb.ca/minsci/finding/electromag1.htm

Edwards Air Force Base Web Site. Plume Example. http://www.edwards.af.mil/penvmng/documents/rts/1999rts/may99/maypge5.htm,

Electrical Resistance Tomography, Innovative Technology Summary Report. DOE/EM-0538 http://apps.em.doe.gov/ost/pubs/itsrs/itsr17.pdf

EM and Radar Uses for Plumes. http://www.on.ec.gc.ca/pollution/ecnpd/tabs/tab03-e.html

EM Induction Surveys Near the Norman Landfill, USGS EM31/EM34 Data and Images. http://ok.water.usgs.gov/norlan/em31_34.html

G.P.R. Geophysical Services. Ground Penetrating Radar. www.geosurvey.co.nz/cases.htm

GEOE 475. Advanced Hydrogeology Course Notes. http://www.engr.usask.ca/classes/GEOE/475/notes/geoe475contamenant.ppt

Geosurvey Web Site. GPR Image of Oil Plume. http://www.geosurvey.co.nz/cases.htm,

Godwin, M., and Monks, K., Sample Design Optimization and Identification of Contaminant Plumes and Subsurface Structures Through Use of Multi-tool Surface Geophysics. http://www.containment.fsu.edu/cd/content/pdf/187.pdf

Griesemer, J. Diving Plumes. http://www.state.nj.us/dep/srp/news/2001/0105_04.htm,

Johnson, C., J. Lane, J. Williams, and F. Haeni, 2001. Application of Geophysical Methods to Delineate Contamination in Fractured Rock at the University of Connecticut Landfill, Storrs, Connecticut. http://water.usgs.gov/ogw/bgas/publications/SAGEEP01_135/

U.S. Geological Survey. Contaminate Plumes and Geophysics. Denver, CO. http://earth.agu.org/revgeophys/phillj01/node17.html

USGS Web Site. Assessment of Natural Attenuation in the East Branch Canal Creek Area, Aberdeen Proving Ground, Maryland. http://md.usgs.gov/projects/md135.html,

Unexploded Ordnance (UXO)

Anderson , M., and G. Hollyer. Development of a Geophysical Mapping Platform for Real-Time UXO Data Acquisition. www.geosoft.com/support/Papers/pdfs/RealTimeUXODataAcquisition.pdf

Blackhawk Web Site. UXO Information. http://www.blackhawk-uxo.com/index.html,

Gamey, T., W. Doll, D. Bell, A. Duffy, and S. Millhouse. Evaluation of Improved Airborne Techniques for Detection of UXO. http://www.esd.ornl.gov/people/gamey/papers/HM3%20BBR.pdf

Hollyer, G., and L. Racic. Enhancing Geophysical Data Acquisition, Quality Control, Processing, Analysis and Visualization for UXO Detection, Characterization and Discrimination. www.geosoftx.com/support/Papers/pdfs/enhancinggeophysicsforuxo.pdf

Innovative Seismic System for Buried Unexploded Ordnance Detection and Classification. http://www.uxo.com/

Krumhansl, P. E. Dorfman, P. Remington, H. Allik, R. Mullen, M. Goldsmith, and R. Barile. Innovative Seismic System for Buried Unexploded Ordnance Detection and Classification. CU-1091 Final Report, BBN Technologies Report No. 8313. http://www.uxo.com/finalreport/Report8313_UXO.pdf

Pawlowski, J., R. Lewis, T. Dobush, and N. Valleau, 1995. An Integrated Approach for Measuring and Processing Geophysical Data for the Detection of Unexploded Ordinance. Proceedings of the Symposium on the Application of Geophysics to Engineering and Environmental Problems, Orlando, FL. www.geosoftx.com/support/Papers/pdfs/integratedgeophysical.pdf

Powers, M., and G. Olhoeft, 1996. Computer Modeling to Transfer GPR UXO Detectability Knowledge Between Sites. Proceedings UXO Forum 1996 Conference, Williamsburg, VA. http://www.g-p-r.com/uxo96.pdf

U.S. Army Corps of Engineers, 2000. Ordnance and Explosives Response. Pamphlet EP 1110-1-18. http://www.usace.army.mil/inet/usace-docs/eng-regs/er1110-1-8153/toc.htm

Warren, J., and G. Fields, 2002. Digital Geophysical Mapping for UXO. RTLP/ITAM Conference-Digital Geophysical Mapping for UXO. www.quality-geophysics.com/DGMforUXO.pdf

CHAPTER 7

Vibration

American National Standard Institute (ANSI), 1996. Guide to the Evaluation of Human Exposure to Vibration in Buildings, S3.29-1983. http://webstore.ansi.org/ansidocstore/default.asp

American National Standard Institute (ANSI), 1997. Vibration of Buildings – Guidelines for the Measurement of Vibrations and Evaluation of their Effects on Buildings, S2.47-1990. http://webstore.ansi.org/ansidocstore/default.asp

American National Standard Institute ANSI, 1999. Guide for the Evaluation of Human Exposure to Whole-Body Vibration, S3.18-1979. http://webstore.ansi.org/ansidocstore/default.asp

American National Standard Institute ANSI, 1999. Mechanical Vibration and Shock Affecting Man – Vocabulary, S3.32-1982. http://webstore.ansi.org/ansidocstore/default.asp

Bollinger, G., 1971. Blast Vibration Analysis. Southern Illinois University Press, 1971.

Design Procedures for Dynamically Loaded Structures (Ch. 10), Prentice-Hall Inc, Englewood Cliffs, NJ.

Dowding, C., 1996. Construction Vibrations. Prentice Hall, NJ.

Federal Transit Administration, 1995. Transit Noise and Vibration Impact Assessment. Available from Harris Miller Miller & Hanson Inc. http://www.hmmh.com/rail05.html#top

Griffin, M., 1990. Handbook of Human Vibrations. Academic Press Inc, San Diego, CA.

Rosenthal, M., and G. Morlock., 1978. Blasting Guidance Manual, Office of Surface Mining and Reclamation and Enforcement, US Dept of the Interior.

Siskind, D., 2000. Vibrations from Blasting. International Society of Explosives Engineers, Cleveland. http://www.isee.org

PART II

CHAPTER 8

Geophysical Quantities

Annan, A., and S. Cosway, 1991. Ground Penetrating Radar Survey Design. Paper presented to the 53rd annual meeting of the European Association of Exploration Geophysicists, Florence, Italy.

Coetzee, V., R. Meyer, C. Elphinstone, H. Bezuidenhout, and A. Watson, 1991. Hydraulic Aquifer Characteristics from Resistivity Sounding Parameters Using Empirical Formulae and Geostatistical Techniques. Proceedings of SAGEEP, Oakbrook, Illinois, pp 291-307.

Grant and West, 1965. Interpretation Theory in Applied Geophysics. McGraw Hill, Toronto, 582 pp.

Hearst, J., and P. Nelson, 1985. Well Logging for Physical Properties. McGraw Hill, 571 pp.

Mazac, O., W. Kelly, and I. Landa, 1986. A Hydrogeophysical Model for Relationships between Electrical and Hydraulic Properties of Aquifers. J. Hydrology, No. 79, pp. 1-19.

Nelson, P., and G. Van Voorhis, 1983. Estimation of Sulfide Content from Induced Polarization Data. Geophysics, Vol. 48, pp 62-75.

Olhoeft, G., 1986. Direct Detection of Hydrocarbon and Organic Chemicals with Ground Penetrating Radar and Complex Resistivity. Proceedings of the National Water Well Assoc. Conference on Petroleum Hydrocarbons and Organic Chemicals in Ground Water, Houston, TX.

CHAPTER 9

Geophysics

American Society for Testing and Materials, 1988. Standard Test Methods for Crosshole Seismic Testing. ASTM D-4428 M-84, American Society for Testing and Materials.

Allen, N. F., F. Richart, and R. Woods, 1980. Fluid Wave Propagation in Saturated and Nearly Saturated Sand. Journal of the Geotechnical Engineering Division, ASCE, Vol 106, No. GT3, pp 235-254.

Annan, A. P., 1992. Ground Penetrating Radar, Workshop Notes. Sensors and Software, Inc., Ontario, Canada.

Arzi, A. A., 1975. Microgravimetry for Engineering Applications. Geophysical Prospecting, Vol 23, No. 3, pp 408-425.

Avery, T. E., and G. Berlin, 1985. Interpretation of Aerial Photographs. Burgess Publishing Co., Minneapolis, MN.

Ballard, R. F., R. McGee, and R. Whalin, 1992. A High-Resolution Subbottom Imaging System. Proceedings of US/Japan Marine Facilities Panel of UNJR, Washington, DC.

Ballard, R. F., K. Sjostrom, R. McGee, and R. Leist, 1993. A Rapid Geophysical Technique for Subbottom Imaging., Dredging Research Technical Notes DRP-2-07, U.S. Army Engineer Waterways Experiment Station, Vicksburg, MS.

Barker, R. D., 1990. Investigation of Groundwater Salinity by Geophysical Methods. Geotechnical and Environmental Geophysics, Vol 2, Society of Exploration Geophysicists, pp 201-212, Tulsa, OK.

Bateman, R. M., 1985. Log Quality Control. Boston International Human Resources Development Corp.

Belknap, W. B., J. Dewan, C. Kirkpatrick, W. Mott, A. Pearson, and W. Robson, 1959. API Calibration Facility for Nuclear Logs. Drilling and Production Practice, American Petroleum Institute, pp 289-316.

Benson, R. C., R. Glaccum, and M. Noel, 1983. Geophysical Techniques for Sensing Buried Wastes and Waste Migrations, U.S. Environmental Protection Agency, Washington, DC, Contract No. 68-03-3050, National Water Well Association, Worthington, OH.

Blake L. S. (Editor), 1975. Civil Engineer's Reference Book, 3rd Edition, Butterworths, London.

Blizkovsky, M., 1979. Processing and Applications in Microgravity Surveys. Geophysical Prospecting, Vol 27, No. 4, pp 848-861.

Bodmer, R., S. Ward, and H. Morrison, 1968. On Induced Electrical Polarization and Ground Water. Geophysics, Vol 33, No. 5, pp 805-821.

Bradshaw, J. M., 1976. New Casing Log Defines Internal/External Corrosion. World Oil, Vol 183, No. 4, pp 53-55.

Broding, R. A., 1984. Application of the Sonic Volumetric Scan Log to Cement Evaluation. Procedings of 25 Symposium of Society of Professional Well Log Analysts, New Orleans, 1984, Transactions: Houston, Society of Professional Well Log Analysts, Vol 2, pp JJ1-JJ17.

Butler, D. K., 1983. Cavity Detection and Delineation Research; Report 1, Microgravimetric Surveys, Medford Caul Site, Florida. Technical Report GL-83-1, U.S. Army Engineer Waterways Experiment Station, Vicksburg, MS.

Butler, D. K., 1984. Microgravimetric and Gravity-Gradient Techniques for Detection of Subsurface Cavities. Geophysics, Vol 49, No. 7, pp 1084-1096.

Butler, D. K., 1986. Assessment and Field Examples of Continuous Wave Electromagnetic Surveying for Ground Water; Report 10, Military Hydrology, Miscellaneous Paper EL-79-6, U.S. Army Engineer Waterways Experiment Station, Vicksburg, MS.

Butler, D. K., 1986. Transient Electromagnetic Methods for Ground-Water Assessment. Miscellaneous Paper GL-86-27, U.S. Army Engineer Waterways Experiment Station, Vicksburg, MS.

Butler, D. K., D. Yule, J. Llopis, and M. Sharp, 1989. Geophysical Assessment of Foundation Conditions, Mill Creek Dam. Technical Report GL-89-12, U.S. Army Engineer Waterways Experiment Station, Vicksburg, MS.

Butler, D. K., J. Simms, and D. Cook, 1994. Archaeological Geophysics Investigation of the Wright Brothers 1910 Hanger Site Technical Report GL-89-13, U.S. Army Engineer Waterways Experiment Station, Vicksburg, MS.

Butler, D. K., 1992. Proceedings of the Government Users Workshop on Ground Penetrating Radar Applications and Equipment. Miscellaneous Paper GL-92-40, U.S. Army Engineer Waterways Experiment Station, Vicksburg, MS.

Cahyna, F., O. Mazac, and D. Vendhodova, D., 1990. Determination of the Extent of Cyanide Contamination by Surface Geoelectrical Methods. Geotechnical and Environmental Geophysics, Vol 2, Society of Exploration Geophysicists, Tulsa, OK, pp 97-99.

Colwel, R. N., 1983. Manual of Remote Sensing, Volumes 1 and 2, American Society of Photogrammetry, Falls Church, VA.

Corwin, R. W., 1989. Geotechnical Applications of the Self-Potential Method. Technical Report REMRGT-6, U.S. Army Engineer Waterways Experiment Station, Vicksburg, MS.

Corwin, R. F., and D. Hoover, 1979. The Self-Potential Method in Geothermal Exploration, Geophysics, Vol 44, No. 2, pp 226-245.

Craig, J. T., Jr., and B. Randall, 1976. Directional Survey Calculation. Petroleum Engineer International, March 1976, pp 38-54.

Crowder, R. E., F. Paillet, and A. Hess, 1994. High Resolution Flowmeter Logging - A Unique Combination of Borehole Geophysics and Hydraulics; Part I, Flowmeter Techniques and Equipment Development: Borehole Applications with the Heat Pulse Flowmeter. Proceedings of Symposium on the Application of Geophysics to Engineering and Environmental Problems, Vol 1.

Das, B. M., 1994. Principles of Geotechnical Engineering. 3rd edition, PWS Publishing Company, Boston, MA.

Davison, C. C., W. Keys, and F. Paillet, 1982. Use of Borehole-Geophysical Logs and Hydrologic Tests to Characterize Crystalline Rock for Nuclear-Waste Storage, Whiteshell Nuclear Research Establishment, Manitoba and Chalk River Nuclear Laboratory, Ontario, Canada. Technical Report 418, Battelle Project Management Division Office of Nuclear Waste Isolation, Columbus, OH.

Dobrin, M. B., 1960. Introduction to Geophysical Prospecting. 2nd edition, McGraw-Hill Book Co, Inc., New York.

Dodds, A. R., and D. Ivic, 1990. Integrated Geophysical Methods Used for Groundwater Studies in the Murray Basin, South Australia in Geotechnical and Environmental Geophysics. Society of Exploration Geophysicists.

Dudgeon, C. R., M. Green, and W. Smedmor, 1975. Heat-Pulse Flowmeter for Boreholes. Technical Report 4, Water Research Centre, Medmenham, England.

Duska, L., 1963. A Rapid Curved Path Method for Weathering and Drift Corrections. Blondeau Swartz, Vol 28, No. 6, pp 925-947.

Eastman Kodak Co., 1982. Kodak for Aerial Photography. Kodak Publication No. M-29, Rochester, NY.

Eastman Kodak Co., 1983. Characteristics of Kodak Films. Kodak Publication No. M-57, Rochester, NY.

Edwards, J. M., and S. Stroud, 1964. A Report on Field Results of the Electromagnetic Casing Inspection Log. Paper SPE 664, Society of Petroleum Engineers of the American Institute of Mining, Metallurgical, and Petroleum Engineers.

Elifrits, C. D., T. Barney, D. Barr, and C. Johannsen, 1979. Low Cost Method of Mapping Land Cover Using Satellite Images. In Learning to Use Our Environment, The Institute of Environmental Studies, Mt. Prospect, IL.

Erchul, Ronald A., and D. Slifer, 1989. The Use of Self Potential to Detect Ground-Water Flow in Karst. Technical Report REMR-GT-6, U.S. Army Engineer Waterways Experiment Station, Vicksburg, MS.

Ewing, S., 1939. The Copper-Copper Sulfate Half Cell for Measuring Potentials in the Earth. American Gas Association Proc.

Fajklewicz, Z., 1983. Rock-Burst Forecasting and Genetic Research in Coal-Mines by Microgravity Method. Geophysical Prospecting, Vol 31, No. 5, pp 748-765.

Frische, R. H., and H. Von Buttlar, 1957. A Theoretical Study of Induced Electrical Polarization. Geophysics, Vol 22, No. 3, pp. 688-706.

Gal'perin, E. I., 1974. Vertical Seismic Profiling. Special Publication No. 12, Society of Exploration Geophysicists.

Geonics, 1993. Buried-Metal Detection with the EM61. Geonics Limited, Ontario, Canada.

Geotechnical Applications of Remote Sensing and Remote Data Transmission, STP 967, A. I. Johnson and C. B. Pettersson, ed., Philadelphia, PA.

Ghosh, D. P., 1971a. Inverse Filter Coefficient for the Computation of Apparent Resistivity Standard Curves for a Horizontally Stratified Earth. Geophysical Prospecting, Vol 19, No. 4, pp 769-775.

Ghosh, D. P., 1971b. The Application of Linear Filter Theory to the Direct Interpretation of Geoelectrical Resistivity Sounding Measurements. Geophysical Prospecting, Vol 19, pp 192-217.

Grant, F. S., and G. West, 1965. Interpretation Theory in Applied Geophysics. McGraw-Hill, New York.

Guyod, H,, 1966. Interpretation of Electric and Gamma Ray Logs in Water Wells, The Log Analyst, Vol 6, No. 5, pp 29-44.

Hallof, P., 1980. Grounded Electrical Methods in Geophysical Exploration, Practical Geophysics for the Exploration Geologist, Northwest Mining Association, Spokane, WA, pp 39-152.

Hardage, B. A., 1983. Vertical Seismic Profiling, Part A: Principles. Geophysical Press, London.

Hardage, B. A., and J. DiSiena, 1984. Vertical Seismic Profiling. Society of Exploration Geophysicists Continuing Education Program, Denver, CO.

Hearst, J. R., and P. Nelson, 1985. Well Logging for Physical Properties, McGraw-Hill, New York.

Heiland, C. A., 1940. Geophysical Exploration, Prentice-Hall, New York.

Hempen, G., and A. Hatheway, 1992. Geophysical Methods for Hazardous Waste Site Characterization. Special Publication No. 3, Association of Engineering Geologists, Sudbury, MA.

Hess, A. E., 1982. A Heat-Pulse Flowmeter for Measuring Low Velocities in Boreholes. U.S. Geological Survey Open-File Report 82-699.

Hilchie, D. W. 1968. Caliper Logging--Theory and Practice. The Log Analyst, Vol 9, No. 1, pp 3-12.

Hoar, J. H., 1982. Field Measurement of Seismic Wave Velocity and Attenuation for Dynamic Analyses. Ph.D. dissertation, University of Texas at Austin.

Hodges, R. E., and W. Teasdale, 1991. Considerations Related to Drilling Methods in Planning and Performing Borehole-Geophysical Logging for Ground-water Studies. Water-Resources Investigations Report 91-4090, U.S. Geological Survey.

Hoffman, G. L., M. Fenton, and J. Pawlowicz, 1991. Downhole Geophysics Project 1986-1990, Final Report. Alberta Research Council Information Series No. 110.

Hollister, J. C., 1967. A Curved Path Refractor Method, in Seismic Refraction Prospecting. A. W. Musgrave, editor, Society of Exploration Geophysicists, Tulsa, OK, pp 217-230.

Hudson, D. D., 1976. A Cost/Benefit Study of Several Land Use Mapping Methodologies Using Remotely Sensed Data. Unpublished M.S. thesis, Department of Geological Engineering, University of Missouri at Rolla.

Hudson, D. D., C. Elifrits, and D. Barr, 1976. Investigation of the Use of Remote Sensor Imagery for Land Resource Mapping. Office of Administration, State of Missouri, Jefferson City, MO.

Johannsen, H. K., 1975. An Interactive Computer/Graphic-Display-Terminal System for Interpretation of Resistivity Soundings. Geophysical Prospecting, Vol 23, pp 449-458.

Johannsen, C. J., and J. Sanders, 1982. Remote Sensing and Resource Management, Soil Conservation Society of America, Ankeny, IA.

Jones, P. H., 1961. Hydrology of Waste Disposal, National Reactor Testing Station, Idaho. US Geological Survey IDO 22042, Issued by US Atomic Energy Commission Technical Information Service, Oak Ridge, TN.

Jorgensen, D. G., 1989. Using Geophysical Logs to Estimate Porosity, Water Resistivity, and Intrinsic Permeability. U.S. Geological Survey Water Supply Paper 2321.

Joyce, A. T., 1978. Procedures for Gathering Ground Truth. Information for a Supervised Approach to a Computer-Implemented Land Cover Classification of Landsat-Acquired Multispectral Scanner Data. NASA Reference Publication No. 1015, National Aeronautics and Space Administration, Lyndon B. Johnson Space Center, Houston, TX.

Kaufman, A. A., and G. Keller, 1983. Frequency and Transient Soundings. Elsevier, New York.

Keller, G. V., and F. Frischknecht, 1966. Electrical Methods in Geophysical Prospecting. Pergamon Press, New York.

Kendall, H. A., 1965. Application of SP Curves to Corrosion Detection. Journal of Petroleum Technology, pp 1029-1032.

Kennett, P., and R. Ireson, 1982. Vertical Seismic Profiles. European Association of Exploration Geophysicists, 44th Annual Meeting, Cannes, France.

Kerfoot, W. B., 1982. Comparison of 2-D and 3-D Ground-water Flowmeter Probes in Fully Penetrating Monitoring Wells. Proceedings of Second National Aquifer and Ground Water Monitoring Symposium, National Water Well Association, pp 264-268.

Keys, W. S., 1963. Pressure Cementing of Water Wells on the National Reactor Testing Station, Idaho. US Atomic Energy Commission, IDO 12022.

Keys, W. S., 1979. Borehole Geophysics in Igneous and Metamorphic Rocks. Transactions, Society of Professional Well Loggers 20th Annual Logging Symposium, Tulsa, Society of Professional Well Log Analysts, pp 001-0026.

Keys, W. S., 1984. A Synthesis of Borehole Geophysical Data at the Underground Research Laboratory, Manitoba, Canada. Technical Report 15, Battelle Project Management Division Office of Crystalline Repository Development, Columbus, OH.

Keys, W. S., 1986. Analysis of Geophysical Logs of Water Wells with a Microcomputer. Ground Water, Vol 24, No. 6, pp 750-760.

Keys, W. S., 1990. Borehole Geophysics Applied to Ground-water Investigations. Techniques of Water Resources Investigations of the U.S. Geological Survey, Book 2, Chapter E2. (Also published in 1989 by the National Water Well Association.)

Keys, W. S., 1993. The Role of Borehole Geophysics in a Superfund Lawsuit. Transactions, 5th International Symposium, Minerals and Geotechnical Logging Society.

Keys, W. S., and A. Boulogne, 1969. Well Logging with Californium-252. Transactions, Society of Professional Well Log Analysts 10th Annual Logging Symposium, Houston, Society of Professional Well Log Analysts, pp 1-25.

Keys, W. S., and R. Brown, 1978. The Use of Temperature Logs to Trace the Movement of Injected Water. Ground Water, Vol 16, No. 1, pp 32-48.

Keys, W. S., R. Wolff, J. Bredehoeft, E. Shuter, and J. Healy, 1979. In-situ Stress Measurements Near the San Andreas Fault in Central California. Journal of Geophysical Research, Vol 84, No. B4, pp 1583-1591.

Keys, W. S., R. Crowder, and W. Henrich, 1993. Selecting Logs for Environmental Applications. Seventh Annual Outdoor Action Conference on Aquifer Restoration, Groundwater Monitoring, and Geophysical Methods, National Groundwater Association.

Klein, Jan, and J. Lajoie, 1980. Electromagnetic Prospecting for Minerals. Practical Geophysics for the Exploration Geologist, Northwest Mining Association, Spokane, WA, pp 239-290.

Komarov, V. A., H. Pishpareva, M. Semenov, and L. Khloponina, 1966. Theoretical Fundamentals for Interpretation of Survey Data Obtained with the Induced Polarization Method. Leningrad, Isdatel'stov Nedra.

Krige, J. J., 1939. Borehole Temperatures in the Transvaal and Orange Free State. Royal Society (London) Procedures Series A, Vol 173, pp 450-474.

Kuzmina, E. N., and A. Ogil'vi, 1965. On the Possibility of Using the Induced Polarization Method to Study Ground Water. Razvedochnaya i Promyslovaya Geofizika, No. 9, pp 47-69.

Ladwig, K. J., 1982. Electromagnetic Induction Methods for Monitoring Acid Mine Drainage. Ground Water Monitoring Review, Winter Issue, pp 46-57.

Lillisand, T. M., and R. Keifer, 1994. Remote Sensing and Image Interpretation. 3rd edition, Wiley, New York.

Llopis, J. L., and D. Butler, 1988. Geophysical Investigation in Support of Beaver Dam Comprehensive Seepage Investigation. Technical Report GL-88-6, U.S. Army Engineer Waterways Experiment Station, Vicksburg, MS.

Llopis, J., and K. Sjostrom, 1989. Geophysical Investigation at Hazardous Waste Management Site 16, Radford Army Ammunition Plant, Radford, Virginia. Miscellaneous Paper GL-89-18, U.S. Army Engineer Waterways Experiment Station, Vicksburg, MS.

Loelkes, G. L., G. Howard, E. Schwertz, P. Lampart, and W. Miller, 1983. Land Use/Land Cover and Environmental Photointerpretation Keys. USGS Bulletin 1600, U.S. Geological Survey, Alexandria, VA.

McNeill, J. D., 1980. Electromagnetic Terrain Conductivity Measurement at Low Induction Numbers. Technical Note TN-6, Geonics Limited, Ontario, Canada.

McNeill, J. D., 1986. Rapid, Accurate Mapping of Soil Salinity Using Electromagnetic Ground Conductivity Meters. Technical Note TN-20, Geonics Limited, Ontario, Canada.

McNeill, J. D., 1990. Use of Electromagnetic Methods for Groundwater Studies. Geotechnical and Environmental Geophysics, Vol 1, Society of Exploration Geophysicists, Tulsa, OK, pp 191-218.

Mooney, H. M., 1984. Handbook of Engineering Geophysics; Volume 1: Seismic. Bison Instruments Inc., Minneapolis, MN, (612/926-1846).

Mooney, H. M., and W. Wetzel, 1956. The Potentials About a Point Electrode and Apparent Resistivity Curves for a Two-, Three-, and Four Layer Earth. University of Minnesota Press, Minneapolis, MN.

Nettleton, L. L., 1971. Elementary Gravity and Magnetics for Geologists and Seismologists. Society of Exploration Geophysicists, Tulsa, OK.

Nielsen, David M., and L. Aller, 1984. Methods for Determining the Mechanical Integrity of Class II Injection Wells. Robert S. Kerr Environmental Research Laboratory Report EPA-600/2-84-121, US Environmental Protection Agency Office of Research and Development, Ada, OK.

Orellana, E., and H. Mooney, 1966. Master Tables and Curves for Vertical Electrical Sounding Over Layered Structures. Madrid Interciecia.

Paillet, F. L., 1980. Acoustic Propagation in the Vicinity of Fractures Which Intersect a Fluid-Filled Borehole. Transactions, Society of Professional Well Log Analysts 21st Annual Logging Symposium, pp DD1-DD33.

Paillet, F. L., 1981. A Comparison of Fracture Characterization Techniques Applied to Near-Vertical Fractures in a Limestone Reservoir. Transactions, Society of Professional Well Log Analysts 22nd Annual Logging Symposium, pp XX1-XX29.

Paillet, F. L., and J. White, 1982. Acoustic Modes of Propagation in the Borehole and Their Relationship to Rock Properties. Geophysics, Vol. 47, No. 8, pp 1215-1228.

Paillet, F. L., W. Keys, and A. Hess, 1985. Effects of Lithology on Televiewer-Log Quality and Fracture Interpretation. Transactions, Society of Professional Well Log Analysts 26th Annual Logging Symposium, pp JJJ1-JJJ31.

Paillet, F. L., and K. Kim, 1985. The Character and Distribution of Borehole Breakouts and Their Relationship to In-Situ Stresses in Deep Columbia River Basalts. Journal of Geophysical Research.

Paillet, F. L., 1994. Application of Borehole Geophysics in the Characterization of Flow in Fractured Rocks. US Geological Survey, Water Resources Investigations Report 93-4214.

Paillet, F. L., R. Crowder, and A. Hess, 1994. High-Resolution Flowmeter Logging - A Unique Combination of Borehole Geophysics and Hydraulics; Part II, Borehole Applications with the Heat Pulse Flowmeter. Proceedings of Symposium on the Application of Geophysics to Engineering and Environmental Problems, Vol 1.

Palacky, G. J., I. Ritsema, and S. De Jong, 1981. Electromagnetic Prospecting for Groundwater in Precambrian Terrains in the Republic of Upper Volta. Geophysical Prospecting, Vol 29, pp 932-955.

Palmer, D., 1980. The Generalized Reciprocal Method of Seismic Refraction Interpretation. Society of Exploration Geophysicists, Tulsa, OK.

Parasnis, D. S., 1962. Principles of Applied Geophysics. Methuen and Co., Ltd, London.

Parasnis, D. S., 1973. Mining Geophysics. Elsevier Scientific Publishing, New York.

Patten, E. P., and G. Bennett, 1963. Application of Electrical and Radioactive Well Logging to Ground Water Hydrology. US Geological Survey Water Supply Paper 1544-D.

Pedler, W. H., M. Barvenik, C. Tsang, and F. Hale, 1990. Determination of Bedrock Hydraulic Conductivity and Hydrochemistry Using a Wellbore Fluid Logging Method. Proceedings of 4th National Water Well Association Outdoor Action Conference.

Pedler, W. H., C. Head, and L. Williams, 1992. Hydrophysical Logging: A New Wellbore Technology for Hydrogeologic and Contaminant Characterization of Aquifers. Proceedings of National Groundwater Association 6th National Outdoor Action Conference, pp 1701-1715.

Pirson, S. J., 1963. Handbook of Well Log Analysis, Prentice-Hall, Englewood Cliffs, NJ.

Prakash, S., 1981. Soil Dynamics, McGraw-Hill Book Company, New York.

Redpath, B. B., 1973. Seismic Refraction Exploration for Engineering Site Investigations. Technical Report E-73-4, U.S. Army Engineer Waterways Experiment Station, Vicksburg, MS.

Redpath, B. B., R. Edwards, R. Hale, and F. Kintzer, 1982. Development of Field Techniques to Measure Damping Values for Near-surface Rocks and Soils. Unpublished report prepared for the National Science Foundation Earthquake Hazards Mitigation, New York.

Schimschal, U., 1986. VSP Interpretation and Applications. Schlumberger Educational Services, Houston, TX.

Scott, J. H., 1977. Borehole Compensation Algorithms for a Small-Diameter, Dual-Detector Density Well-Logging Probe. Transactions, Society of Professional Well Log Analysts 18th Annual Logging Symposium, Society of Professional Well Log Analysts, pp S1-S17.

Seigel, H. O., 1959. Mathematical Formulation and Type Curves for Induced Polarization. Geophysics, Vol 24, No. 3, pp 547-565.

Seigel, H. O., 1970. The Induced Polarization Method in Mining and Groundwater Geophysics. Geological Survey Canada, Economic Geology Report 26.

Sharp, M. K., D. Yule, and D. Butler, 1990. Geophysical Investigation of Burial Site 3-A, Defense Depot, Ogden, Utah. Miscellaneous Paper GL-90-6, U.S. Army Engineer Waterways Experiment Station, Vicksburg, MS.

Sirles, P. C., and A. Viksne, 1990. Site-Specific Shear Wave Velocity Determinations for Geotechnical Engineering Applications. Geotechnical and Environmental Geophysics,

Investigations in Geophysics No. 5, Society of Exploration Geophysicists, Tulsa, OK, pp 121-131.

Sirles, P. C., D. Custer, and D. McKisson, 1993. CROSSIT Version 2, (computer program for data reduction and presentation of crosshole seismic measurements), US Bureau of Reclamation, Denver, CO.

Society of Professional Well Log Analysts, Houston Chapter, 1979. The Art of Ancient Log Analysis. Houston, TX.

Sternberg, B. K., and others, 1990. Geophysical Investigations in Support of the Arizona SSc Project. Geotechnical and Environmental Geophysics, Vol 3, Society of Exploration Geophysicists, Tulsa, OK, pp 211-228.

Stokoe, K. H., 1980. Field Measurement of Dynamic Soil Properties. Specialty Conference on Civil Engineering and Nuclear Power, ASCE, Sept. 15-17, Knoxville, TN.

Telford, W. M., and others, 1976. Applied Geophysics. Cambridge University Press.

Telford, W. M., L. Geldart, and R. Sheriff, 1990. Applied Geophysics, Cambridge University Press, New York.

Toksoz, M. N., 1984. Vertical Seismic Profiling; Part B: Advanced Concepts. Geophysical Press, London.

Tsang, C. H., P. Hufschmied, and F. Hale, 1990. Determination of Fracture Inflow Parameters with a Borehole Fluid Conductivity Method. Water Resources Research, Vol 26, No. 4, pp 561-578.

U.S. Bureau of Reclamation, 1989. Seismic Design and Analysis, Design Standards for Embankment Dams, US Bureau of Reclamation, Denver, CO.

U.S. Bureau of Reclamation, 1992. Geophysical Investigations at Tabor Dam, Unpublished report D-3611, Seismotectonics and Geophysics Section, US Bureau of Reclamation, Denver, CO.

Vacquier, V., C. Holmes, P. Kintzinger, and M. Lavergne, 1957. Prospecting for Ground Water by Induced Electrical Polarization. Geophysics, Vol 12, No. 3, pp 660-687.

Van Blaricom, R., 1980. Practical Geophysics for the Exploration Geologist. Northwest Mining Association, Spokane, WA.

Van Nostrand, R. G., and K. Cook, 1966. Interpretation of Resistivity Data. US Geological Survey Prof. Paper 499.

Vernon, J. H., F. Paillet, W. Pedler, and W. Griswold, 1993. Application of Borehole Geophysics in Defining the Wellhead Protection Area for a Fractured Crystalline Bedrock Aquifer. The Log Analyst, Vol 35, No. 1, pp 41-57.

Wetzel, W. W., and H. McMurray, 1937. A Set of Curves to Assist in the Interpretation of the Three Layer Resistivity Problem. Geophysics, Vol 2, pp 329-341.

White, J. E., 1983. Underground Sound, Application of Seismic Waves. Elsevier Science Publishing Co., New York.

Wilt, M. J., and D. Butler, 1990. Geotechnical Applications of the Self Potential (SP) Method; Report 4, Numerical Modeling of SP Anomalies: Documentation of Program SPPC and Applications. Technical Report REMR-GT-6, U.S. Army Engineer Waterways Experiment Station, Vicksburg, MS.

Wolff, R. G., J. Bredehoeft, W. Keys, and E. Shuter,, 1974. Tectonic Stress Determinations, Northern Piceance Creek Basin, Colorado. Denver Rocky Mountain Association of Geologists Guidebook, pp 193-198.

Wood, R. C., 1987. Uses of the EM31 Terrain Conductivity Meter for Mapping Surficial Geology and Groundwater Features in Dryland Salinity Investigations--a Discussion Paper. Internal Report, Prairie Farm Rehabilitation Adminstration, Lethbridge, Alberta, Canada.

Wright, J., 1988. VLF Interpretation Manual. EDA Instruments Inc., Englewood, CO.

Wyllie, M. R. J., 1963. The Fundamentals of Well Log Interpretation. Academic Press, New York.

Yearsley, E. N., and R. Crowder, 1990. Acoustic Spectrum Analysis of Borehole Sonic Logs for Engineering Properties and Fracture Characterization: A Case History. Proceedings of 1990 Annual Symposium on Engineering Geology and Geotechnical Engineering, No. 26.

Yearsley, E. N., R. Crowder, and L. Irons, 1991. Monitoring Well Completion Evaluation with Borehole Geophysical Density Logging, Ground Water Monitoring Review, Winter.

Zemanek, J., R. Caldwell, E. Glenn, S. Holcomb, L. Norton, and A. Straus, 1969. The Borehole Televiewer - A New Logging Concept for Fracture Location and Other Types of Borehole Inspection. Journal of Petroleum Technology, Vol 21, No. 6, pp 762-774.

Zhang, G., and Y. Luo, 1990. The Application of IP and Resistivity Methods to Detect Underground Metal Pipes and Cables. Geotechnical and Environmental Geophysics, Vol 3, Society of Exploration Geophysicists, Tulsa, OK, pp 239-248.

Zohdy, A., 1965. The Auxiliary Point Method of Electrical Sounding Interpretation, and Its Relationship to the Dar Zarrouk Parameters. Geophysics, Vol 30, pp 644-660.

Zohdy, A., 1968. The Effect of Current Leakage and Electrode Spacing Errors on Resistivity Measurements. U.S. Geological Survey, Prof. Paper 600-D, pp 822-833.

Zohdy, A., 1973. A Computer Program for the Automatic Interpretation of Schlumberger Sounding Curves Over Horizontally Stratified Media. U.S. Geological Survey Open File Report No. USGS-GD-74-017.

Zohdy, A., 1974. A Computer Program for the Calculation of Schlumberger Sounding Curves by Convolution. U.S. Geological Survey Open File Report No. USGS-GD-74-010.

Zohdy, A., 1974. Electrical Methods in US Geological Survey, Tech Water Resources Investigation, Book 2, Chapter D1.

Zohdy, A., 1975. Automatic Interpretation of Schlumberger Sounding Curves, Using Modified Dar Zarrouk Functions. U.S. Geological Survey Bulletin 1313-E.

Zohdy, A., and R. Bisdorf, 1975. Computer Programs for the Forward Calculation and Automatic Inversion of Wenner Sounding Curves. U.S. Geological Survey.

Spectral Analysis of Surface Waves (SASW)

Brown, L.T., 1998. Comparison of V_S Profiles from SASW and Borehole Measurements at Strong Motion Sites in Southern California. Master's thesis, University of Texas at Austin.

Gabriels, P., R. Snieder, and G. Nolet, 1987. In-situ Measurements of Shear-Wave Velocity in Sediments with Higher-Mode Rayleigh Waves. Geophysical Prospecting, Vol. 35, pp. 187-196.

Geovision Web Site. Spectral Analysis of Surface Waves (SASW). http://www.geovision.com/SASW.htm

Gucunski, N., and R. D. Woods, 1991. Instrumentation for SASW Testing. Geotechnical Special Publication No. 29, Recent Advances in Instrumentation, Data Acquisition, and Testing in Soil Dynamics, New York: American Society of Civil Engineers, pp. 1–16.

Joh, S. H., 1997. Advances in Interpretation and Analysis Techniques for Spectral-Analysis-of-Surface-Waves (SASW) Measurements. Ph.D. Dissertation, University of Texas at Austin.

Kalinski, M.E., 1998. Determination of V_S and G_{MAX} Using Surface Wave Measurements in Cased and Uncased Boreholes. Ph.D. Dissertation, University of Texas at Austin.

Lai, C.J., 1998. Simultaneous Inversion of Rayleigh Phase Velocity and Attenuation for Near-surface Site Characterization. Ph.D. Dissertation, Georgia Institute of Technology.

Nolet, G., 1975 Higher Rayleigh Modes in Western Europe. Geophysical Research Letters, Vol. 2, No. 60.

Olson Engineering Web Site. Spectral Analysis of Surface Waves (SASW). http://www.olsonengineering.com/sasw.html

Park., C.B., R. D. Miller, and J. Xia, 1999. Multichannel Analysis of Surface Waves. Geophysics, Vol. 64, No. 3, pp. 800-808.

Phillips, C., G. Casante, D. Hutchinson, 2002. The Innovative Use of Seismic Surface Waves for Void Detection and Material Characterization. Proceedings of SAGEEP '02, Las Vegas, NV.

Richart., F. E., Jr., J. R. Hall, Jr., and R. D. Woods, 1970. Vibrations of Soils and Foundations. Prentice Hall, Englewood Cliffs, N.J.

Rix, G. J., and E. A. Leipski, 1991. Accuracy and Resolution of Surface Wave Inversion. Geotechnical Special Publication No. 29: Recent Advances in Instrumentation, Data Acquisition, and Testing in Soil Dynamics, New York: American Society of Civil Engineers, pp 17–32.

Roesset, J.M., D. Chang, and K. H. Stokoe, II, 1991. Comparison of 2-D and 3-D Models for Analysis of Surface Wave Tests. Proceedings of Fifth International Conference on Soil Dynamics and Earthquake Engineering, pp. 111-126.

Roubal, M., 2000. Evaluating and Locating Engineering Structures Using Non-destructive Testing Technology. Proceedings of First International Conference on the Application of Geophysical Methodologies & NDT to Transportation Facilities and Infrastructure, Dec 2000. www.modot.state.mo.us/g2000/PAPERS/CAT2/GEOPH51.PDF

Spectral Analysis of Surface Waves (SASW), http://www.force-institute.com/ciad/sasw.htm

Stokoe, K. H., II, S. G. Wright, J. M. Roesset, R. C. Gauer, and M. Sedighi-Manesh, 1990. In situ Measurements of Stiffness Profiles in Ocean Bottom Materials Using the SASW Method. Proceedings of Offshore Technology Conference, Houston, Texas, OTC Paper No. 6234, pp. 299-305.

Stokoe, K. H.,II, G. L. Rix, and S. Nazarian, 1989. In situ Seismic Testing with Surface Waves. Proceedings of Twelfth International Conference on Soil Mechanics and Foundation Engineering, Vol. 1, Rio de Janeiro, Brazil, pp. 330-334.

Tokimatsu, K., 1995. Geotechnical Site Characterization Using Surfaces Waves. Proceedings of First International Conference on Earthquake Geotechnical Engineering, IS-Tokyo, '95, Tokyo, Balkema, Rotterdam, pp. 1333-1368.

Woods, R. D., 1968. Screening of Surface Waves in Soils. Journal of Soil Mechanics and Foundation Engineering, Proceedings of ASCE, 94 (SM4), pp. 951–979.

Zywicki, D. J., 1999. Advanced Signal Processing Methods Applied to Engineering Analysis of Seismic Surface Waves. Ph.D. Dissertation, Georgia Institute of Technology.

Zywicki, D. J. Advanced Signal Processing Methods Applied to Engineering Analysis of Seismic Surface Waves. http://www.zywicki.com/dissert.htm

The Seismoelectrical Method

Butler, K. E., R. Russell, A. Kepic, M. and Maxwell, 1996. Measurement of the Seismoelectric Response from a Shallow Boundary. Geophysics, Vol. 61, No. 06, pp. 1769-1778.

Haartsen, M. and R. Pride, 1994. Modeling of Coupled Electroseismic Wave Propagation from Point Sources in Layered Media. Abstracts, Annual Meeting, Society Of Exploration Geophysicists, pp. 1155-1158.

Haartsen, M. W., Z. Zhu, and M. Toksoz,, 1995. Seismoelectric Experimental Data and Modeling in Porous Layer Models at Ultrasonic Frequencies. Abstracts, Annual Meeting, Society Of Exploration Geophysicists, pp. 696-699.

Kindij, E., 1960. Discussion of the Electroseismic Effect, by Martner, S. T., et al (GEO-24-02-0297-0308). Geophysics, Vol. 25, No. 01, p. 325.

Long, L. T., and W. Rivers, 1975. Field Measurement of the Electroseismic Response. Geophysics, Vol. 40, No. 02, pp. 233-245.

Martner, S. T., and N. Sparks, 1959. The Electroseismic Effec. Geophysics, Vol. 24, No. 02, pp. 297-308. (* Discussion in GEO-25-01-0325-0325)

Mikhailov, O. V., J. Queen, and N. Toksoz, 1997a. Using Borehole Electroseismic Measurements to Detect and Characterize Fractured (permeable) zones. Abstracts, Annual Meeting, Society Of Exploration Geophysicists, pp. 1981-1984.

Mikhailov, O. V., M. Haartsen, and N. Toksoz, 1997b. Electroseismic Investigation of the Shallow Subsurface: Field Measurements and Numerical Modeling. Geophysics, Vol. 62, No. 01, pp. 97-105.

Millar, J, and R. Clarke. Electrokinetic Techniques for Measurement of Rock Permeability. Company Brochure from GroundFlow Ltd.

Murthy, Y. S., 1985. First Results on the Direct Detection of Groundwater by Seismoelectric Effect - A Field Experiment. ASEG 13th Geophysical Conference, Australian Society Of Exploration Geophysicists, Vol. 16, pp. 254-256.

Pride, S. and W. Haartsen, 1993. Modeling Electroseismic Wave Phenomena in Layered Media. 61st Meeting of the European Association of Exploration Geophysicists, Extended Abstracts, European Association Of Exploration Geophysicists, Session:D017.

Pride, S. R., and F. Morgan, 1991. Electrokinetic Dissipation Induced by Seismic Waves. Geophysics, Vol. 56, No. 07, pp. 914-925.

Pride, S. R., T. Madden, and N. Toksoz, 1992. Theoretical Modeling of the Electroseismic Effect. 61st Meeting of the European Association of Exploration Geophysicists, Extended Abstracts, European Association Of Exploration Geophysicists, pp. 348-349.

Ramboll Web Site. New Seismic Method for Mapping of Groundwater, http://www.ramboll.dk/other/uk/geotechnology/pulled_array_seismic.htm.

Russell, R. D., K. Butler, A. Kepic, and M. Maxwell, 1997. Seismoelectric Exploration. The Leading Edge, Vol. 16, No. 11, pp. 1611-1615.

Schirov, M., and A. Legchenko, 1991. A New Direct Non-invasive Groundwater Detection Technology for Australia. Exploration Geophysics.

Shankar, R.K., Groundwater Exploration. 20th WEDC Conference, http://www.lboro.ac.uk/departments/cv/wedc/papers/20/sessiong/ravi.pdf.

Thompson, A. H., and G. Gist, 1991. Electroseismic Prospecting. Abstracts, Annual Meeting, Society Of Exploration Geophysicists, pp. 425-427.

Thompson, A. H., and G. Gist, 1993. Geophysical Applications of Electrokinetic Conversion. The Leading Edge, Vol. 12, No. 12, pp. 1169-1173.

Zhu, Z., and D. Toksoz, 1999. Seismoelectric and Seismomagnetic Measurements in Fractured Borehole Models. Abstracts, Annual Meeting, Society Of Exploration Geophysicists, pp. 144-147.

Nuclear Magnetic Resonance (NMR)

Bernard, J., 1997. The Proton Magnetic Resonance Method for Groundwater Investigations. IRIS Document.

Fox, R. A., 1987. Magnetic Resonance Imaging of the Body. ASEG 13th Geophysical Conference, Australian Society Of Exploration Geophysicists, Vol. 18, pp. 58-59.

GEO ENG Web Site. Groundwater Geophysics Solutions. http://www.geo-eng.com.au/mine resource/download/Geo-Eng gwater geophys brochure2.pdf.

Goldman, G., M. Rabinovich, and I. Rabinovich, 1996. Detection of the Water Level in Fractured Phreatic Aquifers using NMR Geophysical Measurements. Journal of Applied Geophysics.

Goldman, M., B. Rabinovich, M. Rabinovich, D. Gilad, I. Gev, and M. Hurlimann, 1997. Advances in the Characterization of Pore Geometry and Pore Fluids by Nuclear Magnetic Resonance. Abstracts, Annual Meeting, Society Of Exploration Geophysicists, pp. 1934-1937.

Hurlimann, M. D., 1997. Advances in the Characterization of Pore Geometry and Pore Fluids by Nuclear Magnetic Resonance. Abstracts, Annual Meeting, Society Of Exploration Geophysicists, pp. 1934-1937.

IRIS Instruments, 1997. NUMIS-Surface PMR System for Water Prospecting-Maintenance Manual.

IRIS Instruments, 1997. Some Recent Publications on the Proton Magnetic Resonance Method Applied to Groundwater Investigations. Prepared for US Department of Energy. Agreement No. DE-FG07-96ER14732.

IRIS Instruments. NUMIS Sounding Inversion Program Manual.

IRIS Instruments. NUMIS-Surface PMR System for Water Prospecting, Users Guide.

Jackson, J. A., 1981. New NMR Well-logging/Fracture Mapping Technique with Possible Application of Squid NMR Detection. In Overton, W. C., Jr., Ed., SQUID Applications in Geophysics, Society Of Exploration Geophysicists, pp. 161-165.

Knight, R., T. Bryar, and C. Daughney, 1999. Laboratory Studies to Assess the Use of Nuclear Magnetic Resonance for Near surface Applications. Abstracts, Annual Meeting, Society of Exploration Geophysicists.

Legchenko, A. V., Shushakov, O. A., Perrin, J. A. and Portselan, A. A., 1995, Noninvasive NMR study of subsurface aquifers in France: Annual Meeting Abstracts, Society Of Exploration Geophysicists, 364-367.

Legchenko, A., 1996a. Some Aspects of the Performance of the Surface NMR Method. Abstracts, Annual Meeting, Society of Exploration Geophysicists, pp. 936-939.

Legchenko, A., 1996b. A Practical Accuracy of the Surface NMR Measurements. 61st Meeting European Association of Exploration Geophysicists, Extended Abstracts, European Association Of Exploration Geophysicists, Session:M025.

Legchenko, A., 1998. Inversion of Surface NMR Data. Geophysics, Vol. 63, No. 01, pp. 75 84.

Maxwell, S. and Segel, S. L., 1985, A superfast NMR determination of the proton content of rocks: Annual Meeting Abstracts, Society Of Exploration Geophysicists, Session BHG5.6.

Mohnke, O. and U. Yaramanci, 1999. A New Inversion Scheme for Surface NMR Amplitudes Using Simulated Annealing. 61st Meeting of the European Association of Exploration Geophysicists, Extended Abstracts, European Association Of Exploration Geophysicists, Session 2027.

Nes, O., P. Horsrud, and T. Skjetne, 1993. Shale Porosities as Determined by NMR. Abstracts, Annual Meeting, Society Of Exploration Geophysicists, pp. 88-91.

New Mexico Institute of Mining and Technology, 1998. Nuclear Magnetic Resonance Imaging of Water Content in the Subsurface. Blackhawk Geometrics, Inc.

Schirov, M., A. Legchenko, and G. Creer, 1991. A New Direct Non-invasive Groundwater Detection Technology for Australia. ASEG 13th Geophysical Conference, Australian Society Of Exploration Geophysicists, Vol. 12, pp. 333-338.

Shushakov, O. A., 1996. Groundwater NMR in Conductive Water. Geophysics, Vol. 61, No. 04, pp. 998-1006.

Trushkin, D. V., O. Shushakov, and A. Legchenko, 1994. The Potential of a Noise-Reducing Antenna for Surface NMR Groundwater Surveys in the Earth's Magnetic Field. Geophysical Prospecting, Vol. 42, No. 07, pp. 855-862.

Trushkin, D. V., O. Shushakov, and A. Legchenko, 1995. Surface NMR Applied to an Electroconductive Medium. Geophysical Prospecting, Vol. 43, No. 05, pp. 623-633.

Yaramanci, U., G. Lange, and K. Knodel, 1998. Effects of Regularization in the Inversion of Surface NMR Measurements. 61st Meeting of the European Association of Exploration Geophysicists, Extended Abstracts, European Association Of Exploration Geophysicists, Session:10-18.

Yaramanci, U., G. Lange, and M. Hertrich, 1999. Surface NMR Combined with Geoelectrics and Radar for Aquifer Studies in Nauen, Berlin. 61st Meeting European Association of Exploration Geophysicists, Extended Abstracts, European Association Of Exploration Geophysicists, Session:2028.

CHAPTER 10

Crosshole Sonic Logging (CSL), CSL Tomography (CSLT)

Finno, R. J., and P. Champy, 1997. Cross-hole Sonic Logging Evaluation of Drilled Shafts at the Northwestern University National GeoTechnical Experimentation Site, Final Report to the Infrastructure Technology Institute. http://www.iti.northwestern.edu/projects/NDE/

Hanna, K., K. Haramy, K, A. Rock, and B. Hoekstra, 2001. Three-Dimensional Tomographic Imaging for Deep Foundation Integrity Testing Case Studies. Proceedings of 52nd Highway Geology Symposium, Allegheny County, Maryland.

Hanna, K., K. Haramy, K, A. Rock, and B. Hoekstra, 2000. Three-Dimensional Tomographic Imaging for Deep Foundation Integrity Testing. Proceedings of First International Conference on the Application of Geophysical Methodologies & NDT to Transportation Facilities and Infrastructure.
http://www.modot.state.mo.us/g2000/PAPERS/CAT4/GEOPH54.PDF

Haramy, K. Y, and N. Mekic-Stall, 2000. Cross-hole Sonic Logging and Tomographic Imaging Surveys to Evaluate the Integrity of Deep Foundations – Case Studies. FHWA, www.cflhd.gov/CSL-Tomo/

Haramy, K. Y, and N. Mekic-Stall, 2000. Evaluation of Drilled Shafts at Piney Creek Bridge Using Cross-hole Sonic Logging Data and 3D Tomographic Imaging Method. Proceedings of First International Conference on the Application of Geophysical Methodologies & NDT to Transportation Facilities and Infrastructure. www.modot.state.mo.us/g2000/PAPERS/CAT4/GEOPH49.PDF

InfraSeis Web Site, www.infraseis.com/ust.htm

Jalinoos, F., et al, 1995. Ultrasonic Cross-hole and Cross-medium Tomography for the Detection of Defects in Structural Concrete. Proceedings of SAGEEP '95, Orlando, FL.

Mekic-Stall, N., P. Sirles, and R. Grimm, 2002. 2D and 3D Cross-hole Sonic Logging Tomography (CSLT) versus Cross-hole Sonic Logging (CSL) for Drilled Shafts. U.S. Department of Transportation, Federal Highways Administration, Geophysics 2002, Los Angeles, California.

Olson Engineering Web Site. Cross-hole Sonic Logging. http://www.olsonengineering.com/CSL.html

Piletest.com, Pile Integrity Sonic Analyzer and Cross-hole Ultrasonic Analyzer. Products and Services- Network Advertisement.

Test Method Review- A Comparison of Gamma/gamma and Cross-hole Sonic Logging. http://members.aol.com/ndtman1/papers/gammacsl.zip

GLOSSARY

A electrode. One of the current-emitting electrodes of a resistivity-logging system (A); the current return electrode is labeled B.

API unit. The American Petroleum Institute (API) has established test pits for calibrating neutron and gamma logs. The API neutron unit is defined as 1/1,000 of the difference between electrical zero and the logged value opposite the Indiana limestone in the calibration pit that has an average porosity of 19 percent. The API gamma unit is defined as 1/200 of the deflection between intervals of high and low radioactivity in the calibration pit.

Accuracy. Refers to closeness of a measurement to the true value.

Acoustic impedance. Reflects the ability of a boundary to reflect seismic energy. It is the contrast of density multiplied by velocity across the boundary. A measure of the seismic inertia of the medium.

Acoustic log. Also called sonic log; a record of changes in the character of sound waves as they are transmitted through liquid-filled rock; a record of the transit time (t) is the most common; amplitude and the full acoustic-wave form also are recorded.

Acoustic televiewer log. A record of the amplitude of high-frequency acoustic pulses reflected by the borehole wall; provides location and orientation of bedding, fractures, and cavities.

Acoustic wave. A sound wave transmitted through material by elastic deformation.

Activation log. Also called neutron-activation logs; a record of radiation from radionuclides that are produced in the vicinity of a well by irradiation with neutrons; the short half-life radioisotopes usually are identified by the energy of their gamma radiation or decay time.

Alluvium. A general term for unconsolidated material (e.g. clay, silt, sand, gravel) deposited from running water. Often a sorted or semi-sorted sediment in the bed of a stream or on its floodplain or delta. The deposit may be in the form of an alluvial fan.

Amplitude. The maximum departure of a wave from the average value.

Analog recording. Data are represented as a continuous record of physical variables instead of discrete values, as in digital recording.
Anisotropic. Having a physical property, which varies with direction.

Annulus. The space between the drill pipe or casing and the wall of the drill hole; in rocks saturated with hydrocarbons, the annulus is the transition interval between the invaded zone and the uncontaminated zone.

Anomaly. Refers to deviation from uniformity in a physical property.

Apparent resistivity/conductivity. The resistivity of a homogeneous isotropic ground that would give the same voltage/current or secondary/primary field ratios as observed in the field with resistivity or EM methods. The apparent conductivity is the reciprocal of the apparent resistivity.

Aquifer. Rocks or unconsolidated sediments that are capable of yielding a significant amount of water to a well or a spring.

Aquitard. Geologic formation/s of low hydraulic conductivity, typically saturated, but yielding a limited amount of water to wells. Also referred to as a confining unit.

Archie's Law. An empirical relationship linking formation resistivity (ρ_t), formation water resistivity (ρ_w) and porosity. The form of the relationship is $\rho_t = a \rho_w^{-m}$ where a and m are experimentally determined constants.

Atomic number (Z). The number of protons in the nucleus of an atom equal to the number of electrons in a neutral atom.

Atomic weight. The total number of protons and neutrons in the nucleus of an atom.

Attenuation, attenuate. A reduction in energy or amplitude caused by the physical characteristics of a transmitting system.

Automatic Gain Control (AGC). A process for increasing the amplitude of a trace with time, thus making all events on the trace appear to be of approximately the same amplitude. Note that this process will expand the amplitudes even if no data are present. Various window lengths are used; the appearance of the data may be greatly affected by the window used in the calculation.

Back-up curve. A curve on the analog record that displays log data on a new scale when deflections on the main curve exceed the width of the paper; usually displayed with a different pattern or color.

Bedrock. A general term referring to rock that underlies unconsolidated material.

Borehole-compensated. Probes designed to reduce the extraneous effects of the borehole and of probe position are called borehole-compensated.

Borehole television or video. A downhole television camera; see acoustic-televiewer definition.

Bottom-hole temperature. The bottom-hole temperature (BHT) usually is measured with maximum recording thermometers attached to a logging probe.

Bouguer correction. The process of correcting gravity data for the mass of the rock between a given station and its reference (base) station. Application of the Bouguer

correction to the data set, as well as corrections for latitude, topography, meter drift and elevation, yields the Bouguer anomaly.

Brute stack. A common midpoint stack with only preliminary static corrections (often none) and preliminary normal-moveout corrections (often constant velocity). This stack is often done by field computers to verify the existence of actual reflections.

Bulk density. Bulk density is the mass of material per unit volume; in logging, it is the density, in grams per cubic centimeter, of the rock with pore volume filled with fluid.

Bulk modulus. A modulus of elasticity, relating change in volume to the hydrostatic state of stress. It is the reciprocal of compressibility.

CERCLA. Comprehensive environmental response, compensation and liability act (1980). Provides for the cleanup of and liability for hazardous substances released into the environment, regardless of fault.

Calibration. Determination of the log values that correspond to environmental units, such as porosity or bulk density; calibration usually is carried out in pits or by comparison with laboratory analyses of core.

Caliper log. A continuous record of hole diameter, usually made with a mechanical probe having from one to six arms.

Casing-collar locator. An electromagnetic device (CCL) that usually is run with other logs to record the location of collars or other changes in casing or pipe.

Cementation factor. The cementation exponent (m) in Archie's equation relating formation-resistivity factor and porosity; cementation factor as relates to many aspects of pore and grain geometry that affect permeability.

Cement bond log. An acoustic amplitude log that is used to determine the location of cement behind the casing and, under some conditions, the quality of the bonding to casing and rock.

Centralizer. A device designed to maintain a probe in the center of a borehole.

Chargeability. The normalized (using the primary voltage) area under an induced polarization (IP) decay curve, between two times, after the transmitted current is stopped in a time domain survey. Usually expressed in millivolt-seconds per volt.

Coherence. A measure of the similarity of two oscillating functions.

Collimation. The technique for forcing radiation, like gamma photons, into a beam.

Complex number. Comprised of a real and imaginary part.

Complex resistivity (CR). A geophysical effect, also the basis of the CR method, in which polarization within the medium results in the voltage and applied current being out of phase - that is, their ratio is complex. Also known as spectral IP. Induced polarization (IP) is one form of complex resistivity.

Compressibility. The relative volume reduction that geological material can undergo when a force is applied or water is removed from the vicinity by pumping.

Compressional wave. Compressional acoustic waves (P) are propagated in the same direction as particle displacement; they are faster than shear waves and are used for measuring acoustic velocity or transit

Compton scattering. The inelastic scattering of gamma photons by orbital electrons; Compton scattering is related to electron density and is a significant process in gamma-gamma (density) logging.

Conductance. The product of conductivity and thickness [Siemens].

Conduction currents. Electrical current resulting from the movement of free charges (contrast with displacement current).

Conductivity (electrical). The ability of a material to conduct electrical current. In isotropic material, it is the reciprocal of resistivity. Units are Siemens/m.

Correlation. Determination of the position of stratigraphically equivalent rock units in different wells, often done by matching the character of geophysical logs; also the matching of variables, such as log response and core analyses.

Cross-hole. Geophysical methods carried out between boreholes (see also tomography).

Crossplot. A term used in log analysis for a plot of one parameter versus another, usually two different types of logs. Useful for the identification of lithology.

Cultural environment. The part of the environment which represents man-made features (e.g. roads, buildings, canals, bridges) as opposed to natural features.

Curie. The quantity of any radionuclide that produces 3.70 x 1010 disintegrations per second.

Current channeling/gathering. Channeling is a restriction of current flow due to an insulating barrier or narrowing of a conductor. Current gathering is a concentration of current in a locally, more conductive zone. The disproportionate influence of lakes and swamps on VLF surveys is a well-known example.

Current density. A measure of current flow through a given (oriented) area [Amperes/ m^2].

Cycle skip. In acoustic-velocity logging, cycle skips are caused by only one of a pair of receivers being triggered by an arriving wave, which causes sharp deflections on the log.

Dead time. In nuclear logging, dead time is the amount of time required for the system to be ready to count the next pulse; pulses occurring during dead time are not counted.

Decay. In nuclear physics, the process of disintegration of an unstable radioisotope by the spontaneous emission of charged particles or photons.

Decentralize. Forcing a logging probe against one side of the drill hole.

Deconvolution. A data processing technique applied to seismic reflection data to improve the detection and resolution of reflected events. The process reverses the effect of linear filtering processes (convolution) that have been applied to the data by recording instruments or other processes.

Dense-non-aqueous-phase liquids (DNAPLs). Organic liquids that are more dense than water. They often coalesce in an immiscible layer at the bottom of a saturated geologic unit.

Density log. Also called gamma-gamma log; gamma photons from a radioactive source in the sonde are backscattered to a detector; the backscattering is related to the bulk density of the material around the sonde.

Departure curves. Graphs that show the correction that may be made to logs for some extraneous effects, such as hole diameter, bed thickness, temperature, etc.

Depth of invasion. Radial distance from the wall of the hole to which mud filtrate has invaded.

Depth of investigation. See volume of investigation, also called radius or diameter of investigation.

Depth reference or datum. Zero reference for logs of a well; kelly bushing may be used if the rig is still on the well; ground level or top of casing is frequently used.

Depth section. A cross section to which a velocity function has been applied, thus converting arrival times of reflections to depths.

Detector. Can be any kind of a sensor used to detect a form of energy, but usually refers to nuclear detectors, such as scintillation crystals.

Deviation. The departure in degrees between the drill hole or probe axis and vertical.

Dielectric constant. A measure of the ability of a material to store charge when an electric field is applied.

Dielectric permittivity. Describes the charge separation or polarization in a medium.

Differential log. A log that records the rate of change of some logged value as a function of depth; the differential log is sensitive to very small changes in absolute value.

Digital log. A log recorded as a series of discrete numerical values (compare analog recording).

Dipmeter. A multielectrode, contact-resistivity probe that provides data from which the strike and dip of bedding can be determined.

Dipole. A pair of equal charges or poles of opposite signs.

Directional survey. A log that provides data on the azimuth and deviation of a borehole from the vertical.

Dispersion. A property of seismic surface waves in which their velocity (as well as their penetration into the subsurface) is dependent on their frequency. The basis of methods such as SASW in which seismic wave velocity is analyzed as a function of wave frequency.

Displacement currents. The movement of charge within a material by polarization, as opposed to the flow of free ions or electrons. Related to the applied electric field by the electric permittivity (dielectric constant).

Dual laterolog. A focused resistivity log with both shallow and deep investigation; usually gamma, SP, and microfocused logs are run simultaneously.

Effective porosity. The amount of interconnected pore space through which fluids can pass. Effective porosity is usually less than total porosity because some dead-end pores may be occupied by static fluid.

Elastic moduli (elastic constants). Elastic moduli specify the stress- strain properties of isotropic materials in which stress is proportional to strain. They include bulk and shear moduli.

Electric field. A vector field describing the force on a unit electrical charge [newtons/coulomb = volts/meter].

Electrical logs. Provide information on porosity, hydraulic conductivity, and fluid content of formations drilled in fluid-filled boreholes. This record is based on the dielectric properties (e.g., electrical resistivity) of the aquifer materials measured by geophysical devices lowered down boreholes or wells.

Electrode. A piece of metallic material that acts as an electric contact with a non-metal. In chemistry, it refers to an instrument designed to measure an electrical response that is proportional to the condition being assessed (e.g. pH, resistivity).

Electromagnetic-casing inspection log. The effects of eddy currents on a magnetic field are used to provide a record of the thickness of the casing wall.

Electromagnetic method. A method which measures magnetic and/or electric fields associated with subsurface currents.

Electron volt. The energy acquired by an electron passing through a potential difference of one volt (eV); used for measuring the energy of nuclear radiation and particles, usually expressed as million electron volts (MeV).

Epithermal neutron. A neutron source emits fast neutrons that are slowed by moderation to an energy level just above thermal equilibrium, where they are available for capture; most modern neutron probes measure epithermal neutrons, because they are less affected by chemical composition than thermal neutrons.

Equipotential map. A plot in which points of equal hydraulic head are connected.

F-K filtering. As frequency filtering removes components of a signal with particular time variations (low-frequency cut, etc.), F-K filtering removes components of seismic records with particular variations in both time (frequency) and space (K or wave number). As an example, ground roll will often be of low frequency and, due to the low velocity, have short wavelengths (high wave number). Thus, a low frequency, high-wave number cut filter will attenuate ground roll.

Fan shooting. A seismic refraction technique where the sensors (geophones) are deployed on a segment of a circle centered on the seismic source. Variations in the time of arrival are caused by radial variations in the velocity structure. Could be used, for example, to search for low velocity anomalies caused by buried waste.

Ferrimagnetic. Substances having positive and relatively large magnetic susceptibility as well as generally large hysteresis and remanence. This is due to the interaction of atoms and the coupling of magnetic moments aligned in opposition, which result in non-zero net moments. Ferrimagnetic minerals have this property.

Field. That space in which an effect, such as gravity or magnetism, is measurable.

Field print. A copy of a log obtained at the time of logging that has not been edited or corrected.

Filtering. a) The attenuation of a signal's components based on a measurable property (usually frequency). Filtering usually involves a numerical operation that enhances only a portion of the signal. b) Fluid passage through a material that retains particles or colloids above a certain size.

First reading. The depth at which logging began at the bottom of the hole.

Flexural Waves. Flexural waves occur in bars and refers to the 'flexing, or bending, of a bar. Thus they can be created in shafts by impacting the side of a shaft. The velocity of flexural waves depends on their wavelength.

Flowmeter. A logging device designed to measure the rate, and usually the direction, of fluid movement in a well; most are designed to measure vertical flow.

Fluid sampler. An electronically controlled device that can be run on a logging cable to take water samples at selected depths in the well.

Flushed zone. The zone in the borehole wall behind the mudcake that is considered to have had all mobile native fluids flushed from it.

Focused log. A resistivity log that employs electrodes designed to focus the current into a sheet that provides greater penetration and vertical resolution than unfocused logs.

Formation. Used in well-logging literature in a general sense to refer to all material penetrated by a drill hole without regard to its lithology or structure; used in a stratigraphic sense, formation refers to a named body of rock strata with unifying lithologic features.

Formation-resistivity factor. Formation factor (F) is the ratio of the electrical resistivity of a rock 100 percent saturated with water (Ro) to the resistivity of the water with which it is saturated (Rw). $F = Ro/Rw$.

Frequency domain. In geophysics, refers to measurements analyzed according to their constituent frequencies. The usual alternative is time domain measurements.

Galvanic. Describes geophysical techniques that require direct contact with the ground in order to pass current. The alternative is to induce currents in the earth.

Gamma. The common unit of magnetic field intensity, equal to one nanoTesla (a Tesla is the SI unit). The Earth's magnetic field strength is about 50,000 gammas (γ) in mid-latitudes.

Gamma log. Also called gamma-ray log or natural-gamma log; log of the natural radioactivity of the rocks penetrated by a drill hole; also will detect gamma-emitting artificial radioisotopes (see spectral-gamma log).

Gamma ray. A photon that has neither mass nor electrical charge that is emitted by the nucleus of an atom; measured in gamma logging and output from a source used in gamma-gamma logging.

Geomagnetic field. The Earth's magnetic field.

Geophones. Receivers used to record the seismic energy arriving from a source, in seismic geophysical methods.

Geophysical mapping. Locating geophysical anomalies in space (as opposed to time, which is geophysical monitoring).

Geophysical monitoring. Observing the change in a geophysical measurement with time.

Grain density. Also called matrix density; the density of a unit volume of rock matrix at zero porosity, in grams per cubic centimeter.

Ground electrode. A surface electrode used for SP and resistivity logging.

Ground penetrating radar (GPR). A geophysical method in which bursts of electromagnetic energy are transmitted downwards from the surface, to be reflected and refracted by velocity contrasts within the subsurface. Also known as Ground Probing Radar.

Guard log. A type of focused resistivity log that derives its name from guard electrodes that are designed to focus the flow of current.

Half-life. Radioactively, half-life is the time required for half of a given quantity of material to decay. Chemically, it is the time required for half of a given quantity of material to undergo a chemical reaction.

Imaging work station. Consists of a microcomputer with a high-resolution color monitor and accompanying software which allows the manipulation, enhancement and visual display of digital data.

Induced magnetization. Magnetization caused by an applied magnetic field. Contrast with remanent magnetization.

Induced polarization (IP). A geophysical effect whereby electrical charge is momentarily polarized within a material, usually a disseminated ore or a clay. This effect is the basis for the IP method, in which a decaying voltage due to this polarization is measured following the turn-off of the activating current in time domain surveying. See also complex resistivity.

Induction (EM), induce. The process, described by Faraday's Law, whereby a variable magnetic field generates an electric field (voltage) that, in the presence of a conductor, will produce electric currents.

Induction log. A method for measuring resistivity or conductivity that uses an electromagnetic technique to induce a flow of current in the rocks around a borehole; can be used in nonconductive-borehole fluids.

Induction number. A quantitative measure of the quality of a target for EM methods. The formulation varies for different targets but in general it involves the product of target conductivity, magnetic permeability, frequency of the transmitter and a cross-sectional dimension of the target. Dimensionless.

In-phase. That part of a periodic signal that has zero phase shift with a reference signal. See also quadrature.

Interpolation. A method to determine intermediate values from surrounding known values.

Interpretation. Transforming geophysical measurements into subsurface structure. More general term than inversion.

Interval transit time. The time required for a compressional acoustic wave to travel a unit distance (t); transit time usually is measured by acoustic or sonic logs, in microseconds per foot, and is the reciprocal of velocity.

Invaded zone. The annular interval of material around a drill hole where drilling fluid has replaced all or part of the native interstitial fluids.

Inversion, inverting. The process of deriving a model of the subsurface that is consistent with the geophysical data obtained. Generally refers to a more specific methodology than interpretation.

Isotopes. Atoms of the same element that have the same atomic number, but a different mass number; unstable isotopes are radioactive and decay to become stable isotopes.

Karst. Topographic area which has been created by the dissolution of carbonate rock terrain. It is characterized by caverns, sinkholes, and the absence of surface streams.

Lag. The distance a nuclear logging probe moves during one time constant.

Last reading. The depth of the shallowest value recorded on a log.

Lateral log. A multielectrode, resistivity-logging technique that has a much greater radius of investigation than the normal techniques, but requires thick beds and produces an unsymmetrical curve.

Laterolog. A focused-resistivity logging technique; see also guard log.

Light-non-aqueous phase liquids (LNAPLs). Organic fluids that are less dense than water. They are capable of forming an immiscible layer that floats on the water table (e.g. petroleum hydrocarbons or other organic liquids). Also referred to as Floaters.

Long normal log. A resistivity log with AM spacing usually 64 in.; see normal logs.

M electrode. The potential electrode nearest to the A electrode in a resistivity device.

Magnetics, geomagnetics. Geophysical methodology for studying anomalies in the geomagnetic field due to non-uniform magnetization of the subsurface. Uses magnetometers.

Magnetic permeability. Characteristic of a material, it is proportional to the magnetism induced in that material divided by strength of the magnetic field used.

Magnetic susceptibility. A measure of the extent to which a substance may be magnetized; it represents the ratio of magnetization to magnetic field strength.

Magnetization. The magnetic moment per unit volume. It is a vector quantity. See also magnetic susceptibility.

Magnetometer. A device for measuring the earth's magnetic geomagnetic field. Variations in the field strength may indicate changes in magnetic properties of soil and rock or presence of ferrous metals.

Mapping. Locating geological, chemical or geophysical information in space (as opposed to time, which is monitoring). The results are usually summarized as maps.

Matrix. The solid framework of rock or mineral grains that surrounds the pore spaces.

Mho. A unit of electrical conductance that is the reciprocal of ohm.

Micro-gravity survey. A surface geophysical survey method, undertaken on a very small scale (typically station spacings of a few meters), and requiring a high meter sensitivity. Measures the earth's gravitational field at different points over an area of interest. Variations in the field are related to differences in subsurface density distributions, which in turn are associated with changes in soil, rock, and cultural factors. Typically used for cavern or fracture detection.

Microresistivity log. Refers to a group of short-spaced resistivity logs that are used to make measurements of the mud cake and invaded zone.

Migration. The movement of chemicals, bacteria, gases, etc. in flowing water or vapor in the subsurface. Also, a seismic/radar term whose general meaning is the correction of the recorded image for the effects of reflector dip. A very typical result of migration is the removal of hyperbolic events on the record resulting from diffractions from faults and other discontinuities.

Monitoring. Observing the change in a geophysical, hydrogeological or geochemical measurement with time.

Mud cake. Also called filter cake; the layer of mud particles that builds up on the wall of a rotary-drilled hole as mud filtrate is lost to the formation.

Mud filtrate. The liquid effluent of drilling mud that penetrates the wall of the hole.

Muting. Change in the amplitude of all or part of a trace before additional processing. Noisy or clearly erroneous traces are given zero amplitude. Data before the first break and the known refraction arrivals are also often reduced to zero amplitude.

N electrode. The potential electrode distant from the A electrode in a resistivity device.

Neutron log. Neutrons from an isotopic source are measured at one or several detectors after they migrate through material in, and adjacent to, the borehole. Log response primarily results from hydrogen content, but it can be related to saturated porosity and moisture content.

Noise. Any unwanted signal; a disturbance that is not part of signal from a specified source. In electrical or induced polarization (IP) surveys, noise may result from interference of power lines, motor-generators, atmospheric electrical discharges, etc. See cultural noise.

Non-aqueous-phase-liquid (NAPL). Elements or compounds in the liquid phase other than water. This phase is immiscible in water. Examples include petroleum hydrocarbons, like gasoline, and solvents such as trichloroethylene.

Non-unique. In geophysical interpretation and mathematical modeling, a problem for which two or more subsurface models satisfy the data equally well.

Normal log. A quantitative-resistivity log, made with four electrodes, which employs spacings between 4 and 64 in. to investigate different volumes of material around the borehole; see also long-normal log and short-normal log.

Normal moveout corrections. Time shift corrections to reflection arrivals because of variation in shotpoint-to-geophone distance (offset). The amount of shift depends on 1) the length of the raypath from shot to reflection point to receiver, and 2) the velocity of the material traversed. Deeper reflections are corrected using velocities indicative of the deeper section.

Nuclear log. Well logs using nuclear reactions either measuring response to radiation from sources in the probe or measuring natural radioactivity present in the rocks.

Ohm (Ω). The unit of electrical resistance through which 1 amp of current will flow when the potential difference is 1 V.

Ohm-meter (Ωm). Unit of electrical resistivity; the resistivity of 1 m^3 of material, which has a resistance of 1 ohm when electrical current flows between opposite faces; the standard unit of measurement for resistivity logs.

Open hole. Uncased intervals of a drill hole.

Optimum offset. Seismic reflection technique employing optimum window.

P-wave. An elastic body wave in which particles move in the direction of propagation. It is the wave assumed in most seismic surveys. Also called primary or push-pull wave.

Percentage frequency effect (PFE). The percent difference in resistivity measured at two frequencies (one high, one low). It is the basic polarization parameter measured in frequency domain resistivity surveys. Equivalent to chargeability in time domain surveys.

Permafrost. Perennially frozen ground in areas where the temperature remains at or below 0^{o} C for two or more years in a row.

Permittivity. The property which enables a three-dimensional material to store electrical charge; i.e. its capacitivity.

Phase II study. Common nomenclature for the part of an environmental investigation that first involves on-site activities (i.e. geophysics, soil gas surveys and drilling)

Phase shift. A measure of the offset between two periodic signals of the same frequency. Measured in degrees or radians/milliradians.

Polarize, polarization, polarizable. Separation of charge, as in induced polarization or IP.
Porosity. The ratio of the void volume of a porous rock to the total volume, usually expressed as a percentage.

Precision. The reproducibility of a measurement; the closeness of each of a set of similar measurements to the arithmetic mean of that set.

Primary (magnetic field). The magnetic field generated by an EM transmitter. May induce a secondary magnetic field.

Probe. Also called sonde or tool; downhole well-logging instrument package.

Processing. Geophysically, to change data so as to emphasize certain aspects or correct for known influences, thereby facilitating interpretation.

Profiling. In geophysics, a survey method whereby an array of sensors is moved along the Earth's surface without change in its configuration, in order to detect lateral changes in the properties of the subsurface (faults, buried channels, etc.) The alternative is usually a sounding.

Proton. The nucleus of a hydrogen atom; a positively charged nuclear particle with a mass of one; see neutron.

Pseudosection. A cross section showing the distribution of a geophysical property, such as seismic travel time, from which the distribution of the geological property of interest (depth to bedrock, for example) can be interpreted.

Quadrature. That part of a periodic signal that is 90 degrees out of phase with a reference signal. See also in-phase.

RCRA. The Resource Conservation and Recovery Act, passed by the US Congress in 1976 to regulate solid and hazardous waste disposal.

RI/FS. Remedial investigation/feasibility study.

Radar. A system whereby short electromagnetic waves are transmitted and any energy which is scattered back by reflecting objects is detected. Acronym for radio detection and ranging.

Radioactivity. Energy emitted as particles or rays during the decay of an unstable isotope to a stable isotope.

Receiver. The part of an acquisition system that senses the information signal.

Reflection coefficient. A term used in seismic reflection and GPR to describe the ratio of the reflected to incident amplitudes of a pulse reflected from an interface.

Remanent magnetization (Remanence). Magnetization remaining after the application of magnetic field has ceased.

Repeat section. A short interval of log that is run a second time to establish repeatability and stability.

Resistivity (electrical). Electrical resistance to the passage of a current, expressed in ohm-meters; the reciprocal of conductivity.

Resistivity logs. Any of a large group of logs that are designed to make quantitative measurements of the specific resistance of a material to the flow of electric current; calibrated in ohm-meters.

Resolution. Refers to the smallest unit of measurement that can be distinguished using a particular instrument or method; based on the ability to separate two measurements which are very close together.

Reversal. A typical distortion of normal-resistivity logs opposite beds that are thinner than the AM spacing; the effect is an apparent decrease in resistivity in the center of a resistive unit.

Rugosity. The irregularity or roughness of the wall of a borehole.

SASW. Spectral analysis of surface waves. An in situ seismic method that analyzes dispersion of surface waves and inverts it in terms of mechanical properties of the soil.

S-wave. A body wave in which particles move perpendicular to the direction of propagation. Also known as secondary or shear wave.

Saturation. The percentage of the pore space occupied by a fluid, usually water in hydrologic applications.

Scintillation detector. An efficient detector used in nuclear-logging equipment; radiation causes flashes of light that are amplified and output in a crystal as electronic pulses by a photo multiplier tube to which it is coupled.

Secondary (magnetic field). The magnetic field that is generated by currents that are induced to flow in the ground by time variations in the primary magnetic field of the transmitter.

Secondary porosity. Porosity developed in a rock after its deposition as a result of fracturing or solution; usually not uniformly distributed.

Seismic reflection. A surface geophysical method recording seismic waves reflected from geologic strata, giving an estimate of their depth and thickness.

Seismic refraction. A surface geophysical method recording seismic waves refracted by geological strata.

Self potential (SP). A geophysical method measuring the natural, static voltage existing between sets of points on the ground surface.

Shale base line. A line drawn through the SP log deflections that represent shale; a similar technique can be used on gamma logs and can represent the average log response of sand.

Shear modulus. The stress-strain ratio for simple shear in isotropic materials which obey Hooke's law.

Shear wave. An acoustic wave with direction of propagation at right angles to the direction of particle vibration (S wave).

Short-normal log. One of a group of normal-resistivity logs usually with AM spacing of 16 in. or less.

Single-point resistance log. A single electrode device used to make measurements of resistance that cannot be used quantitatively.

Skin depth. The effective depth of penetration in a conducting medium of electromagnetic energy (when displacement currents can be ignored); the depth at which the amplitude of a plane wave has been attenuated to 1/e or 0.37.

Sort. Data in shot record form are sorted for display as common offset records, common shot records, common receiver records, or common depth point records.

Sounding. In geophysics, a survey method whereby the geometry and/or frequency of an array of sensors is varied so as to measure the physical properties of the earth as a function of depth beneath the configuration. The alternative is usually profiling.

Spacing. The distance between sources or transmitters and detectors or receivers on a logging probe.

Specific conductance. Strictly speaking identical to electrical conductivity; the term is used in hydrogeology to refer to the conductivity of surface and ground water and expressed in micro Siemens per centimeter. It is a direct function of the total dissolved solids in the water.

Spectral-gamma log. A log of gamma radiation as a function of its energy that permits the identification of the radioisotopes present.

Spectral induced polarization (IP). See complex resistivity.

Spine and ribs plot. A plot of long-spaced detector output versus short-spaced detector output for a dual detector gamma-gamma probe; permits correction for some extraneous effects.

Spinner survey. A log made with an impeller flowmeter.

Spontaneous-potential log. A log of the difference in DC voltage between an electrode in a well and one at the surface; most of the voltage results from electrochemical potentials that develop between dissimilar borehole and formation fluids.

Stacking. Adding together two or more signals. This process is often used in geophysics to improve the signal to noise ratio. A common application is stacking seismic signals in seismic refraction data recording.

Standoff. Distance separating a probe from the wall of a borehole.

Statics. Time shift corrections to individual traces to compensate for the effects of variations in elevation, surface layer thickness or velocity, or datum references.

Streaming potential. A voltage resulting from flow of an ionic fluid.

Surface wave. A wave that travels along, or near to, the surface; its motion dropping off rapidly with distance from it. A distinct seismic mode from the body waves, P- and S.

Survey. Oil-industry term used for the performance or result of a well-logging operation.

Target. The object at which a survey sighting is aimed.

Temperature log. A log of the temperature of the fluids in the borehole; a differential

temperature log records the rate of change in temperature with depth and is sensitive to very small changes.

Terrain conductivity. Geophysical method in which EM methods measure directly the average electrical conductivity of the ground. Operates at low induction number.

Thermal neutron. A neutron that is in equilibrium with the surrounding medium such that it will not change energy (average 0.025 eV) until it is captured.

Time constant. The time in seconds required for an analog system to record 63 percent of the change that actually occurred from one signal level to another.

Time domain. In geophysics refers to measurements analyzed according to their behavior in time. The usual alternative is frequency domain measurements.

Time domain reflectometry (TDR). A device, which measures electrical characteristics of wideband transmission systems. Commonly used to measure soil moisture content.

Tomography. A method for determining the distribution of physical properties within the earth by inverting the results of a large number of measurements made in three dimensions (e.g. seismic, radar, resistivity, EM) between different source and receiver locations.

Tracer log. Also called tracejector log; a log made for the purpose of measuring fluid movement in a well by means of following a tracer injected into the well bore; tracers can be radioactive or chemical.

Track. Term used for the areas in the American Petroleum Institute log grid that are tandard for most large well-logging companies; track 1 is to the left of the depth column, and tracks 2 and 3 are to the right of the depth column, but are not separated.

Transducer. Any device that converts an input signal to an output signal of a different form; it can be a transmitter or receiver in a logging probe.

Transient. Occurring when the system is still changing with time; i.e., a steady state has not been attained. Most groundwater flow systems are transient, not steady state.

Variable-density log (VDL). Also called 3-dimensional log; a log of the acoustic wave train that is recorded photographically, so that variations in darkness are related to the relative amplitude of the waves.

Velocity panels. A set of stacked test sections with a progression of assumed normal-moveout velocities applied. A powerful method for determining velocities if distinct reflection events are present, as the reflections will be coherent where the velocities are correct and be degraded in appearance at higher or lower NMO velocities.

Well log. A record describing geologic formations and well testing or development techniques used during well construction. Often refers to a geophysical well log in which the physical properties of the formations are measured by geophysical tools, E-logs, neutron logs, etc.

Z/A effect. Ratio of the atomic number (Z) to the atomic weight (A), which affects the relation between the response of gamma-gamma logs and bulk density.

Errata to
Application of Geophysical Methods to Highway Related Problems

Page number		Change	
		From	**to**
ii		object	objective
34		Figure 19	Figure 21
37		for	either
Figure 46		Woke	Wake
Figure 46		etal	et al
142		Calculate	To calculate
142		*add text*	use the equation
142		*delete*	Calculate
142		Calculate	To calculate
143		Calculate	*remove word*
182		Sting/Swift automated	SuperSting R1 IP
193		Sting/Swift	SuperSting R1 IP resistivity
227		Sting/Swift	SuperSting R1 IP resistivity
266	Figure 154 caption	figure 153	figure 152
272		Sting/Swift	SuperSting R1 IP resistivity instrument
285		Sting/Swift system	SuperSting R1 IP Resistivity meter
296		GroundFlow 1500	GroundFlow 2500
296		GroundFlow 1500	GroundFlow 2500
419		materialshigher	materials higher
426		equa tions	equations
427		vubrations	vibrations
529		GroundFlow 1500	GroundFlow 2500
529		The GroundFlow 1500	The GroundFlow 2500
529	Figure 324 caption	Ground Flow 1500	GroundFlow 2500